VOLUME 29 / NUMBER 6
MARCH 23, 1991
ACC. NOS. N91-14273 TO N91-15122

STAR

AN ABSTRACT JOURNAL

Scientific and Technical Aerospace Reports

PRODUCED BY THE
SCIENTIFIC AND TECHNICAL
INFORMATION
DIVISION

NASA

NATIONAL AERONAUTICS AND SPACE ADMINISTRATION

***Scientific and Technical Aerospace Reports* (*STAR*)** is an abstract journal that provides comprehensive coverage of worldwide aerospace-related reports. It is a major product of the International Aerospace Database managed by the NASA Scientific and Technical Information (STI) Program. The coverage includes reports on aeronautics, space, and supporting disciplines. *STAR* lists current, publicly available reports entered into the NASA STI Database during the 2-week period preceding publication. An explanation of items that appear in each citation is given on the last page of each volume.

NASA sponsors a companion journal, *International Aerospace Abstracts* (*IAA*), that lists abstracts of the open literature on aerospace subjects available worldwide. *IAA* is available through the American Institute of Aeronautics and Astronautics.

Entries found in *STAR* and *IAA* are available through NASA's online service, RECON, as the International Aerospace Database and through DIALOG as the Aerospace Database.

Information on aerospace and related subjects is gathered by the NASA STI Program through national and international agreements and exchanges and is made available to the NASA community as well as to the public in many forms through various outlets. The section on NASA STI Program Products and Services contains additional information.

US ISSN 0036-8741

Volume 29 Number 6 / March 23, 1991

TABLE OF CONTENTS

AERONAUTICS For related information see also *Astronautics.*

01 AERONAUTICS (GENERAL) **771**

02 AERODYNAMICS **771**
Includes aerodynamics of bodies, combinations, wings, rotors, and control surfaces; and internal flow in ducts and turbomachinery. For related information see also *34 Fluid Mechanics and Heat Transfer.*

03 AIR TRANSPORTATION AND SAFETY **778**
Includes passenger and cargo air transport operations; and aircraft accidents. For related information see also *16 Space Transportation* and *85 Urban Technology and Transportation.*

04 AIRCRAFT COMMUNICATIONS AND NAVIGATION **779**
Includes digital and voice communication with aircraft; air navigation systems (satellite and ground based); and air traffic control. For related information see also *17 Space Communications, Spacecraft Communications, Command and Tracking* and *32 Communications and Radar.*

05 AIRCRAFT DESIGN, TESTING AND PERFORMANCE **780**
Includes aircraft simulation technology. For related information see also *18 Spacecraft Design, Testing and Performance* and *39 Structural Mechanics.* For land transportation vehicles see *85 Urban Technology and Transportation.*

06 AIRCRAFT INSTRUMENTATION **784**
Includes cockpit and cabin display devices; and flight instruments. For related information see also *19 Space craft Instrumentation* and *35 Instrumentation and Photography.*

07 AIRCRAFT PROPULSION AND POWER **785**
Includes prime propulsion systems and systems components, e.g., gas turbine engines and compressors; and onboard auxiliary power plants for aircraft. For related information see also *20 Spacecraft Propulsion and Power, 28 Propellants and Fuels,* and *44 Energy Production and Conversion.*

08 AIRCRAFT STABILITY AND CONTROL **785**
Includes aircraft handling qualities; piloting; flight controls; and autopilots. For related information see also *05 Aircraft Design, Testing and Performance.*

09 RESEARCH AND SUPPORT FACILITIES (AIR) **787**
Includes airports, hangars and runways; aircraft repair and overhaul facilities; wind tunnels; shock tubes; and aircraft engine test stands. For related information see also *14 Ground Support Systems and Facilities (Space).*

ASTRONAUTICS For related information see also *Aeronautics.*

12 ASTRONAUTICS (GENERAL) **788**
For extraterrestrial exploration see *91 Lunar and Planetary Exploration.*

13 ASTRODYNAMICS **789**
Includes powered and free-flight trajectories; and orbital and launching dynamics.

14 GROUND SUPPORT SYSTEMS AND FACILITIES (SPACE) **790**
Includes launch complexes, research and production facilities; ground support equipment, e.g., mobile transporters; and simulators. For related information see also *09 Research and Support Facilities (Air).*

15 LAUNCH VEHICLES AND SPACE VEHICLES ..... **N.A.**
Includes boosters; operating problems of launch/space vehicle systems; and reusable vehicles. For related information see also *20 Spacecraft Propulsion and Power.*

16 SPACE TRANSPORTATION ..... **N.A.**
Includes passenger and cargo space transportation, e.g., shuttle operations; and space rescue techniques. For related information see also *03 Air Transportation and Safety* and *18 Spacecraft Design, Testing and Performance.* For space suits see *54 Man/System Technology and Life Support.*

17 SPACE COMMUNICATIONS, SPACECRAFT COMMUNICATIONS, COMMAND AND TRACKING . **790**
Includes telemetry; space communications networks; astronavigation and guidance; and radio blackout. For related information see also *04 Aircraft Communications and Navigation* and *32 Communications and Radar.*

N.A.—no abstracts were assigned to this category for this issue.

18 SPACECRAFT DESIGN, TESTING AND PERFORMANCE **791**
Includes satellites; space platforms; space stations; spacecraft systems and components such as thermal and environmental controls; and attitude controls. For life support systems see *54 Man/System Technology and Life Support.* For related information see also *05 Aircraft Design, Testing and Performance, 39 Structural Mechanics,* and *16 Space Transportation.*

19 SPACECRAFT INSTRUMENTATION **792**
For related information see also *06 Aircraft Instrumentation* and *35 Instrumentation and Photography.*

20 SPACECRAFT PROPULSION AND POWER **800**
Includes main propulsion systems and components, e.g., rocket engines; and spacecraft auxiliary power sources. For related information see also *07 Aircraft Propulsion and Power, 28 Propellants and Fuels, 44 Energy Production and Conversion,* and *15 Launch Vehicles and Space Vehicles.*

CHEMISTRY AND MATERIALS

23 CHEMISTRY AND MATERIALS (GENERAL) **801**

24 COMPOSITE MATERIALS **801**
Includes physical, chemical, and mechanical properties of laminates and other composite materials. For ceramic materials see *27 Nonmetallic Materials.*

25 INORGANIC AND PHYSICAL CHEMISTRY **804**
Includes chemical analysis, e.g., chromatography; combustion theory; electrochemistry; and photochemistry. For related information see also *77 Thermodynamics and Statistical Physics.*

26 METALLIC MATERIALS **806**
Includes physical, chemical, and mechanical properties of metals, e.g., corrosion; and metallurgy.

27 NONMETALLIC MATERIALS **810**
Includes physical, chemical, and mechanical properties of plastics, elastomers, lubricants, polymers, textiles, adhesives, and ceramic materials. For composite materials see *24 Composite Materials.*

28 PROPELLANTS AND FUELS **814**
Includes rocket propellants, igniters and oxidizers; their storage and handling procedures; and aircraft fuels. For related information see also *07 Aircraft Propulsion and Power, 20 Spacecraft Propulsion and Power,* and *44 Energy Production and Conversion.*

29 MATERIALS PROCESSING **814**
Includes space-based development of products and processes for commercial application. For biological materials see *55 Space Biology.*

ENGINEERING For related information see also *Physics.*

31 ENGINEERING (GENERAL) **815**
Includes vacuum technology; control engineering; display engineering; cryogenics; and fire prevention.

32 COMMUNICATIONS AND RADAR **817**
Includes radar; land and global communications; communications theory; and optical communications. For related information see also *04 Aircraft Communications and Navigation* and *17 Space Communications, Spacecraft Communications, Command and Tracking.* For search and rescue see *03 Air Transportation and Safety,* and *16 Space Transportation.*

33 ELECTRONICS AND ELECTRICAL ENGINEERING **819**
Includes test equipment and maintainability; components, e.g., tunnel diodes and transistors; microminiaturization; and integrated circuitry. For related information see also *60 Computer Operations and Hardware* and *76 Solid-State Physics.*

34 FLUID MECHANICS AND HEAT TRANSFER **824**
Includes boundary layers; hydrodynamics; fluidics; mass transfer and ablation cooling. For related information see also *02 Aerodynamics* and *77 Thermodynamics and Statistical Physics.*

35 INSTRUMENTATION AND PHOTOGRAPHY **828**
Includes remote sensors; measuring instruments and gauges; detectors; cameras and photographic supplies; and holography. For aerial photography see *43 Earth Resources and Remote Sensing.* For related information see also *06 Aircraft Instrumentation* and *19 Spacecraft Instrumentation.*

36 LASERS AND MASERS **831**
Includes parametric amplifiers. For related information see also *76 Solid-State Physics.*

37 MECHANICAL ENGINEERING **832**
Includes auxiliary systems (nonpower); machine elements and processes; and mechanical equipment.

38 QUALITY ASSURANCE AND RELIABILITY **835**
Includes product sampling procedures and techniques; and quality control.

39 STRUCTURAL MECHANICS **836**
Includes structural element design and weight analysis; fatigue; and thermal stress. For applications see *05 Aircraft Design, Testing and Performance* and *18 Spacecraft Design, Testing and Performance.*

GEOSCIENCES For related information see also *Space Sciences.*

42 GEOSCIENCES (GENERAL) ..... **N.A.**

43 EARTH RESOURCES AND REMOTE SENSING **839**
Includes remote sensing of earth resources by aircraft and spacecraft; photogrammetry; and aerial photography. For instrumentation see *35 Instrumentation and Photography.*

44 ENERGY PRODUCTION AND CONVERSION **840**
Includes specific energy conversion systems, e.g., fuel cells; global sources of energy; geophysical conversion; and windpower. For related information see also *07 Aircraft Propulsion and Power, 20 Spacecraft Propulsion and Power,* and *28 Propellants and Fuels.*

45 ENVIRONMENT POLLUTION **843**
Includes atmospheric, noise, thermal, and water pollution.

46 GEOPHYSICS **844**
Includes aeronomy; upper and lower atmosphere studies; ionospheric and magnetospheric physics; and geomagnetism. For space radiation see *93 Space Radiation.*

47 METEOROLOGY AND CLIMATOLOGY **848**
Includes weather forecasting and modification.

48 OCEANOGRAPHY **850**
Includes biological, dynamic, and physical oceanography; and marine resources. For related information see also *43 Earth Resources and Remote Sensing.*

LIFE SCIENCES

51 LIFE SCIENCES (GENERAL) **851**

52 AEROSPACE MEDICINE **853**
Includes physiological factors; biological effects of radiation; and effects of weightlessness on man and animals.

53 BEHAVIORAL SCIENCES **854**
Includes psychological factors; individual and group behavior; crew training and evaluation; and psychiatric research.

54 MAN/SYSTEM TECHNOLOGY AND LIFE SUPPORT **855**
Includes human engineering; biotechnology; and space suits and protective clothing. For related information see also *16 Space Transportation.*

55 SPACE BIOLOGY **856**
Includes exobiology; planetary biology; and extraterrestrial life.

MATHEMATICAL AND COMPUTER SCIENCES

59 MATHEMATICAL AND COMPUTER SCIENCES (GENERAL) **856**

60 COMPUTER OPERATIONS AND HARDWARE **857**
Includes hardware for computer graphics, firmware, and data processing. For components see *33 Electronics and Electrical Engineering.*

61 COMPUTER PROGRAMMING AND SOFTWARE **857**
Includes computer programs, routines, algorithms, and specific applications, e.g., CAD/CAM.

62 COMPUTER SYSTEMS **862**
Includes computer networks and special application computer systems.

63 CYBERNETICS **864**
Includes feedback and control theory, artificial intelligence, robotics and expert systems. For related information see also *54 Man/System Technology and Life Support.*

64 NUMERICAL ANALYSIS **864**
Includes iteration, difference equations, and numerical approximation.

65 STATISTICS AND PROBABILITY **867**
Includes data sampling and smoothing; Monte Carlo method; and stochastic processes.

66 SYSTEMS ANALYSIS ..... **N.A.**
Includes mathematical modeling; network analysis; and operations research.

67 THEORETICAL MATHEMATICS ..... **N.A.**
Includes topology and number theory.

PHYSICS For related information see also *Engineering.*

70 PHYSICS (GENERAL) ..... **N.A.**
For precision time and time interval (PTTI) see *35 Instrumentation and Photography;* for geophysics, astrophysics or solar physics see *46 Geophysics, 90 Astrophysics,* or *92 Solar Physics.*

71 ACOUSTICS **868**
Includes sound generation, transmission, and attenuation. For noise pollution see *45 Environment Pollution.*

72 ATOMIC AND MOLECULAR PHYSICS **870**
Includes atomic structure, electron properties, and molecular spectra.

73 NUCLEAR AND HIGH-ENERGY PHYSICS **871**
Includes elementary and nuclear particles; and reactor theory. For space radiation see *93 Space Radiation.*

74 OPTICS **872**
Includes light phenomena and optical devices. For lasers see *36 Lasers and Masers.*

75 PLASMA PHYSICS **874**
Includes magnetohydrodynamics and plasma fusion. For ionospheric plasmas see *46 Geophysics.* For space plasmas see *90 Astrophysics.*

76 SOLID-STATE PHYSICS **878**
Includes superconductivity. For related information see also *33 Electronics and Electrical Engineering* and *36 Lasers and Masers.*

77 THERMODYNAMICS AND STATISTICAL PHYSICS **884**
Includes quantum mechanics; theoretical physics; and Bose and Fermi statistics. For related information see also *25 Inorganic and Physical Chemistry* and *34 Fluid Mechanics and Heat Transfer.*

SOCIAL SCIENCES

80 SOCIAL SCIENCES (GENERAL) ..... **N.A.**
Includes educational matters.

81 ADMINISTRATION AND MANAGEMENT **884**
Includes management planning and research.

82 DOCUMENTATION AND INFORMATION SCIENCE **885**
Includes information management; information storage and retrieval technology; technical writing; graphic arts; and micrography. For computer documentation see *61 Computer Programming and Software.*

83 ECONOMICS AND COST ANALYSIS ..... **N.A.**
Includes cost effectiveness studies.

84 LAW, POLITICAL SCIENCE AND SPACE POLICY **886**
Includes NASA appropriation hearings; aviation law; space law and policy; international law; international cooperation; and patent policy.

85 URBAN TECHNOLOGY AND TRANSPORTATION ..... **N.A.**
Includes applications of space technology to urban problems; technology transfer; technology assessment; and surface and mass transportation. For related information see *03 Air Transportation and Safety, 16 Space Transportation,* and *44 Energy Production and Conversion.*

SPACE SCIENCES For related information see also *Geosciences.*

88 SPACE SCIENCES (GENERAL) **886**

89 ASTRONOMY **912**
Includes radio, gamma-ray, and infrared astronomy; and astrometry.

90 ASTROPHYSICS **915**
Includes cosmology; celestial mechanics; space plasmas; and interstellar and interplanetary gases and dust. For related information see also *75 Plasma Physics.*

91 LUNAR AND PLANETARY EXPLORATION **929**
Includes planetology; and manned and unmanned flights. For spacecraft design or space stations see *18 Spacecraft Design, Testing and Performance.*

92 SOLAR PHYSICS **930**
Includes solar activity, solar flares, solar radiation and sunspots. For related information see *93 Space Radiation.*

93 SPACE RADIATION **932**
Includes cosmic radiation; and inner and outer earth's radiation belts. For biological effects of radiation see *52 Aerospace Medicine.* For theory see *73 Nuclear and High-Energy Physics.*

GENERAL

Includes aeronautical, astronautical, and space science related histories, biographies, and pertinent reports too broad for categorization; histories or broad overviews of NASA programs.

99 GENERAL **933**

SUBJECT INDEX **I-1**

PERSONAL AUTHOR INDEX **I-57**

CORPORATE SOURCE INDEX **I-65**

CONTRACT NUMBER INDEX **I-75**

REPORT/ACCESSION NUMBER INDEX **I-77**

APPENDIX **A-1**

VOLUME 29 NUMBER 6 / MARCH 23, 1991

Scientific and Technical Aerospace Reports

A Semimonthly Publication of the National Aeronautics and Space Administration

01 AERONAUTICS (GENERAL)

N91-14273*# National Aeronautics and Space Administration. Ames Research Center, Moffett Field, CA.
TABULATION OF DATA FROM THE TIP AERODYNAMICS AND ACOUSTICS TEST
Jeffrey L. Cross and Wilson Tu (DeAnza Coll., Cupertino, CA.) Nov. 1990 410 p
(NASA-TM-102280; A-90069; NAS 1.15:102280) Avail: NTIS HC/MF A18 CSCL 01B

In a continuing effort to understand helicopter rotor tip aerodynamics and acoustics, researchers at Ames Research Center conducted a flight test. The test was performed using the NASA White Cobra and a set of highly instrumented blades. Tabular and graphic summaries of two data subsets from the Tip Aerodynamics and Acoustics Test are given. The data presented are for airloads, blade structural loads, blade vibrations, with summary tables of the aircraft states for each test point. The tabular data consist of the first 15 harmonics only, whereas the plots contain the entire measured frequency content. Author

02 AERODYNAMICS

Includes aerodynamics of bodies, combinations, wings, rotors, and control surfaces; and internal flow in ducts and turbomachinery.

For related information see also *34 Fluid Mechanics and Heat Transfer.*

N91-14274*# National Aeronautics and Space Administration. Langley Research Center, Hampton, VA.
FLOW VISUALIZATION STUDIES OF BLOWING FROM THE TIP OF A SWEPT WING
Jeannette W. Smith, Raymond E. Mineck, and Dan H. Neuhart (Lockheed Engineering and Sciences Co., Hampton, VA.) Washington Nov. 1990 31 p Original contains color illustrations
(NASA-TM-4217; L-16767; NAS 1.15:4217) Avail: NTIS HC/MF A03; 8 functional color pages CSCL 01A

Flow visualization studies of blowing from the tip of a swept wing were conducted in the Langley 16- by 24-inch water tunnel. Four wing tips, each with two independent blowing slots, were tested. The two slots were located one behind the other in the chordwise direction. The wing tips were designed to vary systematically the jet length, the jet in-plane exhaust direction (sweep), and the jet out-of-plane exhaust direction (anhedral). Each blowing slot was tested separately at two angles of attack and at four ratios of jet to free stream velocity ratios. Limited tests were conducted with blowing from both slots simultaneously. Blowing from the tip inhibited inboard spanwise flow on the upper wing surface near the tip. The jet path moved farther away from the tip with increasing jet to free stream velocity ratio and moved closer to the tip with increasing angle of attack. Author

N91-14275*# National Aeronautics and Space Administration. Langley Research Center, Hampton, VA.
INTERNAL PERFORMANCE OF A HYBRID AXISYMMETRIC/NONAXISYMMETRIC CONVERGENT-DIVERGENT NOZZLE
John G. Taylor Washington Jan. 1991 57 p
(NASA-TM-4230; L-16816; NAS 1.15:4230) Avail: NTIS HC/MF A04 CSCL 01A

An investigation was conducted in the static test facility of the Langley 16-foot transonic tunnel to determine the internal performance of a hybrid axisymmetric/nonaxisymmetric nozzle in forward-thrust mode. Nozzle cross-sections in the spherical convergent section were axisymmetric whereas cross-sections in the divergent flap area nonaxisymmetric (two-dimensional). Nozzle concepts simulating dry and afterburning power settings were investigated. Both subsonic cruise and supersonic cruise expansion ratios were tested for the dry power nozzle concepts. Afterburning power configurations were tested at an expansion ratio typical for subsonic acceleration. The spherical convergent flaps were designed in such a way that the transition from axisymmetric to nonaxisymmetric cross-section occurred in the region of the nozzle throat. Three different nozzle throat geometries were tested for each nozzle power setting. High-pressure air was used to simulate jet exhaust at nozzle pressure ratios up to 12.0. Author

N91-14276 Texas Univ., Austin.
DYNAMICS OF SEPARATION AND REATTACHMENT IN A MACH 5 UNSWEPT COMPRESSION RAMP FLOW Ph.D. Thesis
Richard Anthony Gramann 1989 301 p
Avail: Univ. Microfilms Order No. DA9016890

The unsteadiness of a Mach 5 unswept compression ramp induced shock wave turbulent boundary layer interaction was examined experimentally. The wall pressure fluctuations at different locations in the interaction were measured simultaneously. These fluctuations were analyzed using a conditional cross correlation method to determine flow directions at different locations in the interaction. Data from a cylinder-induced turbulent interaction were also similarly analyzed. Conditionally acquired data from a specialized data acquisition program were used to determine the dynamics of the separation bubble and outgoing boundary layer on the ramp surface. The conditional cross correlation analysis showed that the flow downstream of the instantaneous separation shock position, in both cylinder and ramp interactions, is separated for all locations within the region of separation shock motion. The conditionally acquired data and subsequent analysis showed that the reattachment location correlates with the separation location. Therefore, the separation bubble expands and contracts at frequencies in the same range as that of the separation shock motion. The mean pressures and fluctuation intensities of the outgoing boundary layer on the ramp surface also correlate with the separation shock position, indicating that the entire interaction undergoes large amplitude, relatively low frequency changes. Since the unsteadiness is such a dominant feature, computations should include it in the solutions. Furthermore, the mean CFD results and time-averaged experimental results should be calculated the same way using time-dependent data in the experimental case, and unsteady, time-dependent computations for the CFD case.
Dissert. Abstr.

N91-14277*# Nevada Univ., Reno. Engineering Research and Development Center.
NUMERICAL INVESTIGATIONS IN THREE-DIMENSIONAL INTERNAL FLOWS Semiannual Status Report, 1 Jul. - 31 Dec. 1990
William C. Rose Dec. 1990 39 p
(Contract NCC2-507)
(NASA-CR-187373; NAS 1.26:187373) Avail: NTIS HC/MF A03 CSCL 01A

The application of the SCRAM2D code to investigating the flow fields that might be expected to occur in a representative Mach 10, two dimensional (ramp-compression) inlet is described. This Mach number allows the use of existing Navier-Stokes codes without the additional complexity of air chemistry and the associated large increases in computational time required to achieve numerical simulations of such flow fields. The CFD simulation consists of a two-dimensional inlet geometry that has an overall geometric turning of 36 degrees. The cowl for this inlet is assumed to be aligned with the oncoming freestream flow, turning the ramp flow field back parallel to the freestream, thus producing the overall 36 degree turning angle. The primary subject is the cowl shock wave-ramp boundary layer interaction effects. The results of numerical simulations carried out at the design Mach number of 10 and two other off-design Mach numbers, 7.2 and 5.0 are described. K.S.

N91-14278# Advisory Group for Aerospace Research and Development, Neuilly-Sur-Seine (France). Fluid Dynamics Panel.
MISSILE AERODYNAMICS
Oct. 1990 391 p In ENGLISH and FRENCH Symposium held in Friedrichshafen, Fed. Republic of Germany, 23-26 Apr. 1990
(AGARD-CP-493; ISBN-92-835-0589-1) Copyright Avail: NTIS HC/MF A17; Non-NATO Nationals requests available only from AGARD/Scientific Publications Executive

Current progress and achievements were reviewed, outstanding problems highlighted, and pointers established for planning future research programs. Topics considered were: computational methods and validation; empirical tools and experimental techques; flow separation and interference effects; unconventional shapes and projectiles; propulsion and base flows; aerothermodynamics; and hypersonics. For individual titles, see N91-14279 through N91-14305.

N91-14279# Aerospatiale, Chatillon (France). Div. Engins Tactiques.
SOME TRENDS IN MISSILE AERODYNAMICS
R. G. Lacau and M. Robert *In* AGARD, Missile Aerodynamics Oct. 1990 24 p (For primary document see N91-14278 06-02)
Copyright Avail: NTIS HC/MF A17; Non-NATO Nationals requests available only from AGARD/Scientific Publications Executive

The requirements for the next generation of tactical missiles, the corresponding new aerodynamic problems, and the new wind tunnel testing techniques and computational methods were highlighted. Special attention is focused on unconventional shapes as airbreathing missiles, stealth considerations, pyrotechnical lateral jet control, high angles of attack, and non-rigid airframe. The computational codes presented are based on the resolution of the Euler equations; they are illustrated by numerous industrial examples. Author

N91-14280# Royal Aerospace Establishment, Farnborough (England). Dept. of Attack Weapons.
REVIEW OF THE SPRING 1988 AGARD FMP SYMPOSIUM
H. A. Torode *In* AGARD, Missile Aerodynamics Oct. 1990 8 p (For primary document see N91-14278 06-02)
Copyright Avail: NTIS HC/MF A17; Non-NATO Nationals requests available only from AGARD/Scientific Publications Executive

Missile stability and control topics summarized include aerodynamic prediction codes; high incidence dynamics; wind tunnel experiments; configuration and control; aeroelasticity; test and evaluation; and project descriptions. B.G.

N91-14281# Royal Aeronautical Society, London (England). Aerodynamics Group Committee.
STORE CARRIAGE, INTEGRATION, AND RELEASE c05
A. B. Haines *In* AGARD, Missile Aerodynamics Oct. 1990 8 p (For primary document see N91-14278 06-02)
Copyright Avail: NTIS HC/MF A17; Non-NATO Nationals requests available only from AGARD/Scientific Publications Executive

The highlights of the conference are summarized and a balanced view of recent developments and prospects for the future in both design and prediction are given. New design concepts (internal carriage, improved launch systems, and active control during launch); mathematical modeling for predictions of store release; development and application of experimental and engineering level prediction methods for installed drag, carriage loads, effects on aircraft stability, and store release trajectories; the RAE Tornado flight research programs to provide data for the evaluation of prediction methods (aircraft flow fields, store carriage loads, and release trajectories); and application of computational fluid dynamics to problems of store carriage and release - design and prediction are discussed. Author

N91-14282# Royal Aerospace Establishment, Bedford (England). Weapon Systems Aerodynamics Div.
PRESSURE MEASUREMENTS ON SLENDER BODIES AT SUPERSONIC SPEEDS AND DEVELOPMENT OF FLOW SEPARATION CRITERA FOR EULER CODES
J. Hodges, L. C. Ward, and T. J. Birch *In* AGARD, Missile Aerodynamics Oct. 1990 12 p Previously announced as X90-72605 (For primary document see N91-14278 06-02)
Copyright Avail: NTIS HC/MF A17; Non-NATO Nationals requests available only from AGARD/Scientific Publications Executive

Surface pressure measurements on a cylindrical body with a tangent-ogive nose are described. The Mach number range is 0.7 to 4.5 with incidence angles up to 26 degrees. The high density of the measurements has allowed surface pressure contours to be constructed and detailed flow features can be observed. The measurements have suggested the use of a 2-element approximation to represent the line along which flow separation occurs. Calculations were made using a space-marching Euler code (ZEUSB) both with and without forcing flow separation. Comparisons with experimental data are presented which show that forcing flow separation significantly improves both the surface pressure and force predictions. Conclusions are drawn regarding the use of a 2-element separation line representation within Euler codes. Author

N91-14283# Imperial Coll. of Science and Technology, London (England). Dept. of Aeronautics.
COMPUTATION OF VISCOUS SUPERSONIC FLOWS
Y. Noguchi, J. M. R. Graham, and R. Hillier *In* AGARD, Missile Aerodynamics Oct. 1990 6 p Sponsored in part by Ministry of Defence, England (For primary document see N91-14278 06-02)
Copyright Avail: NTIS HC/MF A17; Non-NATO Nationals requests available only from AGARD/Scientific Publications Executive

Finite difference computations aimed at the prediction of the viscous flow field around projectiles and slender bodies at transonic and low supersonic speeds are described. Following a step by step validation process to ensure reliability in the computer program development, the code is tested with an axisymmetric body of revolution at a free stream Mach number of 1.4 and length based Reynolds number of Rex = 1.0 x 10(exp 7). Results using Baldwin-Lomax and Johnson-King turbulence models are shown. Author

N91-14284# Naval Surface Warfare Center, Silver Spring, MD. Information and Mathematical Sciences Branch.
SUPERSONIC TACTICAL MISSILE COMPUTATION USING EULER'S EQUATION WITH CROSSFLOW SEPARATION MODELING
F. J. Priolo and A. B. Wardlaw, Jr. *In* AGARD, Missile Aerodynamics Oct. 1990 11 p (For primary document see

N91-14278 06-02)
Copyright Avail: NTIS HC/MF A17; Non-NATO Nationals requests available only from AGARD/Scientific Publications Executive

The space-marching Euler solver, ZEUS, is coupled with a separation model to predict the fully three-dimensional separated flows for supersonic tactical missiles. ZEUS incorporates a multiple zone, gridding technique and a second-order extension of Godunov's method. The separation model assumes a vortex sheet leaves the surface at the experimentally observed separation point. Computations are performed on missiles which have bodies of circular and elliptic cross sections at incidences high enough to exhibit boundary layer separation. Results show that the separation model was most effective in improving predictions on missiles with circular bodies at Mach numbers below 3.5; but, at higher Mach numbers, predicted loads are not significantly affected. Qualitatively, calculated and measured flow field structures exhibit improved agreement which increases the accuracy of the predicted body and fin loads, however, quantitative flow field differences remain. For elliptic bodies, inviscid solutions are in close agreement with measured surface pressures except near the shoulder where calculations display a crossflow shock. Inclusions of the separation model diminishes the strength of the inviscid crossflow shock in the vicinity of the shoulder but has little influence on the missile loads. Author

N91-14285# Nielsen Engineering and Research, Inc., Mountain View, CA.
AERODYNAMIC DESIGN OF PEGASUS (TRADEMARK): CONCEPT TO FLIGHT WITH CFD **c20**
Michael R. Mendenhall, Daniel J. Lesieutre, Steven C. Caruso, Marnix F. E. Dillenius, and Gary D. Kuhn *In* AGARD, Missile Aerodynamics Oct. 1990 11 p Sponsored in part by Orbital Sciences Corp., Vienna, VA (For primary document see N91-14278 06-02)
Copyright Avail: NTIS HC/MF A17; Non-NATO Nationals requests available only from AGARD/Scientific Publications Executive

Pegasus (trademark), a three-stage, air-launched, winged space booster is currently under development to provide fast and efficient commercial launch services for small satellites. The aerodynamic design and analysis of the vehicle was conducted without benefit of wind tunnel and subscale model testing using only computational aerodynamic and fluid dynamic methods. All levels of codes, ranging in complexity from empirical database methods to three-dimensional Navier-Stokes codes, were used in the design. The design and analysis requirements, the unique and conservative design philosophy, and the analysis methods considered for the various technical areas of interest and concern are described. Author

N91-14286# National Aeronautical Establishment, Ottawa (Ontario).
APPLICATION OF EULER AND NAVIER-STOKES CODES TO MISSILE TYPE BODIES WITH HIGH L/D RATIOS
D. J. Jones, J. Evans, F. J. Priolo, Walter B. Sturek, and A. B. Wardlaw, Jr. (Naval Surface Warfare Center, Silver Spring, MD.) *In* AGARD, Missile Aerodynamics Oct. 1990 15 p (For primary document see N91-14278 06-02)
Copyright Avail: NTIS HC/MF A17; Non-NATO Nationals requests available only from AGARD/Scientific Publications Executive

Several Euler codes and a parabolized Navier-Stokes code are used to predict normal forces, pitching moments, and centers of pressure on long axisymmetric bodies which are cone cylinders or tangent ogive cylinders one of which has 3 fins. Only supersonic flow situations are considered so that downstream marching methods are valid. The Mach number range is from 2 to 5 and the incidence range is up to 15 degrees. Author

N91-14287# British Aerospace Public Ltd. Co., Bristol (England). Dept. of Aerodynamics and Vulnerability Research.
NUFA: A SEMI-EMPIRICAL METHOD FOR THE PREDICTION OF ISOLATED WEAPON AERODYNAMICS
S. McDougall, A. J. Press, and P. S. Barratt *In* AGARD, Missile Aerodynamics Oct. 1990 18 p (For primary document see N91-14278 06-02)
Copyright Avail: NTIS HC/MF A17; Non-NATO Nationals requests available only from AGARD/Scientific Publications Executive

The NUFA method was developed from the ABACUS program to provide estimates of weapon aerodynamic loads when immersed in nonuniform, as well as uniform, onset flows. Being semi-empirical in nature, the method is relatively simple and inexpensive to use. The body load prediction method within NUFA has recently undergone significant development to both the inviscid and viscous load contributions including the introduction of an initial square body capability. Results from each of these developments are presented. A feature of NUFA is the ability to provide estimates of body load distributions. This capability was exploited to predict pitch damping derivatives. A comparison with experiment demonstrates a first application of NUFA to aerodynamic derivative prediction. The load distribution facility is further illustrated by predictions using a nonuniform flow as input. It is hoped that the flexibility of the body load prediction method was demonstrated. Author

N91-14288# Dornier-Werke G.m.b.H., Friedrichshafen (Germany, F.R.).
A SEMI-EMPIRICAL PREDICTION METHOD FOR MISSILE AERODYNAMICS
K.-W. Bock *In* AGARD, Missile Aerodynamics Oct. 1990 11 p (For primary document see N91-14278 06-02)
Copyright Avail: NTIS HC/MF A17; Non-NATO Nationals requests available only from AGARD/Scientific Publications Executive

The calculation procedure of the new semiempirical computer code AAVEX (Aerodynamics of Air Vehicles, Extended version) for the static aerodynamic coefficients of missiles with a body of revolution and up to three cross wings is described. The range of application is: Mach-number M is equal or less than 4, angle of incidence i is equal to or less than 90 degrees, roll angle arbitrary, and all fins independently deflectable. An existing program for missiles at zero roll angle with wings in + position is extended with respect to the roll angle influence and an improved front to rear wing interference. Special emphasis is set on this extension because it is applicable to other zero roll angle codes and thus might be of general interest. The whole procedure can be roughly divided into three different stages: calculation for wings in + position at zero roll angle; empirical modification of forces and moments for wings in arbitrary position, at given roll angle; and calculation of front to rear wing interference. Especially the second stage is based on a wide data base with systematically varied cross wings at a body of revolution. Although the code is new and has a potential for improvement, the examples presented agree well with experiments. Author

N91-14289# Istanbul Univ. (Turkey). Dept. of Aeronautics and Astronautics.
AERODYNAMIC CHARACTERISTICS OF CYLINDRICAL BODIES WITH POINTED AND TRUNCATED CONICAL NOSES
V. Atli *In* AGARD, Missile Aerodynamics Oct. 1990 12 p (For primary document see N91-14278 06-02)
Copyright Avail: NTIS HC/MF A17; Non-NATO Nationals requests available only from AGARD/Scientific Publications Executive

The aerodynamic characteristics of cylindrical bodies, with pointed and truncated conical noses, are investigated experimentally and theoretically, at a low Mach number, over the range of angle of attack from 0 to 20 deg. The Reynolds number, based on the maximum body diameter is about 4.1 x 10(exp 4). The surface-flow visualization is performed by applying the oil method. The balance measurements are made by using a sting-type strain-gage balance which is designed and constructed under the project T40 of FDP of AGARD. The results of the balance measurements are compared with the potential theory and the method of viscous crossflow analogy. It is observed that the method of viscous cross flow analogy is applicable to the cylindrical bodies with pointed and truncated conical noses even at high angles of attack, unlike the potential theory. The nose-cone angle and the bluntness are the parameters affecting the flowfield around and

the aerodynamic characteristics of a pointed or truncated one-cylinder body. Author

N91-14290# Deutsche Forschungsanstalt fuer Luft- und Raumfahrt, Goettingen (Germany, F.R.). Inst. fuer Experimentelle Stroemungsmechanik.

SYSTEMATIC INVESTIGATIONS OF BODY-WING-TAIL INTERFERENCE AT HIGH ANGLES OF ATTACK

K. Hartmann and D. Nikolitsch (Messerschmitt-Boelkow-Blohm G.m.b.H., Munich, Germany, F.R.) *In* AGARD, Missile Aerodynamics Oct. 1990 16 p (For primary document see N91-14278 06-02)

Copyright Avail: NTIS HC/MF A17; Non-NATO Nationals requests available only from AGARD/Scientific Publications Executive

Six component measurements were carried out on several combinations of an ogive-circular cylinder body without and with lifting surfaces having rectangular planform and sharp leading and trailing edges. These experiments were performed in the subsonic compressible speed range at various Reynolds numbers up to high angles of attack. For the same geometries the forces and moments were calculated and compared with the experimental results. It was the aim of this combined investigation to get a better understanding of the vortex flows over such body-wing-tail combinations and to generate a reliable data base for the validation and improvement of prediction methods and to obtain hints for a more accurate theoretical modeling of the flow fields. Author

N91-14291# Aerospatiale, Chatillon (France). Div. Engins Tactiques.

SUPERSONIC VORTEX FLOWS AROUND A MISSILE BODY: BASIC EXPERIMENT AND EULER NUMERICAL COMPUTATION

Jerome Lordon, Jean-Christopher Fare, and Didier Pagan (Office National d'Etudes et de Recherches Aerospatiales, Paris, France) *In* AGARD, Missile Aerodynamics Oct. 1990 15 p Sponsored in part by Direction des Recherches, Etudes et Techniques, France Original contains color illustrations (For primary document see N91-14278 06-02)

Copyright Avail: NTIS HC/MF A17; Non-NATO Nationals requests available only from AGARD/Scientific Publications Executive

At high or moderate angles of attack, boundary layers separate and vortices develop on the leeside of tactical missile bodies. The purpose is to validate a numerical approach simulating these supersonic separated flows. In this iterating coupling technique, the inviscid flow is computed by means of an Euler solver in which separation is forced by a parietal treatment. The location of the separation line is given by a boundary layer calculation based on a three-dimensional field method. A detailed experimental study was performed to provide a wide range of comparisons with computations over an ogive-cylinder configuration at Mach 2. Experiments are first described, then computational results are presented for different angles of attack. Calculations over a body-tail configuration finally evaluate the vortical flow interaction with wings. Author

N91-14292*# National Aeronautics and Space Administration. Langley Research Center, Hampton, VA.

ASYMMETRIC SUPERSONIC FLOW AROUND CONES WITH NONCIRCULAR SECTIONS

Osama A. Kandil, Tin-Chee Wong (Old Dominion Univ., Norfolk, VA.), and C. H. Liu *In* AGARD, Missile Aerodynamics Oct. 1990 11 p (For primary document see N91-14278 06-02) (Contract NAS1-18584)

Copyright Avail: NTIS HC/MF A17; Non-NATO Nationals requests available only from AGARD/Scientific Publications Executive CSCL 01A

The unsteady, compressible, single and double thin-layer, Navier-Stokes equations are used to solve for steady and unsteady, asymmetric, supersonic flow around pointed bodies with noncircular sections at high incidence and zero side slip. The equations are solved by using an implicit, upwind, flux-difference splitting finite-volume scheme. Since the flow is locally conical, the solutions are presented on a cross-flow plane at the axial station of unit. The grid is generated by using a modified Joukowski transformation. The computational applications cover noncircular sections with elliptic and diamond shapes. Unsteady asymmetric vortex shedding has been captured at large angles of attack. It is shown that for the same flow conditions and same cross-section fineness ratio, the diamond-section cones develop less flow asymmetry than the elliptic-section cones. Passive control of flow asymmetry was also demonstrated computationally. Author

N91-14293# Office National d'Etudes et de Recherches Aerospatiales, Paris (France).

COMPARISON OF DIFFERENT CALCULATION METHODS APPLIED TO A LENTICULAR FUSELAGE SECTION [COMPARASON DE DIFFENENTES METHODES DE CALCUL APPLIQUEES A UN FUSELAGE DE SECTION LENTICULAIRE]

P. dEspiney *In* AGARD, Missile Aerodynamics Oct. 1990 15 p In FRENCH; ENGLISH summary (For primary document see N91-14278 06-02)

Copyright Avail: NTIS HC/MF A17; Non-NATO Nationals requests available only from AGARD/Scientific Publications Executive

Measurements on a non-circular body were made in the ONERA wind tunnels. This model representative of non-conventional missile shapes, was studied for Mach numbers from 0.4 to 4.5, angles of attack up to 20 deg and sideslip angles up to 10 deg. The data base mainly consists of wall static pressure measurements but also of flowfield measurements at Mach number 2 for angles of attack 10 deg and 20 deg. Comparisons between calculations and experiments obtained with different codes are reported: SHABP (a semi-empirical prediction method), ECOPAN, HISSS (panel method), and FLU3C (Euler method). After a brief survey of the codes their advantages and drawbacks in terms of accuracy and cost-time are shown. Author

N91-14294# Ballistic Research Labs., Aberdeen Proving Ground, MD. Launch and Flight Div.

THREE DIMENSIONAL FLOW CALCULATIONS FOR A PROJECTILE WITH STANDARD AND DOME BASES

Jubaraj Sahu and Charles J. Nietubicz *In* AGARD, Missile Aerodynamics Oct. 1990 9 p (For primary document see N91-14278 06-02)

Copyright Avail: NTIS HC/MF A17; Non-NATO Nationals requests available only from AGARD/Scientific Publications Executive

Test firings of the 155 mm XM825 artillery projectile have shown that its flight performance was affected by configurational changes to the base cavity. This was an unexpected result and a clear understanding of why these changes affected the flight behavior did not exist. A computational study was made for the two different base cavity configurations which were flight tested. Flowfield computations were performed at 0.8 is less than M is less than 1.5 and alpha was 4.0 deg using a recently developed 3D Navier-Stokes code. The computed results show the qualitative features of the base region flow field for the two base cavities. The base changes are found to alter the recirculation patterns in the wake which in turn affect the expansion at the base corner. These changes in the flow structure contribute to small changes in the base pressure. Aerodynamic force and moment coefficients were obtained from the computed pressures and are presented as a function of Mach number. Computed results show small differences in normal force and pitching moment coefficients similar to that found in the range data. Author

N91-14295# Ballistic Research Labs., Aberdeen Proving Ground, MD. Launch and Flight Div.

NAVIER-STOKES PREDICTIONS OF STATIC AND DYNAMIC AERODYNAMIC DERIVATIVES FOR HIGH L/D FINNED PROJECTILES

Paul Weinacht and Walter B. Sturek *In* AGARD, Missile Aerodynamics Oct. 1990 12 p (For primary document see N91-14278 06-02)

Copyright Avail: NTIS HC/MF A17; Non-NATO Nationals requests available only from AGARD/Scientific Publications Executive

The current research effort has examined several aspects of the aerodynamics of finned projectiles. These are (1) static

aerodynamics at angle of attack, (2) aerodynamics in pure rolling motion, and (3) aerodynamics in steady coning motion. In each case, three-dimensional viscous flow field computations were performed over a range of supersonic Mach numbers using the parabolized Navier-Stokes technique of Schiff and Steger. The computational approach were applied to two high L/D finned projectiles. From the flow field predictions at constant angle of attack, determination of the normal force, pitching moment, and side moment coefficients were made. Computation of the flow field about the projectile in rolling motion has allowed the determination of the roll producing and roll damping moment coefficients, and the equilibrium spin rate. Finally, the predictions of the flow field about the projectile in steady coning motion has allowed prediction of the pitch-damping aerodynamic coefficients. Where possible, comparisons were made between computational results and results obtained from range fringe. Author

N91-14296# Naval Weapons Center, China Lake, CA. Airbreathing Propulsion Branch.

OVERVIEW OF PROPULSION CONCEPTS FOR TACTICAL MISSILES **c20**

Frederick C. Zarlingo *In* AGARD, Missile Aerodynamics Oct. 1990 12 p (For primary document see N91-14278 06-02)

Copyright Avail: NTIS HC/MF A17; Non-NATO Nationals requests available only from AGARD/Scientific Publications Executive

Several propulsion concepts lend themselves to application in tactical missiles; many of them can improve missile system performance by means of longer range, high speed, or both. Tactical missile propulsion systems generally fall into one of two categories: rockets that carry all their fuel and oxidizer and airbreathing engines that have to carry only their fuel since their oxidizer is obtained from the surrounding air. Tactical missiles were typically propelled by conventional solid propellant powered rockets or, occasionally, liquid propellant powered rockets. However, newly emerging requirements and needs are placing more emphasis on sustained high speed and longer ranges, as well as reduced cost and improved reliability and safety. In addition, there is more emphasis on launcher (aircraft or ground based) survivability. Survivability can be enhanced by longer ranges or reduced visibility. These needs can be implemented either singly or in combination by using selected propulsion systems. Pulse rockets, ramjets (both liquid fueled and solid fueled), turbojets, and air-turborockets (or turboramjets) possess the potential of long range and high speeds. An overview is provided for the various propulsion concepts considered applicable to tactical missiles and describes and discusses the merits of each. Author

N91-14297# Office National d'Etudes et de Recherches Aerospatiales, Paris (France).

ANTICIPATION OF AERODYNAMIC COEFFICIENTS OF MISSILE AIR INTAKES [PREVISION DES COEFFICIENTS AERODYNAMIQUES DE MISSILES MUNIS DE PROSES D'AIR]

P. Champigny, D. Baudin, and P. Gonidec (Laboratoire de Recherches Balistiques et Aerodynamiques, Vernon, France) *In* AGARD, Missile Aerodynamics Oct. 1990 11 p In FRENCH; ENGLISH summary (For primary document see N91-14278 06-02)

Copyright Avail: NTIS HC/MF A17; Non-NATO Nationals requests available only from AGARD/Scientific Publications Executive

One of the most promising systems for the propulsion of high performance (velocity, range) missiles of the next generation is the airbreathing propulsion concept (turbojet or ramjet), but it leads to complex configuration with air-intakes. That is why parametric experimental studies were conducted in the LRBA (Laboratoire de Recherches Ballistiques et Aerodynamiques) C4 wind-tunnel in order to evaluate air-intake influence on body lift and center of pressure. Some of the results obtained during this study as well as the prediction method included in the MISSILE code for airbreathing missiles calculations are presented. Author

N91-14298# Dornier-Werke G.m.b.H., Friedrichshafen (Germany, F.R.). Dept. of Aerodynamics.

COMPUTATION OF AXISYMMETRIC BASE FLOW WITH DIFFERENT TURBULENCE MODELS

F. Magagnato *In* AGARD, Missile Aerodynamics Oct. 1990 10 p (For primary document see N91-14278 06-02)

Copyright Avail: NTIS HC/MF A17; Non-NATO Nationals requests available only from AGARD/Scientific Publications Executive

The flow past axisymmetrical missile afterbodies with base is calculated using a finite-volume technique. The compressible Reynolds-averaged Navier-Stokes equations are solved with different turbulence models for the approximation of the Reynolds-stresses. Two algebraic eddy-viscosity models, which were adjusted for the use in free-shearlayers, as well as the well known K-epsilon low Reynolds number turbulence model are used. Calculations were done on a conical afterbody with and without a centered propulsive jet. The results are found in good agreement with the experiments although some discrepancies occur in critical flow regions. The algebraic turbulence models were extended to allow a meaningful application in those regions where the performance formerly was poor. Author

N91-14299# Office National d'Etudes et de Recherches Aerospatiales, Paris (France).

RESULTS OF GARTEUR ACTION GROUP AG09 ON FLOW PAST MISSILE AFTERBODIES

J. Delery and B. Wagner (Dornier-Werke G.m.b.H., Friedrichshafen, Germany, F.R.) *In* AGARD, Missile Aerodynamics Oct. 1990 35 p Original contains color illustrations (For primary document see N91-14278 06-02)

Copyright Avail: NTIS HC/MF A17; Non-NATO Nationals requests available only from AGARD/Scientific Publications Executive

Accurate prediction of the aerodynamic behavior of missiles is still hampered by the lack of knowledge of afterbody flow, the influence of which increases with the complexity of the geometrical configuration. In a recent past, the AGARD Working Group 8 made a rather thorough review of afterbody flow studies by examining both the experimental and the theoretical sides of the question. However, the large majority of calculations were relative to aircraft afterbodies. Thus, due to the lack of reliable information on the aerodynamics of missile afterbodies, the GARTEUR Group of Responsibles for Aerodynamics decided in 1986 the creation of an Action Group (AG09) on this subject. In the course of its activity, the AG has executed the following tasks: constitution of a comprehensive data base on base pressure results containing 158 test cases, testing of 12 semiempirical or multicomponent methods by comparison with the data base, constitution of a data base made of 6 well documented experiments including LDV measurements to test Euler and Navier-Stokes calculation, execution of Navier-Stokes calculations and confrontation of their results with the data base. Author

N91-14300# Rheinmetall G.m.b.H., Duesseldorf (Germany, F.R.).

EXPERIMENTAL AERODYNAMICS FOR HOT GAS JET REACTION CONTROL SYSTEMS

H. Schilling, R. Friedrichs, and D. Christ (Deutsche Forschungsanstalt fuer Luft- und Raumfahrt, Brunswick, Germany, F.R.) *In* AGARD, Missile Aerodynamics Oct. 1990 13 p (For primary document see N91-14278 06-02)

Copyright Avail: NTIS HC/MF A17; Non-NATO Nationals requests available only from AGARD/Scientific Publications Executive

The aerodynamic interferences which arise from the interactions between the flow around a configuration and the flow of lateral blowing thrusters are well-known in the supersonic case due to many missile applications. Here some results and experimental investigations which are planned for the very near future, are reported for the case of a subsonic configuration. The EPHRAM concept is a terminal guided submunition which is designed to improve the hit accuracy and effectiveness of conventional artillery rounds. The flight condition for this concept is typically Mach 0.5 in low altitudes. EPHRAM is controlled by four lateral hot gas thrusters with a design based on mechanical

valve switching technology. By applying lateral forces, the configuration develops an angle of attack which is utilized for flight path corrections. Extrapolations from the literature show that there might be a negative jet spoiler effect reducing the aerodynamic normal forces due to interferences between the lateral jet and the configuration flow field. Therefore, experimental investigations have to be performed in order to learn more about the aerodynamic behavior of such systems. In a first test series, the complete model with the operating jet control system was installed in a low speed wind tunnel. The results showed that in the case under investigation there were no severe interferences. However, only a few tests could be performed for a single configuration. So additionally an experimental research program was launched in order to learn more about the basic effects. The experimental apparatus which shall be used is presented and the facilities that are involved in the planned tests are described. The investigations show the importance of a thorough understanding of the phenomena. There is some evidence that by a suitable design the perfomance of subsonic concepts using jet reaction control systems can be improved considerably. Author

N91-14301# Bodenseewerk Geraetetechnik G.m.b.H., Ueberlingen (Germany, F.R.). Intelligent Systems Div.

LAMINAR/TURBULENT FLOW TRANSITION EFFECTS ON HIGH-SPEED MISSILE DOMES

Uwe G. Hingst *In* AGARD, Missile Aerodynamics Oct. 1990 8 p (For primary document see N91-14278 06-02)

Copyright Avail: NTIS HC/MF A17; Non-NATO Nationals requests available only from AGARD/Scientific Publications Executive

The new generation of high-speed short range missile has to withstand extreme aerokinetic heating. For IR seeking missiles with its fragile domes the aerokinetic heating effects make further velocity increase difficult. The main driving parameter is the aerothermodynamically imposed stress within the IR-window material. The induced thermal stress is a function of the aerodynamic flow properties around the missile dome, the relevant local boundary layer characteristics and the resulting aerokinetic heating. The analysis of the heat transfer coefficients and resulting temperature fields on hemispherical domes for the laminar and turbulent flow and especially for the transient behavior in between are examined. It will be demonstrated that just the boundary transition from the laminar to the turbulent flow has a significant influence on the imposed window stress. The different influences of the characteristic Reynolds-Numbers, start and end of transition zone, and the resulting stress parameters are investigated. Problems related to the definition of correct transition behavior are discussed. Author

N91-14302# Royal Aerospace Establishment, Farnborough (England).

INVESTIGATIONS OF AEROTHERMODYNAMIC EFFECTS ON AXISYMMETRIC BODIES AT HIGH MACH NUMBERS

J. D. Regan and T. J. Rooke *In* AGARD, Missile Aerodynamics Oct. 1990 12 p (For primary document see N91-14278 06-02)

Copyright Avail: NTIS HC/MF A17; Non-NATO Nationals requests available only from AGARD/Scientific Publications Executive

This memorandum describes experimental studies carried out at RAE in the Shock Tunnel and Gun Tunnel to measure the heat transfer rates to a 7 deg blunted cone, to provide data for validation of flow field prediction codes. The tests were carried out at Mach numbers of 7.1 in the Shock Tunnel and at 12.8 in the Gun Tunnel at angles of incidence of up to 25 deg. Some observations are made about the general nature of the flow around the body that can be deduced from surface heat transfer contours and flow field photographs and exemplified for 0, 1, 5, and 20 deg of incidence, and some comparisons between experimental results and theoretical predictions are presented. Author

N91-14303# Deutsche Forschungs- und Versuchsanstalt fuer Luft- und Raumfahrt, Goettingen (Germany, F.R.). Inst. for Experimental Fluid Mechanics.

THERMAL IMAGING ON MISSILES IN HYPERSONIC FLOW

Henning Schoeler *In* AGARD, Missile Aerodynamics Oct. 1990 8 p Original contains color illustrations (For primary document see N91-14278 06-02)

Copyright Avail: NTIS HC/MF A17; Non-NATO Nationals requests available only from AGARD/Scientific Publications Executive

The method of thermal imaging with liquid crystals developed at DLR Goettingen is briefly described, and some applications in the DLR Ludwieg tube are presented. As the temperature sensor is sprayed on the model no expensive instrumentation is required. Responding to temperature variation the liquid crystals show a color play which directly visualizes surface temperature fields. For qualitative heat transfer measurements, it is sufficient to photograph or video record the model while it is exposed to the flow. Author

N91-14304# Nielsen Engineering and Research, Inc., Mountain View, CA. Engineering Aerodynamics Div.

CHORDWISE AND SPANWISE CENTERS OF PRESSURE OF MISSILE FINS

Daniel J. Lesieutre and Marnix F. E. Dillenius *In* AGARD, Missile Aerodynamics Oct. 1990 12 p (For primary document see N91-14278 06-02)

(Contracts N00014-80-C-0700; F33615-86-C-3626)

Copyright Avail: NTIS HC/MF A17; Non-NATO Nationals requests available only from AGARD/Scientific Publications Executive

The extensive triservice experimental data base was investigated and used to obtain a fin chordwise and spanwise center of pressure data base for use in the preliminary analysis and design of missile fins. Correlations and curve fits of the center of pressure data were performed to reduce the storage and computation time required to obtain engineering level predictions of fin hinge and bending moments. The method developed is simple to use and is easily incorporated into comprehensive missile aeroprediction methods. The method is extremely valuable because it includes effects due to real flow and fin-body gaps inherent in the experimental data base. The experimental data base, its manipulation, and its implementation into a prediction method are described. Author

N91-14305# Science Applications International Corp., Fort Washington, PA. Fluid Sciences Div.

COMPUTATIONAL MODELS WITH ADVANCED THERMOCHEMISTRY FOR THE ANALYSIS OF MISSILE/PLUME FLOWFIELD INTERACTIONS

S. M. Dash, N. Sinha, and B. J. York *In* AGARD, Missile Aerodynamics Oct. 1990 30 p (For primary document see N91-14278 06-02)

(Contract N00014-87-C-0549)

Copyright Avail: NTIS HC/MF A17; Non-NATO Nationals requests available only from AGARD/Scientific Publications Executive

Advanced computational models which solve the full (FNS) and parabolized (PNS) Navier-Stokes equations for the analysis of missile aerodynamic problems with exhaust plume interactions are described. The models utilize conservative implicit algorithms and include finite-rate chemistry, two-equation turbulence models, and preliminary multi-phase flow capabilities. In the tactical missile arena, a 3D Navier-Stokes code, PARCH, was developed to analyze missile/plume interactions with both conventional nozzle exhausts, as well as with bifurcated/scarfed nozzle exhausts. The PNS work has focused on supersonic/hypersonic applications utilizing time-iterative upwind numerics for enhanced robustness and accuracy, and has included the analysis of aerodynamic, plume, and propulsive problems for missiles as well as for reentry and aerospace vehicles. Author

N91-14306# Messerschmitt-Boelkow-Blohm G.m.b.H., Munich (Germany, F.R.). Hubschrauber und Flugzeuge.
HYPERSONIC AERODYNAMICS: AN APPROXIMATION METHOD FOR THE CALCULATION OF REAL GAS EFFECTS AND WALL TEMPERATURES Thesis - Tech. Univ. Munich [HYPERSCHALLAERODYNAMIK: EINE APPROXIMATIVE METHODE ZUR BERECHNUNG VON REALGASEFFEKTEN UND WANDTEMPERATUREN]
Roland Schreiner 31 May 1990 90 p In GERMAN
(MBB/FE127/S/PUB/0403; ETN-90-98153) Copyright Avail: NTIS HC/MF A05

A program existing for ideal gases is adapted to real gases at high Mach numbers. The calculation equations for the Prandtl-Meyer motion were derived for the vertical and oblique impacts and a subroutine was achieved which calculates the pressure, density and temperature distribution at the boundary layer edge for any geometry, and two dimensional or three dimensional configurations. Good results were obtained for surface temperatures for Mach numbers lower than 20. ESA

N91-14307*# Institute for Computer Applications in Science and Engineering, Hampton, VA.
THE INVISCID STABILITY OF SUPERSONIC FLOW PAST HEATED OR COOLED AXISYMMETRIC BODIES Final Report
Stephen J. Shaw and Peter W. Duck (Manchester Univ., England) Nov. 1990 54 p Submitted for publication Sponsored in cooperation with Science Research Council, and by Manchester Univ.
(Contract NAS1-18605)
(NASA-CR-187475; NAS 1.26:187475; ICASE-90-81) Avail: NTIS HC/MF A04 CSCL 01A

The inviscid, linear, nonaxisymmetric, temporal stability of the boundary layer associated with the supersonic flow past axisymmetric bodies (with particular emphasis on long thin, straight circular cylinders), subject to heated or cooled wall conditions is investigated. The eigenvalue problem is computed in some detail for a particular Mach number or 3.8, revealing that the effect of curvature and the choice of wall conditions both have a significant effect on the stability of the flow. Both the asymptotic, large azimuthal wavenumber solution and the asymptotic, far downstream solution are obtained for the stability analysis and compared with numerical results. Additionally, asymptotic analyses valid for large radii of curvature with cooled/heated wall conditions, are presented. In general, important differences were found to exist between the wall temperature conditions imposed and the adiabatic wall conditions considered previously. Author

N91-14308*# Institute for Computer Applications in Science and Engineering, Hampton, VA.
THE EFFECT OF WALL COMPLIANCE ON THE GOERTLER VORTEX INSTABILITY Final Report
J. P. Denier and Philip Hall Dec. 1990 18 p Submitted for publication Sponsored by Science Research Council
(Contract NAS1-18605)
(NASA-CR-187477; NAS 1.26:187477; ICASE-90-84) Avail: NTIS HC/MF A03 CSCL 01A

The stability of the flow of a viscous incompressible fluid over a curved compliant wall to longitudinal Goertler vortices is investigated. The compliant wall is modeled by a particularly simple equation relating the induced wall displacement to the pressure in the overlying fluid. Attention is restricted to the large Goertler number regime; this regime being appropriate to the most unstable Goertler mode. The effect of wall compliance on this most unstable mode is investigated. Author

N91-14309*# National Aeronautics and Space Administration. Lewis Research Center, Cleveland, OH.
RESULTS OF A SUB-SCALE MODEL ROTOR ICING TEST
Robert J. Flemming, Thomas H. Bond, and Randall K. Britton (Sverdrup Technology, Inc., Brook Park, OH.) 1991 31 p Presented at the 29th Aerospace Sciences Meeting, Reno, NV, 7-10 Jan. 1991; sponsored by AIAA
(NASA-TM-103709; E-5935; NAS 1.15:103709; AIAA-91-0660) Avail: NTIS HC/MF A03 CSCL 01A

A heavily instrumented sub-scale model of a helicopter main rotor was tested in the NASA Lewis Research Center Icing Research Tunnel (IRT) in September and November 1989. The four-bladed main rotor had a diameter of 1.83 m (6.00 ft) and the 0.124 m (4.9 in) chord rotor blades were specially fabricated for this experiment. The instrumented rotor was mounted on a Sikorsky Aircraft Powered Force Model, which enclosed a rotor balance and other measurement systems. The model rotor was exposed to a range of icing conditions that included variations in temperature, liquid water content, and median droplet diameter, and was operated over ranges of advance ratio, shaft angle, tip Mach number (rotor speed) and weight coefficient to determine the effect of these parameters on ice accretion. In addition to strain gage and balance data, the test was documented with still, video, and high speed photography, ice profile tracings, and ice molds. The sensitivity of the model rotor to the test parameters, is given, and the result to theoretical predictions are compared. Test data quality was excellent, and ice accretion prediction methods and rotor performance prediction methods (using published icing lift and drag relationships) reproduced the performance trends observed in the test. Adjustments to the correlation coefficients to improve the level of correlation are suggested. Author

N91-14310*# National Aeronautics and Space Administration. Lewis Research Center, Cleveland, OH.
NUMERICAL SIMULATION OF ICE GROWTH ON A MS-317 SWEPT WING GEOMETRY
M. G. Potapczuk and C. S. Bidwell Jan. 1991 24 p Presented at the 29th Aerospace Sciences Meeting, Reno, NV, 7-10 Jan. 1991; sponsored in part by AIAA
(NASA-TM-103705; E-5928; NAS 1.15:103705; AIAA-91-0263) Avail: NTIS HC/MF A03 CSCL 01A

An effort to develop a 3-D ice accretion modeling method was initiated. This first step towards creation of a complete aircraft icing simulation code builds on previously developed methods for calculating 3-D flow fields and particle trajectories combined with a 2-D ice accretion calculation along coordinate locations corresponding to streamlines. The types of calculations necessary to predict 3-D ice accretion is demonstrated. Results of calculations using 3-D method for a MS-317 swept wing geometry are projected onto a 2-D plane parallel to the free stream direction and compared to experimental results for the same geometry. It is anticipated that many modifications will be made to this approach, however this effort will lay the groundwork for future modeling efforts. Results indicate that rime ice shapes indicate a difficulty in accurately calculating the ice shape in the runback region. Author

N91-14311*# Johnson Aeronautics, Palo Alto, CA.
FEASIBILITY INVESTIGATION OF GENERAL TIME-DOMAIN UNSTEADY AERODYNAMICS OF ROTORS
Wayne Johnson Oct. 1990 220 p
(Contract NAS2-13125)
(NASA-CR-177570; A-90304; NAS 1.26:177570) Avail: NTIS HC/MF A10 CSCL 01A

The feasibility of a general theory for the time-domain unsteady aerodynamics of helicopter rotors is investigated. The wake theory gives a linearized relation between the downwash and the wing bound circulation, in terms of the impulse response obtained directly in the time domain. This approach makes it possible to treat general wake configurations, including discrete wake vorticity with rolled-up and distorted geometry. The investigation establishes the approach for model order reduction; determines when a constrained identification method is needed; verifies the formulation of the theory for rolled-up, distorted trim wake geometry; and verifies the formulation of the theory for wake geometry perturbations. The basic soundness of the approach is demonstrated by the results presented. A research program to complete the development of the method is outlined. The result of this activity will be an approach for analyzing the aeroelastic stability and

response of helicopter rotors, while retaining the important influence of the complicated rotor wake configuration. Author

N91-14312# Naval Postgraduate School, Monterey, CA.
NUMERICAL STUDIES OF COMPRESSIBLE FLOW OVER A DOUBLE-DELTA WING AT HIGH ANGLES OF ATTACK M.S. Thesis
Raymond L. Coutley Mar. 1990 171 p
(AD-A226931) Avail: NTIS HC/MF A08 CSCL 01/1

The objective of this work is the investigation of vortical flows at high angles of attack using numerical techniques. The first step for a successful application of a numerical technique, such as finite difference or finite volume, is the generation of a computational mesh which can capture adequately and accurately the important physics of the flow. Therefore, the first part of this work deals with the grid generation over a double-delta wing and the second part deals with the visualization of the computed flow field over the double-delta wing at different angles of attack. The surface geometry of the double-delta wing is defined algebraically. The developed surface grid generator provides flexibility in distributing the surface points along the axial and circumferential directions. The hyperbolic grid generation method is chosen for the field grid generation and both cylindrical and spherical grids are constructed. The computed low speed (M = 0.2) flow results at different angles of attack over the double-delta wing are visualized. Important flow characteristics of the leeward side flow field are discussed while the development of vortex interaction, occurrence and progression of vortex breakdown as the angle of attack increases is demonstrated. The computed results at different fixed angles of attack are presented. GRA

N91-14313# Air Force Academy, CO.
AN EXPERIMENTAL INVESTIGATION INTO THE USE OF HOT-FILM ANEMOMETRY TO MEASURE VORTICAL VELOCITY BEHIND A PITCHING WING
C. Bruce Harmon and William Dieterich Aug. 1990 17 p
(AF Proj. 2307)
(AD-A227177; FJSRL-TR-90-0002) Avail: NTIS HC/MF A03 CSCL 14/2

Much has been done in the instrumentation of airfoils and wings to obtain surface pressure data in support of the characterization of the transient lift augmentation due to unsteady aerodynamic effects. These effects have usually been the result of rapidly rotating wings to high angles of attack or periodic oscillation. Integration of the acquired pressure coefficients leads to the airfoil or wing coefficient of lift. Researchers Walker and Robinson asked for other researchers to explore the use of hot-film anemometry as a confirming technique. In such a role, the anemometry is capable of mapping velocity vs. position, which is used to compute circulation via a line integral. The computed circulation is directly proportional to lift coefficient for a given freestream velocity. The investigation is described into the use of hot-film anemometry, strengths and weaknesses of the approach are identified, and specific recommendations are made regarding its use. GRA

N91-14314# Wright Research Development Center, Wright-Patterson AFB, OH. High Speed Aero Performance Branch.
COMMENTS ON HYPERSONIC BOUNDARY-LAYER TRANSITION Final Report, 1 Oct. 1984 - 31 Jul. 1990
Kenneth F. Stetson Sep. 1990 114 p Presented at the 3rd Joint Europe/US Short Course in Hypersonics, Aachen, Fed. Republic of Germany, Oct. 1990
(AF Proj. 2307)
(AD-A227242; WRDC-TR-90-3057) Avail: NTIS HC/MF A06 CSCL 20/4

This is a survey paper on the subject of hypersonic boundary-layer transition. Part 1 discusses boundary-layer stability theory, hypersonic boundary-layer stability experiments, and a comparison between theory and experiment. Part 2 contains comments on how many configuration and flow parameters influence transition. Part 3 discusses some additional general aspects of transition. Part 4 discusses problems of predicting transition and comments on three prediction methods. Part 5 contains some general guidelines for prediction methodology. GRA

N91-14315# University of Southern California, Los Angeles. Dept. of Aerospace Engineering.
CONTROL OF UNSTEADY AERODYNAMIC FORCES Final Report, 1 May 1988 - 30 Apr. 1990
Chih-Ming Ho 26 Jul. 1990 67 p
(Contract F49620-88-C-0061)
(AD-A227365; AFOSR-90-0924TR) Avail: NTIS HC/MF A04 CSCL 01/1

The aerodynamic properties of an airfoil under unsteady conditions are very different from ones in steady conditions because the vortex generated by unsteady separation greatly modifies the loading on the wing. In this study, a fundamental approach was taken to investigate the lift and the velocity field of unsteady airfoils. GRA

N91-14316*# National Aeronautics and Space Administration. Langley Research Center, Hampton, VA.
PARAMETRIC STUDY OF AFTERBODY/NOZZLE DRAG ON TWIN TWO-DIMENSIONAL CONVERGENT-DIVERGENT NOZZLES AT MACH NUMBERS FROM 0.60 TO 1.20
Odis C. Pendergraft, Jr., James R. Burley, II, and E. Ann Bare Oct. 1986 267 p
(NASA-TP-2640; L-16158; NAS 1.60:2640) Avail: NTIS HC/MF A12 CSCL 01A

An investigation has been conducted in the Langley 16-Foot Transonic Tunnel to determine the effects of upper and lower external nozzle flap geometry on the external afterbody/nozzle drag of nonaxisymmetric two-dimensional convergent-divergent exhaust nozzles having parallel external sidewalls installed on a generic twin-engine, fighter-aircraft model. Tests were conducted over a Mach number range from 0.60 to 1.20 and over an angle-of-attack range from -5 to 9 deg. Nozzle pressure ratio was varied from jet off (1.0) to approximately 10.0, depending on Mach number. Author

N91-14331# Deutsche Forschungsanstalt fuer Luft- und Raumfahrt, Goettingen (Germany, F.R.). Inst. for Aeroelasticity.
UNSTEADY AERODYNAMIC FORCES ON AN OSCILLATING WING AT HIGH INCIDENCES AND FLOW SEPARATION
H. W. Foersching *In* AGARD, Aircraft Dynamic Loads Due to Flow Separation Sep. 1990 18 p (For primary document see N91-14324 06-05)
Copyright Avail: NTIS HC/MF A12; Non-NATO Nationals requests available only from AGARD/Scientific Publications Executive

N91-14340*# National Aeronautics and Space Administration. Langley Research Center, Hampton, VA.
UNSTEADY AIRLOADS DUE TO SEPARATED FLOW ON AIRFOILS AND WINGS
John W. Edwards *In* AGARD, Aircraft Dynamic Loads Due to Flow Separation Sep. 1990 18 p Previously announced in IAA as A90-33311 (For primary document see N91-14324 06-05)
Copyright Avail: NTIS HC/MF A12; Non-NATO Nationals requests available only from AGARD/Scientific Publications Executive CSCL 01A

03 AIR TRANSPORTATION AND SAFETY

Includes passenger and cargo air transport operations; and aircraft accidents.

For related information see also *16 Space Transportation* and *85 Urban Technology and Transportation.*

N91-14317# Federal Aviation Administration, Atlantic City, NJ.
SMOKE AND EXTINGUISHER AGENT DISSIPATION IN A

SMALL PRESSURIZED FUSELAGE Final Report
G. Slusher, A. Abramowitz, and W. Neese Nov. 1990 43 p
(DOT/FAA/CT-89/31) Avail: NTIS HC/MF A03

A test study was conducted using Halon 1211 and Halon 1301 fire extinguishing agents and aerosol smoke to study their behavior in a pressurized Cessna C-421B aircraft. Halon fire extinguishers were discharged and monitored at various locations to determine the concentrations of neat halon gases present, their dissipation rates and any resultant toxic threat to the occupants. Artificial smoke was also generated at various locations and was measured at three fixed locations in the aircraft, thereby providing localized visibility information as well as ventilation data. Peak halon concentrations were considered adequate to extinguish most fires. Halon dosages for the pilot and copilot were low or zero and those for the passengers were also low in relation to the toxic limits recommended. The high ventilation rates in the cockpit area contributed to clearing smoke from the cockpit quickly. It also prevented the smoke from entering the cockpit when it was released in the passenger cabin. Author

04 AIRCRAFT COMMUNICATIONS AND NAVIGATION

Includes digital and voice communication with aircraft; air navigation systems (satellite and ground based); and air traffic control.

For related information see also *17 Space Communications, Spacecraft Communications, Command and Tracking* and *Communications and Radar.*

N91-14318# Federal Aviation Administration, Atlantic City, NJ.
USING SIMULATION TO EVALUATE THE SAFETY OF PROPOSED ATC OPERATIONS AND PROCEDURES
Lee E. Paul Oct. 1990 26 p
(Contract FAA-F2006-D)
(DOT/FAA/CT-TN90/22) Avail: NTIS HC/MF A03

Some problems are considered that arise when simulation is used to evaluate capacity enhancing system changes that may also affect safety. A safety standard is proposed that is not based on meeting a predetermined or absolute criterion, but on the ability to demonstrate that the proposed system is as safe as the present one assuming the present system is considered safe. Conversely, a change intended to increase safety would be required to show significantly safe operations vis-a-vis the present standard and, perhaps, no loss of capacity. Author

N91-14319# Sandia National Labs., Albuquerque, NM. Advanced Technology Div.
OPTIMAL SENSOR FUSION FOR LAND VEHICLE NAVIGATION
J. Dan Morrow Oct. 1990 33 p
(Contract DE-AC04-76DP-00789)
(DE91-002586; SAND-89-0816) Avail: NTIS HC/MF A03

Position location is a fundamental requirement in autonomous mobile robots which record and subsequently follow x,y paths. The Dept. of Energy, Office of Safeguards and Security, Robotic Security Vehicle (RSV) program involves the development of an autonomous mobile robot for patrolling a structured exterior environment. A straight-forward method for autonomous path-following has been adopted and requires digitizing the desired road network by storing x,y coordinates every 2m along the roads. The position location system used to define the locations consists of a radio beacon system which triangulates position off two known transponders, and dead reckoning with compass and odometer. This paper addresses the problem of combining these two measurements to arrive at a best estimate of position. Two algorithms are proposed: the optimal algorithm treats the measurements as random variables and minimizes the estimate variance, while the average error algorithm considers the bias in dead reckoning and attempts to guarantee an average error. Data collected on the algorithms indicate that both work well in practice. DOE

N91-14320# MiTech, Inc., Washington, DC.
AUTOMATIC DEPENDENT SURVEILLANCE BENEFIT AND COST ANALYSIS Interim Report
G. J. Couluris Nov. 1990 74 p
(Contract DTFA01-88-Y-D-01025)
(DOT/FAA/RD-90/34; IAT-ADS-BC-1) Avail: NTIS HC/MF A04

A benefit and cost analysis of the economic and operational impacts of automatic dependent surveillance (ADS) is given. The ADS function is currently under development and is designed to use satellite communications and advanced air traffic control (ATC) automation to improve air traffic services in oceanic and other airspaces. ADS will provide direct communication between pilots and air traffic controllers and enhanced ATC flight monitoring and airspace management capabilities. The study identifies the operational benefits and implementation requirements of ADS and analyzes their potential impacts on users and providers of air traffic services. Potential safety benefits are qualitatively assessed. Potential cost savings due to ADS operations are quantitatively estimated as are ADS system implementation costs. The expenditures considered in the analysis include user flight operating costs, air-ground communication user costs, aircraft ADS communication equipage costs, and ATC system enhancement costs. The study examines ADS implementation and potential operational impacts for the North Atlantic and Pacific oceanic areas. The resulting estimated cost savings due to ADS exceed the estimated implementation costs. Author

N91-14321* National Aeronautics and Space Administration. Pasadena Office, CA.
EFFICIENT DETECTION AND SIGNAL PARAMETER ESTIMATION WITH APPLICATION TO HIGH DYNAMIC GPS RECEIVER Patent
Rajendra Kumar, inventor (to NASA) (Jet Propulsion Lab., California Inst. of Tech., Pasadena.) 25 Sep. 1990 11 p Filed 31 Oct. 1989
(NASA-Case-NPO-17820-1-CU; US-Patent-4,959,656;
US-Patent-Appl-SN-429734; US-Patent-Class-342-418;
US-Patent-Class-342-352; US-Patent-Class-342-357;
US-Patent-Class-329-306; US-Patent-Class-375-80;
US-Patent-Class-375-94; Int-Patent-Class-G01S-5/02) Avail: US Patent and Trademark Office CSCL 17G

In a system for deriving position, velocity, and acceleration information from a received signal emitted from an object to be tracked wherein the signal comprises a carrier signal phase modulated by unknown binary data and experiencing very high Doppler and Doppler rate, this invention provides combined estimation/detection apparatus for simultaneously detecting data bits and obtaining estimates of signal parameters such as carrier phase and frequency related to receiver dynamics in a sequential manner. There is a first stage for obtaining estimates of the signal parameters related to phase and frequency in the vicinity of possible data transitions on the basis of measurements obtained within a current data bit. A second stage uses the estimates from the first stage to decide whether or not a data transition has actually occurred. There is a third stage for removing data modulation from the received signal when a data transition has occurred and a fourth stage for using the received signal with data modulation removed therefrom to update global parameters which are dependent only upon receiver dynamics and independent of data modulation. Finally, there is a fifth stage for using the global parameters to determine the position, velocity, and acceleration of the object.
Official Gazette of the U.S. Patent and Trademark Office

N91-14322*# National Aeronautics and Space Administration. Ames Research Center, Moffett Field, CA.
FLIGHT DATA ACQUISITION METHODOLOGY FOR VALIDATION OF PASSIVE RANGING ALGORITHMS FOR OBSTACLE AVOIDANCE
Phillip N. Smith Oct. 1990 17 p Presented at the 46th Annual Forum and Technology Display of the American Helicopter Society, Washington, DC, 21-23 May 1990

(NASA-TM-102809; A-90124; NAS 1.15:102809) Avail: NTIS HC/MF A03 CSCL 01D

The automation of low-altitude rotorcraft flight depends on the ability to detect, locate, and navigate around obstacles lying in the rotorcraft's intended flightpath. Computer vision techniques provide a passive method of obstacle detection and range estimation, for obstacle avoidance. Several algorithms based on computer vision methods have been developed for this purpose using laboratory data; however, further development and validation of candidate algorithms require data collected from rotorcraft flight. A data base containing low-altitude imagery augmented with the rotorcraft and sensor parameters required for passive range estimation is not readily available. Here, the emphasis is on the methodology used to develop such a data base from flight-test data consisting of imagery, rotorcraft and sensor parameters, and ground-truth range measurements. As part of the data preparation, a technique for obtaining the sensor calibration parameters is described. The data base will enable the further development of algorithms for computer vision-based obstacle detection and passive range estimation, as well as provide a benchmark for verification of range estimates against ground-truth measurements. Author

05 AIRCRAFT DESIGN, TESTING AND PERFORMANCE

Includes aircraft simulation technology.

For related information see also *18 Spacecraft Design, Testing and Performance* and *39 Structural Mechanics*. For land transportation vehicles see *85 Urban Technology and Transportation*.

N91-14323*# National Aeronautics and Space Administration. Langley Research Center, Hampton, VA.

A METHOD FOR THE DESIGN OF TRANSONIC FLEXIBLE WINGS

Leigh Ann Smith and Richard L. Campbell Washington Dec. 1990 41 p

(NASA-TP-3045; L-16762; NAS 1.60:3045) Avail: NTIS HC/MF A03 CSCL 01C

Methodology was developed for designing airfoils and wings at transonic speeds which includes a technique that can account for static aeroelastic deflections. This procedure is capable of designing either supercritical or more conventional airfoil sections. Methods for including viscous effects are also illustrated and are shown to give accurate results. The methodology developed is an interactive system containing three major parts. A design module was developed which modifies airfoil sections to achieve a desired pressure distribution. This design module works in conjunction with an aerodynamic analysis module, which for this study is a small perturbation transonic flow code. Additionally, an aeroelastic module is included which determines the wing deformation due to the calculated aerodynamic loads. Because of the modular nature of the method, it can be easily coupled with any aerodynamic analysis code. Author

N91-14324# Advisory Group for Aerospace Research and Development, Neuilly-Sur-Seine (France). Structures and Materials Panel.

AIRCRAFT DYNAMIC LOADS DUE TO FLOW SEPARATION

Sep. 1990 274 p In ENGLISH and FRENCH Meeting held in Sorrento, Italy, 1-6 Apr. 1990

(AGARD-CP-483; ISBN-92-835-0582-4) Copyright Avail: NTIS HC/MF A12; Non-NATO Nationals requests available only from AGARD/Scientific Publications Executive

A state-of-the-art review of all types of separated-flow dynamic problems to be encountered in present and future aircraft is provided. In particular, the following topics are presented: evaluation of aerodynamic buffet input characteristics; in-flight and wind tunnel buffeting measurements; and aeroelastic buffeting prediction techniques. For individual titles, see N91-14325 through N91-14340.

N91-14325# National Aeronautical Establishment, Ottawa (Ontario).

WIND TUNNEL INVESTIGATION AND FLIGHT TESTS OF TAIL BUFFET ON THE CF-18 AIRCRAFT **c08**

B. H. K. Lee, D. Brown, M. Zgela, and D. Poirel *In* AGARD, Aircraft Dynamic Loads Due to Flow Separation Sep. 1990 26 p (For primary document see N91-14324 06-05)

Copyright Avail: NTIS HC/MF A12; Non-NATO Nationals requests available only from AGARD/Scientific Publications Executive

Investigations of tail buffet on the CF-18 were conducted at the National Aeronautical Establishment (NAE) and the Aerospace Engineering Test Establishment (AETE). Flow visualization of the vortex burst phenomenon was carried out in a low speed water tunnel using a modified 1/72 scaled plastic model. In wind tunnel tests, a rigid 6 percent model was used for measurements in the NAE 5 x 5 ft Trisonic Tunnel. Unsteady pressure measurements on the vertical fin were made by means of 24 fast response transducers on each surface. Results of the acceleration experienced by the fin are presented. The vortex flow structure was studied with the aid of a 49 pressure-sensor-rake mounted behind the fin. In addition to measuring steady pitot pressure values, to deduce pressure contours, unsteady pressure fluctuations were obtained from 13 fast response transducers. The leading edge extension (LEX) was also instrumented with pressure orifices and fast response transducers. The investigation was carried out with LEX fences on and off to note their effect on tail buffet loads. Flight tests were conducted at AETE on a test aircraft with accelerometers installed on the vertical fins and horizontal stabilators and strain gauges mounted on the aft fuselage structures and fin root attachment stubs. Flight test data are presented showing the effectiveness of the LEX fence in reducing aft fuselage structural response to buffet loads. Author

N91-14326# McDonnell Aircraft Co., Saint Louis, MO.

A UNIFIED APPROACH TO BUFFET RESPONSE OF FIGHTER AIRCRAFT EMPENNAGE **c08**

M. A. Ferman, S. R. Patel, and N. H. Zimmerman *In* AGARD, Aircraft Dynamic Loads Due to Flow Separation Sep. 1990 18 p (For primary document see N91-14324 06-05)

Copyright Avail: NTIS HC/MF A12; Non-NATO Nationals requests available only from AGARD/Scientific Publications Executive

A unified approach was derived for predicting buffet response of fighter aircraft empennage operating in high angle of attack maneuvering conditions. Since the advent of high angle of attack flight using controlled vortex flows, incidences of severe structural stress, and in some cases, damages have resulted. This was pronounced on twin tailed aircraft, including McDonnell's F-15 and F/A-18 aircraft which required structural beef-ups to their empennage. Two concepts are shown for predicting buffet response of empennage. The first approach uses elastically scaled models in wind tunnel tests to provide full scale prediction. The second approach is based on calculations using measured pressure data from wind tunnel tests. The latter method is more versatile. Detailed applications are shown for the F/A-18 empennage, while other applications at McDonnell are noted. This work covers many years and is believed to be a mature approach. Author

N91-14327# National Aeronautical Establishment, Ottawa (Ontario).

EFFECTS OF TRAILING-EDGE FLAP ON BUFFET CHARACTERISTICS OF A SUPERCRITICAL AIRFOIL **c08**

B. H. K. Lee *In* AGARD, Aircraft Dynamic Loads Due to Flow Separation Sep. 1990 14 p (For primary document see N91-14324 06-05)

Copyright Avail: NTIS HC/MF A12; Non-NATO Nationals requests available only from AGARD/Scientific Publications Executive

The buffet characteristics of a 16 percent thickness-to-chord ratio supercritical airfoil were investigated in the High Reynolds Number Two-Dimensional Test Facility of the National Aeronautical Establishment. The trailing-edge flap dimension was 13.5 percent chord and it was deflected at various angles to study the effect of modifying the downstream pressure on controlling flow separation over the airfoil. The unsteady normal force was

measured and the buffet boundary was determined from the divergence of the fluctuating normal force. The investigation was conducted quite deep into the buffet regime. Spectral analyses of the normal force were carried out and the frequencies of shock wave oscillations were measured. They were found to be Mach number dependent and varied between 50 to 80 Hz for M = 0.612 to 0.792. The effects of varying the flap angles on the shock wave position and drag of the airfoil were also investigated. Results for an off-design Mach number of 0.612 were given in some details. Author

N91-14328# Deutsche Forschungsanstalt fuer Luft- und Raumfahrt, Goettingen (Germany, F.R.). Institut fuer Experimentelle Stroemungsmechanik.

EXPERIMENTAL INVESTIGATION OF BUFFET ONSET AND PENETRATION ON A SUPERCRITICAL AIRFOIL AT TRANSONIC SPEEDS c08

E. Stanewsky and D. Basler (Holtronic G.m.b.H., Ottersberg, Germany, F.R.) *In* AGARD, Aircraft Dynamic Loads Due to Flow Separation Sep. 1990 11 p (For primary document see N91-14324 06-05)

Copyright Avail: NTIS HC/MF A12; Non-NATO Nationals requests available only from AGARD/Scientific Publications Executive

An experimental investigation was carried out on the supercritical airfoil CAST 7/DOA1 to determine the influence of three parameters, Mach number, angle of attack and most of all Reynolds number, on the buffet process and especially on the shock oscillation frequency and amplitude. For this investigation, the model was equipped with regular pressure orifices, dynamic pressure transducers and hot-film sensors, the latter utilized to determine transition location and regions of separation. The flow field was observed by a holographic high-speed, real-time interferometer. The analysis of the results revealed that the buffet process is essentially driven by the interaction of the upper surface shock wave with the boundary layer, especially as it influences the development of the shock-induced separation bubble, and the resultant change in flow conditions at the airfoil trailing edge and that, within the domain of intensive buffet, the shock oscillation frequency decreases with Reynolds number while the amplitude increases. It was furthermore found that the amplitude of the shock oscillation, hence the magnitude of the change in the dynamic load on the airfoil, seems to be dependent on the airfoil geometry. Author

N91-14329# Deutsche Forschungsanstalt fuer Luft- und Raumfahrt, Goettingen (Germany, F.R.). Inst. for Aeroelasticity.

EXPERIMENTAL INVESTIGATIONS OF BUFFET EXCITATION FORCES ON A LOW ASPECT RATIO TRAPEZOIDAL HALF WING IN INCOMPRESSIBLE FLOW c08

P. Bublitz and H. Zingel (Deutsche Airbus G.m.b.H., Bremen, Germany, F.R.) *In* AGARD, Aircraft Dynamic Loads Due to Flow Separation Sep. 1990 19 p (For primary document see N91-14324 06-05)

Copyright Avail: NTIS HC/MF A12; Non-NATO Nationals requests available only from AGARD/Scientific Publications Executive

The problem of determining the steady and unsteady airloads is determined for swept wings of low aspect ratios at high incidences. Despite great progress in the field of computational fluid dynamics (CFD), this problem is not yet accessible to computer-supported methods, at least with respect to unsteady airloads. First, the information will be discussed which is necessary for buffeting prediction. The reasons for performing pressure measurements are outlined. Then, a brief description of the test set-up and instrumentation will be given. The steady and unsteady test results will be presented and their strong mutual interdependency will be demonstrated. The question as to whether it is possible to separate the unsteady pressures due to flow separation from those due to oscillatory motion of the model will be answered on the basis of experimental results. The usefulness of such investigations and their limitations with respect to the buffeting problem will be discussed. Author

N91-14330# Deutsche Airbus G.m.b.H., Bremen (Germany, F.R.).

EXPERIMENTAL INVESTIGATION AND SEMI-EMPIRICAL PREDICTION OF THE DYNAMIC RESPONSE OF A LOW-ASPECT-RATIO TRAPEZOIDAL WING DUE TO FLOW SEPARATION c08

H. Zingel *In* AGARD, Aircraft Dynamic Loads Due to Flow Separation Sep. 1990 16 p (For primary document see N91-14324 06-05)

Copyright Avail: NTIS HC/MF A12; Non-NATO Nationals requests available only from AGARD/Scientific Publications Executive

The buffet response of a low-aspect-ratio trapezoidal half-wing model was measured in the low speed wind tunnel of the DLR-Research Center in Goettingen at different model natural frequencies of pitch and roll both separately and coupled and at different angles of incidence up to 40 degrees. On the basis of linear aeroelastic equations of motion and measured structural dynamic and unsteady aerodynamic input data, the buffet response was calculated and compared with the measurement. The comparison shows a satisfactory coincidence. Consequently the adopted way for the semi-empirical calculation of the buffet response proves to be practicable. Author

N91-14331# Deutsche Forschungsanstalt fuer Luft- und Raumfahrt, Goettingen (Germany, F.R.). Inst. for Aeroelasticity.

UNSTEADY AERODYNAMIC FORCES ON AN OSCILLATING WING AT HIGH INCIDENCES AND FLOW SEPARATION c02

H. W. Foersching *In* AGARD, Aircraft Dynamic Loads Due to Flow Separation Sep. 1990 18 p (For primary document see N91-14324 06-05)

Copyright Avail: NTIS HC/MF A12; Non-NATO Nationals requests available only from AGARD/Scientific Publications Executive

Based on wind tunnel measurements on a low-aspect-ratio trapezoidal half-wing model in incompressible flow, some characteristic features of motion-induced unsteady airloads at high incidences and flow separation are presented and discussed. Special emphasis is placed on the effect of the motion of the wing on the flow separation processes and on the investigation of the interactions between the separated flow phenomena on the stationary wing and the motion-induced unsteady airloads on the oscillating wing. It is shown that these airloads are strongly affected by the flow separations and that their prediction from inviscid potential-flow theory may lead to rather unrealistic results in buffeting response calculations. Author

N91-14332# Bristol Univ. (England). Dept. of Aerospace Engineering.

THE FORWARD MOUNTED SPOILER AS A SOURCE OF BUFFET EXCITATION c08

P. G. Myers and D. L. Birdsall *In* AGARD, Aircraft Dynamic Loads Due to Flow Separation Sep. 1990 13 p Sponsored by Department of Trade and Industry, England (For primary document see N91-14324 06-05)

Copyright Avail: NTIS HC/MF A12; Non-NATO Nationals requests available only from AGARD/Scientific Publications Executive

Tests were made with fixed transition at low Reynolds Numbers (usually 0.56 x 10(exp 6), based on chord) on a wing with a spoiler of length 8 percent chord hinged at 13 percent chord. Different classes of flow leading to differing spoiler performance have been identified. However signal analysis has shown that the non-dimensional frequency n(sub 1) can be used to correlate results from these classes of flow and that the peak frequencies will lie within a narrow band. Now n(sub 1) = fl(sub b)/V where f is the frequency, l(sub b) the length of separated flow from the spoiler free edge lying over the wing (in the case of a closed bubble, l(sub b) is the bubble length) and V the freestream velocity. Since n(sub 1) depends on l(sub b), a good idea of the nature of buffet excitation can be formed from an observation of the scale of separated flow lying over the wing. With one class of flow, there was no change in steady state lift following spoiler deployment, but the formation of a separation bubble over much of the wing upper surface led to a high level of buffet excitation. This underlines

the difficulty of trying to deduce the fluctuating component of lift from a steady mean. Author

N91-14333# National Aerospace Lab., Amsterdam (Netherlands).
INVESTIGATION OF A SEMI-EMPIRICAL METHOD TO PREDICT LIMIT CYCLE OSCILLATIONS OF MODERN FIGHTER AIRCRAFT **c08**
J. J. Meijer and R. J. Zwaan *In* AGARD, Aircraft Dynamic Loads Due to Flow Separation Sep. 1990 8 p (For primary document see N91-14324 06-05)
Copyright Avail: NTIS HC/MF A12; Non-NATO Nationals requests available only from AGARD/Scientific Publications Executive

Requirements of modern fighter aircraft to operate with high maneuverability in the transonic speed regime may lead under certain conditions to limit cycle oscillations (LCO), produced by a structural/aerodynamic interaction. Conditions of transonic LCO are moderate angel of attack and Mach numbers ranging from 0.9 to 1.1. An analysis of steady wind tunnel data, obtained for a fighter type aircraft in a typical configuration, has indicated that shock-induced separation plays a dominant role. A semi-empirical prediction method is presented which makes use of these steady data, and some results are shown. Possibilities are discussed to extend the method to the use of unsteady wind tunnel data. Author

N91-14334# Royal Aerospace Establishment, Bedford (England).
INTERACTION BETWEEN THE CANARD AND WING FLOW ON A MODEL OF A TYPICAL COMBAT AIRCRAFT
D. G. Mabey, B. L. Welsh, and C. R. Pyne *In* AGARD, Aircraft Dynamic Loads Due to Flow Separation Sep. 1990 19 p (For primary document see N91-14324 06-05)
Copyright Avail: NTIS HC/MF A12; Non-NATO Nationals requests available only from AGARD/Scientific Publications Executive

The main features of canard/wing interaction were established by a comprehensive test of a half model of a typical combat aircraft in the RAE 13 x 9 ft Low Speed Wind Tunnel. The measurements comprised overall steady forces, buffeting on the wing and the canard, and steady and unsteady pressure distributions on the wing. The results show that the canard effective incidence (determined by the canard setting and the body/wing upwash) controls the canard/wing interaction. With attached flow the canard produces a downwash field which has significant effects when the wing flow is attached. With separated flow on the canard the downwash field is still produced but in addition there is vigorous mixing which inhibits the development of wing flow separations, increasing the overall lift, reducing the wing buffeting and reducing the drag. The process by which this favorable effect is achieved is illustrated by an analysis of the steady and unsteady pressure distributions on the wing at three spanwise sections. These results have important implications with respect to the development and optimization of other canard/wing configurations, particularly at high angles of incidence. Author

N91-14335*# General Dynamics Corp., Fort Worth, TX.
PREDICTIONS OF F-111 TACT AIRCRAFT BUFFET RESPONSE **c08**
Atlee M. Cunningham, Jr. and Charles F. Coe (Coe Engineering, Inc., Los Altos, CA.) *In* AGARD, Aircraft Dynamic Loads Due to Flow Separation Sep. 1990 16 p (For primary document see N91-14324 06-05)
(Contract NAS2-11420)
Copyright Avail: NTIS HC/MF A12; Non-NATO Nationals requests available only from AGARD/Scientific Publications Executive CSCL 01C

A summary is presented for the prediction method development and correlations of predicted response with flight test measurements. The prediction method was based on refinements to the method described by Cunningham. One improvement made use of direct time integration of the correlated fluctuating pressure data to obtain buffet excitation for the various modes of interest. Another improvement incorporated a hybrid technique for scaling measured wind tunnel damping data to full-scale for the modes of interest. A third improvement made use of the diagonalized form of the fully coupled equations of motion. Finally, a mechanism was described for explaining an apparent coupling between the aircraft wing torsion modes and shock induced trailing edge separation that led to very high wing motion on the aircraft that was not observed on the wind tunnel model. Author

N91-14336# National Aeronautical Establishment, Ottawa (Ontario).
THE EFFECT OF WING PLANFORM ON LOW SPEED BUFFET **c08**
S. J. Zan and D. J. Maull (Cambridge Univ., England) *In* AGARD, Aircraft Dynamic Loads Due to Flow Separation Sep. 1990 15 p Sponsored by Department of Trade and Industry, England (For primary document see N91-14324 06-05)
Copyright Avail: NTIS HC/MF A12; Non-NATO Nationals requests available only from AGARD/Scientific Publications Executive

A parametric experimental investigation into low speed buffet is presented. The influence of wing generalized mass, reduced frequency, aspect ratio, dynamic pressure and wing sweep on the buffet excitation parameter, the square root of nG(n), was studied for a simple wing model with sharp leading and trailing edges. The investigation was limited to buffeting response in the fundamental bending mode. The angle of incidence range for the experiments was 0 to 40 deg, however the paper will concentrate on results at 10 deg incidence (near stall) and at 30 deg incidence. The influence of aspect ratio on the buffet excitation parameter was found to be significant at high incidences at values of reduced frequency below those common for subsonic flight. Author

N91-14337# Office National d'Etudes et de Recherches Aerospatiales, Paris (France).
NEW METHOD TO DETERMINE IN WIND TUNNEL THE BUFFETING FORCES **c08**
Roger Destuynder and Roland Barreau (Aerospatiale, Toulouse, France) *In* AGARD, Aircraft Dynamic Loads Due to Flow Separation Sep. 1990 16 p In FRENCH; ENGLISH Summary (For primary document see N91-14324 06-05)
Copyright Avail: NTIS HC/MF A12; Non-NATO Nationals requests available only from AGARD/Scientific Publications Executive

Among the usual criteria used to qualify the airplane buffet onset, it is classical to use the acceleration values measured at the pilot seat and limited at + or - 0.2g. This acceleration is the result of two excitation systems. The first one, due to the external forces, is created by the random unsteady field of pressure on the airplane and acting in a large frequency range. The second excitation is due to the induced pressures coming from the airplane motions and characterizing principally the eigen modes of the structure. It seems interesting to separate the two pressure fields to improve the buffet knowledge not only to have the correct buffet onset forces but also to obtain the forces distribution. For this target a closed loop system using a parameter of the wing (unsteady bending moment or accelerometers) permits in wind tunnel to reduce the wing motion introducing damping forces, in the model with the help of actuator. It is necessary to translate these results to the aircraft, the static deformation of the model and aircraft being similar. In a second phase, always under buffet conditions, sinusoidal excitations are applied on the wind tunnel model, giving a field of pressure uncorrelated with the buffeting pressure. In this manner the possibility of extraction, using an FFT, is given for the induced complex pressure and forces. Some examples are given. Author

N91-14338# Office National d'Etudes et de Recherches Aerospatiales, Paris (France).
COUPLED AERODYNAMIC LOADS DUE TO UNSTEADY STALL ON A LARGE ASPECT RATIO WING OSCILLATING AT GREAT AMPLITUDE [FORCES AERODYNAMIQUES COUPLEES DUES AU DECROCHAGE INSTATIONNAIRE SUR UNE AILE DE GRAND ALLONGEMENT OSCILLANT A GRANDE AMPLITUDE] **c08**
J.-J. Costes and D. Petot *In* AGARD, Aircraft Dynamic Loads

Due to Flow Separation Sep. 1990 15 p In FRENCH; ENGLISH Summary (For primary document see N91-14324 06-05)
Copyright Avail: NTIS HC/MF A12; Non-NATO Nationals requests available only from AGARD/Scientific Publications Executive

Experimental results which were obtained on a rectangular wing oscillating in pitch around the quarter chord line are presented. Normal flow as well as skewed flow cases were investigated. The comparison with a simple theory used in helicopter applications showed the influence of the tip wing vortex and the importance, in the skewed flow case, of the component of the wind velocity directed along the wing span. Author

N91-14339# Lockheed Missiles and Space Co., Sunnyvale, CA.
UNSTEADY SEPARATED FLOW PHENOMENA CAUSING SELF-EXCITED STRUCTURAL OSCILLATIONS **c08**
L. E. Ericsson *In* AGARD, Aircraft Dynamic Loads Due to Flow Separation Sep. 1990 16 p (For primary document see N91-14324 06-05)
Copyright Avail: NTIS HC/MF A12; Non-NATO Nationals requests available only from AGARD/Scientific Publications Executive

Because of steadily increasing performance demands both aircraft and missiles operate at high angles of attack where separated flow often has a dominant influence on especially the unsteady aerodynamics. The penetration of the buffet boundary usually changes the structural response from the buffet-type to the self-excited type. This transfer occurs when the structural response starts interacting with the unsteady flow separation, generating negative aerodynamic damping. Separated flow aerodynamics are usually very nonlinear, and the self-excited response frequently takes the form of a limit-cycle oscillation. Author

N91-14340*# National Aeronautics and Space Administration. Langley Research Center, Hampton, VA.
UNSTEADY AIRLOADS DUE TO SEPARATED FLOW ON AIRFOILS AND WINGS **c02**
John W. Edwards *In* AGARD, Aircraft Dynamic Loads Due to Flow Separation Sep. 1990 18 p Previously announced in IAA as A90-33311 (For primary document see N91-14324 06-05)
Copyright Avail: NTIS HC/MF A12; Non-NATO Nationals requests available only from AGARD/Scientific Publications Executive CSCL 01A

Experimental and computational studies of airloads due to separated flows over airfoils and wings conducted at the NASA Langley Research Center are surveyed. Results are presented for cases involving local flow separation such as shock-induced separation, for the initiation of leading-edge vortex flows, and for cases involving unsteady airloads due to flows separating over remote aircraft components. Good correlation is obtained between experiment and computation for cases of locally separating flow and steady computations of vortex flow over delta wings and complex forebody geometries are shown. Physical flow modeling issues and computational requirements for the case of vertical tail buffeting are developed. Author

N91-14341# Royal Aerospace Establishment, Farnborough (England).
IN-FLIGHT MEASUREMENTS ON A TORNADO AIRCRAFT FOR STORES CARRIAGE AND RELEASE RESEARCH
G. W. Foster 25 May 1990 21 p Presented at RAeS Conference on Store Carriage, Integration and Release, Bath, England, 4-6 Apr. 1990
(RAE-TM-AERO-2180; BR114548; AD-A226742; ETN-91-98366)
Copyright Avail: NTIS HC/MF A03

Flight trials with a Tornado aircraft to produce full scale experimental data for stores carriage loads, release trajectories and flow surveys are described. Among the instrumentation used for the tests were position transducers on all the aircraft control surfaces, a set of accelerometers and gyroscopes near the aircraft center of gravity, an inertial navigation system, the fuel state, the aircraft air data system and an additional air data system based on a pair of 5-hole conical yawmeters. A modular data acquisition system was used for the data capture. Aircraft and store instrumentation were proved and if necessary, calibrated in flight. Flow fields below pylons were measured using a specially constructed rig. The results show that flight trials provide high quality full scale data of stores during carriage and release. ESA

N91-14342# Naval Postgraduate School, Monterey, CA.
DEVELOPMENT OF AN UNMANNED AIR RESEARCH VEHICLE FOR SUPERMANEUVERABILITY STUDIES M.S. Thesis
Christopher M. Cleaver 29 Mar. 1990 53 p
(AD-A227165) Avail: NTIS HC/MF A04 CSCL 01/3

With the advent of all-aspect missiles and highly maneuverable threat aircraft, maintaining air superiority in the future will require innovative solutions to current aerodynamic and propulsive limitations. Unmanned Air Vehicles (UAV's) provide an excellent experimental alternative for supermaneuverability investigations, providing dynamic flight measurements not available in wind tunnels. A 1/8 geometrically scaled F-16A was constructed and test flown in order to provide a proven, highly maneuverable of airspeed, angle of attack, sideslip angle, and control surface deflection. A seven-channel telemetry system was designed to transmit the flight measurement data to a ground station for display and recording. Follow-on research will complete the on-board systems and perform a baseline evaluation for comparison with future flight tests with varied control configurations. GRA

N91-14343# McDonnell-Douglas Helicopter Co., Mesa, AZ.
ADVANCED TECHNOLOGY LANDING GEAR. VOLUME 1: DESIGN Final Report, Sep. 1985 - Dec. 1989
J. K. Sen Aug. 1990 185 p
(Contract DAAJ02-85-C-0049)
(AD-A227196; MDHC-89-17-Vol-1;
USAAVSCOM-TR-89-D-13A-Vol-1) Avail: NTIS HC/MF A09
CSCL 01/3

The development is described of a retractable, crashworthy, main landing gear system for an LHX-size utility helicopter. The landing gear is of a tricycle configuration and is designed to absorb 60 percent of the energy from a 42 fps level impact condition. The landing gear extends automatically in less than two seconds in an emergency. In the event that the hydraulic and electrical systems fail, the gear is extended with the hydraulic accumulator that primarily supports the helicopter Auxialiary Power Unit. Five sets of landing gears were fabricated in the program. The tests included single gear platform drop tests with level and simulated roll and pitch conditions, and combined pitch (+15 deg) and roll (10 deg) conditions with an iron-bird fixture simulating a helicopter. The tests were conducted for five impact velocities from 10 to 42 fps. The crashworthiness results was very good and demonstrated how analyses can be used to predict the response of landing gears without utilizing expensive tests. The cost of 5000 shipsets over a 13-year production cycle was projected from the cost of fabricated landing gears. GRA

N91-14344# McDonnell-Douglas Helicopter Co., Mesa, AZ.
ADVANCED TECHNOLOGY LANDING GEAR. VOLUME 2: TEST Final Report, Sep. 1985 - Dec. 1989
J. K. Sen Aug. 1990 151 p
(Contract DAAJ02-85-C-0049)
(AD-A227197; MDHC-89-17-Vol-2;
USAAVSCOM-TR-89-D-13B-Vol-2) Avail: NTIS HC/MF A08
CSCL 01/3

The development is described of retractable, crashworthy, main landing gear system for an LHX-size helicopter. The landing gear is of a tricycle configuration and is designed to absorb 60 percent of the energy from a 42 fps level impact condition. The landing gear extends automatically in less than two seconds in an emergency. In the event that the hydraulic and electrical systems fail, the gear is extended with the hydraulic accumulator that primarily supports the helicopter APU. Five sets of landing gears were fabricated in the program. The tests included single gear platform drop tests with level and simulated roll and pitch conditions, and combined pitch (+15 deg) and roll (10 deg)

conditions with an iron-bird fixture simulating a helicopter. The tests were conducted for five impact velocities from 10 to 42 fps. The crashworthiness analyses were conducted using program KRASH. The correlation between test and crashworthiness analysis results was very good and demonstrated how analyses can be used to predict the response of landing gears without utilizing expensive tests. The cost of 5000 shipsets over a 13 year production cycle was projected from the cost of the fabricated landing gears. GRA

N91-14345* National Aeronautics and Space Administration. Langley Research Center, Hampton, VA.
WINGTIP VORTEX TURBINE Patent
James C. Patterson, Jr., inventor (to NASA) 17 Apr. 1990 7 p Filed 28 Oct. 1988 Continuation-in-part of abandoned US-Patent-Appl-SN-004304, filed 5 Jan. 1987 which is a continuation-in-part of abandoned US-Patent-Appl-SN-243685, filed 16 Mar. 1981
(NASA-Case-LAR-14116-1; US-Patent-4,917,332; US-Patent-Appl-SN-264993; US-Patent-Appl-SN-004304; US-Patent-Appl-SN-243685; US-Patent-Class-244-58; US-Patent-Class-244-199; US-Patent-Class-290-44; US-Patent-Class-290-55; Int-Patent-Class-B64D-33/00) Avail: US Patent and Trademark Office CSCL 01C

A means for extracting rotational energy from the vortex created at aircraft wing tips which consists of a turbine with blades located in the crossflow of the vortex and attached downstream of the wingtip. The turbine has blades attached to a core. When the aircraft is in motion, rotation of a core transmits energy to a centrally attached shaft. The rotational energy thus generated may be put to use within the airfoil or aircraft fuselage.
Official Gazette of the U.S. Patent and Trademark Office

N91-14346*# Douglas Aircraft Co., Inc., Long Beach, CA.
STRUCTURAL DEVELOPMENT OF LAMINAR FLOW CONTROL AIRCRAFT CHORDWISE WING JOINT DESIGNS Final Report
J. E. Fischler, N. M. Jerstad, F. H. Gallimore, Jr., and T. J. Pollard Apr. 1989 195 p
(Contract NAS1-18037)
(NASA-CR-181888; NAS 1.26:181888) Avail: NTIS HC/MF A09 CSCL 01C

For laminar flow to be achieved, any protuberances on the surface must be small enough to avoid transition to turbulent flow. However, the surface must have joints between the structural components to allow assembly or replacement of damaged parts, although large continuous surfaces can be utilized to minimize the number the number of joints. Aircraft structural joints usually have many countersunk bolts or rivets on the outer surface. To maintain no mismatch on outer surfaces, it is desirable to attach the components from the inner surface. It is also desirable for the panels to be interchangeable, without the need for shims at the joint, to avoid surface discontinuities that could cause turbulence. Fabricating components while pressing their outer surfaces against an accurate mold helps to ensure surface smoothness and continuity at joints. These items were considered in evaluating the advantages and disadvantages of the joint design concepts. After evaluating six design concepts, two of the leading candidates were fabricated and tested using many small test panels. One joint concept was also built and tested using large panels. The small and large test panel deflections for the leading candidate designs at load factors up to +1.5 g's were well within the step and waviness requirements for avoiding transition.The small panels were designed and tested for compression and tension at -65 F, at ambient conditions, and at 160 F. The small panel results for the three-rib and the sliding-joint concepts indicated that they were both acceptable. The three-rib concept, with tapered splice plates, was considered to be the most practical. A modified three-rib joint that combined the best attributes of previous candidates was designed, developed, and tested. This improved joint met all of the structural strength, surface smoothness, and waviness criteria for laminar flow control (LFC). The design eliminated all disadvantages of the initial three-rib concept except for unavoidable eccentricity, which was reduced and reacted satisfactorily by the rib supports. It should also result in a relatively simple low-cost installation, and makes it easy to replace any panels damaged in the field. Author

N91-14281# Royal Aeronautical Society, London (England). Aerodynamics Group Committee.
STORE CARRIAGE, INTEGRATION, AND RELEASE
A. B. Haines *In* AGARD, Missile Aerodynamics Oct. 1990 8 p (For primary document see N91-14278 06-02)
Copyright Avail: NTIS HC/MF A17; Non-NATO Nationals requests available only from AGARD/Scientific Publications Executive

06 AIRCRAFT INSTRUMENTATION

Includes cockpit and cabin display devices; and flight instruments.

For related information see also *19 Spacecraft Instrumentation* and *35 Instrumentation and Photography.*

N91-14347*# General Electric Co., Daytona Beach, FL. Simulation and Control Systems Dept.
RASTER GRAPHIC HELMET-MOUNTED DISPLAY STUDY Final Report
William S. Beamon and Susanna I. Moran Washington NASA Dec. 1990 126 p
(Contract NAS1-18711)
(NASA-CR-4331; NAS 1.26:4331; AVSCOM-TR-90-B-008) Avail: NTIS HC/MF A07 CSCL 01D

A design of a helmet mounted display system is presented, including a design specification and development plan for the selected design approach. The requirements for the helmet mounted display system and a survey of applicable technologies are presented. Three helmet display concepts are then described which utilize lasers, liquid crystal display's (LCD's), and subminiature cathode ray tubes (CRT's), respectively. The laser approach is further developed in a design specification and a development plan. Author

N91-14348# Optech, Inc., Downsview (Ontario).
HELICOPTER LIDAR BATHYMETER SYSTEM. CONCEPTUAL DESIGN Final Report
Jun. 1990 213 p
(Contract DACW39-88-D-0039)
(AD-A227057; CERC-90-2) Avail: NTIS HC/MF A10 CSCL 08/3

A technical evaluation is presented of the likely performance of a Helicopter Lidar Bathymeter System (HLBS) that is being developed through an international agreement between the United States and Canada and is implemented through a joint Memorandum of Understanding under the U.S./Canadian Defense Development Sharing Program. Optech, Inc., is developing the HLBS, and the U.S. Army Engineer Waterways Experiment Station is directing the overall development program. The program is in two phases. Phase 1, the developement of a conceptual design, was initiated in March 1988 and completed in March 1989. Phase 2 provides for the detailed design, fabrication, and field testing of an operational prototype system. The conceptual design is presented of the HLBS, which is designed for use from a Bell 212 helicopter at altitudes ranging from 100 to 1,000 m. The system is intended for use in water depths from approx. 1.5 to 35 m. Horizontal control will be provided either by microwave or the NAVSTAR Global Positioning System. GRA

07 AIRCRAFT PROPULSION AND POWER

Includes prime propulsion systems and systems components, e.g., gas turbine engines and compressors; and onboard auxilliary power plants for aircraft.

For related information see also *20 Spacecraft Propulsion and Power, 28 Propellants and Fuels,* and *44 Energy Production and Conversion.*

N91-14349*# National Aeronautics and Space Administration. Lewis Research Center, Cleveland, OH.
COMBUSTOR TECHNOLOGY FOR FUTURE AIRCRAFT
Robert R. Tacina 1990 17 p Presented at the 26th Joint Propulsion Conference, Orlando, FL, 16-18 Jul. 1990; cosponsored by AIAA, SAE, ASME, and ASEE Previously announced in IAA as A90-47219
(NASA-TM-103268; E-5707; NAS 1.15:103268; AIAA-90-2400) Avail: NTIS HC/MF A03 CSCL 21E

The continuing improvement of aircraft gas turbine engine operating efficiencies involves increases in overall engine pressure ratio increases that will result in combustor inlet pressure and temperature increases, greater combustion temperature rises, and higher combustor exit temperatures. These conditions entail the development of fuel injectors generating uniform circumferential and radial temperature patterns, as well as combustor liner configurations and materials capable of withstanding increased thermal radiation even as the amount of cooling air is reduced. Low NO(x)-emitting combustor concepts are required which will employ staged combustion. The development status of component technologies answering these requirements are presently evaluated. Author

N91-14350# Purdue Univ., West Lafayette, IN. Thermal Sciences and Propulsion Center.
RESEARCH AS PART OF THE AIR FORCE RESEARCH IN AERO-PROPULSION TECHNOLOGY (AFRAPT) PROGRAM Annual Summary Report, 15 Aug. 1988 - 14 Oct. 1990
Sanford Fleeter 1 Aug. 1990 5 p
(Grant AF-AFOSR-0261-88; AF Proj. 2308)
(AD-A226893; AFOSR-90-0961TR) Avail: NTIS HC/MF A01 CSCL 21/5

Nine graduate students participated in the AFRAPT Program during this time period. Two students have completed their M.S.M.E. programs and are currently employed at one of the AFRAPT participating companies. Four students have nearly completed their thesis research, with one student having withdrawn. The other two continuing and new students have initiated their thesis research and are making good progress. GRA

N91-14351# Detroit Diesel Allison, Indianapolis, IN.
FATIGUE AND FRACTURE OF TITANIUM ALUMINIDES, VOLUME 2 Final Report, 1 Jul. 1985 - 31 Jul. 1989
M. L. Gambone Feb. 1990 235 p
(Contract F33615-85-C-5111; AF Proj. 2420)
(AD-A227353; ALLISON-EDR-14249-Vol-2; WRDC-TR-89-4145-Vol-2) Avail: NTIS HC/MF A11 CSCL 11/6

Titanium aluminide composites hold great promise for application in the later stages of advanced compressor systems. This conclusion is based on the assumption that Ti3Al composites can achieve the fatigue strength levels projected from data for the SiC/Ti 6Al-4V composite system yet remain stable to 650 C or higher temperatures. In the limited results to date, Ti3Al composite specimens have exhibited a minimum of fiber/matrix interaction, good strength stiffness, and significantly better fatigue strength than monolithic Ti3Al. The good fatigue and high stiffness are essential for application to the high temperature compressor spacers in the minimum-weight rotor configuration being developed. The key material design parameters for titanium aluminides and titanium aluminide composites must be identified and understood. These parameters include the fatigue and fracture behavior (crack initiation and propagation as a function of temperature, frequency, size, and stress ratio), the near threshold stress intensity crack growth rates, and the thermomechanical fatigue behavior. GRA

08 AIRCRAFT STABILITY AND CONTROL

Includes aircraft handling qualities; piloting; flight controls; and autopilots.

For related information see also *05 Aircraft Design, Testing and Performance.*

N91-14352# Messerschmitt-Boelkow-Blohm G.m.b.H., Munich (Germany, F.R.). Hubschrauber und Flugzeuge.
ROLE OF SEPARATION AUTOPILOTS FOR MODERN MISSILE CONCEPTS
Ronald Deslandes 23 Jul. 1990 20 p Presented at Store Carriage and Release Conference, Bath, England, 4 Apr. 1990; sponsored by Royal Aeronautical Society
(MBB/FE121/S/PUB/409/A; ETN-90-98150) Copyright Avail: NTIS HC/MF A03

It is demonstrated that for certain weapon stations on modern fighter aircraft the roll disturbance induced by interference effects is a quite sensitive area as far as risk of collision and or roll sensor limitations are concerned. Based on the experience gathered on the field of passive and active control for missiles, the concept of a typical separation autopilot is discussed in detail and highlighted by some results. Safe separation of missiles from fighter aircraft is concluded to still be restricted to a smaller envelope. The use of autopilots in the missiles with combined roll and pitch authority is concluded to greatly improve separation behavior. ESA

N91-14353*# Calspan-State Univ. of New York Joint Venture, Buffalo, NY.
INTERACTION OF FEEL SYSTEM AND FLIGHT CONTROL SYSTEM DYNAMICS ON LATERAL FLYING QUALITIES Final Report
R. E. Bailey and L. H. Knotts Dec. 1990 391 p
(NASA Order A-43049-C)
(NASA-CR-179445; H-1584; NAS 1.26:179445; Calspan-7205-26) Avail: NTIS HC/MF A17 CSCL 01C

An experimental investigation of the influence of lateral feel system characteristics on fighter aircraft roll flying qualities was conducted using the variable stability USAF NT-33. Forty-two evaluation flights were flown by three engineering test pilots. The investigation utilized the power approach, visual landing task and up-and-away tasks including formation, gun tracking, and computer-generated compensatory attitude tracking tasks displayed on the Head-Up Display. Experimental variations included the feel system frequency, force-deflection gradient, control system command type (force or position input command), aircraft roll mode time constant, control system prefilter frequency, and control system time delay. The primary data were task performance records and evaluation pilot comments and ratings using the Cooper-Harper scale. The data highlight the unique and powerful effect of the feel system of flying qualities. The data show that the feel system is not 'equivalent' in flying qualities influence to analogous control system elements. A lower limit of allowable feel system frequency appears warranted to ensure good lateral flying qualities. Flying qualities criteria should most properly treat the feel system dynamic influence separately from the control system, since the input and output of this dynamic element is apparent to the pilot and thus, does not produce a 'hidden' effect. Author

N91-14325# National Aeronautical Establishment, Ottawa (Ontario).
WIND TUNNEL INVESTIGATION AND FLIGHT TESTS OF TAIL BUFFET ON THE CF-18 AIRCRAFT
B. H. K. Lee, D. Brown, M. Zgela, and D. Poirel *In* AGARD, Aircraft Dynamic Loads Due to Flow Separation Sep. 1990

26 p (For primary document see N91-14324 06-05)
Copyright Avail: NTIS HC/MF A12; Non-NATO Nationals requests available only from AGARD/Scientific Publications Executive

N91-14326# McDonnell Aircraft Co., Saint Louis, MO.
A UNIFIED APPROACH TO BUFFET RESPONSE OF FIGHTER AIRCRAFT EMPENNAGE
M. A. Ferman, S. R. Patel, and N. H. Zimmerman *In* AGARD, Aircraft Dynamic Loads Due to Flow Separation Sep. 1990 18 p (For primary document see N91-14324 06-05)
Copyright Avail: NTIS HC/MF A12; Non-NATO Nationals requests available only from AGARD/Scientific Publications Executive

N91-14327# National Aeronautical Establishment, Ottawa (Ontario).
EFFECTS OF TRAILING-EDGE FLAP ON BUFFET CHARACTERISTICS OF A SUPERCRITICAL AIRFOIL
B. H. K. Lee *In* AGARD, Aircraft Dynamic Loads Due to Flow Separation Sep. 1990 14 p (For primary document see N91-14324 06-05)
Copyright Avail: NTIS HC/MF A12; Non-NATO Nationals requests available only from AGARD/Scientific Publications Executive

N91-14328# Deutsche Forschungsanstalt fuer Luft- und Raumfahrt, Goettingen (Germany, F.R.). Institut fuer Experimentelle Stroemungsmechanik.
EXPERIMENTAL INVESTIGATION OF BUFFET ONSET AND PENETRATION ON A SUPERCRITICAL AIRFOIL AT TRANSONIC SPEEDS
E. Stanewsky and D. Basler (Holtronic G.m.b.H., Ottersberg, Germany, F.R.) *In* AGARD, Aircraft Dynamic Loads Due to Flow Separation Sep. 1990 11 p (For primary document see N91-14324 06-05)
Copyright Avail: NTIS HC/MF A12; Non-NATO Nationals requests available only from AGARD/Scientific Publications Executive

N91-14329# Deutsche Forschungsanstalt fuer Luft- und Raumfahrt, Goettingen (Germany, F.R.). Inst. for Aeroelasticity.
EXPERIMENTAL INVESTIGATIONS OF BUFFET EXCITATION FORCES ON A LOW ASPECT RATIO TRAPEZOIDAL HALF WING IN INCOMPRESSIBLE FLOW
P. Bublitz and H. Zingel (Deutsche Airbus G.m.b.H., Bremen, Germany, F.R.) *In* AGARD, Aircraft Dynamic Loads Due to Flow Separation Sep. 1990 19 p (For primary document see N91-14324 06-05)
Copyright Avail: NTIS HC/MF A12; Non-NATO Nationals requests available only from AGARD/Scientific Publications Executive

N91-14330# Deutsche Airbus G.m.b.H., Bremen (Germany, F.R.).
EXPERIMENTAL INVESTIGATION AND SEMI-EMPIRICAL PREDICTION OF THE DYNAMIC RESPONSE OF A LOW-ASPECT-RATIO TRAPEZOIDAL WING DUE TO FLOW SEPARATION
H. Zingel *In* AGARD, Aircraft Dynamic Loads Due to Flow Separation Sep. 1990 16 p (For primary document see N91-14324 06-05)
Copyright Avail: NTIS HC/MF A12; Non-NATO Nationals requests available only from AGARD/Scientific Publications Executive

N91-14332# Bristol Univ. (England). Dept. of Aerospace Engineering.
THE FORWARD MOUNTED SPOILER AS A SOURCE OF BUFFET EXCITATION
P. G. Myers and D. L. Birdsall *In* AGARD, Aircraft Dynamic Loads Due to Flow Separation Sep. 1990 13 p Sponsored by Department of Trade and Industry, England (For primary document see N91-14324 06-05)
Copyright Avail: NTIS HC/MF A12; Non-NATO Nationals requests available only from AGARD/Scientific Publications Executive

N91-14333# National Aerospace Lab., Amsterdam (Netherlands).
INVESTIGATION OF A SEMI-EMPIRICAL METHOD TO PREDICT LIMIT CYCLE OSCILLATIONS OF MODERN FIGHTER AIRCRAFT
J. J. Meijer and R. J. Zwaan *In* AGARD, Aircraft Dynamic Loads Due to Flow Separation Sep. 1990 8 p (For primary document see N91-14324 06-05)
Copyright Avail: NTIS HC/MF A12; Non-NATO Nationals requests available only from AGARD/Scientific Publications Executive

N91-14335*# General Dynamics Corp., Fort Worth, TX.
PREDICTIONS OF F-111 TACT AIRCRAFT BUFFET RESPONSE
Atlee M. Cunningham, Jr. and Charles F. Coe (Coe Engineering, Inc., Los Altos, CA.) *In* AGARD, Aircraft Dynamic Loads Due to Flow Separation Sep. 1990 16 p (For primary document see N91-14324 06-05)
(Contract NAS2-11420)
Copyright Avail: NTIS HC/MF A12; Non-NATO Nationals requests available only from AGARD/Scientific Publications Executive CSCL 01C

N91-14336# National Aeronautical Establishment, Ottawa (Ontario).
THE EFFECT OF WING PLANFORM ON LOW SPEED BUFFET
S. J. Zan and D. J. Maull (Cambridge Univ., England) *In* AGARD, Aircraft Dynamic Loads Due to Flow Separation Sep. 1990 15 p Sponsored by Department of Trade and Industry, England (For primary document see N91-14324 06-05)
Copyright Avail: NTIS HC/MF A12; Non-NATO Nationals requests available only from AGARD/Scientific Publications Executive

N91-14337# Office National d'Etudes et de Recherches Aerospatiales, Paris (France).
NEW METHOD TO DETERMINE IN WIND TUNNEL THE BUFFETING FORCES
Roger Destuynder and Roland Barreau (Aerospatiale, Toulouse, France) *In* AGARD, Aircraft Dynamic Loads Due to Flow Separation Sep. 1990 16 p In FRENCH; ENGLISH Summary (For primary document see N91-14324 06-05)
Copyright Avail: NTIS HC/MF A12; Non-NATO Nationals requests available only from AGARD/Scientific Publications Executive

N91-14338# Office National d'Etudes et de Recherches Aerospatiales, Paris (France).
COUPLED AERODYNAMIC LOADS DUE TO UNSTEADY STALL ON A LARGE ASPECT RATIO WING OSCILLATING AT GREAT AMPLITUDE [FORCES AERODYNAMIQUES COUPLEES DUES AU DECROCHAGE INSTATIONNAIRE SUR UNE AILE DE GRAND ALLONGEMENT OSCILLANT A GRANDE AMPLITUDE]
J.-J. Costes and D. Petot *In* AGARD, Aircraft Dynamic Loads Due to Flow Separation Sep. 1990 15 p In FRENCH; ENGLISH Summary (For primary document see N91-14324 06-05)
Copyright Avail: NTIS HC/MF A12; Non-NATO Nationals requests available only from AGARD/Scientific Publications Executive

N91-14339# Lockheed Missiles and Space Co., Sunnyvale, CA.
UNSTEADY SEPARATED FLOW PHENOMENA CAUSING SELF-EXCITED STRUCTURAL OSCILLATIONS
L. E. Ericsson *In* AGARD, Aircraft Dynamic Loads Due to Flow Separation Sep. 1990 16 p (For primary document see N91-14324 06-05)
Copyright Avail: NTIS HC/MF A12; Non-NATO Nationals requests available only from AGARD/Scientific Publications Executive

09 RESEARCH AND SUPPORT FACILITIES (AIR)

Includes airports, hangars and runways; aircraft repair and overhaul facilities; wind tunnels; shock tubes; and aircraft engine test stands.

For related information see also *14 Ground Support Systems and Facilities (Space).*

N91-14354# Brookhaven National Lab., Upton, NY.
A CABLE VEHICLE BARRIER FOR ALERT AIRCRAFT PROTECTION
J. P. Indusi, D. R. Dougherty, and C. H. Waide 1990 11 p Presented at the Institute of Nuclear Materials Management Conference, Los Angeles, CA, 15-18 Jul. 1990
(Contract DE-AC02-76CH-00016)
(DE91-001723; BNL-44994; CONF-9007106-75) Avail: NTIS HC/MF A03

A cable vehicle barrier (CVB) for the protection of Strategic Air Command (SAC) alert aircraft parking areas was conceived, designed and tested under a program managed by the Weapons Laboratory of the U.S. Air Force. A barrier with proven capability against vehicles and readily removable in all situations was required to support the security police and, in time, reduce manpower requirements. The CVB spans a 300 ft gap across a taxiway used by alert tankers and bombers and must be capable of being lowered quickly to meet defense or emergency vehicle needs. The barrier consists of three impact cables linked together by nylon straps, supported by posts and pulleys, and held under tension using nylon rope shock absorbers. The barrier is raised and lowered using an electric winch; a manual winch provides for adjustment and emergency operation in the event of electric winch failure. The CVB was proven in vehicle impact tests at Kirtland AFB, NM, and the prototype unit has been tested operationally at Wurtsmith AFB, MI. DOE

N91-14355# Massachusetts Inst. of Tech., Cambridge. Dept. of Ocean Engineering.
MEASUREMENT OF HYDRODYNAMIC FORCES AND MOMENTS AND FLOW FIELD MAPPING OF A MODEL IN CONING MOTION M.S. Thesis
Thomas John Eccles Jun. 1990 146 p Sponsored by General Dynamics Corp.
(Contract N00123-89-G-0580)
(AD-A226684) Avail: NTIS HC/MF A07 CSCL 13/10

A method of captive model testing using an axisymmetric marine vehicle model in steady motion with constant roll and yaw rates has been used experimentally to obtain functional relationships between certain motion parameters and the resultant hydrodynamic forces and moments on the body. Specifically, cross coupling terms in roll rate and yaw rate have been investigated for non-planar cross-flow. An instrumented slender body of revolution with length/diameter of 9.5 was tested at Reynolds number of about 5 million, based on length. The tests were conducted at free stream velocity of 25 ft/s for coning angles between zero and -20 deg in 2 deg increments, at rotation rates of up to 200 rpm in 12.5 rpm increments in both rotational directions. The character of force and moment terms varying with rotation rate and coning angle was determined. The results may be translated to functional relationships between the hydrodynamic coefficients and the angular velocities in roll and yaw. The data showed a transition in the forms of the sway force and the pitch moment after the coning angle exceeded -10 deg, due to body lift in the cross flow. A method for measuring the velocity field about the model using laser Doppler velocimetry has been developed. The flow field was mapped for two model coning angles at one moderate rotation rate. The flow field representation portrays perturbations in cross flow velocity at five sections in a body-fixed reference frame. This method is useful in understanding the vortex mechanisms at work to influence body forces and moments. The data showed formation of asymmetric body vortices after the coning angle exceeded -10 deg. GRA

N91-14356* National Aeronautics and Space Administration. Langley Research Center, Hampton, VA.
ELECTRO-OPTICAL SPIN MEASUREMENT SYSTEM Patent
Robert Fodale, inventor (to NASA) and Herbert R. Hampton, inventor (to NASA) 12 Jun. 1990 7 p Filed 30 Sep. 1988
(NASA-Case-LAR-13629-1; US-Patent-4,932,777;
US-Patent-Appl-SN-251411; US-Patent-Class-356-152;
US-Patent-Class-33-263; US-Patent-Class-73-147;
US-Patent-Class-342-54; US-Patent-Class-356-1;
US-Patent-Class-356-141; US-Patent-Class-364-433) Avail: US Patent and Trademark Office CSCL 14B

An electro-optical spin measurement system for a spin model in a spin tunnel includes a radio controlled receiver/transmitter, targets located on the spin model, optical receivers mounted around the perimeter of the spin tunnel and the base of the spin tunnel for receiving data from the targets, and a control system for accumulating data from the radio controlled receiver and receivers. Six targets are employed. The spin model includes a fuselage, wings, nose, and tail. Two targets are located under the fuselage of the spin model at the nose tip and tail. Two targets are located on the side of the fuselage at the nose tip and tail, and a target is located under each wing tip. The targets under the fuselage at the nose tip and tail measure spin rate of the spin model, targets on the side of the fuselage at the nose tip and tail measure angle of attack of the spin model, and the targets under the wing tips measure roll angle of the spin model. Optical receivers are mounted at 90 degree increments around the periphery of the spin tunnel to determine angle of attack and roll angle measurements of the spin model. Optical receivers are also mounted at the base of the spin tunnel to define quadrant and position of the spin model and to determine the spin rate of the spin model.

Official Gazette of the U.S. Patent and Trademark Office

N91-14357* National Aeronautics and Space Administration. Ames Research Center, Moffett Field, CA.
WIND TUNNEL BALANCE Patent
Warren L. Horne, inventor (to NASA), Nans Kunz, inventor (to NASA), Phillip M. Luna, inventor (to NASA), Andrew C. Roberts, inventor (to NASA), Kenneth M. Smith, inventor (to NASA), and Ronald C. Smith, inventor (to NASA) 11 Jul. 1989 10 p Filed 18 May 1988
(NASA-Case-ARC-11877-1-SB; US-Patent-4,845,993;
US-Patent-Appl-SN-195563; US-Patent-Class-73-147;
Int-Patent-Class-G01M-9/00) Avail: US Patent and Trademark Office CSCL 14B

A flow-through balance is provided which includes a non-metric portion and a metric portion which form a fluid-conducting passage in fluid communication with an internal bore in the sting. The non-metric and metric portions of the balance are integrally connected together by a plurality of flexure beams such that the non-metric portion, the metric portion and the flexure beams form a one-piece construction which eliminates mechanical hysteresis between the non-metric and the metric portion. The system includes structures for preventing the effects of temperature, pressure and pressurized fluid from producing asymmetric loads on the flexure beams. A temperature sensor and a pressure sensor are located within the fluid-conducting passage of the balance. The system includes a longitudinal bellows member connected at two ends to one of the non-metric portion and the metric portion and at an intermediate portion thereof to the other of (1) and (2). A plurality of strain gages are mounted on the flexure beams to measure strain forces on the flexure beams. The flexure beams are disposed so as to enable symmetric forces on the flexure beams to cancel out so that only asymmetric forces are measured as deviations by the strain gages.

Official Gazette of the U.S. Patent and Trademark Office

12 ASTRONAUTICS (GENERAL)

For extraterrestrial exploration see *91 Lunar and Planetary Exploration.*

N91-14358*# Boeing Aerospace Co., Huntsville, AL. Advanced Civil Space Systems.

SPACE TRANSFER CONCEPTS AND ANALYSIS FOR EXPLORATION MISSIONS Quarterly Review No. 2

23 Mar. 1990 605 p

(Contract NAS8-37857)

(NASA-CR-183943; NAS 1.26:183943; D615-10009) Avail: NTIS HC/MF A99 CSCL 22A

The progress and results are summarized for mission/system requirements database; mission analysis; GN and C (Guidance, Navigation, and Control), aeroheating, Mars landing; radiation protection; aerobrake mass analysis; Shuttle-Z, TMIS (Trans-Mars Injection Stage); Long Duration Habitat Trade Study; evolutionary lunar and Mars options; NTR (Nuclear Thermal Rocket); NEP (Nuclear Electric Propulsion) update; SEP (Solar Electric Propulsion) update; orbital and space-based requirements; technology; piloted rover; programmatic task; and evolutionary and innovative architecture. B.G.

N91-14359*# Jet Propulsion Lab., California Inst. of Tech., Pasadena.

PROCEEDINGS OF THE MARS GLOBAL NETWORK MISSION WORKSHOP

Francis M. Sturms, Jr., ed. 1 Jun. 1990 429 p Workshop held in Pasadena, CA, 6-7 Feb. 1990

(Contract NAS7-918)

(NASA-CR-186844; JPL-Publ-90-5; NAS 1.26:186844) Avail: NTIS HC/MF A19 CSCL 22A

A workshop on the Mars Global Network Mission held at the Jet Propulsion Laboratory (JPL) on February 6 and 7, 1990, was attended by 68 people from JPL, National Aeronautics and Space Administration centers, universities, national laboratories, and industry. Three working sessions on science and exploration objectives, mission and system design concepts, and subsystem technology readiness each addressed three specific questions on implementation concepts for the mission. The workshop generated conclusions for each of the nine questions and also recommended several important science and engineering issues to be studied subsequent to the workshop. For individual titles, see N91-14360 through N91-14364.

N91-14360*# California Univ., Los Angeles. Dept. of Earth and Space Sciences.

SPECIFICATION GOALS FOR A MARS SEISMIC NETWORK **c91**

Paul M. Davis *In* JPL, Proceedings of the Mars Global Network Mission Workshop 1 Jun. 1990 p 159-173 (For primary document see N91-14359 06-12)

Avail: NTIS HC/MF A19 CSCL 03B

A seismic network on Mars should have enough stations (e.g., 24) to characterize the seismicity of the planet for comparison with a diversity of structural features; be comprised of low noise stations, preferably underground, 3 to 4 orders of magnitude more sensitive than those used on Viking; record over a sufficient band-width (DC-30 Hz) to detect micro-earthquakes to normal modes; and record for a sufficient duration (10 years) and data rate (10(exp 8) Mb/day/station) to obtain a data set comparable to that from the Apollo mission to the Moon so that locations of major internal boundaries can be inferred, such as those in the Earth, i.e., crust - lithosphere - asthenosphere - upper - lower phase transitions - outer - inner core. The proposed Mars Global Network Mission provides an opportunity to sense the dynamics and probe the interior of the planet. The seismic objectives, the availability of the instrumentation and trade-offs to meet them are discussed. Author

N91-14361*# Jet Propulsion Lab., California Inst. of Tech., Pasadena.

A POLAR ORBIT FOR THE MARS GLOBAL NETWORK MISSION **c91**

Philip Knocke *In its* Proceedings of the Mars Global Network Mission Workshop 1 Jun. 1990 p 177-189 (For primary document see N91-14359 06-12)

Avail: NTIS HC/MF A19 CSCL 03B

The purpose of the Global Network Mission (GNM) is to deploy simple landers on the Martian surface in late 1998. The objective is to create a globally distributed network of ground stations which will collect environmental data, perhaps for as long as several years. The GNM presents unique mission design challenges, which are addressed by the following essay. The GNM mission concept calls for two carrier spacecraft, each equipped with a number of simple landers. Some of the landers may be deployed from approach, either to reduce carrier mass prior to orbit insertion, or to reach latitudes not available from the carrier orbit. The remaining landers are deployed from orbit. One configuration for the Global Network Mission was proposed in a report from the Exploration Precursors Task Team to the Office of Space Science and Applications. This formed the basis of a previous orbit design for the GNM. This mission scenario is used as a point of reference, but results from the current study are generally applicable to a wide range of GNM mission variants. The analysis concluded that a 1/5 sol, polar orbit with a periapse altitude of 275 km offers the best circumstances for orbital deployment of the Global Network Mission landers. It allows easy polar access at nominal entry angles, and global dispersal of landing sites at lighting angles suitable for descent imaging. The polar orbit allows the option of deploying all the landers from orbit. A wait interval of 160 days after arrival is required before deployment can commence. Author

N91-14362*# Science Applications International Corp., Schaumburg, IL.

A GLOBAL VIEW OF LANDER-TO-ORBITER COMMUNICATIONS ACCESSIBILITY FOR A MARS GLOBAL NETWORK MISSION **c91**

Alan L. Friedlander *In* JPL, Proceedings of the Mars Global Network Mission Workshop 1 Jun. 1990 p 205-221 (For primary document see N91-14359 06-12)

Avail: NTIS HC/MF A19 CSCL 03B

Given the mission objective to deploy a number of small landers to the surface of Mars at various latitude/longitude locations, it is of interest to obtain a global perspective of the communications link geometry between the landers and a data relay orbiter. Specifically, the question to be answered is what is the total time interval over one Martian day (1 sol) that a lander at any given latitude and longitude can communicate data to the orbiter. Results should be obtained for more than one elevation angle constraint (lander antenna design issue), and also for several time points into the mission since the orbiter's periapsis location moves under the influence of Mars' oblateness perturbation. Such information is presented in terms of global contour maps of available communications time per sol summed over all orbiter pases on that day. Global data of this type complements more detailed local site data such as communications range and elevation vs time per pass. Communications time contour maps are included here for sol grids of 180, 232, 318, 361, and 404 corresponding to orbiter periapsis latitudes of 35 S, 90 S, equatorial, 45 N, and 90 N. For each of these days, there is a map for both a 15 deg and 45 deg minimum elevation constraint on the lander-to-orbiter line of sight. The jagged appearance of the contour lines is due to computational resolution in interpolating between a finite number of latitude/longitude grid points. Although the contours should really be smooth, the general information content is represented by the lower resolution maps shown here. An example of the tabulated, finite-grid data points is also given. Communication with all sites is possible at the 15 deg elevation constraint, at times only for several minutes per sol but more generally for a much longer time up to 14 hours per sol. Significantly less time is available with a 45 deg elevation constraint, and at certain times in the mission some localized regions of the planet are inaccessible.

Still, one may conclude that the reference orbit selection will support a more than adequate communications link through the mission timeline with landers emplaced at any desired location on Mars. Author

N91-14363*# Science Applications International Corp., Schaumburg, IL.
ANALYSIS OF SUCCESS PROBABILITY/COST TRADES FOR SMALL LANDERS IN A MARS NETWORK c83
Alan L. Friedlander *In* JPL, Proceedings of the Mars Global Network Mission Workshop 1 Jun. 1990 p 229-243 (For primary document see N91-14359 06-12)
Avail: NTIS HC/MF A19 CSCL 05C

The premise to be tested in this analysis is whether cost economics may accrue by delivering more landers designed to lower reliability of operation (compared to fewer landers of higher reliability) to obtain a desired probability of achieving a given number of lander successes. Generally, the application in mind is a network of penetrators, although the analysis may apply as well to other small lander concepts or even to simple rovers. The method of analysis is based on a probabilistic model of lander success and a related probabilistic model of project cost including the lander, spacecraft carrier, and integration, but not launch or operations costs. Quantitative results are obtained in a normalized and parametric fashion. Sensitivity to the assumed model parameters is also examined. Author

N91-14364*# National Aeronautics and Space Administration. Lyndon B. Johnson Space Center, Houston, TX.
A GNM MISSION AND SYSTEM DESIGN PROPOSAL
Stephen Bailey *In* JPL, Proceedings of the Mars Global Network Mission Workshop 1 Jun. 1990 p 349-366 (For primary document see N91-14359 06-12)
Avail: NTIS HC/MF A19 CSCL 22A

Here, the author takes an advocacy position for the proposed Mars Global Network Mission (GNM); it is not intended to be an objective review, although both pros and cons are presented in summary. The mission consists of launches from earth in the '96, '98, and '01 opportunities on Delta-class launch vehicles (approx. 1000 kg injected to Mars in 8 to 10 ft diameter shroud). The trans Mars boost stage injects a stack of small independent, aeroshelled spacecraft. The stack separates from the boost stage and each rigid (as opposed to deployable) aeroshell flies to Mars on its own, performing midcourse maneuvers as necessary. Each spacecraft flies a unique trajectory which is targeted to achieve approach atmospheric interface at the desired latitude and lighting conditions; arrival times may vary by a month or more. A direct entry is performed, there is no propulsive orbit capture. The aeroshelled rough-landers are targeted to achieve a desired attitude and entry flight path angle, and then follow a passive ballistic trajectory until terminal descent. Based on sensed acceleration (integrated to deduce altitude), the aft aeroshell skirt is jettisoned; a short later a supersonic parachute is deployed. The ballistic coefficient of the parachute is sized to achieve terminal velocity at about 8 km. However the parachute is not deployed until a few Km above the surface to minimize wind-induced drift. The nose cap descent imaging begins, a laser altimeter also measures true altitude. Based on range and range rate to the surface, the parachute is jettisoned and the lander uses descent engines to achieve touchdown velocity. A contact sensor shuts down the motors to avoid cratering, and the lander rough-lands at less than 5 m/sec. The remaining aeroshell and a deployable bladder attenuate landing loads and minimize the possibility of tip over. Science instruments are deployed and activated, and the network is established. Author

13 ASTRODYNAMICS

Includes powered and free-flight trajectories; and orbital and launching dynamics.

N91-14365*# Rice Univ., Houston, TX.
GAMMA GUIDANCE OF TRAJECTORIES FOR COPLANAR, AEROASSISTED ORBITAL TRANSFER
A. Miele and T. Wang 1990 97 p
(Grant NAG8-820)
(NASA-CR-187732; NAS 1.26:187732; AA-246) Avail: NTIS HC/MF A05 CSCL 22A

The optimization and guidance of trajectories for coplaner, aeroassisted orbital transfer (AOT) from high Earth orbit (HEO) to low Earth orbit (LEO) are examined. In particular, HEO can be a geosynchronous Earth orbit (GEO). It is assumed that the initial and final orbits are circular, that the gravitational field is central and is governed by the inverse square law, and that at most three impulses are employed: one at HEO exit, one at atmospheric exit, and one at LEO entry. It is also assumed that, during the atmospheric pass, the trajectory is controlled via the lift coefficient. The presence of upper and lower bounds on the lift coefficient is considered. First, optimal trajectories are computed by minimizing the total velocity impulse (hence, the propellant consumption) required for AOT transfer. The sequential gradient-restoration algorithm (SGRA) is used for optimal control problems. The optimal trajectory is shown to include two branches: a relatively short descending flight branch (branch 1) and a long ascending flight branch (branch 2). Next, attention is focused on guidance trajectories capable of approximating the optimal trajectories in real time, while retaining the essential characteristics of simplicity, ease of implementation, and reliability. For the atmospheric pass, a feedback control scheme is employed and the lift coefficient is adjusted according to a two-stage gamma guidance law. Further improvements are possible via a modified gamma guidance which is more stable with respect to dispersion effects arising from navigation errors, variations of the atmospheric density, and uncertainties in the aerodynamic coefficients than gamma guidance trajectory. A byproduct of the studies on dispersion effects is the following design concept. For coplaner aeroassisted orbital transfer, the lift-range-to-weight ratio appears to play a more important role than the lift-to-drag ratio. This is because the lift-range-to-weight ratio controls mainly the minimum altitude (hence, the peak heating rate) of the guidance trajectory; on the other hand, the lift-to-drag ratio controls mainly the duration of the atmospheric pass of the guidance trajectory. Author

N91-14366*# Rice Univ., Houston, TX.
PROPERTIES OF THE OPTIMAL TRAJECTORIES FOR COPLANAR, AEROASSISTED ORBITAL TRANSFER
A. Miele, T. Wang, and A. W. Deaton 1990 58 p
(Grant NAG8-820)
(NASA-CR-187733; NAS 1.26:187733; AA-249) Avail: NTIS HC/MF A04 CSCL 22A

The optimization of trajectories for coplaner, aeroassisted orbital transfer (AOT) from a high Earth orbit (HEO) to a low Earth orbit (LEO) is examined. In particular, HEO can be a geosynchronous Earth orbit (GEO). It is assumed that the initial and final orbits are circular, that the gravitational field is central and is governed by the inverse square law, and that two impulses are employed, one at HEO exit and one at LEO entry. During the atmospheric pass, the trajectory is controlled via the lift coefficient in such a way that the total characteristic velocity is minimized. First, an ideal optimal trajectory is determined analytically for lift coefficient unbounded. This trajectory is called grazing trajectory, because the atmospheric pass is made by flying at constant altitude along the edge of the atmosphere until the excess velocity is depleted. For the grazing trajectory, the lift coefficient varies in such a way that the lift, the centrifugal force due to the Earth's curvature, the weight, and the Coriolis force due to the Earth's rotation are in static balance. Also, the grazing trajectory minimizes the total characteristic velocity and simultaneously nearly minimizes the peak values of the altitude drop, dynamic pressure, and heating

rate. Next, starting from the grazing trajectory results, a real optimal trajectory is determined numerically for the lift coefficient bounded from both below and above. This trajectory is characterized by atmospheric penetration with the smallest possible entry angle, followed by flight at the lift coefficient lower bound. Consistently with the grazing trajectory behavior, the real optimal trajectory minimizes the total characteristic velocity and simultaneously nearly minimizes the peak values of the altitude drop, the dynamic pressure, and the heating rate. Author

N91-14367*# Rice Univ., Houston, TX.
DECOMPOSITION TECHNIQUE AND OPTIMAL TRAJECTORIES FOR THE AEROASSISTED FLIGHT EXPERIMENT
A. Miele, T. Wang, and A. W. Deaton 1990 68 p
(Grant NAG8-820)
(NASA-CR-187734; NAS 1.26:187734; AA-250) Avail: NTIS HC/MF A04 CSCL 22A

An actual geosynchronous Earth orbit-to-low Earth orbit (GEO-to-LEO) transfer is considered with reference to the aeroassisted flight experiment (AFE) spacecraft, and optimal trajectories are determined by minimizing the total characteristic velocity. The optimization is performed with respect to the time history of the controls (angle of attack and angle of bank), the entry path inclination and the flight time being free. Two transfer maneuvers are considered: direct ascent (DA) to LEO and indirect ascent (IA) to LEO via parking Earth orbit (PEO). By taking into account certain assumptions, the complete system can be decoupled into two subsystems: one describing the longitudinal motion and one describing the lateral motion. The angle of attack history, the entry path inclination, and the flight time are determined via the longitudinal motion subsystem. In this subsystem, the difference between the instantaneous bank angle and a constant bank angle is minimized in the least square sense subject to the specified orbital inclination requirement. Both the angles of attack and the angle of bank are shown to be constant. This result has considerable importance in the design of nominal trajectories to be used in the guidance of AFE and aeroassisted orbital transfer (AOT) vehicles. Author

N91-14368*# Rice Univ., Houston, TX.
GUIDANCE TRAJECTORIES FOR AEROASSISTED ORBITAL TRANSFER Final Report
A. Miele 1990 22 p
(Grant NAG8-820)
(NASA-CR-187735; NAS 1.26:187735; AA-251) Avail: NTIS HC/MF A03 CSCL 22A

Research on aerobraking guidance schemes is presented. The intent is to produce aerobraking guidance trajectories exhibiting many of the desirable characteristics of optimal aerobraking trajectories. Both one-control schemes and two-control schemes are studied. The research is in the interest of aeroassisted flight experiment vehicles (AFE) and aeroassisted orbital transfer (AOT) vehicles. Author

14 GROUND SUPPORT SYSTEMS AND FACILITIES (SPACE)

Includes launch complexes, research and production facilities; ground support equipment, e.g., mobile transporters; and simulators.

For related information see also *09 Research and Support Facilities (Air).*

N91-14369# Stanford Linear Accelerator Center, CA.
HIGH GRADIENT ELECTRON GUNS
K. S. Fant, G. Caryotakis, R. F. Koontz, A. E. Vlieks, and G. Miram (Miram, G., Atherton, CA) Aug. 1990 2 p Presented at the 14th International Symposium on Discharges and Electrical Insulation in Vacuum, Santa Fe, NM, 16-20 Sep. 1990
(Contract DE-AC03-76SF-00515)
(DE91-000056; SU-SLAC-PUB-5325; CONF-9009192-14) Avail: NTIS HC/MF A01

Experiments have been conducted to determine peak operating gradients attainable in thermionic electron guns. These tests are part of a study of high-current-density, long-life cathodes suitable for use in high power klystrons. We also investigated the use of chromium oxide coating as a means of inhibiting electronic breakdown across the focus electrode anode gap. Field gradients in excess of 280 kV/cm have been achieved for a gun operating at 240 kV with a beam current of 228 A, at pulse widths of the order of 1 micron. DOE

15 LAUNCH VEHICLES AND SPACE VEHICLES

Includes boosters; operating problems of launch/space vehicle systems; and reusable vehicles.

For related information see also *20 Spacecraft Propulsion and Power.*

No abstracts in this category.

16 SPACE TRANSPORTATION

Includes passenger and cargo space transportation, e.g., shuttle operations; and space rescue techniques.

For related information see also *03 Air Transportation and Safety* and *18 Spacecraft Design, Testing and Performance.* For space suits see *54 Man/System Technology and Life Support.*

N91-15064*# Iowa Univ., Iowa City. Dept. of Physics and Astronomy.
PLASMA WAVES ASSOCIATED WITH THE SPACE SHUTTLE
I. H. Cairns and D. A. Gurnett *In* ESA, Plasma Astrophysics Aug. 1990 p 87-92 (For primary document see N91-15046 06-90)
(Grants NAGw-1488; NAG3-449)
Copyright Avail: NTIS HC/MF A14 CSCL 03B

17 SPACE COMM., SPACECRAFT COMM., COMMAND & TRACKING

Includes telemetry; space communications networks; astronavigation and guidance; and radio blackout.

For related information see also *04 Aircraft Communications and Navigation* and *32 Communications and Radar.*

N91-14370# Los Alamos National Lab., NM.
THE VERTICAL VAN DE GRAAFF TELEMETRY SYSTEM
Jeff T. Gray 1990 10 p Presented at the SNEAP '90, Manhattan, KS, 22-25 Oct. 1990
(Contract W-7405-eng-36)
(DE91-001960; LA-UR-90-3535; CONF-9010228-1) Avail: NTIS HC/MF A02

With the push on to take the machine to higher and higher potentials, it quickly became apparent that the existing telemetry system was simply not acceptable. Therefore, in 1988 a new multichannel telemetry system was specified for bid. The new system was to provide a control interface for the operator in the control room connected via fiber optic cables to three remote I/O devices located on two different (electrically isolated) decks on the ion terminal. The system was received in early 1989 and is based on the General Electric FANUC Division's Series One Plus programmable controller (GE FANUC was recently bought out by Texas Instruments who now offer the Series 305 programmable

controller which is the same as GE's Series One Plus). This paper describes this system and its implementations. DOE

N91-14371* National Aeronautics and Space Administration. Lyndon B. Johnson Space Center, Houston, TX.
ADAPTIVE DATA ACQUISITION MULTIPLEXING SYSTEM AND METHOD Patent
Richard L. Sinderson, inventor (to NASA), George A. Salazar, inventor (to NASA), Clyde M. Haddick, Jr., inventor (to NASA), Caroll J. Spahn, inventor (to NASA), and Chikkabelarangala N. Venkatesh, inventor (to NASA) (Lockheed Engineering and Management Services Co., Inc., Houston, TX.) 27 Nov. 1990 10 p Filed 15 Apr. 1988
(NASA-Case-MSC-21170-1; US-Patent-4,974,181; US-Patent-Appl-SN-182266; US-Patent-Class-364-550; US-Patent-Class-324-115; US-Patent-Class-364-487; Int-Patent-Class-G06F-15/20) Avail: US Patent and Trademark Office CSCL 09F

A reconfigurable telemetry multiplexer is described which includes a monitor-terminal and a plurality of remote terminals. The remote terminals each include signal conditioning for a plurality of sensors for measuring parameters which are converted by an analog to digital converter. CPU's in the remote terminals store instructions for prompting system configuration and reconfiguration commands. The measurements, instructions, and the terminal's present configuration and status data are transmitted to the monitor-terminal and displayed. In response to menu-driven prompts generated and displayed at the monitor-terminal, data generation request commands, status and health commands, and the like are input at the monitor-terminal and transmitted to the remote terminals. The CPU in each remote terminal receives the various commands, stores them in electrically alterable memory, and reacts in accordance with the commands to reconfigure a plurality of aspects of the system. The CPU in each terminal also generates parameter measurements, status and health signals, and transmits these signals of the respective terminals to the monitor-terminal for low data rate operator viewing and to higher rate external transmission/monitor equipment. Reconfiguration may be in real time during the general period of parameter measurement acquisition, and may include alteration of the gain, automatic gain rescaling, bias, and or sampling rates associated with one or more of the parameter measurements made by the remote terminals.
Official Gazette of the U.S. Patent and Trademark Office

18 SPACECRAFT DESIGN, TESTING AND PERFORMANCE

Includes satellites; space platforms; space stations; spacecraft systems and components such as thermal and environmental controls; and attitude controls.

For life support systems see *54 Man/System Technology and Life Support.* For related information see also *05 Aircraft Design, Testing and Performance, 39 Structural Mechanics,* and *16 Space Transportation.*

N91-14372*# National Aeronautics and Space Administration. Goddard Space Flight Center, Greenbelt, MD.
SATELLITE SITUATION REPORT, VOLUME 30, NO. 1
31 Mar. 1990 90 p
(NASA-TM-101105; NAS 1.15:101105) Avail: NTIS HC/MF A05 CSCL 22B

Space objects are listed as well as those which decayed during this reporting period. Data provided include international designation and catalog number, nation of source, launch data, inclination, apogee, and perigee. Transmitting frequencies for satellites being monitored by NASA's space flight tracking and data network are given. Author

N91-14373*# Martin Marietta Corp., Denver, CO. Astronautics Group.
SPACE STATION COMMON MODULE NETWORK TOPOLOGY AND HARDWARE DEVELOPMENT Final Report
P. Anderson, L. Braunagel, S. Chwirka, M. Fishman, K. Freeman, D. Eason, D. Landis, L. Lech, J. Martin, and J. McCorkle et al Jul. 1990 226 p
(Contract NAS8-36583)
(NASA-CR-184034; NAS 1.26:184034; MCR-90-536) Avail: NTIS HC/MF A11 CSCL 22B

Conceptual space station common module power management and distribution (SSM/PMAD) network layouts and detailed network evaluations were developed. Individual pieces of hardware to be developed for the SSM/PMAD test bed were identified. A technology assessment was developed to identify pieces of equipment requiring development effort. Equipment lists were developed from the previously selected network schematics. Additionally, functional requirements for the network equipment as well as other requirements which affected the suitability of specific items for use on the Space Station Program were identified. Assembly requirements were derived based on the SSM/PMAD developed requirements and on the selected SSM/PMAD network concepts. Basic requirements and simplified design block diagrams are included. DC remote power controllers were successfully integrated into the DC Marshall Space Flight Center breadboard. Two DC remote power controller (RPC) boards experienced mechanical failure of UES 706 stud-mounted diodes during mechanical installation of the boards into the system. These broken diodes caused input to output shorting of the RPC's. The UES 706 diodes were replaced on these RPC's which eliminated the problem. The DC RPC's as existing in the present breadboard configuration do not provide ground fault protection because the RPC was designed to only switch the hot side current. If ground fault protection were to be implemented, it would be necessary to design the system so the RPC switched both the hot and the return sides of power. K.S.

N91-14374* National Aeronautics and Space Administration. Lyndon B. Johnson Space Center, Houston, TX.
SMART TUNNEL: DOCKING MECHANISM Patent
John A. Schliesing, inventor (to NASA) and Kevin L. Edenborough, inventor (to NASA) 29 Aug. 1989 9 p Filed 30 Dec. 1988
(NASA-Case-MSC-21360-1; US-Patent-4,860,975; US-Patent-Appl-SN-292131; US-Patent-Class-244-161; US-Patent-Class-405-188; US-Patent-Class-14-71.5; US-Patent-Class-244-137.2; Int-Patent-Class-B64G-1/64) Avail: US Patent and Trademark Office CSCL 22B

A docking mechanism is presented for the docking of a space vehicle to a space station comprising a flexible tunnel frame structure which is deployable from the space station. The tunnel structure comprises a plurality of series connected frame sections, one end section of which is attached to the space station and the other end attached to a docking module of a configuration adapted for docking in the payload bay of the space vehicle. The docking module is provided with trunnions, adapted for latching engagement with latches installed in the vehicle payload bay and with hatch means connectable to a hatch of the crew cabin of the space vehicle. Each frame section comprises a pair of spaced ring members, interconnected by actuator-attenuator devices which are individually controllable by an automatic control means to impart relative movement of one ring member to the other in six degrees of freedom of motion. The control means includes computer logic responsive to sensor signals of range and attitude information, capture latch condition, structural loads, and actuator stroke for generating commands to the onboard flight control system and the individual actuator-attenuators to deploy the tunnel to effect a coupling with the space vehicle and space station after coupling. A tubular fluid-impervious liner, preferably fabric, is disposed through the frame sections of a size sufficient to accommodate the passage of personnel and cargo.
Official Gazette of the U.S. Patent and Trademark Office

N91-14375# Cincinnati Univ., OH. Dept. of Aerospace Engineering and Engineering Mechanics.
MULTIVARIABLE METHODS FOR THE DESIGN, IDENTIFICATION, AND CONTROL OF LARGE SPACE STRUCTURES. VOLUME 2: OPTIMAL AND SUB-OPTIMAL ESTIMATION APPLIED TO LARGE FLEXIBLE STRUCTURES Final Report, Jul. 1987 - Feb. 1989
S. Dumbacher Jul. 1989 114 p
(Contract F33615-86-C-3216; AF Proj. 2302)
(AD-A226699; WRDC-TR-90-3037-Vol-2) Avail: NTIS HC/MF A06 CSCL 22/2

This report investigates the integrated control/structure design optimization problem for large flexible structures subject to stochastic disturbance forces. The full state feedback control of truss type structures is considered. The problem is formulated as a mathematical programming problem, and solved using a sequential approximations solution technique along with a scaling procedure. Due to the special nature of full state feedback control, it is shown that the controller can be assumed to be an LQR controller, where the control and state weightings are Lagrange multipliers from the mathematical programming optimality conditions. The design space is therefore effectively reduced to the truss element cross-sectional areas and these Lagrange multipliers, significantly reducing the computational effort required for solution. In this report, the solution algorithm is applied to the DRAPER I tetrahedral truss structure. GRA

N91-14376# Naval Postgraduate School, Monterey, CA.
THE EFFECTS OF LIQUID PROPELLANT MOTION ON THE ATTITUDE STABILITY OF SPIN STABILIZED SPACECRAFT M.S. Thesis
Jack W. Myers, Jr. Mar. 1990 92 p
(AD-A227002) Avail: NTIS HC/MF A05 CSCL 22/3

An analysis of the effects of liquid motion on the attitude stability of spin stabilized spacecraft is presented. The effects of varying the fuel load and the asymmetry of the platform are emphasized. The energy sink stability criteria are derived and applied to a marginally stable spacecraft. The stability predictions based on the energy sink stability criteria are compared to the results of a computer simulation. Based on this comparison the limitations of the energy sink stability criteria are identified. GRA

N91-14377# Integrated Systems, Inc., Santa Clara, CA.
ADAPTIVE CONTROL OF LARGE SPACE STRUCTURES Final Technical Report, 1 Feb. 1989 - 31 Mar. 1990
Robert L. Kosut 15 Aug. 1990 39 p
(Contract F49620-89-C-0043; AF Proj. 2302)
(AD-A227304; ISI-5877-01; AFOSR-90-0921TR) Avail: NTIS HC/MF A03 CSCL 12/4

Preliminary results are presented for set estimation of uncertain nonlinear systems. Set estimation is a process in an adaptive robust control system which produces a set of models from the measured data. The set is then used in an on-line robust control design to implement a controller which is guaranteed to achieve performance goals for all members on the set. The scheme works whenever the actual system which produced the data is a member of the estimated set. The results of this report extend some previous work in linear set estimation to nonlinear systems. This report also summarizes an analysis of an adaptive nonlinear system using the method of averaging. The aim of adaptive control is to implement in real-time and on-line as many as possible of the design functions now performed off-line by the control engineer. Although it is easy to configure an adaptive system by connecting an estimator and control design rule, research is essential to identify the performance limitations of adaptive strategies for LSS control. The long range goal of this research program is to establish guidelines for selecting the appropriate strategy, to evaluate performance improvements over fixed-gain mechanizations, and to examine the architecture necessary to produce a practical hardware realization. The initial and continuing thrust, however, is to build a strong theoretical foundation without losing sight of the practical implementation issues. GRA

N91-14378*# Battelle Columbus Labs., OH.
DEFINITION OF EXPERIMENTS TO INVESTIGATE FIRE SUPPRESSANTS IN MICROGRAVITY Final Report
James J. Reuther Dec. 1990 64 p
(Contract NAS3-25362)
(NASA-CR-185295; NAS 1.26:185295; BCO-JJR-90-1348) Avail: NTIS HC/MF A04 CSCL 22B

Defined and justified here are the conceptual design and operation of a critical set of experiments expected to yield information on suppressants and on suppressant delivery systems under realistic spacecraft-fire conditions (smoldering). Specific experiment parameters are provided on the solid fuel (carbon), oxidants (habitable spacecraft atmospheres), fuel/oxidant supply, mixing mode, and rate (quiescent and finite; ventilated and replenishable), ignition mode, event, and reignition tendency, fire-zone size, fire conditions, lifetime, and consequences (toxicity), suppressants (CO2, H2O, N2) and suppressant delivery systems, and diagnostics. Candidate suppressants were identified after an analysis of how reduced gravity alters combustion, and how these alterations may influence the modes, mechanisms, and capacities of terrestrial agents to suppress unwanted combustion, or fire. Preferred spacecraft suppression concepts included the local, near-quiescent application of a gas, vapor, or mist that has thermophysical fire-suppression activity and is chemically inert under terrestrial (normal gravity) combustion conditions. The scale, number, and duration (about 1 hour) of the proposed low-gravity experiments were estimated using data not only on the limitations imposed by spacecraft-carrier (Shuttle or Space Station Freedom) accommodations, but also data on the details and experience of standardized smolder-suppression experiments at normal gravity. Deliberately incorporated into the conceptual design was sufficient interchangeability for the prototype experimental package to fly either on Shuttle now or Freedom later. This flexibility is provided by the design concept of up to 25 modular fuel canisters within a containment vessel, which permits both integration into existing low-gravity in-space combustion experiments and simultaneous testing of separate experiments to conserve utilities and time.
Author

19 SPACECRAFT INSTRUMENTATION

For related information see also *06 Aircraft Instrumentation* and *35 Instrumentation and Photography.*

N91-14379*# Jet Propulsion Lab., California Inst. of Tech., Pasadena.
INNOVATIVE LONG WAVELENGTH INFRARED DETECTOR WORKSHOP PROCEEDINGS
Frank J. Grunthaner 1 Jul. 1990 498 p Workshop held in Pasadena, CA, 24-26 Apr. 1990; sponsored by NASA, Washington, Strategic Defense Initiative Organization, Army Lab. Command, and DARPA
(Contract NAS7-918)
(NASA-CR-187433; JPL-Publ-90-22; NAS 1.26:187433) Avail: NTIS HC/MF A21 CSCL 14B

The focus of the workshop was on innovative long wavelength (lambda less than 17 microns) infrared (LWIR) detectors with the potential of meeting future NASA and DoD long-duration space application needs. Requirements are for focal plane arrays which operate near 65K using active refrigeration with mission lifetimes of five to ten years. The workshop addressed innovative concepts, new material systems, novel device physics, and current progress in relation to benchmark technology. It also provided a forum for discussion of performance characterization, producibility, reliability, and fundamental limitations of device physics. It covered the status of the incumbent HgCdTe technology, which shows encouraging progress towards LWIR arrays, and provided a snapshot of research and development in several new contender technologies. For individual titles, see N91-14380 through N91-14411.

N91-14380*# Jet Propulsion Lab., California Inst. of Tech., Pasadena.
SENSOR REQUIREMENTS FOR EARTH AND PLANETARY OBSERVATIONS
Moustafa T. Chahine *In its* Innovative Long Wavelength Infrared Detector Workshop Proceedings 1 Jul. 1990 p 3-31 (For primary document see N91-14379 06-19)
Avail: NTIS HC/MF A21 CSCL 14B

Future generations of Earth and planetary remote sensing instruments will require extensive developments of new long-wave and very long-wave infrared detectors. The upcoming NASA Earth Observing System (EOS) will carry a suite of instruments to monitor a wide range of atmospheric and surface parameters with an unprecedented degree of accuracy for a period of 10 to 15 years. These instruments will observe Earth over a wide spectral range extending from the visible to nearly 17 micrometers with a moderate to high spectral and spacial resolution. In addition to expected improvements in communication bandwidth and both ground and on-board computing power, these new sensor systems will need large two-dimensional detector arrays. Such arrays exist for visible wavelengths and, to a lesser extent, for short wavelength infrared systems. The most dramatic need is for new Long Wavelength Infrared (LWIR) and Very Long Wavelength Infrared (VLWIR) detector technologies that are compatible with area array readout devices and can operate in the temperature range supported by long life, low power refrigerators. A scientific need for radiometric and calibration accuracies approaching 1 percent translates into a requirement for detectors with excellent linearity, stability and insensitivity to operating conditions and space radiation. Current examples of the kind of scientific missions these new thermal IR detectors would enhance in the future include instruments for Earth science such as Orbital Volcanological Observations (OVO), Atmospheric Infrared Sounder (AIRS), Moderate Resolution Imaging Spectrometer (MODIS), and Spectroscopy in the Atmosphere using Far Infrared Emission (SAFIRE). Planetary exploration missions such as Cassini also provide examples of instrument concepts that could be enhanced by new IR detector technologies.
Author

N91-14381*# Strategic Defense Initiative Organization, Washington, DC.
SDIO LONG WAVELENGTH INFRARED DETECTOR REQUIREMENTS
Dwight Duston *In* JPL, California Inst. of Tech., Innovative Long Wavelength Infrared Detector Workshop Proceedings 1 Jul. 1990 p 33-44 (For primary document see N91-14379 06-19)
Avail: NTIS HC/MF A21 CSCL 14B

The Strategic Defense Initiative Organization (SDIO) has a significant requirement for infrared sensors for surveillance, tracking and discrimination of objects in space. Projected SDIO needs cover the range from short wavelengths out to 30 microns. Large arrays are required, and producibility and cost are major factors. The SDIO is pursuing several approaches including innovative concepts based on semiconductors and superconductors.
Author

N91-14382*# Aerospace Corp., Los Angeles, CA.
LWIR DETECTOR REQUIREMENTS FOR LOW-BACKGROUND SPACE APPLICATIONS
Frank J. DeLuccia *In* JPL, California Inst. of Tech., Innovative Long Wavelength Infrared Detector Workshop Proceedings 1 Jul. 1990 p 45-58 (For primary document see N91-14379 06-19)
Avail: NTIS HC/MF A21 CSCL 14B

Detection of cold bodies (200 to 300 K) against space backgrounds has many important applications, both military and non-military. The detector performance and design characteristics required to support low-background applications are discussed, with particular emphasis on those characteristics required for space surveillance. The status of existing detector technologies under active development for these applications is also discussed. In order to play a role in future systems, new, potentially competing detector technologies such as multiple quantum well detectors must not only meet system-derived requirements, but also offer distinct performance or other advantages over these incumbent technologies.
Author

N91-14383*# Loral Infrared and Imaging Systems, Lexington, MA.
STATUS OF LWIR HgCdTe INFRARED DETECTOR TECHNOLOGY
M. B. Reine *In* JPL, California Inst. of Tech., Innovative Long Wavelength Infrared Detector Workshop Proceedings 1 Jul. 1990 p 61-77 (For primary document see N91-14379 06-19)
Avail: NTIS HC/MF A21 CSCL 14B

The performance requirements that today's advanced Long Wavelength Infrared (LWIR) focal plane arrays place on the HgCdTe photovoltaic detector array are summarized. The theoretical performance limits for intrinsic LWIR HgCdTe detectors are reviewed as functions of cutoff wavelength and operating temperature. The status of LWIR HgCdTe photovoltaic detectors is reviewed and compared to the focal plane array (FPA) requirements and to the theoretical limits. Emphasis is placed on recent data for two-layer HgCdTe PLE heterojunction photodiodes grown at Loral with cutoff wavelengths ranging between 10 and 19 microns at temperatures of 70 to 80 K. Development trends in LWIR HgCdTe detector technology are outlined, and conclusions are drawn about the ability for photovoltaic HgCdTe detector arrays to satisfy a wide variety of advanced FPA array applications.
Author

N91-14384*# Rockwell International Science Center, Thousand Oaks, CA.
LWIR HgCdTe: INNOVATIVE DETECTORS IN AN INCUMBENT TECHNOLOGY
William E. Tennant *In* JPL, California Inst. of Tech., Innovative Long Wavelength Infrared Detector Workshop Proceedings 1 Jul. 1990 p 79-91 (For primary document see N91-14379 06-19)
Avail: NTIS HC/MF A21 CSCL 14B

HgCdTe is the current material of choice for high performance imagers operating at relatively high temperatures. Its lack of technological maturity compared with silicon and wide-band gap III-V compounds is more than offset by its outstanding IR sensitivity and by the relatively benign effect of its materials defects. This latter property has allowed non-equilibrium growth techniques, metal oxide chemical vapor deposition (MOCVD) and molecular beam epitaxy (MBE), to produce device quality long wavelength infrared (LWIR) HgCdTe even on common substrates like GaAs and GaAs/Si. Detector performance in these exotic materials structures is comparable in many ways with devices in equilibrium-grown material. Lifetimes are similar. RoA values at 77K as high as several hundred have been seen in HgCdTe/GaAs/Si with 9.5 micron cut-off wavelength. HgCdTe/GaAs layers with approx. 15 micron cut-off wavelengths have given average 77K RoAs of greater than 2. Hybrid focal plane arrays have been evaluated with excellent operability.
Author

N91-14385*# Santa Barbara Research Center, Goleta, CA.
HgCdTe FOR NASA EOS MISSIONS AND DETECTOR UNIFORMITY BENCHMARKS Abstract Only
Paul R. Norton *In* JPL, California Inst. of Tech., Innovative Long Wavelength Infrared Detector Workshop Proceedings 1 Jul. 1990 p 93-94 (For primary document see N91-14379 06-19)
Avail: NTIS HC/MF A21 CSCL 14B

Important NASA Earth Observing System (EOS) missions, Atmospheric Infrared Sounder (AIRS) and Moderate Resolution Imaging Spectrometer (MODIS-N), which require detector spectral response in the range of 14 to 17 microns at medium background flux levels and operation in the range of temperatures between 65 to 95 K, will be flown beginning in the next few years. Currently, a prime candidate detector technology for these missions is trapping-mode photoconductive HgCdTe devices. These devices can be tailored to the exact cutoff wavelengths required by those

missions, and thus offer the performance advantages of an intrinsic detector which is ideally matched to the mission wavelength. Under the long wavelength-background-temperature conditions of these EOS missions, any detector will at best be thermal generation-recombination noise limited. Photoconductive devices are generally preferred under these circumstances, since at elevated temperatures their performance degrades with n(sub i) while for photovoltaic detectors performance degrades as n sub i(exp 2) n sub i is the intrinsic carrier concentration which is a function of alloy composition and temperature, but not doping. Very high performance trapping-mode photoconductive HgCdTe detectors have been developed which can be reproducibly fabricated. Detectivity (D asterisk) at 80K and 16 micron cutoff wavelength in excess of 10(exp 11) Jones has been measured for these devices. Power dissipation is at least two orders of magnitude less than conventional HgCdTe photoconductors - on the order of 0.12 W/cm(exp 2) compared with 12 W/cm(exp 2). EOS missions define thermal noise limited conditions for the long wavelength operating bands. Trapping-mode photoconductive HgCdTe detectors are linear under such conditions and responsivity is independent of background flux. At lower temperatures or high flux conditions in which background flux limits detector performance, trapping-mode detectors have a responsivity which varies with background flux. Internal calibration must be provided for radiometric measurements under the latter conditions (not an EOS mission concern). Liquid phase epitaxy is used to grow these HgCdTe device structures. This technique has been shown to give control of the cutoff wavelength on the order of 16 plus or minus 1 micron or less, both from run to run and across wafer dimensions of several centimeters on a side. Author

N91-14386*# Arizona Univ., Tucson. Optical Sciences Center.
DETECTOR ARRAY EVALUATION AND FIGURES OF MERIT
Eustace L. Dereniak *In* JPL, California Inst. of Tech., Innovative Long Wavelength Infrared Detector Workshop Proceedings 1 Jul. 1990 p 99-116 (For primary document see N91-14379 06-19)
Avail: NTIS HC/MF A21 CSCL 14B

The commonly used methods to evaluate the performance of a two-dimensional focal-plane array using charge transfer devices are reviewed. Two figures of merit that attempt to combine quantum efficiency, read noise and dark-current generation into a single parameter are discussed. The figures of merit are suggested as possible alternatives to the D asterisk. Author

N91-14387*# Columbia Univ., New York, NY. Dept. of Electrical Engineering.
ISSUES AND DIRECTIONS IN IR DETECTOR READOUT ELECTRONICS
Eric R. Fossum *In* JPL, California Inst. of Tech., Innovative Long Wavelength Infrared Detector Workshop Proceedings 1 Jul. 1990 p 117-147 (For primary document see N91-14379 06-19)
Avail: NTIS HC/MF A21 CSCL 14B

An introduction to the major issues encountered in the readout of imaging detector arrays in the infrared are presented. These include circuit issues such as multiplexing, buffering, and noise, as well as materials issues. Future directions in infrared readout electronics will also be discussed. These include on-chip signal processing and advanced hybridization schemes. Finally, recent work at Columbia on 2DEG-charge coupled devices for IR detector multiplexing are described. Author

N91-14388*# Mission Research Corp., Colorado Springs, CO.
RADIATION RESPONSE ISSUES FOR INFRARED DETECTORS
Arne H. Kalma *In* JPL, California Inst. of Tech., Innovative Long Wavelength Infrared Detector Workshop Proceedings 1 Jul. 1990 p 149-157 Sponsored in part by Systems Science and Software (For primary document see N91-14379 06-19)
(Contract F729601-88-C-0025)
Avail: NTIS HC/MF A21 CSCL 14B

Researchers describe the most important radiation response issues for infrared detectors. In general, the two key degradation mechanisms in infrared detectors are the noise produced by exposure to a flux of ionizing particles (e.g.; trapped electronics and protons, debris gammas and electrons, radioactive decay of neutron-activated materials) and permanent damage produced by exposure to total dose. Total-dose-induced damage is most often the result of charge trapping in insulators or at interfaces. Exposure to short pulses of ionization (e.g.; prompt x rays or gammas, delayed gammas) will cause detector upset. However, this upset is not important to a sensor unless the recovery time is too long. A few detector technologies are vulnerable to neutron-induced displacement damage, but fortunately most are not. Researchers compare the responses of the new technologies with those of the mainstream technologies of PV HgCdTe and IBC Si:As. One important reason for this comparison is to note where some of the newer technologies have the potential to provide significantly improved radiation hardness compared with that of the mainstream technologies, and thus to provide greater motivation for the pursuit of these technologies. Author

N91-14389*# California Univ., Berkeley. Dept. of Physics.
FABRICATION OF SENSITIVE HIGH Tc BOLOMETERS
Michael Nahum, S. Verghese, Qing Hu, Paul L. Richards, K. Char, N. Newman, and Scott A. Sachtjen (Conductus, Inc., Sunnyvale, CA.) *In* JPL, California Inst. of Tech., Innovative Long Wavelength Infrared Detector Workshop Proceedings 1 Jul. 1990 p 161-181 Prepared in cooperation with California Univ., Berkeley. Lawrence Berkeley Lab. (For primary document see N91-14379 06-19)
(Contract DE-AC03-76SF-00098)
Avail: NTIS HC/MF A21 CSCL 14B

The rapid change of resistance with temperature of high quality films of high T sub c superconductors can be used to make resistance thermometers with very low temperature noise. Measurements on c-axis yttrium barium copper oxide (YBCO) films have given a spectral intensity of temperature noise less than 4 times 10(exp -8) K/Hz(exp 1/2) at 10 Hz. Consequently, the opportunity exists to make useful bolometric infrared detectors that operate near 90 K which can be cooled with liquid nitrogen. The fabrication and measurement of two bolometer architectures are discussed. The first is a conventional bolometer which consists of a 3000 A thick YBCO film deposited in situ by laser ablation on top of a 500 A thick SrTiO3 thickness and diced into 1x1 mm(exp 2) bolometer chips. Gold black smoke was used as the radiation absorber. The voltage noise was less than the amplifier noise when the film was current biased. Optical measurements gave an NEP of 5 times 10(exp -11) W/Hz(exp 1/2) at 10 Hz. The second architecture is that of an antenna-coupled microbolometer which consists of a small (5x10 cubic microns) YBCO film deposited directly on a bulk substrate with a low thermal conductance (YSZ) and an impedance matched planar lithographed spiral or log-periodic antenna. This structure is produced by standard photolithographic techniques. Measurements gave an electrical NEP of 4.7 times 10(exp -12) W/Hz(exp 1/2) at 10 kHz. Measurements of the optical efficiency are in progress. The measured performance of both bolometers will be compared to other detectors operating at or above liquid nitrogen temperatures so as to identify potential applications. Author

N91-14390*# National Aeronautics and Space Administration. Ames Research Center, Moffett Field, CA.
PYROELECTRIC DETECTORS
Eugene E. Haller, Jeffrey Beeman, William L. Hansen (California Univ., Berkeley. Lawrence Berkeley Lab.), G. Scott Hubbard, and Robert E. McMurray, Jr. *In* JPL, California Inst. of Tech., Innovative Long Wavelength Infrared Detector Workshop Proceedings 1 Jul. 1990 p 183-196 (For primary document see N91-14379 06-19)
Avail: NTIS HC/MF A21 CSCL 14B

The multi-agency, long-term Global Change programs, and specifically NASA's Earth Observing system, will require some new and advanced photon detector technology which must be specifically tailored for long-term stability, broad spectral range, cooling constraints, and other parameters. Whereas MCT and GaAs

alloy based photovoltaic detectors and detector arrays reach most impressive results to wavelengths as long as 12 microns when cooled to below 70 K, other materials, such as ferroelectrics and pyroelectrics, appear to offer special opportunities beyond 12 microns and above 70 K. These materials have found very broad use in a wide variety of room temperature applications. Little is known about these classes of materials at sub-room temperatures and no photon detector results have been reported. From the limited information available, researchers conclude that the room temperature values of D asterisk greater than or equal to 10(exp 9) cm Hz(exp 1/2)/W may be improved by one to two orders of magnitude upon cooling to temperatures around 70 K. Improvements of up to one order of magnitude appear feasible for temperatures achievable by passive cooling. The flat detector response over a wavelength range reaching from the visible to beyond 50 microns, which is an intrinsic advantage of bolometric devices, makes for easy calibration. The fact that these materials have been developed for reduced temperature applications makes ferro- and pyroelectric materials most attractive candidates for serious exploration. Author

N91-14391*# Jet Propulsion Lab., California Inst. of Tech., Pasadena.
A NOVEL ELECTRON TUNNELING INFRARED DETECTOR
T. W. Kenny, S. B. Waltman, J. K. Reynolds, and W. J. Kaiser *In its* Innovative Long Wavelength Infrared Detector Workshop Proceedings 1 Jul. 1990 p 197-207 Sponsored by DARPA and Strategic Defense Initiative Organization (For primary document see N91-14379 06-19)
Avail: NTIS HC/MF A21 CSCL 14B

The pneumatic infrared detector, originally developed by Golay in the late 1940s, uses the thermal expansion of one cm(exp 3) of xenon at room temperature to detect the heat deposited by infrared radiation. This detector was limited by thermal fluctuations within a 10 Hz bandwidth, but suffered from long thermal time constants and a fragile structure. Nevertheless, it represents the most sensitive room temperature detector currently available in the long wavelength infrared (LWIR). Fabrication of this type of detector on smaller scales has been limited by the lack of a suitably sensitive transducer. Researchers designed a detector based on this principle, but which is constructed entirely from micromachined silicon, and uses a vacuum tunneling transducer to detect the expansion of the trapped gas. Because this detector is fabricated using micromachining techniques, miniaturization and integration into one and two-dimensional arrays is feasible. The extreme sensitivity of vacuum tunneling to changes in electrode separation will allow a prototype of this detector to operate in the limit of thermal fluctuations over a 10 kHz bandwidth. A calculation of the predicted response and noise of the prototype is presented with the general formalism of thermal detectors. At present, most of the components of the prototype have been fabricated and tested independently. In particular, a characterization of the micromachined electron tunneling transducer has been carried out. The measured noise in the tunnel current is within a decade of the limit imposed by shot noise, and well below the requirements for the operation of an infrared detector with the predicted sensitivity. Assembly and characterization of the prototype infrared detector will be carried out promptly. Author

N91-14392*# Bell Telephone Labs., Inc., Murray Hill, NJ.
QUANTUM WELL INFRARED PHOTODETECTORS (QWIP)
B. F. Levine *In* JPL, California Inst. of Tech., Innovative Long Wavelength Infrared Detector Workshop Proceedings 1 Jul. 1990 p 211-229 (For primary document see N91-14379 06-19)
Avail: NTIS HC/MF A21 CSCL 14B

There has been a lot of interest in III-V long wavelength detectors in the lambda = 8 to 12 micron spectral range as alternatives to HgCdTe. Recently high performance quantum well infrared photodetectors (QWIP) have been demonstrated. They have a responsivity of R = 1.2 A/W, and a detectivity D(exp asterisk) sub lambda = 2 times 10(exp 10) cm Hz(exp 1/2)/W at 68 K for a QWIP with a cutoff wavelength of lambda sub c = 10.7 micron and a R = 1.0 A/W, and D(exp asterisk) sub lambda = 2 times 10(exp 10) cm Hz(exp 1/2)/W at T = 77 K for lambda sub c = 8.4 micron. These detectors consist of 50 periods of molecular beam epitaxy (MBE) grown layers doped n = 1 times 10(exp 18)cm(exp -3) having GaAs quantum well widths of 40 A and barrier widths of 500 A of Al sub x Ga sub 1-x As. Due to the well-established GaAs growth and processing techniques, these detectors have the potential for large, highly uniform, low cost, high performance arrays as well as monolithic integration with GaAs electronics, high speed and radiation hardness. Latest results on the transport physics, device performance and arrays are discussed. Author

N91-14393*# Princeton Univ., NJ. Dept. of Electrical Engineering.
PHOTOVOLTAIC QUANTUM WELL INFRARED PHOTODETECTORS
Steve A. Lyon, Keith Goossen, Sanjay Parihar, Kambiz Alavi, Mike Santos, and Mansour Shayegan *In* JPL, California Inst. of Tech., Innovative Long Wavelength Infrared Detector Workshop Proceedings 1 Jul. 1990 p 231-241 (For primary document see N91-14379 06-19)
Avail: NTIS HC/MF A21 CSCL 14B

Quantum well infrared photodetectors (QWIP) are a promising new approach to long-wavelength infrared detector arrays. Both single-well photovoltaic and multiple-well photoconductive devices have been demonstrated. The author discusses noise considerations as they apply to photovoltaic devices, grating coupling of the infrared light into QWIPs, and recently demonstrated electrically tunable detectors. The use of light trapping to enhance the quantum efficiency and reduce cross-talk in an array is addressed. Author

N91-14394*# Aerospace Corp., Los Angeles, CA.
CHARACTERISTICS OF AlGaAs/GaAs MULTIPLE QUANTUM WELL INFRARED DETECTORS
Bruce K. Janousek, Mary L. Rosenbluth, Michael J. OLoughlin, Walter L. Bloss, Frank J. DeLuccia, Helmut Kanter, L. Elaine Perry, and Michael J. Daugherty *In* JPL, California Inst. of Tech., Innovative Long Wavelength Infrared Detector Workshop Proceedings 1 Jul. 1990 p 243-255 (For primary document see N91-14379 06-19)
Avail: NTIS HC/MF A21 CSCL 14B

Researchers fabricated and characterized several AlGaAs/GaAs multiple quantum well infrared detectors to evaluate the ultimate performance of these devices for low infrared background applications. The detectors were designed to have a single bound state in the quantum well and the first excited state in the continuum above the AlGaAs conduction band edge. The difference in energy between the two levels, as determined by the quantum well width and aluminum mole fraction in the barrier, was chosen such that peak absorption would occur near 8 microns. The initial structures studied comprised 50 periods with 40 A well widths and 300 A Al(0.28)Ga(0.72)As barriers. The performance of these detectors are summarized. To better interpret these results and design optimized detectors, researchers modeled both the detector noise and tunneling currents. The noise model correctly predicts that multiple quantum well detectors will, indeed, exhibit noise lower than full shot noise. The tunneling current model predicts the dark current versus bias for any choice of design parameters in a multiple quantum well detector. This model predicts a substantially reduced dark current (x 10(exp 04)) for samples with 400 A barriers. To evaluate structures with thicker barriers, researchers fabricated and characterized detectors with 400 A and 500 A barriers; a comparison of detector dark currents is shown. These results are consistent with the predictions of the dark current model. Author

N91-14395*# International Business Machines Corp., Yorktown Heights, NY.
RESONANT TUNNELING IR DETECTORS
Jerry M. Woodall and T. P. Smith, III *In* JPL, California Inst. of Tech., Innovative Long Wavelength Infrared Detector Workshop

Proceedings 1 Jul. 1990 p 257-262 (For primary document see N91-14379 06-19)
Avail: NTIS HC/MF A21 CSCL 14B

Researchers propose a novel semiconductor heterojunction photodetector which would have a very low dark current and would be voltage tunable. A schematic diagram of the device and its band structure are shown. The two crucial components of the device are a cathode (InGaAs) whose condition band edge is below the conduction band edge of the quantum wells and a resonant tunneling filter (GaAs-AlGaAs). In a standard resonant tunneling device the electrodes are made of the same material as the quantum wells, and this device becomes highly conducting when the quantum levels in the wells are aligned with the Fermi level in the negatively biased electrode. In contrast, the researchers device is essentially non-conducting under the same bias conditions. This is because the Fermi Level of the cathode (InGaAs) is still well below the quantum levels so that no resonant transport occurs and the barriers (AlGaAs) effectively block current flow through the device. However, if light with the same photon energy as the conduction-band discontinuity between the cathode and the quantum wells, E sub c3-E sub c1, is shone on the sample, free carriers will be excited to an energy corresponding to the lowest quantum level in the well closest to the cathode (hv plue E sub c1 = E sub o). These electrons will resonantly tunnel through the quantum wells and be collected as a photocurrent in the anode (GaAs). To improve the quantum efficiency, the cathode (InGaAs) should be very heavily doped and capped with a highly reflective metal ohmic contact. The thickness of the device should be tailored to optimize thin film interference effects and afford the maximum absorption of light. Because the device relies on resonant tunneling, its response should be very fast, and the small voltages needed to change the responsivity should allow for very high frequency modulation of the photocurrent. In addition, the device is tuned to a specific photon energy so that it can be designed to detect a fairly narrow range of wavelengths. This selectivity is important for reducing the photocurrent due to spurious light sources. Author

N91-14396*# Hughes Aircraft Co., Torrance, CA.
LOW DARK CURRENT PHOTOVOLTAIC MULTIQUANTUM WELL LONG WAVELENGTH INFRARED DETECTORS
C. S. Wu, Cheng P. Wen, R. N. Sato, and M. Hu *In* JPL, California Inst. of Tech., Innovative Long Wavelength Infrared Detector Workshop Proceedings 1 Jul. 1990 p 263-274 (For primary document see N91-14379 06-19)
Avail: NTIS HC/MF A21 CSCL 14B

The authors have, for the first time, demonstrated photovoltaic detection for an multiple quantum well (MQW) detector. With a blocking layer, the MQW detector exhibits Schottky I-V characteristics with extremely low dark current and excellent ideality factor. The dark current is 5 times 10(exp -14) A for an 100x100 square micron 10 micron detector at 40 K, 8 to 9 orders of magnitude lower than that of a similar 10 micron MQW detector without blocking layer. The ideality factor is about 1.01 to 1.05 at T = 40 to 80 K. The measured barrier height is consistent with the energy difference between first excited states and ground states, or the peak of spectral response. The authors also, for the first time, report the measured effective Richardson constant (A asterisk asterisk) for the GaAs/AlGaAs heterojunction using this blocking layer structure. The A asterisk asterisk is low approx. 2.3 A/sq cm/K(exp 2). Author

N91-14397*# Jet Propulsion Lab., California Inst. of Tech., Pasadena.
FUNDAMENTAL LIMITS TO PERFORMANCE OF QUANTUM WELL INFRARED DETECTORS
Amnon Yariv, Michael Kinch, S. Borenstain, and I. Grave (California Inst. of Tech., Pasadena.) *In its* Innovative Long Wavelength Infrared Detector Workshop Proceedings 1 Jul. 1990 p 275-290 (For primary document see N91-14379 06-19)
Avail: NTIS HC/MF A21 CSCL 14B

Radiometric, density of states (material), and thermal considerations are used to obtain the figure of merit of the quantum-well GaAs/GaAlAs infrared detectors described by Smith et. al. The results are compared with HgCdTe, the present industry standard, as well as with recent experiments at other laboratories. Author

N91-14398*# Jet Propulsion Lab., California Inst. of Tech., Pasadena.
NEW HETEROJUNCTION LWIR DETECTOR OPTIONS
Joseph Maserjian *In its* Innovative Long Wavelength Infrared Detector Workshop Proceedings 1 Jul. 1990 p 291-301 Sponsored in part by Strategic Defense Initiative Organization (For primary document see N91-14379 06-19)
Avail: NTIS HC/MF A21 CSCL 14B

Researchers investigate the heterojunction internal photoemission (HIP) approach that potentially offers long wavelength infrared (LWIR) photovoltaic detector performance (single pixel) that is competitive with the best of other approaches being considered. Most significantly, this approach offers a relatively simple device technology that promises producible and uniform FPA's. Researchers emphasize an exciting process based on intervalence band absorption. They investigate both III-V and Si-based heterojunctions grown by molecular beam epitaxy (MBE) in which the barrier can be tailored to the desired cutoff wavelength. In addition, MBE allows one to optimize the device structure with precise control of doping profiles and layer thicknesses, and perform band structure engineering by control of composition and heterojunction strain. Researchers also consider free carrier absorption in heterojunctions. Acceptable absorption coefficients can be achieved in very heavily n(exp +) doped semiconductor layers (approx. equals 10(exp 20)cm(exp -3). However, in this case the appreciable filling of conduction band states leads to a Schottky-like photoresponse with a gradual (quadratic) turn-on above threshold. A more satisfactory approach would be to use p(exp +) doping so that with the higher density of states in the heavy hole valence band there would be a narrow band of occupied states. This gives the desirable effect of a more rapid (linear) turn-on above threshold. Unfortunately, the higher hole effective mass also reduces (inversely) the free carrier absorption. For this and other reasons, the intervalence band absorption process looks much more promising. Author

N91-14399*# California Inst. of Tech., Pasadena.
INTERSUBBAND ABSORPTION IN Si(1-x)Ge(x/Si SUPERLATTICES FOR LONG WAVELENGTH INFRARED DETECTORS
Yasantha Rajakarunanayake and Tom C. McGill *In* JPL, California Inst. of Tech., Innovative Long Wavelength Infrared Detector Workshop Proceedings 1 Jul. 1990 p 305-321 (For primary document see N91-14379 06-19)
Avail: NTIS HC/MF A21 CSCL 14B

Researchers calculated the absorption strengths for intersubband transitions in n-type Si(1-x)Ge(x)/Si superlattices. These transitions can be used for the detection of long-wavelength infrared radiation. A significant advantage in Si(1-x)Ge(x)/Si supperlattice detectors is the ability to detect normally incident light; in Ga(1-x)Al(x)As/GaAs superlattices, intersubband absorption is possible only if the incident light contains a polarization component in the growth direction of the superlattice. Researchers present detailed calculation of absorption coefficients, and peak absorption wavelengths for (100), (111) and (110) Si(1-x)Ge(x)/Si superlattices. Peak absorption strengths of about 2000 to 6000 cm(exp -1) were obtained for typical sheet doping concentrations (approx. equals 10(exp 12)cm(exp -2)). Absorption comparable to that in Ga(1-x)Al(x)As/GaAs superlattice detectors, compatibility with existing Si technology, and the ability to detect normally incident light make these devices promising for future applications. Author

N91-14400*# Hughes Research Labs., Malibu, CA.
POSSIBILITIES FOR LWIR DETECTORS USING MBE-GROWN Si(/Si(1-x)Ge(x) STRUCTURES
Robert J. Hauenstein, Richard H. Miles, and Mary H. Young *In* JPL, California Inst. of Tech., Innovative Long Wavelength Infrared

Detector Workshop Proceedings 1 Jul. 1990 p 323-337 (For primary document see N91-14379 06-19)
Avail: NTIS HC/MF A21 CSCL 14B

Traditionally, long wavelength infrared (LWIR) detection in Si-based structures has involved either extrinsic Si or Si/metal Schottky barrier devices. Molecular beam epitaxially (MBE) grown Si and Si/Si(1-x)Ge(x) heterostructures offer new possibilities for LWIR detection, including sensors based on intersubband transitions as well as improved conventional devices. The improvement in doping profile control of MBE in comparison with conventional chemical vapor deposited (CVD) Si films has resulted in the successful growth of extrinsic Si:Ga, blocked impurity-band conduction detectors. These structures exhibit a highly abrupt step change in dopant profile between detecting and blocking layers which is extremely difficult or impossible to achieve through conventional epitaxial growth techniques. Through alloying Si with Ge, Schottky barrier infrared detectors are possible, with barrier height values between those involving pure Si or Ge semiconducting materials alone. For both n-type and p-type structures, strain effects can split the band edges, thereby splitting the Schottky threshold and altering the spectral response. Measurements of photoresponse of n-type Au/Si(1-x)Ge(x) Schottky barriers demonstrate this effect. For intersubband multiquntum well (MQW) LWIR detection, Si(1-x)Ge(x)/Si detectors grown on Si substrates promise comparable absorption coefficients to that of the Ga(Al)As system while in addition offering the fundamental advantage of response to normally incident light as well as the practical advantage of Si-compatibility. Researchers grew Si(1-x)Ge(x)/Si MQW structures aimed at sensitivity to IR in the 8 to 12 micron region and longer, guided by recent theoretical work. Preliminary measurements of n- and p-type Si(1-x)Ge(x)/Si MQW structures are given. Author

N91-14401*# Jet Propulsion Lab., California Inst. of Tech., Pasadena.
NOVEL Si(1-x)Ge(x)/SI HETEROJUNCTION INTERNAL PHOTOEMISSION LONG WAVELENGTH INFRARED DETECTORS
T. L. Lin, Joseph Maserjian, A. Ksendzov, Mark L. Huberman, R. Terhune, and T. N. Krabach *In its* Innovative Long Wavelength Infrared Detector Workshop Proceedings 1 Jul. 1990 p 339-349 Sponsored in part by Strategic Defense Initiative Organization (For primary document see N91-14379 06-19)
Avail: NTIS HC/MF A21 CSCL 14B

There is a major need for long-wavelength-infrared (LWIR) detector arrays in the range of 8 to 16 microns which operate with close-cycle cryocoolers above 65 K. In addition, it would be very attractive to have Si-based infrared (IR) detectors that can be easily integrated with Si readout circuitry and have good pixel-to-pixel uniformity, which is critical for focal plane array (FPA) applications. Here, researchers report a novel Si(1-x)Ge(x)/Si heterojunction internal photoemission (HIP) detector approach with a tailorable long wavelength infrared cutoff wavelength, based on internal photoemission over the Si(1-x)Ge(x)/Si heterojunction. The HIP detectors were grown by molecular beam epitaxy (MBE), which allows one to optimize the device structure with precise control of doping profiles, layer thickness and composition. The feasibility of a novel Si(1-x)Ge(x)/Si HIP detector has been demonstrated with tailorable cutoff wavelength in the LWIR region. Photoresponse at wavelengths 2 to 10 microns are obtained with quantum efficiency (QE) above approx. 1 percent in these non-optimized device structures. It should be possible to significantly improve the QE of the HIP detectors by optimizing the thickness, composition, and doping concentration of the Si(1-x)Ge(x) layers and by configuring the detector for maximum absorption such as the use of a cavity structure. With optimization of the QE and by matching the barrier energy to the desired wavelength cutoff to minimize the thermionic current, researchers predict near background limited performance in the LWIR region with operating temperatures above 65K. Finally, with mature Si processing, the relatively simple device structure offers potential for low-cost producible arrays with excellent uniformity. Author

N91-14402*# Hughes Aircraft Co., Torrance, CA.
MBE HgCdTe HETEROSTRUCTURE DETECTORS
Joel N. Schulman and Owen K. Wu *In* JPL, California Inst. of Tech., Innovative Long Wavelength Infrared Detector Workshop Proceedings 1 Jul. 1990 p 351-362 (For primary document see N91-14379 06-19)
Avail: NTIS HC/MF A21 CSCL 14B

HgCdTe has been the mainstay for medium (3 to 5 micron) and long (10 to 14 micron) wavelength infrared detectors in recent years. Conventional growth and processing techniques are continuing to improve the material. However, the additional ability to tailor composition and placement of doped layers on the tens of angstroms scale using molecular beam epitaxy (MBE) provides the opportunity for new device physics and concepts to be utilized. MBE-based device structures to be discussed here can be grouped into two categories: tailored conventional structures and quantum structures. The tailored conventional structures are improvements on familiar devices, but make use of the ability to create layers of varying composition, and thus band gap, at will. The heterostructure junction can be positioned independently of doping p-n junctions. This allows the small band gap region in which the absorption occurs to be separated from a larger band gap region in which the electric field is large and where unwanted tunneling can occur. Data from hybrid MBE/liquid phase epitaxy (LPE)/bulk structures are given. Quantum structures include the HgTe-CdTe superlattice, in which the band gap and transport can be controlled by alternating thin layers (tens of angstroms thick) of HgTe and CdTe. The superlattice has been shown to exhibit behavior which is non-alloy like, including very high hole mobilities, two-dimensional structure in the absorption coefficient, resonant tunneling, and anisotropic transport. Author

N91-14403*# North Carolina State Univ., Raleigh. Dept. of Physics.
GROWTH AND PROPERTIES OF Hg-BASED QUANTUM WELL STRUCTURES AND SUPERLATTICES
J. F. Schetzina *In* JPL, California Inst. of Tech., Innovative Long Wavelength Infrared Detector Workshop Proceedings 1 Jul. 1990 p 363-379 (For primary document see N91-14379 06-19)
(Contract N00014-89-5-2024; NSF DMR-88-13525)
Avail: NTIS HC/MF A21 CSCL 14B

An overview of the properties of HgTe-CdTe quantum well structures and superlattices (SL) is presented. These new quantum structures are candidates for use as new long wavelength infrared (LWIR) and very long wavelength infrared (VLWIR) detectors, as well as for other optoelectronic applications. Much has been learned within the past two years about the physics of such structures. The valence band offset has been determined to be approx. 350 meV, independent of temperature. The occurrence of electron and hole mobilities in excess of 10(exp 5)cm(exp 2)/V center dot s is now understood on the basis of SL band structure calculations. The in-plane and out-of-plane electron and hole effective masses have been measured and interpreted theoretically for HgTe-CdTe superlattices. Controlled substitutional doping of superlattices has recently been achieved at North Carolina State University (NCSU), and modulation-doped SLs have now been successfully grown and studied. Most recently, a dramatic lowering of the growth temperature of Hg-based quantum well structure and SLs (to approx. 100 C) has been achieved by means of photoassisted molecular beam epitaxy (MBE) at NCSU. A number of new devices have been fabricated from these doped multilayers. Author

N91-14404*# Santa Barbara Research Center, CA.
HgZnTe-BASED DETECTORS FOR LWIR NASA APPLICATIONS
Elizabeth A. Patten and Murray H. Kalisher *In* JPL, Californa Inst. of Tech., Innovative Long Wavelength Infrared Detector Workshop Proceedings 1 Jul. 1990 p 381-397 Sponsored by NASA, Langley Research Center (For primary document see N91-14379 06-19)
Avail: NTIS HC/MF A21 CSCL 14B

The initial goal was to grow and characterize HgZnTe and determine if it indeed had the advantageous properties that were predicted. Researchers grew both bulk and liquid phase epitaxial HgZnTe. It was determined that HgZnTe had the following properties: (1) microhardness at least 50 percent greater than HgCdTe of equivalent bandgap; (2) Hg annealing rates of at least 2 to 4 times longer than HgCdTe; and (3) higher Hg vacancy formation energies. This early work did not focus on one specific composition (x-value) of HgZnTe since NASA was interested in HgZnTe's potential for a variety of applications. Since the beginning of 1989, researchers have been concentrating, however, on the liquid phase growth of very long wavelength infrared (VLWIR) HgZnTe (cutoff approx. equals 17 microns at 65K) to address the requirements of the Earth Observing System (EOS). Since there are no device models to predict the advantages in reliability one can gain with increased microhardness, surface stability, etc., one must fabricate HgZnTe detectors and assess their relative bake stability (accelerated life test behavior) compared with HgCdTe devices fabricated in the same manner. Researchers chose to fabricate HIT detectors as a development vehicle for this program because high performance in the VLWIR has been demonstrated with HgCdTe HIT detectors and the HgCdTe HIT process should be applicable to HgZnTe. HIT detectors have a significant advantage for satellite applications since these devices dissipate much less power than conventional photoconductors to achieve the same responsivity. Author

N91-14405*# Los Alamos National Lab., NM.
SMALL BAND GAP SUPERLATTICES AS INTRINSIC LONG WAVELENGTH INFRARED DETECTOR MATERIALS
Darryl L. Smith and C. Mailhiot (Lawrence Livermore National Lab., CA.) *In* JPL, California Inst. of Tech., Innovative Long Wavelength Infrared Detector Workshop Proceedings 1 Jul. 1990 p 401-411 (For primary document see N91-14379 06-19)
Avail: NTIS HC/MF A21 CSCL 14B

Intrinsic long wavelength (lambda greater than or equal to 10 microns) infrared (IR) detectors are currently made from the alloy (Hg, Cd)Te. There is one parameter, the alloy composition, which can be varied to control the properties of this material. The parameter is chosen to set the band gap (cut-off wavelength). The (Hg, Cd)Te alloy has the zincblend crystal structure. Consequently, the electron and light-hole effective masses are essentially inversely proportional to the band gap. As a result, the electron and light-hole effective masses are very small (M sub(exp asterisk)/M sub o approx. M sub lh/M sub o approx. less than 0.01) whereas the heavy-hole effective mass is ordinary size (M sub hh(exp asterisk)/M sub o approx. 0.4) for the alloy compositions required for intrinsic long wavelength IR detection. This combination of effective masses leads to rather easy tunneling and relatively large Auger transition rates. These are undesirable characteristics, which must be designed around, of an IR detector material. They follow directly from the fact that (Hg, Cd)Te has the zincblend crystal structure and a small band gap. In small band gap superlattices, such as HgTe/CdTe, In(As, Sb)/InSb and InAs/(Ga,In)Sb, the band gap is determined by the superlattice layer thicknesses as well as by the alloy composition (for superlattices containing an alloy). The effective masses are not directly related to the band gap and can be separately varied. In addition, both strain and quantum confinement can be used to split the light-hole band away from the valence band maximum. These band structure engineering options can be used to reduce tunneling probabilities and Auger transition rates compared with a small band gap zincblend structure material. Researchers discuss the different band structure engineering options for the various classes of small band gap superlattices. Author

N91-14406*# Sandia National Labs., Albuquerque, NM.
LWIR DETECTOR RESEARCH IN InAsSb/InAs
Paul S. Peercy *In* JPL, California Inst. of Tech., Innovative Long Wavelength Infrared Detector Workshop Proceedings 1 Jul. 1990 p 413-430 (For primary document see N91-14379 06-19)
Avail: NTIS HC/MF A21 CSCL 14B

The InAsSb/InSb strained-layer system forms a type-II superlattice in the Sb-rich region of the phase diagram. The band gap of InAsSb/InSb strained-layer superlattices grown on lattice-matched buffers can be varied continuously to produce semiconducting systems with band gaps ranging from that of InSb (0.23 eV with an absorption edge at 5.5 microns at 77 K) to 0. The semiconductor to semimetal transition occurs at As concentrations of approximately 33 percent, with the precise value dependent upon the strain and quantum well dimensions. At higher As content, the system is a semimetal. The authors fabricated photovoltaic detectors with high D asterisk at 77 K at wavelengths beyond 10 microns, and both photovoltaic and photoconductive detectors have been demonstrated with response to 15 microns. The photoconductive detectors exhibit gain of up to 100. Details of the materials growth, studies of the band structure and properties, device processing and the detector performance observed to date in these systems are discussed. Author

N91-14407*# Hughes Aircraft Co., Torrance, CA.
InAs/Ga(1-x)In(x)Sb SUPERLATTICES FOR INFRARED DETECTOR APPLICATIONS
Richard H. Miles, Joel N. Schulman, D. H. Chow, and Tom C. McGill (California Inst. of Tech., Pasadena.) *In* JPL, California Inst. of Tech., Innovative Long Wavelength Infrared Detector Workshop Proceedings 1 Jul. 1990 p 431-445 (For primary document see N91-14379 06-19)
Avail: NTIS HC/MF A21 CSCL 14B

The successful growth of InAs/Ga(1-x)In(x)Sb superlattices and their optical and structural characterization is discussed. Samples were grown by molecular beam epitaxy at fairly low substrate temperatures (less than 400 C). Structural quality was assessed by reflection high energy electron difrraction, transmission electron microscopy, and x ray diffraction. Excellent structures were achieved for growth on thick, strain relaxed GaSb buffer layers on GaAs substrates, despite a residual threading dislocation density of 10(exp 9)cm(exp -2) originating at the GaSb/GaAs interface. Despite a lattice mismatch of 1.7 percent, InAs/Ga(0.75)In(0.25)Sb superlattices are observed to be free of misfit dislocations at the thicknesses examined here, owing to the close lattice match between the superlattice and GaSb, which evenly distributes compressive and tensile stresses between the InAs and Ga(0.75)In(0.25)Sb layers. Photoluminescence and photoconductivity measurements indicate that the energy gaps of the strain-layer superlattices are smaller than those of InAs/GaSb superlattices with the same layer thicknesses, and are in agreement with the theoretical predictions of Smith and Mailhiot. Energy gaps of 80 to 250 meV (15 to 15 microns) have been measured for InAs/Ga(0.75)In(0.25)Sb superlattices with 45 to 25 A/25 A layer thickness. Results demonstrate that far-infrared cutoff wavelengths are compatible with the thin superlattice layers required for strong optical absorption in type-II superlattices. Author

N91-14408*# Minnesota Univ., Minneapolis. Dept. of Electrical Engineering.
IR DETECTORS BASED ON n-i-p-i SUPERLATTICES
P. Paul Ruden *In* JPL, California Inst. of Tech., Innovative Long Wavelength Infrared Detector Workshop Proceedings 1 Jul. 1990 p 447-462 (For primary document see N91-14379 06-19)
Avail: NTIS HC/MF A21 CSCL 14B

The principles of operation of n-i-p-i photodetectors are discussed. Special consideration is given to issues that are relevant to the performance of IR detectors such as noise, dark current, and surface effects. In addition, a novel IR detector that promises to provide information about the spectral distribution of the infrared radiation emitted from an object and, consequently, about its temperature, independent of the distance between detector and object is discussed. This detector makes use of the possibility to modulate the internal electric fields of an n-i-p-i superlattice with an applied voltage. By this technique the spectral responsivity of the detector may be controlled electrically and some information about the shape of the emission spectrum may be obtained. Author

N91-14409*# Jet Propulsion Lab., California Inst. of Tech., Pasadena.
InAs/GaAs AND InAs DOPING SUPERLATTICES
Frank J. Grunthaner, Bruce R. Hancock, and Joseph Maserjian *In its* Innovative Long Wavelength Infrared Detector Workshop Proceedings 1 Jul. 1990 p 463-478 (For primary document see N91-14379 06-19)
Avail: NTIS HC/MF A21 CSCL 14B

The extension of the optical response of narrow band gap III-V semiconductors into the long wavelength infrared radiation (LWIR) regime for high sensitivity sensor applications is a challenging problem. Recent advances in nipi doped GaAs superlattices, lattice mismatched epitaxy and the heteroepitaxial growth of III-V compound semiconductors on silicon substrates offer a number of opportunities. Researchers describe two different device approaches based on the molecular beam epitaxy (MBE) growth of superlattice materials which are directed to LWIR focal plane array technology. The first of these uses nipi superlattices fabricated in bulk InAs which has been grown on either GaAs or Si substrates. The second is based on the growth of a new pseudomorphic tetragonal phase of InAs on GaAs to create a semimetal/semiconductor superlattice material. Author

N91-14410*# Utah Univ., Salt Lake City. Dept. of Materials Science and Engineering.
InAsSbBi, A DIRECT BAND-GAP, III-V, LWIR MATERIAL
G. B. Stringfellow, Colin E. Jones, and John Frodsham (Space Systems Engineering, Logan, UT.) *In* JPL, California Inst. of Tech., Innovative Long Wavelength Infrared Detector Workshop Proceedings 1 Jul. 1990 p 481-493 (For primary document see N91-14379 06-19)
Avail: NTIS HC/MF A21 CSCL 14B

In the last several years Dr. Stringfellow's group at the University of Utah has reported success in incorporating over 3 percent Bi in InAs and 1.5 percent in InAsSb using Organometallic Vapor Phase Epitaxy (OMVPE) growth techniques. For InAs the lattice constant increase is linear with a=6.058+0.966x (InAs(1-x)Bi(x)), and a decrease in band gap energy of dEg / dx = -55meV / at a percentage Bi. Extrapolating this to the ternary minimum band gap at InAs(0.35)Sb(0.65), an addition of 1 to 2 percent Bi should drop the band gap to the 0.1 to 0.05eV range (10 to 20 microns). These alloys are direct band gap semiconductors making them candidates for far IR detectors. The current status of the InAsSbBi alloys is that good crystal morphology and x ray diffraction data has been obtained for up to 3.4 percent Bi. The Bi is metastable at these concentrations but the OMVPE grown material has been able to withstand the 400 C growth temperature for several hours without phase separation. Author

N91-14411*# California Univ., Santa Barbara. Dept. of Electrical and Computer Engineering.
AlSb/InAs/AlSb QUANTUM WELLS
Herbert Kroemer *In* JPL, California Inst. of Tech., Innovative Long Wavelength Infrared Detector Workshop Proceedings 1 Jul. 1990 p 495-509 (For primary document see N91-14379 06-19)
Avail: NTIS HC/MF A21 CSCL 14B

Researchers studied the InAs/AlSb system recently, obtaining 12nm wide quantum wells with room temperature mobilities up to 28,000 cm(exp 2)/V center dot S and low-temperature mobilities up to 325,000 cm(exp 2)/V center dot S, both at high electron sheet concentrations in the 10(exp 12)/cm(exp 2) range (corresponding to volume concentrations in the 10(exp 18)/cm(exp 2) range). These wells were not intentionally doped; the combination of high carrier concentrations and high mobilities suggest that the electrons are due to not-intentional modulation doping by an unknown donor in the AlSb barriers, presumably a stoichiometric defect, like an antisite donor. Inasmuch as not intentionally doped bulk AlSb is semi-insulating, the donor must be a deep one, being ionized only by draining into the even deeper InAs quantum well. The excellent transport properties are confirmed by other observations, like excellent quantum Hall effect data, and the successful use of the quantum wells as superconductive weak links between Nb electrodes, with unprecendentedly high critical current densities. The system is promising for future field effect transistors (FETs), but many processing problems must first be solved. Although the researchers have achieved FETs, the results so far have not been competitive with GaAs FETs. Author

N91-14412* National Aeronautics and Space Administration. Langley Research Center, Hampton, VA.
METHOD AND APPARATUS FOR DETERMINING TIME, DIRECTION, AND COMPOSITION OF IMPACTING SPACE PARTICLES Patent
William H. Kinard, inventor (to NASA), Jim J. Wortman, inventor (to NASA), Philip C. Kassel, Jr., inventor (to NASA), Fred S. Singer, inventor (to NASA), Donald H. Humes, inventor (to NASA), and John E. Stanley, inventor (to NASA) (Virginia Univ., Charlottesville.) 23 Oct. 1990 9 p Filed 21 Jun. 1989
(NASA-Case-LAR-13392-1-CU; US-Patent-4,964,300; US-Patent-Appl-SN-369490; US-Patent-Class-73-170R; Int-Patent-Class-G01W-1/00) Avail: US Patent and Trademark Office CSCL 22B

A space particle collector for recording the time specific particles are captured, and its direction at the time of capture, utilizes an array of targets, each comprised of an MOS capacitor on a chip charged from an external source and discharged upon impact by a particle through a tab on the chip that serves as a fuse. Any impacting particle creates a crater, but only the first will cause a discharge of the capacitor. A substantial part of the metal film around the first crater is burned off by the discharge current. The time of the impulse which burns the tab, and the identification of the target, is recorded together with data from flight instruments. The metal film is partitioned into pie sections to provide a plurality of targets on each of an array of silicon wafers, thus increasing the total number of identified particles that can be collected. It is thus certain which particles were captured at what specific times. NASA

N91-14413# Air Force Geophysics Lab., Hanscom AFB, MA. Space Physics Div.
THE AIS: A SPECTROGRAPH/IMAGER ENSEMBLE FOR SPACE FLIGHT
R. A. Viereck, D. J. Knecht, A. L. Broadfoot, and B. Sandel (Arizona Univ., Tucson.) 17 May 1990 62 p
(AF Proj. 7601)
(AD-A227009; GL-TR-90-0158; GL-IP-340) Avail: NTIS HC/MF A04 CSCL 20/5

An instrument, the Arizona Imager/Spectrograph (AIS), developed for the Geophysics Laboratory by the University of Arizona for use on the space shuttle is described. The instrument is a combination of spectrographs and imagers intended for the study of optical emissions in the vicinity of spacecraft. It includes nine spectrographs, which cover the spectral range from 115 to 1100 nm, with spectral resolutions ranging from 0.5 nm at short wavelengths to 1.3 nm at long wavelengths, and twelve imagers which have narrow, medium, and wide fields of view and optical bandpass filters to select particular wavelengths. The images and spectra are focused onto intensified charge coupled devices. The design of this instrument is discussed and examples of test data are presented. GRA

20 SPACECRAFT PROPULSION AND POWER

Includes main propulsion systems and components, e.g., rocket engines; and spacecraft auxilliary power sources.

For related information see also *07 Aircraft Propulsion and Power, 28 Propellants and Fuels, 44 Energy Production and Conversion,* and *15 Launch Vehicles and Space Vehicles.*

N91-14414*# Minnesota Univ., Minneapolis.
ONE- AND TWO-DIMENSIONAL STIRLING MACHINE SIMULATION USING EXPERIMENTALLY GENERATED FLOW TURBULENCE MODELS Final Report
Louis F. Goldberg Aug. 1990 198 p
(Grant NAG3-693)
(NASA-CR-185285; NAS 1.26:185285) Avail: NTIS HC/MF A09 CSCL 10A

Investigations of one- and two-dimensional (1- or 2-D) simulations of Stirling machines centered around experimental data generated by the U. of Minnesota Mechanical Engineering Test Rig (METR) are covered. This rig was used to investigate oscillating flows about a zero mean with emphasis on laminar/turbulent flow transitions in tubes. The Space Power Demonstrator Engine (SPDE) and in particular, its heater, were the subjects of the simulations. The heater was treated as a 1- or 2-D entity in an otherwise 1-D system. The 2-D flow effects impacted the transient flow predictions in the heater itself but did not have a major impact on overall system performance. Information propagation effects may be a significant issue in the simulation (if not the performance) of high-frequency, high-pressure Stirling machines. This was investigated further by comparing a simulation against an experimentally validated analytic solution for the fluid dynamics of a transmission line. The applicability of the pressure-linking algorithm for compressible flows may be limited by characteristic number (defined as flow path information traverses per cycle); this warrants further study. Lastly the METR was simulated in 1- and 2-D. A two-parameter k-w foldback function turbulence model was developed and tested against a limited set of METR experimental data. Author

N91-14415*# Thiokol Corp., Brigham City, UT. Space Operations.
FLIGHT SET 360L006 STS-34 FIELD JOINT PROTECTION SYSTEM, THERMAL PROTECTION SYSTEM, AND SYSTEMS TUNNEL COMPONENTS, VOLUME 4 Final Report
J. P. Wilkinson Aug. 1990 26 p
(Contract NAS8-30490)
(NASA-CR-184050; NAS 1.26:184050; TWR-17545-Vol-4; Publ-91211) Avail: NTIS HC/MF A03 CSCL 21H

The performance of the thermal protection system, field joint protection system, and systems tunnel components of Flight Set 360L006, are documented, as evaluated by postflight hardware inspection. The condition of both motors was similar to previous flights. Sixteen aft edge hits were noted on the ground environment instrumentation thermal protection system. Each hit left a clean substrate, indicating that the damage was caused by nozzle severance debris and/or water impact. No National Space and Transporation System debris criteria for missing thermal protection system were violated. One 5.0 by 1.0 in. unbond was observed on the left hand center field joint K5NA closeout and was elevated to an in-flight anomaly (STS-34-M-4) by the NASA Ice/Debris team. Aft edge damage to the K5NA and an associated black streak indicate that burning debris from the nozzle severance system was the likely cause of the damage. Minor divots caused by debris were seen on previous flights, but this is the first occurrence of a K5NA unbond. Since the unbond occurred after booster separation there is no impact on flight safety and no corrective actions was taken. The right hand center field joint primary heater failed the dielectric withstanding voltage test after joint closeout. The heater was then disabled by opening the circuit breaker, and the redundant heater was used. The redundant heater performed nominally during the launch countdown. A similar condition occurred on Flight 4 when a secondary joint heater failed the dielectric withstanding voltage test. Author

N91-14416*# Thiokol Corp., Brigham City, UT. Space Operations.
SPACE SHUTTLE REDESIGNED SOLID ROCKET MOTOR CERTIFICATE OF QUALIFICATION (COQ) DATA REPORT
Fred Duersch, Jr. Aug. 1990 103 p
(Contract NAS8-30490)
(NASA-CR-184051; NAS 1.26:184051; TWR-18764/13) Avail: NTIS HC/MF A06 CSCL 21H

The Space Shuttle Redesigned Solid Rocket Motor (RSRM) Certification Program provides confidence that the RSRM and its components/subsystems meet or exceed Mission Oriented Requirements when manufactured per design requirements and specified/approved processes. Certification is based on documented results of tests, analyses, inspections, similarity, and demonstrations. Evidencing information is provided to certify that each RSRM component/subsystem satisfies design, mission related requirements and objectives. Author

N91-14417# Naval Postgraduate School, Monterey, CA.
DETERMINATION OF SPEAR-1 ROCKET BODY POTENTIAL DURING HIGH-VOLTAGE EXPERIMENTS M.S. Thesis
Thurston VanHorn Jun. 1990 170 p
(AD-A226971) Avail: NTIS HC/MF A08 CSCL 22/1

The space power experiment aboard rockets (SPEAR) 1 payload was launched on December 13, 1987. It had a primary objective of providing guidelines in designing high-voltage (HV) systems for use in low-earth orbit (LEO). The experiment consisted of 24 HV bias operations using two 20 cm diameter spheres attached to the rocket by booms. The SPEAR-1 rocket charged to substantial negative potentials during the flight when the spheres were biased positive with respect to the rocket. This thesis uses the electrostatic analyzer ion data to determine the charging response of the rocket body. The peak potential was reached during a 45 kV sphere bias sequence resulting in a 17.4 kV rocket body potential at 361 km altitude. The rocket body potential varied between 7 an 38 percent of sphere potential. Geomagnetic orientation, vice altitude, had greater effect on rocket body potential. The flight data also indicated that neutral gas emissions from the rocket attitude control system (ACS) triggered transient discharge currents that effectively grounded the rocket body potential. ACS firings resulted in an order of magnitude change in the rocket body potential. GRA

N91-14285# Nielsen Engineering and Research, Inc., Mountain View, CA.
AERODYNAMIC DESIGN OF PEGASUS (TRADEMARK): CONCEPT TO FLIGHT WITH CFD
Michael R. Mendenhall, Daniel J. Lesieutre, Steven C. Caruso, Marnix F. E. Dillenius, and Gary D. Kuhn *In* AGARD, Missile Aerodynamics Oct. 1990 11 p Sponsored in part by Orbital Sciences Corp., Vienna, VA (For primary document see N91-14278 06-02)
Copyright Avail: NTIS HC/MF A17; Non-NATO Nationals requests available only from AGARD/Scientific Publications Executive

N91-14296# Naval Weapons Center, China Lake, CA. Airbreathing Propulsion Branch.
OVERVIEW OF PROPULSION CONCEPTS FOR TACTICAL MISSILES
Frederick C. Zarlingo *In* AGARD, Missile Aerodynamics Oct. 1990 12 p (For primary document see N91-14278 06-02)
Copyright Avail: NTIS HC/MF A17; Non-NATO Nationals requests available only from AGARD/Scientific Publications Executive

23 CHEMISTRY AND MATERIALS (GENERAL)

N91-14418* National Aeronautics and Space Administration. Langley Research Center, Hampton, VA.
BIS (4-(3,4-DIMETHYLENE-PYRROLIDYL)-PHENYL) METHANE Patent
Raphael M. Ottenbrite, inventor (to NASA) (Virginia Commonwealth Univ., Richmond.) 23 Jan. 1990 4 p Filed 16 Feb. 1989 Division of US-Patent-Appl-SN-221386, filed 19 Jul. 1988
(NASA-Case-LAR-13965-2-CU; US-Patent-4,895,915; US-Patent-Appl-SN-311551; US-Patent-Appl-SN-221386; US-Patent-Class-526-262; US-Patent-Class-528-322; Int-Patent-Class-C08G-73/10) Avail: US Patent and Trademark Office CSCL 07A

The primary objective is to prepare high temperature polymeric materials, especially linear aromatic polyimides, which maintain their integrity and toughness during long exposure times at elevated temperatures. The attained benefits are obtained by first providing the bis (exocyclodiene) bis (4-(3,4-dimethylene-pyrrolidyl)-phenyl) methane, which is a novel material formed from the monomer N-phenyl-3,4-dimethylene-pyrrolidine. This compound undergoes Diels-Alder reaction with a bismaleimide, without the evolution of gaseous by-products, to form the aromatic polyimide bis (4-(3,4-dimethylene-pyrrolidyl)-phenyl) methane.
Official Gazette of the U.S. Patent and Trademark Office

N91-14419* National Aeronautics and Space Administration. Langley Research Center, Hampton, VA.
N-(3-ETHYNYLPHENYL)MALEIMIDE Patent
Paul M. Hergenrother, inventor (to NASA), John W. Connell, inventor (to NASA), and Stephen J. Havens, inventor (to NASA) 26 Jun. 1990 7 p Filed 10 Aug. 1989 Division of US-Patent-Appl-SN-328392, filed 24 Mar. 1989 which is a continuation-in-part of abandoned US-Patent-Appl-SN-087375, filed 20 Aug. 1987
(NASA-Case-LAR-14188-2; US-Patent-4,937,356; US-Patent-Appl-SN-391692; US-Patent-Appl-SN-328392; US-Patent-Appl-SN-087375; US-Patent-Class-548-549; Int-Patent-Class-C07D-207/44) Avail: US Patent and Trademark Office CSCL 07A

Acetylene terminated aspartimides are prepared using two methods. In the first, an amino-substituted aromatic acetylene is reacted with an aromatic bismaleimide in a solvent of glacial acetic acid and/or m-cresol. In the second method, an aromatic diamine is reacted with an ethynyl containing maleimide, such as N-(3-ethynylphenyl) maleimide, in a solvent of glacial acetic acid and/or m-cresol. In addition, acetylene terminated aspartimides are blended with various acetylene terminated oligomers and polymers to yield composite materials exhibiting improved mechanical properties.
Official Gazette of the U.S. Patent and Trademark Office

24 COMPOSITE MATERIALS

Includes physical, chemical, and mechanical properties of laminates and other composite materials.
For ceramic materials see *27 Nonmetallic Materials.*

N91-14420 Mississippi Univ., University.
A STATISTICALLY-BASED MODEL OF THE INTERACTING PROCESSES WHICH LEAD TO CREEP-RUPTURE IN FILAMENT-WOUND COMPOSITE PRESSURE VESSELS Ph.D. Thesis
Kerry Timothy Slattery 1989 207 p
Avail: Univ. Microfilms Order No. DA9019281

Advanced filamentary composite materials suffer loss of strength and stiffness when subjected to service loads. This loss can be attributed to the effect of several mechanisms which include matrix microcrack growth, fiber/matrix debonding, and fiber breakage. Consequently, any time that a composite material system is subjected to a relatively high load its structural integrity is significantly diminished. Advanced composites can also fail when they are subjected to constant-magnitude loads that are substantially lower than the ultimate strength of the composite if the loads are sustained for long periods of time. This phenomenon, which is commonly referred to as creep-rupture, stress-rupture, or static fatigue is accelerated if the structure was initially subjected to a proof-test load. The effect of this test on the reliability of the vessel is a major concern. A better understanding of proof-test damage and creep-rupture requires a great deal of study and modeling of the interacting damaging processes. The approach taken herein is to model the interactions between the constituent materials in micromechanical detail using the finite element method. Fibers are divided into a series of bar elements whose nodes are connected transversely by shear elements representing the matrix. Random strengths are assigned to the fiber elements and randomly dispersed matrix elements are damaged during the application of load. An iterative, time-stepping procedure is employed in the solution. At the end of each time step, stresses are calculated in the constituent materials, time and stress dependent damage is assessed, the stiffness matrix is updated accordingly, and the load is adjusted as required. This process is repeated until failure. The solution is carried out on a supercomputer. Dissert. Abstr.

N91-14421 British Petroleum Co. Ltd., London (England).
METHOD FOR MANUFACTURING COMPOSITE MATERIAL Patent Application
Adrian Wilfred Melton, inventor (to British Petroleum Co. Ltd.) 14 Oct. 1988 8 p
(EP-Patent-0-314-353-A2; EP-Patent-Appl-SN-88309670-3; Int-Patent-Class-B29C-67/18; Int-Patent-Class-B29D-28/00; Int-Patent-Class-B29C-33/00; ETN-90-97605) Avail: UK Patent Office, 254 Southhampton Buildings, London WC2A 1A4, England

A method and apparatus for manufacturing perforate fiber reinforced composite material is presented A problem associated with the manufacture of composite materials with intricate shapes where the material may be difficult to remove from the mold is addressed. The material is perforated by needles and the mold has a stripper plate whereby the composite material bends to withdraw from the mold with the plate rather than with the mold part having needles. The invention is described by way of example with reference to accompanying drawings. ESA

N91-14422*# California Univ., Santa Barbara. Dept. of Mechanical and Environmental Engineering.
OPTIMIZATION OF INTERFACE LAYERS IN THE DESIGN OF CERAMIC FIBER REINFORCED METAL MATRIX COMPOSITES Final Report
I. Doghri, S. Jansson, F. A. Leckie, and J. Lemaitre (Paris VI Univ., France) Nov. 1990 35 p
(Grant NAG3-894)
(NASA-CR-185307; NAS 1.26:185307) Avail: NTIS HC/MF A03 CSCL 11D

The potential of using an interface layer to reduce thermal stresses in the matrix of composites with a mismatch in coefficients of thermal expansion (CTE) of fiber and matrix was investigated. It was found that the performance of the layer can be defined by the product of the CTE and the thickness, and that a compensating layer with a sufficiently high CTE can reduce the thermal stresses in the matrix significantly. A practical procedure offering a window of candidate layer materials is proposed. Author

N91-14423# Oxford Univ. (England). Dept. of Engineering Science.
THE INTERLAMINAR SHEAR STRENGTH OF WOVEN CARBON, WOVEN GLASS AND WOVEN CARBON/GLASS HYBRID LAMINATES UNDER STATIC AND IMPACT LOADING
Y. L. Li, J. Harding, and M. E. C. Taylor 1990 65 p Previously announced as A90-45967 Submitted for publication
(Grant AF-AFOSR-0129-87)
(OUEL-1831/90; ETN-90-98222) Avail: NTIS HC/MF A04

Double-lap shear specimens are prepared from woven carbon

and woven glass plies and one carbon and one glass ply specimens prepared from dry woven mats hand lay-up in an epoxy resin matrix. All carbon specimens are prepared from a satin weave carbon/epoxy pre-preg. Tests are performed under static loading using an Instron testing machine and under impact loading using a tensile split Hopkinson bar. The results show that the interlaminar shear stress is highest for the specimens prepared from the carbon/epoxy pre-preg under both static loading and impact loading. For the specimens prepared from dry woven mats and epoxy resin under static loading the interlaminar shear strength is highest for the hybrid hand lay-up and is lowest for the all glass hand lay-up. For the all carbon hand lay-up the interlaminar shear strength is slightly less than that of the hybrid specimen. The results show that interlaminar shear strength is slightly less than that of the hybrid specimen. The results show that interlaminar shear strength is remarkably strain rate dependent. The interlaminar shear strength increases by about 72.6 percent under impact loading for the all glass material, 70.4 percent for the all carbon material, and 55.6 percent for the hybrid material. Under impact loading the interlaminar shear strength is highest for the all carbon hand lay-up and lowest for the all glass hand lay-up. For the hybrid specimen it is slightly less than for the all carbon hand lay-up. ESA

N91-14424*# Virginia Polytechnic Inst. and State Univ., Blacksburg. Center for Composite Materials and Structures.
AN ANALYSIS OF INTERLAMINAR STRESSES IN UNSYMMETRICALLY LAMINATED PLATES Interim Report No. 81
D. S. Norwood, M. J. Shuart, and Carl T. Herakovich (Virginia Univ., Charlottesville.) Nov. 1990 355 p
(Grant NAG1-343)
(NASA-CR-187657; NAS 1.26:187657; CCMS-90-11; VPI-E-90-18) Avail: NTIS HC/MF A16 CSCL 11D

The results of a numerical study of the interlaminar stress fields within unsymmetrically laminated anisotropic plates is presented. The focus of the study is upon the linear thermoelastic response of thin square laminated composite plates subjected to extensional, compressive, or thermal loading. Symmetric and unsymmetric 0/90, +45/-45, and 0/+45 laminate stacking sequences are examined to determine the effects of mismatch between adjacent layers in Poisson's ratio, coefficient of mutual influence, and coefficients of thermal expansion. Since the out-of-plane (transverse) deflections of unsymmetric laminates are typically large, a geometrically nonlinear kinematic description is used to account for the large displacements and large rotations. The geometrically nonlinear three dimensional boundary value problems are formulated from nonlinear elasticity theory and approximate solutions are determined using the finite element method. A total Lagrangian, displacement-based, incremental finite element formulation is implemented using Newton's method. Geometrically nonlinear global/local finite element analysis is used to obtain improved free edge stress predictions. The conclusions apply to extensional, compressive (prior to a change in mode shape), and thermal loading. Author

N91-14425# Illinois Univ., Urbana-Champaign.
ALUMINUM NITRIDE-SILICON CARBIDE WHISKER COMPOSITES: PROCESSING, PROPERTIES, AND MICROSTRUCTURAL STABILITY M.S. Thesis
Michael Thomas Cross 1990 100 p
(Contract DE-AC02-76ER-01198)
(DE91-001907; DOE/ER-01198/T43) Avail: NTIS HC/MF A05

Aluminum nitride-silicon carbide whisker composites with up to 20 vol percent whiskers were fabricated by pressureless sintering (1750 to 1800 C) and by hot-pressing (1700 to 1800 C). Silicon carbide whiskers were found to degrade depending on the type of protective powder bed used during sintering. Whiskers were found degraded in high oxygen containing samples by reaction with sintering additives. Whisker degradation was also due to the formation of silicon carbide -- aluminum nitride solid solution. No whisker degradation was observed in hot-pressed samples. For these samples Young's modulus and fracture toughness were measured. A 33 percent increase in the fracture toughness was measured by the indentation technique for a 20 vol percent whisker composite. Operative toughening mechanisms were investigated using scanning electron microscopy. Crack deflection and whisker bridging were the dominant mechanisms. It was also shown that load transfer from matrix to whiskers can be a contributing factor to toughening. DOE

N91-14426*# National Aeronautics and Space Administration. Lewis Research Center, Cleveland, OH.
LOW VELOCITY IMPACT ANALYSIS WITH NASTRAN
Daniel A. Trowbridge (Analex Corp., Fairview Park, OH.), Joseph E. Grady, and Robert A. Aiello Apr. 1990 17 p Presented at the NASTRAN User's Colloquium, Portland OR, 23-27 Apr. 1990; sponsored in part by COSMIC, and Georgia Univ. Previously announced as N90-24647
(NASA-TM-103169; E-5541; NAS 1.15:103169) Avail: NTIS HC/MF A03 CSCL 11D

A nonlinear elastic force-displacement relationship is used to calculate the transient impact force and local deformation at the point of contact between impactor and target. The nonlinear analysis and transfer function capabilities of NASTRAN are used to define a finite element model that behaves globally linearly elastic, and locally nonlinear elastic to model the local contact behavior. Results are presented for two different structures: a uniform cylindrical rod impacted longitudinally; and an orthotropic plate impacted transversely. Calculated impact force and transient structural response of the targets are shown to compare well with results measured in experimental tests. Author

N91-14427# Edgerton, Germeshausen and Grier, Inc., Idaho Falls, ID.
DYNAMIC CONSOLIDATION OF ALUMINUM-SILICON CARBIDE COMPOSITES
B. H. Rabin, G. E. Korth, and R. L. Williamson 1990 20 p Presented at the 119th Minerals, Metals and Metallurgical Society Annual Meeting and Exhibit, Anaheim, CA, 18-22 Feb. 1990
(Contract DE-AC07-76ID-01570)
(DE91-001929; EGG-M-89129; CONF-900206-12) Avail: NTIS HC/MF A03

Dynamic consolidation was investigated as a potential method for producing P/M metal matrix composites. In this study, 2124 aluminum powders were mixed with silicon carbide particulate and consolidated using explosives. Numerical simulations were performed to provide insight into the consolidation process and to aid in the selection of experimental conditions. The microstructure of the as-consolidated product was dependent upon processing variables. Careful control of the shock parameters allowed full density, crack free composites to be achieved in cylindrical geometries. Although full density was obtained, low fracture strengths suggested a lack of interparticle bonding, probably resulting from the limited ability to redistribute surface oxides during consolidation. DOE

N91-14428# Lawrence Livermore National Lab., CA.
AC-130H GUNSHIP ARMOR UPGRADE PROJECT
Thomas E. Shell and Robert L. Landingham 19 Sep. 1990 18 p
(Contract W-7405-eng-48)
(DE91-002567; UCRL-ID-106022) Avail: NTIS HC/MF A03

This report covers the test methods and equipment for testing both hard and soft aircraft armor. The hard armor are the typical ceramic type while the soft armor are various types of layered composite materials. DOE

N91-14429*# Utah Univ., Salt Lake City. Dept. of Materials Science and Engineering.
SURFACE AND INTERFACIAL PROPERTIES OF CARBON FIBERS Final Report
Willard D. Bascom 2 Jan. 1991 75 p
(Grant NAG1-1049)
(NASA-CR-184916; NAS 1.26:184916) Avail: NTIS HC/MF A04 CSCL 11D

The adhesion strength of AS4 fibers to thermoplastic polymers was determined. The specific polymers were polycarbonate, polyphenylene oxide, polyetherimide, polyphenylene oxide blends with polystyrene, and polycarbonate blends with a polycarbonate-polysiloxan copolymer. Data are also included for polysulfone. It was recognized at the outset that an absolute measure of the fiber matrix adhesion would be difficult. However, it is feasible to determine the fiber bond strengths to the thermoplastics relative to the bond strengths of the same fibers to epoxy polymers. It was anticipated, and in fact realized, that the adhesion of AS4 to the thermoplastic polymers was relatively low. Therefore, further objectives of the study were to identify means of increasing fiber/matrix adhesion and to try to determine why the adhesion of AS4 to thermoplastics is significantly less than to epoxy polymers. Author

N91-14430* National Aeronautics and Space Administration. Langley Research Center, Hampton, VA.
DELAMINATION TEST APPARATUS AND METHOD Patent
John H. Crews, Jr., inventor (to NASA) and James R. Reeder, inventor (to NASA) 22 May 1990 7 p Filed 28 Jul. 1989
(NASA-Case-LAR-13985-1; US-Patent-4,926,694; US-Patent-Appl-SN-386172; US-Patent-Class-73-794; Int-Patent-Class-G01N-3/00) Avail: US Patent and Trademark Office CSCL 11D

A delamination test apparatus and method uses a single beam to simultaneously apply opening and shear stresses to a test specimen. A fulcrum extending downwardly from the beam produces shear stress in the specimen by downward movement, and opening stress by pivotal upward movement of the beam, which results by virtue of the fact that the applied load is on one side of the fulcrum while the test specimen is connected to the beam on the opposite side of the fulcrum.
Official Gazette of the U.S. Patent and Trademark Office

N91-14431# Carnegie Inst. of Tech., Pittsburgh, PA. Dept. of Metallurgy and Materials Science.
FUNDAMENTALS OF INTERFACIAL STRENGTH IN COMPOSITE MATERIALS Final Report, 1 Jul. 1986 - 30 Sep. 1989
A. W. Thompson and I. M. Bernstein 1 May 1990 57 p
(Grant AF-AFOSR-0238-86; AF Proj. 2306)
(AD-A226701; MEMS-ACL-13; AFOSR-90-1002TR) Avail: NTIS HC/MF A04 CSCL 11/4

Research in the third program year has examined fatigue and toughness behavior of composites with 6061 and 7090 or 7191 alloy matrix material, with the goal being better understanding of relationships between microstructure and mechanical properties of these matrices with particulate SiC reinforcement. Tensile and fatigue testing results, in air and in corrosive environments, of the various microstructures (i.e., aging conditions) chosen are presented, along with toughness results and finite-element studies to interpret the observed toughness levels. The strong microstructural dependence of mechanical properties is emphasized, along with possible avenues for improvement of these properties. GRA

N91-14432# Toronto Univ. (Ontario). Dept. of Chemical Engineering and Applied Chemistry.
MESOMECHANICAL MODEL FOR FIBRE COMPOSITES Annual Progress Report, 1 Jul. 1989 - 31 May 1990
Michael R. Piggott 30 Jul. 1990 21 p
(Grant AF-AFOSR-0365-89; AF Proj. 2302)
(AD-A226792; AFOSR-90-1040TR) Avail: NTIS HC/MF A03 CSCL 11/4

Carbon fiber interfaces with epoxy resins have been examined using the pull out method. This method can now be reliably and reproducibly used to measure the bond strength. Shear strengths can be very high, up to nearly 150 MPa in individual experiments, with average values for 50 or more tests of up to 100 MPa. The strengths are little different for Hercules AS1, AS2 and AS4. The sizing appears to have little effect (but this needs to be confirmed). The strengths observed are up to three times the shear strength of the polymer. Carbon and glass interfaces with thermoplastics (polyethylene and nylon) can also be measured using this method. Results here are up to four times the estimated shear strength of the polymer. To explain the high results an equivalent work of fracture is involved. This has never exceeded 300 Jm-2, indicating that the interphases are quite brittle. GRA

N91-14433# Naval Postgraduate School, Monterey, CA.
THERMOMECHANICAL PROCESSING AND AMBIENT TEMPERATURE PROPERTIES OF A 6061 ALUMINUM 10 VOLUME PERCENT ALUMINA METAL MATRIX COMPOSITE M.S. Thesis
Thomas A. Schaefer Mar. 1990 54 p
(AD-A227004) Avail: NTIS HC/MF A04 CSCL 11/4

Thermomechanical processing was conducted on a cast aluminum-based metal matrix composite. The material studied was 6061 aluminum containing 10 volume percent of alumina (Al_2O_3) particles, fabricated by casting and subsequently extruded by DURALCAN, Inc. Processing included isothermal rolling of an extruded bar to large strain values. As a result of rolling at 500 C, strength was increased, but with a substantial loss of ductility. Further strengthening was realized by rolling at 350 C and no further ductility loss was seen. Homogeneity of the particle dispersion was considerably improved with no evidence of microstructural damage. Upon subsequent solution heat treatment, ductility of the rolled materials was restored to values greater than obtained in material experiencing only extrusion. Also, the strength of the rolled material exceeded that of material heat treated after extrusion. Upon subsequent aging treatment (aging at 160 C), the increased strength and ductility enhancement persisted. GRA

N91-14434# Massachusetts Inst. of Tech., Cambridge. Dept. of Ocean Engineering.
STRUCTURAL RESPONSE OF MARINE SANDWICH PANELS TO UNIFORM PRESSURE LOADING M.S. Thesis
J. Rowland Huss Jun. 1990 234 p
(Contract N00123-89-G-0580)
(AD-A227038) Avail: NTIS HC/MF A11 CSCL 11/4

Deflection and strain responses of six marine sandwich panels to uniform pressure loading are investigated. Panels are full scale typical of those found in a 40-foot high performance deep-vee monohull. Three combinations of matrix-reinforcement are used in the panel faces: bi-axial (0 deg to 90 deg) E-glass in a fire retardent vinyl ester resin (DERAKANE 510A), bi-axial and double bias (+ or - 45 deg) Kevlar in DERAKANE 510A, and bi-axial and double bias Kevlar with an elastomer modified vinyl ester resin (DERAKANE 8084). Polyvinyl chloride foam AIREX is the core material. A panel test mechanism applies uniform pressure to panels 90 in. wide by 120 in. long. The central test section is 30 by 60 in. and is isolated by one panel span to simulate in situ boundary conditions. Two pressure loading rates (static and cyclic) are employed allowing examination of viscoelastic effects. A material and mechanical characterization of the sandwich panel lower faces is conducted. Membrane behavior is not evident on a per cycle basis, yet its effect can be seen over successive cycles. The non-linearity and hysteresis diminish with repeated loading. After relatively few cycles, the deflection and strain responses become linear, the rate-normalized bending stiffness lessens, and the overall panel response approaches that recorded during static tests. GRA

N91-14435# Utah Univ., Salt Lake City. Dept. of Mechanical Engineering.
FAILURE IN LAMINATED COMPOSITE PLATES CONTAINING A HOLE Final Report, 1987 - 1990
E. S. Folias 25 Jul. 1990 72 p
(Grant AF-AFOSR-0204-87; AF Proj. 2302)
(AD-A227307; AFOSR-90-0937TR) Avail: NTIS HC/MF A04 CSCL 11/4

This investigation concerns the 3D stresses in a laminated composite plate weakened by a circular hole. The analysis is based on 3D macromechanical considerations. The debonding aspects

are investigated between a fiber/matrix interface particularly in the region where the fiber intersects a free edge, e.g., the surface of a hole. The results, which are based on micromechanical considerations, are then used to predict the critical applied load stress which may cause initiation of ply-delamination. GRA

N91-14436# Oak Ridge National Lab., TN.
INTERFACIAL PUSH-OUT MEASUREMENTS OF FULLY-BONDED SiC/Sc COMPOSITES
Lance L. Snead, Don Steiner (Rensselaer Polytechnic Inst., Troy, NY.), and Steven J. Zinkle 1990 7 p Presented at the Symposium on Composites, Orlando, FL, 15 Nov. 1990
(Contract DE-AC05-84OR-21400)
(DE91-004527; CONF-9011122-2) Avail: NTIS HC/MF A02

The direct measurement of interfacial bond strength and frictional resistance to sliding in a fully-bonded SiC/SiC composite is measured. It is shown that a fiber push-out technique can be utilized for small diameter fibers and very thin composite sections. Results are presented for a 22 micron thick section for which 37 out of 44 Nicalon fibers tested were pushed-out within the maximum nanoindentor load of 120 mN. Fiber interfacial yielding, push-out and sliding resistance were measured for each fiber. The distribution of interfacial strengths is treated as being Weibull in form. DOE

N91-14437*# National Aeronautics and Space Administration. Goddard Space Flight Center, Greenbelt, MD.
OUTGASSING DATA FOR SELECTING SPACECRAFT MATERIALS, REVISION 2
William A. Campbell, Jr. and John J. Scialdone Washington Nov. 1990 398 p
(NASA-RP-1124-Rev-2; Rept-90B00138-Rev-2; NAS 1.61:1124-Rev-2) Avail: NTIS HC/MF A17 CSCL 11D

Outgassing data, derived from tests at 398 K (125 C) for 24 hours in vacuum as per ASTM E 595-77, were compiled for numerous materials for spacecraft use. The data presented are the total mass loss (TML) and the collected volatile condensable materials (CVCM). The various materials are listed by likely usage and alphabetically. Author

25 INORGANIC AND PHYSICAL CHEMISTRY

Includes chemical analysis, e.g., chromatography; combustion theory; electrochemistry; and photochemistry.

For related information see also *77 Thermodynamics and Statistical Physics.*.

N91-14438# Oak Ridge National Lab., TN.
IN-LINE SENSORS FOR ELECTROLYTIC MAGNESIUM CELLS
J. P. Young and Gleb Mamantov 12 Nov. 1990 8 p
(Contract DE-AC05-84OR-21400)
(DE91-002561; ORNL/M-1323) Avail: NTIS HC/MF A02

MgCl2 purification and molten salt preparation facilities have been completed at both the University of Tennessee, Knoxville, and Oak Ridge National Laboratory. The purification of MgCl2 is being studied. Initial Raman spectral results have been obtained at both facilities. Two analytical spectral techniques involving near-infrared (NIR) and IR reflectance spectral measurements show promise for identifying and quantifying OH species in solid salts of interest. A sealed IR reflectance cell has been developed for use in the project. An electrochemical cell for use in voltammetric studies concerned with the project has been designed and fabricated. DOE

N91-14439# California Univ., Berkeley. Lawrence Berkeley Lab. Combustion Group.
STATISTICAL ERRORS IN THE FRACTAL ANALYSIS OF FLAME BOUNDARIES
Ian G. Shepherd and Robert K. Cheng Oct. 1990 20 p Presented at the 1990 Combustion Institute Fall Meeting, San Diego, CA, 14-16 Oct. 1990 Submitted for publication
(Contract DE-AC03-76SF-00098)
(DE91-001795; LBL-29666; CONF-9010207-3) Avail: NTIS HC/MF A03

A high speed tomographic technique is used to evaluate the effect of spatial resolution, and requirements for statistical convergence on the fractal analysis of a turbulent, premixed, stoichiometric methane/air flame at high Damkoehler number. The gas velocity at the nozzle exit is 5 m/s, the turbulence intensity is 7 percent, the integral length scale 3 mm and hence the turbulence Reynolds number is 70. The light source is a copper vapor laser which produces 20ns, 5 mJ pulses at a 4KHz repetition rate. Cylindrical lenses transform the 38mm circular laser beam to a sheet 50 mm high and 0.6 mm thick. A high speed Fastax camera is used to record the tomographic images formed by the scattering of light from oil droplets seeded in the reactant flow. The films are digitized and the flame front extracted from the images by a thresholding technique. Digitization noise, which appears in the fractal plots at approximately twice the pixel resolution, can obscure the inner cutoff. Simple smoothing can remove this problem if the spatial resolution is sufficient. At insufficient resolution smoothing produces plausible resolutes which are in fact erroneous. If the inner cutoff is ambiguous, the range over which the fractal dimension is determined will be unclear. The wide distribution of fractal dimensions obtained from the individual images indicates the necessity of ensemble averaging the fractal plots if reliable statistical results are to be obtained. DOE

N91-14440# Louisville Univ., KY. Dept. of Chemical Engineering.
MECHANISM OF HYDRODENITROGENATION. PART 4: INFRARED SPECTROSCOPY OF ACIDIC MOLYBDENA CATALYSTS
Raul Miranda 1990 14 p
(Contract DE-FG22-89PC-89771)
(DE91-002496; DOE/PC-89771/4) Avail: NTIS HC/MF A03

Mo oxide catalysts supported over a complete series of silica-aluminas have been characterized in the oxidic and reduced states, by means of total acidity measurements and by infrared spectroscopy. Ammonia chemisorption was used to titrate the total acidity of the catalysts, and IR absorption of adsorbed pyridine to distinguish Bronsted from Lewis acid sites. The formation of new acidity upon deposition of molybdena on silica-alumina supports was then explained on the basis of a simple surface model. The new acidity is of both Lewis and Bronsted type with the preponderance of one over the other depending on support composition, as well as loading and state of oxidation of Mo. High-alumina supports and low Mo loading favor dispersed Mo species, in particular bidentate and monodentate di-oxo Mo species. The latter is responsible for the new Bronsted acidity. Coordinative unsaturation of polymolybdates is responsible for the new Lewis acidity, which is increased upon reduction of Mo. High-silica supports favor monodentate species (high Bronsted acidity) up to 4 wt percent MoO3. Beyond that, polymolybdates species and Lewis acidity predominate. DOE

N91-14441# California Inst. of Tech., Pasadena.
INVESTIGATION OF COMBUSTION IN LARGE VORTICES Final Report, Sep. 1986 - Sep. 1989
Edward E. Zukoski 15 Aug. 1990 13 p
(Grant AF-AFOSR-0286-84; AF Proj. 2308)
(AD-A226791; AFOSR-90-1038TR) Avail: NTIS HC/MF A03 CSCL 21/2

This research consists of an experimental study of the time dependent combustion in vortex structures. Large vortices were formed utilizing pulsed flow over a downstream facing step. The technique for simultaneous shadowgraph, chemiluminescence, and laser Doppler velocimeter measurements has been developed and is used regularly. For a pressure oscillation of fixed amplitude, the diameter of the vortex grows linearly with time at a rate that increases linearly with the pressure amplitude of the oscillation generating the vortex formation. The onset of chemiluminescence - and we believe combustion - is delayed for several milliseconds,

close to our estimates for the chemical time for the systems under study here. GRA

N91-14442# Aerospace Corp., El Segundo, CA. Chemistry and Physics Lab.
CONVERSION OF ALKOXIDE SOLUTIONS TO OXIDES: EVAPORATION OF PRODUCTS
R. A. Lipeles and D. J. Coleman 15 Nov. 1989 23 p
(Contract F04701-88-C-0089)
(AD-A226927; TR-0089(4945-02)-1; SSD-TR-90-27) Avail: NTIS HC/MF A03 CSCL 07/3

The evaporation kinetics of methanol depended on the drying rate achieved by flowing dry air over the gel. Cracking of the gel during drying was used to indicate the degree of stress. At low drying rates, minor cracking was observed near the edges of the gel. At high flow rates, extensive cracking was observed. GRA

N91-14443# Utah Univ., Salt Lake City. Dept. of Material Sciences and Engineering.
USE OF D2 TO ELUCIDATE OMVPE GROWTH MECHANISMS Final Report, 15 Jun. 1987 - 14 Jun. 1990
G. B. Stringfellow 11 Jul. 1990 13 p
(Grant AF-AFOSR-0233-80; AF Proj. 2306)
(AD-A226966; AFOSR-90-0950TR) Avail: NTIS HC/MF A03 CSCL 07/4

The reaction mechanisms were determined for the pyrolysis of the group III precursors trimethylgallium (TMGa) and trimethylindium (TMIn) and the grup V precursors AsH3. PH3, trimethylarsine (TMAs), dimethylarsin (DMAs), triethylarsin (TEAs), diethylarsine DEAs), monoethylarsine (MEAs), tertiarybutylarsin (TBAs), and tertiarybutylophospine (TBP). The reaction mechanisms were also studied for combinations of the group III and group V precursors which result in the production of GaAs and InP. The technique used was mass spectrometry with the pyrolysis occurring in various ambients including H2, He, and D2. The latter allows labelling of reaction products involving interactions with the ambient. The reaction mechanisms observed are surprisingly diverse. The pyrolysis temperatures for the various As precursors can be compared. GRA

N91-14444# Aerospace Corp., El Segundo, CA. Materials Sciences Lab.
PROCEDURES FOR THE PREPARATION OF SAMPLES FOR CROSS-SECTIONAL TRANSMISSION ELECTRON MICROSCOPY
Sue Y. Teng and Paul M. Adams 6 Aug. 1990 36 p
(Contract F04701-88-C-0089)
(AD-A227013; TR-0090(5945-07)-1; SSD-TR-90-18) Avail: NTIS HC/MF A03 CSCL 14/2

Cross sectional transmission electron microscopy (XTEM) is an important technique for studying the morphology and local chemistry of the interfaces of thin film materials. The preparation of samples for XTEM analysis can be summarized as follows: Samples are cleaved or sawed into 2 mm x 7 mm strips. A sandwich consisting of four strips is glued together. Fifty-mil thick slices are cut from the sandwich. The slices are ground and polished to a thickness of 100 micrometers. The thin slice is glued to a TEM grid and is dimpled until a perforation is achieved. The dimpled specimen is thinned to electron transparency with an ion-milling machine. A detailed account of the procedures used to prepare XTEM samples of Si-Ge superlattices is given. Selected micrographs of these samples show how the XTEM technique can be used to study interfaces. GRA

N91-14445# State Univ. of New York, Buffalo. Dept. of Chemistry.
PHOTODISSOCIATION NEAR A ROUGH METAL SURFACE: EFFECT OF REACTION FIELDS
Purna C. Das, Ashok Puri (New Orleans Univ., LA.), and Thomas F. George Sep. 1990 35 p Submitted for publication
(Contract N00014-90-J-1193; NSF CHE-89-22288)
(AD-A227030; UBUFFALO/DC/90/TR-23) Avail: NTIS HC/MF A03 CSCL 07/4

The modification of the photochemical dissociation rate of molecules in the presence of a rough metal surface is explored. Classical electromagnetic calculations are presented for the photodissociation rate of a point dipole near a rough surface modeled as a hemispheroidal pump on a semi-infinite flat plane. A correction is introduced by accounting for the reaction fields due to the dipole-substrate system radiating photons and coupling to delocalized surface plasmons. The effect of the shape and size of the bump and the separation of the molecule from the bump on the rate of photodissociation of the molecule are studied numerically. GRA

N91-14446# California Univ., Berkeley. Dept. of Mechanical Engineering.
OPPOSED JET TURBULENT DIFFUSION FLAMES Final Report, 1 Oct. 1987 - 31 Mar. 1990
L. Talbot 5 Sep. 1990 68 p
(Grant AF-AFOSR-0011-88; AF Proj. 2308)
(AD-A227048; AFOSR-90-1026TR) Avail: NTIS HC/MF A04 CSCL 21/2

A Hydrogen-Helium mixture was chosen to investigate the structure of a counterflow diffusion flame. Reacting and non reacting conditions were studied at the same Reynolds number. To study the reaction zone structure, high speed tomography based on Mie scattering was employed using a copper vapor laser and a Fastax high speed camera. Laser Doppler Velocimeter (LDV) measurements were also obtained. Different seeding techniques were used to visualize both the turbulent air and fuel jets. The tomographic records were digitized and recorded in a digital computer for statistical treatment. Significant differences in the wrinkle scales between the reacting and non reacting flows were found. A fractal statistical analysis of the tomography records was done to quantify these differences. Seeding of both fuel and air jets provided a mean for the evaluation of the reaction zone thickness. The strain of the reaction zone was obtained from the time resolved tomographic records. Local flame extinction and reignition were observed for different H2/Helium fuel mixtures. GRA

N91-14447# Naval Research Lab., Washington, DC. Lab. for Computational Physics.
DYNAMICS OF AN UNSTEADY DIFFUSION FLAME: EFFECTS OF HEAT RELEASE AND GRAVITY
Janet L. Ellzey (Berkeley Research Association, Springfield, VA.) and Elaine S. Oran 27 Sep. 1990 19 p
(AD-A227348; NRL-MR-6716) Avail: NTIS HC/MF A03 CSCL 21/2

This report presents time-dependent axisymmetric numerical simulations of an unsteady diffusion flame formed between a jet and a coflowing air stream. The computations include the effects of convection, molecular diffusion, thermal conduction, viscosity, gravitational forces, and chemical reactions with energy release. Previous work has shown that viscous effects are important in these flames and, therefore, all of the viscous terms in the compressible Navier-Stokes equations are included. In addition, the resolution is increased so that the large, vortical structures in the coflowing gas are resolved and the boundary conditions are improved so that the velocity field near the jet is more realistic. Computations with and without chemical reactions and heat release, and with and without gravity, are compared. Gravitational effects are insignificant in the nonreacting jet but in the reacting jet gravity produced the relatively low-frequency instabilities typically associated with flame flicker. Kelvin-Helmholtz instabilities develop in the region between the high-velocity and low-velocity fluid when there are no chemical reactions, but heat release dampens these instabilities to produce a mixing region which is almost steady in time. GRA

N91-14448# Texas A&M Univ., College Station. Dept. of Chemistry.
DEVELOPMENT OF LASER-ION BEAM PHOTODISSOCIATION METHODS

D. H. Russell Aug. 1990 5 p
(Contract DE-FG05-85ER-13434)
(DE91-000680; DOE/ER-13434/5) Avail: NTIS HC/MF A01

During this report period our research efforts have concentrated on studies of the dissociation reactions of model peptides and other biologically important molecules. In addition, a considerable amount of research effort has been directed toward improving the apparatus used for laser-ion beam photodissociation. The instrumental improvements include some changes on the original apparatus, but most of this effort involved designing a second generation laser-ion beam photodissociation instrument. DOE

N91-14449# California Univ., Berkeley. Lawrence Berkeley Lab. Combustion Group.
THE APPLICATION OF THE TURBULENT BURNING SPEED CONCEPT TO LABORATORY FLAMES
Robert K. Cheng Oct. 1990 15 p Presented at the 1990 Combustion Institute Fall Meeting, La Jolla, CA, 14-16 Oct. 1990 Submitted for publication
(Contract DE-AC03-76SF-00098)
(DE91-001789; LBL-29665; CONF-9010207-4) Avail: NTIS HC/MF A03

The purpose of this paper is to review and critique previous and current practices of applying the turbulent burning speed concept to different laboratory flames. Also evaluated and discussed are the suitability and limitations of the flame configurations, and conventional and novel experimental methods for determining S(sub T). The survey shows that most of the currently available S(sub T) data obtained by flame geometry methods tend to be high and need to be corrected for the effects of flow divergence. This emphasizes the significance of the flowfield on flame propagation. DOE

N91-14450# Sandia National Labs., Albuquerque, NM.
LASER STUDIES OF THE INTERACTION OF SIO WITH THE SURFACE OF A THIN FILM
Pauline Ho, Richard J. Buss, and M. E. Weber (Texas Instruments, Inc., Dallas.) 1990 9 p Presented at the Fall Meeting of the Materials Research Society, Boston, MA, 24 Nov. - 1 Dec. 1990
(Contracts DE-AC04-76DP-00789; F33615-88-C-5448)
(DE91-004562; SAND-90-1789C; CONF-901105-26) Avail: NTIS HC/MF A02

The interaction of SiO radicals from a SiCl4/O2 plasma with the surface of a depositing thin film is studied with the Imaging of Radicals Interacting with Surfaces (IRIS) technique, which combines spatially-resolved laser-induced fluorescence with molecular beam methods. In contrast to previous results for SiH, SiO appears not to react at the surface of the depositing film, but desorbs with a cosine spatial distribution for a wide range of substrate temperatures. No evidence is observed for specular scattering of the molecules. DOE

N91-14451# National Research Inst. for Pollution and Resources, Tokyo (Japan).
HYDROCARBON GROUP-TYPE ANALYSIS OF PETROLEUM DISTILLATES AND RESIDUES BY HIGH-PERFORMANCE LIQUID CHROMATOGRAPHY
S. Matsuzawa, E. Nakamura, T. Yamamoto, O. Setoguchi, M. Sato, Y. Shimizu, S. Sato, S. Takahashi, M. Enomoto, and M. Tamura et al 29 Mar. 1990 134 p In JAPANESE; ENGLISH summary
(DE91-727527; ETDE/JP-mf-1727527) Avail: NTIS (US Sales Only) HC/MF A07

On the hydrocarbon group-type separation and analysis by a high-performance liquid chromatography (HPLC), the improvement of a separation performance and a sensitivity correction method for a differential refractometer (RI detector) was synthetically reported. Problems of the separation and analysis by a HPLC, and effects of various factors on a separation efficiency were summarized, and the enhancement of a separation accuracy for olefin and heavy oil was reported. As pretreatment methods of specimens to enhance the accuracy, new separation methods of polar compounds were reported. The improvement of the sensitivity correction method for the detector, and the calculation method of response factors from the specific gravity of specimens were reported in detail, and analysis results of middle distillate, residue of petroleum, and cracked oil were reported with the calculated factors. Furthermore, applications of the analysis to the low-pressure hydroretorting of oil shale and the quantitative analysis of polycyclic aromatic hydrocarbon isomers were also reported. DOE

N91-14993*# National Aeronautics and Space Administration. Goddard Space Flight Center, Greenbelt, MD.
LABORATORY STUDIES OF REFRACTORY METAL OXIDE SMOKES
Joseph A. Nuth, R. N. Nelson (College of Southern Georgia, Statesboro.), and Bertram Donn *In* NASA, Ames Research Center, Interstellar Dust: Contributed Papers Dec. 1989 p 373-374 (For primary document see N91-14897 06-88)
Avail: NTIS HC/MF A22 CSCL 07D

N91-14994*# Los Alamos National Lab., NM.
INFRARED SPECTRA OF CRYSTALLINE AND GLASSY SILICATES AND APPLICATION TO INTERSTELLAR DUST
John R. Stephens, A. Blanco, A. Borghesi, Sergio Fonti, and E. Bussoletti (Istituto Universitario Navale, Naples, Italy) *In* NASA, Ames Research Center, Interstellar Dust: Contributed Papers Dec. 1989 p 375-380 (For primary document see N91-14897 06-88)
Avail: NTIS HC/MF A22 CSCL 07D

N91-15014*# York Univ. (Ontario). Dept. of Chemistry.
GAS-PHASE FORMATION OF SILICON CARBIDES, OXIDES, AND SULPHIDES FROM ATOMIC SILICON IONS
Diethard K. Bohme, Stanislaw Wlodek, and Arnold Fox *In* NASA, Ames Research Center, Interstellar Dust: Contributed Papers Dec. 1989 p 473-478 Sponsored in part by Natural Sciences and Engineering Research Council of Canada (For primary document see N91-14897 06-88)
Avail: NTIS HC/MF A22 CSCL 07D

N91-15015*# Pennsylvania State Univ., University Park. Dept. of Astronomy.
PAH FORMATION IN CARBON-RICH CIRCUMSTELLAR ENVELOPES
Eric D. Feigelson and Michael Frenklach *In* NASA, Ames Research Center, Interstellar Dust: Contributed Papers Dec. 1989 p 479-483 (For primary document see N91-14897 06-88)
Avail: NTIS HC/MF A22 CSCL 07D

26 METALLIC MATERIALS

Includes physical, chemical, and mechanical properties of metals, e.g., corrosion; and metallurgy.

N91-14452 Maryland Univ., College Park.
FUNDAMENTAL STUDIES ON MICROSTRUCTURAL EVOLUTION OF TWO-PHASE TITANIUM ALLOYS Ph.D. Thesis
Gurpreet Singh Grewal 1990 182 p
Avail: Univ. Microfilms Order No. DA9030904

A systematic study was undertaken to determine the affect of temperature and diffusivity of alloying elements on the particle coarsening and grain growth kinetics of various two phase materials using Ti-Mn and Ti-V alloys as the model systems. During the course of this investigation, it was found that the titanium end of the Ti-V phase diagram is incorrect. Based on the results of this investigation, a new phase diagram was proposed. A model was proposed for two phase materials where solute and solvent atoms move in opposite directions resulting in coarsening of particles. In addition to this bulk diffusion mechanism, additional mechanisms were considered. It is found that mixed diffusion (grain boundary + lattice) controls the coarsening of particles at 973 K for the Ti-Mn system whereas predominantly grain boundary diffusion is the controlling mechanism for the Ti-V system at 973 K. Studies on the effect of temperature on particle coarsening showed that

the activation energy for particle coarsening process increases with an increase in temperature. In addition, it is found that the coarsening exponents also increase with increase in temperature. It is proposed that the particle coarsening mechanism changes from mixed diffusion control towards bulk diffusion control as the temperature increases from 973 to 1108 K for the Ti-Mn system. It is also suggested that the coarsening mechanism changes from predominantly grain boundary diffusion control to mixed diffusion control as the temperature is increased from 973 to 1073 K for the Ti-V system. The growth of matrix grains in the presence of growing second phase particles was also studied. A model based on classical driving force for grain growth and a modified form of Zener retardation is proposed for the growth of matrix grains.
Dissert. Abstr.

N91-14453 British Petroleum Co. Ltd., London (England).
SURFACE TREATMENT OF METALS Patent Application
Richard Arthur Cayless, inventor (to British Petroleum Co. Ltd.) 26 Oct. 1989 6 p
(EP-Patent-0-367-504-A2; EP-Patent-Appl-SN-89311025-9; Int-Patent-Class-C23C-22/68; Int-Patent-Class-C23C-22/83; ETN-90-97972) Avail: UK Patent Office, 254 Southampton Buildings, London WC2A 1A4, England

A patent is claimed for an invention relating to a method of treating metal surfaces, in particular steel, aluminum and zinc. Metal surfaces are heated with an aqueous treatment medium which is a solution of yttrium and metal of the lanthanum series or a suspension of particles or alumina with bound chromate followed by treatment with a solution of organosilane. Bonding of adhesives of surface coatings is improved. The invention is illustrated with reference to described adhesion tests. ESA

N91-14454*# National Aeronautics and Space Administration. Lewis Research Center, Cleveland, OH.
THERMAL STABILITY OF THE MICROSTRUCTURE OF AN AGED Nb-Zr-C ALLOY Final Report
Mehmet Uz (Lafayette Coll., Easton, PA.) and Robert H. Titran Oct. 1990 18 p Presented at the 8th Symposium on Space Nuclear Power Systems, Albuquerque, NM, 7-10 Jan. 1991; sponsored by New Mexico Univ.
(Contract DE-A103-86SF-16310)
(NASA-TM-103647; DOE/NASA/16310-14; E-5829; NAS 1.15:103647) Avail: NTIS HC/MF A03 CSCL 11F

The effects of thermal aging with and without an applied stress on the microstructure of a Nb-Zr-C alloy containing 0.9 wt percent Zr and 0.06 wt percent C were studied. Chemical analysis, metallographic examination, energy dispersive x-ray spectra of the bulk material, and chemical and x-ray analyses of the phase-extracted residue were used to characterize the microstructure. The samples examined were from a creep strength study involving hot and cold working, and various combinations of exposure to temperatures ranging from 1350 to 1755 K with and without applied load for times as long as 34,000 plus hours. The results showed that the initial microstructure consisted primarily of orthorombic precipitates of Nb sub 2 C which were partially or completely transformed to face-centered cubic carbides of nb and Zr, (Zr, Nb)C, upon prolonged exposure to elevated temperatures. Furthermore, it was found that the microstructure of the alloy is extremely stable owing to the very finely distributed precipitates throughout its matrix and along the grain boundaries. The lattice parameters of the cubic carbides were determed to vary from 0.458 to 0.465 nm as the Zr/Nb ratio varied from 38/62 to 75/25. Author

N91-14455# Lawrence Livermore National Lab., CA.
A MODIFICATION OF 4330 ALLOY STEEL
Raymond P. Gogolewski, Bruce J. Cunningham, Robert Gentile, and Scott Fleming (Norton Defense Systems, Mahwah, NJ.) Aug. 1990 17 p Presented at the 12th International Symposium on Ballistics, San Antonio, TX, 30 Oct. - 1 Nov. 1990 Submitted for publication Sponsored by DARPA
(Contract W-7405-eng-48)
(DE91-001764; UCRL-103008; CONF-9010190-2) Avail: NTIS HC/MF A03

We have developed a modification of 4330 alloy steel which does not have an exact equivalent expressed in any standard specification. When we compare the ballistic performance of our modified cast steel in thicknesses of about 120 mm with that of stacked, 24 mm thick rolled 4340 alloy steel plates of comparable hardness and the same total thickness, we do not find a significant difference in terminal ballistic performance against either heavy metal kinetic energy penetrators or precision shaped charges. This result is surprising in relation to contemporary experience in which cast steel has been found to be ballistically inferior to rolled steel against either kinetic energy projectiles or shaped charge warheads. DOE

N91-14456# California Univ., Berkeley. Lawrence Berkeley Lab. Materials and Chemical Sciences Div.
ANOMALOUS SURFACE PHASE FORMATION ON Pt3Sn WITH ZONE AXES GROUP (100)
Alexandra N. Haner, Philip N. Ross, and Ugo Bardi (Florence Univ., Italy) Jun. 1990 12 p Presented at the 2nd International Conference on the Structure of Surfaces, Amsterdam, Netherlands, 22-25 Jun. 1987
(Contract DE-AC03-76SF-00098)
(DE91-001794; LBL-29473; CONF-8706159-4) Avail: NTIS HC/MF A03

LEED analysis of the clean annealed surface of a group of zone axes (100) oriented Pt3Sn single crystal surface indicates the formation of a multilayer surface phase which does not have the L1(sub 2) bulk structure. LEISS analysis indicates a surface stoichiometry of ca. 1:1 with Sn atoms displaced ca. 1.4 above the plane of Pt atoms. The surface phase is hypothesized to be a rhombic distortion of the group of zone axes (0001) plant of PtSn, which has a B8(sub 1) (NiAs-type) bulk structure. It is not clear whether the phase forms by precipitation of PtSn due to a slight (0.5 percent) stoichiometric excess of Sn in the bulk, or due to multilayer reconstruction driven by surface segregation. DOE

N91-14457# Oak Ridge Gaseous Diffusion Plant, TN.
ELECTROLESS NICKEL BATH RECOVERY BY CATION EXCHANGE AND PRECIPITATION
R. W. Anderson and W. A. Neff 1991 9 p Presented at the 12th AESF/EPA Conference on Environmental Control for the Surface Finishing Industry, Orlando, FL, 28-30 Jan. 1991
(Contract DE-AC05-84OT-21400)
(DE91-001988; CONF-910147-1) Avail: NTIS HC/MF A02

A method has been discovered to remove accumulated phosphite, sodium, and sulfate from spent electroless nickel plating baths without significant loss of plating reagents or discharge of hazardous chemicals to the environment. A hydrogen-form, strongly-acidic cation resin sorbs sodium and nickel from spent baths to produce effluent containing hypophosphorous, phosphorous, lactic, sulfuric acids, and anti-pit wetting agent. Treatment of the effluent with CaO and CaCO3 removes sulfate as CaSO4-0.5H20, and MgO removes phosphite as MgHPO3-3H2O solids. Following stripping of sodium from the resin with dilute sulfuric acid, more concentrated magnesium sulfate or sulfuric acid recovers nickel sulfate in a sulfuric acid solution. After concentration by evaporation, sulfuric acid is removed by CaSO4-0.5H2O precipitation. Treated solutions are combined to produce rejuvenated baths which have given excellent electroless nickel plates, and plating rates equal to or exceeding those for initial fresh baths. DOE

N91-14458# Los Alamos National Lab., NM.
SHORT TERM CREEP RUPTURE PREDICTIONS FOR TANTALUM ALLOY T-3
John J. Stephens 1991 8 p Presented at the 8th Symposium on Space Nuclear Power Systems, Albuquerque, NM, 6-10 Jan. 1991
(Contract DE-AC04-76DP-00789)
(DE91-002338; SAND-90-2778C; CONF-910116-3) Avail: NTIS HC/MF A02

A knowledge of the short term creep rupture behavior of Tantalum alloy T-111 is necessary to predict device integrity in the heat source section of Radioisotope Thermoelectric Generators (RTG's) at the end of service life, in the event of a fuel fire. High pressures exist in RTG's near the end of service life. These are caused by gas generation resulting from radioactive decay of the nuclear fuel. The internal pressure exerts a significant hoop stress on the T-111 alloy structural containment member. This paper analyses the short term creep behavior (rupture times up to approximately 2 times 10(exp 3) hrs.) of cold worked (CW) T-111 alloy, using the existing data of Stephenson (1967). Correlations for the time to rupture, time to 1 percent strain and minimum creep rate have been obtained from this data using multivariable linear regression analysis. These results are compared to other short term rupture data for T-111 alloy. Finally, at the stress/temperature levels relevant to the RTG fuel fire scenario near the end of service life, the rupture time correlation for T-111 alloy predicts a rupture time of approximately 100 hrs. DOE

N91-14459# Oak Ridge National Lab., TN.
THE EFFECT OF SCANDIUM ON THE PHASE STABILITY OF Al3Nb AND Al3Zr
D. M. Nicholson, J. H. Schneibel, W. A. Shelton, P. Sterne, and W. M. Temmerman (Daresbury Nuclear Physics Lab., England) 1990 12 p Presented at the Spring Meeting of the Materials Research Society, San Francisco, CA, 16-21 Apr. 1990
(Contract DE-AC05-84OR-21400)
(DE91-002657; CONF-900466-92) Avail: NTIS HC/MF A03

A series of Al-25 (Nb,Sc), at. percent, and Al-25 (Zr,Sc), at. percent, alloy buttons were arc-cast in argon and homogenized for 2 h in vacuum at temperatures ranging from 1473 to 1573K. X-ray powder-diffraction indicated that almost all the Nb in Al-25 Nb (DO sub 22) had to be replaced by Sc in order to obtain the L1(sub 2) structure. In the case of Al3Zr much less Sc was required - the single phase L1(sub 2) composition is approximately Al-16Zr-8Sc. Recent calculations show that once the tetragonality is properly included in the phase stability of the Tri-Aluminide transition-metal binary alloys can be understood in terms of their electronic density of states. The dominating feature is a deep minimum in the density of states just below the major transition metal d-band peak. The exact position of the minimum changes with structure type (i.e., L1(sub 2), DO sub 22, or DO sub 23, and with c/a). The alignment of the Fermi energy with the minimum appears to determine the equilibrium structure. The results of linearized-muffin-tin-orbital (LMTO) electronic structure calculations are compared to the rigid band model and checked against the experimentally determined phase boundaries. DOE

N91-14460# Mound Lab., Miamisburg, OH.
ELUCIDATION OF FUNDAMENTAL PROPERTIES OF HELIUM IN METALS BY NUCLEAR MAGNETIC RESONANCE TECHNIQUES
G. C. Abell 1990 21 p Presented at the NATO Advanced Research Workshop on Fundamental Aspects of Inert Gases in Solids, Bonas, France, 16-22 Sep. 1990
(Contract DE-AC04-88DP-43495)
(DE91-002715; MLM-3658(OP); CONF-9009256-2) Avail: NTIS HC/MF A03

The nuclear magnetic resonance (NMR) properties of very high density He-3 in metals are discussed in the context of the corresponding properties in relatively high density bulk He-3. In particular, the effects of the He-3 diffusion on the contribution of the He-3 - He-s dipolar interaction to the lineshape and to the spin-lattice relaxation parameter (T sub 1) are described. It is shown that the temperature dependence of the lineshape and of T sub 1 are independent sources of information about helium density and also about helium diffusivity. Moreover, T sub 1 is shown to be a sensitive indicator of melting transitions in bulk He-3. Palladium tritide is presented as a model system for NMR studies of He-3 in metals. Experimental NMR studies of this system reveal behavior analogous to what has been observed for bulk helium. Evidence for a He-3 phase transition near 250 K is provided by the temperature dependence of T sub 1. Assuming this to be a melting transition, a density is obtained from the bulk helium EOS that is in good agreement with theory and with swelling measurements on related metal tritides. He-3 NMR measurements have also provided information about the density distribution, helium diffusivity, and mean bubble size in palladium tritide. DOE

N91-14461# Oak Ridge National Lab., TN.
ION IMPLANTATION FOR CORROSION INHIBITION OF ALUMINUM ALLOYS IN SALINE MEDIA
J. M. Williams, A. Gonzales, J. Quintana, I.-S. Lee, R. A. Buchanan, F. C. Burns, R. J. Culbertson, M. Levy, and J. R. Treglio (ISM Technologies, Inc., San Diego, CA.) 1990 16 p Presented at the 7th International Conference on Ion Beam Modification of Materials, Knoxville, TN, 9-14 Sep. 1990
(Contract DE-AC05-84OR-21400)
(DE91-002887; CONF-900936-18) Avail: NTIS HC/MF A03

The effects of ion implantation treatments on corrosion of 2014 and 1100 aluminum in saline media were investigated. Implanted ions were N, Si, Ti and Cr. Techniques included salt spray testing, electrochemical studies, Rutherford backscattering spectrometry, and profilometry. It was concluded that ion implantation of Cr is of potential practical benefit for corrosion inhibition of 2014 Al in salt environments. DOE

N91-14462* National Aeronautics and Space Administration. Marshall Space Flight Center, Huntsville, AL.
DIRECTIONAL SOLIDIFICATION OF SUPERALLOYS Patent
Deborah Diane Schmidt, inventor (to NASA), Wendy Sue Alter, inventor (to NASA), and William David Hamilton, inventor (to NASA) 23 Oct. 1990 6 p Filed 7 Sep. 1989
(NASA-Case-MFS-28314-1; US-Patent-4,964,453;
US-Patent-Appl-SN-404289; US-Patent-Class-164-122.1;
US-Patent-Class-164-338.1; Int-Patent-Class-B22D-27/04) Avail: US Patent and Trademark Office CSCL 11F

This invention relates to the directional solidification of superalloys, in particular nickel-based superalloys, by imposition of a predetermined temperature profile in the solidification front and, depending on the desired results, a predetermined rate of advance of said solidification front, whereas castings of markedly superior fatigue resistance are produced.
Official Gazette of the U.S. Patent and Trademark Office

N91-14463# Bristol Univ. (England). Dept. of Inorganic Chemistry.
HETERONUCLEAR METAL CLUSTER COMPOUNDS SYNTHESIS AND REACTIVITY Final Report, Mar. 1986 - Jul. 1990
F. G. Stone 10 Aug. 1990 22 p
(Grant AF-AFOSR-0125-86; AF Proj. 2303)
(AD-A226815; AFOSR-90-0960TR) Avail: NTIS HC/MF A03 CSCL 07/2

This final report describes the synthesis and characterisation of compounds containing metal-metal bonds between dissimilar transition elements. The new compounds reported included species with chains or rings of metal atoms, involving tungsten or molybdenum bonded to the elements nickel, platinum, rhodium, or iridium. The report also describes numerous mixed-metal compounds in which the metal-metal bonds are bridged by the carbaborane group C2B9H9R2 (R = H or Me). A variety of unprecedented molecular structures have been identified by x ray crystallographic studies. GRA

N91-14464# Naval Postgraduate School, Monterey, CA.
AN EXAMINATION OF DELTA PRIME GROWTH IN AN ALUMINUM-LITHIUM ALLOY BY X RAY DIFFRACTION M.S. Thesis
Clark E. Whitman Mar. 1990 58 p
(AD-A227254) Avail: NTIS HC/MF A04 CSCL 11/6

A previously manufactured hot rolled sheet of Al-Li-Zr alloy of composition Al(2.5 percent)-Li(.15 percent)- Zr, by weight, was solution treated and artificially aged at 194 C from 0 to 32 hours. X ray diffraction analysis of the alloy was conducted to observe the growth characteristics of the delta prime precipitate (the

precipitate hardening phase). Transmission electron microscopy was used to verify x ray results. Significant superlattice intensity and line broadening occurred in the as-quenched sample. This observation supports a possible order/disorder reaction and a spinodal decomposition as opposed to the typical nucleation and precipitation reaction usually observed in a precipitation hardened alloy. The Scherrer equation was used to determine delta prime particle size from diffraction line broadening, and this size was found to coarsen following conventional Ostwald ripening theory once the initial effects of the spinodal had aged out. The delta phase (considered cause of low toughness) was observed in the as quenched sample and throughout the heat treatment. It was surmised that this may be the origin of he low-short transverse fracture toughness which is typical of some of these alloys.

GRA

N91-14465# Naval Postgraduate School, Monterey, CA.
PROCESSING STUDIES OF ALUMINUM-MAGNESIUM AND ALUMINUM-COPPER-LITHIUM ALLOYS M.S. Thesis
Frank J. Harsacky, Jr. Mar. 1990 86 p
(AD-A227255) Avail: NTIS HC/MF A05 CSCL 11/4

Investigation into the effect on superplastic behavior of two aluminum alloys produced by variations of thermomechanical processing parameters was conducted. The alloys in this study are Al-10Mg-0.1Zr (weight percent) and 2090, which is Al-2.56Cu-2.03Li-0.12Zr (weight percent). Determination of the existence of an optimum balance between deformation and recovery for the Al-10Mg-0.1Zr alloy was accomplished by extending the annealing interval to 60 minutes during warm rolling at 300 C. The optimum balance is a 30 minute annealing interval between rolling passes. Processing of Al-10Mg-0.1Zr with a rolling temperature lower than the annealing temperature produced ductilities which are less than those obtained by utilization of the optimum process. The extension of annealing intervals in the processing of 2090 resulted in increased superplastic response when compared with results obtained employing shorter annealing intervals. By application of a two-temperature process which incorporates rolling at a lower temperature than the annealing temperature, the determination has been made that enhanced ductility results however, the annealing interval of 14 minutes should be extended.

GRA

N91-14466# Ames Lab., IA.
APPLICATION OF ULTRASONIC GUIDED WAVES TO THE CHARACTERIZATION OF TEXTURE IN METAL SHEETS OF CUBIC AND HEXAGONAL CRYSTALLITES Ph.D. Thesis - Iowa State Univ.
Yan Li Oct. 1990 251 p
(Contract W-7405-eng-82)
(DE91-001107; IS-T-1515) Avail: NTIS HC/MF A12

Ultrasonic techniques have recently been applied to the texture characterization in polycrystalline aggregates of hexagonal crystals. The basis of this application lies in the relations between the elastic constants of the aggregates, which can be inferred from ultrasonic wave velocity measurements and the orientation distribution coefficients. This communication presents such relations for aggregates which possess orthotopic material symmetry and hexagonal crystal symmetry for Voigt, Reuss, and Hill averaging methods in a unified and concise representation.

DOE

N91-14467# Oak Ridge National Lab., TN. Metals and Ceramics Div.
EFFECTS OF IRRADIATION ON INITIATION AND CRACK-ARREST TOUGHNESS OF TWO HIGH-COPPER WELDS AND ON STAINLESS STEEL CLADDING
Randy K. Nanstad, Shafik K. Iskander, and Fahmy M. Haggag 1990 19 p Presented at the 16th MPA Seminar, Stuttgart, Fed. Republic of Germany, 4-5 Oct. 1990
(Contracts DE-AC05-84OR-21400; DOE-1886-8189-8L)
(DE91-001272; CONF-9010217-1) Avail: NTIS HC/MF A03

The objective of the study on the high-copper welds is to determine the effect of neutron irradiation on the shift and shape of the ASME K(sub Ic) and K(sub Ia) toughness curves. Two submerged-arc welds with copper contents of 0.23 and 0.31 wt percent were commercially fabricated in 220 mm-thick plate. Compact specimens fabricated from these welds were irradiated at a nominal temperature of 288 C to fluences from 1.5 to 1.9x10(exp 19) neutrons/sq cm (less than 1 MeV). The fracture toughness test results show that the irradiation-induced shifts at 100 MPa/m were greater than the Charpy 41-J shifts by about 11 and 18 C. Mean curve fits indicate mixed results regarding curve shape changes, but curves constructed as lower boundaries to the data do indicate curves of lower slopes. A preliminary evaluation of the crack-arrest results shows that the neutron-irradiation induced crack-arrest toughness temperature shift is about the same as the Charpy V-notch impact temperature shift at the 41-J energy level. The shape of the lower bound curves (for the range of test temperatures covered), compared to those of the ASME K(sub Ia) curve did not appear to have been altered by the irradiation. Three-wire stainless steel weld overlay cladding was irradiated at 288 C to fluences of 2 and 5x10(exp 19) neutrons/sq cm (less than 1 MeV) Charpy 41-J temperature shifts of 13 and 28 C were observed, respectively. For the lower fluence only, 12.7-mm thick compact specimens showed decreases in both J(sub Ic) and the tearing modulus. Comparison of the fracture toughness results with typical plate and a low upper-shelf weld reveals that the irradiated stainless steel cladding possesses low ductile initiation fracture toughness comparable to the low upper-shelf weld.

DOE

N91-14468# Westinghouse Hanford Co., Richland, WA.
CORROSION BEHAVIOR OF COPPER-BASE MATERIALS IN A GAMMA-IRRADIATED ENVIRONMENT Final Report
Wayne H. Yunker Sep. 1990 115 p
(Contract DE-AC06-87RL-10930)
(DE91-001286; WHC-EP-0188) Avail: NTIS HC/MF A06

Specimens of three copper-base materials were corrosion tested with gamma radiation exposure dose rates in the range of 1.9x10(exp 3) R/h to 4.9x10(exp 5) R/h. Materials used were pure copper, 7 percent aluminum bronze and 30 percent copper-nickel. Exposures were performed in moist air at 95 C and 150 C and liquid well water (J-13) at 95 C, for periods of up to 16 months. Specimens were monitored for uniform weight loss, stress-induced corrosion and crevice corrosion. Specimen surfaces were examined visually at 10X magnification as well as by auger electron spectroscopy, x ray diffraction, and metallography. Corrosion was not severe in any of the cases. In general, the pure copper was corroded most uniformly while the copper-nickel was the least reproducibly corroded.

DOE

N91-14469# Sandia National Labs., Albuquerque, NM.
AMORPHIZATION OF C-IMPLANTED Fe(Cr) ALLOYS
J. A. Knapp, D. M. Follstaedt, N. R. Sorensen, and L. E. Pope 1990 13 p Presented at the 7th International Conference on Ion Beam Modification of Materials, Knoxville, TN, 9-14 Sep. 1990
(Contract DE-AC04-76DP-00789)
(DE91-001338; SAND-90-1068C; CONF-900936-15) Avail: NTIS HC/MF A03

The amorphous phase formed by implanting C into Fe alloyed with Cr, which is prototype for the amorphous phase formed by implanting C into stainless steels, is compared to that formed by implanting C plus Ti into Fe and steels. The composition range of the phase has been examined; higher Cr and C concentrations are required than needed with Ti and C. The friction and wear benefits obtained by implanting stainless steels with C alone do not persist for the long durations and high wear loads found with Ti and C. However, the amorphous Fe-Cr-C alloys exhibits good aqueous corrosion resistance.

DOE

N91-14470# Pacific Northwest Lab., Richland, WA.
RADIATION RESISTANCE OF COPPER ALLOYS AT HIGH EXPOSURE LEVELS
F. A. Garner and Steven J. Zinkle (Oak Ridge National Lab., TN.) Aug. 1990 17 p Presented at the Conference on the Effect of

Irradiation on Materials of Fusion Reactors, Leningrad, USSR, 18-20 Sep. 1990
(Contracts DE-AC06-76RL-01830; DE-AC05-84OR-21400)
(DE91-001563; PNL-SA-18576; CONF-9009264-2) Avail: NTIS HC/MF A03

Copper alloys are currently being considered for high heat flux applications in fusion power devices. A review is presented of the results of two separate series of experiments on the radiation response of copper and copper alloys. One of these involved pure copper and boron-doped copper in the ORR mixed spectrum reactor. The other series included pure copper and a wide array of copper alloys irradiated in the FFTF fast reactor. DOE

N91-14471# Northwestern Univ., Evanston, IL.
USE OF ANOMALOUS SMALL ANGLE X RAY SCATTERING TO INVESTIGATE MICROSTRUCTURAL FEATURES IN COMPLEX ALLOYS Technical Progress Report, 1 Aug. 1989 - 1 Aug. 1990
J. R. Weertman Aug. 1990 20 p
(Contract DE-FG02-86ER-45229)
(DE91-002397; DOE/ER-45229/T3) Avail: NTIS HC/MF A03

The research thrust has been directed into two areas. The principal effort has been spent in an investigation of the use of anomalous small angle x ray scattering (ASAXS) to observe changes in the microstructure of a relatively complex alloy produced by high temperature deformation or aging. A second effort involves a study of the high temperature behavior of several ferritic steels. In particular, we are investigating the precursors and earliest stages of fatigue crack initiation, especially how initiation is affected by hold times and by environment. We have been studying carbides in two ferritic steel alloys. The first is Fe9CrlMo modified by the addition of small amounts of the strong carbide formers, V and Nb. This alloy, which has been studied at ORNL and in the course of this grant, is used in power-generating equipment. The second alloy is AF1410 (primarily Fel4Col0Ni), an ultra high-strength, high toughness steel. DOE

N91-14472# Argonne National Lab., IL. Materials Science Div.
ION-INDUCED GRAIN GROWTH IN MULTILAYER AND COEVAPORATED METAL ALLOY THIN FILMS
D. E. Alexander, G. S. Was (Michigan Univ., Ann Arbor.), and L. E. Rehn Sep. 1990 10 p Presented at the 7th International Conference on Ion Beam Modification of Materials, Knoxville, TN, 9-14 Sep. 1990
(Contract W-31-109-eng-38; NSF DMR-86-03174; NSF DMR-89-03138)
(DE91-004489; CONF-900936-22) Avail: NTIS HC/MF A02

Irradiation experiments were conducted on multilayer (ML) and coevaporated (CO) thin films in order to examine the role that the heat of mixing (Del H sub mix) has in ion-induced grain growth. Room temperature irradiations using 1.7 MeV Xe were performed in the High Voltage Electron Microscope at Argonne National Laboratory. The alloys studied (Pt-Ti, Pt-V, Pt-Ni, Au-Co and Ni-Al) spanned a large range of Del H sub mix values. Comparison of grain growth rates between ML and CO films of a given alloy confirmed a heat of mixing effect. Differences in grain growth rates between ML and CO films scaled according to the sign and magnitude of Del H sub mix of the system (with exception of the Pt-V system). Substantial variations in growth rates among CO alloy films experiencing similar irradiation damage demonstrated that a purely collisional approach is inadequate for describing ion-induced grain growth and consideration must also be given to material-specific properties. Results from CO alloy films were consistent with a thermal spike model of ion-induced grain growth. The grain boundary mobility was observed to be proportional to the thermal spike-related parameter, (F sub D(exp 2))/(Del H sub coh)(exp 3), where F sub D is the deposited damage energy and Del H sub coh is the cohesive energy. DOE

N91-14473# Sandia National Labs., Albuquerque, NM.
FLOW BEHAVIOR OF Ti-24Al-11Nb AT HIGH STRAIN RATES
L. S. Harbison, D. A. Koss (Pennsylvania State Univ., University Park.), and R. J. Bourcier 1990 19 p Presented at the TMS Symposium on Microstructure/Property Relationships in Titanium Alloys and Titanium Aluminides, Detroit, MI, 7-11 Oct. 1990
(Contracts DE-AC04-76DP-00789; SNL-06-9583)
(DE91-004506; SAND-90-2909C; CONF-9010258-1) Avail: NTIS HC/MF A03

The deformation and crack initiation behavior of Ti-24Al-11Nb has been examined over a temperature range of 298 to 923 K and for strain rates from 10(exp -4)/s to 10(exp 2)/s. Tests performed in compression indicate much lower strain hardening at 10(exp 2)/s than at either 10(exp -1)/s or 10(exp -4)/s at all temperatures. Associated with this behavior is the occurrence of non-uniform, localized deformation bands at 10(exp 2)/s. An analysis indicates that adiabatic deformation conditions predominate at 10(exp 2)/s and that these result in adiabatic softening. Furthermore, as a result of non-uniform deformation and adiabatic heating, this Ti3-Al-based alloy is actually more resistant to strain-induced microcrack initiation at 10(exp 2)/s than at 10(exp -4)/s during room temperature testing. DOE

N91-14474*# Virginia Univ., Charlottesville. Dept. of Materials Science.
NASA-UVA LIGHT AEROSPACE ALLOY AND STRUCTURES TECHNOLOGY PROGRAM Progress Report, 1 Jan. - 30 Jun. 1989
Richard P. Gangloff, John K. Haviland, Carl T. Herakovich, Walter D. Pilkey, Marek-Jerzy Pindera, Earl A. Thornton, Glenn E. Stoner, Robert E. Swanson (Virginia Polytechnic Inst. and State Univ., Blacksburg.), Franklin E. Wawner, Jr., and John A. Wert Aug. 1989 169 p
(Grant NAG1-745)
(NASA-CR-187321; NAS 1.26:187321; UVA/528266/MS90/104)
Avail: NTIS HC/MF A08 CSCL 11F

The report on progress achieved in accomplishing of the NASA-UVA Light Aerospace Alloy and Structures Technology Program is presented. The objective is to conduct interdisciplinary graduate student research on the performance of next generation, light weight aerospace alloys and associated thermal gradient structures in close collaboration with researchers. The efforts will produce basic understanding of material behavior, new monolithic and composite alloys, processing methods, solid and fluid mechanics analyses, measurement advances, and a pool of educated graduate students. The presented accomplishments include: research on corrosion fatigue of Al-Li-Cu alloy 2090; research on the strengthening effect of small In additions to Al-Li-Cu alloys; research on localized corrosion of Al-Li alloys; research on stress corrosion cracking of Al-Li-Cu alloys; research on fiber-matrix reaction studies (Ti-1100 and Ti-15-3 matrices containing SCS-6, SCS-9, and SCS-10 fibers); and research on methods for quantifying non-random particle distribution in materials that has led to generation of a set of computer programs that can detect and characterize clusters in particles. Y.S.

27 NONMETALLIC MATERIALS

Includes physical, chemical, and mechanical properties of plastics, elastomers, lubricants, polymers, textiles, adhesives, and ceramic materials.

For composite materials see *24 Composite Materials.*

N91-14475*# Michigan Univ., Ann Arbor. Radiation Lab.
[TASK REPORTS ON DEVELOPING TECHNIQUES FOR SCATTERING BY 3D COMPOSITE STRUCTURES AND TO GENERATE NEW SOLUTIONS IN DIFFRACTION THEORY USING HIGHER ORDER BOUNDARY CONDITIONS] Semiannual Report, Feb. - Sep. 1990
John L. Volakis Sep. 1990 73 p
(Grant NAG2-541)
(NASA-CR-186899; NAS 1.26:186899; UMICH-025921-13-T)
Avail: NTIS HC/MF A04 CSCL 11C

There are two tasks described in this report. First, an extension of a two dimensional formulation is presented for a three dimensional body of revolution. With the introduction of a Fourier

expansion of the vector electric and magnetic fields, a coupled two dimensional system is generated and solved via the finite element method. An exact boundary condition is employed to terminate the mesh and the fast fourier transformation is used to evaluate the boundary integrals for low O(n) memory demand when an iterative solution algorithm is used. Second, the diffraction by a material discontinuity in a thick dielectric/ferrite layer is considered by modeling the layer as a distributed current sheet obeying generalized sheet transition conditions (GSTC's). For individual titles, see N91-14476 through N91-14477.

N91-14476*# Michigan Univ., Ann Arbor. Radiation Lab.
A FINITE ELEMENT CONJUGATE GRADIENT FFT METHOD FOR SCATTERING
Jeffery D. Collins, John Zapp, Chang-Yu Hsa, and John L. Volakis *In its* Task Reports on Developing Techniques for Scattering by 3D Composite Structures and to Generate New Solutions in Diffraction Theory Using Higher Order Boundary Conditions Sep. 1990 24 p (For primary document see N91-14475 06-27)
Avail: NTIS HC/MF A04 CSCL 11C

An extension of a two dimensional formulation is presented for a three dimensional body of revolution. With the introduction of a Fourier expansion of the vector electric and magnetic fields, a coupled two dimensional system is generated and solved via the finite element method. An exact boundary condition is employed to terminate the mesh and the fast fourier transformation (FFT) is used to evaluate the boundary integrals for low O(n) memory demand when an iterative solution algorithm is used. By virtue of the finite element method, the algorithm is applicable to structures of arbitrary material composition. Several improvements to the two dimensional algorithm are also described. These include: (1) modifications for terminating the mesh at circular boundaries without distorting the convolutionality of the boundary integrals; (2) the development of nonproprietary mesh generation routines for two dimensional applications; (3) the development of preprocessors for interfacing SDRC IDEAS with the main algorithm; and (4) the development of post-processing algorithms based on the public domain package GRAFIC to generate two and three dimensional gray level and color field maps. Author

N91-14477*# Michigan Univ., Ann Arbor. Radiation Lab.
ANALYTICAL SOLUTIONS WITH GENERALIZED IMPEDANCE BOUNDARY CONDITIONS (GIBC)
Mark A. Ricoy and John L. Volakis *In its* Task Reports on Developing Techniques for Scattering by 3D Composite Structures and to Generate New Solutions in Diffraction Theory Using Higher Order Boundary Conditions Sep. 1990 43 p (For primary document see N91-14475 06-27)
Avail: NTIS HC/MF A04 CSCL 11C

The diffraction by a material discontinuity in a thick dielectric/ferrite layer is considered by modeling the layer as a distributed current sheet obeying generalized sheet transition conditions (GSTC's). The sheet currents are then formulated and solved via the standard dual integral equation approach. This yields the diffracted field in terms of unknown constants which underscore the non-uniqueness of the GSTC current sheet representation. The constants are dependent on the geometry and properties of the discontinuity and are determined by enforcing field continuity across the material junction. This requires the field internal to the slab which are determined from the external ones via analytic continuity. Results are given which validate the solution and demonstrate the importance of the constants. Author

N91-14478 Department of the Navy, Washington, DC.
FABRICATION BY FILAMENT WINDING WITH AN ELASTOMERIC MATERIAL Patent
Wayne H. Nakamura, inventor (to Navy) 1 May 1990 8 p Filed 13 Jul. 1988
(AD-D014570; US-Patent-4,921,557; US-Patent-Appl-SN-209143; US-Patent-Class-156-169) Avail: US Patent and Trademark Office CSCL 11/4

This patent discloses an invention that relates in general to fabricating fiber-reinforced membranes using elastometric materials and, in particular, to a filament winding process suitable for fabricating flexible fiber-reinforced membranes for inflatable deployable or expandable structures capable of sustaining high structural loads or providing thermal insulation to the structure. The invention relates especially to a filament winding process for fabricating a flexible membrane which may be inflated to provide a flexible membrane which may be inflated to provide a conically shaped deployable nose fairing for a missile. GRA

N91-14479# Department of the Navy, Washington, DC.
METHOD OF GROWING DIAMOND FILM ON SUBSTRATES Patent Application
Arthur A. Morrish, inventor (to Navy), Paul M. Natishan, inventor (to Navy), and William A. Carrington, inventor (to Navy) 30 Apr. 1990 27 p
(AD-D014632; US-Patent-Appl-SN-516585) Avail: NTIS HC/MF A03 CSCL 11/3

The deposition of diamond on a substrate is enhanced by coating the substrate surface with a thin layer of carbon before deposition. Preferably, the substrate is scratched before being coated with diamond. The carbon layer may be formed by applying an oil coating to the substrate and then heating the substrate to carbonize the coating, or by the evaporative deposition of carbon. GRA

N91-14480# Sandia National Labs., Albuquerque, NM.
ADHESION AT CERAMIC INTERFACES
T. A. Michalske, J. E. Houston, and S. A. Joyce 1990 3 p Presented at the Frontiers of Chemistry: Materials By Design, Columbus, OH, 12-14 Nov. 1990
(Contract DE-AC04-76DP-00789)
(DE91-001660; SAND-90-2557C; CONF-9011123-1) Avail: NTIS HC/MF A01

Many of the properties associated with ceramic materials such as high hardness, high dielectric constant, refractoriness, and good optical properties will play a critical role in the development of devices for new and emerging technologies. In many cases, the combination of properties that is required demands that a composite material be designed to fulfill these complex materials needs. The increasing emphasis upon composite materials design and performance necessarily focuses greater attention upon the structure and properties of interfaces in ceramic materials. One on the most important aspects of interfacial behavior is the adhesive stability. As an example, high hardness ceramic coatings for tribological applications require a high degree of interfacial adhesion with the underlying substrate material. Alternatively it has been shown that fiber reinforced ceramic composites that are designed for high fracture toughness must contain weak interfaces that allow for fiber pull-out to toughen the instrinsically brittle ceramic matrix. Our ability to design ceramic interfaces for specific interfacial adhesive behavior dictates that we develop a full understanding of the factors that control the adhesive bond in these systems. We report on the use of continuum fracture mechanics techniques to identify the molecular source of adhesion between oxide surfaces and introduce a new approach to measuring interfacial adhesive forces using an Interfacial Force Microscope. DOE

N91-14481# Lawrence Livermore National Lab., CA.
COMPUTER STUDIES OF THE DYNAMIC STRENGTH OF CERAMICS
Daniel Steinberg 24 Sep. 1990 25 p
(Contract W-7405-eng-48)
(DE91-002568; UCRL-ID-106004) Avail: NTIS HC/MF A03

Using a new constitutive model, we performed computer studies concerning the dynamic yield strength of six ceramics, SiC, TiB2 AlN, two types of B4C, and partially stabilized zirconia. The relative importance of the thermomechanical variables, strain, strain-rate, pressure, and temperature, as well as the Bauschinger effect, is demonstrated in determining the time response of ceramics to high-train-rate deformation. The constitutive model is easy to implement in a hydrodynamic computer code, and it successfully reproduces a variety of data for these six materials. DOE

N91-14482*# National Aeronautics and Space Administration. Lewis Research Center, Cleveland, OH.
EFFECT OF HYDROGEN ON THE STRENGTH AND MICROSTRUCTURE OF SELECTED CERAMICS
Thomas P. Herbell, Andrew J. Eckel, David R. Hull, and Ajay K. Misra (Sverdrup Technology, Inc., Brook Park, OH.) 1990 16 p Presented at the Fall Meeting of the Metallurgical Society, Detroit, MI, 7-11 Oct. 1990
(NASA-TM-103674; E-5702; NAS 1.15:103674) Avail: NTIS HC/MF A03 CSCL 11C

Ceramics in monolithic form and as composite constituents in the form of fibers, matrices, and coatings are currently being considered for a variety of high-temperature applications in aeronautics and space. Many of these applications involve exposure to a hydrogen-containing environment. The compatibility of selected ceramics in gaseous high-temperature hydrogen is assessed. Environmental stability regimes for the long term use of ceramic materials are defined by the parameters of temperature, pressure, and moisture content. Thermodynamically predicted reactions between hydrogen and several monolithic ceramics are compared with actual performance in a controlled environment. Morphology of hydrogen attack and the corresponding strength degradation is reported for silicon carbide, silicon nitride, alumina, magnesia, and mullite. Author

N91-14483*# Old Dominion Univ., Norfolk, VA. Dept. of Electrical and Computer Engineering.
STUDY OF DIAMOND FILM GROWTH AND PROPERTIES Final Report, period ending 5 Jul. 1989
Sacharial Albin Dec. 1990 40 p
(Grant NAG1-791)
(NASA-CR-187709; NAS 1.26:187709) Avail: NTIS HC/MF A03 CSCL 11C

The objective was to study diamond film growth and its properties in order to enhance the laser damage threshold of substrate materials. Calculations were performed to evaluate laser induced thermal stress parameter, R(sub T) of diamond. It is found that diamond has several orders of magnitude higher in value for R(sub T) compared to other materials. Thus, the laser induced damage threshold (LIDT) of diamond is much higher. Diamond films were grown using a microwave plasma enhanced chemical vapor deposition (MPECVD) system at various conditions of gas composition, pressure, temperature, and substrate materials. A 0.5 percent CH4 in H2 at 20 torr were ideal conditions for growing of high quality diamond films on substrates maintained at 900 C. The diamond films were polycrystalline which were characterized by scanning electron microscopy (SEM) and Raman scattering spectroscopy. The top surface of the growing film is always rough due to the facets of polycrystalline film while the back surface of the film replicates the substrate surface. An analytical model based on two dimensional periodic heat flow was developed to calculate the effective in-plane (face parallel) diffusivity of a two layer system. The effective diffusivity of diamond/silicon samples was measured using a laser pulse technique. The thermal conductivity of the films was measured to be 13.5 W/cm K, which is better than that of a type Ia natural diamond. Laser induced damage experiments were performed on bare Si substrates, diamond film coated Si, and diamond film windows. Significant improvements in the LIDT were obtained for diamond film coated Si compared to the bare Si. Author

N91-14484* National Aeronautics and Space Administration. Langley Research Center, Hampton, VA.
PROCESS FOR LOWERING THE DIELECTRIC CONSTANT OF POLYIMIDES USING DIAMIC ACID ADDITIVES Patent
Diane M. Stoakley, inventor (to NASA) and Anne K. St.Clair, inventor (to NASA) 23 Jan. 1990 7 p Filed 1 Sep. 1988
(NASA-Case-LAR-13902-1; US-Patent-4,895,972; US-Patent-Appl-SN-239259; US-Patent-Class-528-353; US-Patent-Class-528-125; US-Patent-Class-528-126; US-Patent-Class-528-128; US-Patent-Class-528-172; US-Patent-Class-528-185; US-Patent-Class-528-188) Avail: US Patent and Trademark Office CSCL 11C

Linear aromatic polyimides with low dielectric constants are produced by adding a diamic acid additive to the polyamic acid resin formed by the condensation of an aromatic dianhydride with an aromatic diamine. The resulting modified polyimide is a better electrical insulator than state-of-the-art commercially available polyimides.
Official Gazette of the U.S. Patent and Trademark Office

N91-14485# Lowell Univ., MA. Dept. of Chemistry and Physics.
APPROACHES TO THE DESIGN OF A NOVEL MACROMOLECULAR SYSTEM WITH TAILORED OPTICAL PROPERTIES
Sukant Tripathy, Jayant Kumar, R. Sal Kumar, and A. Blumstein 1990 20 p Submitted for publication
(Contract N00014-90-J-1148)
(AD-A226952; TR-6) Avail: NTIS HC/MF A03 CSCL 09/6

A systematic approach towards the development of polymeric nonlinear optical material has been presented. The optimally designed functional molecular elements are carefully assembled to incorporate large second and third order optical nonlinearities, paying attention to the processing needs. Preliminary results from the measurement of the optical properties is also presented. GRA

N91-14486# Walowit (Jed A.), Inc., Clifton Park, NY.
A CONTINUUM APPROACH TOWARD MODELING THE MECHANICS OF SOLID LUBRICATING FILMS Final Report, Mar. - Sep. 1990
Jed A. Walowit 21 Sep. 1990 55 p
(Contract N00014-90-C-0087)
(AD-A226961; JAW-90-TR-1) Avail: NTIS HC/MF A04 CSCL 11/8

Analyses are developed to predict the tractive forces that will occur in a rolling-sliding contact between one body of a single material and a second body containing a thin coating of solid lubricant. Isotropic materials and conditions of plane strain are assumed. The loaded coating thickness is taken to be large compared with asperity heights but small compared with contact dimensions. Contact pressures are assumed to be high compared with the shear yield stress of the coating which in turn is taken to be small compared with those of the substrates. An initial analysis is presented for approximating tractions under conditions of low slide to roll ratios which includes elastic, plastic, creep and thermal interactions. This analysis implements an approach developed for elastohydrodynamic lubrication at pressures and shear rates where the lubricant exhibits solid-like behavior but is oriented toward solid lubrication and includes a more extensive thermal analysis. Solutions are presented which show the influence of elastic modulus, rheological model, yield stress and pressure and temperature dependence of mechanical properties on predicted traction and shear stress behavior. An analysis is presented which reduces the Levy-Von Mises equations for a plastic-rigid system so as to approximate thin film behavior under conditions of high slip rate. This analysis shows the expected development of a nearly hydrostatic state of stress for the coating in the contact zone but also shows that the film cannot support a pressure gradient when yielding occurs inside the coating. GRA

N91-14487# Ultrasystems Defense and Space Systems, Inc., Irvine, CA. Dept. of Chemicals and Materials.
HETEROCYCLES BASED ON GROUP 3, 4, AND 5 ELEMENTS: PRECURSORS FOR NOVEL GLASSES AND CERAMICS Final Report, 1 Mar. 1985 - 28 Feb. 1990
K. L. Paciorek, J. H. Nakahara, S. R. Masuda, J. G. Shih, L. A. Hoferkamp, and R. H. Kratzer Aug. 1990 130 p
(Contract F49620-85-C-0042)
(AD-A226988; SN-3503-F; AFOSR-90-0917TR) Avail: NTIS HC/MF A07 CSCL 09/1

The general objective was to explore the feasibility of synthesizing novel heterocyclics from the group of elements consisting of Boron, Carbon, Nitrogen, Aluminum, Silicon, and Phosphorous, the ultimate goal being the production of processible precursors for novel ceramics of unusual properties. The major

efforts were devoted to development of processible preceramic systems leading to aluminum nitride and multi-element nitride ceramics and ceramic materials. Aluminum nitride, in view of its high thermal conductivity, among other considerable properties, is of the interest in electronic applications, in particular in packaging of electronic microcircuits. GRA

N91-14488# Technion Research and Development Foundation Ltd., Haifa (Israel).
ELECTROPHORETIC AND ELECTROLYTIC DEPOSITION OF CERAMIC PARTICLES ON POROUS SUBSTRATES Annual Report, 1 Jul. 1989 - 30 Jun. 1990
L. Gal-Or, S. Haber, and S. Liubovich 30 Aug. 1990 94 p
(Grant AF-AFOSR-0474-89; AF Proj. 2306)
(AD-A227371; AFOSR-90-1047TR) Avail: NTIS HC/MF A05
CSCL 11/2

Electrophoretic deposition of ceramic particles on porous graphite and their penetration into the pores was demonstrated and studied both theoretically and experimentally. The theoretical analysis enables us to predict the penetration depth of the particles as function of two non-dimensional parameters based on solvent properties, field strength and particle size and concentration. In the experimental studies the amount of induced material was found to increase with the ratio of dielectric constant to viscosity of the solvent, as well as with particle concentration and field intensity. However, due to simultaneous buildup of an overlying deposit penetration as function of deposition time reaches a plateau. In parallel studies on electrolytic deposition, ZrO2 coatings were deposited on porous graphite from an aqueous solution of ZrO(NO3)2. The deposition kinetics and microstructure of the deposit were studied. The initial amorphous deposits transformed into crystalline ZrO2 polymorphs with nanocrystalline dimensions following heat treatment. GRA

N91-14489* National Aeronautics and Space Administration. Pasadena Office, CA.
HIGH TEMPERATURE REFRACTORY MEMBER WITH RADIATION EMISSIVE OVERCOAT Patent
William D. Deininger, inventor (to NASA) and David Q. King, inventor (to NASA) (Jet Propulsion Lab., California Inst. of Tech., Pasadena.) 22 May 1990 6 p Filed 20 Aug. 1987
(NASA-Case-NPO-17122-1-CU; US-Patent-4,928,027; US-Patent-Appl-SN-087376; US-Patent-Class-310-11; Int-Patent-Class-H02K-44/10) Avail: US Patent and Trademark Office CSCL 11C

A radiation type heat dissipator for use in a plasma engine is formed of a refractory metal layer upon which there is deposited a radiation emissive coating made of a high emissivity material such as zirconium diboride. The radiation emissive coating has a surface emissivity coefficient substantially greater than the emissivity coefficient of the refractory metal and thereby enhances the optical radiating efficiency of the heat dissipator.
Official Gazette of the U.S. Patent and Trademark Office

N91-14490# Los Alamos National Lab., NM.
NEW MULTIPHASE EQUATION OF STATE FOR POLYCRYSTALLINE QUARTZ
J. C. Boettger and S. P. Lyon Oct. 1990 14 p
(Contract W-7405-eng-36)
(DE91-001048; LA-11918-MS) Avail: NTIS HC/MF A03

We have generated separate equations of state (EOS's) for the alpha quartz, coesite, and stishovite phases of polycrystalline quartz, SiO2, using the computer program GRIZZLY. We also modified the program GRIZZLY to combine two single-phase EOS's for a given material into a single two-phase EOS via minimization of the Gibbs free energy. This new version of GRIZZLY has been used to generate a three-phase SESAME type EOS for polycrystalline quartz using the three EOS's mentioned above. All four of the EOS's produced for SiO2 are now available on request. DOE

N91-14491# Brandeis Univ., Waltham, MA.
SYNTHESIS AND PROPERTIES OF NOVEL ORGANOMETALLIC POLYMERS Final Report, 7 Mar. 1985 - 6 May 1990
31 May 1990 9 p
(Contract DE-FG02-85ER-45193)
(DE91-001978; DOE/ER-45193/1) Avail: NTIS HC/MF A02

A 1,1'-Diruthenocenylnaphthalene compound was prepared and its molecular structure has been determined by x ray diffraction, in order to compare its structure with that of its iron analog. The molecular structure of the half oxidized form of 1,1'-diferocenylnaphthalene has also been determined. Comparison of these structures has made it possible to assign the origins of observed deformations in these substances. Polymeric, face-to-face metallocenes related to the 1,8-dimetallocenylnaphthalenes (M=Fe, Ru) have also been prepared by coupling of 1,1'-bis(chlorozinc)metallocenes with 1,8- diiodonaphthalene. A more general approach to the synthesis of polymeric face-to-face metallocenes incorporating other transition metals has been developed. This involves the sequential replacement of iodo groups in 1,8-diiodonaphthalene with cyclopentadiene and the complexation of these rings with metals. A short synthesis of 4-n-butyl-1,8-diiodonaphthalene has been achieved. The molecular structure of a 2,3-oligomeric face-to-face ferrocene has been determined and shown to have the unexpected cis arrangement of naphthalene rings. DOE

N91-14492# EG and G Mound Applied Technologies, Miamisburg, OH.
CHARACTERIZATION OF PHENOLIC RESINS WITH THERMOGRAVIMETRY-MASS SPECTROMETRY
Cherng Chang and Juanita R. Tackett 1990 12 p Presented at the 19th Annual North American Thermal Analysis Society Conference, Boston, MA, 23-26 Sep. 1990
(Contract DE-AC04-88DP-43495)
(DE91-002710; MLM-3668(OP); CONF-9009223-4) Avail: NTIS HC/MF A03

As part of an advanced material research program, thermogravimetry-mass spectrometry (TG-MS) analysis of a phenolic resin was carried out recently for the study of the curing of the prepolymer, solvent extraction, and carbonization of the polymer at high temperature in inert atmosphere. These steps are critical to the quality of the produced advanced material. In addition to TG-MS, several other complementary techniques were also employed for the analysis of the phenolic resin prepolymer and its curing and thermal degradation products. These techniques include pyrolysis-gas chromatography-mass spectrometry, direct insertion probe-mass spectrometry and gas chromatography-mass spectrometry. DOE

N91-14493# Sandia National Labs., Albuquerque, NM.
KINETICS OF MOLECULAR BEAM EPITAXY: EFFECT OF ION-INDUCED SPUTTERING
Peter M. Richards 1990 13 p Presented at the Fall Meeting of the Materials Research Society, Boston, MA, 24 Nov. - 1 Dec. 1990
(Contract DE-AC04-76DP-00789)
(DE91-004511; SAND-90-2884C; CONF-901105-25) Avail: NTIS HC/MF A03

Steady state roughness of surfaces growing by molecular beam epitaxy is investigated by Monte Carlo simulations under conditions where an ion beam is also present which sputters adatoms off the surface. If the sputtering is random, it only increases the roughness. But if the sputtering probability is strongly dependent on the binding energy of an adatom within a cluster or island, the ions can have a smoothening effect. Physical arguments are given in support of the results. DOE

N91-14494*# National Aeronautics and Space Administration. Goddard Space Flight Center, Greenbelt, MD.
AN EVALUATION OF TWO FLAT-BLACK SILICONE PAINTS FOR SPACE APPLICATION
Carroll H. Clatterbuck and John J. Scialdone Washington Dec.

1990 23 p
(NASA-TM-100768; Rept-91E00700; NAS 1.15:100768) Avail: NTIS HC/MF A03 CSCL 11C

Tests were conducted on two flat-black silicone paints suggested for space applications to determine their optical, electrical, and mechanical properties. Three different types of substrate materials were chosen for these paint tests; the application of the paints onto the primed substrates was carried out by spray coating. The adhesion properties were verified by thermal shock and sudden immersion into liquid nitrogen. A controlled thermal vacuum tests was also carried out by varying the temperature of the paint from -100 to 225 C. The measured optical properties included normal and hemispherical emittance, and solar absorption/reflectance. A simultaneous exposure to low-energy proton/UV irradiation in vacuum, and high-energy proton/electron irradiation was carried out. Additional tests of the paints are described. Author

28 PROPELLANTS AND FUELS

Includes rocket propellants, igniters, and oxidizers; their storage and handling procedures; and aircraft fuels.

For related information see also *07 Aircraft Propulsion and Power, 20 Spacecraft Propulsion and Power,* and *44 Energy Production and Conversion.*

N91-14495* National Aeronautics and Space Administration. John F. Kennedy Space Center, Cocoa Beach, FL.
LIQUID HYDROGEN POLYGENERATION SYSTEM AND PROCESS Patent
Peter A. Minderman, inventor (to NASA), Gary P. Gutkowski, inventor (to NASA), Lawrence Manfredi, inventor (to NASA), Julian V. King, inventor (to NASA), and Frank S. Howard, inventor (to NASA) 26 Jun. 1990 9 p Filed 15 Nov. 1985 Continuation of abandoned US-Patent-Appl-SN-603375, filed 24 Apr. 1984
(NASA-Case-KSC-11304-2; US-Patent-4,936,869; US-Patent-Appl-SN-798713; US-Patent-Appl-SN-603375; US-Patent-Class-48-77; US-Patent-Class-48-197R; US-Patent-Class-48-203; US-Patent-Class-60-39.12; US-Patent-Class-60-39.182; US-Patent-Class-423-655) Avail: US Patent and Trademark Office CSCL 21D

An integrated polygeneration system and process is disclosed for generating liquid hydrogen as a main energy product for use as a propellant for space vehicles. Secondary energy products and commodities for supporting a space center complex and launching of the space vehicle includes the production of electrical and thermal energy and gaseous nitrogen. The integrated process includes a coal gasification and gas cleanup system, a combined cycle power generation system, a hydrogen production and liquefaction system and an air separation system. A medium BTU gas is produced by the coal gasification system. Steam also produced in the coal gasification process is delivered to a steam turbine in the combined cycle power generation system.
Official Gazette of the U.S. Patent and Trademark Office

N91-14496# Case Western Reserve Univ., Cleveland, OH.
SOLID FUEL COMBUSTION Final Report, 1 Aug. 1985 - 31 Oct. 1989
James S. Tien Aug. 1990 82 p
(Grant AF-AFOSR-0340-85; AF Proj. 2308)
(AD-A227170; AFOSR-90-0946TR) Avail: NTIS HC/MF A05 CSCL 21/4

Theoretical analyses were performed on several different types of diffusion flames to study the flame radiation effect. In the first problem, a soot formation and oxidation scheme was incorporated into a turbulent diffusion flame model adjacent to a solid fuel. The computed results for the natural convective fire showed good agreement with experimentally measured solid fuel burning rate. Soot radiation increased its importance with flame height. With flames greater than 1 m, the radiative heat flux exceeded that by convection. In the second problem, matched asymptotic expansions were employed to study the spherical diffusion flame around a droplet or solid particle with flame radiation. It was found that the importance of radiation increased with droplet radius. The theory predicted that there was a maximum droplet or particle size above which a spherical flame could not be supported due to radiative loss. In the third problem, the thermophoretic motion of small particles (e.g., soot) were studied in a stagnation-point laminar flow next to a heated plate with and without combustion. It was found that both the thermophoretic motion and this Brownian particle diffusion can have a profound effect on the particle concentration distributions. GRA

N91-14497# Ballistic Research Labs., Aberdeen Proving Ground, MD.
ANALYSIS OF HYDROXYLAMMONIUM NITRATE BASED LIQUID PROPELLANTS Final Report, Jan. - Dec. 1989
Ronald Sasse Sep. 1990 27 p
(AD-A227300; BRL-TR-3154) Avail: NTIS HC/MF A03 CSCL 21/8

Chemical analysis of hydroxlammonium nitrate (HAN) based liquid propellants have matured over the past twenty years, and various techniques have been offered to meet particular requirements at particular times. This has resulted in a plethora of technology built by several authors, and it now seems prudent to summarize those methods selected by our laboratory to best characterize the propellant. GRA

29 MATERIALS PROCESSING

Includes space-based development of products and processes for commercial applications.

For biological materials see *55 Space Biology.*

N91-14498*# National Aeronautics and Space Administration. Lewis Research Center, Cleveland, OH.
MANIPULATION HARDWARE FOR MICROGRAVITY RESEARCH
J. N. Herndon, R. L. Glassell, P. L. Butler, D. M. Williams, D. A. Rohn, and J. H. Miller (Sverdrup Technology, Inc., Brook Park, OH.) 1990 14 p Presented at the American Nuclear Society Winter Meeting, Washington, DC, 11-15 Nov. 1990
(Contract DE-AC05-84OR-21400)
(NASA-TM-103423; NAS 1.15:103423; DE91-002871; CONF-901101-46) Avail: NTIS HC/MF A03 CSCL 22A

The establishment of permanent low earth orbit occupation on the Space Station Freedom will present new opportunities for the introduction of productive flexible automation systems into the microgravity environment of space. The need for robust and reliable robotic systems to support experimental activities normally intended by astronauts will assume great importance. Many experimental modules on the space station are expected to require robotic systems for ongoing experimental operations. When implementing these systems, care must be taken not to introduce deleterious effects on the experiments or on the space station itself. It is important to minimize the acceleration effects on the experimental items being handled while also minimizing manipulator base reaction effects on adjacent experiments and on the space station structure. NASA Lewis Research Center has been performing research on these manipulator applications, focusing on improving the basic manipulator hardware, as well as developing improved manipulator control algorithms. By utilizing the modular manipulator concepts developed during the Laboratory Telerobotic Manipulator program, Oak Ridge National Laboratory has developed an experimental testbed system called the Microgravity Manipulator, incorporating two pitch-yaw modular positioners to provide a 4 dof experimental manipulator arm. A key feature in the design for microgravity manipulation research was the use of traction drives for torque transmission in the modular pitch-yaw differentials.
DOE

31 ENGINEERING (GENERAL)

Includes vacuum technology; control engineering; display engineering; cryogenics; and fire prevention.

N91-14499 State Univ. of New York, Buffalo.
ON THE MODELING AND CONTROL OF SLEWING FLEXIBLE STRUCTURES Ph.D. Thesis
Ephrahim Garcia 1990 150 p
Avail: Univ. Microfilms Order No. DA9022156

The slewing control of a single link flexible structure is investigated. First a simple model of a slewing beam is examined. This structure is modeled as an Euler-Bernoulli beam which is pinned at one end with the other end free. A model summation procedure is applied to determine the response of the structure. A servo system acting at the pinned end is idealized as a spring. It is shown that the effects of the spring can be modeled through the boundary conditions for the flexible structure, or, the pin-free (open loop) modes of vibration can be assumed and the effects of the spring are included through the use of a position feedback matrix. The slewing equations of motions are derived from Hamilton's principle. The feedback closed loop system matrices are derived for the angular position and velocity, and structural strain signal. The controllability norm of a system with various degree of actuator structure interaction is investigated to determine the degree of controllability of the higher modes of vibration. The nonlinear equations of motion are derived and a summary of nonlinear dynamics in slewing is given. A parameter for gauging the speed of response of slewing structures is proposed, and an example is given which shows the divergence of the linear and nonlinear models as this parameter is increased. The optimal control of the slewing system is discussed and an example using optimal output feedback is presented. The proposed model which accounts for the actuator structure interaction is used to model an experimental slewing structure in a direct drive configuration. It is shown that by taking advantage of the interaction between actuator and structure, vibration attenuation of the flexible modes can be achieved using only angular position and velocity sensors.
Dissert. Abstr.

N91-14500*# National Aeronautics and Space Administration. Lewis Research Center, Cleveland, OH.
A NUMERICAL AND EXPERIMENTAL ANALYSIS OF REACTOR PERFORMANCE AND DEPOSITION RATES FOR CVD ON MONOFILAMENTS
S. A. Gokoglu, M. Kuczmarski, L. Veitch, P. Tsui (Sverdrup Technology, Inc., Brook Park, OH.), and A. Chait 1990 9 p Presented at the 11th International Conference on Chemical Vapor Deposition, Seattle, WA, 14-19 Oct. 1990; sponsored by Electrochemical Society
(Contract NAS3-25266)
(NASA-TM-103631; E-5801; NAS 1.15:103631) Avail: NTIS HC/MF A02 CSCL 13B

The computational fluid dynamics (CFD) code FLUENT is adopted to simulate a cylindrical upflow reactor designed for chemical vapor deposition (CVD) on monofilaments. Equilibrium temperature profiles along the fiber and quartz reactor wall are experimentally measured and used as boundary conditions in numerical simulations. Two-dimensional axisymmetric flow and temperature fields are calculated for hydrogen and argon; the effect of free convection is assessed. The gas and surface chemistry is included for predicting silicon deposition from silane. The model predictions are compared with experimentally measured silicon CVD rates. Inferences are made for optimum conditions to obtain uniformity.
Author

N91-14501# Pask Research and Engineering, Inc., Pinole, CA.
JOINING ALUMINA TO SAPPHIRE FOR COPPER VAPOR LASER TUBES Final Report
Antonia P. Tomsia, Andreas M. Glaeser, and Joseph A. Pask 10 Sep. 1990 75 p
(Contract N61331-90-C-0005)
(AD-A226619) Avail: NTIS HC/MF A04 CSCL 09/3

The technology for building copper vapor lasers has existed for years; the joining technology for producing sealed copper vapor lasers did not. Thus, our focus during Phase 1 research was to explore means of joining alumina to alumina and alumina to sapphire for high temperature applications. We felt that it was imperative to explore more than one joining technique, and for a given technique, to investigate a range of conditions of compositions, or both. The motivation for this approach was twofold. First, it was beyond the scope of Phase 1 research to exhaustively explore the mechanical and chemical stability of all joints produced by a broad assortment of joining techniques, particularly for the timeframes of interest for a sealed copper vapor laser. We recognized that joining methods that produced bonds of adequate quality to survive limited thermal cycling and limited exposure to copper might prove to be inadequate for long-term use. Thus, if the method that appeared most satisfactory in Phase 1 testing proved inadequate for fabrication of sealed copper vapor lasers, we would have the needed experience with alternative joining approaches to adjust and adapt rapidly. Second, we felt that it was possible that more than one joining approach would be suitable in producing the total system. Those who had chosen to explore only one joining method would lack this flexibility.
GRA

N91-14502# Consiglio Nazionale delle Ricerche, Frascati (Italy). Ist. di Fisica dello Spazio Interplanetario.
DESIGN OF A He4 COOLING SYSTEM FOR A CRYOSTAT WORKING AT 1K [PROGETTAZIONE DI UN REFRIGERATORE A 4 HE LIQUIDO PER UN CRIOSTATO OPERANTE A1K]
P. Baldetti, C. Ceccarelli, B. Nisini, and E. Saraceno Sep. 1989 18 p In ITALIAN
(IFSI-89-17; ETN-90-97778) Avail: NTIS HC/MF A03

A description is presented of the systems design which includes thermodynamic curves illustrating the discussed phenomena. The basic components are a pump and the expansion chamber. Absorption and desorption from active carbon is used for helium handling (cryopump). The dimensions of the cooling chamber are determined by the request to keep the system at 1 K for 12 hours.
ESA

N91-14503# American Foundreymens' Society, Des Plaines, IL.
EXPENDABLE PATTERN CASTING TECHNOLOGY Final Report
Jul. 1990 80 p
(Contract DE-FC07-89ID-12869)
(DE91-001348; DOE/ID-12869/1) Avail: NTIS HC/MF A05

The expendable pattern casting (EPC) process is a potential casting process breakthrough which could dramatically improve the competitiveness of the U.S. foundry industry. Cooperatively supported by U.S. Industry and the Department of Energy and managed by the American Foundrymen's Society, a project was started in May 1989 to develop and optimize expendable pattern casting technology. Four major tasks were conducted in the first phase of the project. Those tasks involved: (1) reviewing published literature to determine the major problems in the EPC process; (2) evaluating factors influencing sand flow and compaction; (3) evaluating and comparing casting precision obtained in the EPC process with that obtained in other processes; and (4) identifying critical parameters that control dimensional precision and defect formation in EP castings.
DOE

N91-14504# Sandia National Labs., Albuquerque, NM.
MANUFACTURING TECHNOLOGY: A SANDIA TECHNOLOGY BULLETIN, VOLUME 1, NO. 1
R. C. Maydew, ed., J. A. Leonard, ed., and N. S. Hey, ed. Aug. 1990 7 p
(Contract DE-AC04-76DP-00789)
(DE91-002518; SAND-90-2168) Avail: NTIS HC/MF A02

Welcome to this first issue of Manufacturing Technology, one of three new technology bulletins published at Sandia National Laboratories in which we seek to share information with U.S. industry about applications of technology. Inside this issue: industry/DOE/Sandia agreement to strengthen specialty metals competitiveness; silicon micromachining produces microscopic

parts; Sandia develops state-of-the-art capacitor winding machine; new robotic system spells finis to manual edge finishing; and milling assistant speeds numerically controlled machine programming. DOE

N91-14505# Edgerton, Germeshausen and Grier, Inc., Idaho Falls, ID.
THIN STEEL SECTION CASTING ON A NEAR-HORIZONTAL TWIN-BELT CASTER
S. S. Daniel, P. E. Hamill, A. Vassilicos, J. H. Baker, T. W. Lewis, and C. D Dykes (Hazelett Strip Casting Corp., Colchester, VT.) 1990 12 p Presented at the Conference on New Smelting Reduction and Near Net Casting Technology for Steel, Phoang, Republic of Korea, Oct. 1990
(Contract DE-FC07-84ID-12545)
(DE91-001883; EGG-M-90402; CONF-9010240-1) Avail: NTIS HC/MF A03

As part of a program to develop a high productivity casting process for thin steel sections for direct hot rolling into high quality sheet, a process was devised where a closed-pool injection feeding system was coupled with a Hazelett twin-belt casting machine. Pilot facilities were built to determine the feasibility of closed-pool feeding. The facility was designed to cast up to 13.5 tons of steel into 25-mm thick and 430-mm wide steel sections at rates ranging from 4 to 15 m/min. Closed-pool feeding was attained in parts of seven casts. Under certain casting conditions, closed-pool feeding resulted in improvement in strand surface quality over open-pool feeding. However in nearly all cases of closed-pool feeding, the casts had to be terminated prematurely due to feeding nozzle breakage. This failure appears to be caused by frequent steel skull formation on, and subsequent detachment from the nozzle tip. In general, horizontal thin sections casting of steel with closed-pool feeding is a very complicated technology which is extremely labor and and material intensive, and not deemed economically viable. DOE

N91-14506# Los Alamos National Lab., NM.
TRANSIENT ANALYSIS OF A TWO-PHASE HYDROGEN HEAT SWITCH
Coyne Prenger and Walter Stewart 1990 15 p Presented at the 6th International Cryocooler Conference, Plymouth, MA, 25-26 Oct. 1990 Sponsored in part by Naval Ship Research and Development Center
(Contract W-7405-eng-36)
(DE91-002314; LA-UR-90-2156; CONF-901029-3) Avail: NTIS HC/MF A03

A transient, thermal analysis of a two-phase hydrogen heat switch is presented. The heat switch has application to a zero-g, no-moving-part magnetic refrigerator that operates between 7 K and 25 K and provides a one-way thermal path for heat rejection from the refrigerator to the 20 K heat sink. Incorporation of the heat switch is dependent on operating frequency. However, the thermal diode operating characteristic and the high axial thermal conductivity of the heat switch provide advantages over other methods. DOE

N91-14507# Lawrence Livermore National Lab., CA.
A VIBRATING RAZOR BLADE MACHINING TOOL FOR MATERIAL REMOVAL ON LOW-DENSITY FOAMS
D. F. Hillyer, Jr. 1 Oct. 1990 26 p
(Contract W-7405-eng-48)
(DE91-002996; UCRL-ID-105063) Avail: NTIS HC/MF A03

The Lawrence Livermore National Laboratory (LLNL) has developed an accurate method of machining low-density foams into rectangular blank shapes by using a commercial oscillating razor blade machining tool concept marketed as a Vibratome. Since 1970, Vibratome has been used by medical laboratories to section fresh or fixed animal and plant tissues without freezing or embedding. By employing a vibrating razor blade principle, Vibratome sectioning avoids the alteration of morphology and the destruction of enzyme activities. The patented vibrating blade principle moves the sectioning razor blade in a reciprocating arcuate path as it penetrates the specimen. Sectioning takes place in a liquid bath using an ordinary injector-type razor blade. Although other commercial products may accomplish the same task, the Vibratome concept is currently being used at LLNL to obtain improved foam surface qualities from razor machining by combining state-of-the-art air bearing hardware with precise linear motion and an electrodynamic exciter that generates sinusoidal excitation. Razor cut foam surfaces of less than 25 microns (0.001 in.) flatness are achieved over areas of 8.75 sq in. (2.5 x 3.5 in.). Razor machining of wide or narrow foam surfaces is generally characterized by a continuous curl chip for the full length of the material removed. This continuous chip facilitates flatness and prevents increased surface densities caused by material chip collection often left in the surface cells by conventional machine tools. This report covers the design evolution of razor machining of non-metallic soft materials. Hardware that maintains close dimensional tolerances and concurrently leaves the machined surface free of physical property changes is described. DOE

N91-14508* National Aeronautics and Space Administration. Marshall Space Flight Center, Huntsville, AL.
ELECTROSTATICALLY SUSPENDED ROTOR FOR ANGULAR ENCODER Patent
Walter Polstorff, inventor (to NASA) 23 Oct. 1990 13 p Filed 21 Aug. 1989
(NASA-Case-MFS-28294-1; US-Patent-4,965,429;
US-Patent-Appl-SN-396262; US-Patent-Class-219-121.68;
Int-Patent-Class-B23K-26/00) Avail: US Patent and Application Office CSCL 13B

An apparatus for engraving a code strip with coded markings is disclosed. The code strip is attached for rotation to a cylindrical rotor which is mounted within the cavity of a stator. The stator carries electrodes on its top and side walls to which high potentials are applied to electrostatically suspend the rotor. Circuit means sense the position of the rotor with respect to the stator electrodes and adjust the potential to maintain the rotor at its desired location. A drive motor is connected to the rotor through a drive shaft to initially lift the rotor into the desired location within the stator and to rotate it at the desired speed. Thereafter, the drive shaft is disconnected from the rotor, and the rotor continues to spin at a highly stable angular velocity, supported only by the electrostatic fields. Official Gazette of the U.S. Patent and Trademark Office

N91-14509# Army Armament Research and Development Command, Watervliet, NY.
HAZARDS AND SAFEGUARDS OF HIGH PRESSURE HYDRAULIC FATIGUE TESTING Final Report
Bruce B. Brown Jul. 1990 27 p
(AD-A226767; ARCCB-TR-90020) Avail: NTIS HC/MF A03 CSCL 14/2

The creation and transfer of hydraulic pressure at the 690-MPa (100,000-psi) level is in itself hazardous. When this is used to fatigue cycle large pressure vessels to failure, the potential for catastrophic accidents is always present. This report summarizes the experience gained over several years of this operation wherein several hundred pressure vessels have been successfully taken to fatigue failure. Although accidents still take place, we have eliminated most of the personnel hazards, greatly reduced equipment damage, and are constantly striving to detect and eliminate any existing or new hazards. The hazards and safeguards are grouped into four areas of consideration: high pressure fluids, fragments, large components, and material handling. GRA

N91-14510# New Mexico Univ., Albuquerque. Engineering Research Inst.
NEXT-GENERATION FIRE EXTINGUISHING AGENT. PHASE 2: LABORATORY TESTS AND SCOPING TRIALS Final Report, Aug. 1986 - Jun. 1988
Robert E. Tapscott, John H. May, Joanne P. Moore, Michael E. Lee, and Joseph L. Walker Apr. 1990 136 p
(Contract F29601-84-C-0080)
(AD-A227347; NMERI-WA3-78-(3.21); AFESC/ESL-TR-87-03)
Avail: NTIS HC/MF A07 CSCL 13/12

Concepts were orginated for next-generation fire extinguishing

agents. In Phase 2, laboratory tests and scoping trials were performed to initiate a program for replacement of halon fire extinguishants in Air Force fire protection and firefighter training. Facilities were also established to perform laser Raman spectroscopic investigations of flame suppression halon agents, and initial, baseline Raman studies were carried out. GRA

N91-14511*# Case Western Reserve Univ., Cleveland, OH.
CHEMICAL VAPOR DEPOSITION MODELING: AN ASSESSMENT OF CURRENT STATUS Final Report
Suleyman A. Gokoglu Jan. 1991 10 p Presented at the 11th International Conference on Chemical Vapor Deposition (CVD-XI), Seattle, WA, 14-19 Oct. 1990; sponsored in part by the Electrochemical Society Original contains color illustrations
(Contract NCC3-73)
(NASA-CR-185301; E-5792; NAS 1.26:185301) Avail: NTIS HC/MF A02; 1 functional color page CSCL 13H

The shortcomings of earlier approaches that assumed thermochemical equilibrium and used chemical vapor deposition (CVD) phase diagrams are pointed out. Significant advancements in predictive capabilities due to recent computational developments, especially those for deposition rates controlled by gas phase mass transport, are demonstrated. The importance of using the proper boundary conditions is stressed, and the availability and reliability of gas phase and surface chemical kinetic information are emphasized as the most limiting factors. Future directions for CVD are proposed on the basis of current needs for efficient and effective progress in CVD process design and optimization. Author

32 COMMUNICATIONS AND RADAR

Includes radar; land and global communications; communications theory; and optical communications.

For related information see also *04 Aircraft Communications and Navigation* and *17 Space Communications, Spacecraft Communications, Command and Tracking.* For search and rescue see *03 Air Transportation and Safety,* and *16 Space Transportation.*

N91-14512 Department of the Navy, Washington, DC.
TAPERED FIBER AMPLIFIER Patent
Stephen D. Russell, inventor (to Navy) and Timothy C. Stamnitz, inventor (to Navy) 17 Jul. 1990 6 p Filed 31 Aug. 1988
(AD-D014629; US-Patent-4,941,726; US-Patent-Appl-SN-239158; US-Patent-Class-350-9615) Avail: US Patent and Trademark Office CSCL 20/6

A tapered optical fiber amplifier is designed to provide for long-distance, un-repeatered fiber optic communications. Two single-mode fiber portions are tapered to efficiently intensify and couple an information signal from a laser diode and a pump signal at a shorter wavelength into a fused, tapered single-mode fiber optic coupler. The concentrated information signal and concentrated pump signal are combined via the coupler which is coupled to a several-kilometer length of a relatively small core diametered single-mode fiber to create nonlinear optical effect (stimulated Raman scattering) (SRS). The SRS causes Raman shift of the pump light into the small core diametered single-mode fiber length, thereby generating SRS to result in a signal amplification and an efficient extraction of the amplified signal via the tapered output fiber portion or pigtail. GRA

N91-14513*# Lawrence Livermore National Lab., CA.
A SYSTEM ARCHITECTURE FOR LONG DURATION FREE FLOATING FLIGHT FOR MILITARY APPLICATIONS
L. E. Epley (CIRRUS Aerospace Corp., Burke, VA.) 31 Aug. 1990 60 p Sponsored by NASA
(Contract W-7405-eng-48)
(NASA-CR-187435; NAS 1.26:187435; DE91-002668; UCRL-CR-105118) Avail: NTIS HC/MF A04 CSCL 17B

Accessibility is today's space frontier. Our need for wide-band global communications, earth imaging and sensing, atmospheric measurements and military reconnaissance is endless, but growing dependence on space-based systems raises concerns about potential vulnerability. Military commanders want space assets more accessible and under direct local control. As a result, a robust and low cost access to space-like capability has become a national priority. Buoyant vehicles, free floating in the middle stratosphere could provide the kind of cost effective access to space-like capability needed for a variety of missions. These vehicles are inexpensive, invisible and easily launched. Developments in payload electronics, atmospheric wind modeling and materials combined with ever-improving communications and navigation infrastructure are making balloon-borne concepts more attractive. The fundamental question is whether a free floating balloon, used in a pseudo-satellite role, has value in a military system. Flight tests are ongoing under NASA sponsorship. Following these tests NASA intends to use the vehicles for research in the Antarctic. The concept is being reviewed by other agencies interested in stratospheric research. We believe that LDFFF systems have applications in areas of communications, surveillance and other traditional satellite missions. Dialogue with the broader community of space users is needed to expand the applications. This report reviews the status of the recent flight tests and presents an overview of the concept of Long Duration Free Floating Flight for military applications. DOE

N91-14514# Technische Hochschule, Darmstadt (Germany, F.R.). Fachbereich Regelungs- und Datentechnik.
SYSTEM INTEGRATION OF A BLOCK CODE Ph.D. Thesis
Hans Peter Foerster 1989 131 p In GERMAN; ENGLISH summary
(ETN-91-98169) Avail: NTIS HC/MF A07

The integration of a simple single parity check code for communication systems was considered under systems aspects. With respect to the implementation several interactions between communication system and coding scheme were analyzed. The quantization of the amplitude of the received signal, the influence of the increase of bandwith in band limited systems due to the coded transmissions, the problems of symbol time recovery, and the support of word synchronization were investigated theoretically or using simulations. It is shown that with soft decision decoding an error detecting code can also be used for error correction. A realization of a decoding circuit using an application specific integrated circuit is described, and the results of measurements via Intelsat 5 are given. ESA

N91-14515# Missouri Univ., Saint Louis.
QUANTUM 1/f NOISE IN HIGH TECHNOLOGY APPLICATIONS INCLUDING ULTRASMALL STRUCTURES AND DEVICES Annual Report No. 1, 15 Jul. 1989 - 14 Jul. 1990
Peter H. Handel 15 Jul. 1990 43 p
(Grant AF-AFOSR-0416-89; AF Proj. 2305)
(AD-A226739; AFOSR-90-0938TR) Avail: NTIS HC/MF A03 CSCL 20/10

Quantum 1/f noise is a basic property of physical cross sections and process rates and a form of quantum chaos in the nonlinear system of the charged particles plus the electromagnetic field. Therefore, the present report starts with a consideration of the general problem of 1/f spectra in nonlinear systems, derives for the first time a general sufficient criterion which tells us if a system will show 1/f noise, and applies the new criterion to transport in semiconductors, in metals, on highways, and in quantum electrodynamics. In all these cases 1/f spectra follow from the same criterion, in the same way. This is, for the first time, a unifying principle. In addition, the report contains the first rigorous first principles derivation of quantum 1/f mobility fluctuations in semiconducting materials (analytical) and reference to a Monte Carlo simulation of the same problem. Finally, a solution for the long-standing problem of quantum 1/f noise in the collector of bipolar junction transmitters (BJT's) is proposed. GRA

N91-14516# Rome Air Development Center, Griffiss AFB, NY.
SYSTOLIC EMULATOR EXPERIMENTATION Report, Apr. 1987 - Apr. 1990

Richard N. Smith and Michael W. Fenton Jul. 1990 135 p
(AF Proj. 4519)
(AD-A226746; RADC-TR-90-181) Avail: NTIS HC/MF A07
CSCL 12/5

Adaptive spatial filtering or adaptive antenna nulling techniques have been used to remove or eliminate directional electromagnetic interferences or unwanted signals from getting into radio receivers. This signal processing technique has been studied for many years. Many systems have been proposed, some have built and a few have been fielded. High speed parallel processors are beginning to show promise in providing real-time solutions for meeting the processing requirements needed for space applications. One type of high speed parallel processor architecture is called systolic. The name arises from the way the data pulses through the cell-like structure of the processor in a prescribed pipelined manner. Effective implementation of adaptive signal processing techniques using systolic array processors, especially, required careful matching between the algorithm to be performed and the processor architecture. This process of matching algorithm and architecture can be facilitated by computer emulation. GRA

N91-14517# Calspan Advanced Technology Center, Buffalo, NY.
DESCRIPTION OF THE BISTATIC RADAR TERRAIN MEASUREMENTS SYSTEM EQUIPMENT Interim Report, 1 May 1985 - 1 May 1989
Edward H. Jocoy, J. R. Gucwa, M. A. Rude, N. E. Schweitzer, and L. M. Sheldon Jun. 1990 211 p
(Contract F33615-84-C-1517; AF Proj. 691X)
(AD-A226808; Rept-7277-1; WRDC-TR-90-1067) Avail: NTIS HC/MF A10 CSCL 17/9

The objective of this program was to collect a data base of X-band, bistatic terrain reflectivity data to aid in the design and evaluation of the Electronic Warfare (EW) Systems. Airborne radar platforms were used to obtain data from various types of terrain at various incidence, reflection and out-of-plane angles. Both static and dynamic tests were conducted. The principal reflectivity measure derived from the data was the bistatic reflection coefficient as a function of angle. Spectra were obtained from the dynamic tests. GRA

N91-14518# Stanford Univ., CA. Information Systems Lab.
STUDIES IN STATISTICAL SIGNAL PROCESSING Final Report, 1 Jul. 1988 - 30 Jun. 1990
Thomas Kailath 30 Jun. 1990 34 p
(Grant AF-AFOSR-0327-88; AF Proj. 2304)
(AD-A226825; AFOSR-90-0955TR) Avail: NTIS HC/MF A03
CSCL 12/3

The primary objective of our research is to develop efficient and numerically stable algorithms for nonstationary signal processing problems by understanding and exploiting special structures, both deterministic and stochastic, in the problems. We also strive to establish and broaden links with related disciplines, such as cascade filter synthesis, scattering theory, numerical linear algebra, and mathematical operator theory for the purpose of cross fertilization of ideas and techniques. These explorations have led to new results both in estimation theory and in these other fields, e.g., to new algorithms for triangular and QR factorization of structured matrices, new techniques for root location and stability testing, new realizations for multiple-input/multiple-output (MIMO) transfer functions, and new recursions for orthogonal polynomials on the unit circle and the real line as well as on other curves. GRA

N91-14519# Alaska Univ., Fairbanks. Geophysical Inst.
RADIO FREQUENCY INTERFERENCE (RFI) MEASUREMENTS MADE NEAR THE PROPOSED ALASKA OTH RECEIVING SITE
Steven A. Estes, DuWayne Bostow, and Robert D. Hunsucker Jul. 1990 68 p
(Contract F19628-87-K-0048; AF Proj. 4140)
(AD-A226922; GL-TR-89-0296; SR-1) Avail: NTIS HC/MF A04
CSCL 17/9

As part of our AFGL contract on auroral clutter and radio frequency interference (RFI) studies in Alaska, we were requested to make field measurements of RFI and atmospheric radio noise in the vicinity of the proposed Alaska OTH radar site near Tok, Alaska as described by Task 2 in our proposal. Extensive measurements of RFI and radio noise were made during the period 23 September to 9 October 1987 in the vicinity of the planned OTH radar site. Figure 1 shows the location of the proposed OTH receiver antenna systems and the 10 sites where measurements made in relation to the Greater Tok Metropolitan Area. GRA

N91-14520# Naval Research Lab., Washington, DC. Propagation Staff.
PERSPECTIVES ON MODELING ELECTROMAGNETIC SEA SCATTER Memorandum Report
Lewis B. Wetzel 28 Sep. 1990 15 p Presented at the NSF Workshop on Future Directions in Electromagnetics Research, Boston, MA, 27 Jul. 1989 Sponsored by ONR, Arlington, VA
(AD-A226939; NRL-MR-6720) Avail: NTIS HC/MF A03 CSCL 20/14

The purpose of this report is to provide a brief perspective on the status of various theories used to predict the scattering of electromagnetic waves from the sea surface. The three theoretical approaches discussed are the Global Boundary Value Problem (GBVP), the Composite Surface Model (CSM), and the Surface Feature Scattering Model (SFSM). It is concluded, among other things, that (1) the GBVP approaches are inadequate without further consideration of surface sharpness in the scattering integral; (2) the basic conceptual difficulties that prevent the CSM from being a satisfactory physical theory should be confronted; and (3) while the SFSMs can account for scattering behavior inexplicable by the other methods, there is still no way to relate the generation and distribution of the scattering features to measurable environmental variables. The present state of understanding of sea scatter is judged to be inadequate as a basis for reliable predictions. GRA

N91-14521# Institute of Electrical and Electronics Engineers, New York, NY.
INTERNATIONAL SYMPOSIUM ON INFORMATION THEORY Abstracts Only
Jan. 1990 216 p Sponsored by ARO; NSF; and ONR
(AD-A226957; IEEE-90CH2711-0; LC-72-179437) Avail: NTIS HC/MF A10 CSCL 12/9

Some of the main topics presented at the symposium include: spread spectrum communications, detection theory, neural networks, data compression, channel capacity, coding theory, trellis coding, communication systems, broadcast channels, estimation, quantization, error-control and other coding, communication theory, modulation, optical communications, and source coding. GRA

N91-14522# Raytheon Co., Lexington, MA.
MMIC COMPENSATION NETWORK FOR PHASED ARRAY ELEMENT MISMATCH Final Report, Oct. 1987 - Jun. 1988
K. Simon, J. Wendler, R. Pozgay, and M. Schindler 14 Sep. 1990 73 p
(Contract N00014-87-C-2517)
(AD-A227437; RAY/RD/S-4248A) Avail: NTIS HC/MF A04
CSCL 09/1

A tuning scheme was developed that compensates the radiating element input mismatch that occurs in broadband phased arrays. The compensated radiator has an input VSWR less than 2.0 from 8 to 18 GHz and antenna scan angles from 0 to 60. GRA

N91-14523* National Aeronautics and Space Administration. Pasadena Office, CA.
TRELLIS CODED MODULATION FOR TRANSMISSION OVER FADING MOBILE SATELLITE CHANNEL Patent
Marvin K. Simon, inventor (to NASA) and Dariush Divasalar, inventor (to NASA) (Jet Propulsion Lab., California Inst. of Tech., Pasadena.) 3 Jul. 1990 21 p Filed 15 Sep. 1988 Continuation of abandoned US-Patent-Appl-SN-929876, filed 13 Nov. 1986
(NASA-Case-NPO-16904-2-CU; US-Patent-4,945,549;
US-Patent-Appl-SN-246032; US-Patent-Appl-SN-929876;

US-Patent-Class-375-53; US-Patent-Class-375-57; US-Patent-Class-371-43; Int-Patent-Class-H04L-27/18) Avail: US Patent and Trademark Office CSCL 17B

The combination of trellis coding and multiple phase-shift keyed (MPSK) signaling with asymmetry (nonuniform spacing) to the signal set is disclosed with regard to its suitability for a fading mobile satellite communication channel. For MPSK signaling, introducing nonuniformity in the phase spacing between signal points provides an improvement in performance over that achievable with trellis codes symmetric MPSK signaling, all this without increasing the average or peak power, or changing the bandwidth constraints imposed on the system. Block interleaving may be used to reduce error and pilot tone(s) may be used for improving the error correction performance of the trellis decoder in the presence of channel fading.

Official Gazette of the U.S. Patent and Trademark Office

N91-14524# Sandia National Labs., Albuquerque, NM. Radiation and Electromagnetic Analysis Div.

THE INCLUSION OF WALL LOSS IN ELECTROMAGNETIC FINITE-DIFFERENCE TIME-DOMAIN THIN-SLOT ALGORITHMS

Douglas J. Riley and C. David Turner Sep. 1990 46 p

(Contract DE-AC04-76DP-00789)

(DE91-001046; SAND-90-2091) Avail: NTIS HC/MF A03

Sub-gridding techniques enable finite-difference time-domain (FDTD) electromagnetic codes to model apertures that are much narrower than the spatial resolution of the FDTD mesh. Previous thin-slot methods have assumed that the slot walls are perfectly conducting. As the slot depth-to-width ratio becomes large, interior wall losses for realistic materials can significantly affect the coupling through the slot, and therefore these loss effects should not be neglected. This paper presents two methods for incorporating loss for walls with good, but not perfect conductivity, into the FDTD calculations. The first method modifies an FDTD equation internal to the slot to include a surface-impedance contribution. This method is appropriate for the usual FDTD thin-slot formalisms. The second method includes the losses into a 'half-space' integral equation that can be used by the recently introduced Hybrid Thin-Slot Algorithm. Results based on the two methods are compared for a variety of slot parameters and wall conductivities. DOE

N91-14525# Sandia National Labs., Albuquerque, NM. Electronic Development Div.

AN INVESTIGATION OF USING A PHASE-CHANGE MATERIAL TO IMPROVE THE HEAT TRANSFER IN A SMALL ELECTRONIC MODULE FOR AN AIRBORNE RADAR APPLICATION

Keith W. Snyder Oct. 1990 51 p

(Contract DE-AC04-76DP-00789)

(DE91-002597; SAND-90-2316) Avail: NTIS HC/MF A04

Finding new and improved means of cooling small electronic packages are of great importance to today's electronic packaging engineer. Thermal absorption through the use of a material which changes phase is an attractive alternative. Taking advantage of the heat capacity of a material's latent heat of fusion is shown to absorb heat away from the electronics, thus decreasing the overall temperature rise of the system. The energy equation is formulated in terms of enthalpy and discretized using a finite-difference method. A FORTRAN program to solve the discretized equations is presented which can be used to analyze heat conduction in a rectangular region undergoing an isothermal phase change. An analysis of heat transfer through a miniature radar electronic module cooled by a phase-change reservoir is presented, illustrating the method's advantages over conventional heat sinks. DOE

N91-14526# Los Alamos National Lab., NM.

A SIMPLE PLANE-WAVE EXPLOSIVE LENS

J. N. Fritz Dec. 1990 21 p

(Contract W-7405-eng-36)

(DE91-004297; LA-11956-MS) Avail: NTIS HC/MF A03

A simple plane-wave lens, using an inert central plastic wave shaper, has been designed. An experiment was done with a 4-in. diam, zeroth-order design. An iterative technique that uses measured time deviations to correct the next wave shape was developed. Two identical versions of the first iterated shape were fired. Arrival-time deviations in these first iterates fell within 50-ns bounds. With greater care and further iteration, lenses bound by 10-ns deviations seem possible. DOE

N91-15074# Abastumani Astrophysical Observatory, Georgia (USSR).

AMPLIFICATION OF ALFVEN WAVES IN FREE SHEAR FLOWS

G. D. Chagelishvili, R. G. Chanishvili, L. G. Filipov, T. S. Khristov (Bulgarian Academy of Sciences, Sofia.), and J. G. Lominadze *In* ESA, Plasma Astrophysics Aug. 1990 p 147-152 (For primary document see N91-15046 06-90)

Copyright Avail: NTIS HC/MF A14

N91-15076# Abastumani Astrophysical Observatory, Georgia (USSR).

EXCITATION OF LANGMUIR WAVE BY TRANSVERSAL NONLINEAR WAVE IN THE ELECTRON-POSITRON INHOMOGENEOUS PLASMA IN THE PRESENCE OF POSITRON BEAM

A. D. Pataraya, T. A. Pataraya, and M. Z. Zedginidze (Tbilisi State Univ., USSR) *In* ESA, Plasma Astrophysics Aug. 1990 p 159-162 (For primary document see N91-15046 06-90)

Copyright Avail: NTIS HC/MF A14

N91-15086# Academy of Sciences, Potsdam (German D.R.). Zentralinstitut fuer Astrophysik.

ENERGY DISSIPATION OF SHEAR ALFVEN WAVES IN EXTENDED COSMIC JETS

T. M. Kirchner *In* ESA, Plasma Astrophysics Aug. 1990 p 215-220 (For primary document see N91-15046 06-90)

Copyright Avail: NTIS HC/MF A14

N91-15092# Academy of Sciences (USSR), Moscow. Inst. of Space Research.

ON THE THEORY OF LARGE-SCALE MICROPULSE STRUCTURE OF PULSAR RADIO RADIATION

O. G. Onishchenko *In* ESA, Plasma Astrophysics Aug. 1990 p 251-253 (For primary document see N91-15046 06-90)

Copyright Avail: NTIS HC/MF A14

33 ELECTRONICS AND ELECTRICAL ENGINEERING

Includes test equipment and maintainability; components, e.g., tunnel diodes and transistors; microminiaturization; and integrated circuitry.

For related information see also *60 Computer Operations and Hardware* and *76 Solid-State Physics.*

N91-14527*# Rochester Univ., NY. Lab. for Laser Energetics.

ELECTRO-OPTIC NETWORK ANALYZER Final Technical Report

Todd A. Jackson 15 Jun. 1990 17 p

(Contract NCC3-107)

(NASA-CR-186613; NAS 1.26:186613) Avail: NTIS HC/MF A03 CSCL 09A

The bandwidth of frequency domain measurement methods of electrical signals has usually been far greater than the bandwidth of time domain methods. The primary limits of the time domain approach have been the 20 to 30 GHz bandwidth limit for electronic waveform acquisition instrumentation, and the lack of usable electrical pulse generators for excitation of a test device. The bandwidth of frequency domain network analysis appears to have reached a plateau of between 100 to 200 GHz, while time domain measurement have improved markedly in both bandwidth and sensitivity with the introduction of the pulsed laser based electro-optic sampling approach. Network analysis or the measurement of device scattering parameters provides information necessary to the design of electronic network such as high

frequency amplifiers, mixers, and phase shifter. The bandwidth of frequency domain network analysis is currently being exceeded by the next generations of high frequency transistors and devices. Thus the electro-optic approach is a natural means of extending network analysis into the range above 100 GHz by employing time domain methods. In this approach, a suitable electrical excitation pulse is generated and propagated along a transmission line toward a test device. In the picosecond domain, laser driven photoconductive switches provide a unique method of generating electrical transients. Several materials were studied for generating short electrical pulses using photoconductive switches. The various semiconductive materials tested for photoconductive switching, and the electro-optic measurement technique used to characterize the material performance are described. E.R.

N91-14528 Department of the Navy, Washington, DC.
MONOLITHIC MULTICHANNEL DETECTOR AMPLIFIER ARRAYS AND CIRCUIT Patent
Gordon E. Anderson, inventor (to Navy), John B. Boos, inventor (to Navy), David I. Ma, inventor (to Navy), Ingham A. Mack, inventor (to Navy), and Nicholas A. Papanicolaou, inventor (to Navy) 8 May 1990 7 p Filed 25 Oct. 1988 Supersedes AD-D013932 (AD-D014566; US-Patent-4,924,285; US-Patent-Appl-SN-262765; US-Patent-Class-357-30) Avail: US Patent and Trademark Office CSCL 09/1

An integrated planar, single-channel, photodetector-amplifier device is disclosed. The single-channel device includes a photodetector layer and an amplifier layer above the photodetector layer. The photodetector layer is low-doped to give a low dark current and is sufficiently thick to give a high quantum efficiency. The amplifier layer is of a smaller thickness and is a more highly doped material than the photodetector layer, to provide an amplifier having high gain. An insulating layer is included between the photodetector and amplifier layers for electrically isolating the photodetector and amplifier layers. The layers are fabricated on a substrate. Isolation regions are also included for electrically laterally isolating a photodetector, amplifier, and other circuit components comprising the single channel device from each other. GRA

N91-14529 Department of the Navy, Washington, DC.
UNIDIRECTIONAL AMPLITUDE SENSITIVE NOISE RIDING THRESHOLD CIRCUIT Patent
William P. Huntley, inventor (to Navy) 24 Apr. 1990 6 p Filed 30 Jun. 1989
(AD-D014568; US-Patent-4,920,346; US-Patent-Appl-SN-373955; US-Patent-Class-342-91) Avail: US Patent and Trademark Office CSCL 25/2

An RF multiplexer divides an incoming signal from an RF antenna into discrete frequency bands. Each frequency band has its own separate circuit on separate lines to operate on the frequency band and determine if a radar signal is present or if only noise is present on the line. This is done by comparing the incoming signal for magnitude with a dc signal that is generated within the circuit and is proportional to the noise within the frequency band. An indication that any of the signals within the discrete frequency bands exceed the dc signal generated within the same band results in an alarm indication. GRA

N91-14530 Department of the Navy, Washington, DC.
EDDY CURRENT METHOD FOR MEASURING ELECTRICAL RESISTIVITY AND DEVICE FOR PROVIDING ACCURATE PHASE DETECTION Patent
Susan N. Vernon, inventor (to Navy) and Paul M. Gammell, inventor (to Navy) 1 May 1990 13 p Filed 9 Jan. 1989
(AD-D014571; US-Patent-4,922,201; US-Patent-Appl-SN-294622; US-Patent-Class-320-236) Avail: US Patent and Trademark Office CSCL 14/2

This invention relates to a method and devices for measuring the resistivity of materials. In particular, the methods measure resistivity in carbon fiber reinforced composites as well as any materials with a relative magnetic permeability of 1. The measurement may be made with access restricted to a single side of the material under test. The present invention relates to the field of nondestructive inspection of materials. In particular, this invention involves methods and a device of eddy current inspection for estimating the electrical resistivity of materials. While the method applies to all materials with a relative magnetic permeability of 1, it is particularly useful when the test material falls in one or more of three categories: (1) the resistivity falls within a range for which there are no calibration standards; (2) only one surface of the test material is accessible; and (3) the resistivity is frequency dependent and must be determined over a particular range of frequencies. GRA

N91-14531# Sandia National Labs., Albuquerque, NM. Battery Development Div.
A MATERIALS DATABASE FOR Li(Si)/FeS2 THERMAL BATTERIES
Ronald A. Guidotti Sep. 1990 52 p
(Contract DE-AC04-76DP-00789)
(DE91-002592; SAND-90-1302) Avail: NTIS HC/MF A04

The establishment of a database for the materials that are used in production Li(Si)/FeS2 thermal batteries designed at Sandia National Laboratories is described. The database is a Hewlett-Packard (HP) network type (IMAGE) designed to run on an HP3000 computer. Heavy emphasis is placed on the use of screen forms for entry, editing, and retrieval of data. Custom screen forms were used for the various materials in the battery. For the purposes of the materials database, each battery is composed of four mixes: cathode, separator, anode, and heat (pyrotechnic) powders. A consistent lot-numbering system was adopted for both the mixes and the discrete components that make up the mixes. Each serial number of a particular battery is linked to the lot numbers of the four mixes used in the battery. Each mix, in turn, is linked to the lot numbers of the discrete components that are contained within the mix. This allows traceability of each of the components used in any given serial number of a particular battery. The materials database provides the necessary traceability, as required by the Department of Energy, for the lifetime of the program associated with the battery. DOE

N91-14532# Sandia National Labs., Albuquerque, NM.
TRIGGERING GaAs LOCK-ON SWITCHES WITH LASER DIODE ARRAYS
G. M. Loubriel, M. T. Buttram, W. D. Helgeson, D. L. McLaughlin, M. W. OMalley, F. J. Zutavern, A. Rosen, and P. J. Stabile (David Sarnoff Research Center, Princeton, NJ.) 1990 8 p Presented at the SPIE Symposium on Laser Science and Applications of Optics, Optically Activate Switching Conference, Boston, MA, 4-9 Nov. 1990
(Contract DE-AC04-76DP-00789)
(DE91-002419; SAND-90-0953C; CONF-9011125-2) Avail: NTIS HC/MF A02

Laser diode arrays have been used to trigger GaAs Photoconducting Semiconductor Switches (PCSS) charged to voltages of up to 60 kV and conducting currents of 580 A. The driving forces behind the use of laser diode arrays are compactness, elimination of complicated optics, and the ability to run at high repetition rates. Laser diode arrays are compactness, elimination of complicated optics, and the ability to run at high repetition rates. Laser diode arrays can trigger GaAs at high fields as the result of a new switching mode (lock-on) with very high carrier number gain. We have achieved switching of up to 10 MW in a 60 Ohm system, with a pulse rise time of 500 ps. At 1.2 MW we have achieved repetition rates of 1 kHz with switch rise time of 500 ps for 10(exp 5) shots. The laser diode array used for these experiments delivers a 166 W pulse. In a single shot mode we have switched 4 kA with a flash lamp pumped laser and 600 A with the 166 W array. DOE

N91-14533# Sandia National Labs., Albuquerque, NM.
TOTAL-DOSE RADIATION HARDNESS ASSURANCE FOR SPACE ELECTRONICS
Peter S. Winokur and Daniel M. Fleetwood 1990 4 p Presented at the 8th Symposium on Space Nuclear Power Systems, Albuquerque, NM, 6-10 Jan. 1991 Sponsored in part by Defense

Nuclear Agency
(Contract DE-AC04-76DP-00789)
(DE91-002425; SAND-90-2724C; CONF-910116-5) Avail: NTIS HC/MF A01

An improved standard total-dose test method is described to qualify electronics for a low-dose radiation environment typical of space systems. The method consists of Co-60 irradiation at a dose rate of 1 to 3 Gy(Si)/s (100 to 300 rad(Si)/s) and a subsequent 373 K (100 C) bake. New initiatives in radiation hardness assurance are also briefly discussed, including the Qualified Manufacturers List (QML) test methodology and the possible use of 1/f noise measurements as a nondestructive screen for oxide-trap charge related failure. DOE

N91-14534# Tri-Univ. Meson Facility, Vancouver (British Columbia).
A VERSATILE RF CAVITY MODE DAMPER
W. R. Smythe (Colorado Univ., Boulder.), T. A. Enegren, and R. L. Poirier Jun. 1990 3 p Presented at the 2nd European Particle Accelerator Conference, Nice, France, 12-16 Jun. 1990
(DE91-002947; TRI-PP-90-43; CONF-900603-46) Avail: NTIS (US Sales Only) HC/MF A01

The ferrite tuned KAON booster synchrotron cavity is coaxial with the beam and operates from 46 to 61 MHz. Higher order modes can be strongly damped by including one or more 50 Ohm resistors shunted by a 250 MHz annular slot cavity within the acceleration cavity. The parameters are chosen so that the resistance dissipates a tolerable amount of power at the acceleration frequency. Immediately above the acceleration frequency, the damping shunt resistance decreases rapidly, approximately as the inverse fourth power of the frequency. Both calculation and measurement have shown very strong damping of all modes between the fundamental and 1000 MHz. DOE

N91-14535# Lawrence Livermore National Lab., CA. Field Test Systems Div.
AVALANCHE TRANSISTOR SELECTION FOR LONG TERM STABILITY IN STREAK CAMERA SWEEP AND PULSER APPLICATIONS
S. W. Thomas, R. L. Griffith, and A. T. Teruya Sep. 1990 13 p Presented at the 19th International Congress on High Speed Photography and Photonics, Cambridge, England, 16-22 Sep. 1990 Submitted for publication
(Contract W-7405-eng-48)
(DE91-004195; UCRL-102844; CONF-9009248-4) Avail: NTIS HC/MF A03

We have identified the Motorola 2N4014 and 2N5551 and the Raytheon RS3944 as three transistor types that exhibit avalanche characteristics and have long term collector breakdown voltage stability superior to other transistors tested. Stability on all types has been improved by power burnin. An automatic avalanche transistor burnin tester has been constructed to allow power burnin of up to 1008 transistors at a time. The tester is controlled by an IBM Personal Computer (PC) and can be programmed to acquire data, unattended, at any desired rate or period. Data are collected from each run and stored on a floppy disk in ASCII format. The data analysis software, RS/1, was used for analysis and display. Data runs were typically 3 to 4 months long, with readings taken weekly. The transistors were biased into the avalanche or Zener region by individual current sources set to about 20 percent of the self-avalanche current for each type of transistor. Motorola, Zetex and National transistors were operated at 100 micro-A, and the Raytheon units were operated at 20 micro-A. The electric field causes migration of material in the high field region at the surface near the collector-base junction, creating the voltage instability. DOE

N91-14536* National Aeronautics and Space Administration. Pasadena Office, CA.
ORGANIC CATHODE FOR A SECONDARY BATTERY Patent
Ratnakumar V. Bugga, inventor (to NASA), Salvador DiStefano, inventor (to NASA), Roger M. Williams, inventor (to NASA), and Clyde P. Bankston, inventor (to NASA) (Jet Propulsion Lab., California Inst. of Tech., Pasadena.) 7 Sep. 1989 9 p Filed 7 Sep. 1989 Prepared in cooperation with Jet Propulsion Lab., California Inst. of Tech., Pasadena
(NASA-Case-NPO-17604-1-CU; US-Patent-4,966,823; US-Patent-Appl-SN-404288; US-Patent-Class-429-104; US-Patent-Class-429-213; US-Patent-Class-252-62.2; Int-Patent-Class-H07M-10/39; Int-Patent-Class-H07M-4/60)
Avail: US Patent and Trademark Office CSCL 09A

A liquid catholyte for a battery based on liquid metal such as sodium anode and a solid, ceramic separator such as beta alumina (BASE) comprises a mixture of a Group I-III metal salt such as sodium tetrachloroaluminate and a minor amount of an organic carbonitrile depolarizer having at least one adjacent ethylenic band such as 1 to 40 percent by weight of tetracyanoethylene. The tetracyanoethylene forms an adduct with the molten metal salt.
Official Gazette of the U.S. Patent and Trademark Office

N91-14537* National Aeronautics and Space Administration. Lyndon B. Johnson Space Center, Houston, TX.
THERMAL SWITCH DISC FOR SHORT CIRCUIT PROTECTION OF BATTERIES Patent
Eric C. Dimpault-Darcy, inventor (to NASA) and Bobby J. Bragg, inventor (to NASA) 27 Nov. 1990 5 p Filed 27 Apr. 1989
(NASA-Case-MSC-21428-1; US-Patent-Appl-SN-343652; US-Patent-Class-338-32; US-Patent-Class-320-51; US-Patent-Class-338-221; Int-Patent-Class-H01L-43/00) Avail: US Patent and Trademark Office CSCL 09A

A protective device for one battery or serially arranged battery cells is disclosed and is adapted to fit between one battery and its terminal connector or between adjacent battery cells. The device incorporates a disk of positive temperature coefficient material having a pair of circular end faces for contact. The disk is supported by a ring adhesively joined thereto, the ring having a central axial opening to enable the button terminal of a battery cell to contact against the disk as the disk and battery cell are arranged in a single battery application or in serial contact with similar battery cells. Official Gazette of the U.S. Patent and Trademark Office

N91-14538* National Aeronautics and Space Administration. Pasadena Office, CA.
COPPER CHLORIDE CATHODE FOR A SECONDARY BATTERY Patent
Ratnakumar V. Bugga, inventor (to NASA), Salvador DiStefano, inventor (to NASA), Ganesan Nagasubramanian, inventor (to NASA), and Clyde P. Bankston, inventor (to NASA) (Jet Propulsion Lab., California Inst. of Tech., Pasadena.) 31 Jul. 1990 6 p Filed 11 Sep. 1989
(NASA-Case-NPO-17640-1-CU; US-Patent-4,945,012; US-Patent-Appl-SN-405169; US-Patent-Class-429-103; US-Patent-Class-429-120; Int-Patent-Class-H01M-6/20) Avail: US Patent and Trademark Office CSCL 09A

Higher energy and power densities are achieved in a secondary battery based on molten sodium and a solid, ceramic separator such as a beta alumina and a molten catholyte such as sodium tetrachloroaluminate and a copper chloride cathode. The higher cell voltage of copper chloride provides higher energy densities and the higher power density results from increased conductivity resulting from formation of copper as discharge proceeds.
Official Gazette of the U.S. Patent and Trademark Office

N91-14539* National Aeronautics and Space Administration. Pasadena Office, CA.
IMPROVED HIGH POWER/HIGH FREQUENCY INDUCTOR Patent
W. T. McLyman, inventor (to NASA) (Jet Propulsion Lab., California Inst. of Tech., Pasadena.) 4 Dec. 1990 5 p Filed 30 Nov. 1989
(NASA-Case-NPO-17830-1-CU; US-Patent-4,975,672; US-Patent-Appl-SN-443297; US-Patent-Class-336-198; US-Patent-Class-336-205; US-Patent-Class-336-229; Int-Patent-Class-H01F-27/30) Avail: US Patent and Trademark Office CSCL 09A

A toroidal core is mounted on an alignment disc having uniformly

distributed circumferential notches or holes therein. Wire is then wound about the toroidal core in a uniform pattern defined by the notches or holes. Prior to winding, the wire may be placed within shrink tubing. The shrink tubing is then wound about the alignment disc and core and then heat-shrunk to positively retain the wire in the uniform position on the toroidal core.

Official Gazette of the U.S. Patent and Trademark Office

N91-14540*# National Aeronautics and Space Administration. Ames Research Center, Moffett Field, CA.

MODELING AND CONTROL DESIGN OF A WIND TUNNEL MODEL SUPPORT

David A. Howe Nov. 1990 11 p Prepared for presentation at the 9th International Model Analysis Conference, Florence, Italy, 15-16 Apr. 1991

(NASA-TM-103829; A-91008; NAS 1.15:103829) Avail: NTIS HC/MF A03 CSCL 09C

The 12-Foot Pressure Wind Tunnel at Ames Research Center is being restored. A major part of the restoration is the complete redesign of the aircraft model supports and their associated control systems. An accurate trajectory control servo system capable of positioning a model (with no measurable overshoot) is needed. Extremely small errors in scaled-model pitch angle can increase airline fuel costs for the final aircraft configuration by millions of dollars. In order to make a mechanism sufficiently accurate in pitch, a detailed structural and control-system model must be created and then simulated on a digital computer. The model must contain linear representations of the mechanical system, including masses, springs, and damping in order to determine system modes. Electrical components, both analog and digital, linear and nonlinear must also be simulated. The model of the entire closed-loop system must then be tuned to control the modes of the flexible model-support structure. The development of a system model, the control modal analysis, and the control-system design are discussed. Author

N91-14541# Scientific Research Associates, Inc., Glastonbury, CT.

STUDYING QUANTUM PHASE-BASED ELECTRONIC DEVICES Final Report, 20 May 1987 - 14 Jun. 1990

H. L. Grubin, M. Cahay, and J. P. Kreskovsky 15 Aug. 1990 107 p

(Contract F49620-87-C-0055; AF Proj. 2386)

(AD-A226809; SRA/R90-910023-F; AFOSR-90-0923TR) Avail: NTIS HC/MF A06 CSCL 20/10

A study was undertaken to examine, theoretically, quantum phase-based electronic devices. The study was implemented through examination of moments of the Wigner Distribution Function, time dependent solutions to Schrodingers equation in two dimensions and solutions to the equation of motion of the Density Matrix. Solutions were obtained using numerical methods. A variety of problems were considered including simulation of resonant tunneling structures, electron diffraction through an aperture in a potential well, and examination of the Aharanov-Bohm effect. GRA

N91-14542# Texas Univ., Austin. Microwave Lab.

THE APPLICATION OF DETERMINISTIC SPECTRAL DOMAIN METHOD TO THE ANALYSIS OF PLANAR CIRCUIT DISCONTINUITIES ON OPEN SUBSTRATES

James Stuart McLean and Tatsuo Itoh Aug. 1990 130 p

(Contract N00014-89-C-1006)

(AD-A226901; MW-90-P-5) Avail: NTIS HC/MF A07 CSCL 09/1

A deterministic formulation of the method of moments carried out in the spectral domain is extended to include the effects of two-dimensional, two-component current flow in planar transmission line discontinuities on open substrates. The method includes the effects of space-wave and surface-wave radiation through the use of the exact spectral domain Green's function. The procedure and formulation of the method are described in detail. Also, techniques used to increase the numerical efficiency are described in detail. The method is used to determine accurate circuit models of three types of planar circuit discontinuities on open substrates: microstrip open-end discontinuities, slotline short-circuit discontinuities, and microstrip gap discontinuities. The analysis is then applied to gap-coupled resonators. The coupling between cascaded gap discontinuities is shown to be significant when the substrate is electrically thick since surface wave excitation is strong. Possibilities for further applications of the method to more complicated discontinuities are discussed. GRA

N91-14543# SoHaR, Inc., Los Angeles, CA.

INTEGRATION OF SNEAK ANALYSIS WITH DESIGN, VOLUME 1 Final Technical Report, Oct. 1987 - Oct. 1989

Jeff Miller Jun. 1990 104 p Prepared for Fail-Safe Technology Corp., Los Angeles, CA

(Contract F30602-87-C-0193; AF Proj. 2338)

(AD-A226902; RADC-TR-90-109-Vol-1) Avail: NTIS HC/MF A06 CSCL 12/5

This report documents the work in the creation of a software package to be used by a design engineer to prevent sneak circuit failures in a new design. Sneak Circuit Analysis for the Common Man was an interim report that was issued representing the manual procedure for identifying possible sneak circuits. This report presents the automated version to be used on an IBM PC under MS/DOS. The Sneak Circuit Analysis (SCA) software package uses the ORCAD II schematic capture program to analyze the circuitry. SCA will search for potential sneak paths and identify them for the user. SCA will then offer suggestions to the user to correct the design weaknesses. The software package handles analog as well as digital circuits and for very large networks, a sectional analysis is possible. GRA

N91-14544# Naval Academy, Annapolis, MD. Dept. of Systems.

DEVELOPMENT OF A TACTION SYSTEM USING PIEZOELECTRIC FILM Final Report, 1989 - 1990

Lyle E. Hoag 22 May 1990 62 p

(AD-A227076; USNA-TSPR-168) Avail: NTIS HC/MF A04 CSCL 09/1

The piezoelectric properties of materials such as naturally occurring quartz have been used in pressure and vibration sensors for many decades. Over the last twenty years synthetic crystals have been developed with improved mechanical properties and improved machinability over naturally occurring quartz. A more recent development is a plastic film which displays the piezoelectric property. The film is finding application in areas where crystals would be impossible or difficult to use because of its flexibility and ruggedness as compared to quartz. A taction system is a multi-sensor touch sensing system. A taction system was designed using piezoelectric film. Digital signal processing techniques were used to acquire and display the voltage produced by an array of sixteen tactile sensors. It was demonstrated that the taction system could be used in a variety of applications requiring multiple pressure measurements such as touch sensing in robotics and in prosthetic devices. GRA

N91-14545# Science Applications International Corp., Torrance, CA.

ELECTRIC PROPULSION STUDY Final Report, 21 Sep. 1988 - 30 Nov. 1989

Dennis J. Cravens Aug. 1990 169 p

(Contract F04611-88-C-0014)

(AD-A227121; AL-TR-89-040) Avail: NTIS HC/MF A08 CSCL 21/3

Inductive theories and experimental approaches which provide for interactions between gravitational and electromagnetic fields are reviewed. The theoretical section develops a general relativistic five dimensional theory to the point that electromagnetic effects can be interpreted. Emphasis is placed on modifications to the classical Maxwell equations and field vector equations. The theories are then often used to propose specific experimental studies which can verify the electromagnetic and gravitational interactions. Specific recommendations are made for experiments that would

both verify the theories and serve as a basis for electric propulsive systems that would convert between electromagnetic and inertial momentum. GRA

N91-14546# Toledo Univ., OH. Dept. of Electrical Engineering.
A STUDY OF TWO CONTROL METHODS FOR FULL BRIDGE CONVERTERS: SOFT SWITCH BYPASS AND CURRENT MODE CONTROL Final Report, 1 May 1989 - 11 Mar. 1990
Thomas A. Stuart Jun. 1990 61 p
(Contract F33615-86-C-2720; AF Proj. 3145)
(AD-A227136; WRDC-TR-90-2026) Avail: NTIS HC/MF A04 CSCL 10/2

In a broad sense, there are now 3 basic categories for high power (above several KW) DC/DC converters: (1) Forced commutation (FC); (2) Resonant (R); and (3) Soft switch (SS). Some topologies that are combinations of the above also have been proposed, such as certain pulse width modulation (PWM)-resonant arrangements. The first part of this project was a proposed improvement of the third category, the soft switch. The basic idea of this new converter was to use two additional switches that would bypass the loading during part of the operating cycle if the current decreased below a certain level. The motivation for this was to retain the soft switching characteristic at light loads (a common problem with soft switch converters). Although the bypass circuit proved functional, certain problems were uncovered which raise doubts about its ultimate feasibility. Because of these problems, the research emphasis was shifted from the bypass to an improve current mode control (CMC) converter that promised better results. GRA

N91-14547# Naval Postgraduate School, Monterey, CA.
COMPUTER AIDED DESIGN MODELS FOR MILLIMETER-WAVE SUSPENDED SUBSTRATE MICROSTRIP LINE M.S. Thesis
Man S. Choi Mar. 1990 89 p
(AD-A227259) Avail: NTIS HC/MF A05 CSCL 12/5

An equivalent circuit model was derived for the series gap discontinuity in shielded suspended-substrate transmission line. Numerical values of the circuit parameters were computed for various sets of line dimensions, over a range of operating frequencies. The shielded suspended-substrate line is a transmission medium useful for radar and microwave circuits in the Ka band frequency range, 30 to 40 GHz. In order to utilize this transmission medium in the construction of microwave circuits and filters, it is necessary to have valid circuit models for typical discontinuous change in width. These discontinuity characteristics may be deduced on the basis of a calculation of their scattering coefficients for propagating waves in the medium. The approach chosen in this thesis, however, is that of placing the selected discontinuity in an open-ended strip resonator in the transmission medium. An appropriate circuit model is adopted for the given discontinuity, and its circuit elements are then deduced on the basis of the perturbation of the resonance frequency of the strip resonator which is induced by the mode. The boundary-value problem associated with the microstrip resonator structure has been approached in a rigorous manner based on a full-wave analysis which utilizes a process of solving the electromagnetic (EM) boundary value problem with inclusion of all the field components. GRA

N91-14548# Cree Research, Inc., Durham, NC.
DEVELOPMENT AND TESTING OF RADIATION AND ELECTROMAGNETIC PULSE HARDENED SILICON CARBIDE BASED ELECTRONICS Quarterly Report, 1 Jun. - 31 Aug. 1990
J. A. Edmond and J. W. Palmour 19 Sep. 1990 11 p
(Contract N00014-90-C-0037)
(AD-A227309; TR-901008-4) Avail: NTIS HC/MF A03 CSCL 09/1

There were three primary objectives. The first was the reverse avalanche testing of diodes exhibiting the following: (1) microplasma dominated breakdown; (2) a combination of microplasma and bulk avalanche breakdown; and (3) bulk avalanche breakdown only. These glass encapsulated devices were tested at approximately 1, 10, and 100 microsec pulses. The second objective was to fabricate and characterize Shockley diodes in chip form showing proper breakdown in forward and reverse bias and a forward bias turn-on of approximately 2.6 V. The third objective was to fabricate and characterize 6H-SiC JFET structures in chip form. GRA

N91-14549# Utah Univ., Salt Lake City. Dept. of Physics.
CONDUCTIVITY FLUCTUATIONS IN FAST IONIC CONDUCTORS Final Report, 1 Aug. 1982 - 30 Sep. 1990
James J. Brophy Sep. 1990 7 p
(Contract N00014-82-K-0603)
(AD-A227379) Avail: NTIS HC A02/MF A01 CSCL 07/4

Electrical conductivity fluctuations in superionic solids provide a new way of examining transport and electrode properties of solid electrolytes. Of particular interest are the Na Beta and Na Beta double primed aluminas because of their high ionic conductivity, potentially important technological applications, and the ease with which the mobile sodium ions can be exchanged for a number of mono- and di-valent cations. Single crystal and ceramic specimens of sodium, silver, lead, and calcium Beta double primed aluminas, as well as mixed Na/Ag and Na/Ca conductors, have been found to exhibit conductivity fluctuations associated with diffusion of the mobile ions. Also, in the absence of electric current and at frequencies above about 100 Hz Nyquist noise corresponding to the bulk electrolyte resistance is observed. Below 100 Hz noise associated with amalgamation reactions at the electrolyte/contact interface or noise associated with ionic shot noise during the build-up of an electric double layer at the interface are dominant. Experimental diffusion noise levels can be quantitatively explained by focusing on the diffusion of ion-vacancy pairs in single conduction planes. Fluctuations in adjacent planes are correlated and corrections arising from in-plane coulomb forces are negligible. GRA

N91-14550* National Aeronautics and Space Administration. Goddard Space Flight Center, Greenbelt, MD.
DIGITIZED SYNCHRONOUS DEMODULATOR Patent
Christopher E. Woodhouse, inventor (to NASA) 27 Nov. 1990 6 p Filed 10 Oct. 1989
(NASA-Case-GSC-13237-1; US-Patent-4,973,914;
US-Patent-Appl-SN-418612; US-Patent-Class-329-363;
US-Patent-Class-328-151; Int-Patent-Class-H03D-1/00) Avail: US Patent and Trademark Office CSCL 09A

A digitized synchronous demodulator is constructed entirely of digital components including timing logic, an accumulator, and means to digitally filter the digital output signal. Indirectly, it accepts, at its input, periodic analog signals which are converted to digital signals by traditional analog-to-digital conversion techniques. Broadly, the input digital signals are summed to one of two registers within an accumulator, based on the phase of the input signal and medicated by timing logic. At the end of a predetermined number of cycles of the inputted periodic signals, the contents of the register that accumulated samples from the negative half cycle is subtracted from the accumulated samples from the positive half cycle. The resulting difference is an accurate measurement of the narrow band amplitude of the periodic input signal during the measurement period. This measurement will not include error sources encountered in prior art synchronous demodulators using analog techniques such as offsets, charge injection errors, temperature drift, switching transients, settling time, analog to digital converter missing code, and linearity errors.
Official Gazette of the U.S. Patent and Trademark Office

N91-14551* National Aeronautics and Space Administration. Pasadena Office, CA.
MILLIMETER-WAVE MONOLITHIC DIODE-GRID FREQUENCY MULTIPLIER Patent
Joseph Maserjian, inventor (to NASA) (Jet Propulsion Lab., California Inst. of Tech., Pasadena.) 4 Sep. 1990 7 p Filed 13 Dec. 1988
(NASA-Case-NPO-17258-1-CU; US-Patent-4,954,864;
US-Patent-Appl-SN-283673; US-Patent-Class-357-30;

US-Patent-Class-357-15; US-Patent-Class-357-29; US-Patent-Class-357-32; US-Patent-Class-357-58; Int-Patent-Class-H01L-27/14) Avail: US Patent and Trademark Office CSCL 09A

A semiconductor diode structure useful for harmonic generation of millimeter or submillimeter wave radiation from a fundamental input wave is fabricated on a GaAs substrate. A heavily doped layer of n(sup ++) GaAs is produced on the substrate and then a layer of intrinsic GaAs on said heavily doped layer on top of which a sheet of heavy doping (++) is produced. A thin layer of intrinsic GaAs grown over the sheet is capped with two metal contacts separated by a gap to produce two diodes connected back to back through the n(sup ++) layer for multiplication of frequency by an odd multiple. If only one metal contact caps the thin layer of intrinsic GaAs, the second diode contact is produced to connect to the n(sup ++) layer for multiplication of frequency by an even number. The odd or even frequency multiple is selected by a filter. A phased array of diodes in a grid will increase the power of the higher frequency generated.

Official Gazette of the U.S. Patent and Trademark Office

N91-14552* National Aeronautics and Space Administration. Lewis Research Center, Cleveland, OH.

UNIVERSAL NONDESTRUCTIVE mm-WAVE INTEGRATED CIRCUIT TEST FIXTURE Patent

Robert R. Romanofsky, inventor (to NASA) and Kurt A. Shalkhauser, inventor (to NASA) 25 Dec. 1990 9 p Filed 10 Aug. 1989

(NASA-Case-LEW-14746-1; US-Patent-4,980,636; US-Patent-Appl-SN-392239; US-Patent-Class-324-158F; US-Patent-Class-324-158P; US-Patent-Class-324-601; US-Patent-Class-333-247; Int-Patent-Class-G01R-1/04) Avail: US Patent and Trademark Office CSCL 09C

Monolithic microwave integrated circuit (MMIC) test includes a bias module having spring-loaded contacts which electrically engage pads on a chip carrier disposed in a recess of a base member. RF energy is applied to and passed from the chip carrier by chamfered edges of ridges in the waveguide passages of housings which are removably attached to the base member. Thru, Delay, and Short calibration standards having dimensions identical to those of the chip carrier assure accuracy and reliability of the test. The MMIC chip fits in an opening in the chip carrier with the boundaries of the MMIC lying on movable reference planes thereby establishing accuracy and flexibility.

Official Gazette of the U.S. Patent and Trademark Office

N91-14553# Sandia National Labs., Albuquerque, NM.

OPTICALLY-TRIGGERED GaAs THYRISTOR SWITCH S: INTEGRATED STRUCTURES FOR ENVIRONMENTAL HARDENING

R. F. Carson, H. T. Weaver, R. C. Hughes, T. E. Zipperian, T. M. Brennan, and B. E. Hammons 1990 11 p Presented at the Annual Meeting of the Optical Society of America, Inc., Boston, MA, 4-9 Nov. 1990

(Contract DE-AC04-76DP-00789)

(DE91-001355; SAND-90-0736C; CONF-901102-1) Avail: NTIS HC/MF A03

Optically-triggered thyristor switches often operate in adverse environments, such as high temperature and high dose-rate transient radiation, which can result in lowered operating voltage and premature triggering. These effects can be reduced by connecting or monolithically integrating a reverse-biased compensating photodiode or phototransistor into the gate of the optically-triggered thyristor. We have demonstrated the effectiveness of this hardening concept in silicon thyristors packaged with photodiodes, and in gallium arsenide optically-triggered thyristors monolithically integrated with compensating phototransistors. DOE

N91-14554# Fermi National Accelerator Lab., Batavia, IL.

SUPERCONDUCTING CURRENT TRANSDUCER

M. Kuchnir and J. P. Ozelis Oct. 1990 3 p Presented at the 1990 Applied Superconductivity Conference, Snowmass, CO, 24-28 Sep. 1990

(Contract DE-AC02-76CH-03000)

(DE91-004674; FNAL-TM-1688) Avail: NTIS HC/MF A01

The construction and performance of an electric current meter that operates in liquid He and mechanically splits apart to permit replacement of the current carrying conductor is described. It permits the measurement of currents induced in a loop of superconducting cable and expeditious exchange of such loops. It is a key component for a short sample cable testing facility that requires no high current power supplies nor high current leads. Its superconducting pickup circuit involves a non-magnetic core toroidal split-coil that surrounds the conductor and a solenoid whose field is sensed by a Hall probe. This toroidal split-coil is potted inside another compensating toroidal split-coil. The C shaped half toroids can be separated and brought precisely together from outside the cryostat. The Hall probe is energized and sensed by a lock-in amplifier whose output drives a bipolar power supply which feeds the compensating coil. The output is the voltage across a resistor in this feedback circuit. Currents of up to 10 kA can be measured with a precision of 150 mA. DOE

34 FLUID MECHANICS AND HEAT TRANSFER

Includes boundary layers; hydrodynamics; fluidics; mass transfer; and ablation cooling.

For related information see also *02 Aerodynamics* and *77 Thermodynamics and Statistical Physics.*

N91-14555 Michigan Univ., Ann Arbor.

ACCELERATION TECHNIQUES FOR EXPLICIT EULER CODES Ph.D. Thesis

Chang Hsien Tai 1990 175 p

Avail: Univ. Microfilms Order No. DA9023650

Two steps in the acceleration of Euler computations to steady solutions are studied: (1) using full multi-grid to march from an arbitrary initial guess to within the range of attraction of the steady solution; and (2) using vector-sequencing to converge to the steady solution from a nearby state. Regarding the first step, in order to design schemes that combine well with multi-grid acceleration, a method was developed for designing optimally smoothing multi-stage time-marching schemes, given any spatial-differencing operator. The analysis was extended to the Euler and Navier-Stokes equations in one space-dimension by use of characteristic time-stepping. Convergence rates independent of the number of cells in the finest grid were achieved with these optimal schemes, for transonic flow with and without a shock. Besides characteristic time-stepping, local time-stepping was tested with these schemes. Good convergence was obtained with local time-stepping. Finally, the analysis was extended to scalar, Burgers, and Euler equations in two space dimensions. The successful application to multi-dimensional scalar equations turns out to depend on the possibility of damping numerical signals that move normal to the physical transport direction. Several techniques that were tested do this. Regarding the second step, two vector-sequencing strategies, generalized minimum residuals (GMRES) and minimum polynomial extrapolation (MPE), which can quickly converge to the steady solution from a nearby state, were explored and applied to linear and nonlinear problems. The results obtained with GMRES and MPE in nested iterations suggest that there is an advantage in the combination of the multi-grid strategy with vector-sequencing ideas. Dissert. Abstr.

N91-14556*# National Aeronautics and Space Administration. Lewis Research Center, Cleveland, OH.

SURFACE SETTLING IN PARTIALLY FILLED CONTAINERS UPON STEP REDUCTION IN GRAVITY

Marl M. Weislogel and Howard D. Ross Nov. 1990 19 p Submitted for publication

(NASA-TM-103641; E-4998; NAS 1.15:103641) Avail: NTIS HC/MF A03 CSCL 20D

A large literature exists concerning the equilibrium configurations of free liquid/gas surfaces in reduced gravity environments. Such conditions generally yield surfaces of constant curvature meeting the container wall at a particular (contact) angle. The time required to reach and stabilize about this configuration is less studied for the case of sudden changes in gravity level, e.g. from normal- to low-gravity, as can occur in many drop tower experiments. The particular interest here was to determine the total reorientation time for such surfaces in cylinders (mainly), as a function primarily of contact angle and kinematic viscosity, in order to aid in the development of drop tower experiment design. A large parametric range of tests were performed and, based on an accompanying scale analysis, the complete data set was correlated. The results of other investigations are included for comparison. Author

N91-14557*# Alabama Univ., Huntsville. Dept. of Mechanical Engineering.

CFD CODE EVALUATION FOR INTERNAL FLOW MODELING Final Report

T. J. Chung Dec. 1990 78 p

(Grant NAG8-095)

(NASA-CR-187677; NAS 1.26:187677) Avail: NTIS HC/MF A05 CSCL 20D

Research on the computational fluid dynamics (CFD) code evaluation with emphasis on supercomputing in reacting flows is discussed. Advantages of unstructured grids, multigrids, adaptive methods, improved flow solvers, vector processing, parallel processing, and reduction of memory requirements are discussed. As examples, researchers include applications of supercomputing to reacting flow Navier-Stokes equations including shock waves and turbulence and combustion instability problems associated with solid and liquid propellants. Evaluation of codes developed by other organizations are not included. Instead, the basic criteria for accuracy and efficiency have been established, and some applications on rocket combustion have been made. Research toward an ultimate goal, the most accurate and efficient CFD code, is in progress and will continue for years to come. Author

N91-14558*# Eloret Corp., Palo Alto, CA.

COMPUTATION OF THERMOCHEMICAL NONEQUILIBRIUM FLOWS AROUND A SIMPLE AND A DOUBLE ELLIPSE

Tahir Gokcen 1990 25 p

(Contract NCC2-420)

(NASA-CR-187702; NAS 1.26:187702) Avail: NTIS HC/MF A03 CSCL 20D

The nonequilibrium viscous reactive flows over a simple and a double ellipse at a 30 degree angle of attack were computed. The geometry and the free stream conditions are given by INRIA/GAMNI/SMAI workshop test cases 6.2-2 and 6.2-4. The governing Navier-Stokes equations coupled with thermochemical nonequilibrium processes are solved numerically using a fully coupled, implicit, finite volume technique with a dynamically adaptive grid. The nonequilibrium gas model and the numerical method used in the calculations are briefly described. Author

N91-14559*# National Aeronautics and Space Administration. Lewis Research Center, Cleveland, OH.

NUMERICAL STUDY OF SHOCK-WAVE/BOUNDARY LAYER INTERACTIONS IN PREMIXED HYDROGEN-AIR HYPERSONIC FLOWS

Shaye Yungster Nov. 1990 21 p Presented at the 29th Aerospace Sciences Meeting, Reno, NV, 7-10 Jan. 1991; sponsored by AIAA Original contains color illustrations

(NASA Order C-99066-G)

(NASA-TM-103273; E-5715; ICOMP-90-22; NAS 1.15:103273; AIAA-91-0413) Avail: NTIS HC/MF A03; 3 functional color pages CSCL 20D

A computational study of shock wave/boundary layer interactions involving premixed combustible gases, and the resulting combustion processes is presented. The analysis is carried out using a new fully implicit, total variation diminishing (TVD) code developed for solving the fully coupled Reynolds-averaged Navier-Stokes equations and species continuity equations in an efficient manner. To accelerate the convergence of the basic iterative procedure, this code is combined with vector extrapolation methods. The chemical nonequilibrium processes are simulated by means of a finite-rate chemistry model for hydrogen-air combustion. Several validation test cases are presented and the results compared with experimental data or with other computational results. The code is then applied to study shock wave/boundary layer interactions in a ram accelerator configuration. Results indicate a new combustion mechanism in which a shock wave induces combustion in the boundary layer, which then propagates outwards and downstream. At higher Mach numbers, spontaneous ignition in part of the boundary layer is observed, which eventually extends along the entire boundary layer at still higher values of the Mach number. Author

N91-14560# Lawrence Livermore National Lab., CA.

A NUMERICAL THEORY OF LATTICE GAS AND LATTICE BOLTZMANN METHODS IN THE COMPUTATION OF SOLUTIONS TO NONLINEAR ADVECTIVE-DIFFUSIVE SYSTEMS Ph.D. Thesis - California Univ., Davis

Altamont Bracy Hamil Elton 24 Sep. 1990 265 p

(Contract W-7405-eng-48)

(DE91-002566; UCRL-LR-105090) Avail: NTIS HC/MF A13

A numerical theory for the massively parallel lattice gas and lattice Boltzmann methods for computing solutions to nonlinear advective-diffusive systems is introduced. The convergence theory is based on consistency and stability arguments that are supported by the discrete Chapman-Enskog expansion (for consistency) and conditions of monotonicity (in establishing stability). The theory is applied to four lattice methods: Two of the methods are for some two-dimensional nonlinear diffusion equations. One of the methods is for the one-dimensional lattice method for the one-dimensional viscous Burgers equation. And one of the methods is for a two-dimensional nonlinear advection-diffusion equation. Convergence is formally proven in the L(sub 1)-norm for the first three methods, revealing that they are second-order, conservative, conditionally monotone finite difference methods. Computational results which support the theory for lattice methods are presented. In addition, a domain decomposition strategy using mesh refinement techniques is presented for lattice gas and lattice Boltzmann methods. The strategy allows concentration of computational resources on regions of high activity. Computational evidence is reported for the strategy applied to the lattice gas method for the one-dimensional viscous Burgers equation. DOE

N91-14561# Sandia National Labs., Albuquerque, NM.

A FAST SOLVER FOR SYSTEMS OF AXISYMMETRIC RING VORTICES

James H. Strickland and Donald E. Amos Sep. 1990 54 p

(Contract DE-AC04-76DP-00789)

(DE91-002594; SAND-90-1925) Avail: NTIS HC/MF A04

A method which is capable of efficient calculation of the axisymmetric flow field produced by a large system of ring vortices is presented in this report. The system of ring vortices can, in turn, be used to model body surfaces and wakes in incompressible unsteady axisymmetric flow fields. This method takes advantage of source point and field point series expansions which enables one to make calculations for interactions between groups of vortices which are in well separated spatial domains rather than having to consider interactions between every pair of vortices. In this work, series expansions for the stream function of the ring vortex system are obtained. Such expansions explicitly contain the radial and axial velocity components. A FORTRAN computer code RSOLV has been written to execute the fast solution technique to calculate the stream function and the axial and radial velocity components at points in the flow field. Test cases have been run to optimize the code and to benchmark the truncation errors and CPU time savings associated with the method. Non-dimensional truncation errors for the stream function and total velocity field are on the order of 5 times 10(exp -5) and 3 times 10(exp -3) respectively. Single precision accuracy produces errors in these quantities up to about 1 times 10(exp -5). For 100 vortices in the field, there is virtually no CPU time savings with the fast

solver. For 10,000 vortices in the flow, the fast solver obtains solutions in about 1 to 3 percent of the time required for the direct solution technique. Simulations of vortices with square and circular cores were run in order to obtain expressions for the self-induced velocities of such vortices. DOE

N91-14562* National Aeronautics and Space Administration. Langley Research Center, Hampton, VA.
ACTIVE CONTROL OF BOUNDARY LAYER TRANSITION AND TURBULENCE Patent
Lucio Maestrello, inventor (to NASA) 12 Jun. 1990 7 p Filed 11 Mar. 1986
(NASA-Case-LAR-13532-1; US-Patent-4,932,610; US-Patent-Appl-SN-838649; US-Patent-Class-244-203; US-Patent-Class-244-204; US-Patent-Class-244-130; US-Patent-Class-114-67A; Int-Patent-Class-B64B-21/00) Avail: US Patent and Trademark Office CSCL 20D

The invention is a system and method for controlling boundary layer flow such that flow separation can be delayed and skin friction drag can be reduced. The invention consists of heater elements used to trigger turbulent flow and audio speakers used to suppress turbulent oscillations. By inducing turbulent oscillations into the flow in a region of positive pressure gradient, pressure patterns became more regular. The suppression of these patterns can be accomplished by imposing an out-of-phase suppressing wave. This wave is the audio output generated by a feedback amplifier using inputs from a hot-wire anemometer reading downstream turbulence. The novel features of the present invention are the tripping of boundary layer flow in a region of positive pressure gradient and the cooperative use of the feedback means to control turbulence. The result is a significant reduction in drag and separation problems.
Official Gazette of the U.S. Patent and Trademark Office

N91-14563* National Aeronautics and Space Administration. Marshall Space Flight Center, Huntsville, AL.
LOW-NOISE NOZZLE VALVE Patent
Hal S. Gwin, inventor (to NASA) and James Aaron, inventor (to NASA) 18 Sep. 1990 8 p Filed 7 Sep. 1989
(NASA-Case-MFS-28383-1; US-Patent-4,957,139; US-Patent-Appl-SN-404290; US-Patent-Class-137-556; US-Patent-Class-251-212; Int-Patent-Class-F16K-3/32; Int-Patent-Class-F16K-37/00; Int-Patent-Class-F16K-3/316)
Avail: US Patent and Trademark Office CSCL 20D

A low noise, variable discharage area, valve is constructed having opposed recesses within which a pair of gates are slidably disposed. Each of the gates is provided with upstream edges having a radius thereon, the radius enabling smooth, accelerated, low noise flow therebetween. The gates are further provided with tracks along each side, which in turn slide along splines set in the side walls of the valve. A threaded rod which rotates in a threaded insert in a rear wall of each of the gates, serves to move the gates within their respective recesses.
Official Gazette of the U.S. Patent and Trademark Office

N91-14564# Ballistic Research Labs., Aberdeen Proving Ground, MD.
DIRECT NUMERICAL SIMULATION OF TURBULENT COUETTE FLOW, PART 2 Final Report, Dec. 1989 - Jun. 1990
John D. Kuzan and Phillip C. Dykstra Aug. 1990 40 p
(AD-A226770; BRL-MR-3857) Avail: NTIS HC/MF A03 CSCL 20/4

A direct simulation of fully developed turbulent channel flow has been performed, through a direct solution of the time-varying, incompressible, Navier-Stokes equations. Reynolds shear stress appears to mark structures that are similar to those marked by hydrogen bubbles in the near-wall region of wall bounded shear flows. This has been observed by others, but not from animated views that match closely the physical experiments. Three-dimensional views of the Reynolds shear stress reveal elongated structures in the near-wall region that do not appear to be connected at larger normal distances. GRA

N91-14565# Massachusetts Inst. of Tech., Cambridge. Dept. of Ocean Engineering.
VARIATION OF WALL SHEAR STRESS AND REYNOLDS STRESS OVER A FLAT PLATE DOWNSTREAM OF A BOUNDARY LAYER MANIPULATOR M.S. Thesis
Francis James Camelio Jun. 1990 160 p
(AD-A226875) Avail: NTIS HC/MF A08 CSCL 20/4

An experiment to measure the variation of wall shear stress and Reynolds stress over a flat plate downstream of a honeycomb manipulator was conducted. Two velocity components of the flow were measured with an X-configured hot-wire probe, and wall shear stress was obtained from a surface differential pressure gauge or surface fence. Unmanipulated boundary layer data was collected at eight different free stream speeds to establish boundary layer characteristics and to calibrate the surface differential pressure gauge by making use of Coles' law of the wall for the mean velocity profile. Manipulated boundary layer data was obtained at three free stream speeds and six manipulator positions. Although manipulator hole size and length remained constant, height was varied to determine the influence of this length scale upon the surface friction coefficient. Manipulated stream and vertical mean and fluctuating velocity profiles and Reynolds stress profiles were compared to their unmanipulated counterparts to map the influence of the manipulator in the streamwise direction. Immediately downstream of the manipulations the transport of turbulent energy to the wall via the working of Reynolds stresses was sharply reduced. Complete restoration of Reynolds stress profiles to unmanipulated form was not observed out to the farthest downstream measurement position. Local drag reduction up to 40 percent was verified via comparison of the unmanipulated and manipulated friction coefficients obtained from the wall shear stress measurements. GRA

N91-14566# Rensselaer Polytechnic Inst., Troy, NY. Dept. of Chemical Engineering.
EFFECT OF INTERLINE HEAT FLOW PARAMETER ON CONTACT LINE HEAT TRANSFER Interim Report, Apr. 1988 - Jun. 1989
Peter C. Wayner, Jr. Apr. 1990 36 p
(Contract F33615-88-C-2821; AF Proj. 0581)
(AD-A226944; RPI-CHE/PCW-89-01; WRDC-TR-90-2008) Avail: NTIS HC/MF A03 CSCL 20/13

A circular heat transfer cell was designed and fabricated to study fluid flow and change of phase heat transfer in the contact line region. The cell incorporates the use of ellipsometry and interferometry to measure ultra-thin film thickness profiles, which give the local pressure field for fluid flow. In addition, the total fluid flow rate and therefore, the integral heat sink of the evaporating meniscus can be measured. A theoretical equation that includes the effects of capillarity, disjoining pressure, gravity, and temperature on the thin film heat transfer process has been developed and used. GRA

N91-14567# Naval Research Lab., Washington, DC. Center for Fluid/Structure Interactions.
INNOVATIVE METHODOLOGY FOR CANCELLING CONTAMINATING NOISE IN TURBULENT FLUID FLOW ENVIRONMENTS Memorandum Report
Michael P. Horne and Robert A. Handler 19 Sep. 1990 31 p
Sponsored by ONR, Arlington, VA
(AD-A227028; NRL-MR-6683) Avail: NTIS HC/MF A03 CSCL 20/1

A method is presented for the cancellation of wide band contaminating noise occurring within internal flow configurations such as rectangular channels and pipes. Facility generated noise within these flow systems contaminates the turbulent wall pressure signature at low frequencies thus preventing the possible extraction of useful information. The proposed methodology utilizes the signals from two flush mounted wall pressure transducers. A first estimate for the one and two-point spectral densities is obtained using a least mean square algorithm. A secondary correction to this estimate is obtained by taking advantage of the planar homogeneity of the turbulence. The application of the technique is demonstrated

in a fully developed turbulent channel flow for which more than 40 dB cancellation is obtained at low frequencies. In this low frequency range, the power spectral density is shown to have an approximate quadratic dependence, substantiating past theoretical predictions reported in the literature. In addition, the two-point spectral densities are adequately resolved, substantiating a convective pattern which rapidly loses coherence which is typical in such flow configurations. GRA

N91-14568# Naval Academy, Annapolis, MD. Dept. of Mechanical Engineering.
ON THE BREAKDOWN OF A VORTEX Final Report, 1989 - 1990
Douglas E. Reckamp 22 May 1990 93 p
(AD-A227066; USNA-TSPR-171) Avail: NTIS HC/MF A05 CSCL 20/4

The physical problem presented is water rotating steadily in a vertical cylinder with a specified tangential influx. Water is withdrawn through a sink in the center of the base of the cylinder. Laser Doppler velocimetry is utilized to obtain velocity data in and near the viscous vortex core region, the viscous boundary layer, and the near irrotational region. Of particular interest is the region near the sink where the viscous core interacts with the bottom boundary layer. The core radius is measured for various circulations with fixed sink radius and water column depth. Tangential and axial velocity measurements are taken through the viscous core and into the near irrotational region for various circulations with fixed sink radius and water column depth and at various radial and axial locations. Axial and tangential velocities are measured near and in the bottom boundary layer. A flow visualization technique is developed to display qualitative data on the flow where the boundary layer and viscous core interact. GRA

N91-14569# Illinois Univ., Urbana. Aerothermal Simulations Lab.
EFFECTS OF TURBULENCE ON STATIONARY AND NONSTATIONARY PROCESSES IN C-SYSTEMS Final Technical Report, 1 Sep. 1985 - 31 Aug. 1989
Robert A. Beddini and Ted A. Roberts 23 Jul. 1990 77 p
(Contract F04611-86-K-0081; AF-AFOSR-0319-86; AF Proj. 2308)
(AD-A227067; AAE-87-1; UILU-ENG-870501; AFOSR-90-0936TR) Avail: NTIS HC/MF A05 CSCL 21/2

Turbularization of an acoustic boundary layer (Strokes layer) on impermeable and permeable surfaces is analytically considered. The theoretical approach utilizes a second-order closure model of turbulence. An approximate, closed form solution and a more comprehensive finite difference solution of the time dependent, parabolic, one dimensional governing equations is obtained. For simple acoustic boundary layers on impermeable surfaces, the approximate solution and the numerical results for the critical acoustic Mach number required for turbulent transition are qualitatively confirmed. Calculations for acoustic boundary layers with transpiration (injection) indicate a substantial reduction for the acoustic Mach number required for transition, up to a frequency dependent limiting injection velocity. The results may provide a practical mechanism for flow related combustion instability in solid propellent rockets, since turbularization of near surface combustion zone could result in relatively low acoustic Mach numbers. An analysis of the transitional and turbulent reactive acoustic boundary layer on a homogenous solid propellant surface investigates potential mechanisms of combustion instability. A new technique is developed for the condensed phase thermal layer, in which the propellant space is mapped onto the gas space and efficiently solved using the same adaptive numerical grid. An acoustic pressure node is obtained in the absence of a mean axial flow. GRA

N91-14570# California Univ., San Diego, La Jolla.
INVESTIGATIONS OF EQUILIBRIA, LATTICES, AND CHAOTIC DYNAMICS OF 2-D HAMILTONIAN POINT VORTICES Final Report, 1 Nov. 1988 - 31 Oct. 1989
James Kadtke 8 Aug. 1990 108 p
(Grant AF-AFOSR-0072-87; AF Proj. 2304)
(AD-A227364; AFOSR-90-0944TR) Avail: NTIS HC/MF A06 CSCL 20/4

The aim of the proposed research effort involved theoretical work, both analytic and numerical, on a number of different problems which were all loosely tied together as involving some aspect of vortex systems, and their relation to chaos in fluid flows. Significant results were obtained during this funding period in several major topics. The first topic which was investigated was a continuation of the author's previous work on vortex lattices. Results consisted of the refinement of the analytic expression for the lattice summation of an infinite lattice of point vortices, and use of this expression to calculate the allowed lattice structures of two-component triangular lattice. It was also shown how these expressions can be used to calculate the bulk physical properties of vortex lattices, by calculating the energy of slip displacement for the triangular lattice. GRA

N91-14571# Brookhaven National Lab., Upton, NY. Dept. of Applied Sciences.
PHASE PORTRAIT METHODS FOR VERIFYING FLUID DYNAMIC SIMULATIONS
H. Bruce Stewart 1989 20 p Presented at the US-Korea Joint Seminar on Fluids Engineering and Science, Seoul, Republic of Korea, 3-9 Sep. 1989
(Contract DE-AC02-76CH-00016)
(DE91-001129; BNL-45182; CONF-8909178-2) Avail: NTIS HC/MF A03

As computing resources become more powerful and accessible, engineers more frequently face the difficult and challenging engineering problem of accurately simulating nonlinear dynamic phenomena. Although mathematical models are usually available, in the form of initial value problems for differential equations, the behavior of the solutions of nonlinear models is often poorly understood. A notable example is fluid dynamics: while the Navier-Stokes equations are believed to correctly describe turbulent flow, no exact mathematical solution of these equations in the turbulent regime is known. Differential equations can of course be solved numerically, but how are we to assess numerical solutions of complex phenomena without some understanding of the mathematical problem and its solutions to guide us. DOE

N91-14572# Midwest Research Inst., Golden, CO. Wind Energy Research Branch.
A DISCUSSION OF THE RESULTS OF AN IN-SITU COMPARISON OF THREE FULL-VECTOR ANEMOMETERS
N. D. Kelley, G. N. Scott, and J. S. Allread Oct. 1990 6 p Presented at the 7th International Conference on Interactive Information and Processing Systems for Meteorology, Oceanography, and Hydrology, New Orleans, LA, 13-18 Jan. 1991
(Contract DE-AC02-83CH-10093)
(DE91-002113; SERI/TP-257-4019; CONF-910108-2) Avail: NTIS HC/MF A02

Extensive field measurements and the numerical modeling of dynamic responses associated with wind turbine rotor blades have pointed to strong interactions with coherent turbulent structures in the turbine inflow. These interactions are thought to be a major source of high-cycle fatigue in the primary structural components of wind turbines. The sources of such turbulent structures are not only natural terrain features but also the wakes from upwind turbines. Many unsteady aerodynamic processes are excited by turbulent eddies ranging in size from several rotor diameters down to the dimensions of the mean blade chord. These processes are responsible for inducing large, fluctuating loads on the turbine rotor blades. For the wind turbine generators now in use, this encompasses a spatial range of about 0.1 to 300 m. To assess our ability to measure the coherent properties of inflow turbulence over such a wide range of spatial range, we performed a study to compare three full-vector anemometers. We believe that to identify the dominant fluid dynamic properties of such flows, the instrumentation used must be capable of good fidelity measurements over the desired spatial range. The sonic

anemometer is a primary candidate; we also wanted to compare the results associated with a well-designed mechanical instrument which is available at considerably less cost. Two sonic designs and a propeller-bivane were exposed to turbulent flows downstream of both extremely complex and moderately rolling terrain. This paper discusses some of the results of these comparisons with an emphasis on the measurements of turbulent fluctuations. DOE

N91-14573# Sandia National Labs., Albuquerque, NM. Solid Mechanics Div.
DYNAMIC STABILITY OF A SPINNING TUBE CONVEYING A FLUID THROUGH A SYMMETRICAL NONCIRCULAR CROSS-SECTION
G. A. Benedetti Nov. 1990 45 p
(Contract DE-AC04-76DP-00789)
(DE91-004146; SAND-90-8015) Avail: NTIS HC/MF A03

When a fluid flows inside a tube, the deformations of the tube can interact with the fluid flowing within it and these dynamic interactions can result in significant lateral motions of the tube and the flowing fluid. The purpose of this report is to examine the dynamic stability of a spinning tube through which an incompressible frictionless fluid is flowing. The tube can be considered as either a hollow beam or a hollow cable. The analytical results can be applied to spinning or stationary tubes through which fluids are transferred; e.g., liquid coolants, fuels and lubricants, slurry solutions, and high explosives in paste form. The coupled partial differential equations are determined for the lateral motion of a spinning Bernoulli-Euler beam or a spinning cable carrying an incompressible flowing fluid. The beam, which spins about an axis parallel to its longitudinal axis and which can also be loaded by a constant axial force, is straight, uniform, simply supported, and rests on a massless, uniform elastic foundation that spins with the beam. Damping for the beam and foundation is considered by using a combined uniform viscous damping coefficient. The fluid, in addition to being incompressible, is frictionless, has a constant density, and flows at a constant speed relative to the longitudinal beam axis. The Galerkin method is used to reduce the coupled partial differential equations for the lateral motion of the spinning beam to a coupled set of 2N, second order, ordinary differential equations for the generalized beam coordinates. By simplifying these equations and examining the roots of the characteristic equation, an analytical solution is obtained for the lateral dynamic instability of the beam (or cable). The analytical solutions determined the minimum critical fluid speed and the critical spin speeds, for a specified fluid speed, in terms of the physical parameters of the system. DOE

N91-15080# Abastumani Astrophysical Observatory, Georgia (USSR).
EXPERIMENTS WITH COLLISION OF VORTICES IN ROTATING AND STILL FREE-SURFACE SHALLOW WATER
R. A. Antonova, B. P. Zhvania, J. G. Lominadze, J. I. Nanobashvili, and V. I. Petviashvili (Kurchatov, I. V. Inst. of Atomic Energy, Moscow, USSR) *In* ESA, Plasma Astrophysics Aug. 1990 p 183-187 (For primary document see N91-15046 06-90)
Copyright Avail: NTIS HC/MF A14

35 INSTRUMENTATION AND PHOTOGRAPHY

Includes remote sensors; measuring instruments and gages; detectors; cameras and photographic supplies; and holography.

For aerial photography see *43 Earth Resources and Remote Sensing*. For related information see also *06 Aircraft Instrumentation*, and *19 Spacecraft Instrumentation*.

N91-14574*# National Aeronautics and Space Administration. Lewis Research Center, Cleveland, OH.
HIGH RESOLUTION, HIGH FRAME RATE VIDEO TECHNOLOGY
Washington May 1990 102 p Workshop held in Cleveland, OH, 11-12 May 1988 List of attendees included as supplement (NASA-CP-3080; E-5044; NAS 1.55:3080) Avail: NTIS HC/MF A06 CSCL 14B

Papers and working group summaries presented at the High Resolution, High Frame Rate Video (HHV) Workshop are compiled. HHV system is intended for future use on the Space Shuttle and Space Station Freedom. The Workshop was held for the dual purpose of: (1) allowing potential scientific users to assess the utility of the proposed system for monitoring microgravity science experiments; and (2) letting technical experts from industry recommend improvements to the proposed near-term HHV system. The following topics are covered: (1) State of the art in the video system performance; (2) Development plan for the HHV system; (3) Advanced technology for image gathering, coding, and processing; (4) Data compression applied to HHV; (5) Data transmission networks; and (6) Results of the users' requirements survey conducted by NASA. For individual titles, see N91-14575 through N91-14580.

N91-14575*# National Aeronautics and Space Administration. Lewis Research Center, Cleveland, OH.
RESULTS OF THE USERS' REQUIREMENTS SURVEY
Robert L. Butcher *In its* High Resolution, High Frame Rate Video Technology May 1990 p 3-17 (For primary document see N91-14574 06-35)
Avail: NTIS HC/MF A06 CSCL 14B

The objectives of the High Resolution, High Frame Rate Video Technology (HHVT) Users' Requirements Survey were the following: (1) Document the requirements of potential users of the HHVT system; (2) Establish a data base relating key video parameters to HHVT users; (3) Guide the development of a high resolution, high frame rate video system offering high data storage capacity and high data transmission rates; (4) Allow users to compare their requirements to those of other users and to the state-of-the-art technology; and (5) Allow users to reassess, if necessary, their requirements in the light of existing and near-term technology. The results of the Users' Requirements Survey are presented. The diversity of these requirements indicates a need for developing a video system with great flexibility. Y.S.

N91-14576*# Analex Corp., Cleveland, OH.
DATA TRANSMISSION NETWORKS
Robert Alexovich *In* NASA, Lewis Research Center, High Resolution, High Frame Rate Video Technology May 1990 p 18-26 (For primary document see N91-14574 06-35)
Avail: NTIS HC/MF A06 CSCL 14B

A task order was written by the High Resolution, High Frame Rate Video Technology (HHVT) project engineers to investigate data compression techniques that could be applied to the HHVT system, and both existing and planned downlink/uplink capabilities of the Space Shuttle and Space Station Freedom. The following tasks were included: (1) Investigate signal channel availability and determine both the maximum possible data rate and the average data rate; (2) Identify time blocks for HHVT video transmission assuming time sharing and interruptions in the communication links; (3) Determine the bit error rates to be expected; and (4) Define the transmit and receive interfaces. A summary chart of the data transmission capabilities for Tracking and Data Relay Satellite System (TDRSS), the Space Shuttle, Space Station Freedom, Spacelab, and USLab are also presented. Y.S.

N91-14577*# Analex Corp., Cleveland, OH.
DATA COMPRESSION APPLIED TO HHVT
William K. Thompson *In* NASA, Lewis Research Center, High Resolution, High Frame Rate Video Technology May 1990 p 27-36 (For primary document see N91-14574 06-35)
Avail: NTIS HC/MF A06 CSCL 14B

A task order was written by the High Resolution, High Frame Rate Video Technology (HHVT) project engineers to study data compression techniques that could be applied to the HHVT system. Specifically, the goals of the HHVT data compression study are to accomplish the following: (1) Determine the downlink capabilities

of the Space Shuttle and Space Station Freedom to support HHVT data (i.e., determine the maximum data rates and link availability); (2) Determine current and projected capabilities of high speed storage media to support HHVT data by determining their maximum data acquisition/transmission rates and volumes; (3) Identify which experiment in the HHVT Users' Requirement data base need data compression, based on the experiments' imaging requirements; (4) Select the best data compression technique for each of these users by identifying a technique that provides compression but minimizes distortion; and (5) Investigate state-of-the-art technologies for possible implementation of selected data compression techniques. Data compression will be needed because of the high data rates and larger volumes of data that will result from the use of digitized video onboard the Space Shuttle and Space Station Freedom. Y.S.

N91-14578*# National Aeronautics and Space Administration. Lewis Research Center, Cleveland, OH.
STATE OF THE ART IN VIDEO SYSTEM PERFORMANCE
Michael J. Lewis *In its* High Resolution, High Frame Rate Video Technology May 1990 p 37-48 (For primary document see N91-14574 06-35)
Avail: NTIS HC/MF A06 CSCL 14B

The closed circuit television (CCTV) system that is onboard the Space Shuttle has the following capabilities: camera, video signal switching and routing unit (VSU); and Space Shuttle video tape recorder. However, this system is inadequate for use with many experiments that require video imaging. In order to assess the state-of-the-art in video technology and data storage systems, a survey was conducted of the High Resolution, High Frame Rate Video Technology (HHVT) products. The performance of the state-of-the-art solid state cameras and image sensors, video recording systems, data transmission devices, and data storage systems versus users' requirements are shown graphically. Y.S.

N91-14579*# National Aeronautics and Space Administration. Langley Research Center, Hampton, VA.
ADVANCED TECHNOLOGY DEVELOPMENT FOR IMAGE GATHERING, CODING, AND PROCESSING
Friedrich O. Huck *In* NASA, Lewis Research Center, High Resolution, High Frame Rate Video Technology May 1990 p 49-58 (For primary document see N91-14574 06-35)
Avail: NTIS HC/MF A06 CSCL 14B

Three overlapping areas of research activities are presented: (1) Information theory and optimal filtering are extended to visual information acquisition and processing. The goal is to provide a comprehensive methodology for quantitatively assessing the end-to-end performance of image gathering, coding, and processing. (2) Focal-plane processing techniques and technology are developed to combine effectively image gathering with coding. The emphasis is on low-level vision processing akin to the retinal processing in human vision. (3) A breadboard adaptive image-coding system is being assembled. This system will be used to develop and evaluate a number of advanced image-coding technologies and techniques as well as research the concept of adaptive image coding. Author

N91-14580*# National Aeronautics and Space Administration. Lewis Research Center, Cleveland, OH.
HIGH RESOLUTION, HIGH FRAME RATE VIDEO TECHNOLOGY DEVELOPMENT PLAN AND THE NEAR-TERM SYSTEM CONCEPTUAL DESIGN
Robert A. Ziemke *In its* High Resolution, High Frame Rate Video Technology May 1990 p 59-88 (For primary document see N91-14574 06-35)
Avail: NTIS HC/MF A06 CSCL 14B

The objective of the High Resolution, High Frame Rate Video Technology (HHVT) development effort is to provide technology advancements to remove constraints on the amount of high speed, detailed optical data recorded and transmitted for microgravity science and application experiments. These advancements will enable the development of video systems capable of high resolution, high frame rate video data recording, processing, and transmission. Techniques such as multichannel image scan, video parameter tradeoff, and the use of dual recording media were identified as methods of making the most efficient use of the near-term technology. Author

N91-14581*# Thiokol Corp., Brigham City, UT. Space Operations.
NOVA 201 ULTRASONIC THICKNESS GAGE (NOVA GAGE) Final Test Report
Diane Garecht Aug. 1990 132 p
(Contract NAS8-30490)
(NASA-CR-184031; NAS 1.26:184031; TWR-60533; Publ-90654)
Avail: NTIS HC/MF A07 CSCL 14B

The measurement integrity of the NOVA 201 digital ultrasonic thickness gage (NOVA gage) was demonstrated by comparing the NOVA gage measurements to the thickness gage measurements, and determining the bias and uncertainty of the NOVA gage when measuring redesigned solid rocket motor (RSRM) hardware per engineering test plans (ETP). The NOVA gage was tested by three different operators on steel and aluminum RSRM hardware for wall thickness. The results show that the measurement bias is not consistent. The uncertainty of the bias is caused by the heterogeneous material properties of the RSRM components that influence the time of flight of ultrasonic waves. The measurement uncertainty inherent to the design and operation of the NOVA gage is less in comparison to the uncertainty of the bias. The total measurement uncertainty cannot be substantially reduced by taking more than one measurement. There is no correlation between bias and the surface finish range of this test unless 3-in-One oil is used as a couplant, in which case there appears to be a slight trend. There is no correlation between uncertainty and the surface finish range. The measurement uncertainty of the NOVA gage can be reduced using 3-in-One oil as a couplant. B.G.

N91-14582# Laboratoire d'Automatique et d'Analyse des Systemes, Toulouse (France). Groupe Systemes Integrees de Perception.
DYNAMIC BEHAVIOR OF THIN SILICON PLATE: APPLICATION TO SILICON SENSORS Ph.D. Thesis - Inst. National des Sciences Appliquees de Toulouse
Patrick Pons 1990 176 p In FRENCH; ENGLISH summary
(LAAS-90144; ETN-91-98212) Avail: NTIS HC/MF A09

The small amplitude deflection of thin silicon plates are modeled by means of a Lagrange/Newton's equation. An approximated polynomial solution is obtained from the virtual displacement theorem, for rectangular plates fully clamped on their edges. For free vibration, the expression of the first fifteen natural modes of vibration are given. The responses to uniform harmonic, step and pulse type excitations are computed. Validation of the model is achieved with the help of capacitive structures realized using micro electronic and micro machining of silicon. The twenty to forty micron thick silicon membrane and a rigid metallic plate are assembled to obtain a variable capacitor. Using these devices as mixer and modulator, the first for natural modes of vibration are characterized. The application of the model to the analysis of the dynamic behavior of the piezoresistive and capacitive pressure sensors shows that they can be assimilated to second order systems when submitted to uniform pressure steps. The response time of pressure sensors is minimized by increasing the rectangularity ratio of the membranes and by realizing the latter in silicon rather than steel. ESA

N91-14583# Lawrence Livermore National Lab., CA.
SHOT REPORT, HOLO-17-HOLO-22 REX-9
Charles McMillan, Richard Whipkey, and Peter Vance 25 Oct. 1990 14 p
(Contract W-7405-eng-48)
(DE91-002575; UCRL-ID-105117) Avail: NTIS HC/MF A03

We report on a series of holographic shots using explosives to generate ejecta from lead. These experiments covered a range of geometries including point initiation and plane wave initiation for the holograms of ejecta (H.E.). and using a gas-fill in the cavity where the ejecta was produced. The final experiment, Rex-9,

was a Fabry-Perot experiment at Site 300 which provided the velocity history of the lead surface for the purpose of normalizing the code being used to calculate the position of the lead surface in these experiments. The focus of this report is on the experimental technique rather than on the size measurements. We want to insure that the advances in mechanical design and experimental technique that were made during these experiments are preserved in future experiments. DOE

N91-14584# Colorado School of Mines, Golden. Dept. of Chemical and Petroleum Refining Engineering.
AN AUTOMATED FLOW CALORIMETER FOR HEAT CAPACITY AND ENTHALPY MEASUREMENTS AT ELEVATED TEMPERATURES AND PRESSURES Final Report, 1 Mar. 1987 - 31 May 1990
Victor F. Yesavage 31 Aug. 1990 86 p
(Contract DE-FG02-87ER-13683)
(DE91-002759; DOE/ER-13683/3) Avail: NTIS HC/MF A05

The need for highly accurate thermal property data for a broad range of new application fluids is well documented. To facilitate expansion of the current thermophysical database, an automated flow calorimeter was developed for the measurement of highly accurate isobaric heat capacities and enthalpies of fluids at elevated temperatures and pressures. The experimental technique utilizes traditional electrical power input, adiabatic flow calorimetry with a precision metering pump that eliminates the need for on-line flow rate monitoring. In addition, a complete automation system greatly simplifies the operation of the apparatus and increases the rapidity of the measurement process. The range over which the instrument was tested was 300 to 600 K and 0 to 12 Mpa, although the calorimeter should perform up to the original design goals of 700 K and 30 MPa. The new flow calorimeter was evaluated by measuring the mean, isobaric, specific heat capacities of liquid water and n-pentane. These experiments yielded an average deviation from the standard literature data of +0.02 percent and a total variation of 0.05 percent. Additional data analysis indicated that the overall measurement uncertainty was conservatively estimated as 0.2 percent with an anticipated precision of 0.1 to 0.15 percent at all operating conditions. DOE

N91-14585# Texas A&M Univ., College Station.
A STUDY OF LIQUID SCINTILLATOR AND FIBER MATERIALS FOR USE IN A FIBER CALORIMETER
Peter Parker Altice, Jr. Apr. 1990 63 p
(Contract DE-AS05-81ER-40039)
(DE91-004229; DOE/ER-40039/45) Avail: NTIS HC/MF A04

This reports an investigation into the performance of selected scintillation oils and fiber materials to test their applicability in high energy, liquid scintillator calorimetry. Two scintillating oils, Bicron BC-517 and an oil mixed for the MACRO experiment, and two fiber materials, Teflon and GlassClad PS-252, were tested for the following properties: light yield, attenuation length and internal reflection angle. The results of these tests indicated that the scintillation oils and the fiber materials had an overall good performance with lower energies and would meet the requirements of liquid scintillator detection at Superconducting Super Collider (SSC) energies. DOE

N91-14586*# Santa Barbara Research Center, CA.
EARTH OBSERVING SCANNING POLARIMETER (EOSP), PHASE B Final Report
Dec. 1990 60 p
(Contract NAS5-30756)
(NASA-CR-187715; NAS 1.26:187715; DMLB87-0016) Avail: NTIS HC/MF A04 CSCL 14B

Evaluations performed during a Phase B study directed towards defining an optimal design for the Earth Observing Scanning Polarimeter (EOSP) instrument is summarized. An overview of the experiment approach is included which provides a summary of the scientific objectives, the background of the measurement approach, and the measurement method. In the instrumentation section, details of the design are discussed starting with the key instrument features required to accomplish the scientific objectives and a system characterization in terms of the Stokes vector/Mueller matrix formalism. This is followed by a detailing of the instrument design concept, the design of the individual elements of the system, the predicted performance, and a summary of appropriate instrument testing and calibration. The selected design makes use of key features of predecessor polarimeters and is fully compatible with the Earth Observing System spacecraft requirements.
Author

N91-14587* National Aeronautics and Space Administration. Pasadena Office, CA.
APPARATUS AND METHOD FOR CHARACTERIZING THE TRANSMISSION EFFICIENCY OF A MASS SPECTROMETER Patent
Santash Srivasytava, inventor (to NASA) (Jet Propulsion Lab., California Inst. of Tech., Pasadena.) 27 Nov. 1990 9 p Filed 26 May 1989
(NASA-Case-NPO-16989-1-CU; US-Patent-4,973,840; US-Patent-Appl-SN-358027; US-Patent-Class-250-281; US-Patent-Class-250-282; US-Patent-Class-250-286; US-Patent-Class-250-287; US-Patent-Class-250-288; US-Patent-Class-250-305; US-Patent-Class-250-423) Avail: US Patent and Trademark Office CSCL 14B

An electron/ion coincidence technique is employed to characterize the absolute mass dependent transmission efficiency of mass spectrometers. The technique is not dependent upon the partial pressure of the sample beam or the ionization cross sections of calibrant gases.
Official Gazette of the U.S. Patent and Trademark Office

N91-14588* National Aeronautics and Space Administration. Pasadena Office, CA.
FIELD INDUCED GAP INFRARED DETECTOR Patent
C. Thomas Elliott, inventor (to NASA) (Jet Propulsion Lab., California Inst. of Tech., Pasadena.) 28 Aug. 1990 14 p Filed 21 Jun. 1989
(NASA-Case-NPO-17526-1-CU; US-Patent-4,952,811; US-Patent-Appl-SN-369403; US-Patent-Class-250-370.13; US-Patent-Class-250-338.1; US-Patent-Class-250-338.2; US-Patent-Class-250-493.1; US-Patent-Class-250-370.12; US-Patent-Class-357-30; US-Patent-Class-357-27) Avail: US Patent and Trademark Office CSCL 14B

A tunable infrared detector which employs a vanishing band gap semimetal material provided with an induced band gap by a magnetic field to allow intrinsic semiconductor type infrared detection capabilities is disclosed. The semimetal material may thus operate as a semiconductor type detector with a wavelength sensitivity corresponding to the induced band gap in a preferred embodiment of a diode structure. Preferred semimetal materials include Hg(1-x)Cd(x)Te, x is less than 0.15, HgCdSe, BiSb, alpha-Sn, HgMgTe, HgMnTe, HgZnTe, HgMnSe, HgMgSe, and HgZnSe. The magnetic field induces a band gap in the semimetal material proportional to the strength of the magnetic field allowing tunable detection cutoff wavelengths. For an applied magnetic field from 5 to 10 tesla, the wavelength detection cutoff will be in the range of 20 to 50 micrometers for Hg(1-x)Cd(x)Te alloys with x about 0.15. A similar approach may also be employed to generate infrared energy in a desired band gap and then operating the structure in a light emitting diode or semiconductor laser type of configuration.
Official Gazette of the U.S. Patent and Trademark Office

N91-14589# Mechanical Technology, Inc., Latham, NY.
COMPUTER-ASSISTED STRAIN-GAGE MONITORING AND DATA REDUCTION SYSTEM Final Report, Jul. 1985 - May 1990
Lawrence Lagace and Peter Hayes Aug. 1990 63 p
(Contract F33615-85-C-2503; AF Proj. 3066)
(AD-A226894; MTI-89TR19; WRDC-TR-90-2064) Avail: NTIS HC/MF A04 CSCL 09/1

The objective of this program was to design and build a computer-based strain gage monitoring system (SGMS) for the Wright-Patterson Air Force Base (WPAFB) using state-of-the-art

electronics to assist in real-time monitoring and subsequent reduction and analysis of compressor analog data. During aerodynamic and aeromechanical testing at the WPAFB Compressor Research Facility (CRF), the SGMS monitors blade and vane stress level data provided by sensors attached to a turbine engine compressor. The system monitors vibratory responses, provides ample warning of compressor component failure, and assists test engineers in data analysis. On-line data are presented to the test engineers via a graphics display terminal and printed reports. GRA

N91-14590* National Aeronautics and Space Administration. Langley Research Center, Hampton, VA.
THERMAL COMPENSATING MOUNT Patent
Antony Jalink, Jr., inventor (to NASA) and Scott R. Campbell, inventor (to NASA) 23 Jan. 1990 4 p Filed 12 Jun. 1989 Continuation of abandoned US-Patent-Appl-SN-168065, filed 14 Mar. 1988
(NASA-Case-LAR-14207-1; US-Patent-4,895,430; US-Patent-Appl-SN-366205; US-Patent-Appl-SN-168065; US-Patent-Class-350-287; US-Patent-Class-350-500; Int-Patent-Class-G02B-7/18; Int-Patent-Class-G02B-27/64) Avail: US Patent and Trademark Office CSCL 14B

The main objective is to provide a device for maintaining the alignment integrity of an alignment sensitive component over a wide range of temperatures. A thermal compensating mount is presented. A cylindrical extension is integrally formed to the alignment sensitive component. Both the extension and component share the same coefficient of thermal expansion. The cylindrical extension is placed into a mounting structure which has a diameter greater than that of the extension. An adhesive secures the cylindrical extension to the mount. The difference between the diameters of the cylindrical extension and the cylindrical receptacle is such that the differential thermal expansion across the extension and the receptacle edges is exactly compensated for by the thermal compensation of the adhesive between them. Accordingly, the alignment sensitive component does not change position when subjected to temperature variations. One application of this invention is laser optical-path folding prisms, which are fixed to the mounting surface by a small amount of epoxy adhesive.
Official Gazette of the U.S. Patent and Trademark Office

N91-14591* National Aeronautics and Space Administration. Ames Research Center, Moffett Field, CA.
MULTIPLE AXIS RETICLE Patent
Chris E. Barns, inventor (to NASA) and William D. Gunter, inventor (to NASA) (Photon Applications, San Jose, CA.) 18 Sep. 1990 9 p Filed 6 Oct. 1989
(NASA-Case-ARC-11886-1-SB; US-Patent-4,957,357; US-Patent-Appl-SN-418374; US-Patent-Class-350-576; US-Patent-Class-33-261; Int-Patent-Class-G02B-23/00; Int-Patent-Class-F41G-11/00) Avail: US Patent and Trademark Office CSCL 14B

A reticle permits the alignment of three orthogonal axes (X, Y and Z) that intersect at a common target point. Thin, straight filaments are supported on a frame. The filaments are each contained in a different orthogonal plane (S sub xy, S sub xz, and S sub yz) and each filament intersects two of the three orthogonal axes. The filaments, as viewed along the frame axis, give the appearance of a triangle with a V extending from each triangle vertex. When axial alignment is achieved, the filament portions adjacent to a triangle vertex are seen (along the axis of interest) as a right-angle cross, whereas these filament portions are seen to intersect at an oblique angle when axial misalignment occurs. The reticle is open in the region near the target point leaving ample space for alignment aids such as a pentaprism or a cube mirror. Official Gazette of the U.S. Patent and Trademark Office

N91-14592# Lawrence Livermore National Lab., CA.
RECENT LONG-PULSE AND HIGH-AVERAGE-POWER TESTS ON A 140 GHz GYROTRON
K. Felch, C. Hess, H. Huey, E. Jongewaard, H. Jory, J. Neilson, R. Pendleton, and M. Tsirulnikov (Varian Associates, Palo Alto, CA.) Oct. 1990 5 p
(Contract W-7405-eng-48)
(DE91-001680; UCRL-CR-104813) Avail: NTIS HC/MF A01

Varian is carrying out the development of high-power, CW gyrotrons at frequencies ranging from 100 to 140 GHz. Initial test vehicles at 140 GHz have been designed to generate short-pulse power levels of 1 MW and up to 400 kW CW. Thus far, short-pulse power levels of 1040 kW have been measured at 38 percent efficiency and average powers of 200 kW have been achieved. Output power levels of 400 kW have been obtained for pulse durations of 0.5 sec. DOE

N91-14593# Joensuu Univ. (Finland). Dept. of Physics.
THE OPTICAL PARAMETRIZATION OF AN AERIAL MULTISPECTRAL CAMERA Ph.D. Thesis
R. Silvennoinen 1989 139 p
(DE91-003017; JOY-LT-16; ISSN-0781-0342; ISBN-9-51696-8678) Avail: NTIS (US Sales Only) HC/MF A07

This work presents a parametric study of an aerial multispectral camera produced with the aid of small cameras. The effects of the filter, spectrum of light, image motion and vibrations to the resolving power, contrast transfer function and resolution of the multispectral camera under examination are presented in this study. The estimated optical parameters of the aerial multispectral camera under examination are compared with the results from test flights and from practical aerial multispectral photography. Finally, some results of the interpreted variables of natural objects derived from the aerial multispectral pictures produced with the aerial multispectral camera under examination are presented also during the course of this work. DOE

36 LASERS AND MASERS

Includes parametric amplifiers.
For related information see also *76 Solid-State Physics.*

N91-14594# Plesscor Optronics, Inc., Chatsworth, CA.
QUANTUM WELL LASER Final Technical Report, Sep. 1985 - Mar. 1988
P. J. Williams, A. C. Marshall, and D. J. Robbins Feb. 1990 128 p
(Contract F19628-85-C-0172; AF Proj. 2306)
(AD-A227303; RADC-TR-89-352) Avail: NTIS HC/MF A07 CSCL 09/3

During the first year of the program, basic materials growth experiments were carried out in order to develop the necessary capability of the growth of quantum well lasers by atmospheric pressure MOVPE (AP-MOVPE). In the latter part of the program, this technology was transferred to a low pressure MOVPE (LP-MOVPE) reactor which demonstrated superior materials and interface qualities with respect to structures prepared by AP-MOVPE. By correlating SIMS data and Hall analysis, conditions were determined for the growth of high quality and abrupt p-doped and n-doped InP of known carrier concentration. In this way p-doped InP over the range mid 10(exp 17)/cc to 2x10(exp 18)/cc could be grown, with carrier concentrations extended up to 10(exp 19)/cc for p++ InGaAs contact layers. Quantum well laser structures were grown and tested. GRA

N91-14595# Texas Univ., Austin. Dept. of Physics.
PICOSECOND LASER SYSTEM FOR HIGH SPEED CHARACTERIZATION OF MONOLITHIC DEVICES Final Report, 1 Dec. 1988 - 31 Dec. 1989
M. C. Downer, T. Itol, and D. P. Nelkirk 31 Dec. 1989 4 p
(Grant AF-AFOSR-0209-89; AF Proj. 2305; AF Proj. 3842)
(AD-A227372; AFOSR-90-1046TR) Avail: NTIS HC/MF A01 CSCL 09/3

Accurate characterization of high-speed electronic circuitry requires the introduction of optical sampling as a method of generating and measuring large electrical bandwidths. The optical sampling techniques that can be employed for measuring the electrical response of a circuit consist of electro-optic sampling

and photoconductive switching. In electro-optic sampling, the fields of a propagating electrical pulse induce a transient birefringence in an electro-optic crystal which, in turn, rotates the polarization of an optical probe pulse transmitted through the crystal. The time resolution of the polarization rotation is an indirect measurement of the time evolution of the propagating pulse as it passes the crystal. In addition, the crystal can be dipped into the fringing fields of the propagating electrical pulse above the circuit substrate, allowing for high spatial resolution while remaining noncontacting. In photoconductive switching, a small gap between two biased, transmission line conductors laid down on a semiconducting substrate can be electrically closed by an optical pulse focused onto the gap. This results in the generation of an electrical pulse whose shape and duration are determined by the laser pulsewidth, the circuit characteristics of the gap and transmission line and the photo-excited carrier lifetime of the substrate. GRA

N91-14596# Oregon Univ., Eugene. Dept. of Physics.
NONLINEAR DYNAMICS OF BROAD-BAND LASERS Progress Report, 1 Sep. 1988 - 31 Aug. 1990
Michael G. Raymer Feb. 1990 7 p
(Contract DE-FG06-88ER-13973)
(DE91-001143; DOE/ER-13973/3) Avail: NTIS HC/MF A02

Significant progress has been made in several areas. The source of mode-intensity fluctuations in a three-mirror, multimode dye laser has been identified in the typical operating regime well above threshold. It was found experimentally that deterministic four-wave mixing interactions are the underlying cause. We have also made new theoretical studies concerning the regime just above threshold and predicted that the mode fluctuations will be dominated by quantum noise in this regime. We have constructed a preliminary-design short-cavity dye laser in an attempt to enhance this quantum effect, and are now beginning to characterize its output. We have also constructed a Ti:Sapphire laser, and are beginning its study. DOE

N91-14597# Rochester Univ., NY. Lab. for Laser Energetics.
LLE (LABORATORY FOR LASER ENERGETICS) REVIEW Quarterly Report, Apr. - Jun. 1990
S. A. Kumpan, ed. 1990 72 p Sponsored by Empire State Electric Energy Research Corp., New York, NY; New York State Energy Research and Development Authority, Albany, NY; and Hydro-Electric Power Commission, Toronto, Ontario
(Contracts DE-FC03-85DP-40200; DE-FG02-88ER-45376; AF-AFOSR-0327-87)
(DE91-001254; DOE/DP-40200/132) Avail: NTIS HC/MF A04

This volume of the LLE Review, covering the period April to June 1990, contains articles in two main sections, Progress in Laser Fusion and Advanced Technology Developments. The first article presents the theoretical interpretation of the glass-ablator cryogenic-implosion experiments recently conducted on OMEGA. It is followed by an article describing the analysis of neutron time-of-flight data taken during DT and DD experiments; and a discussion of the improvements to laser diagnostics that now provide for precise control of the OMEGA laser is given. This paper contains a report on the development of transparent conductive coatings for KDP crystals, and a discussion of the study of the transient-surface Debye-Waller effect in materials irradiated with an ultrafast laser. DOE

N91-14598# Sandia National Labs., Albuquerque, NM.
CHARACTERIZATION OF SEMICONDUCTOR SURFACE-EMITTING LASER WAFERS
P. L. Gourley, G. A. Vawter, T. M. Brennan, and B. E. Hammons 1990 11 p Presented at the 178th Meeting of the Electrochemical Society, Seattle, WA, 14-19 Oct. 1990
(Contract DE-AC04-76DP-00789)
(DE91-001336; SAND-90-1770C; CONF-901073-8) Avail: NTIS HC/MF A03

The development of epitaxial semiconductor surface-emitting lasers has begun in recent years. These lasers are ultra-short (a few microns) Fabry-Perot resonators comprising epitaxial multilayer semiconductor mirrors and quantum well active regions. The resonators are single crystals grown along the lasing axis by molecular beam epitaxy (MBE) or chemical vapor deposition (CVD). They offer significant advances over conventional cleaved, edge-emitting lasers for creating lasers with single elements of 2 dimensional arrays, low beam divergence, engineered active regions, single longitudinal modes, and improved temperature characteristics. To realize the high potential of these new laser structures, techniques for characterizing the laser wafer after growth and between fabrication, steps must be developed. In this paper we discuss several optical techniques that we have developed for this emerging surface-emitting laser technology. DOE

N91-14599# Minnesota Univ., Minneapolis.
STATE-TO-STATE DYNAMICS OF MOLECULAR ENERGY TRANSFER Annual Report, 1 Apr. 1990 - 31 Mar. 1991
W. Ronald Gentry 26 Nov. 1990 4 p
(Contract DE-FG02-86ER-13515)
(DE91-004589; DOE/ER-13515/6) Avail: NTIS HC/MF A01

Progress on this DOE project during the 1990--91 budget year can be divided into three distinct parts. In chronological order: we completed both experimental and theoretical work on vibrational-rotational excitation of glyoxal, (CHO)(sub 2) in collisions with He. We then moved the crossed molecular beam apparatus to a new laboratory, in order to provide access to the lasers needed for stimulated-emission pumping (SEP) experiments. In the process, we upgraded both the detector and data acquisition electronics. Finally, we carried out the first crossed beam experiments anywhere in which SEP was used to selectively prepare a highly excited initial state of reactants. DOE

37 MECHANICAL ENGINEERING

Includes auxiliary systems (nonpower); machine elements and processes; and mechanical equipment.

N91-14600*# Jet Propulsion Lab., California Inst. of Tech., Pasadena.
MARS ROVER/SAMPLE RETURN (MRSR) MISSION: MARS ROVER TECHNOLOGY WORKSHOP
1987 806 p Workshop held in Pasadena, CA, 28-30 Apr. 1987
(NASA-TM-101129; JPL-D-4788; NAS 1.15:101129) Avail: NTIS HC/MF A99 CSCL 13F

A return to the surface of Mars has long been an objective of NASA mission planners. The ongoing Mars Rover and Sample Return (MRSR) mission study represents the latest stage in that interest. As part of NASA's preparation for a possible MRSR mission, a technology planning workshop was held to attempt to define technology requirements, options, and preliminary plans for the principal areas of Mars rover technology. The proceedings of that workshop are presented. Author

N91-14601 California Univ., Davis.
EVALUATION OF PERFORMANCE AND FEEDBACK CONTROL DESIGN FOR VEHICLE SUSPENSIONS WITH VARIABLE COMPLIANCE ELEMENTS Ph.D. Thesis
Douglas Alan Baker 1990 231 p
Avail: Univ. Microfilms Order No. DA9026818

Vehicle suspension design for vibration isolation is discussed. Specifically, a nonlinear suspension element called a variable compliance element is investigated. Feedback control laws are designed, and the vibration isolation performance is evaluated. This involves computer simulation, because analytical results are difficult or impossible to obtain for nonlinear feedback systems. In addition, Bilinear System Theory is studied because of its close relation to variable parameter systems. Two example problems are studied. The first is a switched-damper-controlled compliance. Optimal open loop control is computed numerically for initial condition (IC) response and for a bump input. Feedback control laws are designed and evaluated for the IC case, bump input, random roadway input, and random external force input. A quadratic performance index weighting acceleration, suspension travel

(rattlespace), and road contact force is used. The second example is based on a linear passive tuned isolator. The objective of the variable compliance is to extend the isolation to a wider frequency range. First a variable air compliance is shown to yield very good results if the time-varying input frequency is measurable (feedforward control). A device for varying the effective compliance is also suggested. Then the model is changed by incorporating a lever which has a movable fulcrum (called the Variable Fulcrum Isolator (VFI)). Feedback control is then studied with the VFI model. An important characteristic of the VFI with acceleration feedback is the response to inputs of 1 or 2 distinct frequencies. The fulcrum will move to the optimum position, and then remain virtually stationary. Thus, it will use very little control power under these conditions and achieve very good performance. Dissert. Abstr.

N91-14602*# Illinois Univ., Chicago.
STRADDLE DESIGN OF SPIRAL BEVEL AND HYPOID PINIONS AND GEARS
Faydor L. Litvin, Chihping Kuan, Jonathan Kieffer, Robert Bossler, and Robert F. Handschuh (Army Aviation Systems Command, Cleveland, OH.) Nov. 1990 12 p
(DA Proj. 1L1-62211-A-47-A)
(NASA-TM-103621; L-5467; NAS 1.15:103621;
AVSCOM-TR-90-C-010) Avail: NTIS HC/MF A03 CSCL 13H

The design of spiral bevel and hypoid gears that have a shaft extended from both sides of the cone apex (straddle design) is considered. A main difficulty of such a design is determining the length and diameter of the shaft that might be undercut by the head cutter during gear tooth generation. A method that determines the free space available for the gear shaft is proposed. The approach avoids collision between the shaft being designed and the head cutter during tooth generation. The approach is illustrated with a numerical example. Author

N91-14603*# Scientific Research Associates, Inc., Glastonbury, CT.
INTELLIGENT MANIPULATION TECHNIQUE FOR MULTI-BRANCH ROBOTIC SYSTEMS Quarterly Progress Report, 1 Sep. - 30 Nov. 1990
Alexander Y. K. Chen and Eugene Y. S. Chen Dec. 1990 26 p
(Contract NAS7-1072)
(NASA-CR-187651; NAS 1.26:187651; R90-900077-4) Avail: NTIS HC/MF A03 CSCL 13I

New analytical development in kinematics planning is reported. The INtelligent KInematics Planner (INKIP) consists of the kinematics spline theory and the adaptive logic annealing process. Also, a novel framework of robot learning mechanism is introduced. The FUzzy LOgic Self Organized Neural Networks (FULOSONN) integrates fuzzy logic in commands, control, searching, and reasoning, the embedded expert system for nominal robotics knowledge implementation, and the self organized neural networks for the dynamic knowledge evolutionary process. Progress on the mechanical construction of SRA Advanced Robotic System (SRAARS) and the real time robot vision system is also reported. A decision was made to incorporate the Local Area Network (LAN) technology in the overall communication system. Author

N91-14604# Institut National Polytechnique, Grenoble (France). Lab. d'Informatique Fondamentale et d'Intelligence Artificielle.
CONTRIBUTION TO THE SPECIFICATION AND IMPLEMENTATION OF COMPLEX ROBOT TASKS Ph.D. Thesis [CONTRIBUTION A LA SPECIFICATION ET L'IMPLANTATION DES TACHES ROBOTIQUES COMPLEXES]
Jean-Marc Lefebvre 1989 162 p In FRENCH
(ETN-90-98209) Avail: NTIS HC/MF A08

Three aspects of robot commands are addressed. Control of complex movements of manipulator arms is discussed. Sensor data is taken into account in the study of control movements. The interplay of a complex of multi-sensors with multi-effectors is considered. A trajectory generator able to transform an external image, understandable by an operator, into an internal image usable by an algorithm is described. It is demonstrated that a complex of multi-effectors and multi-sensors can be specified with the help of sequential communicating processes. A series of primitive outlines, allowing for commands and parallelism to be taken into account in the control of robots, are presented ESA

N91-14605# Oxford Univ. (England). Robotics Research Group.
ROBOT CONTROL STRATEGIES
Inaki Arocena 25 May 1990 65 p
(OUEL-1754/89; ETN-90-98221) Avail: NTIS HC/MF A04

Work on adaptive control of robot manipulators is described. Fast and light manipulators requiring direct drive systems and compliance control are investigated. A full dynamics controller is the final goal of the research. The proposed robotics regulator requires full dynamics because with the ideal parameters, it linearizes and decouples each joint. The direct drive flexible manipulator Rotabot and eight T800 transputers 32 bit floating points are used in the search for a full dynamics adaptive controller on a flexible direct drive robot for trajectory control. ESA

N91-14606# Lawrence Livermore National Lab., CA.
ENABLE KIT (MC-4246) FOR THE DOT CHARGED LINE SYSTEM: WELDING DEVELOPMENT REPORT FOR 1/4-INCH TUBES AND FITTINGS
D. D. Kautz and R. P. Decofano Jun. 1990 6 p
(Contract W-7405-eng-48)
(DE91-002577; UCRL-ID-104523) Avail: NTIS HC/MF A02

The Enable Kit (MC-4246) is a high-pressure assembly that has several welds on 1/4-inch tubes and fittings. A series of sample welds that were well outside the expected process variability were made. These were then tested to determine the sensitivity of the welding process to variations in heat input. Test results showed satisfactory welds with no microstructural defects and a sufficient high-pressure safety factor after welding. From the information obtained, we are able to certify that production process variation is well within acceptable limits. DOE

N91-14607* National Aeronautics and Space Administration. Lyndon B. Johnson Space Center, Houston, TX.
VIBRATION ANALYZER Patent
Richard J. Bozeman, Jr., inventor (to NASA) 11 Dec. 1990 9 p Filed 31 Jan. 1989
(NASA-Case-MSC-21408-1; US-Patent-4,977,395;
US-Patent-Appl-SN-304154; US-Patent-Class-340-683;
US-Patent-Class-73-658; Int-Patent-Class-G08B-21/00) Avail: US Patent and Trademark Office CSCL 13I

The invention relates to monitoring circuitry for the real time detection of vibrations of a predetermined frequency and which are greater than a predetermined magnitude. The circuitry produces an instability signal in response to such detection. The circuitry is particularly adapted for detecting instabilities in rocket thrusters, but may find application with other machines such as expensive rotating machinery, or turbines. The monitoring circuitry identifies when vibration signals are present having a predetermined frequency of a multi-frequency vibration signal which has an RMS energy level greater than a predetermined magnitude. It generates an instability signal only if such a vibration signal is identified. The circuitry includes a delay circuit which responds with an alarm signal only if the instability signal continues for a predetermined time period. When used with a rocket thruster, the alarm signal may be used to cut off the thruster if such thruster is being used in flight. If the circuitry is monitoring tests of the thruster, it generates signals to change the thruster operation, for example, from pulse mode to continuous firing to determine if the instability of the thruster is sustained once it is detected.
Official Gazette of the U.S. Patent and Trademark Office

N91-14608* National Aeronautics and Space Administration. Marshall Space Flight Center, Huntsville, AL.
TURBOMACHINERY ROTOR SUPPORT WITH DAMPING Patent
George L. VonPragenau, inventor (to NASA) 22 May 1990 8 p Filed 26 May 1989
(NASA-Case-MFS-28345-1; US-Patent-4,927,326;

US-Patent-Appl-SN-364743; US-Patent-Class-415-170.1; US-Patent-Class-415-174.5; US-Patent-Class-415-229; Int-Patent-Class-F01D-11/08) Avail: US Patent and Trademark Office CSCL 13I

Damping seals, damping bearings, and a support sleeve are presented for the ball bearings of a high speed rotor. The ball bearings consist of a duplex set having the outer races packaged tightly within the sleeve while the sleeve provides a gap with a support member so that the bearings may float with the sleeve. The sleeve has a web extending radially between the pair of outer races and acts in conjunction with one or more springs to apply an axial preload to the outer races. The sleeves have a series of slits which provide the sleeve with a spring-like quality so that the spring acts to center the rotor upon which the bearings are mounted during start up and shut down. A damping seal or a damping bearing may be used in conjunction with the ball bearings and supporting sleeve, the damping seal and damping bearing having rotor portions including rigid outer surfaces mounted within the bore of a stator portion having triangular shaped pockets on the surface facing the rotor. Axial gates are provided between adjacent pockets in sections of the stator permitting fluid to flow with less resistance axially relative to the flow of fluids circumferentially between the rotor and the stator.

Official Gazette of the U.S. Patent and Trademark Office

N91-14609* National Aeronautics and Space Administration. John C. Stennis Space Center, Bay Saint Louis, MS.

HYBRID BUTTERFLY VALVE Patent

Laurence deQuay, inventor (to NASA) 1 May 1990 7 p Filed 7 Sep. 1989

(NASA-Case-SSC-00004-1; US-Patent-4,921,212; US-Patent-Appl-SN-404292; US-Patent-Class-251-163; US-Patent-Class-251-160; Int-Patent-Class-F16K-1/22) Avail: US Patent and Trademark Office CSCL 13I

A hybrid butterfly valve has a stationary seat and a valve closure disk which may rotate together with an actuating shaft from the fully open position to a position wherein the disk is aligned with the seat, and may be moved linearly into a sealing relationship with the seat. The disk is supported by brackets having an elongated slot through which the shaft extends, the brackets being adapted to move linearly relative to the shaft. Cams fastened to the shaft initiate a 90 degree rotation of the disk from the fully open position to the position where the valve disk is aligned with the seat, and the cams act in conjunction with followers carried by the disk to move the disk and the brackets linearly. The disk carries guide members which are positioned in a guide slot, the guide slot having an arcuate portion and a linear portion, and the disk is guided by the guide members guided in the arcuate portion when the disk is fully opened to and until the disk is aligned with the seat, and the guide members are guided by the linear portion of the slot. A portion of each cam is spring biased so that the cams tightly engage follower rollers carried by the brackets during the rotational portion of the movement of the disk.

Official Gazette of the U.S. Patent and Trademark Office

N91-14610* National Aeronautics and Space Administration. Lyndon B. Johnson Space Center, Houston, TX.

QUICK CONNECT COUPLING Patent

Benny B. Sprague, inventor (to NASA) 20 Nov. 1990 5 p Filed 30 Mar. 1990

(NASA-Case-MSC-21539-1; US-Patent-4,971,474; US-Patent-Appl-SN-503410; US-Patent-Class-403-331; US-Patent-Class-285-327; US-Patent-Class-403-327; US-Patent-Class-403-317; US-Patent-Class-403-381; Int-Patent-Class-B25G-3/00; Int-Patent-Class-F16B-1/00) Avail: US Patent and Trademark Office CSCL 13I

A coupling device has a transversely arranged, open-end groove in a flange attached to a pipe end. The groove in the flange receives a circumferentially arranged locking flange element on the other coupling member and permits alignment of the bores of the coupling members when the locking flange element is in the open end groove. Upon alignment of the bores of the coupling members, a trigger member is activated to automatically release a spring biased tubular member in one of the coupling members. The tubular member has a conical end which is displaced into the other coupling member to lock the coupling members to one another. A tensioning nut is threadedly movable on a coupling member so as to be moved into tightening engagement with the other coupling member.

Official Gazette of the U.S. Patent and Trademark Office

N91-14611# Naval Postgraduate School, Monterey, CA.

VALIDATION OF A COMPUTATIONAL MODEL FOR AUTOGENOUS ARC WELDING M.S. Thesis

Eugene B. Sedy Mar. 1990 58 p

(AD-A227258) Avail: NTIS HC/MF A04 CSCL 11/6

A three dimensional transient computational model of heat transfer arc welding is generalized, and then validated by comparison to Rosenthal's solution for moving point sources of heat. The current version of the code allows much greater flexibility in the specification of the thermal input from the arc. The resulting surface temperature profiles and fusion zone shapes are compared to those measured experimentally for several input power levels for autogenous gas tungsten arc welding. Arc efficiency is experimentally determined using change of phase of a liquid fluorocarbon. The model is shown to be useful for modeling autogenous welding of thick plates. Weld seam misalignment and surface flaw detection are shown to be possible ahead of the arc with accurate surface temperature detection methods. The potential of the model for creating a database of fusion and heat zone sizes, temperature profiles, and coding rates for various materials, processes, and power levels is indicated. GRA

N91-14612# Coordinating Research Council, Inc., Atlanta, GA.

CRC PROGRAM FOR QUANTIFYING PERFORMANCE OF KNOCK-SENSOR-EQUIPPED VEHICLES WITH VARYING OCTANE LEVEL

Aug. 1990 46 p

(Contract DAAK70-89-C-0022)

(AD-A227340) Avail: NTIS HC/MF A03 CSCL 21/4

A pilot study was conducted under the auspices of the Coordinating Research Council, Inc. (CRC) to assess the potential effects of gasoline octane quality on acceleration performance, fuel economy and driveability in vehicles equipped with electronic spark control systems (knock sensors). Fourteen vehicles were tested by five participating laboratories on CRC unleaded reference fuels of varying octane quality (78 to 104 RON). The test vehicles included nine naturally-aspirated and five turbocharged models. The results showed that acceleration performance was the parameter most sensitive to octane quality changes, particularly in the turbocharged models. GRA

N91-14613* National Aeronautics and Space Administration. Marshall Space Flight Center, Huntsville, AL.

SYSTEM FOR CONNECTING FLUID COUPLINGS Patent

Joseph C. Cody, inventor (to NASA) and Paul R. Matthews, inventor (to NASA) (Spectra Research Systems, Inc., Huntsville, AL.) 12 Jun. 1990 7 p Filed 29 Feb. 1988

(NASA-Case-MFS-26042-1-SB; US-Patent-4,932,688; US-Patent-Appl-SN-161682; US-Patent-Class-285-82; US-Patent-Class-285-361; Int-Patent-Class-F16L-35/00) Avail: US Patent and Trademark Office CSCL 13I

A system for mating fluid transfer couplings is constructed having a male connector which is provided with a pair of opposed rollers mounted to an exterior region thereof. A male half of a fluid transfer coupling is rotatably supported in an opening in an end of the connector and is equipped with an outwardly extending forward portion. The forward portion locks into an engagement and locking region of a female half of the fluid transfer coupling, with female half being rotatably supported in a receptacle. The receptacle has an opening aligned with locking region, with this opening having a pair of concentric, annularly disposed ramps extending around an interior portion of opening. These ramps are inclined toward the interior of the receptacle and are provided with slots through which rollers of the connector pass. After the connector is inserted into the receptacle (engaging forward portion

into engagement region), relative rotation between the connector and receptacle causes the rollers to traverse ramps until the rollers abut and are gripped by retainers. This axially forces the forward portion into locked, sealed engagement with the engagement region. Official Gazette of the U.S. Patent and Trademark Office

N91-14614* National Aeronautics and Space Administration. Langley Research Center, Hampton, VA.
MECHANICAL END JOINT SYSTEM FOR CONNECTING STRUCTURAL COLUMN ELEMENTS Patent
Harold G. Bush, inventor (to NASA), Martin M. Mikulas, Jr., inventor (to NASA), and Richard E. Wallsom, inventor (to NASA) 16 Oct. 1990 12 p Filed 30 Mar. 1990 Continuation-in-part of abandoned US-Patent-Appl-SN-388264, filed 1 Aug. 1989 which is a continuation-in-part of abandoned US-Patent-Appl-SN-223122, filed 22 Jul. 1988
(NASA-Case-LAR-14465-1; US-Patent-4,963,052;
US-Patent-Appl-SN-501910; US-Patent-Appl-SN-388264;
US-Patent-Appl-SN-223122; US-Patent-Class-403-322;
US-Patent-Class-403-327; US-Patent-Class-403-331;
US-Patent-Class-403-171; Int-Patent-Class-B25G-3/18) Avail: US Patent and Trademark Office CSCL 13I

A mechanical end joint system is presented that eliminates the possibility of free movements between the joint halves during loading or vibration. Both node joint body (NJB) and column end joint body (CEJB) have cylindrical engaging ends. Each of these ends has an integral semicircular tongue and groove. The two joint halves are engaged transversely - the tongue of the NJB mating with the groove of the CEJB and vice versa. The joint system employs a spring loaded internal latch mechanism housed in the CEJB. During mating, this mechanism is pushed away from the NJB and enters the NJB when mating is completed. In order to lock the joint and add a preload across the tongue and groove faces, an operating ring collar is rotated through 45 deg causing an internal mechanism to compress a Belleville washer preload mechanism. This causes an equal and opposite force to be exerted on the latch bolt and the latch plunger. This force presses the two joint halves tightly together. In order to prevent inadvertent disassembly, a secondary lock is also engaged when the joint is closed. Plungers are carried in the operating ring collar. When the joint is closed, the plungers fall into tracks on the CEJB, which allows the joint to be opened only when the operating ring collar and plungers are pushed directly away from the joining end. One application of this invention is the rapid assembly and disassembly of diverse skeletal framework structures which is extremely important in many projects involving the exploration of space.
Official Gazette of the U.S. Patent and Trademark Office

N91-14615* National Aeronautics and Space Administration. Langley Research Center, Hampton, VA.
SPIRAL LEAD PLATEN ROBOTIC END EFFECTOR Patent
David C. Beals, inventor (to NASA) 11 Sep. 1990 7 p Filed 28 Sep. 1988
(NASA-Case-LAR-13855-1; US-Patent-4,955,653;
US-Patent-Appl-SN-250662; US-Patent-Class-294-119.1;
US-Patent-Class-901-38; US-Patent-Class-901-39;
Int-Patent-Class-B25J-15/08) Avail: US Patent and Trademark Office CSCL 13I

A robotic end effector is disclosed which makes use of a rotating platen with spiral leads used to impact lateral motion to gripping fingers. Actuation is provided by the contact of rolling pins with the walls of the leads. The use of the disclosed method of actuation avoids jamming and provides excellent mechanical advantage while remaining light in weight and durable. The entire end effector is compact and easily adapted for attachment to robotic arms currently in use.
Official Gazette of the U.S. Patent and Trademark Office

N91-14616* National Aeronautics and Space Administration. Pasadena Office, CA.
MULTI-FINGERED ROBOTIC HAND Patent
Carl F. Ruoff, inventor (to NASA) and Kenneth Salisbury, Jr., inventor (to NASA) (Jet Propulsion Lab., California Inst. of Tech., Pasadena.) 1 May 1990 10 p Filed 12 Dec. 1984 Continuation of abandoned US-Patent-Appl-SN-364774, filed 2 Apr. 1982
(NASA-Case-NPO-15959-2; US-Patent-4,921,293;
US-Patent-Appl-SN-680605; US-Patent-Appl-SN-364774;
US-Patent-Class-294-111; US-Patent-Class-74-479;
US-Patent-Class-74-665G; US-Patent-Class-294-106;
US-Patent-Class-414-7; US-Patent-Class-414-729) Avail: US Patent and Trademark Office CSCL 13I

A robotic hand is presented having a plurality of fingers, each having a plurality of joints pivotally connected one to the other. Actuators are connected at one end to an actuating and control mechanism mounted remotely from the hand and at the other end to the joints of the fingers for manipulating the fingers and passing externally of the robot manipulating arm in between the hand and the actuating and control mechanism. The fingers include pulleys to route the actuators within the fingers. Cable tension sensing structure mounted on a portion of the hand are disclosed, as is covering of the tip of each finger with a resilient and pliable friction enhancing surface.
Official Gazette of the U.S. Patent and Trademark Office

N91-14617* National Aeronautics and Space Administration. Lewis Research Center, Cleveland, OH.
POST CLAMP Patent
John K. Ramsey, inventor (to NASA) and Erwin H. Meyn, inventor (to NASA) 7 Aug. 1990 9 p Filed 29 Sep. 1989
(NASA-Case-LEW-14862-1; US-Patent-4,946,122;
US-Patent-Appl-SN-414816; US-Patent-Class-248-229;
US-Patent-Class-248-230; US-Patent-Class-403-385;
US-Patent-Class-403-391; Int-Patent-Class-F16M-13/00) Avail: US and Trademark Office CSCL 13I

A pair of spaced collars are mounted at right angles on a clamp body by retaining rings which enable the collars to rotate with respect to the clamp body. Mounting posts extend through aligned holes in the collars and clamp body. Each collar can be clamped onto the inserted post while the clamp body remains free to rotate about the post and collar. The clamp body is selectively clamped onto each post.
Official Gazette of the U.S. Patent and Trademark Office

38 QUALITY ASSURANCE AND RELIABILITY

Includes product sampling procedures and techniques; and quality control.

N91-14618*# National Aeronautics and Space Administration. Langley Research Center, Hampton, VA.
AXISYMMETRIC SHELL ANALYSIS OF THE SPACE SHUTTLE SOLID ROCKET BOOSTER FIELD JOINT
Michael P. Nemeth and Melvin S. Anderson (Old Dominion Univ., Norfolk, VA.) Washington Jan. 1991 55 p
(NASA-TP-3033; L-16746; NAS 1.60:3033) Avail: NTIS HC/MF A04 CSCL 20K

The Space Shuttle Challenger (STS 51-L) accident led to an intense investigation of the structural behavior of the solid rocket booster (SRB) tang and clevis field joints. Results are presented of axisymmetric shell analyses that parametrically assess the structural behavior of SRB field joints subjected to quasi-steady-state internal pressure loading for both the original joint flown on mission STS 51-L and the redesigned joint flown for the first time after the STS 51-L accident on the Space Shuttle Discovery. Discussion of axisymmetric shell modeling issues and details is presented and a generic method for simulating contact between adjacent shells of revolution is described. Results are presented that identify the performance trends of the joints for a wide range of joint parameters. An important finding is that the redesigned joint exhibits significantly smaller O-ring gap changes and much less sensitivity to joint clearances than the original joint. For a wide range of joint parameters, the result presented indicate that the redesigned joint provides a much better pressure seal than the original joint. Author

N91-14619# Oak Ridge National Lab., TN.
ULTRASONIC DETECTION OF FATIGUE DAMAGE IN GLASS-EPOXY COMPOSITES
W. A. Simpson, Jr. and R. W. McClung 1990 42 p Presented at the Damage Detection and Quality Assurance Conference, San Antonio, TX, 13-14 Nov. 1990
(Contract DE-AC05-84OR-21400)
(DE91-002652; CONF-9011135-1) Avail: NTIS HC/MF A03

Energy storage flywheels fabricated of S2 glass-epoxy composite were studied to determine the behavior of the ultrasonic properties as a function of strain history and to identify possible predictors of incipient failure. Tensile specimens of the flywheel material were loaded uniaxially, and the ultrasonic properties (i.e., the shear and longitudinal wave velocities and the attenuation) were measured as a function of strain. Finished flywheels were similarly tested at various stages during cyclic spin testing; in addition, the polar backscattering intensity as a function of fatigue cycle was recorded. The velocities are excellent indicators of the maximum strain incurred at each point of the flywheel, and the attenuation delineates the region in which the stress is high enough to initiate microcracking in the matrix. DOE

N91-14620# Harry Diamond Labs., Adelphi, MD.
EFFECT OF LASER FLUCTUATIONS IN AUTOMATED SOLDER JOINT INSPECTION Final Report, Sep. 1989 - Mar. 1990
Andrew J. Bayba Aug. 1990 17 p Sponsored by Army Material Command, Alexandria, VA
(AD-A226685; HDL-TM-90-13) Avail: NTIS HC/MF A03 CSCL 09/3

A study was performed to assess the significance of potential fluctuations in power output of the heating laser in automated laser inspection systems. So that the effect of variations in power output could be determined, heat-transfer analysis was conducted on a simplified model of a solder connection using finite-element methods. The study indicates that 10-percent modulation about some mean power input produces the same frequency of modulation as the input, but slightly damped amplitude, in the infrared emissions measured during the heat-up phase; the error is negligible after the laser is terminated. The study also indicates that a 10-percent increase or decrease in average power input produces an error in measured infrared emissions of approximately 11 percent throughout the process. The latter results were corroborated by a mathematical model. GRA

N91-14621# Midwest Research Inst., Golden, CO.
THE HIGH COST OF LOW QUALITY IN R/D (RESEARCH AND DEVELOPMENT)
Chester V. Wells Oct. 1990 10 p Presented at the 17th Annual Conference of the American Society for Quality Control, Tucson, AZ, 9-12 Sep. 1990
(Contract DE-AC02-83CH-10093)
(DE91-002118; SERI/TP-215-3975; CONF-9009153-4) Avail: NTIS HC/MF A02

The principles of quality assurance and quality control yield high payoffs when applied to research activities. Researchers are usually highly motivated individuals who earnestly desire to produce excellent results. The nature of research and the temperament of researchers are such that considerable freedom and latitude are usually required so that the creative processes are not impeded. These are approaches that can be used in applying quality assurance and control that researchers will accept and use when they see the payoff. Some examples are given, with particular emphasis on quality cost systems applied to measurement processes in Research and Development. DOE

N91-14622# EG and G Mound Applied Technologies, Miamisburg, OH.
THERMAL ANALYSES FOR QUALITY CONTROL OF PLASTICS, CERAMICS, AND EXPLOSIVES
C. R. Brown, M. J. Garrod, and R. B. Whitaker 1990 4 p Presented at the 19th Annual North American Thermal Analysis Society Conference, Boston, MA, 23-26 Sep. 1990
(Contract DE-AC04-88DP-43495)
(DE91-002701; MLM-3667(OP); CONF-9009223-3) Avail: NTIS HC/MF A01

Thermal analyses are performed for production quality control and for surveillance at Mound on plastic, ceramic, explosive, and pyrotechnic materials. For the weapons surveillance program, weapon components are disassembled after varying times in the field; thermal and other analyses are then performed on the component materials. The types of thermal analyses done include: differential scanning calorimetry (DSC), differential thermal analysis (DTA), thermogravimetry (TG), thermomechanical analysis (TMA), and high temperature TG/DTA. DOE

N91-14623# Oak Ridge National Lab., TN.
QUALITY CONTROL AND NONDESTRUCTIVE TEST PROCEDURES FOR WELDED PRODUCTS Foreign Trip Report
C. E. Childress Nov. 1990 5 p
(Contract DE-AC05-84OR-21400)
(DE91-004530; ORNL/FTR-3815) Avail: NTIS HC/MF A01

The International Institute of Welding is composed of some 600 technical experts from 36 countries. These individuals are divided by talent and personal interest into fifteen separate groups called Commissions, each with its own charter and goals. The title, and by inference the charter, of Commission V is: Quality Control and Quality Assurance of Welded Products. In pursuit of its charter, Commission V has several subcommissions engaged in the development of drafts, procedures, and standards. Those documents subsequently considered suitable may be submitted to the International Organization for Standards (ISO), an organization similar to the American Society for Testing Materials, for acceptance as international standards. All ISO procedures and standards which have been in effect for five years must undergo review by the initiating body. The results from review of five-year-old standards and procedures and the discussion of other documents proposed for international publication are presented. DOE

39 STRUCTURAL MECHANICS

Includes structural element design and weight analysis; fatigue; and thermal stress.

For applications see *05 Aircraft Design, Testing and Performance* and *18 Spacecraft Design, Testing and Performance.*

N91-14624*# Alabama Univ., Huntsville. Center for Microgravity and Materials Research.
VIBRATION ISOLATION TECHNOLOGY: SENSITIVITY OF SELECTED CLASSES OF EXPERIMENTS TO RESIDUAL ACCELERATIONS Semiannual Progress Report No. 4, 30 Dec. 1989 - 30 Jun. 1990
J. Iwan D. Alexander 23 Aug. 1990 138 p
(Grant NAG8-724)
(NASA-CR-186902; NAS 1.26:186902) Avail: NTIS HC/MF A07 CSCL 20K

The solution was sought of a 2-D axisymmetric moving boundary problem for the sensitivity of isothermal and nonisothermal liquid columns and the sensitivity of thermo-capillary flows to buoyancy driven convection caused by residual accelerations. The sensitivity of a variety of space experiments to residual accelerations are examined. In all the cases discussed, the sensitivity is related to the dynamic response of a fluid. In some cases the sensitivity can be defined by the magnitude of the response of the velocity field. This response may involve motion of the fluid associated with internal density gradients, or the motion of a free liquid surface. For fluids with internal density gradients, the type of acceleration to which the experiment is sensitive will depend on whether buoyancy driven convection must be small in comparison to other types of fluid motion (such as thermocapillary flow), or fluid motion must be suppressed or eliminated (such as in diffusion studies, or directional solidification experiments). The effect of the velocity on the composition and temperature field must be considered, particularly in the vicinity of the melt crystal

interface. As far as the response to transient disturbances is concerned the sensitivity is determined by both the magnitude and frequency the acceleration and the characteristic momentum and solute diffusion times. Author

N91-14625 Michigan Univ., Ann Arbor.
SOME PROBLEMS IN ELASTIC CONTACT AND FRACTURE Ph.D. Thesis
Xiaoping Lu 1990 97 p
Avail: Univ. Microfilms Order No. DA9023592

Three problems in elastic contact and fracture mechanics are studied. The first problem is the perturbation of the elastic compliances of a solid of two bonded dissimilar materials due to interacting cracks at the interface. The problem is formulated using Betti's reciprocal theorem. The analysis provides the equivalent elastic compliances in terms of the geometric parameters of the interface cracks for various loadings and material combinations. The results show that the interaction between cracks is significant only when the crack spacing is less than four times the crack length. Also, contact between crack faces introduces coupling between applied shear stress and normal stress, but the coupling is significant only when the ratio of the magnitudes of the shear and normal stresses exceeds two. The second problem concerns the stress evaluation of an elastic half space with periodically-distributed hemispherical holes at the free surface; the analysis is based upon the Galerkin's strain potentials approach. At infinity the body is assumed to be in a state of uniform plane stress parallel to the free surface. The solution is presented by three sets of double Fourier series. The numerical results are given for two cases: uniform tensile stress and uniform shear stress at infinity. It is found that stress concentration is greatest at the bottom of holes; it increases with spacing and approaches to the value for a single hole for large spacing. The last problem involves the effect on crack propagation, of mixed mode and partial crack closure due to curvature; the effect is examined by analyzing a simple sinusoidal crack model. For a slightly curved crack under applied shear stress, a small mode I stress intensity factor is obtained. Cracks under combined tension-and-shear loads, and compression-and-shear loads are also studied. Dissert. Abstr.

N91-14626 Kentucky Univ., Lexington.
A BOUNDARY ELEMENT METHOD FOR ELASTOSTATIC AND ELASTODYNAMIC CRACK PROBLEMS IN TWO AND THREE DIMENSIONS Ph.D. Thesis
Zhenhong Jia 1990 201 p
Avail: Univ. Microfilms Order No. DA9017321

The direct boundary element method is applied to the stress analysis of cracked structures of both two and three dimensions. Complications arising from the singular stress field at the crack tip (front) are addressed. It is well known from the theory of fracture mechanics that the displacement and stresses in the vicinity of a crack tip (front) behave like sq root of r and 1/sq root of r and that such behaviors are not representable by ordinary polynomials. Consequently, isoparametric elements fail in a small neighborhood of the crack. Special shape functions containing the correct terms are developed based on a three-noded line element and an eight-noded quadrilateral element to be used at a crack tip (front). This special treatment not only improves the accuracy but also enables a direct computation of the stress intensity factors. Singularities arising from both the kernels and the special shape functions are removed analytically before numerical integration. Coordinate transformation and element subdivision are used to accomplish this task. Detailed discussions are presented to explain the step-by-step procedures. In the current formulation, cracks of arbitrary shapes can be handled, and numerical problems of straight and curved cracks are investigated in the two-dimensional, elastostatic context. For three-dimensional problems involving penny-shaped cracks, both static and time-harmonic loading are considered. Stress intensity factors of modes I, II, and III are obtained for a variety of problems. In solving mixed-mode problems and problems dealing with infinite bodies, a multidomain strategy is utilized. This new concept of infinite body subdivision is important in treating wave-scattering problems. The fictitious eigen-frequency difficulty is encountered in solving elastodynamic problems, and the combined Helmholtz integral equation formulation (CHIEF) technique is used to overcome this difficulty. Dissert. Abstr.

N91-14627 Texas Univ., Austin.
FRACTURE ANALYSIS OF CATHODIC DELAMINATION IN RUBBER-TO-METAL BONDS Ph.D. Thesis
Chih Lin 1989 188 p
Avail: Univ. Microfilms Order No. DA9016923

A fracture mechanics approach was taken to examine the durability of rubber to metal bonds that are subject to cathodic delamination. The particular application considered here was the rubber window in sonar transducers which is bonded to steel and aluminum and subjected to various mechanical loads which give rise to large deformations even in the absence of delaminations. The neoprene rubber used in sonar transducers displayed the characteristic nonlinear elastic response of rubberlike materials in uniaxial and strip biaxial experiments. The data was used to obtain a number of representations of the strain energy function for the neoprene. A number of more general stress states were used to determine the most suitable representation. Other experiments were used to validate the finite deformation finite element analysis. Various crack geometries in the sonar transducers were analyzed to examine the range of energy release rates and fracture mode mixity that can arise. The double strip blister specimen was then developed as a simple, self-loading fracture property specimen for cathodic delamination experiments. The experiments were conducted in artificial seawater and 1N sodium hydroxide environments with specimens having various rubber thicknesses and load levels. A commercially available primer adhesive system with and without a silane coupling agent was used to bond the rubber to steel. Crack growth rates were correlated with the energy release rate. The results indicated that the energy rate was not a unifying correlating parameter for all rubber thicknesses and loadings, suggesting that fracture mode mixity has a strong effect. The sodium hydroxide environment was clearly a more aggressive environment than the artificial seawater. However, the results suggest that different debonding mechanisms were active because the degree of adhesion as well as debonding rates were affected. Dissert. Abstr.

N91-14628 Rochester Univ., NY.
THE BUCKLING OF OFF-AXIS, ORTHOTROPIC, CYLINDRICAL SHELLS IN TORSION Ph.D. Thesis
Zbigniew Hakiel 1989 143 p
Avail: Univ. Microfilms Order No. DA9019818

The stability of thin, off-axis orthotropic, circular, cylindrical shells under torsion in the presence of axial loads is investigated. Buckling and post-buckling experiments are performed on orthotropic polyester shells and torque versus twist measurements are made from which the critical loads are determined. Detailed measurements of the shape of the buckled surface are made and contour plots are generated. A Galerkin solution is developed to the linearized Donnell equations. The dependence of the critical load and buckle shape on the angle between the material coordinates and the shell coordinates is determined and an unexpected reversal in the difference between the critical shear loads in the two directions of twist is found in both the measured and predicted results. Parametric studies are made with the Galerkin solution to determine the effect of elastic properties, axial loading, and geometry. It is found that the level of orthotropy of the shell has a pronounced effect on both the critical load and buckle shape. Off-axis orthotropic shells are generally found to have fewer circumferential buckles and higher values of critical load when twisted in the direction which puts the shell in compression along its stronger material axis. It is also found that the observed reversal of the difference between the critical shear loads in the two directions of twist is affected by the level of the shear modulus and the level of orthotropy of the shell. Axial tension is found to stabilize the shells, as expected. Twisting of the off-axis orthotropic shells in their strong direction is found to stabilize them in axial compression. It is found that geometry affects the

dependence of the critical load and buckle shape on the orthotropy of the shell, but that this effect is small for long, thin and slender shells. Dissert. Abstr.

N91-14629*# National Aeronautics and Space Administration. Langley Research Center, Hampton, VA.
A PARAMETRIC SHELL ANALYSIS OF THE SHUTTLE 51-L SRB AFT FIELD JOINT
Randall C. Davis, Lynn M. Bowman, Robert M. Hughes, IV, and Brian J. Jackson (Old Dominion Univ., Norfolk, VA.) Oct. 1990 19 p
(NASA-TM-102748; NAS 1.15:102748) Avail: NTIS HC/MF A03 CSCL 20K

Following the Shuttle 51-L accident, an investigation was conducted to determine the cause of the failure. Investigators at the Langley Research Center focused attention on the structural behavior of the field joints with O-ring seals in the steel solid rocket booster (SRB) cases. The shell-of-revolution computer program BOSOR4 was used to model the aft field joint of the solid rocket booster case. The shell model consisted of the SRB wall and joint geometry present during the Shuttle 51-L flight. A parametric study of the joint was performed on the geometry, including joint clearances, contact between the joint components, and on the loads, induced and applied. In addition combinations of geometry and loads were evaluated. The analytical results from the parametric study showed that contact between the joint components was a primary contributor to allowing hot gases to blow by the O-rings. Based upon understanding the original joint behavior, various proposed joint modifications are shown and analyzed in order to provide additional insight and information. Finally, experimental results from a hydro-static pressurization of a test rocket booster case to study joint motion are presented and verified analytically. Author

N91-14630*# Engineering Mechanics Association, Inc., Torrance, CA.
METHODS FOR EVALUATING THE PREDICTIVE ACCURACY OF STRUCTURAL DYNAMIC MODELS Quarterly Report No. 6, 1 Sep. - 30 Nov. 1990
T. K. Hasselman and Jon D. Chrostowski 9 Dec. 1990 60 p Sponsored by NASA
(NASA-CR-187649; NAS 1.26:187649; EMA-TR-89-1152-6)
Avail: NTIS HC/MF A04 CSCL 20K

Uncertainty of frequency response using the fuzzy set method and on-orbit response prediction using laboratory test data to refine an analytical model are emphasized with respect to large space structures. Two aspects of the fuzzy set approach were investigated relative to its application to large structural dynamics problems: (1) minimizing the number of parameters involved in computing possible intervals; and (2) the treatment of extrema which may occur in the parameter space enclosed by all possible combinations of the important parameters of the model. Extensive printer graphics were added to the SSID code to help facilitate model verification, and an application of this code to the LaRC Ten Bay Truss is included in the appendix to illustrate this graphics capability. K.S.

N91-14631# Naval Postgraduate School, Monterey, CA. Dept. of Mechanical Engineering.
THE RESPONSE AND FAILURE MECHANISMS OF CIRCULAR METAL AND COMPOSITE PLATES SUBJECTED TO UNDERWATER SHOCK LOADING M.S. Thesis
Robert A. Jones Mar. 1990 105 p
(AD-A226759) Avail: NTIS HC/MF A06 CSCL 11/4

The response and failure mechanism of circular aluminum and S-2 glass fiber/polyester resin matrix composite panels in response to underwater shock loading were investigated. The response of the aluminum panels was compared to the characteristic response of thin circular metal plates subjected to shock loading with a good degree of correlation. The response of the aluminum panels was then used as a reference with which to compare the response of the composite panels. The response and failure mechanism of the composite panels were found to be highly dependent on the boundary conditions of the panel. For the conditions of this test series, in which the panel boundary was allowed limited motion in the radial direction, the response of the composite panel was determined to be generally similar to the response of the aluminum panels, mitigated by the high strength in tension of the glass fiber. The failure mechanism appeared to be localized matrix failure in compression due to the high circumferential stresses generated as a result of the panel being forced into the smaller diameter test fixture by the shock wave. The radial motion of the panel edge, allowed by the boundary conditions, appears to have exacerbated the circumferential stresses. GRA

N91-14632*# National Aeronautics and Space Administration. Lewis Research Center, Cleveland, OH.
AXIAL-TORSIONAL FATIGUE: A STUDY OF TUBULAR SPECIMEN THICKNESS EFFECTS
Peter J. Bonacuse and Sreeramesh Kalluri (Sverdrup Technology, Inc., Brook Park, OH.) Dec. 1990 19 p
(NASA-TM-103637; E-5814; NAS 1.15:103637;
AVSCOM-TM-90-C-014) Avail: NTIS HC/MF A03 CSCL 20K

A room-temperature experimental program was conducted on AISI type 316 stainless steel to determine the effect of wall thickness on the cyclic deformation behavior and fatigue life of thin-wall, tubular, axial-torsional fatigue specimens. The following experimental variables were examined in this study: the depth of the surface work-hardened layer produced in specimen machining, and the effects of strain range and axial-torsional strain phasing. Tubular fatigue specimens were fabricated with wall thicknesses of 1.5, 2.0, and 2.5 mm. One as-fabricated specimen from each wall thickness was sectioned for microstructural examination and microhardness measurement. A specimen of each wall thickness was tested at each of three conditions - high strain range in-phase, low strain range in-phase, and low strain range out-of-phase - for a total of nine axial-torsional fatigue experiments. The machining-induced work-hardened zone, as a percentage of the gage section material, was found to have a minimal effect on both deformation behavior and fatigue life. Also, little or no variation in fatigue life or deformation behavior as a function of wall thickness was observed. Out-of-phase fatigue tests displayed shorter fatigue lives and more cyclic hardening than in-phase tests. Author

N91-14633# Sandia National Labs., Albuquerque, NM.
THE USE OF LIGHT EMISSION IN FAILURE ANALYSIS OF CMOS ICS
Charles F. Hawkins (New Mexico Univ., Albuquerque.), Jerry M. Soden, Edward I. Cole, Jr., and Eric S. Snyder 1990 13 p Presented at the 16th International Symposium and Exposition for Testing and Failure Analysis, Los Angeles, CA, 26 Oct. - 7 Nov. 1990
(Contract DE-AC04-76DP-00789)
(DE91-001234; SAND-90-1169C; CONF-9010148-1) Avail: NTIS HC/MF A03

The use of photon emission for analyzing failure mechanisms and defects in CMOS IC's is presented. Techniques are given for accurate identification and spatial localization of failure mechanisms and physical defects, including defects such as short and open circuits which do not themselves emit photons. DOE

42 GEOSCIENCES (GENERAL)

No abstracts in this category.

43 EARTH RESOURCES AND REMOTE SENSING

Includes remote sensing of earth resources by aircraft and spacecraft; photogrammetry; and aerial photography.

For instrumentation see *35 Instrumentation and Photography.*

N91-14634*# National Aeronautics and Space Administration. Langley Research Center, Hampton, VA.
ADVANCED TECHNOLOGY NEEDS FOR A GLOBAL CHANGE SCIENCE PROGRAM: PERSPECTIVE OF THE LANGLEY RESEARCH CENTER
Lawrence F. Rowell and Thomas J. Swissler (ST Systems Corp., Hampton, VA.) Washington Jan. 1991 134 p
(NASA-TM-4196; L-16705; NAS 1.15:4196) Avail: NTIS HC/MF A07 CSCL 08E

The focus of the NASA program in remote sensing is primarily the Earth system science and the monitoring of the Earth global changes. One of NASA's roles is the identification and development of advanced sensing techniques, operational spacecraft, and the many supporting technologies necessary to meet the stringent science requirements. Langley Research Center has identified the elements of its current and proposed advanced technology development program that are relevant to global change science according to three categories: sensors, spacecraft, and information system technologies. These technology proposals are presented as one-page synopses covering scope, objective, approach, readiness timeline, deliverables, and estimated funding. In addition, the global change science requirements and their measurement histories are briefly discussed. Author

N91-14635*# Massachusetts Inst. of Tech., Cambridge. Center for Electromagnetic Theory and Applications.
REMOTE SENSING OF EARTH TERRAIN Progress Report, 1 Jan. - 30 Jun. 1990
Jin Au Kong, Robert T. Shin, Son V. Nghiem, Herng-Aung Yueh, Hsiu C. Han, Harold H. Lim, and David V. Arnold 1990 20 p
(Grant NAGw-1617)
(NASA-CR-186904; NAS 1.26:186904) Avail: NTIS HC/MF A03 CSCL 08B

Remote sensing of earth terrain is examined. The layered random medium model is used to investigate the fully polarimetric scattering of electromagnetic waves from vegetation. The model is used to interpret the measured data for vegetation fields such as rice, wheat, or soybean over water or soil. Accurate calibration of polarimetric radar systems is essential for the polarimetric remote sensing of earth terrain. A polarimetric calibration algorithm using three arbitrary in-scene reflectors is developed. In the interpretation of active and passive microwave remote sensing data from the earth terrain, the random medium model was shown to be quite successful. A multivariate K-distribution is proposed to model the statistics of fully polarimetric radar returns from earth terrain. In the terrain cover classification using the synthetic aperture radar (SAR) images, the applications of the K-distribution model will provide better performance than the conventional Gaussian classifiers. The layered random medium model is used to study the polarimetric response of sea ice. Supervised and unsupervised classification procedures are also developed and applied to synthetic aperture radar polarimetric images in order to identify their various earth terrain components for more than two classes. These classification procedures were applied to San Francisco Bay and Traverse City SAR images. B.G.

N91-14636*# Ohio State Univ., Columbus. Dept. of Geodetic Science and Surveying.
ESTIMABILITY OF GEODETIC PARAMETERS FROM SPACE VLBI OBSERVABLES
Jozsef Adam Jul. 1990 118 p
(Grant NsG-5265)
(NASA-CR-187413; NAS 1.26:187413; OSU-406) Avail: NTIS HC/MF A06 CSCL 08E

The feasibility of space very long base interferometry (VLBI) observables for geodesy and geodynamics is investigated. A brief review of space VLBI systems from the point of view of potential geodetic application is given. A selected notational convention is used to jointly treat the VLBI observables of different types of baselines within a combined ground/space VLBI network. The basic equations of the space VLBI observables appropriate for convariance analysis are derived and included. The corresponding equations for the ground-to-ground baseline VLBI observables are also given for a comparison. The simplified expression of the mathematical models for both space VLBI observables (time delay and delay rate) include the ground station coordinates, the satellite orbital elements, the earth rotation parameters, the radio source coordinates, and clock parameters. The observation equations with these parameters were examined in order to determine which of them are separable or nonseparable. Singularity problems arising from coordinate system definition and critical configuration are studied. Linear dependencies between partials are analytically derived. The mathematical models for ground-space baseline VLBI observables were tested with simulation data in the frame of some numerical experiments. Singularity due to datum defect is confirmed. Author

N91-14637# Beleidscommissie Remote Sensing, Delft (Netherlands).
STRATEGIC PLAN COMMERCIALIZATION REMOTE SENSING BY NEDECO [STRATEGISCH PLAN COMMERCIALISERING REMOTE SENSING NEDECO]
Feb. 1990 96 p In DUTCH
(BCRS-89-35; ETN-90-97684) Avail: NTIS HC/MF A05

The task given to NEDECO to draw up a strategic plan on the commercialization of remote sensing (in the framework of the National Remote Sensing Program) is described. The strategic plan contains the following items: acceptance by the public, marketing, product development, demonstration projects, work organization, personnel, education, facilities, and finance. It is concluded that the competitivity of the Dutch Remote Sensing is fairly favorable. ESA

N91-14638*# Michigan Univ., Ann Arbor. Radiation Lab.
MULTIBAND RADAR CHARACTERIZATION OF FOREST BIOMES Final Report, 1 Mar. 1985 - 28 Feb. 1990
M. Craig Dobson and Fawwaz T. Ulaby Feb. 1990 12 p
(Grant NAGw-733)
(NASA-CR-185101; NAS 1.26:185101; UM-022486-1-F) Avail: NTIS HC/MF A03 CSCL 02F

The utility of airborne and orbital SAR in classification, assessment, and monitoring of forest biomes is investigated through analysis of orbital synthetic aperature radar (SAR) and multifrequency and multipolarized airborne SAR imagery relying on image tone and texture. Preliminary airborne SAR experiments and truck-mounted scatterometer observations demonstrated that the three dimensional structural complexity of a forest, and the various scales of temporal dynamics in the microwave dielectric properties of both trees and the underlying substrate would severely limit empirical or semi-empirical approaches. As a consequence, it became necessary to develop a more profound understanding of the electromagnetic properties of a forest scene and their temporal dynamics through controlled experimentation coupled with theoretical development and verification. The concatenation of various models into a physically-based composite model treating the entire forest scene became the major objective of the study as this is the key to development of a series of robust retrieval algorithms for forest biophysical properties. In order to verify the performance of the component elements of the composite model, a series of controlled laboratory and field experiments were undertaken to: (1) develop techniques to measure the microwave dielectric properties of vegetation; (2) relate the microwave dielectric properties of vegetation to more readily measured characteristics such as density and moisture content; (3) calculate the radar cross-section of leaves, and cylinders; (4) improve backscatter models for rough surfaces; and (5) relate attenuation and phase delays during propagation through canopies to canopy properties. These modeling efforts, as validated by the

measurements, were incorporated within a larger model known as the Michigan Microwave Canopy Scattering (MIMICS) Model.

Author

N91-14639*# Georgia Univ., Athens. Dept. of Agronomy.
COMPARISON OF GROUND AND SATELLITE BASED MEASUREMENTS OF THE FRACTION OF PHOTOSYNTHETICALLY ACTIVE RADIATION INTERCEPTED BY TALL-GRASS PRAIRIE
T. H. Demetriades-Shah, E. T. Kanemasu, I. Flitcroft, and H. Su (Kansas State Univ., Manhattan.) 1990 17 p
(Grant NAG5-1192)
(NASA-CR-187696; NAS 1.26:187696) Avail: NTIS HC/MF A03 CSCL 02C

The fraction, of photosynthetically active radiation absorbed by vegetation, F sub ipar, is an important requirement for estimating vegetation biomass productivity and related quantities. This was an integral part of a large international effort; the First ISLSCP Field Experiment (FIFE). The main objective of FIFE was to study the effects of vegetation on the land atmosphere interactions and to determine if these interactions can be assessed from satellite spectral measurements. The specific purpose of this experiment was to find out how well measurements of F sub ipar relate to ground, helicopter, and satellite based spectral reflectance measurements. Concurrent measurements of F sub ipar and ground, helicopter, and satellite based measurements were taken at 13 tall grass prairie sites in Kansas. The sites were subjected to various combinations of burning and grazing managements.

Author

N91-14640# Technische Univ., Delft (Netherlands). Werkeeheid Fotogrammetrie en Remote Sensing.
FITTING OF PHOTOGRAMMETRY AND FIELD COMPLETION Thesis [AFSTEMMING FOTOGRAMMETRIE EN NAVERKENNING]
J. C. M. Leijten Nov. 1989 106 p In DUTCH; ENGLIGH summary
(ETN-91-98144) Avail: NTIS HC/MF A06

The fitting of photogrammetry and field completion for the large scale digital topographic map of the Netherlands was investigated with a view to a reduction of the total map making costs. Presently the costs of field completion are as high as 45 percent of the total costs. The accuracy requirement results in a requirement for the accuracy of the photogrammetric product, the conceptual map and the map itself. The quality of the photogrammetric product can be improved using an analytical plotter, supporting software, of a lower flying altitude. The new mapping process is described. Two tests show that the method satisfies all the demands. It is expected that fitting the field completion to the accuracy requirements and the better photogrammetric product will result in less field completion.

ESA

N91-14641# National Environmental Satellite Service, Washington, DC.
EVALUATION OF DATA REDUCTION AND COMPOSING OF THE NOAA GLOBAL VEGETATION INDEX PRODUCT: A CASE STUDY
K. P. Gallo and J. F. Brown Jul. 1990 32 p Prepared in cooperation with EROS Data Center, Sioux Falls, SD
(AD-A227397; NESIDS-54) Avail: NTIS HC/MF A03 CSCL 17/5

Data acquired by the AVHRR onboard the TIROS/NOAA series of satellites are spatially degraded from a 1 km resolution at nadir (LAC) to several coarser resolutions. Global Area Coverage Coverage (GAC) data are processed onboard the satellites and have a resolution of approximately 4 km. Global Vegetation Index (GVI) data are processed from sampled GAC data and have a resolution of approximately 15 km. The objectives of this study were to examine the effects of spatial degradation of NOAA AVHRR data on monitoring of land surface or related processes over large areas and to examine alternative procedures for computation and compositing of the GVI data product. While differences existed between the vegetation index values computed for the examined data resolutions, a portion of the observed difference was not due directly to reduction of the satellite data. The mean values of the low resolution (GAC or GVI) data were representative of the full resolution data. Thus, low resolution data used in monitoring activities would likely provide the same results as full resolution data (LAC). The difference index would be the recommended algorithm for satellite zenith angle selection if advantages exist for selection of backscatter views of vegetation from satellites.

GRA

N91-14642* National Aeronautics and Space Administration. Pasadena Office, CA.
METHOD FOR DETECTING SURFACE MOTIONS AND MAPPING SMALL TERRESTRIAL OR PLANETARY SURFACE DEFORMATIONS WITH SYNTHETIC APERTURE RADAR
Patent
Andrew K. Gabriel, inventor (to NASA), Richard M. Goldstein, inventor (to NASA), and Howard A. Zebker, inventor (to NASA) (Jet Propulsion Lab., California Inst. of Tech., Pasadena.) 4 Dec. 1990 9 p Filed 26 Jan. 1990
(NASA-Case-NPO-17831-1-CU; US-Patent-4,975,704; US-Patent-Appl-SN-470665; US-Patent-Class-342-25; Int-Patent-Class-G01S-13/90) Avail: US Patent and Trademark Office CSCL 08B

A technique based on synthetic aperture radar (SAR) interferometry is used to measure very small (1 cm or less) surface deformations with good resolution (10 m) over large areas (50 km). It can be used for accurate measurements of many geophysical phenomena, including swelling and buckling in fault zones, residual, vertical and lateral displacements from seismic events, and prevolcanic swelling. Two SAR images are made of a scene by two spaced antennas and a difference interferogram of the scene is made. After unwrapping phases of pixels of the difference interferogram, surface motion or deformation changes of the surface are observed. A second interferogram of the same scene is made from a different pair of images, at least one of which is made after some elapsed time. The second interferogram is then compared with the first interferogram to detect changes in line of sight position of pixels. By resolving line of sight observations into their vector components in other sets of interferograms along at least one other direction, lateral motions may be recovered in their entirety. Since in general, the SAR images are made from flight tracks that are separated, it is not possible to distinguish surface changes from the parallax caused by topography. However, a third image may be used to remove the topography and leave only the surface changes.

Official Gazette of the U.S. Patent and Trademark Office

44 ENERGY PRODUCTION AND CONVERSION

Includes specific energy conversion systems, e.g., fuel cells; global sources of energy; geophysical conversion; and windpower.

For related information see also *07 Aircraft Propulsion and Power, 20 Spacecraft Propulsion and Power,* and *28 Propellants and Fuels.*

N91-14643# Midwest Research Inst., Golden, CO.
HIGH EFFICIENCY CADMIUM AND ZINC TELLURIDE-BASED THIN FILM SOLAR CELLS
A. Rohatgi, C. J. Summers, A. Erbil, R. Sudharsanan, and S. Ringel Oct. 1990 83 p Prepared in cooperation with Georgia Inst. of Tech., Atlanta, GA
(Contract DE-AC02-83CH-10093)
(DE91-002112; SERI/TP-211-3952) Avail: NTIS HC/MF A05

Polycrystalline Cd(1-x)Zn(x)Te and Cd(1-x)Mn(x)Te films with a band gap of 1.7 eV were successfully grown on glass/SnO2/CdS substrates by molecular beam epitaxy (MBE) and metal-organic chemical vapor deposition (MOCVD), respectively. Polycrystalline Cd(1-x)Zn(x)Te films grown by MBE resulted in uniform composition and sharp interfaces. However, polycrystalline Cd(1-x)Mn(x)Te films

grown by MOCVD showed nonuniform compositions and evidence of manganese accumulation at the Cd(1-x)Mn(x)Te/CdS interface. We found that manganese interdiffuses and replaces cadmium in the CdS film. By improving the CdTe/CdS interface and, thus, reducing the collection function effects, the efficiency of the MOCVD CdTe cell can be improved to about 13.5 percent. MBE-grown CdTe cells also produced 8 to 9 percent efficiencies. The standard CdTe process was not optimum for ternary films and resulted in a decrease in the band gap. Recent results indicate that CdCl2 + ZnCl2 chemical treatment may prevent the band-gap reduction, and that chromate etch (rather than bromine etch) may provide the solution to contact resistance in the ternary cells. DOE

N91-14644# Midwest Research Inst., Golden, CO.
LOAD RESPONSE OF HORIZONTAL-AXIS WIND TURBINES TO TURBULENCE
R. E. Wilson, S. N. Walker, J. R. Hartin, and T. L. Weber Sep. 1990 76 p Prepared in cooperation with Oregon State Univ., Corvallis, OR
(Contract DE-AC02-83CH-10093)
(DE90-000375; SERI/TP-257-3891) Avail: NTIS HC/MF A05

A structural and aerodynamic model of a three-bladed rigid-hub wind turbine is described. The model includes four structural degrees of freedom; one for each blade in flapping, and tower translation. The aerodynamic model includes the effects of wind turbulence as well as the unsteady aerodynamic effects caused by the airfoil shed and trailing wakes. A separate code developed at the Pacific Northwest Laboratory is used to simulate wind turbulence for input to the model described in this report. This model is validated by comparison of code predictions to measured blade bending moments for two different field test turbines. Comparisons are made between measured data and predictions for both mean loads and cyclic flatwise bending moments. The comparisons for the cyclic bending moments include (1) the history of bending moment over one revolution of blade rotation, (2) the power spectral density of the bending moment, and (3) rainflow counting of the bending moment. Conclusions are then made as to the accuracy of the code predictions. DOE

N91-14645# Sandia National Labs., Albuquerque, NM.
PROCESSING EXPERIMENTS FOR DEVELOPMENT OF HIGH-EFFICIENCY SILICON SOLAR CELLS
J. M. Gee, P. A. Basore, D. L. King, J. D. McBrayer, D. S. Ruby, M. E. Buck, and J. W. Tingley 1990 4 p Presented at the 2nd Sunshine Workshop for Crystalline Silicon Solar Cells, Shizuoka, Japan, 23-24 Nov. 1990
(Contract DE-AC04-76DP-00789)
(DE91-002698; SAND-90-2587C; CONF-9011138-1) Avail: NTIS HC/MF A01

Fabrication of high-efficiency silicon solar cells requires processing technology capable of maintaining long bulk carrier lifetime and low surface recombination. Development of long-lifetime processing techniques using experimental designs based on statistical methods is described. The first three experiments investigated pre-oxidation cleans, phosphorus gettering, and a comparison of different phosphorus diffusion sources. Optimal processing parameters were found to depend on the type of silicon material. DOE

N91-14646# Sandia National Labs., Albuquerque, NM. Modal and Structural Dynamics Testing.
DAMPING MEASUREMENTS USING OPERATIONAL DATA
G. H. James, T. G. Carne, and P. S. Veers 1991 10 p Presented at the 10th ASME Wind Energy Symposium, Houston, TX, 20-24 Jan. 1991
(Contract DE-AC04-76DP-00789)
(DE91-002781; SAND-90-2670C; CONF-910154-1) Avail: NTIS HC/MF A02

We have measured modal damping using strain-gauge data from an operating wind turbine. Previously, such measurements were difficult and expensive. Auto-correlation and cross-correlation functions of the strain-gauge data have been shown to consist of decaying sinusoids which correspond to the modal frequencies and damping ratios of the wind turbine. We have verified the method by extracting damping values from an analytically generated data set. Actual operating response data from the DOE/Sandia 34-meter Test Bed has been used to calculate modal damping ratios as a function of rotor rotation rate. This capability will allow more accurate fatigue life prediction and control. DOE

N91-14647*# Oak Ridge National Lab., TN. Metals and Ceramics Div.
HIGH-TEMPERATURE THERMAL STORAGE SYSTEMS FOR ADVANCED SOLAR RECEIVERS MATERIALS SELECTIONS
D. F. Wilson, J. H. DeVan, and M. Howell Sep. 1990 23 p Sponsored by NASA, Lewis Research Center
(Contract DE-AC05-84OR-21400)
(NASA-CR-187750; NAS 1.26:187750; DE91-002969; ORNL/TM-11587) Avail: NTIS HC/MF A03 CSCL 10A

Advanced space power systems that use solar energy and Brayton or Stirling heat engines require thermal energy storage (TES) systems to operate continuously through periods of shade. The receiver storage units, key elements in both Brayton and Stirling systems, are designed to use the latent heat of fusion of phase-change materials (PCMs). The power systems under current consideration for near-future National Aeronautics and Space Administration space missions require working fluid temperatures in the 1100 to 1400 K range. The PCMs under current investigation that gave liquid temperatures within this range are the fluoride family of salts. However, these salts have low thermal conductivity, which causes large temperature gradients in the storage systems. Improvements can be obtained, however, with the use of thermal conductivity enhancements or metallic PCMs. In fact, if suitable containment materials can be found, the use of metallic PCMs would virtually eliminate the orbit associated temperature variations in TES systems. The high thermal conductivity and generally low volume change on melting of germanium and alloys based on silicon make them attractive for storage of thermal energy in space power systems. An approach to solving the containment problem, involving both chemical and physical compatibility, preparation of NiSi/NiSi2, and initial results for containment of germanium and NiSi/NiSi2, are presented. DOE

N91-14648# Pacific Northwest Lab., Richland, WA.
EFFECTS OF WIND SHEAR AND TURBULENCE ON WIND TURBINE POWER CURVES
D. L. Elliott and J. B. Cadogan (Department of Energy, Washington, DC.) Sep. 1990 6 p Presented at the European Community Wind Energy Conference and Exhibition, Madrid, Spain, 10-14 Sep. 1990
(Contract DE-AC06-76RL-01830)
(DE91-004072; PNL-SA-18354; CONF-900989-2) Avail: NTIS HC/MF A02

It is a common practice to use wind speeds at hub height in determining wind turbine power curves. Although the possible influence of other variables (such as turbulence and wind shear) is generally neglected in power curve measurements, we discovered the importance of other variables in an analysis of power curves for three 2.5 MW wind turbines. When the power curves were stratified by turbulence intensity. Such a large sensitivity to turbulence was not expected, and further analyses were conducted to determine if other factors accompanying the change in turbulence level could cause or contribute to the observed sensitivity of the power curves to turbulence. In summary, the sensitivity of the observed power curves was largely due to two factors: (1) an actual sensitivity to turbulence in determining the power curve and (2) the deviation of the disk-averaged velocity from the hub-height velocity under low turbulence conditions that were most prevalent at the site. An examination of the wind shear profiles over the height of the rotor disk revealed that low turbulence conditions were characterized by strong shear in the lower half of the rotor disk and weak or negative shear in the upper half. Implications of this analysis are that significant errors in power curve measurements can result if the effects of wind shear and turbulence are ignored. DOE

N91-14649# Sandia National Labs., Albuquerque, NM.
SOLAR CONCENTRATOR DEVELOPMENT IN THE US
D. J. Alpert, T. R. Mancini, R. M. Houser, J. W. Crossman, P. Schissel, M. Carasso, G. Jorgensen, and M. Scheve (Department of Defense, Washington, DC.) 1990 22 p Presented at the 5th International Symposium on Solar High-Temperature Technologies, Davos, Switzerland, 27-31 Aug. 1990
(Contracts DE-AC04-76DP-00789; DE-AC02-83CH-10093)
(DE91-001232; SAND-90-0903C; CONF-9008139-2) Avail: NTIS HC A03/MF A01

Sandia National Laboratories leads the U.S. Department of Energy's solar concentrator development program in a joint effort with the Solar Energy Research Institute. The goal of DOE's program is to develop, build and test solar concentrators that are low in cost, have high performance, and long lifetimes. Efforts are currently focused on three areas: low-cost heliostats, point-focus parabolic dishes, and durable reflective films. The status and future plans of DOE's program in each area are reviewed. DOE

N91-14650# Sandia National Labs., Albuquerque, NM. Wind Energy Research Div.
FATIGUE RELIABILITY OF WIND TURBINE COMPONENTS
P. S. Veers 1990 8 p Presented at the Windpower 1990, Washington, DC, 25-28 Sep. 1990
(Contract DE-AC04-76DP-00789)
(DE91-001262; SAND-90-2538C; CONF-9009107-3) Avail: NTIS HC/MF A02

Fatigue life estimates for wind turbine components can be extremely variable due to both inherently random and uncertain parameters. A structural reliability analysis is used to qualify the probability that the fatigue life will fall short of a selected target. Reliability analysis also produces measures of the relative importance of the various sources of uncertainty and the sensitivity of the reliability to each input parameter. The process of obtaining reliability estimates is briefly outlined. An example fatigue reliability calculation for a blade joint is formulated; reliability estimates, importance factors, and sensitivities are produced. Guidance in selecting distribution functions for the random variables used to model the random and uncertain parameters is also provided. DOE

N91-14651# Sandia National Labs., Albuquerque, NM.
RELIABILITY OF PHOTOVOLTAIC CONCENTRATOR MODULES
Elizabeth H. Richards and Clement J. Chiang 1990 7 p Presented at the 21st IEEE Photovoltaic Specialists Conference, Kissimmee, FL, 21-25 May 1990
(Contract DE-AC04-76DP-00789)
(DE90-012754; SAND-90-1259C; CONF-900542-11) Avail: NTIS HC/MF A02

The cost goals and calculations in the Five-Year Plan for the National Photovoltaics Program assume that photovoltaic (PV) concentrator modules will have a reliable output and an operational life expectancy of 30 years. Although the modules in the few PV concentrator systems fielded to date have so far been reliable, they have not been in the field long enough to establish performance levels for 30 years and are not necessarily representative of newer concentrator designs. Thus, extensive testing and analysis are required to evaluate and establish the reliability of current concentrator module designs. Considerable research has been done to establish appropriate qualification tests, to understand component failure mechanisms, and to obtain reliable materials and designs. Surveys of fielded systems have been conducted and new test and analysis techniques have been developed in the process. This paper discusses the reliability of photovoltaic concentrator modules with an emphasis on the issues that are currently of most concern. DOE

N91-14652# Sandia National Labs., Albuquerque, NM.
THE SYNTHESIS OF SOLAR RADIATION DATA FOR SIZING STAND-ALONE PHOTOVOLTAIC SYSTEMS
Richard N. Chapman 1990 19 p Presented at the 21st IEEE Photovoltaic Specialists Conference, Kissimmee, FL, 21-25 May 1990
(Contract DE-AC04-76DP-00789)
(DE90-012758; SAND-90-1201C; CONF-900542-12) Avail: NTIS HC/MF A03

Research has shown that long-term hourly insolation data are necessary to properly size stand-alone photovoltaic systems. Even if these data are available, their direct use requires extensive computing capabilities and is not practical on a routine basis. This paper describes a three-step model that generates realistic long-term hourly insolations from average monthly insolations. The model executes rapidly on a personal computer and generates the hourly data needed to properly size stand-alone systems. The approach used to develop this model was unique in that system performance predictions rather than statistical properties were used to verify that the synthetic data were representative of actual data. Results of verification tests show that array sizes resulting from the synthetic data are within 6 percent of the array sizes resulting from actual hourly data for any system with at least two days of energy storage. DOE

N91-14653# Department of Defense, Washington, DC.
OFFICE OF BASIC ENERGY SCIENCES 1990 SUMMARY REPORT
Oct. 1990 56 p
(DE91-002971; DOE/ER-0475P) Avail: NTIS HC/MF A04

Basic research is an important investment in the future which will help the U.S. maintain and enhance its economic strength. The Office of Basic Energy Sciences' (BES) basic research activities, carried out mainly in universities and Department of Energy (DOE) laboratories, are critical to the Nation's leadership in science, for training future scientists, and to fortify the Nation's foundations for social and economic well-being. Attainment of the national goals -- energy self-sufficiency, improved health and quality of life for all, economic growth, national security -- depends on both technological research achievements and the ability to exploit them rapidly. Basic research is a necessary element for technology development and economic growth. This report presents the Department of Energy's Office of Basic Energy Sciences program. The BES mission is to develop understanding and to stimulate innovative thinking needed to fortify the Department's missions. DOE

N91-14654# Institute of Applied Energy, Tokyo (Japan).
PROSPECTS OF NEW ENERGY [PROSPECTS OF NEW ENERGY]
Mar. 1990 38 p In JAPANESE; In JAPANESE
(DE91-727567; ETDE/JP-mf-1727567) Avail: NTIS (US Sales Only) HC/MF A03

With the oil crisis, development of new energy became an important issue in Japan and abroad, but with the fall of the petroleum price, the time to put new energy to use is prolonged. On the other hand, with the rise of the worldwide issue of the Earth environment, it is now required that we give greatest consideration to the environment in using energy. Fuel cells are especially important from the viewpoint of effective utilization of energy and prevention of air pollution. A fuel cell, which generates power with the chemical reaction of natural gas and others, emits little material which causes air pollution, and it does not require cooling water. Development of fuel cells is being pushed forward energetically in Japan, the USA and Europe, but it is necessary to reduce the cost further to put them to practical use. Among the fuel cells which are being developed at present for commercial use, a phosphoric acid fuel cell is on the step just before commercialization, and the research and development of a molten carbonate fuel cell and a solid oxide fuel cell is under way. DOE

45 ENVIRONMENT POLLUTION

Includes atmospheric, noise, thermal, and water pollution.

N91-14655*# Maryland Univ., College Park. Dept. of Geography.
ANALYSIS OF THE BOREAL FOREST-TUNDRA ECOTONE: A TEST OF AVIRIS CAPABILITIES IN THE EASTERN CANADIAN SUBARCTIC Final Report, 1 Jun. 1987 - 31 Dec. 1989
Samuel N. Goward and Donald E. Petzold 31 Dec. 1989 69 p
(Grant NAGw-1142)
(NASA-CR-187335; NAS 1.26:187335) Avail: NTIS HC/MF A04 CSCL 13B

A comparison was conducted between ground reflectance spectra collected in Schefferville, Canada and imaging spectrometer observations acquired by the AVIRIS sensor in a flight of the ER-2 Aircraft over the same region. The high spectral contrasts present in the Canadian Subarctic appeared to provide an effective test of the operational readiness of the AVIRIS sensor. Previous studies show that in this location various land cover materials possess a wide variety of visible/near infrared reflectance properties. Thus, this landscape served as an excellent test for the sensing variabilities of the newly developed AVIRIS sensor. An underlying hypothesis was that the unique visible/near infrared spectral reflectance patterns of Subarctic lichens could be detected from high altitudes by this advanced imaging spectrometer. The relation between lichen occurrence and boreal forest-tundra ecotone dynamics was investigated. Author

N91-14656# Pacific Northwest Lab., Richland, WA.
ATMOSPHERIC SOURCE-RECEPTOR RELATIONSHIPS: CONCEPTS AND TERMINOLOGY
J. M. Hales and D. S. Renne Sep. 1990 43 p
(Contract DE-AC06-76RL-01830)
(DE91-001033; PNL-7470) Avail: NTIS HC/MF A04

This report reviews a number of conceptual bases for the interpretation of atmospheric source-receptor phenomena, including spatial attributes, nonlinearity, and temporal attributes. Source-receptor properties are commonly expressed and interpreted in terms of statistical parameters. Definitions of these parameters often vary from one user to the next, however, and the resulting potential for confusion suggests the need for a standard and accepted set of terms for applied use. Time-averaging is an important consideration in describing system linearity/nonlinearity as well as temporal and spatial variability. Unless expressed in terms of a conceptual model (such as a steady-state system) where a time-averaging is implied, explicit statement of the averaging time, or period of observation, is necessary for satisfactory definition of pertinent statistical features. This plus a number of additional contributing factors tend to complicate the description of source-receptor phenomena and underline the need for consistent terminology. This report provides a description of source-receptor linearity as well as several statistical measures of spatial and temporal variability in the source-receptor sequence. These are suggested for use as standard terminology in future source-receptor studies and in applied emission-control policy analyses. DOE

N91-14657*# Colorado Univ., Boulder. Dept. of Astrophysical, Planetary and Atmospheric Sciences.
STUDIES OF THE OBSERVED AND THEORETICAL VARIATIONS OF ATMOSPHERIC OZONE Final Report, 1 Jan. 1977 - 30 Jun. 1990
Julius London 30 Jun. 1990 8 p
(Grant NsG-5153)
(NASA-CR-187703; NAS 1.26:187703) Avail: NTIS HC/MF A02 CSCL 13B

The four related topics covered include: (1) distributions of total and upper atmospheric ozone and their time and space variations; (2) observed and theoretical models of the quasi-biennial oscillation (QBO) ozone variation; (3) radiative processes in the upper atmosphere; and (4) relations between ozone and solar variations. The results of these studies are presented. They come from twenty-three published papers. Author

N91-14658# Oak Ridge National Lab., TN.
ACIDIC DEPOSITION: ITS NATURE AND IMPACTS Foreign Trip Report
Robert B. Cook, Robert S. Turner, and Patrick F. Ryan (Science Applications International Corp., Oak Ridge, TN.) 18 Oct. 1990 13 p
(Contract DE-AC05-84OR-21400)
(DE91-001984; ORNL/FTR-3791) Avail: NTIS HC/MF A03

The travelers presented papers on various aspects of modeling performed as part of the U.S. National Acidic Precipitation Assessment Program (NAPAP) at the Fourth International Conference on Acidic Deposition: Its Nature and Impacts. The meeting was sponsored by the Royal Society of Edinburgh and was attended by over 800 scientists, primarily from Europe and North America. The conference focused on nine aspects of the nature and impacts of atmospheric pollutants, including ozone, chemistry of atmospheric pollutants, processes controlling the deposition of pollutants, effects of pollutants on soils, physiology of plant responses to pollutants, effects of pollutants in agricultural and natural or seminatural ecosystems, atmospheric pollutants and forests, effects of pollutants on the chemistry of freshwater streams and lakes, effects of pollutants on freshwater plants and animals, and effects of pollutants, indoors and outdoors, on materials and buildings. DOE

N91-14659# Lawrence Livermore National Lab., CA.
THE EFFECTS OF CLIMATE CHANGE ON THE NITROGEN CYCLE AND ACID DEPOSITION
J. E. Penner, J. J. Walton, and B. C. Graboske (California Univ., Berkeley.) Sep. 1990 5 p Presented at the 7th International Conference on Interactive Information and Processing Systems for Meteorology, Oceanography, and Hydrology, New Orleans, LA, 13-17 Jan. 1991
(Contract W-7405-eng-48)
(DE91-002785; UCRL-JC-106083; CONF-910108-1) Avail: NTIS HC/MF A01

Increases in greenhouse gases are expected to lead to a number of changes to the atmosphere which may impact regional and global chemical cycles. With the increasing awareness of climate change and the possibility of global chemical changes to the atmosphere, it becomes important to ask whether these changes to global climate and chemical cycles might benefit or hinder control programs aimed at reducing acid deposition. In the following, we review several possible changes to climate that may be expected to impact the global cycle of reactive nitrogen. We then use our global model of the reactive nitrogen cycle to estimate the effects of several of the more important changes on the continental-scale deposition of nitric acid. DOE

N91-14660# Oak Ridge National Lab., TN.
VALIDITY OF ENVIRONMENTAL TRANSFER MODELS
B. Gordon Blaylock, F. Owen Hoffman, and Robert H. Gardner Nov. 1990 12 p
(Contract DE-AC05-84OR-21400)
(DE91-002929; ORNL/FTR-3812) Avail: NTIS HC/MF A03

BIOspheric MOdel Validation Study (BIOMOVS) is an international cooperative study initiated in 1985 by the Swedish National Institute of Radiation Protection to test models designed to calculate the environmental transfer and bioaccumulation of radionuclides and other trace substances. The objective of the symposium and workshop was to synthesize results obtained during Phase 1 of BIOMOVS (the first five years of the study) and to suggest new directions that might be pursued during Phase 2 of BIOMOVS. The travelers were an instrumental part of the development of BIOMOVS. This symposium allowed the travelers to present a review of past efforts at model validation and a synthesis of current activities and to refine ideas concerning future development of models and data for assessing the fate, effect, and human risks of environmental contaminants. R. H. Gardner also visited the Free University, Amsterdam, and the National

Institute of Public Health and Environmental Protection (RIVM) in Bilthoven to confer with scientists about current research in theoretical ecology and the use of models for estimating the transport and effect of environmental contaminants and to learn about the European efforts to map critical loads of acid deposition. DOE

N91-14661# Sandia National Labs., Albuquerque, NM.
A BALLOON-BORNE AEROSOL SPECTROMETER FOR HIGH ALTITUDE LOW AEROSOL CONCENTRATION MEASUREMENTS
G. S. Brown and R. E. Weiss (Radiance Research, Seattle, WA.) Aug. 1990 118 p
(Contract DE-AC04-76DP-00789)
(DE91-002563; SAND-88-2466; TTC-0836) Avail: NTIS HC/MF A06

Funded by Air Force Wright Aeronautical Laboratory, a new balloon-borne high altitude aerosol spectrometer, for the measurement of cirrus cloud ice crystals, has been developed and successfully flown by Sandia National Laboratories and Radiance Research. This report (1) details the aerosol spectrometer design and construction, (2) discusses data transmission and decoding, (3) presents data collected on three Florida flights in tables and plots. DOE

N91-14662* National Aeronautics and Space Administration. John C. Stennis Space Center, Bay Saint Louis, MS.
COMBINED AIR AND WATER POLLUTION CONTROL SYSTEM Patent
Billy C. Wolverton, inventor (to NASA) and Lamont Jarrell, inventor (to NASA) 25 Sep. 1990 8 p Filed 26 May 1989
(NASA-Case-NST-00007-1; US-Patent-4,959,084;
US-Patent-Appl-SN-357938; US-Patent-Class-55-68;
US-Patent-Class-55-74; US-Patent-Class-55-84;
US-Patent-Class-55-89; US-Patent-Class-55-228;
US-Patent-Class-55-242; US-Patent-Class-210-615) Avail: US Patent and Trademark Office CSCL 13B

A bioaquatic air pollution control system for controlling both water and atmospheric pollution is disclosed. The pollution control system includes an exhaust for directing polluted gases out of a furnace and a fluid circulating system which circulates fluid, such as waste water, from a source, past the furnace where the fluid flow entrains the pollutants from the furnace. The combined fluid and pollutants are then directed through a rock/plant/microbial filtering system. A suction pump pumps the treated waste water from the filter system past the exhaust to again entrain more pollutants from the furnace where they are combined with the fluid (waste water) and directed to the filter system.
Official Gazette of the U.S. Patent and Trademark Office

N91-14663# Oak Ridge National Lab., TN. Environmental Sciences Div.
THE RESPONSE OF ATMOSPHERIC CO2 TO CHANGES IN LAND USE
A. W. King, W. R. Emanuel, and W. M. Post 1990 52 p Presented at the Chapman Conference on Global Biomass Burning: Atmospheric, Climatic, and Biospheric Implications, Williamsburg, VA, 19-23 Mar. 1990
(Contract DE-AC05-84OR-21400)
(DE91-001212; CONF-900355-1) Avail: NTIS HC/MF A04

The burning of biomass that often accompanies deforestation and other changes in land use is believed to be a major contributor to documented increases in the concentration of atmospheric CO2. Using three models of carbon turnover in the atmosphere and ocean, we simulate changes in atmospheric CO2 that result from the addition of CO2 from industrial sources and terrestrial ecosystems disturbed by changes in land use. We simulate atmospheric response to different histories of terrestrial biospheric CO2 release, and we compare these simulations with the history of atmospheric CO2 obtained from ice core measurements and atmospheric monitoring stations. DOE

N91-14664# Oak Ridge National Lab., TN.
ENVIRONMENTAL IMPACT ASSESSMENT AS APPLIED TO POLICIES, PLANS, AND PROGRAMS Foreign Trip Report
Lorene L. Sigal 19 Oct. 1990 11 p
(Contract DE-AC05-84OR-21400)
(DE91-001372; ORNL/FTR-3784) Avail: NTIS HC/MF A03

A proposal to study the application of the principles of environmental impact assessment (EIA) to policy, plans, and programs was submitted by the U.S. Environmental Protection Agency (EPA) to the Senior Advisors on Environmental and Water Problems of the United Nations Economic Commission. On approval, EPA asked Oak Ridge National Laboratory (ORNL) to support its efforts as lead participant on an international task force. ORNL is responsible for overall project management, including development of the report. At the first meeting in Geneva on June 18 to 19, there were representatives from Austria, Canada, Finland, Norway, Poland, Sweden, and the United Kingdom. The administrative/legal setting for EIA in each country was reviewed. The objectives of the task force were defined, and issues related to the application of EIA at the policy level were discussed. At the second meeting, in addition to those countries represented at the first meeting the Commission of Economic Communities, Czech and Slovak Federal Republic, Remark, Federal Republic of Germany, Hungary, and The Netherlands were represented. A brief review was given by the new participants of legal/administrative requirements for EIA in their countries. Case studies were presented by Canada, Finland, The Netherlands, Norway, Sweden, and the United States. DOE

46 GEOPHYSICS

Includes aeronomy; upper and lower atmosphere studies; ionospheric and magnetospheric physics; and geomagnetism.

For space radiation see *93 Space Radiation.*

N91-14665*# Stanford Univ., CA. Dept. of Geophysics.
[REPORTS ON BLOCK ROTATIONS, FAULT DOMAINS AND CRUSTAL DEFORMATION]
Amos Nur 28 Feb. 1990 89 p
(Grant NAG5-926)
(NASA-CR-186756; NAS 1.26:186756) Avail: NTIS HC/MF A05 CSCL 08G

Studies of block rotations, fault domains and crustal deformation in the western United States, Israel, and China are discussed. Topics include a three-dimensional model of crustal fracture by distributed fault sets, distributed deformation and block rotation in 3D, stress field rotation, and multiple strike slip fault sets. For individual titles, see N91-14666 through N91-14669.

N91-14666*# Stanford Univ., CA. Dept. of Geophysics.
BLOCK ROTATIONS, FAULT DOMAINS AND CRUSTAL DEFORMATION IN THE WESTERN US Final Report, 15 Sep. 1987 - 28 Feb. 1990
Amos Nur *In its* Reports on Block Rotations, Fault Domains and Crustal Deformation 28 Feb. 1990 6 p (For primary document see N91-14665 06-46)
(Grant NAG5-926)
Avail: NTIS HC/MF A05 CSCL 08G

The aim of the project was to develop a 3D model of crustal deformation by distributed fault sets and to test the model results in the field. In the first part of the project, Nur's 2D model (1986) was generalized to 3D. In Nur's model the frictional strength of rocks and faults of a domain provides a tight constraint on the amount of rotation that a fault set can undergo during block rotation. Domains of fault sets are commonly found in regions where the deformation is distributed across a region. The interaction of each fault set causes the fault bounded blocks to rotate. The work that has been done towards quantifying the rotation of fault sets in a 3D stress field is briefly summarized. In the second part of the project, field studies were carried out in Israel, Nevada and China. These studies combined both paleomagnetic and structural

information necessary to test the block rotation model results. In accordance with the model, field studies demonstrate that faults and attending fault bounded blocks slip and rotate away from the direction of maximum compression when deformation is distributed across fault sets. Slip and rotation of fault sets may continue as long as the earth's crustal strength is not exceeded. More optimally oriented faults must form, for subsequent deformation to occur. Eventually the block rotation mechanism may create a complex pattern of intersecting generations of faults. Author

N91-14667*# Stanford Univ., CA. Dept. of Geophysics.
DISTRIBUTED DEFORMATION AND BLOCK ROTATION IN 3D
Oona Scotti, Amos Nur, and Raul Estevez *In its* Reports on Block Rotations, Fault Domains and Crustal Deformation 28 Feb. 1990 38 p (For primary document see N91-14665 06-46)
Avail: NTIS HC/MF A05 CSCL 08G

The authors address how block rotation and complex distributed deformation in the Earth's shallow crust may be explained within a stationary regional stress field. Distributed deformation is characterized by domains of sub-parallel fault-bounded blocks. In response to the contemporaneous activity of neighboring domains some domains rotate, as suggested by both structural and paleomagnetic evidence. Rotations within domains are achieved through the contemporaneous slip and rotation of the faults and of the blocks they bound. Thus, in regions of distributed deformation, faults must remain active in spite of their poor orientation in the stress field. The authors developed a model that tracks the orientation of blocks and their bounding faults during rotation in a 3D stress field. In the model, the effective stress magnitudes of the principal stresses (sigma sub 1, sigma sub 2, and sigma sub 3) are controlled by the orientation of fault sets in each domain. Therefore, adjacent fault sets with differing orientations may be active and may display differing faulting styles, and a given set of faults may change its style of motion as it rotates within a stationary stress regime. The style of faulting predicted by the model depends on a dimensionless parameter phi = (sigma sub 2 - sigma sub 3)/(sigma sub 1 - sigma sub 3). Thus, the authors present a model for complex distributed deformation and complex offset history requiring neither geographical nor temporal changes in the stress regime. They apply the model to the Western Transverse Range domain of southern California. There, it is mechanically feasible for blocks and faults to have experienced up to 75 degrees of clockwise rotation in a phi = 0.1 strike-slip stress regime. The results of the model suggest that this domain may first have accommodated deformation along preexisting NNE-SSW faults, reactivated as normal faults. After rotation, these same faults became strike-slip in nature. Author

N91-14668*# Stanford Univ., CA.
STRESS FIELD ROTATION OR BLOCK ROTATION: AN EXAMPLE FROM THE LAKE MEAD FAULT SYSTEM Final Report, 8 Aug. 1989
Hagai Ron, Amos Nur, and Atilla Aydin (Purdue Univ., West Lafayette, IN.) *In its* Reports on Block Rotations, Dault Domains and Crustal Deformation 28 Feb. 1990 19 p (For primary document see N91-14665 06-46)
Avail: NTIS HC/MF A05 CSCL 08G

The Coulomb criterion, as applied by Anderson (1951), has been widely used as the basis for inferring paleostresses from in situ fault slip data, assuming that faults are optimally oriented relative to the tectonic stress direction. Consequently if stress direction is fixed during deformation so must be the faults. Freund (1974) has shown that faults, when arranged in sets, must generally rotate as they slip. Nur et al., (1986) showed how sufficiently large rotations require the development of new sets of faults which are more favorably oriented to the principal direction of stress. This leads to the appearance of multiple fault sets in which older faults are offset by younger ones, both having the same sense of slip. Consequently correct paleostress analysis must include the possible effect of fault and material rotation, in addition to stress field rotation. The combined effects of stress field rotation and material rotation were investigated in the Lake Meade Fault System (LMFS) especially in the Hoover Dam area. Fault inversion results imply an apparent 60 degrees clockwise (CW) rotation of the stress field since mid-Miocene time. In contrast structural data from the rest of the Great Basin suggest only a 30 degrees CW stress field rotation. By incorporating paleomagnetic and seismic evidence, the 30 degrees discrepancy can be neatly resolved. Based on paleomagnetic declination anomalies, it is inferred that slip on NW trending right lateral faults caused a local 30 degrees counter-clockwise (CCW) rotation of blocks and faults in the Lake Mead area. Consequently the inferred 60 degrees CW rotation of the stress field in the LMFS consists of an actual 30 degrees CW rotation of the stress field (as for the entire Great Basin) plus a local 30 degrees CCW material rotation of the LMFS fault blocks. Author

N91-14669*# Stanford Univ., CA. Dept. of Geophysics.
MULTIPLE STRIKE SLIP FAULTS SETS: A CASE STUDY FROM THE DEAD SEA TRANSFORM
Hagai Ron, Amos Nur, and Y. Eyal (Beersheva Univ., Israel) *In its* Reports on Block Rotations, Fault Domains and Crustal Deformation 28 Feb. 1990 25 p (For primary document see N91-14665 06-46)
Avail: NTIS HC/MF A05 CSCL 08G

In many strike slip tectonic settings, large rotations of crust blocks about vertical axes have been inferred from paleomagnetic data. These blocks are bounded by sets of parallel faults which presumably accommodate the relative motion between the blocks as regional deformation progress. A mechanical model by Nur et al., (1986) suggests that rotations greater than phi sub c equals 25 to 45 degrees must be accommodated by more than one set of faults, with angle phi sub c between their direction; consequently the sum of the angles between sets must be roughly equal to the total tectonic material rotation. To test this model, the authors investigated the fault geometry and field relation of fault sets in the Mt. Hermon area in northern Israel, where paleomagnetic declination implies data 69 degrees plus or minus 13 degrees counter-clockwise block rotation. The statistical and field relation analysis of over 315 faults shows that the faulting is predominantly right lateral strike slip consisting of three distinct sets. The oldest set strikes 253 degrees, the second oldest set strikes 293 degrees and the youngest strikes 339 degrees. This last direction is consistent also with the current north-south direction of the maximum principle stress axis. The angle phi sub c between the first and second sets is 39 degrees and between the second and third sets 46 degrees, in good agreement with the phi sub c angle predicted from mechanical considerations. The sum of the two angles is 85 degrees, in good agreement with the 69 degrees plus or minus 13 degrees CCW paleomagnetically derived rotation. The results suggest specifically that the sequential development of multiple intersecting fault sets is responsible for the faulting in the Mt. Hermon area; and generally that the model of block rotation with multiple faults provides very good simple rules for analyzing very complex fault patterns. Author

N91-14670# Consiglio Nazionale delle Ricerche, Frascati (Italy). Ist. di Fisica dello Spazio Interplanetario.
MEASUREMENT OF THE GRAVITOMAGNETIC FIELD USING A PAIR OF LASER RANGED SATELLITES Final Report
Ignazio Ciufolini 1989 128 p
Avail: NTIS HC/MF A07

A detailed study of the non-gravitational perturbation of the LAGEOS node, and the estimate of the corresponding modeling errors and of the consequent error in the measurement of the gravitomagnetic field (Lense-Thirring effect) using the pair of satellite LAGEOS-1 and LAGEOS-3 are presented. The main results from previous studies regarding the LAGEOS-gravitomagnetic experiment are summarized. The major sources of errors in the experiment are identified and a preliminary limit for the statistical error is established from basic physical and analytical considerations. A comprehensive computerized simulation was undertaken. The main non-gravitational perturbations are analyzed. The quantities to be measured are identified and the kind of

measurements needed to minimize the modeling errors associated with these non-gravitational perturbations are studied. The final results are presented. B.G.

N91-14671 Michigan Univ., Ann Arbor.
THEORY AND MEASUREMENTS OF NIGHTTIME HORIZONTAL GRADIENTS IN THE MID-LATITUDE F REGION Ph.D. Thesis
Daniel J. Melendez-Alvira 1990 345 p
Avail: Univ. Microfilms Order No. DA9023600

The theoretical servo model of Rishbeth, Ganguly, and Walker (1978) is extended to fit horizontal gradients in the nighttime F2-layer measured during solar maximum. The model fits are made by adjusting the model zonal current to match the measured peak height variations. The following results are obtained: (1) the model reproduces the observed overhead values; (2) the additional servo-height equation terms affect the computation by less than 10 percent on average; (3) the generally eastward model current reverses westward during layer descents; (4) the differences between model and Fabry-Perot meridional winds are related to large vertical shears in the wind; (5) the model and measured peak densities agree to within 20 to 40 percent on average; and (6) variable plasmaspheric fluxes on the order of 10(exp 13) (m(exp -2)s(exp -1) can be important to the maintenance and variability of the nighttime ionosphere. In addition, the model fit is improved by increasing the O(+) O(-) collision cross-section. Similarly, the gradients are fitted by adjusting the model current gradients to match the measured peak height gradients. The following results are obtained: (1) the model reproduces the observed horizontal gradients; (2) the model peak density gradients result from peak height gradients; (3) the current can be divergent; (4) the zonal current can have significant meridional shear; (5) the current appears to be either irrotational or to have constant vorticity; (6) the current gradients are due to both neutral and electric drifts; (7) very large wind accelerations would be required to account for the Fabry-Perot wind gradients; and (8) there appears to be significant electrodynamic changes during the descents of the F2-layer. Consideration is also given to the possible current closure involving conjugate ionospheres and between E and F regions. Furthermore, model equations are developed to calculate the vorticity and divergence of the wind. Dissert. Abstr.

N91-14672*# Massachusetts Inst. of Tech., Cambridge. Dept. of Earth, Atmospheric, and Planetary Sciences.
PLATE MOTIONS AND DEFORMATIONS FROM GEOLOGIC AND GEODETIC DATA Semiannual Report, 1 Jan. - 30 Jun. 1990
Thomas H. Jordan Jun. 1990 33 p
(Grant NAG5-459)
(NASA-CR-187379; NAS 1.26:187379) Avail: NTIS HC/MF A03 CSCL 08G

An analysis of geodetic data in the vicinity of the Crustal Dynamics Program (CDP) site at Vandenberg Air Force Base (VNDN) is presented. The utility of space-geodetic data in the monitoring of transient strains associated with earthquakes in tectonically active areas like California is investigated. Particular interest is in the possibility that space-geodetic methods may be able to provide critical new data on deformations precursory to large seismic events. Although earthquake precursory phenomena are not well understood, the monitoring of small strains in the vicinity of active faults is a promising technique for studying the mechanisms that nucleate large earthquakes and, ultimately, for earthquake prediction. Space-geodetic techniques are now capable of measuring baselines of tens to hundreds of kilometers with a precision of a few parts in 108. Within the next few years, it will be possible to record and analyze large-scale strain variations with this precision continuously in real time. Thus, space-geodetic techniques may become tools for earthquake prediction. In anticipation of this capability, several questions related to the temporal and spatial scales associated with subseismic deformation transients are examined. Author

N91-14673*# Massachusetts Inst. of Tech., Cambridge. Dept. of Earth, Atmospheric, and Planetary Sciences.
CRUSTAL DYNAMICS PROJECT: THE INTERPRETATION OF CRUSTAL DYNAMICS DATA IN TERMS OF PLATE MOTIONS AND REGIONAL DEFORMATION NEAR PLATE BOUNDARIES Semiannual Status Report No. 8, 22 Mar. - 21 Sep. 1990
Sean C. Solomon 19 Dec. 1990 42 p
(Grant NAG5-814)
(NASA-CR-187691; NAS 1.26:187691) Avail: NTIS HC/MF A03 CSCL 08G

The focus of the research was in two broad areas: (1) the nature and dynamics of time-dependent deformation and stress along major seismic zones, and (2) the nature of long-wavelength oceanic geoid anomalies in terms of lateral variations in upper mantle temperature and composition. The principal findings are described in the appendices. Author

N91-14674# Colorado School of Mines, Golden. Center for Wave Phenomena.
STABLE EXPLICIT DEPTH EXTRAPOLATION OF SEISMIC WAVEFIELDS
Dave Hale 1990 24 p
(Contract DE-FG02-89ER-14079)
(DE91-001445; DOE/ER-14079/2; CWP-095) Avail: NTIS HC/MF A03

Stable explicit filters for depth extrapolation of seismic wavefields may be derived through a modification of the conventional Taylor series method. The modified Taylor series method described here yields extrapolators with maximally-flat amplitude spectra in their passband, while ensuring that no spectral components in the wavefield are amplified by any factor greater than one. The price for stability is increased phase error. For low normalized frequencies, implicit extrapolators are more accurate than the 39-coefficient stable explicit extrapolator described here. However, the small spatial sampling intervals required to obtain high phase accuracy in implicit extrapolation imply that this accuracy is rarely achieved in practice. Over the wide range of normalized frequencies likely to be encountered in practice, stable explicit extrapolators outperform implicit ones. The method presented here for deriving stable explicit extrapolators is in no formal sense optimal. It is only guaranteed to yield stable extrapolators. In my limited experience with alternative methods for designing stable extrapolators, the method presented here produced the least phase error while ensuring stability. Nevertheless, a simple method for designing optimal (in some sense) stable explicit extrapolators would be preferred over the method presented here. DOE

N91-14675# Colorado School of Mines, Golden. Center for Wave Phenomena.
THE 3-D DEPTH MIGRATION VIA MCCLELLAN TRANSFORMATIONS
Dave Hale 1990 18 p
(Contract DE-FG02-89ER-14079)
(DE91-001446; DOE/ER-14079/3; CWP-096) Avail: NTIS HC/MF A03

Three-dimensional seismic wavefields may be extrapolated in depth, one frequency at a time, by two-dimensional convolution with a circularly symmetric, frequency- and velocity-dependent filter. This depth extrapolation, performed for each frequency independently, lies at the heart of 3-D finite-difference depth migration. The computational efficiency of 3-D depth migration depends directly on the efficiency of this depth extrapolation. McClellan transformations provide an efficient method for both designing and implementing two-dimensional digital filters that have a particular form of symmetry, such as the circularly symmetric depth extrapolation filters used in 3-D depth migration. Given the coefficients of one-dimensional, frequency- and velocity-dependent filters used to accomplish 2-D depth migration, McClellan transformations lead to a simple and efficient algorithm for 3-D depth migration. DOE

N91-14676# Geological Survey, Menlo Park, CA.
FEASIBILITY STUDY OF THE SEISMIC REFLECTION METHOD IN AMARGOSA DESERT, NYE COUNTY, NEVADA
Thomas M. Brocher, Patrick E. Hart, and Steven F. Carle 1990 150 p
(Contract DE-AI08-78ET-44802)
(DE91-001646; USGS-OFR-89-133) Avail: NTIS HC/MF A07

The U.S. Geological Survey (USGS) working under an Interagency agreement with the Department of Energy is engaged in a broad geoscience program to assess and identify potential repositories for high level nuclear waste at Yucca Mountain, Nye County, Nevada. The USGS program, referred to as the Yucca Mountain Projects, or YMP, consists of integrated geologic, hydrologic and geophysical studies which range in nature from site specific to regional. This report is an evaluation of different acquisition methods for future regional seismic reflection studies to be conducted in the vicinity of Yucca Mountain, located in the southwestern corner of the Nevada Test Site (NTS). In January 1988, field studies were conducted to investigate the feasibility of using the common-depth point (CDP) seismic reflection method to map subsurface geological horizons within the Amargosa Desert, Nye County, Nevada. The goal of the field study was to investigate which seismic reflection method(s) should be used for mapping shallow to lower-crustal horizons. Therefore, a wide-variety of field acquisition parameters were tested, included point versus linear receiver group arrays; Vibroseis (service and trademark of Conoco, Inc.) versus explosive sources; Vibroseis array patterns; and Vibroseis sweep and frequency range. DOE

N91-14677# SRI International Corp., Menlo Park, CA.
JOULE HEATING INVESTIGATIONS USING THE SONDRESTROM RADAR AND DMSP SATELLITES Final Report, 10 Dec. 1989 - 9 May 1990
Juergen Watermann and Odile delaBeaujardiere Jun. 1990 52 p
(Contract F19628-87-K-0006)
(AD-A227425; GL-TR-90-0172) Avail: NTIS HC/MF A04
CSCL 04/1

The objective was to cross validate Joule heating rates derived from Defense Meteorological Satellite Program (DMSP) F7 observations through comparison with incoherent scatter radar measurements from Sondre Stromfjord, Greenland. In spite of obvious difficulties encountered within localized and dynamic structures such as discrete auroral arcs, where electric field and Pederson current estimates did not match, good agreement was found within relatively stable structures like the poleward edge of the diffuse aurora. Unrelated to spatial and temporal ambiguity problems, a systematic discrepancy in a summer daytime Pedersen conductance calculations from spacecraft and radar data was found. Although the conditions for comparison were generally not optimal because the temporal and spatial coincidences between spacecraft and radar measurements were not perfect, 50 percent of the cases examined were in good agreement. Possible error source for the remaining cases of disagreement are identified and explanations for the disagreement are offered. The necessity of further efforts to cross validate measurements of ionospheric parameters is emphasized and ways for improvements of the comparison method are suggested. GRA

N91-14678# Brookhaven National Lab., Upton, NY. Global Studies Program.
OVERVIEW OF THE US DEPARTMENT OF ENERGY'S ARM (ATMOSPHERIC RADIATION MEASUREMENT) PROGRAM
Gerald M. Stokes (Pacific Northwest Lab., Richland, WA.) and Joyce L. Tichler Jun. 1990 8 p Presented at the 12th International CODATA Conference: Data for Discovery, Columbus, OH, 17-19 Jul. 1990
(Contract DE-AC02-76CH-00016)
(DE91-001126; BNL-44375; CONF-900762-1) Avail: NTIS HC/MF A02

The Department of Energy (DOE) is initiating a major atmospheric research effort, the Atmospheric Radiation Measurement Program (ARM). The program is a key component of DOE's research strategy to address global climate change and is a direct continuation of DOE's decade-long effort to improve the ability of General Circulation Models (GCMs) to provide reliable simulations of regional, and long-term climate change in response to increasing greenhouse gases. The effort is multi-disciplinary and multi-agency, involving universities, private research organizations and more than a dozen government laboratories. The objective of the ARM Research is to provide an experimental testbed for the study of important atmospheric effects, particularly cloud and radiative processes, and to test parameterizations of these processes for use in atmospheric models. This effort will support the continued and rapid improvement of GCM predictive capability. DOE

N91-14679*# National Aeronautics and Space Administration. Goddard Space Flight Center, Greenbelt, MD.
CRUSTAL DYNAMICS PROJECT DATA ANALYSIS, 1990
D. S. Caprette (ST Systems Corp., Lanham, MD.), C. Ma, and J. W. Ryan Washington Dec. 1990 384 p
(NASA-TM-100765; Rept-91E00714; NAS 1.15:100765) Avail: NTIS HC/MF A17; also available as magnetic tape and as floppy disk from the Crustal Dynamic Project Data Information System, NASA, Goddard Space Flight Center, Greenbelt, MD
CSCL 08G

The Goddard Very Long Baseline Interferometry (VLBI) group reports the results of analyzing 1073 Mark 3 data sets acquired from fixed and mobile observing sites through the end of 1989 and available to the Crustal Dynamics Project. Two large solutions, GLB656 and GLB657, were used to establish a VLBI reference frame with an origin coincident with the ITRF89. Another large solution, GLB658, was used to obtain Earth rotation parameters, nutation offsets, and global source positions. Site velocities were obtained from another large solution, GLB659. A fifth large solution, GLB660, was used to obtain baseline evolution. Site positions are tabulated on a yearly basis from 1979 through 1992. Site velocities are presented in both Cartesian and topocentric coordinates. The results include 76 sources, 80 sites, and 422 baselines. Author

N91-15058# Abastumani Astrophysical Observatory, Georgia (USSR).
BURSTS OF ENERGETIC PROTONS IN THE EARTH'S MAGNETOTAIL
A. L. Taktakishvili and L. M. Zelenyi (Academy of Sciences, USSR, Moscow) *In* ESA, Plasma Astrophysics Aug. 1990 p 51-55 (For primary document see N91-15046 06-90)
Copyright Avail: NTIS HC/MF A14

N91-15059# Ruhr Univ., Bochum (Germany, F.R.). Theoretische Physik IV.
THREE-DIMENSIONAL MAGNETIC RECONNECTION AT THE EARTH'S MAGNETOPAUSE
A. Otto *In* ESA, Plasma Astrophysics Aug. 1990 p 57-62 Sponsored by DFG (For primary document see N91-15046 06-90)
Copyright Avail: NTIS HC/MF A14

N91-15061# Johns Hopkins Univ., Laurel, MD. Applied Physics Lab.
IMPLICATIONS OF MULTIPOINT OBSERVATIONS OF SUBSTORMS IN THE INNER MAGNETOTAIL
R. E. Lopez *In* ESA, Plasma Astrophysics Aug. 1990 p 69-75 (For primary document see N91-15046 06-90)
Copyright Avail: NTIS HC/MF A14

N91-15107# Abastumani Astrophysical Observatory, Georgia (USSR).
INVESTIGATION OF THE NIGHT SKY AIRGLOW NEAR THE EPICENTER OF THE EARTHQUAKE
G. G. Didebulidze, L. M. Fishkova, A. D. Pataraya, and T. I. Toroshelidze *In* ESA, Plasma Astrophysics Aug. 1990 p 321-327 (For primary document see N91-15046 06-90)
Copyright Avail: NTIS HC/MF A14

N91-15109# Academy of Sciences (USSR), Irkutsk. Inst. of Terrestrial Magnetism and Radio Wave Propagation.
INTERRELATIONSHIP BETWEEN THE TEARING-INSTABILITY AND MAGNETIC ISLAND MERGING
A. T. Altyntsev and N. V. Lebedev *In* ESA, Plasma Astrophysics Aug. 1990 p 335-338 (For primary document see N91-15046 06-90)
Copyright Avail: NTIS HC/MF A14

47 METEOROLOGY AND CLIMATOLOGY

Includes weather forecasting and modification.

N91-14680*# New Mexico Inst. of Mining and Technology, Socorro.
AIRCRAFT MEASUREMENTS OF ELECTRIFIED CLOUDS AT KENNEDY SPACE CENTER Final Report, 1 Sep. 1988 - 31 Aug. 1990
J. J. Jones, W. P. Winn, S. J. Hunyady, C. B. Moore, and J. W. Bullock (AIRO, Inc., Colorado Springs, CO.) 27 Apr. 1990 133 p
(Grant NAG8-751)
(NASA-CR-186536; NAS 1.26:186536) Avail: NTIS HC/MF A07 CSCL 04B

The space-vehicle launch commit criteria for weather and atmospheric electrical conditions in us at Cape Canaveral Air Force Station and Kennedy Space Center (KSC) have been made restrictive because of the past difficulties that have arisen when space vehicles have triggered lightning discharge after their launch during cloudy weather. With the present ground-base instrumentation and our limited knowledge of cloud electrification process over this region of Florida, it has not been possible to provide a quantitative index of safe launching conditions. During the fall of 1988, a Schweizer 845 airplane equipped to measure electric field and other meteorological parameters flew over KSC in a program to study clouds defined in the existing launch restriction criteria. All aspects of this program are addressed including planning, method, and results. A case study on the November 4, 1988 flight is also presented. For individual titles, see N91-14681 through N91-14682.

N91-14681*# New Mexico Inst. of Mining and Technology, Socorro.
AIRCRAFT MEASUREMENTS OF ELECTRIFIED CLOUDS AT KENNEDY SPACE CENTER. PART 1: 1988 FLIGHTS
J. J. Jones, W. P. Winn, S. J. Hunyady, C. B. Moore, and J. W. Bullock (AIRO, Inc., Colorado Springs, CO.) *In its* Aircraft Measurements of Electrified Clouds at Kennedy Space Center 27 Apr. 1990 109 p (For primary document see N91-14680 06-47)
Avail: NTIS HC/MF A07 CSCL 04B

During the fall of 1988, a Schweizer 845 airplane equipped to measure electric field and other meteorological parameters flew over Kennedy Space Center in a program to study clouds defined in the existing launch retriction requirements. The special purpose test vehicle for atmospheric research (SPTVAR) was suitable for flights through thunderclouds and was instrumented to measure all three components of the ambient electric vector. The main goals of the project were: (1) to develop and demonstrate techniques for measuring the electric field aloft and locate regions of charge during flight; (2) to characterize the electrical conditions within and near clouds that are presently identified as a threat to space launch vehicles; and (3) to study the correlation between the electric field aloft and that at Kennedy Space Center's ground-based field mill network for a variety of electrified clouds.
K.S.

N91-14682*# New Mexico Inst. of Mining and Technology, Socorro.
AIRCRAFT MEASUREMENTS OF ELECTRIFIED CLOUDS AT KENNEDY SPACE CENTER. PART 2: CASE STUDY: 4 NOVEMBER 1988 (88309)
J. J. Jones, W. P. Winn, S. J. Hunyady, C. B. Moore, and J. W. Bullock (AIRO, Inc., Colorado Springs, CO.) *In its* Aircraft Measurements of Electrified Clouds at Kennedy Space Center 27 Apr. 1990 17 p (For primary document see N91-14680 06-47)
Avail: NTIS HC/MF A07 CSCL 04B

During the fall of 1988, a Schweizer airplane equipped to measure electric field and other meteorological parameters flew over Kennedy Space Center (KSC) in a program to study clouds defined in the existing launch restriction criteria. A case study is presented of a single flight over KSC on November 4, 1988. This flight was chosen for two reasons: (1) the clouds were weakly electrified, and no lightning was reported during the flight; and (2) electric field mills in the surface array at KSC indicated field strengths greater than 3 kV/m, yet the aircraft flying directly over them at an altitude of 3.4 km above sea level measured field strengths of less than 1.6 kV/m. A weather summary, sounding description, record of cloud types, and an account of electric field measurements are included.
K.S.

N91-14683*# National Aeronautics and Space Administration. Langley Research Center, Hampton, VA.
LIMB-DARKENING FUNCTIONS AS DERIVED FROM ALONG-TRACK OPERATION OF THE ERBE SCANNING RADIOMETERS FOR AUGUST 1985
G. Louis Smith, Natividad D. Manalo (Lockheed Engineering and Sciences Co., Hampton, VA.), and Lee M. Avis Washington Dec. 1990 41 p
(NASA-RP-1243; L-16779; NAS 1.61:1243) Avail: NTIS HC/MF A03 CSCL 04B

During August 1985, the scanning radiometers of the Earth Radiation Budget Experiment aboard the Earth Radiation Budget Satellite (ERBS) and the NOAA-9 satellite were operated in along-track scanning modes. These data were analyzed to produce limb darkening functions for Earth-emitted radiation, which relates the radiance in any given direction to the radiant exitence. Limb darkening functions are presented and shown as figures for day and night for each spacecraft. The scene types were computed using measurements within 10 deg of zenith. The models have values near zenith of 1.02 to 1.09, with values near 1.06 being typical. The typical value of the model is 1.06 for both day and night for ERBS, and for NOAA-9, the typical value at zenith is 1.06 for day and 1.05 for night. Mean models are formed for the ERBS and for the NOAA-9 results and are found to differ less than 1 percent, the ERBS results being the higher. The models vary about 1 percent with latitude near zenith.
Author

N91-14684*# Columbia Univ., New York, NY.
[CLIMATE AND ATMOSPHERIC MODELING STUDIES. CLIMATE APPLICATIONS OF EARTH AND PLANETARY OBSERVATIONS. CHEMISTRY OF EARTH AND ENVIRONMENT] Semiannual Progress Report, Apr. - Sep. 1990
Sep. 1990 75 p
(Contract NCC5-29)
(NASA-CR-187326; NAS 1.26:187326) Avail: NTIS HC/MF A04 CSCL 04B

The research conducted during the past year in the climate and atmospheric modeling programs concentrated on the development of appropriate atmospheric and upper ocean models, and preliminary applications of these models. Principal models are a one-dimensional radiative-convective model, a three-dimensional global climate model, and an upper ocean model. Principal applications have been the study of the impact of CO2, aerosols and the solar 'constant' on climate. Progress was made in the 3-D model development towards physically realistic treatment of these processes. In particular, a map of soil classifications on 1 degree x 1 degree resolution has been digitized, and soil properties have been assigned to each soil type. Using this information about soil properties, a method was developed to simulate the hydraulic behavior of soils of the world. This improved treatment of soil hydrology, together with the seasonally varying vegetation cover, will provide a more realistic study of the role of

the terrestrial biota in climate change. A new version of the climate model was created which follows the isotopes of water and sources of water (or colored water) throughout the planet. Each isotope or colored water source is a fraction of the climate model's water. It participates in condensation and surface evaporation at different fractionation rates and is transported by the dynamics. A major benefit of this project has been to improve the programming techniques and physical simulation of the water vapor budget of the climate model. Author

N91-14685 Illinois Univ., Urbana-Champaign.
MODELING STUDY OF TROPICAL NONSQUALL AND SQUALL CLUSTERS Ph.D. Thesis
Hung-Neng Steve Chin 1990 229 p
Avail: Univ. Microfilms Order No. DA9026157

A numerical cloud model in both two dimensional and three dimensional form is used to investigate the dynamical differences between non-squall and squall line convection in the tropics. Two dimensional simulations with cold-pool dynamics indicate that the simulated convective system propagates as a slow-moving multicellular squall line, in contrast to the nearly stationary observed non-squall convective line. Environmental winds are not included in the two dimensional simulations. To assess their effect on the behavior and general structure of non-squall convection, three-dimensional simulations are performed. In addition, oceanic squall lines are also studied. The results indicate that the dynamic structure of tropical mesoscale convective systems is strongly controlled by the environmental wind and moisture structure. Model simulations also show that the dominant easterly shear and weak convectively unstable environment favor the occurrence of non-squall line convection. Both the bell-shaped large-scale ascent and the environmental winds together play a crucial role in aligning the initially random distributed convective cells. Author

N91-14686# National Academy of Sciences - National Research Council, Washington, DC. Panel on Snow Avalanches.
SNOW AVALANCHE HAZARDS AND MITIGATION IN THE UNITED STATES
1990 94 p
(Contracts DI-J-5130-137; EMW-85-K-2202; GS-14-08-0001-G1101; NSF NAS-82-05616; DTFH61-85-P-00311) (LC-90-62814; ISBN-0-309-04335-2) Avail: NTIS HC/MF A05

Avalanche-prone areas can be delineated with some accuracy, although exceptional weather conditions can produce avalanches that overrun normal path boundaries or create new paths. Snow avalanches can build and be triggered many times in a given winter season. Avalanche activity occurs in about one-third of the states and is a significant hazard in much of the West. Avalanche hazard can have a negative impact on the economy and affects the management of Federal lands. Hazard mitigation requires appropriate land use management, effective building codes, timely issuance of emergency warnings, programs of public education, secure funding, improved standards and operational procedures for the safe release of built up snow cover, and a coordinated national leadership on avalanche issues. The panel recommends: (1) the formation of a short-lived interagency committee to initiate interagency program coordination; (2) the formation of a committee with representatives from government, academia, industry, and professional organizations to coordinate avalanche management and research nationwide; and (3) the study and use of ideas from programs already in operation in other countries. J.P.S.

N91-14687# Sandia National Labs., Albuquerque, NM.
A BALLOON-BORNE INTEGRATING NEPHELOMETER
G. S. Brown, M. L. Apple, and R. E. Weiss (Radiance Research, Seattle, WA.) Sep. 1990 61 p
(Contract DE-AC04-76DP-00789)
(DE91-001037; SAND-90-0404; TTC-0959) Avail: NTIS HC/MF A04

A balloon-borne integrating nephelometer has been successfully developed and flown by Sandia National Laboratories and Radiance Research. This report details instrument design, calibration and data conversion procedure. Free and tethered balloon transport and telemetry systems are described. Data taken during March 1989 South-Central New Mexico free flight ascents are presented as vertical profiles of atmospheric particle scattering coefficient, temperature and balloon heading. Data taken during December 1989 Albuquerque, New Mexico tethered flights are also presented as vertical profiles. Data analysis shows superior instrument performance. DOE

N91-14688# Oak Ridge National Lab., TN.
MODIFIED SEASONAL FACTORS IN EXPONENTIAL SMOOTHING
J. Scott Armstrong, Ho-Ling Hwang, and Jeff Bandy (Tennessee Univ., Knoxville.) Sep. 1990 46 p
(Contract DE-AC05-84OR-21400)
(DE91-002802; ORNL/M-1262) Avail: NTIS HC/MF A03

Current practice uses statistical tests to determine whether seasonal factors should be applied in a given forecasting situation. Research suggests that an optimal policy might lie somewhere between using full seasonal factors and using no seasonal factors on series. This research proposes and tests use of a modified seasonality factor. Modified seasonal factors reduce the emphasis on the seasonal adjustments when forecasts are made. The adjustments account for errors in the estimation of the factors and for possible changes in the factors over the forecast horizon. An analysis of data from U.S. Navy personnel inventories was conducted to test the use of a modified seasonality factor. Modified seasonal factors led to improved accuracy for predictions of inventories by paygrade using quarterly data from the Navy Personnel Research and Development Center (NPRDC). Under certain selections of factors, the mean absolute percent error (MAPE) was reduced by 4.4 percent. No gain was obtained, however, for the inventories by length of service. It is expected, but not shown here, that the modified seasonal factors will only be of value for series where the estimated seasonal factors show a substantial variation across the year. DOE

N91-14689# Wisconsin Univ., Madison. Space Science and Engineering Center.
CLOUD COVER STATISTICS Final Report, 15 Mar. 1989 - 14 Mar. 1990
Donald P. Wylie May 1990 35 p
(Contract F19628-89-K-0031; AF Proj. 6670)
(AD-A226892; GL-TR-90-0146) Avail: NTIS HC/MF A03
CSCL 04/2

Cloud height data has been collected for 4 years over the CONUS and one year globally using the multi-spectral infrared sensors GOES/VAS and NOAA/HIRS. The analysis technique distinguished partially transmissive cirrus from other cloud forms. Cirrus were commonly found from 13 to 40 percent of the time over the CONUS. Seasonal and diurnal variations were small over the CONUS. More significant seasonal variations were found over the oceans from the movement of the subtropical high pressure systems and cyclonic storms and fronts in high latitudes. One half of the cirrus was associated with radar echoes in the summer while the other half was not. In winter only 22 percent of the cirrus were associated with radar echoes because of the lack of echo activity. Cirrus were slightly more numerous in winter than in summer. One half of the cirrus detected over the CONUS in January also were associated with jet streams. In summer this reduced to 10 to 30 percent because of weaker upper air winds. GRA

N91-14690# Manchester Univ. (England). Dept. of Physics.
POLARIZATION RADAR STUDIES OF PRECIPITATION: IMPLEMENTATION OF THE TECHNIQUE AND DATA INTERPRETATION Final Scientific Report, 15 Feb. 1988 - 14 Feb. 1990
Anthony J. Illingworth 25 Jul. 1990 113 p
(Grant AF-AFOSR-0121-88; AF Proj. 2310)
(AD-A227073; AFOSR-90-0941TR) Avail: NTIS HC/MF A06
CSCL 09/2

Polarization radar observations provide information on characteristics of precipitation particles not available with conventional weather radar. Observations are reported for four

parameters made with the 25 m Chilbolton dish the largest steerable meteorological radar in the world. These are the first S-band measurements of the linear depolarization ratio and the most accurate co- copolar correlations yet reported. Ten publications describe the work in more detail. It is demonstrated how the new parameters can be used to: differentiate ice from water, differentiate the different forms of ice (snow, hail pellets), locate areas where large hail is forming, and identify clouds posing a threat of triggered lightning before natural lightning or breakdown has occurred. GRA

N91-14691# Naval Academy, Annapolis, MD. Dept. of Oceanography.
EXPLOSIVE CYCLOGENESIS: A CASE STUDY OF THE VETERANS' DAY STORM OF 11-12 NOVEMBER 1987 Final Report, 1989 - 1990
Russell S. McCormack 22 May 1990 80 p
(AD-A227077; USNA-TSPR-169) Avail: NTIS HC/MF A05 CSCL 04/2

An important breeding ground for explosive cyclone development is off the east coast of the United States, near Cape Hatteras. An important factor in cyclone development is the enormous energy requirement needed for explosive deepening of these systems. The presence of the warm Gulf Stream current in the western Atlantic provides a significant portion of this energy. This energy source, coupled with strong upper and lower level forcing, provides the mechanisms responsible for rapid intensification of these significant weather producing storms. A case of explosive cyclogenesis is examined. It was discovered that the intensification phase of this storm, called the Veteran's Day Storm of November 1987, was related to the strong sea surface temperature (SST) gradient present off the east coast of the United States. The SST gradient was analyzed using Advanced Very High Resolution Radiometer (AVHRR) data. The upper and lower level forcing mechanisms were studied using conventional weather products from the National Meteorological Center and special analyses made available from the NASA Goddard Laboratory for Atmospheric Sciences in Greenbelt, MD. The presence of strong positive vorticity advection, significant upper level divergence, and an atmospheric lid were among the major contributors responsible for intensification of this storm. GRA

N91-14692# Air Force Geophysics Lab., Hanscom AFB, MA.
MESOSCALE FEATURES OF A WINTER STORM: DUAL DOPPLER VELOCITY FIELDS AND DIFFERENTIAL REFLECTIVITY Final Report
James I. Metcalf and Frank H. Ruggiero 10 Apr. 1990 40 p
(AD-A227342; GL-TR-90-0091; ERP-1061) Avail: NTIS HC/MF A03 CSCL 04/2

Doppler radars were used to observe a winter coastal storm on 12 February 1988. Measurements of the polarization differential reflectivity by radar yielded information about the changing thermodynamic phase of precipitation as the change from snow to rain progressed northward from the southern New England coast in a strongly stable environment. Doppler velocity measurements by the two radars were used to synthesize the two-dimensional wind fields. These wind fields revealed an upper-level mesoscale trough and ridge moving across the surveillance area during a two-hour period, closely preceding the large-scale clearing of the precipitation, well ahead of the surface low-pressure center. This case represents the first use of these radars for dual-Doppler wind field analysis. GRA

48 OCEANOGRAPHY

Includes biological, dynamic, and physical oceanography; and marine resources.

For related information see also *43 Earth Resources and Remote Sensing.*

N91-14693# Naval Oceanographic and Atmospheric Research Lab., Bay Saint Louis, MS. Remote Sensing Branch.
OCEANOGRAPHIC EXPERT SYSTEM VALIDATION USING GOAP MESOSCALE PRODUCTS AND GULF/DART VALIDATION TEST DATA Final Report
Matthew Lybanon Jun. 1990 36 p Sponsored by Space and Naval Warfare Systems Command, Washington, DC
(AD-A226929; NOARL-5) Avail: NTIS HC/MF A03 CSCL 12/5

A prototype oceanographic expert system is being developed by the Remote Sensing Branch of the Naval Oceanographic and Atmospheric Research Laboratory (NOARL). System performance for eddy motion was tested using GEOSAT Ocean Applications Program (GOAP) mesoscale products. A second data set was used to validate the Harvard Gulfcast and the NOARL DART (Data Assimilation Research and Transition program) models. Several types of performance measures were calculated for both warm- and cold-core Gulf Stream eddies. Statistics compiled from the analysis results are presented in both tabular and graphical form. The analysis shows that the expert system performs reasonably well with respect to both eddy motion and eddy size. The expert system's projections are superior to an assumption of no motion out to 14 days. Results with the second (better) data set indicate performance superior to no motion in about two-thirds of the cases. The GOAP results, which used longer than 2 weeks. The expert system tracks ring sizes to within 10 percent for periods up to 7 to 11 weeks. Discussion of the results identifies factors that interfere with the validation and strongly indicates factors that interfere with the validation and strongly indicates the need for more data to continue and refine the analysis. A first-order correction to the rule base is proposed, based on the results of this study. That correction should significantly improve the expert system's average eddy motion performance. Changes based upon a more detailed evaluation may also be feasible and could lead to greater improvements. GRA

N91-14694# Massachusetts Inst. of Tech., Cambridge.
SHIPBOARD AND SATELLITE OBSERVATIONS OF UPPER OCEAN VELOCITY AND TRANSPORT VARIABILITY IN THE GULF STREAM M.S. Thesis
David Michael Schubert, Jr. Sep. 1990 105 p Prepared in cooperation with Woods Hole Oceanographic Inst., MA
(Contract N00123-89-G-0580)
(AD-A226974) Avail: NTIS HC/MF A06 CSCL 08/3

Acoustic Doppler velocities are combined with velocity profiles generated from XBT measurements to produce estimates of the flow field between Bermuda and Eastern United States. Repeated shipboard measurements along an ascending GEOSAT subtrack between Bermuda and Cape cod allow study of rapid Gulf Stream variability along the track, and comparison of sea surface and velocity measurements with those computer on the R/V Oceanus in April and December 1989. Using mass conservation constraints and inverse techniques, the transport across the Cape Cod-Bermuda track has been balanced with transport across additional ship tracks between Bermuda and Cape Hatteras, and between Bermuda and Nova Scotia. The shipboard results show evidence of a rapid barotropic mode which caused changes in transport along the Cape Cod-Bermuda track on the order of 8 Sverdrups in a week period. Comparisons of sea surface velocity and dynamic height determined from the ship's data with measurements made from the GEOSAT altimeter showed a consistent picture of the Gulf Stream location and were also consistent in showing smaller scale variations in flow. The dynamic height difference across the Gulf Stream was approximately 10 percent higher for the GEOSTAT measurements than for the

shipboard measurements, which is within the expected errors of the analysis techniques. GRA

N91-14695# Massachusetts Inst. of Tech., Cambridge.
OBSERVATIONS OF OCEAN FLUCTUATIONS BETWEEN 15 AND 23 HOUR PERIODS IN THE PACIFIC
Wayne Richard Blanding Sep. 1990 45 p Prepared in cooperation with Woods Hole Oceanographic Inst., MA
(Contract N00123-89-G-0580)
(AD-A227017) Avail: NTIS HC/MF A03 CSCL 20/1

Pulse-like acoustic signals were transmitted from an acoustic source near Oahu to seven receivers off the west coast of the United States for a 124-day period in 1988. Acoustic travel-time oscillations were observed in the received signal at periods between 15 and 23 hours, which were caused by barotropic (or first or second mode baroclinic) fluctuations in the ocean. It is shown that these fluctuations cannot be local processes isolated to either the source or to the receivers. It is further shown that resonant barotropic gravity wave modes (Platzman et al., 1981) are not consistent with the data. The cause of these fluctuations remains unresolved, but the data and other oceanographic measurements put many constraints on the process causing these fluctuations. GRA

N91-14696# Massachusetts Inst. of Tech., Cambridge.
THE DISTRIBUTION OF WAVE HEIGHTS AND PERIODS FOR SEAS WITH UNIMODAL BIMODAL POWER DENSITY SPECTRA M.S. Thesis
Matthew Michael Sharpe Sep. 1990 116 p Prepared in cooperation with Woods Hole Oceanographic Inst., MA
(Contract N00123-89-G-0580)
(AD-A227040) Avail: NTIS HC/MF A06 CSCL 08/3

Observed distributions of wave heights and periods taken from one year of surface wave monitoring near Martha's Vineyard are compared to distributions based on narrow-band theory. The joint distributions of wave heights and periods and the marginal height distributions are examined. The observed significant wave heights and periods of the extreme waves are also studied. Seas are classified by the shapes of their power density spectra. Spectra with a single peak are designated as unimodal and spectra with two peaks as bimodal. Seas are further classified by spectral width, a function of the thee lowest spectral moments. The joint distributions of wave heights and periods from seas with narrow spectral widths take the general shape predicted by narrow-band theory and the statistics of extreme waves for these seas are well described. As spectral width increases, agreement between the theoretical and observed distributions diminishes and the significant wave heights and statistics of extreme waves show increasingly variability. Bimodal seas with wide-banded spectra are found to have larger significant and extreme wave heights and shorter extreme wave periods than unimodal seas of the same width. GRA

N91-14697# Naval Oceanographic and Atmospheric Research Lab., Bay Saint Louis, MS.
MULTISPECTRAL IMAGERY SUPPORT FOR OCEAN VENTURE 90 Interim Report
C. L. Walker, D. Byman, M. T. Kalcic, and T. Beaubouef Aug. 1990 65 p
(AD-A227119; NOARL-SP-058-351-90) Avail: NTIS HC/MF A04 CSCL 08/3

The Naval Oceanographic and Atmospheric Research Laboratory's Mapping, Charting and Geodesy Division performs research and development in new and improved methods for gathering navigational bathymetric data in coastal areas. One area of special interest is the development of algorithms to derive bathymetry from multispectral data. Currently, multispectral imagery can be derived from airborne scanners or from satellite sensors, such as the thematic mapper on board LANDSAT. Multispectral bathymetry has the potential for gathering data much more rapidly that present shipboard systems; in particular, satellite systems can gather data from many parts of the world that are denied to other collection systems. The results are presented of applying multispectral bathymetry algorithms and image enhancement and classification techniques developed at NOARL to support a joint amphibious exercise. GRA

N91-14698# Naval Academy, Annapolis, MD. Dept. of Oceanography.
UPWELLING SOUTHWEST OF ICELAND DUE TO QUASI-GEOSTROPHIC FLOW Final Report, 1989 - 1990
Maria K. Filonczuk 22 May 1990 63 p
(AD-A227129; USNA-TSPR-167) Avail: NTIS HC/MF A04 CSCL 08/3

Investigation of unusual oceanographic upwelling occurrences southwest of Iceland (64 deg N, 26 deg W) suggests causes due to quasi-geostrophic flow over submarine bathymetry. Complex circulation patterns occur in this region and no predominant pattern has been recognized to account for the upwelling. Two submarine canyons are located 30 km northeast of the approximate location of the upwelling center. It is postulated that quasi-geostrophic flow over the canyons and a resulting conservation of potential vorticity is the cause of the upwelling. Satellite imagery, hydrographic data, wind patterns, and mean currents all point to a temperature doming. This suggests a persistent bottom-generated feature. Submarine bathymetry appears to play the dominant role in the upwelling. GRA

N91-14699# Rhode Island Univ., Narragansett. School of Oceanography.
THE SYNOP EXPERIMENT: INVERTED ECHO SOUNDER DATA REPORT FOR OCTOBER 1987 TO MAY 1988 Summary Report, Oct. 1987 - May 1988
Xiaoshu Qian, Karen Tracey, Erik Fields, and D. Randolph Watts Jul. 1990 163 p
(Contract N00014-87-K-0235; NSF OCE-87-17144)
(AD-A227232; GSO-TR-90-3) Avail: NTIS HC/MF A08 CSCL 08/3

The Synoptic Ocean Prediction experiment (SYNOP) was undertaken with the goal that increased understanding of the Gulf Stream obtained through coordinated observations could be integrated with numerical models, including predictive models of the Gulf Stream. Our moored experiment, which began in fall of 1987, consists of two separate arrays in the Gulf Stream. The Inlet array consists of inverted echo sounders (IES) and deep current meters in a 120 x 150 km rectangle Cape Hatteras. It measures key parameters that describe the variability of the Gulf Stream and Deep Western Boundary Current (DWBC). In this region the Gulf first flows into deeper water and crosses over the DWBC. The Central array of IESs, a 300x320 km rectangle centered on the Gulf Stream near 68W, monitors the thermocline structure of the Gulf Stream in the region of large meanders and frequent interactions with rings. IES data are documented here by plots and tables of basic statistics and pertinent deployment information. Altogether 22 IES records are presented, plus pressure and temperature records at 5 sites. The plots are time series of measured travel time, pressure, and temperature; the residual pressure; and low-pass filtered records of residual pressure, thermocline depth, and temperature. GRA

51 LIFE SCIENCES (GENERAL)

N91-14700*# Center for Blood Research, Boston, MA.
INITIAL BLOOD STORAGE EXPERIMENT
Douglas MacN. Surgenor 1 Apr. 1988 445 p Prepared in cooperation with Little (Arthur D.), Inc., Boston, MA; Childrens Hospital Medical Center, Boston, MA; Lahey Clinic Medical Center, Boston, MA and Massachusetts Univ., Boston
(Contract NAS9-17222)
(NASA-CR-185513-Pt-1; NAS 1.26:185513-Pt-1) Avail: NTIS HC/MF A19 CSCL 06C

The design of the Initial Blood Storage Experiment (IBSE) was based upon a carefully controlled comparison between

identical sets of human blood cell suspensions - red cells, white cell, and platelets - one set of which was transported aboard the Columbia on a 6 day 11 hour mission, and the other held on the ground. Both sets were carried inside stainless steel dewars within specially fabricated flight hardware. Individual bags of cell suspensions were randomly assigned with respect to ground vs orbit status, dewar chamber, and specific location within the dewar. To foster optimal preservation, each cell type was held under specific optimal conditions of pH, ionic strength, solute concentration, gas tension, and temperature. An added variable in this initial experiment was provided by the use of three different polymer/plasticizer formulations for the sealed bags which held the blood cells. At termination of the experiment, aliquots of the suspensions, identified only by code, were distributed to be assayed. Assays were selected to constitute a broad survey of cellular properties and thereby maximize the chances of detection of gravitational effects. A total of 74 different outcome measurements were reported for statistical analysis. When the measurements were completed, the results were entered into the IBSE data base, at which time the data were matched with the original blood bag numbers to determine their status with respect to polymer/plasticizer type, orbit status (orbit or ground), and storage position within the experimental hardware. The data were studied by analysis of variance. Initially, type of bag and orbital status were main factors; later more detailed analyses were made on specific issues such as position in the hardware and specific plastic. If the analysis of variance indicated a statistical significance at the 5 percent level the corresponding p-value was reported.

Author

N91-14701*# Center for Blood Research, Boston, MA.
INITIAL BLOOD STORAGE EXPERIMENT
Douglas MacN. Surgenor 1 Apr. 1988 301 p Prepared in cooperation with Little (Arthur D.), Inc., Boston, MA; Childrens Hospital Medical Center, Boston, MA; Lahey Clinic Medical Center, Boston, MA and Massachusetts Univ., Boston
(Contract NAS9-17222)
(NASA-CR-185513-Pt-2; NAS 1.26:185513-Pt-2) Avail: NTIS HC/MF A14 CSCL 06C

The possibility of conducting experiments with the formed elements of the blood under conditions of microgravity opens up important opportunities to improve the understanding of basic formed element physiology, as well as, contribution to improved preservation of the formed elements for use in transfusion. The physiological, biochemical, and physical changes of the membrane of the erythrocyte, platelet, and leukocyte was studied during storage under two specific conditions: standard blood bank conditions and microgravity, utilizing three FDA approved plastic bags. Storage lesions; red cell storage on Earth; platelet storage on Earth; and leukocyte storage Earth were examined. The interaction of biomaterials and blood cells was studied during storage. B.G.

N91-14702*# Washington Univ., Saint Louis, MO. Dept. of Pharmacology.
COSMOS 2044 Final Report
Oliver H. Lowry, Igor Krasnov, E. Ilyina Kakueva, Patti M. Nemeth, David B. McDougal, Jr., Rati Choksi, Joyce G. Carter, Maggie M. Y. Chi, Jill K. Manchester, and Mary Ellen Pusateri 14 Sep. 1990 51 p
(Grant NAG2-615)
(NASA-CR-187003; NAS 1.26:187003) Avail: NTIS HC/MF A04 CSCL 06C

The effects of microgravity and hind limb suspension on the enzyme patterns are assessed within a slow twitch muscle (soleus) and a fast twitch muscle (tibialis anterior). Studies were made on 95 soleus fibers and about 300 tibialis anterior (TA) fibers. Over 2200 individual enzyme measurements were made. Six key metabolic enzymes (hexokinase, pyruvate kinease, citrate kinase, beta-hydroxyacyl CoA dehydrogenase, glucose-6-P dehydrogenase, and aspartate aminotransferase) plus glutaminase and glutamate decarboxylase, as well as glutamate, aspartate, and GABA, were measured in 11 regions of the hippocampal formation of synchronous, flight, and tail suspension rats. Major differences were observed in the normal distribution of each enzyme and amine acid, but no substantive effects of either microgravity or tail suspension on these patterns were clearly demonstrated.

B.G.

N91-14703* National Aeronautics and Space Administration. Lyndon B. Johnson Space Center, Houston, TX.
BIO-REACTOR CHAMBER Patent
Joseph A. Chandler, inventor (to NASA) 13 Jun. 1989 8 p Filed 20 Aug. 1987
(NASA-Case-MSC-20929-1; US-Patent-4,839,046; US-Patent-Appl-SN-087358; US-Patent-Class-210-355; US-Patent-Class-210-414; US-Patent-Class-435-311; US-Patent-Class-435-316; Int-Patent-Class-B01D-29/04; Int-Patent-Class-B01D-29/42) Avail: US Patent and Trademark Office CSCL 06B

A bioreactor for cell culture is disclosed which provides for the introduction of fresh medium without excessive turbulent action. The fresh medium enters the bioreactor through a filter with a backwash action which prevents the cells from settling on the filter. The bioreactor is sealed and depleted medium is forced out of the container as fresh medium is added.

Official Gazette of the U.S. Patent and Trademark Office

N91-14704# Princeton Univ., NJ.
BIOREACTIVITY: STUDIES ON A SIMPLE BRAIN STEM REFLEX IN BEHAVING ANIMALS Final Report, 1 Jun. 1987 - 31 May 1990
Barry L. Jacobs 10 Aug. 1990 7 p
(Grant AF-AFOSR-0301-87; AF Proj. 2312)
(AD-A226823; AFOSR-90-0967TR) Avail: NTIS HC/MF A02 CSCL 06/5

A major problem in attempting to understand complex physiological processes, such as brain neuromodulation, or complex behavioral processes, such as arousal, is finding a simple system that will permit such analyses. The brain stem masseteric (jaw closure) reflex in cats is such a system. It is simple, containing only one synapse in the brain, and receives dense inputs from two neurochemical systems important in neuromodulation and arousal. Initial pharmacologic studies showed that locally applied norepinephrine facilitated the reflex response. More importantly, physiologic conditions, known to activate the brain norepinephrine system, also facilitated the response. This latter finding was shown to be causal, rather than correlative, by a study which found that the facilitation could be blocked by prior destruction of the norepinephrine input specifically to the reflex circuitry. These data represent the first definitive example of an activational effect in an intact and behaving organism being attributable to a particular central neurotransmitter acting at a specific brain site. GRA

N91-14705# Naval Medical Research Inst., Bethesda, MD.
DEVELOPMENT OF AN ANIMAL MODEL OF HUMAN NON-FREEZING COLD INJURY: CHANGES IN THERMAL SENSITIVITY FOLLOWING COLD EXPOSURE Technical Report, Oct. 1988 - Sep. 1989
Stephen T. Ahlers, John R. Thomas, Karl F. VanOrden, John Schrot, and Mark P. McAndrew 17 Aug. 1990 17 p
(AD-A227174; NMRI-90-63) Avail: NTIS HC/MF A03 CSCL 06/10

Non-freezing cold injury (NFCI) is a debilitating injury that results from damage to peripheral tissues exposed to cold temperatures for a prolonged period of time. NFCI continues to be a major operational hazard for personnel who must perform in cold environments. Despite considerable research, the mechanisms underlying NFCI have remained elusive. The objective of the research described represents the initial efforts to develop an animal model that adequately reflects the symptomatology observed in human NFCI. A salient feature in the post cold exposure manifestation of NFCI in humans is that, following an initial period of sensation loss in the affected limb, an increased, often permanent, thermal sensitivity develops. This is one of the more debilitating aspects of NFCI since personnel are unable to tolerate

even minor alterations in temperature of the hands or feet and are thus greatly restricted from performing in inclement weather conditions. Thermal sensitivity was measured in the tail of adult rats before and after the tail and a portion of the hind flank were exposed to cold (1 to 4 C) or warm (28 C) water for one to nine hours. GRA

52 AEROSPACE MEDICINE

Includes physiological factors; biological effects of radiation; and effects of weightlessness on man and animals.

N91-14706# Joint Publications Research Service, Arlington, VA.
JPRS REPORT: SCIENCE AND TECHNOLOGY. USSR: LIFE SCIENCES
B. A. Atchabarov and B. A. Abeuov 18 Apr. 1990 45 p
(JPRS-ULS-89-003) Avail: NTIS HC/MF A03

Life sciences research in the U.S.S.R. is discussed. Topics covered include aerospace medicine, biochemistry, genetics, laser bioeffects, physiology, public health, psychology, radiation biology, virology, and veternary medicine. Author

N91-14707# Ohio State Univ., Columbus. Dept. of Speech and Hearing Science.
DEMODULATION PROCESSES IN AUDITORY PERCEPTION
Annual Report, 1 Dec. 1988 - 30 Nov. 1989
Lawrence L. Feth 1 Mar. 1990 6 p
(Grant AF-AFOSR-0227-89; AF Proj. 2313)
(AD-A226824; AFOSR-90-0966TR) Avail: NTIS HC/MF A02
CSCL 06/4

The overall goal of this project is to understand the ability of the human listener to extract information from complex, time-varying sounds such as speech, music or other environmentally important signals. Specifically, we are interested in the listener's ability to process modulations of frequency and amplitude which are thought to carry the information of such signals. This report represents the continuation and extension of work begun at the University of Kansas in 1987. Preliminary work to determine the temporal acuity of normal hearing listeners for spectrally-dynamic signals is complete. Pilot work on processing of frequency transitions in a proving frequency paradigm has been started; and work on listeners with cochlear hearing impairments has been added to the scope of work undertaken on the project. GRA

N91-14708# Army Research Inst. of Environmental Medicine, Natick, MA.
THE EFFECTS OF SLEEP LOSS ON INDIVIDUAL AND GROUP PERFORMANCE
Robert H. Stretch and David W. Jamieson (Defence and Civil Inst. of Environmental Medicine, Downsview, Ontario) May 1990 46 p
(DA Proj. 3M1-61102-BS-15)
(AD-A226963; USARIEM-T16-90) Avail: NTIS HC/MF A03
CSCL 06/10

This experiment was part of a study designed to assess the effects of two-hour naps on cognitive performance during sustained operation conditions. It was conducted using 12 young, military subjects who performed operations officer duties in a simulated brigade-level command post. They worked continuously processing military messages over a 4.5 day period and were tested on several recurring cognitive tasks. This paper reports the results of tasks and questionnaires assessing the effects of sleep loss on both individual and group performance. Across subjects, the results indicate significant sleep loss effects on perceived physical health, sleep quality, sleep value, and attributions of performance on mental tasks and individual and group cognitive performance. Significant individual differences in the effects of sleep loss are also noted. A discussion of the results is presented and is asserted that there is a need to individualize the placement of naps in future studies to maximize performance. GRA

N91-14709* National Aeronautics and Space Administration. Lyndon B. Johnson Space Center, Houston, TX.
DUAL PHYSIOLOGICAL RATE MEASUREMENT INSTRUMENT
Patent
Tommy G. Cooper, inventor (to NASA) 26 Jun. 1990 6 p
Filed 15 Apr. 1988 Continuation of abandoned US-Patent-Appl-SN-585627, filed 7 Mar. 1984 which is a continuation of US-Patent-Appl-SN-394343, filed 1 Jul. 1982
(NASA-Case-MSC-20078-3; US-Patent-4,936,309;
US-Patent-Appl-SN-183475; US-Patent-Appl-SN-585627;
US-Patent-Appl-SN-394343; US-Patent-Class-128-671;
US-Patent-Class-128-689; US-Patent-Class-128-706;
US-Patent-Class-128-716; US-Patent-Class-331-1) Avail: US Patent and Trademark Office CSCL 06E

The object of the invention is to provide an instrument for converting a physiological pulse rate into a corresponding linear output voltage. The instrument which accurately measures the rate of an unknown rectangular pulse wave over an extended range of values comprises a phase-locked loop including a phase comparator, a filtering network, and a voltage-controlled oscillator, arranged in cascade. The phase comparator has a first input responsive to the pulse wave and a second input responsive to the output signal of the voltage-controlled oscillator. The comparator provides a signal dependent on the difference in phase and frequency between the signals appearing on the first and second inputs. A high-input impedance amplifier accepts an output from the filtering network and provides an amplified output DC signal to a utilization device for providing a measurement of the rate of the pulse wave.
Official Gazette of the U.S. Patent and Trademark Office

N91-14710# Oak Ridge National Lab., TN.
PREDICTION OF HELICOPTER SIMULATOR SICKNESS
Roger D. Horn, J. Douglas Birdwell (Tennessee Univ., Knoxville.), and Glenn O. Allgood 1990 11 p Presented at the 29th IEEE Conference on Decision and Control, Honolulu, HI, 5-7 Dec. 1990
(Contract DE-AC05-84OR-21400)
(DE90-016530; CONF-901209-2) Avail: NTIS HC/MF A03

Machine learning methods from artificial intelligence are used to identify information in sampled accelerometer signals and associative behavioral patterns which correlates pilot simulator sickness with helicopter simulator dynamics. These simulators are used to train pilots in fundamental procedures, tactics, and response to emergency conditions. Simulator sickness induced by these systems represents a risk factor to both the pilot and manufacturer. Simulator sickness symptoms are closely aligned with those of motion sickness. Previous studies have been performed by behavioral psychologists using information gathered with surveys and motor skills performance measures; however, the results are constrained by the limited information which is accessible in this manner. In this work, accelerometers were installed in the simulator cab, enabling a complete record of flight dynamics and the pilot's control response as a function of time. Given the results of performance measures administered to detect simulator sickness symptoms, the problem was then to find functions of the recorded data which could be used to help predict the simulator sickness level and susceptibility. Methods based upon inductive inference were used, which yield decision trees whose leaves indicate the degree of simulator-induced sickness. The long-term goal is to develop a gauge which can provide an on-line prediction of simulator sickness level, given a pilot's associative behavioral patterns (learned expectations). This will allow informed decisions to be made on when to terminate a hop and provide an effective basis for determining training and flight restrictions placed upon the pilot after simulator use. DOE

N91-14711* National Aeronautics and Space Administration, Washington, DC.
AEROSPACE MEDICINE AND BIOLOGY: A CONTINUING BIBLIOGRAPHY WITH INDEXES (SUPPLEMENT 343)
Dec. 1990 82 p

(NASA-SP-7011(343); NAS 1.21:7011(343)) Avail: NTIS HC A05; NTIS standing order as PB90-912300, $11.50 domestic, $23.00 foreign CSCL 06E

This bibliography lists 125 reports, articles and other documents introduced into the NASA Scientific and Technical Information System during January, 1989. Subject coverage includes: aerospace medicine and psychology, life support systems and controlled environments, safety equipment, exobiology and extraterrestrial life, and flight crew behavior and performance.

Author

N91-14712* National Aeronautics and Space Administration, Washington, DC.

AEROSPACE MEDICINE AND BIOLOGY: A CONTINUING BIBLIOGRAPHY WITH INDEXES (SUPPLEMENT 344)

Jan. 1991 92 p

(NASA-SP-7011(344); NAS 1.21:7011(344)) Avail: NTIS HC A05; NTIS standing order as PB91-912300, $15.00 domestic, $30.00 foreign CSCL 06E

This bibliography lists 125 reports, articles and other documents introduced into the NASA Scientific and Technical Information System during January, 1989. Subject coverage includes: aerospace medicine and psychology, life support systems and controlled environments, safety equipment, exobiology and extraterrestrial life, and flight crew behavior and performance.

Author

53 BEHAVIORAL SCIENCES

Includes psychological factors; individual and group behavior; crew training and evaluation; and psychiatric research.

N91-14713# PERI, Inc., Princeton, NJ.

AIR TRAFFIC CONTROLLER MEMORY ENHANCEMENT Technical Report, Oct. 1989 - Sep. 1990

P. J. Vingelis, E. Schaeffer, P. Stringer, S. Gromelski, and B. Ahmed Dec. 1990 85 p Prepared in cooperation with Essex Corp., Alexandria, VA

(Contract DTFA08-89-0050)

(DOT/FAA/CT-TN90/38) Avail: NTIS HC/MF A05

The Federal Aviation Administration is engaged in an ongoing research effort to help air traffic controllers reduce the frequency of operational errors. The results of the first year's efforts in a three-year project to develop practical, effective memory aids to improve controller performance of tasks where memory is a critical element are given. Literature on controller memory and performance is reviewed and operational errors are analyzed to determine the nature and frequency of controller memory lapses. Several potential memory aids are identified and evaluated for effectiveness, feasibility, usability, acceptability, cost, and testability. The highest ranking memory aids are recommended for further evaluation in controlled experiments. Author

N91-14714# Rutgers - The State Univ., New Brunswick, NJ. Dept. of Psychology.

EYE MOVEMENTS AND VISUAL INFORMATION PROCESSING Interim Progress Report, Apr. 1989 - Apr. 1990

Eileen Kowler 22 Aug. 1990 4 p

(Grant AF-AFOSR-0171-88; AF Proj. 2313)

(AD-A226782; AFOSR-90-0978TR) Avail: NTIS HC/MF A01 CSCL 06/4

This research extended our understanding of the visual and cognitive process controlling saccadic and smooth eye movements, and the role of these eye movements in visual information acquisition. Experiments showed that: (1) saccades are biased toward likely locations of targets, suggesting that previous reports of center-of-gravity reflexes are actually due to search of attentional strategies; (2) saccades can be directed to spatially-extended targets with an accuracy and precision as good as those found for single point targets; (3) predictive smooth eye movements are caused by cognitive expectations about future path of target motion, not by learned oculomotor habits; (4) slow control is not sensitive to position error; (5) smooth eye movements are sensitive to the expected direction of future target motion; (6) strategies of scanning the boundaries of difficult texture patterns are more effective than strategies of scanning the symmetric axis; (7) normal reading is carried out by a coordinated pattern of eye movements and head movements. GRA

N91-14715# Oregon Univ., Eugene. Dept. of Psychology.

INVESTIGATING INDIVIDUAL DIFFERENCES IN GENERAL COMPREHENSION SKILL: THE ROLE OF SUPPRESSION AND ENHANCEMENT Final Technical Report, 1 Apr. 1989 - 1 Apr. 1990

Morton A. Gernsbacher 1 Aug. 1990 69 p

(Grant AF-AFOSR-0305-89; AF Proj. 2313)

(AD-A226788; AFOSR-90-0945TR) Avail: NTIS HC/MF A04 CSCL 05/8

Investigation into whether the cognitive mechanism of suppression underlies differences in adult comprehension skills are reported. Less-skilled comprehenders less-efficiently reject the inappropriate meaning of ambiguous words (e.g., the playing card vs garden tool meaning of spade), the incorrect forms of homophones (e.g., patients vs patience), the highly-typical-but-absent members of scenes (e.g., tractor in a farm scene), and words superimposed on pictures of pictures surrounding words. However, less-skilled comprehenders are not less cognizant of what is contexually appropriate; in fact, they benefit from a biasing context just as much (and perhaps more) as more-skilled comprehenders do. So, comprehenders do no have difficulty enhancing contexually appropriate information. Instead, it is suggested that less-skilled comprehenders suffer from less-efficient suppression mechanism, which we conclude is an important component of general comprehension skill. GRA

N91-14716# Harvard Univ., Cambridge, MA. Dept. of Psychology.

PERCEPTION AND TEMPORAL PROPERTIES OF SPEECH Annual Technical Report, Jul. 1989 - Jul. 1990

Peter C. Gordon 26 Jul. 1990 67 p

(Grant AF-AFOSR-0461-89; AF Proj. 2313)

(AD-A226958; AFOSR-90-0943TR) Avail: NTIS HC/MF A04 CSCL 05/7

Two series of experiments are reported on the role of prosody in human speech comprehension. One series looked at the role of prosodic information in listeners' ability to recognize adjacent vowels and consonants cued by the common temporal feature of vowel duration. The stimuli consisted of syllables from a large sample of natural speech which listeners heard with prosodic context or without. Prosodic context was found to aid listeners in correctly attributing the phonological source of vowel duration. The second series of experiments examines the role of stress in syllable accessibility during the on-line comprehension of language and from short-term memory. During on-line comprehension stress is found to interact with lexical processing, while the effect of stress on syllable accessibility from short-term memory is not dependent on lexical effects. Partial contents: Disambiguation of segmental dependencies by extended phonetic context; and coming to terms with stress -- Effects of stress location in sentence processing. GRA

N91-14717# Naval Aerospace Medical Research Lab., Pensacola, FL.

VALIDATION OF DICHOTIC LISTENING AND PSYCHOMOTOR TASK PERFORMANCE AS PREDICTORS OF PRIMARY FLIGHT TRAINING CRITERIA: HIGHLIGHTING RELEVANT STATISTICAL ISSUES Interim Report, Jun. - Aug. 1989

Harold D. Delaney Jul. 1990 26 p Sponsored by Naval Medical Research and Development Command, Bethesda, MD

(AD-A227010; NAMRL-1357) Avail: NTIS HC/MF A03 CSCL 05/8

A statistical evaluation of the automated dichotic listening (DLT) and psychomotor tasks (PMT) indicated that both contributed to the prediction of primary flight training criteria. Prior to the main

analyses, the extreme skewness-squadron differences in flight grades were removed by tranformations based on z-scores. Primary flight grades were highly correlated with the psychomotor scores (r's between -.26 and -.41) and moderately related with the dichotic listening scores (r's between -.22 and -.28). These r's were significant at an experiment wise alpha of .05. Multiple regression analysis indicated an even stronger validity coefficient when a combination of the performance measures was used (R = .442). Furthermore, the 19.5 percent of flight grade variance accounted for by the performance based tests was largely independent of the 16.6 percent variance accounted for by a combination of current selection tests and demographic variables. For the pass/fail criterion, a statistically optimal combination of DLT/PMT variables, selection tests scores, and demographic variables was specified that could be used to identify individuals who are relatively more likely to attrite. Classification matrices illustrate how such predictions could reduce attrition. GRA

N91-14718# EEG Systems Lab., San Francisco, CA.
EMPIRICAL NETWORK MODEL OF HUMAN HIGHER COGNITIVE BRAIN FUNCTIONS Final Technical Report, 1 Apr. 1987 - 31 Mar. 1990
Alan S. Gevins, Brian A. Cutillo, Judy Illes, Steven L. Bressler, and Paul A. Brickett 31 Mar. 1990 207 p
(Contract F49620-87-C-0047; AF Proj. 2313)
(AD-A227193; EEG-88001; AFOSR-90-1028TR) Avail: NTIS HC/MF A10 CSCL 05/8

EEG Systems Laboratory (EEGSL) develops and applies advanced technologies for measuring neurocognitive signals in the human brain. Results included: (1) measurement of leading indicator neuroelectric patterns preceding performance decrements in five Air Force fighter test pilots who performed difficult cognitive tasks for 10 to 14 hours; (2) measurement of split-second neurocognitive patterns of basic linguistic operations which distinguished letter from non-letter, word from non-word, and syntactic from non-syntactic processing; and (3) functional anatomical localization based on 124-channel evoked potential recordings and three dimensional finite element brain models constructed from magnetic resonance images. GRA

54 MAN/SYSTEM TECHNOLOGY AND LIFE SUPPORT

Includes human engineering; biotechnology; and space suits and protective clothing.

For related information see also *16 Space Transportation.*

N91-14719*# Jeanneret and Associates, Inc., Houston, TX.
POSITION REQUIREMENTS FOR SPACE STATION PERSONNEL AND LINKAGES TO PORTABLE MICROCOMPUTER PERFORMANCE ASSESSMENT
P. R. Jeanneret Feb. 1988 103 p Prepared in cooperation with Essex Corp., Orlando, FL
(Contract NAS9-17326)
(NASA-CR-185606; NAS 1.26:185606; EOTR-88-11) Avail: NTIS HC/MF A06 CSCL 05H

The development and use of a menu of performance tests that can be self-administered on a portable microcomputer are investigated. In order to identify, develop, or otherwise select the relevant human capabilities/attributes to measure and hence include in the performance battery, it is essential that an analysis be conducted of the jobs or functions that will be performed throughout a space shuttle mission. The primary job analysis instrument, the Position Analysis Questionnaire (PAQ), is discussed in detail so the reader will have sufficient background for understanding the application of the instrument to the various work activities included within the scope of the study, and the derivation of the human requirements (abilities/attributes) from the PAQ analyses. The research methodology is described and includes the procedures used for gathering the PAQ data. The results are presented in detail with specific emphasis on identifying critical requirements that can be measured with a portable computerized assessment battery. A discussion of the results is given with implications for future research. Author

N91-14720# Carlow Associates, Inc., Fairfax, VA.
HUMAN FACTORS ENGINEERING. PART 1: TEST PROCEDURES Final Report
15 May 1990 866 p
(AD-A226480; TOP-1-2-610-Pt-1) Avail: NTIS HC/MF A99 CSCL 23/2

The material in this Test Operations Procedure (TOP) is intended to be used for the Human Factors Engineering (HFE) assessment of all types of materiel and systems tested by the U.S. Army Test and Evaluation Command (TECOM). Supplementary sources of guidance are indicated when required. TOP 1-2-610 encompasses the HFE procedures for the testing of design, functional performance, and environmental considerations for the major test functions (operability, maintainability, transportability, portability/usability, erectability, and habitability) applicable to the HFE assessment. This TOP contains two parts: Part 1, Test Procedures and Part 2, Human Factors Engineering Data Guide for Evaluation (HEDGE). Part 1, Test Procedures, provides guidance on how to plan and conduct an HFE test. Part 1 includes specific test procedures for measurement and assessment of environmental, design, and performance characteristics of test items and sample data collection forms such as checklists, questionnaire/interview forms, and other data collection forms. Part 2, the Human Factors Engineering Data Guide for Evaluation (HEDGE) provides planning guidance concerning what to test. HEDGE includes guidance on classification of the test item, identification of applicable test functions, test conditions, performance tasks, and detailed design criteria. GRA

N91-14721# Virginia Polytechnic Inst. and State Univ., Blacksburg.
ADAPTIVE HUMAN-COMPUTER INTERFACES USING EXPERT PROFILES Final Report, Sep. 1986 - Sep. 1987
Robert C. Williges, Jay Elkerton, Kim J. Vicente, and Brian C. Hayes Jul. 1990 131 p
(Contract MDA903-84-C-2017)
(AD-A226906; HCI-87-01; ARI-RN-90-83) Avail: NTIS HC/MF A07 CSCL 23/2

Adaptive human-computer systems accommodate a wide variety of users learning to interact with computers because they adjust to different skill levels and provide novices with appropriate levels of expertise needed to perform certain tasks. This effort was directed toward developing improved models of experts based on goal-based models and toward assaying and isolating individual differences of inexperienced users in order to adapt the software interface to these individual differences. Results show that inexperienced users and that slower users were more variable in their search times than experienced users and that slower users selected more inefficient search commands. Two performance-based and one cognitive-based command selection aid improved search performance and strategies of slower, inexperienced users. Since spatial and verbal ability were found to correlate of slower, positively with search strategies, inexperienced users learned to select fewer and more efficient commands when provided with spatial augmentation (graphic presentation). GRA

N91-14722# Illinois Univ., Champaign. Dept. of Psychology.
INFORMATION EXTRACTION FROM VISUAL DISPLAYS AND THE EVENT-RELATED BRAIN POTENTIAL Interim Report, Aug. 1985 - Sep. 1986
Christopher D. Wickens, Carla Bosco, Amir Mane, Arthur F. Kramer, Michael Coles, and Emanuel Donchin Sep. 1990 41 p
(Contract MDA903-83-K-0255)
(AD-A227063; ARI-RN-90-120) Avail: NTIS HC/MF A03 CSCL 06/5

Three experiments, of increasing levels of complexity, are reported which examine two questions: (1) Will subjects extract more information from progressively more information stimuli in a

probabilistic state estimation task, as inferred from reaction time measures; and (2) Will the amplitude of the P300 component of the event-related brain potential, reflect the amount of information extracted. The three experiments used different versions of a process monitoring task in which the process could be in one of two states, and information bearing on the expectancy of one state or the other was conveyed by discrete informative cues. Occasional probes signalled imperative responses to the expected or unexpected states. The data indicated that in the simplest version of the task with only two levels of information value (Experiment 1), both questions were answered affirmatively. GRA

N91-14723* National Aeronautics and Space Administration. Lyndon B. Johnson Space Center, Houston, TX.
VALVE FOR WASTE COLLECTION AND STORAGE Patent
William E. Thornton, Jr., inventor (to NASA) and Henry B. Whitmore, inventor (to NASA) 3 Jul. 1990 15 p Filed 10 Aug. 1989 Division of US-Patent-Appl-SN-035401, filed 7 Apr. 1989
(NASA-Case-MSC-21025-4; US-Patent-4,937,891; US-Patent-Appl-SN-392228; US-Patent-Appl-SN-035401; US-Patent-Class-4-209R; US-Patent-Class-4-482; US-Patent-Class-4-316; Int-Patent-Class-E03D-9/04) Avail: US Patent and Trademark Office CSCL 06K

A method and valve apparatus for collection of fecal matter designed to operate efficiently in a zero gravity environment is presented. The system comprises a waste collection area within a body having a seat opening. Low pressure within the waste collection area directs fecal matter away from the user's buttocks and prevents the escape of undersirable gases. The user actuates a piston covered with an absorbent pad that sweeps through the waste collection area to collect the fecal matter, scrub the waste collection area, press the waste against an end of the waste collection area and retracts, leaving the used pad. Multiple pads are provided on the piston to accommodate multiple uses of the system. Also a valve allows air to be drawn through the body, so the valve will not be plugged with fecal matter. A sheet feeder feeds fresh sheets of absorbent pads to a face of the piston with each actuation.
Official Gazette of the U.S. Patent and Trademark Office

N91-14724* National Aeronautics and Space Administration. Lyndon B. Johnson Space Center, Houston, TX.
METHOD FOR WASTE COLLECTION AND STORAGE Patent
William E. Thornton, Jr., inventor (to NASA) and Henry B. Whitmore, inventor (to NASA) 24 Jul. 1990 15 p Filed 10 Aug. 1989 Division of US-Patent-Appl-SN-035401, filed 7 Apr. 1989
(NASA-Case-MSC-21025-2; US-Patent-4,942,632; US-Patent-Appl-SN-391911; US-Patent-Appl-SN-035401; US-Patent-Class-4-661; US-Patent-Class-4-482; US-Patent-Class-4-316; US-Patent-Class-4-DIG.9; Int-Patent-Class-A47K-11/00) Avail: US Patent and Trademark Office CSCL 06K

A method for collection of fecal matter designed to operate efficiently in a zero gravity environment was invented. The system consists of a waste collection area within a body having a seat opening. Low pressure within the waste collection area directs fecal matter away from the user's buttocks and prevents the escape of waste gases. The user actuates a piston covered with an absorbent pad that sweeps through the waste collection area to collect fecal matter, scrub the waste collector area, press the waste against an end of the waste collection area and retracts, leaving the used pad. Multiple pads are provided on the piston to accommodate multiple usages. Also a valve allows air to be drawn through the body, which keeps the valve from becomming plugged with the feces. A sheet feeder feeds fresh sheets of absorbent pads to a face of the piston with each actuation.
Official Gazette of the U.S. Patent and Trademark Office

55 SPACE BIOLOGY

Includes exobiology; planetary biology; and extraterrestrial life.

N91-14725*# National Aeronautics and Space Administration. Ames Research Center, Moffett Field, CA.
EXOBIOLOGY IN EARTH ORBIT: THE RESULTS OF SCIENCE WORKSHOPS HELD AT NASA, AMES RESEARCH CENTER
D. DeFrees, ed., D. Brownlee, ed., J. Tarter, ed., D. Usher, ed., W. Irvine, ed., and H. Klein, ed. 1989 142 p Original contains color illustrations
(NASA-SP-500; NAS 1.21:500) Avail: NTIS HC/MF A07; also available SOD HC $6.50 as 033-000-01057-5; 5 functional color pages CSCL 06C

The Workshops on Exobiology in Earth Orbit were held to explore concepts for orbital experiments of exobiological interest and make recommendations on which classes of experiments should be carried out. Various observational and experimental opportunities in Earth orbit are described including those associated with the Space Shuttle laboratories, spacecraft deployed from the Space Shuttle and expendable launch vehicles, the Space Station, and lunar bases. Specific science issues and technology needs are summarized. Finally, a list of recommended experiments in the areas of observational exobiology, cosmic dust collection, and in situ experiments is presented. M.G.

59 MATHEMATICAL AND COMPUTER SCIENCES (GENERAL)

N91-14726*# Institute for Computer Applications in Science and Engineering, Hampton, VA.
[RESEARCH IN PROGRESS IN APPLIED MATHEMATICS, NUMERICAL ANALYSIS, AND COMPUTER SCIENCE]
Semiannual Final Report, 1 Apr. - 30 Sep. 1990
Nov. 1990 84 p
(Contract NAS1-18605)
(NASA-CR-187474; NAS 1.26:187474) Avail: NTIS HC/MF A05 CSCL 12A

Research conducted at the Institute in Science and Engineering in applied mathematics, numerical analysis, and computer science is summarized. The Institute conducts unclassified basic research in applied mathematics in order to extend and improve problem solving capabilities in science and engineering, particularly in aeronautics and space. Author

N91-14727*# National Aeronautics and Space Administration. Ames Research Center, Moffett Field, CA.
NASA's SUPERCOMPUTING EXPERIENCE
F. Ron Bailey Dec. 1990 30 p Presented at the Singapore Supercomputing Conference, Singapore, 11-12 Dec. 1990
(NASA-TM-102890; A-91024; NAS 1.15:102890) Avail: NTIS HC/MF A03 CSCL 12A

A brief overview of NASA's recent experience in supercomputing is presented from two perspectives: early systems development and advanced supercomputing applications. NASA's role in supercomputing systems development is illustrated by discussion of activities carried out by the Numerical Aerodynamical Simulation Program. Current capabilities in advanced technology applications are illustrated with examples in turbulence physics, aerodynamics, aerothermodynamics, chemistry, and structural mechanics. Capabilities in science applications are illustrated by examples in astrophysics and atmospheric modeling. Future directions and NASA's new High Performance Computing Program are briefly discussed. Author

60 COMPUTER OPERATIONS AND HARDWARE

Includes hardware for computer graphics, firmware, and data processing.

For components see *33 Electronics and Electrical Engineering.*

N91-14728# Federal Aviation Administration, Atlantic City, NJ.
DATAS HARDWARE DIAGNOSTIC TESTS
John Zvanya Oct. 1990 43 p
(Contract FAA-T-2001-F)
(DOT/FAA/CT-TN90/44) Avail: NTIS HC/MF A03

Reference material is presented for personnel using the Data Link Test and Analysis System (DATAS) for hardware diagnostic testing. Included is a brief overall description of the DATAS, and a thorough description of how to operate the hardware diagnostic tests. The National Airspace System plan, which is used to handle the increased air traffic, includes and Advanced Automation System (AAS) that will provide computer assistance to air traffic controllers, increased reliability via a digital Data Link between ground sensors and aircraft which will be provided by a Secondary Surveillance Radar (SSR) known as the Mode Select Beacon System (Mode S). DATAS will test these integrated and complex systems. E.R.

N91-14729# Stanford Univ., CA. Dept. of Computer Science.
COMPUTATIONAL EQUIPMENT FOR THE DEVELOPMENT OF NUMERICAL ALGORITHMS COMPUTATION Final Report, 1 Oct. 1986 - 31 Mar. 1988
Gene H. Golub Aug. 1990 4 p
(Grant AF-AFOSR-0084-87; AF Proj. 2917)
(AD-A226702; AFOSR-90-0998TR) Avail: NTIS HC/MF A01 CSCL 12/6

Under this grant, the following equipment was purchased: 7 SUN 3/50 workstations; 1 SUN 3/260 workstation; 1 SUN 3/180 file server; 1 CDC disk; 1 Eagle disk; 2 Apple Laser Writer printers. This equipment was of utmost importance in our research in the Scientific Computing and Computational Mathematics Program at Stanford. In particular, it allowed us to analyze, devise, and study various numerical algorithms associated with our research activity. I enclose a list of recent reports which depended heavily on the use of this equipment. Here are some special activities: The Lanczos method is a well known method for computing the eigen-values of symmetric matrices. For many years there has been an attempt to generalize this algorithm for matrices that are non-symmetric. There have been inherent difficulties, and for a long time it was not understood how to modify the algorithm for the non-symmetric case. In the last year, it has finally been understood how to formulate a stable and robust algorithm. We were able to develop numerical software for operating on non-symmetric matrices. GRA

N91-14730# Stanford Univ., CA. Dept. of Computer Science.
A MEDIATOR ARCHITECTURE FOR ABSTRACT DATA ACCESS Final Report, 1985 - 1990
Gio Wiederhold, Tore Risch, Peter Rathmann, Linda DeMichiel, and Surajit Chaudhuri 23 Feb. 1990 171 p
(Contract N00039-84-C-0211)
(AD-A227362; SU-STAN-CS-90-1303) Avail: NTIS HC/MF A08 CSCL 12/7

This report contains some concept papers describing the general architecture that we envisage to be appropriate for further information systems, as well as a number of papers with specific research results. The architecture presented here is conceived to deal with a wide variety of users, in many locals, served by many distinct experts, and using a wide variety of databases. It is not feasible for any single institution to address the entire problem. At Stanford, within the KBMS project, we have addressed a number of critical subtasks, but much more work needs to be done. While some results are ready for prototype implementation, the main motivation for issuing this report is to provide an overview with enough detail in some areas to allow the reader to gain insights into a direction that future information systems research needs to pursue. GRA

61 COMPUTER PROGRAMMING AND SOFTWARE

Includes computer programs, routines, alogorithms, and specific applications, e.g., CAD/CAM.

N91-14731*# Cornell Univ., Ithaca, NY.
ISIS AND META PROJECTS Progress Report
Kenneth Birman, Robert Cooper, and Keith Marzullo 22 Feb. 1990 14 p
(Contract NAG2-593; N00140-87-C-8904; ARPA Order 6037)
(NASA-CR-186413; NAS 1.26:186413) Avail: NTIS HC/MF A03 CSCL 09B

The ISIS project has developed a new methodology, virtual synchony, for writing robust distributed software. High performance multicast, large scale applications, and wide area networks are the focus of interest. Several interesting applications that exploit the strengths of ISIS, including an NFS-compatible replicated file system, are being developed. The META project is distributed control in a soft real-time environment incorporating feedback. This domain encompasses examples as diverse as monitoring inventory and consumption on a factory floor, and performing load-balancing on a distributed computing system. One of the first uses of META is for distributed application management: the tasks of configuring a distributed program, dynamically adapting to failures, and monitoring its performance. Recent progress and current plans are reported. B.G.

N91-14732*# Cornell Univ., Ithaca, NY. Dept. of Computer Science.
THE ISIS PROJECT: REAL EXPERIENCE WITH A FAULT TOLERANT PROGRAMMING SYSTEM
Kenneth Birman and Robert Cooper Jul. 1990 8 p
(Grant NAG2-593)
(NASA-CR-187029; NAS 1.26:187029; TR-90-1138) Avail: NTIS HC/MF A02 CSCL 09B

The ISIS project has developed a distributed programming toolkit and a collection of higher level applications based on these tools. ISIS is now in use at more than 300 locations world-wise. The lessons (and surprises) gained from this experience with the real world are discussed. Author

N91-14733*# Southwest Research Inst., San Antonio, TX.
DISTRIBUTED SYSTEMS STATUS AND CONTROL Final Report
David Kreidler and David Vickers 27 Sep. 1990 34 p
(Grant NAG9-387; SwRI Proj. 05-2985)
(NASA-CR-187014; NAS 1.26:187014) Avail: NTIS HC/MF A03 CSCL 09B

Concepts are investigated for an automated status and control system for a distributed processing environment. System characteristics, data requirements for health assessment, data acquisition methods, system diagnosis methods and control methods were investigated in an attempt to determine the high-level requirements for a system which can be used to assess the health of a distributed processing system and implement control procedures to maintain an accepted level of health for the system. A potential concept for automated status and control includes the use of expert system techniques to assess the health of the system, detect and diagnose faults, and initiate or recommend actions to correct the faults. Therefore, this research included the investigation of methods by which expert systems were developed for real-time environments and distributed systems. The focus is on the features required by real-time expert systems and the tools available to develop real-time expert systems. Author

N91-14734*# California Univ., Los Angeles.
RANDOMLY SAMPLED-DATA CONTROL SYSTEMS Ph.D. Thesis
Kuoruey Han 1990 117 p
(Contract NCC2-374)
(NASA-CR-187425; NAS 1.26:187425) Avail: NTIS HC/MF A06 CSCL 09B

The purpose is to solve the Linear Quadratic Regulator (LQR) problem with random time sampling. Such a sampling scheme may arise from imperfect instrumentation as in the case of sampling jitter. It can also model the stochastic information exchange among decentralized controllers to name just a few. A practical suboptimal controller is proposed with the nice property of mean square stability. The proposed controller is suboptimal in the sense that the control structure is limited to be linear. Because of i. i. d. assumption, this does not seem unreasonable. Once the control structure is fixed, the stochastic discrete optimal control problem is transformed into an equivalent deterministic optimal control problem with dynamics described by the matrix difference equation. The N-horizon control problem is solved using the Lagrange's multiplier method. The infinite horizon control problem is formulated as a classical minimization problem. Assuming existence of solution to the minimization problem, the total system is shown to be mean square stable under certain observability conditions. Computer simulations are performed to illustrate these conditions. Author

N91-14735# Consiglio Nazionale delle Ricerche, Frascati (Italy). Ist. di Fisica dello Spazio Interplanetario.
GRAPHICS SOFTWARE FOR THE HP825/9000 IFSI SYSTEM [SOFTWARE GRAFICO PER IL SISTEMA HP825/9000 DELL'IFSI]
R. Bruno Oct. 1989 35 p In ITALIAN
(IFSI-89-18; ETN-90-97779) Avail: NTIS HC/MF A03

The computer system working on the UNIX operating system includes plotters, laserjet printers and other graphics peripheries. The utilization of some of the graphics routines included in the Starbase graphics library is described. Illustrations and the corresponding code examples using those routines are included. ESA

N91-14736# Utrecht State Univ. (Netherlands). Dept. of Computer Science.
HIDDEN SURFACE REMOVAL FOR AXIS-PARALLEL POLYHEDRA
Mark deBerg and Mark H. Overmars May 1990 15 p Sponsored by Netherlands Organization for Scientific Research, and in part by EEC
(RUU-CS-90-21; ETN-90-98134) Avail: NTIS HC/MF A03

A new, efficient, output sensitive method for computing the visibility map of a set of axis parallel polyhedra (i.e., polyhedra with their faces and edges parallel to the coordinate axes) as seen from a given viewpoint is presented. For non intersecting polyhedra with n edges in total, the algorithm runs in time O((n + k)log n), where n k is the complexity of the visibility map. The method can handle cyclic overlap of the polyhedra and perspective views without any problem. The method can be extended to c-oriented polyhedra (with faces and edges in c orientations, for some constant c) and to intersecting polyhedra with only a slight increase in the time bound. ESA

N91-14737# Geological Survey, Denver, CO.
COLOR PALETTE: PLOTTING GUIDE FOR USE WITH GSMAP AND GSDRAW DIGITAL CARTOGRAPHIC SOFTWARE
Steven P. Schilling and Ren A. Thompson 1989 11 p
(Contract DE-AI08-78ET-44802)
(DE91-001643; USGS-OFR-88-553) Avail: NTIS HC/MF A03

Guidelines for plotting a variety of colors and patterns using GSMAP and GSDRAW digital cartographic programs have been developed. These color and pattern variations can be used to fill polygons (areas) on maps, charts, or diagrams. Batch processing file for plotting a sample color/pattern palette on a Hewlett Packard 7585B 8-pen plotter using GSDRAW software are provided on the disk. The detailed instructions, batch processing files, and variables used to construct the palette will provide the user ready access to 99 fill patterns, and aid in designing other useful combinations. DOE

N91-14738# Technische Univ., Delft (Netherlands). Faculty of Geodesy.
RECONSTRUCTION OF VECTORIZED RASTER DATA Thesis [RECONSTRUCTUE VAN GEVECTORISEERDE RASTERGEGEVENS]
H. F. Duursma Feb. 1990 104 p In DUTCH
(ETN-91-98143) Avail: NTIS HC/MF A06

The generation and correction of errors in the reconstruction of vectorized raster data for cartographic applications are treated. The digitation techniques for large scale maps are presented. The acquisition of data in raster form and the errors due to raster vector conversion are discussed. A computer program was written to detect these errors automatically and to reconstruct the original inventory. The program RADAMES (Reconstruction of Automatically Digitized Analog Maps and Editing and Squaring) consists of two parts: a program to detect, test and correct possible errors, and a program to test squaring relations within larger partial areas. ESA

N91-14739# Los Alamos National Lab., NM.
A CLOS (COMMON LISP OBJECT SYSTEM) IMPLEMENTATION ON TOP OF KEE (KNOWLEDGE ENGINEERING ENVIRONMENT)
H. W. Egdorf 1990 6 p Presented at the Artificial Intelligence in DOE Complex Annual Meeting, Idaho Falls, ID, 9-11 Oct. 1990
(Contract W-7405-eng-36)
(DE91-001957; LA-UR-90-3541; CONF-9010211-2) Avail: NTIS HC/MF A02

IntelliCorp's Knowledge Engineering Environment (KEE) is a popular AI shell running on top of Common Lisp. KEE implements a message-passing style of object-oriented programming. Common Lisp has adopted the different style of the Common Lisp Object System (CLOS) as the standard object-oriented programming style. This paper describes an implementation of a subset of CLOS on top of KEE that uses the CLOS-style of programming to construct and manipulate KEE objects. The subset has been used to construct a moderate-sized discrete-event simulation of some facilities at the Rocky Flats Plant in Colorado. Experiences constructing this model will be discussed. Several reasons are examined for use of such a system. Programmers may have to maintain and extend an existing KEE application, but wish to do so using the newer CLOS style of programming while staying within the KEE environment. A requirement may exist for support of a mixed CLOS/KEE system where CLOS is not available. Programmers may wish to begin developing in CLOS with a view toward migration from KEE when CLOS becomes more available. DOE

N91-14740# Lawrence Livermore National Lab., CA.
CONSTRUCTION OF LARGE-SCALE SIMULATION CODES USING ALPAL (A LIVERMORE PHYSICS APPLICATIONS LANGUAGE)
Grant Cook Oct. 1990 18 p Presented at the 2nd International Conference for Expert Systems in Numerical Analysis, West Lafayette, IN, 24-26 Apr. 1990
(Contract W-7405-eng-48)
(DE91-002783; UCRL-102469; CONF-9004189-2) Avail: NTIS HC/MF A03

A Livermore Physics Applications Language (ALPAL) is a new computer tool that is designed to leverage the abilities and creativity of the computational scientist. Some of the ways that ALPAL provides this leverage are noted. First, it eliminates many sources of errors; second, it permits building code modules with far greater speed than is otherwise possible; third, it provides a means of specifying almost any numerical algorithm; and fourth, it is a language that is close to a journal-style presentation of physics models and numerical methods for solving them. DOE

N91-14741* National Aeronautics and Space Administration. Lyndon B. Johnson Space Center, Houston, TX.
DISCRETE EVENT SIMULATION TOOL FOR ANALYSIS OF QUALITATIVE MODELS OF CONTINUOUS PROCESSING SYSTEMS Patent
Jane T. Malin, inventor (to NASA), Bryan D. Basham, inventor (to NASA), and Richard A. Harris, inventor (to NASA) (Mitre Corp., McLean, VA.) 23 Oct. 1990 29 p Filed 14 Jul. 1988
(NASA-Case-MSC-21465-1; US-Patent-4,965,743; US-Patent-Appl-SN-219295; US-Patent-Class-364-513; US-Patent-Class-364-578; Int-Patent-Class-G06F-15/18) Avail: US Patent and Trademark Office CSCL 09B

An artificial intelligence design and qualitative modeling tool is disclosed for creating computer models and simulating continuous activities, functions, and/or behavior using developed discrete event techniques. Conveniently, the tool is organized in four modules: library design module, model construction module, simulation module, and experimentation and analysis. The library design module supports the building of library knowledge including component classes and elements pertinent to a particular domain of continuous activities, functions, and behavior being modeled. The continuous behavior is defined discretely with respect to invocation statements, effect statements, and time delays. The functionality of the components is defined in terms of variable cluster instances, independent processes, and modes, further defined in terms of mode transition processes and mode dependent processes. Model construction utilizes the hierarchy of libraries and connects them with appropriate relations. The simulation executes a specialized initialization routine and executes events in a manner that includes selective inherency of characteristics through a time and event schema until the event queue in the simulator is emptied. The experimentation and analysis module supports analysis through the generation of appropriate log files and graphics developments and includes the ability of log file comparisons.

Official Gazette of the U.S. Patent and Trademark Office

N91-14742# Carnegie-Mellon Univ., Pittsburgh, PA. Software Engineering Inst.
EXPERIENCES PORTING THE DISTRIBUTED Ada REAL-TIME KERNEL
Brian Smith (Boeing Military Airplane Development, Seattle, WA.) and James E. Tomayko Jun. 1990 25 p
(Contract F19628-89-C-0003)
(AD-A226693; CMU/SEI-90-TR-17; ESD-90-TR-217) Avail: NTIS HC/MF A03 CSCL 12/7

The Distributed Ada Real-Time Kernel (DARK) is a mechanism for supporting the execution of distributed real-time Ada applications in embedded computer systems. It provides a solution to scheduling and distributing tasks without modifying the Ada language or vendor-supplied runtime systems. An important test of the utility of the Kernel is whether or not it can be ported to different hardware architectures and still function effectively. As part of an independent research and development project, Boeing Military Airplanes and The Wichita State University became co-acceptors of a copy of DARK for the purpose of demonstrating a part of 68000-based distributed architecture. This report describes the experiences in accomplishing the port. GRA

N91-14743# Carnegie-Mellon Univ., Pittsburgh, PA. Software Engineering Inst.
NATIONAL SOFTWARE CAPACITY: NEAR-TERM STUDY
Jane A. L. Siegel, Shelby Stewman, Suresh Konda (Purdue Univ., West Lafayette, IN.), Patrick D. Larkey, and W. Gary Wagner May 1990 85 p
(Contract F19628-89-C-0003)
(AD-A226694; CMU/SEI-90-TR-12; ESD-90-TR-13) Avail: NTIS HC/MF A05 CSCL 12/5

This study provides an initial assessment of the U.S.'s industrial capacity to produce MCCR software. A survey of senior government and industry people showed that 90 percent of them expected a serious problem with the nation's capacity to produce military software over the next 5 years. They ranked acquisition and labor factors as contributing most to the failure of military system development contracts to meet schedule or costs. The study team also analyzed available data about the supply of labor (new graduates and experienced scientists and engineers) and three aspects of demand (Ada systems, PDSS, and related commercial applications) before concluding there is a serious capacity problem. The report describes, organizational, and technological issues affecting software production capacity and concludes with some preliminary recommendations for DoD and industry initiatives. GRA

N91-14744# Carnegie-Mellon Univ., Pittsburgh, PA. Software Engineering Inst.
DARK TECHNOLOGY TRANSITION PLAN
Judy Bamberger Apr. 1990 35 p
(AD-A226695; CMU/SEI-90-SR-6) Avail: NTIS HC/MF A03 CSCL 12/5

The original goal of the DARK Project was to provide a set of artifacts, documents and code (to demonstrate that it is possible to develop application code entirely in Ada that has acceptable quality and real time performance) in a manner that avoids or mitigates the efficiency and maturity problems found in current Ada runtime implementations. To demonstrate, as required above, the transition activity to occur, i.e., individuals, groups, and organizations has to review DARK documents and code to become convinced that DARK did (or did not) provide that capability. The DARK Project was not out to develop any radically new technological breakthroughs, but to demonstrate that well understood, familiar, and reliable methods of building real time, distributed systems could be done in Ada as well as in any programming language. GRA

N91-14745# Carnegie-Mellon Univ., Pittsburgh, PA. Software Engineering Inst.
CLASSIFYING SOFTWARE DESIGN METHODS
John P. Long, William G. Wood, and David P. Wood Aug. 1989 27 p
(AD-A226696; CMU/SEI-89-TR-25; ESD-89-TR-33) Avail: NTIS HC/MF A03 CSCL 09/2

A few mature and popular methods are currently being used to specify and design real time embedded systems software, and these methods are the basis for a large number of tools automating the process. Unfortunately, some of the tools support only parts of a method, while others support a mixture of different methods. Because of the large number of tools involved, companies selecting tools for their particular needs are faced with a significant problem. As a result, the choice of tools often depends on the best salesperson rather than on the most appropriate method, leading to disappointment on the part of end users of the tools. The Software Engineering Institute (SEI) has had a project underway for some time that provides a basis for selecting methods and tools. Some of the results with respect to classifying design methods for Ada based software are described. Author

N91-14746# Army Electronic Proving Ground, Fort Huachuca, AZ.
METHODOLOGY INVESTIGATION OF SOFTWARE MATURITY MODEL VALIDATION Final Report
Ken VanKarsen 13 Nov. 1989 81 p Sponsored by Army Test and Evaluation Command, Aberdeen Proving Ground, MD
(AD-A226697) Avail: NTIS HC/MF A05 CSCL 12/5

This report covers phase 1 of an investigation to identify methods of quantitatively assessing software reliability. A set of candidate software reliability models were screened for potential use in estimating reliability parameters. Other techniques were examined briefly. Finally, the various methods were evaluated with respect to applicability during developmental testing. GRA

N91-14747# Naval Postgraduate School, Monterey, CA. Dept. of Compter Science.
DEVELOPING PORTABLE USER INTERFACES FOR Ada COMMAND CONTROL SOFTWARE M.S. Thesis

Chien Hsiung Sun Jun. 1990 135 p
(AD-A226712) Avail: NTIS HC/MF A07 CSCL 12/5

DoD mandated use of Ada for embedded systems include Combat and Control System such as shipboard Combat Direction System (CDS). A Low Cost CDS (LCCDS) which will use commercial workstation platforms will require interfacing Ada real time programs with portable windowing environment such as X Windows. Several methods are explored for building X Windows based user interface for Ada C2 programs and provides a step-by-step approach to user interface design for future CDS developers. GRA

N91-14748# Carnegie-Mellon Univ., Pittsburgh, PA. Software Engineering Inst.
AN ANALYSIS OF INPUT/OUTPUT PARADIGMS FOR REAL-TIME SYSTEMS Final Report
Mark H. Klein and Thomas Ralya Jul. 1990 62 p
(Contract F19628-90-C-0003)
(AD-A226724; CMU/SEI-90-TR-19; ESD-90-TR-220) Avail: NTIS HC/MF A04 CSCL 12/7

The correctness of a real-time system with hard deadline requirements depends both on the logical correctness and on the timing correctness of the system. The principles of rate monotonic scheduling have proven to be very useful in providing a framework for designing, analyzing, and modifying the timing and concurrency aspects of real-time systems. This paper illustrates how to build a mathematical model of the schedulability of a real-time system, taking into consideration such factors as preemption, synchronization, non-preemptibility, interrupts, and process idle time. In particular, this paper illustrates how these principles can be applied to input/output interfaces (e.g., to devices or local area networks) to predict the timing of various design alternatives. The primary characteristic that distinguishes real-time system from non-real-time systems is the importance of time. The correctness of a real-time system depends not only upon its logical correctness but also its timing correctness. System complexity tends to compromise correctness unless there are techniques and methods for managing the complexity. Basic software engineering principles such as abstraction, encapsulation, and information hiding form the basis of methods and techniques that are used to manage logical complexity. Rate monotonic scheduling theory offers a set of engineering principles for managing timing complexity. GRA

N91-14749# Martin Marietta Aerospace, Denver, CO. Astronautics Group.
SOFTWARE COST ESTIMATION STUDY Final Report
Aaron N. Silver Aug. 1990 10 p
(Contract N00014-85-C-0892)
(AD-A226777; MCR-90-523) Avail: NTIS HC/MF A02 CSCL 12/5

The documentation described in this summary refers to both reports and software products, i.e., computer prototype programs, generated during the entire Software Cost Estimation Study. The period of performance covered is from 2 January 1986 to 31 August 1990. During this time frame, both the Naval Center for Cost Analysis (under the auspices of the office the Naval Research) and the Air Force Center for Cost Analysis funded several additional enhancements to the program, which resulted in producing the Software Architecture Sizing and Estimating Tool (SASET). These specific enhancements along with the initial Software Cost Estimation Study comprise the overall scope of this investigation. GRA

N91-14750# Princeton Univ., NJ. Cognitive Science Lab.
PEDAGOGICAL STRATEGIES FOR HUMAN AND COMPUTER TUTORING Interim Report, Jul. 1987 - Jun. 1990
Brian J. Reiser Aug. 1990 35 p
(Contract MDA903-87-K-0652)
(AD-A226886; ARI-RN-90-90) Avail: NTIS HC/MF A03 CSCL 12/5

This report considers the pedagogical strategies of human tutors and examines the implications of this work for research in intelligent tutoring systems. It briefly describes GIL, an intelligent tutor for simple LISP programming, and considers its effectiveness from the perspective of human tutoring strategies. Finally, it discusses the implications of research on human tutoring for the design of intelligent tutoring systems for problem solving. GRA

N91-14751# KAB Labs, Inc., San Diego, CA.
FEATURE SET EVALUATION FOR CLASSIFIERS Final Report, 15 Sep. 1988 - 1 Mar. 1989
John Konotchick 1 Mar. 1989 25 p
(Contract DAAB07-88-C-F415)
(AD-A226903) Avail: NTIS HC/MF A03 CSCL 09/2

The activity proposed meeting the following five technical objectives: (1) to identify and propose a collection of feature set evaluation algorithmic tools which address unique characteristics of feature sets used in ATR applications; (2) to implement at least one new promising feature set evaluation algorithm in FORTRAN and integrate it within the on-line pattern analysis and recognition system (OLPARS), which is an existing commercial software system that provides general purpose feature set evaluation and classifier design capabilities; (3) to demonstrate the performance of the new feature set evaluation algorithms already within OLPARS using feature sets derived from both real and simulated E/O imagery; (4) to provide DoD with a licensed Vax-compatible copy of the augmented OLPARS software package; and (5) to document the proposed new feature set evaluation algorithm and the test results obtained with the newly implemented algorithm within a final technical report. GRA

N91-14752# KAB Labs, Inc., San Diego, CA.
FEATURE SET EVALUATION FOR CLASSIFIERS Progress Report No. 1, 15 Sep. - 15 Nov. 1988
20 Nov. 1988 12 p
(Contract DAAB07-88-C-F415)
(AD-A226904) Avail: NTIS HC/MF A03 CSCL 09/2

The activity proposed meeting the following five objectives: (1) to identify and propose a collection of feature set evaluation algorithmic tools which address unique characteristics of feature sets used in ATR applications; (2) to implement at least one new promising feature set evaluation algorithm in FORTRAN and integrate it within the on-line pattern analysis and recognition system (OLPARS), which is an existing commercial software system that provides general purpose feature set evaluation and classifier design capabilities; (3) to demonstrate the performance of the new feature set evaluation algorithms already within OLPARS using feature sets derived from both real and simulated E/O imagery; (4) to provide DoD with a licensed VAX-compatible copy of the augmented OLPARS software package; and (5) to document the proposed new feature set evaluation algorithm and the test results obtained with the newly implemented algorithm within a final technical report. GRA

N91-14753# KAB Labs, Inc., San Diego, CA.
FEATURE SET EVALUATION FOR CLASSIFIERS Progress Report No. 2, 16 Nov. 1988 - 15 Jan. 1989
John Konotchick 20 Jan. 1989 13 p
(Contract DAAB07-88-C-F415)
(AD-A226905) Avail: NTIS HC/MF A03 CSCL 09/2

The activity proposed meeting the following five technical objectives: (1) to identify and propose a collection of feature set evaluation algorithmic tools which assress unique characteristics of feature sets used in ATR applications; (2) to implement at least one new promising feature wet evaluation algorithm in FORTRAN and integrate it within the on-line pattern analysis and recognition system (OLPARS), which is an existing commercial software system which provides general purpose feature set evaluation and classifier design capabilities; (3) to demonstrate the performance of the new feature set evaluation algorithms already within OLARS using feature sets derived from both real and simulated E/O imagery; (4) to provide DoD with a licensed VAX-compatible copy of the qugmented OLPARS software package; and (5) to document the proposed new feature set evaluation algorithm and the test results obtained with the newly implemented algorithm within a final technical report. GRA

N91-14754# Nevada Univ., Las Vegas. Dept. of Computer Science.
PLANNING MONOTONE PATHS TO VISIT A SET OF OBSTACLES
Laxmi P. Gewali Jun. 1990 17 p
(Contract DAAL03-87-G-0004)
(AD-A226923; CSR-90-36; ARO-24960.50-MA-REP) Avail: NTIS HC/MF A03 CSCL 12/9

Computing a shortest collision-free path connecting points s and t that visits a given set of obstacles in two dimensions is like the travelling salesman problem and is NP-hard. We consider a restricted version of the above problem called the s-t-monotone visit problem that asks for a monotone path connecting s and t that visits the maximum number of obstacles. We give an O(n squared) time algorithm to solve this problem, where n is the size of the obstacle scene. GRA

N91-14755# Naval Postgraduate School, Monterey, CA.
EVALUATIONS OF SOME SCHEDULING ALGORITHMS FOR HARD REAL-TIME SYSTEMS M.S. Thesis
Bao-Hua Fan Jun. 1990 124 p
(AD-A226930) Avail: NTIS HC/MF A06 CSCL 12/5

The computer aided prototyping system (CAPS) and the prototype system description language (PSDL) represent a pioneering effort in the field of software development. Execution support system (ESS) within the framework of CAPS. The static scheduler is one of the critical elements of the ESS which extracts critical timing constraints and precedence constraints for operators and schedules the time-critical operators to guarantee that their timing constraints will be met. The static scheduler uses the information of timing constraints and precedence constraints to determine whether a feasible schedule can be built. This construction provides the foundation for handling the execution for real-time systems. The goal of this thesis is to provide improved versions of the static scheduler. GRA

N91-14756# Naval Postgraduate School, Monterey, CA.
A PERFORMANCE STUDY OF THE CONCURRENCY CONTROL ALGORITHMS IN HIERARCHICAL NETWORK WITH PARTITIONED DATABASE M.S. Thesis
Eon S. Shin Mar. 1990 48 p
(AD-A227055) Avail: NTIS HC/MF A03 CSCL 12/7

It is common to have a hierarchical communication network in a military environment. If we consider each node in the network as a computer site then we have a hierarchical computer network. In a hierarchical computer network, because the need of resource sharing, we now have a distributed processing system. In this system a parent node may have duplicate records of all its children. Any update of a record has to be reflected in other nodes that keep the duplicates. We need a concurrency control mechanism to guarantee the integrity of the distributed database and the serializability of concurrent updates. This thesis is the first to investigate the performance in hierarchical networks of two widely-cited concurrency control mechanisms, locking based and timestamp. Various parameters are investigated in our research: number of nodes, level of network, transaction arrival rates, and message transmission speeds, etc. We present the problem, explain the algorithms used in our simulation, analyze the results, and discuss the findings. GRA

N91-14757# Maryland Univ., College Park. Inst. for Advanced Computer Studies.
A SOFTWARE-SYSTEM VISUALIZATION TOOL
John R. Callahan and James M. Purtilo Apr. 1990 20 p
(AD-A227145; UMIACS-TR-90-51; CS-TR-2450) Avail: NTIS HC/MF A03 CSCL 12/5

Minion is a visual link editor used to configure and instrument software systems. It was originally developed as a general purpose graph editor for use in many task domains where connected graphs appropriately model logical structures. A software system, for example, can be represented by a connected graph - nodes and edges of the graph correspond respectively to large-grain software modulus (e.g. programs, files, databased, servers) and the dependencies established between these modules (e.g. procedure calls, message passing channels). We use the tool to write, visualize, and execute specifications for heterogenous, distributed software applications in the Polylith module interconnection environment. Our tool complements use of the Polylith textual module interconnection environment. Our tool complements use of the Polylith textual module interconnection language (MIL) because Minion is used as a link editor that reads and writes MIL specifications. Through the use of windows, icons, menus, and other means of direct manipulation, users can edit MIL specs as graphs in order to perform complex configuration management tasks which may be tedious to denote directly in the MIL. GRA

N91-14758# Stanford Univ., CA. Dept. of Computer Science.
MECHANIZING PROOF THEORY: RESOURCE-AWARE LOGICS AND PROOF TRANSFORMATIONS TO EXTRACT IMPLICIT INFORMATION Ph.D. Thesis
Gianluigi Bellin Jun. 1990 243 p
(Contract N00039-84-C-0211; NSF CCR-87-18605)
(AD-A227147; SU-STAN-CS-90-1319) Avail: NTIS HC/MF A11 CSCL 12/5

Few systems for mechanical proof-checking have been used so far to transform formal proofs rather than to formalize informal arguments and to verify correctness. The unwinding of proofs, namely, the process of applying lemmata and extracting explicit values for the parameters within a proof, is an obvious candidate for mechanization. It corresponds to the procedures of Cut-elimination and functional interpretation in proof-theory and allows the extraction of the constructive content of a proof, sometimes yielding information useful in mathematics and in computing. Resource-aware logics restrict the number of times an assumption may be used in a proof and are of interest for proof-checking not only in relation to their decidability or computational complexity, but also because they efficiently solve the practical problem of representing the structure of relevance in a derivation. In particular, in Direct Logic only one subformula-occurrence of the input is allowed, and the connections established during a successful proof-verification can be represented on the input without altering it. In addition, the values for the parameters obtained from unwinding are read off directly. In Linear Logic, where classical logic is regarded as the limit of a resource-aware logic, long-standing issues in proof-theory have been successfully attacked. We are particularly interested in the system of proof-nets as a multiple-conclusion Natural Deduction system for Linear Logic. GRA

N91-14759# Naval Academy, Annapolis, MD. Dept. of Physics.
DEVELOPMENT OF PHENOMENOLOGICAL FITTING PROCEDURE FOR THE FAST MICROCOMPUTER Final Report, 1989 - 1990
David F. Clipsham 22 May 1990 56 p
(AD-A227168; USNA-TSPR-166) Avail: NTIS HC/MF A04 CSCL 12/6

Currently available fitting techniques for both linear and nonlinear models are slow, require expensive equipment that is not widely available, and shield the modeler from an in-depth understanding of the fitting procedure. New high speed microcomputer technology has opened the door for development of microcomputer based fitting techniques that eliminate some of these shortcomings. Fitting in general is discussed with an emphasis on the distinction between the linear fitting problem and the non-linear fitting problem. The suitability of existing fitting techniques to handle these fitting problems is analyzed, and the strengths and weaknesses of each technique are noted. A case is made to justify the development of a microcomputer based phenomenological fitting procedure, and the technique is developed. The various stages in the development of the technique are described including the arrangement of a user-friendly display, the choice and testing of the cybernetic interface, and the writing of the computer code in Turbo Pascal 5.5. The technique is validated by fitting a number of real world data sets, and two of these validation tests are discussed in detail. Finally, speculation

is made about the future of the phenomenological fitting technique. The phenomenological fitting algorithm developed is included on disk with a brief user's manual. GRA

N91-14760# Naval Postgraduate School, Monterey, CA.
CYCLOMATIC COMPLEXITY AS A UTILITY FOR PREDICTING SOFTWARE FAULTS M.S. Thesis
Edwin A. Shuman, IV Mar. 1990 96 p
(AD-A227313) Avail: NTIS HC/MF A05 CSCL 12/5

The cyclomatic complexity metric provides a means of quantifying intra-modular software complexity, and its utility has been suggested in the software development and testing process. In this thesis, an empirical analysis was undertaken to examine the relationship between the cyclomatic complexity and the incidence of faults in a series of eight relatively large (from 1200 to 2400 LOC) complex programs. Each of these programs was developed from a single program specification and subsequently subjected to rigorous unit level testing. A comparison was also made between the relationship of cyclomatic complexity to faults and the relationship of lines of codes (LOC) to faults. The results of this study support a relationship between the cyclomatic complexity and the incidence of faults. Further, a relationship between LOC and faults is demonstrated. It could not be shown that there exists a stronger relationship between cyclomatic complexity and faults than LOC and faults. GRA

N91-14761# George Washington Univ., Washington, DC. Joint Inst. for Advancement of Flight Sciences.
NONLINEAR FINITE ELEMENT DYNAMICS ON MULTIPROCESSOR COMPUTERS Final Report, 1 Apr. 1988 - 30 Jun. 1990
Ahmed K. Noor 31 Jul. 1990 40 p
(Grant AF-AFOSR-0136-88; AF Proj. 2304)
(AD-A227409; AFOSR-90-1033TR) Avail: NTIS HC/MF A03 CSCL 12/1

A computational procedure is presented for the nonlinear dynamic analysis of unsymmetric structures on vector multiprocessor systems. The procedure is based on novel hierarchical partitioning strategy in which the response of the unsymmetric structure at any time instant is approximated by a linear combination of symmetric and antisymmetric response vectors, each obtained by using only a fraction of the degrees of freedom of the original finite element model. The three key elements of the procedure which result in a high degree of concurrency throughout the solution process are: (1) mixed (or primitive variable) formulation with independent shape functions for the different fields; (2) operator splitting or restructuring of the discrete equations at each time step to delineate the symmetric and antisymmetric vectors constituting the response; and (3) two-level iterative process for generating the response of the structure. An assessment is made of the effectiveness of the procedure on the CRAY X-MP/4 computers. GRA

N91-14762# Carnegie-Mellon Univ., Pittsburgh, PA. Software Engineering Inst.
THE ROLE OF ASSESSMENT IN SOFTWARE PROCESS IMPROVEMENT Final Report
David H. Kitson and Watts S. Humphrey Dec. 1989 48 p
(Contract F19628-85-C-0003)
(AD-A227426; CMU/SEI-89-TR-3; ESD-TR-89-3) Avail: NTIS HC/MF A03 CSCL 12/5

The role is discussed of assessment in improving an organization's software capabilities; specifically, the ability of the organization's projects to consistently meet cost, schedule, and quality objectives. Software process assessments are described from both a conceptual and pragmatic point of view. Underlying concepts of software process, software process management, and software process maturity are discussed. Collectively, these constitute a framework for software process assessment and improvement. GRA

N91-14763# Stanford Linear Accelerator Center, CA.
SOFTWARE MANAGEMENT ISSUES
Paul F. Kunz Jun. 1990 7 p Presented at the International Conference on Computing in High Energy Physics, Oxford, England, 10-14 Apr. 1989
(Contract DE-AC03-76SF-00515)
(DE91-001031; SU-SLAC-PUB-5293; CONF-890415-14) Avail: NTIS HC/MF A02

The difficulty of managing the software in large high energy physics (HEP) collaborations appears to becoming progressively worse with each new generation of detector. If one were to extrapolate to the superconducting super collider (SSC), it will become a major problem. This paper explores the possible causes of the difficulty and makes suggestions on what corrective actions should be taken. DOE

N91-14764# Stanford Univ., CA. Systems Optimization Lab.
COVERS BY POLARS OF ARRANGEMENTS
B. Curtis Eaves and Alan J. Hoffman (IBM Watson Research Center, Yorktown Heights, NY.) Aug. 1990 28 p
(Contract DE-FG03-87ER-25028; NSF DMS-89-02662)
(DE91-001358; SU-SOL-90-14) Avail: NTIS HC/MF A03

For a collection of hyperplanes passing through the origin in euclidean space let S be the induced subdivision. Let T be the collection of polars of the full cells of S. If only the origin lies in all hyperplanes, T forms a (kappa) (approximately) fold cover of euclidean space. If, in addition, the collection of hyperplanes is of size m and is regular, then kappa is m-1 choose n-1. Other similar results relate to spheres, hemispheres, and linear programming. DOE

N91-14765# Argonne National Lab., IL. Mathematics and Computer Science Div.
AN ACCURATE PRODUCT SVD (SINGULAR VALUE DECOMPOSITION) ALGORITHM
Adam W. Bojanczyk, Franklin T. Luk, Mangus Ewerbring, and Paul VanDooren (Philips Research Labs., Brussels, Belgium) 1990 19 p Presented at the 2nd International Workshop on SVD and Signal Processing, Providence, RI, 25-27 Jun. 1990 Sponsored by AFOSR
(Contracts W-31-109-eng-38; DAAL03-90-G-0092)
(DE91-004448; CONF-9006295-1) Avail: NTIS HC/MF A03

In this paper, we propose a new algorithm for computing a singular value decomposition of a product of three matrices. We show that our algorithm is numerically desirable in that all relevant residual elements will be numerically small. DOE

62 COMPUTER SYSTEMS

Includes computer networks and special application computer systems.

N91-14766*# California Univ., Los Angeles. School of Engineering and Applied Science.
A STUDY OF STRONG STABILITY OF DISTRIBUTED SYSTEMS Ph.D. Thesis
Tayfun Cataltepe Dec. 1989 102 p
(Grants NAG2-303; AF-AFOSR-0132-86)
(NASA-CR-187421; NAS 1.26:187421) Copyright Avail: NTIS HC/MF A06 CSCL 09B

The strong stability of distributed systems is studied and the problem of characterizing strongly stable semigroups of operators associated with distributed systems is addressed. Main emphasis is on contractive systems. Three different approaches to characterization of strongly stable contractive semigroups are developed. The first one is an operator theoretical approach. Using the theory of dilations, it is shown that every strongly stable contractive semigroup is related to the left shift semigroup on an L(exp 2) space. Then, a decomposition for the state space which identifies strongly stable and unstable states is introduced. Based on this decomposition, conditions for a contractive semigroup to be strongly stable are obtained. Finally, extensions of Lyapunov's equation for distributed parameter systems are investigated. Sufficient conditions for weak and strong stabilities of uniformly

bounded semigroups are obtained by relaxing the equivalent norm condition on the right hand side of the Lyanupov equation. These characterizations are then applied to the problem of feedback stabilization. First, it is shown via the state space decomposition that under certain conditions a contractive system (A,B) can be strongly stabilized by the feedback -B(*). Then, application of the extensions of the Lyapunov equation results in sufficient conditions for weak, strong, and exponential stabilizations of contractive systems by the feedback -B(*). Finally, it is shown that for a contractive system, the first derivative of x with respect to time = Ax + Bu (where B is any linear bounded operator), there is a related linear quadratic regulator problem and a corresponding steady state Riccati equation which always has a bounded nonnegative solution. Author

N91-14767# Utrecht State Univ. (Netherlands). Dept. of Computer Science.
MATRIX TECHNIQUES FOR FASTER ROUTING OF AFFINE PERMUTATIONS ON A MESH INTERCONNECTION NETWORK
Jop F. Sibeyn 1 May 1990 12 p Sponsored by Netherlands Foundation for Computer Science, and in part by EEC
(RUU-CS-90-19; ETN-90-98132) Avail: NTIS HC/MF A03

The problem of routing affine permutations on a SIMD MESH connected network without wrap around connections is studied. An algorithm with 4.(square root of n)-4 routing steps at most is obtained. The permutation is performed by a sequence of selective bit complementations but they are no longer invertible and the two datasets reside in the same processing unit. The algorithm is optimal for some affine permutations and on average the number of routine steps is only O(1) from a lower bound. ESA

N91-14768# Institut National Polytechnique, Grenoble (France).
BOOLEAN GROBNER BASES, CALCULATION METHODS. APPLICATIONS AND PARALLEL PROCESSING Ph.D. Thesis [BASES DE GROEBNER BOOLEENNES: METHODES DE CALCUL. APPLICATIONS PARALLELISATION]
Pascale Senechaud 1990 230 p In FRENCH
(ETN-90-98208) Avail: NTIS HC/MF A11

Grobner bases, their applications and the parallel workings of the algorithms used in calculating the bases when applied to boolean polynomials, are discussed. A formal proving algorithm is presented for hierarchic combinatory circuits. This sequential algorithm is adapted to a boolean situation. Two parallel processing methods with different granularity are proposed. Several parallel systems are compared and experimental results are presented. A spreading method for the polynomials is presented based on shortest path analysis on an oriented graph. This method allows conclusions to be made about the different algorithms presented. ESA

N91-14769* National Aeronautics and Space Administration. Lyndon B. Johnson Space Center, Houston, TX.
METHOD OF UP-FRONT LOAD BALANCING FOR LOCAL MEMORY PARALLEL PROCESSORS Patent
Paul Thomas Baffes, inventor (to NASA) 24 Apr. 1990 10 p Filed 12 Dec. 1988
(NASA-Case-MSC-21348-1; US-Patent-4,920,487;
US-Patent-Appl-SN-283106; US-Patent-Class-364-300;
US-Patent-Class-364-228.3; US-Patent-Class-364-231.9;
US-Patent-Class-364-280; US-Patent-Class-364-281;
Int-Patent-Class-G06F-9/46; Int-Patent-Class-G06F-15/16) Avail: US Patent and Trademark Office CSCL 09B

In a parallel processing computer system with multiple processing units and shared memory, a method is disclosed for uniformly balancing the aggregate computational load in, and utilizing minimal memory by, a network having identical computations to be executed at each connection therein. Read-only and read-write memory are subdivided into a plurality of process sets, which function like artificial processing units. Said plurality of process sets is iteratively merged and reduced to the number of processing units without exceeding the balance load. Said merger is based upon the value of a partition threshold, which is a measure of the memory utilization. The turnaround time and memory savings of the instant method are functions of the number of processing units available and the number of partitions into which the memory is subdivided. Typical results of the preferred embodiment yielded memory savings of from sixty to seventy five percent.
Official Gazette of the U.S. Patent and Trademark Office

N91-14770# Science Applications International Corp., San Diego, CA.
LITERATURE SURVEY ON TOOLS
C. G. Murphy Jul. 1990 140 p
(Contract N66001-87-D-0039)
(AD-A226933; NOSC/TD-1853) Avail: NTIS HC/MF A07
CSCL 12/5

This literature survey of parallel programming tools, including more than 200 references, is designed to allow continued browsing and probing of different specific areas of interest. Therefore, the first look at parallel programming tools is a broad one, where each reference article is briefly described. Keywords (or phrases) were assigned and provided in sorts by author and by assignment to a hierarchy of high performance computing technology. This hierarchy ranges from algorithms through tools environments to architectures and technology. A table of commercial programming tools is also provided. At the most focuses level, a review is made of articles providing information which is important to support signal processing parallel tools. A general discussion of the state-of-the-technology, and definitions and discussions of key terms, and concepts of parallel computing are also given. Designing and building multiprocessors has proceeded at a dramatic pace; the development of effective ways to program them generally has not. Yet, software development is the most critical element in a system's design. The immense complexity of parallel computation can only increase our dependency on software. GRA

N91-14771# Maryland Univ., College Park. Inst. for Advanced Computer Studies.
EFFICIENT PARALLEL ALGORITHMS ON THE NETWORK MODEL Ph.D. Thesis
Kwan Woo Ryu Mar. 1990 108 p
(AD-A227144; UMIACS-TR-90-37; CS-TR-2426) Avail: NTIS HC/MF A06 CSCL 12/7

We develop efficient parallel algorithms for several fundamental problems on the hypercube, the shuffle-exchange, the cube-connected cycles and the butterfly. Those problems are related to load balancing, packet routing list ranking, graph theory and Very Large Scale Integration (VLSI) routing. Load balancing, sorting routing problems have been studied heavily on various parallel models. There are some optimal algorithms for these problems on few networks. We introduce a new simple and efficient algorithm for load balancing on our networks, and show that load balancing requires more time on our bounded-degree networks than on the weak hypercube. GRA

N91-14772* National Aeronautics and Space Administration. Pasadena Office, CA.
DISTRIBUTED COMPUTING SYSTEM WITH DUAL INDEPENDENT COMMUNICATIONS PATHS BETWEEN COMPUTERS AND EMPLOYING SPLIT TOKENS Patent
Robert D. Rasmussen, inventor (to NASA), Robert M. Manning, inventor (to NASA), Blair F. Lewis, inventor (to NASA), Gary S. Bolotin, inventor (to NASA), and Richard S. Ward, inventor (to NASA) (Jet Propulsion Lab., California Inst. of Tech., Pasadena.) 12 Jun. 1990 18 p Filed 17 Aug. 1987
(NASA-Case-NPO-17185-1-CU; US-Patent-4,933,936;
US-Patent-Appl-SN-085833; US-Patent-Class-370-85.9;
US-Patent-Class-370-85.6; US-Patent-Class-370-85.4;
US-Patent-Class-370-94.3; US-Patent-Class-340-825.5;
Int-Patent-Class-H04J-3/02) Avail: US Patent and Trademark Office CSCL 09B

This is a distributed computing system providing flexible fault tolerance; ease of software design and concurrency specification; and dynamic balance of the loads. The system comprises a plurality of computers each having a first input/output interface and a second input/output interface for interfacing to communications

networks each second input/output interface including a bypass for bypassing the associated computer. A global communications network interconnects the first input/output interfaces for providing each computer the ability to broadcast messages simultaneously to the remainder of the computers. A meshwork communications network interconnects the second input/output interfaces providing each computer with the ability to establish a communications link with another of the computers bypassing the remainder of computers. Each computer is controlled by a resident copy of a common operating system. Communications between respective ones of computers is by means of split tokens each having a moving first portion which is sent from computer to computer and a resident second portion which is disposed in the memory of at least one of computer and wherein the location of the second portion is part of the first portion. The split tokens represent both functions to be executed by the computers and data to be employed in the execution of the functions. The first input/output interfaces each include logic for detecting a collision between messages and for terminating the broadcasting of a message whereby collisions between messages are detected and avoided.

Official Gazette of the U.S. Patent and Trademark Office

63 CYBERNETICS

Includes feedback and control theory, artificial intelligence, robotics and expert systems.

For related information see also *54 Man/System Technology and Life Support.*

N91-14773# Oxford Univ. (England). Robotics Research Group.

ANALOGUE COMPUTATION USING VLSI NEURAL NETWORK DEVICES

Michael Brownlow, Lionel Tarassenko, and Alan Murray (Edinburgh Univ., Scotland) May 1990 9 p Previously announced in IAA as A90-45967 Sponsored by United Kingdom Science and Engineering Research Council and EEC

(OUEL-1835/90; ETN-90-98223) Avail: NTIS HC/MF A02

Results are presented demonstrating analog neural network computation using VLSI (Very Large Scale Integration) pulse-stream devices. Synapse weight storage is dynamic, and the multiply and add function is performed by a switched capacitor circuit. Used on a mobile robot localization task, the neural VLSI devices achieve results within 1.2 percent of those from a SUN workstation. It is concluded that it is now possible to solve pattern recognition or signal processing problems in real time with the neural network architecture. ESA

N91-14774# Laboratoire d'Automatique et d'Analyse des Systemes, Toulouse (France).

PROTOTYPING OF A PROTOCOL VALIDATION ENVIRONMENT: APPLICATION TO THE ESTELLE APPROACH Ph.D. Thesis - Toulouse Univ.

Pierre deSaqui-Sannes 1990 148 p In FRENCH; ENGLISH summary

(LAAS-90113; ETN-91-98210) Avail: NTIS HC/MF A07

The Estelle formal description technique and the prototyping of an environment for the validation of protocols described with the aid of this technique are described. Two extension proposals enhance Estelle's power of abstraction from the viewpoint of the expression of parallel behaviors and that of the description of data structures exchanged by application processes. Based on previous works, a rendezvous mechanism is formally defined to bring Estelle closer to Petri nets, the latter being a modeling tool for which well proven validation techniques are available. The extension of these techniques to Estelle descriptions is carried out within the framework of the development of the ESTIM tool which offers simulation functionalities for interactive analysis as a protocol as well as verification functionalities for automatic generation of the quotient automaton, which characterizes the service provided by the protocol. The tests have shown that the methodology proposed for the ESTIM tool bridges the gap between the validation step and the actual implementation of a protocol. Developed in ML, on the basis of an Estelle's formal semantics, the prototype obtained remains a support tool for evaluating Estelle and its extensions. ESA

N91-14775# Laboratoire d'Automatique et d'Analyse des Systemes, Toulouse (France). Groupe Robotique et Intelligence Artificielle.

REASONING OF THE GEOMETRIC AND UNCERTAINTY CONSTRAINTS IN PLANNING ROBOT MANIPULATION TASKS Ph.D. Thesis - Toulouse Univ.

Isabelle Mazon 1990 149 p In FRENCH; ENGLISH summary Sponsored by Matra Datadivision

(LAAS-90143; ETN-91-98211) Avail: NTIS HC/MF A07

The problem of automatic programming for robotic systems is discussed. The design of a system which automatically plans pick and place tasks is reviewed. The interdependencies due to the decomposition of the task into actions as transfer notions, local motions and grasping and placement operations are taken into account. The state of the art in the field of automatic task level programming is reviewed. The basis modules of the system SPARA and the problems induced by the specific algorithms chosen are outlined. The positioning uncertainty propagation modules used to resolve interdependencies due to the imperfections of the models used by the system and ensure that the generated plan is robust are described. A set of techniques that guarantee compatibility between the approach and depart motions and the transfer motions are presented. The current implementation of the system is discussed. The architecture of the controller, which is partially constrained by the techniques used to take into account the geometric interdependencies is outlined. ESA

N91-14776# Boston Univ., MA. Coll. of Engineering.

SENSOR BASED CONTROL OF ROBOTIC MECHANISMS Final Report, 1 Dec. 1988 - 31 May 1990

John Baillieul 15 Aug. 1990 14 p

(Grant AF-AFOSR-0135-89; AF Proj. 3842)

(AD-A226784; AFOSR-90-0970TR) Avail: NTIS HC/MF A03

CSCL 09/1

This report provides a detailed account of equipment purchases made under a DoD University Research Instrumentation Grant (AFOSR-89-0135). The equipment includes a Silicon Graphics IRIS 4D/120GTX workstation and a variety of hardware components which have been selected as components of real-time server network designed to support a graphical interface to experiments in the control of mechanical systems. A brief description is provided of the resulting hardware implementation and its use in controlling three different experimental systems - a flexible beam, a rotating kinematic chain, and a six axis industrial robot. A detailed breakdown of expenditures is provided. GRA

64 NUMERICAL ANALYSIS

Includes iteration, difference equations, and numerical approximation.

N91-14777# Utrecht State Univ. (Netherlands). Dept. of Computer Science.

FINDING SHORTEST PATHS IN THE PRESENCE OF ORTHOGONAL OBSTACLES USING A COMBINED L SUB 1 AND LINK METRIC

Mark deBerg, Marc vanKreveld, Bengt J. Nilsson (Lund Univ., Sweden), and Mark H. Onermars Apr. 1990 17 p Sponsored by EEC, and Netherlands Organization for Scientific Research

(RUU-CS-90-20; ETN-90-98133) Avail: NTIS HC/MF A03

The problem of computing shortest paths in obstacle environments is studied for a new metric that generalizes the L sub 1 metric and the link metric. In this combined metric, the length of a path is defined as its L sub 1 length plus some non negative constant C times the number of turns the path makes. Given an environment of n axis parallel line segments and a target point, a data structure is presented in which an obstacle free

shortest rectilinear path from a query point to the target can be computed efficiently. The data structure uses O(n log n) storage and its construction takes O(n squared) time. Queries can be performed in O(log n) time, and the shortest path can be reported in additional time proportional to its size. ESA

N91-14778# Technische Hochschule, Darmstadt (Germany, F.R.). Fachbereich Mathematik.
EXTREMAL RAYS OF CONVEX CONES AND COMPLEMENTARY INEQUALITIES Ph.D. Thesis [EXTREMALSTRAHLEN KONVEXER KEGEL UND KOMPLEMENTAERE UNGLEICHUNGEN]
Martin Petschke 1989 110 p In GERMAN
(ETN-91-98166) Avail: NTIS HC/MF A06

The maximum principles for extremal rays on convex cones and inequalities for concave functions are treated. The methods of convex analysis and the Choquet theory were used. Concerning extremal rays of convex cones a semiconvex optimization problem, minimal and maximal points and Krein-Milman sets, a minimum principle for concave and quasiconcave functions, quasiconvex restrictions, for concave and monotonically concave functions as well as for monotonic functions are treated. Radon-concave functions and inequalities of the Favard-Berwald type are presented. Minimum principles for multidimensional spaces are discussed. ESA

N91-14779# Technische Hochschule, Darmstadt (Germany, F.R.). Fachbereich Mathematik.
THE INTEGRAL EQUATION METHOD FOR AN ELLIPTIC BOUNDARY VALUE OF THE HALF INTEGER CHARACTERISTIC Ph.D. Thesis [DIE INTEGRALGLEICHUNGSMETHODE FUER EIN ELLIPTISCHES RANDWERTPROBLEM HALBZAHLIGER CHARAKTERISTIK]
Brigitte Karin Becker 1989 64 p In GERMAN
(ETN-91-98167) Avail: NTIS HC/MF A04

The integral equation method was used to solve an elliptical boundary value problem with a matrix with half integer characteristic. The integral equation system is presented. The calculation of the Fredholm index is outlined. The conditions under which the boundary value problem can be solved are discussed. The boundary value problem in multiple connected regions is presented. Some examples of boundary value problems whose defect pair can be determined are given. An equivalent integral equation for the weak boundary value problem was deduced. ESA

N91-14780# Technische Hochschule, Darmstadt (Germany, F.R.). Fachbereich Mathematik.
BOUNDARY VALUE PROBLEMS OF THE ELASTICITY THEORY FOR POLYHEDRA: SINGULARITIES AND APPROXIMATION WITH BOUNDARY ELEMENT METHODS Ph.D. Thesis [RANDWERTPROBLEME DER ELASTIZITAETSTHEORIE FUER POLYEDER: SINGULARITAETEN UND APPROXIMATION MIT RANDELEMENTMETHODEN]
Tobias vonPetersdorff 1989 137 p In GERMAN
(ETN-91-98168) Avail: NTIS HC/MF A07

A mixed boundary value problem, the elasticity theory with Drichlet and Neumann conditions for a polyhedral domain, in which cracks are allowed, was treated. A splitting in a regular part and corner and edge singularities was obtained following the Dauge method. The edge singularities contain convolution terms. The splitting was modified in such a way that the edge singularities have a simpler tensor product form without convolution terms. Using the direct method an equivalent boundary integral equation was deduced for the general boundary value problem with Dirichlet Neumann and transmission conditions whereby cracks are allowed. It is shown that the singularities can be compensated by a refinement of the finite element grid at the edges. Hence, the same convergence rate as in the absence of singularities is obtained. The theoretical convergence rates are confirmed by numerical calculations for several crack and inclusion problems. ESA

N91-14781*# National Aeronautics and Space Administration. Lewis Research Center, Cleveland, OH.
MAPPINGS AND ACCURACY FOR CHEBYSHEV PSEUDO-SPECTRAL APPROXIMATIONS
Alvin Bayliss and Eli Turkel (Tel-Aviv Univ., Israel) Dec. 1990 21 p
(Grants NASA Order C-99066-G; NSF ASC-87-19573; NSF DMS-87-01543)
(NASA-TM-103630; ICOMP-90-24; E-5798; NAS 1.15:103630)
Avail: NTIS HC/MF A03 CSCL 12A

The effect of mappings on the approximation, by Chebyshev collocation, of functions which exhibit localized regions of rapid variation is studied. A general strategy is introduced whereby mappings are adaptively constructed which map specified classes of rapidly varying functions into low order polynomials which can be accurately approximated by Chebyshev polynomial expansions. A particular family of mappings constructed in this way is tested on a variety of rapidly varying functions similar to those occurring in approximations. It is shown that the mapped function can be approximated much more accurately by Chebyshev polynomial approximations than in physical space or where mappings constructed from other strategies are employed. Author

N91-14782# Universal Energy Systems, Inc., Dayton, OH.
ENGINEERING DESIGN WITH DECISION SUPPORT: AN APPLICATION OF GOAL DECOMPOSITION Final Technical Report, Jan. 1988 - Jul. 1990
Charles E. Wells Sep. 1990 39 p
(Contract F49620-85-C-0013)
(AD-A226730; AFHRL-TP-90-65) Avail: NTIS HC/MF A03 CSCL 12/4

Mathematical modeling is becoming a vital tool in engineering design. These models have been used to provide decision support to designers of systems characterized by many design choices. However, for the design of complex systems, these models become too large and cumbersome to be of significant value. As a result, research has progressed in the decomposition of the design problem. A decision support system, serving as a computer-based aid for engineers designing weapon systems, must integrate procedures dealing with designing for producibility and designing for supportability with those dealing with designing for performance cost and schedule (ULCE Implementation Plan, 1987). One of the characteristics of large weapon system development that causes difficulties in achieving this integration is the hierarchical nature of the design process. Typically, a system is designed in terms of subsystems which are required to meet certain specifications. Problems begin to arise when these specifications cannot be met. Consequently, these design processes may be enhanced by a computer-based system that supports the hierarchical nature of design. This research examines the application of mathematical modeling and knowledge-based system techniques to the development of decision support systems to support engineering design. GRA

N91-14783# Nevada Univ., Las Vegas. Dept. of Computer Science and Electrical Engineering.
CAPTURING STRONG REDUCTION IN DIRECTOR STRING CALCULUS
Vugranam Sreedhar and Kazem Taghva 5 Jul. 1990 30 p
(Contract DAAL03-87-G-0004)
(AD-A226738; CSR-90-38; ARO-24960.52-MA-REP) Avail: NTIS HC/MF A03 CSCL 12/1

A modified version of Director String Calculus (MDSC) is introduced which preserves the applicative structure of the original lambda terms and captures the strong reduction as opposed to weak reduction of the original Director String Calculus (DSC). Furthermore, MDSC provides an environment which supports the nonatomic nature of the substitution operation and hence can lend itself to parallel and optimal reduction. GRA

N91-14784# Arizona State Univ., Tempe. Dept. of Mathematics.
(DURIP) EXPLORING AND CONTROLLING SPATIO TEMPORAL CHAOS UNDER COMPLEX STRUCTURES THROUGH VISUALIZATION: A MINI-SUPERCOMPUTER APPROACH Final Report, 1 Dec. 1988 - 30 Nov. 1989
William T. Trotter 30 Nov. 1989 4 p
(Grant AF-AFOSR-0155-89; AF Proj. 3842)
(AD-A226793; AFOSR-90-1035TR) Avail: NTIS HC/MF A01 CSCL 12/6

The goal of the grant was to assist the Mathematics Program at Arizona State University in acquiring equipment for an Advanced Graphics Computing Facility. Our computers have made possible a breakthrough in unravelling the topology and geometry of some critical phenomena in turbulence, which closely blend chaotic dynamics with classical moderate turbulence. Interactive graphics visualization enabled us to describe the qualitative global nature of numerical solutions and interpret key features from the huge volume of numerical output. GRA

N91-14785# ST Systems Corp., Lexington, MA.
SEMI-IMPLICIT TIME INTEGRATION IN LIMITED AREA MODEL Report, 1 May 1988 - Apr. 1989
Isidore Halberstam 12 Nov. 1989 30 p
(Contract F19628-88-C-0072)
(AD-A226818; GL-TR-89-0324; SR-1) Avail: NTIS HC/MF A03 CSCL 12/3

An analysis of the Australian Bureau of Meteorology Research Center (BMRC) semi-implicit scheme is presented. The scheme is discussed for possible adaptation to the Relocatable Limited-Area Model (RLAM). It is found that the scheme has certain peculiarities which make it difficult to blend with the other versions of RLAM. It is shown, for example, that a small change in representing vertical differencing can have a severely damaging impact on the surface pressure forecast. GRA

N91-14786# Maryland Univ., College Park. Inst. for Advanced Computer Studies.
THE DEFINITION OF NECESSARY HIDDEN UNITS IN NEURAL NETWORKS FOR COMBINATORIAL OPTIMIZATION
Benjamin J. Hellstrom and Laveen N. Kanal Jan. 1990 57 p
(Grant NSF DCR-85-04011)
(AD-A227142; UMIACS-TR-90-6; CS-TR-2388) Avail: NTIS HC/MF A04 CSCL 12/3

Among the earliest successful applications of multi-layered neural networks are combinatorial optimization problems, most notably, the travelling salesman problem. Hopfield-type thermodynamic networks comprised of functionally homogenous visible units have been applied to a variety of structurally simple NP-hard optimization problems. A fundamental obstacle to the application of neural networks to difficult problems is that these problems must first be reduced to 0 to 1 Hamiltonian optimization problems. We show that certain optimization problems cannot be embedded in networks composed entirely of visible units and present a method for defining necessary hidden units together with their best features. We derive a knapsack-packing network of O(n) units with both standard and conjunctive synapses. Encouraging simulation results are cited. GRA

N91-14787# Brown Univ., Providence, RI. Center for Control Sciences.
CONTROL OF DISTRIBUTED PARAMETER SYSTEMS Final Technical Report, 15 Sep. 1986 - 20 Sep. 1989
H. T. Banks 1 Aug. 1990 51 p
(Contract F49620-86-C-0111; AF Proj. 3484)
(AD-A227306; AFOSR-90-0927TR) Avail: NTIS HC/MF A04 CSCL 12/1

A unified approximation framework for parameter estimation in general linear partial differential equators models has been completed. This framework has provided the theoretical basis for a number of identification problems on which these investigators have made significant progress. These include: (1) nondestructive evaluation techniques of composite materials using thermal probes; (2) estimation of damping in composite material beams from vibration experiments; and (3) conclusive evidence that an identification of damping mechanisms in the partial differential equation of a composite beam cannot be accomplished by the use of experimental model analysis. This is a major result in the theory of identifying damping mechanisms in flexible structures. The group has also studied questions related to the determination of irregularities (corrosion, cracks, delaminations, etc.) in composite materials using boundary observations of temperatures after known heat fluxes have been applied to the boundary. Successful efforts using experimental data with the theoretical and computational ideas developed by this group are reported. Substantial progress has been made on the development of a statistical framework (including hypothesis testing algorithms) to use in comparing the suitability of PDE models in least squares fits to data. A number of results on feedback stabilization of distributed parameter model have been obtained. GRA

N91-14788# Carnegie-Mellon Univ., Pittsburgh, PA. Robotics Inst.
PLANNING THE BEHAVIOR OF DYNAMICAL SYSTEMS
Nicola Muscettola Apr. 1990 17 p
(AD-A227381; CMU-RI-TR-90-10) Avail: NTIS HC/MF A03 CSCL 12/9

Two important factors hinder our ability to address large planning problems. On one hand, our understanding of planning is not independent from specific planning frameworks. On the other hand, current planning frameworks lack modularity, a key factor for 'divide and conquer' approaches to large problems. This paper addresses the formal definition of planning, points out some limitations of the current planning frameworks, and describes a new planning framework that overcomes these limitations. Our formal definition relies on the hypothesis that the problem solver's model of the world is dynamical system. On this basis, we can clearly separate the knowledge about how the world works from the heuristic knowledge needed to solve problems quickly. Our definition is also independent from any particular planning representation framework. Our analysis of modularity indicates which features can support it in a planning framework. We describe how these features are implemented in the HSTS planning framework, a general purpose facility integrated in the HSTS scheduling architecture. Its effectiveness to address complex 'real world' domains has been successfully demonstrated on the problem of building executable observation schedules for the Hubble Space Telescope. GRA

N91-14789*# Michigan Univ., Ann Arbor. Radiation Lab.
A COMBINED FINITE ELEMENT-BOUNDARY ELEMENT FORMULATION FOR SOLUTION OF AXIALLY SYMMETRIC BODIES Technical Report, Sep. 1990 - Feb. 1991
Jeffery D. Collins and John L. Volakis Jan. 1991 69 p
(Grant NAG2-541)
(NASA-CR-185852; NAS 1.26:185852; Rept-025921-18-T) Avail: NTIS HC/MF A04 CSCL 12A

A new method is presented for the computation of electromagnetic scattering from axially symmetric bodies. To allow the simulation of inhomogeneous cross sections, the method combines the finite element and boundary element techniques. Interior to a fictitious surface enclosing the scattering body, the finite element method is used which results in a sparse submatrix, whereas along the enclosure the Stratton-Chu integral equation is enforced. By choosing the fictitious enclosure to be a right circular cylinder, most of th resulting boundary integrals are convolutional and may therefore be evaluated via the Fast Fourier Transformation (FFT) when the system is iteratively solved. In view of the sparse matrix associated with the interior fields, this reduces the storage requirement of the entire system to O(N) making the method attractive for large scale computations. The details of the corresponding formulation and its numerical implementation are described. Author

N91-14790# International Centre for Theoretical Physics, Trieste (Italy).
THE COMPUTER ALGEBRA APPROACH OF THE FINITE DIFFERENCE METHODS FOR PDES
Liu Ruxun Jan. 1990 21 p
(DE90-631581; IC-90/12) Avail: NTIS (US Sales Only) HC/MF A03

In this paper, a first attempt has been made to realize the computer algebra construction of the finite difference methods or the finite difference schemes for constant coefficient partial differential equations. DOE

N91-14791# Lawrence Livermore National Lab., CA.
PROJECTED IMPLICIT RUNGE-KUTTA METHODS FOR DIFFERENTIAL-ALGEBRAIC BOUNDARY VALUE PROBLEMS
U. Ascher and L. Petzoid Sep. 1990 9 p Presented at the 29th IEEE Conference on Decision and Control, Honolulu, HI, 5-7 Dec. 1990
(Contract W-7405-eng-48)
(DE91-000660; UCRL-JC-104926; CONF-901209-5) Avail: NTIS HC/MF A02

Differential-algebraic boundary value problems arise in the modelling of singular optimal control problems and in parameter estimation for singular systems. A new class of numerical methods for these problems is introduced, and shown to overcome difficulties with previously defined numerical methods. DOE

N91-14792# Minnesota Univ., Minneapolis. Supercomputer Inst.
PIECEWISE-PARABOLIC METHODS FOR SYSTEMS OF HYPERBOLIC CONSERVATION LAWS IN MULTIPROCESSING ENVIRONMENTS Progress Report
Paul R. Woodward 28 Nov. 1990 13 p
(Contract DE-FG02-87ER-25035)
(DE91-004582; DOE/ER-25035/2) Avail: NTIS HC/MF A03

In this section we shall briefly summarize our progress in a number of different areas. These areas of research are all tied together by a common approach, which is expressed in the underlying mathematics embodied in our Piecewise-Parabolic Method (PPM) and in the construction of our numerical laboratory. The breadth of subjects which we have addressed is an indication of the power of this common approach to research in computational fluid dynamics. DOE

65 STATISTICS AND PROBABILITY

Includes data sampling and smoothing; Monte Carlo method; and stochastic processes.

N91-14793# Utrecht State Univ. (Netherlands). Dept. of Computer Science.
ON PROBABILITY INTERVALS AND THEIR UPDATING
Linda vanderGaag Jun. 1990 20 p
(RUU-CS-90-22; ISSN-0924-3275; ETN-90-98135) Avail: NTIS HC/MF A03

The adversaries of probability theory for dealing with uncertainty in Artificial Intelligence (AI) systems often argue that it is not expressive enough to distinguish between uncertainty and ignorance due to incompleteness of information. Probability intervals, however, have proven to be suitable for expressing incompleteness of information. A new method for computing such intervals from a partial specification of a joint probability distribution is presented. The method allows for the successive updating of probability intervals as evidence becomes available. ESA

N91-14794# Stanford Univ., CA. Dept. of Statistics.
IMPROVED ESTIMATION OF VARIANCE COMPONENTS IN MIXED MODELS
Alan E. Gelfand and Dipak K. Dey 30 Aug. 1990 22 p
(Contract N00014-89-J-1627; NR Proj. 042-267)
(AD-A226854; SU-TR-434) Avail: NTIS HC/MF A03 CSCL 12/3

Taking Albert's (1976) formulation of a mixed model Analysis of variance, we consider improved estimation of the variance components for balanced designs under squared error loss. Two approaches are presented. One extends the ideas of Stein (1964). The other is developed from the fact that variance components can be expressed as linear combinations of chi-scale parameters. Encouraging simulation results are presented. GRA

N91-14795# Colorado Univ., Boulder. Inst. of Cognitive Science.
INVESTIGATIONS OF PROBABILISTIC INFERENCE Interim Report, Sep. 1986 - Sep. 1987
Robert M. Hamm Jul. 1990 16 p
(Contract MDA903-86-K-0265)
(AD-A226882; ARI-RN-90-73) Avail: NTIS HC/MF A03 CSCL 12/3

A report on the first-year results of The Use of Protocol Analysis and Process Tracing Techniques to Investigate Probabilistic Inference Project are presented. Research indicates that the most recently presented information is given more attention in situations that require the integration of information about expectancies with uncertain information about what is happening at present. In addition, subjects have difficulty distinguishing two types of conditional probability information: the reliability p(evidence/hypothesis) and the probability that the hypothesis is true if the evidence is observed, p(hypothesis/evidence). GRA

N91-14796# Illinois Univ., Champaign. Dept. of Psychology.
THE OBJECT DISPLAY: PRINCIPLES AND REVIEW OF EXPERIMENTAL FINDINGS Interim Report, Aug. 1983 - Sep. 1986
Christopher D. Wickens Sep. 1990 22 p
(Contract MDA903-83-K-0255)
(AD-A226883; ARI-RN-90-119) Avail: NTIS HC/MF A03 CSCL 12/9

This report summarizes and integrates the results of several experiments that have been conducted during the contract period comparing object displays of multidimensional information with more conventional bargraph displays. The context in which this summary is presented is a theory of information integration which proposes that the benefits of object displays will be enhanced to the extent that information from multiple channels must be integrated, and will be diminished to the extent that separate channels must either be processed independently, or information in certain channels must be filtered out. The experiments described involve rectangular, triangular, pentagon and single point objects, conveying data in paradigms related to statistical data analysis, decision making, and process control. The results generally support the theory of an object-display benefit for integrated information; furthermore they indicate that the object display effects are independent of the degree of correlation between variables. GRA

N91-14797# Colorado Univ., Boulder. Inst. of Cognitive Science.
INTERPRETATION OF CONDITIONAL PROBABILITIES IN PROBABILISTIC INTERFERENCE WORD PROBLEMS Final Report, Sep. 1986 - Aug. 1988
Robert M. Hamm and Michelle A. Miller Jul. 1990 82 p
(Contract MDA903-86-K-0265)
(AD-A226907; ICS-88-15; ARI-RN-90-63) Avail: NTIS HC/MF A05 CSCL 05/7

People's strategies on probabilistic inference word problems were investigated in an attempt to determine which of three theories explains their neglect of base rate information when estimating the probability of a hypothesis. These word problems present a base rate or prior probability (p(h)), some evidence (e) that typically conflicts with the prior expectation, and information on the reliability of the evidence, which is stated as p(e/h), the conditional probability of the evidence being seen if the hypothesis is true. The three theories are: (1) subjects believe that the base rate is irrelevant; (2) they integrate base rate and evidence in a manner that underweighs the base rate; or (3) they misinterpret the reliability

information p(e/h) as if it were p(h/e). Data using four distinct methods support the theory that subjects confuse the conditional probabilities. GRA

N91-14798# Purdue Univ., West Lafayette, IN. Dept. of Statistics.
APPROXIMATELY INTEGRABLE LINEAR STATISTICAL MODELS IN NON-PARAMETRIC ESTIMATION
B. Ya. Levit Aug. 1990 23 p
(Contract N00014-89-K-0170; NSF DMS-89-23071)
(AD-A227395; TR-90-37C) Avail: NTIS HC/MF A03 CSCL 12/3

The notion of approximately integrable linear statistical models is introduced to analyze the higher order optimality properties of some common nonparametric estimators. The approximately integrable models suggest a useful approach to a unified treatment of both regular and irregular non-parameter problems. It is shown that with such models any rate of improvement ranging from (log n)(exp alpha)/n(exp 2) to 1/(n(log...log n)(exp alpha)), alpha greater than 0, of the classical non-parametric procedures can be anticipated. Both an example of a first order asymptotically optimal estimator with the unusual rate n(exp -1) log n and an estimator with an extremely slow unimprovable rate of convergence 1/(log...log n) (exp alpha) are presented. GRA

N91-14799# Naval Postgraduate School, Monterey, CA.
MINIMIZATION ON STOCHASTIC MATROIDS
Michael P. Bailey Jul. 1990 37 p
(AD-A227413; NPS55-90-14) Avail: NTIS HC/MF A03 CSCL 12/3

A methodology is given for analyzing matroids with random element weights, with emphasis placed on independent, exponentially distributed element weights. The minimum weight basic element in such a structure is shown to be an absorbing state in a Markov chain, while the distribution of weight of the minimum weight element is shown to be of phase-type. Two sided bounds are presented for matroids with new better than used (NBUE) distributed weights, as well as for weights with bounded positive hazard rates. The method is illustrated using the transversal matroid to solve stochastic assignment problems. GRA

66 SYSTEMS ANALYSIS

Includes mathematical modeling; network analysis; and operations research.

No abstracts in this category.

67 THEORETICAL MATHEMATICS

Includes topology and number theory.

No abstracts in this category.

70 PHYSICS (GENERAL)

For precision time and time interval (PTTI) see *35 Instrumentation and Photography;* for geophysics, astrophysics or solar physics see *46 Geophysics, 90 Astrophysics,* or *92 Solar Physics.*

No abstracts in this category.

71 ACOUSTICS

Includes sound generation, transmission and attenuation. For noise pollution see *45 Environmental Pollution.*

N91-14800 Georgia Inst. of Tech., Atlanta.
AN INVESTIGATION OF THE DIFFRACTION OF AN ACOUSTIC PLANE WAVE BY A CURVED SURFACE OF FINITE IMPEDANCE Ph.D. Thesis
James Andrew Kearns 1990 247 p
Avail: Univ. Microfilms Order No. DA9023818

The diffraction effects which would occur near the tops of hills and ridges was analyzed. The diffraction of a high frequency plane wave due to its grazing of a two-dimensional curved surface of finite impedance was studied. Laboratory scale models were constructed and measurements were made of the field on, above, and behind either of two curved surfaces possessing distinctly different impedances; that is, one was soft while the other was hard. The experimental technique consisted of simultaneously measuring the pressure at a reference point and at a field point due to a transient pulse generated by an electric spark. The pressure waveforms were digitized and processed. The ratio of the discrete Fourier transforms of the two waveforms provided an estimate of the insertion loss between them. The results of the measurements were compared with the predictions of theory which was derived by Pierce using the method of matched asymptotic expansions (MAE). The predictions relied upon the experimental evaluation of the impedance of each surface at grazing angles of incidence. This evaluation was achieved by a fairly standard technique involving empirical models of various generic types of surfaces. An example was shown of the important role that the structural intricacies of a surface play in the determination of an appropriate model. The comparison between the measurements and predictions clearly indicated that the theory gives an excellent description of the field anywhere near a curved surface. The theory was also shown to give nearly as good of a description of the field surrounding a curved surface even at distances far behind the surface yet near the line of sight. Dissert. Abstr.

N91-14801 Arizona Univ., Tucson.
IN-FLIGHT METHODS FOR SATELLITE SENSOR ABSOLUTE RADIOMETRIC CALIBRATION Ph.D. Thesis
Stuart Frick Biggar 1990 153 p
Avail: Univ. Microfilms Order No. DA9028144

Three methods for the in-flight absolute radiometric calibration of satellite sensors are presented. The thematic mapper (TM) on the LANDSAT satellites and the high resolution visibility (HRV) on the SPOT satellite were calibrated using the three methods. Ground and airborne measurements of ground reflectance, radiance, atmospheric, and weather parameters are made coincident with satellite image acquisition. The data are analyzed to determine inputs to radiative transfer codes. The codes compute the radiance at the sensor entrance pupil which is compared to the average digital count from the measured ground area. The three methods are the reflectance-based, radiance-based, and irradiance-based methods. Radiative transfer through an atmosphere is reviewed. The partition of extinction optical depth into Rayleigh, aerosol, and absorption optical depths is discussed. The reflectance-based method is described along with the assumptions made. The radiance-based method is described. The standard for the radiance method is a standard of spectral irradiance used to calibrate a radiometer. The calibration of a radiometer is discussed along with the use of radiative transfer computations to correct for the residual atmosphere above the radiometer. The irradiance-based method is described. It uses the measurement of the downward direct and total irradiance at ground level to determine the apparent reflectance seen by a sensor. This method uses an analytic approximation to compute the reflectance without the use of an exact radiative transfer code. The direct-to-total irradiance ratio implicitly gives the description of the scattering normally calculated from the size distribution and assumption of Mie scattering by the aerosols. Dissert. Abstr.

N91-14802*# Texas A&M Univ., College Station. Dept. of Mechanical Engineering.
EFFECT OF ATMOSPHERICS ON BEAMFORMING ACCURACY Final Report, 1 Oct. 1988 - 31 Aug. 1990
Richard M. Alexander 10 Dec. 1990 75 p
(Grant NAG1-911)
(NASA-CR-187695; NAS 1.26:187695) Avail: NTIS HC/MF A04 CSCL 20A

Two mathematical representations of noise due to atmospheric turbulence are presented. These representations are derived and used in computer simulations of the Bartlett Estimate implementation of beamforming. Beamforming is an array processing technique employing an array of acoustic sensors used to determine the bearing of an acoustic source. Atmospheric wind conditions introduce noise into the beamformer output. Consequently, the accuracy of the process is degraded and the bearing of the acoustic source is falsely indicated or impossible to determine. The two representations of noise presented here are intended to quantify the effects of mean wind passing over the array of sensors and to correct for these effects. The first noise model is an idealized case. The effect of the mean wind is incorporated as a change in the propagation velocity of the acoustic wave. This yields an effective phase shift applied to each term of the spatial correlation matrix in the Bartlett Estimate. The resultant error caused by this model can be corrected in closed form in the beamforming algorithm. The second noise model acts to change the true direction of propagation at the beginning of the beamforming process. A closed form correction for this model is not available. Efforts to derive effective means to reduce the contributions of the noise have not been successful. In either case, the maximum error introduced by the wind is a beam shift of approximately three degrees. That is, the bearing of the acoustic source is indicated at a point a few degrees from the true bearing location. These effects are not quite as pronounced as those seen in experimental results. Sidelobes are false indications of acoustic sources in the beamformer output away from the true bearing angle. The sidelobes that are observed in experimental results are not caused by these noise models. The effects of mean wind passing over the sensor array as modeled here do not alter the beamformer output as significantly as expected.
Author

N91-14803*# Cornell Univ., Ithaca, NY. Fluid Dynamics and Aerodynamics Program.
PREDICTION OF XV-15 TILT ROTOR DISCRETE FREQUENCY AEROACOUSTIC NOISE WITH WOPWOP
Charles D. Coffen and Albert R. George Jan. 1990 39 p
(Grant NAG2-554)
(NASA-CR-187684; NAS 1.26:187684; FDA-90-10) Avail: NTIS HC/MF A03 CSCL 20A

The results, methodology, and conclusions of noise prediction calculations carried out to study several possible discrete frequency harmonic noise mechanisms of the XV-15 Tilt Rotor Aircraft in hover and helicopter mode forward flight are presented. The mechanisms studied were thickness and loading noise. In particular, the loading noise caused by flow separation and the fountain/ground plane effect were predicted with calculations made using WOPWOP, a noise prediction program developed by NASA Langley. The methodology was to model the geometry and aerodynamics of the XV-15 rotor blades in hover and steady level flight and then create corresponding FORTRAN subroutines which were used an input for WOPWOP. The models are described and the simplifying assumptions made in creating them are evaluated, and the results of the computations are presented. The computations lead to the following conclusions: The fountain/ground plane effect is an important source of aerodynamic noise for the XV-15 in hover. Unsteady flow separation from the airfoil passing through the fountain at high angles of attack significantly affects the predicted sound spectra and may be an important noise mechanism for the XV-15 in hover mode. The various models developed did not predict the sound spectra in helicopter forward flight. The experimental spectra indicate the presence of blade vortex interactions which were not modeled in these calculations. A need for further study and development of more accurate aerodynamic models, including unsteady stall in hover and blade vortex interactions in forward flight. Author

N91-14804# Ohio State Univ., Columbus.
INVESTIGATIONS OF ULTRASONIC WAVE INTERACTIONS WITH GRAIN BOUNDARIES AND GRAIN IMPERFECTIONS
1990 106 p
(Contract DE-FG02-84ER-45057)
(DE91-002695; DOE/ER-45057/6) Avail: NTIS HC/MF A06

The main objective of our research is to obtain a better understanding of ultrasonic wave interaction with interfaces in polycrystalline materials. This report discusses two recently developed experimental techniques: scanning acoustic microscope and optical point sensors. As for general wave propagation problems in anisotropic media, four major topics are discussed in separate sections. First, single boundaries between large bicrystals are considered. The reflection and transmission coefficients of such interfaces are calculated for imperfect boundary conditions by using the finite interface stiffness approach. Ultrasonic transmission through multiple-grain structures are investigated by computer simulation based on the statistical evaluation of repeated acoustical wave interactions with individual grain boundaries. The number of grains interacting with the propagating acoustical wave is considered to be high enough to approximate the wave-material interaction as scattering on elastic inhomogeneities. The grain scattering induced attenuation of Rayleigh waves is investigated in polycrystalline materials. DOE

N91-14805# Johns Hopkins Univ., Baltimore, MD.
MASSIVELY PARALLEL NETWORK ARCHITECTURES FOR AUTOMATIC RECOGNITION OF VISUAL SPEECH SIGNALS Final Technical Report
Terrence J. Sejnowski and Moise Goldstein 1990 16 p
(Grant AF-AFOSR-0246-86; AF Proj. 2305)
(AD-A226968; AFOSR-90-0949TR) Avail: NTIS HC/MF A03 CSCL 25/4

This research sought to produce a massively parallel network architecture that could interpret speech signals from video recordings of human talkers. The project's results are summarized: (1) A corpus of video recordings from two human speakers was analyzed with image processing techniques and used as the data for this study; (2) It was demonstrated that a feedforward network could be trained to categorize vowels from these talkers (The performance was comparable to that of the nearest neighbors techniques and to trained humans on the same data); (3) A novel approach was developed to sensory fusion by training a network to transform from facial images to short-time spectral amplitude envelopes. This information can be used to increase the signal to noise ratio and hence the performance of acoustic speech recognition systems in noisy environments; and (4) The use was explored of recurrent networks to perform the same mapping for continuous speech. Results demonstrate the feasibility of adding a visual speech recognition component to enhance existing speech recognition systems. Such a combined system could be used in noisy environments, such as cockpits, where improved communication is needed. This demonstration of presymbolic fusion of visual and acoustic speech signals is consistent with the current understanding of human speech perception. GRA

N91-14806# Naval Academy, Annapolis, MD. Dept. of Oceanography.
A MODEL OF THE ACOUSTIC INTERACTIONS OCCURRING UNDER ARCTIC ICE Final Report, 1989 - 1990
Roger R. Ullman, II 22 May 1990 109 p
(AD-A227128; USNA-TSPR-173) Avail: NTIS HC/MF A06 CSCL 20/1

Underwater sound interacting with the Arctic ice cover is reflected from the plane surface as well as scattered due to small scale roughness elements and large pressure-ridge keel structures. Experiments modeled the acoustic ice interactions using burst transmissions from omnidirectional underwater point sources. Floating acrylic plates were employed to represent the Arctic ice

due to similarity in impedance characteristics and other physical properties to known ice values. Geometrical properties of the ice were accurately scaled in the acrylic by maintaining the appropriate wavelength ratios. Reflection and forwardscatter effects were analyzed and compared with existing theories for the Arctic.
GRA

N91-14807* National Aeronautics and Space Administration. Pasadena Office, CA.
ACOUSTIC POSITIONING AND ORIENTATION PREDICTION Patent
Martin B. Barmatz, inventor (to NASA), Glenn Aveni, inventor (to NASA), Seth Putterman, inventor (to NASA), and Joseph Rudnick, inventor (to NASA) (Jet Propulsion Lab., California Inst. of Tech., Pasadena.) 23 Oct. 1990 10 p Filed 15 Nov. 1988
(NASA-Case-NPO-17511-1-CU; US-Patent-4,964,303; US-Patent-Appl-SN-271265; US-Patent-Class-73-505; Int-Patent-Class-G01K-15/00) Avail: US Patent and Trademark Office CSCL 20A

A method is described for use with an acoustic positioner, which enables a determination of the equilibrium position and orientation which an object assumes in a zero gravity environment, as well as restoring forces and torques of an object in an acoustic standing wave field. An acoustic standing wave field is established in the chamber, and the object is held at several different positions near the expected equilibrium position. While the object is held at each position, the center resonant frequency of the chamber is determined, by noting which frequency results in the greatest pressure of the acoustic field. The object position which results in the lowest center resonant frequency is the equilibrium position. The orientation of a nonspherical object is similarly determined, by holding the object in a plurality of different orientations at its equilibrium position, and noting the center resonant frequency for each orientation. The orientation which results in the lowest center resonant frequency is the equilibrium orientation. Where the acoustic frequency is constant, but the chamber length is variable, the equilibrium position or orientation is that which results in the greatest chamber length at the center resonant frequency.
Official Gazette of the U.S. Patent and Trademark Office

N91-14808* National Aeronautics and Space Administration. Pasadena Office, CA.
ACOUSTIC TRANSDUCER APPARATUS WITH REDUCED THERMAL CONDUCTION Patent
Ernst G. Lierke, inventor (to NASA), Emily W. Leung, inventor (to NASA), and Balakrishna T. Bhat, inventor (to NASA) (Jet Propulsion Lab., California Inst. of Tech., Pasadena.) 9 Oct. 1990 6 p Filed 21 Mar. 1989
(NASA-Case-NPO-17620-1-CU; US-Patent-4,962,330; US-Patent-Appl-SN-326756; US-Patent-Class-310-323; US-Patent-Class-310-325; US-Patent-Class-310-334; US-Patent-Class-181-0.5; Int-Patent-Class-H01L-41/08) Avail: US Patent and Trademark Office CSCL 20A

A horn is described for transmitting sound from a transducer to a heated chamber containing an object which is levitated by acoustic energy while it is heated to a molten state, which minimizes heat transfer to thereby minimize heating of the transducer, minimize temperature variation in the chamber, and minimize loss of heat from the chamber. The forward portion of the horn, which is the portion closest to the chamber, has holes that reduce its cross-sectional area to minimize the conduction of heat along the length of the horn, with the entire front portion of the horn being rigid and having an even front face to efficiently transfer high frequency acoustic energy to fluid in the chamber. In one arrangement, the horn has numerous rows of holes extending perpendicular to the length of horn, with alternate rows extending perpendicular to one another to form a sinuous path for the conduction of heat along the length of the horn.
Official Gazette of the U.S. Patent and Trademark Office

72 ATOMIC AND MOLECULAR PHYSICS

Includes atomic structure, electron properties, and molecular spectra.

N91-14809# Colorado Univ., Boulder. Dept. of Physics.
INTERMEDIATE ENERGY NUCLEAR PHYSICS
1 Oct. 1990 68 p
(Contracts DE-FG02-86ER-40269; DE-FG02-87ER-40335)
(DE91-002758; DOE/ER-40269/7) Avail: NTIS HC/MF A04

This report summarizes work carried out between October 1, 1989 and October 1, 1990 at the Nuclear Physics Laboratory of the University of Colorado, Boulder, under contracts FG02-86ER-40269 and FG02-87ER-40335 with the United States Department of Energy. These contracts support experimental and theoretical work in intermediate energy nuclear physics. The experimental program is very broadly based; it includes pion-nucleon studies at TRIUMF, inelastic pion scattering and charge exchange reactions at LAMPF, and nucleon charge exchange at LAMPF/NTOF. This has been an especially important year for the LAMPF/NTOF program as the first experimental results are becoming available after an extensive commissioning process. The theoretical program continues to emphasize Dirac-based models of nuclear structure and scattering as well as the extension of techniques in nuclear reaction theory to problems at the interface between nuclear and high energy physics such as (vector p)p yields (vector lambda)lambda and (e,e(prime)d) reactions. We have also begun investigations of chiral models of baryon structure.
DOE

N91-14810# Oak Ridge National Lab., TN.
STATUS OF THE ADVANCED NEUTRON SOURCE
John B. Hayter 1990 12 p Presented at the International Collaboration on Advanced Neutron Sources, Tsukuba, Japan, 21-26 Oct. 1990
(Contract DE-AC05-84OR-21400)
(DE91-002870; CONF-9010243-2) Avail: NTIS HC/MF A03

Research reactors in the United States are becoming more and more outdated, at a time when neutron scattering is being recognized as an increasingly important technique in areas vital to the US scientific and technological future. The last US research reactor was constructed over 25 years ago, whereas new facilities have been built or are under construction in Japan, Russia and, especially, Western Europe, which now has a commanding lead in this important field. Concern over this situation in the early 1980's by a number of organizations, including the National Academy of Sciences, led to a recommendation that design work start urgently on an advanced US neutron research facility. This recommendation is realized in the Advanced Neutron Source Project. The centerpiece of the Advanced Neutron Source will be a new research reactor of unprecedented flux (>7.5 x 10(exp 19) m(exp -2) s(exp -1), equipped with a wide variety of state-of-the-art spectrometers and diffractometers on hot, thermal, and cold neutron beams. Very cold and ultracold neutron beams will also be provided for specialized experiments. This paper will discuss the current status of the design and the plans for scattering instrumentation.
DOE

N91-14811# Brookhaven National Lab., Upton, NY. Dept. of Physics.
NUCLEUS-NUCLEUS COLLISIONS AT VERY HIGH ENERGIES
Ole Hansen 1990 18 p Presented at the 1990 Mikolajki Summer School on Nuclear Physics, Mikolajki, Poland, 25 Aug. - 5 Sep. 1990
(Contract DE-AC02-76CH-00016)
(DE91-004003; BNL-45312; CONF-900857-2) Avail: NTIS HC/MF A03

The present report covers the material of two lectures. The first part, contains a collection of useful formulae from relativistic kinematics and deals with invariant cross sections and multiplicities. The remainder of the paper is on strangeness production in relativistic heavy ion collisions. Some elementary rules for particle production in nucleon-nucleon interactions are presented. This paper also contains arguments on why one expects enhanced

strange particle production from the quark-gluon plasma. Next is presented some selected data on strangeness production in Si + Au and other interactions at 14.6 GeV/c per nucleon and from S + S at 200 GeV/c per nucleon. Some conclusions drawn from the experimental results are presented. DOE

N91-14812# Brookhaven National Lab., Upton, NY. National Nuclear Data Center.
DATA REQUIREMENTS FOR INTERMEDIATE ENERGY NUCLEAR APPLICATIONS
Sol Pearlstein 1990 17 p Presented at the Advisory Group Meeting on Intermediate Energy Nuclear Data for Applications, Vienna, Austria, 9-12 Oct. 1990 Submitted for publication
(Contract DE-AC02-76CH-00016)
(DE91-004005; BNL-45308; CONF-9010199-2) Avail: NTIS HC/MF A03

Several applications that include spallation neutron sources, space radiation effects, biomedical isotope production, accelerator shielding and radiation therapy make use of intermediate energy nuclear data extending to several GeV. The overlapping data needs of these applications are discussed in terms of what projectiles, targets and reactions are of interest. Included is a discussion of what is generally known about these data and what is needed to facilitate their use in intermediate energy applications. DOE

N91-14813* National Aeronautics and Space Administration. Pasadena Office, CA.
SURFACE MODIFICATION USING LOW ENERGY GROUND STATE ION BEAMS Patent
Ara Chutjian, inventor (to NASA), Michael H. Hecht, inventor (to NASA), and Otto J. Orient, inventor (to NASA) (Jet Propulsion Lab., California Inst. of Tech., Pasadena.) 20 Feb. 1990 5 p Filed 21 Oct. 1988
(NASA-Case-NPO-17498-1-CU; US-Patent-4,902,647; US-Patent-Appl-SN-260762; US-Patent-Class-437-239; US-Patent-Class-437-225; US-Patent-Class-437-228; US-Patent-Class-437-930; US-Patent-Class-437-936; US-Patent-Class-437-235; US-Patent-Class-437-238) Avail: US Patent and Trademark Office CSCL 20H

A method of effecting modifications at the surfaces of materials using low energy ion beams of known quantum state, purity, flux, and energy is presented. The ion beam is obtained by bombarding ion-generating molecules with electrons which are also at low energy. The electrons used to bombard the ion generating molecules are separated from the ions thus obtained and the ion beam is directed at the material surface to be modified. Depending on the type of ion generating molecules used, different ions can be obtained for different types of surface modifications such as oxidation and diamond film formation. One area of application is in the manufacture of semiconductor devices from semiconductor wafers. Official Gazette of the U.S. Patent and Trademark Office

N91-14814# Carnegie-Mellon Univ., Pittsburgh, PA. Dept. of Metallurgical Engineering and Materials Science.
EQUILIBRIUM COMPOSITION OF INTERPHASE BOUNDARIES Progress Report, 1 Aug. 1988 - 31 Oct. 1990
Paul Wynblatt 1990 7 p
(Contract DE-FG02-88ER-45358)
(DE91-002470; DOE/ER-45358/2) Avail: NTIS HC/MF A02

Two modeling approaches have been used to investigate segregation effects at interphase boundaries. The first approach is based on the nearest neighbor bond model, used in conjunction with the regular solution approximation, and is an extension of an earlier framework developed to address segregation phenomena at free surfaces. In order to model a semicoherent interphase boundary, we have employed a second modeling approach, based on Monte Carlo simulation, in conjunction with the embedded atom method (EAM). The EAM is a powerful new method for describing interatomic interactions in metallic systems. It includes certain many-body interactions that depend on the local environment of an atom. The Monte Carlo approach has been applied to semicoherent interphase boundaries in Cu-Ag-Au alloys dilute in Au. These alloys consist of coexisting Cu-rich and Ag-rich phases, which differ in lattice constant by about 12 percent, such that good matching across in interface occurs when nine structural units of the Cu-rich phase are opposed to eight structural units of the Ag-rich phase. Thus far, interfaces with two different orientations have been studied. DOE

N91-14815# Argonne National Lab., IL.
INITIAL DATA FROM THE SOUDAN 2 EXPERIMENT
David S. Ayres 12 Oct. 1990 2 p Presented at the 25th IUPAP International Conference on High Energy Physics, Singapore, Singapore, 2-8 Aug. 1990 Submitted for publication
(Contract W-31-109-eng-38)
(DE91-004454; ANL-HEP-CP-90-87; CONF-900822-15) Avail: NTIS HC/MF A01

Soudan 2 is an 1100-ton tracking calorimeter which is being built 713 m underground to search for nucleon decay and to study neutrino and cosmic-ray physics. The detector is assembled from 256 identical 4.3-ton calorimeter modules. Each module consists of finely segmented iron and drift tubes, and records three space coordinates and dE/dx for every tube crossing. It is surrounded on all sides by a 1700 m(exp 2) active shield of proportional tubes. The first atmospheric neutrino interactions and a magnetic monopole search are described. Prospects for cosmic ray studies are summarized. DOE

73 NUCLEAR AND HIGH-ENERGY PHYSICS

Includes elementary and nuclear particles; and reactor theory.

For space radiation see *93 Space Radiation.*

N91-14816# Continuous Electron Beam Accelerator Facility, Newport New, VA.
A BEAM POSITION MONITOR FOR LOW CURRENT dc BEAMS
P. Adderley, W. Barry, J. Heefner, P. Kloeppel, R. Rossmanith, M. Wise, and S. Jachim (Los Alamos National Lab., NM.) 1989 6 p
(CEBAF-PR-89-004) Avail: NTIS HC/MF A02

The 4 GeV recirculating linac, Continuous Electron Beam Accelerator Facility (CEBAF), is presently under construction and will produce a continuous wave beam with average current between 0.1 and 200 micro-A. In order to measure beam position, the beam current will be amplitude modulated at a frequency 10 MHz. The modulation is detected by an inductive loop type monitor with electronics sensitive only to the modulation frequency. The first tests with beam from the CEBAF injector indicate that beam position can be measured with an accuracy of 0.1 mm at a modulated beam current of 1 micro-A. Author

N91-14817*# Jet Propulsion Lab., California Inst. of Tech., Pasadena.
PRELIMINARY SURVEY OF 21ST CENTURY CIVIL MISSION APPLICATIONS OF SPACE NUCLEAR POWER
John C. Mankins, J. Olivieri, and A. Hepenstal Mar. 1987 123 p Sponsored by NASA, Washington, DC
(NASA-TM-101249; JPL-D-3547; NAS 1.15:101249) Avail: NTIS HC/MF A06 CSCL 20H

The purpose was to collect and categorize a forecast of civilian space missions and their power requirements, and to assess the suitability of an SP-100 class space reactor power system to those missions. A wide variety of missions were selected for examination. The applicability of an SP-100 type of nuclear power system was assessed for each of the selected missions; a strawman nuclear power system configuration was drawn up for each mission. The main conclusions are as follows: (1) Space nuclear power in the 50 kW sub e plus range can enhance or enable a wide variety of ambitious civil space mission; (2) Safety issues require additional analyses for some applications; (3) Safe space nuclear reactor disposal is an issue for some applications; (4) The current baseline SP-100 conical radiator configuration is not applicable in all cases;

(5) Several applications will require shielding greater than that provided by the baseline shadow-shield; and (6) Long duration, continuous operation, high reliability missions may exceed the currently designed SP-100 lifetime capabilities. Author

N91-14818# Oak Ridge National Lab., TN. Physics Div.
STUDY OF SPIN-TEMPERATURE EFFECTS USING ENERGY-ORDERED CONTINUUM GAMMA RAY SPECTROSCOPY TECHNIQUE
C. Baktash, M. L. Halbert, D. C. Hensley, N. R. Johnson, I. Y. Lee, J. W. McConnell, and F. K. McGowan 1990 11 p Presented at the Nuclear Structure in the 1990's, Oak Ridge, TN, 23-27 Apr. 1990
(Contract DE-AC05-84OR-21400)
(DE91-002854; CONF-900450-12) Avail: NTIS HC/MF A03

We have investigated a new continuum (gamma)-ray spectroscopy technique which is based on the detection of all emitted (gamma) rays in a 4(pi) detector system, and ordering them according to their energies on an event-by-event basis. The technique allows determination of gamma strength functions, and rotational damping width as a function of spin and temperature. Thus, it opens up the possibility of studying the onset of motional narrowing, order-to-chaos transition, and the mapping of the evolution of nuclear collectivity with a spin and temperature. Application of the technique for preferential entry-state population, exit-channel selection, and feeding of the discrete states via selective pathways will be discussed. DOE

N91-14819# Stanford Linear Accelerator Center, CA.
HEM(SUB 11) MODES REVISITED
J. W. Wang and G. A. Loew Sep. 1990 4 p Presented at the Linear Accelerator Conference, Albuquerque, NM, 9-14 Sep. 1990
(Contract DE-AC03-76SF-00515)
(DE91-001028; SU-SLAC-PUB-5321; CONF-9009123-37) Avail: NTIS HC/MF A01

Concern with emittance growth in future multi-bunch linear colliders has rekindled interest in HEM(sub 11) dipole modes (sometimes also called 'TM(sub 11)-like' or 'TE(sub 11)-like') in disk-loaded waveguides. The availability of modern computer codes (URMEL, MAFIA) makes it possible to gain a deeper understanding of these modes and their properties. This paper presents omega-beta dispersion diagrams, field configurations, and transverse shunt impedances for the HEM(sub 11) modes as a function of iris aperture. The transition between forward and backward waves of the various branches is explored. This information serves as background material for another paper at this conference which reports recent work on linac structures in which these modes are damped or detuned. DOE

74 OPTICS

Includes light phenomena; and optical devices.
For lasers see *36 Lasers and Masers*.

N91-14820 Department of the Navy, Washington, DC.
OPTICAL PHASE CONJUGATE BEAM MODULATOR AND METHOD THEREFOR Patent
L. S. Ditman, Jr., inventor (to Navy) 1 May 1990 6 p Filed 1 Sep. 1988 Supersedes AD-D013882
(AD-D014569; US-Patent-4,921,335; US-Patent-Appl-SN-239498; US-Patent-Class-350-354) Avail: US Patent and Trademark Office CSCL 09/5

The present invention relates to the modulation of a phase conjugate beam. A writing beam is directed incident to phase conjugate reflector. A modulating beam is also directed incident to the phase conjugate reflector for amplitude modulation of the phase conjugate beam. The modulating beam can also be steerable for effecting the amplitude of the phase conjugate beam according to spatial distribution so as to spatially modulate the phase conjugate beam. The phase conjugate modulation thus can be accomplished by opto-optical means and without modulation of or effect on the incident writing beam. GRA

N91-14821# Department of the Navy, Washington, DC.
OPTICAL ENCODING OF IMAGING DATA Patent Application
Joseph P. Garcia, inventor (to Navy) 16 Jul. 1990 10 p
(AD-D014617; US-Patent-Appl-SN-553058; Navy-Case-72146)
Avail: NTIS HC/MF A02 CSCL 20/6

Optical imaging data sampled through a sensing array of spaced receiving end faces of optic fiber bundles is encoded by the different signal delay lengths of the fibers forming the respective bundles. The geometry of such end faces in the array is such as to effect encoding in dependence on the angular orientation and position of sampled segments of the optical data relative to the end faces on which such sampled segments impinge. GRA

N91-14822# Department of the Navy, Washington, DC.
OPTOELECTRONIC DEVICES Patent Application
Leslie H. Sperling, inventor (to Navy), Clarence J. Murphy, inventor (to Navy), Warren A. Rosen, inventor (to Navy), and Himanshu Jain, inventor (to Navy) 16 Jul. 1990 29 p
(AD-D014618; US-Patent-Appl-SN-554051; Navy-Case-72676)
Avail: NTIS HC/MF A03 CSCL 07/6

This invention relates to acrylic polymers and more specifically to polyacrylamides and polyacrylates such as poly(2-((N-2-methyl-5-nitrophenylamino) ethyl acrylate)) and poly((N-2-methyl-4-nitrophenyl)acrylamide). These acrylic polymers are particularly useful as nonlinear optical components in various electrical devices for processing optical signals including interferometors, optical switches, optical amplifiers, generators, computational devices and the like. GRA

N91-14823# Department of the Army, Washington, DC.
DEVICE AND METHOD FOR MONITORING THE PRESENCE OF AN OBJECT IN SPACE Patent Application
Walter E. Miller, Jr., inventor (to Army), Robert R. Mitchell, inventor (to Army), and Donald E. Lovelace, inventor (to Army) 3 May 1990 18 p
(AD-D014621; US-Patent-Appl-SN-518620) Avail: NTIS HC/MF A03 CSCL 17/7

An optically transparent cylinder, having a hemispherical cavity at one end thereof and containing at least one light source and one light detector inside the hemispherical cavity, utilizes the prismatic effect of the cylinder to locate an object in space. The light source and detector are located on a disk whose insertion depth into the cavity and tilt angle inside the cavity can be varied to control the sharpness, width, and direction of the conical beam output, which is searching space for the location of the desired object, from the cylinder. GRA

N91-14824 Department of the Navy, Washington, DC.
AUTOMATED SYSTEM FOR MEASURING THE STRENGTH OF OPTICAL FIBERS Patent
Howard E. Rast, inventor (to Navy) 10 Jul. 1990 8 p Filed 22 Aug. 1989
(AD-D014626; US-Patent-4,940,891; US-Patent-Appl-SN-397074; US-Patent-Class-250-227.15) Avail: US Patent and Trademark Office CSCL 20/6

A system automatically measures the strength of optical fibers by initiating a series of breaks in an optical fiber delivered from a supply spool. The fiber is stressed to failure in an automatically displacable jaw mechanism and the fiber is advanced and the measurement repeated. A computer-controlled mechanism advances the fiber, records data and monitors jaw mechanism fracture parameters so that the strength distribution of a length of optical fibers is reliably determined. GRA

N91-14825*# Auburn Univ., AL. Engineering Experiment Station.
THE DESIGN OF OPTICAL SENSOR FOR THE PINHOLE/OCCULTER FACILITY Final Report
Michael E. Greene 20 Dec. 1990 59 p
(Grant NAG8-636)
(NASA-CR-187694; NAS 1.26:187694) Avail: NTIS HC/MF A04 CSCL 20F

Three optical sight sensor systems were designed, built and

tested. Two optical lines of sight sensor system are capable of measuring the absolute pointing angle to the sun. The system is for use with the Pinhole/Occulter Facility (P/OF), a solar hard x ray experiment to be flown from Space Shuttle or Space Station. The sensor consists of a pinhole camera with two pairs of perpendicularly mounted linear photodiode arrays to detect the intensity distribution of the solar image produced by the pinhole, track and hold circuitry for data reduction, an analog to digital converter, and a microcomputer. The deflection of the image center is calculated from these data using an approximation for the solar image. A second system consists of a pinhole camera with a pair of perpendicularly mounted linear photodiode arrays, amplification circuitry, threshold detection circuitry, and a microcomputer board. The deflection of the image is calculated by knowing the position of each pixel of the photodiode array and merely counting the pixel numbers until threshold is surpassed. A third optical sensor system is capable of measuring the internal vibration of the P/OF between the mask and base. The system consists of a white light source, a mirror and a pair of perpendicularly mounted linear photodiode arrays to detect the intensity distribution of the solar image produced by the mirror, amplification circuitry, threshold detection circuitry, and a microcomputer board. The deflection of the image and hence the vibration of the structure is calculated by knowing the position of each pixel of the photodiode array and merely counting the pixel numbers until threshold is surpassed. Y.S.

N91-14826# Brookhaven National Lab., Upton, NY.
SCATTERING BY ANISOTROPIC GRAINS IN BERYLLIUM MIRRORS
Eugene L. Church, Peter Z. Takacs, and J. C. Stover (TMA Technologies, Inc., Bozeman, MT.) Aug. 1990 8 p Presented at the SPIE's International Symposium on Optical and Optoelectronic Applied Science and Engineering Exhibit, San Diego, CA, 8-13 Jul. 1990
(Contract DE-AC02-76CH-00016)
(DE91-001724; BNL-45154; CONF-900756-52) Avail: NTIS HC/MF A02

Scattering from mirror surfaces arises from topographic and non-topographic sources. This paper considers the nontopographic scattering of beryllium mirrors modelled as a collection of randomly oriented bireflective grains. Simple scattering theory shows that this type of scattering scales as lambda(exp -2), rather than as lambda(exp -4) for topographic scattering, which means that it is relatively more important at long radiation wavelengths. Estimates of the intensity based an available short-wavelength values of the anisotropic optical constants of beryllium indicate that this type of scattering could dominate the topographic scattering from smooth surfaces at CO2 wavelengths. DOE

N91-14827# British Columbia Univ., Vancouver. TRIUMF Facility.
AN INTENSE OPTICALLY PUMPED H(-) ION SOURCE
L. Buchmann, R. Burge, C. D. P. Levy, M. McDonald, R. Ruegg, P. W. Schmor, A. Belov, V. G. Polushkin, and A. Zelinskii (Academy of Sciences, USSR, Moscow) Jun. 1990 3 p Presented at the 2nd European Particle Accelerator Conference, Nice, France, 12-16 Jun. 1990
(DE91-002949; TRI-PP-90-42; CONF-900603-45) Avail: NTIS (US Sales Only) HC/MF A01

An optically pumped polarized ion source producing a DC H(-) current of 20 microA with a polarization in excess of 50 percent has been developed at TRIUMF. A 28 GHz Electron Cyclotron Resonance (ECR) source is used to provide an initial proton beam. A significant increase in polarized beam current was obtained using multihole extraction electrodes in an accel-accel mode. Three dye lasers were used to polarize the sodium charge exchange target. Recent laser optimization has significantly increased the power from the dye lasers. The sodium target has been lengthened from 10 to 23 cm and immersed in a 2.1 T longitudinal field to increase the H(-) polarization at the higher currents. The source design and recent pumping results are presented. DOE

N91-14828# Lawrence Livermore National Lab., CA.
INTEGRATED OPTICAL DEVICES FOR PHOTONICS INSTRUMENTATION SYSTEMS
G. M. McWright, D. A. Lafaw, M. Lowry, and W. Tindall 1990 8 p Presented at the International Conference on Optical Science and Engineering, Hague, Netherlands, 12-16 Mar. 1990 Submitted for publication
(Contract W-7405-eng-48)
(DE91-004192; UCRL-101486; CONF-900368-11) Avail: NTIS HC/MF A02

We discuss the design, fabrication, and evaluation of high speed integrated optical devices for application to photonics instrumentation systems. Specifically, we have demonstrated integrated optical devices with bandwidths in excess of 25 GHz and implemented these devices in single-shot, streak camera based recording schemes. DOE

N91-14829*# National Aeronautics and Space Administration. Lewis Research Center, Cleveland, OH.
VIBRATIONAL TESTING OF OPTICAL FIBER CONNECTOR JOINTS
Amy L. Sovie and George C. Madzsar 1990 10 p Presented at the 2nd Annual Conference on Health Monitoring for Space Propulsion Systems, Cincinnati, OH, 14-15 Nov. 1990; sponsored by Cincinnati Univ.
(NASA-TM-103654; E-5845; NAS 1.15:103654) Avail: NTIS HC/MF A02 CSCL 20F

An experimental study was performed to determine the effects of vibration on the propagation of light through SMA- and ST-type fiber-optic connectors. A multimode, fiber-optic link was vibrated from 0 to 10,000 Hz at a constant peak acceleration along the connector transverse and longitudinal axes. All other environmental parameters were ambient. Transfer characteristics through the connection were examined as a function of vibrational frequency using both laser and light-emitting diode (LED) light to illuminate the system. Slight differences in operation between the SMA and ST connectors were observed with no appreciative attenuation as a result of vibration. Vibration did cause the constant-amplitude input light to be modulated in the connector; however, the amplitude of vibration-induced noise was less than 3 standard deviations from the mean. Author

N91-14830# Columbia Univ., New York, NY. Radiation Lab.
SPONTANEOUS AND INDUCED COHERENT RADIATION GENERATION IN ATOMIC VAPORS Annual Report, 1 Nov. 1989 - 31 Oct. 1990
Sven Hartmann 14 Sep. 1990 7 p
(Contract N00014-88-K-0299)
(AD-A226776) Avail: NTIS HC/MF A02 CSCL 20/6

Experiments have been performed to study the nonlinear behavior of intense incoherent light propagating in an optical fiber; to study time delayed four-wave-mixing in semiconductor doped glasses and organic dyes and coherent light to generate attosecond beats in potassium vapor; to calculate the effect of the dynamic Lorentz shift on four-wave parametric interactions in a strongly driven two-level system as well as the distinct problem of the nonlinear intensity dependent frequency shift of the reflectivity from a gas dielectric interface; and to consider the problem of induced phase modulation by an incoherent pump, a diversion in studying an aspect of optical memories using photon echoes. GRA

N91-14831# Lowell Univ., MA. Dept. of Chemistry.
NONLINEAR OPTICS AND ORGANIC MATERIALS
Sukant Tripathy, Elizabeth Cavicchi, Jayant Kumar, and R. Sai Saikumar Oct. 1989 14 p Submitted for publication
(Contract N00014-90-J-1148)
(AD-A226953; TR-5) Avail: NTIS HC/MF A03 CSCL 20/6

In glancing through a flat windowpane we confront light's interaction with glass, but ignore it. We assume that the world's image is not perceptibly altered when light passes through the glass. Yet glass does play tricks with light: A penny viewed through a variety of lenses may appear the same size, magnified, reduced, or blurred. The shape of glass dictates the distortion of the image.

The 14th century craftsmen who first formed lenses from glass to aid those with deteriorating vision progressed by trial and error. Even Galileo used the exacting labor of grinding glass, without benefit of a practical theory of optics, to improve his pioneering telescope. The optics industry flourished for centuries before theory could minutely chart the interaction between light and glass. In this paper we will follow some of the newly laid routes into the domain of organic materials-materials that have such unusual responses to light that they undermine some of our intuitive assumptions about optics. The molecular structure of these organic materials can be custom designed to amplify their optical properties. Novel devices based on the optical phenomena manifested by organic materials may change communications and information processing. GRA

N91-14832# State Univ. of New York, Buffalo. Dept. of Chemistry.
SCALE-INVARIANT THEORY OF OPTICAL PROPERTIES OF FRACTAL CLUSTERS
Vadim A. Markel, Leonid S. Muratov, Mark I. Stockman, and Thomas F. George Sep. 1990 9 p
(Contract N00014-90-J-1193)
(AD-A227031; UBUFFALO/DC/90/TR-25) Avail: NTIS HC/MF A02 CSCL 20/6

Optical properties of fractal clusters are considered by means of a scale-invariant theory. Numerical simulations are carried out for three fractal types: self-avoiding walks, random walks and Witten-Sander's. Fractals are scale self-similar mathematical objects possessing nontrivial geometrical properties. There exist various physical realizations of fractals, and here we shall consider optical properties of what we believe to be one the most important such realizations, namely fractal clusters. A fractal cluster is a system of interacting material particles called monomers. GRA

N91-14833# Air Force Inst. of Tech., Wright-Patterson AFB, OH. School of Engineering.
OPTICAL PHASE CONJUGATION VIA STIMULATED BRILLOUIN SCATTERING IN MULTIMODE OPTICAL FIBER M.S. Thesis
Patrick T. Ryan Sep. 1990 70 p Sponsored in part by AFOSR and AFWL
(AD-A227054; AFIT/GEP/ENP/90S-1) Avail: NTIS HC/MF A04 CSCL 20/6

The main objective was to obtain phase conjugation of laser beam using the process of stimulated Brillouin scattering (SBS) in optical fiber and to characterize the parameters involved. SBS in fiber is used for several reasons: high conversion efficiency, nanosecond response time, only the signal beam is required and fiber has a lower SBS threshold and superior power handling capabilities compared to either crystals or liquids. SBS theory is briefly described along with some results from previous work. Experimental results show the multimode fiber losses at coupled powers below about 2 W to be 16.4 + or - 0.3 dB/km at 514.5 nm. The transmitted and backscattered power exhibited behavior similar to that previously reported for single-mode fiber. The SBS threshold power increased for shorter fibers and when index matching liquid was used. The Stokes shift was 32.78 + or - 0.02 GHz and the measured gain coefficient was 10.2 x (exp -9) cm/W with an error of 10 percent. Most importantly, nonlinear optical phase conjugation was demonstrated for the first time. The polarization state of the pump beam was not reproduced, however. In addition, the SBS power exhibited bursts of strong fluctuations. GRA

N91-14834# Dove Electronics, Inc., Rome, NY.
HYBRID OPTICAL PROCESSOR Final Technical Report, 1 Jul. 1987 - 30 Jul. 1990
J. F. Dove, F. T. Yu, and C. Eldering Aug. 1990 110 p
(Contract F19628-87-C-0086; AF Proj. 2305)
(AD-A227163; RADC-TR-90-256) Avail: NTIS HC/MF A06 CSCL 20/6

Recent advances of programmable spatial light modulators (SLM) have permitted the synthesis of hybrid signal processors for various computational needs. In accordance with this research program, various types of hybrid optical architectures were developed and synthesized which are capable of performing tasks such as: multiple matrix computation, hybrid optical computing, optical binary adder, optical perfect shuffle, application of associative memory to symbolic substitution, acousto optic joint transform correlator for space integration and frequency shift keying applications, hard clipping joint transform correlator, and programmable multichannel optical correlator for automatic scanning image detection. The basic architecture of these hybrid optical processors is a microcomputer-based design utilizing various types of spatial light modulators. The configuration of these hybrid optical architectures and discussion of the operation of these systems are presented. GRA

N91-14835* National Aeronautics and Space Administration. Marshall Space Flight Center, Huntsville, AL.
X RAY SENSITIVE AREA DETECTION DEVICE Patent
Daniel C. Carter, inventor (to NASA), William K. Witherow, inventor (to NASA), Marc L. Pusey, inventor (to NASA), and Vaughn H. Yost, inventor (to NASA) 12 Jun. 1990 14 p Filed 31 Jan. 1989
(NASA-Case-MFS-28232-1; US-Patent-4,933,558; US-Patent-Appl-SN-304155; US-Patent-Class-250-327.2; US-Patent-Class-250-484.1; Int-Patent-Class-G01N-23/20; Int-Patent-Class-H05B-33/00) Avail: US Patent and Trademark Office CSCL 20F

A radiation sensitive area detection device is disclosed which comprises a phosphor-containing film capable of receiving and storing an image formed by a pattern of incoming x rays, UV, or other radiation falling on the film. The device is capable of fluorescing in response to stimulation by a light source in a manner directly proportional to the stored radiation pattern. The device includes: (1) a light source capable of projecting light or other appropriate electromagnetic wave on the film so as to cause it to fluoresce; (2) a means to focus the fluoresced light coming from the phosphor-containing film after light stimulation; and (3) at least one charged coupled detector or other detecting element capable of receiving and digitizing the pattern of fluoresced light coming from the phosphor-containing film. The device will be able to generate superior x ray images of high resolution from a crystal or other sample and will be particularly advantageous in that instantaneous near-real-time images of rapidly deteriorating samples can be obtained. Furthermore, the device can be made compact and sturdy, thus capable of carrying out x ray or other radiation imaging under a variety of conditions, including those experienced in space.
Official Gazette of the U.S. Patent and Trademark Office

N91-14995*# Laboratoire d'Astronomie Spatiale, Marseille (France).
OPTICAL PROPERTIES OF IRREGULAR INTERSTELLAR GRAINS
J. M. Perrin and P. L. Lamy *In* NASA, Ames Research Center, Interstellar Dust: Contributed Papers Dec. 1989 p 381-388
(For primary document see N91-14897 06-88)
Avail: NTIS HC/MF A22 CSCL 20F

75 PLASMA PHYSICS

Includes magnetohydrodynamics and plasma fusion.
For ionospheric plasmas see *46 Geophysics*. For space plasmas see *90 Astrophysics*.

N91-14836# Ceskoslovenska Akademie Ved, Prague. Inst. of Plasma Physics.
LINEAR RESONANT INTERACTION OF AN ELECTROMAGNETIC WAVE WITH A COLLISIONAL INHOMOGENEOUS PLASMA
J. Lacina Nov. 1989 37 p
(IPPCZ-298) Avail: NTIS HC/MF A03

A solution of the time evolution to the steady state for an

obliquely incident P-polarized wave on an inhomogeneous collisional plasma with resonant density is presented. The solution reveals a close connection between the collisionless interaction with the steady state collisional one. The time-asymptotic evolution of total energies is given. An analogy between this process and that of Landau damping is presented. Author

N91-14837# Ceskoslovenska Akademie Ved, Prague. Inst. of Plasma Physics.
PHASE CHANGES DURING PLASMA SPRAY DEPOSITION
P. Chraska, J. Dubsky, B. Kolman, and P. Raus Nov. 1990 20 p
(IPPCZ-297) Avail: NTIS HC/MF A03

Plasma sprayed coatings are now widely used in various fields of application and therefore a considerable effort is aimed toward the description, understanding, and control of particular processes and mechanisms governing the formation and properties of coating. Generally, there are several tens of process variables determining the output, but very often the struggle for a required property is solved only through a chemical modification of the injected powder. Concentrations of the accompanying stabilizing elements in a certain powder are optimized but frequently this is only from the equilibrium data while the plasma spraying is definitely a nonequilibrium process. Experimental evidence shows a great variety of phase changes taking place during the plasma duration. Sometimes they can be beneficial as in the case of the formation of amorphous phases for certain purposes. At other times they can be very detrimental as in the case of alpha/gamma Al2O3 formation. Hence it is very important to study all the possible mechanisms of phase changes during the plasma deposition (what can cause them, and at what stage of the process they can occur). A contribution in this direction is presented describing results obtained from detailed studies of several metallic as well as ceramic materials. Author

N91-14838# Los Alamos National Lab., NM.
FAST ELECTRON STUDIES IN THE ZT-40M EDGE PLASMA
J. C. Ingraham, R. F. Ellis, J. N. Downing, G. Miller, C. P. Munson, M. M. Pickrell, K. F. Schoenberg, P. G. Weber, and G. A. Wurden 1990 20 p Presented at the International School of Plasma Physics, Varenna, Italy, 15-19 Oct. 1990
(Contract W-7405-eng-36)
(DE91-002323; LA-UR-90-3456; CONF-9010230-4) Avail: NTIS HC/MF A03

Measurements of the edge plasma on the ZT-40M Reversed Field Pinch (RFP) show the presence of a dilute (1 to 10 percent of the edge density), fast (T(sub H) approximately equal to (2-3)T(sub (epsilon)0)) electron tail with a nearly unidirectional flow along B in a toroidal sense that is against the external applied electric field force. These studies have been extended over a wide range of operating conditions including high density and krypton-injected radiation-dominated (P(sub RAD) approximately equal to 0.9 P(sub IN)) discharges. In all cases the current density of the fast electrons is sufficient to account for the current density required to maintain the RFP. For low current 60 kA discharges this result has been confirmed in to a depth 20 mm inside of the reversal surface suggesting that the source of the fast electrons is the core of the discharge. The fast electrons also carry a large power flux parallel to B (several hundreds of MW/sq m, typically), and radial transport measurements of the fast electrons in the shadow of a movable limiter for 120 kA standard discharges indicate that the fast electrons are the primary electron energy loss channel. The fast electrons are a significant energy loss channel for a broad range of other cases as well. The collisionality of the fast electrons varies widely over the range of cases studied and it is noted that a small backflowing component of fast electrons increases in relative size as the collisionality increases. An estimate of the magnetic field stochastic diffusivity at the edge is made from the fast electron limiter shadow measurements and shows that the stochasticity of the magnetic field is low at the edge relative to the core. This is in agreement with magnetic fluctuation diffusivity measurements and MHD simulations. DOE

N91-14839# Oak Ridge National Lab., TN.
FUELING OF MAGNETICALLY CONFINED PLASMAS BY SINGLE- AND TWO-STAGE REPEATING PNEUMATIC PELLET INJECTORS
M. J. Gouge, S. K. Combs, C. R. Foust, and S. L. Milora 1990 14 p Presented at the Annual Meeting of the Aeroballistic Range Association, San Diego, CA, 22-25 Oct. 1990
(Contract DE-AC05-84OR-21400)
(DE91-002635; CONF-9010227-2) Avail: NTIS HC/MF A03

Advanced plasma fueling systems for magnetic fusion confinement experiments are under development at Oak Ridge National Laboratory (ORNL). The general approach is that of producing and accelerating frozen hydrogenic pellets to speeds in the kilometer-per-second range using single shot and repetitive pneumatic (light-gas gun) pellet injectors. The millimeter-to-centimeter size pellets enter the plasma and continuously ablate because of the plasma electron heat flux, depositing fuel atoms along the pellet trajectory. This fueling method allows direct fueling in the interior of the hot plasma and is more efficient than the alternative method of injecting room temperature fuel gas at the wall of the plasma vacuum chamber. Single-stage pneumatic injectors based on the light-gas gun concept have provided hydrogenic fuel pellets in the speed range of 1 to 2 km/s in single-shot injector designs. Repetition rates up to 5 Hz have been demonstrated in repetitive injector designs. Future fusion reactor-scale devices may need higher pellet velocities because of the larger plasma size and higher plasma temperatures. Repetitive two-stage pneumatic injectors are under development at ORNL to provide long-pulse plasma fueling in the 3 to 5 km/s speed range. Recently, a repeating, two-stage light-gas gun achieved repetitive operation at 1 Hz with speeds in the range of 2 to 3 km/s. DOE

N91-14840# Oak Ridge National Lab., TN.
CHARACTERISTICS AND POTENTIAL APPLICATIONS OF AN ORNL MICROWAVE ECR MULTICUSP PLASMA ION SOURCE
C. C. Tsai 1990 22 p Presented at the 10th International Workshop on ECR Ion Sources, Knoxville, TN, 1-2 Nov. 1990
(Contract DE-AC05-84OR-21400)
(DE91-002649; CONF-9011136-1) Avail: NTIS HC/MF A03

A new microwave electron cyclotron resonance (ECR) multicusp plasma ion source that has two ECR plasma production regions and uses multicusp plasma confinement has been developed at Oak Ridge National Laboratory. This source has been operated to produce uniform and dense plasma over large areas of 300 to 400 sq cm and could be scaled up to produce uniform plasma over 700 sq cm or larger. The plasma source has been operated with continuous argon gas feed and pulsed microwave power. The working gases used were argon, helium, hydrogen, and oxygen. The discharge initiation phenomena and plasma properties have been investigated and studied as functions of the discharge parameters. The discharge characteristics and a hypothetical discharge mechanism for this plasma source are described and discussed. Potential applications, including plasma and ion-beam sources for manufacturing advanced microelectronics, space electric propulsion, and fusion research, are discussed. DOE

N91-14841# KMS Fusion, Inc., Ann Arbor, MI.
EXPERIMENTAL DEVELOPMENT, TESTING AND RESEARCH WORK IN SUPPORT OF THE INERTIAL CONFINEMENT FUSION PROGRAM Semiannual Report, Oct. 1989 - Mar. 1990
Roy Johnson, ed., Ruth Luckhardt, ed., Nancy Terry, ed., Douglas Drake, ed., and James Gaines, ed. 27 Apr. 1990 184 p
(Contract DE-AC03-87DP-10560)
(DE91-002771; KMSF-U-2375) Avail: NTIS HC/MF A09

This KMS Fusion Semi-Annual Technical Report covers the period October 1989 through March 1990. It contains a review of work performed by KMS Fusion, Inc. (KMSF), in support of the national program to achieve inertially confined fusion (ICF). A major section of the report is devoted to target technology, a field which is expected to play an increasingly important role in the overall KMSF fusion effort. Among the highlights of our efforts in this area covered in this report are: improvements and new

developments in target fabrication techniques, including a discussion of techniques for introducing Gaussian bumps and bands on target surfaces; development of a single automated system for the interferometric characterization of transparent shells; residual gas analysis of the blowing gases contained in glass shells made from xerogels. These usually include CO2, O2 and N2, and are objectionable because they dilute the fuel. Efforts to observe the ice layers formed in the beta-layering process in cryogenic targets, and to simulate the formation of these layers. In addition to our work on target technology, we conducted experiments with the Chroma laser and supported the ICF effort at other labs with theoretical and computational support as well as diagnostic development. Included in the work covered in this report are: experiments on Chroma to study interpenetration of and ionization balance in laser generated plasmas; diagnostic development, including an optical probe for the Aurora laser at Los Alamos National Laboratory, and a high energy x ray continuum spectrograph for Aurora; investigation of the radiation cooling instability as a possible mechanism for the generation of relatively cold, dense jets observed in ICF experiments. DOE

N91-14842# Lawrence Livermore National Lab., CA.
PHYSICS DATA BASE FOR THE BEAM PLASMA NEUTRON SOURCE (BPNS)
F. H. Coensgen, T. A. Casper, D. L. Correll, C. C. Damm, A. H. Futch, and A. W. Molvik 12 Oct. 1990 21 p Presented at the Workshop on Physics of Alternative Magnetic Confinement Schemes, Varenna, Italy, 15-24 Oct. 1990
(Contract W-7405-eng-48)
(DE91-002796; UCRL-JC-103736; CONF-9010209-5) Avail: NTIS HC/MF A03

A 14-MeV deuterium-tritium (D-T) neutron source for accelerated end-of-life testing of fusion reactor materials has been designed on the basis of a linear two-component collisional plasma system. An intense flux (up to 5 x 10(exp 18)/sq m sec) of 14 MeV neutrons is produced in a fully ionized high-density (n sub e approx. = 3 x 10(exp 21) per cu m) tritium target by transverse injection of 60 MW of neutral beam power. Power deposited in the target is removed by thermal electron conduction to large end chambers, where it is deposited in gaseous plasma collectors. We show in this paper that the major physics issues have now been experimentally demonstrated. These include magnetohydrodynamic (MHD) equilibrium and stability, microstability, startup, fueling, Spitzer electron thermal conductivity, and power deposition in a gaseous plasma collector. However, an integrated system was not demonstrated. DOE

N91-14843# Ohio State Univ., Columbus. Dept. of Aeronautical and Astronautical Engineering.
IR AND FIR LASER DIAGNOSTICS FOR PLASMA THRUSTERS USING A CW CO2 RADIATION SOURCE Final Report, 1 May 1989 - 30 Apr. 1990
Thomas M. York Jul. 1990 42 p
(Grant AF-AFOSR-0297-89; AF Proj. 2308)
(AD-A226816; AFOSR-90-1030TR) Avail: NTIS HC/MF A03 CSCL 21/3

The accomplishments during this contract period have been related to the development of a multi-beam interferometer system, which would utilize a CO2 laser system for high sensitivity, to eventually be used to diagnose plasma in the electromagnetic expansion region of a plasma thruster. Since the application of interest is a 1/4 Scale MPD experiment, funded by NASA, where plasma is poorly known, the CO2 laser interferometer will first be tested with a single beam on a DC discharge experiment whose plasma characteristics are well known. That experiment has been assembled and tested. The CO2 laser system has been tested and found to be satisfactory. GRA

N91-14844# Sandia National Labs., Albuquerque, NM.
CHARACTERIZATION OF ELECTRON CYCLOTRON RESONANCE HYDROGEN PLASMAS
C. A. Outten (Michigan Univ., Ann Arbor.), J. C. Barbour, and W. R. Wampler 1990 20 p Presented at the 37th National American Vacuum Society Symposium, Toronto, Ontario, 8-12 Oct. 1990
(Contract DE-AC04-76DP-00789)
(DE91-001250; SAND-90-1387C; CONF-901035-9) Avail: NTIS HC/MF A03

Electron cyclotron resonance (ECR) plasmas yield low energy and high ion density plasmas. The characteristics downstream of an ECR hydrogen plasma were investigated as a function of microwave power and magnetic field. A fast-injection Langmuir probe and a carbon resistance probe were used to determine plasma potential (V(sub p)), electron density (N(sub e)), electron temperature (T(sub e)), ion energy (T(sub i)), and ion fluence. Langmuir probe results showed that at 17 cm downstream from the ECR chamber the plasma characteristics are approximately constant across the center 7 cm of the plasma for 50 Watts of absorbed power. These results gave V(sub p) = 30 +/- 5 eV, N(sub e) = 1x10(exp 8) cm(exp -3), and T(sub e) = 10-13 eV. In good agreement with the Langmuir probe results, carbon resistance probes have shown that T(sub i) is less than or equal to 50 eV. Also, based on hydrogen chemical sputtering of carbon, the hydrogen (ion and energetic neutrals) fluence rate was determined to be 1x10(exp 16)/sq cm-sec at a pressure of 1x10(exp -4) Torr and for 50 watts of absorbed power. DOE

N91-14845# Oak Ridge National Lab., TN. Fusion Energy Div.
ITER GLOBAL STABILITY LIMITS
J. T. Hogan and N. A. Uckan 1990 16 p Presented at the 9th Topical Meeting on Technology of Fusion Energy, Oak Brook, IL, 7-11 Oct. 1990
(Contract DE-AC05-84OR-21400)
(DE91-001488; CONF-901007-19) Avail: NTIS HC/MF A03

The MHD stability limits to the International Thermonuclear Experimental Reactor (ITER) operational space have been examined with the PEST ideal stability code. Constraints on ITER operation have been examined for the nominal operational scenarios and for possible design variants. Rather than rely on evaluation of a relatively small number of sample cases, the approach has been to construct an approximation to the overall operational space, and to compare this with the observed limits in high-beta tokamaks. An extensive database with approximately 20,000 stability results has been compiled for use by the ITER design team. Results from these studies show that the design values of the Troyon factor (g approximately 2.5 for ignition studies, and g approximately 3 for the technology phase) are also expected to be attainable for ITER conditions which differ in configuration and wall-stabilization environment from those in present experiments. Strongly peaked pressure profiles lead to degraded high-beta performance. Values of g approximately equal to 4 are found for a higher safety factor (q(sub psi) greater than or equal to 4) than that of the present design (q(sub psi) approximately equal to 3). Profiles with q(0) less than 1 are shown to give g approximately equal to 2.5, if the current density profile provides optimum shear. The overall operational spaces are presented for g-q(sub psi), q(sub psi)-1(sub i), q-alpha(sub p) and l(sub i)-q(sub psi). DOE

N91-14846# General Atomic Co., San Diego, CA.
WALL CONDITIONING AND PLASMA SURFACE INTERACTIONS IN DIII-D
G. L. Jackson, P. I. Petersen, M. S. Schaffer, P. L. Taylor, T. S. Taylor, B. L. Doyle, D. S. Walsh, D. N. Hill, W. L. Hsu, and J. Winter (Kernforschungsanlage, Juelich, Germany, F.R.) Sep. 1990 5 p Presented at the 16th Symposium on Fusion Technology, London, England, 3-7 Sep. 1990 Submitted for publication
(Contract DE-AC03-89ER-51114; GA Proj. 3466)
(DE91-001547; GA-A-20250; CONF-900918-14) Avail: NTIS HC/MF A01

Wall conditioning is used in DIII-D for both reduction of impurity influxes and particle control. The methods used include: baking, pulsed discharge cleaning, hydrogen glow cleaning, helium and neon glow conditioning, and carbonization. Helium glow wall conditioning applied before every tokamak discharge has been

effective in impurity removal and particle control and has significantly expanded the parameter space in which DIII-D operates to include limiter and ohmic H-mode discharges and higher (beta)(sub T) at low q. The highest values of divertor plasma current (3.0 MA) and stored energy (3.6 MJ) and peaked density profiles in H-mode discharges have been observed after carbonization. Divertor physics studies in DIII-D include sweeping the X-point to reduce peak heat loads, measurement of particle and heat fluxes in the divertor region, and erosion studies. The DIII-D Advanced Divertor has been installed and bias and baffle experiments will begin in the fall of 1991. DOE

N91-14847# General Atomic Co., San Diego, CA.
DIII-D RESULTS AND PLANS
R. Callis, P. Anderson, A. Colleraine, J. Smith, P. I. Petersen, and P. L. Taylor Sep. 1990 7 p Presented at the 16th Symposium on Fusion Technology, London, England, 3-7 Sep. 1990
(Contract DE-AC03-89ER-51114; GA Proj. 3466)
(DE91-001548; GA-A-20219; CONF-900918-13) Avail: NTIS HC/MF A02

The completion of additional radiation shielding in the spring of 1989 has allowed the DIII-D tokamak to enter a new phase of experimental operation, in which the potential of injecting deuterium beam injection into deuterium plasmas has been exploited. The benefit of the isotope effect in increased energy confinement time, and increased power delivery by the neutral beam injectors, has been used to extend the machine performance. Plasma beta values (beta(sub T) less than or equal to 10.7 percent) near expected theoretical limits (3.5 I/aB) have been obtained and high energy content discharges with beta(sub T) = 5.2 percent have been achieved at full magnetic field (2.1 T). The stored energy has reached 3.6 MJ and diverted plasmas with 3 MA have been produced. Enhanced (H-mode) energy confinement plasmas have been maintained for over 10 seconds with no indication of impurity accumulation. This paper presents a brief description of the shielding design; a discussion of the performance improvements of the neutral beam ion sources with deuterium; an overall review of plasma parameters achieved recently in the DIII-D tokamak; and a presentation of new hardware systems being brought on line (e.g., Advanced Divertor, Fast Wave Current Drive, and 110 GHz ECH). DOE

N91-14848# Massachusetts Inst. of Tech., Cambridge. Plasma Fusion Center.
A METHOD FOR ESTIMATING TOKAMAK POLOIDAL FIELD COIL CURRENTS WHICH INCORPORATES ENGINEERING CONSTRAINTS M.S. Thesis
William Andrew Stewart May 1990 147 p
(Contract DE-AC02-78ET-51013)
(DE91-001662; DOE/ET-51013/T231; PFC/RR-90-8) Avail: NTIS HC/MF A07

This thesis describes the development of a design tool for the poloidal field magnet system of a tokamak. Specifically, an existing program for determining the poloidal field coil currents has been modified to support the general case of asymmetric equilibria and coil sets, determine the coil currents subject to constraints on the maximum values of those currents, and determine the coil currents subject to limits on the forces those coils may carry. The equations representing the current limits and coil force limits are derived and an algorithm based on Newton's method is developed to determine a set of coil currents which satisfies those limits. The resulting program allows the designer to quickly determine whether or not a given coil set is capable of supporting a given equilibrium. DOE

N91-14849# Oak Ridge National Lab., TN.
TOKAMAK FLUIDLIKE EQUATIONS, WITH APPLICATIONS TO TURBULENCE AND TRANSPORT IN H MODE DISCHARGES
Y. B. Kim, H. Biglari, B. A. Carreras, P. H. Diamond, R. J. Groebner, O. J. Kwon, D. A. Spong, J. D. Callen, Z. Chang, and J. B. Hollenberg (Wisconsin Univ., Madison.) et al 1990 14 p Presented at the 13th International Conference on Plasma Physics and Controlled Nuclear Fusion Research, Washington, DC, 1-6 Oct. 1990 Submitted for publication
(Contract DE-AC05-84OR-21400)
(DE91-002632; IAEA-CN-53/D-4-13; CONF-901025-21) Avail: NTIS HC/MF A03

Significant progress has been made in developing tokamak fluidlike equations which are valid in all collisionality regimes in toroidal devices, and their applications to turbulence and transport in tokamaks. The areas highlighted in this paper include: the rigorous derivation of tokamak fluidlike equations via a generalized Chapman-Enskog procedure in various collisionality regimes and on various time scales; their application to collisionless and collisional drift wave models in a sheared slab geometry; applications to neoclassical drift wave turbulence (i.e. neoclassical ion-temperature-gradient-driven turbulence and neoclassical electron-drift-wave turbulence); applications to neoclassical bootstrap-current-driven turbulence; numerical simulation of nonlinear bootstrap-current-driven turbulence and tearing mode turbulence; and transport in Hot-Ion H mode discharges. DOE

N91-15050# Academy of Pedagogical Sciences of the USSR, Moscow. Dept. of Physics.
A NEW KIND OF MAGNETIC BUOYANCY INSTABILITY
N. I. Kleeorin and I. V. Rogachevskii (Academy of Sciences, USSR, Troitsk) *In* ESA, Plasma Astrophysics Aug. 1990 p 21-23 (For primary document see N91-15046 06-90)
Copyright Avail: NTIS HC/MF A14

N91-15057# Universidad de Los Andes, Merida (Venezuela). Facultad de Ciencias.
ON THE THERMAL STABILITY OF SLABS, CYLINDERS, AND SPHERES
M. H. Ibanez and F. Plachco *In* ESA, Plasma Astrophysics Aug. 1990 p 45-48 (For primary document see N91-15046 06-90)
Copyright Avail: NTIS HC/MF A14

N91-15063# Academy of Sciences (USSR), Moscow. Inst. of Space Research.
DETECTION OF NONLINEAR FEATURES IN PLASMA AND FIELD MEASUREMENTS BY PROGNOZ-8
A. Yu. Sokolov, I. Kh. Khabibrakhmanov, M. M. Kuznetsova, J. Lemaire, M. Roth, J. M. Lesceux, and F. Verheest (Ghent Univ., Belgium) *In* ESA, Plasma Astrophysics Aug. 1990 p 81-85 (For primary document see N91-15046 06-90)
Copyright Avail: NTIS HC/MF A14

N91-15065# Academy of Sciences (USSR), Moscow. Inst. of Space Research.
GRADIENT CATASTROPHE OF THE SUPERSONIC MASS-LOADED MAGNETISED PLASMA FLOW AND THE FORMATION OF BOW SHOCK
A. A. Galeev and I. Kh. Khabibrakhmanov *In* ESA, Plasma Astrophysics Aug. 1990 p 95-98 (For primary document see N91-15046 06-90)
Copyright Avail: NTIS HC/MF A14

N91-15067# Academy of Sciences (USSR), Troitsk. Inst. of Terrestrial Magnetism, Ionosphere, and Radio Wave Propagation.
NONSTATIONARY PROCESSES IN THE FRONT OF HIGH MACH NUMBER COLLISIONLESS QUASIPERPENDICULAR SHOCK: DYNAMICS OF THE ION DISTRIBUTION
V. V. Krasnoselskikh, V. V. Lobzin, and V. B. Roznov (Academy of Sciences, USSR, Moscow) *In* ESA, Plasma Astrophysics Aug. 1990 p 103-107 (For primary document see N91-15046 06-90)
Copyright Avail: NTIS HC/MF A14

N91-15071# Kharkov State Univ. (USSR).
DESCRIPTION OF NONLINEAR EFFECTS IN A RELATIVISTIC PLASMA USING HAMILTONIAN FORMALISM
V. V. Gulenko and V. V. Gushchin *In* ESA, Plasma Astrophysics Aug. 1990 p 129-131 (For primary document see N91-15046 06-90)
Copyright Avail: NTIS HC/MF A14

N91-15072# Abastumani Astrophysical Observatory, Georgia (USSR).
HYDRODYNAMICS OF COLLISIONLESS RELATIVISTIC PLASMA IN A STRONG MAGNETIC FIELD
J. G. Lominadze, J. I. Javakhishvili (Tbilisi State Univ., USSR), and E. G. Tsikarishvili *In* ESA, Plasma Astrophysics Aug. 1990 p 133-137 (For primary document see N91-15046 06-90)
Copyright Avail: NTIS HC/MF A14

N91-15073# Academy of Sciences (USSR), Moscow. Inst. of Space Research.
WAVE COLLAPSE AT LOWER HYBRID RESONANCE
V. P. Kalinen, R. Z. Sagdeev, V. D. Shapiro, V. I. Shevchenko, G. I. Soloviev, and M. Ashour-Abdalla (California Univ., Los Angeles.) *In* ESA, Plasma Astrophysics Aug. 1990 p 139-145 (For primary document see N91-15046 06-90)
Copyright Avail: NTIS HC/MF A14

N91-15075# Academy of Sciences (USSR), Leningrad. Inst. of Physics and Technology.
MASER CYCLOTRON INSTABILITY IN A PLASMA WITH ANISOTROPIC DISTRIBUTION FUNCTION
V. G. Bezchastanov and G. G. Pavlov *In* ESA, Plasma Astrophysics Aug. 1990 p 153-158 (For primary document see N91-15046 06-90)
Copyright Avail: NTIS HC/MF A14

N91-15077# Academy of Sciences (USSR), Gorky. Inst. of Applied Physics.
GENERATION OF INDUCTIVE FIELDS BY AN OBLIQUE MAGNETIC ROTATOR IN COLLISIONLESS PLASMA
V. M. Gubchenko and M. L. Khodachenko *In* ESA, Plasma Astrophysics Aug. 1990 p 163-168 (For primary document see N91-15046 06-90)
Copyright Avail: NTIS HC/MF A14

N91-15078# Academy of Sciences (USSR), Leningrad. A.F. Ioffe Inst. of Physics and Technology.
ANNIHILATION RADIATION OF STRONGLY-MAGNETISED ELECTRON-POSITRON PLASMA WITH POWER-LAW DISTRIBUTIONS OF PARTICLES
A. D. Kaminker, G. G. Pavlov, and P. G. Mamradze (Abastumani Astrophysical Observatory, Georgia, USSR) *In* ESA, Plasma Astrophysics Aug. 1990 p 169-173 (For primary document see N91-15046 06-90)
Copyright Avail: NTIS HC/MF A14

N91-15079# Nagoya Univ. (Japan). Dept. of Electrical Engineering.
OBSERVATION OF ELECTRON HOLE, DOUBLE LAYER, AND TURBULENT HEATING IN A LABORATORY PLASMA
T. Tsukishima and H. Inuzuka *In* ESA, Plasma Astrophysics Aug. 1990 p 177-182 (For primary document see N91-15046 06-90)
Copyright Avail: NTIS HC/MF A14

N91-15081# Academy of Sciences (USSR), Novosibirsk. Inst. of Pure and Applied Mechanics.
LABORATORY SIMULATION OF THE ASTROPHYSICAL BURST PROCESSES IN NON-UNIFORM MAGNETISED MEDIA
V. M. Antonov, Yu. P. Zakharov, A. M. Orishich, A. G. Ponomarenko, V. G. Posukh, V. N. Snytnikov, and V. O. Stoyanovsky *In* ESA, Plasma Astrophysics Aug. 1990 p 189-190 (For primary document see N91-15046 06-90)
Copyright Avail: NTIS HC/MF A14

N91-15082# Academy of Sciences (USSR), Novosibirsk. Inst. of Pure and Applied Mechanics.
LABORATORY AND COMPUTER SIMULATIONS OF WAVE GENERATION PROCESSES IN NON-STATIONARY ASTROPHYSICAL PHENOMENA
G. I. Dudnikova, A. M. Orishich, A. G. Ponomarenko, V. A. Vshivkov, and Yu. P. Zakharov *In* ESA, Plasma Astrophysics Aug. 1990 p 191-194 (For primary document see N91-15046 06-90)
Copyright Avail: NTIS HC/MF A14

N91-15084# Texas Univ., Austin. Inst. for Fusion Studies.
MAGNETICALLY DRIVEN JETS AND WINDS
R. V. E. Lovelace (Cornell Univ., Ithaca, NY.) *In* ESA, Plasma Astrophysics Aug. 1990 p 201-206 Sponsored by the Guggenheim Foundation (For primary document see N91-15046 06-90)
(Contract DE-FG05-80ET-53088)
Copyright Avail: NTIS HC/MF A14

N91-15085# Ecole Polytechnique, Palaiseau (France). Centre de Physique Theorique.
NONLINEAR PLASMA EFFECTS IN THE ENVIRONMENT OF ACTIVE GALACTIC NUCLEI
E. Asseo, G. Pelletier, and H. Sol (Observatoire de Paris-Meudon, France) *In* ESA, Plasma Astrophysics Aug. 1990 p 207-213 (For primary document see N91-15046 06-90)
Copyright Avail: NTIS HC/MF A14

N91-15095# Abastumani Astrophysical Observatory, Georgia (USSR).
LARGE-SCALE VORTICES IN COMPRESSIBLE TURBULENT MEDIUM WITH THE MAGNETIC FIELD
V. V. Gvaramadze and B. G. Dimitrov (Bulgarian Academy of Sciences, Sofia.) *In* ESA, Plasma Astrophysics Aug. 1990 p 263-267 (For primary document see N91-15046 06-90)
Copyright Avail: NTIS HC/MF A14

76 SOLID-STATE PHYSICS

Includes superconductivity.

For related information, see also *33 Electronics and Electrical Engineering* and *36 Lasers and Masers.*

N91-14850*# National Aeronautics and Space Administration. Lewis Research Center, Cleveland, OH.
SILICON CARBIDE, A SEMICONDUCTOR FOR SPACE POWER ELECTRONICS
J. Anthony Powell and Lawrence G. Matus 1991 8 p Presented at the 8th Symposium on Space Nuclear Power Systems, Albuquerque, NM, 6-10 Jan. 1991; cosponsored by New Mexico Univ., Strategic Defense Initiative Organization, DOE, and AF
(NASA-TM-103655; NAS 1.15:103655) Avail: NTIS HC/MF A02 CSCL 20L

After many years of promise as a high temperature semiconductor, silicon carbide (SiC) is finally emerging as a useful electronic material. Recent significant progress that has led to this emergence has been in the areas of crystal growth and device fabrication technology. High quality single-crystal SiC wafers, up to 25 mm in diameter, can now be produced routinely from boules grown by a high temperature (2700 K) sublimation process. Device fabrication processes, including chemical vapor deposition (CVD), in situ doping during CVD, reactive ion etching, oxidation, metallization, etc. have been used to fabricate p-n junction diodes and MOSFETs. The diode was operated to 870 K and the MOSFET to 770 K. Author

N91-14851# Devcom, Inc., Framingham, MA.
PROGRAM TO STUDY THE PROCESS PARAMETERS OF OMVPE AND THEIR RELATIONSHIP TO THE PROPERTIES OF Ga(0.47)In(0.53) AS ON InP SUBSTRATES Final Technical Report, Jun. 1984 - Mar. 1988
I. Ahmed Nov. 1989 175 p
(Contract F19628-84-C-0066; AF Proj. 4600)
(AD-A226618; RADC-TR-89-224) Avail: NTIS HC/MF A08 CSCL 11/6

The purpose of the work was a study of the process parameters of the organometallic vapor phase epitaxy technique and their relationship to the properties of gallium indium arsenide lattice matched to indium phosphide. The study was an extension of an

earlier study at atmospheric to low pressure conditions and shows that the effects of parasitic reactions can be essentially eliminated by low pressures. The work has established ranges of operation (temperature and pressures) for high quality material with a high degress of compositional uniformity over the substrate. Some problem areas have been designated which can be encountered in the growth of the lattice matched composition. Methods for their resolution have been presented. Specific criteria for scale-up have been identified and methods for their implementation presented. GRA

N91-14852# Lawrence Livermore National Lab., CA.
A CHARACTERIZATION OF INTERNAL-Sn Nb3 Sn SUPERCONDUCTORS FOR USE IN THE PROOF OF PRICIPLES (PoP) COIL
L. T. Summers, A. R. Duenas, C. E. Karlsen, G. M. Ozeryansky, and E. Gregory (Intermagnetics General Corp., Waterbury, CT.) 21 Sep. 1990 6 p Presented at the Applied Superconductivity Conference, Aspen, CO, 24-28 Sep. 1990
(Contract W-7405-eng-48)
(DE91-001743; UCRL-JC-103491; CONF-900944-13) Avail: NTIS HC/MF A02

High performance Ti-alloyed internal-Sn superconductors have been selected for use in the Proof of Principles (PoP) coil, and a 1.0 m o.d., 0.4 m i.d., solenoid designed to produce fields up to 15 T. The PoP coil, which will use forced-flow Cable-In-Conduit Conductors (CICC), will operate at 4.2 K and moderate levels of conductor strain. Here we report the results of detailed characterizations of two proposed PoP coil Nb(sub 3)Sn 19 subelement superconductor wires of different topology. We have investigated the critical current as a function of applied field, and applied strain. The wires were found to have excellent high field properties, providing a high performance margin for the proposed PoP coil. The field and strain dependence of J(sub c) have been found to compare favorably with predictions from a wire performance model recently developed for Nb(sub 3)Sn superconductors. DOE

N91-14853# Sandia National Labs., Albuquerque, NM.
FTIR (FOURIER TRANSFORM INFRARED) SPECTROPHOTOMETRY FOR THIN FILM MONITORS: COMPUTER AND EQUIPMENT INTEGRATION FOR ENHANCED CAPABILITIES
J. N. Cox, J. Sedayao, G. Shergill, R. Villasol, and D. M. Haaland 1990 10 p Presented at the International Semiconductor Manufacturing Science Symposium, Burlingame, CA, 21-23 May 1990 Prepared in cooperation with INTEL Corp., Santa Clara, CA
(Contract DE-AC04-76DP-00789)
(DE91-001228; SAND-89-2738C; CONF-9005284-1) Avail: NTIS HC/MF A02

Fourier transform infrared spectrophotometry (FTIR) is a valuable technique for monitoring thin films used in semiconductor device manufacture. Determinations of the constituent contents in borophosphosilicate (BPSG), phosphosilicate (PSG), silicon oxynitride (SiON:H,OH), and spin-on-glass (SOG) thin films are a few applications. Due to the nature of the technique, FTIR instrumentation is one of the most extensively computer-dependent pieces of equipment that is likely to be found in a microelectronics plant. In the role of fab monitor or reactor characterization tool, FTIR instruments can rapidly generate large amounts of data. By linking a local FTIR data station to a remote minicomputer its capabilities are greatly improved. We discuss three caused of enhancement. First, the FTIR in the fab area communicates and interacts in real time with the minicomputer: transferring data segments to it, instructing it to perform sophisticated processing, and returning the result to the operator in the fab. Characterizations of PSG thin films by this approach are discussed. Second, the spectra of large numbers of samples are processed locally. The large database is then transmitted to the minicomputer for study by statistical/graphics software. Results of CVD-reactor spatial profiling experiments for plasma SiON are presented. Third, processing of calibration spectra is performed on the minicomputer to optimize the accuracy and precision of a Partial Least Squares analysis mode. This model is then transferred to the data station in the fab. The analysis of BPSG thin films is discussed in this regard. The prospects for fully automated at-line monitoring and for real-time, in-situ monitoring will be discussed. DOE

N91-14854# Sandia National Labs., Albuquerque, NM.
RISE TIME AND RECOVERY OF GaAs PHOTOCONDUCTIVE SEMICONDUCTOR SWITCHES
F. J. Zutavern, G. M. Loubriel, M. W. OMalley, D. L. McLaughlin, and W. D. Helgeson 1990 17 p Presented at the SPIE Symposium on LaserScience a nd Applications of Optics, Optically Activate Switching Conference, Boston, MA, 4-9 Nov. 1990 Sponsored in part by Navy
(Contract DE-AC04-76DP-00789)
(DE91-001267; SAND-90-1131C; CONF-9011125-1) Avail: NTIS HC/MF A03

Fast rise time applications have encouraged us to look at the rise time dependences of lock-on switching. Our tests have shown rise time and delay effects which decrease dramatically with increasing electric field across the switch and/or optical energy used in activating lock-on. Interest in high repetition rate photoconductive semiconductor switches (PCSS), which require very little trigger energy (our 1.5-cm long switches have been triggered with as little as 20 (mu)J), has also led us to investigate recovery from lock-on. Several circuits have been used to induce fast recovery, the fastest being 30 ns. The most reliable circuit produced a 4-pulse burst of +/(minus) 10-kV pulses at 7 MHz with 100-(mu)J trigger energy per pulse. DOE

N91-14855# Florida State Univ., Tallahassee. Helium Atom Surface Scattering Group.
He ATOM SURFACE SPECTROSCOPY: SURFACE LATTICE DYNAMICS OF INSULATORS, METALS, AND METAL OVERLAYERS Progress Report, 1 May 1985 - 30 Apr. 1991
S. A. Safron and J. G. Skofronick 1990 34 p
(Contract DE-FG05-85ER-45208)
(DE91-001993; DOE/ER-45208/6) Avail: NTIS HC/MF A03

During the first three years of this grant (1985 to 1988) the effort was devoted to the construction of a state-of-the-art He atom scattering (HAS) instrument which would be capable of determining the structure and dynamics of metallic, semiconductor or insulator crystal surfaces. The second three year grant period (1988 to 1991) has been dedicated to measurements. The construction of the instrument went better than proposed; it was within budget, finished in the proposed time and of better sensitivity and resolution than originally planned. The same success has been carried over to the measurement phase where the concentration has been on studies of insulator surfaces, as discussed in this paper. The experiments of the past three years have focused primarily on the alkali halides with a more recent shift to metal oxide crystal surfaces. Both elastic and inelastic scattering experiments were carried out on LiF, NaI, NaCl, RbCl, KBr, RbBr, RbI, CsF, CsI and with some preliminary work on NiO and MgO. DOE

N91-14856# Los Alamos National Lab., NM.
SUPERCONDUCTING PROPERTIES OF Tl-Ba-Ca-Cu-O FILMS ON SILVER SUBSTRATES
R. C. Dye, P. N. Arendt, J. A. Martin, K. M. Hubbard, N. Elliott, and G. Reeves 1990 5 p Presented at the Applied Superconductivity Conference, Aspen, CO, 24-28 Sep. 1990
(Contract W-7405-eng-36)
(DE91-002304; LA-UR-90-3408; CONF-900944-15) Avail: NTIS HC/MF A01

Films of Ba-Ca-Cu-O have been RF magnetron sputtered onto Consil 995 substrates. A post deposition anneal in an over pressure of Tl produces the superconducting 1212 and 2212 phases. Varying the annealing procedures changes the electrical properties of the final films dramatically. Dynamic impedance, a novel approach to the electrical characterization of these films on a conductive substrate is discussed and compared with SEM, XRD and RBS

measurements as a function of differing annealing protocols. DOE

N91-14857# Mound Lab., Miamisburg, OH.
SOLID STATE RADIOLUMINESCENT SOURCES USING ZEOLITES
John T. Gill, Daniel B. Hawkins, and Clifford L. Renschler (Sandia National Labs., Albuquerque, NM.) 1990 7 p Presented at the Radioluminescent Technology Conference, Annapolis, MD, 25-26 Sep. 1990
(Contracts DE-AC04-88DP-43495; DE-AC04-76DP-00789)
(DE91-002703; MLM-3663(OP); CONF-9009201-9) Avail: NTIS HC/MF A02

Inorganic zeolites show promise as an alternative to traditional tritium gas tube light sources. Greater proximity of tritium atoms and luminescing centers, as well as greater tritium loading density, have been obtained within the zeolite aluminosilicate matrix. Zeolites are in addition optically clear and radiation stable. The zeolite radioluminescence program is described. Procedures for obtaining light sources are presented and results are discussed. DOE

N91-14858# Colorado Univ., Boulder.
INVESTIGATION OF REDOX PROCESSES AT SEMICONDUCTOR ELECTRODE LIQUID JUNCTIONS Research Report, 15 Jul. 1987 - 14 Feb. 1991
Carl A. Koval Aug. 1990 16 p
(Contract DE-FG02-84ER-13247)
(DE91-001787; DOE/ER-13247/6) Avail: NTIS HC/MF A03

Research in fundamental aspects of photoelectrochemical cells has been in the following areas: chemical probes for hot carrier processes, electrostatic theory for describing electrical interactions at interfaces, and kinetics of electron transfer at ideal semiconductor solution interfaces. Our goal is to achieve a better understanding of dark and photo-induced current flow at the semiconductor electrode/redox electrolyte interface (SEI) so that devices and processes utilizing this interface for solar energy conversion can be developed or improved. Our most important accomplishment has been the development of a redox system capable of detecting hot electrons at the p-InP/acetonitrile interface. Also, we have examined electrostatic theory for the image potential of an ion as a function of distance from the SEI. Finally, our group was one of the first to realize that the 2-dimensional metal chalcogenides (MC) are excellent materials for fundamental studies of electron transfer at the SEI. One of the chief potential advantages for use of MC's is the formation of semiconductor/liquid junctions with nearly ideal electrochemical properties. DOE

N91-14859# City Univ. of New York Research Foundation, NY.
MAGNETIC PROPERTIES OF DOPED SEMICONDUCTORS
1990 9 p
(Contract DE-FG02-84ER-45153)
(DE91-002395; DOE/ER-45153/T3) Avail: NTIS HC/MF A02

Research continued on the transport behavior of doped semiconductors on both sides of the metal-insulator transition, and the approach to the transition from both the insulating and the metallic side. Work is described on magneto resistance of a series of metallic Si:B samples and CdSe. DOE

N91-14860# Oak Ridge National Lab., TN.
ION BEAM INDUCED DIFFUSION AND CRYSTALLIZATION IN HIGH DOSE Er IMPLANTED Si
A. Golanski (Centre National d'Etudes des Telecommunications, Meylan, France), W. H. Christie, M. D. Galloway, J. L. Park, S. J. Pennycook, D. B. Poker, J. L. Moore, H. E. Harmon, and C. W. White 1990 18 p Presented at the 7th International Conference on Ion Beam Modification of Materials, Knoxville, TN, 9-14 Sep. 1990
(Contract DE-AC05-84OR-21400)
(DE91-002869; CONF-900936-19) Avail: NTIS HC/MF A03

High doses (1x10(exp 16)-1x10(exp 17)/sq cm) of 145 keV and 175 keV Er(+) ions were implanted into single-crystal Si using implantation temperatures, T(sub i), between room temperature and 500 C. Implanted samples were subsequently annealed using thermal annealing at 800 C under vacuum as well as a 1 MeV As(+) ion beam assisted annealing (IBAA) at 300 C. During Er(+) implantation, we find evidence for ion beam induced mobility for T(sub i) as low as 300 C. A measurable redistribution of the implanted Er also occurs during the IBAA for Er doses greater than 5x10(exp 16)/sq cm. During Er(+) implantation at T(sub i) greater than 300 C a polycrystalline ErSi2 phase is formed. For T(sub i) greater than 400 C, the coherent precipitation of ErSi2 phase occurs within the crystalline Si matrix. During subsequent thermal annealing of samples implanted at T(sub i) greater than 400 C, the Er distribution narrows due to Ostwald ripening, and preferential alignment occurs to form a discontinuous buried layer of a single crystalline Er silicide. DOE

N91-14861# Brookhaven National Lab., Upton, NY.
IRREVERSIBILITY TEMPERATURES IN OXIDE- AND METALLIC SUPERCONDUCTORS
M. Suenaga, A. K. Ghosh, Youwen Xu, and D. O. Welch 1990 5 p Presented at the 3rd International Symposium on Superconductivity, Sendai, Japan, 6-9 Nov. 1990
(Contract DE-AC02-76CH-00016)
(DE91-004021; BNL-45324; CONF-901169-1) Avail: NTIS HC/MF A01

We measured the irreversibility temperatures, T sub r (H) for both oxides (pure and alloyed Y(123) and Bi(2212, 2223)) and metallic (Nb, NbTi, and Nb(sub 3)Sn) superconductors. These results are compared and discussed in terms of T sub r (H) being the depinning line and/or the melting line of the flux line (crystalline or disordered) lattice in the H-T plane. DOE

N91-14862# Massachusetts Inst. of Tech., Cambridge. Dept. of Materials Science and Engineering.
INVESTIGATION OF NEW SEMIINSULATING BEHAVIOR OF 3-5 COMPOUNDS Final Technical Report, 16 Aug. 1986 - 28 Feb. 1990
Jacek Lagowski 28 Feb. 1990 50 p
(Grant AF-AFOSR-0342-86; AF Proj. 2306)
(AD-A226787; AFOSR-90-0939TR) Avail: NTIS HC/MF A03 CSCL 20/6

Study of transition metal impurities have defined direct effects associated with deep donor/acceptor levels acting as compensating centers. Electrical and optical properties of vanadium and titanium levels were determined in GaAs. The experimental data provided basis for the verification of chemical trends and defined compositional range for III-V mixed crystals whereby semiinsulating behavior can be achieved using transition elements deep levels and a suitable codoping with shallow donor/acceptor impurities. GRA

N91-14863# Cornell Univ., Ithaca, NY.
ULTRA HIGH SPEED COMPOUND SEMICONDUCTORS AND REAL TIME SIGNAL PROCESSING Final Report, 1 May 1988 - 30 Apr. 1990
J. Peter Krusius 30 Jun. 1990 16 p
(Contract F49620-87-C-0044)
(AD-A226790; AFOSR-90-0914TR) Avail: NTIS HC/MF A03 CSCL 20/12

This report is the final report on research conducted under the auspices of the Joint Services Electronics Program at Cornell University. The research is grouped under two themes: (1) ultra high speed compound semiconductors, and (2) real time signal processing. Results on organometallic vapor phase epitaxy materials growth, femtosecond laser probing of hot carriers, and ensemble Monte Carlo simulations are reported on for the first theme. Accomplishments on VLSI algorithms, fault tolerant architectures, and architectures with multiple functional units for signal processing are given under the second theme. GRA

N91-14864# General Electric Co., Syracuse, NY. Electronics Lab.
PSEUDOMORPHIC InGaAs MATERIALS Final Technoical Report, Mar. 1988 - Jul. 1990

J. M. Ballingall, P. Ho, P. Martin, and T. Yu Aug. 1990 48 p
(Contract F49620-88-C-0054; AF Proj. 2305)
(AD-A226895; AFOSR-90-1037TR) Avail: NTIS HC/MF A03
CSCL 20/2

The objective of this program is to evaluate the dependence of pseudomorphic In(x)Ga(1-x)As quality on epitaxial growth conditions and In(x)Ga(1-x)As composition. All of the structures were fabricated by molecular beam epitaxy (MBE). The effects of different growth conditions were evaluated with a combination of characterization techniques, including Hall effect, Shubnikov-de Hass, photoreflectance, microwave reflectance, photoluminescence, transmission electron microscopy (TEM), and in-situ reflection high energy electron diffraction (RHEED). Critical layer thickness is shown to be a function of MBE growth temperature. Also, the interruption of In(x)Ga(1-x)As growth with a few monolayers of GaAs is shown to smoothen the In(x)Ga(1-x)As surface to provide strain relief, substantially extending the critical layer thickness. Modulation enhanced epitaxy is demonstrated to yield high quality pseudomorphic structures at temperatures as low as 300 C. Extensive materials characterization and modeling were applied to the structures, and excellent agreement was often obtained without resorting to adjustable parameters. GRA

N91-14865# Naval Weapons Center, China Lake, CA. Chemistry Div.
CRYSTAL STRUCTURE OF ZnGa2S4, A DEFECT SPHALERITE-DERIVATIVE Technical Report No. 1, Oct. 1989 - Sep. 1990
Charlotte K. Lowe-Ma and Terrell A. Vanderah Oct. 1990 23 p
Submitted for publication
(AD-A226937) Avail: NTIS HC/MF A03 CSCL 20/2

ZnGa2S4 crystallizes in the defect stannite structure which is related to sphalerite. Refinement of different models of cation distribution gave R values of 0.041 to 0.043 for 360 independent reflections. Of the models considered, the ordered model with Zn only at point set 2a and Ga only at point set at 4d was found to be worse, statistically, than models with some degree of cation disorder. Models with cation disorder are consistent with a previous review in which is was suggested that the displacement of the anion from the ideal (1/4, 1/4, 1/8) was insufficient in ZnGa2S4 to indicate cation ordering. Disorder amongst the cation sites is also consistent with reported Raman and photoluminescence results. The slight difference observed between the metal-sulfur bond lengths for the two crystallographic cation sites attributed to the differing effect of the vacancy on these sites rather than to cation ordering. GRA

N91-14866# Naval Weapons Center, China Lake, CA. Chemistry Div.
ON THE CRYSTAL STRUCTURE OF KInS2-I Technical Report No. 4, Oct. 1989 - Oct. 1990
Charlotte K. Lowe-Ma, D. O. Kipp, and Terrell A. Vanderah 5 Sep. 1990 17 p Submitted for publication Sponsored by ONR, Arlington, VA
(AD-A226940) Avail: NTIS HC/MF A03 CSCL 20/2

An x ray single-crystal structure determination has confirmed that KInS2-I has the TlGaSe2 structure. The bonding in KInS2-I is highly covalent and exhibits both two-dimensional and three-dimensional features. The structure is comprised of layers of vertex-sharing (In4S10) adamantane-like units built of (InS4) tetrahedra. The stacking arrangement of these layers creates channels that contain the potassium ions in distorted trigonal prismatic sites that provide the three-dimensionality of the structure. The covalent nature of the interlayer potassium-sulfur bonding is reflected in the non-micaceous morphology and water-stability of the transparent light-yellow crystals. GRA

N91-14867# Brown Univ., Providence, RI. Div. of Engineering.
SIMULATION OF TRANSIENT GLIDE OF A THREADING DISLOCATION IN AN EMBEDDED STRAINED EXPITAXIAL LAYER
Jean-Claude Ramirez, Allan Bower, and L. B. Freund Jul. 1990 59 p Sponsored by IBM
(Contract N00014-87-K-0481; NSF DMR-87-14665)
(AD-A226965) Avail: NTIS HC/MF A04 CSCL 20/12

The material configuration is a thin strained layer embedded between two relatively thick, unstrained layers. The interfaces between the strained layer and the unstrained layers are assumed to be epitaxial, and the strain in the layer is assumed to arise from a mismatch in lattice parameters between the strained layer material and the surrounding material. The crystalline materials are assumed to have cubic symmetry, oriented so that (001) direction is normal to the interfaces. Initially, a long straight 60 deg dislocation exits on a (111) plane, extending from one otherwise strain-free region, through the strained layer, and into the other strain-free region. The process of glide of this dislocation is modeled under the action of the stress associated with the mismatch strain in the layer. The shape of the dislocation during glide is approximated by a continuous piecewise linear curve, and the location of the vertices of this curve are viewed as generalized coordinates of the system. A corresponding generalized force is defined at each node as the variation in total energy of the system due to variation in position of that node. A kinetic law of motion, suitable for thermally activated glide of the dislocation, is then cast into a form involving the nodal velocities and the corresponding generalized forces. The governing equations have been integrated numerically for material parameters representative of the GeSi/Si(001) strained layer systems. GRA

N91-14868# California Univ., Los Angeles. Dept. of Physics.
ELECTROMAGNETIC PROPERTIES OF HIGH Tc SUPERCONDUCTORS Final Report
George Gruener 17 Apr. 1990 6 p
(Contract N00014-85-K-0617)
(AD-A227006) Avail: NTIS HC/MF A02 CSCL 20/3

The high frequency properties of various high T(c) superconductors was investigated. The key parameter which is studied in the microwave and millimeter wave spectral range is the surface impedance Z(s). It is one of the parameters which reflects the electrodynamics of the superconducting state. At the same time it is perhaps the most important technical parameter which determines the application potential of the superconductors for high frequency passive components and devices. GRA

N91-14869# Air Force Weapons Lab., Kirtland AFB, NM.
TRANSIENT X RAY IRRADIATION OF HIGH TRANSITION TEMPERATURE SUPERCONDUCTING MATERIAL Final Report, Feb. 1988 - Mar. 1990
Robert M. Pelzl and David C. Koller Jul. 1990 30 p
(AD-A227090; WL-TR-90-47) Avail: NTIS HC/MF A03 CSCL 20/12

Transient radiation studies performed on high critical temperature (Tc) superconductors by Weapons Laboratory (WL) personnel in the WI Flash X ray Facility are described. The objective was to detect any transient effects on the superconductivity of high Tc material during irradiation by an x ray pulse. Each sample of high Tc material was cooled to a temperature below its Tc and then irradiated with a 20-ns pulse from a Febetron 705 flash x ray machine. Each pulse delivered 85 rad(Si) to the sample. The samples were current biased and their conductivity measured during irradiation. Within instrumentation limits, measurements made on thin film high Tc material revealed no changes in conductivity during or after irradiation. GRA

N91-14870# Stanford Univ., CA. High Temperature Gasdynamics Lab.
AN INVESTIGATION OF DIAMOND SYNTHESIS IN AN OXYGEN-ACETYLENE DIFFUSION FLAME
M. A. Cappelli Sep. 1990 7 p
(Contract N00014-89-J-1197)
(AD-A227224; SU-TR-4) Avail: NTIS HC/MF A02 CSCL 21/2

Diamond synthesis is demonstrated in an oxygen-acetylene diffusion flame. The acetylene flame is diluted with argon to suppress sooting tendencies and is sustained and stabilized by overventilation with a surrounding oxygen flow. The result is a

relatively cold flame, and the carbon film is deposited on a free-standing silicon wafer without the need for substrate cooling. Deposition patterns observed so far are nonuniform, with diamond deposited within a small annular ring surrounding a predominantly amorphous carbon film. Particle growth rates observed are in the range of 20 to 50 micrometer/hour, and deposit patterns are qualitatively similar to those observed in premixed oxygen-acetylene flames, however, unlike in premixed flame deposition, the temperature distribution appears to be much more nonuniform, with heat generated primarily at the diffusion flame boundary. GRA

N91-14871# North Carolina State Univ., Raleigh. Dept. of Materials Science and Engineering.
GROWTH, CHARACTERIZATION AND DEVICE DEVELOPMENT IN MONOCRYSTALLINE DIAMOND FILMS Quarterly Letter Report, 1 Jul. - 30 Sep. 1990
Robert F. Davis 30 Sep. 1990 50 p
(Contract N00014-90-J-1604)
(AD-A227238) Avail: NTIS HC/MF A03 CSCL 20/2

Diamond films were deposited on various polycrystalline metal and (001) Si substrates by biased hot filament chemical vapor deposition, the films characterized by TEM, x ray diffraction and Raman and Auger spectroscopies and devices (specifically IMATTs and MESFETs) modeled from the properties of diamond. Films grown on Si, Ni and W exhibited the highest quality diamond films from the viewpoint of Raman characterization. The model of the MESFET device with gate length = 1 micron and width = 1 mm showed that significant degradation in RF performance is not expected at 10 GHz. GRA

N91-14872* National Aeronautics and Space Administration. Marshall Space Flight Center, Huntsville, AL.
PIEZOELECTROSTATIC GENERATOR Patent
Glen A. Robertson, inventor (to NASA) 28 Aug. 1990 10 p Filed 27 Apr. 1989
(NASA-Case-MFS-28298-1; US-Patent-4,952,836;
US-Patent-Appl-SN-343656; US-Patent-Class-310-339;
US-Patent-Class-310-330; US-Patent-Class-310-331;
US-Patent-Class-310-340; Int-Patent-Class-H01L-41/08) Avail: US Patent and Trademark Office CSCL 20L

A piezoelectrostatic generator includes a plurality of elongated piezoelectric elements having first and second ends, with the first ends fixedly mounted in a cylindrical housing and the second extending radially inwardly toward an axis. A shaft movable along the axis is connected to the inner ends of the elements to produce bending forces in piezoelectric strips within the elements. Each element includes a pair of strips mounted in surface contact and in electrical series to produce a potential upon bending. Electrodes spaced from the strips by a solid dielectric material act as capacitor plates to collect the potential charge.
Official Gazette of the U.S. Patent and Trademark Office

N91-14873# Ames Lab., IA.
LOW-ENERGY ELECTRON DIFFRACTION INVESTIGATION OF EPITAXIAL GROWTH: Pt AND Pd(100) Ph.D. Thesis
Diane K. Flynn-Sanders 21 Sep. 1990 235 p
(Contract W-7405-eng-82)
(DE91-000750; IS-T-1415) Avail: NTIS HC/MF A11

We investigate the epitaxial growth of Pt and Pd and Pd(100) via spot profile analysis using conventional low-energy electron diffraction (LEED). We resolve a central-spike and diffuse component in the spot profiles, reflecting the layer-occupations and pair-correlations, respectively. Kinetic limitations inhibit layer-by-layer growth at low temperatures. Our data suggest diffusion switches on at ca. 150 K for Pt and ca. 170 K for Pd indicating activation barriers to surface diffusion of ca. 10 and ca. 13 kcal/mol, respectively. To clarify the role of diffusion in determining the resulting film morphology, we develop a growth model that incorporates the adsorption-site requirement and predicts intensity oscillations. We present a new procedure to experimentally determine out-of-phase scattering conditions. At these energies, ring-structure is evident in the profiles during Pd growth between ca. 200 and 400 K. We report ring intensity oscillations as a function of coverage, which demonstrate the filling of individual layers. DOE

N91-14874# Minnesota Univ., Minneapolis. Dept. of Chemical Engineering and Materials Science.
THEORY OF THE ELECTRONIC AND STRUCTURAL PROPERTIES OF SOLID STATE OXIDES Annual Report, 1 Jul. 1989 - 1 May 1990
J. R. Chelikowsky 1990 75 p
(Contract DE-FG02-89ER-45391)
(DE91-001192; DOE/ER-45391/1) Avail: NTIS HC/MF A04

Studies on electronic and structural properties of solid state oxides continued. This quarter, studies have concentrated on silica. Progress is discussed in the following sections: interatomic potentials and the structural properties of silica; chemical reactivity and covalent/metallic bonding on Si clusters; and surface and thermodynamic interatomic forces fields for silicon. DOE

N91-14875# Sandia National Labs., Albuquerque, NM.
EFFECT OF STEP EDGE TRANSITION RATES AND ANISOTROPY IN SIMULATIONS OF EPITAXIAL GROWTH
E. Chason and B. W. Dodson 1990 23 p Presented at the 37th National American Vacuum Society Symposium, Toronto, Ontario, 8-12 Oct. 1990
(Contract DE-AC04-76DP-00789)
(DE91-001251; SAND-90-1239C; CONF-901035-10) Avail: NTIS HC/MF A03

We present the results of a hybrid rate equation/Monte Carlo simulation of epitaxial growth on vicinal surfaces. We have studied the effect on surface morphology of changing transition rates at step edges, of changing detachment rates from step edges and clusters, and of adding anisotropy to the diffusion and incorporation kinetics at step edges and islands. The effect of the transition rates on surface morphology are discussed in terms of a balance between growth by nucleation and coalescence of islands and by the propagation of steps. DOE

N91-14876# Oak Ridge National Lab., TN. Solid State Div.
DEFECT AND IMPURITY EFFECTS ON THE INITIAL GROWTH OF Ag ON Si(111)
J.-K. Zuo and J. F. Wendelken Oct. 1990 23 p Presented at the 37th National American Vacuum Society Symposium, Toronto, Ontario, 8-12 Oct. 1990
(Contract DE-AC05-84OR-21400)
(DE91-001277; CONF-901035-8) Avail: NTIS HC/MF A03

Step and impurity effects on the initial growth of a thin film have been demonstrated in the (sq root of 3 x sq root of 3)R30 degree domain growth of Ag on Si(111) using high angular resolution LEED. Anisotropy in the sq root of 3 domain shape and growth during deposition are found on the stepped Si(111) with the preferential growth along the step edge direction. The sq root of 3 superlattice grows with coverage principally by domain coalescence at the approximate temperature of 450 C and is self-similar at different coverages (scaling) as observed on a flat Si(111). The size distribution is shown to follow a gamma distribution by a simple model calculation. A dramatic change in the growth mechanism is observed when oxygen impurities (less than 0.02 ML) appear. The sq root of 3 domains in the presence of impurities grow with coverage more randomly and isotropically in contrast with the step edge effects and coalescence is inhibited. As a result, the sq root of 3 superlattice stays in a microdomain morphology without long range order. DOE

N91-14877# Sandia National Labs., Albuquerque, NM.
IRRADIATION-INDUCED PINNING IN SINGLE-CRYSTAL AND THIN-FILM Tl2Ca2Ba2Cu3O10 SUPERCONDUCTORS
J. C. Barbour, E. L. Venturini, and D. S. Ginley 1990 15 p Presented at the 7th International Conference on Ion Beam Modification of Materials, Knoxville, TN, 9-14 Sep. 1990
(Contract DE-AC04-76DP-00789)
(DE91-001342; SAND-90-1094C; CONF-900936-14) Avail: NTIS HC/MF A03

Magnetization relaxation measurements were used to directly measure the effects of ion irradiation on magnetic flux pinning. The pinning potential (U) in a Tl2Ca2Ba2Cu3O(sub y) single crystal irradiated with 4.5 MeV protons, to a damage level of 4x10(exp -4) dpa, increased by approximately 25 percent at 25 K. In contrast, U for a highly oriented polycrystalline thin film irradiated with 300 keV He ions to a damage level of 2x10(exp -4) dpa increased by only 5 percent at 25 K (and less at higher temperatures). Enhancement of the magnetization critical current density, J(sub cm), is determined as a function of temperature and damage in the single crystal and thin film. High energy proton irradiation increased J(sub cm) in the single crystal by an order of magnitude at 25 K but had only a small effect on J(sub cm) in the thin film. DOE

N91-14878# Columbia Univ., New York, NY. Microelectronics Sciences Labs.

PHOTOGENERATED CARRIER-INDUCED REACTION ON SEMICONDUCTOR SURFACES Progress Report, 15 Dec. 1989 - 30 Jul. 1990

Richard M. Osgood, Jr. Aug. 1990 13 p
(Contract DE-FG02-90ER-14104)
(DE91-001349; DOE/ER-14104/1) Avail: NTIS HC/MF A03

We have begun studying the effect of illumination on the chemical interaction of molecular chlorine with a well-defined GaAs(110) surface under ultra-high vacuum (UHV) conditions. We have found that chlorine adsorbs dissociatively at temperatures as low as 85 K. Illumination of molecular chlorine-covered surface at 85 K with 193-nm radiation led to desorption of Cl-atoms accompanied by Cl2 molecules, as well as formation of AsCl2/AsCl3, which desorbed at 180 K. Illumination with 351-nm excimer-laser radiation caused exclusively Cl-atoms ejection, at a lower rate. It also resulted in smaller amounts of arsenic chloride formed on the surface. No new species were observed when the surface was irradiated with a 535-nm laser. We suggest that the surface reaction is initiated by dissociation of adsorbed molecular chlorine, which we believe, is mediated by photoemission of electrons from the substrate upon 193-nm irradiation. Finally, we have nearly completed the construction of a second UHV system for the study of laser-induced dissociation of metal alkyls on GaAs surfaces. This system will incorporate total-internal-reflection Fourier-transform IR spectroscopy to follow reaction intermediates, a time of flight mass spectrometer, low electron energy diffraction, and Auger Electron spectroscopy. DOE

N91-14879# Pacific Northwest Lab., Richland, WA. Molecular Science Research Center.

A LEED STUDY OF THE MgO(001) SURFACE STRUCTURE

D. L. Blanchard, D. L. Lessor, J. P. LaFemina, D. R. Baer, W. K. Ford, and T. Guo (Montana State Univ., Bozeman.) Oct. 1990 21 p Presented at the 37th National American Vacuum Society Symposium, Toronto, Ontario, 8-12 Oct. 1990
(Contract DE-AC06-76RL-01830)
(DE91-002811; PNL-SA-18242; CONF-901035-12) Avail: NTIS HC/MF A03

Low-energy electron diffraction (LEED) beam intensities were measured from the freshly cleaved (in UHV) MgO(001) surface using beam energy modulation to avoid electrical charging. Dynamic LEED analysis of the data indicates: (1) an interlayer relaxation of 1 + or - 2 percent and a rumple of the first layer ions of 5 + or - 2.5 percent; (2) a new attenuation model containing no adjustable parameters gives fits to the data that are comparable to those using a constant V(sub i); (3) a weak dependence of the optimum rumpling on the energy range of the data used. The structure determined in this study is compared to others reported in the literature for this surface, and the effects of lattice vibrations, attenuation length and number of surface layers treated exactly are considered. DOE

N91-14880# Massachusetts Inst. of Tech., Cambridge. Dept. of Materials Science and Engineering.

GROUND BOUNDARIES Progress Report, 15 Feb. - 15 Oct. 1990

R. W. Balluffi and P. D. Bristowe 1990 17 p
(Contract DE-FG02-87ER-45310)
(DE91-004027; DOE/ER-45310/21) Avail: NTIS HC/MF A03

The present document is a progress report describing the work accomplished on the study of grain boundaries in Ag, Au, Ni, Si, and Ge. Research was focused on the following four major efforts: study of the atomic structure of grain boundaries by means of x-ray diffraction, transmission electron microscopy and computer modeling; grain boundary migration; short-circuit diffusion along grain boundaries; and development of Thin-Film Deposition/Bonding Apparatus for the manufacture of high purity bicrystals. DOE

N91-14881# Argonne National Lab., IL. Engineering Physics Div.

DESIGN AND APPLICATION POSSIBILITIES OF SUPERCONDUCTING RADIO-FREQUENCY QUADRUPOLES

A. Schempp, H. Deitinghoff (Johann-Wolfgang-Goethe-Univ., Frankfurt am Main, Germany, F.R.), J. R. Delayen, and K. W. Shepard 1990 4 p Presented at the Linear Accelerator Conference, Albuquerque, NM, 9-14 Sep. 1990
(Contract W-31-109-eng-38)
(DE91-004477; CONF-9009123-56) Avail: NTIS HC/MF A01

In recent experiments, CW surface electric fields in excess of 100 MV/m have been obtained in a superconducting RF quadrupole (SCRFQ) device. In this paper we explore some design and application possibilities of SCRFQs which have been opened by these results. For example, SCRFQs may be able to accelerate higher CW currents than is now possible. Also, highly-modulated SCRFQs could be designed to provide compact, high-longitudinal-gradient devices. Some conceptual designs and applications will be discussed. DOE

N91-14882# Argonne National Lab., IL. Engineering Physics Div.

EXPERIMENTAL RESULTS IN SUPERCONDUCTING NIOBIUM RESONATORS FOR HIGH-BRIGHTNESS ION BEAM ACCELERATION

J. R. Delayen, C. L. Bohn, and C. T. Roche 1990 4 p Presented at the Linear Accelerator Conference, Albuquerque, NM, 9-14 Sep. 1990 Sponsored by Army Strategic Defense Command
(Contract W-31-109-eng-38)
(DE91-004478; CONF-9009123-58) Avail: NTIS HC/MF A01

Two niobium resonant cavities for high-brightness ion beam acceleration have been constructed and tested. The first was based on a coaxial quarter-wave geometry and was optimized for phase velocity beta(sub 0) = 0.15. This cavity, which resonates at 400 MHz in the fundamental mode, operated at an average (wall-to-wall) accelerating gradient of 12.9 MV/m under continuous-wave (CW) fields. At his gradient, a cavity Q of 1.4 x 10(exp 8) was measured. The second was based on a coaxial half-wave geometry and was optimized for beta(sub 0) = 0.12. This cavity, which resonates at 355 MHz in the fundamental mode, operated at an average accelerating gradient of 18.0 MV/m under CW fields. This is the highest average accelerating gradient achieved to date in low-velocity structures designed for CW operation. At this gradient, a cavity Q of 1.2 x 10(exp 8) was measured. DOE

N91-14883# Argonne National Lab., IL. Engineering Physics Div.

FIRST TESTS OF A SUPERCONDUCTING RFQ (RADIO FREQUENCY QUADRUPOLE) STRUCTURE

J. R. Delayen and K. W. Shepard 1990 4 p Presented at the Linear Accelerator Conference, Albuquerque, NM, 9-14 Sep. 1990
(Contract W-31-109-eng-38)
(DE91-004483; CONF-9009123-54) Avail: NTIS HC/MF A01

High surface electric fields have been obtained in the first tests of a superconducting rf quadrupole device. The rf quadrupole fields were generated between niobium vanes 6.5 cm in length, with an edge radius of 2 mm, and with a beam aperture of 6 mm diameter. In tests at 4.2 K, the 64 MHz device operated cw at peak surface electric fields of 128 MV/m. Virtually no electron loading was observed at fields below 100 MV/m. It was possible

to operate at surface fields of 210 MV/m in pulses of 1 msec duration using a 2.5 kW rf source. For the vane geometry tested, more than 10 square centimeters of surface support a field greater than 90 percent of the peak field. The present result indicates that electric fields greater than 100 MV/m can be obtained over an appreciable area, sufficient for some accelerator applications. It also shows that superconducting rf technology may provide an extended range of options for rf quadrupole design. DOE

N91-14884# Argonne National Lab., IL. Materials Science Div.
AN ION-CHANNELING STUDY OF IRRADIATION-INDUCED AMORPHIZATION OF YBa2Cu3O(7-x)
L. E. Rehn, R. P. Sharma, P. M. Baldo, and Y. Fang Sep. 1990 13 p Presented at the 7th International Conference on Ion Beam Modification of Materials, Knoxville, TN, 9-14 Sep. 1990
(Contract W-31-109-eng-38)
(DE91-004488; CONF-900936-21) Avail: NTIS HC/MF A03

We previously employed Brillouin scattering to demonstrate that the irradiation-induced crystalline-to-amorphous (c-a) transformation in several intermetallic compounds was preceded by a large (greater than 50 percent) decrease in shear elastic constant, indicative of an elastic instability. In situ electron diffraction revealed that the elastic softening was caused by static atom displacements. Here we report the results of an ion-channeling study designed to examine whether parallel changes occur during ion irradiation of single crystals of YBa2Cu3O(7-x). The (static plus thermal) atomic displacements introduced during 1.5 MeV He-4 irradiation at a temperature of 100 K were determined from zone axes (001) axial channeling scans taken after several irradiation increments between 0 and 0.04 dpa. It was possible to obtain reliable channeling information at quite low doses, as low as 0.0004 dpa, because of the excellent minimum yields (X sub min less than 3 percent) obtained from the high-quality single crystals. In agreement with the previous observations in intermetallic compounds, large atomic displacements, implying a drop in elastic modulus of approximately greater than 90 percent, were found prior to the onset of amorphization. However, X sub min was found to be directly proportional to dose over a very broad range. The observed linear dependence on dose indicates that the irradiation-induced disorder develops continuously, and at the same rate, from the very onset of the irradiation to nearly complete amorphization. DOE

77 THERMODYNAMICS AND STATISTICAL PHYSICS

Includes quantum mechanics; theoretical physics; and Bose and Fermi statistics.

For related information see also *25 Inorganic and Physical Chemistry* and *34 Fluid Mechanics and Heat Transfer.*

N91-14885*# Clarkson Univ., Potsdam, NY. Center for Crystal Growth in Space.
A NOVEL APPROACH TO DETERMINE THE HEAT TRANSFER COEFFICIENT IN DIRECTIONAL SOLIDIFICATION FURNACES
Mohsen Banan, Ross T. Gray, and William R. Wilcox 1990 27 p
(Grant NAG8-831)
(NASA-CR-187648; NAS 1.26:187648) Avail: NTIS HC/MF A03 CSCL 13M

The heat transfer coefficient between a molten charge and its surroundings in a Bridgman furnace was determined using an approach utilizing in-situ temperature measurement. The ampoule containing an isothermal melt was suddenly moved from a higher temperature zone to a lower temperature zone. The temperature-time history was used in a lumped-capacity cooling model to evaluate the heat transfer coefficient between the charge and the furnace. The experimentally determined heat transfer coefficient was of the same order of magnitude as the value estimated by standard heat transfer calculations. Author

N91-14886# Messerschmitt-Boelkow-Blohm G.m.b.H., Munich (Germany, F.R.). Theoretical Aerodynamics Dept.
NEW ACCURATE, VECTORIZED APPROXIMATIONS OF STATE SURFACES FOR THE THERMODYNAMIC AND TRANSPORT PROPERTIES OF EQUILIBRIUM AIR
C. Mundt, R. Keraus, and J. Fischer (Technische Univ., Munich, Germany, F.R.) 18 Jul. 1990 27 p Submitted for publication
(MBB/FE122/S/PUB/0389; ETN-90-98151) Copyright Avail: NTIS HC/MF A03

The chemical equilibrium assumption eases the calculation of flows with real gas effects. In equilibrium all quantities are functions of two thermodynamic parameters only. This leads to the possibility of using a 2-D interpolation to approximate the state surfaces. Considering their complex shape, a piecewise bicubic interpolation is appropriate. The determination of the coefficients is described with emphasis placed on a smooth, vectorizable representation. State surfaces for both the thermodynamic and transport properties of air are evaluated, and a selection of them is presented. A discussion of the gains encountered in applications shows the advantages of this approach. ESA

N91-14887# California Univ., Berkeley. Lawrence Berkeley Lab. Earth Sciences Div.
COUPLED TRANSPORT PROCESSES IN SEMIPERMEABLE MEDIA. PART 1: ANALYTICAL SOLUTIONS OF THE LINEARIZED GOVERNING EQUATIONS
Janet S. Jacobsen and Chalon L. Carnahan Mar. 1990 21 p
(Contract DE-AC03-76SF-00098)
(DE91-004138; LBL-24725-Pt-1) Avail: NTIS HC/MF A03

The thermodynamics of irreversible processes leads to nonlinear governing equations for direct and coupled mass transport processes. Analytical solutions of linearized versions of these equations can be used to verify numerical solutions of the nonlinear equations under conditions such that nonlinear terms are relatively small. This report presents derivations of the analytical solutions for one-dimensional and axisymmetric geometries. DOE

80 SOCIAL SCIENCES (GENERAL)

Includes educational matters.

No abstracts in this category.

81 ADMINISTRATION AND MANAGEMENT

Includes management planning and research.

N91-14888# Purdue Univ., West Lafayette, IN. Dept. of Psychology.
THE EVALUATION OF LONG RANGE CONSEQUENCES IN DECISION MAKING Final Report, Aug 1985 - Aug. 1987
Mary Kay Stevenson-Busemeyer Aug. 1990 11 p
(Contract MDA903-85-K-0366)
(AD-A226949; ARI-RN-90-113) Avail: NTIS HC/MF A03 CSCL 05/8

The purpose of this research program is to develop a general model of how individuals make decisions that involve temporally remote or long range consequences. The primary focus of this project is to define the form of the subjective time scales as they vary across situations and individuals, to define the type of discounting operation that is used to qualify incentives when they occur in the future, and to test the way that these processes can be analyzed using different tasks or response measures. A measurement model has been used as a framework for investigating the way subjects respond to long-term positive and negative consequences. All five of the experiments described in

the proposal were completed. This summary report will provide and overview of the progress made toward the objectives defined for this phase of the research program. GRA

N91-14889# Illinois Univ., Champaign. Dept. of Psychology.
THE OBJECT DISPLAY IN DECISION MAKING AND JUDGMENT Interim Report, Aug. 1983 - Sep. 1986
Barbara Barnett, Barry P. Goettl, Arthur F. Kramer, and Christopher D. Wickens Aug. 1990 22 p
(Contract MDA903-83-K-0255)
(AD-A227059; CPL-86-7; ARI-RN-90-112) Avail: NTIS HC/MF A03 CSCL 05/8

Three experiments are presented which apply the principle of compatibility of proximity to multicue decision making and judgment. This principle states that when a task requires the integration of information, the display should present the data in close proximity. When, however, the information must be selectively attended or processed, the information should be displayed with low proximity. In the first experiment, subjects processed information cues in a multicue decision making task. The cues varied in their source, diagnosticity and reliability. They were presented either as separate bargraphs, or as rectangles. Their presentation was either simultaneous or sequential. The results indicated that greater proximity in time (simultaneous) and objectness (rectangular cues) lead to improved judgments. Furthermore, the rectangular format did not disrupt the memory for isolated cue values. In experiments 2 and 3, subjects were shown three numerical values and were required to combine them to predict a criterion value. Both equation relating the cues to the criterion and the display format of the cues were varied. Experiment 2 demonstrated that when the cues had to be selectively attended, performance was better with a bargraph display than with an integrated triangle display. No difference was observed when the cues had to be integrated. Experiment 3 demonstrated that the effects of display format are contingent upon the relation between the cues and the criterion. GRA

82 DOCUMENTATION AND INFORMATION SCIENCE

Includes information management; information storage and retrieval technology; technical writing; graphic arts; and micrography.

For computer documentation see *61 Computer Programming and Software.*

N91-14890# National Academy of Sciences - National Research Council, Washington, DC.
INFORMATION TECHNOLOGY AND THE CONDUCT OF RESEARCH: THE USER'S VIEW. REPORT OF THE PANEL ON INFORMATION TECHNOLOGY AND THE CONDUCT OF RESEARCH
1989 84 p
(ISBN-0-309-03888-X; LC-88-28903) Avail: NTIS HC/MF A05

Information technology - the set of computer and telecommunication technologies that makes possible computation, communication, and the storage and retrieval of information - has changed the conduct of scientific, engineering, and clinical research. Present trends, future potential, and impediments to the use of information technology in support of research are examined. Written from the viewpoint of the researcher using information technology and including many examples, a number of recommendations are offered which are directed to two principal audience: policy makers and leaders of institutions responsible for the support and management of research, and researchers themselves. Author

N91-14891 Pittsburgh Univ., PA.
STRATEGIC UTILIZATION OF INFORMATION RESOURCES: A CONTINGENCY APPROACH Ph.D. Thesis
Rajiv Sabherwal 1989 249 p
Avail: Univ. Microfilms Order No. DA9019380

The strategic utilization of information resources, an important but little researched area, is investigated using an information system application as the unit of analysis. The research model includes three levels of the environment (industry, organizational, and information system), the application's characteristics, the decision-making process preceding the application, and the application's success. Hypotheses were proposed for the relationships among these dimensions, using three reference disciplines-strategic decision-making, organizational buying behavior, and innovation adoption. Questionnaire data from 85 senior executives (19.02 percent response rate) of Fortune 1000 companies were analyzed. The analysis supports most research hypotheses as well as the overall model, except the hypotheses concerning the relationship between the environment and the application's characteristics. Hierarchical cluster analysis, used to develop an empirical taxonomy of the decision-making processes, produced five clusters-planned, IS influenced, user-influenced, fluid, and incremental. Discriminant analysis showed that the environmental characteristics discriminate between these decision-making process clusters-the environment correctly classified the decision-making process in 49.38 percent cases. The cluster means for the environmental characteristics, and the application's characteristics and success, were compared to examine the differences among the five clusters. Having systematically utilized knowledge from several reference disciplines, this empirical research on strategic utilization of information resources should help practice and provide a useful foundation for future research. Dissert. Abstr.

N91-14892*# National Aeronautics and Space Administration. Langley Research Center, Hampton, VA.
THE NASA/DOD AEROSPACE KNOWLEDGE DIFFUSION RESEARCH PROJECT: A RESEARCH AGENDA
Thomas E. Pinelli and John M. Kennedy 1990 13 p
(NASA-TM-103439; NAS 1.15:103439; AD-A226502; SAF/AQT-SR-90-011; USAF-STINFO-CONTRIB-90/6) Avail: NTIS HC/MF A03 CSCL 05/2

The project has both immediate and long term purposes. In the first instance it provides a practical and pragmatic basis for understanding how the results of NASA/DoD research diffuse into the aerospace R and D process. Over the long term it provides an empirical basis for understanding the aerospace knowledge diffusion process itself, and its implications at the individual, organizational, national, and international levels. The project is studying the major barriers to effective knowledge diffusion. This project will provide descriptive and analytical data regarding the flow of scientific and technical information (STI). It will examine both channels used to communicate information and the social system of the aerospace knowledge diffusion process. GRA

N91-14893# Naval Postgraduate School, Monterey, CA. Dept. of Computer Science.
DEMON: A MEDIA OBJECT MODEL INCORPORATING NATURAL LANGUAGE DESCRIPTIONS FOR RETRIEVAL SUPPORT Progress Report, Apr. - Dec. 1989
Bernhard Holtkamp, Vincent Y. Lum, and Neil C. Rowe Feb. 1990 25 p
(AD-A226711; NPS52-90-019) Avail: NTIS HC/MF A03 CSCL 13/5

The DEMOM (Description based Media Object data Model) media object data model aims at providing a uniform framework for managing different types of media data, i.e., images, text, sound or graphics. According to DEMOM media objects are defined as a class hierarchy of objects, i.e., images, text, sound, and graphics being subtypes of the general type media object. Representation specific objects are regarded as subordinate types of the corresponding subtype, e.g., a SUN raster image in pixrect format is an instance of the subtype pixrect which is in turn a subtype of image. Using images as an example, the media object hierarchy, the corresponding access operations and implementation issues are discussed. Content oriented search of media data on the basis of predicate calculus is considered as an essential part of DEMOM and hence discussed as well. GRA

N91-14894# Naval Postgraduate School, Monterey, CA.
DEFENSE DATA NETWORK (DDN) PERFORMANCE ANALYSIS USING PROBABILITY MODELING M.S. Thesis
Donald P. Gaver and Patricia A. Jacobs Jul. 1990 67 p
(AD-A226856; NPS55-90-13) Avail: NTIS HC/MF A04 CSCL 05/2

The data defense network (DDN) is a large packet switching network that services elements of the U.S. Department of Defense (DOD). The emphasis of this report is to perform probabilistic analysis of certain features of the DDN system with a view of enhancing or optimizing measures of service such as data base throughput and the waiting times experienced by data-base-transfer customers. The particular questions addressed, and the models constructed, are in response to tasking statements supplied by personnel from the Defense Communications Engineering Center, Reston, Virginia. In Section 2 models are presented to study the optimal length of a packet subject to transmission errors. When a data transfer is to occur the total collection of bits that comprise the data base is divided into packets, i.e., subcollections of contiguous bits from the data base plus a header carrying address information. In Section 3 models are introduced to study the effect on D's buffer of all sources retransmitting at a retransmission interval of length 8. We also model the behavior of one form of congestion control, exponential backoff, a procedure that increases successive time-out intervals possibly from 8 to 28, 28 to 48, etc. In summary, probabilistic models have been constructed to study the effect of packet size and message size on system throughput and response time of a data-transfer operation. The effect of packet retransmission on response times has also been evaluated. GRA

N91-14895# Naval Underwater Systems Center, Newport, RI. Dept. of Command Support.
TIPS ON HOW TO CUT TECHNICAL PUBLICATIONS COSTS
4 Sep. 1990 10 p
(AD-A227334; NUSC-TD-8771) Avail: NTIS HC/MF A02 CSCL 05/1

This document presents a brief collection of tips on how to cut the editing and production costs of technical publications. The tips presented were contributed and complied by the Naval Underwater Systems Center publications editors and are directed primarily at the authors of technical reports, technical articles, and other Navy documentation. GRA

83 ECONOMICS AND COST ANALYSIS

Includes cost effectiveness studies.

N91-14363*# Science Applications International Corp., Schaumburg, IL.
ANALYSIS OF SUCCESS PROBABILITY/COST TRADES FOR SMALL LANDERS IN A MARS NETWORK
Alan L. Friedlander *In* JPL, Proceedings of the Mars Global Network Mission Workshop 1 Jun. 1990 p 229-243 (For primary document see N91-14359 06-12)
Avail: NTIS HC/MF A19 CSCL 05C

84 LAW, POLITICAL SCIENCE AND SPACE POLICY

Includes NASA appropriation hearings; aviation law; space law and policy; international law; international cooperation; and patent policy.

N91-14896# Congressional Research Service, Washington, DC.
OUTER SPACE: WHAT SHOULD BE THE US GOVERNMENT POLICY TOWARD THE REGION BEYOND EARTH'S ATMOSPHERE. NATIONAL DEBATE TOPIC FOR HIGH SCHOOLS, 1990-1991
1990 726 p
(PB90-255464; Doc-101-24) Avail: NTIS HC/MF A99 CSCL 05D

The 1990-1991 high school debate topic is: 'What Should be the United States Government Policy Toward the Region Beyond Earth's Atmosphere'. The three official debate propositions within the topic are: (1) Resolved: That the United States Government should significantly increase space exploration; (2) Resolved: That the United States should significantly increase commercial development of space; (3) Resolved: That the United States Government should significantly increase its military use of space. In compliance with Public Law 88-246, the Congressional Research Service of the Library of Congress prepared the compilation of materials and bibliographic references to assist high school debaters in researching the topic. Excerpts from documents were selected to provide background information, an overview of the principal issues, and a balance of opposing views. Some materials are included that are not readily available in public or research libraries. In selecting items for this reader and bibliography, the Congressional Research Service (CRS) has attempted to sample the wide spectrum of opinions reflected in current literature on these questions. No preference for any policy is indicated by the selection or positioning of articles herein, nor is CRS disapproval of any policy or article to be inferred from its omission. Author

85 URBAN TECHNOLOGY AND TRANSPORTATION

Includes applications of space technology to urban problems; technology transfer; technology assessment; and surface and mass transportation.

For related information see also *03 Air Transportation and Safety, 16 Space Transportation,* and *44 Energy Production and Conversion.*

No abstracts in this category.

88 SPACE SCIENCES (GENERAL)

N91-14897*# National Aeronautics and Space Administration. Ames Research Center, Moffett Field, CA.
INTERSTELLAR DUST: CONTRIBUTED PAPERS
Alexander G. G. M. Tielens, ed. and Louis J. Allamandola, ed. Dec. 1989 512 p Symposium held in Santa Clara, CA, 26-30 Jul. 1988; sponsored by NASA. Ames Research Center, NSF, and the International Astronomical Union
(NASA-CP-3036; A-89050; NAS 1.55:3036) Avail: NTIS HC/MF A22 CSCL 03B

A coherent picture of the dust composition and its physical characteristics in the various phases of the interstellar medium was the central theme. Topics addressed included: dust in diffuse interstellar medium; overidentified infrared emission features; dust in dense clouds; dust in galaxies; optical properties of dust grains; interstellar dust models; interstellar dust and the solar system; dust formation and destruction; UV, visible, and IR observations of interstellar extinction; and quantum-statistical calculations of IR emission from highly vibrationally excited polycyclic aromatic hydrocarbon (PAH) molecules. For individual titles, see N91-14898 through N91-15033.

N91-14898*# Observatoire de Marseille (France).
REDDENING AND EXTINCTION TOWARDS H II REGIONS
Progress Report **c90**
James Caplan and Lise DeHarveng *In* NASA, Ames Research Center, Interstellar Dust: Contributed Papers Dec. 1989 p 3-4 (For primary document see N91-14897 06-88)
Avail: NTIS HC/MF A22 CSCL 03B

The light emitted by the gas in H II regions is attenuated by dust. This extinction can be measured by comparing H alpha, H beta, and radio continuum fluxes, since the intrinsic ratios of the Balmer line and thermal radio continuum emissivities are nearly constant for reasonable conditions in H II regions. In the case of giant extragalactic H II regions, the extinction was found to be considerably greater than expected. The dust between the Earth and the emitting gas may have an optical thickness which varies. The dust may be close enough to the source that scattered light contributes to the flux, or the dust may be actually mixed with the emitting gas. It is difficult to decide which configuration is correct. A rediscussion of this question in light of recent observations, with the Fabry-Perot spectrophotometers, of the large Galactic H II region is presented. The color excesses are compared for stars embedded in these H II regions with those derived (assuming the standard law) from the nebular extinction and reddening. Author

N91-14899*# Wisconsin Univ., Madison. Dept. of Astronomy.
THE RELATIONSHIP BETWEEN IR, OPTICAL, AND UV EXTINCTION **c89**
Jason A. Cardelli, Geoffrey C. Clayton, and John S. Mathis *In* NASA, Ames Research Center, Interstellar Dust: Contributed Papers Dec. 1989 p 5-10 (For primary document see N91-14897 06-88)
Avail: NTIS HC/MF A22 CSCL 03A

An analysis is presented for the variability of absolute IR, optical, and UV extinction, A(sub lambda), derived through the ratio of total-to-selective extinction, R, for 31 lines of sight for which reliable UV extinction parameters were derived. These data sample a wide range of environments and are characterized by 2.5 is less than or equal to R is less than or equal to 6.0. It was found that there is a strong linear dependence between extinction expressed as A(sub lambda)/A(sub V) and 1/R for 1.25 micron is less than or equal to lambda is less than or equal to 0.12 micron. Differences in the general shape of extinction curves are largely due to variations in shape of optical/near-UV extinction corresponding to changes in R, with A(sub lambda)/A(sub V) decreasing for increasing R. From a least-squares fit of the observed R-dependence as a function of wavelength for 0.8/micron is less than or greater than 1/lambda is less than or equal to 8.3/micron, an analytic expression was generated from which IR, optical, and UV extinction curves of the form A(sub lambda)/A(sub V) can be reproduced with reasonable accuracy from a knowledge of R. It was also found that the absolute bump strength normalized to A(sub V) shows a general decrease with increasing R, suggesting that some fraction of bump grains may be selectively incorporated into coagulated grains. Finally, it was found that absolute extinction normalized by suitably chosen color indices results in a minimization of the R-dependence of portions of the UV curve, allowing A(sub lambda) to be estimated for these wavelengths independent of R. Author

N91-14900*# University Coll., London (England). Dept. of Physics and Astronomy.
THE DETECTION OF A BROAD INTERSTELLAR EXTINCTION FEATURE NEAR 1700 A **c89**
David J. Carnochan *In* NASA, Ames Research Center, Interstellar Dust: Contributed Papers Dec. 1989 p 11-16 (For primary document see N91-14897 06-88)
Avail: NTIS HC/MF A22 CSCL 03A

A statistical examination of 126 extinction curves has revealed the presence of a second broad absorption feature similar in nature to the 2200 A feature. The feature is centered on wavelength 1706 A, has a full half-width of 350 A, and a mean central height of 0.21 magnitudes. The strength of the feature increases with E(B-V) supporting an interstellar origin, and on average it is 18 times weaker than the 2200 A feature. Author

N91-14901*# Copenhagen Observatory (Denmark).
THE AUTOCORRELATION FUNCTION OF THE NORTH POLE DUST **c90**
Jens Knude *In* NASA, Ames Research Center, Interstellar Dust: Contributed Papers Dec. 1989 p 17-20 (For primary document see N91-14897 06-88)
Avail: NTIS HC/MF A22 CSCL 03B

The angular scales on which local interstellar dust is distributed are so far rather unknown as are the geometrical shapes of the dust features. From the about 5000 color excesses resulting from a north polar survey with 4 to 5 stars per square degree the two-point autocorrelation function is derived for separations ranging from 10 min to 3 deg. For intercloud lines of sight, -0.020 is less than E(b - y) is less than -0.010 mag, the average cross products (E sub 1 x E sub 2)(sub theta) show no variation with separation theta(1,2) whereas products of cloud column densities, 0.030 is less than E(b - y) is less than 0.040 mag, seem to prefer discrete separations either less than 20 min, around 75 min, or finally at about 150 min. Surprisingly the two point autocorrelation function omega(sub E) = E(sub 1) x E(sub 2)/E squared - 1 equals 0 except for any separation except theta = 0. Omega(sub E)(theta)'s absence of variation is unexpected because omega(sub H)(theta) is known to vary exponentially above b = 40 deg for separations less than 3 deg. Atomic hydrogen and dust may thus not be entirely mixed or the moments (E sub 1 x E sub 2)(sub theta) may not characterize the dust distribution. Author

N91-14902*# Applied Research Corp., Landover, MD.
THE DEPENDENCE OF UV EXTINCTION PROPERTIES ON DUST ENVIRONMENT Abstract Only **c90**
Derck Massa *In* NASA, Ames Research Center, Interstellar Dust: Contributed Papers Dec. 1989 p 21 (For primary document see N91-14897 06-88)
Avail: NTIS HC/MF A22 CSCL 03B

UV extinction data, derived from the Savage et al. (1985) ANS extinction catalog, are analyzed. The data include the normalized extinction at 1550 A, the strength of the 2175 A bump, and a crude estimate of the bump width. The results confirm the systematic increase of far-UV extinction with galactic altitude first uncovered by Kiszkurno-Koziej and Lequeux (1987) and verify that this effect is in fact a result of the dust being away from the plane, and not a generalized density dependence. It is also shown that the width of the 2175 A bump is systematically broader in denser regions (defined by large values of E(B-V) per Kpc), implying that a similar galactic altitude effect seen in this parameter may only be a reflection of the lower densities encountered away from the plane. The dependence of bump width upon bump strength is also examined. It is shown that a relationship between these two parameters is expected for certain models of the bump, but none is found. However, two factors which could be complicating a straightforward interpretation of the observations are identified and discussed. Author

N91-14903*# Vilnius Kapsukas State Univ. (Lithuania).
PROPERTIES OF INTERSTELLAR DUST IN THE REGION OF THE CEP OB4 ASSOCIATION **c90**
J. Sudzius *In* NASA, Ames Research Center, Interstellar Dust: Contributed Papers Dec. 1989 p 23-28 (For primary document see N91-14897 06-88)
Avail: NTIS HC/MF A22 CSCL 03B

Regional variations in the interstellar extinction law was examined. The region of Cyg was noted among the areas with abnormal interstellar extinction law (IEL). An attempt was made to study interstellar extinction in the region of the Cep OB4 association. The Vilnius seven color photometric system was used for this purpose. The effective wavelengths and their reciprocals for the Vilnius photometric system are presented. This system was applied for the study of variations in the IEL in four regions of the sky: Cyg, Cep, Per, and Mon (Sudzius, 1974). The results of multicolor photometry were combined with the data of Whiteoak (1966) and detailed interstellar extinction curves were derived for Cyg and for Cep-Per-Mon (average) regions in the wavelengths interval of 3000 to 8000 A (Sudzius, 1974). The obtained IEL for the Cep OB4 association does not match any of the laws determined for other regions of the sky. However, it is very close to Cyg OB2 law in the ultraviolet. Results suggest that Cep OB4

IEL have no very broadband structure (VBS) in the interval of wavenumbers 1.84 to 2.15/micron. Author

N91-14904*# Universidad Nacional Autonoma de Mexico, Ensenada. Inst. de Astronomia.
THREE-MICRON SPECTROSCOPY OF HIGHLY REDDENED FIELD STARS Abstract Only **c90**
Mauricio Tapia, P. Persi, M. Roth, and M. Ferrari-Toniolo (Consiglio Nazionale delle Ricerche, Frascati, Italy) *In* NASA, Ames Research Center, Interstellar Dust: Contributed Papers Dec. 1989 p 29 (For primary document see N91-14897 06-88)
Avail: NTIS HC/MF A22 CSCL 03B

Broad absorption features centered at 3.45 microns and at 3.0-3.0 microns towards a number of late-type supergiants in the vicinity of the galactic center were repeatedly reported. Here, 2.0 to 2.5 and 3.0 to 4.0 micron spectra are presented for field late-type highly reddened (A sub V is approximately 17-27) stars located in different regions of the galactic plane more than 20 deg away from the galactic center direction. The observations, made with the 3.6, 2.2, and 1.0 m ESO telescopes at La Silla, Chile, consists of CVF spectra with resolution lambda/delta lambda is approximately or equal to 100 and IRSPEC spectra with resolution lambda/delta lambda is approximately or equal to 700. In the direction of the most highly reddened stars, definitive detections of the 3.45 and the 3.0 to 3.1 micron absorption features are reported. The 3.45 micron feature was attributed to absorption arising in a vibrational transition resulting from the C-H stretching in organic compounds, while the 3.0 to 3.1 micron broader feature are tentatively attributed to O-H bonds. The observations strongly support that the agent producing the 3.45 micron feature, presumably organic molecules, is an important component of the diffuse interstellar medium and is not characteristic only of the galactic center environment. Author

N91-14905*# Kapteyn Astronomical Lab., Groningen (Netherlands).
INTERSTELLAR CIRCULAR POLARIZATION AND THE DIELECTRIC NATURE OF DUST GRAINS Abstract Only **c90**
Grzegorz Chlewicki and J. Mayo Greenberg (Leiden Univ., Netherlands) *In* NASA, Ames Research Center, Interstellar Dust: Contributed Papers Dec. 1989 p 33 (For primary document see N91-14897 06-88)
Avail: NTIS HC/MF A22 CSCL 03B

The implications of the observed relationship between the wavelength dependence of interstellar circular and linear polarization were reexamined. Mie theory calculations for grains with various optical constants demonstrate that any population of grains which matches the observed wavelength dependence of linear polarization also yields the correct cross-over wavelength of circular polarization. The coincidence of the peak wavelength of linear polarization and the cross-over of circular polarization is therefore independent of the optical constants of the grains and cannot be used as a critical constraint on grain properties. The observed relationship instead reflects a more fundamental connection between linear and circular polarization which was derived from the Kramers-Kronig relations by Shapiro (1975). Numerical results fully support Shapiro's conclusions and demonstrate that the apparent upper limit on the visual absorptivity of polarizing grains deduced from earlier Mie theory calculations (Martin, 1972) was spurious and resulted from a violation of the Kramers-Kronig relations in the assumed optical constants of the particles. The Kramers-Kronig interpretation of circular polarization can be used to place constraints on linear polarization outside the wavelength range in which it was observed. This approach was used to show that the peak observed in the visual is likely to be the only significant feature in the linear polarization curve, which therefore appears to be well approximated at all wavelengths by the Serkowski formula. A synthesis of available laboratory data was used to analyze the properties of dielectric core-mantel grains as the source of visual extinction and polarization. Author

N91-14906*# Belgian Royal Observatory, Brussels.
NEW RESULTS IN THE THEORY OF DUST GRAIN ALIGNMENT **c90**
Pierre Cugnon *In* NASA, Ames Research Center, Interstellar Dust: Contributed Papers Dec. 1989 p 35-36 (For primary document see N91-14897 06-88)
Avail: NTIS HC/MF A22 CSCL 03B

Two complementary approaches are used in an attempt to propose an appropriate formulation of the solution to the problem of magnetic alignment of grains in the diffuse and/or the more denser clouds, whatever the mechanism of rotational excitation can be. The interest of such a unified formulation is mainly that the same theoretical expression for polarization can be used everywhere, allowing for easier comparisons between regions where the physical conditions are highly different. The first consists in applying a Monte-Carlo method to a limited number of representative cases, for which all the torques acting on the grain are taken into account: impulsive random torques due to direct collisions with gas atoms, to evaporation of atoms from the surface, and to exo-energetic recombinations forming hydrogen molecules, followed by violent ejections from peculiar sites; magnetic torques. Three characteristic times are associated with these torques: the collisional damping time, the time necessary to change completely the actual sites configuration narrowly bound to the correlation time of the suprathermal torque; and the magnetic damping time. The second approach starts from a heuristic point of view. It consists in a generalization of results (Cugnon, 1983; see also Purcell and Spitzer, 1971; Greenberg, 1978) obtained for thermal alignment to the suprathermal case. It appears indeed that in two extreme cases, the thermal formulation may be used after redefinition of involved times and temperatures. Author

N91-14907*# Tohoku Univ., Sendai (Japan). Astronomical Inst.
POLARIZATION AND EXTINCTION BY ALIGNED GRAINS **c90**
Masafumi Matsumura and Munezo Seki *In* NASA, Ames Research Center, Interstellar Dust: Contributed Papers Dec. 1989 p 37-40 (For primary document see N91-14897 06-88)
Avail: NTIS HC/MF A22 CSCL 03B

Correlations between ultraviolet extinction and visual polarization are studied. No correlations are found for 272 sampled stars. UV extinction and visual polarization are quite independent phenomena. Author

N91-14908*# Tohoku Univ., Sendai (Japan). Coll. of General Education.
ALIGNMENT MECHANISMS OF PARAMAGNETIC GRAINS REVISITED **c90**
Munezo Seki *In* NASA, Ames Research Center, Interstellar Dust: Contributed Papers Dec. 1989 p 41-44 (For primary document see N91-14897 06-88)
Avail: NTIS HC/MF A22 CSCL 03B

Taking into account the tight coupling of grain axis with angular momentum due to effective dissipation of rotation energy, the alignment of spheroidal grains was investigated by paramagnetic relaxation. Alignment degree will be significantly improved in diffuse clouds. The inclusions of superparamagnetic (SPM) substances may play a key role in grain alignment in dark clouds as well as in diffuse clouds. Author

N91-14909*# California Univ., Berkeley. Space Sciences Lab.
NEW MEASUREMENTS OF THE FAR ULTRAVIOLET SCATTERING PROPERTIES OF INTERSTELLAR DUST Abstract Only **c89**
Mark Hurwitz, Stuart Bowyer, and Christopher Martin *In* NASA, Ames Research Center, Interstellar Dust: Contributed Papers Dec. 1989 p 47 (For primary document see N91-14897 06-88)
(Grants NGR-05-003-805; NGT-50185)
Avail: NTIS HC/MF A22 CSCL 03B

An analysis is presented for the spectra of the diffuse ultraviolet background taken during shuttle flight STS-61C (January 1986). Eight regions of the sky were observed for approximately 20 minutes each, using a spectrograph designed specifically to perform measurements of the UV background. The field of view was 3.8

deg x 8 min, with imaging along the slit to confine stellar contamination. The instrument featured a shutter mechanism to measure internal background during flight, a low-scatter holographically ruled diffraction grating, photon counting microchannel plate detectors, through baffling, and a crystal window to further attenuate stray light. The spectra covered the range 1400 to 1850 A and was binned in 50 A bands. The procedure for substracting the contribution of stars too faint to be detected as discrete sources during the observations (in general this represents a small fraction of the total intensity detected except at the longest wavelengths). A radiative transfer model used to interpret the data and set confidence intervals on the relevant parameters is described. It was found that the continuum component of the diffuse ultraviolet background arises primarily from two sources. One source is scattering of starlight by interstellar dust with an albedo of about 12 percent and a relatively isotropic phase function. A second source consists of about 150 photons/cm/sec/ster/A of extragalactic light which is attenuated by the dust in the galaxy. Although emission features possibly associated with molecular H2 are detected in one look direction, fluorescence of H2 is not a major contributor to the diffuse UV background, at least at galactic latitudes greater than -10 degrees. Author

N91-14910*# Academy of Sciences (USSR), Dushanbe. Inst. of Astrophysics.

INTERSTELLAR DUST AS GENERATOR OF X RAY RADIATION **c93**

Subhon Ibadov *In* NASA, Ames Research Center, Interstellar Dust: Contributed Papers Dec. 1989 p 49-54 (For primary document see N91-14897 06-88)

Avail: NTIS HC/MF A22 CSCL 03B

The x ray generation due to arising of hot dense plasma balls at high-velocity (greater than or equal to 70 km/s) collisions of dust grains in the interstellar medium is considered. Analytical expressions for efficiency of conversions of colliding dust particle kinetic energy into x ray radiation are presented. The observed intensity distribution of the diffuse component of soft cosmic x rays (0.1 to 1 keV) may be partly caused by collisions between the dusty components of high velocity clouds and of the disk of the Galaxy. Author

N91-14911*# Helsinki Univ. (Finland).

THE SPECTRAL ENERGY DISTRIBUTION OF THE SCATTERED LIGHT FROM DARK CLOUDS **c90**

Kalevi Mattila and G. F. O. Schnur (Ruhr Univ., Bochum, Germany, F.R.) *In* NASA, Ames Research Center, Interstellar Dust: Contributed Papers Dec. 1989 p 55-56 (For primary document see N91-14897 06-88)

Avail: NTIS HC/MF A22 CSCL 03B

A dark cloud is exposed to the ambient radiation field of integrated starlight in the Galaxy. Scattering of starlight by the dust particles gives rise to a diffuse surface brightness of the dark nebula. The intensity and the spectrum of this diffuse radiation can be used to investigate, e.g., the scattering parameters of the dust, the optical thickness of the cloud, and as a probe of the ambient radiation field at the location of the cloud. An understanding of the scattering process is also a prerequisite for the isolation of broad spectral features due to fluorescence or to any other non-scattering origin of the diffuse light. Model calculations are presented for multiple scattering in a spherical cloud. These calculations show that the different spectral shapes of the observed diffuse light can be reproduced with standard dust parameters. The possibility to use the observed spectrum as a diagnostic tool for analyzing the thickness of the cloud and the dust particle is discussed. Author

N91-14912*# National Aeronautics and Space Administration. Goddard Space Flight Center, Greenbelt, MD.

OBSERVATIONS OF THE DIFFUSE UV RADIATION FIELD **c93**

Jayant Murthy, R. C. Henry, P. D. Feldman, and P. D. Tennyson (Massachusetts Inst. of Tech., Lexington.) *In* NASA, Ames Research Center, Interstellar Dust: Contributed Papers Dec. 1989 p 57-58 (For primary document see N91-14897 06-88) (Grant NAG5-619)

Avail: NTIS HC/MF A22 CSCL 03B

Spectra are presented for the diffuse UV radiation field between 1250 to 3100 A from eight different regions of the sky, which were obtained with the Johns Hopkins UVX experiment. UVX flew aboard the Space Shuttle Columbia (STS-61C) in January 1986 as part of the Get-Away Special project. The experiment consisted of two 1/4 m Ebert-Fastie spectrometers, covering the spectral range 1250 to 1700 A at 17 A resolution and 1600 to 3100 A at 27 A resolution, respectively, with a field of view of 4 x .25 deg, sufficiently small to pick out regions of the sky with no stars in the line of sight. Values were found for the diffuse cosmic background ranging in intensity from 300 to 900 photons/sq cm/sec/sr/A. The cosmic background is spectrally flat from 1250 to 3100 A, within the uncertainties of each spectrometer. The zodiacal light begins to play a significant role in the diffuse radiation field above 2000 A, and its brightness was determined relative to the solar emission. Observed brightnesses of the zodiacal light in the UV remain almost constant with ecliptic latitude, unlike the declining visible brightnesses, possibly indicating that those (smaller) grains responsible for the UV scattering have a much more uniform distribution with distance from the ecliptic plane than do those grains responsible for the visible scattering. Author

N91-14913*# National Aeronautics and Space Administration. Goddard Space Flight Center, Greenbelt, MD.

THE CAPABILITY OF THE ULTRAVIOLET IMAGING TELESCOPE FOR OBSERVING INTERSTELLAR DUST Abstract Only **c89**

Theodore P. Stecher *In* NASA, Ames Research Center, Interstellar Dust: Contributed Papers Dec. 1989 p 59 (For primary document see N91-14897 06-88)

Avail: NTIS HC/MF A22 CSCL 03A

The Ultraviolet Imaging Telescope (UIT) was designed to be able to obtain deep images of nearby galaxies with a single frame. This ability makes it ideal for many imaging problems of the interstellar dust. The instrument has a forty arc-minute field of view with two arc-second resolution. It has 11 ultraviolet filters and a grating which is used as a grism for full field spectroscopy. In a thirty minute exposure (one orbital night) the limiting magnitude for hot objects is V = 25, or a UV mag of 22 for point sources and a UV mag of 26 for extended sources. Programs are planned for the observation of dust in reflection nebulae H II regions, planetaries, dark nebulae, the diffuse galactic light, and dust in other galaxies are planned. The UIT was integrated into the Astro Spacelab Payload and is scheduled to be launched on the Columbia in Nov. 1989. Author

N91-14914*# Applied Research Corp., Landover, MD.

DIFFUSE GALACTIC LIGHT OBSERVATIONS AT 206 SELECTED AREAS **c89**

Gary N. Toller *In* NASA, Ames Research Center, Interstellar Dust: Contributed Papers Dec. 1989 p 61-65 (For primary document see N91-14897 06-88)

Avail: NTIS HC/MF A22 CSCL 03A

Space-based, observational diffuse galactic light (DGL) levels at 4400 A are presented as a function of galactic latitude (b). A peak in the ratio of DGL to direct starlight is apparent at the absolute value of b = 5 to 15 deg, where one third of the celestial brightness is due to scattered light. Another salient feature is the general decrease in the relative contribution of the DGL at intermediate and high galactic latitudes. The relationship DGL (S sub 10(V)sub G2V, 4400 A) = 2.4 x 10 (exp -20 N(sub H I) atoms/sq cm may be used to estimate the brightness of DGL from neutral hydrogen column densities when N(sub H I) is less than 2 x 10(exp 21) atoms/sq cm. The results presented here have been used to characterize the interstellar dust in the general interstellar medium. A galaxy model that reproduces observed brightness levels was used to compare theoretical and observed DGL values. This determines two grain parameters - the albedo

and the asymmetry of the scattering phase function (g). The results are albedo = .61 + or - .07, and g = .6 + or - .2. Author

N91-14915*# Arizona Univ., Tucson. Dept. of Physics.
SIMULTANEOUS INFRARED AND UV-VISIBLE ABSORPTION SPECTRA OF MATRIX-ISOLATED CARBON VAPOR **c90**
Joe Kurtz and Donald R. Huffman *In* NASA, Ames Research Center, Interstellar Dust: Contributed Papers Dec. 1989 p 71-75 (For primary document see N91-14897 06-88)
Avail: NTIS HC/MF A22 CSCL 03B

Carbon molecules were suggested as possible carriers of the diffuse interstellar bands. In particular, it was proposed that the 443 nm diffuse interstellar band is due to the same molecule which gives rise to the 447 nm absorption feature in argon matrix-isolated carbon vapor. If so, then an associated C-C stretching mode should be seen in the IR. By doing spectroscopy in both the IR and UV-visible regions on the same sample, the present work provides evidence for correlating UV-visible absorption features with those found in the IR. Early data indicates no correlation between the strongest IR feature (1997/cm) and the 447 nm band. Correlation with weaker IR features is being investigated. Author

N91-14916*# University Coll., London (England). Dept. of Physics and Astronomy.
CORRELATION PROPERTIES OF INTERSTELLAR DUST: DIFFUSE INTERSTELLAR BANDS **c90**
W. B. Somerville *In* NASA, Ames Research Center, Interstellar Dust: Contributed Papers Dec. 1989 p 77-81 (For primary document see N91-14897 06-88)
Avail: NTIS HC/MF A22 CSCL 03B

Results are presented from a research program in which an attempt was made to establish the physical nature of the interstellar grains, and the carriers of the diffuse interstellar bands, by comparing relations between different observed properties; the properties used include the extinction in the optical and ultraviolet (including wavelength 2200 and the far-UV rise), cloud density, atomic depletions, and strengths of the diffuse bands. Observations and also data from literature were used, selecting particularly sight-lines where some observed property was found to have anomalous behavior. Author

N91-14917*# Texas Univ., Austin. Dept. of Astronomy.
HIGH RESOLUTION SPECTROSCOPY OF THE 11.3 MICRON EMISSION BAND Abstract Only **c89**
Jeff M. Achtermann, J. H. Lacy, and D. E. Bruce *In* NASA, Ames Research Center, Interstellar Dust: Contributed Papers Dec. 1989 p 85 (For primary document see N91-14897 06-88)
Avail: NTIS HC/MF A22 CSCL 03A

High resolution spectra of the 11.3 micron emission band in M82 and NGC 7027 were obtained using the University of Texas IR echelle spectrometer on the IRTF in April 1988. The spectral resolution was 0.004 micron, with coverage from 11.0 to 11.6 microns. Spectra were measured at ten positions along a 10 min. long slit. Analysis of the data is still in progress, but initial results show no clear evidence of narrow structure within the feature. The analysis will involve comparison of the observed spectra to laboratory and predicted spectra of Polycylic Aromatic Hydrocarbons (PAHs) and Quenched Carbonaceous Composite (QCCs) to determine which may be responsible for the emission. The spectra will be examined with a goal of determining whether the emission is caused by molecular or solid state material. The data are also examined for evidence of variations in the shape and strength of the 11.3 micron feature with position on the sky. In NGC 7027 the 10 min. long slit went across the edge of the ionized nebulae, allowing comparison of emission from both ionized and neutral regions. Author

N91-14918*# National Aeronautics and Space Administration. Ames Research Center, Moffett Field, CA.
INFRARED IMAGES OF REFLECTION NEBULAE AND ORION'S BAR: FLUORESCENT MOLECULAR HYDROGEN AND THE 3.3 MICRON FEATURE **c89**
Michael G. Burton, Alan Moorhouse, P. W. J. L. Brand, Patrick F. Roche, and T. R. Geballe (Joint Astronomy Centre, Hilo, HI.) *In its* Interstellar Dust: Contributed Papers Dec. 1989 p 87-92 (For primary document see N91-14897 06-88)
Avail: NTIS HC/MF A22 CSCL 03A

Images were obtained of the (fluorescent) molecular hydrogen 1-0 S(1) line, and of the 3.3 micron emission feature, in Orion's Bar and three reflection nebulae. The emission from these species appears to come from the same spatial locations in all sources observed. This suggests that the 3.3 micron feature is excited by the same energetic UV-photons which cause the molecular hydrogen to fluoresce. Author

N91-14919*# National Aeronautics and Space Administration. Ames Research Center, Moffett Field, CA.
AIRBORNE OBSERVATIONS OF THE INFRARED EMISSION BANDS Abstract Only **c89**
M. Cohen, Diane Wooden, Alexander G. G. M. Tielens, Jesse D. Bregman, Fred C. Witteborn, D. Rank, and Louis J. Allamandola *In its* Interstellar Dust: Contributed Papers Dec. 1989 p 93 (For primary document see N91-14897 06-88)
Avail: NTIS HC/MF A22 CSCL 03A

Earlier airborne studies of the infrared bands between 5 and 8 microns have now been extended to a sample of southern sources selected from the IRAS Low Resolution Spectra (LRS) atlas. The correlation between the strongest bands at 6.2 and 7.7 microns is now based on a total sample of 40 sources and is very strong. A new emission band at 5.2 microns, previously predicted for polycyclic aromatic hydrocarbons (PAHs), is recognized in 27 sources; it too correlates with the dominant 7.7 micron band, showing that the 5.2 micron feature also belongs to the generic spectrum of PAH features at 3.3, 5.6, 6.2, 6.2, 7.7, 8.7, 11.3, and 12.7 microns. Sufficient sources are had now to define the relative strengths of most of these bands in three separate nebular environments: planetaries, H II regions, and reflection nebulae. Significant variations are detected in the generic spectra of PAHs in these different environments which are echoed by variations in the exact wavelength of the strong 7.7 micron peak. The earlier suggestion that, in planetaries, the fraction of total emission observed by IRAS that is carried by the PAH emissions is correlated with nebular gas-phase C/O ratio is supported by the addition of newly-observed southern planetaries, including the unusually carbon-rich (WC10) nebular nuclei. These (WC10) nuclei also exhibit a strong plateau of emission linking the 6.2 and 7.7 micron features. Author

N91-14920*# Leiden Univ. (Netherlands).
A SURVEY FOR PAH EMISSION IN H II REGIONS, PLANETARY AND PROTO-PLANETARY NEBULAE **c93**
M. deMuizon, P. Cox, and J. Lequeux (Ecole Normale Superieure, Paris, France) *In* NASA, Ames Research Center, Interstellar Dust: Contributed Papers Dec. 1989 p 95-99 Previously announced as N90-19129 (For primary document see N91-14897 06-88)
Avail: NTIS HC/MF A22 CSCL 03B

The results of a systematic investigation of polycyclic aromatic hydrocarbon (PAH) emission in H II regions, planetary nebulae (PN), and proto-planetary nebulae (PNN), are reported. Data is obtained from the low resolution spectra (LRS) of IRAS. The results show that: PAHs are formed in carbon rich objects; and PAH emission is ubiquitous in general interstellar medium and requires the presence of ultraviolet photons, in planetary and proto-planetary nebulae, PAH emission is seen only where an ionizing flux is present and in carbon rich objects. Author

N91-14921*# Mount Stromlo and Siding Spring Observatory, Canberra (Australia).
PAH EMISSION FROM NOVA CEN 1986 **c93**
A. R. Harry Hyland and P. J. McGregor *In* NASA, Ames Research Center, Interstellar Dust: Contributed Papers Dec. 1989 p 101-106 (For primary document see N91-14897 06-88)
Avail: NTIS HC/MF A22 CSCL 03B

The discovery of broad emission features between 3.2 and 3.6

microns were reported in the spectrum of Nova Cen 1986 (V842 Cen) some 300 days following outburst and remaining prominent for several months. The general characteristics of these features are similar to those attributed to polycyclic hydrocarbon (PAH) molecules in other dusty sources, although the relative strengths are different, and these observations provide the first clear evidence for molecular constituents other than graphite particles in the ejecta of novae. Author

N91-14922*# National Aeronautics and Space Administration. Ames Research Center, Moffett Field, CA.
SPATIAL VARIATIONS OF THE 3 MICRON EMISSION FEATURES WITHIN NEBULAE Abstract Only **c89**
Alan Moorhouse, T. R. Geballe (Joint Astronomy Centre, Hilo, HI.), and Louis J. Allamandola *In its* Interstellar Dust: Contributed Papers Dec. 1989 p 10 (For primary document see N91-14897 06-88)
Avail: NTIS HC/MF A22 CSCL 03A

The 3 micron spectra is presented for the Orion bar region and the Red Rectangle. In both objects spectra were obtained at more than one location, corresponding to different distances from the excitation source. The well known 3.3 and 3.4 micron emission bands are seen in both objects as well as the recently discovered features at 3.46, 3.51, and 3.57 microns in the Orion bar spectra. The spectra show that the relative strengths of the 3 micron emission features vary within the Orion bar. As distance from the exciting star increases, the 3.4 and 3.51 micron features increase, and the 3.46 micron feature decreases in strength, relative to the strong 3.3 micron feature. These are two possible interpretations which are postulated, each of which involves the breaking of bonds by UV radiation, which removes the modes responsible for the 3.4 micron emission near the star. The two possible bond ruptures are the CH bond in small polycyclic aromatic hydrocarbons (PAHs), or the bond to an aliphatic subgroup. It has to be pointed out that neither interpretation appears entirely satisfactory. The vibrational overtone interpretation cannot explain the presence or behavior of the 3.46 micron feature, whereas the laboratory spectra of aliphatic sidegroups contain many more features in the 3 micron region than are observed in the astronomical sources. Author

N91-14923*# Durham Univ. (England). Dept. of Physics.
THE WAVELENGTH DEPENDENCE OF POLARIZATION IN NGC 2023 **c89**
C. D. Rolph and S. M. Scarrott *In* NASA, Ames Research Center, Interstellar Dust: Contributed Papers Dec. 1989 p 109-110 (For primary document see N91-14897 06-88)
Avail: NTIS HC/MF A22 CSCL 03A

NGC 2023 is a bright reflection nebula illuminated by the central star HD37903. At 2 microns the nebula is seen solely by reflected light from the central star but in the NIR there is excess radiation that is supposed to arise from thermal emission from a population of small grains (Sellgren, 1984). The unexpectedly high surface brightness at R and I wavelengths has led to the suggestion that even at these wavelengths there is a significant contribution from this thermal emission process (Witt, Schild, and Kraiman, 1984). If the nebula is seen by reflected starlight then this radiation will be linearly polarized. The level of polarization depends on the scattering geometry, grain size distribution, etc., and is typically 20 to 40 percent for nebulae such as NGC 1999 which is morphologically similar to NGC 2023. If, in any waveband, there is a contribution of radiation from emission processes this radiation will be unpolarized and will serve to dilute the scattered radiation to give a lower level of observed polarization. A study of the wavelength dependence of polarization in nebulae in which there may be thermal emission from grains will indicate the contribution from this process to the total luminosity. Polarization maps were produced in BVRI wavebands for the NGC 2023 nebulosity which confirm that at all wavelengths it is a reflection nebula illuminated by a central star. The wavelength dependence of polarization at representative points in the nebula and in a scatter plot of polarization in V and I wavebands at all points at which measurements are given. Results indicate that throughout the nebula there is a general trend for the level of polarization to increase with wavelength and that maximum levels of polarization occur at the longest wavelengths. No evidence is seen in the data for any significant contribution from the thermal emission from grains in the BVRI luminosity of NGC 2023. Author

N91-14924*# Commissariat a l'Energie Atomique, Gif-sur-Yvette (France). Service d'Astrophysique.
RED FLUORESCENCE AND 3-12 MICRON EMISSION IN NGC 2023, HD 44179, M 82, AND LYNDS 1780 **c93**
Charles Ryter and Louis B. dHendecourt (Paris VII Univ., France) *In* NASA, Ames Research Center, Interstellar Dust: Contributed Papers Dec. 1989 p 111-114 (For primary document see N91-14897 06-88)
Avail: NTIS HC/MF A22 CSCL 03B

A red excess observed in the Red Rectangle (HD 44179), was attributed to a possible molecular fluorescence mechanism was discovered in NGC 2023 and analyzed in subsequent work in this and other nebulae. An unexpected red light excess was also noticed in a high latitude dark cloud L 1780. The fluorescence was attributed to hydrogenated amorphous carbon by Duley (1985), on the basis of laboratory work. Alternatively, transitions between electronic states of free polycyclic aromatic hydrocarbon molecules, by-passing the cascade along the vibrational states was considered. In L 1780, the red excess was related to the 12 micron emission detected by IRAS. A quantitative comparison of the intensity of the red fluorescence and that of the 3 to 12 micron features is thus warranted in helping assess the physical properties of large interstellar molecules. The red fluorescence radiation, F(R), appears as a bump on the spectra between 0.6 and 0.9 micron. Values were deduced from the spectra for HD 44179, and for the high latitude cloud L 1780. Corrections for the extinction, both interstellar and internal to the nebulae, were included. The 3 to 12 micron brightness, F(IR), was obtained through integration of the spectra for NGC 2023, and for HD 44179 after removal of a smooth continuum due to hot large grains. The values of the ratio of fluorescence flux to the infrared flux, F(R)/F(IR), are summarized. Red fluorescence and infrared radiation are two separate ways to access to the size of the molecules through observation, and it is rewarding that both approaches give similar results. These findings bring a striking coherence into the physical description of the particles, and add further support to the initial attribution of the infrared features to polycyclic aromatic hydrocarbons (PAHs). Author

N91-14925*# Hawaii Univ., Honolulu. Inst. for Astronomy.
HIGH-SPECTRAL RESOLUTION OBSERVATIONS OF THE 3.29 MICRON EMISSION FEATURE: COMPARISON TO QCC AND PAHS **c89**
Alan T. Tokunaga, Kris Sellgren, Akira Sakata, S. Wada, Takashi Onaka, Y. Nakada, and T. Nagata (Kyoto Univ., Japan) *In* NASA, Ames Research Center, Interstellar Dust: Contributed Papers Dec. 1989 p 115-118 (For primary document see N91-14897 06-88)
Avail: NTIS HC/MF A22 CSCL 03A

Two of the most promising explanations for the origin of the interstellar emission features observed at 3.29, 3.4, 6.2, 7.7, 8.6, and 11.3 microns are: quenched carbonaceous composite (QCC) and polycyclic aromatic hydrocarbons (PAHs). High resolution spectra are given of the 3.29 micron emission feature which were taken with the Cooled Grating Array Spectrometer at the NASA Infrared Telescope Facility and previously published. These spectra show that the peak wavelength of the 3.29 micron feature is located at 3.295 + or - 0.005 micron and that it is coincident with the peak absorbance of QCC. The peak wavelength of the 3.29 micron feature appears to be the same in all of the sources observed thus far. However, the width of the feature in HD 44179 and Elias 1 is only 0.023 micron, which is smaller than the 0.043 micron width in NGC 7027, IRAS 21282+5050, the Orion nebula, and BD+30 deg 3639. Spectra of NGC 7027, QCC, and PAHs is shown. QCC matches the 3.29 micron interstellar emission feature very closely in the wavelength of the peak, and it produces a single feature. On the other hand, PAHs rarely match the peak of

the interstellar emission feature, and characteristically produce multiple features. Author

N91-14926*# National Aeronautics and Space Administration. Ames Research Center, Moffett Field, CA.
SPECTRAL STRUCTURE NEAR THE 11.3 MICRON EMISSION FEATURE Abstract Only **c93**
Fred C. Witteborn, Scott A. Sandford, Jesse D. Bregman, Louis J. Allamandola, M. Cohen, and Diane Wooden *In its* Interstellar Dust: Contributed Papers Dec. 1989 p 11 (For primary document see N91-14897 06-88)
Avail: NTIS HC/MF A22 CSCL 03B

If the 11.3 micron emission feature seen in the spectra of many planetary nebulae, H II regions, and reflection nebulae is attributable to polycyclic aromatic hydrocarbons (PAHs), then additional features should be present between 11.3 and 13.0 microns. Moderate resolution spectra of NGC 7027, HD 44179, BD+30 deg 3639, and IRAS 21282+5050 are presented which show evidence for new emission features centered near 12.0 and 12.7 microns. These are consistent with an origin from PAHs and can be used to constrain the molecular structure of the family of PAHs responsible for the infrared features. There is an indication that coronene-like PAHs contribute far more to the emission from NGC 7027 than to the emission from HD 44179. The observed asymmetric profile of the 11.3 micron band in all the spectra is consistent with the slight anharmonicity expected in the C-H out-of-plane bending mode in PAHs. A series of repeating features between 10 and 11 microns in the spectrum of HD 44179 suggests a simple hydride larger than 2 atoms is present in the gas phase in this object. Author

N91-14927*# Ecole Normale Superieure, Paris (France). Lab. de Physique.
SMALL SCALE VARIATIONS OF ABUNDANCES OF TRANSIENTLY HEATED GRAINS IN MOLECULAR CLOUDS **c90**
F. Boulanger, E. Falgarone, G. Helou (California Inst. of Tech., Pasadena.), and J. L. Puget *In* NASA, Ames Research Center, Interstellar Dust: Contributed Papers Dec. 1989 p 123-127 (For primary document see N91-14897 06-88)
Avail: NTIS HC/MF A22 CSCL 03B

IRAS images of a variety of fragments in nearby molecular clouds show that the energy distribution of their IR emission varies widely from cloud to cloud and from place to place within a given cloud. These variations at small scale are all the more unexpected since the colors of the IR emission of cold material differ very little at large scale: the colors of the cirrus emission above the 3kpc molecular ring are the same as those of the cirrus emission in the solar neighborhood. To quantitatively study these variations, 12, 60, and 100 microns brightnesses were obtained of small areas centered at different positions within the set of clouds and complexes. The range of observed 12/100 micron colors is given for each cloud. Variations by an order of magnitude are found in most clouds. Variations by a factor of 2 to 3 are observed within a cloud on scales as small as 0.5pc, the resolution of this study. It is concluded that large variations of the abundances of small particles with respect to those of the large grains responsible for the 100 micron emission are required to explain the observed color variations and that these abundances have to vary by large factors; an order of magnitude from cloud to cloud. Author

N91-14928*# Centre d'Etude Spatiale des Rayonnements, Toulouse (France).
THE 3.3 MICRON EMISSION FEATURE: MAP OF THE GALACTIC DISK, 10 DEG LESS THAN 1 LESS THAN 35 DEG, - 6 DEG LESS THAN B LESS THAN 6 DEG **c93**
Martin Giard, F. Pajot, Emanuel Caux, J. M. Lamarre (Centre National de la Recherche Scientifique, Verrieres-Le Buisson, France), G. Serra *In* NASA, Ames Research Center, Interstellar Dust: Contributed Papers Dec. 1989 p 129-130 (For primary document see N91-14897 06-88)
Avail: NTIS HC/MF A22 CSCL 03B

The 3.3 micron aromatic feature has been detected in the diffuse galactic emission with the AROME balloon-borne instrument. The results are presented in the form of an map of the 3.3 micron feature's intensity. The AROME instrument consists in a Cassegrain telescope with wobbling secondary mirrors and a liquid/solid nitrogen cooled photometer. The instrumental output is modified by the impulse response of the system. So the galactic surface brightness was restored in Fourier space by an inverse optimal filtering. The map of the feature's intensity is presented for a region of galactic coordinates. All the known H II giant molecular cloud complexes are visible in the 3.3 micron feature emission showing a good correlation with the infrared dust emission. Author

N91-14929*# Aerospace Corp., Los Angeles, CA. Space Sciences Lab.
IR EMISSION AND UV EXTINCTION IN TWO OPEN CLUSTERS Abstract Only **c93**
James A. Hackwell and James H. Hecht *In* NASA, Ames Research Center, Interstellar Dust: Contributed Papers Dec. 1989 p 131 (For primary document see N91-14897 06-88)
Avail: NTIS HC/MF A22 CSCL 03B

Recent models of interstellar extinction have shown the importance of understanding both the UV and IR properties of interstellar dust grains. IRAS data have shown variations in 60 and 100 micron emissions presumably due to the presence of IR cirrus, while recent observations in the UV by Fitzpatrick and Massa have identified components in the UV extinction curve which vary in different star regions. A Draine and Anderson model connects these results by proposing that different size variations in interstellar grains would cause distinct changes in both the IR emission and the UV extinction. In order to test this model it is necessary to make observations in well defined locations away from peculiar extinction regions. In the infrared this means looking away from the galactic plane so as to limit non-local sources of IR radiation. Two open clusters that are out of the galactic plane and which contain a number of late B and early A stars suitable for UV extinction studies, and whose IRAS data show variations in the 60/100 micron ratio were studied. Based on the Drain and Anderson model, variations were expected in their UV extinction curves that correlate with the IR cirrus emission. Author

N91-14930*# Kapteyn Astronomical Lab., Groningen (Netherlands).
DUST EMISSION FROM HIGH LATITUDE CIRRUS CLOUDS Abstract Only **c90**
Rene J. Laureijs, Grzegorz Chlewicki, F. O. Clark, and P. R. Wesselius *In* NASA, Ames Research Center, Interstellar Dust: Contributed Papers Dec. 1989 p 133 (For primary document see N91-14897 06-88)
Avail: NTIS HC/MF A22 CSCL 03B

In order to study dust emission from grains in the interstellar medium, the infrared properties were analyzed in a number of isolated high latitude dust clouds which contain no dominant internal heating sources. The clouds are spatially resolved, have a simple geometry, and are mapped in the IRAS bands at 12, 25, 60, and 100 microns. For a number of these clouds, extinction data (A sub B) were obtained from starcounts. A large part (30 to 50 percent) of the infrared radiation of the clouds in the IRAS wavelength range of 8 to 130 micron is emitted in the short wavelength bands at 12 and 25 micron. The 60/100 micron ratios for the integrated fluxes of the clouds have a typical value of 0.19 + or - 0.05. Author

N91-14931*# National Aeronautics and Space Administration. Ames Research Center, Moffett Field, CA.
THE SPATIAL DISTRIBUTION OF INFRARED RADIATION FROM VISIBLE REFLECTION NEBULAE **c89**
Ling Luan, Michael W. Werner, Eli Dwek, and Kris Sellgren (Hawaii Univ., Honolulu.) *In its* Interstellar Dust: Contributed Papers Dec. 1989 p 135-140 (For primary document see N91-14897 06-88)
(Contract NCA2-269)
Avail: NTIS HC/MF A22 CSCL 03A

The emission at IRAS 12 and 25 micron bands of reflection nebulae is far in excess of that expected from the longer wavelength equilibrium thermal emission. The excess emission in the IRAS 12 micron band is a general phenomenon, seen in various components of interstellar medium such as IR cirrus clouds, H II regions, atomic and molecular clouds, and also normal spiral galaxies. This excess emission has been attributed to UV excited fluorescence in polycyclic aromatic hydrocarbon (PAH) molecules or to the effect of temperature fluctuations in very small grains. Results are presented of studies of IRAS data on reflection nebulae selected from the van den Bergh reflection nebulae sample. Detailed scans of flux ratio and color temperature across the nebulae were obtained in order to study the spatial distribution of IR emission. A model was used to predict the spatial distribution of IR emission from dust grains illuminated by a B type star. The model was also used to explore the excitation of the IRAS 12 micron band emission as a function of stellar temperature. The model predictions are in good agreement with the analysis of reflection nebulae, illuminated by stars with stellar temperature ranging from 21,000 down to 3,000 K. Author

N91-14932*# Centre National de la Recherche Scientifique, Verrieres-Le Buisson (France). Lab. de Physique Stellaire et Planetaire.

INFLUENCE OF TEMPERATURE ON THE INFRARED SPECTRUM OF THE CORONENE MOLECULE **c89**

Jean-Phillipe Bernard, Louis B. DHendecourt, and Alain Leger (Paris VII Univ., France) *In* NASA, Ames Research Center, Interstellar Dust: Contributed Papers Dec. 1989 p 143-148 Previously announced in IAA as A89-53607 (For primary document see N91-14897 06-88)

Avail: NTIS HC/MF A22 CSCL 03A

Laboratory experiments were performed to study the temperature dependence of the absorption spectrum of the coronene molecule (C24H12), believed to be representative of the polycyclic aromatic hydrocarbon (PAH) molecules present in the interstellar medium. The main results is that both line positions and total intensities are almost unchanged when varying the temperature so that the spectrum is mostly temperature independent in the explored range, supporting the modeling of the IR emission originally made by Leger and Puget where room temperature was used in the calculations. In the structure of the band shape, small temperature correlated changes are observed. Qualitative arguments are given to interpret them. Author

N91-14933*# Lecce Univ. (Italy). Dept. of Physics.

RAMAN PROPERTIES OF VARIOUS CARBONACEOUS MATERIALS AND THEIR ASTROPHYSICAL IMPLICATIONS Abstract Only **c93**

A. Blanco, A. Borghesi, E. Bussoletti, Luigi Colangeli, Sergio Fonti, M. Lugara, Vincenso Orofino, and G. Scamarcio (Bari Univ., Italy) *In* NASA, Ames Research Center, Interstellar Dust: Contributed Papers Dec. 1989 p 149-150 (For primary document see N91-14897 06-88)

Avail: NTIS HC/MF A22 CSCL 03B

It is well known that a large number of celestial objects exhibit, in the range 3 to 12 micron, a family of emission features called unidentified infrared bands (UIR). They usually appear together and are associated with UV sources. Recently various authors have suggested that these features could be attributed to solid carbonaceous materials. Following this interest, a systematic analysis was performed of various types of amorphous carbon grains and polycyclic aromatic hydrocarbons (PAH), produced in lab. Updating results of Raman measurements performed on several carbonaceous materials, chosen according to their astrophysical interest, are presented. The measurements were made by means of a Jobin-Yvon monochromator HG2S and standard DC electronic. The line at 5145 A of an Ar+ laser was used as excitation source. Author

N91-14934*# Michigan Univ., Ann Arbor. Space Physics Research Lab.

INFRARED FLUORESCENCE FROM PAHS IN THE LABORATORY **c93**

Isabelle Cherchneff and John R. Barker *In* NASA, Ames Research Center, Interstellar Dust: Contributed Papers Dec. 1989 p 151-156 Sponsored in part by NSF (For primary document see N91-14897 06-88)

Avail: NTIS HC/MF A22 CSCL 03B

Several celestial objects, including UV rich regions of planetary and reflection nebulae, stars, H II regions, and extragalactic sources, are characterized by the unidentified infrared emission bands (UIR bands). A few years ago, it was proposed that polycyclic aromatic hydrocarbon species (PAHs) are responsible for most of the UIR bands. This hypothesis is based on a spectrum analysis of the observed features. Comparisons of observed IR spectra with lab absorption spectra of PAHs support the PAH hypothesis. An example spectrum is represented, where the Orion Bar 3.3 micron spectrum is compared with the absorption frequencies of the PAHs Chrysene, Pyrene, and Coronene. The laser excited 3.3 micron emission spectrum is presented from a gas phase PAH (azulen). The infrared fluorescence theory (IRF) is briefly explained, followed by a description of the experimental apparatus, a report of the results, and discussion. Author

N91-14935*# Aerospace Corp., Los Angeles, CA. Space Sciences Lab.

SI3N4 EMISSIVITY AND THE UNIDENTIFIED INFRARED BANDS **c93**

Ray W. Russell, M. A. Chatelain, James H. Hecht, and John R. Stephens (Los Alamos National Lab., NM.) *In* NASA, Ames Research Center, Interstellar Dust: Contributed Papers Dec. 1989 p 157-162 (For primary document see N91-14897 06-88)

Avail: NTIS HC/MF A22 CSCL 03B

Infrared spectroscopy of warm (about 150 to 750 K), dusty astronomical sources has revealed a structured emission spectrum which can be diagnostic of the composition, temperature, and in some cases, even size and shape of the grains giving rise to the observed emission. The identifications of silicate emission in oxygen rich objects and SiC in carbon rich object are two examples of this type of analysis. Cometary spectra at moderate resolution have similarly revealed silicate emission, tying together interstellar and interplanetary dust. However, Goebel has pointed out that some astronomical sources appear to contain a different type of dust which results in a qualitatively different spectral shape in the 8 to 13 micron region. The spectra shown make it appear unlikely that silicon nitride can be identified as the source of the 8 to 13 micron emission in either NGC 6572 or Nova Aql 1982. The similarity between the general wavelength and shape of the 10 micron emission from some silicates and that from the two forms of silicon nitride reported could allow a mix of cosmic grains which include some silicon nitride if only the 8 to 13 micron data are considered. Author

N91-14936*# Alabama Univ., Birmingham. Dept. of Physics.

PAH IN THE LABORATORY AND INTERSTELLAR SPACE **c93**

Thomas J. Wdowiak, Gregory C. Flickinger, and David A. Boyd *In* NASA, Ames Research Center, Interstellar Dust: Contributed Papers Dec. 1989 p 163-167 (For primary document see N91-14897 06-88)

(Grant NAGw-749)

Avail: NTIS HC/MF A22 CSCL 03B

The theory that polycyclic aromatic hydrocarbons (PAHs) are a constituent of the interstellar medium, and a source of the IR emission bands at 3.3, 6.2, 7.7, 8.6, and 11.3 microns is being studied using PAH containing acid insoluble residue of the Orgueil CI meteorite and coal tar. FTIR spectra of Orgueil PAH material that has undergone thermal treatment, and a solvent insoluble fraction of coal tar that has been exposed to hydrogen plasma are presented. The UV excided luminescence spectrum of a solvent soluble coal tar film is also shown. Comparison of the lab

measurements with observations appears to support the interstellar PAH theory, and shows the process of dehydrogenation expected to take place in the interstellar medium. Author

N91-14937*# Molecular Research Inst., Palo Alto, CA.
THE EFFECT OF IONIZATION ON THE INFRARED ABSORPTION SPECTRA OF PAHS: A PRELIMINARY REPORT **c93**

Doug J. DeFrees and M. D. Miller (International Business Machines Corp., San Jose, CA.) *In* NASA, Ames Research Center, Interstellar Dust: Contributed Papers Dec. 1989 p 173-176 (For primary document see N91-14897 06-88)
Avail: NTIS HC/MF A22 CSCL 03B

The emission lines observed in many interstellar IR sources at 3.28, 6.2, 7.7, 8.7, and 11.3 microns are theorized to originate from polycyclic aromatic hydrocarbons (PAHs). These assignments are based on analyses of lab IR spectra of neutral PAHs. However, it is likely that in the interstellar medium that PAHs are ionized, i.e., are positively charged. Besides, as pointed out by Allamandola et al., although the IR emission band spectrum resembles what one might expect from a mixture of PAHs, it does not match in details such as frequency, band profile, or relative intensities predicted from the absorption spectra of any known PAH molecule. One source of more information to test the PAH theory is ab initio molecular orbital theory. It can be used to compute, from first principles, the geometries, vibrational frequencies, and vibrational intensities for model PAH compounds which are difficult to study in the lab. The Gaussian 86 computer program was used to determine the effect of ionization on the infrared absorption spectra of several small PAHs: naphthalene and anthracene. A preliminary report is presented of the results of these calculations. Author

N91-14938*# Observatoire de Paris-Meudon (France). Lab. de Recherches Spatiales.
ANGULAR MOTION OF A PAH MOLECULE IN INTERSTELLAR ENVIRONMENT **c93**

D. Rouan, Alain Leger, A. Omont, and Martin Giard (Centre d'Etude Spatiale des Rayonnements, Toulouse, France) *In* NASA, Ames Research Center, Interstellar Dust: Contributed Papers Dec. 1989 p 177-181 (For primary document see N91-14897 06-88)
Avail: NTIS HC/MF A22 CSCL 03B

Polycyclic aromatic hydrocarbon (PAH) molecules have recently been proposed as an important and hitherto undetected component of the Interstellar Medium (ISM). The theory was based on an explanation of the Unidentified IR Emission Bands by Leger et al. It has already led to a verified prediction on extended galactic and extragalactic emissions measured by IRAS, or by a recent balloon borne experiment. The physics that rules the motion of such molecules in the ISM was studied, taking into account their coupling with the ambient gas, the radiation field (absorption and emission) and the static magnetic field. This is important for many implications of the PAH theory such as the radio emission by these molecules or the expected polarization of their IR emission. A reflection nebulae is considered where the situation is rather well known. Every day life of a mean PAH molecule in such a region is as follows: every 3 hrs a UV photon is absorbed heating the molecule to a thousand degs; the temperature decay due to cooling by IR emission follows then within a few seconds. A collision with a molecule of gas occurs typically once a week, while an H atom is ejected or captured at the same rate. A typical cooling cycle after a heat impulse is given. The PAH molecules studied as representative of the family has typically 50 atoms, a radius of 4.5 A, is circular and has a molecular mass of M = 300; its permanent dipole moment is 3 Debye. Author

N91-14939*# Paris VII Univ. (France). Groupes de Physique des Solides de l'ENS.
PAHS MOLECULES AND HEATING OF THE INTERSTELLAR GAS **c93**

Laurent Verstraete, Alain Leger, Louis B. dHendecourt, O. Dutuit (Laboratoire de Chimie-Physique, Orsay, France), and D. Defourneau *In* NASA, Ames Research Center, Interstellar Dust: Contributed Papers Dec. 1989 p 183-188 (For primary document see N91-14897 06-88)
Avail: NTIS HC/MF A22 CSCL 03B

Until now it has remained difficult to account for the rather high temperatures seen in many diffuse interstellar clouds. Various heating mechanisms have been considered: photoionization of minor species, ionization of H by cosmic rays, and photoelectric effect on small grains. Yet all these processes are either too weak or efficient under too restricting conditions to balance the observed cooling rates. A major heat source is thus still missing in the thermal balance of the diffuse gas. Using photoionization cross sections measured in the lab, it was shown that in order to balance the observed cooling rates in cold diffuse clouds (T approx. 80 K) the PAHs would have to contain 15 percent of the cosmic abundance of carbon. This value does not contradict the former estimation of 6 percent deduced from the IR emission bands since this latter is to be taken as a lower limit. Further, it was estimated that the contribution to the heating rate due to PAH's in a warm HI cloud, assuming the same PAH abundance as for a cold HI cloud, would represent a significant fraction of the value required to keep the medium in thermal balance. Thus, photoionization of PAHs might well be a major heat source for the cold and warm HI media. Author

N91-14940*# Texas Univ., Austin. Dept. of Astronomy.
THE COMPACT FAR INFRARED EMISSION FROM THE YOUNG STELLAR OBJECT IRAS 16293-2422 **c93**

Harold M. Butner, N. J. Evans, III, D. F. Lester, L. G. Mundy, P. M. Harvey, and M. F. Campbell (Colby Coll., Waterville, ME.) *In* NASA, Ames Research Center, Interstellar Dust: Contributed Papers Dec. 1989 p 191-192 (For primary document see N91-14897 06-88)
Avail: NTIS HC/MF A22 CSCL 03B

High resolution far IR observations at 50 and 100 microns were made of the young stellar object (YSO), IRAS 16293-2422. The observations are part of a systematic high resolution study of nearby YSO's. The purpose is to obtain resolution in the far IR comparable to that at other wavelengths. Until recently, the high resolution that has been available in the far IR has been from either IRAS (angular resolution of approx 4 min) or the KAO using standard FIR photometry (approx 35 sec). With scanning techniques, it is possible to obtain 10 sec resolution on bright sources. Such a resolution is necessary to better determine the physical conditions of the YSO, and to compare with model of star formation. In order to better constrain the models for the source, the YSO was observed at both 50 and 100 microns on several flights in 1988 April from the KAO. Estimates are presented of the size both along the major and minor axis of the disk, as well as estimates of the dust temperature and 100 micron opacity for the YSO. Author

N91-14941*# Academy of Sciences (USSR), Leningrad. Special Astrophysical Observatory.
DUST CLOUDS IN ORION AND THE INTERSTELLAR NEUTRAL HYDROGEN DISTRIBUTION Abstract Only **c90**

N. V. Bystrova *In* NASA, Ames Research Center, Interstellar Dust: Contributed Papers Dec. 1989 p 193 (For primary document see N91-14897 06-88)
Avail: NTIS HC/MF A22 CSCL 03B

According to published examples of the far IR observations in the Orion and its surroundings, several well defined dust clouds of different sizes and structure are present. For comparison of these clouds with the neutral hydrogen distribution on the area of approx. 1000 sq degs, the data from Pulkovo Sky Survey in the interstellar neutral Hydrogen Radio Line as well as special observations with the RATAN-600 telescope in 21 cm line were used. From the materials of Pulkovo HI Survey, the data were taken near the line emission at ten velocities between -21.8 and +25.6 km/s LSR for the structural component of the interstellar hydrogen emission. The results given concern mainly the Orion's Great Dust Cloud and the Lambda Orionis region where the

information about the situation with the dust and interstellar hydrogen is very essential for interpretation. Author

N91-14942*# Wisconsin Univ., Madison. Dept. of Astronomy.
INFRARED EMISSION FROM ULTRACOMPACT H II REGIONS **c93**
Abstract Only
Ed Churchwell, Mark G. Wolfire (Chicago Univ., IL.), and Douglas O. S. Wood *In* NASA, Ames Research Center, Interstellar Dust: Contributed Papers Dec. 1989 p 195 (For primary document see N91-14897 06-88)
Avail: NTIS HC/MF A22 CSCL 03B

Models of circumstellar dust shells around ultracompact (UC) H II regions were constructed that accurately fit the observed IR flux distributions. The models assume spherically symmetric dust shells illuminated by stars whose bolometric luminosity is inferred from the integrated FIR flux densities. Assuming ionization by a single zero age main sequence (ZAMS) star, the relations of Panagia were used to infer the stellar radius and effective temperature for a given luminosity. The grain mixture in the dust shell consists of bare graphite and silicate grains with the optical properties of Draine and Lee and the size distribution of Mathis et al. The computer code of Wolfire et al was used to solve the radiative transfer equations through a spherical dust shell. The model provides monochromatic luminosities, dust temperatures, and opacities through the shell. Aside from the stellar and dust properties, the only other input parameters to the model are the distance to the shell, the form of its density distribution, and its outer radius. Predictions of the model are compared with observations of a typical UC H II region and the run of dust temperature with radius and the optical depth with frequency are discussed. Author

N91-14943*# Tata Inst. of Fundamental Research, Bombay (India).
DUST IN A FEW SOUTHERN H II REGIONS **c90**
Swarna Kanti Ghosh, K. V. K. Iyengar, T. N. Rengarajan, S. N. Tandon, R. P. Verma, and R. R. Daniel *In* NASA, Ames Research Center, Interstellar Dust: Contributed Papers Dec. 1989 p 197-198 (For primary document see N91-14897 06-88)
Avail: NTIS HC/MF A22 CSCL 03B

The property of dust in four southern H II region/molecular cloud complexes (RCW 108, RCW 57, RCW 122, and G351.6-1.3) was discussed. These regions were observed at an effective wavelength of 150 micron using TIFR balloon borne 1 m telescope and deconvolved maps with a resolution of 1 min were obtained. The data were combined with other available data to derive the properties of the infrared emitting dust in these regions. Author

N91-14944*# Tata Inst. of Fundamental Research, Bombay (India).
DISTRIBUTION OF DUST IN W31 COMPLEX **c90**
Swarna Kanti Ghosh, K. V. K. Iyengar, T. N. Rengarajan, S. N. Tandon, R. P. Verma, and R. R. Daniel *In* NASA, Ames Research Center, Interstellar Dust: Contributed Papers Dec. 1989 p 199-200 (For primary document see N91-14897 06-88)
Avail: NTIS HC/MF A22 CSCL 03B

W31 is a H II region/molecular cloud complex in the galactic plane at a distance of 6 Kpc. This complex consists of two prominent radio continuum sources (G10.2-0.3 and G10.3-0.1) representing H II regions. An extended region covering both these H II regions was mapped in the Far IR (FIR) using the TIFR 1 m balloon-borne telescope with an angular resolution of approx. 1 min and a dynamic range of 100. The resulting flux density distribution at an effective wavelength of 160 microns is presented. The coadded IRAS survey scan data at 60 and 100 microns were deconvolved using a maximum entropy method to generate the flux density maps of the same region. These 60 and 100 micron maps are given and are briefly discussed. Author

N91-14945*# National Radio Astronomy Observatory, Tucson, AZ.
LONGWAVE SPECTRAL DEPENDENCE OF EMISSION FROM WARM DUST CLOUDS **c93**
M. A. Gordon *In* NASA, Ames Research Center, Interstellar Dust: Contributed Papers Dec. 1989 p 201-202 (For primary document see N91-14897 06-88)
Avail: NTIS HC/MF A22 CSCL 03B

Observations of the continuum emission from warm dust clouds at 230 GHz, or 1300 microns, enables the determination of the frequency dependence of the optically thin longwave emission. Integrating the emission over the solid angle of the clouds gives a flux independent of the beam size and of the internal temperature structure of the clouds. The frequency resolving power of 64 allows the correction of these fluxes for the contribution of free-free emission from nearby H II regions at a price of reduced sensitivity. These observations were combined with similar observations made by others in the submillimeter and far infrared regimes to determine the continuum spectra of the dust clouds. Mean characteristics were determined for these clouds, fitting the spectra with simple transfer equations. Results are briefly discussed. Author

N91-14946*# Helsinki Univ. (Finland). Observatory and Astrophysics Lab.
H I AND DUST IN THE HIGH LATITUDE DARK CLOUD L1642 **c90**
Tarja Liljestroem and Kalevi Mattila *In* NASA, Ames Research Center, Interstellar Dust: Contributed Papers Dec. 1989 p 203-204 (For primary document see N91-14897 06-88)
Avail: NTIS HC/MF A22 CSCL 03B

The high latitude dark cloud L1642 in the 21 cm H I region was mapped using a 100 m radio telescope. A remarkable H I line broadening from 2.5 to 2.9 km/s is observed over a small area on the bright side of L1642, i.e., the side facing the galactic plane. Results are presented concerning the effects of the asymmetrical UV radiation field of OB stars on the H I gas and the very small dust grains associated with L1642. Author

N91-14947*# Five-College Astronomy Dept., Amherst, MA.
DUST EMISSION IN THE SAGITTARIUS B2 MOLECULAR CLOUD CORE **c90**
Dariusz C. Lis and Paul F. Goldsmith *In* NASA, Ames Research Center, Interstellar Dust: Contributed Papers Dec. 1989 p 205-209 (For primary document see N91-14897 06-88)
Avail: NTIS HC/MF A22 CSCL 03B

A model is presented for the dust emission from the Sagittarius B2 molecular cloud core which reproduces the observed spectrum between 30 and 1300 micron, as well as the distribution of the emission at 1300 micron. The model is based on the assumption that Sgr B2(N) continuum source is located behind the dust cloud associated with Sgr B2(M) continuum source. The fact that Sgr B2(N) is stronger at 1300 micron can be attributed to a local column density maximum at the position of this source. Absence of a 53 micron emission peak at the position of Sgr B2(N) suggests that the luminosity of the north source is lower than that of the middle source. Author

N91-14948*# Indian Inst. of Astrophysics, Bangalore.
ADDITIONAL RED AND REDDENED STARS IN CYG OB2 ASSOCIATION **c89**
M. Parthasarathy and S. K. Jain *In* NASA, Ames Research Center, Interstellar Dust: Contributed Papers Dec. 1989 p 211-217 (For primary document see N91-14897 06-88)
Avail: NTIS HC/MF A22 CSCL 03B

Several new red and reddened stars are detected in the most heavily reddened associations Cyg OB2. About 47 IRAS sources are detected in Cyg OB2. Their flux distributions, and colors, suggest that they are young stellar objects embedded in dust envelopes or disks (some of them may be proto stars) and are most likely members of the Cyg OB2 association. The large values of the flux ratio L sub IR/L sub VIS suggests that the central objects are obscured because of very large extinction. Author

N91-14949*# Groningen Rijksuniv. (Netherlands). Lab. for Space Research.
THE EMBEDDED OBJECTS IN EPSILON CHA I CLOUD **c90**
Abstract Only

Timo Prusti, R. Assendorp, and P. R. Wesselius *In* NASA, Ames Research Center, Interstellar Dust: Contributed Papers Dec. 1989 p 219 (For primary document see N91-14897 06-88)
Avail: NTIS HC/MF A22 CSCL 03B

A study was made of the embedded objects in the epsilon Cha I cloud. General shapes of the spectra were constructed for the members in the cloud. The near infrared data were compiled from the literature and combined with the IRAS Point Source Catalog information. Pointed observations by the IRAS were used in the regions of high source density where the Point Source Catalog is confused. Member objects near the late B star HD 97300 were measured recently in the 3 to 10 micron bands using the ESO 2.2 m telescope in order to study the effects of disks seen in other young stellar objects. A picture is presented of the complete initial luminosity function in the epsilon Cha I cloud. The observations were compared with the theoretical views on low mass star formation. Author

N91-14950*# California Univ., Berkeley. Radio Astronomy Lab.
INTERFEROMETRIC MOLECULAR LINE OBSERVATIONS OF W51 **c89**
Alexander Rudolph, William J. Welch, Patrick Palmer, and Berengere Dubrulle (Ecole Normale Superieure, Paris, France) *In* NASA, Ames Research Center, Interstellar Dust: Contributed Papers Dec. 1989 p 221-226 (For primary document see N91-14897 06-88)
Avail: NTIS HC/MF A22 CSCL 03A

Observations are presented of the H II region complex in W51 made with a mm interferometer. W51 is a region of massive star formation approx. 7 kpc distant from the sun. This region has been well studied in both the IR and submillimeter, the radio, as well as the maser transitions. These previous observations have revealed three regions of interest: (1) W51MAIN, a know of bright maser emission near two compact H II regions W51e1 and W51e2 (W51MAIN is also the peak of the 400 micron emission indicating that the bulk of the mass is centered there; (2) W51IRS1 is a long curving structure seen at 20 micron and at 2 and 6 cm but not at 400 micron; (3) W51IRS2 (also known as W51NORTH) is another compact H II region slightly offset from an 8 and a 20 micron peak and a collection of masers. Some conclusions are as follows: (1) SO and H(13)CN emission are similar and coincide with outflow activity; (2) HCO+ spectra show evidence for overall collapse of the W51 cloud toward W51MAIN; (3) A previously undetected continuum peak, W51DUST, coincides with the molecular peak H(13)CN-4; and (4) Dust emission at 3.4 mm reveals that about half of the 400 micron emission comes from the ultracompact H II region e2, and the rest from W51e1 and W51DUST. Author

N91-14951*# Naval Research Lab., Washington, DC.
DUST EMISSION FROM BARNARD 35: GAS HEATING ANOMALY RESOLVED **c90**
Howard A. Smith *In* NASA, Ames Research Center, Interstellar Dust: Contributed Papers Dec. 1989 p 227-232 (For primary document see N91-14897 06-88)
Avail: NTIS HC/MF A22 CSCL 03B

The molecular cloud B35 has puzzled observers because it contains gas which is, at T sub g approx. = 23 K, hotter that the surrounding dust whose T sub d approx. = 10 K. An investigation of the IRAS data, however, shows a previously unreported dust component at T sub d approx. 33 K, whose luminosity is ample to heat the gas. IRAS also finds that about 12 percent of the total luminosity around the core, and about 20 percent along the rim, arises from the small grain component with T less than or = 300 K. The temperature of these two components vary across the source, and this behavior is discussed. The results illustrate the presence of multiple components of dust in these clouds, and emphasize the need for data at multiple wavelengths. Author

N91-14952*# Kyoto Univ. (Japan).
A TWO MICRON POLARIZATION SURVEY TOWARD DARK CLOUDS **c89**
M. Tamura, S. Sato, I. Gatley, and J. H. Hough (Hatfield Polytechnic, England) *In* NASA, Ames Research Center, Interstellar Dust: Contributed Papers Dec. 1989 p 233-234 (For primary document see N91-14897 06-88)
Avail: NTIS HC/MF A22 CSCL 03A

A near infrared (2.2 micron) polarization survey of about 190 sources was conducted toward nearby dark clouds. The sample includes both background field stars and embedded young stellar objects. The aim is to determine the magnetic field structure in the densest regions of the dark clouds and study the role of magnetic fields in various phases of star formation processes, and to study the grain alignment efficiency in the dark cloud cores. From the polarization of background field stars and intrinsically unpolarized embedded sources, the magnetic field structure was determined in these clouds. From the intrinsic polarization of young stellar objects, the spatial distribution was determined of circumstellar dust around young stars. Combining the perpendicularity between the disks and magnetic fields with perpendicularity between the cloud elongation and magnetic fields, it is concluded that the magnetic fields might have dominated nearly all aspects of cloud dynamics, from the initial collapse of the clouds right through to the formation of disks/tori around young stars in these low to intermediate mass star forming clouds of the Taurus, Ophiuchus, and Perseus. Author

N91-14953*# California Inst. of Tech., Pasadena.
IRAS RESULTS ON OUTER GALAXY STAR FORMATION Abstract Only **c89**
Susan Terebey and Michel Fich (Waterloo Univ., Ontario) *In* NASA, Ames Research Center, Interstellar Dust: Contributed Papers Dec. 1989 p 235 (For primary document see N91-14897 06-88)
Avail: NTIS HC/MF A22 CSCL 03A

An infrared defined (60 micron) sample of IRAS sources were systematically studied in order to investigate star formation in the outer Galaxy. Five percent of the sample are point sources with IRAS spectra that suggest the emission is from a dust shell surrounding a mature star. Ninety five percent have spectra where flux density strictly rises with wavelength. The sources are extended, and it is shown that Point Source Catalog fluxes seriously underestimate total fluxes. CO kinematic distances were reliably assigned to two thirds of the sources. Most of the infrared luminosities correspond to B spectral types. Six cm continuum emission were detected from all sources inferred to have spectral type B1 or earlier. The combined IRAS/CO/6 cm data show these sources are young, moderately massive stars that are embedded in interstellar clouds. The young embedded sources define a distinct band in an IRAS color-colar diagram. Normal IRAS galaxies fall in the same band, consistent with the interpretation that their infrared emission is due to star formation. Author

N91-14954*# Max-Planck-Inst. fuer Radioastronomie, Bonn (Germany, F.R.).
HIGH RESOLUTION OBSERVATIONS OF COMPACT H II REGIONS AT 230 GHz **c89**
Joern-E. Wink (Institut de Radio Astronomie Millimetrique, Grenoble, France), P. G. Mezger, and R. Zylka *In* NASA, Ames Research Center, Interstellar Dust: Contributed Papers Dec. 1989 p 237-238 (For primary document see N91-14897 06-88)
Avail: NTIS HC/MF A22 CSCL 03A

Based on the idea that star formation goes on progressively in molecular clouds, a search was conducted for protostars by mapping compact H II regions at a frequency of 250 GHz. The IRAM 30 m radio telescope was used with a (3)He cooled bolometer. Twenty compact H II regions usually obtaining twice the expected free-free flux density, positionally coincident with the H II region, were observed. Even fine structure within the H II regions can be traced in the maps as in the case of G75.84+0.40 near ON-2. The high degree of coincidence between the 250 and 5 GHz map of Harris shows that the excess flux density observed must come from dust mixed with the ionized gas. Part of the dust must however be accumulated in the outer part of the H II region, since in some cases the contours are shifted outwards relative to

the radio maps. This is consistent with the fact that in those cases where enough information is available to make a model fit, temperatures were derived of 80 + or - 30 K. Author

N91-14955*# Bandung Inst. of Tech. (Indonesia). Dept. of Astronomy.
SURVEY OBSERVATIONS OF EMISSION-LINE STARS IN THE ORION REGION Abstract Only **c89**
Suhardja D. Wiramihardja, T. Kogure, S. Yoshida, K. Ogura, and M. Nakano (Oita Univ., Japan) *In* NASA, Ames Research Center, Interstellar Dust: Contributed Papers Dec. 1989 p 239 (For primary document see N91-14897 06-88)
Avail: NTIS HC/MF A22 CSCL 03A

Survey observations were conducted for H alpha-emission stars in the Orion region using the Kiso Schmidt telescope and partly the CTIO Curtis Schmidt telescope. In the area of about 25 square degrees, a total of 236 H alpha-emission objects, mostly supposed to be T Tau type stars, have been detected among which 155 are new ones including 6 non-stellar objects. Celestial coordinates and V-magnitude are measured for the detected objects. Eye estimation of the H alpha-emission intensity is also made at three epochs in a time span of about two years, where notable variation of H alpha intensity was found in 68 out of 236 objects. Besides a remarkable concentration along the northern dark cloud complex, a loose concentration is noticed near the Orion Belt region, fairly well coinciding with the distribution of the Orion OBIb association members. A comparison with the Av-map is also made to see the relationship between the distribution of emission-line objects and that of interstellar dust. Author

N91-14956*# Rice Univ., Houston, TX. Dept. of Chemistry.
MATRIX ISOLATION AS A TOOL FOR STUDYING INTERSTELLAR CHEMICAL REACTIONS Abstract Only **c90**
David W. Ball, Bryan J. Ortman, Robert H. Hauge, and John L. Margrave *In* NASA, Ames Research Center, Interstellar Dust: Contributed Papers Dec. 1989 p 243-244 (For primary document see N91-14897 06-88)
Avail: NTIS HC/MF A22 CSCL 03B

Since the identification of the OH radical as an interstellar species, over 50 molecular species were identified as interstellar denizens. While identification of new species appears straightforward, an explanation for their mechanisms of formation is not. Most astronomers concede that large bodies like interstellar dust grains are necessary for adsorption of molecules and their energies of reactions, but many of the mechanistic steps are unknown and speculative. It is proposed that data from matrix isolation experiments involving the reactions of refractory materials (especially C, Si, and Fe atoms and clusters) with small molecules (mainly H2, H2O, CO, CO2) are particularly applicable to explaining mechanistic details of likely interstellar chemical reactions. In many cases, matrix isolation techniques are the sole method of studying such reactions; also in many cases, complexations and bond rearrangements yield molecules never before observed. The study of these reactions thus provides a logical basis for the mechanisms of interstellar reactions. A list of reactions is presented that would simulate interstellar chemical reactions. These reactions were studied using FTIR-matrix isolation techniques. Author

N91-14957*# Leiden Univ. (Netherlands). Lab. Astrophysics.
NEW INSIGHTS IN THE PHOTOCHEMISTRY OF GRAIN MANTLES: THE IDENTIFICATION OF THE 4.62 AND 6.87 MICRON BANDS **c90**
Ruud Grim, Willem A. Schutte, Bernard Schmitt, and J. Mayo Greenberg *In* NASA, Ames Research Center, Interstellar Dust: Contributed Papers Dec. 1989 p 245-246 (For primary document see N91-14897 06-88)
Avail: NTIS HC/MF A22 CSCL 03B

The mid-IR spectral region of molecular clouds is known to show the fingerprints of molecules frozen in the icy mantles of the interstellar grains. To study the complex chemical and physical interactions on the ice mantles accreted on grains in molecular clouds numerous UV irradiation and diffusion experiments were performed. The irradiation of binary ices was studied. Using isotopic labelling on NH3/CO and NH3/O2 ices numerous compounds were identified, of which OCN(-), NO2(-), NO3(-), and NH4(+) ions reveal a new type of chemical reactions. It appeared that these compounds were formed by proton transfer reactions induced by the interaction between an acid (HNCO, HNO2, HNO3) and a base (NH3) through a hydrogen bond. This mechanism was confirmed by a study of photolyzed diluted argon mixtures. The main astrophysically relevant data from the overall study are presented. The 4.62 micron band in W33A can be reproduced with NH3/CO containing irradiated ices and was identified with OCN(-). The 6.87 micron band in W33A and other photostellar objects is reproduced with NH3/O2 containing ices and is identified with NH4(+). Y.S.

N91-14958*# Hawaii Univ., Honolulu. Inst. for Astronomy.
DISTRIBUTION OF THE 3.1 MICRON FEATURE IN CEPHEUS A **c89**
Klaus-Werner Hodapp and Carlos Eiroa (Observatorio Astronomico Nacional, Madrid, Spain) *In* NASA, Ames Research Center, Interstellar Dust: Contributed Papers Dec. 1989 p 247-248 (For primary document see N91-14897 06-88)
Avail: NTIS HC/MF A22 CSCL 03A

Near-IR absorption features produced by core-mantle dust grains are observed in many protostellar objects. The high spatial resolution observations (less or equal to 3 in.) could be helpful to monitor the expected changes of the features. Cep A/IRS 6 is a suitable candidate to carry out such a kind of study. It is located in an active star formation region and consists of a young object associated with an extended reflection nebula. The ice feature was observed in four positions of Cep A/IRS 6 with a 2.7 in. aperture. The observations were carried out at the IRTF using the cooled grating array spectrometer CGAS. The 2.4 to 3.8 micron spectra of two positions are presented. Y.S.

N91-14959*# Manchester Coll. of Science and Technology (England). Dept. of Mathematics.
GRAIN GROWTH, OPTICAL POLARISATION, AND EXTINCTION IN INTERSTELLAR CLOUDS Abstract Only **c90**
A. P. Jones *In* NASA, Ames Research Center, Interstellar Dust: Contributed Papers Dec. 1989 p 249 (For primary document see N91-14897 06-88)
Avail: NTIS HC/MF A22 CSCL 03B

Increases in the wavelength of maximum polarization and the ratio of total to selective extinction are generally assumed to be the result of grain growth in interstellar clouds. Using a grain model in which the interstellar extinction is explained by amorphous carbon (a-C) and hydrogenated amorphous carbon (a-C:H) mantles on silicate cores the effects of these absorbing carbonaceous mantles on the polarizing properties of large (500 to 2500 A radius) silicate grains were theoretically studied. The polarization model of Mathis was adopted and it was shown that carbon-coated silicate grains can explain the relationship between the wavelength of maximum polarization and R observed toward dark clouds. Y.S.

N91-14960*# Princeton Univ. Observatory, NJ.
GRAIN MANTLES: THE IMPACT ON GRAIN EVOLUTION AND SELECTIVE EXTINCTION **c90**
Charles L. Joseph *In* NASA, Ames Research Center, Interstellar Dust: Contributed Papers Dec. 1989 p 251-255 (For primary document see N91-14897 06-88)
Avail: NTIS HC/MF A22 CSCL 03B

Depletion studies are used to infer the presence of mantles and to constrain grain evolutionary models in the diffuse interstellar medium. The presence of these mantles appears to be important in the evolution of the grains inside diffuse as well as dense clouds. In dense clouds where the element-to-element abundances sometimes differ from those found in diffuse clouds, empirical relationships are starting to emerge between gas abundances and various types of peculiar selective extinction. These peculiar extinction curves may be the results of nonvolatile mantle formation on grain cores or may reflect chemical differences due to variations in the intrinsic metalicity from one cloud to another. A simple model of the time evolution of a parcel of gas and dust as observed

by the depletion of two elements is presented. Different studies of grain evolution and selective extinction are discussed and compared. Y.S.

N91-14961*# Leiden Univ. (Netherlands). Lab. Astrophysics.
MOLECULAR AND MASS SPECTROSCOPIC ANALYSIS OF ISOTOPICALLY LABELED ORGANIC RESIDUES **c90**
Celia X. Mendoza-Gomez, J. Mayo Greenberg, P. McCain, J. P. Ferris, R. Briggs (New York State Dept. of Health, Albany.), M. S. deGroot, and Willem A. Schutte *In* NASA, Ames Research Center, Interstellar Dust: Contributed Papers Dec. 1989 p 257-260 (For primary document see N91-14897 06-88)
(Grant NGR-33-018-148)
Avail: NTIS HC/MF A22 CSCL 03B

Experimental studies aimed at understanding the evolution of complex organic molecules on interstellar grains were performed. The photolysis of frozen gas mixtures of various compositions containing H2O, CO, NH3, and CH4 was studied. These species were chosen because of their astrophysical importance as deducted from observational as well as theoretical studies of ice mantles on interstellar grains. These ultraviolet photolyzed ices were warmed up in order to produce refractory organic molecules like the ones formed in molecular clouds when the icy mantles are being irradiated and warmed up either by a nearby stellar source or impulsive heating. The laboratory studies give estimates of the efficiency of production of such organic material under interstellar conditions. It is shown that the gradual carbonization of organic mantles in the diffuse cloud phase leads to higher and higher visual absorptivity - yellow residues become brown in the laboratory. The obtained results can be applied to explaining the organic components of comets and their relevance to the origin of life. Y.S.

N91-14962*# Calabria Univ., Arcavacta di Rende (Italy). Dipartimento di Fisica.
SYNTHESIS OF H2 IN DIRTY ICE MANTLES BY FAST ION ENERGY LOSS: NEW EXPERIMENTAL RESULTS INCREASE THE RELEVANCE OF THIS MECHANISM **c90**
Valero Pirranello, W. L. Brown, L. J. Lanzerotti, and D. A. Averna (Catania Univ., Italy) *In* NASA, Ames Research Center, Interstellar Dust: Contributed Papers Dec. 1989 p 261-264 (For primary document see N91-14897 06-88)
Avail: NTIS HC/MF A22 CSCL 03B

Recent experimental results support the importance of H2 production in molecular clouds by cosmic ray bombardment of the mantles of grains. The formation of molecules different from those originally present in the irradiated layer can be explained by the production of molecular fragments induced by the release of energy if the impinging fast particle. One way of considering the process is in terms of a transiently hot cylinder, initially about 50 A in diameter, that exists around the track of an individual fast ion. Since ice has a relatively low thermal conductivity, energy lost by the ion in the ice layers remains confined around the track for time long enough to be thermalized. The hot cylinder increases in diameter and decreases in temperature on a time scale of 10(exp -11) to 10(exp -10) sec. Molecular fragments that are formed in this high temperature region acquire enough mobility to recombine with different partners, forming new molecules. A Monte Carlo simulation of the interaction between cosmic rays and grain mantles, at various depths in the core of a spherical molecular cloud, was performed. The simulation was continued until 40,000 ions had hit each grain of the type and size chosen. During the performed experiments thin icy films made of H2O and CD4 mixed in the gas phase and deposited on a cold finger at 9 K were irradiated with 1.5 MeV helium beams. Among synthesized molecules were found H2, HD, and D2. Y.S.

N91-14963*# Leiden Univ. (Netherlands). Lab. Astrophysics.
DIFFUSION AND INFRARED PROPERTIES OF MOLECULES IN ICE MANTLES Abstract Only **c90**
Bernard Schmitt, Ruud Grim, and J. Mayo Greenberg *In* NASA, Ames Research Center, Interstellar Dust: Contributed Papers Dec. 1989 p 265 (For primary document see N91-14897 06-88)
Avail: NTIS HC/MF A22 CSCL 03B

Within dense molecular clouds the formation of frozen icy mantles on interstellar dust grains is thought to be the result of various growth conditions. The molecules, which make up the ice mantles are probably completely mixed. To study the physical properties of such ice mixtures the experiments were performed on the evaporation processes and on the spectroscopic properties of CO, CO2, and CH4 in water rich ices. The decrease in concentration of volatile molecules in ice samples deposited at 10 K and subsequently heated is found to occur essentially in two steps. The first one, corresponding to an evaporation of part of the volatile molecules, starts at about 25 K for CO, 32 K for CH4, and 70 K for CO2. During the crystallization of H2O ice at temperatures greater than 120 K a second evaporation occurs leading to the complete disappearance of the volatile molecules in the solid phase. The main astrophysical implications of the diffusion and spectroscopic behaviors are presented. The possible effects of a heating source on the fraction of volatile molecules, such as CO trapped in grain mantles, are discussed. Y.S.

N91-14964*# Leiden Univ. (Netherlands). Lab. Astrophysics.
THE EVOLUTION OF ORGANIC MANTLES ON INTERSTELLAR GRAINS **c90**
Willem A. Schutte and J. Mayo Greenberg *In* NASA, Ames Research Center, Interstellar Dust: Contributed Papers Dec. 1989 p 267-268 (For primary document see N91-14897 06-88)
Avail: NTIS HC/MF A22 CSCL 03B

By laboratory simulation of the chemical processes on dust grains it was investigated how solid organic materials can be produced in the interstellar medium. The ice mantles that accrete on grains in molecular clouds, consisting primarily of H2O, CO, H2CO, NH3, and O2, are irradiated by the internal UV field, resulting in the storage of radicals upon photodissociation of the original molecules. Transient heating events lead to the production of oxygen-rich organic species by recombination reactions. The experiments indicated that in this way the observed amount of organic material can be produced if a grain passes a few times through a molecular cloud during its life. After the destruction of the cloud the grains enter a more diffuse medium. Here they are subjected to the interstellar UV field as well as to collisions with atomic hydrogen. Experiments show that the intense photoprocessing results in the removal of small species like H2O and NH3 as well as in carbonization of the organic molecules. Contrary to this, the atomic H flux will maintain a certain hydrogen level in the mantle. These processes likely convert the original, oxygen-rich organics into an unsaturated hydrocarbon type material such as that observed towards IRS 7 and in Comet Halley grains. Y.S.

N91-14965*# Max-Planck-Inst. fuer Extraterrestrische Physik, Garching (Germany, F.R.).
ABSORPTION FEATURES IN THE 3 MICRON SPECTRA OF HIGHLY OBSCURED OBJECTS **c90**
Robert G. Smith, Kris Sellgren, and Alan T. Tokunaga (Hawaii Univ., Honolulu.) *In* NASA, Ames Research Center, Interstellar Dust: Contributed Papers Dec. 1989 p 269-270 (For primary document see N91-14897 06-88)
Avail: NTIS HC/MF A22 CSCL 03B

Using the IRTF cooled-grating spectrometer moderate resolution 2.4 to 3.8 micron spectra of a selection of IR protostars and one object located behind the Taurus dark cloud were obtained. Two examples of the spectra are presented. It is clear that the absorption near 3.07 micron is dominated by H2O ice and a comparison between the spectra and a simple H2O ice model allows a temperature estimate for the hottest ice-coated grains in these sources. Higher resolution observations showed no indication of the absorption due to the N-H stretching vibration of NH3 near 2.963 micron. The most plausible explanation for the 3.3 and 3.45 micron features appears to be absorption by the mixture of hydrocarbons, although they cannot be identified with features already attributed to hydrocarbons in the ISM, reflection nebulae

and Comets. However these features appear the same for all sources in the sample, including Elias 16, thus implying a very similar mixture of molecules in each source. Y.S.

N91-14966*# Florence Univ. (Italy). Dipartimento di Fisica.
PRODUCTION AND TRANSFER OF UV PHOTONS IN NON-HOMOGENEOUS SPHERICAL CLOUDS **c90**
Santi Aiello, C. Cecchi-Pestellini, Francesco Mencaraglia, Bruno Barsella, and F. Ferrini (Pisa Univ., Italy) *In* NASA, Ames Research Center, Interstellar Dust: Contributed Papers Dec. 1989 p 273-278 (For primary document see N91-14897 06-88)
Avail: NTIS HC/MF A22 CSCL 03B

Due to screening by dust particles, the UV radiation field of interstellar origin is practically inexistent within very dense interstellar clouds. However, it appears possible that the cosmic-ray excitation of the Lyman and Werner systems of the hydrogen molecule could originate a chemically-significant flux of UV photons even within such dense clouds. Computations of photon fluxes were carried out for two different models of radial density distribution inside the cloud (gas and dust densities were assumed to have the same density distribution). The result strongly support the suggestion that the low energy cosmic rays may generate inside dense interstellar clouds UV radiation fields that may significantly contribute to the gas and dust evolution. Y.S.

N91-14967*# Observatoire de Paris-Meudon (France).
GRAINS CHARGES IN INTERSTELLAR CLOUDS **c90**
N. Bel, J. P. Lafon, and Y. P. Viala *In* NASA, Ames Research Center, Interstellar Dust: Contributed Papers Dec. 1989 p 279-280 (For primary document see N91-14897 06-88)
Avail: NTIS HC/MF A22 CSCL 03B

The charge of cosmic grains could play an important role in many astrophysical phenomena. It probably has an influence on the coagulation of grains and more generally on grain-grain collisions, and on interaction between charged particles and grains which could lead to the formation of large grains or large molecules. The electrostatic charge of grains depends mainly on the nature of constitutive material of the grain and on the physical properties of its environment: it results from a delicate balance between the plasma particle collection and the photoelectron emission, both of them depending on each other. The charge of the grain is obtained in two steps: (1) using the numerical model the characteristics of the environment of the grain are computed; (2) the charge of a grain which is embedded in this environment is determined. The profile of the equilibrium charge of some typical grains through different types of interstellar clouds is obtained as a function of the depth of the cloud. It is shown that the grain charge can reach high values not only in hot diffuse clouds, but also in clouds with higher densities. The results are very sensitive to the mean UV interstellar radiation field. Three parameters appear to be essential but with different levels of sensitivity of the charge: the gas density, the temperature, and the total thickness of the cloud. Y.S.

N91-14968*# National Aeronautics and Space Administration. Ames Research Center, Moffett Field, CA.
DUST COAGULATION IN ISM **c90**
Arati Chokshi, Alexander G. G. M. Tielens, and David Hollenbach *In its* Interstellar Dust: Contributed Papers Dec. 1989 p 281-282 (For primary document see N91-14897 06-88)
Avail: NTIS HC/MF A22 CSCL 03B

Coagulation is an important mechanism in the growth of interstellar and interplanetary dust particles. The microphysics of the coagulation process was theoretically analyzed as a function of the physical properties of the coagulating grains, i.e., their size, relative velocities, temperature, elastic properties, and the van der Waal interaction. Numerical calculations of collisions between linear chains provide the wave energy in individual particles and the spectrum of the mechanical vibrations set up in colliding particles. Sticking probabilities are then calculated using simple estimates for elastic deformation energies and for the attenuation of the wave energy due to absorption and scattering processes. Y.S.

N91-14969*# Montreal Univ. (Quebec). Departement de Physique.
ON THE POLARIZATION MECHANISM IN THE R MON/NGC 2261 COMPLEX **c90**
Francois Menard and Pierre Bastien *In* NASA, Ames Research Center, Interstellar Dust: Contributed Papers Dec. 1989 p 283-288 (For primary document see N91-14897 06-88)
Avail: NTIS HC/MF A22 CSCL 03B

The detection of circular polarization in R Mon and NGC 2261 is reported. This detection implies that the mechanism responsible for the linear and circular polarization is most likely multiple scattering in a flattened distribution. It replaces the previously suggested scenario where dichroic extinction by elongated dust grains aligned by a toroidal magnetic field was producing the polarization. The multiple scattering interpretation of linear polarization maps also means that these maps now provide direct evidence for a circumstellar disk around R Mon and possibly around many other young stellar objects. Author

N91-14970*# National Aeronautics and Space Administration. Ames Research Center, Moffett Field, CA.
INFRARED STUDIES OF DUST GRAINS IN INFRARED REFLECTION NEBULAE **c90**
Yvonne J. Pendleton, Alexander G. G. M. Tielens, and Michael W. Werner *In its* Interstellar Dust: Contributed Papers Dec. 1989 p 289-290 (For primary document see N91-14897 06-88)
Avail: NTIS HC/MF A22 CSCL 03B

IR reflection nebulae, regions of dust which are illuminated by nearby embedded sources, were observed in several regions of ongoing star formation. Near IR observation and theoretical modelling of the scattered light form IR reflection nebulae can provide information about the dust grain properties in star forming regions. IR reflection nebulae were modelled as plane parallel slabs assuming isotropically scattering grains. For the grain scattering properties, graphite and silicate grains were used with a power law grain size distribution. Among the free parameters of the model are the stellar luminosity and effective temperature, the optical depth of the nebula, and the extinction by foreground material. The typical results from this model are presented and discussed. Y.S.

N91-14971*# Prague Observatory (Czechoslovakia).
LABORATORY INVESTIGATION OF ELECTRIC CHARGING OF DUST PARTICLES BY ELECTRONS, IONS, AND UV RADIATION **c90**
Jiri Svestka, S. Pinter, and E. Gruen (Max-Planck-Inst. fuer Kernphysik, Heidelberg, Germany, F.R.) *In* NASA, Ames Research Center, Interstellar Dust: Contributed Papers Dec. 1989 p 291-292 (For primary document see N91-14897 06-88)
Avail: NTIS HC/MF A22 CSCL 03B

In many cosmic environments electric charging of dust particles occurs by electrons, ions, and UV radiation. In case of interstellar dust particles the value of their electric charge can have, for instance, very important consequences for their destruction rate in supernova remnant's shock waves and can globally influence the overall life cycle of dust particles in galaxies. For experimental simulation of charging processes a vacuum chamber was used in which the particles fall through an electron or ion beam of energies up to 10 KeV. The aim of the experiments was to attain maximum charge of dust particles. Furthermore the influence of the rest gas was also determined because electrons and ions produced by collisional ionization of the rest gas can result in significant effects. For measurement particles from 1 to 100 microns from glass, carbon, Al, Fe, MgO, and very loosely bound conglomerates of Al2O3 were used. Y.S.

N91-14972*# Chicago Univ., IL. Astronomy and Astrophysics Center.
DUST IN REGIONS OF MASSIVE STAR FORMATION **c90**
Mark G. Wolfire and J. P. Cassinelli (Wisconsin Univ., Madison.) *In* NASA, Ames Research Center, Interstellar Dust: Contributed

Papers Dec. 1989 p 293-294 (For primary document see N91-14897 06-88)
Avail: NTIS HC/MF A22 CSCL 03B

It is suggested that protostars increase mass by accreting the surrounding gas and dust. Grains are destroyed as they near the central protostar creating a dust shell or cocoon. Radiation pressure acting on the grains can halt the inflow of material thereby limiting the amount of mass accumulated by the protostar. General constraints were considered on the initial dust-to-gas ratio and mass accretion rates that permit inflow. These results were constrained further by constructing a numerical model, including radiative deceleration on grains and grain destruction processes. Also the constraints on dust properties were investigated which allow the formation of massive stars. The obtained results seem to suggest that massive star formation requires rather extreme preconditioning of the grain and gas environment. Y.S.

N91-14973*# National Aeronautics and Space Administration. Goddard Space Flight Center, Greenbelt, MD.
DOES CO TRACE H2 AT HIGH GALACTIC LATITUDE c90
David Bazell, L. Blitz (Maryland Univ., College Park.), and Francois-Xavier Desert *In* NASA, Ames Research Center, Interstellar Dust: Contributed Papers Dec. 1989 p 297-298 (For primary document see N91-14897 06-88)
Avail: NTIS HC/MF A22 CSCL 03B

A CO survey of 342 Infrared Excess Clouds (IRECs) distributed uniformly across the sky is presented. Following comparison of the integrated CO brightness with the 100 micron infrared brightness B(sub 4) obtained from the IRAS data, evidence was found for a threshold in B(sub 4) of 4-5 MJy sr(exp -1) below which CO does not form. Evidence is also presented that the threshold effect can be seen within an individual cloud, providing evidence for a phase transition between atomic and molecular gas. While the main thrust was to examine the CO content of the IRECs, it was also attempted to detect CO toward a number of UV stars so that CO brightness could be correlated with direct measurements of H2 column density and E(B-V). Of the 26 observed stars CO was detected toward 6. It is consistent with the results obtained using infrared data. Y.S.

N91-14974*# Centre d'Etude Spatiale des Rayonnements, Toulouse (France).
THE ORIGIN OF THE GALACTIC EMISSION IN IRAS DATA c93
Emanuel Caux, P. M. Solomon, and T. J. Mooney (State Univ. of New York, Stony Brook.) *In* NASA, Ames Research Center, Interstellar Dust: Contributed Papers Dec. 1989 p 299-300 (For primary document see N91-14897 06-88)
Avail: NTIS HC/MF A22 CSCL 03B

Using the high resolution IRAS data and the radial distribution of gaseous material and those of the interstellar radiation field (ISRF), a model of the Galactic infrared emission was built. The first step consisted of a separation of the diffuse emission in IRAS data from that of the well-defined strong Galactic sources. A well accepted idea is that IR emission comes from dust heated either by the ISRF and/or by internal cloud heating sources. Thus the IR galactic emission was modelled from radial distributions of gas and ISRF and the following three main hypothesis: (1) the dust-to-gas ration is the same in the whole Galaxy; (2) IR emission is proportional to local dust density; and (3) IR emission is also proportional to the local ISRF. The IR emission as modelled was integrated over each line of sight and compared with observed IRAS data. The results show that the IR diffuse component comes from dust associated with H1 and heated by the general ISRF. For the dust embedded in cold H2 component, the heating source is also the general ISRF while the warm component is explained by dust embedded in molecular clouds and heated by high-mass stars born in the close vicinity of the clouds and by disc population ISRF. Y.S.

N91-14975*# California Univ., Berkeley. Dept. of Astronomy.
MOLECULES, GRAINS, AND SHOCKS: A COMPARISON OF CO, H I, AND IRAS DATA Abstract Only c90
Carl Heiles, William T. Reach, and Bon-Chul Koo *In* NASA, Ames Research Center, Interstellar Dust: Contributed Papers Dec. 1989 p 301 (For primary document see N91-14897 06-88)
Avail: NTIS HC/MF A22 CSCL 03B

The IR and H I properties, and CO content were compared for a set of 26 isolated, degree-sized interstellar clouds. The comparisons offer some conclusions concerning the effects of kinematics on molecular content and grain size distribution. It was also found that some clouds must have very large fractions of their total Carbon in the form of polycyclic aromatic hydrocarbons. Y.S.

N91-14976*# California Univ., Berkeley. Dept. of Physics.
A ROCKET-BORNE MEASUREMENT OF INTERSTELLAR DUST EMISSION AT HIGH GALACTIC LATITUDE c89
Andrew E. Lange, D. Alsop, S. Hayakawa, T. Matsumoto, H. Matsuo, H. Murakami, Paul L. Richards, and S. Sato (Nagasaki Univ., Japan) *In* NASA, Ames Research Center, Interstellar Dust: Contributed Papers Dec. 1989 p 303-305 Sponsored by Japan Society for the Promotion of Science, Tokyo; NSF; Ministry of Education, Science and Culture, Sagamihara, Japan; and California Space Inst. (For primary document see N91-14897 06-88)
(Grant NGL-05-003-497)
Avail: NTIS HC/MF A22 CSCL 03A

The diffuse brightness of the sky was measured in six submillimeter passbands, using a rocket-borne, liquid helium-cooled, absolute radiometer. The average brightness was reported which was observed in each of the passbands, and the dominant source of emission was tentatively identified in the three shortest wavelength bands as interstellar dust (ISD). Spacial structure was observed in these bands, as would be expected for emission from the ISD. The average column density of H I was calculated in each field of view along the scan path. All three bands show a significant correlation with H I. The obtained values are in excellent agreement with those computed for a mixture of graphite and silicate grains. A significant residual emission, not correlated with the H I column density, is evident in all three channels. Y.S.

N91-14977*# Bonn Univ. (Germany, F.R.). Radioastronomisches Inst.
MOLECULES IN AN INFRARED CIRRUS CLOUD c90
Horst Meyerdierks and Nathalie Brouillet (Bordeaux Univ., France) *In* NASA, Ames Research Center, Interstellar Dust: Contributed Papers Dec. 1989 p 307-308 (For primary document see N91-14897 06-88)
Avail: NTIS HC/MF A22 CSCL 03B

One of the clouds that form the Polar Loop was observed in the 1(sub 10)-1(sub 11) 4.8 GHz transition of formaldehyde and in J equal to 1-0 transitions of CO-12 and CO-13 at 115 and 110 GHz resp. The cloud consists of several filaments. From the correlation of IRAS 60 and 100 microns intensities a color temperature of the dust of 21 K and a maximum optical depth of 3 x 10(exp -4) were derived. At one local maximum of the 100 micron intensity, the hyperfine structure of formaldehyde could be resolved. Since the infrared optical depth is small, the 100 micron intensity can be used as a measure of dust column density. Y.S.

N91-14978*# California Univ., Berkeley. Dept. of Astronomy.
INFRARED CIRRUS POINT SOURCES Abstract Only c90
William T. Reach, Carl Heiles, and Bon-Chul Koo *In* NASA, Ames Research Center, Interstellar Dust: Contributed Papers Dec. 1989 p 309 (For primary document see N91-14897 06-88)
Avail: NTIS HC/MF A22 CSCL 03B

The IRAS discovered a large number of unresolved sources which were more intense at 100 microns than at shorter IR wavelengths. A sample of these point sources was isolated which are located in regions of very low Galactic H I column density. Whereas it was initially believed these sources to be prime candidates for a class of previously unknown astronomical object, the observations has proven that most of these sources are associated with the interstellar medium (ISM) of our Galaxy. Y.S.

N91-14979*# Space Telescope Science Inst., Baltimore, MD.
DUST IN STELLAR WIND BOW SHOCKS Abstract Only **c90**
Dave VanBuren *In* NASA, Ames Research Center, Interstellar Dust: Contributed Papers Dec. 1989 p 311 Prepared in cooperation with Johns Hopkins Univ., Baltimore, MD (For primary document see N91-14897 06-88)
Avail: NTIS HC/MF A22 CSCL 03B

A number of high velocity O stars have associated parsec-sized structure visible in the IRAS infrared. They can most readily be explained as the dense shells of stellar wind bow shocks. The IR emission arises from starlight-heated post-shock dust, and possibly also from ionic lines. Emission from pre-shock dust is often seen as well, and allows in principle the empirical determination of the effects of shocks on dust. Since the observed bow shocks span a range of velocities a comparison with theories for shock destruction of dust is possible. Author

N91-14980*# National Aeronautics and Space Administration. Ames Research Center, Moffett Field, CA.
STUDYING THE SPATIAL DISTRIBUTION OF INTERSTELLAR DUST **c90**
Helen J. Walker, Michael W. Werner, C. Allen, R. C. Henry, R. Kimble, J. Wofford, and Jayant Murthy (National Aeronautics and Space Administration. Goddard Space Flight Center, Greenbelt, MD.) *In its* Interstellar Dust: Contributed Papers Dec. 1989 p 313-316 (For primary document see N91-14897 06-88)
Avail: NTIS HC/MF A22 CSCL 03B

The spacial distribution of interstellar dust reflects both interstellar dynamics and the processes which form and destroy dust in the interstellar medium (ISM). The IRAS survey, because of its high sensitivity to thermal emission from dust in the IR, provides new approaches to determining the spatial distribution of dust. The initial results are reported of an attempt to use the IRAS data to probe the spatial distribution of dust - by searching for thermal emission from dust in the vicinity of bright stars. These results show that this technique (which relies on finding IR emission associated with randomly selected stars) can ultimately be used to study the distribution of dust in the ISM. The density of the cloud producing the IR emission may be derived by assuming that the dust is at its projected distance from the star and that the heating is due to the star's (known) radiation field. The heating radiation is folded into a grain model, and the number of emitting grains adjusted to reproduce the observed energy distribution. It is noted that this technique is capable in principle of detecting dust densities much lower than those typical of the cirrus clouds. Y.S.

N91-14981*# Five-College Astronomy Dept., Amherst, MA.
THERMAL EMISSION FROM INTERSTELLAR DUST IN AND NEAR THE PLEIADES **c90**
Richard E. White *In* NASA, Ames Research Center, Interstellar Dust: Contributed Papers Dec. 1989 p 317-321 Prepared in cooperation with Wyoming Univ., Laramie (For primary document see N91-14897 06-88)
Avail: NTIS HC/MF A22 CSCL 03B

IRAS survey coadds for a 8.7 deg x 4.3 deg field near the Pleiades provide evidence for dynamical interaction between the cluster and the surrounding interstellar medium. The far-infrared images show large region of faint emission with bright rims east of the cluster, suggestive of a wake. Images of the far-infrared color temperature and 100 micron optical depth reveal temperature maxima and optical depth minima near the bright cluster stars, as well as a strong optical depth peak at the core of the adjacent CO cloud. Models for thermal dust emission near the stars indicate that most of the apparent optical depth minima near stars are illusory, but also provide indirect evidence for small interaction between the stars and the encroaching dust cloud. Author

N91-14982*# California Inst. of Tech., Pasadena. Lab. of Physics.
TEMPERATURE DISTRIBUTION OF DUST IN LUMINOUS IRAS GALAXIES **c90**
David P. Carico *In* NASA, Ames Research Center, Interstellar Dust: Contributed Papers Dec. 1989 p 325-329 (For primary document see N91-14897 06-88)
Avail: NTIS HC/MF A22 CSCL 03B

Work is currently in progress to obtain temperature distributions of dust in the most infrared-luminous galaxies. The results presented are of a preliminary nature, representing a zeroth-order approximation. The objects which have been analyzed so far are all galaxies from the Infrared Astronomy Satellite (IRAS) Bright Galaxy Sample with infrared luminosities L sub IR greater than or equal to 10(exp 11) solar luminosity. They are: Arp 220, Mrk 231, Mrk 273, NGC 1614, NGC 3690, NGC 6285/6, and Zw 049.057. The analysis utilized 3.7 micron data from the Palomar 5 m Hale telescope, IRAS data at 12, 25, 60, and 100 microns, and 1 mm continuum data from the CalTech Submillimeter Observatory on Mauna Kea. Author

N91-14983*# Yerkes Observatory, Williams Bay, WI.
THE 100 AND 160 MICRON MAPS OF THE DUST REEMISSION FROM THE NUCLEUS AND INNER-ARM REGIONS OF NGC 6946 **c90**
Gregory Engargiola, D. A. Harper, and D. T. Jaffe (Texas Univ., Austin.) *In* NASA, Ames Research Center, Interstellar Dust: Contributed Papers Dec. 1989 p 331-338 (For primary document see N91-14897 06-88)
Avail: NTIS HC/MF A22 CSCL 03B

Dust reemission from the Scd galaxy NGC 6946 has been measured at 100 and 160 microns with the 32-channel University of Chicago Far-Infrared Camera. Researchers present fully sampled maps of the nucleus and inner spiral arms at 45 seconds resolution. The far-infrared morphology of the galaxy is a bright peak centered on a diffuse disk, where the peak occurs about 24 seconds NE of the Dressel and Condon optical center. The 100/160 micron color temperature is correlated with the H alpha surface brightness. Assuming the distance from Earth to the galaxy is 10.1 Mpc, researchers determine that Tc is 32 K at the nucleus and at radius 5.4 kpc, where there is a concentration of H II regions. In the intermediate annulus of relatively low H alpha surface brightness, the temperature drops to a local minimum of 25 K at radius 3 kpc. The ratio of reradiated to transmitted stellar luminosity is approx. 3.0 at the nucleus and approx. 0.9 for the disk. The optical depth at 100 micron increases from .0005 at the edges of our map to .0035 at the far infrared radiation (FIR) peak. Combining our observations with a fully sampled map of similar spatial extent in CO(1 greater than 0), researchers determine that the ratio F sub IR/I sub CO at the center of the galaxy is almost twice that for the disk, where the value is more or less constant. Author

N91-14984*# Pisa Univ. (Italy). Ist. di Astronomia.
GRAINS IN GALACTIC HALOES **c90**
Andrea Ferrara, Bruno Barsella, F. Ferrini, J. Mayo Greenberg, and Santi Aiello (Florence Univ., Italy) *In* NASA, Ames Research Center, Interstellar Dust: Contributed Papers Dec. 1989 p 339-343 (For primary document see N91-14897 06-88)
Avail: NTIS HC/MF A22 CSCL 03B

Researchers considered the effect of extensive forces on dust grains subjected to the light and matter distribution of a spiral galaxy (Greenberg et al. (1987), Ferrini et al. (1987), Barsella et al (1988). Researchers showed that the combined force on a small particle located above the plane of a galactic disk may be either attractive or repulsive depending on a variety of parameters. They found, for example, that graphite grains from 20 nm to 250 nm radius are expelled from a typical galaxy, while silicates and other forms of dielectrics, after initial expulsion, may settle in potential minimum within the halo. They discuss only the statistical behavior of the forces for 17 galaxies whose luminosity and matter distribution in the disk, bulge and halo components are reasonably well known. The preliminary results of the study of the motion of a dust grain for NGC 3198 are given. Author

N91-14985*# Mullard Radio Astronomy Observatory, Cambridge (England).
DOES THE FAR-INFRARED/RADIO CORRELATION IN SPIRAL GALAXIES EXTEND TO THE SPATIAL DOMAIN **c90**

Neil A. Howarth and A. J. Fitt *In* NASA, Ames Research Center, Interstellar Dust: Contributed Papers Dec. 1989 p 345-346 (For primary document see N91-14897 06-88)
Avail: NTIS HC/MF A22 CSCL 03B

A comparison is made between the spatial distribution of the thermal far-infrared and non-thermal radio emission of nearby spiral galaxies. This is done in an attempt to improve our understanding of the well known correlation between the integrated Infrared Astronomy Satellite (IRAS) far-infrared and radio emission of spiral galaxies, e.g., de Jong et al., 1985, Helou et al., 1986. A physical explanation for this correlation is not straight forward due to the ambiguous nature of the origin of the far-infrared and radio, and the dependence of the non-thermal radio on each galaxies' magnetic field. It is now widely believed that the infrared emission detected in the longer wavelength IRAS wavebands (less than 50 microns) arises from at least two distinct sources, e.g., Cox et al., 1986, Persson and Helou, 1987: (1) a warm (T approx. 40 K) component associated with dense dust clouds heated by embedded O and B type stars; and (2) a cooler (T approx. 20 K) component associated with diffuse dust distributed throughout the interstellar matter (ISM) heated by the interstellar radiation field. A link between the warm component and the radio via electrons originating in Type II supernovae (the ultimate fate of many of the O and B type stars responsible for the warm component) has been suggested by numerous authors. The supporting evidence is scarce and inconclusive. Researchers have attempted to provide some insight into the problem by looking at the spatial distribution of the different components in some nearby spiral galaxies, starting with the face-on spiral M51. The source of the far-infrared data is the IRAS chopped photometric channel (CPC) instrument. Warm and cold far-infrared fluxes integrated over all wavelengths and the radio intensity at two frequencies are plotted against radius. All plots are to a common resolution of 100 arcsec, the radio data originating from the Cambridge Low Frequency Synthesis Telescope (151 MHz) and the VLA (1490 MHz, from Condon, 1987). The warm and cold regions are assumed to be representedby a single galactic wide temperatures of 50 K and 20 K respectively. A dust emissivity of 1 has been assumed. The form of the plots is little effected by varying these assumptions. The radio and cold component curves appear to follow each other most closely, in contradiction to the simple OB star/type II supernovae hypothesis. Author

N91-14986*# Sao Paulo Univ. (Brazil). Inst. Astronomico de e Geofisico.
MULTICOLOR OPTICAL POLARIMETRY OF REDDENED STARS IN THE SMALL MAGELLANIC CLOUD **c89**
Antonio M. Magalhaes, G. V. Coyne, Valero Piirola (Helsinki Univ., Finland), and C. V. Rodrigues *In* NASA, Ames Research Center, Interstellar Dust: Contributed Papers Dec. 1989 p 347-352 Sponsored in part by International Astronomical Union and Fundacao de Amparo a pesquisa do Estado de Sao Paulo (For primary document see N91-14897 06-88)
Avail: NTIS HC/MF A22 CSCL 03A

First results of an on-going program to determine the wavelength dependence of the interstellar optical polarization of reddened stars in the Small Magellanic Cloud (SMC) are presented. IUE observations of reddened stars in the SMC (Bouchet et al. 1985) generally show marked differences in the extinction law as compared to both the Galaxy and the Large Megallanic Cloud. The aim here is to determine the wavelength dependence of the optical linear polarization in the direction of several such stars in the SMC in order to further constrain the dust composition and size distribution in that galaxy. Author

N91-14987*# National Aeronautics and Space Administration. Goddard Space Flight Center, Greenbelt, MD.
ON THE ORIGIN OF EXTINCTION IN THE COMA CLUSTER OF GALAXIES **c89**
Y. Rephaeli (California Univ., La Jolla.), Eli Dwek, and John C. Mather *In* NASA, Ames Research Center, Interstellar Dust: Contributed Papers Dec. 1989 p 353-356 (For primary document see N91-14897 06-88)
Avail: NTIS HC/MF A22 CSCL 03A

Visual extinction of distant clusters seen through the Coma cluster seem to suggest that dust may be present in the hot x ray emitting intracluster gas. However, the Infrared Astronomy Satellite (IRAS) failed to detect any infrared emission from the cluster at the level expected from the extinction measurements. Researchers carried out a detailed analysis of the properties of intracluster dust in the context of a model which includes continuous injection of dust by the cluster galaxies, grain destruction by sputtering, and transient grain heating by the hot plasma. Computed infrared fluxes are in agreement with the upper limit obtained from the IRAS. The calculations, and the constraint implied by the IRAS observations, suggest that the intracluster dust must be significantly depleted compared to interstellar abundances. Researchers discuss possible explanations for the discrepancy between the observed visual extinction and the IRAS upper limit. Author

N91-14988*# National Aeronautics and Space Administration. Ames Research Center, Moffett Field, CA.
FAR INFRARED STRUCTURE OF SPIRAL GALAXIES FROM THE IRAS CPC IMAGES Abstract Only **c90**
Richard J. Wainscoat, Arati Chokshi (National Academy of Sciences - National Research Council, Washington, DC.), and Laurance R. Doyle *In its* Interstellar Dust: Contributed Papers Dec. 1989 p 35 (For primary document see N91-14897 06-88)
Avail: NTIS HC/MF A22 CSCL 03A

Significant extended far infrared (50 micron and 100 micron) structure was found for five face-on spiral galaxies (NGC2403, M51, M83, NGC6946, and IC342) from fourteen galaxies searched in the Infrared Astronomy Satellite (IRAS) chopped photometric channel (CPC) catalogue. Images were initially processed to remove instrumental and background artifacts, the isophotal centroids of each image determined, and multiple images of each galaxy (for each wavelength) superimposed and averaged to improve signal-to-noise. Calibration of these images was performed using IRAS survey array data. Infrared isophotes were then superimposed on optical (blue) images so that direct structural comparisons could be made. Author

N91-14989*# Harvard-Smithsonian Center for Astrophysics, Cambridge, MA.
GALAXY FORMATION BY DUST Abstract Only **c90**
Boqi Wang and Goerge B. Field *In* NASA, Ames Research Center, Interstellar Dust: Contributed Papers Dec. 1989 p 359 (For primary document see N91-14897 06-88)
Avail: NTIS HC/MF A22 CSCL 03A

It has been known since the early 1940's that radiation can cause an instability in the interstellar medium. Absorbing dust particles in an isotropic radiation field shadow each other by a solid angle which is inversely proportional to the square of the distance between the two particles, leading to an inverse-square attractive force - mock gravity. The effect is largest in an optically thin medium. Recently Hogan and White (HW, hereafter) proposed that if the pre-galactic universe contained suitable sources of radiation and dust, instability in the dust distribution caused by mock gravity may have led to the formation of galaxies and galaxy clusters. In their picture of a well-coupled dust-gas medium, HW show that mock gravity begins to dominate gravitational instability when the perturbation becomes optically thin, provided that the radiation field at the time is strong enough. The recent rocket observation of the microwave background at submillimeter wavelengths by Matsumoto et al. might be from pre-galactic stars, the consequence of the absorption of ultraviolet radiation by dust, and infrared reemission which is subsequently redshifted. HW's analysis omits radiative drag, incomplete collisional coupling of gas and dust, finite dust albedo, and finite matter pressure. These effects could be important. In a preliminary calculation including them, the authors have confirmed that mock gravitational instability is effective if there is a strong ultraviolet radiation at the time, but any galaxies that form would be substantially enriched in heavy elements because the contraction of the dust is more rapid than that of the gas. Moreover, since the dust moves with supersonic

velocity through the gas soon after the perturbation becomes optically thin, the sputtering of dust particles by gas is significant, so the dust could disappear before the instability develops significantly. They conclude that the mock gravity by dust is not important in galaxy formations. Author

N91-14990*# Lecce Univ. (Italy). Dept. of Physics.
VUV-VISIBLE MEASUREMENTS ON DIFFERENT SAMPLES OF AMORPHOUS CARBON **c89**
A. Blanco, A. Borghesi, E. Bussoletti, Luigi Colangeli, Sergio Fonti, H. E. Gumlich, Ch. Jung, Vincenso Orofino, and G. Schwehm (European Space Agency. European Space Research and Technology Center, ESTEC, Noordwijk, Netherlands) *In* NASA, Ames Research Center, Interstellar Dust: Contributed Papers Dec. 1989 p 363-368 (For primary document see N91-14897 06-88)
Avail: NTIS HC/MF A22 CSCL 03A

Among various candidate materials for interstellar dust, amorphous carbon (AC) is playing an increasingly important role (Greenstein, 1981; Hecht et al., 1984; Jura, 1983, 1986). Furthermore, recent in situ measurements have clearly shown the presence of carbonaceous grains in the coma of comet Halley (Kissel et al., 1986). Laboratory investigations on AC grains may be very useful to better interpret observations and to support theoretical elaborations. Recently, the authors started an international research program which also includes UV extinction analyses on AC samples, by using synchrotron light. Preliminary results obtained in a first shift of measurements, last June, are given. At the present stage of the data analysis, the authors can only draw some preliminary considerations. A wide band falling at around 240 nm is detected in all the analyzed samples. It intensity seems to decrease with increasing the dust collecting distance. A peak at 150 nm decreases in intensity with increasing the collecting distance. The band seems absent in the samples characterized by a larger amount of dust. A feature at about 200 nm is detected in some samples. At the moment the authors tend to attribute it to the transmission properties of the LiF substrates at the wavelength and/or to some problems in the experimental setup. It is unclear if a hump at 120 nm is real or due to instrumental effects. The profile of the spectra does not show substantial changes when the samples are cooled down to about 100 K. The present results appear to be in general agreement with previous findings, but their analysis is in progress and the interpretation is still on the way. Author

N91-14991*# Universitaets-Sternwarte, Jena (German D.R.).
STEPS TOWARD INTERSTELLAR SILICATE DUST MINERALOGY **c90**
J. Dorschner, J. Guertler, and Th. Henning *In* NASA, Ames Research Center, Interstellar Dust: Contributed Papers Dec. 1989 p 369-370 (For primary document see N91-14897 06-88)
Avail: NTIS HC/MF A22 CSCL 03B

One of the most certain facts on interstellar dust is that it contains grains with silicon oxygen tetrahedra (SOT), the internal vibrations of which cause the well known silicate bands at 10 and 18 microns. The broad and almost structureless appearance of them demonstrates lack of translation symmetry in these solids that must be considered amorphous or glassy silicates. There is no direct information on the cations in these interstellar silicates and on the number of bridging oxygens per tetrahedron (NBO). Comparing experimental results gained on amorphous silicates, e.g., silicate glasses, of cosmically most abundant metals (Mg, Fe, Ca, Al) with the observations is the only way to investigate interstellar silicate dust mineralogy (cf, Dorschner and Henning, 1986). At Jena University Observatory IR spectra of submicrometer-sized grains of pyroxene glasses (SSG) were studied. Pyroxenes are common minerals in asteroids, meteorites, interplanetary, and supposedly also cometary dust particles. Pyroxenes consist of linearly connected SOT (NBO=2). In the vitreous state reached by quenching melted minerals, the SOT remain nearly undistorted (Si-O bond length unchanged); the Si-O-Si angles at the bridging oxygens of pyroxenes, however, scatter statistically. Therefore, the original cation oxygen symmetry of the crystal (octahedral and hexahedral coordination by O) is completely lost. The blended bands at 10 and 18 microns lose their diagnostic differences and become broad and structureless. This illustrates best the basic problem of interstellar silicate mineral diagnostics. Optical data of glasses of enstatite, bronzite, hypersthene, diopside, salite, and hedenbergite have been derived. Results of enstatite (E), bronzite (B), and hypersthene (H) show very good agreement with the observed silicate features in the IR spectra of evolutionarily young objects that show P-type silicate signature according to the classification by Gurtler and Henning (1986). Compositional parameters and main characteristics of experimental SSG spectra in IR for the glasses E, B, and H are shown in tabular form. Results fit excellently the relations derived by Koike and Hasegawa (1987) and suggest that the band ratio of the astronomical silicate by Draine and Lee (1984) is too low. Author

N91-14992*# Leiden Univ. (Netherlands). Lab. Astrophysics.
SCATTERING BY FLUFFY GRAINS Abstract Only **c90**
J. I. Hage and J. Mayo Greenberg *In* NASA, Ames Research Center, Interstellar Dust: Contributed Papers Dec. 1989 p 371 (For primary document see N91-14897 06-88)
Avail: NTIS HC/MF A22 CSCL 03B

There are indications (Greenberg et al., 1988), that fluffy (i.e., porous) particles are responsible for the observed 3.4 and 10 micron emissions of comet Halley. The absorption characteristics of small particles both solid and fluffy are needed in order to explain the Halley emissions. How isolated small solid particles react to an external radiation field is well known - the Rayleigh approximation. How these same small particles emit when assembled as fluffy aggregates in another question. To what degree are the emission spectra of isolated and aggregated particles comparable. In order to quantify the assertion that fluffy particles produce the observed Halley infrared emission features, the authors are performing calculations to determine the effect of porosity on the absorption characteristics of aggregates of interstellar grain-type particles. The calculations are based on an integral representation of the scattered electromagnetic field. Results are given with application to comet Halley. Author

N91-14993*# National Aeronautics and Space Administration. Goddard Space Flight Center, Greenbelt, MD.
LABORATORY STUDIES OF REFRACTORY METAL OXIDE SMOKES **c25**
Joseph A. Nuth, R. N. Nelson (College of Southern Georgia, Statesboro.), and Bertram Donn *In* NASA, Ames Research Center, Interstellar Dust: Contributed Papers Dec. 1989 p 373-374 (For primary document see N91-14897 06-88)
Avail: NTIS HC/MF A22 CSCL 07D

Studies of the properties of refractory metal oxide smokes condensed from a gas containing various combinations of SiH4, Fe(CO)5, Al(CH3)3, TiCl4, O2 and N2O in a hydrogen carrier stream at 500 K greater than T greater than 1500 K were performed. Ultraviolet, visible and infrared spectra of pure, amorphous SiO(x), FeO(x), AlO(x) and TiO(x) smokes are discussed, as well as the spectra of various co-condensed amorphous oxides, such as FE(x)SiO(y) or Fe(x)AlO(y). Preliminary studies of the changes induced in the infrared spectra of iron-containing oxide smokes by vacuum thermal annealing suggest that such materials become increasingly opaque in the near infrared with increased processing: hydration may have the opposite effect. More work on the processing of these materials is required to confirm such a trend: this work is currently in progress. Preliminary studies of the ultraviolet spectra of amorphous Si2O3 and MgSiO(x) smokes revealed no interesting features in the region from 200 to 300 nm. Studies of the ultraviolet spectra of both amorphous, hydrated and annealed SiO(x), TiO(x), AlO(x) and FeO(x) smokes are currently in progress. Finally, data on the oxygen isotopic composition of the smokes produced in the experiments are presented, which indicate that the oxygen becomes isotopically fractionated during grain condensation. Oxygen in the grains is as much as 3 percent per amu lighter than the oxygen in the original

gas stream. The authors are currently conducting experiments to understand the mechanism by which fractionation occurs.
Author

N91-14994*# Los Alamos National Lab., NM.
INFRARED SPECTRA OF CRYSTALLINE AND GLASSY SILICATES AND APPLICATION TO INTERSTELLAR DUST **c25**
John R. Stephens, A. Blanco, A. Borghesi, Sergio Fonti, and E. Bussoletti (Istituto Universitario Navale, Naples, Italy) *In* NASA, Ames Research Center, Interstellar Dust: Contributed Papers Dec. 1989 p 375-380 (For primary document see N91-14897 06-88)
Avail: NTIS HC/MF A22 CSCL 07D

The infrared spectra of crystalline minerals predicted in theoretical condensation sequences do not match the astronomical observations. Since the astronomical spectra are a closer match to glassy silicates, the authors undertook a study to measure the infrared spectra of glassy silicates that have compositions similar to silicate minerals predicted in theoretical condensation sequences. The data should support observations aimed at elucidating condensation chemistry in dust forming regions. The authors measured the mass absorption coefficients, from 2.5 to 25 microns, of ground samples of olivine, diopside, and serpentine and also smoke samples that were prepared from these minerals. The smoke samples prepared in this way are predominantly glassy with nearly the same composition as the parent minerals. The crystalline samples consisted of pure olivine ((Fe(0.1)Mg(0.9))-(2)SiO(4)), serpentine, diopside. Sample purity was confirmed by x ray diffraction. Each mineral was ground for 10 hours and a measured mass of the powder was mixed with KBr powder for absorption measurements using the method of Borghesi et a. (1985). The smoke samples were prepared from the same samples used for grinding by vaporizing the minerals using pulsed laser radiation in air. The smoke samples formed by condensation of the resulting vapor. The smoke settled onto infrared transparent KRS-5 substrates and onto a quartz crystal microbalance used to obtain mass measurements. A description of the preparation method is given in Stephens (1980). The glassy diopside showed only diffuse electron diffraction peaks and hence was nearly amorphous, while the serpentine smoke showed a weak diffraction pattern corresponding to MgO. The smoke from olivine showed a weak diffraction pattern corresponding to Fe2O3 and/or Fe3O4. The mass absorption coefficients, from 2.5 to 25 microns, of crystalline diopside, olivine, and serpentine and their corresponding smoke samples are shown in figures. Author

N91-14995*# Laboratoire d'Astronomie Spatiale, Marseille (France).
OPTICAL PROPERTIES OF IRREGULAR INTERSTELLAR GRAINS **c74**
J. M. Perrin and P. L. Lamy *In* NASA, Ames Research Center, Interstellar Dust: Contributed Papers Dec. 1989 p 381-388 (For primary document see N91-14897 06-88)
Avail: NTIS HC/MF A22 CSCL 20F

In order to study the interaction of light with interstellar grains, the authors represent an irregular particle by a network of interacting dipoles whose polarizability is determined in a first approach by the Clausius-Mossoti relationship. Typically, 10,000 dipoles are considered. In the case of spherical particles, the results from Mie theory are fully recovered. The main interest of this method is to study with good accuracy the implications of surface roughness and/or inhomogeneities on optical properties in the infrared spectral range, particularly of the silicate emission features. Author

N91-14996*# Aerospace Corp., Los Angeles, CA. Space Sciences Lab.
OBSERVATIONAL CONSTRAINTS ON INTERSTELLAR DUST MODELS **c89**
James H. Hecht, James A. Hackwell, and Ray W. Russell *In* NASA, Ames Research Center, Interstellar Dust: Contributed Papers Dec. 1989 p 391-393 (For primary document see N91-14897 06-88)
Avail: NTIS HC/MF A22 CSCL 03A

No single model has been able to account for all of the observed spectroscopic properties of interstellar or circumstellar dust. The reason for this is that, despite the agreement that the grains are composed of silicaceous/metal oxide and carbonaceous material, there is strong disagreement as to their exact structure and composition. This led Draine and Lee (1984) to use interstellar extinction data to define an interstellar graphitic material; new observational findings have made even that identification uncertain. But the great advantage of their approach is that they used observations at all of the wavelengths available to define the material. Here, the authors attempt a variation of that approach. They examine recent UV and IR data and attempt to put constraints on the possible types of interstellar grain composition, and to connect these constraints with grain models. A summary of some of the important constraints imposed by the observations is given.
Author

N91-14997*# Universitaets-Sternwarte, Jena (German D.R.).
SIZE DISTRIBUTION OF DUST GRAINS: A PROBLEM OF SELF-SIMILARITY **c90**
Th. Henning, J. Dorschner, and J. Guertler *In* NASA, Ames Research Center, Interstellar Dust: Contributed Papers Dec. 1989 p 395-396 (For primary document see N91-14897 06-88)
Avail: NTIS HC/MF A22 CSCL 03B

Distribution functions describing the results of natural processes frequently show the shape of power laws, e.g., mass functions of stars and molecular clouds, velocity spectrum of turbulence, size distributions of asteroids, micrometeorites and also interstellar dust grains. It is an open question whether this behavior is a result simply coming about by the chosen mathematical representation of the observational data or reflects a deep-seated principle of nature. The authors suppose the latter being the case. Using a dust model consisting of silicate and graphite grains Mathis et al. (1977) showed that the interstellar extinction curve can be represented by taking a grain radii distribution of power law type n(a) varies as a(exp -p) with 3.3 less than or equal to p less than or equal to 3.6 (example 1) as a basis. A different approach to understanding power laws like that in example 1 becomes possible by the theory of self-similar processes (scale invariance). The beta model of turbulence (Frisch et al., 1978) leads in an elementary way to the concept of the self-similarity dimension D, a special case of Mandelbrot's (1977) fractal dimension. In the frame of this beta model, it is supposed that on each stage of a cascade the system decays to N clumps and that only the portion beta N remains active further on. An important feature of this model is that the active eddies become less and less space-filling. In the following, the authors assume that grain-grain collisions are such a scale-invarient process and that the remaining grains are the inactive (frozen) clumps of the cascade. In this way, a size distribution n(a) da varies as a(exp -(D+1))da (example 2) results. It seems to be highly probable that the power law character of the size distribution of interstellar dust grains is the result of a self-similarity process. We can, however, not exclude that the process leading to the interstellar grain size distribution is not fragmentation at all. It could be, e.g., diffusion-limited growth discussed by Sander (1986), who applied the theory of fractal geometry to the classification of non-equilibrium growth processes. He received D=2.4 for diffusion-limited aggregation in 3d-space.
Author

N91-14998*# National Aeronautics and Space Administration. Ames Research Center, Moffett Field, CA.
STOCHASTIC HISTORIES OF DUST GRAINS IN THE INTERSTELLAR MEDIUM **c90**
Kurt Liffman and D. D. Clayton (Rice Univ., Houston, TX.) *In its* Interstellar Dust: Contributed Papers Dec. 1989 p 397-398 (For primary document see N91-14897 06-88)
Avail: NTIS HC/MF A22 CSCL 03B

The purpose is to study an evolving system of refractory dust

grains within the Interstellar Medium (ISM). This is done via a combination of Monte Carlo processes and a system of partial differential equations, where refractory dust grains formed within supernova remnants and ejecta from high mass loss stars are subjected to the processes of sputtering and collisional fragmentation in the diffuse media and accretion within the cold molecular clouds. In order to record chemical detail, the authors take each new particle to consist of a superrefractory core plus a more massive refractory mantle. The particles are allowed to transfer to and fro between the different phases of the interstellar medium (ISM) - on a time scale of 10(exp 8) years - until either the particles are destroyed or the program finishes at a Galaxy time of 6x10(exp 9) years. The resulting chemical and size spectrum(s) are then applied to various astrophysical problems with the following results. For an ISM which has no collisional fragmentation of the dust grains, roughly 10 percent by mass of the most refractory material survives the rigors of the ISM intact, which leaves open the possibility that fossilized isotopically anomalous material may have been present within the primordial solar nebula. Stuctured or layered refractory dust grains within the model cannot explain the observed interstellar depletions of refractory material. Fragmentation due to grain-grain collisions in the diffuse phase plus the accretion of material in the molecular cloud phase can under certain circumstances cause a bimodal distribution in grain size. Author

N91-14999*# Manuel (Lawrence R.), Berkeley, CA.
SUPERAROMATICS: THE KEY TO A UNIFIED COSMIC DUST THEORY **c90**
Lawrence R. Manuel *In* NASA, Ames Research Center, Interstellar Dust: Contributed Papers Dec. 1989 p 399-404 (For primary document see N91-14897 06-88)
Avail: NTIS HC/MF A22 CSCL 03B

The theory of Superaromatics, the key to a unified cosmic dust theory, was constructed by analyzing several thousand astronomical features covering every major aspect of astrophysics and astrochemistry relating to dust. To insure consistency between disciplines, the logical structure of the conclusions in each field was checked rather than accepting the current consensus. No substantial contradictory features are known to the author. The analysis falls into seven major parts: (1) kinetics of grain formation and destruction; (2) optical spectra of the interstellar medium (ISM); (3) meteorite interplanetary dust particle (IPD) chemistry; (4) structure and chemistry of the interstellar medium arising from surface catalysis; (6) dynamics of circumstellar and interstellar dust clouds, including galactic morphology; and (7) the chemistry and physics of previously unidentified compounds. Only tentative conclusions are presented here. The principle conclusion is that quantum mechanics as it is normally formulated is incomplete. The probable cause is that it is formulated with complex numbers rather than the more fundamental quaternion system. The manifestation in astrochemistry is that the most stable compounds are superaromatic and exotic enough to confound most classical analysis. Author

N91-15000*# Colorado Univ., Boulder. Center for Astrophysics and Space Astronomy.
THE ORIGIN OF MICROGRAINS **c90**
Theodore P. Snow, Jr., C. Gregory Seab, Richard H. Buss, Jr., Karl Josafatsson, and Kris Sellgren (Hawaii Univ., Honolulu.) *In* NASA, Ames Research Center, Interstellar Dust: Contributed Papers Dec. 1989 p 405-406 (For primary document see N91-14897 06-88)
Avail: NTIS HC/MF A22 CSCL 03B

Using ultraviolet and infrared techniques, researchers investigated the origins of the tiny (approx. 10A) grains whose presence in the interstellar medium (ISM) is inferred from near-infrared photometry (Sellgren, Werner, and Dinerstein 1983; Sellgren 1984). The authors consider two possibilities: (1) that the grains are formed by condensation in stellar atmospheres; or (2) that they are formed by fragmentation of larger grains in interstellar shocks. They searched for evidence of very small grains in circumstellar environments by analyzing ultraviolet extinction curves in binaries containing hot companions, and by searching for the 3.3-micron emission feature in similar systems. The ultraviolet extinction curve analysis could be applied only to oxygen-rich systems, where small carbonaceous grains would not be expected, so these results provide only indirect information. Researchers find a deficiency of grains smaller than 800A in oxygen-rich systems, consistent with theoretical models of grain condensation which suggest that grains grow to large sizes before injection into the interstellar medium. More direct information on carbonaceous micrograins was obtained from the search for the 3.3-micron feature in carbon-rich binaries with hot companions, whose ultraviolet flux should excite the tiny grains to emit in the infrared. No 3.3-micron feature was found, suggesting that the micrograins are absent in these systems. In addition to the negative search for micrograins in circumstellar environments, researchers have also studied the possible association of these grains with shocks in the diffuse interstellar medium. Using Infrared Astronomy Satellite (IRAS) colors as indicators of the presence or absence of the small grains (e.g., Ryter, Puget, and Perault 1987 and references cited therein), researchers systematically searched for them in regions (reflection nebulae) expected to have sufficient ultraviolet flux to make them glow in the infrared. They found that the distribution is not uniform. The researchers propose that production of micrograins by fragmentation of larger grains in shocks could explain this uneven distribution. Author

N91-15001*# Kapteyn Astronomical Lab., Groningen (Netherlands).
PROPERTIES OF GRAINS DERIVED FROM IRAS OBSERVATIONS OF DUST **c90**
P. R. Wesselius, Grzegorz Chlewicki, and Rene J. Laureijs *In* NASA, Ames Research Center, Interstellar Dust: Contributed Papers Dec. 1989 p 407 (For primary document see N91-14897 06-88)
Avail: NTIS HC/MF A22 CSCL 03B

The authors used the results of Infrared Astronomy Satellite (IRAS) observations of diffuse medium dust to develop a theoretical model of the infrared properties of grains. Recent models based entirely on traditional observations of extinction and polarization include only particles whose equilibrium temperatures do not exceed 20 K in the diffuse interstellar medium. These classical grains, for which the authors have adopted the multipopulation model developed by Hong and Greenberg (1980), can explain only the emission in the IRAS 100 micron band. The measurements at shorter wavelengths (12, 25 and 60 microns) require two new particle populations. Vibrational fluorescence from aromatic molecules provides the most likely explanation for the emission observed at 12 microns, with polycyclic aeromatic hydrocarbons (PAHs) containing about 10 percent of cosmic carbon. A simplified model of the emission process shows that PAH molecules can also explain most of the emission measured by IRAS at 25 microns. The authors identified the warm particles responsible for the excess 60 microns emission with small (a approx. equals 0.01 microns) iron grains. A compilation of the available data on the optical properties of iron indicates that the diffuse medium temperature of small iron particles should be close to 50 K and implies that a large, possibly dominant, fraction of cosmic iron must be locked up in metallic particles in order to match the observed 60 microns intensities. The model matches the infrared fluxes typically observed by IRAS in the diffuse medium and can also reproduce the infrared surface brightness distribution in individual clouds. In particular, the combination of iron and classical cool grains can explain the surprising observations of the 60/100 microns flux ratio in clouds, which is either constant or increases slightly towards higher opacities. The presence of metallic grains has significant implications for the physics of the interstellar medium, including catalytic H2 formation, for which iron grains could be the main site; differences in depletion patterns between iron and other refractory elements (Mg, Si); and superparamagnetic behavior of large grains with embedded iron clusters giving rise to the observed high degree of alignment by the galactic magnetic field. Author

N91-15002*# Planetary Science Inst., Tucson, AZ.
A SPECTRAL DIFFERENCE BETWEEN SILICATES IN COMET HALLEY AND INTERSTELLAR SILICATES **c90**
Humberto Campins and Eileen V. Ryan *In* NASA, Ames Research Center, Interstellar Dust: Contributed Papers Dec. 1989 p 411-413 Submitted for publication (For primary document see N91-14897 06-88)
Avail: NTIS HC/MF A22 CSCL 03B

The authors obtained an intermediate resolution (1 percent) spectrum of the 8 to 13 micron region in Comet Halley which shows a prominent silicate emission feature with structure not observed before in other comets or in interstellar silicates. They confirm the presence of a strong 11.3 micron peak reported by Bregman et al. (1987) and find evidence for additional structure in the band. The 11.3 micron peak represents the main difference between the Halley Spectrum and that of Comet Kohoutek. The Kohoutek Spectrum is similar to that of the circumstellar shell around mu Ceph. Based on a comparison with the spectra of Interplanetary Dust Particles (Sandford and Walker 1985), most of which are believed to be of cometary origin, the authors attribute the 11.3 micron peak to small crystalline olivine particles, although other minerals cannot be ruled out. Their interpretation is supported by the airborne observation of four emission peaks near 24, 28, 35 and 45 microns which can also be matched with iron-magnesium silicates including crystalline olivine. Other types of silicates (such as hydrated or amorphous) are necessary to explain the width and the 9.7 micron peak of the emission observed in Comet Halley. Author

N91-15003*# National Aeronautics and Space Administration. Ames Research Center, Moffett Field, CA.
THE NATURE OF COMETARY DUST AS DETERMINED FROM INFRARED OBSERVATIONS **c90**
K. S. Krishna Swamy, Scott A. Sandford, Louis J. Allamandola, Fred C. Witteborn, and Jesse D. Bregman *In its* Interstellar Dust: Contributed Papers Dec. 1989 p 415-416 (For primary document see N91-14897 06-88)
Avail: NTIS HC/MF A22 CSCL 03B

The infrared measurements of comets, the compositional information available from interplanetary dust particles (IDPs), and the recent results of flybys to Comet Halley can help in restricting the nature and composition of cometary dust models (c.f., Proceedings of the 20th ESLAB Symposium on Exploration of Halley's Comet, 1986). Researchers tried to incorporate some of these results into a coherent model to account for the observed cometary infrared emission. The presence of 10 and 3.4 micron features in Comet Halley (c.f. Bregman et al. 1987; Wickramasinghe and Allen 1986) indicated the presence of at least two components in the grain material, namely silicates and some form of amorphous carbon. These two components could reside in separate grains or may be parts of composite particles. Both these cases have been considered (see Krishna Swamy el a. 1988a, 1988b). In the absence of refractive index data for cometary analogs, the authors used the optical constants of olivine-rich lunar material 12009.48 (Perry et al. 1972) for the infrared region and that of alpha:C-H film for amorphous carbon (angus et al. 1986). For the visible region, a value of m = 1.38-0.39i was used for the silicates, and values published by Arakawa et al. (1985) were used for the amorphous carbon. These materials should give a representative behavior of the expected results. The model results were compared to observational data. The strength of the 3.4 micron and 10 micron features relative to the adjacent continuum, as well as the slope of the continuum between 2500 and 1250 cm(exp -1) (4 to 8 microns), were used as criteria for comparison. Model calculations with alpha approx. equals -3.5, and also the size distribution function inferred for Comet Halley, with a mass fraction (X) of silicate to amorphous carbon grains of about 40 to 1 can fit the data. A good match is obtained for the infrared spectra of Comets Halley and West from a 40 to 1 mixture of silicate and amorphous carbon grains with a a(exp -3.5) size distribution function. The results are consistent with compositional constraints provided by interplanetary dust particles (IPDs) and Halley flyby data. The variation of grain temperature with heliocentric distance appears to account for the major changes observed in cometary spectra. Author

N91-15004*# Aerospace Corp., Los Angeles, CA. Space Sciences Lab.
THE 10 MICRON SPECTRAL STRUCTURE IN COMETS **c90**
David K. Lynch, Ray W. Russell, and Humberto Campins (Planetary Science Inst., Tucson, AZ.) *In* NASA, Ames Research Center, Interstellar Dust: Contributed Papers Dec. 1989 p 417-422 Sponsored by NSF (For primary document see N91-14897 06-88)
(Contract NAS2-12370)
Avail: NTIS HC/MF A22 CSCL 03B

The 10 micron spectra of comets Halley (1982i), Wilson (1986l), Kohoutek (1973f) and Bradfield (1987s) are presented and compared. The silicate emission profiles of Halley and Bradfield are seen to be remarkably similar in that both contain a sharp break in the spectrum at 11.3 microns. Comet Bradfield does not show the same double peak structure seen in olivine and reported in Comet Halley be Campins and Ryan (1988) and Bregman, et al. (1987). The authors interpret the 11.3 micron signature as being due to olivine-type dust grains with at least some degree of crystallinity. Olivine alone is not enough to reproduce the shape of the 10 micron structure. However, in view of the authors' past success in fitting interstellar dust features with the emissivity profile obtained from amorphous grains produced by laser-vaporizing olivine, this is a very appealing identification. They note that there are significant variations in olivine spectra due to compositional differences, grain size distribution and related grain temperature variations to make the olivine identification tentative. They further tentatively identify the 9.8 micron feature in Halley as being due to either amorphorous olivine or a phyllosilicate (layer lattice). Neither the spectra of Halley, Kohoutek, nor Bradfield exhibited the 12.2 micron feature seen in Comet Wilson, which may prove diagnostic of the composition or thermal history differences between these comets. IR spectra of various mineral samples are discussed in terms of their match to cometary spectra. Author

N91-15005*# Leiden Univ. (Netherlands). Lab. of Astrophysics.
A COMPARATIVE STUDY OF THE CONTINUUM AND EMISSION CHARACTERISTICS OF COMET DUST. 1: ARE THE SILICATES IN COMET HALLEY AND KOHOUTEK AMORPHOUS OR CRYSTALLINE **c90**
Zhao Nansheng, J. Mayo Greenberg, and J. I. Hage *In* NASA, Ames Research Center, Interstellar Dust: Contributed Papers Dec. 1989 p 423-427 (For primary document see N91-14897 06-88)
Avail: NTIS HC/MF A22 CSCL 03B

A continuum emission was subtracted from the 10 micron emission observed towards comets Halley and Kohoutek. The 10 micron excess emissions were compared with BN absorption and laboratory amorphous silicates. The results show that cometary silicates are predominantly amorphous which is consistent with the interstellar dust model of comets. It is concluded that cometary silicates are predominantly similar to interstellar silicates. For a periodic comet like Comet Halley, it is to be expected that some of the silicate may have been heated enough to convert to crystalline form. But apparently, this is only a small fraction of the total. A comparison of Comet Halley silicates with a combination of the crystalline forms observed in interplanetary dust particles (IPDs) seemed reasonable at first sight (Walker 1988, Brownlee 1988). But, if true, it would imply that the total silicate mass in Comet Halley dust is lower than that given by mass spectrometry data of Kissel and Krueger (1987). They estimated m sub org/m sub sil = 0.5 while using crystalline silicate to produce the 10 micron emission would give m sub org/m sub sil = 5 (Greenberg et al. 1988). This is a factor of 10 too high. Author

N91-15006*# State Univ. of New York, Stony Brook. Dept. of Earth and Space Sciences.
THE 3.4 MICRON EMISSION IN COMETS Abstract Only **c90**
Tim Y. Brooke, Roger F. Knacke, T. C. Owen, and Alan T. Tokunaga (Hawaii Univ., Honolulu.) *In* NASA, Ames Research Center,

Interstellar Dust: Contributed Papers Dec. 1989 p 431 (For primary document see N91-14897 06-88)
Avail: NTIS HC/MF A22 CSCL 03B

Emission features near 3.4 microns were detected in comet Bradfield (1987s) on 17 Nov. 1987 UT, and, marginally, on two earlier dates, with the Cooled Grating Array Spectrometer at the NASA Infrared Radio Telescope Facility (IRTF) (Brooke et al., 1988b). The central wavelength (3.36 microns) and width (approx. 0.15 microns) of the strongest feature coincide with those observed in comet Halley. A weaker emission feature at 3.52 microns and a strong feature extending shortward of 2.9 microns were also detected. This brings the number of comets in which these three features have been seen to three, two new (Bradfield, Wilson) and one old (Halley). It seems almost certain that the 3.4 micron features are emissions by C-H groups in complex molecules. Based on the similarity of the 3.4 micron features in comets Halley and Wilson, the authors suggest that a particular set of organic compounds may be common to all comets (Brooke et al. 1988a). The absence of the feature in some comets could then be due to photodestruction or evaporation of the organics when the comet approaches the sun, in combination with a predominance of thermal emission from non C-H emitting grains. Detection of the 3.4 micron emission feature in comet Bradfield at 4 = 0.9 AU provides support for this argument. Complex organics in comets could have been formed by particle irradiation of parent ices in the nucleus or been incorporated as grains at the time the comets formed. Since the most heavily irradiated layers of Halley would have been lost in its hundreds of perihelion passages, the authors believe the more likely explanation is that the 3.4 micron emitting material was incorporated in comet nuclei at the time of formation. The 3.4 micron comet feature resembles, but is not identical to, the interstellar 3.29 micron (and longer wavelength) emission features and the broad 3.4 micron feature seen in absorption toward the Galactic center. Detailed comparisons of cometary and interstellar organics will require comet spectra with signal-to-noise and spectral resolution comparable to that available in spectra of the interstellar medium. Such observations are currently being planned. Author

N91-15007*# Cornell Univ., Ithaca, NY. Lab. for Planetary Studies.
THE PRE- AND POST-ACCRETION IRRADIATION HISTORY OF COMETARY ICES **c90**
Christopher Chyba and Carl Sagan *In* NASA, Ames Research Center, Interstellar Dust: Contributed Papers Dec. 1989 p 433-435 (For primary document see N91-14897 06-88)
Avail: NTIS HC/MF A22 CSCL 03B

Comets Halley and Wilson exhibited similar 3.4 micron emission features at approx. 1 AU from the Sun. A simple model of thermal emission from organic grains fits the feature, provides optical depths in good agreement with spacecraft measurements, and explains the absence of longer-wavelength organic features as due to spectral heliocentric evolution (Chyba and Sagan, 1987). The model utilizes transmission spectra of organics synthesized in the laboratory by irradiation of candidate cometary ices; the authors have long noted that related gas-phase syntheses yield polycyclic aromatic hydrocarbons, among other organic residues (Sagan et al., 1967). The authors previously concluded (Chyba and Sagan, 1987) that Halley's loss of several meters' depth with each perihelion passage, combined with the good fit of the Halley 3.4 micron feature to that of comet Wilson (Allen and Wickramasinghe, 1987), argues for the primordial - but not necessarily interstellar - origin of cometary organics. The authors examine the relative importance to the formation of organics of the variety of radiation environments experienced by comets. They conclude that there is at present no compelling reason to choose any of three contributing mechanisms (pre-accretion UV, pre-accretion cosmic ray, and post-accretion radionuclide processing) as the most important.
Author

N91-15008*# European Space Agency. European Space Research and Technology Center, ESTEC, Noordwijk (Netherlands). Dept. of Space Science.
EXPERIMENTAL EVIDENCE FOR AMORPHOUS CARBON GRAINS IN COMETS **c90**
Luigi Colangeli, G. Schwehm, E. Bussoletti, A. Blanco, A. Borghesi, Sergio Fonti, and Vincenso Orofino (Lecce Univ., Italy) *In* NASA, Ames Research Center, Interstellar Dust: Contributed Papers Dec. 1989 p 437-442 (For primary document see N91-14897 06-88)
Avail: NTIS HC/MF A22 CSCL 03B

Amorphous carbon grains similar to those produced in the laboratory, but with a higher hydrogen content, appear to be good candidates to simulate both the IR continuum emission and the 3.4 micron band measured for P/Halley. The comparison of the cometary features with those detected in the laboratory for carbon grains characterized by various sp(exp 2)/sp(exp 3) ratios seems to indicate that a prevalent diamond-like (sp(exp 3)) structure should be present in cometary particles. These kinds of solid particles seem also suitable to explain the daily and monthly variations of the 3.4 micron band intensity, relative to the continuum, and, at the same time,- to fulfill the abundance constraints. The same grains appear to be able to reproduce the absorption bands detected in the IR galactic source IRS 7. This result may be considered as a first experimental evidence of a relation existing between interstellar dust and cometary materials. Author

N91-15009*# Warsaw Univ. (Poland). Dept. of Chemistry.
VEGA-GIOTTO FLYBY MISSIONS AND COMETARY COSMOGONY **c90**
Bruno Lang *In* NASA, Ames Research Center, Interstellar Dust: Contributed Papers Dec. 1989 p 445-450 (For primary document see N91-14897 06-88)
Avail: NTIS HC/MF A22 CSCL 03B

The most important implication of the Vega/Giotto flyby missions to Halley's Comet for cometary cosmogony is the opportunity to absorb the results of the in-situ measurements as made onboard the spacecrafts. Unfortunately the exploration of ejecta form the nucleus was unable to provide an unambiguous definition of the chemical-mineralogical nature of the nucleus: it failed to provide information comparable to that which was expected from a sample return mission. However, the obtained results are significant enough to affect and redirect cosmogonical thinking. Accordingly, the understanding of the cometary-matter dichotomy is modified as deduced from the distiction of water-dominated volitiles and silicate-based non-volitiles. Organic carbon compounds emerge as a major constituent of cometary nuclei. Presently, it is likely that the revision of Whipple's classic concept of the icy conglomerate cannot be avoided. Affected by the Vega/Giotto flyby missions to Hally's Comet, cometary cosmogony seems to enter a new conceptual period. The results of the in-situ measurements (mass spectrometric, UV spectroscopic, and IR spectroscopic) appear to be of basic importance. A chemical explanation is employed to explain the occurrence inside the nuclei of the variety of species, as inferred from the mass spectrometric data, to predict the results of the processes possibly involved. A cosmochemical factor is postulated to operate behind the observed cometary phenomena. The chemistry of the interstellar medium, covering the circumstellar and interstellar dust, advances cometary cosmogony.
Author

N91-15010*# California Univ., Berkeley. Space Sciences Lab.
THE COMPOSITION OF HEAVY MOLECULAR IONS INSIDE THE IONOPAUSE OF COMET HALLEY **c90**
David L. Mitchell, R. P. Lin, K. A. Anderson, C. W. Carlson, D. W. Curtis, A. Korth, H. Reme, J. A. Sauvaud, C. dUston, and D. A. Mendis (California Univ., San Diego.) *In* NASA, Ames Research Center, Interstellar Dust: Contributed Papers Dec. 1989 p 451-452 (For primary document see N91-14897 06-88)
Avail: NTIS HC/MF A22 CSCL 03B

The RPA2-PICCA instrument aboard the Giotto spacecraft obtained 10-210 amu mass spectral of cold thermal molecular ions in the coma of Comet Halley. The dissociation products of

the long chain formaldehyde polymer polyoxymethylene (POM) have recently been proposed as the dominant complex molecules in the coma of Comet Halley; however, POM alone cannot account for all of the features of the high resolution spectrum. An important component of the dust at Comet Halley is particles highly enriched in carbon, hydrogen, oxygen, and nitrogen relative to the composition of carbonaceous chondrites. Since this dust could be a source for the heavy molecules observed by PICCA, a search was conducted for other chemical species by determining all the molecules with mass between 20 and 120 amu which can be made from the relatively abundant C, H, O, and N, without regard to chemical structure. Author

N91-15011*# British Museum of Natural History, London (England). Dept. of Mineralogy.
ATOMIC ENVIRONMENTS IN IRON METEORITES USING EXAFS **c90**
G. Cressey, A. J. Dent, B. Dobson, A. Evans, G. N. Greaves, C. M. B. Henderson, R. Hutchison, R. N. Jenkins, S. P. Thompson, and R. Zhu (Science Research Council, Daresbury, England) *In* NASA, Ames Research Center, Interstellar Dust: Contributed Papers Dec. 1989 p 455-461 (For primary document see N91-14897 06-88)
Avail: NTIS HC/MF A22 CSCL 03B

Extended x ray absorption fine structure (EXAFS) is observed as a modulation on the high energy side of an x ray absorption edge. It occurs when the photo-ejected electron wave is scattered by neighboring atoms in a solid, and interference occurs between the outgoing and scattered waves. The result is that the absorption spectrum carries a signature that is characteristic of the identity and disposition of scattering atoms around the absorbing atom. Therefore, it may be shown that the Fourier transform of the normalized EXAFS can provide detailed information about the immediate environment of specific atoms in a solid and is ideally suited to the study of cosmic dusts. A study of cosmic dust was initiated using EXAFS and other techniques. The simplest type of cosmic material, namely iron meteorites, was investigated. Author

N91-15012*# Abastumani Astrophysical Observatory, Georgia (USSR).
DUST OF ORIONID METEOR SHOWER IN THE EARTH ATMOSPHERE BEFORE AND AFTER HALLEY'S COMET **c90**
G. Mateshvili and Yu. Mateshvili *In* NASA, Ames Research Center, Interstellar Dust: Contributed Papers Dec. 1989 p 463-468 (For primary document see N91-14897 06-88)
Avail: NTIS HC/MF A22 CSCL 03B

Among the interesting questions concerning meteor streams associated with Comet Halley is the question of whether or not the activity of a meteor stream was connected with the approach of the comet to the terrestrial orbit in 1985 to 1986. Meteoric aerosols getting to the upper atmosphere can be detected by twilight sounding, as has been done previously. It turns out that not only parameters describing some properties of aerosol can be obtained by twilight sounding, but also characteristics concerning the structure of the stream can be derived. Among the yearly active streams, the Orionides have always attracted the attention of scientists. The period of activity of the Orionides is October 18 to 26, and the maximum stream activity is October 21. In detecting aerosol layers in the terrestrial atmosphere, a notion of the logarithmic intensity gradient of scattered twilight light is used, d log I/dH, where I is intensity and H is the real twilight beam height, which is a function of the wavelength observed. A photoelectric photometer with an interference filter at the wavelength of 610 nm is used. The observation were carried out in two points of the solar vertical; the zenith angle of the observation points was + or - 60 degrees. The recording was carried on continuously in each direction during a minute, then the system was switched to the other direction. A calibration standard was recorded before each observation. The observation dates in the Orionid periods of 1984, 1986, and 1987 are given. Author

N91-15013*# California Univ., Berkeley. Dept. of Astronomy.
INFRARED EMISSION FROM INTERPLANETARY DUST **c89**
William T. Reach *In* NASA, Ames Research Center, Interstellar Dust: Contributed Papers Dec. 1989 p 469-470 (For primary document see N91-14897 06-88)
Avail: NTIS HC/MF A22 CSCL 03A

The infrared sky is dominated on large scales by emission from interplanetary dust, which produces the zodiacal emission (ZE), and interstellar dust. These two components of the infrared background differ in angular and spectral distribution, allowing the two to be separated easily in some places. A method of determining the emission from interplanetary dust near the Earth's orbit is described, and the results are compared to predictions for realistic materials with the interplanetary size distribution measured in situ. Author

N91-15014*# York Univ. (Ontario). Dept. of Chemistry.
GAS-PHASE FORMATION OF SILICON CARBIDES, OXIDES, AND SULPHIDES FROM ATOMIC SILICON IONS **c25**
Diethard K. Bohme, Stanislaw Wlodek, and Arnold Fox *In* NASA, Ames Research Center, Interstellar Dust: Contributed Papers Dec. 1989 p 473-478 Sponsored in part by Natural Sciences and Engineering Research Council of Canada (For primary document see N91-14897 06-88)
Avail: NTIS HC/MF A22 CSCL 07D

A systematic experimental study of the kinetics and mechanisms of the chemical reactions in the gas phase between ground-state Si(+)2p and a variety of astrophysical molecules. The aim of this study is to identify the reactions which trigger the formation of chemical bonds between silicon and carbon, oxygen and sulphur, and the chemical pathways which lead to further molecular growth. Such knowledge is valuable in the identification of new extraterrestrial silicon-bearing molecules and for an assessment of the gas-phase transition from atomic silicon to silicon carbide and silicate grain particles in carbon-rich and oxygen-rich astrophysical environments. Author

N91-15015*# Pennsylvania State Univ., University Park. Dept. of Astronomy.
PAH FORMATION IN CARBON-RICH CIRCUMSTELLAR ENVELOPES **c25**
Eric D. Feigelson and Michael Frenklach *In* NASA, Ames Research Center, Interstellar Dust: Contributed Papers Dec. 1989 p 479-483 (For primary document see N91-14897 06-88)
Avail: NTIS HC/MF A22 CSCL 07D

While there is growing observational evidence that some fraction of interstellar carbon is in polycyclic aromatic hydrocarbons (PAH's), the mechanisms by which these molecules might be formed have not been extensively studied. A detailed investigation of PAH production in the outflowing molecular envelopes of carbon-rich red giant star is presented. The gasphase kinetics of a chemical reaction mechanism developed to study soot production in hydrocarbon flames is modified to apply in circumstellar environments. It was found that astrophysically significant quantities of PAH's can be formed in carbon star envelopes provided the gas is sufficiently dense and resides for a long time in the temperature range of 900 to 1100 k. The precise yield of PAH's is very sensitive to astronomical parameters of the envelope (e.g., mass loss rate, outflow velocity, and acetylene abundance) and certain poorly determined chemical reaction rates. Author

N91-15016*# National Aeronautics and Space Administration. Ames Research Center, Moffett Field, CA.
SUBLIMATING ICY PLANETESIMALS AS THE SOURCE OF NUCLEATION SEEDS FOR GRAIN CONDENSATION IN CLASSICAL NOVAE **c90**
John J. Matese, D. P. Whitmire (University of Southwestern Louisiana, Lafayette.), and R. T. Reynolds *In its* Interstellar Dust: Contributed Papers Dec. 1989 p 485-488 (For primary document see N91-14897 06-88)
Avail: NTIS HC/MF A22 CSCL 03B

The problem of grain nucleation during novae outbursts is a

major obstacle to our understanding of dust formation in these systems. How nucleation seeds can form in the hostile post-outburst environment remains an unresolved matter. It is suggested that the material for seeding the condensation of ejecta outflow is stored in a primordial disk of icy planetesimals surrounding the system. Evidence is presented that the requisite number of nucleation seeds can be released by sublimation of the planetesimals during outbursts. Author

N91-15017*# Tokyo Univ. (Japan). Dept. of Astronomy.
DUST FORMATION AROUND M-TYPE STARS **c90**
Takashi Onaka *In* NASA, Ames Research Center, Interstellar Dust: Contributed Papers Dec. 1989 p 489-494 Sponsored in part by Ministry of Education, Science and Culture, Sagamihara, Japan (For primary document see N91-14897 06-88)
Avail: NTIS HC/MF A22 CSCL 03B

IRAS LRS spectra of M Mira variable have shown variation in the appearance of the 9.7 micron silicate feature, which is correlated with the shape of light curve. The LRS spectra of 100 Mira variables have been studied using simple dust shell models containing mixtures of silicate and aluminum oxide dust grains. It has been shown that the aluminum oxide grains account for the observed broad feature around 12 microns and that the variation of the spectra can be interpreted in terms of the variation of the temperature at the inner boundary of silicate dust shell. It has been proposed that silicate mantle growth on aluminum oxide grains is a possible explanation for the results. In this report, the model spectra are calculated taking account of silicate mantle growth, and the physical parameters which may determine the appearance of the 9.7 micron feature in M Mira variables are investigated. In the model calculation it is assumed that aluminum oxide grains are already formed at the bottom of the circumstellar envelope because of their high condensation temperature. The growth of silicate mantle and the motion of gas and grains from r=r(sub 0), where the mantle growth starts, are investigated. Sticking and sputtering processes due to the relative motion of grain to the ambient gas are taken into account. The thermal velocity is assumed to be negligible to the drift velocity. Acceleration by radiation pressure is considered in the gas motion equation. The formal solution is integrated to obtain the emergent spectra. Physical conditions inside r(sub 0) are regarded as boundary conditions. Observed spectra are compared to model spectra to investigate the conditions at the bottom of circumstellar envelope. In modeling the envelope, a parameter C(sub l) is introduced to take account of the density fluctuation of the envelope phenomenologically. Author

N91-15018*# National Aeronautics and Space Administration. Ames Research Center, Moffett Field, CA.
SUBLIMATING COMETS AS THE SOURCE OF NUCLEATION SEEDS FOR GRAIN CONDENSATION IN THE GAS OUTFLOW FROM AGB STARS **c90**
D. P. Whitmire, John J. Matese (University of Southwestern Louisiana, Lafayette.), and R. T. Reynolds *In its* Interstellar Dust: Contributed Papers Dec. 1989 p 495-501 (For primary document see N91-14897 06-88)
Avail: NTIS HC/MF A22 CSCL 03B

A growing amount of observational and theoretical evidence suggests that most main sequence stars are surrounded by disks of cometary material. The dust production by comets in such disks is investigated when the central stars evolve up the red giant and asymptotic giant branch (AGB). Once released, the dust is ablated and accelerated by the gas outflow and the fragments become the seeds necessary for condensation of the gas. The origin of the requisite seeds has presented a well known problem for classical nucleation theory. This model is consistent with the dust production observed in M giants and supergiants (which have increasing luminosities) and the fact that earlier supergiants and most WR stars (whose luminosities are unchanging) do not have significant dust clouds even though they have significant stellar winds. Another consequence of the model is that the spatial distribution of the dust does not, in general, coincide with that of the gas outflow, in contrast to the conventional condensation model. A further prediction is that the condensation radius is greater that that predicted by conventional theory which is in agreement with IR interferometry measurements of alpha-Ori. Author

N91-15019*# Lecce Univ. (Italy). Dept. of Physics.
IR EMISSION FROM CIRCUMSTELLAR ENVELOPES OF C-RICH STARS **c89**
A. Blanco, A. Borghesi, E. Bussoletti, Luigi Colangeli (European Space Agency. European Space Research and Technology Center, ESTEC, Noordwijk, Netherlands), Sergio Fonti, and Vincenso Orofino *In* NASA, Ames Research Center, Interstellar Dust: Contributed Papers Dec. 1989 p 505-506 (For primary document see N91-14897 06-88)
Avail: NTIS HC/MF A22 CSCL 03A

The reliability of a theoretical model that solves the radiative transfer equation in dust clouds surrounding a central star is checked. In particular, it is found that both classical scattering by dust and the back-heating effects are negligible in the radiative transfer when envelopes similar to IRC+10216 are taken into consideration. In addition, new fits of IRC+10216 spectra are presented which were obtained, when the source is in different luminosity phases, under the assumption that amorphous carbon grains are in the circumstellar envelope. The same model is currently used to simulate the emission from carbon-rich sources showing the silicon carbide feature at 11.3 microns. Author

N91-15020*# Crimean Astrophysical Observatory (USSR).
THE INFLUENCE OF GRAIN GROWTH IN CIRCUMSTELLAR DUST ENVELOPES ON OBSERVED COLORS AND POLARIZATION OF SOME ERUPTIVE STARS **c90**
Yu. S. Efimov *In* NASA, Ames Research Center, Interstellar Dust: Contributed Papers Dec. 1989 p 507-514 (For primary document see N91-14897 06-88)
Avail: NTIS HC/MF A22 CSCL 03B

R CrB stars are classical examples of stars where dust envelope formation takes place. Dust envelope formation was detected around the Kuwano-Honda object (PU Vul) in 1980 to 1981 when the star's brightness fell to 8(sup m). Such envelopes are also formed at nova outbursts. The process of dust envelope formation leads to appreciable variations in optical characteristics, which are seen in specific color and polarization variations in the course of light fading and the appearance of IR radiation. It is shown that the model of a circumstellar dust envelope with aligned particles of changing size can be successfully applied to explain most phenomena observed at the time of light minima for a number of eruptive stars. The polarization may arise in a nonspherical dust envelope or be produced by alignment of nonspherical particles. K.S.

N91-15021*# Rensselaer Polytechnic Inst., Troy, NY.
USING INFRARED SPECTRAL FEATURES TO PROBE CIRCUMSTELLAR DUST SHELLS AROUND COOL STARS **c89**
Michael P. Egan and Chun Ming Leung *In* NASA, Ames Research Center, Interstellar Dust: Contributed Papers Dec. 1989 p 515-516 (For primary document see N91-14897 06-88)
(Grant NAGw-1103)
Avail: NTIS HC/MF A22 CSCL 03A

IRAS observations of cool stars provide low resolution spectra in the mid-infrared and also give fluxes at four wavelength bands from which color-color diagrams are constructed. The later have been used to study the evolution of these stars: as an O-rich star evolves to become a C-rich star and its detached dust shell moves further away, its evolution can be tracked on a color-color diagram. A major factor in determining the position of either C-rich or O-rich stars on the 12-25-60 micron color-color diagram is the presence of spectral features in the mid-IR. O-rich stars show a 9.8 micron silicate feature, while C-rich stars have a SiC feature at 11.2 microns. IRAS observations indicate that the SiC feature is quite narrow and uniform in shape showing little variation from star to star. The full width at half maximum (FWHM) is 1.6 + or - 0.15 microns. On the other hand, the shape of the silicate feature varies widely among the O-rich stars, with a FWHM ranging from

2 to 3 microns. The characteristics of circumstellar dust shells should manifest themselves both in the flux spectrum and in the details of the spectral features. To provide a coherent interpretation for these IRAS observations, models were constructed (using a radiative transfer code) of dust shells around O-rich and C-rich stars. Realistic grain opacities were used which include spectral features of varying intrinsic widths (e.g., Gaussian features at 10 microns with half width at half maximum of 0.5 and 1.0 microns). Author

N91-15022*# National Aeronautics and Space Administration. Ames Research Center, Moffett Field, CA.
CARBON STARS WITH ALPHA-C:H EMISSION Abstract Only **c90**
Florence Gerbault and John H. Goebel *In its* Interstellar Dust: Contributed Papers Dec. 1989 p 51 (For primary document see N91-14897 06-88)
Avail: NTIS HC/MF A22 CSCL 03B

Many carbon stars in the IRS low resolution spectra (LRS) catalog were found which display emission spectra that compare favorable with the absorption spectrum of alpha-C:H. These stars have largely been classified as 4X in the LRS which has led to their interpretation by others in terms of displaying a mixture of the UIRF's 8.6 micron band and SiC at 11.5 microns. It was also found that many of these stars have a spectral upturn at 20+ microns which resembles the MgS band seen in carbon stars and planetary nebulae. It was concluded that this group of carbon stars will evolve into planetary nebulae like NGC 7027 and IC 418. In the presence of hard ultraviolet radiation the UIRF's will light up and be displayed as narrow emission bands on top of the broad alpha-C:H emission bands. Author

N91-15023*# National Aeronautics and Space Administration. Ames Research Center, Moffett Field, CA.
NEW CIRCUMSTELLAR DUST COMPONENT IN OXYGEN RICH ENVIRONMENTS Abstract Only **c90**
John H. Goebel and Florence Gerbault *In its* Interstellar Dust: Contributed Papers Dec. 1989 p 51 (For primary document see N91-14897 06-88)
Avail: NTIS HC/MF A22 CSCL 03B

Spectra of oxygen rich stars in the IRAS low-resolution spectra (LRS) catalog were found to display two distinct classes of curcumstellar excess emission. The first group has the normal silicate with emission peaking at 10 and 18 microns. The second group has an emission spectrum peaking at 13 and 20 microns. There are also spectra with a mixture of the above types. Generally the continuum temperature associated with the second group is much warmer than that associated with the normal silicate group. Laboratory spectra are compared with the new excess which associates the emission with a class of materials represented by hydrated aluminates and silicates. Possible interpretations include equilibrium condensation sequences and peculiar metal abundance ratios. Author

N91-15024*# Tata Inst. of Fundamental Research, Bombay (India).
TYPE OF SILICATE FEATURE IN OXYGEN RICH STELLAR ENVELOPES **c90**
K. V. K. Iyengar and T. N. Rengarajan *In* NASA, Ames Research Center, Interstellar Dust: Contributed Papers Dec. 1989 p 521-522 (For primary document see N91-14897 06-88)
Avail: NTIS HC/MF A22 CSCL 03B

In many astronomical studies, the emissivity function derived from the Trapezium emission feature has been used. A statistical study of a large sample of objects is described that deals with the applicability of this function (hereafter TR). For comparison, another emissivity function derived for lunar silicate (LS) sample 14321 was used which has a maximum at 10.2 microns instead of at 9.7 microns as for TR. The IRAS low resolution spectra sources classified as 7n was used which has a silicate absorption feature without any atomic line emission. Most of these sources are likely to be oxygen rich stellar envelopes or hotspots in molecular clouds. The central source as assumed to emit a Plankian spectrum characterized by a temperature (t) and an absorbing envelope with an emissivity dependence of type TR or LS. Values of t and tau, the absorption optical depth were obtained by minimizing chi(exp 2) between the observed and fitted spectra in the 7 to 13 micron range. Values of reduced chi(exp 2) were obtained by taking the noise listed in the LRS Catalog as standard deviation. The tau values obtained correspond to 9.7 microns for TR and 10.2 for LS. Author

N91-15025*# National Aeronautics and Space Administration. Ames Research Center, Moffett Field, CA.
INTERSTELLAR EXTINCTION AT 10-20 MICRONS **c90**
Janet P. Simpson and Robert H. Rubin (California Univ., Los Angeles.) *In its* Interstellar Dust: Contributed Papers Dec. 1989 p 523-526 (For primary document see N91-14897 06-88)
Avail: NTIS HC/MF A22 CSCL 03B

The IRAS low-resolution spectra (LRS) spectra of 117 stars of excellent signal/noise with optically thin silicate dust shells were analyzed. The stellar continua (assumed to be a cool black body) were subtracted, and the resulting dust shell spectra were fit with simple models F(sub lambda) assuming uniform mass loss and dust temperature as a function of distance from the star, calculated using the optical constants for silcates of Draine (1985). From the comparison of the spectra and the models, functions for the emissivity, kappa(sub lambda), were derived. Author

N91-15026*# Amsterdam Univ. (Netherlands). Astronomical Inst.
DUST AROUND MIRA VARIABLES: AN ANALYSIS OF IRAS LRS SPECTRA **c90**
S. Slijkhuis *In* NASA, Ames Research Center, Interstellar Dust: Contributed Papers Dec. 1989 p 527-528 (For primary document see N91-14897 06-88)
Avail: NTIS HC/MF A22 CSCL 03B

The spatial extent and spectral appearance of the thin dust shell around Mira variables is determined largely by the dust absorptivity, Q(sub abs)(lambda), and the dust condensation temperature T(sub cond). Both Q(sub abs)(lambda) and T(sub cond) are extracted from IRAS low-resolution spectra (LRS) spectra. In order to do this, the assumption that the ratio of total power in the 10 micron feature to that in the 20 micron feature should be equal to that measured in other amorphous silicates (e.g., synthesized amorphous Mg2SiO4). It was found that T(sub cond) decreases with decreasing strength of the 10 micron feature, from T(sub cond) = 1000 K to 500 K (estimated error 20 percent). A value for the near-infrared dust absorptivity could not be determined. Although this parameter strongly affects the condensation radius, it hardly affects the shape of the LRS spectrum (as long as the optically thin approximation is valid), because it scales the spatial distribution of the dust. Information on the magnitude of the near-infrared dust absorptivity may be deduced from the unique carbon star BM Gem. This star has a LRS spectrum with silicate features indication an inner dust shell temperature of at least 1000 K. However, on the basis of observations in the 1920s-30s one may infer an inner dust shell radius of at least 6x10(exp 12)m. To have this high temperature at such a large distance, the near-infrared absorptivity of the dust must be high. Author

N91-15027*# Indian Inst. of Astrophysics, Bangalore.
POLARIZATION DUE TO DUST SCATTERING IN THE PLANETARY NEBULA Cn1-1 **c90**
Harish C. Bhatt *In* NASA, Ames Research Center, Interstellar Dust: Contributed Papers Dec. 1989 p 531-532 (For primary document see N91-14897 06-88)
Avail: NTIS HC/MF A22 CSCL 03B

The peculiar emission-line object Cn1-1 (=HDE330036=PK330+4 degrees 1), classified both as a symbiotic star and as a planetary nebula, was detected by the Infrared Astronomical Satellite (IRAS) as a strong source of far-infrared dust in the system. Bhatt and Mallik (1986) discussed the nature of the dust in Cn1-1 and argued that the object is a

Type I protoplanetary nebula in a binary system. The argument presented here is that the polarization is intrinsic to Cn1-1 and is due to scattering by large (compared to interstellar) dust grains in the protoplanetary nebula that are asymmetrically distributed around the central star. The large degree of polarization (approximately 3 percent for the Cn1-1 distance of approximately 450 pc) with a large lambda(sub max) is naturally explained if it is caused by scattering by large dust grains in the Cn1-1 nebula. Since the H(sub alpha) line is also polarized at the same level and position angle as the continuum, the dust must be asymmetrically distributed around the central star. The morphology of the protoplanetary nebula in Cn1-1 may be bipolar. Thus, the polarization observations support the suggestion that Cn1-1 is a bipolar Type I planetary nebula. Author

N91-15028*# Colorado Univ., Boulder. Center for Astrophysics and Space Astronomy.

CIRCUMSTELLAR GRAIN EXTINCTION PROPERTIES OF RECENTLY DISCOVERED POST AGB STARS **c89**

Richard H. Buss, Jr., Henny J. G. L. M. Lamers (Space Research Organization Netherlands, Utrecht.), and Theodore P. Snow, Jr. *In* NASA, Ames Research Center, Interstellar Dust: Contributed Papers Dec. 1989 p 533-534 (For primary document see N91-14897 06-88)

Avail: NTIS HC/MF A22 CSCL 03A

The circumstellar grains of two hot evolved post asymptotic giant branch (post AGB) stars, HD 89353 and HD 213985 were examined. From ultraviolet spectra, energy balance of the flux, and Kurucz models, the extinction around 2175 A was derived. With visual spectra, an attempt was made to detect 6614 A diffuse band absorption arising from the circumstellar grains so that we could examine the relationship of these features to the infrared features. For both stars, we did not detect any diffuse band absorption at 6614 A, implying the carrier of this diffuse band is not the carrier of the unidentified infrared features not of the 2175 A bump. The linear ultraviolet extinction of the carbon-rich star HD 89353 was determined to continue across the 2175 A region with no sign of the bump; for HD 213985 it was found to be the reverse: a strong, wide bump in the mid-ultraviolet. The 213985 bump was found to be positioned at 2340 A, longward of its usual position in the interstellar medium. Since HD 213985 was determined to have excess carbon, the bump probably arises from a carbonaceous grain. Thus, in view of the ultraviolet and infrared properties of the two post AGB stars, ubiquitous interstellar infrared emission features do not seem to be associated with the 2175 A bump. Instead, the infrared features seem related to the linear ultraviolet extinction component: hydrocarbon grains of radius less than 300 A are present with the linear HD 89353 extinction; amorphous anhydrous carbonaceous grains of radius less than 50 A might cause the shifted ultraviolet extinction bump of HD 213985. Author

N91-15029*# Beijing Observatory, Huairou (China).

COMPACT REFLECTION NEBULAE, A TRANSIT PHASE OF EVOLUTION FROM POST-AGB TO PLANETARY NEBULAE Abstract Only **c90**

J. Y. Hu and S. Slijkhuis (Amsterdam Univ., Netherlands) *In* NASA, Ames Research Center, Interstellar Dust: Contributed Papers Dec. 1989 p 535 (For primary document see N91-14897 06-88)

Avail: NTIS HC/MF A22 CSCL 03B

In a search of the optical counter-part of candidates of protoplanetary nebulae on the plates of UK Schmidt, ESO Schmidt, and POSS, five compact reflection nebulae associated with post-AGB stars were found. A simplified model (dust shell is spherical symmetric, expansion velocity of dust shell is constant, Q(sub sca)(lambda) is isotropic, and the dust grain properties are uniform) is used to estimate the visible condition of the dust shell due to the scattering of the core star's light. Under certain conditions the compact reflection nebulae can be seen of the POSS or ESO/SRC survey plates. Author

N91-15030*# Polish Academy of Sciences, Torun. Lab. of Astrophysics.

CONTINUOUS INFRARED EMISSION OF PROTO- AND YOUNG-PLANETARY NEBULAE Abstract Only **c90**

Ryszard Szczerba *In* NASA, Ames Research Center, Interstellar Dust: Contributed Papers Dec. 1989 p 537-538 (For primary document see N91-14897 06-88)

Avail: NTIS HC/MF A22 CSCL 03B

Evolutionary sequences of planetary nebulae (PNe) were calculated beginning from the moment of shell ejection to its dissipation and IR spectra of the outgoing radiation were obtained for different stages of the evolution. To solve the coupled hydrodynamical and radiation transfer problem a computer code was used in which gas and dust are treated as two separate hydrodynamical components. The models, which are calculated for two grain materials (graphite and silicate) have a size distribution of particles based on that found for the interstellar medium. In the computations, the recent optical properties of graphite and astronomical silicate grains tabulated by Draine (1987) were employed. It was assumed that silicate of graphite grains exist below some critical temperature equal to 1300 or to 1700 K, respectively. Infrared model spectra are compared with the IR radiation emitted by some proto- and some young-planetary nebulae. The observed IR continua can be quite well matched with our models with grains having a reasonable size range. Author

N91-15031*# Royal Observatory, Edinburgh (Scotland).

THE DISCOVERY OF A HIGHLY POLARIZED BIPOLAR NEBULA **c90**

Ramon D. Wolstencroft, S. M. Scarrott, and J. Menzies (South African Astronomical Observatory, Cape Town.) *In* NASA, Ames Research Center, Interstellar Dust: Contributed Papers Dec. 1989 p 539-540 (For primary document see N91-14897 06-88)

Avail: NTIS HC/MF A22 CSCL 03B

During a search for the optical counterparts of IRAS sources whose flux peaks at 25 microns, a small faint bipolar nebula was discovered in Monoceros at the position of IRAS 07131-0147. The CCD images display the object's considerable structure. The central star seems relatively free of closeby nebulosity: the two lobes have a bow-tie structure with those parts nearest to the star consisting of series of small knots. The outer parts of the lobes seem to be made up of filaments streaming away from knots. On the basis of its optical spectrum, the central star was classified as a M5-6 giant. In the IRAS color classification scheme of Van der Veen and Habing (1988), the central star is VIb which indicates that there are distinct hot and cold components of circumstellar dust and that the mass loss process may have temporarily abated. Therefore, it is proposed that the object is in the post main sequence stage of evolution and is a protoplanetary nebulae. Young protoplanetary nebulae have totally obscured central stars illuminating reflective lobes whereas older ones such as M2-9 have lobes seen in emission from gas ionized by the central hot star which is clearly visible. Since the central object of IRAS07131-0147 is a relatively unobscured late type star and the lobes are seen only by reflection, it is suggested that this nebula is a protoplanetary nebula in an evolutionary stage intermediate between that of CRL2688 and M2-9. Author

N91-15032*# National Aeronautics and Space Administration. Goddard Space Flight Center, Greenbelt, MD.

INFRARED EMISSION FROM THE SUPERNOVA REMNANT PUPPIS A: DUST AND GAS PARAMETERS **c90**

Richard G. Arendt (Illinois Univ., Urbana.), Eli Dwek, and R Petre *In* NASA, Ames Research Center, Interstellar Dust: Contributed Papers Dec. 1989 p 543-548 (For primary document see N91-14897 06-88)

Avail: NTIS HC/MF A22 CSCL 03B

The infrared (IR) spectra of collisionally heated dust at several regions across the supernova remnant (SNR) Puppis A were modelled. Through the comparison of the actual and model spectra, the possible range of gas density and temperature within these

areas was narrowed down. From the models, information on the minimum and maximum dust grain sizes and the amount of sputtering which has occurred was found. Finally the mass of gas and dust, the IR luminosity, the effective thickness, and the length of time since the dust was swept up by the SNR were derived for these regions. Author

N91-15033*# National Aeronautics and Space Administration. Goddard Space Flight Center, Greenbelt, MD.
ON THE DETECTABILITY OF INFRARED ECHO ARCS AROUND SUPERNOVA 1987A c89
James E. Felten and Eli Dwek *In* NASA, Ames Research Center, Interstellar Dust: Contributed Papers Dec. 1989 p 549-552 (For primary document see N91-14897 06-88)
Avail: NTIS HC/MF A22 CSCL 03A

The ring-like interstellar visual echoes of radii 33 and 54 arcsec detected around SN 1987A should coincide with infrared echoes (thermal reradiation) from dust at T approximately equal to 15 to 30 K. Whether these infrared echoes are detectable at present is considered. They will be brightest at approximately 100 microns, the range of the Texas infrared photometer. Detectability depends on the ratio zeta congruent to tan(sub a)/tan(sub s)P(theta), where tan(sub a) and tan(sub s) are the visual absorption and scattering optical thicknesses of the echo layer, and P is the phase function function for small-angle scattering (theta approximately equal to 2 to 4 degrees). Zeta approximately greater than 1 is needed for a detectable signal (approximately 0.3 Jy), but zeta cannot be much less than 1; otherwise the visual echoes could not be as bright as they are. Typical dust mixtures of Mathis-Rumpl-Nordsieck type have zeta much less than 1. Zeta remains small even if a population of very small grains with power-law index as steep as approximately 5.5 is added. A population with even more small grains and/or fewer large grains could have a zeta similar to 1 and be detectable at present, but this seems unlikely. The echoes will move, but should remain accessible for many years and should be detected eventually. Author

N91-15034*# National Aeronautics and Space Administration, Washington, DC.
A BIBLIOGRAPHY OF PLANETARY GEOLOGY AND GEOPHYSICS PRINCIPAL INVESTIGATORS AND THEIR ASSOCIATES, 1989-1990
Dec. 1990 54 p
(NASA-TM-4221; NAS 1.15:4221) Avail: NTIS HC/MF A04 CSCL 03C

This is a compilation of selected bibliographic data specifically relating to recent publications submitted by principle investigators and their associates, supported through the NASA Office of Space Science and Applications, Solar System Exploration Division, Planetary Geology and Geophysics Program. Author

89 ASTRONOMY

Includes radio, gamma-ray, and infrared astronomy, and astrometry.

N91-15035# Nautical Almanac Office, Washington, DC.
ASTRONOMICAL PHENOMENA FOR THE YEAR 1990
1988 76 p Prepared in cooperation with Royal Greenwich Observatory, Cambridge, England
Avail: NTIS HC/MF A05

This publication contains information extracted from the Astronomical Almanac for the Year 1990. Dates and times of planetary and lunar phenomena and other astronomical data of general interest are presented. M.G.

N91-15036# Nautical Almanac Office, Washington, DC.
THE AIR ALMANAC, 1990
1989 907 p Prepared in cooperation with Royal Greenwich Observatory, Cambridge, England
Avail: NTIS HC/MF A99

The object of this almanac is to provide, in convenient form, the astronomical data required for air navigation. Ephemeris data for the year are presented along with auxiliary tables and graphs, and a brief explanation of the use of the volume. Data for each day are provided for the Sun, Aries, planets, and Moon. The magnitudes, sidereal hour angles, and declinations of 57 reference stars are also given. M.G.

N91-15037# Naval Observatory, Washington, DC.
THE AIR ALMANAC, 1989
1989 907 p Prepared in cooperation with Royal Greenwich Observatory, Cambridge, England
Avail: NTIS HC/MF A99

The object of this almanac is to provide, in convenient form, the astronomical data required for air navigation. Ephemeris data for the year are presented along with auxiliary tables and graphs, and a brief explanation of the use of the volume. Data for each day are provided for the Sun, Aries, planets, and Moon. Data for 57 reference stars are also given. M.G.

N91-15038# Nautical Almanac Office, Washington, DC.
THE ASTRONOMICAL ALMANAC FOR THE YEAR 1989
1989 546 p Prepared in cooperation with Science Research Council, London, England
(ISBN-0-11-886932-9) Avail: NTIS HC/MF A23

Ephemerides and other astronomical data are presented along with information related to various astronomical phenomena, time scales and coordinate systems. M.G.

N91-15039# Nautical Almanac Office, Washington, DC.
THE ASTRONOMICAL ALMANAC FOR THE YEAR 1990
1990 548 p Prepared in cooperation with Science Research Council, London, England
(ISBN-0-11-886934-5) Avail: NTIS HC/MF A23; also available SOD HC $23.00 as 008-054-00129-7

Ephemerides and other astronomical data are presented along with information related to various astronomical and geophysical phenomena, time scales, and coordinate systems. M.G.

N91-15040*# National Aeronautics and Space Administration. Ames Research Center, Moffett Field, CA.
WIND TUNNEL STUDY OF AN OBSERVATORY DOME WITH A CIRCULAR APERTURE
Gregory G. Zilliac and Ethan W. Cliffton (Monoptec Corp., San Francisco, CA.) Nov. 1990 18 p
(NASA-TM-102888; A-91019; NAS 1.15:102888) Avail: NTIS HC/MF A03 CSCL 03A

Results of a wind tunnel test of a new concept in observatory dome design, the Fixed Shutter Dome are presented. From an aerodynamic standpoint, the new dome configuration is similar in overall shape to conventional observatory domes, with the exception of the telescope viewing aperture. The new design consists of a circular aperture of reduced area in contrast to conventional domes with rectangular or slotted openings. Wind tunnel results of a side-by-side comparison of the new dome with a conventional dome demonstrate that the mean and fluctuating velocity through the aperture and in the center of the new dome configuration are lower than those of conventional domes, thus reducing the likelihood of telescope flow-induced vibration. Author

N91-15041# Massachusetts Inst. of Tech., Lexington. Lincoln Lab.
A PROPOSED ASTRONOMICAL REFERENCE CATALOG OF INFRARED SOURCES
J. M. Sorvari 6 Aug. 1990 57 p
(Contract F19628-90-C-0002)
(AD-A226757; TR-884; ESD-TR-90-085) Avail: NTIS HC/MF A04 CSCL 03/1

Data requirements are derived for stellar infrared spectra to be used for calibration reference in a generalized, defense-related program. A program to create such a data set is outlined. The data set would be usable by a variety of users and would both

simplify the calibration process and facilitate program-to-program comparisons. GRA

N91-14899*# Wisconsin Univ., Madison. Dept. of Astronomy.
THE RELATIONSHIP BETWEEN IR, OPTICAL, AND UV EXTINCTION
Jason A. Cardelli, Geoffrey C. Clayton, and John S. Mathis *In* NASA, Ames Research Center, Interstellar Dust: Contributed Papers Dec. 1989 p 5-10 (For primary document see N91-14897 06-88)
Avail: NTIS HC/MF A22 CSCL 03A

N91-14900*# University Coll., London (England). Dept. of Physics and Astronomy.
THE DETECTION OF A BROAD INTERSTELLAR EXTINCTION FEATURE NEAR 1700 A
David J. Carnochan *In* NASA, Ames Research Center, Interstellar Dust: Contributed Papers Dec. 1989 p 11-16 (For primary document see N91-14897 06-88)
Avail: NTIS HC/MF A22 CSCL 03A

N91-14909*# California Univ., Berkeley. Space Sciences Lab.
NEW MEASUREMENTS OF THE FAR ULTRAVIOLET SCATTERING PROPERTIES OF INTERSTELLAR DUST Abstract Only
Mark Hurwitz, Stuart Bowyer, and Christopher Martin *In* NASA, Ames Research Center, Interstellar Dust: Contributed Papers Dec. 1989 p 47 (For primary document see N91-14897 06-88)
(Grants NGR-05-003-805; NGT-50185)
Avail: NTIS HC/MF A22 CSCL 03B

N91-14913*# National Aeronautics and Space Administration. Goddard Space Flight Center, Greenbelt, MD.
THE CAPABILITY OF THE ULTRAVIOLET IMAGING TELESCOPE FOR OBSERVING INTERSTELLAR DUST Abstract Only
Theodore P. Stecher *In* NASA, Ames Research Center, Interstellar Dust: Contributed Papers Dec. 1989 p 59 (For primary document see N91-14897 06-88)
Avail: NTIS HC/MF A22 CSCL 03A

N91-14914*# Applied Research Corp., Landover, MD.
DIFFUSE GALACTIC LIGHT OBSERVATIONS AT 206 SELECTED AREAS
Gary N. Toller *In* NASA, Ames Research Center, Interstellar Dust: Contributed Papers Dec. 1989 p 61-65 (For primary document see N91-14897 06-88)
Avail: NTIS HC/MF A22 CSCL 03A

N91-14917*# Texas Univ., Austin. Dept. of Astronomy.
HIGH RESOLUTION SPECTROSCOPY OF THE 11.3 MICRON EMISSION BAND Abstract Only
Jeff M. Achtermann, J. H. Lacy, and D. E. Bruce *In* NASA, Ames Research Center, Interstellar Dust: Contributed Papers Dec. 1989 p 85 (For primary document see N91-14897 06-88)
Avail: NTIS HC/MF A22 CSCL 03A

N91-14918*# National Aeronautics and Space Administration. Ames Research Center, Moffett Field, CA.
INFRARED IMAGES OF REFLECTION NEBULAE AND ORION'S BAR: FLUORESCENT MOLECULAR HYDROGEN AND THE 3.3 MICRON FEATURE
Michael G. Burton, Alan Moorhouse, P. W. J. L. Brand, Patrick F. Roche, and T. R. Geballe (Joint Astronomy Centre, Hilo, HI.) *In its* Interstellar Dust: Contributed Papers Dec. 1989 p 87-92 (For primary document see N91-14897 06-88)
Avail: NTIS HC/MF A22 CSCL 03A

N91-14919*# National Aeronautics and Space Administration. Ames Research Center, Moffett Field, CA.
AIRBORNE OBSERVATIONS OF THE INFRARED EMISSION BANDS Abstract Only
M. Cohen, Diane Wooden, Alexander G. G. M. Tielens, Jesse D. Bregman, Fred C. Witteborn, D. Rank, and Louis J. Allamandola *In its* Interstellar Dust: Contributed Papers Dec. 1989 p 93 (For primary document see N91-14897 06-88)
Avail: NTIS HC/MF A22 CSCL 03A

N91-14922*# National Aeronautics and Space Administration. Ames Research Center, Moffett Field, CA.
SPATIAL VARIATIONS OF THE 3 MICRON EMISSION FEATURES WITHIN NEBULAE Abstract Only
Alan Moorhouse, T. R. Geballe (Joint Astronomy Centre, Hilo, HI.), and Louis J. Allamandola *In its* Interstellar Dust: Contributed Papers Dec. 1989 p 10 (For primary document see N91-14897 06-88)
Avail: NTIS HC/MF A22 CSCL 03A

N91-14923*# Durham Univ. (England). Dept. of Physics.
THE WAVELENGTH DEPENDENCE OF POLARIZATION IN NGC 2023
C. D. Rolph and S. M. Scarrott *In* NASA, Ames Research Center, Interstellar Dust: Contributed Papers Dec. 1989 p 109-110 (For primary document see N91-14897 06-88)
Avail: NTIS HC/MF A22 CSCL 03A

N91-14925*# Hawaii Univ., Honolulu. Inst. for Astronomy.
HIGH-SPECTRAL RESOLUTION OBSERVATIONS OF THE 3.29 MICRON EMISSION FEATURE: COMPARISON TO QCC AND PAHS
Alan T. Tokunaga, Kris Sellgren, Akira Sakata, S. Wada, Takashi Onaka, Y. Nakada, and T. Nagata (Kyoto Univ., Japan) *In* NASA, Ames Research Center, Interstellar Dust: Contributed Papers Dec. 1989 p 115-118 (For primary document see N91-14897 06-88)
Avail: NTIS HC/MF A22 CSCL 03A

N91-14931*# National Aeronautics and Space Administration. Ames Research Center, Moffett Field, CA.
THE SPATIAL DISTRIBUTION OF INFRARED RADIATION FROM VISIBLE REFLECTION NEBULAE
Ling Luan, Michael W. Werner, Eli Dwek, and Kris Sellgren (Hawaii Univ., Honolulu.) *In its* Interstellar Dust: Contributed Papers Dec. 1989 p 135-140 (For primary document see N91-14897 06-88)
(Contract NCA2-269)
Avail: NTIS HC/MF A22 CSCL 03A

N91-14932*# Centre National de la Recherche Scientifique, Verrieres-Le Buisson (France). Lab. de Physique Stellaire et Planetaire.
INFLUENCE OF TEMPERATURE ON THE INFRARED SPECTRUM OF THE CORONENE MOLECULE
Jean-Phillipe Bernard, Louis B. DHendecourt, and Alain Leger (Paris VII Univ., France) *In* NASA, Ames Research Center, Interstellar Dust: Contributed Papers Dec. 1989 p 143-148 Previously announced in IAA as A89-53607 (For primary document see N91-14897 06-88)
Avail: NTIS HC/MF A22 CSCL 03A

N91-14948*# Indian Inst. of Astrophysics, Bangalore.
ADDITIONAL RED AND REDDENED STARS IN CYG OB2 ASSOCIATION
M. Parthasarathy and S. K. Jain *In* NASA, Ames Research Center, Interstellar Dust: Contributed Papers Dec. 1989 p 211-217 (For primary document see N91-14897 06-88)
Avail: NTIS HC/MF A22 CSCL 03B

N91-14950*# California Univ., Berkeley. Radio Astronomy Lab.
INTERFEROMETRIC MOLECULAR LINE OBSERVATIONS OF W51
Alexander Rudolph, William J. Welch, Patrick Palmer, and Berengere Dubrulle (Ecole Normale Superieure, Paris, France) *In* NASA, Ames Research Center, Interstellar Dust: Contributed Papers Dec. 1989 p 221-226 (For primary document see N91-14897 06-88)
Avail: NTIS HC/MF A22 CSCL 03A

N91-14952*# Kyoto Univ. (Japan).
A TWO MICRON POLARIZATION SURVEY TOWARD DARK CLOUDS
M. Tamura, S. Sato, I. Gatley, and J. H. Hough (Hatfield Polytechnic, England) *In* NASA, Ames Research Center, Interstellar Dust: Contributed Papers Dec. 1989 p 233-234 (For primary document see N91-14897 06-88)
Avail: NTIS HC/MF A22 CSCL 03A

N91-14953*# California Inst. of Tech., Pasadena.
IRAS RESULTS ON OUTER GALAXY STAR FORMATION Abstract Only
Susan Terebey and Michel Fich (Waterloo Univ., Ontario) *In* NASA, Ames Research Center, Interstellar Dust: Contributed Papers Dec. 1989 p 235 (For primary document see N91-14897 06-88)
Avail: NTIS HC/MF A22 CSCL 03A

N91-14954*# Max-Planck-Inst. fuer Radioastronomie, Bonn (Germany, F.R.).
HIGH RESOLUTION OBSERVATIONS OF COMPACT H II REGIONS AT 230 GHz
Joern-E. Wink (Institut de Radio Astronomie Millimetrique, Grenoble, France), P. G. Mezger, and R. Zylka *In* NASA, Ames Research Center, Interstellar Dust: Contributed Papers Dec. 1989 p 237-238 (For primary document see N91-14897 06-88)
Avail: NTIS HC/MF A22 CSCL 03A

N91-14955*# Bandung Inst. of Tech. (Indonesia). Dept. of Astronomy.
SURVEY OBSERVATIONS OF EMISSION-LINE STARS IN THE ORION REGION Abstract Only
Suhardja D. Wiramihardja, T. Kogure, S. Yoshida, K. Ogura, and M. Nakano (Oita Univ., Japan) *In* NASA, Ames Research Center, Interstellar Dust: Contributed Papers Dec. 1989 p 239 (For primary document see N91-14897 06-88)
Avail: NTIS HC/MF A22 CSCL 03A

N91-14958*# Hawaii Univ., Honolulu. Inst. for Astronomy.
DISTRIBUTION OF THE 3.1 MICRON FEATURE IN CEPHEUS A
Klaus-Werner Hodapp and Carlos Eiroa (Observatorio Astronomico Nacional, Madrid, Spain) *In* NASA, Ames Research Center, Interstellar Dust: Contributed Papers Dec. 1989 p 247-248 (For primary document see N91-14897 06-88)
Avail: NTIS HC/MF A22 CSCL 03A

N91-14976*# California Univ., Berkeley. Dept. of Physics.
A ROCKET-BORNE MEASUREMENT OF INTERSTELLAR DUST EMISSION AT HIGH GALACTIC LATITUDE
Andrew E. Lange, D. Alsop, S. Hayakawa, T. Matsumoto, H. Matsuo, H. Murakami, Paul L. Richards, and S. Sato (Nagasaki Univ., Japan) *In* NASA, Ames Research Center, Interstellar Dust: Contributed Papers Dec. 1989 p 303-305 Sponsored by Japan Society for the Promotion of Science, Tokyo; NSF; Ministry of Education, Science and Culture, Sagamihara, Japan; and California Space Inst. (For primary document see N91-14897 06-88)
(Grant NGL-05-003-497)
Avail: NTIS HC/MF A22 CSCL 03A

N91-14986*# Sao Paulo Univ. (Brazil). Inst. Astronomico de e Geofisico.
MULTICOLOR OPTICAL POLARIMETRY OF REDDENED STARS IN THE SMALL MAGELLANIC CLOUD
Antonio M. Magalhaes, G. V. Coyne, Valero Piirola (Helsinki Univ., Finland), and C. V. Rodrigues *In* NASA, Ames Research Center, Interstellar Dust: Contributed Papers Dec. 1989 p 347-352 Sponsored in part by International Astronomical Union and Fundacao de Amparo a pesquisa do Estado de Sao Paulo (For primary document see N91-14897 06-88)
Avail: NTIS HC/MF A22 CSCL 03A

N91-14987*# National Aeronautics and Space Administration. Goddard Space Flight Center, Greenbelt, MD.
ON THE ORIGIN OF EXTINCTION IN THE COMA CLUSTER OF GALAXIES
Y. Rephaeli (California Univ., La Jolla.), Eli Dwek, and John C. Mather *In* NASA, Ames Research Center, Interstellar Dust: Contributed Papers Dec. 1989 p 353-356 (For primary document see N91-14897 06-88)
Avail: NTIS HC/MF A22 CSCL 03A

N91-14990*# Lecce Univ. (Italy). Dept. of Physics.
VUV-VISIBLE MEASUREMENTS ON DIFFERENT SAMPLES OF AMORPHOUS CARBON
A. Blanco, A. Borghesi, E. Bussoletti, Luigi Colangeli, Sergio Fonti, H. E. Gumlich, Ch. Jung, Vincenso Orofino, and G. Schwehm (European Space Agency. European Space Research and Technology Center, ESTEC, Noordwijk, Netherlands) *In* NASA, Ames Research Center, Interstellar Dust: Contributed Papers Dec. 1989 p 363-368 (For primary document see N91-14897 06-88)
Avail: NTIS HC/MF A22 CSCL 03A

N91-14996*# Aerospace Corp., Los Angeles, CA. Space Sciences Lab.
OBSERVATIONAL CONSTRAINTS ON INTERSTELLAR DUST MODELS
James H. Hecht, James A. Hackwell, and Ray W. Russell *In* NASA, Ames Research Center, Interstellar Dust: Contributed Papers Dec. 1989 p 391-393 (For primary document see N91-14897 06-88)
Avail: NTIS HC/MF A22 CSCL 03A

N91-15013*# California Univ., Berkeley. Dept. of Astronomy.
INFRARED EMISSION FROM INTERPLANETARY DUST
William T. Reach *In* NASA, Ames Research Center, Interstellar Dust: Contributed Papers Dec. 1989 p 469-470 (For primary document see N91-14897 06-88)
Avail: NTIS HC/MF A22 CSCL 03A

N91-15019*# Lecce Univ. (Italy). Dept. of Physics.
IR EMISSION FROM CIRCUMSTELLAR ENVELOPES OF C-RICH STARS
A. Blanco, A. Borghesi, E. Bussoletti, Luigi Colangeli (European Space Agency. European Space Research and Technology Center, ESTEC, Noordwijk, Netherlands), Sergio Fonti, and Vincenso Orofino *In* NASA, Ames Research Center, Interstellar Dust: Contributed Papers Dec. 1989 p 505-506 (For primary document see N91-14897 06-88)
Avail: NTIS HC/MF A22 CSCL 03A

N91-15021*# Rensselaer Polytechnic Inst., Troy, NY.
USING INFRARED SPECTRAL FEATURES TO PROBE CIRCUMSTELLAR DUST SHELLS AROUND COOL STARS
Michael P. Egan and Chun Ming Leung *In* NASA, Ames Research Center, Interstellar Dust: Contributed Papers Dec. 1989 p 515-516 (For primary document see N91-14897 06-88)
(Grant NAGw-1103)
Avail: NTIS HC/MF A22 CSCL 03A

N91-15028*# Colorado Univ., Boulder. Center for Astrophysics and Space Astronomy.
CIRCUMSTELLAR GRAIN EXTINCTION PROPERTIES OF RECENTLY DISCOVERED POST AGB STARS
Richard H. Buss, Jr., Henny J. G. L. M. Lamers (Space Research Organization Netherlands, Utrecht.), and Theodore P. Snow, Jr. *In* NASA, Ames Research Center, Interstellar Dust: Contributed Papers Dec. 1989 p 533-534 (For primary document see N91-14897 06-88)
Avail: NTIS HC/MF A22 CSCL 03A

N91-15033*# National Aeronautics and Space Administration. Goddard Space Flight Center, Greenbelt, MD.
ON THE DETECTABILITY OF INFRARED ECHO ARCS AROUND SUPERNOVA 1987A

James E. Felten and Eli Dwek *In* NASA, Ames Research Center, Interstellar Dust: Contributed Papers Dec. 1989 p 549-552 (For primary document see N91-14897 06-88)
Avail: NTIS HC/MF A22 CSCL 03A

N91-15103# Sternberg Astronomical Inst., Moscow (USSR).
THE OPTICAL OBSERVATIONS OF X RAY NOVA GS2023+33 = V404 CYG
O. A. Osminkina, E. Yu. Osminkin, N. I. Shakura, and S. Yu. Shugarov *In* ESA, Plasma Astrophysics Aug. 1990 p 301-302 (For primary document see N91-15046 06-90)
Copyright Avail: NTIS HC/MF A14

90 ASTROPHYSICS

Includes cosmology; celestial mechanics; space plasmas; and interstellar and interplanetary gases and dust.
For related information see also *75 Plasma Physics*.

N91-15042 Illinois Univ., Urbana-Champaign.
AN INTERFEROMETRIC STUDY OF MOLECULAR EMISSION AROUND NGC 7538 AT MILLIMETER WAVELENGTHS Ph.D. Thesis
Preethi Pratap 1990 172 p
Avail: Univ. Microfilms Order No. DA9026296

NGC 7538 is a visible H II region with an associated molecular cloud, situated in the Perseus arm of the Galaxy. A group of infrared sources, IRS 1, IRS 2, and IRS 3, is situated at the interface between the molecular cloud and the visible nebula. Maser emission from OH, H2O, H2CO, CH3OH, and NH3 were detected toward IRS 1. In order to examine the model for the excitation of the formaldehyde (H2CO) maser, proposed by Boland and de Jong (1981), interferometric observations of the cloud around IRS 1 have been made in the J = 1-0 transitions of HCN, HCO(+), and (13)CO. The HCN and HCO(+) maps show the presence of a cavity around IRS 1 which is not seen in the (13)CO maps. Since HCN and HCO(+) trace densities greater than 10(exp 5)cm(exp -3), the cavity indicates a lack of high density material around the H II region. Continuum observations at 88 GHz and 110 GHz result in a 2-component model for the H II region. There is a cool, extended component toward which all the masers are seen. The parameters calculated for this component, along with the H2 densities from the molecular observations, were put into the H2CO master model. The results show that the H2CO gas must be at a distance of 0.011 pc from the H II region for maximum inversion in the H2CO transition and the abundance of H2CO relative to H2 must be approximately 4x10(exp -7). The molecular observations also show that the molecular cloud is extremely clumpy. These clumps around IRS 1 could provide the varying densities required for the other masers observed in the region. The HCO(+) results also indicate the presence of a high density molecular outflow which originates about 15 sec south of IRS 1. The position angle of the outflow agrees with that of a CO outflow detected toward this source. The results imply that there may be another source powering the outflow which is situated south of IRS 1. Dissert. Abstr.

N91-15043 California Univ., Berkeley.
CONTINUUM RADIATIVE TRANSFER IN ACCRETION-POWERED PULSARS Ph.D. Thesis
David James Burnard 1989 194 p
Avail: Univ. Microfilms Order No. DA9028763

A new technique is described for studying the flow of radiation through one dimensional slabs of the strongly magnetized thermal plasma in the polar regions of accreting, magnetized neutron stars. This method allows rapid computation of one dimensional atmospheres with arbitrary orientation of the magnetic field, as well as arbitrary inhomogeneity. The effects of coherent and incoherent scattering in the continuum, bremsstrahlung emission and absorption, and a net continuum emissivity from the cyclotron line are included. Comptonization is assumed to be important only in regions where the radiation field is almost isotropic. This solution technique was applied to an analytical model of the accretion flow near the polar caps of the neutron stars. It is demonstrated how the emission from such an accretion mound model can be computed from a series of one dimensional slabs of non-uniform material. It is concluded that single models are inadequate for representing all but the lowest luminosity x ray pulsars. Author

N91-15044*# Arizona Univ., Tucson.
A STUDY OF EXTENDED ZODIACAL STRUCTURES Final Report, 15 Aug. 1989 - 14 Aug. 1990
Mark V. Sykes 1990 14 p
(Grant NAG5-1236)
(NASA-CR-187687; NAS 1.26:187687) Avail: NTIS HC/MF A03 CSCL 03B

Observations of cometary dust trails and zodiacal dust bands, discovered by the Infrared Astronomical Satellite (IRAS) were analyzed in a continuing effort to understand their nature and relationship to comets, asteroids, and processes effecting those bodies. A survey of all trails observed by IRAS has been completed, and analysis of this phenomenon continues. A total of 8 trails have been associated with known short-period comets (Churyumov-Gerasimenko, Encke, Gunn, Kopff, Pons-Winnecke, Schwassmann-Wachmann 1, Tempel 1, and Tempel 2), and a few faint trails have been detected which are not associated with any known comet. It is inferred that all short-period comets may have trails, and that the trails detected were seen as a consequence of observational selection effects. Were IRAS launched today, it would likely observe a largely different set of trails. The Tempel 2 trail exhibits a small but significant excess in color temperature relative to a blackbody at the same heliocentric distance. This excess may be due to the presence of a population of small, low-beta particles deriving from large particles within the trail, or a temperature gradient over the surface of large trail particles. Trails represent the very first stage in the formation and evolution of a meteor stream, and may also be the primary mechanism by which comets contribute to the interplanetary dust complex. A mathematical model of the spatial distribution of orbitally evolved collisional debris was developed which reproduces the zodiacal dust band phenomena and was used in the analysis of dust band observations made by IRAS. This has resulted in the principal zodiacal dust bands being firmly related to the principal Hirayama asteroid families. In addition, evidence for the collisional diffusion of the orbital elements of the dust particles has been found in the case of dust generated in the Eos asteroid family. Author

N91-15045*# Institute for Scientific Research, Lexington, MA.
THEORETICAL STUDIES OF IMPORTANT PROCESSES IN PLANETARY AND COMET ATMOSPHERES Semiannual Status Report
Steven L. Guberman 1990 19 p
(Grants NAGw-1404; NAGw-496)
(NASA-CR-187692; NAS 1.26:187692) Avail: NTIS HC/MF A03 CSCL 03B

Dissociative recombination (DR) reactions in planetary and comet atmospheres are discussed. A computer program was developed which determines DR cross sections and rates using potential curves and electronic capture widths. It uses Multi-Channel Quantum Defect Theory (MQDT) to include excited Rydberg resonance levels in the DR cross section and rate calculations. Each vibrational level of a molecular ion is the limit for an infinite series of Rydberg states. Above each ion vibrational level are Rydberg vibrational levels having higher ion levels as their series limit. These Rydberg vibrational levels are resonances, i.e., neutral states which are imbedded in the electron-molecular ion continuum. The process in which the Rydberg level causes an abrupt perturbation in the cross section for DR (because of interference between capture into the Rydberg level and capture into the repulsive dissociative state) is referred to as indirect recombination. The process in which the Rydberg levels are excluded and recombination goes from the entrance channel to the repulsive state is called direct recombination. The full DR process, i.e., both direct and indirect recombination, is the process of importance for

planetary atmospheres. These ideas are illustrated with the new results for DR from excited ion vibrational levels of O2(+) into the dissociative state which leads to O(1S) + O(1D). Y.S.

N91-15046# European Space Agency, Paris (France).
PLASMA ASTROPHYSICS
T. Duc Guyenne, ed. and James J. Hunt, ed. Aug. 1990 321 p A joint Varenna-Abastumani-ESA-Nagoya-Potsdam workshop held in Telavi, USSR, 4-12 Jun. 1990; sponsored in cooperation by International School of Plasma Physics, Abastumani Astrophysical Observatory, Academy of Sciences (USSR), Moscow, ESA, Nagoya Univ., and Academy of Sciences, Potsdam, German D.R.
(ESA-SP-311; ISBN-92-9092-086-6; ISSN-0879-6566;
ETN-91-98344) Copyright Avail: NTIS HC/MF A14

Studies in plasma astrophysics are presented. The Sun and heliosphere were addressed, including solar flux tubes, flare acceleration, spicules and coronal loops. Planetary magnetospheres and cometary plasmas were studied. Bow shock, cosmic ray acceleration and plasma effects were addressed. Numerical and laboratory simulation was reported. Astrophysics studies included black holes, pulsars, accretion, compact objects, jets, x ray, gamma ray, and star evolution. Supernova 1987A studies were included. For individual titles, see N91-15047 through N91-15110.

N91-15047# European Space Agency. European Space Research and Technology Center, ESTEC, Noordwijk (Netherlands). Dept. of Space Science.
SOLAR MAGNETIC FLUX-TUBES AND CORONAL LOOPS **c92**
B. H. Foing *In its* Plasma Astrophysics Aug. 1990 p 1-6 (For primary document see N91-15046 06-90)
Copyright Avail: NTIS HC/MF A14

High resolution observations show that the solar magnetic field is structured in flux-tubes from the photosphere to the corona. These tubes can be diagnosed with EUV images such as those obtained with the transition region camera rocket experiment in Ly alpha or in different continua. Constraints on flux-tube models are presented. Observations of loops in the corona show the confining role of the magnetic field, but also the coexistence of plasmas at different temperatures. Relevant diagnosis and models of coronal loops are discussed. The study of these magnetic structures on the Sun, considered as a plasma laboratory, is of interest for stellar magnetic fields and coronae and in other astrophysical contexts. For discriminating between different processes at work in flux-tubes and coronal loops, the expected contribution of the SOHO observatory and of the SIMURIS interferometric project under study for ultrahigh resolution, is stressed. ESA

N91-15048# Toyama Univ. (Japan). Dept. of Applied Maths and Physics.
HIGH-ENERGY PARTICLE ACCELERATION DURING THE IMPLOSION DRIVEN BY 3-DIMENSIONAL X-TYPE CURRENT LOOP COALESCENCE IN SOLAR FLARES **c92**
Jun-Ichi Sakai *In* ESA, Plasma Astrophysics Aug. 1990 p 7-12 (For primary document see N91-15046 06-90)
Copyright Avail: NTIS HC/MF A14

A model for high energy solar flares is presented to explain prompt proton and electron acceleration within one second to relativistic energies. It is shown that both protons and electrons can be promptly (within than one second) accelerated to approximately 100 GeV and approximately 100 MeV, respectively during the implosion driven by a three dimensional X-type current loop coalescence. The fact that a well developed high energy flare has three phases of particle acceleration is accentuated. The present acceleration mechanism can explain the first phase. ESA

N91-15049# Nagoya Univ. (Japan). Plasma Science Center.
SOLAR FLARES AND PARTICLE ACCELERATION **c92**
Y. Ohsawa and Y. Terashima *In* ESA, Plasma Astrophysics Aug. 1990 p 13-19 (For primary document see N91-15046 06-90)
Copyright Avail: NTIS HC/MF A14

Observations of rapid particle acceleration in solar flares are reviewed. The theory and simulation of ion acceleration in a large amplitude magnetosonic wave is described. It is shown that relativistic protons can be produced in a time much shorter than one second, if large amplitude magnetosonic waves are excited in coronal magnetic tubes in association with solar flares. Those protons can have very hard energy spectrum. The energy spectra of gamma rays generated through the decay of neutral pions are discussed. ESA

N91-15050# Academy of Pedagogical Sciences of the USSR, Moscow. Dept. of Physics.
A NEW KIND OF MAGNETIC BUOYANCY INSTABILITY **c75**
N. I. Kleeorin and I. V. Rogachevskii (Academy of Sciences, USSR, Troitsk) *In* ESA, Plasma Astrophysics Aug. 1990 p 21-23 (For primary document see N91-15046 06-90)
Copyright Avail: NTIS HC/MF A14

The quantitative theory of a new type of magnetic buoyancy instability is presented. This instability is connected with the large scale magnetic force reversal in plasma with fully developed magnetohydrodynamic turbulence. The energy of the instability is provided by fine scale fluctuations. Isothermal plasma for beta much greater than 1 is considered, beta being the ratio of the plasma pressure to the pressure of the large scale magnetic field. ESA

N91-15051# Abastumani Astrophysical Observatory, Georgia (USSR).
A NEW MODEL OF SPICULE FORMATION IN THE SUN CHROMOSPHERE **c92**
A. D. Pataraya, A. L. Taktakishvili, and B. B. Chargeishvili *In* ESA, Plasma Astrophysics Aug. 1990 p 25-27 (For primary document see N91-15046 06-90)
Copyright Avail: NTIS HC/MF A14

The physical processes occurring in the supergranule boundary cylinder layer are investigated. Taking into account the Coriolis force an expression for the phi component of the magnetic field and velocity are obtained. The estimated number of the spicules coming on each supergranule cell depends on the solar latitude theta. The time scale of the formation and the coalescence of the magnetic tubes is of the order of the observed life time of the spicules. ESA

N91-15052# Kharkov State Univ. (USSR).
NONLINEAR SURFACE MHD WAVES IN THE INHOMOGENEOUS PLASMA WITH CUSP-RESONANCE IN UPPER SOLAR ATMOSPHERE **c92**
E. A. Fedutenko, V. I. Lapshin, and K. N. Stepanov *In* ESA, Plasma Astrophysics Aug. 1990 p 29-32 (For primary document see N91-15046 06-90)
Copyright Avail: NTIS HC/MF A14

The weakly nonlinear surface MHD (magnetohydrodynamic) waves propagation along the plane narrow nonuniform layer is considered. The existence of new type surface waves in the case when cusp velocity has an extremum in this layer is shown. Nonlinear evolution of these surface waves is considered. ESA

N91-15053# Academy of Sciences (USSR), Moscow. Inst. of the Physics of the Earth.
FILAMENTARY STRUCTURES IN THE SUN'S ATMOSPHERE AS SINGULAR ALFVEN WAVES **c92**
N. V. Petviashvili *In* ESA, Plasma Astrophysics Aug. 1990 p 33-34 (For primary document see N91-15046 06-90)
Copyright Avail: NTIS HC/MF A14

A model is proposed which treats filamentary structures observed in the Sun's chromosphere as thin beams of energetic electrons. The structures are corresponded to Alfven waves with filamentary singularity. The set of integro-differential equations describing dynamics of the beams are derived from the ordinary

magnetohydrodynamic equations. Some solutions of this set are obtained. ESA

N91-15054# Abastumani Astrophysical Observatory, Georgia (USSR).
ON SOME PECULIARITIES OF SOLAR DIFFERENTIAL ROTATION **c92**
M. Sh. Gigolashvili and E. V. Khutsishvili *In* ESA, Plasma Astrophysics Aug. 1990 p 35-37 (For primary document see N91-15046 06-90)
Copyright Avail: NTIS HC/MF A14

It is found that for large spots differential rotation effects are more markedly expressed in the solar Northern Hemisphere for uneven cycles (numbers 19, 21) than in the southern one. For an even cycle (number 20) the picture is vice versa. There is no doubt that there is a solid body rotation of large spots in even and uneven cycles of the solar activity alternatively in the Northern and Southern Hemispheres respectively. The asymmetry found in solid body rotation of large solar spots might be a help to solve the question of the solar activity mechanism and explain the essence of the solar differential rotation. ESA

N91-15055# Kharkov State Univ. (USSR).
NONLINEARITY INFLUENCE IN LOCAL RESONANCE REGIONS ON THE ALFVEN WAVES PROPAGATION IN SOLAR CORONA **c92**
V. I. Lapshin, K. N. Stepanov, and V. O. Strasser *In* ESA, Plasma Astrophysics Aug. 1990 p 39-40 (For primary document see N91-15046 06-90)
Copyright Avail: NTIS HC/MF A14

The Alfven wave propagation in the homogeneous solar corona in the presence of local resonance is considered. The striction nonlinearity and effect of the finite ion Larmour radius are taken into account. Results of numerical calculations which illustrated the nonlinear waves conversion in the resonance region are given. ESA

N91-15056# Universidad de Los Andes, Merida (Venezuela). Grupo de Astrofisica.
LINEAR STABILITY AND MHD WAVE PROPAGATION IN PLASMAS WITH SOLAR ABUNDANCES **c92**
M. H. Ibanez and O. B. Escalona *In* ESA, Plasma Astrophysics Aug. 1990 p 41-44 (For primary document see N91-15046 06-90)
Copyright Avail: NTIS HC/MF A14

The local stability and the MHD (magnetohydrodynamic) propagation of linear waves in optically thin plasmas are analyzed. From Hurwitz's criteria the critical wave numbers for unstable disturbances are found. For the wave driven case, a dispersion relation for propagation of thermal and magnetosonic waves were obtained. Analytical conditions for amplification and damping are given for several asymptotic cases. ESA

N91-15057# Universidad de Los Andes, Merida (Venezuela). Facultad de Ciencias.
ON THE THERMAL STABILITY OF SLABS, CYLINDERS, AND SPHERES **c75**
M. H. Ibanez and F. Plachco *In* ESA, Plasma Astrophysics Aug. 1990 p 45-48 (For primary document see N91-15046 06-90)
Copyright Avail: NTIS HC/MF A14

The critical values of slab like, cylindrical and spherical configurations, in which a diffusion mechanism of heat transport is balanced by a source or a sink term, are determined. The heating and loss (radiative) terms as well as the diffusion coefficient are assumed to be local functions of the density and the temperature. The configurations are assumed to be kept within a constant boundary temperature. ESA

N91-15058# Abastumani Astrophysical Observatory, Georgia (USSR).
BURSTS OF ENERGETIC PROTONS IN THE EARTH'S MAGNETOTAIL **c46**
A. L. Taktakishvili and L. M. Zelenyi (Academy of Sciences, USSR, Moscow) *In* ESA, Plasma Astrophysics Aug. 1990 p 51-55 (For primary document see N91-15046 06-90)
Copyright Avail: NTIS HC/MF A14

Initial non zero temperature particle distribution (Maxwellian and kappa) are considered and its influence on the spectrum of the protons accelerated in the vicinity of the magnetic X-line in the course of the explosive tearing mode development in the magnetotail is investigated. The evolution of the temporal structure of the particle bursts are studied and theoretical results are compared with inverse velocity dispersion events observed by the onboard spacecraft instruments. ESA

N91-15059# Ruhr Univ., Bochum (Germany, F.R.). Theoretische Physik IV.
THREE-DIMENSIONAL MAGNETIC RECONNECTION AT THE EARTH'S MAGNETOPAUSE **c46**
A. Otto *In* ESA, Plasma Astrophysics Aug. 1990 p 57-62 Sponsored by DFG (For primary document see N91-15046 06-90)
Copyright Avail: NTIS HC/MF A14

At the dayside magnetopause of planetary magnetospheres Flux Transfer Events (FTEs) seem to play an important role in connection with magnetospheric activity. Using resistive MHD (magnetohydrodynamic) computations the dynamical evolution of a three dimensional magnetic reconnection process is analyzed. A localized magnetic reconnection process develops if a spot of enhanced resistivity appears in a current layer (e.g., due to suitable fluctuations at a boundary of the layer). The three dimensional reconnection process leads to the formation of structures which represent newly interconnected magnetic flux and show basic properties of the FTEs. A comparison with observations shows that many properties like the magnetic field signatures or pressure variations of FTEs are recovered in the simulations. For special initial conditions it is shown that crater like events (or magnetic holes) may also be formed by the considered process. The influence of fast waves in the solar wind on the process is discussed. ESA

N91-15060*# Johns Hopkins Univ., Laurel, MD. Applied Physics Lab.
SOLAR WIND DYNAMIC PRESSURE VARIATIONS: QUANTIFYING THE STATISTICAL MAGNETOSPHERIC RESPONSE
D. G. Sibeck *In* ESA, Plasma Astrophysics Aug. 1990 p 63-68 Sponsored by NASA, Washington (For primary document see N91-15046 06-90)
(Contract N00039-87-C-5301)
Copyright Avail: NTIS HC/MF A14 CSCL 03B

Solar wind dynamic pressure variations are common and have large amplitudes. Existing models for the transient magnetospheric and ionospheric response to the solar wind dynamic pressure variation are quantified. The variations drive large amplitude (approx 1 R sub E) magnetopause motion with velocities of approx. 60 km/s and transient dayside ionospheric flows of 2 km/s which are organized into double convection vortices. Ground magnetometer signatures are more pronounced under the auroral ionosphere, where they reach 60 to 300 nT, and under the equatorial electrojet. A statistical comparison of transient ground magnetometer events seen at a South Pole station and geosynchronous orbit indicates that all but the weakest ground events are associated with clear compressional signatures at the dayside geosynchronous orbit. ESA

N91-15061# Johns Hopkins Univ., Laurel, MD. Applied Physics Lab.
IMPLICATIONS OF MULTIPOINT OBSERVATIONS OF SUBSTORMS IN THE INNER MAGNETOTAIL **c46**
R. E. Lopez *In* ESA, Plasma Astrophysics Aug. 1990 p 69-75 (For primary document see N91-15046 06-90)
Copyright Avail: NTIS HC/MF A14

Two case studies of substorms in the inner magnetotail during which multipoint observations were available were studied. These

events suggest that the disruption of the cross tail current begins relatively close to the Earth and has a radially outward component of expansion. The following phenomenological models for the evolution of substorms are proposed. At substorm onset at portion of the earthward edge of the cross tail current becomes unstable and begins to disrupt. Within the disruption region, plasma is energized and the magnetic fields relaxes to a more dipolar configuration. The disruption and the resulting current wedge spread longitudinally and radially down the tail, corresponding to the longitudinal and poleward expansion of auroral bulge in the ionosphere. As the disruption spreads down the tail it may evolve into a reconnection region that severs a portion of the plasma sheet and produces a plasmoid; however, this need not occur during every substorm. This scenario for the evolution of substorms reconciles recent observations that suggest that the substorm neutral line rarely forms inside 20 R sub E, although current sheet disruption was frequently observed in the neighborhood of 8 R sub E. ESA

N91-15062# Academy of Sciences (USSR), Moscow. Inst. of Space Research.
SOLITARY VORTICES IN THE VICINITY OF COMETS
A. A. Galeev, V. L. Galinsky, and I. Kh. Khabibrakhmanov *In* ESA, Plasma Astrophysics Aug. 1990 p 77-79 (For primary document see N91-15046 06-90)
Copyright Avail: NTIS HC/MF A14

In situ observations of plasma and magnetic fields in the vicinity of comets have shown existence of diamagnetic disturbances of the plasma of high amplitudes. The physical nature of such disturbances is not yet understood. A study which notes that the same observed features have some kinds of nonlinear solitary vortex type disturbances is presented. This type of motion is supported by plasma density, magnetic field or pressure gradients, which provides effective gravity in system. ESA

N91-15063# Academy of Sciences (USSR), Moscow. Inst. of Space Research.
DETECTION OF NONLINEAR FEATURES IN PLASMA AND FIELD MEASUREMENTS BY PROGNOZ-8 **c75**
A. Yu. Sokolov, I. Kh. Khabibrakhmanov, M. M. Kuznetsova, J. Lemaire, M. Roth, J. M. Lesceux, and F. Verheest (Ghent Univ., Belgium) *In* ESA, Plasma Astrophysics Aug. 1990 p 81-85 (For primary document see N91-15046 06-90)
Copyright Avail: NTIS HC/MF A14

An example of high amplitude electric field oscillations detected by PROGNOZ-8 near the magnetopause at very low frequencies ranging down to fractions of Hz is considered. Observations by other spacecraft including ISEE and AMPTE are discussed. High amplitude fluctuations described are connected with the convection of plasmas in transverse electromagnetic fields. An alternative explanation discussed is a solitary nonlinear structure. The detection of charged dust grains is examined. The additional aim of looking for low frequency phenomena, such as Alfven waves is considered. The precise nature of discontinuities or shocks (tangential or rotational), nonlinear waves and vortices could not be inferred. ESA

N91-15064*# Iowa Univ., Iowa City. Dept. of Physics and Astronomy.
PLASMA WAVES ASSOCIATED WITH THE SPACE SHUTTLE **c16**
I. H. Cairns and D. A. Gurnett *In* ESA, Plasma Astrophysics Aug. 1990 p 87-92 (For primary document see N91-15046 06-90)
(Grants NAGw-1488; NAG3-449)
Copyright Avail: NTIS HC/MF A14 CSCL 03B

Water molecules outgassed from the Space Shuttle suffer collisional charge-exchange with ionospheric oxygen ions, thereby forming unstable distributions of pick-up water ions and leading to high levels of plasma waves near the Shuttle. Liouville's equation with a charge-exchange source term is solved for the water ion distribution function as a function of position relative to the Shuttle. The observational characteristics of the near zone Shuttle waves are summarized. A linear theory in which beam like distributions of water ions drive Doppler shifted lower hybrid waves via the modified two stream instability is developed. This theory explains many characteristics of the near zone waves. Further work on the effects of wave nonlinearities and spatial inhomogeneity is required to explain the detailed frequency spectrum of the waves. The observed wave levels apparently satisfy the threshold condition for modulational instability of lower hybrid waves. ESA

N91-15065# Academy of Sciences (USSR), Moscow. Inst. of Space Research.
GRADIENT CATASTROPHE OF THE SUPERSONIC MASS-LOADED MAGNETISED PLASMA FLOW AND THE FORMATION OF BOW SHOCK **c75**
A. A. Galeev and I. Kh. Khabibrakhmanov *In* ESA, Plasma Astrophysics Aug. 1990 p 95-98 (For primary document see N91-15046 06-90)
Copyright Avail: NTIS HC/MF A14

It is shown that the stationary supersonic flow of mass loaded plasma exhibit singular behavior at the point where Mach number of the flow is equal to 2/(gamma-1) (gamma = specific heat ratio), which results in arbitrary amplitude wave steepening at this point, whereas for greater Mach number values small amplitude disturbances are smoothed. So continuous mass loaded plasma flow is possible until the Mach number reduces to M = 2/(gamma-1) during the slowing down of contaminated flow well before the sonic point M = 1, where stationary solution itself shows ordinary sonic peculiarity (stationary velocity spatial gradient goes to infinity). ESA

N91-15066# Academy of Sciences (USSR), Irkutsk. Inst. of Terrestrial Magnetism and Radio Wave Propagation.
A NUMERICAL CALCULATION OF PARAMETERS OF EXPLOSION MHD SHOCK WAVES FROM MODERATE SOLAR FLARES **c92**
S. V. Uralova and A. M. Urolov *In* ESA, Plasma Astrophysics Aug. 1990 p 99-101 (For primary document see N91-15046 06-90)
Copyright Avail: NTIS HC/MF A14

The calculation of parameters of flare shock waves arriving at Earth with moderate or small intensity by the approximation of nonlinear magnetic acoustics of a moving medium is addressed. Relationships of explosion magnetohydrodynamic shock wave damping in this approximation were previously obtained. The solution starts from the model of an undisturbed solar wind and the importance and position of the flare on the solar disk. The explosion shock parameters are calculated along ray tubes corrected by taking into account the nonlinear factor of ray displacement. Results of the calculations are detailed. ESA

N91-15067# Academy of Sciences (USSR), Troitsk. Inst. of Terrestrial Magnetism, Ionosphere, and Radio Wave Propagation.
NONSTATIONARY PROCESSES IN THE FRONT OF HIGH MACH NUMBER COLLISIONLESS QUASIPERPENDICULAR SHOCK: DYNAMICS OF THE ION DISTRIBUTION **c75**
V. V. Krasnoselskikh, V. V. Lobzin, and V. B. Roznov (Academy of Sciences, USSR, Moscow) *In* ESA, Plasma Astrophysics Aug. 1990 p 103-107 (For primary document see N91-15046 06-90)
Copyright Avail: NTIS HC/MF A14

The analysis of structure and spatial and temporal evolution of ion distribution as an important source of information about the dissipative processes in the front of collisionless shock is addressed. Nonstationarity of ion distribution function and kinetic overturning are investigated. From the results obtained it is evident that the magnetic disturbance due to modulation of the main part of ion flow is nonlinear and cannot be calculated with the aid of the given model. It is proven that the nonstationary ion currents in the strong shock generate intense fast magnetosonic waves in the low frequency waves. ESA

N91-15068# Academy of Sciences (USSR), Moscow. Inst. of Space Research.
EVOLUTION OF HIGH AMPLITUDE ALFVEN WAVES NEAR A BOW SHOCK
V. L. Galinsky *In* ESA, Plasma Astrophysics Aug. 1990 p 109-113 (For primary document see N91-15046 06-90)
Copyright Avail: NTIS HC/MF A14

A model based on the derivative nonlinear Shroedinger equation is used to describe high amplitude parallel propagating Alfven and fast magnetosonic waves subjects to nonlinearity and dispersion. The damping mechanisms considered are either model viscosity or ion cyclotron-resonance absorption. This equation was solved numerically and several types of solutions were obtained as functions of the growth rate and dispersion values as well as a type of dissipation. The application of these results to magnetohydrodynamic wave observations upstream of the comet's bow shock is considered. Nevertheless, the question of the stability of steep front solutions seems to be not yet settled. ESA

N91-15069# Academy of Sciences of the Georgian SSR, Tbilisi. Inst. of Physics.
ON THE PRIMARY COSMIC RAY NUCLEI SPECTRA BEHAVIOUR IN THE 10(EXP 16) eV ENERGY REGION c93
T. T. Barnaveli, I. V. Khaldeeva, S. T. Shargelashvili, and N. A. Eristavi *In* ESA, Plasma Astrophysics Aug. 1990 p 115-120 (For primary document see N91-15046 06-90)
Copyright Avail: NTIS HC/MF A14

On the basis of the investigation of muon group parameters, the conclusion is made on existence of the primary cosmic ray nuclei energy spectra cutoff in the energy range approximately greater than 10 to the 16th power eV. As a mechanism responsible for the effect, the destruction of the nuclei of some objects (elementary particles) of interstallar media is proposed. The mass of these particles is approximately less than 30 eV. The possibility of the identification of these objects with the dark matter is discussed. ESA

N91-15070# Kurchatov (I. V.) Inst. of Atomic Energy, Moscow (USSR).
GENERATION OF COSMIC RAYS IN PINCHES c93
B. Troubnikov *In* ESA, Plasma Astrophysics Aug. 1990 p 121-126 (For primary document see N91-15046 06-90)
Copyright Avail: NTIS HC/MF A14

A hypothesis on the birth of galactic cosmic rays in cosmic plasma cylindrical pinches due to the development of neck-type perturbations from which plasma jets are squeezed out is discussed. It is shown that at the moment of neck breaking in such a jet a function of accelerated particle energy-E distribution is formed. The function is of a power type dN/dE-E/s with the index s = 1 + square root of 3 and it actually coincides with the observed value s sub 0 = 2.7, which makes this hypothesis rather likely, taking into account the evidence for electrical currents in cosmic plasma. ESA

N91-15071# Kharkov State Univ. (USSR).
DESCRIPTION OF NONLINEAR EFFECTS IN A RELATIVISTIC PLASMA USING HAMILTONIAN FORMALISM c75
V. V. Gulenko and V. V. Gushchin *In* ESA, Plasma Astrophysics Aug. 1990 p 129-131 (For primary document see N91-15046 06-90)
Copyright Avail: NTIS HC/MF A14

Hamiltonian formalism is introduced to a relavistic many fluid hydrodynamic model of plasma. With its help, a wide circle on nonlinear effects in plasma astrophysics both in electron-ion plasma and in electron-positron are investigated. Relativistic plasma consisting of N sorts of particle, each sort being charaterized by temperature, charge and mass are considered. ESA

N91-15072# Abastumani Astrophysical Observatory, Georgia (USSR).
HYDRODYNAMICS OF COLLISIONLESS RELATIVISTIC PLASMA IN A STRONG MAGNETIC FIELD c75
J. G. Lominadze, J. I. Javakhishvili (Tbilisi State Univ., USSR), and E. G. Tsikarishvili *In* ESA, Plasma Astrophysics Aug. 1990 p 133-137 (For primary document see N91-15046 06-90)
Copyright Avail: NTIS HC/MF A14

The closed set of relativistic hydrodynamical equations describing relativistic strongly magnetized collisionless plasma with an anisotropic pressure tensor is presented. This model is the generalization of Chew, Goldberger, Low theory for the relativistic case. ESA

N91-15073# Academy of Sciences (USSR), Moscow. Inst. of Space Research.
WAVE COLLAPSE AT LOWER HYBRID RESONANCE c75
V. P. Kalinen, R. Z. Sagdeev, V. D. Shapiro, V. I. Shevchenko, G. I. Soloviev, and M. Ashour-Abdalla (California Univ., Los Angeles.) *In* ESA, Plasma Astrophysics Aug. 1990 p 139-145 (For primary document see N91-15046 06-90)
Copyright Avail: NTIS HC/MF A14

Collapse of low hybrid waves is investigated analytically and by a numerical method both in two dimensional and three dimensional cases. The radial and longitudinal structure of the cavity as well as the angular dependence of the electrical field inside the cavity is investigated. The existence of self similar solution describing the growth of electric field amplitude with time and compression of the cavity is proved. Considered also is the relative role in collapse process of low hybrid waves absorption both by ions and electrons. ESA

N91-15074# Abastumani Astrophysical Observatory, Georgia (USSR).
AMPLIFICATION OF ALFVEN WAVES IN FREE SHEAR FLOWS c32
G. D. Chagelishvili, R. G. Chanishvili, L. G. Filipov, T. S. Khristov (Bulgarian Academy of Sciences, Sofia.), and J. G. Lominadze *In* ESA, Plasma Astrophysics Aug. 1990 p 147-152 (For primary document see N91-15046 06-90)
Copyright Avail: NTIS HC/MF A14

The amplification of Alfven waves in free (unlimited) shear flows is investigated. The initial magnetic field is assumed to be uniform and directed along the velocity of unperturbed flow. The shear present in the flow is assumed to be constant and perpendicular to the velocity itself. The amplification of Alfven waves is shown to have unusual character: it occurs in the limited time interval and is stronger when the initial magnetic field is smaller. ESA

N91-15075# Academy of Sciences (USSR), Leningrad. Inst. of Physics and Technology.
MASER CYCLOTRON INSTABILITY IN A PLASMA WITH ANISOTROPIC DISTRIBUTION FUNCTION c75
V. G. Bezchastanov and G. G. Pavlov *In* ESA, Plasma Astrophysics Aug. 1990 p 153-158 (For primary document see N91-15046 06-90)
Copyright Avail: NTIS HC/MF A14

Electron cyclotron absorption and emission, with allowance for the relativistic effects for propagation along the magnetic field in a plasma with arbitrary refraction index N and anisotropic distribution function of electrons is investigated. This question seems to be important for two reasons: the maser instability is known to arise in nonrelativistic plasmas with anisotropic temperature; accurate allowance for the relativistic effects (which is important even for nonrelativistic plasmas) leads to the conclusion that the negative absorption is strictly forbidden for any distribution function of a tenuous plasma in the case of longitudinal propagation. The study consideration matches these limiting cases. ESA

N91-15076# Abastumani Astrophysical Observatory, Georgia (USSR).
EXCITATION OF LANGMUIR WAVE BY TRANSVERSAL NONLINEAR WAVE IN THE ELECTRON-POSITRON INHOMOGENEOUS PLASMA IN THE PRESENCE OF POSITRON BEAM c32
A. D. Pataraya, T. A. Pataraya, and M. Z. Zedginidze (Tbilisi State

Univ., USSR) *In* ESA, Plasma Astrophysics Aug. 1990 p 159-162 (For primary document see N91-15046 06-90)
Copyright Avail: NTIS HC/MF A14

The elliptically polarized transversal nonlinear wave propagation with the small angle to the magnetic field in the electron-positron and electron-proton plasma in the presence of positron beam is investigated. The nonlinear Langmuir wave propagating with the small angle to the magnetic field is investigated. Investigation of a subpulse drift in the pulsars, the Coriolis force and inhomogeneities of the magnetic field, are reported. ESA

N91-15077# Academy of Sciences (USSR), Gorky. Inst. of Applied Physics.
GENERATION OF INDUCTIVE FIELDS BY AN OBLIQUE MAGNETIC ROTATOR IN COLLISIONLESS PLASMA **c75**
V. M. Gubchenko and M. L. Khodachenko *In* ESA, Plasma Astrophysics Aug. 1990 p 163-168 (For primary document see N91-15046 06-90)
Copyright Avail: NTIS HC/MF A14

The problem of the inductive magnetic field generation by an oblique magnetic rotator with the moment distributed on a given scale, rotating with a given frequency in the plasma with a given plasma frequency and a given thermal velocity is solved. The vector potential field is investigated and its asymptotic behavior in the limiting cases are found. The equations of the magnetic field lines in the equatorial plane of the rotator and their picture are obtained. The power dissipated by the rotator into the plasma and the breaking moment of the forces acting on the dipole are calculated. The expressions for the loss resistance and for the inductive characteristics of the dipole in plasma are obtained. The behavior of the characteristics is investigated depending on the introduced anomalous collisionless magnetic Reynolds number which characterizes the role of the effects of magnetic viscosity and conductivity in a collisionless plasma. The structure of the average velocity field of the plasma particle and of the current system excited is investigated. ESA

N91-15078# Academy of Sciences (USSR), Leningrad. A.F. Ioffe Inst. of Physics and Technology.
ANNIHILATION RADIATION OF STRONGLY-MAGNETISED ELECTRON-POSITRON PLASMA WITH POWER-LAW DISTRIBUTIONS OF PARTICLES **c75**
A. D. Kaminker, G. G. Pavlov, and P. G. Mamradze (Abastumani Astrophysical Observatory, Georgia, USSR) *In* ESA, Plasma Astrophysics Aug. 1990 p 169-173 (For primary document see N91-15046 06-90)
Copyright Avail: NTIS HC/MF A14

Intensity, polarization and cooling rate of the two photon annihilation radiations are studied in the case of one dimensional power law distributions of electron and positrons, assuming that they occupy the ground Landau level in a strong magnetic field. Simple analytical expressions for limiting cases are obtained and numerical calculations of radiations characteristics are presented. Power law electron/positron distributions are shown to generate power law spectra of the annihilation radiation with indices depending on direction of radiation. Power law-like hard tails observed in many gamma ray burst spectra may be associated with the annihilation of a magnetized plasma with the considered electron/proton distributions near the neutron star. ESA

N91-15079# Nagoya Univ. (Japan). Dept. of Electrical Engineering.
OBSERVATION OF ELECTRON HOLE, DOUBLE LAYER, AND TURBULENT HEATING IN A LABORATORY PLASMA **c75**
T. Tsukishima and H. Inuzuka *In* ESA, Plasma Astrophysics Aug. 1990 p 177-182 (For primary document see N91-15046 06-90)
Copyright Avail: NTIS HC/MF A14

Nonlinear phenomena such as electron hole, double layer, and turbulent heating, which were observed in a linear mirror device, THE NU-II, are reviewed. Observations were carried out with a temporal resolution of 2 ns and a spatial resolution of 1 mm, respectively. Upon applying a voltage difference of the order of 10 kV between two electrodes inserted in the cylindrical plasma at a distance of 67 cm, the nonlinear phenomena evolved consecutively. In particular, a strong current limited double layer was formed, and its lifetime was found to satisfy a simple empirical law. One dimensional computer simulations based on a kinetic code were carried out with boundary conditions close to the experimental ones. The effect of magnetic field was taken into consideration in the simulations. ESA

N91-15080# Abastumani Astrophysical Observatory, Georgia (USSR).
EXPERIMENTS WITH COLLISION OF VORTICES IN ROTATING AND STILL FREE-SURFACE SHALLOW WATER **c34**
R. A. Antonova, B. P. Zhvania, J. G. Lominadze, J. I. Nanobashvili, and V. I. Petviashvili (Kurchatov, I. V. Inst. of Atomic Energy, Moscow, USSR) *In* ESA, Plasma Astrophysics Aug. 1990 p 183-187 (For primary document see N91-15046 06-90)
Copyright Avail: NTIS HC/MF A14

Interaction of vortices in rotating and still water were studied. It was found, that in spite of the difference of vortex self localization mechanisms in those media, the qualitative laws of interaction of such structures are identical. ESA

N91-15081# Academy of Sciences (USSR), Novosibirsk. Inst. of Pure and Applied Mechanics.
LABORATORY SIMULATION OF THE ASTROPHYSICAL BURST PROCESSES IN NON-UNIFORM MAGNETISED MEDIA **c75**
V. M. Antonov, Yu. P. Zakharov, A. M. Orishich, A. G. Ponomarenko, V. G. Posukh, V. N. Snytnikov, and V. O. Stoyanovsky *In* ESA, Plasma Astrophysics Aug. 1990 p 189-190 (For primary document see N91-15046 06-90)
Copyright Avail: NTIS HC/MF A14

Under various astrophysical conditions the dynamics of nonstationary burst processes with mass and energy release may be defined by the inhomogeneity of the surrounding medium. In the presence of external magnetic field such a problem in general case becomes a three dimensional one and very complicated both from the observable and theoretical point of view (including the computer simulation method). The application of the laboratory simulation methods in such kinds of problems therefore seems to be rather promising and is demonstrated, mainly on the example of peculiar supernova. ESA

N91-15082# Academy of Sciences (USSR), Novosibirsk. Inst. of Pure and Applied Mechanics.
LABORATORY AND COMPUTER SIMULATIONS OF WAVE GENERATION PROCESSES IN NON-STATIONARY ASTROPHYSICAL PHENOMENA **c75**
G. I. Dudnikova, A. M. Orishich, A. G. Ponomarenko, V. A. Vshivkov, and Yu. P. Zakharov *In* ESA, Plasma Astrophysics Aug. 1990 p 191-194 (For primary document see N91-15046 06-90)
Copyright Avail: NTIS HC/MF A14

The simulation of disturbance generation due to the collisionless interaction of the space plasma clouds with the magnetized medium by the experimental and numerical methods is addressed. In this respect the formulated problem with the effects of the finite Larmor ion radius and interpenetration of plasmas at the expanding spherical cloud boundary differs greatly from the known ones considering the expansion of a super conductive sphere in the magnetohydrodynamic limit. ESA

N91-15083# Academy of Sciences (USSR), Moscow. Inst. of Terrestrial Magnetism, Ionosphere and Radio Wave Propagation.
STERILE NEUTRINOS AND ASTROPHYSICAL AND COSMOLOGICAL CONSTRAINTS ON THE PARAMETERS OF THE EXTENDED ELECTROWEAK MODELS
A. I. Rez and V. B. Semikoz *In* ESA, Plasma Astrophysics Aug. 1990 p 194-198 (For primary document see N91-15046 06-90)
Copyright Avail: NTIS HC/MF A14

In a minimal symmetric model and in an electroweak model

with a charged scalar singlet, the cross section for elastic scattering of a neutrino by leptons with helicity flip is calculated. This cross section can considerably (by more than five orders of magnitude under the specified conditions) exceed the one for neutrino scattering in an electromagnetic channel which is due to the existence of a vacuum magnetic moment of the neutrino. This leads to more stringent astrophysical and cosmological constraints on the parameters of the models. ESA

N91-15084# Texas Univ., Austin. Inst. for Fusion Studies.
MAGNETICALLY DRIVEN JETS AND WINDS **c75**
R. V. E. Lovelace (Cornell Univ., Ithaca, NY.) *In* ESA, Plasma Astrophysics Aug. 1990 p 201-206 Sponsored by the Guggenheim Foundation (For primary document see N91-15046 06-90)
(Contract DE-FG05-80ET-53088)
Copyright Avail: NTIS HC/MF A14

A theory for the formation and propagation of nonrelativistic jets and winds from magnetized accretion disks is derived from the equation of ideal magnetohydrodynamics. The theory allows the self consistent determination of the jet's axial velocity, radius, angular rotation rate, and temperature from the disk surface to infinity. The jets are assumed to carry no net poloidal current. However, the magnetic field is essential in that it acts, in opposition to gravity, to drive matter through the slow magnetosonic critical point. At large distances good collimation of the flow can result from the focusing effect of the external medium. Additionally, the external medium can act, in opposition to gravity, to drive the flow through the fast magnetosonic critical point. ESA

N91-15085# Ecole Polytechnique, Palaiseau (France). Centre de Physique Theorique.
NONLINEAR PLASMA EFFECTS IN THE ENVIRONMENT OF ACTIVE GALACTIC NUCLEI **c75**
E. Asseo, G. Pelletier, and H. Sol (Observatoire de Paris-Meudon, France) *In* ESA, Plasma Astrophysics Aug. 1990 p 207-213 (For primary document see N91-15046 06-90)
Copyright Avail: NTIS HC/MF A14

The physics of beam plasma interaction is investigated in the astrophysical context of jets issued from active galactic nuclei. In this physical situation, the magnetic field plays a significant role and strong Langmuir turbulence develops. This turbulence gives rise to Langmuir solitons which are found to be stable to transverse perturbations if the magnetic field is very strong, whereas they are unstable and collapse if the magnetic field is weak. When collapse occurs, the beam relaxes in the surrounding plasma and it is possible to estimate the power lost by the beam and its relaxation length. The consequences of this analysis for astrophysical jets show that one can associate radio knots observed in several sources and the transition region between relativistic jets, observed on the parsec scale close to the active galactic nuclei, and the classical jet, observed farther on the parsec scale. ESA

N91-15086# Academy of Sciences, Potsdam (German D.R.). Zentralinstitut fuer Astrophysik.
ENERGY DISSIPATION OF SHEAR ALFVEN WAVES IN EXTENDED COSMIC JETS **c32**
T. M. Kirchner *In* ESA, Plasma Astrophysics Aug. 1990 p 215-220 (For primary document see N91-15046 06-90)
Copyright Avail: NTIS HC/MF A14

The question of electron reacceleration in radio jets after their leaving the central power house in the compact cores of the radio galaxies is one of the problems at the heart of the physics of extragalactic radio sources. An interesting heating scheme in magnetically dominated jets is the resonance of MHD (MagnetoHydroDynamics) surface waves, generated by Kelvin-Helmholtz instability, with shear Alfven waves in the body of the jet. The resulting dissipation or convection of wave energy by phase mixing in the frame of ideal MHD for a monotonous profile of plasma parameters is described. Conditions are given for the processes which actually limit the resonance. ESA

N91-15087# Abastumani Astrophysical Observatory, Georgia (USSR).
MATTER PENETRATION AND MOTION THROUGH THE MAGNETOSPHERE OF NEUTRON STAR
P. G. Jincharadze and G. Z. Machabeli *In* ESA, Plasma Astrophysics Aug. 1990 p 221-225 (For primary document see N91-15046 06-90)
Copyright Avail: NTIS HC/MF A14

The adiabatic invariant is shown to conservate through the whole polar column of the neutron star. In the strong magnetic field of pulsars the smoothing process of particles longitudinal and transversal momentum components is therefore highly slowed down. The interface plasma magnetic field is shown to be almost always stable due to the presence of a strong gradient of magnetic field. ESA

N91-15088# Abastumani Astrophysical Observatory, Georgia (USSR).
ON THE EXISTENCE OF CIRCULAR POLARISATION IN THE PULSAR RADIATION
A. Z. Kazbegi, G. Z. Machabeli, and G. I. Melikidze *In* ESA, Plasma Astrophysics Aug. 1990 p 227-233 (For primary document see N91-15046 06-90)
Copyright Avail: NTIS HC/MF A14

A model which explains the existence and properties of the circular polarization in the pulsar emission is presented. Cyclic coordinates are introduced to consider the curvature of magnetic field lines exactly. Some observational features are explained. ESA

N91-15089# Sternberg Astronomical Inst., Moscow (USSR).
THIRTY-FIVE-DAY CYCLE OF HER X-1: SYNTHESISED OPTICAL LIGHT CURVES IN THE MODEL OF FREELY PROCESSING NEUTRON STAR
M. E. Prokhorov, N. I. Shakura, and K. A. Postnov *In* ESA, Plasma Astrophysics Aug. 1990 p 235-237 (For primary document see N91-15046 06-90)
Copyright Avail: NTIS HC/MF A14

Synthesis of the optical light curve of HZ Her is carried out with freely precessing neutron star as a clock mechanism for a 35 day cycle in Her X-1. The rotational axis of the neutron star is tilted to the orbital plane. This results in highly irradiated, twisted accretion disc around the neutron star. Outer disc regions can be slightly tilted to the orbital plane. The disc inclination and the accretion rate onto neutron stars are shown to vary with the precession phase. ESA

N91-15090# Byurakan Observatory, Mount Aragatz (USSR).
ON THE BRAKING MECHANISMS OF PULSARS
D. M. Sedrakyan, A. D. Sedrakyan, and K. M. Shahabasyan (Erivan State Univ., USSR) *In* ESA, Plasma Astrophysics Aug. 1990 p 239-243 (For primary document see N91-15046 06-90)
Copyright Avail: NTIS HC/MF A14

New mechanisms of pulsar spindown arising in the superfluid core of neutron stars are proposed. The evolution, internal and surface temperatures of pulsars are discussed. Pulsars are shown to possibly follow two evolutionary tracks. Calculated surface temperatures lie below the upper limits obtained during HEAO (High Energy Astronomy Observatory) observations. According to this new evolutionary theory, millisecond pulsars are very young ones. The existence of the death line is explained as the consequence of instability of neutron stars with central density higher than the critical one. ESA

N91-15091# Academy of Sciences of the Georgian SSR, Tbilisi. Inst. of Physics.
ULTRARELATIVISTIC LOW-FREQUENCY ELECTROMAGNETIC WAVES IN PULSAR MAGNETOSPHERES
N. L. Tsintsadze, L. N. Tsintsadze, and G. S. Lakshina (Indian Inst. of Geomagnetism, Bombay.) *In* ESA, Plasma Astrophysics Aug. 1990 p 245-249 (For primary document see N91-15046 06-90)
Copyright Avail: NTIS HC/MF A14

Nonlinear propagation of strong low frequency waves, as emitted by pulsar or compact galactic nuclei at their rotation frequencies, in a magnetized plasma is investigated. It is shown that even rather small amplitude waves (resonance effects) which can drive electrons are ultrarelativistic but the ions are immobile, two new types of circularly polarized waves are excited. These new waves are specific in that the frequencies are strongly dependent upon the amplitude. Results on the investigation of the damping of these waves are given. ESA

N91-15092# Academy of Sciences (USSR), Moscow. Inst. of Space Research.
ON THE THEORY OF LARGE-SCALE MICROPULSE STRUCTURE OF PULSAR RADIO RADIATION **c32**
O. G. Onishchenko *In* ESA, Plasma Astrophysics Aug. 1990 p 251-253 (For primary document see N91-15046 06-90)
Copyright Avail: NTIS HC/MF A14

Large scale microstructure of pulsar radiation is shown to be explainable as a result of self interaction of low frequency nonlinear cnoidal waves propagated in inner polar regions along a magnetic field of a neutron star. Stability of these cnoidal waves with respect to two dimensional long wavelength perturbations is discussed. ESA

N91-15093# Bulgarian Academy of Sciences, Sofia. Inst. of Space Research.
STRUCTURE OF ACCRETION FLOW IN CLOSE BINARY SYSTEM: A TWO DIMENSIONAL NUMERICAL MODEL
M. M. Dimitrova and L. G. Filipov *In* ESA, Plasma Astrophysics Aug. 1990 p 255-260 (For primary document see N91-15046 06-90)
Copyright Avail: NTIS HC/MF A14

A two dimensional numerical model forming two spiral shock fronts in accretion flow in close binary star system is presented. The position of these shocks is discussed. In the model, the position of the second shock front depends on the relation between the masses of both stars and the distance between them. Experimental computation based on smaller mass of the second star reveals closer position of the second spiral to the first one. ESA

N91-15094# Commissariat a l'Energie Atomique, Saclay (France). Service d'Astrophysique.
ACCRETION DISK INSTABILITY AND SPOKES IN SATURN'S RINGS **c91**
M. Tagger, R. N. Henriksen, and R. Pellat (Ecole Polytechnique, Palaiseau, France) *In* ESA, Plasma Astrophysics Aug. 1990 p 261-262 (For primary document see N91-15046 06-90)
Copyright Avail: NTIS HC/MF A14

The stability of accretion disks as an important problem concerning various astrophysical objects is addressed. It is shown that, in an ionized disk embedded in a vertical magnetic field, magnetohydrodynamic forces can act as a repulsive force. As a result, magnetosonic waves of low wavenumber can be amplified and produce unstable spiral modes. The amplification mechanism is shown to result from special propagation characteristics, which are explained, given to the waves by the thin disk geometry. The possibility that spokes can be due to waves, driven by a localized perturbation in Saturn's magnetosphere at a specific distance from the synchronous orbit is considered. ESA

N91-15095# Abastumani Astrophysical Observatory, Georgia (USSR).
LARGE-SCALE VORTICES IN COMPRESSIBLE TURBULENT MEDIUM WITH THE MAGNETIC FIELD **c75**
V. V. Gvaramadze and B. G. Dimitrov (Bulgarian Academy of Sciences, Sofia.) *In* ESA, Plasma Astrophysics Aug. 1990 p 263-267 (For primary document see N91-15046 06-90)
Copyright Avail: NTIS HC/MF A14

An averaged equation which describes the large scale vortices and Alfven waves generation in a compressible helical turbulent medium with a constant magnetic field is presented. The presence of the magnetic field leads to anisotropization of the vortex generation. Possible applications of the anisotropic vortex dynamo effect are accretion disks of compact objects. ESA

N91-15096# Academy of Sciences (USSR), Moscow. Inst. of Space Research.
COMPACT OBJECT MASSES IN ACTIVE GALACTIC NUCLEI AND QUASARS AND DURATION OF ACTIVITY STAGE
M. Romanova *In* ESA, Plasma Astrophysics Aug. 1990 p 269-272 (For primary document see N91-15046 06-90)
Copyright Avail: NTIS HC/MF A14

The masses of compact objects in active galactic nuclei (AGN) and quasars derived by different authors are compared. The duration of an activity stage is determined and the slope approximately equal to 4 of the mass function is derived. There is a high dispersion of parameters in each sample, however the samples show the similar dependence of the redshift. The duration of the activity stage of the numerous low massive AGN is possibly about cosmological, whereas the one of the high massive AGN is one or two orders in magnitude less. ESA

N91-15097# Osservatorio Astronomico, Turin (Italy).
A MODEL FOR ONE-SIDED EXTRAGALACTIC JETS
G. Bodo, G. D. Chagelishvili, A. Ferrari, J. G. Lominadze (Abastumani Astrophysical Observatory, Georgia, USSR), and E. Trussoni *In* ESA, Plasma Astrophysics Aug. 1990 p 273-275 (For primary document see N91-15046 06-90)
Copyright Avail: NTIS HC/MF A14

The origin of a possible large scale structure of magnetic field in an active galactic nucleus for which the steady magnetohydrodynamic equations possess non symmetric solutions about the equatorial plane of an axisymmetric accretion disk is discussed. Such asymmetry can be related to the origin of one sided VLBI (very long base interferometry) jets in bright extragalactic radio sources. ESA

N91-15098# Sternberg Astronomical Inst., Moscow (USSR).
ON THE NATURE OF COSMIC GAMMA RAY BURSTS **c93**
N. I. Shakura and N. N. Shakura *In* ESA, Plasma Astrophysics Aug. 1990 p 277-278 (For primary document see N91-15046 06-90)
Copyright Avail: NTIS HC/MF A14

The nature of cosmic gamma ray burst is studied. The sources of the observed gamma bursts are supposed to be presented by the two populations of galactic objects, namely: the old neutron stars concentrated in the galactic disk; and the old degenerated dwarfs that are distributed in the galactic halo. The latter may be responsible for diffuse x ray background in the 100 to 1000 keV energy range. ESA

N91-15099# Byurakan Observatory, Mount Aragatz (USSR).
ON THE GENERATION OF MAGNETIC FIELDS IN ACTIVE STAR ATMOSPHERES
V. S. Hayrapetyan and V. V. Vikharev (Academy of Sciences, USSR, Moscow) *In* ESA, Plasma Astrophysics Aug. 1990 p 279-281 (For primary document see N91-15046 06-90)
Copyright Avail: NTIS HC/MF A14

A simple model of magnetic flux tube emergence is used to show the sharp decrease of plasma beta in the chromosphere of active stars and of the Sun as the heigth increases. This free magnetic field is unstable in relation to compression. It leads to impulsive magnetic energy transformation into thermal and kinetic plasma energy by pinch effect, which can manifest as a flare phenomenon. ESA

N91-15100# Abastumani Astrophysical Observatory, Georgia (USSR).
PREGALACTIC INHOMOGENEITY IN HOT DARK MATTER MODEL OF THE UNIVERSE
T. A. Kahniashvili and K. A. Manukjan (Tbilisi State Univ., USSR) *In* ESA, Plasma Astrophysics Aug. 1990 p 283-285 (For primary document see N91-15046 06-90)
Copyright Avail: NTIS HC/MF A14

The development of small potential perturbations of the

gravitational field and matter of a hot dark matter model in the presence of light weakly interacting particles is considered. Transfer functions and their dependence on the number of massive collisionless particles which today are the dynamical dark matter are found. Effective algorithms for building numerical simulation of the development of small inhomogeneities in this model are investigated. ESA

N91-15101# Academy of Sciences (USSR), Moscow. Inst. of Space Research.
THE PLASMA MODEL OF RADIOEMISSION FROM SN 1987A
G. S. Bisnovatyi-Kogan, A. F. Illarionov, and V. I. Slysh *In* ESA, Plasma Astrophysics Aug. 1990 p 289-295 (For primary document see N91-15046 06-90)
Copyright Avail: NTIS HC/MF A14

The flux of electronic antineutrino from stellar collapse lead to production of relativistic positrons with gamma = 30 outside the shock wave due to reaction p + antineutrino sub e = n + e+. Rapid positrons are additionally accelerated in the shock wave, proceeding the main shock and forming as a result of the decrease of the central mass due to mighty neutrino emission. Close collisions of relativistic e+ with surrounding electrons produce new relativistic particles. Anisotropic distribution of relativistic particles leads to excitation of plasma oscillations which are transformed into photons of plasma and double plasma frequency. This process may explain the observed radioemission during first (approximately) ten days after SN 1987 A explosion. ESA

N91-15102# Abastumani Astrophysical Observatory, Georgia (USSR).
ON THE POSSIBILITY OF DISCOVERING PULSED RADIATION FROM SN 1987A
A. Z. Kazbegi, G. Z. Machabeli, and G. I. Melikidze *In* ESA, Plasma Astrophysics Aug. 1990 p 297-300 (For primary document see N91-15046 06-90)
Copyright Avail: NTIS HC/MF A14

If a pulsar having the rotation period P approximately 0.05/0.1s is formed in the interior of SN (Super Nova) 1987A, it should be a source of energetic radiation. The plasma-maser instabilities should develop in the pulsar magnetosphere. With the increase in the period of the newborn pulsar in SN 1987A the generated frequencies decrease, reaching radio bands for P greater than or equal to 0.1/0.2s. The luminosities in different bands of spectra should not ressemble significantly that of the well known pulsars PSR 0531+21, 0833-45, 0540-69 and 1509-58. The mechanism for the wave escape from the shell of the SN 1987A is offered. ESA

N91-15103# Sternberg Astronomical Inst., Moscow (USSR).
THE OPTICAL OBSERVATIONS OF X RAY NOVA GS2023+33 = V404 CYG **c89**
O. A. Osminkina, E. Yu. Osminkin, N. I. Shakura, and S. Yu. Shugarov *In* ESA, Plasma Astrophysics Aug. 1990 p 301-302 (For primary document see N91-15046 06-90)
Copyright Avail: NTIS HC/MF A14

The results of optical observations of Nova V404 Cyg 1989 are presented in comparison with the outburst in 1938. A possible model in the framework of nonstationary disk accretion is compared with that for Nova Vul 1988. Conclusions include that the outer disk radius in V404 is larger. The system V404 seems to be wider in comparison with Nova Vul 1988. ESA

N91-15104# Academy of Sciences (USSR), Troitsk. Inst. of Terrestrial Magnetism, Ionosphere and Radio Wave Propagation.
NEUTRINO SCATTERING BY NUCLEI IN IMPERFECT MEDIA
L. B. Leinson *In* ESA, Plasma Astrophysics Aug. 1990 p 305-307 (For primary document see N91-15046 06-90)
Copyright Avail: NTIS HC/MF A14

Quasi elastic neutrino scattering by nuclei in the matter and neutrino helicity flip via the scattering by nuclei is investigated. At the neutrino opacity stage the nuclear component of a collapsing star core is highly imperfect. In this case a neutrino scattering by nuclei is reduced to emission and absorption of phonons in the medium. Therefore the cross section of neutrino scattering by nucleus in the collapsing matter is much less than the cross section of the scattering by an isolated nucleus. It may be important for a neutrino opacity approach in the collapsing star core and for correct upper bound evaluation of a neutrino magnetic moment. ESA

N91-15105# Academy of Sciences (USSR), Gorky. Inst. of Applied Physics.
RADIATION-DRIVEN DISKONS AS A NEW ASTROPHYSICAL OBJECT
P. A. Bespalov, A. V. Serber, and V. V. Zheleznyakov *In* ESA, Plasma Astrophysics Aug. 1990 p 309-317 (For primary document see N91-15046 06-90)
Copyright Avail: NTIS HC/MF A14

The plasma envelope of a hot magnetic degenerate with high radiation pressure is investigated. The radiation transfer in the photosphere of an isolated magnetic degenerate star is considered and the radiation pressure force is calculated. The star parameters are determined for the photospheric plasma ejection by the cyclotron radiation pressure to be possible. The mass flux of the matter swept up into the star magnetosphere is estimated and the types of magnetic degenerates with the mass loss driven by the photospheric cyclotron radiation are pointed out. The model of an equatorial plasma disk supported by the high radiation pressure is analyzed. The stationary plasma flow from the star surface to the disk and the radial diffusion of matter to the disk periphery are studied. The disk characteristics are determined for various values of the mass flux. The results were applied to isolated magnetic white dwarfs, evolved planetary nebulae nuclei with strong magnetic field, magnetized x ray bursters and gamma bursters. ESA

N91-15106# Academy of Sciences (USSR), Leningrad. Inst. of Physics and Technology.
SPECTRAL SYNTHESIS CODE LINESPEC: IONISATION EQUILIBRIUM OF PLASMA AND ABSORPTION SPECTRA FORMATION
N. Y. Gnedin, S. A. Levshakov, D. A. Verner, and D. G. Yakovlev *In* ESA, Plasma Astrophysics Aug. 1990 p 319-320 (For primary document see N91-15046 06-90)
Copyright Avail: NTIS HC/MF A14

A modified version of the code LINESPEC designed for many purposes is described. Its main goal is to simulate absorption line spectra of the quasars. The spectras are formed due to passing of continuous quasar radiation through distant intervening clouds situated between the quasar and the observer. Calculation is performed under the assumption that the cloud's plasma is in the state of radiative-collisional equilibrium. LINESPEC includes most recent literature and original data on recombination and ionization rates of atoms and ions of H, He, C, N, O, Ne, Mg, Al, Si, S, Ca, Fe. These may be useful for solving various problems of plasma physics, atomic spectroscopy and astrophysics. ESA

N91-15107# Abastumani Astrophysical Observatory, Georgia (USSR).
INVESTIGATION OF THE NIGHT SKY AIRGLOW NEAR THE EPICENTER OF THE EARTHQUAKE **c46**
G. G. Didebulidze, L. M. Fishkova, A. D. Pataraya, and T. I. Toroshelidze *In* ESA, Plasma Astrophysics Aug. 1990 p 321-327 (For primary document see N91-15046 06-90)
Copyright Avail: NTIS HC/MF A14

Some peculiarities of the upper atmosphere airglow variations according to Abastumani (USSR) observations before and after earthquakes (EQs) near the region of a major shock are given. It is shown that peculiarities of the night intensity variation of atomic oxygen OI 557.7 nm and OI 630 nm lines depend both on the EQ amplitude and region of observations. It is assumed that the reason for such variations is dissipation and dissociation of acoustic-gravitational waves in the middle and upper atmosphere, that in its turn is caused by soil shifting and lava like growth of fractures and spalling of rocks. Or the reason may consist in the periodic amplitude modulation of the high frequency seismic noise on a vast area around the center of a next arterial fracture due to

an increasing tension. Based on the example of observations after the Spitak (USSR) EQ, the possibility of wind generation after the major shock is indicated. ESA

N91-15108# Academy of Sciences (USSR), Irkutsk. Inst. of Terrestrial Magnetism and Radio Wave Propagation.
INFLUENCE OF THE PARAMETER DISTRIBUTION OF THE SOLAR WIND NEAR THE SUN UPON ITS STRUCTURE AT THE EARTH'S ORBIT **c92**
A. P. Kaigorodov and V. G. Fainshtein *In* ESA, Plasma Astrophysics Aug. 1990 p 331-334 (For primary document see N91-15046 06-90)
Copyright Avail: NTIS HC/MF A14

Using numerical calculations of Solar Wind (SW) flow, a study is made of the influence of the azimuthal distribution of its parameters near the Sun upon the SW structure in the space up to the Earth's orbit. It is shown that both the character and intensity of the interaction of fast and slow SW streams in interplanetary space and plasma properties in the region of the heliosphere current sheet which is carried away by the slow SW flow from the Sun to the Earth, depend on solar wind properties at small distances from the Sun and, in particular, on the character of the mass density and magnetic field distribution there. ESA

N91-15109# Academy of Sciences (USSR), Irkutsk. Inst. of Terrestrial Magnetism and Radio Wave Propagation.
INTERRELATIONSHIP BETWEEN THE TEARING-INSTABILITY AND MAGNETIC ISLAND MERGING **c46**
A. T. Altyntsev and N. V. Lebedev *In* ESA, Plasma Astrophysics Aug. 1990 p 335-338 (For primary document see N91-15046 06-90)
Copyright Avail: NTIS HC/MF A14

The merging of current ropes, a problem concerned with processes of magnetic field line reconnection, is studied. A series of experiments with a forced formation of magnetic islands is described. The results show that the magnetic field structure, which is formed when two magnetic fluxes emerge nearby, depends fundamentally on the history of its production and on the rates of reconnection and merging processes. In particular, similar processes are able to take effect in the solar atmosphere. Three stages can be identified in the merging of magnetic islands: a slow, fast and a relaxation stage. ESA

N91-15110# Academy of Sciences (USSR), Novosibirsk. Inst. of Nuclear Physics.
NONLINEAR MAGNETOSONIC WAVES IN AN INHOMOGENEOUS PLASMA
M. Ryutova, M. Kaisig, and T. Tajima (Texas Univ., Austin.) *In* ESA, Plasma Astrophysics Aug. 1990 p 339-343 (For primary document see N91-15046 06-90)
(Contract DE-FG05-80ET-53088; NSF ATM-88-11128)
Copyright Avail: NTIS HC/MF A14

Effects of strong and random inhomogeneities of the magnetic fields, plasma density, and temperature in the solar atmosphere on the properties of magnetoacoustic waves of arbitrary amplitudes are studied. Depending on the statistical properties of the medium, different scenarios of wave propagation arise. In the predominance of dissipative effects, the primary wave is damped away in the linear stage and the efficiency of heating due to inhomogeneities is much greater than that in a homogeneous medium. The process of heating can be accomplished through the formation of shocks or through the storing of the energy of a system of solitons which are later dumped away. Computer simulations were carried out which support and extend the above theoretical investigations. ESA

N91-15111# Chicago Univ., IL.
PARTICLE PHYSICS AND COSMOLOGY Progress Report, Jan. 1988 - Oct. 1990
Michael S. Turner Oct. 1990 21 p
(Contract DE-FG02-90ER-40560)
(DE91-001946; DOE/ER-40560/T2) Avail: NTIS HC/MF A03

This report discusses inflationary cosmology; dark-matter detection; axions, astrophysics, and cosmology; topological defects; and astrophysical/cosmological constraints to particle properties. DOE

N91-14898*# Observatoire de Marseille (France).
REDDENING AND EXTINCTION TOWARDS H II REGIONS Progress Report
James Caplan and Lise DeHarveng *In* NASA, Ames Research Center, Interstellar Dust: Contributed Papers Dec. 1989 p 3-4 (For primary document see N91-14897 06-88)
Avail: NTIS HC/MF A22 CSCL 03B

N91-14901*# Copenhagen Observatory (Denmark).
THE AUTOCORRELATION FUNCTION OF THE NORTH POLE DUST
Jens Knude *In* NASA, Ames Research Center, Interstellar Dust: Contributed Papers Dec. 1989 p 17-20 (For primary document see N91-14897 06-88)
Avail: NTIS HC/MF A22 CSCL 03B

N91-14902*# Applied Research Corp., Landover, MD.
THE DEPENDENCE OF UV EXTINCTION PROPERTIES ON DUST ENVIRONMENT Abstract Only
Derck Massa *In* NASA, Ames Research Center, Interstellar Dust: Contributed Papers Dec. 1989 p 21 (For primary document see N91-14897 06-88)
Avail: NTIS HC/MF A22 CSCL 03B

N91-14903*# Vilnius Kapsukas State Univ. (Lithuania).
PROPERTIES OF INTERSTELLAR DUST IN THE REGION OF THE CEP OB4 ASSOCIATION
J. Sudzius *In* NASA, Ames Research Center, Interstellar Dust: Contributed Papers Dec. 1989 p 23-28 (For primary document see N91-14897 06-88)
Avail: NTIS HC/MF A22 CSCL 03B

N91-14904*# Universidad Nacional Autonoma de Mexico, Ensenada. Inst. de Astronomia.
THREE-MICRON SPECTROSCOPY OF HIGHLY REDDENED FIELD STARS Abstract Only
Mauricio Tapia, P. Persi, M. Roth, and M. Ferrari-Toniolo (Consiglio Nazionale delle Ricerche, Frascati, Italy) *In* NASA, Ames Research Center, Interstellar Dust: Contributed Papers Dec. 1989 p 29 (For primary document see N91-14897 06-88)
Avail: NTIS HC/MF A22 CSCL 03B

N91-14905*# Kapteyn Astronomical Lab., Groningen (Netherlands).
INTERSTELLAR CIRCULAR POLARIZATION AND THE DIELECTRIC NATURE OF DUST GRAINS Abstract Only
Grzegorz Chlewicki and J. Mayo Greenberg (Leiden Univ., Netherlands) *In* NASA, Ames Research Center, Interstellar Dust: Contributed Papers Dec. 1989 p 33 (For primary document see N91-14897 06-88)
Avail: NTIS HC/MF A22 CSCL 03B

N91-14906*# Belgian Royal Observatory, Brussels.
NEW RESULTS IN THE THEORY OF DUST GRAIN ALIGNMENT
Pierre Cugnon *In* NASA, Ames Research Center, Interstellar Dust: Contributed Papers Dec. 1989 p 35-36 (For primary document see N91-14897 06-88)
Avail: NTIS HC/MF A22 CSCL 03B

N91-14907*# Tohoku Univ., Sendai (Japan). Astronomical Inst.
POLARIZATION AND EXTINCTION BY ALIGNED GRAINS
Masafumi Matsumura and Munezo Seki *In* NASA, Ames Research Center, Interstellar Dust: Contributed Papers Dec. 1989 p 37-40 (For primary document see N91-14897 06-88)
Avail: NTIS HC/MF A22 CSCL 03B

N91-14908*# Tohoku Univ., Sendai (Japan). Coll. of General Education.
ALIGNMENT MECHANISMS OF PARAMAGNETIC GRAINS REVISITED
Munezo Seki *In* NASA, Ames Research Center, Interstellar Dust: Contributed Papers Dec. 1989 p 41-44 (For primary document see N91-14897 06-88)
Avail: NTIS HC/MF A22 CSCL 03B

N91-14911*# Helsinki Univ. (Finland).
THE SPECTRAL ENERGY DISTRIBUTION OF THE SCATTERED LIGHT FROM DARK CLOUDS
Kalevi Mattila and G. F. O. Schnur (Ruhr Univ., Bochum, Germany, F.R.) *In* NASA, Ames Research Center, Interstellar Dust: Contributed Papers Dec. 1989 p 55-56 (For primary document see N91-14897 06-88)
Avail: NTIS HC/MF A22 CSCL 03B

N91-14915*# Arizona Univ., Tucson. Dept. of Physics.
SIMULTANEOUS INFRARED AND UV-VISIBLE ABSORPTION SPECTRA OF MATRIX-ISOLATED CARBON VAPOR
Joe Kurtz and Donald R. Huffman *In* NASA, Ames Research Center, Interstellar Dust: Contributed Papers Dec. 1989 p 71-75 (For primary document see N91-14897 06-88)
Avail: NTIS HC/MF A22 CSCL 03B

N91-14916*# University Coll., London (England). Dept. of Physics and Astronomy.
CORRELATION PROPERTIES OF INTERSTELLAR DUST: DIFFUSE INTERSTELLAR BANDS
W. B. Somerville *In* NASA, Ames Research Center, Interstellar Dust: Contributed Papers Dec. 1989 p 77-81 (For primary document see N91-14897 06-88)
Avail: NTIS HC/MF A22 CSCL 03B

N91-14927*# Ecole Normale Superieure, Paris (France). Lab. de Physique.
SMALL SCALE VARIATIONS OF ABUNDANCES OF TRANSIENTLY HEATED GRAINS IN MOLECULAR CLOUDS
F. Boulanger, E. Falgarone, G. Helou (California Inst. of Tech., Pasadena.), and J. L. Puget *In* NASA, Ames Research Center, Interstellar Dust: Contributed Papers Dec. 1989 p 123-127 (For primary document see N91-14897 06-88)
Avail: NTIS HC/MF A22 CSCL 03B

N91-14930*# Kapteyn Astronomical Lab., Groningen (Netherlands).
DUST EMISSION FROM HIGH LATITUDE CIRRUS CLOUDS Abstract Only
Rene J. Laureijs, Grzegorz Chlewicki, F. O. Clark, and P. R. Wesselius *In* NASA, Ames Research Center, Interstellar Dust: Contributed Papers Dec. 1989 p 133 (For primary document see N91-14897 06-88)
Avail: NTIS HC/MF A22 CSCL 03B

N91-14941*# Academy of Sciences (USSR), Leningrad. Special Astrophysical Observatory.
DUST CLOUDS IN ORION AND THE INTERSTELLAR NEUTRAL HYDROGEN DISTRIBUTION Abstract Only
N. V. Bystrova *In* NASA, Ames Research Center, Interstellar Dust: Contributed Papers Dec. 1989 p 193 (For primary document see N91-14897 06-88)
Avail: NTIS HC/MF A22 CSCL 03B

N91-14943*# Tata Inst. of Fundamental Research, Bombay (India).
DUST IN A FEW SOUTHERN H II REGIONS
Swarna Kanti Ghosh, K. V. K. Iyengar, T. N. Rengarajan, S. N. Tandon, R. P. Verma, and R. R. Daniel *In* NASA, Ames Research Center, Interstellar Dust: Contributed Papers Dec. 1989 p 197-198 (For primary document see N91-14897 06-88)
Avail: NTIS HC/MF A22 CSCL 03B

N91-14944*# Tata Inst. of Fundamental Research, Bombay (India).
DISTRIBUTION OF DUST IN W31 COMPLEX
Swarna Kanti Ghosh, K. V. K. Iyengar, T. N. Rengarajan, S. N. Tandon, R. P. Verma, and R. R. Daniel *In* NASA, Ames Research Center, Interstellar Dust: Contributed Papers Dec. 1989 p 199-200 (For primary document see N91-14897 06-88)
Avail: NTIS HC/MF A22 CSCL 03B

N91-14946*# Helsinki Univ. (Finland). Observatory and Astrophysics Lab.
H I AND DUST IN THE HIGH LATITUDE DARK CLOUD L1642
Tarja Liljestroem and Kalevi Mattila *In* NASA, Ames Research Center, Interstellar Dust: Contributed Papers Dec. 1989 p 203-204 (For primary document see N91-14897 06-88)
Avail: NTIS HC/MF A22 CSCL 03B

N91-14947*# Five-College Astronomy Dept., Amherst, MA.
DUST EMISSION IN THE SAGITTARIUS B2 MOLECULAR CLOUD CORE
Dariusz C. Lis and Paul F. Goldsmith *In* NASA, Ames Research Center, Interstellar Dust: Contributed Papers Dec. 1989 p 205-209 (For primary document see N91-14897 06-88)
Avail: NTIS HC/MF A22 CSCL 03B

N91-14949*# Groningen Rijksuniv. (Netherlands). Lab. for Space Research.
THE EMBEDDED OBJECTS IN EPSILON CHA I CLOUD Abstract Only
Timo Prusti, R. Assendorp, and P. R. Wesselius *In* NASA, Ames Research Center, Interstellar Dust: Contributed Papers Dec. 1989 p 219 (For primary document see N91-14897 06-88)
Avail: NTIS HC/MF A22 CSCL 03B

N91-14951*# Naval Research Lab., Washington, DC.
DUST EMISSION FROM BARNARD 35: GAS HEATING ANOMALY RESOLVED
Howard A. Smith *In* NASA, Ames Research Center, Interstellar Dust: Contributed Papers Dec. 1989 p 227-232 (For primary document see N91-14897 06-88)
Avail: NTIS HC/MF A22 CSCL 03B

N91-14956*# Rice Univ., Houston, TX. Dept. of Chemistry.
MATRIX ISOLATION AS A TOOL FOR STUDYING INTERSTELLAR CHEMICAL REACTIONS Abstract Only
David W. Ball, Bryan J. Ortman, Robert H. Hauge, and John L. Margrave *In* NASA, Ames Research Center, Interstellar Dust: Contributed Papers Dec. 1989 p 243-244 (For primary document see N91-14897 06-88)
Avail: NTIS HC/MF A22 CSCL 03B

N91-14957*# Leiden Univ. (Netherlands). Lab. Astrophysics.
NEW INSIGHTS IN THE PHOTOCHEMISTRY OF GRAIN MANTLES: THE IDENTIFICATION OF THE 4.62 AND 6.87 MICRON BANDS
Ruud Grim, Willem A. Schutte, Bernard Schmitt, and J. Mayo Greenberg *In* NASA, Ames Research Center, Interstellar Dust: Contributed Papers Dec. 1989 p 245-246 (For primary document see N91-14897 06-88)
Avail: NTIS HC/MF A22 CSCL 03B

N91-14959*# Manchester Coll. of Science and Technology (England). Dept. of Mathematics.
GRAIN GROWTH, OPTICAL POLARISATION, AND EXTINCTION IN INTERSTELLAR CLOUDS Abstract Only
A. P. Jones *In* NASA, Ames Research Center, Interstellar Dust: Contributed Papers Dec. 1989 p 249 (For primary document see N91-14897 06-88)
Avail: NTIS HC/MF A22 CSCL 03B

N91-14960*# Princeton Univ. Observatory, NJ.
GRAIN MANTLES: THE IMPACT ON GRAIN EVOLUTION AND SELECTIVE EXTINCTION
Charles L. Joseph *In* NASA, Ames Research Center, Interstellar

Dust: Contributed Papers Dec. 1989 p 251-255 (For primary document see N91-14897 06-88)
Avail: NTIS HC/MF A22 CSCL 03B

N91-14961*# Leiden Univ. (Netherlands). Lab. Astrophysics.
MOLECULAR AND MASS SPECTROSCOPIC ANALYSIS OF ISOTOPICALLY LABELED ORGANIC RESIDUES
Celia X. Mendoza-Gomez, J. Mayo Greenberg, P. McCain, J. P. Ferris, R. Briggs (New York State Dept. of Health, Albany.), M. S. deGroot, and Willem A. Schutte *In* NASA, Ames Research Center, Interstellar Dust: Contributed Papers Dec. 1989 p 257-260 (For primary document see N91-14897 06-88)
(Grant NGR-33-018-148)
Avail: NTIS HC/MF A22 CSCL 03B

N91-14962*# Calabria Univ., Arcavacta di Rende (Italy). Dipartimento di Fisica.
SYNTHESIS OF H2 IN DIRTY ICE MANTLES BY FAST ION ENERGY LOSS: NEW EXPERIMENTAL RESULTS INCREASE THE RELEVANCE OF THIS MECHANISM
Valero Pirranello, W. L. Brown, L. J. Lanzerotti, and D. A. Averna (Catania Univ., Italy) *In* NASA, Ames Research Center, Interstellar Dust: Contributed Papers Dec. 1989 p 261-264 (For primary document see N91-14897 06-88)
Avail: NTIS HC/MF A22 CSCL 03B

N91-14963*# Leiden Univ. (Netherlands). Lab. Astrophysics.
DIFFUSION AND INFRARED PROPERTIES OF MOLECULES IN ICE MANTLES Abstract Only
Bernard Schmitt, Ruud Grim, and J. Mayo Greenberg *In* NASA, Ames Research Center, Interstellar Dust: Contributed Papers Dec. 1989 p 265 (For primary document see N91-14897 06-88)
Avail: NTIS HC/MF A22 CSCL 03B

N91-14964*# Leiden Univ. (Netherlands). Lab. Astrophysics.
THE EVOLUTION OF ORGANIC MANTLES ON INTERSTELLAR GRAINS
Willem A. Schutte and J. Mayo Greenberg *In* NASA, Ames Research Center, Interstellar Dust: Contributed Papers Dec. 1989 p 267-268 (For primary document see N91-14897 06-88)
Avail: NTIS HC/MF A22 CSCL 03B

N91-14965*# Max-Planck-Inst. fuer Extraterrestrische Physik, Garching (Germany, F.R.).
ABSORPTION FEATURES IN THE 3 MICRON SPECTRA OF HIGHLY OBSCURED OBJECTS
Robert G. Smith, Kris Sellgren, and Alan T. Tokunaga (Hawaii Univ., Honolulu.) *In* NASA, Ames Research Center, Interstellar Dust: Contributed Papers Dec. 1989 p 269-270 (For primary document see N91-14897 06-88)
Avail: NTIS HC/MF A22 CSCL 03B

N91-14966*# Florence Univ. (Italy). Dipartimento di Fisica.
PRODUCTION AND TRANSFER OF UV PHOTONS IN NON-HOMOGENEOUS SPHERICAL CLOUDS
Santi Aiello, C. Cecchi-Pestellini, Francesco Mencaraglia, Bruno Barsella, and F. Ferrini (Pisa Univ., Italy) *In* NASA, Ames Research Center, Interstellar Dust: Contributed Papers Dec. 1989 p 273-278 (For primary document see N91-14897 06-88)
Avail: NTIS HC/MF A22 CSCL 03B

N91-14967*# Observatoire de Paris-Meudon (France).
GRAINS CHARGES IN INTERSTELLAR CLOUDS
N. Bel, J. P. Lafon, and Y. P. Viala *In* NASA, Ames Research Center, Interstellar Dust: Contributed Papers Dec. 1989 p 279-280 (For primary document see N91-14897 06-88)
Avail: NTIS HC/MF A22 CSCL 03B

N91-14968*# National Aeronautics and Space Administration. Ames Research Center, Moffett Field, CA.
DUST COAGULATION IN ISM
Arati Chokshi, Alexander G. G. M. Tielens, and David Hollenbach *In its* Interstellar Dust: Contributed Papers Dec. 1989 p 281-282 (For primary document see N91-14897 06-88)
Avail: NTIS HC/MF A22 CSCL 03B

N91-14969*# Montreal Univ. (Quebec). Departement de Physique.
ON THE POLARIZATION MECHANISM IN THE R MON/NGC 2261 COMPLEX
Francois Menard and Pierre Bastien *In* NASA, Ames Research Center, Interstellar Dust: Contributed Papers Dec. 1989 p 283-288 (For primary document see N91-14897 06-88)
Avail: NTIS HC/MF A22 CSCL 03B

N91-14970*# National Aeronautics and Space Administration, Ames Research Center, Moffett Field, CA.
INFRARED STUDIES OF DUST GRAINS IN INFRARED REFLECTION NEBULAE
Yvonne J. Pendleton, Alexander G. G. M. Tielens, and Michael W. Werner *In its* Interstellar Dust: Contributed Papers Dec. 1989 p 289-290 (For primary document see N91-14897 06-88)
Avail: NTIS HC/MF A22 CSCL 03B

N91-14971*# Prague Observatory (Czechoslovakia).
LABORATORY INVESTIGATION OF ELECTRIC CHARGING OF DUST PARTICLES BY ELECTRONS, IONS, AND UV RADIATION
Jiri Svestka, S. Pinter, and E. Gruen (Max-Planck-Inst. fuer Kernphysik, Heidelberg, Germany, F.R.) *In* NASA, Ames Research Center, Interstellar Dust: Contributed Papers Dec. 1989 p 291-292 (For primary document see N91-14897 06-88)
Avail: NTIS HC/MF A22 CSCL 03B

N91-14972*# Chicago Univ., IL. Astronomy and Astrophysics Center.
DUST IN REGIONS OF MASSIVE STAR FORMATION
Mark G. Wolfire and J. P. Cassinelli (Wisconsin Univ., Madison.) *In* NASA, Ames Research Center, Interstellar Dust: Contributed Papers Dec. 1989 p 293-294 (For primary document see N91-14897 06-88)
Avail: NTIS HC/MF A22 CSCL 03B

N91-14973*# National Aeronautics and Space Administration. Goddard Space Flight Center, Greenbelt, MD.
DOES CO TRACE H2 AT HIGH GALACTIC LATITUDE
David Bazell, L. Blitz (Maryland Univ., College Park.), and Francois-Xavier Desert *In* NASA, Ames Research Center, Interstellar Dust: Contributed Papers Dec. 1989 p 297-298 (For primary document see N91-14897 06-88)
Avail: NTIS HC/MF A22 CSCL 03B

N91-14975*# California Univ., Berkeley. Dept. of Astronomy.
MOLECULES, GRAINS, AND SHOCKS: A COMPARISON OF CO, H I, AND IRAS DATA Abstract Only
Carl Heiles, William T. Reach, and Bon-Chul Koo *In* NASA, Ames Research Center, Interstellar Dust: Contributed Papers Dec. 1989 p 301 (For primary document see N91-14897 06-88)
Avail: NTIS HC/MF A22 CSCL 03B

N91-14977*# Bonn Univ. (Germany, F.R.). Radioastronomisches Inst.
MOLECULES IN AN INFRARED CIRRUS CLOUD
Horst Meyerdierks and Nathalie Brouillet (Bordeaux Univ., France) *In* NASA, Ames Research Center, Interstellar Dust: Contributed Papers Dec. 1989 p 307-308 (For primary document see N91-14897 06-88)
Avail: NTIS HC/MF A22 CSCL 03B

N91-14978*# California Univ., Berkeley. Dept. of Astronomy.
INFRARED CIRRUS POINT SOURCES Abstract Only
William T. Reach, Carl Heiles, and Bon-Chul Koo *In* NASA, Ames Research Center, Interstellar Dust: Contributed Papers Dec.

1989 p 309 (For primary document see N91-14897 06-88)
Avail: NTIS HC/MF A22 CSCL 03B

N91-14979*# Space Telescope Science Inst., Baltimore, MD.
DUST IN STELLAR WIND BOW SHOCKS Abstract Only
Dave VanBuren *In* NASA, Ames Research Center, Interstellar Dust: Contributed Papers Dec. 1989 p 311 Prepared in cooperation with Johns Hopkins Univ., Baltimore, MD (For primary document see N91-14897 06-88)
Avail: NTIS HC/MF A22 CSCL 03B

N91-14980*# National Aeronautics and Space Administration. Ames Research Center, Moffett Field, CA.
STUDYING THE SPATIAL DISTRIBUTION OF INTERSTELLAR DUST
Helen J. Walker, Michael W. Werner, C. Allen, R. C. Henry, R. Kimble, J. Wofford, and Jayant Murthy (National Aeronautics and Space Administration. Goddard Space Flight Center, Greenbelt, MD.) *In its* Interstellar Dust: Contributed Papers Dec. 1989 p 313-316 (For primary document see N91-14897 06-88)
Avail: NTIS HC/MF A22 CSCL 03B

N91-14981*# Five-College Astronomy Dept., Amherst, MA.
THERMAL EMISSION FROM INTERSTELLAR DUST IN AND NEAR THE PLEIADES
Richard E. White *In* NASA, Ames Research Center, Interstellar Dust: Contributed Papers Dec. 1989 p 317-321 Prepared in cooperation with Wyoming Univ., Laramie (For primary document see N91-14897 06-88)
Avail: NTIS HC/MF A22 CSCL 03B

N91-14982*# California Inst. of Tech., Pasadena. Lab. of Physics.
TEMPERATURE DISTRIBUTION OF DUST IN LUMINOUS IRAS GALAXIES
David P. Carico *In* NASA, Ames Research Center, Interstellar Dust: Contributed Papers Dec. 1989 p 325-329 (For primary document see N91-14897 06-88)
Avail: NTIS HC/MF A22 CSCL 03B

N91-14983*# Yerkes Observatory, Williams Bay, WI.
THE 100 AND 160 MICRON MAPS OF THE DUST REEMISSION FROM THE NUCLEUS AND INNER-ARM REGIONS OF NGC 6946
Gregory Engargiola, D. A. Harper, and D. T. Jaffe (Texas Univ., Austin.) *In* NASA, Ames Research Center, Interstellar Dust: Contributed Papers Dec. 1989 p 331-338 (For primary document see N91-14897 06-88)
Avail: NTIS HC/MF A22 CSCL 03B

N91-14984*# Pisa Univ. (Italy). Ist. di Astronomia.
GRAINS IN GALACTIC HALOES
Andrea Ferrara, Bruno Barsella, F. Ferrini, J. Mayo Greenberg, and Santi Aiello (Florence Univ., Italy) *In* NASA, Ames Research Center, Interstellar Dust: Contributed Papers Dec. 1989 p 339-343 (For primary document see N91-14897 06-88)
Avail: NTIS HC/MF A22 CSCL 03B

N91-14985*# Mullard Radio Astronomy Observatory, Cambridge (England).
DOES THE FAR-INFRARED/RADIO CORRELATION IN SPIRAL GALAXIES EXTEND TO THE SPATIAL DOMAIN
Neil A. Howarth and A. J. Fitt *In* NASA, Ames Research Center, Interstellar Dust: Contributed Papers Dec. 1989 p 345-346 (For primary document see N91-14897 06-88)
Avail: NTIS HC/MF A22 CSCL 03B

N91-14988*# National Aeronautics and Space Administration. Ames Research Center, Moffett Field, CA.
FAR INFRARED STRUCTURE OF SPIRAL GALAXIES FROM THE IRAS CPC IMAGES Abstract Only
Richard J. Wainscoat, Arati Chokshi (National Academy of Sciences - National Research Council, Washington, DC.), and Laurance R. Doyle *In its* Interstellar Dust: Contributed Papers Dec. 1989 p 35 (For primary document see N91-14897 06-88)
Avail: NTIS HC/MF A22 CSCL 03A

N91-14989*# Harvard-Smithsonian Center for Astrophysics, Cambridge, MA.
GALAXY FORMATION BY DUST Abstract Only
Boqi Wang and Goerge B. Field *In* NASA, Ames Research Center, Interstellar Dust: Contributed Papers Dec. 1989 p 359 (For primary document see N91-14897 06-88)
Avail: NTIS HC/MF A22 CSCL 03A

N91-14991*# Universitaets-Sternwarte, Jena (German D.R.).
STEPS TOWARD INTERSTELLAR SILICATE DUST MINERALOGY
J. Dorschner, J. Guertler, and Th. Henning *In* NASA, Ames Research Center, Interstellar Dust: Contributed Papers Dec. 1989 p 369-370 (For primary document see N91-14897 06-88)
Avail: NTIS HC/MF A22 CSCL 03B

N91-14992*# Leiden Univ. (Netherlands). Lab. Astrophysics.
SCATTERING BY FLUFFY GRAINS Abstract Only
J. I. Hage and J. Mayo Greenberg *In* NASA, Ames Research Center, Interstellar Dust: Contributed Papers Dec. 1989 p 371 (For primary document see N91-14897 06-88)
Avail: NTIS HC/MF A22 CSCL 03B

N91-14997*# Universitaets-Sternwarte, Jena (German D.R.).
SIZE DISTRIBUTION OF DUST GRAINS: A PROBLEM OF SELF-SIMILARITY
Th. Henning, J. Dorschner, and J. Guertler *In* NASA, Ames Research Center, Interstellar Dust: Contributed Papers Dec. 1989 p 395-396 (For primary document see N91-14897 06-88)
Avail: NTIS HC/MF A22 CSCL 03B

N91-14998*# National Aeronautics and Space Administration. Ames Research Center, Moffett Field, CA.
STOCHASTIC HISTORIES OF DUST GRAINS IN THE INTERSTELLAR MEDIUM
Kurt Liffman and D. D. Clayton (Rice Univ., Houston, TX.) *In its* Interstellar Dust: Contributed Papers Dec. 1989 p 397-398 (For primary document see N91-14897 06-88)
Avail: NTIS HC/MF A22 CSCL 03B

N91-14999*# Manuel (Lawrence R.), Berkeley, CA.
SUPERAROMATICS: THE KEY TO A UNIFIED COSMIC DUST THEORY
Lawrence R. Manuel *In* NASA, Ames Research Center, Interstellar Dust: Contributed Papers Dec. 1989 p 399-404 (For primary document see N91-14897 06-88)
Avail: NTIS HC/MF A22 CSCL 03B

N91-15000*# Colorado Univ., Boulder. Center for Astrophysics and Space Astronomy.
THE ORIGIN OF MICROGRAINS
Theodore P. Snow, Jr., C. Gregory Seab, Richard H. Buss, Jr., Karl Josafatsson, and Kris Sellgren (Hawaii Univ., Honolulu.) *In* NASA, Ames Research Center, Interstellar Dust: Contributed Papers Dec. 1989 p 405-406 (For primary document see N91-14897 06-88)
Avail: NTIS HC/MF A22 CSCL 03B

N91-15001*# Kapteyn Astronomical Lab., Groningen (Netherlands).
PROPERTIES OF GRAINS DERIVED FROM IRAS OBSERVATIONS OF DUST
P. R. Wesselius, Grzegorz Chlewicki, and Rene J. Laureijs *In* NASA, Ames Research Center, Interstellar Dust: Contributed Papers Dec. 1989 p 407 (For primary document see N91-14897 06-88)
Avail: NTIS HC/MF A22 CSCL 03B

N91-15002*# Planetary Science Inst., Tucson, AZ.
A SPECTRAL DIFFERENCE BETWEEN SILICATES IN COMET HALLEY AND INTERSTELLAR SILICATES
Humberto Campins and Eileen V. Ryan *In* NASA, Ames Research Center, Interstellar Dust: Contributed Papers Dec. 1989 p 411-413 Submitted for publication (For primary document see N91-14897 06-88)
Avail: NTIS HC/MF A22 CSCL 03B

N91-15003*# National Aeronautics and Space Administration. Ames Research Center, Moffett Field, CA.
THE NATURE OF COMETARY DUST AS DETERMINED FROM INFRARED OBSERVATIONS
K. S. Krishna Swamy, Scott A. Sandford, Louis J. Allamandola, Fred C. Witteborn, and Jesse D. Bregman *In its* Interstellar Dust: Contributed Papers Dec. 1989 p 415-416 (For primary document see N91-14897 06-88)
Avail: NTIS HC/MF A22 CSCL 03B

N91-15004*# Aerospace Corp., Los Angeles, CA. Space Sciences Lab.
THE 10 MICRON SPECTRAL STRUCTURE IN COMETS
David K. Lynch, Ray W. Russell, and Humberto Campins (Planetary Science Inst., Tucson, AZ.) *In* NASA, Ames Research Center, Interstellar Dust: Contributed Papers Dec. 1989 p 417-422 Sponsored by NSF (For primary document see N91-14897 06-88)
(Contract NAS2-12370)
Avail: NTIS HC/MF A22 CSCL 03B

N91-15005*# Leiden Univ. (Netherlands). Lab. of Astrophysics.
A COMPARATIVE STUDY OF THE CONTINUUM AND EMISSION CHARACTERISTICS OF COMET DUST. 1: ARE THE SILICATES IN COMET HALLEY AND KOHOUTEK AMORPHOUS OR CRYSTALLINE
Zhao Nansheng, J. Mayo Greenberg, and J. I. Hage *In* NASA, Ames Research Center, Interstellar Dust: Contributed Papers Dec. 1989 p 423-427 (For primary document see N91-14897 06-88)
Avail: NTIS HC/MF A22 CSCL 03B

N91-15006*# State Univ. of New York, Stony Brook. Dept. of Earth and Space Sciences.
THE 3.4 MICRON EMISSION IN COMETS Abstract Only
Tim Y. Brooke, Roger F. Knacke, T. C. Owen, and Alan T. Tokunaga (Hawaii Univ., Honolulu.) *In* NASA, Ames Research Center, Interstellar Dust: Contributed Papers Dec. 1989 p 431 (For primary document see N91-14897 06-88)
Avail: NTIS HC/MF A22 CSCL 03B

N91-15007*# Cornell Univ., Ithaca, NY. Lab. for Planetary Studies.
THE PRE- AND POST-ACCRETION IRRADIATION HISTORY OF COMETARY ICES
Christopher Chyba and Carl Sagan *In* NASA, Ames Research Center, Interstellar Dust: Contributed Papers Dec. 1989 p 433-435 (For primary document see N91-14897 06-88)
Avail: NTIS HC/MF A22 CSCL 03B

N91-15008*# European Space Agency. European Space Research and Technology Center, ESTEC, Noordwijk (Netherlands). Dept. of Space Science.
EXPERIMENTAL EVIDENCE FOR AMORPHOUS CARBON GRAINS IN COMETS
Luigi Colangeli, G. Schwehm, E. Bussoletti, A. Blanco, A. Borghesi, Sergio Fonti, and Vincenso Orofino (Lecce Univ., Italy) *In* NASA, Ames Research Center, Interstellar Dust: Contributed Papers Dec. 1989 p 437-442 (For primary document see N91-14897 06-88)
Avail: NTIS HC/MF A22 CSCL 03B

N91-15009*# Warsaw Univ. (Poland). Dept. of Chemistry.
VEGA-GIOTTO FLYBY MISSIONS AND COMETARY COSMOGONY
Bruno Lang *In* NASA, Ames Research Center, Interstellar Dust: Contributed Papers Dec. 1989 p 445-450 (For primary document see N91-14897 06-88)
Avail: NTIS HC/MF A22 CSCL 03B

N91-15010*# California Univ., Berkeley. Space Sciences Lab.
THE COMPOSITION OF HEAVY MOLECULAR IONS INSIDE THE IONOPAUSE OF COMET HALLEY
David L. Mitchell, R. P. Lin, K. A. Anderson, C. W. Carlson, D. W. Curtis, A. Korth, H. Reme, J. A. Sauvaud, C. dUston, and D. A. Mendis (California Univ., San Diego.) *In* NASA, Ames Research Center, Interstellar Dust: Contributed Papers Dec. 1989 p 451-452 (For primary document see N91-14897 06-88)
Avail: NTIS HC/MF A22 CSCL 03B

N91-15011*# British Museum of Natural History, London (England). Dept. of Mineralogy.
ATOMIC ENVIRONMENTS IN IRON METEORITES USING EXAFS
G. Cressey, A. J. Dent, B. Dobson, A. Evans, G. N. Greaves, C. M. B. Henderson, R. Hutchison, R. N. Jenkins, S. P. Thompson, and R. Zhu (Science Research Council, Daresbury, England) *In* NASA, Ames Research Center, Interstellar Dust: Contributed Papers Dec. 1989 p 455-461 (For primary document see N91-14897 06-88)
Avail: NTIS HC/MF A22 CSCL 03B

N91-15012*# Abastumani Astrophysical Observatory, Georgia (USSR).
DUST OF ORIONID METEOR SHOWER IN THE EARTH ATMOSPHERE BEFORE AND AFTER HALLEY'S COMET
G. Mateshvili and Yu. Mateshvili *In* NASA, Ames Research Center, Interstellar Dust: Contributed Papers Dec. 1989 p 463-468 (For primary document see N91-14897 06-88)
Avail: NTIS HC/MF A22 CSCL 03B

N91-15016*# National Aeronautics and Space Administration. Ames Research Center, Moffett Field, CA.
SUBLIMATING ICY PLANETESIMALS AS THE SOURCE OF NUCLEATION SEEDS FOR GRAIN CONDENSATION IN CLASSICAL NOVAE
John J. Matese, D. P. Whitmire (University of Southwestern Louisiana, Lafayette.), and R. T. Reynolds *In its* Interstellar Dust: Contributed Papers Dec. 1989 p 485-488 (For primary document see N91-14897 06-88)
Avail: NTIS HC/MF A22 CSCL 03B

N91-15017*# Tokyo Univ. (Japan). Dept. of Astronomy.
DUST FORMATION AROUND M-TYPE STARS
Takashi Onaka *In* NASA, Ames Research Center, Interstellar Dust: Contributed Papers Dec. 1989 p 489-494 Sponsored in part by Ministry of Education, Science and Culture, Sagamihara, Japan (For primary document see N91-14897 06-88)
Avail: NTIS HC/MF A22 CSCL 03B

N91-15018*# National Aeronautics and Space Administration. Ames Research Center, Moffett Field, CA.
SUBLIMATING COMETS AS THE SOURCE OF NUCLEATION SEEDS FOR GRAIN CONDENSATION IN THE GAS OUTFLOW FROM AGB STARS
D. P. Whitmire, John J. Matese (University of Southwestern Louisiana, Lafayette.), and R. T. Reynolds *In its* Interstellar Dust: Contributed Papers Dec. 1989 p 495-501 (For primary document see N91-14897 06-88)
Avail: NTIS HC/MF A22 CSCL 03B

N91-15020*# Crimean Astrophysical Observatory (USSR).
THE INFLUENCE OF GRAIN GROWTH IN CIRCUMSTELLAR DUST ENVELOPES ON OBSERVED COLORS AND POLARIZATION OF SOME ERUPTIVE STARS
Yu. S. Efimov *In* NASA, Ames Research Center, Interstellar Dust: Contributed Papers Dec. 1989 p 507-514 (For primary document see N91-14897 06-88)
Avail: NTIS HC/MF A22 CSCL 03B

N91-15022*# National Aeronautics and Space Administration. Ames Research Center, Moffett Field, CA.
CARBON STARS WITH ALPHA-C:H EMISSION Abstract Only
Florence Gerbault and John H. Goebel *In its* Interstellar Dust: Contributed Papers Dec. 1989 p 51 (For primary document see N91-14897 06-88)
Avail: NTIS HC/MF A22 CSCL 03B

N91-15023*# National Aeronautics and Space Administration. Ames Research Center, Moffett Field, CA.
NEW CIRCUMSTELLAR DUST COMPONENT IN OXYGEN RICH ENVIRONMENTS Abstract Only
John H. Goebel and Florence Gerbault *In its* Interstellar Dust: Contributed Papers Dec. 1989 p 51 (For primary document see N91-14897 06-88)
Avail: NTIS HC/MF A22 CSCL 03B

N91-15024*# Tata Inst. of Fundamental Research, Bombay (India).
TYPE OF SILICATE FEATURE IN OXYGEN RICH STELLAR ENVELOPES
K. V. K. Iyengar and T. N. Rengarajan *In* NASA, Ames Research Center, Interstellar Dust: Contributed Papers Dec. 1989 p 521-522 (For primary document see N91-14897 06-88)
Avail: NTIS HC/MF A22 CSCL 03B

N91-15025*# National Aeronautics and Space Administration. Ames Research Center, Moffett Field, CA.
INTERSTELLAR EXTINCTION AT 10-20 MICRONS
Janet P. Simpson and Robert H. Rubin (California Univ., Los Angeles.) *In its* Interstellar Dust: Contributed Papers Dec. 1989 p 523-526 (For primary document see N91-14897 06-88)
Avail: NTIS HC/MF A22 CSCL 03B

N91-15026*# Amsterdam Univ. (Netherlands). Astronomical Inst.
DUST AROUND MIRA VARIABLES: AN ANALYSIS OF IRAS LRS SPECTRA
S. Slijkhuis *In* NASA, Ames Research Center, Interstellar Dust: Contributed Papers Dec. 1989 p 527-528 (For primary document see N91-14897 06-88)
Avail: NTIS HC/MF A22 CSCL 03B

N91-15027*# Indian Inst. of Astrophysics, Bangalore.
POLARIZATION DUE TO DUST SCATTERING IN THE PLANETARY NEBULA Cn1-1
Harish C. Bhatt *In* NASA, Ames Research Center, Interstellar Dust: Contributed Papers Dec. 1989 p 531-532 (For primary document see N91-14897 06-88)
Avail: NTIS HC/MF A22 CSCL 03B

N91-15029*# Beijing Observatory, Huairou (China).
COMPACT REFLECTION NEBULAE, A TRANSIT PHASE OF EVOLUTION FROM POST-AGB TO PLANETARY NEBULAE Abstract Only
J. Y. Hu and S. Slijkhuis (Amsterdam Univ., Netherlands) *In* NASA, Ames Research Center, Interstellar Dust: Contributed Papers Dec. 1989 p 535 (For primary document see N91-14897 06-88)
Avail: NTIS HC/MF A22 CSCL 03B

N91-15030*# Polish Academy of Sciences, Torun. Lab. of Astrophysics.
CONTINUOUS INFRARED EMISSION OF PROTO- AND YOUNG-PLANETARY NEBULAE Abstract Only
Ryszard Szczerba *In* NASA, Ames Research Center, Interstellar Dust: Contributed Papers Dec. 1989 p 537-538 (For primary document see N91-14897 06-88)
Avail: NTIS HC/MF A22 CSCL 03B

N91-15031*# Royal Observatory, Edinburgh (Scotland).
THE DISCOVERY OF A HIGHLY POLARIZED BIPOLAR NEBULA
Ramon D. Wolstencroft, S. M. Scarrott, and J. Menzies (South African Astronomical Observatory, Cape Town.) *In* NASA, Ames Research Center, Interstellar Dust: Contributed Papers Dec. 1989 p 539-540 (For primary document see N91-14897 06-88)
Avail: NTIS HC/MF A22 CSCL 03B

N91-15032*# National Aeronautics and Space Administration. Goddard Space Flight Center, Greenbelt, MD.
INFRARED EMISSION FROM THE SUPERNOVA REMNANT PUPPIS A: DUST AND GAS PARAMETERS
Richard G. Arendt (Illinois Univ., Urbana.), Eli Dwek, and R Petre *In* NASA, Ames Research Center, Interstellar Dust: Contributed Papers Dec. 1989 p 543-548 (For primary document see N91-14897 06-88)
Avail: NTIS HC/MF A22 CSCL 03B

91 LUNAR AND PLANETARY EXPLORATION

Includes planetology; and manned and unmanned flights.
For spacecraft design or space stations see *18 Spacecraft Design, Testing and Performance.*

N91-15112 Council for National Academic Awards (England).
THE ROTATION OF VENUS AND ITS ATMOSPHERE Ph.D. Thesis
John McCue 1989 198 p
Avail: Univ. Microfilms Order No. BRDX88761

The evolutions of both the rotation period and angle of obliquity of the planet Venus are considered. Researchers conclude that the planet's initial configuration may have been a slow period of between 33 and 48 days, with an obliquity of about 170 degrees (i.e., retrograde). Many long-held theories of the origin of the solar system, though, such as the accretion hypothesis, predict an initial regular spin for all the planets, each having a period of about 20 hours and an obliquity of about zero. This present work shows that a collision between Venus and a planetoid, or the capture of a retrograde satellite, are feasible mechanisms for producing the required initial period of between 33 and 48 days. It is then shown that, under the action of two solar gravitational torques (one on the body of the planet and the other on its atmosphere) the spin of Venus can evolve to its current state. It should be noted that the capture hypothesis of the origin of the solar system does, de facto, permit an initial retrograde rotation for Venus after its formation. During the course of this work other substantial aspects were considered. It was shown, for example, that the rapid retrograde rotation of the Venusian atmosphere itself may indeed be maintained by the solar torque on the thermal atmospheric tide. Further, a tephigram was drawn for the Venusian atmosphere for the first time. There emerged predictions that it may be possible for a water condensate to exist at a height of about 60 km, and that Venus' large-scale atmospheric convection occurs between 35 km and 55 km. Also, the aspect was considered of the possible resonance of Venus' present rotation period with that of the Earth. It was concluded that the current near-resonance is coincidental. Finally, the rotation period of Mercury was studied. The conclusion that it is not currently stable implies the existence of an offset between the planet's centre of mass and its geometrical centre.
Dissert. Abstr.

N91-15113 North Carolina State Univ., Raleigh.
A MESOSCALE PLANETARY BOUNDARY LAYER NUMERICAL MODEL FOR SIMULATIONS OF TOPOGRAPHICALLY INDUCED CIRCULATIONS Ph.D. Thesis
Ching-Yuang Albert Huang 1990 268 p
Avail: Univ. Microfilms Order No. DA9023385

A mesoscale planetary boundary layer (PBL) numerical model is developed to investigate airflow over complex topography. The model physics includes PBL turbulent transfer, atmospheric longwave and shortwave radiation, diurnal energy budgets over ground, cloud microphysics, and subgrid cumulus parameterization.

The model utilizes a new fourth order Crowley advection scheme which preserves phase and amplitude much better than other Crowley schemes. Turbulence closures using the turbulent kinetic energy (TKE) and dissipation equations are investigated. One-dimensional (1-D) model results show that the PBL flows under various stability conditions are not significantly sensitive to the modified Blackadar's and Kolmogorov's eddy mixing length formations, although the latter yields excessively large mixing lengths in the entrainment region of the upper PBL. With the same prognostic TKE equation, the model results show insensitivity of the 1-D flow to the details of diagnostic formulations in the closures and to eddy Prandtl numbers. A 2-D model is used to stimulate January 28 cold-air outbreak over the Gulf Stream region during the IOP-2 (Intensive Observation Period) of the 1986 Genesis of Atlantic Lows Experiment (GALE). The modeled 2-D circulation system is found to be sensitive to Prandtl number, in contrast to the 1-D model results. Two cases with 3-D idealized flow are also simulated for the same GALE IOP. The model is also applied to simulate the 3-D airflow past Taiwan mountains. The role of the PBL effects in changing the flow separation and stagnation points is found to be more important for the upstream flow than the downstream flow. Dissert. Abstr.

N91-15114*# State Univ. of New York, Stony Brook. Inst. for Terrestrial and Planetary Atmospheres.
STUDIES OF THE CHEMISTRY OF THE NIGHTSIDE IONOSPHERE OF VENUS Final Report, 1 Jul. 1988 - 30 Nov. 1990
J. L. Fox Jan. 1991 151 p
(Grants NAG2-523; SUNYRF-4313159A)
(NASA-CR-187714; NAS 1.26:187714) Avail: NTIS HC/MF A08 CSCL 03B

A combination of numerical modeling and analysis of the Pioneer Venus UADS data base is studied, specifically data from the orbiter ion mass spectrometer (OIMS), orbiter neutral mass spectrometer (ONMS), and orbiter electron temperature probe (OETP). A one dimensional model of the Venus nightside ionosphere was set up in which downward fluxes of atomic ions are introduced at the upper boundary to simulate transport of ions from the dayside. The model shows that the densities of mass-28 ions, CO(+) + N(2+), resulting from an influx of atomic ions from the dayside are quite small, due to the high ionization potentials of CO and N2 that make chemical production difficult. A look at the data reveals that the actual densities of mass-28 ions are quite variable, from values near 10 to more than 10(exp 4) cm(exp -3). The excess mass-28 ions are assumed to be produced by electron precipitation and that the presence of high densities of mass-28 ions is a signature of auroral precipitation. A discussion of the atomic oxygen green line in the nightglow of Venus, which is produced mainly by dissociative recombination of O(2+), is presented. Original calculations of production rates of excited states for models based on Pioneer Venus data are also presented.
Author

N91-14360*# California Univ., Los Angeles. Dept. of Earth and Space Sciences.
SPECIFICATION GOALS FOR A MARS SEISMIC NETWORK
Paul M. Davis *In* JPL, Proceedings of the Mars Global Network Mission Workshop 1 Jun. 1990 p 159-173 (For primary document see N91-14359 06-12)
Avail: NTIS HC/MF A19 CSCL 03B

N91-14361*# Jet Propulsion Lab., California Inst. of Tech., Pasadena.
A POLAR ORBIT FOR THE MARS GLOBAL NETWORK MISSION
Philip Knocke *In its* Proceedings of the Mars Global Network Mission Workshop 1 Jun. 1990 p 177-189 (For primary document see N91-14359 06-12)
Avail: NTIS HC/MF A19 CSCL 03B

N91-14362*# Science Applications International Corp., Schaumburg, IL.
A GLOBAL VIEW OF LANDER-TO-ORBITER COMMUNICATIONS ACCESSIBILITY FOR A MARS GLOBAL NETWORK MISSION
Alan L. Friedlander *In* JPL, Proceedings of the Mars Global Network Mission Workshop 1 Jun. 1990 p 205-221 (For primary document see N91-14359 06-12)
Avail: NTIS HC/MF A19 CSCL 03B

N91-15094# Commissariat a l'Energie Atomique, Saclay (France). Service d'Astrophysique.
ACCRETION DISK INSTABILITY AND SPOKES IN SATURN'S RINGS
M. Tagger, R. N. Henriksen, and R. Pellat (Ecole Polytechnique, Palaiseau, France) *In* ESA, Plasma Astrophysics Aug. 1990 p 261-262 (For primary document see N91-15046 06-90)
Copyright Avail: NTIS HC/MF A14

92 SOLAR PHYSICS

Includes solar activity, solar flares, solar radiation and sunspots.

For related information see *93 Space Radiation.*

N91-15115*# Texas Univ., Austin. Inst. for Fusion Studies.
CORONAL MASS EJECTIONS
R. S. Steinolfson [1990] 27 p Sponsored by NSF
(Grants NAG5-1092; NAGw-1324)
(NASA-CR-186579; NAS 1.26:186579) Avail: NTIS HC/MF A03 CSCL 03B

Coronal mass ejections (CMEs) are now recognized as an important component of the large-scale evolution of the solar corona. Some representative observations of CMEs are reviewed with emphasis on more recent results. Recent observations and theory are examined as they relate to the following aspects of CMEs: (1) the role of waves in determining the white-light signature; and (2) the mechanism by which the CME is driven (or launched) into the corona. B.G.

N91-15116 California Univ., San Diego.
FLARE HEATING AND IONIZATION OF THE LOW SOLAR CHROMOSPHERE Ph.D. Thesis
Thomas Robert Metcalf 1990 184 p
Avail: Univ. Microfilms Order No. DA9024034

The long-standing question of what mechanisms are responsible for observations of flare heating at the temperature minimum region of the solar atmosphere is examined. Two neutral magnesium spectral lines formed in the temperature minimum region and the low chromosphere, lambda lambda 4571 and 5173 A, were observed and are used to quantify the changes in the atmospheric structure as a function of time. A technique for inverting the MgI lines to yield the vertical temperature and electron density structure in the atmosphere is described. The inversion uses a first order perturbation analysis applied to a model atmosphere to determine the changes in the model's temperature and electron density structures required to bring the calculated and observed spectral lines into agreement. Since small perturbations in the observed lines can yield large changes in the required perturbation of the model atmosphere, the inversion must be stabilized and a smoothness constraint is imposed on the solution to ensure stability. After a discussion of eight proposed heating and ionization mechanisms and predictions of the effects of each on the temperature minimum region, this inversion technique is applied to five separate solar flares, yielding the changes in temperature and electron density as a function of time and atmospheric depth. These observations, along with observations of hard and soft x rays from the SMM and GOES satellites, are compared to the predictions of the eight proposed mechanisms to show that the initial effects in all five flares are consistent with backwarming by enhanced Balmer and Paschen continuum radiation originating in

the upper chromosphere. Extended heating observed in two of the flares is most likely due to UV irradiation. Dissert. Abstr.

N91-15117*# National Aeronautics and Space Administration. Lewis Research Center, Cleveland, OH.
SOLAR RADIATION ON MARS: UPDATE 1990
Joseph Appelbaum (Tel-Aviv Univ., Israel) and Dennis J. Flood Oct. 1990 36 p
(Grant NAGw-2022)
(NASA-TM-103623; E-5783; NAS 1.15:103623) Avail: NTIS HC/MF A03 CSCL 03B

Detailed information on solar radiation characteristics on Mars are necessary for effective design of future planned solar energy systems operating on the surface of Mars. The authors present a procedure and solar radiation related data from which the diurnally and daily variation of the global, direct beam and diffuse insolation on Mars are calculated. The radiation data are based on measured optical depth of the Martian atmosphere derived from images taken of the Sun with a special diode on the Viking Lander cameras and computation based on multiple wavelength and multiple scattering of the solar radiation. This work is an update to NASA-TM-102299 and includes a refinement of the solar radiation model. Author

N91-15118# National Environmental Satellite Service, Washington, DC.
NA-9 SOLAR BACKSCATTER ULTRAVIOLET (SBUV/2) INSTRUMENT AND DERIVED OZONE DATA Status Report, 29 Jan. 1990
Walter G. Planet Jun. 1990 217 p
(AD-A227449; NESDIS-53) Avail: NTIS HC/MF A10 CSCL 04/1

The NOAA ozone monitoring program was initiated by the National Environmental Satellite Data and Information Service (NESDIS) in December 1984 with the launch of the NOAA-9 operational satellite carrying the first operational Solar Backscatter Ultraviolet (SBUV/2) spectrometer. The primary conclusions include the following: (1) The NOAA-9 equator crossing time is continually later in the day due to precession of the orbit. This results in an ever-increasing angle of solar incidence on the diffuser plate, approaching values beyond those used in pre-launch radiometric calibration and testing. (2) The increasing equator crossing times also result in observations at greater solar zenith angles at the observed scenes introducing an uncertain zenith-angle dependency on the retrieved ozone values. (3) Compared to other sources of data (SBUV and TOMS on Nimbus 7 and the ground-base Dobson network), the total ozone amount derived from the SBUV/2 shows an increasing greater difference with SBUV/2 values being higher. Compared to selected subsets of Dobson values, the SBUV/2 - Dobson differences are diverging about 0.3 to 0.5 percent per year. (4) Short-term variations in total ozone derived from SBUV/2 measurements show excellent correlation with SBUV and TOMS data with respect to day-to-day, seasonal and latitudinal variabilities. GRA

N91-15047# European Space Agency. European Space Research and Technology Center, ESTEC, Noordwijk (Netherlands). Dept. of Space Science.
SOLAR MAGNETIC FLUX-TUBES AND CORONAL LOOPS
B. H. Foing *In its* Plasma Astrophysics Aug. 1990 p 1-6 (For primary document see N91-15046 06-90)
Copyright Avail: NTIS HC/MF A14

N91-15048# Toyama Univ. (Japan). Dept. of Applied Maths and Physics.
HIGH-ENERGY PARTICLE ACCELERATION DURING THE IMPLOSION DRIVEN BY 3-DIMENSIONAL X-TYPE CURRENT LOOP COALESCENCE IN SOLAR FLARES
Jun-Ichi Sakai *In* ESA, Plasma Astrophysics Aug. 1990 p 7-12 (For primary document see N91-15046 06-90)
Copyright Avail: NTIS HC/MF A14

N91-15049# Nagoya Univ. (Japan). Plasma Science Center.
SOLAR FLARES AND PARTICLE ACCELERATION
Y. Ohsawa and Y. Terashima *In* ESA, Plasma Astrophysics Aug. 1990 p 13-19 (For primary document see N91-15046 06-90)
Copyright Avail: NTIS HC/MF A14

N91-15051# Abastumani Astrophysical Observatory, Georgia (USSR).
A NEW MODEL OF SPICULE FORMATION IN THE SUN CHROMOSPHERE
A. D. Pataraya, A. L. Taktakishvili, and B. B. Chargeishvili *In* ESA, Plasma Astrophysics Aug. 1990 p 25-27 (For primary document see N91-15046 06-90)
Copyright Avail: NTIS HC/MF A14

N91-15052# Kharkov State Univ. (USSR).
NONLINEAR SURFACE MHD WAVES IN THE INHOMOGENEOUS PLASMA WITH CUSP-RESONANCE IN UPPER SOLAR ATMOSPHERE
E. A. Fedutenko, V. I. Lapshin, and K. N. Stepanov *In* ESA, Plasma Astrophysics Aug. 1990 p 29-32 (For primary document see N91-15046 06-90)
Copyright Avail: NTIS HC/MF A14

N91-15053# Academy of Sciences (USSR), Moscow. Inst. of the Physics of the Earth.
FILAMENTARY STRUCTURES IN THE SUN'S ATMOSPHERE AS SINGULAR ALFVEN WAVES
N. V. Petviashvili *In* ESA, Plasma Astrophysics Aug. 1990 p 33-34 (For primary document see N91-15046 06-90)
Copyright Avail: NTIS HC/MF A14

N91-15054# Abastumani Astrophysical Observatory, Georgia (USSR).
ON SOME PECULIARITIES OF SOLAR DIFFERENTIAL ROTATION
M. Sh. Gigolashvili and E. V. Khutsishvili *In* ESA, Plasma Astrophysics Aug. 1990 p 35-37 (For primary document see N91-15046 06-90)
Copyright Avail: NTIS HC/MF A14

N91-15055# Kharkov State Univ. (USSR).
NONLINEARITY INFLUENCE IN LOCAL RESONANCE REGIONS ON THE ALFVEN WAVES PROPAGATION IN SOLAR CORONA
V. I. Lapshin, K. N. Stepanov, and V. O. Strasser *In* ESA, Plasma Astrophysics Aug. 1990 p 39-40 (For primary document see N91-15046 06-90)
Copyright Avail: NTIS HC/MF A14

N91-15056# Universidad de Los Andes, Merida (Venezuela). Grupo de Astrofisica.
LINEAR STABILITY AND MHD WAVE PROPAGATION IN PLASMAS WITH SOLAR ABUNDANCES
M. H. Ibanez and O. B. Escalona *In* ESA, Plasma Astrophysics Aug. 1990 p 41-44 (For primary document see N91-15046 06-90)
Copyright Avail: NTIS HC/MF A14

N91-15066# Academy of Sciences (USSR), Irkutsk. Inst. of Terrestrial Magnetism and Radio Wave Propagation.
A NUMERICAL CALCULATION OF PARAMETERS OF EXPLOSION MHD SHOCK WAVES FROM MODERATE SOLAR FLARES
S. V. Uralova and A. M. Urolov *In* ESA, Plasma Astrophysics Aug. 1990 p 99-101 (For primary document see N91-15046 06-90)
Copyright Avail: NTIS HC/MF A14

N91-15108# Academy of Sciences (USSR), Irkutsk. Inst. of Terrestrial Magnetism and Radio Wave Propagation.
INFLUENCE OF THE PARAMETER DISTRIBUTION OF THE SOLAR WIND NEAR THE SUN UPON ITS STRUCTURE AT THE EARTH'S ORBIT
A. P. Kaigorodov and V. G. Fainshtein *In* ESA, Plasma Astrophysics Aug. 1990 p 331-334 (For primary document see N91-15046 06-90)
Copyright Avail: NTIS HC/MF A14

93 SPACE RADIATION

Includes cosmic radiation; and inner and outer earth's radiation belts.

For biological effects of radiation see *52 Aerospace Medicine*. For theory see *73 Nuclear and High-Energy Physics*.

N91-14910*# Academy of Sciences (USSR), Dushanbe. Inst. of Astrophysics.
INTERSTELLAR DUST AS GENERATOR OF X RAY RADIATION
Subhon Ibadov *In* NASA, Ames Research Center, Interstellar Dust: Contributed Papers Dec. 1989 p 49-54 (For primary document see N91-14897 06-88)
Avail: NTIS HC/MF A22 CSCL 03B

N91-14912*# National Aeronautics and Space Administration. Goddard Space Flight Center, Greenbelt, MD.
OBSERVATIONS OF THE DIFFUSE UV RADIATION FIELD
Jayant Murthy, R. C. Henry, P. D. Feldman, and P. D. Tennyson (Massachusetts Inst. of Tech., Lexington.) *In* NASA, Ames Research Center, Interstellar Dust: Contributed Papers Dec. 1989 p 57-58 (For primary document see N91-14897 06-88)
(Grant NAG5-619)
Avail: NTIS HC/MF A22 CSCL 03B

N91-14920*# Leiden Univ. (Netherlands).
A SURVEY FOR PAH EMISSION IN H II REGIONS, PLANETARY AND PROTO-PLANETARY NEBULAE
M. deMuizon, P. Cox, and J. Lequeux (Ecole Normale Superieure, Paris, France) *In* NASA, Ames Research Center, Interstellar Dust: Contributed Papers Dec. 1989 p 95-99 Previously announced as N90-19129 (For primary document see N91-14897 06-88)
Avail: NTIS HC/MF A22 CSCL 03B

N91-14921*# Mount Stromlo and Siding Spring Observatory, Canberra (Australia).
PAH EMISSION FROM NOVA CEN 1986
A. R. Harry Hyland and P. J. McGregor *In* NASA, Ames Research Center, Interstellar Dust: Contributed Papers Dec. 1989 p 101-106 (For primary document see N91-14897 06-88)
Avail: NTIS HC/MF A22 CSCL 03B

N91-14924*# Commissariat a l'Energie Atomique, Gif-sur-Yvette (France). Service d'Astrophysique.
RED FLUORESCENCE AND 3-12 MICRON EMISSION IN NGC 2023, HD 44179, M 82, AND LYNDS 1780
Charles Ryter and Louis B. dHendecourt (Paris VII Univ., France) *In* NASA, Ames Research Center, Interstellar Dust: Contributed Papers Dec. 1989 p 111-114 (For primary document see N91-14897 06-88)
Avail: NTIS HC/MF A22 CSCL 03B

N91-14926*# National Aeronautics and Space Administration. Ames Research Center, Moffett Field, CA.
SPECTRAL STRUCTURE NEAR THE 11.3 MICRON EMISSION FEATURE Abstract Only
Fred C. Witteborn, Scott A. Sandford, Jesse D. Bregman, Louis J. Allamandola, M. Cohen, and Diane Wooden *In its* Interstellar Dust: Contributed Papers Dec. 1989 p 11 (For primary document see N91-14897 06-88)
Avail: NTIS HC/MF A22 CSCL 03B

N91-14928*# Centre d'Etude Spatiale des Rayonnements, Toulouse (France).
THE 3.3 MICRON EMISSION FEATURE: MAP OF THE GALACTIC DISK, 10 DEG LESS THAN 1 LESS THAN 35 DEG, - 6 DEG LESS THAN B LESS THAN 6 DEG
Martin Giard, F. Pajot, Emanuel Caux, J. M. Lamarre (Centre National de la Recherche Scientifique, Verrieres-Le Buisson, France), and G. Serra *In* NASA, Ames Research Center, Interstellar Dust: Contributed Papers Dec. 1989 p 129-130 (For primary document see N91-14897 06-88)
Avail: NTIS HC/MF A22 CSCL 03B

N91-14929*# Aerospace Corp., Los Angeles, CA. Space Sciences Lab.
IR EMISSION AND UV EXTINCTION IN TWO OPEN CLUSTERS Abstract Only
James A. Hackwell and James H. Hecht *In* NASA, Ames Research Center, Interstellar Dust: Contributed Papers Dec. 1989 p 131 (For primary document see N91-14897 06-88)
Avail: NTIS HC/MF A22 CSCL 03B

N91-14933*# Lecce Univ. (Italy). Dept. of Physics.
RAMAN PROPERTIES OF VARIOUS CARBONACEOUS MATERIALS AND THEIR ASTROPHYSICAL IMPLICATIONS Abstract Only
A. Blanco, A. Borghesi, E. Bussoletti, Luigi Colangeli, Sergio Fonti, M. Lugara, Vincenso Orofino, and G. Scamarcio (Bari Univ., Italy) *In* NASA, Ames Research Center, Interstellar Dust: Contributed Papers Dec. 1989 p 149-150 (For primary document see N91-14897 06-88)
Avail: NTIS HC/MF A22 CSCL 03B

N91-14934*# Michigan Univ., Ann Arbor. Space Physics Research Lab.
INFRARED FLUORESCENCE FROM PAHS IN THE LABORATORY
Isabelle Cherchneff and John R. Barker *In* NASA, Ames Research Center, Interstellar Dust: Contributed Papers Dec. 1989 p 151-156 Sponsored in part by NSF (For primary document see N91-14897 06-88)
Avail: NTIS HC/MF A22 CSCL 03B

N91-14935*# Aerospace Corp., Los Angeles, CA. Space Sciences Lab.
SI3N4 EMISSIVITY AND THE UNIDENTIFIED INFRARED BANDS
Ray W. Russell, M. A. Chatelain, James H. Hecht, and John R. Stephens (Los Alamos National Lab., NM.) *In* NASA, Ames Research Center, Interstellar Dust: Contributed Papers Dec. 1989 p 157-162 (For primary document see N91-14897 06-88)
Avail: NTIS HC/MF A22 CSCL 03B

N91-14936*# Alabama Univ., Birmingham. Dept. of Physics.
PAH IN THE LABORATORY AND INTERSTELLAR SPACE
Thomas J. Wdowiak, Gregory C. Flickinger, and David A. Boyd *In* NASA, Ames Research Center, Interstellar Dust: Contributed Papers Dec. 1989 p 163-167 (For primary document see N91-14897 06-88)
(Grant NAGw-749)
Avail: NTIS HC/MF A22 CSCL 03B

N91-14937*# Molecular Research Inst., Palo Alto, CA.
THE EFFECT OF IONIZATION ON THE INFRARED ABSORPTION SPECTRA OF PAHS: A PRELIMINARY REPORT
Doug J. DeFrees and M. D. Miller (International Business Machines Corp., San Jose, CA.) *In* NASA, Ames Research Center, Interstellar Dust: Contributed Papers Dec. 1989 p 173-176 (For primary document see N91-14897 06-88)
Avail: NTIS HC/MF A22 CSCL 03B

N91-14938*# Observatoire de Paris-Meudon (France). Lab. de Recherches Spatiales.
ANGULAR MOTION OF A PAH MOLECULE IN INTERSTELLAR ENVIRONMENT
D. Rouan, Alain Leger, A. Omont, and Martin Giard (Centre d'Etude Spatiale des Rayonnements, Toulouse, France) *In* NASA, Ames Research Center, Interstellar Dust: Contributed Papers Dec. 1989 p 177-181 (For primary document see N91-14897 06-88)
Avail: NTIS HC/MF A22 CSCL 03B

N91-14939*# Paris VII Univ. (France). Groupes de Physique des Solides de l'ENS.
PAHS MOLECULES AND HEATING OF THE INTERSTELLAR GAS
Laurent Verstraete, Alain Leger, Louis B. dHendecourt, O. Dutuit (Laboratoire de Chimie-Physique, Orsay, France), and D. Defourneau *In* NASA, Ames Research Center, Interstellar Dust: Contributed Papers Dec. 1989 p 183-188 (For primary document see N91-14897 06-88)
Avail: NTIS HC/MF A22 CSCL 03B

N91-14940*# Texas Univ., Austin. Dept. of Astronomy.
THE COMPACT FAR INFRARED EMISSION FROM THE YOUNG STELLAR OBJECT IRAS 16293-2422
Harold M. Butner, N. J. Evans, III, D. F. Lester, L. G. Mundy, P. M. Harvey, and M. F. Campbell (Colby Coll., Waterville, ME.) *In* NASA, Ames Research Center, Interstellar Dust: Contributed Papers Dec. 1989 p 191-192 (For primary document see N91-14897 06-88)
Avail: NTIS HC/MF A22 CSCL 03B

N91-14942*# Wisconsin Univ., Madison. Dept. of Astronomy.
INFRARED EMISSION FROM ULTRACOMPACT H II REGIONS
Abstract Only
Ed Churchwell, Mark G. Wolfire (Chicago Univ., IL.), and Douglas O. S. Wood *In* NASA, Ames Research Center, Interstellar Dust: Contributed Papers Dec. 1989 p 195 (For primary document see N91-14897 06-88)
Avail: NTIS HC/MF A22 CSCL 03B

N91-14945*# National Radio Astronomy Observatory, Tucson, AZ.
LONGWAVE SPECTRAL DEPENDENCE OF EMISSION FROM WARM DUST CLOUDS
M. A. Gordon *In* NASA, Ames Research Center, Interstellar Dust: Contributed Papers Dec. 1989 p 201-202 (For primary document see N91-14897 06-88)
Avail: NTIS HC/MF A22 CSCL 03B

N91-14974*# Centre d'Etude Spatiale des Rayonnements, Toulouse (France).
THE ORIGIN OF THE GALACTIC EMISSION IN IRAS DATA
Emanuel Caux, P. M. Solomon, and T. J. Mooney (State Univ. of New York, Stony Brook.) *In* NASA, Ames Research Center, Interstellar Dust: Contributed Papers Dec. 1989 p 299-300 (For primary document see N91-14897 06-88)
Avail: NTIS HC/MF A22 CSCL 03B

N91-15069# Academy of Sciences of the Georgian SSR, Tbilisi. Inst. of Physics.
ON THE PRIMARY COSMIC RAY NUCLEI SPECTRA BEHAVIOUR IN THE 10(EXP 16) eV ENERGY REGION
T. T. Barnaveli, I. V. Khaldeeva, S. T. Shargelashvili, and N. A. Eristavi *In* ESA, Plasma Astrophysics Aug. 1990 p 115-120 (For primary document see N91-15046 06-90)
Copyright Avail: NTIS HC/MF A14

N91-15070# Kurchatov (I. V.) Inst. of Atomic Energy, Moscow (USSR).
GENERATION OF COSMIC RAYS IN PINCHES
B. Troubnikov *In* ESA, Plasma Astrophysics Aug. 1990 p 121-126 (For primary document see N91-15046 06-90)
Copyright Avail: NTIS HC/MF A14

N91-15098# Sternberg Astronomical Inst., Moscow (USSR).
ON THE NATURE OF COSMIC GAMMA RAY BURSTS
N. I. Shakura and N. N. Shakura *In* ESA, Plasma Astrophysics Aug. 1990 p 277-278 (For primary document see N91-15046 06-90)
Copyright Avail: NTIS HC/MF A14

99 GENERAL

N91-15119*# Management Services, Inc., Huntsville, AL.
CHRONOLOGY: MSFC SPACE STATION PROGRAM, 1982 - PRESENT. MAJOR EVENTS
Jessie E. Whalen, comp., Sarah L. McKinley, comp., and Thomas G. Gates, comp. Dec. 1988 135 p
(Contract NAS8-35900)
(NASA-CR-184014; NAS 1.26:184014; MHR-12) Avail: NTIS HC/MF A07 CSCL 05D

The Marshall Space Flight Center (MSFC) maintains an active program to capture historical information and documentation on the MSFC's roles regarding Space Shuttle and Space Station. Marshall History Report 12, called Chronology: MSFC Space Station Program, 1982-Present, is presented. It contains synopses of major events listed according to the dates of their occurrence. Indices follow the synopses and provide additional data concerning the events listed. The Event Index provides a brief listing of all the events without synopses. The Element Index lists the specific elements of the Space Station Program under consideration in the events. The Location Index lists the locations where the events took place. The indices and synopses may be cross-referenced by using dates. Y.S.

N91-15120*# Management Services, Inc., Huntsville, AL.
CHRONOLOGY: MSFC SPACE SHUTTLE PROGRAM DEVELOPMENT, ASSEMBLY, AND TESTING MAJOR EVENTS (1969 - APRIL, 1981)
Jessie E. Whalen, comp., Sarah L. McKinley, comp., and Thomas G. Gates, comp. Dec. 1988 190 p
(Contract NAS8-35900)
(NASA-CR-184013; NAS 1.26:184013; MHR-15) Avail: NTIS HC/MF A09 CSCL 05D

Listings of major events directly related to the Space Shuttle Program at Marshall Space Flight Center (MSFC) are presented. This information will provide the researcher with a means of following the chronological progression of the program. The products that the historians have prepared are intended to provide supportive research essential to the writing of formal narrative histories of Marshall's contributions to the Space Shuttle and Space Station. Author

N91-15121# Air Force Office of Scientific Research, Bolling AFB, Washington, DC.
AIR FORCE OFFICE OF SCIENTIFIC RESEARCH TECHNICAL REPORT SUMMARIES: APRIL-JUNE 1990 Quarterly Report
Jun. 1990 201 p
(AD-A227367; AFOSR-90-0928TR) Avail: NTIS HC/MF A10 CSCL 05/2

The Air Force Office of Scientific Research Technical Report Summaries is published quarterly (March, June, September, and December). It contains a brief summary of each technical report received in the Technical Information Division and submitted to the Defense Technical Information Center for the quarter. Three indexes, subject, personal author and title are provided to help the user locate reports that may be of interest. The purpose of this report is to inform Air Force Laboratories about the science that the Air Force Office of Scientific Research is supporting. GRA

N91-15122# Air Force Office of Scientific Research, Bolling AFB, Washington, DC.

AIR FORCE OFFICE OF SCIENTIFIC RESEARCH TECHNICAL REPORT SUMMARIES: JANUARY-MARCH 1990 Quarterly Report

Debra L. Tyrrell Mar. 1990 355 p

(AD-A227368; AFOSR-90-0929TR) Avail: NTIS HC/MF A16

CSCL 05/2

The Air Force Office of Scientific Research Technical Report Summaries is published quarterly (March, June, September, and December). It contains a brief summary of each technical report received in the Technical Information Division and submitted to the Defense Technical Information Center (DTIC) for that quarter. Two indexes, subject and personal author are provided to help the user locate reports that may be of interest. The purpose of this report is to inform Air Force Laboratories about the science that the Air Force Office of Scientific Research is supporting.

GRA

Typical Subject Index Listing

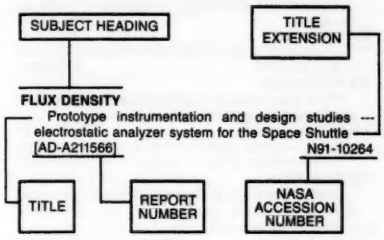

The subject heading is a key to the subject content of the document. Titles, report numbers, and accession numbers of pertinent documents are provided under each subject heading. When the title is insufficiently descriptive of the document content, a title extension has been added, separated from the title by three hyphens. The report number helps to indicate the type of document cited (e.g., NASA report, NASA translation, NASA contractor report). The NASA accession number is the number by which the document abstracts are arranged in this journal and by which the document is sold or requested. The titles, with title extensions if present, are arranged under each subject heading in ascending accession number order. The subject headings have been selected from the latest revision of the *NASA Thesaurus* (NASA SP-7064).

A

A STARS
Three-micron spectroscopy of highly reddened field stars N91-14904
ABILITIES
Investigating individual differences in general comprehension skill: The role of suppression and enhancement
[AD-A226788] N91-14715
Adaptive human-computer interfaces using expert profiles
[AD-A226906] N91-14721
ABSORPTION COOLING
An investigation of using a phase-change material to improve the heat transfer in a small electronic module for an airborne radar application
[DE91-002597] N91-14525
ABSORPTION SPECTRA
Intersubband absorption in Si(1-x)Ge(x/Si superlattices for long wavelength infrared detectors N91-14399
Correlation properties of interstellar dust: Diffuse interstellar bands N91-14916
Spectral structure near the 11.3 micron emission feature N91-14926
Dust emission from high latitude cirrus clouds N91-14930
Infrared fluorescence from PAHs in the laboratory N91-14934
The effect of ionization on the infrared absorption spectra of PAHs: A preliminary report N91-14937
Distribution of the 3.1 micron feature in Cepheus A N91-14958
Absorption features in the 3 micron spectra of highly obscured objects N91-14965
Experimental evidence for amorphous carbon grains in comets N91-15008
Atomic environments in iron meteorites using EXAFS N91-15011
Carbon stars with alpha-C:H emission N91-15022
Spectral synthesis code LINESPEC: Ionisation equilibrium of plasma and absorption spectra formation N91-15106
ABSORPTIVITY
Intersubband absorption in Si(1-x)Ge(x/Si superlattices for long wavelength infrared detectors N91-14399
ABUNDANCE
Small scale variations of abundances of transiently heated grains in molecular clouds N91-14927
ACCELERATED LIFE TESTS
HgZnTe-based detectors for LWIR NASA applications N91-14404
ACCIDENT INVESTIGATION
A parametric shell analysis of the shuttle 51-L SRB AFT field joint
[NASA-TM-102748] N91-14629
ACCIDENT PREVENTION
Snow avalanche hazards and mitigation in the United States
[LC-90-62814] N91-14686
ACCIDENTS
Hazards and safeguards of high pressure hydraulic fatigue testing
[AD-A226767] N91-14509
ACCRETION DISKS
The 3.3 micron emission feature: Map of the galactic disk, 10 deg less than 1 less than 35 deg, - 6 deg less than b less than 6 deg N91-14928
Magnetically driven jets and winds N91-15084
Thirty-five-day cycle of Her X-1: Synthesised optical light curves in the model of freely processing neutron star N91-15089
Structure of accretion flow in close binary system: A two dimensional numerical model N91-15093
Accretion disk instability and spokes in Saturn's rings N91-15094
Large-scale vortices in compressible turbulent medium with the magnetic field N91-15095
The optical observations of x ray Nova GS2023+33 = V404 Cyg N91-15103
Nonlinear magnetosonic waves in an inhomogeneous plasma N91-15110
ACCUMULATORS
Digitized synchronous demodulator
[NASA-CASE-GSC-13237-1] N91-14550
ACETIC ACID
N-(3-ethynylphenyl)maleimide
[NASA-CASE-LAR-14188-2] N91-14419
ACETYLENE
N-(3-ethynylphenyl)maleimide
[NASA-CASE-LAR-14188-2] N91-14419
ACID RAIN
The effects of climate change on the nitrogen cycle and acid deposition
[DE91-002785] N91-14659
Validity of environmental transfer models
[DE91-002929] N91-14660
ACIDITY
Acidic deposition: Its nature and impacts
[DE91-001984] N91-14658
ACOUSTIC ATTENUATION
A LEED study of the MgO(001) surface structure
[DE91-002811] N91-14879
ACOUSTIC EMISSION
Acoustic transducer apparatus with reduced thermal conduction
[NASA-CASE-NPO-17620-1-CU] N91-14808
ACOUSTIC IMPEDANCE
An investigation of the diffraction of an acoustic plane wave by a curved surface of finite impedance N91-14800
A model of the acoustic interactions occurring under Arctic ice
[AD-A227128] N91-14806
ACOUSTIC LEVITATION
Acoustic positioning and orientation prediction
[NASA-CASE-NPO-17511-1-CU] N91-14807
Acoustic transducer apparatus with reduced thermal conduction
[NASA-CASE-NPO-17620-1-CU] N91-14808
ACOUSTIC SCATTERING
A model of the acoustic interactions occurring under Arctic ice
[AD-A227128] N91-14806
ACOUSTICS
Tabulation of data from the tip aerodynamics and acoustics test
[NASA-TM-102280] N91-14273
Research in progress in applied mathematics, numerical analysis, and computer science
[NASA-CR-187474] N91-14726
Effect of atmospherics on beamforming accuracy
[NASA-CR-187695] N91-14802
Acoustic positioning and orientation prediction
[NASA-CASE-NPO-17511-1-CU] N91-14807
ACRYLIC RESINS
Optoelectronic devices
[AD-D014618] N91-14822
ACTIVE CONTROL
Interaction between the canard and wing flow on a model of a typical combat aircraft N91-14334
Smart tunnel: Docking mechanism
[NASA-CASE-MSC-21360-1] N91-14374
Active control of boundary layer transition and turbulence
[NASA-CASE-LAR-13532-1] N91-14562
ACTIVE GALACTIC NUCLEI
Nonlinear plasma effects in the environment of active galactic nuclei N91-15085
Compact object masses in active galactic nuclei and quasars and duration of activity stage N91-15096
A model for one-sided extragalactic jets N91-15097
ACTIVE GALAXIES
On the generation of magnetic fields in active star atmospheres N91-15099
ACTUATORS
Triggering GaAs lock-on switches with laser diode arrays
[DE91-002419] N91-14532
Multi-fingered robotic hand
[NASA-CASE-NPO-15959-2] N91-14616
ACUITY
Demodulation processes in auditory perception
[AD-A226824] N91-14707
ADA (PROGRAMMING LANGUAGE)
Experiences porting the distributed Ada real-time kernel
[AD-A226693] N91-14742
DARK technology transition plan
[AD-A226695] N91-14744
Developing portable user interfaces for Ada command control software
[AD-A226712] N91-14747
ADAPTIVE CONTROL
Adaptive data acquisition multiplexing system and method
[NASA-CASE-MSC-21170-1] N91-14371
Adaptive control of large space structures
[AD-A227304] N91-14377
Robot control strategies
[OUEL-1754/89] N91-14605
ADDITIVES
InAs/GaAs and InAs doping superlattices N91-14409
Process for lowering the dielectric constant of polyimides using diamic acid additives
[NASA-CASE-LAR-13902-1] N91-14484
ADHESION
Adhesion at ceramic interfaces
[DE91-001660] N91-14480
An evaluation of two flat-black silicone paints for space application
[NASA-TM-100768] N91-14494
ADHESION TESTS
Surface and interfacial properties of carbon fibers
[NASA-CR-184916] N91-14429
ADHESIVE BONDING
Surface and interfacial properties of carbon fibers
[NASA-CR-184916] N91-14429
Surface treatment of metals
[EP-PATENT-0-367-504-A2] N91-14453
Fracture analysis of cathodic delamination in rubber-to-metal bonds N91-14627

ADHESIVES
Thermal compensating mount
[NASA-CASE-LAR-14207-1] N91-14590
ADIABATIC CONDITIONS
Flow behavior of Ti-24Al-11Nb at high strain rates
[DE91-004506] N91-14473
ADVANCED VERY HIGH RESOLUTION RADIOMETER
Evaluation of data reduction and composing of the NOAA global vegetation index product: A case study
[AD-A227397] N91-14641
ADVECTION
A numerical theory of lattice gas and lattice Boltzmann methods in the computation of solutions to nonlinear advective-diffusive systems
[DE91-002566] N91-14560
AERIAL PHOTOGRAPHY
The optical parametrization of an aerial multispectral camera
[DE91-003017] N91-14593
AEROACOUSTICS
Prediction of XV-15 tilt rotor discrete frequency aeroacoustic noise with WOPWOP
[NASA-CR-187684] N91-14803
AEROASSIST
Gamma guidance of trajectories for coplanar, aeroassisted orbital transfer
[NASA-CR-187732] N91-14365
Properties of the optimal trajectories for coplanar, aeroassisted orbital transfer
[NASA-CR-187733] N91-14366
Decomposition technique and optimal trajectories for the aeroassisted flight experiment
[NASA-CR-187734] N91-14367
Guidance trajectories for aeroassisted orbital transfer
[NASA-CR-187735] N91-14368
AEROBRAKING
Gamma guidance of trajectories for coplanar, aeroassisted orbital transfer
[NASA-CR-187732] N91-14365
Properties of the optimal trajectories for coplanar, aeroassisted orbital transfer
[NASA-CR-187733] N91-14366
Decomposition technique and optimal trajectories for the aeroassisted flight experiment
[NASA-CR-187734] N91-14367
Guidance trajectories for aeroassisted orbital transfer
[NASA-CR-187735] N91-14368
AERODYNAMIC CHARACTERISTICS
Missile Aerodynamics
[AGARD-CP-493] N91-14278
Some trends in missile aerodynamics N91-14279
A semi-empirical prediction method for missile aerodynamics N91-14288
Aerodynamic characteristics of cylindrical bodies with pointed and truncated conical noses N91-14289
Results of GARTEUR action group AG09 on flow past missile afterbodies N91-14299
Laminar/turbulent flow transition effects on high-speed missile domes N91-14301
Control of unsteady aerodynamic forces
[AD-A227365] N91-14315
Unsteady airloads due to separated flow on airfoils and wings N91-14340
AERODYNAMIC COEFFICIENTS
Three dimensional flow calculations for a projectile with standard and dome bases N91-14294
Anticipation of aerodynamic coefficients of missile air intakes N91-14297
Parametric study of afterbody/nozzle drag on twin two-dimensional convergent-divergent nozzles at Mach numbers from 0.60 to 1.20
[NASA-TP-2640] N91-14316
AERODYNAMIC FORCES
Three dimensional flow calculations for a projectile with standard and dome bases N91-14294
Experimental aerodynamics for hot gas jet reaction control systems N91-14300
Control of unsteady aerodynamic forces
[AD-A227365] N91-14315
Unsteady aerodynamic forces on an oscillating wing at high incidences and flow separation N91-14331
AERODYNAMIC INTERFERENCE
Experimental aerodynamics for hot gas jet reaction control systems N91-14300
Role of separation autopilots for modern missile concepts
[MBB/FE121/S/PUB/409/A] N91-14352
AERODYNAMIC LOADS
Tabulation of data from the tip aerodynamics and acoustics test
[NASA-TM-102280] N91-14273
NUFA: A semi-empirical method for the prediction of isolated weapon aerodynamics N91-14287
A method for the design of transonic flexible wings
[NASA-TP-3045] N91-14323
Experimental investigations of buffet excitation forces on a low aspect ratio trapezoidal half wing in incompressible flow N91-14329
Unsteady aerodynamic forces on an oscillating wing at high incidences and flow separation N91-14331
Coupled aerodynamic loads due to unsteady stall on a large aspect ratio wing oscillating at great amplitude N91-14338
Unsteady airloads due to separated flow on airfoils and wings N91-14340
AERODYNAMIC NOISE
Prediction of XV-15 tilt rotor discrete frequency aeroacoustic noise with WOPWOP
[NASA-CR-187684] N91-14803
AERODYNAMIC STABILITY
Review of the spring 1988 AGARD FMP symposium N91-14280
AERODYNAMIC STALLING
Coupled aerodynamic loads due to unsteady stall on a large aspect ratio wing oscillating at great amplitude N91-14338
Prediction of XV-15 tilt rotor discrete frequency aeroacoustic noise with WOPWOP
[NASA-CR-187684] N91-14803
AERODYNAMICS
Aerodynamic design of Pegasus (trademark): Concept to flight with CFD N91-14285
NUFA: A semi-empirical method for the prediction of isolated weapon aerodynamics N91-14287
Navier-Stokes predictions of static and dynamic aerodynamic derivatives for high L/D finned projectiles N91-14295
Experimental aerodynamics for hot gas jet reaction control systems N91-14300
Hypersonic aerodynamics: An approximation method for the calculation of real gas effects and wall temperatures
[MBB/FE127/S/PUB/0403] N91-14306
Load response of horizontal-axis wind turbines to turbulence
[DE90-000375] N91-14644
Damping measurements using operational data
[DE91-002781] N91-14646
AEROELASTICITY
Feasibility investigation of general time-domain unsteady aerodynamics of rotors
[NASA-CR-177570] N91-14311
A method for the design of transonic flexible wings
[NASA-TP-3045] N91-14323
AERONAUTICAL ENGINEERING
Research as part of the Air Force Research in Aero-Propulsion Technology (AFRAPT) program
[AD-A226893] N91-14350
AEROSOLS
A balloon-borne aerosol spectrometer for high altitude low aerosol concentration measurements
[DE91-002563] N91-14661
Climate and atmospheric modeling studies. Climate applications of Earth and planetary observations. Chemistry of Earth and environment
[NASA-CR-187326] N91-14684
A balloon-borne integrating nephelometer
[DE91-001037] N91-14687
Dust of Orionid meteor shower in the Earth atmosphere before and after Halley's Comet N91-15012
AEROSPACE MEDICINE
JPRS Report: Science and technology. USSR: Life sciences
[JPRS-ULS-89-003] N91-14706
Aerospace medicine and biology: A continuing bibliography with indexes (supplement 343)
[NASA-SP-7011(343)] N91-14711
Aerospace medicine and biology: A continuing bibliography with indexes (supplement 344)
[NASA-SP-7011(344)] N91-14712
AEROSPACE SCIENCES
The NASA/DOD aerospace knowledge diffusion research project: A research agenda
[NASA-TM-103439] N91-14892
AEROTHERMODYNAMICS
Missile Aerodynamics
[AGARD-CP-493] N91-14278
Investigations of aerothermodynamic effects on axisymmetric bodies at high Mach numbers N91-14302
NASA's supercomputing experience
[NASA-TM-102890] N91-14727
AFTERBODIES
Computation of axisymmetric base flow with different turbulence models N91-14298
Results of GARTEUR action group AG09 on flow past missile afterbodies N91-14299
Parametric study of afterbody/nozzle drag on twin two-dimensional convergent-divergent nozzles at Mach numbers from 0.60 to 1.20
[NASA-TP-2640] N91-14316
AGING (MATERIALS)
Fundamentals of interfacial strength in composite materials
[AD-A226701] N91-14431
AIR
Numerical study of shock-wave/boundary layer interactions in premixed hydrogen-air hypersonic flows
[NASA-TM-103273] N91-14559
AIR DATA SYSTEMS
In-flight measurements on a Tornado aircraft for stores carriage and release research
[RAE-TM-AERO-2180] N91-14341
AIR INTAKES
Anticipation of aerodynamic coefficients of missile air intakes N91-14297
AIR LAUNCHING
Aerodynamic design of Pegasus (trademark): Concept to flight with CFD N91-14285
AIR NAVIGATION
Flight data acquisition methodology for validation of passive ranging algorithms for obstacle avoidance
[NASA-TM-102809] N91-14322
The Air Almanac, 1990 N91-15036
The Air Almanac, 1989 N91-15037
AIR POLLUTION
Office of Basic Energy Sciences 1990 summary report
[DE91-002971] N91-14653
Prospects of new energy
[DE91-727567] N91-14654
Atmospheric source-receptor relationships: Concepts and terminology
[DE91-001033] N91-14656
Acidic deposition: Its nature and impacts
[DE91-001984] N91-14658
Combined air and water pollution control system
[NASA-CASE-NST-00007-1] N91-14662
The response of atmospheric CO2 to changes in land use
[DE91-001212] N91-14663
A balloon-borne integrating nephelometer
[DE91-001037] N91-14687
AIR TO AIR MISSILES
Role of separation autopilots for modern missile concepts
[MBB/FE121/S/PUB/409/A] N91-14352
AIR TO SURFACE MISSILES
Role of separation autopilots for modern missile concepts
[MBB/FE121/S/PUB/409/A] N91-14352
AIR TRAFFIC
Using simulation to evaluate the safety of proposed ATC operations and procedures
[DOT/FAA/CT-TN90/22] N91-14318
DATAS hardware diagnostic tests
[DOT/FAA/CT-TN90/44] N91-14728
AIR TRAFFIC CONTROL
Using simulation to evaluate the safety of proposed ATC operations and procedures
[DOT/FAA/CT-TN90/22] N91-14318
Automatic dependent surveillance benefit and cost analysis
[DOT/FAA/RD-90/34] N91-14320
AIR TRAFFIC CONTROLLERS (PERSONNEL)
Air traffic controller memory enhancement
[DOT/FAA/CT-TN90/38] N91-14713
AIR WATER INTERACTIONS
Upwelling southwest of Iceland due to quasi-geostrophic flow
[AD-A227129] N91-14698
AIRBORNE EQUIPMENT
An investigation of using a phase-change material to improve the heat transfer in a small electronic module for an airborne radar application
[DE91-002597] N91-14525
Analysis of the boreal forest-tundra ecotone: A test of AVIRIS capabilities in the Eastern Canadian subarctic
[NASA-CR-187335] N91-14655
In-flight methods for satellite sensor absolute radiometric calibration N91-14801
AIRBORNE SURVEILLANCE RADAR
Multiband radar characterization of forest biomes
[NASA-CR-185101] N91-14638
AIRCRAFT
A cable vehicle barrier for alert aircraft protection
[DE91-001723] N91-14354
AIRCRAFT COMMUNICATION
Automatic dependent surveillance benefit and cost analysis
[DOT/FAA/RD-90/34] N91-14320
AIRCRAFT DESIGN
A method for the design of transonic flexible wings
[NASA-TP-3045] N91-14323
Structural development of laminar flow control aircraft chordwise wing joint designs
[NASA-CR-181888] N91-14346

AIRCRAFT ENGINES
Combustor technology for future aircraft
[NASA-TM-103268] N91-14349
AIRCRAFT EQUIPMENT
Wingtip vortex turbine
[NASA-CASE-LAR-14116-1] N91-14345
AIRCRAFT MANEUVERS
A unified approach to buffet response of fighter aircraft empennage N91-14326
AIRCRAFT MODELS
Results of a sub-scale model rotor icing test
[NASA-TM-103709] N91-14309
Development of an unmanned air research vehicle for supermaneuverability studies
[AD-A227165] N91-14342
Modeling and control design of a wind tunnel model support
[NASA-TM-103829] N91-14540
AIRCRAFT PERFORMANCE
Predictions of F-111 TACT aircraft buffet response N91-14335
AIRCRAFT POWER SUPPLIES
Wingtip vortex turbine
[NASA-CASE-LAR-14116-1] N91-14345
AIRCRAFT SPIN
Electro-optical spin measurement system
[NASA-CASE-LAR-13629-1] N91-14356
AIRFOIL OSCILLATIONS
Unsteady airloads due to separated flow on airfoils and wings N91-14340
AIRFOIL PROFILES
A method for the design of transonic flexible wings
[NASA-TP-3045] N91-14323
Experimental investigation of buffet onset and penetration on a supercritical airfoil at transonic speeds N91-14328
AIRGLOW
Investigation of the night sky airglow near the epicenter of the earthquake N91-15107
ALASKA
Radio Frequency Interference (RFI) measurements made near the proposed Alaska OTH receiving site
[AD-A226922] N91-14519
ALBEDO
Diffuse galactic light observations at 206 selected areas N91-14914
ALDEHYDES
State-to-state dynamics of molecular energy transfer
[DE91-004589] N91-14599
ALGEBRA
The computer algebra approach of the finite difference methods for PDEs
[DE90-631581] N91-14790
ALGORITHMS
Flight data acquisition methodology for validation of passive ranging algorithms for obstacle avoidance
[NASA-TM-102809] N91-14322
Multivariable methods for the design, identification, and control of large space structures. Volume 2: Optimal and sub-optimal estimation applied to large flexible structures
[AD-A226699] N91-14375
The inclusion of wall loss in electromagnetic finite-difference time-domain thin-slot algorithms
[DE91-001046] N91-14524
Remote sensing of Earth terrain
[NASA-CR-186904] N91-14635
Evaluation of data reduction and composing of the NOAA global vegetation index product: A case study
[AD-A227397] N91-14641
The 3-D depth migration via McClellan transformations
[DE91-001446] N91-14675
Multispectral imagery support for ocean venture 90
[AD-A227119] N91-14697
Research in progress in applied mathematics, numerical analysis, and computer science
[NASA-CR-187474] N91-14726
Computational equipment for the development of numerical algorithms computation
[AD-A226702] N91-14729
Hidden surface removal for axis-parallel polyhedra
[RUU-CS-90-21] N91-14736
Feature set evaluation for classifiers
[AD-A226903] N91-14751
Feature set evaluation for classifiers
[AD-A226904] N91-14752
Feature set evaluation for classifiers
[AD-A226905] N91-14753
Planning monotone paths to visit a set of obstacles
[AD-A226923] N91-14754
Evaluations of some scheduling algorithms for hard real-time systems
[AD-A226930] N91-14755
Development of phenomenological fitting procedure for the fast microcomputer
[AD-A227168] N91-14759
An accurate product SVD (singular value decomposition) algorithm
[DE91-004448] N91-14765
Matrix techniques for faster routing of affine permutations on a mesh interconnection network
[RUU-CS-90-19] N91-14767
Boolean Grobner bases, calculation methods. Applications and parallel processing
[ETN-90-98208] N91-14768
Efficient parallel algorithms on the network model
[AD-A227144] N91-14771
Finding shortest paths in the presence of orthogonal obstacles using a combined L sub 1 and link metric
[RUU-CS-90-20] N91-14777
ALIGNMENT
Thermal compensating mount
[NASA-CASE-LAR-14207-1] N91-14590
Multiple axis reticle
[NASA-CASE-ARC-11886-1-SB] N91-14591
New results in the theory of dust grain alignment N91-14906
Polarization and extinction by aligned grains N91-14907
Alignment mechanisms of paramagnetic grains revisited N91-14908
ALIPHATIC HYDROCARBONS
Spatial variations of the 3 micron emission features within nebulae N91-14922
ALLOYING
Fundamental studies on microstructural evolution of two-phase titanium alloys N91-14452
Amorphization of C-implanted Fe(Cr) alloys
[DE91-001338] N91-14469
ALUMINIDES
Fatigue and fracture of titanium aluminides, volume 2
[AD-A227353] N91-14351
The effect of scandium on the phase stability of Al3Nb and Al3Zr
[DE91-002657] N91-14459
ALUMINUM
AlSb/InAs/AlSb quantum wells N91-14411
ALUMINUM ALLOYS
Fundamentals of interfacial strength in composite materials
[AD-A226701] N91-14431
Thermomechanical processing and ambient temperature properties of a 6061 aluminum 10 volume percent alumina metal matrix composite
[AD-A227004] N91-14433
Ion implantation for corrosion inhibition of aluminum alloys in saline media
[DE91-002887] N91-14461
An examination of delta prime growth in an aluminum-lithium alloy by x ray diffraction
[AD-A227254] N91-14464
Processing studies of aluminum-magnesium and aluminum-copper-lithium alloys
[AD-A227255] N91-14465
ALUMINUM GALLIUM ARSENIDES
Characteristics of AlGaAs/GaAs multiple quantum well infrared detectors N91-14394
Resonant tunneling IR detectors N91-14395
Fundamental limits to performance of quantum well infrared detectors N91-14397
ALUMINUM NITRIDES
Aluminum nitride-silicon carbide whisker composites: Processing, properties, and microstructural stability
[DE91-001907] N91-14425
Heterocycles based on group 3, 4, and 5 elements: Precursors for novel glasses and ceramics
[AD-A226988] N91-14487
ALUMINUM OXIDES
Joining alumina to sapphire for copper vapor laser tubes
[AD-A226619] N91-14501
Dust formation around M-type stars N91-15017
ALUMINUM SILICATES
Mechanism of hydrodenitrogenation. Part 4: Infrared spectroscopy of acidic molybdena catalysts
[DE91-002496] N91-14440
AMBIENT TEMPERATURE
Thermomechanical processing and ambient temperature properties of a 6061 aluminum 10 volume percent alumina metal matrix composite
[AD-A227004] N91-14433
AMMONIUM NITRATES
Analysis of hydroxylammonium nitrate based liquid propellants
[AD-A227300] N91-14497
AMORPHOUS MATERIALS
Amorphization of C-implanted Fe(Cr) alloys
[DE91-001338] N91-14469
Phase changes during plasma spray deposition
[IPPCZ-297] N91-14837
VUV-visible measurements on different samples of amorphous carbon N91-14990
The nature of cometary dust as determined from infrared observations N91-15003
A comparative study of the continuum and emission characteristics of comet dust. 1: Are the silicates in Comet Halley and Kohoutek amorphous or crystalline N91-15005
Experimental evidence for amorphous carbon grains in comets N91-15008
AMPLIFIER DESIGN
Monolithic multichannel detector amplifier arrays and circuit
[AD-D014566] N91-14528
AMPLITUDE DISTRIBUTION ANALYSIS
The distribution of wave heights and periods for seas with unimodal bimodal power density spectra
[AD-A227040] N91-14696
AMPLITUDE MODULATION
Optical phase conjugate beam modulator and method therefor
[AD-D014569] N91-14820
Ultrarelativistic low-frequency electromagnetic waves in pulsar magnetospheres N91-15091
ANALOG TO DIGITAL CONVERTERS
X ray sensitive area detection device
[NASA-CASE-MFS-28232-1] N91-14835
ANALYSIS OF VARIANCE
Initial blood storage experiment
[NASA-CR-185513-PT-1] N91-14700
Improved estimation of variance components in mixed models
[AD-A226854] N91-14794
ANGLE OF ATTACK
Systematic investigations of body-wing-tail interference at high angles of attack N91-14290
Numerical studies of compressible flow over a double-delta wing at high angles of attack
[AD-A226931] N91-14312
ANGULAR MOMENTUM
Alignment mechanisms of paramagnetic grains revisited N91-14908
ANGULAR VELOCITY
Angular motion of a PAH molecule in interstellar environment N91-14938
ANISOTROPIC PLATES
An analysis of interlaminar stresses in unsymmetrically laminated plates
[NASA-CR-187657] N91-14424
ANISOTROPY
Scattering by anisotropic grains in beryllium mirrors
[DE91-001724] N91-14826
Effect of step edge transition rates and anisotropy in simulations of epitaxial growth
[DE91-001251] N91-14875
ANNIHILATION REACTIONS
Annihilation radiation of strongly-magnetised electron-positron plasma with power-law distributions of particles N91-15078
ANNUAL VARIATIONS
Studies of the observed and theoretical variations of atmospheric ozone
[NASA-CR-187703] N91-14857
Modified seasonal factors in exponential smoothing
[DE91-002802] N91-14688
ANODES
High gradient electron guns
[DE91-000056] N91-14369
Organic cathode for a secondary battery
[NASA-CASE-NPO-17604-1-CU] N91-14536
ANTENNA ARRAYS
MMIC compensation network for phased array element mismatch
[AD-A227437] N91-14522
ANTENNA DESIGN
A global view of lander-to-orbiter communications accessibility for a Mars Global Network Mission N91-14362
ANTIAIRCRAFT MISSILES
Device and method for monitoring the presence of an object in space
[AD-D014621] N91-14823
ANTICYCLONES
Experiments with collision of vortices in rotating and still free-surface shallow water N91-15080
ANTIMISSILE MISSILES
Device and method for monitoring the presence of an object in space
[AD-D014621] N91-14823
ANTIMONY
LWIR detector research in InAsSb/InAs N91-14406
InAs/Ga(1-x)In(x)Sb superlattices for infrared detector applications N91-14407
InAsSbBi, a direct band-gap, III-V, LWIR material N91-14410
AlSb/InAs/AlSb quantum wells N91-14411

ANTISYMMETRY
Nonlinear finite element dynamics on multiprocessor computers
[AD-A227409] N91-14761
APERTURES
The inclusion of wall loss in electromagnetic finite-difference time-domain thin-slot algorithms
[DE91-001046] N91-14524
Wind tunnel study of an observatory dome with a circular aperture
[NASA-TM-102888] N91-15040
APPLICATIONS PROGRAMS (COMPUTERS)
A finite element conjugate gradient FFT method for scattering N91-14476
New multiphase equation of state for polycrystalline quartz
[DE91-001048] N91-14490
A versatile RF cavity mode damper
[DE91-002947] N91-14534
Integration of sneak analysis with design, volume 1
[AD-A226902] N91-14543
Color palette: Plotting guide for use with GSMAP and GSDRAW digital cartographic software
[DE91-001643] N91-14737
DARK technology transition plan
[AD-A226695] N91-14744
APPROXIMATION
Boundary value problems of the elasticity theory for polyhedra: Singularities and approximation with boundary element methods
[ETN-91-98168] N91-14780
New accurate, vectorized approximations of state surfaces for the thermodynamic and transport properties of equilibrium air
[MBB/FE122/S/PUB/0389] N91-14886
AQUEOUS SOLUTIONS
Surface treatment of metals
[EP-PATENT-0-367-504-A2] N91-14453
Analysis of hydroxylammonium nitrate based liquid propellants
[AD-A227300] N91-14497
ARC WELDING
Validation of a computational model for autogenous arc welding
[AD-A227258] N91-14611
ARCHITECTURE (COMPUTERS)
Adaptive data acquisition multiplexing system and method
[NASA-CASE-MSC-21170-1] N91-14371
Systolic emulator experimentation
[AD-A226746] N91-14516
A mediator architecture for abstract data access
[AD-A227362] N91-14730
The ISIS project: Real experience with a fault tolerant programming system
[NASA-CR-187029] N91-14732
A CLOS (Common Lisp Object System) implementation on top of KEE (Knowledge Engineering Environment)
[DE91-001957] N91-14739
Construction of large-scale simulation codes using ALPAL (A Livermore Physics Applications Language)
[DE91-002783] N91-14740
Literature survey on tools
[AD-A226933] N91-14770
Distributed computing system with dual independent communications paths between computers and employing split tokens
[NASA-CASE-NPO-17185-1-CU] N91-14772
Analogue computation using VLSI neural network devices
[OUEL-1835/90] N91-14773
Reasoning of the geometric and uncertainty constraints in planning robot manipulation tasks
[LAAS-90143] N91-14775
Massively parallel network architectures for automatic recognition of visual speech signals
[AD-A226968] N91-14805
Hybrid optical processor
[AD-A227163] N91-14834
ARCTIC REGIONS
Analysis of the boreal forest-tundra ecotone: A test of AVIRIS capabilities in the Eastern Canadian subarctic
[NASA-CR-187335] N91-14655
A model of the acoustic interactions occurring under Arctic ice
[AD-A227128] N91-14806
ARGON
An investigation of diamond synthesis in an oxygen-acetylene diffusion flame
[AD-A227224] N91-14870
ARMED FORCES (UNITED STATES)
Research as part of the Air Force Research in Aero-Propulsion Technology (AFRAPT) program
[AD-A226893] N91-14350
Air Force Office of Scientific Research technical report summaries: April-June 1990
[AD-A227367] N91-15121
Air Force Office of Scientific Research technical report summaries: January-March 1990
[AD-A227368] N91-15122
ARMOR
AC-130H Gunship Armor Upgrade Project
[DE91-002567] N91-14428
AROMATIC COMPOUNDS
Bis (4-(3,4-dimethylene-pyrrolidyl)-phenyl) methane
[NASA-CASE-LAR-13965-2-CU] N91-14418
PAH formation in carbon-rich circumstellar envelopes N91-15015
ARRAYS
Detector array evaluation and figures of merit N91-14386
Monolithic multichannel detector amplifier arrays and circuit
[AD-D014566] N91-14528
The SYNOP experiment: Inverted echo sounder data report for October 1987 to May 1988
[AD-A227232] N91-14699
ARSENIC
LWIR detector research in InAsSb/InAs N91-14406
InAs/Ga(1-x)In(x)Sb superlattices for infrared detector applications N91-14407
ARTIFICIAL INTELLIGENCE
A CLOS (Common Lisp Object System) implementation on top of KEE (Knowledge Engineering Environment)
[DE91-001957] N91-14739
Discrete event simulation tool for analysis of qualitative models of continuous processing systems
[NASA-CASE-MSC-21465-1] N91-14741
Pedagogical strategies for human and computer tutoring
[AD-A226686] N91-14750
ARTIFICIAL SATELLITES
Satellite situation report, volume 30, no. 1
[NASA-TM-101105] N91-14372
ARTILLERY
Three dimensional flow calculations for a projectile with standard and dome bases N91-14294
ASPECT RATIO
Coupled aerodynamic loads due to unsteady stall on a large aspect ratio wing oscillating at great amplitude N91-14338
ASTEROIDS
Size distribution of dust grains: A problem of self-similarity N91-14997
A study of extended zodiacal structures
[NASA-CR-187687] N91-15044
The rotation of Venus and its atmosphere N91-15112
ASTROMETRY
Estimability of geodetic parameters from space VLBI observables
[NASA-CR-187413] N91-14636
ASTRONOMICAL CATALOGS
The dependence of UV extinction properties on dust environment N91-14902
Astronomical phenomena for the year 1990 N91-15035
The Air Almanac, 1990 N91-15036
The Air Almanac, 1989 N91-15037
The Astronomical Almanac for the year 1989
[ISBN-0-11-886932-9] N91-15038
The Astronomical Almanac for the year 1990
[ISBN-0-11-886934-5] N91-15039
A proposed astronomical reference catalog of infrared sources
[AD-A226757] N91-15041
ASTRONOMICAL MODELS
Interstellar Dust: Contributed Papers
[NASA-CP-3036] N91-14897
Diffuse galactic light observations at 206 selected areas N91-14914
IR emission and UV extinction in two open clusters N91-14929
Dust emission in the Sagittarius B2 molecular cloud core N91-14947
Interstellar extinction at 10-20 microns N91-15025
An interferometric study of molecular emission around NGC 7538 at millimeter wavelengths N91-15042
On the existence of circular polarisation in the pulsar radiation N91-15088
Thirty-five-day cycle of Her X-1: Synthesised optical light curves in the model of freely processing neutron star N91-15089
On the theory of large-scale micropulse structure of pulsar radio radiation N91-15092
Structure of accretion flow in close binary system: A two dimensional numerical model N91-15093
Accretion disk instability and spokes in Saturn's rings N91-15094
Compact object masses in active galactic nuclei and quasars and duration of activity stage N91-15096
A model for one-sided extragalactic jets N91-15097
On the generation of magnetic fields in active star atmospheres N91-15099
ASTRONOMICAL OBSERVATORIES
Wind tunnel study of an observatory dome with a circular aperture
[NASA-TM-102888] N91-15040
ASTRONOMICAL PHOTOGRAPHY
Compact reflection nebulae, a transit phase of evolution from post-AGB to planetary nebulae N91-15029
Coronal mass ejections
[NASA-CR-186579] N91-15115
ASTRONOMICAL SPECTROSCOPY
The 3.4 micron emission in comets N91-15006
ASTROPHYSICS
NASA's supercomputing experience
[NASA-TM-102890] N91-14727
Superaromatics: The key to a unified cosmic dust theory N91-14999
Plasma Astrophysics
[ESA-SP-311] N91-15046
Particle physics and cosmology
[DE91-001946] N91-15111
ASYMMETRY
Asymmetric supersonic flow around cones with noncircular sections N91-14292
Trellis coded modulation for transmission over fading mobile satellite channel
[NASA-CASE-NPO-16904-2-CU] N91-14523
Computational equipment for the development of numerical algorithms computation
[AD-A226702] N91-14729
ASYMPTOTIC GIANT BRANCH STARS
Sublimating comets as the source of nucleation seeds for grain condensation in the gas outflow from AGB stars N91-15018
Circumstellar grain extinction properties of recently discovered post AGB stars N91-15028
Compact reflection nebulae, a transit phase of evolution from post-AGB to planetary nebulae N91-15029
ATMOSPHERIC CHEMISTRY
Atmospheric source-receptor relationships: Concepts and terminology
[DE91-001033] N91-14656
Acidic deposition: Its nature and impacts
[DE91-001984] N91-14658
Studies of the chemistry of the nightside ionosphere of Venus
[NASA-CR-187714] N91-15114
ATMOSPHERIC CIRCULATION
Upwelling southwest of Iceland due to quasi-geostrophic flow
[AD-A227129] N91-14698
Effect of atmospherics on beamforming accuracy
[NASA-CR-187695] N91-14802
The rotation of Venus and its atmosphere N91-15112
A mesoscale planetary boundary layer numerical model for simulations of topographically induced circulations N91-15113
ATMOSPHERIC COMPOSITION
Studies of the observed and theoretical variations of atmospheric ozone
[NASA-CR-187703] N91-14657
The response of atmospheric CO2 to changes in land use
[DE91-001212] N91-14663
ATMOSPHERIC ELECTRICITY
Aircraft measurements of electrified clouds at Kennedy Space Center
[NASA-CR-186536] N91-14680
Aircraft measurements of electrified clouds at Kennedy Space Center. Part 1: 1988 flights N91-14681
Aircraft measurements of electrified clouds at Kennedy Space Center. Part 2: Case study: 4 November 1988 (88309) N91-14682
ATMOSPHERIC ENTRY
Gamma guidance of trajectories for coplanar, aeroassisted orbital transfer
[NASA-CR-187732] N91-14365
Properties of the optimal trajectories for coplanar, aeroassisted orbital transfer
[NASA-CR-187733] N91-14366
Decomposition technique and optimal trajectories for the aeroassisted flight experiment
[NASA-CR-187734] N91-14367
ATMOSPHERIC HEATING
Flare heating and ionization of the low solar chromosphere N91-15116
ATMOSPHERIC IONIZATION
Flare heating and ionization of the low solar chromosphere N91-15116

ATMOSPHERIC MODELS
Studies of the observed and theoretical variations of atmospheric ozone
[NASA-CR-187703] N91-14657
Theory and measurements of nighttime horizontal gradients in the mid-latitude F region N91-14671
Overview of the US Department of Energy's ARM (Atmospheric Radiation Measurement) program
[DE91-001126] N91-14678
Climate and atmospheric modeling studies. Climate applications of Earth and planetary observations. Chemistry of Earth and environment
[NASA-CR-187326] N91-14684
Semi-implicit time integration in limited area model
[AD-A226818] N91-14785
A mesoscale planetary boundary layer numerical model for simulations of topographically induced circulations N91-15113
Studies of the chemistry of the nightside ionosphere of Venus
[NASA-CR-187714] N91-15114
ATMOSPHERIC RADIATION
Overview of the US Department of Energy's ARM (Atmospheric Radiation Measurement) program
[DE91-001126] N91-14678
Limb-darkening functions as derived from along-track operation of the ERBE scanning radiometers for August 1985
[NASA-RP-1243] N91-14683
ATMOSPHERIC SOUNDING
Aircraft measurements of electrified clouds at Kennedy Space Center
[NASA-CR-186536] N91-14680
Aircraft measurements of electrified clouds at Kennedy Space Center. Part 1: 1988 flights N91-14681
Aircraft measurements of electrified clouds at Kennedy Space Center. Part 2: Case study: 4 November 1988 (88309) N91-14682
Cloud cover statistics
[AD-A226892] N91-14689
ATMOSPHERIC TIDES
The rotation of Venus and its atmosphere N91-15112
ATMOSPHERIC TURBULENCE
Effect of atmospherics on beamforming accuracy
[NASA-CR-187695] N91-14802
ATMOSPHERICS
Radio Frequency Interference (RFI) measurements made near the proposed Alaska OTH receiving site
[AD-A226922] N91-14519
ATOMIC INTERACTIONS
Equilibrium composition of interphase boundaries
[DE91-002470] N91-14814
ATOMIC STRUCTURE
The effect of scandium on the phase stability of Al3Nb and Al3Zr
[DE91-002657] N91-14459
Atomic environments in iron meteorites using EXAFS N91-15011
ATOMS
Spontaneous and induced coherent radiation generation in atomic vapors
[AD-A226776] N91-14830
ATTITUDE (INCLINATION)
Interaction of feel system and flight control system dynamics on lateral flying qualities
[NASA-CR-179445] N91-14353
ATTITUDE STABILITY
The effects of liquid propellant motion on the attitude stability of spin stabilized spacecraft
[AD-A227002] N91-14376
AUDITORY PERCEPTION
Demodulation processes in auditory perception
[AD-A226824] N91-14707
Validation of dichotic listening and psychomotor task performance as predictors of primary flight training criteria: Highlighting relevant statistical issues
[AD-A227010] N91-14717
AUDITORY SIGNALS
Demodulation processes in auditory perception
[AD-A226824] N91-14707
Massively parallel network architectures for automatic recognition of visual speech signals
[AD-A226968] N91-14805
AURORAS
Implications of multipoint observations of substorms in the inner magnetotail N91-15061
AUTOCORRELATION
Damping measurements using operational data
[DE91-002781] N91-14646
The autocorrelation function of the North Pole dust N91-14901
AUTOMATA THEORY
Prototyping of a protocol validation environment: Application to the Estelle approach
[LAAS-90113] N91-14774
AUTOMATIC PILOTS
Role of separation autopilots for modern missile concepts
[MBB/FE121/S/PUB/409/A] N91-14352
AUTOMATIC TEST EQUIPMENT
Effect of laser fluctuations in automated solder joint inspection
[AD-A226685] N91-14620
Automated system for measuring the strength of optical fibers
[AD-D014626] N91-14824
AUTOMOBILE FUELS
CRC program for quantifying performance of knock-sensor-equipped vehicles with varying octane level
[AD-A227340] N91-14612
AVALANCHE DIODES
Development and testing of radiation and electromagnetic pulse hardened silicon carbide based electronics
[AD-A227309] N91-14548
AVALANCHES
Snow avalanche hazards and mitigation in the United States
[LC-90-62814] N91-14686
AXIAL STRAIN
Axial-torsional fatigue: A study of tubular specimen thickness effects
[NASA-TM-103637] N91-14632
AXISYMMETRIC BODIES
Investigations of aerothermodynamic effects on axisymmetric bodies at high Mach numbers N91-14302
The inviscid stability of supersonic flow past heated or cooled axisymmetric bodies
[NASA-CR-187475] N91-14307
AXISYMMETRIC FLOW
Computation of axisymmetric base flow with different turbulence models N91-14298
A numerical and experimental analysis of reactor performance and deposition rates for CVD on monofilaments
[NASA-TM-103631] N91-14500
A fast solver for systems of axisymmetric ring vortices
[DE91-002594] N91-14561

B

B STARS
Properties of interstellar dust in the region of the CEP OB4 association N91-14903
Additional red and reddened stars in Cyg OB2 association N91-14948
BACKGROUND RADIATION
New measurements of the far ultraviolet scattering properties of interstellar dust N91-14909
Infrared emission from interplanetary dust N91-15013
BACKSCATTERING
Optical phase conjugation via stimulated Brillouin scattering in multimode optical fiber
[AD-A227054] N91-14833
BAKING
Total-dose radiation hardness assurance for space electronics
[DE91-002425] N91-14533
BALANCE
Wind tunnel balance
[NASA-CASE-ARC-11877-1-SB] N91-14357
Multiple axis reticle
[NASA-CASE-ARC-11886-1-SB] N91-14591
BALL BEARINGS
Turbomachinery rotor support with damping
[NASA-CASE-MFS-28345-1] N91-14608
BALLISTIC TRAJECTORIES
A GNM mission and system design proposal N91-14364
BALLISTICS
A modification of 4330 alloy steel
[DE91-001764] N91-14455
BALLOON-BORNE INSTRUMENTS
A balloon-borne aerosol spectrometer for high altitude low aerosol concentration measurements
[DE91-002563] N91-14661
A balloon-borne integrating nephelometer
[DE91-001037] N91-14687
BALLOONS
A system architecture for long duration free floating flight for military applications
[NASA-CR-187435] N91-14513
BANDPASS FILTERS
Stable explicit depth extrapolation of seismic wavefields
[DE91-001445] N91-14674
BANDWIDTH
Electro-optic network analyzer
[NASA-CR-186613] N91-14527
Picosecond laser system for high speed characterization of monolithic devices
[AD-A227372] N91-14595
BARIUM OXIDES
Fabrication of sensitive high Tc bolometers N91-14389
Superconducting properties of Tl-Ba-Ca-Cu-O films on silver substrates
[DE91-002304] N91-14856
An ion-channeling study of irradiation-induced amorphization of YBa2Cu3O(7-x)
[DE91-004488] N91-14884
BAROCLINITY
Observations of ocean fluctuations between 15 and 23 hour periods in the Pacific
[AD-A227017] N91-14695
BAROTROPISM
Shipboard and satellite observations of upper ocean velocity and transport variability in the Gulf Stream
[AD-A226974] N91-14694
Observations of ocean fluctuations between 15 and 23 hour periods in the Pacific
[AD-A227017] N91-14695
BASE FLOW
Computation of axisymmetric base flow with different turbulence models N91-14298
Direct numerical simulation of turbulent couette flow, part 2
[AD-A226770] N91-14564
BATHS
Electroless nickel bath recovery by cation exchange and precipitation
[DE91-001988] N91-14457
BATHYMETERS
Helicopter lidar bathymeter system. Conceptual design
[AD-A227057] N91-14348
Multispectral imagery support for ocean venture 90
[AD-A227119] N91-14697
BAYES THEOREM
Interpretation of conditional probabilities in probabilistic interference word problems
[AD-A226907] N91-14797
BEAM CURRENTS
Recent long-pulse and high-average-power tests on a 140 GHz gyrotron
[DE91-001680] N91-14592
A beam position monitor for low current dc beams
[CEBAF-PR-89-004] N91-14816
An intense optically pumped H(-) ion source
[DE91-002949] N91-14827
BEAM INJECTION
Characteristics and potential applications of an ORNL microwave ECR multicusp plasma ion source
[DE91-002649] N91-14840
DIII-D results and plans
[DE91-001548] N91-14847
BEAMS (SUPPORTS)
Wind tunnel balance
[NASA-CASE-ARC-11877-1-SB] N91-14357
On the modeling and control of slewing flexible structures N91-14499
BEARING (DIRECTION)
Effect of atmospherics on beamforming accuracy
[NASA-CR-187695] N91-14802
BEHAVIOR
Bioreactivity: Studies on a simple brain stem reflex in behaving animals
[AD-A226823] N91-14704
BEND TESTS
Delamination test apparatus and method
[NASA-CASE-LAR-13985-1] N91-14430
BENDING
The effect of wing planform on low speed buffet N91-14336
BENDING MOMENTS
New method to determine in wind tunnel the buffeting forces N91-14337
BERYLLIUM
Scattering by anisotropic grains in beryllium mirrors
[DE91-001724] N91-14826
BIAS
NOVA 201 ultrasonic thickness gage (NOVA Gage)
[NASA-CR-184031] N91-14581
BIBLIOGRAPHIES
Aerospace medicine and biology: A continuing bibliography with indexes (supplement 343)
[NASA-SP-7011(343)] N91-14711
Aerospace medicine and biology: A continuing bibliography with indexes (supplement 344)
[NASA-SP-7011(344)] N91-14712
A bibliography of planetary geology and geophysics principal investigators and their associates, 1989-1990
[NASA-TM-4221] N91-15034

Air Force Office of Scientific Research technical report summaries: April-June 1990
[AD-A227387] N91-15121
Air Force Office of Scientific Research technical report summaries: January-March 1990
[AD-A227368] N91-15122

BIDIRECTIONAL REFLECTANCE
Scattering by anisotropic grains in beryllium mirrors
[DE91-001724] N91-14826

BINARY STARS
Structure of accretion flow in close binary system: A two dimensional numerical model N91-15093

BIOASTRONAUTICS
Aerospace medicine and biology: A continuing bibliography with indexes (supplement 343)
[NASA-SP-7011(343)] N91-14711
Aerospace medicine and biology: A continuing bibliography with indexes (supplement 344)
[NASA-SP-7011(344)] N91-14712

BIOCHEMISTRY
JPRS Report: Science and technology. USSR: Life sciences
[JPRS-ULS-89-003] N91-14706

BIOGEOCHEMISTRY
The response of atmospheric CO2 to changes in land use
[DE91-001212] N91-14663

BIOLOGICAL EFFECTS
Aerospace medicine and biology: A continuing bibliography with indexes (supplement 343)
[NASA-SP-7011(343)] N91-14711
Aerospace medicine and biology: A continuing bibliography with indexes (supplement 344)
[NASA-SP-7011(344)] N91-14712

BIOREACTORS
Bio-reactor chamber
[NASA-CASE-MSC-20929-1] N91-14703

BIOTECHNOLOGY
Bio-reactor chamber
[NASA-CASE-MSC-20929-1] N91-14703

BIPOLARITY
Polarization due to dust scattering in the planetary nebula Cn1-1 N91-15027
The discovery of a highly polarized bipolar nebula N91-15031

BISMALEIMIDE
Bis (4-(3,4-dimethylene-pyrrolidyl)-phenyl) methane
[NASA-CASE-LAR-13965-2-CU] N91-14418
N-(3-ethynylphenyl)maleimide
[NASA-CASE-LAR-14188-2] N91-14419

BISMUTH
InAsSbBi, a direct band-gap, III-V, LWIR material N91-14410

BISTATIC REFLECTIVITY
Description of the bistatic radar terrain measurements system equipment
[AD-A226808] N91-14517

BLADE-VORTEX INTERACTION
Prediction of XV-15 tilt rotor discrete frequency aeroacoustic noise with WOPWOP
[NASA-CR-187684] N91-14603

BLOOD
Initial blood storage experiment
[NASA-CR-185513-PT-1] N91-14700
Initial blood storage experiment
[NASA-CR-185513-PT-2] N91-14701

BLOWING
Flow visualization studies of blowing from the tip of a swept wing
[NASA-TM-4217] N91-14274
A parametric shell analysis of the shuttle 51-L SRB AFT field joint
[NASA-TM-102748] N91-14629

BODIES OF REVOLUTION
A finite element conjugate gradient FFT method for scattering N91-14476

BODY-WING AND TAIL CONFIGURATIONS
Systematic investigations of body-wing-tail interference at high angles of attack N91-14290

BOLOMETERS
Innovative Long Wavelength Infrared Detector Workshop Proceedings
[NASA-CR-187433] N91-14379
Fabrication of sensitive high Tc bolometers N91-14389
Pyroelectric detectors N91-14390

BOLTZMANN TRANSPORT EQUATION
A numerical theory of lattice gas and lattice Boltzmann methods in the computation of solutions to nonlinear advective-diffusive systems
[DE91-002566] N91-14560
Pregalactic inhomogeneity in hot dark matter model of the universe N91-15100

BONDING
Interfacial push-out measurements of fully-bonded SiC/SC composites
[DE91-004527] N91-14436
Joining alumina to sapphire for copper vapor laser tubes
[AD-A226619] N91-14501
Some problems in elastic contact and fracture N91-14625

BOOLEAN ALGEBRA
Boolean Grobner bases, calculation methods. Applications and parallel processing
[ETN-90-98208] N91-14768
On probability intervals and their updating
[RUU-CS-90-22] N91-14793

BOOSTER ROCKET ENGINES
Flight Set 360L006 STS-34 field joint protection system, thermal protection system, and systems tunnel components, volume 4
[NASA-CR-184050] N91-14415

BORIDES
High temperature refractory member with radiation emissive overcoat
[NASA-CASE-NPO-17122-1-CU] N91-14489

BOUNDARY CONDITIONS
Analytical solutions with Generalized Impedance Boundary Conditions (GIBC) N91-14477

BOUNDARY ELEMENT METHOD
A boundary element method for elastostatic and elastodynamic crack problems in two and three dimensions N91-14626
A combined finite element-boundary element formulation for solution of axially symmetric bodies
[NASA-CR-185852] N91-14789

BOUNDARY LAYER CONTROL
Structural development of laminar flow control aircraft chordwise wing joint designs
[NASA-CR-181888] N91-14346
Active control of boundary layer transition and turbulence
[NASA-CASE-LAR-13532-1] N91-14562

BOUNDARY LAYER FLOW
On the breakdown of a vortex
[AD-A227066] N91-14568

BOUNDARY LAYER SEPARATION
Dynamics of separation and reattachment in a Mach 5 unswept compression ramp flow N91-14276
Aircraft Dynamic Loads Due to Flow Separation
[AGARD-CP-483] N91-14324
Effects of trailing-edge flap on buffet characteristics of a supercritical airfoil N91-14327

BOUNDARY LAYER STABILITY
The inviscid stability of supersonic flow past heated or cooled axisymmetric bodies
[NASA-CR-187475] N91-14307
Comments on hypersonic boundary-layer transition
[AD-A227242] N91-14314

BOUNDARY LAYER TRANSITION
Comments on hypersonic boundary-layer transition
[AD-A227242] N91-14314
Active control of boundary layer transition and turbulence
[NASA-CASE-LAR-13532-1] N91-14562

BOUNDARY LAYERS
Numerical investigations in three-dimensional internal flows
[NASA-CR-187373] N91-14277
Numerical study of shock-wave/boundary layer interactions in premixed hydrogen-air hypersonic flows
[NASA-TM-103273] N91-14559

BOUNDARY VALUE PROBLEMS
Perspectives on modeling electromagnetic sea scatter
[AD-A226939] N91-14520
Computer aided design models for millimeter-wave suspended substrate microstrip line
[AD-A227259] N91-14547
Vibration isolation technology: Sensitivity of selected classes of experiments to residual accelerations
[NASA-CR-186902] N91-14624
The integral equation method for an elliptic boundary value of the half integer characteristic
[ETN-91-98167] N91-14779
Projected implicit Runge-Kutta methods for differential-algebraic boundary value problems
[DE91-000660] N91-14791

BOW WAVES
Dust in stellar wind bow shocks N91-14979
Gradient catastrophe of the supersonic mass-loaded magnetised plasma flow and the formation of bow shock N91-15065

BRAIN
Bioreactivity: Studies on a simple brain stem reflex in behaving animals
[AD-A226823] N91-14704
Empirical network model of human higher cognitive brain functions
[AD-A227193] N91-14718
Information extraction from visual displays and the event-related brain potential
[AD-A227063] N91-14722

BRAIN STEM
Bioreactivity: Studies on a simple brain stem reflex in behaving animals
[AD-A226823] N91-14704

BRIDGMAN METHOD
A novel approach to determine the heat transfer coefficient in directional solidification furnaces
[NASA-CR-187648] N91-14885

BRIGHTNESS
Experimental results in superconducting niobium resonators for high-brightness ion beam acceleration
[DE91-004478] N91-14882
The spectral energy distribution of the scattered light from dark clouds N91-14911
Observations of the diffuse UV radiation field N91-14912
Diffuse galactic light observations at 206 selected areas N91-14914
The wavelength dependence of polarization in NGC 2023 N91-14923
Red fluorescence and 3-12 micron emission in NGC 2023, HD 44179, M 82, and Lynds 1780 N91-14924
A rocket-borne measurement of interstellar dust emission at high galactic latitude N91-14976

BRILLOUIN EFFECT
Optical phase conjugation via stimulated Brillouin scattering in multimode optical fiber
[AD-A227054] N91-14833

BRITTLENESS
Directional solidification of superalloys
[NASA-CASE-MFS-28314-1] N91-14462

BROADBAND
MMIC compensation network for phased array element mismatch
[AD-A227437] N91-14522

BUCKLING
The buckling of off-axis, orthotropic, cylindrical shells in torsion N91-14628

BUFFETING
Aircraft Dynamic Loads Due to Flow Separation
[AGARD-CP-483] N91-14324
Wind tunnel investigation and flight tests of tail buffet on the CF-18 aircraft N91-14325
A unified approach to buffet response of fighter aircraft empennage N91-14326
Effects of trailing-edge flap on buffet characteristics of a supercritical airfoil N91-14327
Experimental investigation of buffet onset and penetration on a supercritical airfoil at transonic speeds N91-14328
Experimental investigations of buffet excitation forces on a low aspect ratio trapezoidal half wing in incompressible flow N91-14329
Experimental investigation and semi-empirical prediction of the dynamic response of a low-aspect-ratio trapezoidal wing due to flow separation N91-14330
Unsteady aerodynamic forces on an oscillating wing at high incidences and flow separation N91-14331
The forward mounted spoiler as a source of buffet excitation N91-14332
Interaction between the canard and wing flow on a model of a typical combat aircraft N91-14334
Predictions of F-111 TACT aircraft buffet response N91-14335
The effect of wing planform on low speed buffet N91-14336
New method to determine in wind tunnel the buffeting forces N91-14337
Unsteady separated flow phenomena causing self-excited structural oscillations N91-14339

BUNDLES
Optical encoding of imaging data
[AD-D014617] N91-14821

BUOYANCY
Vibration isolation technology: Sensitivity of selected classes of experiments to residual accelerations
[NASA-CR-186902] N91-14624
A new kind of magnetic buoyancy instability N91-15050

BURNING RATE
The application of the turbulent burning speed concept to laboratory flames
[DE91-001789] N91-14449
Solid fuel combustion
[AD-A227170] N91-14496

BURSTS
Bursts of energetic protons in the Earth's magnetotail N91-15058

Laboratory simulation of the astrophysical burst processes in non-uniform magnetised media
N91-15081

BUTTERFLY VALVES
Hybrid butterfly valve
[NASA-CASE-SSC-00004-1] N91-14609

C

CABLES (ROPES)
A cable vehicle barrier for alert aircraft protection
[DE91-001723] N91-14354

CADMIUM
HgZnTe-based detectors for LWIR NASA applications
N91-14404
Small band gap superlattices as intrinsic long wavelength infrared detector materials N91-14405

CADMIUM SELENIDES
Magnetic properties of doped semiconductors
[DE91-002395] N91-14859

CADMIUM SULFIDES
High efficiency cadmium and zinc telluride-based thin film solar cells
[DE91-002112] N91-14643

CADMIUM TELLURIDES
MBE HgCdTe heterostructure detectors N91-14402
Growth and properties of Hg-based quantum well structures and superlattices N91-14403
High efficiency cadmium and zinc telluride-based thin film solar cells
[DE91-002112] N91-14643

CALCIUM OXIDES
Superconducting properties of Tl-Ba-Ca-Cu-O films on silver substrates
[DE91-002304] N91-14856

CALCULUS
Capturing strong reduction in director string calculus
[AD-A226738] N91-14783

CALENDARS
Astronomical phenomena for the year 1990
N91-15035

CALIBRATING
Multiple axis reticle
[NASA-CASE-ARC-11886-1-SB] N91-14591
Remote sensing of Earth terrain
[NASA-CR-186904] N91-14635
In-flight methods for satellite sensor absolute radiometric calibration N91-14801
A proposed astronomical reference catalog of infrared sources
[AD-A226757] N91-15041

CALORIMETERS
An automated flow calorimeter for heat capacity and enthalpy measurements at elevated temperatures and pressures
[DE91-002759] N91-14584
A study of liquid scintillator and fiber materials for use in a fiber calorimeter
[DE91-004229] N91-14585
Initial data from the Soudan 2 experiment
[DE91-004454] N91-14815

CANARD CONFIGURATIONS
Interaction between the canard and wing flow on a model of a typical combat aircraft N91-14334

CANCELLATION
Innovative methodology for cancelling contaminating noise in turbulent fluid flow environments
[AD-A227028] N91-14567

CANOPIES (VEGETATION)
Multiband radar characterization of forest biomes
[NASA-CR-185101] N91-14638

CAPACITORS
Method and apparatus for determining time, direction, and composition of impacting space particles
[NASA-CASE-LAR-13392-1-CU] N91-14412

CAPE KENNEDY LAUNCH COMPLEX
Aircraft measurements of electrified clouds at Kennedy Space Center
[NASA-CR-186536] N91-14680
Aircraft measurements of electrified clouds at Kennedy Space Center. Part 1: 1988 flights N91-14681
Aircraft measurements of electrified clouds at Kennedy Space Center. Part 2: Case study: 4 November 1988 (88309) N91-14682

CAPILLARY FLOW
Effect of interline heat flow parameter on contact line heat transfer
[AD-A226944] N91-14566

CAPTIVE TESTS
Measurement of hydrodynamic forces and moments and flow field mapping of a model in coning motion
[AD-A226684] N91-14355

CARBIDES
Dynamic consolidation of aluminum-silicon carbide composites
[DE91-001929] N91-14427
Thermal stability of the microstructure of an aged Nb-Zr-C alloy
[NASA-TM-103647] N91-14454
Use of anomalous small angle x ray scattering to investigate microstructural features in complex alloys
[DE91-002397] N91-14471

CARBON
Amorphization of C-implanted Fe(Cr) alloys
[DE91-001338] N91-14489
Method of growing diamond film on substrates
[AD-D014632] N91-14479
Simultaneous infrared and UV-visible absorption spectra of matrix-isolated carbon vapor N91-14915
VUV-visible measurements on different samples of amorphous carbon N91-14990
Properties of grains derived from IRAS observations of dust N91-15001
Experimental evidence for amorphous carbon grains in comets N91-15008

CARBON DIOXIDE
The response of atmospheric CO2 to changes in land use
[DE91-001212] N91-14663
Overview of the US Department of Energy's ARM (Atmospheric Radiation Measurement) program
[DE91-001126] N91-14678
Climate and atmospheric modeling studies. Climate applications of Earth and planetary observations. Chemistry of Earth and environment
[NASA-CR-187326] N91-14684
Diffusion and infrared properties of molecules in ice mantles N91-14963

CARBON DIOXIDE LASERS
IR and FIR laser diagnostics for plasma thrusters using a CW CO2 radiation source
[AD-A226816] N91-14843

CARBON FIBER REINFORCED PLASTICS
Surface and interfacial properties of carbon fibers
[NASA-CR-184916] N91-14429

CARBON FIBERS
Surface and interfacial properties of carbon fibers
[NASA-CR-184916] N91-14429
Mesomechanical model for fibre composites
[AD-A226792] N91-14432

CARBON MONOXIDE
The response of atmospheric CO2 to changes in land use
[DE91-001212] N91-14663
Diffusion and infrared properties of molecules in ice mantles N91-14963
Does CO trace H2 at high galactic latitude
N91-14973
Molecules, grains, and shocks: A comparison of CO, H I, and IRAS data N91-14975
Molecules in an infrared cirrus cloud N91-14977
Infrared cirrus point sources N91-14978

CARBON STARS
PAH formation in carbon-rich circumstellar envelopes
N91-15015
IR emission from circumstellar envelopes of C-rich stars N91-15019
Carbon stars with alpha-C:H emission N91-15022

CARBONACEOUS MATERIALS
High-spectral resolution observations of the 3.29 micron emission feature: Comparison to QCC and PAHs
N91-14925
Raman properties of various carbonaceous materials and their astrophysical implications N91-14933

CARBONIZATION
Characterization of phenolic resins with thermogravimetry-mass spectrometry
[DE91-002710] N91-14492

CARRIAGES
Store carriage, integration, and release N91-14281

CARRIER MOBILITY
Quantum 1/f noise in high technology applications including ultrasmall structures and devices
[AD-A226739] N91-14515

CASTING
Method for manufacturing composite material
[EP-PATENT-0-314-353-A2] N91-14421
A modification of 4330 alloy steel
[DE91-001764] N91-14455
Thin steel section casting on a near-horizontal twin-belt caster
[DE91-001883] N91-14505

CASTINGS
Expendable Pattern Casting Technology
[DE91-001348] N91-14503

CATALYSIS
Mechanism of hydrodenitrogenation. Part 4: Infrared spectroscopy of acidic molybdena catalysts
[DE91-002496] N91-14440

CATHODE RAY TUBES
Raster graphic helmet-mounted display study
[NASA-CR-4331] N91-14347

CATHODES
High gradient electron guns
[DE91-000056] N91-14369
Organic cathode for a secondary battery
[NASA-CASE-NPO-17604-1-CU] N91-14536
Copper chloride cathode for a secondary battery
[NASA-CASE-NPO-17640-1-CU] N91-14538

CATHODIC COATINGS
Fracture analysis of cathodic delamination in rubber-to-metal bonds N91-14627

CATHOLYTES
Organic cathode for a secondary battery
[NASA-CASE-NPO-17604-1-CU] N91-14536

CATIONS
Electroless nickel bath recovery by cation exchange and precipitation
[DE91-001988] N91-14457

CATS
Bioreactivity: Studies on a simple brain stem reflex in behaving animals
[AD-A226823] N91-14704

CAVITONS
Wave collapse at lower hybrid resonance N91-15073

CAVITY RESONATORS
A versatile RF cavity mode damper
[DE91-002947] N91-14534
Experimental results in superconducting niobium resonators for high-brightness ion beam acceleration
[DE91-004478] N91-14882
First tests of a superconducting RFQ (radio frequency quadrupole) structure
[DE91-004483] N91-14883

CELESTIAL NAVIGATION
The Air Almanac, 1990 N91-15036
The Air Almanac, 1989 N91-15037

CENTER OF PRESSURE
Chordwise and spanwise centers of pressure of missile fins N91-14304

CENTRAL PROCESSING UNITS
Systolic emulator experimentation
[AD-A226746] N91-14516

CERAMIC FIBERS
Fatigue and fracture of titanium aluminides, volume 2
[AD-A227353] N91-14351

CERAMIC MATRIX COMPOSITES
Adhesion at ceramic interfaces
[DE91-001660] N91-14480

CERAMICS
Optimization of interface layers in the design of ceramic fiber reinforced metal matrix composites
[NASA-CR-185307] N91-14422
AC-130H Gunship Armor Upgrade Project
[DE91-002567] N91-14426
Conversion of alkoxide solutions to oxides: Evaporation of products
[AD-A226927] N91-14442
Computer studies of the dynamic strength of ceramics
[DE91-002568] N91-14481
Effect of hydrogen on the strength and microstructure of selected ceramics
[NASA-TM-103674] N91-14482
Heterocycles based on group 3, 4, and 5 elements: Precursors for novel glasses and ceramics
[AD-A226988] N91-14487
Electrophoretic and electrolytic deposition of ceramic particles on porous substrates
[AD-A227371] N91-14488
Thermal analyses for quality control of plastics, ceramics, and explosives
[DE91-002701] N91-14822

CERTIFICATION
Space shuttle redesigned solid rocket motor Certificate of Qualification (COQ) data report
[NASA-CR-184051] N91-14416

CESSNA AIRCRAFT
Smoke and extinguisher agent dissipation in a small pressurized fuselage
[DOT/FAA/CT-89/31] N91-14317

CHANNEL CAPACITY
International Symposium on Information Theory
[AD-A226957] N91-14521

CHANNEL FLOW
Direct numerical simulation of turbulent couette flow, part 2
[AD-A226770] N91-14564
Innovative methodology for cancelling contaminating noise in turbulent fluid flow environments
[AD-A227028] N91-14567

CHAOS
Investigations of equilibria, lattices, and chaotic dynamics of 2-D Hamiltonian point vortices
[AD-A227364] N91-14570
(DURIP) exploring and controlling spatio temporal chaos under complex structures through visualization: A mini-supercomputer approach
[AD-A226793] N91-14784

CHAPMAN-ENSKOG THEORY
A numerical theory of lattice gas and lattice Boltzmann methods in the computation of solutions to nonlinear advective-diffusive systems
[DE91-002566] N91-14560
Tokamak fluidlike equations, with applications to turbulence and transport in H mode discharges
[DE91-002632] N91-14849

CHARGE COUPLED DEVICES
Issues and directions in IR detector readout electronics N91-14387
X ray sensitive area detection device
[NASA-CASE-MFS-28232-1] N91-14835

CHARGE EXCHANGE
Intermediate energy nuclear physics
[DE91-002758] N91-14809

CHARGE TRANSFER DEVICES
Detector array evaluation and figures of merit N91-14386

CHARGED PARTICLES
Grains charges in interstellar clouds N91-14967

CHEBYSHEV APPROXIMATION
Mappings and accuracy for Chebyshev pseudo-spectral approximations
[NASA-TM-103630] N91-14781

CHEMICAL ANALYSIS
Thermal stability of the microstructure of an aged Nb-Zr-C alloy
[NASA-TM-103647] N91-14454
Analysis of hydroxylammonium nitrate based liquid propellants
[AD-A227300] N91-14497
Initial blood storage experiment
[NASA-CR-185513-PT-1] N91-14700
Cosmos 2044
[NASA-CR-187003] N91-14702

CHEMICAL BONDS
Theory of the electronic and structural properties of solid state oxides
[DE91-001192] N91-14874
Ground boundaries
[DE91-004027] N91-14880
Three-micron spectroscopy of highly reddened field stars N91-14904
Simultaneous infrared and UV-visible absorption spectra of matrix-isolated carbon vapor N91-14915

CHEMICAL COMPOSITION
Flow behavior of Ti-24Al-11Nb at high strain rates
[DE91-004506] N91-14473
FTIR (Fourier Transform Infrared) spectrophotometry for thin film monitors: Computer and equipment integration for enhanced capabilities
[DE91-001228] N91-14853
Pseudomorphic InGaAs materials
[AD-A226895] N91-14864
The 10 micron spectral structure in comets N91-15004
Vega-Giotto flyby missions and cometary cosmogony N91-15009
The composition of heavy molecular ions inside the ionopause of Comet Halley N91-15010
An interferometric study of molecular emission around NGC 7538 at millimeter wavelengths N91-15042

CHEMICAL PROPERTIES
Synthesis and properties of novel organometallic polymers
[DE91-001978] N91-14491

CHEMICAL REACTIONS
Use of D2 to elucidate OMVPE growth mechanisms
[AD-A226966] N91-14443
Dynamics of an unsteady diffusion flame: Effects of heat release and gravity
[AD-A227348] N91-14447
Computation of thermochemical nonequilibrium flows around a simple and a double ellipse
[NASA-CR-187702] N91-14558
Matrix isolation as a tool for studying interstellar chemical reactions N91-14956
Gas-phase formation of silicon carbides, oxides, and sulphides from atomic silicon ions N91-15014
PAH formation in carbon-rich circumstellar envelopes N91-15015

CHEMICAL REACTORS
A numerical and experimental analysis of reactor performance and deposition rates for CVD on monofilaments
[NASA-TM-103631] N91-14500

CHEMILUMINESCENCE
Investigation of combustion in large vortices
[AD-A226791] N91-14441

CHEMISORPTION
Mechanism of hydrodenitrogenation. Part 4: Infrared spectroscopy of acidic molybdena catalysts
[DE91-002496] N91-14440

CHLORINE
Photogenerated carrier-induced reaction on semiconductor surfaces
[DE91-001349] N91-14878

CHLOROCARBONS
Next-generation fire extinguishing agent. Phase 2: Laboratory tests and scoping trials
[AD-A227347] N91-14510

CHLOROPRENE RESINS
Fracture analysis of cathodic delamination in rubber-to-metal bonds N91-14627

CHROMIUM
Thermal stability of the microstructure of an aged Nb-Zr-C alloy
[NASA-TM-103647] N91-14454
Ion implantation for corrosion inhibition of aluminum alloys in saline media
[DE91-002687] N91-14461

CHROMIUM ALLOYS
Amorphization of C-implanted Fe(Cr) alloys
[DE91-001338] N91-14469

CHROMOSPHERE
A new model of spicule formation in the Sun chromosphere N91-15051
Filamentary structures in the Sun's atmosphere as singular Alfven waves N91-15053
Flare heating and ionization of the low solar chromosphere N91-15116

CHRONOLOGY
Chronology: MSFC Space Station program, 1982 - present. Major events
[NASA-CR-184014] N91-15119
Chronology: MSFC Space Shuttle program development, assembly, and testing major events (1969 - April, 1981)
[NASA-CR-184013] N91-15120

CIRCUIT PROTECTION
Thermal switch disc for short circuit protection of batteries
[NASA-CASE-MSC-21428-1] N91-14537

CIRCUITS
Issues and directions in IR detector readout electronics N91-14387
Monolithic multichannel detector amplifier arrays and circuit
[AD-D014566] N91-14528
Unidirectional amplitude sensitive noise riding threshold circuit
[AD-D014568] N91-14529

CIRCULAR CYLINDERS
Surface settling in partially filled containers upon step reduction in gravity
[NASA-TM-103641] N91-14556
A combined finite element-boundary element formulation for solution of axially symmetric bodies
[NASA-CR-185852] N91-14789

CIRCULAR PLATES
The response and failure mechanisms of circular metal and composite plates subjected to underwater shock loading
[AD-A226759] N91-14631

CIRCULAR POLARIZATION
Interstellar circular polarization and the dielectric nature of dust grains N91-14905
On the polarization mechanism in the R Mon/NGC 2261 complex N91-14969
On the existence of circular polarisation in the pulsar radiation N91-15088

CIRRUS CLOUDS
Cloud cover statistics
[AD-A226892] N91-14689
Molecules in an infrared cirrus cloud N91-14977

CLADDING
Effects of irradiation on initiation and crack-arrest toughness of two high-copper welds and on stainless steel cladding
[DE91-001272] N91-14467

CLAMPS
Post clamp
[NASA-CASE-LEW-14862-1] N91-14617

CLASSIFICATIONS
Remote sensing of Earth terrain
[NASA-CR-186904] N91-14635

CLEANING
Wall conditioning and plasma surface interactions in DIII-D
[DE91-001547] N91-14846

CLIMATE
The effects of climate change on the nitrogen cycle and acid deposition
[DE91-002785] N91-14659
Climate and atmospheric modeling studies. Climate applications of Earth and planetary observations. Chemistry of Earth and environment
[NASA-CR-187326] N91-14684

CLIMATE CHANGE
Office of Basic Energy Sciences 1990 summary report
[DE91-002971] N91-14653
The effects of climate change on the nitrogen cycle and acid deposition
[DE91-002785] N91-14659
Climate and atmospheric modeling studies. Climate applications of Earth and planetary observations. Chemistry of Earth and environment
[NASA-CR-187326] N91-14684

CLIMATOLOGY
Climate and atmospheric modeling studies. Climate applications of Earth and planetary observations. Chemistry of Earth and environment
[NASA-CR-187326] N91-14684

CLOSED CIRCUIT TELEVISION
State of the art in video system performance N91-14578

CLOUD COVER
Cloud cover statistics
[AD-A226892] N91-14689

CLOUD HEIGHT INDICATORS
Cloud cover statistics
[AD-A226892] N91-14689

CLOUDS (METEOROLOGY)
Aircraft measurements of electrified clouds at Kennedy Space Center
[NASA-CR-186536] N91-14680
Aircraft measurements of electrified clouds at Kennedy Space Center. Part 1: 1988 flights N91-14661
Aircraft measurements of electrified clouds at Kennedy Space Center. Part 2: Case study: 4 November 1988 (88309) N91-14662
Modeling study of tropical nonsquall and squall clusters N91-14685

CLUMPS
Heteronuclear metal cluster compounds synthesis and reactivity
[AD-A226815] N91-14463
Scale-invariant theory of optical properties of fractal clusters
[AD-A227031] N91-14832

CMOS
The use of light emission in failure analysis of CMOS ICs
[DE91-001234] N91-14633

CNOIDAL WAVES
On the theory of large-scale micropulse structure of pulsar radio radiation N91-15092

COAGULATION
Dust coagulation in ISM N91-14968

COAL GASIFICATION
Liquid hydrogen polygeneration system and process
[NASA-CASE-KSC-11304-2] N91-14495

COATINGS
High gradient electron guns
[DE91-000056] N91-14369
Method of growing diamond film on substrates
[AD-D014632] N91-14479
A continuum approach toward modeling the mechanics of solid lubricating films
[AD-A226961] N91-14486

COBALT 60
Total-dose radiation hardness assurance for space electronics
[DE91-002425] N91-14533

COCKPITS
Smoke and extinguisher agent dissipation in a small pressurized fuselage
[DOT/FAA/CT-89/31] N91-14317

CODERS
Electrostatically suspended rotor for angular encoder
[NASA-CASE-MFS-28294-1] N91-14508

CODING
International Symposium on Information Theory
[AD-A226957] N91-14521
Advanced technology development for image gathering, coding, and processing N91-14579
Optical encoding of imaging data
[AD-D014617] N91-14821

COGNITION
Eye movements and visual information processing
[AD-A226782] N91-14714
Investigating individual differences in general comprehension skill: The role of suppression and enhancement
[AD-A226788] N91-14715

Empirical network model of human higher cognitive brain functions
[AD-A227193] N91-14718

COGNITIVE PSYCHOLOGY
The effects of sleep loss on individual and group performance
[AD-A226963] N91-14708
Investigating individual differences in general comprehension skill: The role of suppression and enhancement
[AD-A226788] N91-14715
Adaptive human-computer interfaces using expert profiles
[AD-A226906] N91-14721
Investigations of probabilistic inference
[AD-A226882] N91-14795
The object display: Principles and review of experimental findings
[AD-A226883] N91-14796
Interpretation of conditional probabilities in probabilistic interference word problems
[AD-A226907] N91-14797
The evaluation of long range consequences in decision making
[AD-A226949] N91-14888

COHERENT RADIATION
Spontaneous and induced coherent radiation generation in atomic vapors
[AD-A226776] N91-14830

COHESION
Ion-induced grain growth in multilayer and coevaporated metal alloy thin films
[DE91-004489] N91-14472

COLD NEUTRONS
Status of the advanced neutron source
[DE91-002870] N91-14810

COLD TOLERANCE
Development of an animal model of human non-freezing cold injury: Changes in thermal sensitivity following cold exposure
[AD-A227174] N91-14705

COLLAPSE
Wave collapse at lower hybrid resonance N91-15073

COLLIMATION
Effect of atmospherics on beamforming accuracy
[NASA-CR-187695] N91-14802

COLLISION AVOIDANCE
Planning monotone paths to visit a set of obstacles
[AD-A226923] N91-14754

COLLISIONAL PLASMAS
Linear resonant interaction of an electromagnetic wave with a collisional inhomogeneous plasma
[IPPCZ-298] N91-14836
Physics data base for the Beam Plasma Neutron Source (BPNS)
[DE91-002796] N91-14842

COLLISIONLESS PLASMAS
Nonstationary processes in the front of high Mach number collisionless quasiperpendicular shock: Dynamics of the ion distribution N91-15067
Hydrodynamics of collisionless relativistic plasma in a strong magnetic field N91-15072
Generation of inductive fields by an oblique magnetic rotator in collisionless plasma N91-15077
Laboratory simulation of the astrophysical burst processes in non-uniform magnetised media N91-15081
Laboratory and computer simulations of wave generation processes in non-stationary astrophysical phenomena N91-15082

COLLISIONS
The rotation of Venus and its atmosphere N91-15112

COLLOCATION
Mappings and accuracy for Chebyshev pseudo-spectral approximations
[NASA-TM-103630] N91-14781

COLOR
Color palette: Plotting guide for use with GSMAP and GSDRAW digital cartographic software
[DE91-001643] N91-14737
Reddening and extinction towards H II regions N91-14898

COMBINATORIAL ANALYSIS
The definition of necessary hidden units in neural networks for combinatorial optimization
[AD-A227142] N91-14786

COMBINED CYCLE POWER GENERATION
Liquid hydrogen polygeneration system and process
[NASA-CASE-KSC-11304-2] N91-14495

COMBINED STRESS
Stress field rotation or block rotation: An example from the Lake Mead fault system N91-14668

COMBUSTIBLE FLOW
The application of the turbulent burning speed concept to laboratory flames
[DE91-001789] N91-14449

COMBUSTION
Definition of experiments to investigate fire suppressants in microgravity
[NASA-CR-185295] N91-14378
Statistical errors in the fractal analysis of flame boundaries
[DE91-001795] N91-14439
The response of atmospheric CO2 to changes in land use
[DE91-001212] N91-14663

COMBUSTION CHAMBERS
Combustor technology for future aircraft
[NASA-TM-103268] N91-14349

COMBUSTION PHYSICS
Numerical study of shock-wave/boundary layer interactions in premixed hydrogen-air hypersonic flows
[NASA-TM-103273] N91-14559

COMBUSTION STABILITY
CFD code evaluation for internal flow modeling
[NASA-CR-187677] N91-14557
Effects of turbulence on stationary and nonstationary processes in C-systems
[AD-A227067] N91-14569

COMET NUCLEI
The 3.4 micron emission in comets N91-15006
Vega-Giotto flyby missions and cometary cosmogony N91-15009

COMETARY ATMOSPHERES
A comparative study of the continuum and emission characteristics of comet dust. 1: Are the silicates in Comet Halley and Kohoutek amorphous or crystalline N91-15005
Theoretical studies of important processes in planetary and comet atmospheres
[NASA-CR-187692] N91-15045

COMETS
The 3.4 micron emission in comets N91-15006
Experimental evidence for amorphous carbon grains in comets N91-15008
Sublimating comets as the source of nucleation seeds for grain condensation in the gas outflow from AGB stars N91-15018
A study of extended zodiacal structures
[NASA-CR-187687] N91-15044
Solitary vortices in the vicinity of comets N91-15062
Gradient catastrophe of the supersonic mass-loaded magnetised plasma flow and the formation of bow shock N91-15065

COMMAND AND CONTROL
Developing portable user interfaces for Ada command control software
[AD-A226712] N91-14747

COMMERCE
Strategic plan commercialization remote sensing by NEDECO
[BCRS-89-35] N91-14637

COMMUNICATION NETWORKS
A global view of lander-to-orbiter communications accessibility for a Mars Global Network Mission N91-14362
Data transmission networks N91-14576
A performance study of the concurrency control algorithms in hierarchical network with partitioned database
[AD-A227055] N91-14756
Distributed computing system with dual independent communications paths between computers and employing split tokens
[NASA-CASE-NPO-17185-1-CU] N91-14772

COMMUNICATION THEORY
International Symposium on Information Theory
[AD-A226957] N91-14521

COMPARATORS
Dual physiological rate measurement instrument
[NASA-CASE-MSC-20078-3] N91-14709

COMPLEX SYSTEMS
Engineering design with decision support: An application of goal decomposition
[AD-A226730] N91-14782

COMPONENT RELIABILITY
Fatigue reliability of wind turbine components
[DE91-001262] N91-14650
Reliability of photovoltaic concentrator modules
[DE90-012754] N91-14651

COMPOSITE MATERIALS
Method for manufacturing composite material
[EP-PATENT-0-314-353-A2] N91-14421
AC-130H Gunship Armor Upgrade Project
[DE91-002567] N91-14428
Interfacial push-out measurements of fully-bonded SiC/SC composites
[DE91-004527] N91-14436

COMPOSITE STRUCTURES
Task reports on developing techniques for scattering by 3D composite structures and to generate new solutions in diffraction theory using higher order boundary conditions
[NASA-CR-186899] N91-14475
A finite element conjugate gradient FFT method for scattering N91-14476
Analytical solutions with Generalized Impedance Boundary Conditions (GIBC) N91-14477
The response and failure mechanisms of circular metal and composite plates subjected to underwater shock loading
[AD-A226759] N91-14631

COMPRESSIBLE FLOW
Numerical studies of compressible flow over a double-delta wing at high angles of attack
[AD-A226931] N91-14312
Piecewise-parabolic methods for systems of hyperbolic conservation laws in multiprocessing environments
[DE91-004582] N91-14792
Large-scale vortices in compressible turbulent medium with the magnetic field N91-15095

COMPRESSING
Mechanical end joint system for connecting structural column elements
[NASA-CASE-LAR-14465-1] N91-14614

COMPRESSORS
Fatigue and fracture of titanium aluminides, volume 2
[AD-A227353] N91-14351

COMPUTATION
A fast solver for systems of axisymmetric ring vortices
[DE91-002594] N91-14561
Mechanizing proof theory: Resource-aware logics and proof transformations to extract implicit information
[AD-A227147] N91-14758

COMPUTATIONAL FLUID DYNAMICS
Missile Aerodynamics
[AGARD-CP-493] N91-14278
Store carriage, integration, and release N91-14281
Aerodynamic design of Pegasus (trademark): Concept to flight with CFD N91-14285
Application of Euler and Navier-Stokes codes to missile type bodies with high L/D ratios N91-14286
Supersonic vortex flows aroúnd a missile body: Basic experiment and Euler numerical computation N91-14291
Asymmetric supersonic flow around cones with noncircular sections N91-14292
Three dimensional flow calculations for a projectile with standard and dome bases N91-14294
Computation of axisymmetric base flow with different turbulence models N91-14298
Results of GARTEUR action group AG09 on flow past missile afterbodies N91-14299
Chordwise and spanwise centers of pressure of missile fins N91-14304
Hypersonic aerodynamics: An approximation method for the calculation of real gas effects and wall temperatures
[MBB/FE127/S/PUB/0403] N91-14306
Experimental investigations of buffet excitation forces on a low aspect ratio trapezoidal half wing in incompressible flow N91-14329
A numerical and experimental analysis of reactor performance and deposition rates for CVD on monofilaments
[NASA-TM-103631] N91-14500
CFD code evaluation for internal flow modeling
[NASA-CR-187677] N91-14557
Research in progress in applied mathematics, numerical analysis, and computer science
[NASA-CR-187474] N91-14726
NASA's supercomputing experience
[NASA-TM-102890] N91-14727
Piecewise-parabolic methods for systems of hyperbolic conservation laws in multiprocessing environments
[DE91-004582] N91-14792
New accurate, vectorized approximations of state surfaces for the thermodynamic and transport properties of equilibrium air
[MBB/FE122/S/PUB/0389] N91-14886

COMPUTATIONAL GEOMETRY
Hidden surface removal for axis-parallel polyhedra
[RUU-CS-90-21] N91-14736
Finding shortest paths in the presence of orthogonal obstacles using a combined L sub 1 and link metric
[RUU-CS-90-20] N91-14777

COMPUTATIONAL GRIDS
Numerical studies of compressible flow over a double-delta wing at high angles of attack
[AD-A226931] N91-14312
A fast solver for systems of axisymmetric ring vortices
[DE91-002594] N91-14561
Matrix techniques for faster routing of affine permutations on a mesh interconnection network
[RUU-CS-90-19] N91-14767

COMPUTER AIDED DESIGN
Computer aided design models for millimeter-wave suspended substrate microstrip line
[AD-A227259] N91-14547
Engineering design with decision support: An application of goal decomposition
[AD-A226730] N91-14782
COMPUTER AIDED MANUFACTURING
FTIR (Fourier Transform Infrared) spectrophotometry for thin film monitors: Computer and equipment integration for enhanced capabilities
[DE91-001228] N91-14853
COMPUTER AIDED MAPPING
Graphics software for the HP825/9000 IFSI system
[IFSI-89-18] N91-14735
Color palette: Plotting guide for use with GSMAP and GSDRAW digital cartographic software
[DE91-001643] N91-14737
Reconstruction of vectorized raster data
[ETN-91-98143] N91-14738
COMPUTER ASSISTED INSTRUCTION
Pedagogical strategies for human and computer tutoring
[AD-A226886] N91-14750
COMPUTER GRAPHICS
Raster graphic helmet-mounted display study
[NASA-CR-4331] N91-14347
Graphics software for the HP825/9000 IFSI system
[IFSI-89-18] N91-14735
(DURIP) exploring and controlling spatio temporal chaos under complex structures through visualization: A mini-supercomputer approach
[AD-A226793] N91-14784
COMPUTER NETWORKS
A mediator architecture for abstract data access
[AD-A227362] N91-14730
A performance study of the concurrency control algorithms in hierarchical network with partitioned database
[AD-A227055] N91-14756
Distributed computing system with dual independent communications paths between computers and employing split tokens
[NASA-CASE-NPO-17185-1-CU] N91-14772
Massively parallel network architectures for automatic recognition of visual speech signals
[AD-A226968] N91-14805
Defense Data Network (DDN) performance analysis using probability modeling
[AD-A226856] N91-14894
COMPUTER PROGRAM INTEGRITY
Methodology investigation of software maturity model validation
[AD-A226697] N91-14746
Cyclomatic complexity as a utility for predicting software faults
[AD-A227313] N91-14760
COMPUTER PROGRAMMING
Fitting of photogrammetry and field completion
[ETN-91-98144] N91-14640
Graphics software for the HP825/9000 IFSI system
[IFSI-89-18] N91-14735
A CLOS (Common Lisp Object System) implementation on top of KEE (Knowledge Engineering Environment)
[DE91-001957] N91-14739
Pedagogical strategies for human and computer tutoring
[AD-A226886] N91-14750
Literature survey on tools
[AD-A226933] N91-14770
Reasoning of the geometric and uncertainty constraints in planning robot manipulation tasks
[LAAS-90143] N91-14775
COMPUTER PROGRAMS
Some trends in missile aerodynamics N91-14279
NUFA: A semi-empirical method for the prediction of isolated weapon aerodynamics N91-14287
A semi-empirical prediction method for missile aerodynamics N91-14288
Numerical simulation of ice growth on a MS-317 swept wing geometry
[NASA-TM-103705] N91-14310
A parametric shell analysis of the shuttle 51-L SRB AFT field joint
[NASA-TM-102748] N91-14629
Crustal Dynamics Project data analysis, 1990
[NASA-TM-100765] N91-14679
Research in progress in applied mathematics, numerical analysis, and computer science
[NASA-CR-187474] N91-14726
National software capacity: Near-term study
[AD-A226694] N91-14743
Developing portable user interfaces for Ada command control software
[AD-A226712] N91-14747
Software cost estimation study
[AD-A226777] N91-14749
The role of assessment in software process improvement
[AD-A227426] N91-14762
Software management issues --- superconducting super collider detectors
[DE91-001031] N91-14763
The computer algebra approach of the finite difference methods for PDEs
[DE90-631581] N91-14790
In-flight methods for satellite sensor absolute radiometric calibration N91-14801
COMPUTER SYSTEMS DESIGN
Adaptive data acquisition multiplexing system and method
[NASA-CASE-MSC-21170-1] N91-14371
DATAS hardware diagnostic tests
[DOT/FAA/CT-TN90/44] N91-14728
Literature survey on tools
[AD-A226933] N91-14770
Distributed computing system with dual independent communications paths between computers and employing split tokens
[NASA-CASE-NPO-17185-1-CU] N91-14772
Information technology and the conduct of research: The user's view. Report of the Panel on Information Technology and the Conduct of Research
[ISBN-0-309-03888-X] N91-14890
COMPUTER SYSTEMS PERFORMANCE
DATAS hardware diagnostic tests
[DOT/FAA/CT-TN90/44] N91-14728
COMPUTER SYSTEMS PROGRAMS
Experiences porting the distributed Ada real-time kernel
[AD-A226693] N91-14742
Evaluations of some scheduling algorithms for hard real-time systems
[AD-A226930] N91-14755
COMPUTER TECHNIQUES
Computer-assisted strain-gage monitoring and data reduction system
[AD-A226894] N91-14589
Engineering design with decision support: An application of goal decomposition
[AD-A226730] N91-14782
On probability intervals and their updating
[RUU-CS-90-22] N91-14793
COMPUTER VISION
Flight data acquisition methodology for validation of passive ranging algorithms for obstacle avoidance
[NASA-TM-102809] N91-14322
COMPUTERIZED SIMULATION
Numerical simulation of ice growth on a MS-317 swept wing geometry
[NASA-TM-103705] N91-14310
Using simulation to evaluate the safety of proposed ATC operations and procedures
[DOT/FAA/CT-TN90/22] N91-14318
Phase portrait methods for verifying fluid dynamic simulations
[DE91-001129] N91-14571
A study of liquid scintillator and fiber materials for use in a fiber calorimeter
[DE91-004229] N91-14585
Atmospheric source-receptor relationships: Concepts and terminology
[DE91-001033] N91-14656
Measurement of the gravitomagnetic field using a pair of laser ranged satellites N91-14670
Modeling study of tropical nonsquall and squall clusters N91-14685
Construction of large-scale simulation codes using ALPAL (A Livermore Physics Applications Language)
[DE91-002783] N91-14740
Discrete event simulation tool for analysis of qualitative models of continuous processing systems
[NASA-CASE-MSC-21465-1] N91-14741
Development of phenomenological fitting procedure for the fast microcomputer
[AD-A227168] N91-14759
A combined finite element-boundary element formulation for solution of axially symmetric bodies
[NASA-CR-185852] N91-14789
Piecewise-parabolic methods for systems of hyperbolic conservation laws in multiprocessing environments
[DE91-004582] N91-14792
Effect of atmospherics on beamforming accuracy
[NASA-CR-187695] N91-14802
COMPUTERS
ISIS and META projects
[NASA-CR-186413] N91-14731
(DURIP) exploring and controlling spatio temporal chaos under complex structures through visualization: A mini-supercomputer approach
[AD-A226793] N91-14784
CONCENTRATORS
Reliability of photovoltaic concentrator modules
[DE90-012754] N91-14651
CONCURRENT PROCESSING
A performance study of the concurrency control algorithms in hierarchical network with partitioned database
[AD-A227055] N91-14756
Distributed computing system with dual independent communications paths between computers and employing split tokens
[NASA-CASE-NPO-17185-1-CU] N91-14772
CONDENSATION
Sublimating comets as the source of nucleation seeds for grain condensation in the gas outflow from AGB stars N91-15018
CONDUCTIVE HEAT TRANSFER
Dynamics of an unsteady diffusion flame: Effects of heat release and gravity
[AD-A227348] N91-14447
An investigation of using a phase-change material to improve the heat transfer in a small electronic module for an airborne radar application
[DE91-002597] N91-14525
Acoustic transducer apparatus with reduced thermal conduction
[NASA-CASE-NPO-17620-1-CU] N91-14808
CONES
Extremal rays of convex cones and complementary inequalities
[ETN-91-98166] N91-14778
CONFERENCES
Missile Aerodynamics
[AGARD-CP-493] N91-14278
Review of the spring 1988 AGARD FMP symposium N91-14280
Store carriage, integration, and release N91-14281
Aircraft Dynamic Loads Due to Flow Separation
[AGARD-CP-483] N91-14324
Proceedings of the Mars Global Network Mission Workshop
[NASA-CR-186844] N91-14359
Innovative Long Wavelength Infrared Detector Workshop Proceedings
[NASA-CR-187433] N91-14379
Acidic deposition: Its nature and impacts
[DE91-001984] N91-14658
Interstellar Dust: Contributed Papers
[NASA-CP-3036] N91-14897
Plasma Astrophysics
[ESA-SP-311] N91-15046
CONFIGURATION MANAGEMENT
A software-system visualization tool
[AD-A227145] N91-14757
CONFINEMENT
Fueling of magnetically confined plasmas by single- and two-stage repeating pneumatic pellet injectors
[DE91-002635] N91-14839
CONGRESSIONAL REPORTS
Outer space: What should be the US Government policy toward the region beyond Earth's atmosphere. National debate topic for high schools, 1990-1991
[PB90-255464] N91-14896
CONJUGATE GRADIENT METHOD
A finite element conjugate gradient FFT method for scattering N91-14476
CONNECTORS
Quick connect coupling
[NASA-CASE-MSC-21539-1] N91-14610
System for connecting fluid couplings
[NASA-CASE-MFS-26042-1-SB] N91-14613
Vibrational testing of optical fiber connector joints
[NASA-TM-103654] N91-14829
CONSERVATION LAWS
Piecewise-parabolic methods for systems of hyperbolic conservation laws in multiprocessing environments
[DE91-004582] N91-14792
CONSOLIDATION
Dynamic consolidation of aluminum-silicon carbide composites
[DE91-001929] N91-14427
CONSTITUTIVE EQUATIONS
Influence of the parameter distribution of the solar wind near the Sun upon its structure at the Earth's orbit N91-15108
CONTAINMENT
Definition of experiments to investigate fire suppressants in microgravity
[NASA-CR-185295] N91-14378
CONTAMINANTS
Atmospheric source-receptor relationships: Concepts and terminology
[DE91-001033] N91-14656
Acidic deposition: Its nature and impacts
[DE91-001984] N91-14658

CONTINUOUS RADIATION
A beam position monitor for low current dc beams [CEBAF-PR-89-004] N91-14816
Dust emission in the Sagittarius B2 molecular cloud core N91-14947
CONTINUOUS SPECTRA
Longwave spectral dependence of emission from warm dust clouds N91-14945
CONTINUUMS
A comparative study of the continuum and emission characteristics of comet dust. 1: Are the silicates in Comet Halley and Kohoutek amorphous or crystalline N91-15005
CONTOURS
Wind tunnel investigation and flight tests of tail buffet on the CF-18 aircraft N91-14325
CONTRACTION
Galaxy formation by dust N91-14989
CONTROL EQUIPMENT
Active control of boundary layer transition and turbulence [NASA-CASE-LAR-13532-1] N91-14562
CONTROL STABILITY
A study of strong stability of distributed systems [NASA-CR-187421] N91-14766
CONTROL SYSTEMS DESIGN
Electro-optical spin measurement system [NASA-CASE-LAR-13629-1] N91-14356
The vertical Van de Graaff telemetry system [DE91-001960] N91-14370
Multivariable methods for the design, identification, and control of large space structures. Volume 2: Optimal and sub-optimal estimation applied to large flexible structures [AD-A226699] N91-14375
Adaptive control of large space structures [AD-A227304] N91-14377
Combined air and water pollution control system [NASA-CASE-NST-00007-1] N91-14662
Randomly sampled-data control systems [NASA-CR-187425] N91-14734
Reasoning of the geometric and uncertainty constraints in planning robot manipulation tasks [LAAS-90143] N91-14775
CONTROL VALVES
Low-noise nozzle valve [NASA-CASE-MFS-28383-1] N91-14583
CONTROLLABILITY
On the modeling and control of slewing flexible structures N91-14499
CONTROLLED FUSION
LLE (Laboratory for Laser Energetics) review [DE91-001254] N91-14597
Fast electron studies in the ZT-40M edge plasma [DE91-002323] N91-14838
CONTROLLERS
Randomly sampled-data control systems [NASA-CR-187425] N91-14734
Reasoning of the geometric and uncertainty constraints in planning robot manipulation tasks [LAAS-90143] N91-14775
Sensor based control of robotic mechanisms [AD-A226784] N91-14776
CONVECTION
Dynamics of an unsteady diffusion flame: Effects of heat release and gravity [AD-A227348] N91-14447
Piecewise-parabolic methods for systems of hyperbolic conservation laws in multiprocessing environments [DE91-004582] N91-14792
CONVECTIVE FLOW
Vibration isolation technology: Sensitivity of selected classes of experiments to residual accelerations [NASA-CR-186902] N91-14624
CONVERGENCE
Acceleration techniques for explicit Euler codes N91-14555
An accurate product SVD (singular value decomposition) algorithm [DE91-004448] N91-14785
CONVERGENT-DIVERGENT NOZZLES
Internal performance of a hybrid axisymmetric/nonaxisymmetric convergent-divergent nozzle [NASA-TM-4230] N91-14275
Parametric study of afterbody/nozzle drag on twin two-dimensional convergent-divergent nozzles at Mach numbers from 0.60 to 1.20 [NASA-TP-2640] N91-14316
CONVEXITY
Extremal rays of convex cones and complementary inequalities [ETN-91-98166] N91-14778
COOL STARS
Using infrared spectral features to probe circumstellar dust shells around cool stars N91-15021
COOLING
Pyroelectric detectors N91-14390
COORDINATES
Optimal sensor fusion for land vehicle navigation [DE91-002586] N91-14319
COPOLYMERIZATION
Bis (4-(3,4-dimethylene-pyrrolidyl)-phenyl) methane [NASA-CASE-LAR-13965-2-CU] N91-14418
COPPER
Effects of irradiation on initiation and crack-arrest toughness of two high-copper welds and on stainless steel cladding [DE91-001272] N91-14467
Corrosion behavior of copper-base materials in a gamma-irradiated environment [DE91-001286] N91-14468
Radiation resistance of copper alloys at high exposure levels [DE91-001563] N91-14470
Joining alumina to sapphire for copper vapor laser tubes [AD-A226619] N91-14501
COPPER ALLOYS
Processing studies of aluminum-magnesium and aluminum-copper-lithium alloys [AD-A227255] N91-14485
Corrosion behavior of copper-base materials in a gamma-irradiated environment [DE91-001286] N91-14468
Radiation resistance of copper alloys at high exposure levels [DE91-001563] N91-14470
COPPER CHLORIDES
Copper chloride cathode for a secondary battery [NASA-CASE-NPO-17640-1-CU] N91-14538
COPPER OXIDES
Fabrication of sensitive high Tc bolometers N91-14389
Superconducting properties of Tl-Ba-Ca-Cu-O films on silver substrates [DE91-002304] N91-14856
An ion-channeling study of irradiation-induced amorphization of YBa2Cu3O(7-x) [DE91-004488] N91-14884
CORONAGRAPHS
Coronal mass ejections [NASA-CR-186579] N91-15115
CORRELATION
Prediction of helicopter simulator sickness [DE90-016530] N91-14710
CORROSION
Ion implantation for corrosion inhibition of aluminum alloys in saline media [DE91-002887] N91-14461
Corrosion behavior of copper-base materials in a gamma-irradiated environment [DE91-001286] N91-14468
NASA-UVA light aerospace alloy and structures technology program [NASA-CR-187321] N91-14474
CORROSION PREVENTION
Ion implantation for corrosion inhibition of aluminum alloys in saline media [DE91-002887] N91-14461
CORROSION TESTS
Corrosion behavior of copper-base materials in a gamma-irradiated environment [DE91-001286] N91-14468
COSMIC DUST
Method and apparatus for determining time, direction, and composition of impacting space particles [NASA-CASE-LAR-13392-1-CU] N91-14412
Interstellar Dust: Contributed Papers [NASA-CP-3036] N91-14897
The autocorrelation function of the North Pole dust N91-14901
Properties of interstellar dust in the region of the CEP OB4 association N91-14903
Polarization and extinction by aligned grains N91-14907
Alignment mechanisms of paramagnetic grains revisited N91-14908
New measurements of the far ultraviolet scattering properties of interstellar dust N91-14909
Interstellar dust as generator of x ray radiation N91-14910
The capability of the ultraviolet imaging telescope for observing interstellar dust N91-14913
Diffuse galactic light observations at 206 selected areas N91-14914
Correlation properties of interstellar dust: Diffuse interstellar bands N91-14916
High-spectral resolution observations of the 3.29 micron emission feature: Comparison to QCC and PAHs N91-14925
Small scale variations of abundances of transiently heated grains in molecular clouds N91-14927
The 3.3 micron emission feature: Map of the galactic disk, 10 deg less than l less than 35 deg, - 6 deg less than b less than 6 deg N91-14928
IR emission and UV extinction in two open clusters N91-14929
Dust emission from high latitude cirrus clouds N91-14930
Si3N4 emissivity and the unidentified infrared bands N91-14935
Dust clouds in Orion and the interstellar neutral hydrogen distribution N91-14941
Infrared emission from ultracompact H II regions N91-14942
Dust in a few southern H II regions N91-14943
Distribution of dust in W31 complex N91-14944
Longwave spectral dependence of emission from warm dust clouds N91-14945
H I and dust in the high latitude dark cloud L1642 N91-14946
Dust emission in the Sagittarius B2 molecular cloud core N91-14947
Dust emission from Barnard 35: Gas heating anomaly resolved N91-14951
A two micron polarization survey toward dark clouds N91-14952
IRAS results on outer galaxy star formation N91-14953
High resolution observations of compact H II regions at 230 GHz N91-14954
Survey observations of emission-line stars in the Orion region N91-14955
Matrix isolation as a tool for studying interstellar chemical reactions N91-14956
New insights in the photochemistry of grain mantles: The identification of the 4.62 and 6.87 micron bands N91-14957
Distribution of the 3.1 micron feature in Cepheus A N91-14958
Grain mantles: The impact on grain evolution and selective extinction N91-14960
Molecular and mass spectroscopic analysis of isotopically labeled organic residues N91-14961
Production and transfer of UV photons in non-homogeneous spherical clouds N91-14966
Grains charges in interstellar clouds N91-14967
Dust coagulation in ISM N91-14968
On the polarization mechanism in the R Mon/NGC 2261 complex N91-14969
Infrared studies of dust grains in infrared reflection nebulae N91-14970
Laboratory investigation of electric charging of dust particles by electrons, ions, and UV radiation N91-14971
Dust in regions of massive star formation N91-14972
Does CO trace H2 at high galactic latitude N91-14973
The origin of the galactic emission in IRAS data N91-14974
Molecules, grains, and shocks: A comparison of CO, H I, and IRAS data N91-14975
A rocket-borne measurement of interstellar dust emission at high galactic latitude N91-14976
Molecules in an infrared cirrus cloud N91-14977
Dust in stellar wind bow shocks N91-14979
Studying the spatial distribution of interstellar dust N91-14980
Thermal emission from interstellar dust in and near the Pleiades N91-14981
Temperature distribution of dust in luminous IRAS galaxies N91-14982
The 100 and 160 micron maps of the dust reemission from the nucleus and inner-arm regions of NGC 6946 N91-14983
Grains in galactic haloes N91-14984
On the origin of extinction in the Coma cluster of galaxies N91-14987
Galaxy formation by dust N91-14989
VUV-visible measurements on different samples of amorphous carbon N91-14990
Steps toward interstellar silicate dust mineralogy N91-14991
Observational constraints on interstellar dust models N91-14996
Size distribution of dust grains: A problem of self-similarity N91-14997
Stochastic histories of dust grains in the interstellar medium N91-14998
Superaromatics: The key to a unified cosmic dust theory N91-14999
Properties of grains derived from IRAS observations of dust N91-15001

A comparative study of the continuum and emission characteristics of comet dust. 1: Are the silicates in Comet Halley and Kohoutek amorphous or crystalline N91-15005
Experimental evidence for amorphous carbon grains in comets N91-15008
Atomic environments in iron meteorites using EXAFS N91-15011
Sublimating icy planetesimals as the source of nucleation seeds for grain condensation in classical novae N91-15016
Dust formation around M-type stars N91-15017
Sublimating comets as the source of nucleation seeds for grain condensation in the gas outflow from AGB stars N91-15018
IR emission from circumstellar envelopes of C-rich stars N91-15019
The influence of grain growth in circumstellar dust envelopes on observed colors and polarization of some eruptive stars N91-15020
Using infrared spectral features to probe circumstellar dust shells around cool stars N91-15021
New circumstellar dust component in oxygen rich environments N91-15023
Type of silicate feature in oxygen rich stellar envelopes N91-15024
Interstellar extinction at 10-20 microns N91-15025
Dust around Mira variables: An analysis of IRAS LRS spectra N91-15026
Polarization due to dust scattering in the planetary nebula Cn1-1 N91-15027
Circumstellar grain extinction properties of recently discovered post AGB stars N91-15028
Compact reflection nebulae, a transit phase of evolution from post-AGB to planetary nebulae N91-15029
Continuous infrared emission of proto- and young-planetary nebulae N91-15030
The discovery of a highly polarized bipolar nebula N91-15031
Infrared emission from the supernova remnant Puppis A: Dust and gas parameters N91-15032
On the detectability of infrared echo arcs around supernova 1987A N91-15033

COSMIC GASES
On the origin of extinction in the Coma cluster of galaxies N91-14987
Structure of accretion flow in close binary system: A two dimensional numerical model N91-15093

COSMIC PLASMA
Generation of cosmic rays in pinches N91-15070

COSMIC RAYS
Data requirements for intermediate energy nuclear applications
[DE91-004005] N91-14812
Initial data from the Soudan 2 experiment
[DE91-004454] N91-14815
Synthesis of H2 in dirty ice mantles by fast ion energy loss: New experimental results increase the relevance of this mechanism N91-14962
Production and transfer of UV photons in non-homogeneous spherical clouds N91-14966

COSMIC X RAYS
Interstellar dust as generator of x ray radiation N91-14910

COSMOCHEMISTRY
Vega-Giotto flyby missions and cometary cosmogony N91-15009

COSMOLOGY
Vega-Giotto flyby missions and cometary cosmogony N91-15009
Plasma Astrophysics
[ESA-SP-311] N91-15046
Particle physics and cosmology
[DE91-001946] N91-15111

COST ANALYSIS
Automatic dependent surveillance benefit and cost analysis
[DOT/FAA/RD-90/34] N91-14320
Software cost estimation study
[AD-A226777] N91-14749

COST ESTIMATES
Software cost estimation study
[AD-A226777] N91-14749

COST REDUCTION
Overview of propulsion concepts for tactical missiles N91-14296
Automatic dependent surveillance benefit and cost analysis
[DOT/FAA/RD-90/34] N91-14320
Mechanical end joint system for connecting structural column elements
[NASA-CASE-LAR-14465-1] N91-14614
Tips on how to cut technical publications costs
[AD-A227334] N91-14895

COSTS
Advanced technology needs for a global change science program: Perspective of the Langley Research Center
[NASA-TM-4196] N91-14634

COUETTE FLOW
Direct numerical simulation of turbulent couette flow, part 2
[AD-A226770] N91-14564

COUPLERS
Tapered fiber amplifier
[AD-D014629] N91-14512

COUPLINGS
Quick connect coupling
[NASA-CASE-MSC-21539-1] N91-14610
System for connecting fluid couplings
[NASA-CASE-MFS-26042-1-SB] N91-14613

COWLINGS
Numerical investigations in three-dimensional internal flows
[NASA-CR-187373] N91-14277

CRACK ARREST
Effects of irradiation on initiation and crack-arrest toughness of two high-copper welds and on stainless steel cladding
[DE91-001272] N91-14467

CRACK INITIATION
Effects of irradiation on initiation and crack-arrest toughness of two high-copper welds and on stainless steel cladding
[DE91-001272] N91-14467
Use of anomalous small angle x ray scattering to investigate microstructural features in complex alloys
[DE91-002397] N91-14471

CRACK PROPAGATION
Flow behavior of Ti-24Al-11Nb at high strain rates
[DE91-004506] N91-14473
Some problems in elastic contact and fracture N91-14625
Fracture analysis of cathodic delamination in rubber-to-metal bonds N91-14627

CRACK TIPS
A boundary element method for elastostatic and elastodynamic crack problems in two and three dimensions N91-14626

CRACKING (FRACTURING)
NASA-UVA light aerospace alloy and structures technology program
[NASA-CR-187321] N91-14474

CRACKS
Conversion of alkoxide solutions to oxides: Evaporation of products
[AD-A226927] N91-14442
Ultrasonic detection of fatigue damage in glass-epoxy composites
[DE91-002652] N91-14619
Some problems in elastic contact and fracture N91-14625
A boundary element method for elastostatic and elastodynamic crack problems in two and three dimensions N91-14626

CRASHWORTHINESS
Advanced technology landing gear. Volume 1: Design
[AD-A227196] N91-14343
Advanced technology landing gear. Volume 2: Test
[AD-A227197] N91-14344

CREEP PROPERTIES
Short term creep rupture predictions for Tantalum alloy T-3
[DE91-002338] N91-14458

CREEP RUPTURE STRENGTH
A statistically-based model of the interacting processes which lead to creep-rupture in filament-wound composite pressure vessels N91-14420

CREEP STRENGTH
Thermal stability of the microstructure of an aged Nb-Zr-C alloy
[NASA-TM-103647] N91-14454

CRITICAL EXPERIMENTS
Definition of experiments to investigate fire suppressants in microgravity
[NASA-CR-185295] N91-14378

CRITICAL LOADING
The buckling of off-axis, orthotropic, cylindrical shells in torsion N91-14628

CRITICAL PATH METHOD
Finding shortest paths in the presence of orthogonal obstacles using a combined L sub 1 and link metric
[RUU-CS-90-20] N91-14777

CRITICAL TEMPERATURE
Transient x ray irradiation of high transition temperature superconducting material
[AD-A227090] N91-14869

CROSS CORRELATION
Damping measurements using operational data
[DE91-002781] N91-14646

CROSS FLOW
Supersonic tactical missile computation using Euler's equation with crossflow separation modeling N91-14284
Aerodynamic characteristics of cylindrical bodies with pointed and truncated conical noses N91-14289
Asymmetric supersonic flow around cones with noncircular sections N91-14292

CROSSTALK
Photovoltaic quantum well infrared photodetectors N91-14393

CRUDE OIL
Hydrocarbon group-type analysis of petroleum distillates and residues by high-performance liquid chromatography
[DE91-727527] N91-14451

CRUSTAL FRACTURES
Reports on block rotations, fault domains and crustal deformation
[NASA-CR-186756] N91-14665
Block rotations, fault domains and crustal deformation in the western US N91-14666
Crustal dynamics project: The interpretation of crustal dynamics data in terms of plate motions and regional deformation near plate boundaries
[NASA-CR-187691] N91-14673

CRYOGENICS
Transient analysis of a two-phase hydrogen heat switch
[DE91-002314] N91-14506
Experimental development, testing and research work in support of the inertial confinement fusion program
[DE91-002771] N91-14841

CRYOPUMPING
Design of a He4 cooling system for a cryostat working at 1K
[IFSI-89-17] N91-14502

CRYOSTATS
Design of a He4 cooling system for a cryostat working at 1K
[IFSI-89-17] N91-14502

CRYSTAL DEFECTS
Defect and impurity effects on the initial growth of Ag on Si(111)
[DE91-001277] N91-14876

CRYSTAL DISLOCATIONS
Simulation of transient glide of a threading dislocation in an embedded strained expitaxial layer
[AD-A226965] N91-14867

CRYSTAL GROWTH
Method of growing diamond film on substrates
[AD-D014632] N91-14479
Quantum well laser
[AD-A227303] N91-14594
Processing experiments for development of high-efficiency silicon solar cells
[DE91-002698] N91-14645
Silicon carbide, a semiconductor for space power electronics
[NASA-TM-103655] N91-14850
Pseudomorphic InGaAs materials
[AD-A226895] N91-14864
An investigation of diamond synthesis in an oxygen-acetylene diffusion flame
[AD-A227224] N91-14870
The influence of grain growth in circumstellar dust envelopes on observed colors and polarization of some eruptive stars N91-15020

CRYSTAL LATTICES
Equilibrium composition of interphase boundaries
[DE91-002470] N91-14814
Simulation of transient glide of a threading dislocation in an embedded strained expitaxial layer
[AD-A226965] N91-14867

CRYSTAL OPTICS
Picosecond laser system for high speed characterization of monolithic devices
[AD-A227372] N91-14595

CRYSTAL STRUCTURE
Small band gap superlattices as intrinsic long wavelength infrared detector materials N91-14405
Quantum well laser
[AD-A227303] N91-14594
Equilibrium composition of interphase boundaries
[DE91-002470] N91-14814
Crystal structure of ZnGa2S4, a defect sphalerite-derivative
[AD-A226937] N91-14865
On the crystal structure of KInS2-I
[AD-A226940] N91-14866
Simulation of transient glide of a threading dislocation in an embedded strained expitaxial layer
[AD-A226965] N91-14867
Theory of the electronic and structural properties of solid state oxides
[DE91-001192] N91-14874

A LEED study of the MgO(001) surface structure
[DE91-002811] N91-14879

CRYSTAL SURFACES
Anomalous surface phase formation on Pt3Sn with zone axes group (100)
[DE91-001794] N91-14456
Application of ultrasonic guided waves to the characterization of texture in metal sheets of cubic and hexagonal crystallites
[DE91-001107] N91-14466
Effect of step edge transition rates and anisotropy in simulations of epitaxial growth
[DE91-001251] N91-14875
Defect and impurity effects on the initial growth of Ag on Si(111)
[DE91-001277] N91-14876

CRYSTALLINITY
Infrared spectra of crystalline and glassy silicates and application to interstellar dust N91-14994

CRYSTALLITES
Application of ultrasonic guided waves to the characterization of texture in metal sheets of cubic and hexagonal crystallites
[DE91-001107] N91-14466

CRYSTALLIZATION
Ion beam induced diffusion and crystallization in high dose Er implanted Si
[DE91-002869] N91-14860

CRYSTALLOGRAPHY
Heteronuclear metal cluster compounds synthesis and reactivity
[AD-A226815] N91-14463

CRYSTALS
He atom surface spectroscopy: Surface lattice dynamics of insulators, metals, and metal overlayers
[DE91-001993] N91-14855

CUES
The object display in decision making and judgment
[AD-A227059] N91-14889

CULTURE TECHNIQUES
Bio-reactor chamber
[NASA-CASE-MSC-20929-1] N91-14703

CURING
Characterization of phenolic resins with thermogravimetry-mass spectrometry
[DE91-002710] N91-14492

CURRENT AMPLIFIERS
Monolithic multichannel detector amplifier arrays and circuit
[AD-D014566] N91-14528

CURRENT DENSITY
A method for estimating tokamak poloidal field coil currents which incorporates engineering constraints
[DE91-001662] N91-14848

CURRENT SHEETS
Analytical solutions with Generalized Impedance Boundary Conditions (GIBC) N91-14477
Implications of multipoint observations of substorms in the inner magnetotail N91-15061

CURVATURE
Surface settling in partially filled containers upon step reduction in gravity
[NASA-TM-103641] N91-14556

CURVE FITTING
Development of phenomenological fitting procedure for the fast microcomputer
[AD-A227168] N91-14759

CURVES (GEOMETRY)
The detection of a broad interstellar extinction feature near 1700 A N91-14900

CUTTERS
Straddle design of spiral bevel and hypoid pinions and gears
[NASA-TM-103621] N91-14602

CYBERNETICS
Development of phenomenological fitting procedure for the fast microcomputer
[AD-A227168] N91-14759
Analogue computation using VLSI neural network devices
[OUEL-1835/90] N91-14773
Prototyping of a protocol validation environment: Application to the Estelle approach
[LAAS-90113] N91-14774

CYCLIC HYDROCARBONS
A survey for PAH emission in H II regions, planetary and proto-planetary nebulae N91-14920
PAH emission from Nova Cen 1986 N91-14921
Spatial variations of the 3 micron emission features within nebulae N91-14922
High-spectral resolution observations of the 3.29 micron emission feature: Comparison to QCC and PAHs N91-14925
Spectral structure near the 11.3 micron emission feature N91-14926
The spatial distribution of infrared radiation from visible reflection nebulae N91-14931
Influence of temperature on the infrared spectrum of the coronene molecule N91-14932
Raman properties of various carbonaceous materials and their astrophysical implications N91-14933
Infrared fluorescence from PAHs in the laboratory N91-14934
PAH in the laboratory and interstellar space N91-14936
The effect of ionization on the infrared absorption spectra of PAHs: A preliminary report N91-14937
Angular motion of a PAH molecule in interstellar environment N91-14938
PAHs molecules and heating of the interstellar gas N91-14939
PAH formation in carbon-rich circumstellar envelopes N91-15015

CYCLOGENESIS
Explosive cyclogenesis: A case study of the Veterans' Day storm of 11-12 November 1987
[AD-A227077] N91-14691

CYCLONES
Experiments with collision of vortices in rotating and still free-surface shallow water N91-15080

CYCLOTRON RADIATION
Maser cyclotron instability in a plasma with anisotropic distribution function N91-15075
Radiation-driven diskons as a new astrophysical object N91-15105

CYCLOTRON RESONANCE
An intense optically pumped H(-) ion source
[DE91-002949] N91-14827
Characteristics and potential applications of an ORNL microwave ECR multicusp plasma ion source
[DE91-002649] N91-14840
Characterization of electron cyclotron resonance hydrogen plasmas
[DE91-001250] N91-14844
Evolution of high amplitude Alfven waves near a bow shock N91-15068

CYCLOTRON RESONANCE DEVICES
Recent long-pulse and high-average-power tests on a 140 GHz gyrotron
[DE91-001680] N91-14592

CYGNUS CONSTELLATION
Properties of interstellar dust in the region of the CEP OB4 association N91-14903
Additional red and reddened stars in Cyg OB2 association N91-14948

CYLINDERS
Dynamics of separation and reattachment in a Mach 5 unswept compression ramp flow N91-14276

CYLINDRICAL BODIES
Aerodynamic characteristics of cylindrical bodies with pointed and truncated conical noses N91-14289
Low velocity impact analysis with NASTRAN
[NASA-TM-103169] N91-14426
Thermal compensating mount
[NASA-CASE-LAR-14207-1] N91-14590

CYLINDRICAL PLASMAS
Observation of electron hole, double layer, and turbulent heating in a laboratory plasma N91-15079

CYLINDRICAL SHELLS
The buckling of off-axis, orthotropic, cylindrical shells in torsion N91-14628

D

DAMAGE
Flight Set 360L006 STS-34 field joint protection system, thermal protection system, and systems tunnel components, volume 4
[NASA-CR-184050] N91-14415
Hazards and safeguards of high pressure hydraulic fatigue testing
[AD-A226767] N91-14509

DAMPING
Turbomachinery rotor support with damping
[NASA-CASE-MFS-28345-1] N91-14608
Damping measurements using operational data
[DE91-002781] N91-14646

DARK MATTER
The embedded objects in epsilon Cha I cloud N91-14949
Dust emission from Barnard 35: Gas heating anomaly resolved N91-14951
On the primary cosmic ray nuclei spectra behaviour in the 10(exp 16) eV energy region N91-15069
Pregalactic inhomogeneity in hot dark matter model of the universe N91-15100
Particle physics and cosmology
[DE91-001946] N91-15111

DATA ACQUISITION
Flight data acquisition methodology for validation of passive ranging algorithms for obstacle avoidance
[NASA-TM-102809] N91-14322
In-flight measurements on a Tornado aircraft for stores carriage and release research
[RAE-TM-AERO-2180] N91-14341
Adaptive data acquisition multiplexing system and method
[NASA-CASE-MSC-21170-1] N91-14371
Outgassing data for selecting spacecraft materials, revision 2
[NASA-RP-1124-REV-2] N91-14437
Shot report, Holo-17-Holo-22 Rex-9
[DE91-002575] N91-14583
The synthesis of solar radiation data for sizing stand-alone photovoltaic systems
[DE90-012758] N91-14652
Aircraft measurements of electrified clouds at Kennedy Space Center
[NASA-CR-186536] N91-14680
A balloon-borne integrating nephelometer
[DE91-001037] N91-14687
Human factors engineering. Part 1: Test procedures
[AD-A226480] N91-14720
Distributed systems status and control
[NASA-CR-187014] N91-14733

DATA BASE MANAGEMENT SYSTEMS
A mediator architecture for abstract data access
[AD-A227362] N91-14730
DEMON: A media object model incorporating natural language descriptions for retrieval support
[AD-A226711] N91-14893

DATA BASES
Systematic investigations of body-wing-tail interference at high angles of attack N91-14290
Comparison of different calculation methods applied to a lenticular fuselage section N91-14293
Flight data acquisition methodology for validation of passive ranging algorithms for obstacle avoidance
[NASA-TM-102809] N91-14322
Description of the bistatic radar terrain measurements system equipment
[AD-A226808] N91-14517
A materials database for LI(Si)/FeS2 thermal batteries
[DE91-002592] N91-14531
Initial blood storage experiment
[NASA-CR-185513-PT-1] N91-14700
A mediator architecture for abstract data access
[AD-A227362] N91-14730
A performance study of the concurrency control algorithms in hierarchical network with partitioned database
[AD-A227055] N91-14758
Data requirements for intermediate energy nuclear applications
[DE91-004005] N91-14812
Physics data base for the Beam Plasma Neutron Source (BPNS)
[DE91-002796] N91-14842
A proposed astronomical reference catalog of infrared sources
[AD-A226757] N91-15041

DATA COMPRESSION
International Symposium on Information Theory
[AD-A226957] N91-14521
High Resolution, High Frame Rate Video Technology
[NASA-CP-3080] N91-14574
Data transmission networks N91-14576
Data compression applied to HHVT N91-14577

DATA LINKS
A global view of lander-to-orbiter communications accessibility for a Mars Global Network Mission N91-14362
DATAS hardware diagnostic tests
[DOT/FAA/CT-TN90/44] N91-14728
Distributed computing system with dual independent communications paths between computers and employing split tokens
[NASA-CASE-NPO-17185-1-CU] N91-14772

DATA PROCESSING
Information technology and the conduct of research: The user's view. Report of the Panel on Information Technology and the Conduct of Research
[ISBN-0-309-03888-X] N91-14890

DATA PROCESSING EQUIPMENT
Computational equipment for the development of numerical algorithms computation
[AD-A226702] N91-14729

DATA REDUCTION
Computer-assisted strain-gage monitoring and data reduction system
[AD-A226894] N91-14589
Evaluation of data reduction and composing of the NOAA global vegetation index product: A case study
[AD-A227397] N91-14641

DATA TRANSMISSION
High Resolution, High Frame Rate Video Technology [NASA-CP-3060] N91-14574
Results of the users' requirements survey N91-14575
Data transmission networks N91-14576
Data compression applied to HHVT N91-14577
State of the art in video system performance N91-14578
High resolution, high frame rate video technology development plan and the near-term system conceptual design N91-14580
Finding shortest paths in the presence of orthogonal obstacles using a combined L sub 1 and link metric [RUU-CS-90-20] N91-14777
DEBRIS
A study of extended zodiacal structures [NASA-CR-187687] N91-15044
DECISION MAKING
Information extraction from visual displays and the event-related brain potential [AD-A227063] N91-14722
The object display: Principles and review of experimental findings' [AD-A226883] N91-14796
The evaluation of long range consequences in decision making [AD-A226949] N91-14888
The object display in decision making and judgment [AD-A227059] N91-14889
Strategic utilization of information resources: A contingency approach N91-14891
DECISION THEORY
Interpretation of conditional probabilities in probabilistic interference word problems [AD-A226907] N91-14797
DECLINATION
Stress field rotation or block rotation: An example from the Lake Mead fault system N91-14668
DECODING
System integration of a block code [ETN-91-98169] N91-14514
DEFECTS
Expendable Pattern Casting Technology [DE91-001348] N91-14503
DEFENSE PROGRAM
Defense Data Network (DDN) performance analysis using probability modeling [AD-A226856] N91-14894
A proposed astronomical reference catalog of infrared sources [AD-A226757] N91-15041
DEFORMATION
Low velocity impact analysis with NASTRAN [NASA-TM-103169] N91-14426
Structural response of marine sandwich panels to uniform pressure loading [AD-A227038] N91-14434
Flow behavior of Ti-24Al-11Nb at high strain rates [DE91-004506] N91-14473
Computer studies of the dynamic strength of ceramics [DE91-002568] N91-14481
Axial-torsional fatigue: A study of tubular specimen thickness effects [NASA-TM-103637] N91-14632
Reports on block rotations, fault domains and crustal deformation [NASA-CR-186756] N91-14665
Block rotations, fault domains and crustal deformation in the western US N91-14666
Distributed deformation and block rotation in 3D N91-14667
Multiple strike slip faults sets: A case study from the Dead Sea transform N91-14669
DEGRADATION
Radiation response issues for infrared detectors N91-14388
Aluminum nitride-silicon carbide whisker composites: Processing, properties, and microstructural stability [DE91-001907] N91-14425
DELAMINATING
Delamination test apparatus and method [NASA-CASE-LAR-13985-1] N91-14430
Fracture analysis of cathodic delamination in rubber-to-metal bonds N91-14627
DELAY CIRCUITS
Vibration analyzer [NASA-CASE-MSC-21408-1] N91-14607
DELTA WINGS
Numerical studies of compressible flow over a double-delta wing at high angles of attack [AD-A226931] N91-14312
Control of unsteady aerodynamic forces [AD-A227365] N91-14315
Unsteady airloads due to separated flow on airfoils and wings N91-14340
DEMODULATION
Demodulation processes in auditory perception [AD-A226824] N91-14707
DEMODULATORS
Digitized synchronous demodulator [NASA-CASE-GSC-13237-1] N91-14550
DENITROGENATION
Mechanism of hydrodenitrogenation. Part 4: Infrared spectroscopy of acidic molybdena catalysts [DE91-002496] N91-14440
DENSE PLASMAS
Characteristics and potential applications of an ORNL microwave ECR multicusp plasma ion source [DE91-002649] N91-14840
DENSITY DISTRIBUTION
The distribution of wave heights and periods for seas with unimodal bimodal power density spectra [AD-A227040] N91-14696
Nonlinear magnetosonic waves in an inhomogeneous plasma N91-15110
DEPLETION
Grain mantles: The impact on grain evolution and selective extinction N91-14960
DEPLOYMENT
A GNM mission and system design proposal N91-14364
DEPOSITION
Laser studies of the interaction of SiO with the surface of a thin film [DE91-004562] N91-14450
Acidic deposition: Its nature and impacts [DE91-001984] N91-14658
The effects of climate change on the nitrogen cycle and acid deposition [DE91-002785] N91-14659
Phase changes during plasma spray deposition [IPPCZ-297] N91-14837
Ground boundaries [DE91-004027] N91-14880
DEPTH
Stable explicit depth extrapolation of seismic wavefields [DE91-001445] N91-14674
DESCENT
A GNM mission and system design proposal N91-14364
DESIGN ANALYSIS
Aerodynamic design of Pegasus (trademark): Concept to flight with CFD N91-14285
Integration of sneak analysis with design, volume 1 [AD-A226902] N91-14543
DESTRUCTION
On the origin of extinction in the Coma cluster of galaxies N91-14987
DESTRUCTIVE TESTS
Delamination test apparatus and method [NASA-CASE-LAR-13985-1] N91-14430
DETONATION
A simple plane-wave explosive lens [DE91-004297] N91-14526
Shot report, Holo-17-Holo-22 Rex-9 [DE91-002575] N91-14583
DEUTERIUM
Physics data base for the Beam Plasma Neutron Source (BPNS) [DE91-002796] N91-14842
DIII-D results and plans [DE91-001548] N91-14847
Synthesis of H2 in dirty ice mantles by fast ion energy loss: New experimental results increase the relevance of this mechanism N91-14962
DEUTERIUM PLASMA
DIII-D results and plans [DE91-001548] N91-14847
DIAMAGNETISM
Solitary vortices in the vicinity of comets N91-15062
DIAMINES
N-(3-ethynylphenyl)maleimide [NASA-CASE-LAR-14188-2] N91-14419
DIAMONDS
Method of growing diamond film on substrates [AD-D014632] N91-14479
Study of diamond film growth and properties [NASA-CR-187709] N91-14483
An investigation of diamond synthesis in an oxygen-acetylene diffusion flame [AD-A227224] N91-14870
Growth, characterization and device development in monocrystalline diamond films [AD-A227238] N91-14871
DIELECTRIC PROPERTIES
Adhesion at ceramic interfaces [DE91-001660] N91-14480
Multiband radar characterization of forest biomes [NASA-CR-185101] N91-14638
DIELECTRICS
Flight Set 360L006 STS-34 field joint protection system, thermal protection system, and systems tunnel components, volume 4 [NASA-CR-184050] N91-14415
Spontaneous and induced coherent radiation generation in atomic vapors [AD-A226776] N91-14830
Interstellar circular polarization and the dielectric nature of dust grains N91-14905
Alignment mechanisms of paramagnetic grains revisited N91-14908
DIELS-ALDER REACTIONS
Bis (4-(3,4-dimethylene-pyrrolidyl)-phenyl) methane [NASA-CASE-LAR-13965-2-CU] N91-14418
DIFFERENTIAL EQUATIONS
Some trends in missile aerodynamics N91-14279
Phase portrait methods for verifying fluid dynamic simulations [DE91-001129] N91-14571
Projected implicit Runge-Kutta methods for differential-algebraic boundary value problems [DE91-000660] N91-14791
DIFFRACTION PROPAGATION
An investigation of the diffraction of an acoustic plane wave by a curved surface of finite impedance N91-14800
DIFFUSE RADIATION
Interstellar dust as generator of x ray radiation N91-14910
Observations of the diffuse UV radiation field N91-14912
Simultaneous infrared and UV-visible absorption spectra of matrix-isolated carbon vapor N91-14915
DIFFUSION
Elucidation of fundamental properties of helium in metals by nuclear magnetic resonance techniques [DE91-002715] N91-14460
Low-energy electron diffraction investigation of epitaxial growth: Pt and Pd(100) [DE91-000750] N91-14873
Ground boundaries [DE91-004027] N91-14880
Correlation properties of interstellar dust: Diffuse interstellar bands N91-14916
DIFFUSION ELECTRODES
Conductivity fluctuations in fast ionic conductors [AD-A227379] N91-14549
DIFFUSION FLAMES
Opposed jet turbulent diffusion flames [AD-A227048] N91-14446
Dynamics of an unsteady diffusion flame: Effects of heat release and gravity [AD-A227348] N91-14447
Solid fuel combustion [AD-A227170] N91-14496
An investigation of diamond synthesis in an oxygen-acetylene diffusion flame [AD-A227224] N91-14870
DIFFUSIVITY
Fundamental studies on microstructural evolution of two-phase titanium alloys N91-14452
Study of diamond film growth and properties [NASA-CR-187709] N91-14483
DIGITAL DATA
Trellis coded modulation for transmission over fading mobile satellite channel [NASA-CASE-NPO-16904-2-CU] N91-14523
DIGITAL FILTERS
The 3-D depth migration via McClellan transformations [DE91-001446] N91-14675
DIGITAL SIMULATION
Direct numerical simulation of turbulent couette flow, part 2 [AD-A226770] N91-14564
DIGITAL SYSTEMS
Digitized synchronous demodulator [NASA-CASE-GSC-13237-1] N91-14550
DIMENSIONS
The synthesis of solar radiation data for sizing stand-alone photovoltaic systems [DE90-012758] N91-14652
DIODES
LWIR HgCdTe: Innovative detectors in an incumbent technology N91-14384
DIPOLES
HEM(sub 11) modes revisited [DE91-001028] N91-14819
DIRECTIONAL SOLIDIFICATION (CRYSTALS)
Directional solidification of superalloys [NASA-CASE-MFS-28314-1] N91-14462
A novel approach to determine the heat transfer coefficient in directional solidification furnaces [NASA-CR-187648] N91-14885

DIRICHLET PROBLEM
Boundary value problems of the elasticity theory for polyhedra: Singularities and approximation with boundary element methods
[ETN-91-98168] N91-14780
DISCONTINUITY
Computer aided design models for millimeter-wave suspended substrate microstrip line
[AD-A227259] N91-14547
DISK GALAXIES
Interstellar dust as generator of x ray radiation N91-14910
DISKS
Hybrid butterfly valve
[NASA-CASE-SSC-00004-1] N91-14609
DISPLACEMENT
Dynamic behavior of thin silicon plate: Application to silicon sensors
[LAAS-90144] N91-14582
DISPLAY DEVICES
Information extraction from visual displays and the event-related brain potential
[AD-A227063] N91-14722
The object display: Principles and review of experimental findings
[AD-A226883] N91-14796
The object display in decision making and judgment
[AD-A227059] N91-14889
DISSIPATION
Smoke and extinguisher agent dissipation in a small pressurized fuselage
[DOT/FAA/CT-89/31] N91-14317
DISSOCIATION
Theoretical studies of important processes in planetary and comet atmospheres
[NASA-CR-187692] N91-15045
DISTRIBUTED PARAMETER SYSTEMS
ISIS and META projects
[NASA-CR-186413] N91-14731
A study of strong stability of distributed systems
[NASA-CR-187421] N91-14766
Control of distributed parameter systems
[AD-A227306] N91-14787
DISTRIBUTED PROCESSING
ISIS and META projects
[NASA-CR-186413] N91-14731
The ISIS project: Real experience with a fault tolerant programming system
[NASA-CR-187029] N91-14732
Distributed systems status and control
[NASA-CR-187014] N91-14733
Experiences porting the distributed Ada real-time kernel
[AD-A226693] N91-14742
DARK technology transition plan
[AD-A226695] N91-14744
A performance study of the concurrency control algorithms in hierarchical network with partitioned database
[AD-A227055] N91-14756
Method of up-front load balancing for local memory parallel processors
[NASA-CASE-MSC-21348-1] N91-14769
Distributed computing system with dual independent communications paths between computers and employing split tokens
[NASA-CASE-NPO-17185-1-CU] N91-14772
DISTRIBUTION (PROPERTY)
Grains in galactic haloes N91-14964
DISTRIBUTION FUNCTIONS
Studying quantum phase-based electronic devices
[AD-A226809] N91-14541
Size distribution of dust grains: A problem of self-similarity N91-14997
Maser cyclotron instability in a plasma with anisotropic distribution funotion N91-15075
Matter penetration and motion through the magnetosphere of neutron star N91-15087
On the existence of circular polarisation in the pulsar radiation N91-15088
DIURNAL VARIATIONS
Theory and measurements of nighttime horizontal gradients in the mid-latitude F region N91-14671
DIVERTERS
Wall conditioning and plasma surface interactions in DIII-D
[DE91-001547] N91-14846
DMSP SATELLITES
Joule heating investigations using the sondrestrom radar and DMSP satellites
[AD-A227425] N91-14677
DOCUMENTS
Tips on how to cut technical publications costs
[AD-A227334] N91-14895
DOMES (STRUCTURAL FORMS)
Wind tunnel study of an observatory dome with a circular aperture
[NASA-TM-102888] N91-15040
DONNELL EQUATIONS
The buckling of off-axis, orthotropic, cylindrical shells in torsion N91-14628
DOPED CRYSTALS
Magnetic properties of doped semiconductors
[DE91-002395] N91-14859
Investigation of new semiinsulating behavior of 3-5 compounds
[AD-A226787] N91-14862
DOPPLER EFFECT
Efficient detection and signal parameter estimation with application to high dynamic GPS receiver
[NASA-CASE-NPO-17820-1-CU] N91-14321
DOPPLER RADAR
Mesoscale features of a winter storm: Dual Doppler velocity fields and differential reflectivity
[AD-A227342] N91-14692
DRAG MEASUREMENT
Parametric study of afterbody/nozzle drag on twin two-dimensional convergent-divergent nozzles at Mach numbers from 0.60 to 1.20
[NASA-TP-2640] N91-14316
DRAG REDUCTION
Interaction between the canard and wing flow on a model of a typical combat aircraft N91-14334
Active control of boundary layer transition and turbulence
[NASA-CASE-LAR-13532-1] N91-14562
DROP TESTS
Advanced technology landing gear. Volume 1: Design
[AD-A227196] N91-14343
Advanced technology landing gear. Volume 2: Test
[AD-A227197] N91-14344
DROP TOWERS
Surface settling in partially filled containers upon step reduction in gravity
[NASA-TM-103641] N91-14556
DRYING
Conversion of alkoxide solutions to oxides: Evaporation of products
[AD-A226927] N91-14442
DUAL SPIN SPACECRAFT
The effects of liquid propellant motion on the attitude stability of spin stabilized spacecraft
[AD-A227002] N91-14376
DUCTILITY
Thermomechanical processing and ambient temperature properties of a 6061 aluminum 10 volume percent alumina metal matrix composite
[AD-A227004] N91-14433
Processing studies of aluminum-magnesium and aluminum-copper-lithium alloys
[AD-A227255] N91-14465
DURABILITY
Fracture analysis of cathodic delamination in rubber-to-metal bonds N91-14627
DUST
Reddening and extinction towards H II regions N91-14898
The dependence of UV extinction properties on dust environment N91-14902
Interstellar circular polarization and the dielectric nature of dust grains N91-14905
New results in the theory of dust grain alignment N91-14906
The spectral energy distribution of the scattered light from dark clouds N91-14911
PAH emission from Nova Cen 1986 N91-14921
DYE LASERS
Nonlinear dynamics of broad-band lasers
[DE91-001143] N91-14596
State-to-state dynamics of molecular energy transfer
[DE91-004589] N91-14599
An intense optically pumped H(-) ion source
[DE91-002949] N91-14827
DYNAMIC CHARACTERISTICS
Dynamic stability of a spinning tube conveying a fluid through a symmetrical noncircular cross-section
[DE91-004146] N91-14573
Dynamic behavior of thin silicon plate: Application to silicon sensors
[LAAS-90144] N91-14582
DYNAMIC CONTROL
On the modeling and control of slewing flexible structures N91-14499
DYNAMIC LOADS
Aircraft Dynamic Loads Due to Flow Separation
[AGARD-CP-483] N91-14324
DYNAMIC MODELS
Methods for evaluating the predictive accuracy of structural dynamic models
[NASA-CR-187649] N91-14630
DYNAMIC PRESSURE
Experimental investigation of buffet onset and penetration on a supercritical airfoil at transonic speeds N91-14328
The effect of wing planform on low speed buffet N91-14336
DYNAMIC RESPONSE
Experimental investigation and semi-empirical prediction of the dynamic response of a low-aspect-ratio trapezoidal wing due to flow separation N91-14330
Structural response of marine sandwich panels to uniform pressure loading
[AD-A227038] N91-14434
Vibration isolation technology: Sensitivity of selected classes of experiments to residual accelerations
[NASA-CR-186902] N91-14624
Solar wind dynamic pressure variations: Quantifying the statistical magnetospheric response N91-15060
DYNAMIC STABILITY
Dynamic stability of a spinning tube conveying a fluid through a symmetrical noncircular cross-section
[DE91-004146] N91-14573
DYNAMIC STRUCTURAL ANALYSIS
Low velocity impact analysis with NASTRAN
[NASA-TM-103169] N91-14426
Structural response of marine sandwich panels to uniform pressure loading
[AD-A227038] N91-14434
Axisymmetric shell analysis of the space shuttle solid rocket booster field joint
[NASA-TP-3033] N91-14618
Methods for evaluating the predictive accuracy of structural dynamic models
[NASA-CR-187649] N91-14630
DYNAMICAL SYSTEMS
Planning the behavior of dynamical systems
[AD-A227381] N91-14788

E

EARLY STARS
The compact far infrared emission from the young stellar object IRAS 16293-2422 N91-14940
EARTH ATMOSPHERE
Overview of the US Department of Energy's ARM (Atmospheric Radiation Measurement) program
[DE91-001126] N91-14678
Dust of Orionid meteor shower in the Earth atmosphere before and after Halley's Comet N91-15012
Investigation of the night sky airglow near the epicenter of the earthquake N91-15107
EARTH CRUST
Reports on block rotations, fault domains and crustal deformation
[NASA-CR-186756] N91-14665
Block rotations, fault domains and crustal deformation in the western US N91-14666
Distributed deformation and block rotation in 3D N91-14667
Stress field rotation or block rotation: An example from the Lake Mead fault system N91-14668
Multiple strike slip faults sets: A case study from the Dead Sea transform N91-14669
Plate motions and deformations from geologic and geodetic data
[NASA-CR-187379] N91-14672
Crustal dynamics project: The interpretation of crustal dynamics data in terms of plate motions and regional deformation near plate boundaries
[NASA-CR-187691] N91-14673
Crustal Dynamics Project data analysis, 1990
[NASA-TM-100765] N91-14679
EARTH ENVIRONMENT
Climate and atmospheric modeling studies. Climate applications of Earth and planetary observations. Chemistry of Earth and environment
[NASA-CR-187326] N91-14684
EARTH IONOSPHERE
Determination of SPEAR-1 rocket body potential during high-voltage experiments
[AD-A226971] N91-14417
Theory and measurements of nighttime horizontal gradients in the mid-latitude F region N91-14671
Solar wind dynamic pressure variations: Quantifying the statistical magnetospheric response N91-15060
Investigation of the night sky airglow near the epicenter of the earthquake N91-15107
EARTH MAGNETOSPHERE
Solar wind dynamic pressure variations: Quantifying the statistical magnetospheric response N91-15060
Implications of multipoint observations of substorms in the inner magnetotail N91-15061

EARTH MANTLE
Crustal dynamics project: The interpretation of crustal dynamics data in terms of plate motions and regional deformation near plate boundaries
[NASA-CR-187691] N91-14673
EARTH MOVEMENTS
Crustal dynamics project: The interpretation of crustal dynamics data in terms of plate motions and regional deformation near plate boundaries
[NASA-CR-187691] N91-14673
EARTH OBSERVING SYSTEM (EOS)
Sensor requirements for Earth and planetary observations N91-14380
HgCdTe for NASA EOS missions and detector uniformity benchmarks N91-14385
Pyroelectric detectors N91-14390
HgZnTe-based detectors for LWIR NASA applications N91-14404
Earth Observing Scanning Polarimeter (EOSP), phase B
[NASA-CR-187715] N91-14586
EARTH ORBITS
Guidance trajectories for aeroassisted orbital transfer
[NASA-CR-187735] N91-14368
EARTH RADIATION BUDGET
Limb-darkening functions as derived from along-track operation of the ERBE scanning radiometers for August 1985
[NASA-RP-1243] N91-14683
EARTH RADIATION BUDGET EXPERIMENT
Limb-darkening functions as derived from along-track operation of the ERBE scanning radiometers for August 1985
[NASA-RP-1243] N91-14683
EARTHQUAKES
Plate motions and deformations from geologic and geodetic data
[NASA-CR-187379] N91-14672
Investigation of the night sky airglow near the epicenter of the earthquake N91-15107
ECHO SOUNDING
The SYNOP experiment: Inverted echo sounder data report for October 1987 to May 1988
[AD-A227232] N91-14699
ECLIPTIC
Observations of the diffuse UV radiation field N91-14912
ECOLOGY
Validity of environmental transfer models
[DE91-002929] N91-14660
ECONOMIC IMPACT
Automatic dependent surveillance benefit and cost analysis
[DOT/FAA/RD-90/34] N91-14320
ECONOMICS
Analysis of success probability/cost trades for small landers in a Mars network N91-14363
EDDY CURRENTS
Eddy current method for measuring electrical resistivity and device for providing accurate phase detection
[AD-D014571] N91-14530
EDITING ROUTINES (COMPUTERS)
A software-system visualization tool
[AD-A227145] N91-14757
EDUCATION
NASA-UVA light aerospace alloy and structures technology program
[NASA-CR-187321] N91-14474
Adaptive human-computer interfaces using expert profiles
[AD-A226906] N91-14721
EJECTA
PAH emission from Nova Cen 1986 N91-14921
Stochastic histories of dust grains in the interstellar medium N91-14998
Vega-Giotto flyby missions and cometary cosmogony N91-15009
Sublimating icy planetesimals as the source of nucleation seeds for grain condensation in classical novae N91-15016
ELASTIC PROPERTIES
Application of ultrasonic guided waves to the characterization of texture in metal sheets of cubic and hexagonal crystallites
[DE91-001107] N91-14466
A continuum approach toward modeling the mechanics of solid lubricating films
[AD-A226961] N91-14486
Some problems in elastic contact and fracture N91-14625
Boundary value problems of the elasticity theory for polyhedra: Singularities and approximation with boundary element methods
[ETN-91-98168] N91-14780
An ion-channeling study of irradiation-induced amorphization of YBa2Cu3O(7-x)
[DE91-004488] N91-14884
ELASTIC SCATTERING
Intermediate energy nuclear physics
[DE91-002758] N91-14809
Sterile neutrinos and astrophysical and cosmological constraints on the parameters of the extended electroweak models N91-15083
ELASTODYNAMICS
A boundary element method for elastostatic and elastodynamic crack problems in two and three dimensions N91-14626
ELASTOMERS
Fabrication by filament winding with an elastomeric material
[AD-D014570] N91-14478
ELASTOSTATICS
A boundary element method for elastostatic and elastodynamic crack problems in two and three dimensions N91-14626
ELECTRIC BATTERIES
Organic cathode for a secondary battery
[NASA-CASE-NPO-17604-1-CU] N91-14536
Thermal switch disc for short circuit protection of batteries
[NASA-CASE-MSC-21428-1] N91-14537
Copper chloride cathode for a secondary battery
[NASA-CASE-NPO-17640-1-CU] N91-14538
ELECTRIC BRIDGES
A study of two control methods for full bridge converters: Soft switch bypass and current mode control
[AD-A227136] N91-14546
ELECTRIC COILS
A characterization of internal-Sn Nb3 Sn superconductors for use in the Proof of Priciples (PoP) coil
[DE91-001743] N91-14852
ELECTRIC CONDUCTORS
A characterization of internal-Sn Nb3 Sn superconductors for use in the Proof of Priciples (PoP) coil
[DE91-001743] N91-14852
ELECTRIC CURRENT
Superconducting current transducer
[DE91-004674] N91-14554
ELECTRIC FIELDS
IR detectors based on n-i-p-i superlattices N91-14408
Task reports on developing techniques for scattering by 3D composite structures and to generate new solutions in diffraction theory using higher order boundary conditions
[NASA-CR-186899] N91-14475
The inclusion of wall loss in electromagnetic finite-difference time-domain thin-slot algorithms
[DE91-001046] N91-14524
Aircraft measurements of electrified clouds at Kennedy Space Center
[NASA-CR-186536] N91-14680
Aircraft measurements of electrified clouds at Kennedy Space Center. Part 1: 1988 flights N91-14681
Aircraft measurements of electrified clouds at Kennedy Space Center. Part 2: Case study: 4 November 1988 (88309) N91-14682
Detection of nonlinear features in plasma and field measurements by PROGNOZ-8 N91-15063
Generation of inductive fields by an oblique magnetic rotator in collisionless plasma N91-15077
ELECTRIC GENERATORS
Liquid hydrogen polygeneration system and process
[NASA-CASE-KSC-11304-2] N91-14495
ELECTRIC NETWORKS
Space station common module network topology and hardware development
[NASA-CR-184034] N91-14373
ELECTRIC POTENTIAL
Dual physiological rate measurement instrument
[NASA-CASE-MSC-20078-3] N91-14709
ELECTRIC PROPULSION
Electric propulsion study
[AD-A227121] N91-14545
ELECTRIC SWITCHES
Rise time and recovery of GaAs photoconductive semiconductor switches
[DE91-001267] N91-14854
ELECTRIC WIRE
A characterization of internal-Sn Nb3 Sn superconductors for use in the Proof of Priciples (PoP) coil
[DE91-001743] N91-14852
ELECTRICAL FAULTS
Avalanche transistor selection for long term stability in streak camera sweep and pulser applications
[DE91-004195] N91-14535
ELECTRICAL IMPEDANCE
Analytical solutions with Generalized Impedance Boundary Conditions (GIBC) N91-14477
Electromagnetic properties of high Tc superconductors
[AD-A227006] N91-14868
ELECTRICAL INSULATION
Process for lowering the dielectric constant of polyimides using diamic acid additives
[NASA-CASE-LAR-13902-1] N91-14484
ELECTRICAL MEASUREMENT
Electro-optic network analyzer
[NASA-CR-186613] N91-14527
Eddy current method for measuring electrical resistivity and device for providing accurate phase detection
[AD-D014571] N91-14530
ELECTRICAL PROPERTIES
Investigation of new semiinsulating behavior of 3-5 compounds
[AD-A226787] N91-14862
ELECTRICAL RESISTIVITY
Eddy current method for measuring electrical resistivity and device for providing accurate phase detection
[AD-D014571] N91-14530
Conductivity fluctuations in fast ionic conductors
[AD-A227379] N91-14549
ELECTRO-OPTICS
Electro-optical spin measurement system
[NASA-CASE-LAR-13629-1] N91-14356
Electro-optic network analyzer
[NASA-CR-186613] N91-14527
Picosecond laser system for high speed characterization of monolithic devices
[AD-A227372] N91-14595
Optoelectronic devices
[AD-D014618] N91-14822
Nonlinear optics and organic materials
[AD-A226953] N91-14831
ELECTROACOUSTIC TRANSDUCERS
Acoustic transducer apparatus with reduced thermal conduction
[NASA-CASE-NPO-17620-1-CU] N91-14808
ELECTROCHEMISTRY
Investigation of redox processes at semiconductor electrode liquid junctions
[DE91-001787] N91-14858
ELECTRODEPOSITION
Electrophoretic and electrolytic deposition of ceramic particles on porous substrates
[AD-A227371] N91-14488
ELECTRODES
Resonant tunneling IR detectors N91-14395
Investigation of redox processes at semiconductor electrode liquid junctions
[DE91-001787] N91-14858
ELECTROENCEPHALOGRAPHY
Empirical network model of human higher cognitive brain functions
[AD-A227193] N91-14718
ELECTROLESS DEPOSITION
Electroless nickel bath recovery by cation exchange and precipitation
[DE91-001988] N91-14457
ELECTROLYTIC CELLS
In-line sensors for electrolytic magnesium cells
[DE91-002561] N91-14438
ELECTROMAGNETIC COUPLING
Solar wind dynamic pressure variations: Quantifying the statistical magnetospheric response N91-15060
ELECTROMAGNETIC FIELDS
Electric propulsion study
[AD-A227121] N91-14545
Stable explicit depth extrapolation of seismic wavefields
[DE91-001445] N91-14674
HEM(sub 11) modes revisited
[DE91-001028] N91-14819
Detection of nonlinear features in plasma and field measurements by PROGNOZ-8 N91-15063
Generation of inductive fields by an oblique magnetic rotator in collisionless plasma N91-15077
ELECTROMAGNETIC INTERACTIONS
Laser studies of the interaction of SiO with the surface of a thin film
[DE91-004562] N91-14450
ELECTROMAGNETIC INTERFERENCE
Systolic emulator experimentation
[AD-A226746] N91-14516
ELECTROMAGNETIC NOISE
Quantum 1/f noise in high technology applications including ultrasmall structures and devices
[AD-A226739] N91-14515
Radio Frequency Interference (RFI) measurements made near the proposed Alaska OTH receiving site
[AD-A226922] N91-14519

ELECTROMAGNETIC PROPERTIES
Multiband radar characterization of forest biomes
[NASA-CR-185101] N91-14638
Electromagnetic properties of high Tc superconductors
[AD-A227006] N91-14868
ELECTROMAGNETIC RADIATION
Ultrarelativistic low-frequency electromagnetic waves in pulsar magnetospheres N91-15091
ELECTROMAGNETIC SCATTERING
Task reports on developing techniques for scattering by 3D composite structures and to generate new solutions in diffraction theory using higher order boundary conditions
[NASA-CR-186899] N91-14475
A finite element conjugate gradient FFT method for scattering N91-14476
Analytical solutions with Generalized Impedance Boundary Conditions (GIBC) N91-14477
Perspectives on modeling electromagnetic sea scatter
[AD-A226939] N91-14520
The inclusion of wall loss in electromagnetic finite-difference time-domain thin-slot algorithms
[DE91-001046] N91-14524
A combined finite element-boundary element formulation for solution of axially symmetric bodies
[NASA-CR-185852] N91-14789
ELECTROMAGNETIC SURFACE WAVES
Perspectives on modeling electromagnetic sea scatter
[AD-A226939] N91-14520
ELECTROMAGNETISM
Linear resonant interaction of an electromagnetic wave with a collisional inhomogeneous plasma
[IPPCZ-298] N91-14836
ELECTRON BEAMS
A beam position monitor for low current dc beams
[CEBAF-PR-89-004] N91-14816
Laboratory investigation of electric charging of dust particles by electrons, ions, and UV radiation N91-14971
ELECTRON BOMBARDMENT
Surface modification using low energy ground state ion beams
[NASA-CASE-NPO-17498-1-CU] N91-14813
ELECTRON CYCLOTRON HEATING
Recent long-pulse and high-average-power tests on a 140 GHz gyrotron
[DE91-001680] N91-14592
ELECTRON DIFFRACTION
Studying quantum phase-based electronic devices
[AD-A226809] N91-14541
Low-energy electron diffraction investigation of epitaxial growth: Pt and Pd(100)
[DE91-000750] N91-14873
A LEED study of the MgO(001) surface structure
[DE91-002811] N91-14879
ELECTRON GUNS
High gradient electron guns
[DE91-000056] N91-14369
ELECTRON MICROSCOPY
Procedures for the preparation of samples for cross-sectional transmission electron microscopy
[AD-A227013] N91-14444
ELECTRON PLASMA
Description of nonlinear effects in a relativistic plasma using Hamiltonian formalism N91-15071
ELECTRON STATES
Red fluorescence and 3-12 micron emission in NGC 2023, HD 44179, M 82, and Lynds 1780 N91-14924
ELECTRON TRANSFER
Investigation of redox processes at semiconductor electrode liquid junctions
[DE91-001787] N91-14858
ELECTRON TUNNELING
Innovative Long Wavelength Infrared Detector Workshop Proceedings
[NASA-CR-187433] N91-14379
A novel electron tunneling infrared detector N91-14391
ELECTRON-POSITRON PLASMAS
Description of nonlinear effects in a relativistic plasma using Hamiltonian formalism N91-15071
Excitation of Langmuir wave by transversal nonlinear wave in the electron-positron inhomogeneous plasma in the presence of positron beam N91-15076
Annihilation radiation of strongly-magnetised electron-positron plasma with power-law distributions of particles N91-15078
ELECTRONIC EQUIPMENT
Studying quantum phase-based electronic devices
[AD-A226809] N91-14541
CRC program for quantifying performance of knock-sensor-equipped vehicles with varying octane level
[AD-A227340] N91-14612
ELECTRONIC EQUIPMENT TESTS
Development and testing of radiation and electromagnetic pulse hardened silicon carbide based electronics
[AD-A227309] N91-14548
CRC program for quantifying performance of knock-sensor-equipped vehicles with varying octane level
[AD-A227340] N91-14612
ELECTRONIC MODULES
Space station common module network topology and hardware development
[NASA-CR-184034] N91-14373
An investigation of using a phase-change material to improve the heat transfer in a small electronic module for an airborne radar application
[DE91-002597] N91-14525
Reliability of photovoltaic concentrator modules
[DE90-012754] N91-14651
ELECTRONS
High-energy particle acceleration during the implosion driven by 3-dimensional X-type current loop coalescence in solar flares N91-15048
ELECTROPHORESIS
Electrophoretic and electrolytic deposition of ceramic particles on porous substrates
[AD-A227371] N91-14488
ELECTROPLATING
Electroless nickel bath recovery by cation exchange and precipitation
[DE91-001988] N91-14457
ELECTROSTATIC CHARGE
Grains charges in interstellar clouds N91-14967
ELECTROSTATIC GENERATORS
Piezoelectrostatic generator
[NASA-CASE-MFS-28298-1] N91-14872
ELECTROSTATIC PROBES
Characterization of electron cyclotron resonance hydrogen plasmas
[DE91-001250] N91-14844
ELECTROSTATIC WAVES
Wave collapse at lower hybrid resonance N91-15073
Amplification of Alfven waves in free shear flows N91-15074
Excitation of Langmuir wave by transversal nonlinear wave in the electron-positron inhomogeneous plasma in the presence of positron beam N91-15076
Nonlinear plasma effects in the environment of active galactic nuclei N91-15085
ELECTROSTATICS
Electrostatically suspended rotor for angular encoder
[NASA-CASE-MFS-28294-1] N91-14508
Investigation of redox processes at semiconductor electrode liquid junctions
[DE91-001787] N91-14858
ELEMENTARY PARTICLES
Particle physics and cosmology
[DE91-001946] N91-15111
ELEVATION ANGLE
A global view of lander-to-orbiter communications accessibility for a Mars Global Network Mission N91-14362
ELLIPSES
Computation of thermochemical nonequilibrium flows around a simple and a double ellipse
[NASA-CR-187702] N91-14558
ELLIPTIC DIFFERENTIAL EQUATIONS
The integral equation method for an elliptic boundary value of the half integer characteristic
[ETN-91-98167] N91-14779
EMBEDDED COMPUTER SYSTEMS
Experiences porting the distributed Ada real-time kernel
[AD-A226693] N91-14742
Classifying software design methods
[AD-A226696] N91-14745
EMBEDDING
Equilibrium composition of interphase boundaries
[DE91-002470] N91-14814
EMISSION SPECTRA
IR detectors based on n-i-p-i superlattices N91-14408
The AIS: A spectrograph/imager ensemble for space flight
[AD-A227009] N91-14413
High resolution spectroscopy of the 11.3 micron emission band N91-14917
Airborne observations of the infrared emission bands N91-14919
A survey for PAH emission in H II regions, planetary and proto-planetary nebulae N91-14920
PAH emission from Nova Cen 1986 N91-14921
Spatial variations of the 3 micron emission features within nebulae N91-14922
Red fluorescence and 3-12 micron emission in NGC 2023, HD 44179, M 82, and Lynds 1780 N91-14924
High-spectral resolution observations of the 3.29 micron emission feature: Comparison to QCC and PAHs N91-14925
Spectral structure near the 11.3 micron emission feature N91-14926
The 3.3 micron emission feature: Map of the galactic disk, 10 deg less than 1 less than 35 deg, - 6 deg less than b less than 6 deg N91-14928
IR emission and UV extinction in two open clusters N91-14929
Dust emission from high latitude cirrus clouds N91-14930
Infrared fluorescence from PAHs in the laboratory N91-14934
Si3N4 emissivity and the unidentified infrared bands N91-14935
PAH in the laboratory and interstellar space N91-14936
The effect of ionization on the infrared absorption spectra of PAHs: A preliminary report N91-14937
Longwave spectral dependence of emission from warm dust clouds N91-14945
Dust emission in the Sagittarius B2 molecular cloud core N91-14947
Interferometric molecular line observations of W51 N91-14950
Dust emission from Barnard 35: Gas heating anomaly resolved N91-14951
IRAS results on outer galaxy star formation N91-14953
Scattering by fluffy grains N91-14992
A comparative study of the continuum and emission characteristics of comet dust. 1: Are the silicates in Comet Halley and Kohoutek amorphous or crystalline N91-15005
The 3.4 micron emission in comets N91-15006
Infrared emission from interplanetary dust N91-15013
IR emission from circumstellar envelopes of C-rich stars N91-15019
Carbon stars with alpha-C:H emission N91-15022
New circumstellar dust component in oxygen rich environments N91-15023
Interstellar extinction at 10-20 microns N91-15025
Continuous infrared emission of proto- and young-planetary nebulae N91-15030
Infrared emission from the supernova remnant Puppis A: Dust and gas parameters N91-15032
An interferometric study of molecular emission around NGC 7538 at millimeter wavelengths N91-15042
EMISSIVITY
Reddening and extinction towards H II regions N91-14898
Si3N4 emissivity and the unidentified infrared bands N91-14935
Type of silicate feature in oxygen rich stellar envelopes N91-15024
END EFFECTORS
Contribution to the specification and implementation of complex robot tasks
[ETN-90-98209] N91-14604
Spiral lead platen robotic end effector
[NASA-CASE-LAR-13855-1] N91-14615
Multi-fingered robotic hand
[NASA-CASE-NPO-15959-2] N91-14616
ENERGETIC PARTICLES
Bursts of energetic protons in the Earth's magnetotail N91-15058
ENERGY ABSORPTION
Advanced technology landing gear. Volume 2: Test
[AD-A227197] N91-14344
Linear resonant interaction of an electromagnetic wave with a collisional inhomogeneous plasma
[IPPCZ-298] N91-14836
ENERGY BUDGETS
Limb-darkening functions as derived from along-track operation of the ERBE scanning radiometers for August 1985
[NASA-RP-1243] N91-14683
ENERGY CONVERSION
Wingtip vortex turbine
[NASA-CASE-LAR-14116-1] N91-14345
Copper chloride cathode for a secondary battery
[NASA-CASE-NPO-17640-1-CU] N91-14538
ENERGY CONVERSION EFFICIENCY
New heterojunction LWIR detector options N91-14398
ENERGY DISSIPATION
High temperature refractory member with radiation emissive overcoat
[NASA-CASE-NPO-17122-1-CU] N91-14489
Synthesis of H2 in dirty ice mantles by fast ion energy loss: New experimental results increase the relevance of this mechanism N91-14962
Energy dissipation of shear Alfven waves in extended cosmic jets N91-15086

ENERGY GAPS (SOLID STATE)
Small band gap superlattices as intrinsic long wavelength infrared detector materials N91-14405
InAsSbBi, a direct band-gap, III-V, LWIR material N91-14410
Field induced gap infrared detector [NASA-CASE-NPO-17526-1-CU] N91-14588
ENERGY TECHNOLOGY
Office of Basic Energy Sciences 1990 summary report [DE91-002971] N91-14653
ENERGY TRANSFER
State-to-state dynamics of molecular energy transfer [DE91-004589] N91-14599
ENGINE TESTS
Computer-assisted strain-gage monitoring and data reduction system [AD-A226894] N91-14589
ENGRAVING
Electrostatically suspended rotor for angular encoder [NASA-CASE-MFS-28294-1] N91-14508
ENSTATITE
Infrared spectra of crystalline and glassy silicates and application to interstellar dust N91-14994
ENTHALPY
An automated flow calorimeter for heat capacity and enthalpy measurements at elevated temperatures and pressures [DE91-002759] N91-14584
ENVIRONMENT EFFECTS
Office of Basic Energy Sciences 1990 summary report [DE91-002971] N91-14653
Acidic deposition: Its nature and impacts [DE91-001984] N91-14658
Validity of environmental transfer models [DE91-002929] N91-14660
Environmental impact assessment as applied to policies, plans, and programs [DE91-001372] N91-14664
ENVIRONMENT MODELS
Validity of environmental transfer models [DE91-002929] N91-14660
ENVIRONMENT POLLUTION
Office of Basic Energy Sciences 1990 summary report [DE91-002971] N91-14653
ENVIRONMENT PROTECTION
Environmental impact assessment as applied to policies, plans, and programs [DE91-001372] N91-14664
ENVIRONMENTAL MONITORING
Atmospheric source-receptor relationships: Concepts and terminology [DE91-001033] N91-14656
ENVIRONMENTAL SURVEYS
Environmental impact assessment as applied to policies, plans, and programs [DE91-001372] N91-14664
ENZYME ACTIVITY
Cosmos 2044 [NASA-CR-187003] N91-14702
ENZYMES
Cosmos 2044 [NASA-CR-187003] N91-14702
EPHEMERIDES
The Air Almanac, 1990 N91-15036
The Air Almanac, 1989 N91-15037
The Astronomical Almanac for the year 1989 [ISBN-0-11-886932-9] N91-15038
The Astronomical Almanac for the year 1990 [ISBN-0-11-886934-5] N91-15039
EPITAXY
Simulation of transient glide of a threading dislocation in an embedded strained expitaxial layer [AD-A226965] N91-14867
Low-energy electron diffraction investigation of epitaxial growth: Pt and Pd(100) [DE91-000750] N91-14873
Effect of step edge transition rates and anisotropy in simulations of epitaxial growth [DE91-001251] N91-14875
Defect and impurity effects on the initial growth of Ag on Si(111) [DE91-001277] N91-14876
EPOXY MATRIX COMPOSITES
The interlaminar shear strength of woven carbon, woven glass and woven carbon/glass hybrid laminates under static and impact loading [OUEL-1831/90] N91-14423
Ultrasonic detection of fatigue damage in glass-epoxy composites [DE91-002652] N91-14619
EPOXY RESINS
Mesomechanical model for fibre composites [AD-A226792] N91-14432
EQUATIONS OF MOTION
Predictions of F-111 TACT aircraft buffet response N91-14335
Dynamic stability of a spinning tube conveying a fluid through a symmetrical noncircular cross-section [DE91-004146] N91-14573
Load response of horizontal-axis wind turbines to turbulence [DE90-000375] N91-14644
EQUATIONS OF STATE
New multiphase equation of state for polycrystalline quartz [DE91-001048] N91-14490
EQUIVALENT CIRCUITS
A versatile RF cavity mode damper [DE91-002947] N91-14534
Computer aided design models for millimeter-wave suspended substrate microstrip line [AD-A227259] N91-14547
ERBIUM
Ion beam induced diffusion and crystallization in high dose Er implanted Si [DE91-002869] N91-14860
ERRORS
Statistical errors in the fractal analysis of flame boundaries [DE91-001795] N91-14439
Air traffic controller memory enhancement [DOT/FAA/CT-TN90/38] N91-14713
An accurate product SVD (singular value decomposition) algorithm [DE91-004448] N91-14765
ERYTHROCYTES
Initial blood storage experiment [NASA-CR-185513-PT-1] N91-14700
Initial blood storage experiment [NASA-CR-185513-PT-2] N91-14701
ESTIMATES
NUFA: A semi-empirical method for the prediction of isolated weapon aerodynamics N91-14287
ESTIMATING
A method for estimating tokamak poloidal field coil currents which incorporates engineering constraints [DE91-001662] N91-14848
EUCLIDEAN GEOMETRY
Covers by polars of arrangements [DE91-001358] N91-14764
EULER EQUATIONS OF MOTION
Pressure measurements on slender bodies at supersonic speeds and development of flow separation critera for Euler codes N91-14282
Supersonic tactical missile computation using Euler's equation with crossflow separation modeling N91-14284
Application of Euler and Navier-Stokes codes to missile type bodies with high L/D ratios N91-14286
Supersonic vortex flows around a missile body: Basic experiment and Euler numerical computation N91-14291
Acceleration techniques for explicit Euler codes N91-14555
Dynamic behavior of thin silicon plate: Application to silicon sensors [LAAS-90144] N91-14582
Magnetically driven jets and winds N91-15084
EVAPORATION
Ion-induced grain growth in multilayer and coevaporated metal alloy thin films [DE91-004489] N91-14472
EVAPORATION RATE
Conversion of alkoxide solutions to oxides: Evaporation of products [AD-A226927] N91-14442
EVOKED RESPONSE (PSYCHOPHYSIOLOGY)
Empirical network model of human higher cognitive brain functions [AD-A227193] N91-14718
EXCITATION
Experimental investigations of buffet excitation forces on a low aspect ratio trapezoidal half wing in incompressible flow N91-14329
The forward mounted spoiler as a source of buffet excitation N91-14332
The effect of wing planform on low speed buffet N91-14336
New method to determine in wind tunnel the buffeting forces N91-14337
New results in the theory of dust grain alignment N91-14906
Spatial variations of the 3 micron emission features within nebulae N91-14922
EXHAUST NOZZLES
Internal performance of a hybrid axisymmetric/nonaxisymmetric convergent-divergent nozzle [NASA-TM-4230] N91-14275
EXOBIOLOGY
Aerospace medicine and biology: A continuing bibliography with indexes (supplement 343) [NASA-SP-7011(343)] N91-14711
Aerospace medicine and biology: A continuing bibliography with indexes (supplement 344) [NASA-SP-7011(344)] N91-14712
Exobiology in Earth orbit: The results of science workshops held at NASA, Ames Research Center [NASA-SP-500] N91-14725
EXPANDABLE STRUCTURES
Fabrication by filament winding with an elastomeric material [AD-D014570] N91-14478
EXPERT SYSTEMS
Intelligent manipulation technique for multi-branch robotic systems [NASA-CR-187651] N91-14603
Oceanographic expert system validation using GOAP mesoscale products and Gulf/DART validation test data [AD-A226929] N91-14693
Distributed systems status and control [NASA-CR-187014] N91-14733
Construction of large-scale simulation codes using ALPAL (A Livermore Physics Applications Language) [DE91-002783] N91-14740
Discrete event simulation tool for analysis of qualitative models of continuous processing systems [NASA-CASE-MSC-21465-1] N91-14741
Pedagogical strategies for human and computer tutoring [AD-A226886] N91-14750
EXPLOSIONS
A simple plane-wave explosive lens [DE91-004297] N91-14526
Shot report, Holo-17-Holo-22 Rex-9 [DE91-002575] N91-14583
EXPLOSIVES
Dynamic consolidation of aluminum-silicon carbide composites [DE91-001929] N91-14427
Thermal analyses for quality control of plastics, ceramics, and explosives [DE91-002701] N91-14622
EXPOSURE
Radiation response issues for infrared detectors N91-14388
EXTERNAL STORE SEPARATION
Store carriage, integration, and release N91-14281
EXTERNAL STORES
In-flight measurements on a Tornado aircraft for stores carriage and release research [RAE-TM-AERO-2180] N91-14341
EXTINCTION
Reddening and extinction towards H II regions N91-14898
The relationship between IR, optical, and UV extinction N91-14899
The dependence of UV extinction properties on dust environment N91-14902
Polarization and extinction by aligned grains N91-14907
Correlation properties of interstellar dust: Diffuse interstellar bands N91-14916
Red fluorescence and 3-12 micron emission in NGC 2023, HD 44179, M 82, and Lynds 1780 N91-14924
On the origin of extinction in the Coma cluster of galaxies N91-14987
Properties of grains derived from IRAS observations of dust N91-15001
EXTINGUISHING
Smoke and extinguisher agent dissipation in a small pressurized fuselage [DOT/FAA/CT-89/31] N91-14317
EXTRAGALACTIC RADIO SOURCES
Estimability of geodetic parameters from space VLBI observables [NASA-CR-187413] N91-14636
EXTRAPOLATION
Stable explicit depth extrapolation of seismic wavefields [DE91-001445] N91-14674
The 3-D depth migration via McClellan transformations [DE91-001446] N91-14675
EXTREME ULTRAVIOLET RADIATION
Solar magnetic flux-tubes and coronal loops N91-15047
EYE MOVEMENTS
Eye movements and visual information processing [AD-A226782] N91-14714

F

F 2 REGION
Theory and measurements of nighttime horizontal gradients in the mid-latitude F region N91-14671
F-16 AIRCRAFT
Development of an unmanned air research vehicle for supermaneuverability studies
[AD-A227165] N91-14342
F-111 AIRCRAFT
Predictions of F-111 TACT aircraft buffet response N91-14335
FABRICATION
Fabrication of sensitive high Tc bolometers N91-14389
Development and testing of radiation and electromagnetic pulse hardened silicon carbide based electronics
[AD-A227309] N91-14548
Acoustic positioning and orientation prediction
[NASA-CASE-NPO-17511-1-CU] N91-14807
Acoustic transducer apparatus with reduced thermal conduction
[NASA-CASE-NPO-17620-1-CU] N91-14808
FABRICS
Smart tunnel: Docking mechanism
[NASA-CASE-MSC-21360-1] N91-14374
FAILURE
A parametric shell analysis of the shuttle 51-L SRB AFT field joint
[NASA-TM-102748] N91-14629
ISIS and META projects
[NASA-CR-186413] N91-14731
FAILURE ANALYSIS
Failure in laminated composite plates containing a hole
[AD-A227307] N91-14435
Integration of sneak analysis with design, volume 1
[AD-A226902] N91-14543
The response and failure mechanisms of circular metal and composite plates subjected to underwater shock loading
[AD-A226759] N91-14631
The use of light emission in failure analysis of CMOS ICs
[DE91-001234] N91-14633
Cyclomatic complexity as a utility for predicting software faults
[AD-A227313] N91-14760
FAR INFRARED RADIATION
The compact far infrared emission from the young stellar object IRAS 16293-2422 N91-14940
Far infrared structure of spiral galaxies from the IRAS CPC images N91-14988
FAR ULTRAVIOLET RADIATION
New measurements of the far ultraviolet scattering properties of interstellar dust N91-14909
FAST FOURIER TRANSFORMATIONS
New method to determine in wind tunnel the buffeting forces N91-14337
A finite element conjugate gradient FFT method for scattering N91-14476
A combined finite element-boundary element formulation for solution of axially symmetric bodies
[NASA-CR-185852] N91-14789
FATIGUE (MATERIALS)
Use of anomalous small angle x ray scattering to investigate microstructural features in complex alloys
[DE91-002397] N91-14471
Hazards and safeguards of high pressure hydraulic fatigue testing
[AD-A226767] N91-14509
Ultrasonic detection of fatigue damage in glass-epoxy composites
[DE91-002652] N91-14619
FATIGUE LIFE
Axial-torsional fatigue: A study of tubular specimen thickness effects
[NASA-TM-103637] N91-14632
Fatigue reliability of wind turbine components
[DE91-001262] N91-14650
FATIGUE TESTS
Hazards and safeguards of high pressure hydraulic fatigue testing
[AD-A226767] N91-14509
Axial-torsional fatigue: A study of tubular specimen thickness effects
[NASA-TM-103637] N91-14632
FAULT TOLERANCE
The ISIS project: Real experience with a fault tolerant programming system
[NASA-CR-187029] N91-14732
FEASIBILITY ANALYSIS
Feasibility study of the seismic reflection method in Amargosa Desert, Nye County, Nevada
[DE91-001646] N91-14676
FECES
Valve for waste collection and storage
[NASA-CASE-MSC-21025-4] N91-14723
Method for waste collection and storage
[NASA-CASE-MSC-21025-2] N91-14724
FEEDBACK CONTROL
New method to determine in wind tunnel the buffeting forces N91-14337
Multivariable methods for the design, identification, and control of large space structures. Volume 2: Optimal and sub-optimal estimation applied to large flexible structures
[AD-A226699] N91-14375
On the modeling and control of slewing flexible structures N91-14499
Evaluation of performance and feedback control design for vehicle suspensions with variable compliance elements N91-14601
A study of strong stability of distributed systems
[NASA-CR-187421] N91-14766
FERRITES
A versatile RF cavity mode damper
[DE91-002947] N91-14534
FIBER COMPOSITES
A statistically-based model of the interacting processes which lead to creep-rupture in filament-wound composite pressure vessels N91-14420
Method for manufacturing composite material
[EP-PATENT-0-314-353-A2] N91-14421
Mesomechanical model for fibre composites
[AD-A226792] N91-14432
Failure in laminated composite plates containing a hole
[AD-A227307] N91-14435
Fabrication by filament winding with an elastomeric material
[AD-D014570] N91-14478
Adhesion at ceramic interfaces
[DE91-001660] N91-14480
Eddy current method for measuring electrical resistivity and device for providing accurate phase detection
[AD-D014571] N91-14530
The response and failure mechanisms of circular metal and composite plates subjected to underwater shock loading
[AD-A226759] N91-14631
FIBER OPTICS
Tapered fiber amplifier
[AD-D014629] N91-14512
Optical encoding of imaging data
[AD-D014617] N91-14821
Integrated optical devices for photonics instrumentation systems
[DE91-004192] N91-14828
Vibrational testing of optical fiber connector joints
[NASA-TM-103654] N91-14829
FIBER ORIENTATION
Failure in laminated composite plates containing a hole
[AD-A227307] N91-14435
Optical encoding of imaging data
[AD-D014617] N91-14821
FIBER STRENGTH
Surface and interfacial properties of carbon fibers
[NASA-CR-184916] N91-14429
Automated system for measuring the strength of optical fibers
[AD-D014626] N91-14824
FIBERS
A numerical and experimental analysis of reactor performance and deposition rates for CVD on monofilaments
[NASA-TM-103631] N91-14500
A study of liquid scintillator and fiber materials for use in a fiber calorimeter
[DE91-004229] N91-14585
FIELD ALIGNED CURRENTS
Interrelationship between the tearing-instability and magnetic island merging N91-15109
FIELD COILS
A method for estimating tokamak poloidal field coil currents which incorporates engineering constraints
[DE91-001662] N91-14848
FIELD EFFECT TRANSISTORS
AlSb/InAs/AlSb quantum wells N91-14411
Silicon carbide, a semiconductor for space power electronics
[NASA-TM-103655] N91-14850
FIGHTER AIRCRAFT
Investigation of a semi-empirical method to predict limit cycle oscillations of modern fighter aircraft N91-14333
Interaction of feel system and flight control system dynamics on lateral flying qualities
[NASA-CR-179445] N91-14353
FILAMENT WINDING
A statistically-based model of the interacting processes which lead to creep-rupture in filament-wound composite pressure vessels N91-14420
Fabrication by filament winding with an elastomeric material
[AD-D014570] N91-14478
FILMS
Study of diamond film growth and properties
[NASA-CR-187709] N91-14483
X ray sensitive area detection device
[NASA-CASE-MFS-28232-1] N91-14835
FINE STRUCTURE
Atomic environments in iron meteorites using EXAFS N91-15011
FINITE DIFFERENCE THEORY
Computation of viscous supersonic flows N91-14283
The inclusion of wall loss in electromagnetic finite-difference time-domain thin-slot algorithms
[DE91-001046] N91-14524
An investigation of using a phase-change material to improve the heat transfer in a small electronic module for an airborne radar application
[DE91-002597] N91-14525
A numerical theory of lattice gas and lattice Boltzmann methods in the computation of solutions to nonlinear advective-diffusive systems
[DE91-002566] N91-14560
The 3-D depth migration via McClellan transformations
[DE91-001446] N91-14675
The computer algebra approach of the finite difference methods for PDEs
[DE90-631581] N91-14790
FINITE ELEMENT METHOD
A statistically-based model of the interacting processes which lead to creep-rupture in filament-wound composite pressure vessels N91-14420
An analysis of interlaminar stresses in unsymmetrically laminated plates
[NASA-CR-187657] N91-14424
Low velocity impact analysis with NASTRAN
[NASA-TM-103169] N91-14426
Fundamentals of interfacial strength in composite materials
[AD-A226701] N91-14431
A finite element conjugate gradient FFT method for scattering N91-14476
Effect of laser fluctuations in automated solder joint inspection
[AD-A226685] N91-14620
Fracture analysis of cathodic delamination in rubber-to-metal bonds N91-14627
Nonlinear finite element dynamics on multiprocessor computers
[AD-A227409] N91-14761
A combined finite element-boundary element formulation for solution of axially symmetric bodies
[NASA-CR-185852] N91-14789
FINNED BODIES
Navier-Stokes predictions of static and dynamic aerodynamic derivatives for high L/D finned projectiles N91-14295
FINS
Chordwise and spanwise centers of pressure of missile fins N91-14304
FIRE EXTINGUISHERS
Smoke and extinguisher agent dissipation in a small pressurized fuselage
[DOT/FAA/CT-89/31] N91-14317
Definition of experiments to investigate fire suppressants in microgravity
[NASA-CR-185295] N91-14378
Next-generation fire extinguishing agent. Phase 2: Laboratory tests and scoping trials
[AD-A227347] N91-14510
FIRE FIGHTING
Definition of experiments to investigate fire suppressants in microgravity
[NASA-CR-185295] N91-14378
Next-generation fire extinguishing agent. Phase 2: Laboratory tests and scoping trials
[AD-A227347] N91-14510
FIRES
Smoke and extinguisher agent dissipation in a small pressurized fuselage
[DOT/FAA/CT-89/31] N91-14317
Definition of experiments to investigate fire suppressants in microgravity
[NASA-CR-185295] N91-14378
FLAME PROPAGATION
The application of the turbulent burning speed concept to laboratory flames
[DE91-001789] N91-14449

Solid fuel combustion
[AD-A227170] N91-14496

FLAMES
Statistical errors in the fractal analysis of flame boundaries
[DE91-001795] N91-14439

FLAT PLATES
Variation of wall shear stress and Reynolds stress over a flat plate downstream of a boundary layer manipulator
[AD-A226875] N91-14565

FLEXIBLE BODIES
On the modeling and control of slewing flexible structures N91-14499

FLEXIBLE SPACECRAFT
Multivariable methods for the design, identification, and control of large space structures. Volume 2: Optimal and sub-optimal estimation applied to large flexible structures
[AD-A226699] N91-14375

FLEXIBLE WINGS
A method for the design of transonic flexible wings
[NASA-TP-3045] N91-14323

FLIGHT CHARACTERISTICS
Three dimensional flow calculations for a projectile with standard and dome bases N91-14294
Predictions of F-111 TACT aircraft buffet response N91-14335
Interaction of feel system and flight control system dynamics on lateral flying qualities
[NASA-CR-179445] N91-14353

FLIGHT CONTROL
Interaction of feel system and flight control system dynamics on lateral flying qualities
[NASA-CR-179445] N91-14353

FLIGHT MANAGEMENT SYSTEMS
Automatic dependent surveillance benefit and cost analysis
[DOT/FAA/RD-90/34] N91-14320

FLIGHT PATHS
Experimental aerodynamics for hot gas jet reaction control systems N91-14300

FLIGHT SAFETY
Using simulation to evaluate the safety of proposed ATC operations and procedures
[DOT/FAA/CT-TN90/22] N91-14318
Flight Set 360L006 STS-34 field joint protection system, thermal protection system, and systems tunnel components, volume 4
[NASA-CR-184050] N91-14415

FLIGHT SIMULATORS
Prediction of helicopter simulator sickness
[DE90-016530] N91-14710

FLIGHT TESTS
Tabulation of data from the tip aerodynamics and acoustics test
[NASA-TM-102280] N91-14273
In-flight measurements on a Tornado aircraft for stores carriage and release research
[RAE-TM-AERO-2180] N91-14341
Development of an unmanned air research vehicle for supermaneuverability studies
[AD-A227165] N91-14342
A system architecture for long duration free floating flight for military applications
[NASA-CR-187435] N91-14513

FLIGHT TRAINING
Validation of dichotic listening and psychomotor task performance as predictors of primary flight training criteria: Highlighting relevant statistical issues
[AD-A227010] N91-14717

FLOATING
A system architecture for long duration free floating flight for military applications
[NASA-CR-187435] N91-14513

FLOW CHARACTERISTICS
Laminar/turbulent flow transition effects on high-speed missile domes N91-14301

FLOW DISTRIBUTION
Numerical investigations in three-dimensional internal flows
[NASA-CR-187373] N91-14277
Store carriage, integration, and release N91-14281
Pressure measurements on slender bodies at supersonic speeds and development of flow separation critera for Euler codes N91-14282
Computation of viscous supersonic flows N91-14283
Supersonic tactical missile computation using Euler's equation with crossflow separation modeling N91-14284
Aerodynamic characteristics of cylindrical bodies with pointed and truncated conical noses N91-14289
Systematic investigations of body-wing-tail interference at high angles of attack N91-14290
Comparison of different calculation methods applied to a lenticular fuselage section N91-14293
Navier-Stokes predictions of static and dynamic aerodynamic derivatives for high L/D finned projectiles N91-14295
Results of GARTEUR action group AG09 on flow past missile afterbodies N91-14299
Experimental aerodynamics for hot gas jet reaction control systems N91-14300
Investigations of aerothermodynamic effects on axisymmetric bodies at high Mach numbers N91-14302
Computational models with advanced thermochemistry for the analysis of missile/plume flowfield interactions N91-14305
The inviscid stability of supersonic flow past heated or cooled axisymmetric bodies
[NASA-CR-187475] N91-14307
Numerical simulation of ice growth on a MS-317 swept wing geometry
[NASA-TM-103705] N91-14310
Numerical studies of compressible flow over a double-delta wing at high angles of attack
[AD-A226931] N91-14312
Experimental investigation of buffet onset and penetration on a supercritical airfoil at transonic speeds N91-14328
Measurement of hydrodynamic forces and moments and flow field mapping of a model in coning motion
[AD-A226684] N91-14355
The application of the turbulent burning speed concept to laboratory flames
[DE91-001789] N91-14449
Solid fuel combustion
[AD-A227170] N91-14496
A numerical and experimental analysis of reactor performance and deposition rates for CVD on monofilaments
[NASA-TM-103631] N91-14500
A fast solver for systems of axisymmetric ring vortices
[DE91-002594] N91-14561
Low-noise nozzle valve
[NASA-CASE-MFS-28383-1] N91-14563
Shipboard and satellite observations of upper ocean velocity and transport variability in the Gulf Stream
[AD-A226974] N91-14694
Upwelling southwest of Iceland due to quasi-geostrophic flow
[AD-A227129] N91-14698
New accurate, vectorized approximations of state surfaces for the thermodynamic and transport properties of equilibrium air
[MBB/FE122/S/PUB/0389] N91-14886
Influence of the parameter distribution of the solar wind near the Sun upon its structure at the Earth's orbit N91-i5108

FLOW EQUATIONS
CFD code evaluation for internal flow modeling
[NASA-CR-187677] N91-14557

FLOW MEASUREMENT
Investigation of combustion in large vortices
[AD-A226791] N91-14441
The application of the turbulent burning speed concept to laboratory flames
[DE91-001789] N91-14449
An automated flow calorimeter for heat capacity and enthalpy measurements at elevated temperatures and pressures
[DE91-002759] N91-14584

FLOW REGULATORS
Bio-reactor chamber
[NASA-CASE-MSC-20929-1] N91-14703

FLOW STABILITY
The effect of wall compliance on the Goertler vortex instability
[NASA-CR-187477] N91-14308

FLOW VELOCITY
Flow visualization studies of blowing from the tip of a swept wing
[NASA-TM-4217] N91-14274
The application of the turbulent burning speed concept to laboratory flames
[DE91-001789] N91-14449
Variation of wall shear stress and Reynolds stress over a flat plate downstream of a boundary layer manipulator
[AD-A226875] N91-14565
A discussion of the results of an in-situ comparison of three full-vector anemometers
[DE91-002113] N91-14572
An automated flow calorimeter for heat capacity and enthalpy measurements at elevated temperatures and pressures
[DE91-002759] N91-14584

FLOW VISUALIZATION
Flow visualization studies of blowing from the tip of a swept wing
[NASA-TM-4217] N91-14274
Numerical studies of compressible flow over a double-delta wing at high angles of attack
[AD-A226931] N91-14312
On the breakdown of a vortex
[AD-A227066] N91-14568

FLOWMETERS
The SYNOP experiment: Inverted echo sounder data report for October 1987 to May 1988
[AD-A227232] N91-14699

FLUID DYNAMICS
One- and two-dimensional Stirling machine simulation using experimentally generated flow turbulence models
[NASA-CR-185285] N91-14414
A fast solver for systems of axisymmetric ring vortices
[DE91-002594] N91-14561

FLUID FILMS
A continuum approach toward modeling the mechanics of solid lubricating films
[AD-A226961] N91-14486
Effect of interline heat flow parameter on contact line heat transfer
[AD-A226944] N91-14566

FLUID FLOW
One- and two-dimensional Stirling machine simulation using experimentally generated flow turbulence models
[NASA-CR-185285] N91-14414
An automated flow calorimeter for heat capacity and enthalpy measurements at elevated temperatures and pressures
[DE91-002759] N91-14584

FLUID MECHANICS
NASA-UVA light aerospace alloy and structures technology program
[NASA-CR-187321] N91-14474
Phase portrait methods for verifying fluid dynamic simulations
[DE91-001129] N91-14571

FLUORESCENCE
The spectral energy distribution of the scattered light from dark clouds N91-14911
Infrared images of reflection nebulae and Orion's bar: Fluorescent molecular hydrogen and the 3.3 micron feature N91-14918
Red fluorescence and 3-12 micron emission in NGC 2023, HD 44179, M 82, and Lynds 1780 N91-14924

FLUOROHYDROCARBONS
Next-generation fire extinguishing agent. Phase 2: Laboratory tests and scoping trials
[AD-A227347] N91-14510

FLUX DENSITY
Copper chloride cathode for a secondary battery
[NASA-CASE-NPO-17640-1-CU] N91-14538
Infrared emission from ultracompact H II regions N91-14942
High resolution observations of compact H II regions at 230 GHz N91-14954

FLUX PINNING
Irradiation-induced pinning in single-crystal and thin-film Tl2Ca2Ba2Cu3O10 superconductors
[DE91-001342] N91-14877

FLUX TRANSFER EVENTS
Three-dimensional magnetic reconnection at the Earth's magnetopause N91-15059
Interrelationship between the tearing-instability and magnetic island merging N91-15109

FLYWHEELS
Ultrasonic detection of fatigue damage in glass-epoxy composites
[DE91-002652] N91-14619

FOAMS
A vibrating razor blade machining tool for material removal on low-density foams
[DE91-002996] N91-14507

FOCAL PLANE DEVICES
Innovative Long Wavelength Infrared Detector Workshop Proceedings
[NASA-CR-187433] N91-14379
Status of LWIR HgCdTe infrared detector technology N91-14383
LWIR HgCdTe: Innovative detectors in an incumbent technology N91-14384
Detector array evaluation and figures of merit N91-14386
Novel Si(1-x)Ge(x)/Si heterojunction internal photoemission long wavelength infrared detectors N91-14401
InAs/GaAs and InAs doping superlattices N91-14409

FORCE DISTRIBUTION
Three dimensional flow calculations for a projectile with standard and dome bases N91-14294

FORECASTING
Modified seasonal factors in exponential smoothing
[DE91-002802] N91-14688
Prediction of helicopter simulator sickness
[DE90-016530] N91-14710

FORESTS
Multiband radar characterization of forest biomes [NASA-CR-185101] N91-14638
Analysis of the boreal forest-tundra ecotone: A test of AVIRIS capabilities in the Eastern Canadian subarctic [NASA-CR-187335] N91-14655
Acidic deposition: Its nature and impacts [DE91-001984] N91-14658
FORMALDEHYDE
Molecules in an infrared cirrus cloud N91-14977
FOSSIL FUELS
The effects of climate change on the nitrogen cycle and acid deposition [DE91-002785] N91-14659
The response of atmospheric CO2 to changes in land use [DE91-001212] N91-14663
FOURIER TRANSFORMATION
FTIR (Fourier Transform Infrared) spectrophotometry for thin film monitors: Computer and equipment integration for enhanced capabilities [DE91-001228] N91-14853
FRACTALS
Statistical errors in the fractal analysis of flame boundaries [DE91-001795] N91-14439
Scale-invariant theory of optical properties of fractal clusters [AD-A227031] N91-14832
FRACTIONATION
Laboratory studies of refractory metal oxide smokes N91-14993
FRACTURE MECHANICS
Some problems in elastic contact and fracture N91-14625
A boundary element method for elastostatic and elastodynamic crack problems in two and three dimensions N91-14626
FRACTURE STRENGTH
Fundamentals of interfacial strength in composite materials [AD-A226701] N91-14431
Mesomechanical model for fibre composites [AD-A226792] N91-14432
Directional solidification of superalloys [NASA-CASE-MFS-28314-1] N91-14462
An examination of delta prime growth in an aluminum-lithium alloy by x ray diffraction [AD-A227254] N91-14464
Effects of irradiation on initiation and crack-arrest toughness of two high-copper welds and on stainless steel cladding [DE91-001272] N91-14467
FRACTURING
Distributed deformation and block rotation in 3D N91-14667
FRAGMENTATION
Hazards and safeguards of high pressure hydraulic fatigue testing [AD-A226767] N91-14509
The origin of micrograins N91-15000
FRAMES (DATA PROCESSING)
High Resolution, High Frame Rate Video Technology [NASA-CP-3080] N91-14574
Results of the users' requirements survey N91-14575
Data transmission networks N91-14576
FREDHOLM EQUATIONS
The integral equation method for an elliptic boundary value of the half integer characteristic [ETN-91-98167] N91-14779
FREE FLIGHT
A system architecture for long duration free floating flight for military applications [NASA-CR-187435] N91-14513
FREQUENCIES
Tabulation of data from the tip aerodynamics and acoustics test [NASA-TM-102280] N91-14273
FREQUENCY ANALYZERS
Vibration analyzer [NASA-CASE-MSC-21408-1] N91-14607
FREQUENCY MEASUREMENT
Electro-optic network analyzer [NASA-CR-186613] N91-14527
FREQUENCY MODULATION
Demodulation processes in auditory perception [AD-A226824] N91-14707
FREQUENCY MULTIPLIERS
Millimeter-wave monolithic diode-grid frequency multiplier [NASA-CASE-NPO-17258-1-CU] N91-14551
FRICTION
A continuum approach toward modeling the mechanics of solid lubricating films [AD-A226961] N91-14486
FRONTS (METEOROLOGY)
Explosive cyclogenesis: A case study of the Veterans' Day storm of 11-12 November 1987 [AD-A227077] N91-14691
FUNCTIONAL ANALYSIS
Human factors engineering. Part 1: Test procedures [AD-A226480] N91-14720
FUNCTIONAL DESIGN SPECIFICATIONS
Space station common module network topology and hardware development [NASA-CR-184034] N91-14373
FUNCTIONS (MATHEMATICS)
Mappings and accuracy for Chebyshev pseudo-spectral approximations [NASA-TM-103630] N91-14781
FURNACES
A novel approach to determine the heat transfer coefficient in directional solidification furnaces [NASA-CR-187648] N91-14885
FUSELAGES
Comparison of different calculation methods applied to a lenticular fuselage section N91-14293
FUSION REACTORS
Radiation resistance of copper alloys at high exposure levels [DE91-001563] N91-14470
FUZZY SETS
Methods for evaluating the predictive accuracy of structural dynamic models [NASA-CR-187649] N91-14630

G

GALACTIC CLUSTERS
On the origin of extinction in the Coma cluster of galaxies N91-14987
Galaxy formation by dust N91-14989
GALACTIC COSMIC RAYS
Generation of cosmic rays in pinches N91-15070
GALACTIC EVOLUTION
IRAS results on outer galaxy star formation N91-14953
Galaxy formation by dust N91-14989
Compact object masses in active galactic nuclei and quasars and duration of activity stage N91-15096
Pregalactic inhomogeneity in hot dark matter model of the universe N91-15100
GALACTIC MASS
Compact object masses in active galactic nuclei and quasars and duration of activity stage N91-15096
GALACTIC NUCLEI
The 3.3 micron emission feature: Map of the galactic disk, 10 deg less than 1 less than 35 deg, - 6 deg less than b less than 6 deg N91-14928
GALACTIC RADIATION
The 3.3 micron emission feature: Map of the galactic disk, 10 deg less than 1 less than 35 deg, - 6 deg less than b less than 6 deg N91-14928
The origin of the galactic emission in IRAS data N91-14974
GALACTIC STRUCTURE
Far infrared structure of spiral galaxies from the IRAS CPC images N91-14988
GALAXIES
The spectral energy distribution of the scattered light from dark clouds N91-14911
The capability of the ultraviolet imaging telescope for observing interstellar dust N91-14913
Infrared cirrus point sources N91-14978
Temperature distribution of dust in luminous IRAS galaxies N91-14982
The 100 and 160 micron maps of the dust reemission from the nucleus and inner-arm regions of NGC 6946 N91-14983
Multicolor optical polarimetry of reddened stars in the small Magellanic cloud N91-14986
Stochastic histories of dust grains in the interstellar medium N91-14998
On the nature of cosmic gamma ray bursts N91-15098
GALERKIN METHOD
The buckling of off-axis, orthotropic, cylindrical shells in torsion N91-14628
GALLIUM ARSENIDE LASERS
Quantum well laser [AD-A227303] N91-14594
GALLIUM ARSENIDES
LWIR HgCdTe: Innovative detectors in an incumbent technology N91-14384
Quantum Well Infrared Photodetectors (QWIP) N91-14392
InAs/Ga(1-x)In(x)Sb superlattices for infrared detector applications N91-14407
InAs/GaAs and InAs doping superlattices N91-14409
AlSb/InAs/AlSb quantum wells N91-14411
Triggering GaAs lock-on switches with laser diode arrays [DE91-002419] N91-14532
Millimeter-wave monolithic diode-grid frequency multiplier [NASA-CASE-NPO-17258-1-CU] N91-14551
Optically-triggered GaAs thyristor switch s: Integrated structures for environmental hardening [DE91-001355] N91-14553
Program to study the process parameters of OMVPE and their relationship to the properties of Ga(0.47)In(0.53) as ON InP substrates [AD-A226618] N91-14851
Rise time and recovery of GaAs photoconductive semiconductor switches [DE91-001267] N91-14854
Investigation of new semiinsulating behavior of 3-5 compounds [AD-A226787] N91-14862
Pseudomorphic InGaAs materials [AD-A226895] N91-14864
Photogenerated carrier-induced reaction on semiconductor surfaces [DE91-001349] N91-14878
GALLIUM COMPOUNDS
Crystal structure of ZnGa2S4, a defect sphalerite-derivative [AD-A226937] N91-14865
GAMMA RAY BURSTS
On the nature of cosmic gamma ray bursts N91-15098
GAMMA RAY SPECTROMETERS
Study of spin-temperature effects using energy-ordered continuum gamma ray spectroscopy technique [DE91-002854] N91-14818
GAMMA RAYS
Corrosion behavior of copper-base materials in a gamma-irradiated environment [DE91-001286] N91-14468
Study of spin-temperature effects using energy-ordered continuum gamma ray spectroscopy technique [DE91-002854] N91-14818
Solar flares and particle acceleration N91-15049
GAS ANALYSIS
Apparatus and method for characterizing the transmission efficiency of a mass spectrometer [NASA-CASE-NPO-16989-1-CU] N91-14587
GAS BEARINGS
A vibrating razor blade machining tool for material removal on low-density foams [DE91-002996] N91-14507
GAS DENSITY
Diffuse galactic light observations at 206 selected areas N91-14914
GAS DYNAMICS
Computation of thermochemical nonequilibrium flows around a simple and a double ellipse [NASA-CR-187702] N91-14558
A numerical theory of lattice gas and lattice Boltzmann methods in the computation of solutions to nonlinear advective-diffusive systems [DE91-002566] N91-14560
Structure of accretion flow in close binary system: A two dimensional numerical model N91-15093
GAS EXPANSION
A novel electron tunneling infrared detector N91-14391
GAS FLOW
Computation of thermochemical nonequilibrium flows around a simple and a double ellipse [NASA-CR-187702] N91-14558
New accurate, vectorized approximations of state surfaces for the thermodynamic and transport properties of equilibrium air [MBB/FE122/S/PUB/0389] N91-14886
Structure of accretion flow in close binary system: A two dimensional numerical model N91-15093
GAS JETS
Experimental aerodynamics for hot gas jet reaction control systems N91-14300
GAS LASERS
Statistical errors in the fractal analysis of flame boundaries [DE91-001795] N91-14439
GAS MIXTURES
Numerical study of shock-wave/boundary layer interactions in premixed hydrogen-air hypersonic flows [NASA-TM-103273] N91-14559
Molecular and mass spectroscopic analysis of isotopically labeled organic residues N91-14961
GAS STREAMS
Laboratory studies of refractory metal oxide smokes N91-14993
GAS TRANSPORT
A balloon-borne integrating nephelometer [DE91-001037] N91-14687

GAS TUNGSTEN ARC WELDING
Validation of a computational model for autogenous arc welding
[AD-A227258] N91-14611
GAS TURBINE ENGINES
Combustor technology for future aircraft
[NASA-TM-103268] N91-14349
GASEOUS DIFFUSION
A numerical theory of lattice gas and lattice Boltzmann methods in the computation of solutions to nonlinear advective-diffusive systems
[DE91-002566] N91-14560
GEAR TEETH
Straddle design of spiral bevel and hypoid pinions and gears
[NASA-TM-103621] N91-14602
GEARS
Straddle design of spiral bevel and hypoid pinions and gears
[NASA-TM-103621] N91-14602
GELS
Conversion of alkoxide solutions to oxides: Evaporation of products
[AD-A226927] N91-14442
GENETICS
JPRS Report: Science and technology. USSR: Life sciences
[JPRS-ULS-89-003] N91-14706
GEODESY
Estimability of geodetic parameters from space VLBI observables
[NASA-CR-187413] N91-14636
Plate motions and deformations from geologic and geodetic data
[NASA-CR-187379] N91-14672
GEODYNAMICS
Estimability of geodetic parameters from space VLBI observables
[NASA-CR-187413] N91-14636
Plate motions and deformations from geologic and geodetic data
[NASA-CR-187379] N91-14672
Crustal dynamics project: The interpretation of crustal dynamics data in terms of plate motions and regional deformation near plate boundaries
[NASA-CR-187691] N91-14673
Crustal Dynamics Project data analysis, 1990
[NASA-TM-100765] N91-14679
GEOIDS
Crustal dynamics project: The interpretation of crustal dynamics data in terms of plate motions and regional deformation near plate boundaries
[NASA-CR-187691] N91-14673
GEOLOGICAL FAULTS
Reports on block rotations, fault domains and crustal deformation
[NASA-CR-186756] N91-14665
Block rotations, fault domains and crustal deformation in the western US N91-14666
Distributed deformation and block rotation in 3D N91-14667
Stress field rotation or block rotation: An example from the Lake Mead fault system N91-14668
Multiple strike slip faults sets: A case study from the Dead Sea transform N91-14669
Crustal dynamics project: The interpretation of crustal dynamics data in terms of plate motions and regional deformation near plate boundaries
[NASA-CR-187691] N91-14673
GEOLOGY
Office of Basic Energy Sciences 1990 summary report
[DE91-002971] N91-14653
Feasibility study of the seismic reflection method in Amargosa Desert, Nye County, Nevada
[DE91-001646] N91-14676
Color palette: Plotting guide for use with GSMAP and GSDRAW digital cartographic software
[DE91-001643] N91-14737
GEOMAGNETIC TAIL
Bursts of energetic protons in the Earth's magnetotail N91-15058
Implications of multipoint observations of substorms in the inner magnetotail N91-15061
GEOMAGNETISM
Determination of SPEAR-1 rocket body potential during high-voltage experiments
[AD-A226971] N91-14417
GEOMETRY
Scale-invariant theory of optical properties of fractal clusters
[AD-A227031] N91-14832
GEOPHYSICS
Office of Basic Energy Sciences 1990 summary report
[DE91-002971] N91-14653
A bibliography of planetary geology and geophysics principal investigators and their associates, 1989-1990
[NASA-TM-4221] N91-15034
GEOSTROPHIC WIND
Upwelling southwest of Iceland due to quasi-geostrophic flow
[AD-A227129] N91-14698
GERMANIUM
Intersubband absorption in Si(1-x)Ge(x/Si superlattices for long wavelength infrared detectors N91-14399
Possibilities for LWIR detectors using MBE-grown Si/Si(1-x)Ge(x) structures N91-14400
Novel Si(1-x)Ge(x)/Si heterojunction internal photoemission long wavelength infrared detectors N91-14401
GIANT STARS
Circumstellar grain extinction properties of recently discovered post AGB stars N91-15028
GIBBS FREE ENERGY
New multiphase equation of state for polycrystalline quartz
[DE91-001048] N91-14490
GLASS
Heterocycles based on group 3, 4, and 5 elements: Precursors for novel glasses and ceramics
[AD-A226988] N91-14487
Steps toward interstellar silicate dust mineralogy N91-14991
Infrared spectra of crystalline and glassy silicates and application to interstellar dust N91-14994
GLASS FIBER REINFORCED PLASTICS
Ultrasonic detection of fatigue damage in glass-epoxy composites
[DE91-002652] N91-14619
GLOW DISCHARGES
Wall conditioning and plasma surface interactions in DIII-D
[DE91-001547] N91-14846
GOALS
Advanced technology needs for a global change science program: Perspective of the Langley Research Center
[NASA-TM-4196] N91-14634
GOERTLER INSTABILITY
The effect of wall compliance on the Goertler vortex instability
[NASA-CR-187477] N91-14308
GRAIN BOUNDARIES
Thermal stability of the microstructure of an aged Nb-Zr-C alloy
[NASA-TM-103647] N91-14454
Ion-induced grain growth in multilayer and coevaporated metal alloy thin films
[DE91-004489] N91-14472
Investigations of ultrasonic wave interactions with grain boundaries and grain imperfections
[DE91-002695] N91-14804
Equilibrium composition of interphase boundaries
[DE91-002470] N91-14814
Ground boundaries
[DE91-004027] N91-14880
GRAIN SIZE
The wavelength dependence of polarization in NGC 2023 N91-14923
GRAPH THEORY
Efficient parallel algorithms on the network model
[AD-A227144] N91-14771
GRAPHITE
Electrophoretic and electrolytic deposition of ceramic particles on porous substrates
[AD-A227371] N91-14488
Size distribution of dust grains: A problem of self-similarity N91-14997
GRAPHS (CHARTS)
A software-system visualization tool
[AD-A227145] N91-14757
GRASSES
Comparison of ground and satellite based measurements of the fraction of photosynthetically active radiation intercepted by tall-grass prairie
[NASA-CR-187696] N91-14639
GRASSLANDS
Comparison of ground and satellite based measurements of the fraction of photosynthetically active radiation intercepted by tall-grass prairie
[NASA-CR-187696] N91-14639
GRAVITATION
Galaxy formation by dust N91-14989
GRAVITATIONAL EFFECTS
Determination of SPEAR-1 rocket body potential during high-voltage experiments
[AD-A226971] N91-14417
Dynamics of an unsteady diffusion flame: Effects of heat release and gravity
[AD-A227348] N91-14447
Initial blood storage experiment
[NASA-CR-185513-PT-1] N91-14700
Initial blood storage experiment
[NASA-CR-185513-PT-2] N91-14701
GRAVITATIONAL FIELDS
Electric propulsion study
[AD-A227121] N91-14545
Measurement of the gravitomagnetic field using a pair of laser ranged satellites N91-14670
GRAVITATIONAL WAVE ANTENNAS
Design of a He4 cooling system for a cryostat working at 1K
[IFSI-89-17] N91-14502
GRAVITY WAVES
Observations of ocean fluctuations between 15 and 23 hour periods in the Pacific
[AD-A227017] N91-14695
GRAZING INCIDENCE
An investigation of the diffraction of an acoustic plane wave by a curved surface of finite impedance N91-14800
GREAT BASIN (US)
Stress field rotation or block rotation: An example from the Lake Mead fault system N91-14668
GREEN'S FUNCTIONS
The application of deterministic spectral domain method to the analysis of planar circuit discontinuities on open substrates
[AD-A226901] N91-14542
GREENHOUSE EFFECT
The effects of climate change on the nitrogen cycle and acid deposition
[DE91-002785] N91-14659
Overview of the US Department of Energy's ARM (Atmospheric Radiation Measurement) program
[DE91-001126] N91-14678
GRID GENERATION (MATHEMATICS)
Numerical studies of compressible flow over a double-delta wing at high angles of attack
[AD-A226931] N91-14312
The inclusion of wall loss in electromagnetic finite-difference time-domain thin-slot algorithms
[DE91-001046] N91-14524
GROUND STATE
Surface modification using low energy ground state ion beams
[NASA-CASE-NPO-17498-1-CU] N91-14813
New accurate, vectorized approximations of state surfaces for the thermodynamic and transport properties of equilibrium air
[MBB/FE122/S/PUB/0389] N91-14886
GROUP DYNAMICS
The effects of sleep loss on individual and group performance
[AD-A226963] N91-14708
GUIDANCE (MOTION)
Role of separation autopilots for modern missile concepts
[MBB/FE121/S/PUB/409/A] N91-14352
GULF STREAM
Oceanographic expert system validation using GOAP mesoscale products and Gulf/DART validation test data
[AD-A226929] N91-14693
Shipboard and satellite observations of upper ocean velocity and transport variability in the Gulf Stream
[AD-A226974] N91-14694
The SYNOP experiment: Inverted echo sounder data report for October 1987 to May 1988
[AD-A227232] N91-14699
GUN PROPELLANTS
Analysis of hydroxylammonium nitrate based liquid propellants
[AD-A227300] N91-14497

H

H ALPHA LINE
Survey observations of emission-line stars in the Orion region N91-14955
H I REGIONS
H I and dust in the high latitude dark cloud L1642 N91-14946
Molecules, grains, and shocks: A comparison of CO, H I, and IRAS data N91-14975
Molecules in an infrared cirrus cloud N91-14977
Infrared cirrus point sources N91-14978
H II REGIONS
Reddening and extinction towards H II regions N91-14898
The capability of the ultraviolet imaging telescope for observing interstellar dust N91-14913
Airborne observations of the infrared emission bands N91-14919
A survey for PAH emission in H II regions, planetary and proto-planetary nebulae N91-14920
Infrared emission from ultracompact H II regions N91-14942

Dust in a few southern H II regions N91-14943
Distribution of dust in W31 complex N91-14944
Interferometric molecular line observations of W51 N91-14950
High resolution observations of compact H II regions at 230 GHz N91-14954
An interferometric study of molecular emission around NGC 7538 at millimeter wavelengths N91-15042

HAFNIUM
Study of spin-temperature effects using energy-ordered continuum gamma ray spectroscopy technique [DE91-002854] N91-14818

HAIL
Polarization radar studies of precipitation: Implementation of the technique and data interpretation [AD-A227073] N91-14690

HALL EFFECT
Superconducting current transducer [DE91-004674] N91-14554

HALLEY'S COMET
Scattering by fluffy grains N91-14992
A spectral difference between silicates in Comet Halley and interstellar silicates N91-15002
The nature of cometary dust as determined from infrared observations N91-15003
The 10 micron spectral structure in comets N91-15004
A comparative study of the continuum and emission characteristics of comet dust. 1: Are the silicates in Comet Halley and Kohoutek amorphous or crystalline N91-15005
The 3.4 micron emission in comets N91-15006
The pre- and post-accretion irradiation history of cometary ices N91-15007
Vega-Giotto flyby missions and cometary cosmogony N91-15009
The composition of heavy molecular ions inside the ionopause of Comet Halley N91-15010
Dust of Orionid meteor shower in the Earth atmosphere before and after Halley's Comet N91-15012

HALOS
Grains in galactic haloes N91-14984

HAMILTON-JACOBI EQUATION
Description of nonlinear effects in a relativistic plasma using Hamiltonian formalism N91-15071

HAMILTONIAN FUNCTIONS
Investigations of equilibria, lattices, and chaotic dynamics of 2-D Hamiltonian point vortices [AD-A227364] N91-14570
Description of nonlinear effects in a relativistic plasma using Hamiltonian formalism N91-15071

HARDNESS
A modification of 4330 alloy steel [DE91-001764] N91-14455

HARMONIC GENERATIONS
Millimeter-wave monolithic diode-grid frequency multiplier [NASA-CASE-NPO-17258-1-CU] N91-14551

HARMONICS
Tabulation of data from the tip aerodynamics and acoustics test [NASA-TM-102280] N91-14273

HAZARDS
Hazards and safeguards of high pressure hydraulic fatigue testing [AD-A226767] N91-14509
Snow avalanche hazards and mitigation in the United States [LC-90-62814] N91-14686

HEAD-UP DISPLAYS
Interaction of feel system and flight control system dynamics on lateral flying qualities [NASA-CR-179445] N91-14353

HEARING
Demodulation processes in auditory perception [AD-A226824] N91-14707

HEAT FLUX
Radiation resistance of copper alloys at high exposure levels [DE91-001563] N91-14470

HEAT OF VAPORIZATION
Effect of interline heat flow parameter on contact line heat transfer [AD-A226944] N91-14566

HEAT RESISTANT ALLOYS
Directional solidification of superalloys [NASA-CASE-MFS-28314-1] N91-14462

HEAT SINKS
High temperature refractory member with radiation emissive overcoat [NASA-CASE-NPO-17122-1-CU] N91-14489
Transient analysis of a two-phase hydrogen heat switch [DE91-002314] N91-14506
An investigation of using a phase-change material to improve the heat transfer in a small electronic module for an airborne radar application [DE91-002597] N91-14525
Effect of interline heat flow parameter on contact line heat transfer [AD-A226944] N91-14566

HEAT STORAGE
High-temperature thermal storage systems for advanced solar receivers materials selections [NASA-CR-187750] N91-14647

HEAT TRANSFER
Thermal imaging on missiles in hypersonic flow N91-14303
Transient analysis of a two-phase hydrogen heat switch [DE91-002314] N91-14506
Effect of interline heat flow parameter on contact line heat transfer [AD-A226944] N91-14566
Validation of a computational model for autogenous arc welding [AD-A227258] N91-14611
Effect of laser fluctuations in automated solder joint inspection [AD-A226685] N91-14620
Acoustic transducer apparatus with reduced thermal conduction [NASA-CASE-NPO-17620-1-CU] N91-14808
Coupled transport processes in semipermeable media. Part 1: Analytical solutions of the linearized governing equations [DE91-004138] N91-14887
On the thermal stability of slabs, cylinders, and spheres N91-15057

HEAT TRANSFER COEFFICIENTS
A novel approach to determine the heat transfer coefficient in directional solidification furnaces [NASA-CR-187648] N91-14885

HEAT TREATMENT
Thermomechanical processing and ambient temperature properties of a 6061 aluminum 10 volume percent alumina metal matrix composite [AD-A227004] N91-14433
Outgassing data for selecting spacecraft materials, revision 2 [NASA-RP-1124-REV-2] N91-14437

HEATERS
One- and two-dimensional Stirling machine simulation using experimentally generated flow turbulence models [NASA-CR-185285] N91-14414
Flight Set 360L006 STS-34 field joint protection system, thermal protection system, and systems tunnel components, volume 4 [NASA-CR-184050] N91-14415

HEATING EQUIPMENT
Active control of boundary layer transition and turbulence [NASA-CASE-LAR-13532-1] N91-14562

HEAVY IONS
Nucleus-nucleus collisions at very high energies [DE91-004003] N91-14811
The composition of heavy molecular ions inside the ionopause of Comet Halley N91-15010

HELICAL FLOW
Large-scale vortices in compressible turbulent medium with the magnetic field N91-15095

HELICOPTER DESIGN
Advanced technology landing gear. Volume 2: Test [AD-A227197] N91-14344
Helicopter lidar bathymeter system. Conceptual design [AD-A227057] N91-14348

HELICOPTER PERFORMANCE
Advanced technology landing gear. Volume 1: Design [AD-A227196] N91-14343

HELICOPTERS
Prediction of helicopter simulator sickness [DE90-016530] N91-14710

HELIOSTATS
Solar concentrator development in the US [DE91-001232] N91-14649

HELIUM
He atom surface spectroscopy: Surface lattice dynamics of insulators, metals, and metal overlayers [DE91-001993] N91-14855

HELIUM ISOTOPES
Elucidation of fundamental properties of helium in metals by nuclear magnetic resonance techniques [DE91-002715] N91-14460

HELMET MOUNTED DISPLAYS
Raster graphic helmet-mounted display study [NASA-CR-4331] N91-14347

HETEROCYCLIC COMPOUNDS
Heterocycles based on group 3, 4, and 5 elements: Precursors for novel glasses and ceramics [AD-A226988] N91-14487

HETEROJUNCTION DEVICES
Quantum well laser [AD-A227303] N91-14594

HETEROJUNCTIONS
Innovative Long Wavelength Infrared Detector Workshop Proceedings [NASA-CR-187433] N91-14379
Resonant tunneling IR detectors N91-14395
Low dark current photovoltaic multiquantum well long wavelength infrared detectors N91-14396
New heterojunction LWIR detector options N91-14398
Novel Si(1-x)Ge(x)/Si heterojunction internal photoemission long wavelength infrared detectors N91-14401

HEURISTIC METHODS
Investigations of probabilistic inference [AD-A226882] N91-14795
New results in the theory of dust grain alignment N91-14906

HIERARCHIES
Literature survey on tools [AD-A226933] N91-14770

HIGH ALTITUDE
A balloon-borne aerosol spectrometer for high altitude low aerosol concentration measurements [DE91-002563] N91-14661

HIGH ENERGY ELECTRONS
Fast electron studies in the ZT-40M edge plasma [DE91-002323] N91-14838

HIGH ENERGY INTERACTIONS
Software management issues --- superconducting super collider detectors [DE91-001031] N91-14763
Intermediate energy nuclear physics [DE91-002758] N91-14809
Nucleus-nucleus collisions at very high energies [DE91-004003] N91-14811

HIGH FREQUENCIES
Improved high power/high frequency inductor [NASA-CASE-NPO-17830-1-CU] N91-14539

HIGH PRESSURE
Internal performance of a hybrid axisymmetric/nonaxisymmetric convergent-divergent nozzle [NASA-TM-4230] N91-14275
Hazards and safeguards of high pressure hydraulic fatigue testing [AD-A226767] N91-14509

HIGH RESOLUTION
High Resolution, High Frame Rate Video Technology [NASA-CP-3080] N91-14574
Results of the users' requirements survey N91-14575
Data transmission networks N91-14576
Data compression applied to HHVT N91-14577
High resolution, high frame rate video technology development plan and the near-term system conceptual design N91-14580
High resolution spectroscopy of the 11.3 micron emission band N91-14917
The compact far infrared emission from the young stellar object IRAS 16293-2422 N91-14940

HIGH SPEED
Laminar/turbulent flow transition effects on high-speed missile domes N91-14301

HIGH TEMPERATURE GASES
Experimental aerodynamics for hot gas jet reaction control systems N91-14300
A parametric shell analysis of the shuttle 51-L SRB AFT field joint [NASA-TM-102748] N91-14629
On the origin of extinction in the Coma cluster of galaxies N91-14987

HIGH TEMPERATURE PLASMAS
On the origin of extinction in the Coma cluster of galaxies N91-14987

HIGH TEMPERATURE SUPERCONDUCTORS
Superconducting properties of Tl-Ba-Ca-Cu-O films on silver substrates [DE91-002304] N91-14856
Electromagnetic properties of high Tc superconductors [AD-A227006] N91-14868
Transient x ray irradiation of high transition temperature superconducting material [AD-A227090] N91-14869
An ion-channeling study of irradiation-induced amorphization of YBa2Cu3O(7-x) [DE91-004488] N91-14884

HIGH VOLTAGES
Determination of SPEAR-1 rocket body potential during high-voltage experiments [AD-A226971] N91-14417

HIGHLY MANEUVERABLE AIRCRAFT
Development of an unmanned air research vehicle for supermaneuverability studies
[AD-A227165] N91-14342
HILBERT SPACE
A study of strong stability of distributed systems
[NASA-CR-187421] N91-14766
HIPPOCAMPUS
Cosmos 2044
[NASA-CR-187003] N91-14702
HISTORIES
Chronology: MSFC Space Shuttle program development, assembly, and testing major events (1969 - April, 1981)
[NASA-CR-184013] N91-15120
HOLDERS
Post clamp
[NASA-CASE-LEW-14862-1] N91-14617
HOLES (ELECTRON DEFICIENCIES)
Observation of electron hole, double layer, and turbulent heating in a laboratory plasma N91-15079
HOLES (MECHANICS)
Failure in laminated composite plates containing a hole
[AD-A227307] N91-14435
HOLOGRAPHY
Shot report, Holo-17-Holo-22 Rex-9
[DE91-002575] N91-14583
HOMOGENEOUS TURBULENCE
Effects of turbulence on stationary and nonstationary processes in C-systems
[AD-A227067] N91-14569
HONEYCOMB STRUCTURES
Variation of wall shear stress and Reynolds stress over a flat plate downstream of a boundary layer manipulator
[AD-A226875] N91-14565
HOT PRESSING
Aluminum nitride-silicon carbide whisker composites: Processing, properties, and microstructural stability
[DE91-001907] N91-14425
HOT-FILM ANEMOMETERS
An experimental investigation into the use of hot-film anemometry to measure vortical velocity behind a pitching wing
[AD-A227177] N91-14313
HUBBLE SPACE TELESCOPE
Planning the behavior of dynamical systems
[AD-A227381] N91-14788
HUMAN FACTORS ENGINEERING
Prediction of helicopter simulator sickness
[DE90-016530] N91-14710
Human factors engineering. Part 1: Test procedures
[AD-A226480] N91-14720
Pedagogical strategies for human and computer tutoring
[AD-A226886] N91-14750
HUMAN PERFORMANCE
The effects of sleep loss on individual and group performance
[AD-A226963] N91-14708
Validation of dichotic listening and psychomotor task performance as predictors of primary flight training criteria: Highlighting relevant statistical issues
[AD-A227010] N91-14717
Adaptive human-computer interfaces using expert profiles
[AD-A226906] N91-14721
The evaluation of long range consequences in decision making
[AD-A226949] N91-14888
HYBRID COMPUTERS
Hybrid optical processor
[AD-A227163] N91-14834
HYDRAULIC EQUIPMENT
Hazards and safeguards of high pressure hydraulic fatigue testing
[AD-A226767] N91-14509
HYDROCARBONS
Hydrocarbon group-type analysis of petroleum distillates and residues by high-performance liquid chromatography
[DE91-727527] N91-14451
High resolution spectroscopy of the 11.3 micron emission band N91-14917
HYDRODYNAMICS
Computer studies of the dynamic strength of ceramics
[DE91-002568] N91-14481
HYDROGEN
Effect of hydrogen on the strength and microstructure of selected ceramics
[NASA-TM-103674] N91-14482
Transient analysis of a two-phase hydrogen heat switch
[DE91-002314] N91-14506
Numerical study of shock-wave/boundary layer interactions in premixed hydrogen-air hypersonic flows
[NASA-TM-103273] N91-14559
Infrared images of reflection nebulae and Orion's bar: Fluorescent molecular hydrogen and the 3.3 micron feature N91-14918
Dust clouds in Orion and the interstellar neutral hydrogen distribution N91-14941
Synthesis of H2 in dirty ice mantles by fast ion energy loss: New experimental results increase the relevance of this mechanism N91-14962
Does CO trace H2 at high galactic latitude N91-14973
Molecules, grains, and shocks: A comparison of CO, H I, and IRAS data N91-14975
Laboratory studies of refractory metal oxide smokes N91-14993
HYDROGEN IONS
An intense optically pumped H(-) ion source
[DE91-002949] N91-14827
Characterization of electron cyclotron resonance hydrogen plasmas
[DE91-001250] N91-14844
HYDROGEN PLASMA
Characterization of electron cyclotron resonance hydrogen plasmas
[DE91-001250] N91-14844
HYDROGEN PRODUCTION
Liquid hydrogen polygeneration system and process
[NASA-CASE-KSC-11304-2] N91-14495
HYDROGENATION
Mechanism of hydrodenitrogenation. Part 4: Infrared spectroscopy of acidic molybdena catalysts
[DE91-002496] N91-14440
HYDROGRAPHY
Multispectral imagery support for ocean venture 90
[AD-A227119] N91-14697
HYDROLOGY
Climate and atmospheric modeling studies. Climate applications of Earth and planetary observations. Chemistry of Earth and environment
[NASA-CR-187326] N91-14684
HYDROXYL COMPOUNDS
Analysis of hydroxylammonium nitrate based liquid propellants
[AD-A227300] N91-14497
HYDROXYL RADICALS
Matrix isolation as a tool for studying interstellar chemical reactions N91-14956
HYPERCUBE MULTIPROCESSORS
Method of up-front load balancing for local memory parallel processors
[NASA-CASE-MSC-21348-1] N91-14769
Efficient parallel algorithms on the network model
[AD-A227144] N91-14771
HYPERPLANES
Covers by polars of arrangements
[DE91-001358] N91-14764
HYPERSONIC BOUNDARY LAYER
Comments on hypersonic boundary-layer transition
[AD-A227242] N91-14314
HYPERSONIC FLOW
Thermal imaging on missiles in hypersonic flow N91-14303
Numerical study of shock-wave/boundary layer interactions in premixed hydrogen-air hypersonic flows
[NASA-TM-103273] N91-14559
HYPERSONIC INLETS
Numerical investigations in three-dimensional internal flows
[NASA-CR-187373] N91-14277
HYPERSONIC SPEED
Numerical investigations in three-dimensional internal flows
[NASA-CR-187373] N91-14277
HYPERSONIC VEHICLES
Investigation of combustion in large vortices
[AD-A226791] N91-14441
HYPERSONICS
Missile Aerodynamics
[AGARD-CP-493] N91-14278
Hypersonic aerodynamics: An approximation method for the calculation of real gas effects and wall temperatures
[MBB/FE127/S/PUB/0403] N91-14306
HYSTERESIS
Wind tunnel balance
[NASA-CASE-ARC-11877-1-SB] N91-14357

I

ICE
A model of the acoustic interactions occurring under Arctic ice
[AD-A227128] N91-14806
New insights in the photochemistry of grain mantles: The identification of the 4.62 and 6.87 micron bands N91-14957
Distribution of the 3.1 micron feature in Cepheus A N91-14958
Molecular and mass spectroscopic analysis of isotopically labeled organic residues N91-14961
Synthesis of H2 in dirty ice mantles by fast ion energy loss: New experimental results increase the relevance of this mechanism N91-14962
Diffusion and infrared properties of molecules in ice mantles N91-14963
The evolution of organic mantles on interstellar grains N91-14964
Infrared studies of dust grains in infrared reflection nebulae N91-14970
The pre- and post-accretion irradiation history of cometary ices N91-15007
ICE FORMATION
Results of a sub-scale model rotor icing test
[NASA-TM-103709] N91-14309
Numerical simulation of ice growth on a MS-317 swept wing geometry
[NASA-TM-103705] N91-14310
IGNITION
Definition of experiments to investigate fire suppressants in microgravity
[NASA-CR-185295] N91-14378
ILLUMINATING
The wavelength dependence of polarization in NGC 2023 N91-14923
IMAGE PROCESSING
High Resolution, High Frame Rate Video Technology
[NASA-CP-3080] N91-14574
Advanced technology development for image gathering, coding, and processing N91-14579
High resolution, high frame rate video technology development plan and the near-term system conceptual design N91-14580
The design of optical sensor for the pinhole/occulter facility
[NASA-CR-187694] N91-14825
IMAGES
The AIS: A spectrograph/imager ensemble for space flight
[AD-A227009] N91-14413
Optical encoding of imaging data
[AD-D014617] N91-14821
Far infrared structure of spiral galaxies from the IRAS CPC images N91-14988
IMAGING SPECTROMETERS
HgCdTe for NASA EOS missions and detector uniformity benchmarks N91-14385
Analysis of the boreal forest-tundra ecotone: A test of AVIRIS capabilities in the Eastern Canadian subarctic
[NASA-CR-187335] N91-14655
IMAGING TECHNIQUES
Thermal imaging on missiles in hypersonic flow N91-14303
LWIR HgCdTe: Innovative detectors in an incumbent technology N91-14384
Issues and directions in IR detector readout electronics N91-14387
High Resolution, High Frame Rate Video Technology
[NASA-CP-3080] N91-14574
Data compression applied to HHVT N91-14577
Advanced technology development for image gathering, coding, and processing N91-14579
Optical encoding of imaging data
[AD-D014617] N91-14821
New measurements of the far ultraviolet scattering properties of interstellar dust N91-14909
The capability of the ultraviolet imaging telescope for observing interstellar dust N91-14913
IMIDES
N-(3-ethynylphenyl)maleimide
[NASA-CASE-LAR-14188-2] N91-14419
IMPACT
Method and apparatus for determining time, direction, and composition of impacting space particles
[NASA-CASE-LAR-13392-1-CU] N91-14412
IMPACT LOADS
The interlaminar shear strength of woven carbon, woven glass and woven carbon/glass hybrid laminates under static and impact loading
[OUEL-1831/90] N91-14423
IMPACT TESTS
Low velocity impact analysis with NASTRAN
[NASA-TM-103169] N91-14426
IMPACTORS
Low velocity impact analysis with NASTRAN
[NASA-TM-103169] N91-14426
IMPLOSIONS
LLE (Laboratory for Laser Energetics) review
[DE91-001254] N91-14597
High-energy particle acceleration during the implosion driven by 3-dimensional X-type current loop coalescence in solar flares N91-15048

IMPROVEMENT
Air traffic controller memory enhancement
[DOT/FAA/CT-TN90/38] N91-14713
IN-FLIGHT MONITORING
Development of an unmanned air research vehicle for supermaneuverability studies
[AD-A227165] N91-14342
INCENTIVES
The evaluation of long range consequences in decision making
[AD-A226949] N91-14888
INCOHERENT SCATTER RADAR
Joule heating investigations using the sondrestrom radar and DMSP satellites
[AD-A227425] N91-14677
INCOMPRESSIBLE FLOW
A fast solver for systems of axisymmetric ring vortices
[DE91-002594] N91-14561
Direct numerical simulation of turbulent couette flow, part 2
[AD-A226770] N91-14564
Dynamic stability of a spinning tube conveying a fluid through a symmetrical noncircular cross-section
[DE91-004146] N91-14573
INCOMPRESSIBLE FLUIDS
The effect of wall compliance on the Goertler vortex instability
[NASA-CR-187477] N91-14308
INDEPENDENT VARIABLES
Improved estimation of variance components in mixed models
[AD-A226854] N91-14794
INDEXES (DOCUMENTATION)
Aerospace medicine and biology: A continuing bibliography with indexes (supplement 344)
[NASA-SP-7011(344)] N91-14712
Chronology: MSFC Space Station program, 1982 - present. Major events
[NASA-CR-184014] N91-15119
INDIUM
Resonant tunneling IR detectors N91-14395
LWIR detector research in InAsSb/InAs N91-14406
InAs/Ga(1-x)In(x)Sb superlattices for infrared detector applications N91-14407
AlSb/InAs/AlSb quantum wells N91-14411
INDIUM ARSENIDES
InAs/GaAs and InAs doping superlattices N91-14409
InAsSbBi, a direct band-gap, III-V, LWIR material N91-14410
Pseudomorphic InGaAs materials
[AD-A226895] N91-14864
INDIUM PHOSPHIDES
Quantum well laser
[AD-A227303] N91-14594
Program to study the process parameters of OMVPE and their relationship to the properties of Ga(0.47)In(0.53) as ON InP substrates
[AD-A226618] N91-14851
INDIUM SULFIDES
On the crystal structure of KInS2-I
[AD-A226940] N91-14866
INDUCTORS
Improved high power/high frequency inductor
[NASA-CASE-NPO-17830-1-CU] N91-14539
INDUSTRIAL MANAGEMENT
Strategic utilization of information resources: A contingency approach N91-14891
INDUSTRIES
National software capacity: Near-term study
[AD-A226694] N91-14743
INELASTIC SCATTERING
Intermediate energy nuclear physics
[DE91-002758] N91-14809
INEQUALITIES
Extremal rays of convex cones and complementary inequalities
[ETN-91-98166] N91-14778
INERTIAL CONFINEMENT FUSION
Experimental development, testing and research work in support of the inertial confinement fusion program
[DE91-002771] N91-14841
INFERENCE
Investigations of probabilistic inference
[AD-A226882] N91-14795
INFLATABLE STRUCTURES
Fabrication by filament winding with an elastomeric material
[AD-D014570] N91-14478
INFORMATION
Eye movements and visual information processing
[AD-A226782] N91-14714
INFORMATION DISSEMINATION
The NASA/DOD aerospace knowledge diffusion research project: A research agenda
[NASA-TM-103439] N91-14892
INFORMATION FLOW
The NASA/DOD aerospace knowledge diffusion research project: A research agenda
[NASA-TM-103439] N91-14892
INFORMATION MANAGEMENT
Strategic utilization of information resources: A contingency approach N91-14891
The NASA/DOD aerospace knowledge diffusion research project: A research agenda
[NASA-TM-103439] N91-14892
INFORMATION PROCESSING (BIOLOGY)
Investigating individual differences in general comprehension skill: The role of suppression and enhancement
[AD-A226788] N91-14715
Perception and temporal properties of speech
[AD-A226958] N91-14716
Information extraction from visual displays and the event-related brain potential
[AD-A227063] N91-14722
Investigations of probabilistic inference
[AD-A226882] N91-14795
The object display: Principles and review of experimental findings
[AD-A226883] N91-14796
Interpretation of conditional probabilities in probabilistic interference word problems
[AD-A226907] N91-14797
The object display in decision making and judgment
[AD-A227059] N91-14889
INFORMATION RETRIEVAL
Adaptive human-computer interfaces using expert profiles
[AD-A226906] N91-14721
DEMON: A media object model incorporating natural language descriptions for retrieval support
[AD-A226711] N91-14893
INFORMATION SYSTEMS
Advanced technology needs for a global change science program: Perspective of the Langley Research Center
[NASA-TM-4196] N91-14634
A mediator architecture for abstract data access
[AD-A227362] N91-14730
Information technology and the conduct of research: The user's view. Report of the Panel on Information Technology and the Conduct of Research
[ISBN-0-309-03888-X] N91-14890
Strategic utilization of information resources: A contingency approach N91-14891
INFORMATION THEORY
International Symposium on Information Theory
[AD-A226957] N91-14521
Advanced technology development for image gathering, coding, and processing N91-14579
INFRARED ABSORPTION
Simultaneous infrared and UV-visible absorption spectra of matrix-isolated carbon vapor N91-14915
The effect of ionization on the infrared absorption spectra of PAHs: A preliminary report N91-14937
INFRARED ASTRONOMY
Interstellar Dust: Contributed Papers
[NASA-CP-3036] N91-14897
Spectral structure near the 11.3 micron emission feature N91-14926
The nature of cometary dust as determined from infrared observations N91-15003
Infrared emission from interplanetary dust N91-15013
Using infrared spectral features to probe circumstellar dust shells around cool stars N91-15021
New circumstellar dust component in oxygen rich environments N91-15023
Dust around Mira variables: An analysis of IRAS LRS spectra N91-15026
An interferometric study of molecular emission around NGC 7538 at millimeter wavelengths N91-15042
INFRARED ASTRONOMY SATELLITE
Temperature distribution of dust in luminous IRAS galaxies N91-14982
Does the far-infrared/radio correlation in spiral galaxies extend to the spatial domain N91-14985
On the origin of extinction in the Coma cluster of galaxies N91-14987
Far infrared structure of spiral galaxies from the IRAS CPC images N91-14988
Properties of grains derived from IRAS observations of dust N91-15001
A study of extended zodiacal structures
[NASA-CR-187687] N91-15044
INFRARED CIRRUS (ASTRONOMY)
Small scale variations of abundances of transiently heated grains in molecular clouds N91-14927
Dust emission from high latitude cirrus clouds N91-14930
INFRARED DETECTORS
Innovative Long Wavelength Infrared Detector Workshop Proceedings
[NASA-CR-187433] N91-14379
Sensor requirements for Earth and planetary observations N91-14380
SDIO long wavelength infrared detector requirements N91-14381
LWIR detector requirements for low-background space applications N91-14382
Status of LWIR HgCdTe infrared detector technology N91-14383
Issues and directions in IR detector readout electronics N91-14387
Radiation response issues for infrared detectors N91-14388
A novel electron tunneling infrared detector N91-14391
Quantum Well Infrared Photodetectors (QWIP) N91-14392
Photovoltaic quantum well infrared photodetectors N91-14393
Characteristics of AlGaAs/GaAs multiple quantum well infrared detectors N91-14394
Resonant tunneling IR detectors N91-14395
Low dark current photovoltaic multiquantum well long wavelength infrared detectors N91-14396
Fundamental limits to performance of quantum well infrared detectors N91-14397
New heterojunction LWIR detector options N91-14398
Intersubband absorption in Si(1-x)Ge(x/Si superlattices for long wavelength infrared detectors N91-14399
Possibilities for LWIR detectors using MBE-grown Si(/Si(1-x)Ge(x) structures N91-14400
Novel Si(1-x)Ge(x)/Si heterojunction internal photoemission long wavelength infrared detectors N91-14401
MBE HgCdTe heterostructure detectors N91-14402
Growth and properties of Hg-based quantum well structures and superlattices N91-14403
HgZnTe-based detectors for LWIR NASA applications N91-14404
Small band gap superlattices as intrinsic long wavelength infrared detector materials N91-14405
LWIR detector research in InAsSb/InAs N91-14406
InAs/Ga(1-x)In(x)Sb superlattices for infrared detector applications N91-14407
IR detectors based on n-i-p-i superlattices N91-14408
InAsSbBi, a direct band-gap, III-V, LWIR material N91-14410
Field induced gap infrared detector
[NASA-CASE-NPO-17526-1-CU] N91-14588
Cloud cover statistics
[AD-A226892] N91-14689
INFRARED IMAGERY
Infrared images of reflection nebulae and Orion's bar: Fluorescent molecular hydrogen and the 3.3 micron feature N91-14918
INFRARED INSPECTION
Effect of laser fluctuations in automated solder joint inspection
[AD-A226685] N91-14620
INFRARED INSTRUMENTS
HgCdTe for NASA EOS missions and detector uniformity benchmarks N91-14385
INFRARED LASERS
Effect of laser fluctuations in automated solder joint inspection
[AD-A226685] N91-14620
IR and FIR laser diagnostics for plasma thrusters using a CW CO2 radiation source
[AD-A226816] N91-14843
INFRARED PHOTOMETRY
On the detectability of infrared echo arcs around supernova 1987A N91-15033
INFRARED RADIATION
Sensor requirements for Earth and planetary observations N91-14380
LWIR detector requirements for low-background space applications N91-14382
Status of LWIR HgCdTe infrared detector technology N91-14383
LWIR HgCdTe: Innovative detectors in an incumbent technology N91-14384
Issues and directions in IR detector readout electronics N91-14387
A novel electron tunneling infrared detector N91-14391
IR detectors based on n-i-p-i superlattices N91-14408
InAs/GaAs and InAs doping superlattices N91-14409
Interstellar Dust: Contributed Papers
[NASA-CP-3036] N91-14897

The relationship between IR, optical, and UV extinction N91-14899
Airborne observations of the infrared emission bands N91-14919
The spatial distribution of infrared radiation from visible reflection nebulae N91-14931
IRAS results on outer galaxy star formation N91-14953
Diffusion and infrared properties of molecules in ice mantles N91-14963
Dust in regions of massive star formation N91-14972
Does CO trace H2 at high galactic latitude N91-14973
The origin of the galactic emission in IRAS data N91-14974
Molecules, grains, and shocks: A comparison of CO, H I, and IRAS data N91-14975
Molecules in an infrared cirrus cloud N91-14977
Infrared cirrus point sources N91-14978
Dust in stellar wind bow shocks N91-14979
Studying the spatial distribution of interstellar dust N91-14980
Temperature distribution of dust in luminous IRAS galaxies N91-14982
Does the far-infrared/radio correlation in spiral galaxies extend to the spatial domain N91-14985
On the origin of extinction in the Coma cluster of galaxies N91-14987
Galaxy formation by dust N91-14989
Scattering by fluffy grains N91-14992
The origin of micrograins N91-15000
Properties of grains derived from IRAS observations of dust N91-15001
Infrared emission from interplanetary dust N91-15013
IR emission from circumstellar envelopes of C-rich stars N91-15019

INFRARED REFLECTION
On the detectability of infrared echo arcs around supernova 1987A N91-15033

INFRARED SIGNATURES
Effect of laser fluctuations in automated solder joint inspection
[AD-A226685] N91-14620

INFRARED SOURCES (ASTRONOMY)
Raman properties of various carbonaceous materials and their astrophysical implications N91-14933
Si3N4 emissivity and the unidentified infrared bands N91-14935
PAH in the laboratory and interstellar space N91-14936
The compact far infrared emission from the young stellar object IRAS 16293-2422 N91-14940
Additional red and reddened stars in Cyg OB2 association N91-14948

INFRARED SPECTRA
In-line sensors for electrolytic magnesium cells
[DE91-002561] N91-14438
Small scale variations of abundances of transiently heated grains in molecular clouds N91-14927
Dust emission from high latitude cirrus clouds N91-14930
Influence of temperature on the infrared spectrum of the coronene molecule N91-14932
Raman properties of various carbonaceous materials and their astrophysical implications N91-14933
Infrared fluorescence from PAHs in the laboratory N91-14934
Si3N4 emissivity and the unidentified infrared bands N91-14935
PAH in the laboratory and interstellar space N91-14936
The effect of ionization on the infrared absorption spectra of PAHs: A preliminary report N91-14937
PAHs molecules and heating of the interstellar gas N91-14939
The compact far infrared emission from the young stellar object IRAS 16293-2422 N91-14940
Infrared emission from ultracompact H II regions N91-14942
Distribution of dust in W31 complex N91-14944
The embedded objects in epsilon Cha I cloud N91-14949
New insights in the photochemistry of grain mantles: The identification of the 4.62 and 6.87 micron bands N91-14957
Absorption features in the 3 micron spectra of highly obscured objects N91-14965
Thermal emission from interstellar dust in and near the Pleiades N91-14981
Steps toward interstellar silicate dust mineralogy N91-14991
Laboratory studies of refractory metal oxide smokes N91-14993
Infrared spectra of crystalline and glassy silicates and application to interstellar dust N91-14994
Optical properties of irregular interstellar grains N91-14995
The nature of cometary dust as determined from infrared observations N91-15003
The 10 micron spectral structure in comets N91-15004
Infrared emission from interplanetary dust N91-15013
Using infrared spectral features to probe circumstellar dust shells around cool stars N91-15021
Type of silicate feature in oxygen rich stellar envelopes N91-15024
Dust around Mira variables: An analysis of IRAS LRS spectra N91-15026
Polarization due to dust scattering in the planetary nebula Cn1-1 N91-15027
Circumstellar grain extinction properties of recently discovered post AGB stars N91-15028
Continuous infrared emission of proto- and young-planetary nebulae N91-15030
Infrared emission from the supernova remnant Puppis A: Dust and gas parameters N91-15032
A proposed astronomical reference catalog of infrared sources
[AD-A226757] N91-15041

INFRARED SPECTROMETERS
Analysis of the boreal forest-tundra ecotone: A test of AVIRIS capabilities in the Eastern Canadian subarctic
[NASA-CR-187335] N91-14655

INFRARED SPECTROPHOTOMETERS
FTIR (Fourier Transform Infrared) spectrophotometry for thin film monitors: Computer and equipment integration for enhanced capabilities
[DE91-001228] N91-14853

INFRARED SPECTROSCOPY
Mechanism of hydrodenitrogenation. Part 4: Infrared spectroscopy of acidic molybdena catalysts
[DE91-002496] N91-14440
Distribution of the 3.1 micron feature in Cepheus A N91-14958
Absorption features in the 3 micron spectra of highly obscured objects N91-14965

INHOMOGENEITY
Nonlinear surface MHD waves in the inhomogeneous plasma with cusp-resonance in upper solar atmosphere N91-15052
Nonlinear magnetosonic waves in an inhomogeneous plasma N91-15110

INJECTORS
Fueling of magnetically confined plasmas by single- and two-stage repeating pneumatic pellet injectors
[DE91-002635] N91-14839

INPUT/OUTPUT ROUTINES
An analysis of input/output paradigms for real-time systems
[AD-A226724] N91-14748

INSOLATION
The synthesis of solar radiation data for sizing stand-alone photovoltaic systems
[DE90-012758] N91-14652
Solar radiation on Mars: Update 1990
[NASA-TM-103623] N91-15117

INSULATION
Magnetic properties of doped semiconductors
[DE91-002395] N91-14859

INSULATORS
Process for lowering the dielectric constant of polyimides using diamic acid additives
[NASA-CASE-LAR-13902-1] N91-14484

INTEGRATED CIRCUITS
MMIC compensation network for phased array element mismatch
[AD-A227437] N91-14522
Universal nondestructive mm-wave integrated circuit test fixture
[NASA-CASE-LEW-14746-1] N91-14552
The use of light emission in failure analysis of CMOS ICs
[DE91-001234] N91-14633

INTEGRATED OPTICS
Integrated optical devices for photonics instrumentation systems
[DE91-004192] N91-14828

INTERFACES
Interfacial push-out measurements of fully-bonded SiC/SC composites
[DE91-004527] N91-14436
Investigations of ultrasonic wave interactions with grain boundaries and grain imperfections
[DE91-002695] N91-14804
Investigation of redox processes at semiconductor electrode liquid junctions
[DE91-001787] N91-14858

INTERFACIAL TENSION
Effect of interline heat flow parameter on contact line heat transfer
[AD-A226944] N91-14566

INTERFEROMETRY
Method for detecting surface motions and mapping small terrestrial or planetary surface deformations with synthetic aperture radar
[NASA-CASE-NPO-17831-1-CU] N91-14642
Interferometric molecular line observations of W51 N91-14950
An interferometric study of molecular emission around NGC 7538 at millimeter wavelengths N91-15042

INTERGALACTIC MEDIA
On the origin of extinction in the Coma cluster of galaxies N91-14987

INTERPLANETARY DUST
A spectral difference between silicates in Comet Halley and interstellar silicates N91-15002
The nature of cometary dust as determined from infrared observations N91-15003
The 10 micron spectral structure in comets N91-15004
Vega-Giotto flyby missions and cometary cosmogony N91-15009
The composition of heavy molecular ions inside the ionopause of Comet Halley N91-15010
Dust of Orionid meteor shower in the Earth atmosphere before and after Halley's Comet N91-15012
Infrared emission from interplanetary dust N91-15013

INTERPROCESSOR COMMUNICATION
Experiences porting the distributed Ada real-time kernel
[AD-A226693] N91-14742

INTERSTELLAR CHEMISTRY
Matrix isolation as a tool for studying interstellar chemical reactions N91-14956
Grain growth, optical polarisation, and extinction in interstellar clouds N91-14959
Molecular and mass spectroscopic analysis of isotopically labeled organic residues N91-14961
Production and transfer of UV photons in non-homogeneous spherical clouds N91-14966
Gas-phase formation of silicon carbides, oxides, and sulphides from atomic silicon ions N91-15014
PAH formation in carbon-rich circumstellar envelopes N91-15015

INTERSTELLAR EXTINCTION
Interstellar Dust: Contributed Papers
[NASA-CP-3036] N91-14897
The detection of a broad interstellar extinction feature near 1700 A N91-14900
Properties of interstellar dust in the region of the CEP OB4 association N91-14903
Three-micron spectroscopy of highly reddened field stars N91-14904
IR emission and UV extinction in two open clusters N91-14929
Additional red and reddened stars in Cyg OB2 association N91-14948
Grain growth, optical polarisation, and extinction in interstellar clouds N91-14959
Grain mantles: The impact on grain evolution and selective extinction N91-14960
Multicolor optical polarimetry of reddened stars in the small Magellanic cloud N91-14986
Size distribution of dust grains: A problem of self-similarity N91-14997
Interstellar extinction at 10-20 microns N91-15025
Circumstellar grain extinction properties of recently discovered post AGB stars N91-15028

INTERSTELLAR GAS
PAHs molecules and heating of the interstellar gas N91-14939
Dust clouds in Orion and the interstellar neutral hydrogen distribution N91-14941
H I and dust in the high latitude dark cloud L1642 N91-14946
Production and transfer of UV photons in non-homogeneous spherical clouds N91-14966
Dust in regions of massive star formation N91-14972
Does CO trace H2 at high galactic latitude N91-14973
The origin of the galactic emission in IRAS data N91-14974
Molecules, grains, and shocks: A comparison of CO, H I, and IRAS data N91-14975
A rocket-borne measurement of interstellar dust emission at high galactic latitude N91-14976
The origin of micrograins N91-15000
Dust formation around M-type stars N91-15017
Continuous infrared emission of proto- and young-planetary nebulae N91-15030
Infrared emission from the supernova remnant Puppis A: Dust and gas parameters N91-15032

INTERSTELLAR MATTER
Interstellar Dust: Contributed Papers [NASA-CP-3036] N91-14897
The autocorrelation function of the North Pole dust N91-14901
Properties of interstellar dust in the region of the CEP OB4 association N91-14903
Three-micron spectroscopy of highly reddened field stars N91-14904
Interstellar circular polarization and the dielectric nature of dust grains N91-14905
New measurements of the far ultraviolet scattering properties of interstellar dust N91-14909
Interstellar dust as generator of x ray radiation N91-14910
The capability of the ultraviolet imaging telescope for observing interstellar dust N91-14913
Diffuse galactic light observations at 206 selected areas N91-14914
Simultaneous infrared and UV-visible absorption spectra of matrix-isolated carbon vapor N91-14915
Correlation properties of interstellar dust: Diffuse interstellar bands N91-14916
A survey for PAH emission in H II regions, planetary and proto-planetary nebulae N91-14920
PAH emission from Nova Cen 1986 N91-14921
Red fluorescence and 3-12 micron emission in NGC 2023, HD 44179, M 82, and Lynds 1780 N91-14924
High-spectral resolution observations of the 3.29 micron emission feature: Comparison to QCC and PAHs N91-14925
Spectral structure near the 11.3 micron emission feature N91-14926
IR emission and UV extinction in two open clusters N91-14929
Dust emission from high latitude cirrus clouds N91-14930
The spatial distribution of infrared radiation from visible reflection nebulae N91-14931
Influence of temperature on the infrared spectrum of the coronene molecule N91-14932
Infrared fluorescence from PAHs in the laboratory N91-14934
PAH in the laboratory and interstellar space N91-14936
The effect of ionization on the infrared absorption spectra of PAHs: A preliminary report N91-14937
Angular motion of a PAH molecule in interstellar environment N91-14938
Survey observations of emission-line stars in the Orion region N91-14955
New insights in the photochemistry of grain mantles: The identification of the 4.62 and 6.87 micron bands N91-14957
Distribution of the 3.1 micron feature in Cepheus A N91-14958
Grain growth, optical polarisation, and extinction in interstellar clouds N91-14959
Grain mantles: The impact on grain evolution and selective extinction N91-14960
Molecular and mass spectroscopic analysis of isotopically labeled organic residues N91-14961
The evolution of organic mantles on interstellar grains N91-14964
Grains charges in interstellar clouds N91-14967
Dust coagulation in ISM N91-14968
Infrared studies of dust grains in infrared reflection nebulae N91-14970
Laboratory investigation of electric charging of dust particles by electrons, ions, and UV radiation N91-14971
Infrared cirrus point sources N91-14978
Thermal emission from interstellar dust in and near the Pleiades N91-14981
Galaxy formation by dust N91-14989
VUV-visible measurements on different samples of amorphous carbon N91-14990
Steps toward interstellar silicate dust mineralogy N91-14991
Infrared spectra of crystalline and glassy silicates and application to interstellar dust N91-14994
Optical properties of irregular interstellar grains N91-14995
Observational constraints on interstellar dust models N91-14996
Size distribution of dust grains: A problem of self-similarity N91-14997
Stochastic histories of dust grains in the interstellar medium N91-14998
Superaromatics: The key to a unified cosmic dust theory N91-14999
The origin of micrograins N91-15000
Properties of grains derived from IRAS observations of dust N91-15001
The 3.4 micron emission in comets N91-15006
Experimental evidence for amorphous carbon grains in comets N91-15008
Infrared emission from interplanetary dust N91-15013
PAH formation in carbon-rich circumstellar envelopes N91-15015
Sublimating comets as the source of nucleation seeds for grain condensation in the gas outflow from AGB stars N91-15018
Interstellar extinction at 10-20 microns N91-15025
Polarization due to dust scattering in the planetary nebula Cn1-1 N91-15027
Continuous infrared emission of proto- and young-planetary nebulae N91-15030
On the primary cosmic ray nuclei spectra behaviour in the 10(exp 16) eV energy region N91-15069
Matter penetration and motion through the magnetosphere of neutron star N91-15087
INTERSTELLAR RADIATION
The origin of the galactic emission in IRAS data N91-14974
A rocket-borne measurement of interstellar dust emission at high galactic latitude N91-14976
Molecules in an infrared cirrus cloud N91-14977
Studying the spatial distribution of interstellar dust N91-14980
Does the far-infrared/radio correlation in spiral galaxies extend to the spatial domain N91-14985
INTERSTELLAR SPACE
PAH in the laboratory and interstellar space N91-14936
INTERVALS
On probability intervals and their updating [RUU-CS-90-22] N91-14793
INVARIANCE
Scale-invariant theory of optical properties of fractal clusters [AD-A227031] N91-14832
INVENTORIES
Modified seasonal factors in exponential smoothing [DE91-002802] N91-14688
INVENTORY MANAGEMENT
Modified seasonal factors in exponential smoothing [DE91-002802] N91-14688
INVISCID FLOW
The inviscid stability of supersonic flow past heated or cooled axisymmetric bodies [NASA-CR-187475] N91-14307
ION ACCELERATORS
Design and application possibilities of superconducting radio-frequency quadrupoles [DE91-004477] N91-14881
Experimental results in superconducting niobium resonators for high-brightness ion beam acceleration [DE91-004478] N91-14882
ION BEAMS
Development of laser-ion beam photodissociation methods [DE91-000680] N91-14448
Ion-induced grain growth in multilayer and coevaporated metal alloy thin films [DE91-004489] N91-14472
Surface modification using low energy ground state ion beams [NASA-CASE-NPO-17498-1-CU] N91-14813
Ion beam induced diffusion and crystallization in high dose Er implanted Si [DE91-002869] N91-14860
Design and application possibilities of superconducting radio-frequency quadrupoles [DE91-004477] N91-14881
Experimental results in superconducting niobium resonators for high-brightness ion beam acceleration [DE91-004478] N91-14882
Laboratory investigation of electric charging of dust particles by electrons, ions, and UV radiation N91-14971
ION CURRENTS
Conductivity fluctuations in fast ionic conductors [AD-A227379] N91-14549
ION CYCLOTRON RADIATION
Evolution of high amplitude Alfven waves near a bow shock N91-15068
ION DISTRIBUTION
Plasma waves associated with the space shuttle N91-15064
Nonstationary processes in the front of high Mach number collisionless quasiperpendicular shock: Dynamics of the ion distribution N91-15067
ION IMPLANTATION
Ion implantation for corrosion inhibition of aluminum alloys in saline media [DE91-002887] N91-14461
Amorphization of C-implanted Fe(Cr) alloys [DE91-001338] N91-14469
Ion beam induced diffusion and crystallization in high dose Er implanted Si [DE91-002869] N91-14860
An ion-channeling study of irradiation-induced amorphization of YBa2Cu3O(7-x) [DE91-004488] N91-14884
ION IRRADIATION
Irradiation-induced pinning in single-crystal and thin-film Tl2Ca2Ba2Cu3O10 superconductors [DE91-001342] N91-14877
ION MOTION
Studies of the chemistry of the nightside ionosphere of Venus [NASA-CR-187714] N91-15114
ION SOURCES
The vertical Van de Graaff telemetry system [DE91-001960] N91-14370
Surface modification using low energy ground state ion beams [NASA-CASE-NPO-17498-1-CU] N91-14813
An intense optically pumped H(-) ion source [DE91-002949] N91-14827
Characteristics and potential applications of an ORNL microwave ECR multicusp plasma ion source [DE91-002649] N91-14840
IONIC COLLISIONS
Nucleus-nucleus collisions at very high energies [DE91-004003] N91-14811
IONIC CRYSTALS
Conductivity fluctuations in fast ionic conductors [AD-A227379] N91-14549
IONIC DIFFUSION
Ion beam induced diffusion and crystallization in high dose Er implanted Si [DE91-002869] N91-14860
IONIZATION
Radiation response issues for infrared detectors N91-14388
Experimental development, testing and research work in support of the inertial confinement fusion program [DE91-002771] N91-14841
The effect of ionization on the infrared absorption spectra of PAHs: A preliminary report N91-14937
IONIZATION CROSS SECTIONS
PAHs molecules and heating of the interstellar gas N91-14939
IONOPAUSE
The composition of heavy molecular ions inside the ionopause of Comet Halley N91-15010
IONOSPHERIC CONDUCTIVITY
Joule heating investigations using the sondrestrom radar and DMSP satellites [AD-A227425] N91-14677
IONOSPHERIC ELECTRON DENSITY
Theory and measurements of nighttime horizontal gradients in the mid-latitude F region N91-14671
IONOSPHERIC HEATING
Joule heating investigations using the sondrestrom radar and DMSP satellites [AD-A227425] N91-14677
IONOSPHERIC ION DENSITY
Studies of the chemistry of the nightside ionosphere of Venus [NASA-CR-187714] N91-15114
IONS
Kinetics of molecular beam epitaxy: Effect of ion-induced sputtering [DE91-004511] N91-14493
IRISES (MECHANICAL APERTURES)
HEM(sub 11) modes revisited [DE91-001028] N91-14819
IRON ALLOYS
Amorphization of C-implanted Fe(Cr) alloys [DE91-001338] N91-14469
IRON METEORITES
Atomic environments in iron meteorites using EXAFS N91-15011
IRRADIATION
Corrosion behavior of copper-base materials in a gamma-irradiated environment [DE91-001286] N91-14468
Radiation resistance of copper alloys at high exposure levels [DE91-001563] N91-14470
Photogenerated carrier-induced reaction on semiconductor surfaces [DE91-001349] N91-14878
The evolution of organic mantles on interstellar grains N91-14964
The pre- and post-accretion irradiation history of cometary ices N91-15007
IRREVERSIBLE PROCESSES
Irreversibility temperatures in oxide- and metallic superconductors [DE91-004021] N91-14861

Coupled transport processes in semipermeable media. Part 1: Analytical solutions of the linearized governing equations
[DE91-004138] N91-14887

ISOPHOTES
Far infrared structure of spiral galaxies from the IRAS CPC images N91-14988

ISOTOPE EFFECT
DIII-D results and plans
[DE91-001548] N91-14847

ITERATION
A combined finite element-boundary element formulation for solution of axially symmetric bodies
[NASA-CR-185852] N91-14789

J

JET CONTROL
Experimental aerodynamics for hot gas jet reaction control systems N91-14300

JET EXHAUST
Internal performance of a hybrid axisymmetric/nonaxisymmetric convergent-divergent nozzle
[NASA-TM-4230] N91-14275

JET FLOW
Opposed jet turbulent diffusion flames
[AD-A227048] N91-14446

JFET
Development and testing of radiation and electromagnetic pulse hardened silicon carbide based electronics
[AD-A227309] N91-14548

JOINED WINGS
Structural development of laminar flow control aircraft chordwise wing joint designs
[NASA-CR-181888] N91-14346

JOINTS (JUNCTIONS)
Structural development of laminar flow control aircraft chordwise wing joint designs
[NASA-CR-181888] N91-14346
Joining alumina to sapphire for copper vapor laser tubes
[AD-A226619] N91-14501
Mechanical end joint system for connecting structural column elements
[NASA-CASE-LAR-14465-1] N91-14614
Multi-fingered robotic hand
[NASA-CASE-NPO-15959-2] N91-14616
Axisymmetric shell analysis of the space shuttle solid rocket booster field joint
[NASA-TP-3033] N91-14618
A parametric shell analysis of the shuttle 51-L SRB AFT field joint
[NASA-TM-102748] N91-14629

JUDGMENTS
The object display in decision making and judgment
[AD-A227059] N91-14889

JUNCTION DIODES
Development and testing of radiation and electromagnetic pulse hardened silicon carbide based electronics
[AD-A227309] N91-14548

K

KELVIN-HELMHOLTZ INSTABILITY
Energy dissipation of shear Alfven waves in extended cosmic jets N91-15086

KERNEL FUNCTIONS
Experiences porting the distributed Ada real-time kernel
[AD-A226693] N91-14742

KINEMATICS
Surface settling in partially filled containers upon step reduction in gravity
[NASA-TM-103641] N91-14556
Intelligent manipulation technique for multi-branch robotic systems
[NASA-CR-187651] N91-14603
Sensor based control of robotic mechanisms
[AD-A226784] N91-14776
Nucleus-nucleus collisions at very high energies
[DE91-004003] N91-14811

KINETICS
Kinetics of molecular beam epitaxy: Effect of ion-induced sputtering
[DE91-004511] N91-14493

KLYSTRONS
High gradient electron guns
[DE91-000056] N91-14369

KNOWLEDGE BASES (ARTIFICIAL INTELLIGENCE)
A mediator architecture for abstract data access
[AD-A227362] N91-14730

KNOWLEDGE REPRESENTATION
Discrete event simulation tool for analysis of qualitative models of continuous processing systems
[NASA-CASE-MSC-21465-1] N91-14741

KOHOUTEK COMET
The 10 micron spectral structure in comets N91-15004
A comparative study of the continuum and emission characteristics of comet dust. 1: Are the silicates in Comet Halley and Kohoutek amorphous or crystalline N91-15005

L

LABOR
National software capacity: Near-term study
[AD-A226694] N91-14743

LAMINAR BOUNDARY LAYER
Structural development of laminar flow control aircraft chordwise wing joint designs
[NASA-CR-181888] N91-14346

LAMINAR FLOW
Laminar/turbulent flow transition effects on high-speed missile domes N91-14301
Structural development of laminar flow control aircraft chordwise wing joint designs
[NASA-CR-181888] N91-14346
One- and two-dimensional Stirling machine simulation using experimentally generated flow turbulence models
[NASA-CR-185285] N91-14414

LAMINATES
The interlaminar shear strength of woven carbon, woven glass and woven carbon/glass hybrid laminates under static and impact loading
[OUEL-1831/90] N91-14423
An analysis of interlaminar stresses in unsymmetrically laminated plates
[NASA-CR-187657] N91-14424
Failure in laminated composite plates containing a hole
[AD-A227307] N91-14435

LAND MOBILE SATELLITE SERVICE
Trellis coded modulation for transmission over fading mobile satellite channel
[NASA-CASE-NPO-16904-2-CU] N91-14523

LAND USE
The response of atmospheric CO2 to changes in land use
[DE91-001212] N91-14663

LANDAU DAMPING
Linear resonant interaction of an electromagnetic wave with a collisional inhomogeneous plasma
[IPPCZ-298] N91-14836

LANDING GEAR
Advanced technology landing gear. Volume 1: Design
[AD-A227196] N91-14343
Advanced technology landing gear. Volume 2: Test
[AD-A227197] N91-14344

LANDING LOADS
Advanced technology landing gear. Volume 1: Design
[AD-A227196] N91-14343

LANDING SITES
A polar orbit for the Mars Global Network Mission N91-14361

LANTHANUM
Surface treatment of metals
[EP-PATENT-0-367-504-A2] N91-14453

LARGE SPACE STRUCTURES
Multivariable methods for the design, identification, and control of large space structures. Volume 2: Optimal and sub-optimal estimation applied to large flexible structures
[AD-A226699] N91-14375
Adaptive control of large space structures
[AD-A227304] N91-14377
Methods for evaluating the predictive accuracy of structural dynamic models
[NASA-CR-187649] N91-14630

LASER APPLICATIONS
Raster graphic helmet-mounted display study
[NASA-CR-4331] N91-14347
Electrostatically suspended rotor for angular encoder
[NASA-CASE-MFS-28294-1] N91-14508

LASER BEAMS
Optical phase conjugation via stimulated Brillouin scattering in multimode optical fiber
[AD-A227054] N91-14833

LASER CAVITIES
Nonlinear dynamics of broad-band lasers
[DE91-001143] N91-14596

LASER DAMAGE
Study of diamond film growth and properties
[NASA-CR-187709] N91-14483

LASER FUSION
LLE (Laboratory for Laser Energetics) review
[DE91-001254] N91-14597

LASER INDUCED FLUORESCENCE
Laser studies of the interaction of SiO with the surface of a thin film
[DE91-004562] N91-14450
Infrared fluorescence from PAHs in the laboratory N91-14934

LASER MODE LOCKING
Picosecond laser system for high speed characterization of monolithic devices
[AD-A227372] N91-14595

LASER OUTPUTS
Recent long-pulse and high-average-power tests on a 140 GHz gyrotron
[DE91-001680] N91-14592
Effect of laser fluctuations in automated solder joint inspection
[AD-A226685] N91-14620

LASER PLASMA INTERACTIONS
Experimental development, testing and research work in support of the inertial confinement fusion program
[DE91-002771] N91-14841

LASER PLASMAS
LLE (Laboratory for Laser Energetics) review
[DE91-001254] N91-14597
IR and FIR laser diagnostics for plasma thrusters using a CW CO2 radiation source
[AD-A226816] N91-14843
Laboratory simulation of the astrophysical burst processes in non-uniform magnetised media N91-15081

LASER PUMPING
Picosecond laser system for high speed characterization of monolithic devices
[AD-A227372] N91-14595

LASER RANGE FINDERS
Measurement of the gravitomagnetic field using a pair of laser ranged satellites N91-14670

LASER TARGETS
Experimental development, testing and research work in support of the inertial confinement fusion program
[DE91-002771] N91-14841

LASERS
Development of laser-ion beam photodissociation methods
[DE91-000680] N91-14448
LLE (Laboratory for Laser Energetics) review
[DE91-001254] N91-14597
Measurement of the gravitomagnetic field using a pair of laser ranged satellites N91-14670
JPRS Report: Science and technology. USSR: Life sciences
[JPRS-ULS-89-003] N91-14706
Experimental development, testing and research work in support of the inertial confinement fusion program
[DE91-002771] N91-14841

LATERAL CONTROL
Interaction of feel system and flight control system dynamics on lateral flying qualities
[NASA-CR-179445] N91-14353

LATTICE PARAMETERS
Thermal stability of the microstructure of an aged Nb-Zr-C alloy
[NASA-TM-103647] N91-14454
Simulation of transient glide of a threading dislocation in an embedded strained expitaxial layer
[AD-A226965] N91-14867

LATTICE VIBRATIONS
A LEED study of the MgO(001) surface structure
[DE91-002811] N91-14879

LATTICES
Investigations of equilibria, lattices, and chaotic dynamics of 2-D Hamiltonian point vortices
[AD-A227364] N91-14570

LATTICES (MATHEMATICS)
A numerical theory of lattice gas and lattice Boltzmann methods in the computation of solutions to nonlinear advective-diffusive systems
[DE91-002566] N91-14560

LAUNCHING
Analysis of success probability/cost trades for small landers in a Mars network N91-14363

LEAST SQUARES METHOD
FTIR (Fourier Transform Infrared) spectrophotometry for thin film monitors: Computer and equipment integration for enhanced capabilities
[DE91-001228] N91-14853
The relationship between IR, optical, and UV extinction N91-14899

LENSES
A simple plane-wave explosive lens
[DE91-004297] N91-14526

LEUKOCYTES
Initial blood storage experiment
[NASA-CR-185513-PT-2] N91-14701

LIAPUNOV FUNCTIONS
A study of strong stability of distributed systems
[NASA-CR-187421] N91-14766
LIFE (DURABILITY)
Reliability of photovoltaic concentrator modules
[DE90-012754] N91-14651
LIFE SCIENCES
JPRS Report: Science and technology. USSR: Life sciences
[JPRS-ULS-89-003] N91-14706
LIFE SUPPORT SYSTEMS
Aerospace medicine and biology: A continuing bibliography with indexes (supplement 343)
[NASA-SP-7011(343)] N91-14711
LIFT
An experimental investigation into the use of hot-film anemometry to measure vortical velocity behind a pitching wing
[AD-A227177] N91-14313
LIFT DRAG RATIO
Application of Euler and Navier-Stokes codes to missile type bodies with high L/D ratios N91-14286
Navier-Stokes predictions of static and dynamic aerodynamic derivatives for high L/D finned projectiles N91-14295
LIGHT ALLOYS
NASA-UVA light aerospace alloy and structures technology program
[NASA-CR-187321] N91-14474
LIGHT AMPLIFIERS
Tapered fiber amplifier
[AD-D014629] N91-14512
Optoelectronic devices
[AD-D014618] N91-14822
LIGHT BEAMS
Optical phase conjugate beam modulator and method therefor
[AD-D014569] N91-14820
LIGHT CURVE
On the detectability of infrared echo arcs around supernova 1987A N91-15033
Thirty-five-day cycle of Her X-1: Synthesised optical light curves in the model of freely processing neutron star N91-15089
LIGHT EMISSION
The AIS: A spectrograph/imager ensemble for space flight
[AD-A227009] N91-14413
The use of light emission in failure analysis of CMOS ICs
[DE91-001234] N91-14633
The 100 and 160 micron maps of the dust reemission from the nucleus and inner-arm regions of NGC 6946 N91-14983
LIGHT EMITTING DIODES
Field induced gap infrared detector
[NASA-CASE-NPO-17526-1-CU] N91-14588
Integrated optical devices for photonics instrumentation systems
[DE91-004192] N91-14828
LIGHT MODULATION
Optical phase conjugate beam modulator and method therefor
[AD-D014569] N91-14820
Hybrid optical processor
[AD-A227163] N91-14834
LIGHT SCATTERING
Scattering by anisotropic grains in beryllium mirrors
[DE91-001724] N91-14826
LIGHT SOURCES
Solid state radioluminescent sources using zeolites
[DE91-002703] N91-14857
LIGHT TRANSMISSION
Vibrational testing of optical fiber connector joints
[NASA-TM-103654] N91-14829
Spontaneous and induced coherent radiation generation in atomic vapors
[AD-A226776] N91-14830
LIGHTNING
Aircraft measurements of electrified clouds at Kennedy Space Center
[NASA-CR-186536] N91-14680
Aircraft measurements of electrified clouds at Kennedy Space Center. Part 1: 1988 flights N91-14681
Aircraft measurements of electrified clouds at Kennedy Space Center. Part 2: Case study: 4 November 1988 (88309) N91-14682
LIMB DARKENING
Limb-darkening functions as derived from along-track operation of the ERBE scanning radiometers for August 1985
[NASA-RP-1243] N91-14683
LINE SPECTRA
High-spectral resolution observations of the 3.29 micron emission feature: Comparison to QCC and PAHs N91-14925
Raman properties of various carbonaceous materials and their astrophysical implications N91-14933
H I and dust in the high latitude dark cloud L1642 N91-14946
Interferometric molecular line observations of W51 N91-14950
LINEAR ACCELERATORS
High gradient electron guns
[DE91-000056] N91-14369
A beam position monitor for low current dc beams
[CEBAF-PR-89-004] N91-14816
HEM(sub 11) modes revisited
[DE91-001028] N91-14819
LINEAR ARRAYS
The design of optical sensor for the pinhole/occulter facility
[NASA-CR-187694] N91-14825
LINEAR EQUATIONS
Experimental investigation and semi-empirical prediction of the dynamic response of a low-aspect-ratio trapezoidal wing due to flow separation N91-14330
Control of distributed parameter systems
[AD-A227306] N91-14787
LINEAR POLARIZATION
Alignment mechanisms of paramagnetic grains revisited N91-14908
On the polarization mechanism in the R Mon/NGC 2261 complex N91-14969
LINEAR PROGRAMMING
Covers by polars of arrangements
[DE91-001358] N91-14764
LINEAR QUADRATIC REGULATOR
Multivariable methods for the design, identification, and control of large space structures. Volume 2: Optimal and sub-optimal estimation applied to large flexible structures
[AD-A226699] N91-14375
Randomly sampled-data control systems
[NASA-CR-187425] N91-14734
LINEAR SYSTEMS
A study of strong stability of distributed systems
[NASA-CR-187421] N91-14766
Approximately integrable linear statistical models in non-parametric estimation
[AD-A227395] N91-14798
LINEARITY
Improved estimation of variance components in mixed models
[AD-A226854] N91-14794
Linear stability and MHD wave propagation in plasmas with solar abundances N91-15056
LINKAGES
Position requirements for space station personnel and linkages to portable microcomputer performance assessment
[NASA-CR-185606] N91-14719
LIQUID BEARINGS
Turbomachinery rotor support with damping
[NASA-CASE-MFS-28345-1] N91-14608
LIQUID CHROMATOGRAPHY
Hydrocarbon group-type analysis of petroleum distillates and residues by high-performance liquid chromatography
[DE91-727527] N91-14451
LIQUID HELIUM
Design of a He4 cooling system for a cryostat working at 1K
[IFSI-89-17] N91-14502
LIQUID HYDROGEN
Liquid hydrogen polygeneration system and process
[NASA-CASE-KSC-11304-2] N91-14495
LIQUID METALS
Organic cathode for a secondary battery
[NASA-CASE-NPO-17604-1-CU] N91-14536
LIQUID PHASE EPITAXY
HgCdTe for NASA EOS missions and detector uniformity benchmarks N91-14385
LIQUID ROCKET PROPELLANTS
The effects of liquid propellant motion on the attitude stability of spin stabilized spacecraft
[AD-A227002] N91-14376
CFD code evaluation for internal flow modeling
[NASA-CR-187677] N91-14557
LIQUID SURFACES
Surface settling in partially filled containers upon step reduction in gravity
[NASA-TM-103641] N91-14556
LIQUID-SOLID INTERFACES
Effect of interline heat flow parameter on contact line heat transfer
[AD-A226944] N91-14566
LIQUIDS
Investigation of redox processes at semiconductor electrode liquid junctions
[DE91-001787] N91-14858
LISP (PROGRAMMING LANGUAGE)
Pedagogical strategies for human and computer tutoring
[AD-A226886] N91-14750
LITHIUM ALLOYS
An examination of delta prime growth in an aluminum-lithium alloy by x ray diffraction
[AD-A227254] N91-14464
Processing studies of aluminum-magnesium and aluminum-copper-lithium alloys
[AD-A227255] N91-14465
LITHOSPHERE
Specification goals for a Mars seismic network N91-14360
LOAD TESTING MACHINES
Delamination test apparatus and method
[NASA-CASE-LAR-13985-1] N91-14430
LOAD TESTS
Delamination test apparatus and method
[NASA-CASE-LAR-13985-1] N91-14430
Structural response of marine sandwich panels to uniform pressure loading
[AD-A227038] N91-14434
LOADS (FORCES)
Wind tunnel balance
[NASA-CASE-ARC-11877-1-SB] N91-14357
A continuum approach toward modeling the mechanics of solid lubricating films
[AD-A226961] N91-14486
Load response of horizontal-axis wind turbines to turbulence
[DE90-000375] N91-14644
LOCAL AREA NETWORKS
An analysis of input/output paradigms for real-time systems
[AD-A226724] N91-14748
LOCKING
Quick connect coupling
[NASA-CASE-MSC-21539-1] N91-14610
System for connecting fluid couplings
[NASA-CASE-MFS-26042-1-SB] N91-14613
LOGIC CIRCUITS
Intelligent manipulation technique for multi-branch robotic systems
[NASA-CR-187651] N91-14603
LONG WAVE RADIATION
Innovative Long Wavelength Infrared Detector Workshop Proceedings
[NASA-CR-187433] N91-14379
LWIR detector requirements for low-background space applications N91-14382
LWIR HgCdTe: Innovative detectors in an incumbent technology N91-14384
New heterojunction LWIR detector options N91-14398
Intersubband absorption in Si(1-x)Ge(x/Si superlattices for long wavelength infrared detectors N91-14399
Possibilities for LWIR detectors using MBE-grown Si(/Si(1-x)Ge(x) structures N91-14400
Novel Si(1-x)Ge(x)/Si heterojunction internal photoemission long wavelength infrared detectors N91-14401
HgZnTe-based detectors for LWIR NASA applications N91-14404
Small band gap superlattices as intrinsic long wavelength infrared detector materials N91-14405
LWIR detector research in InAsSb/InAs N91-14406
InAsSbBi, a direct band-gap, III-V, LWIR material N91-14410
Longwave spectral dependence of emission from warm dust clouds N91-14945
LOW ASPECT RATIO
Experimental investigations of buffet excitation forces on a low aspect ratio trapezoidal half wing in incompressible flow N91-14329
LOW ASPECT RATIO WINGS
Experimental investigation and semi-empirical prediction of the dynamic response of a low-aspect-ratio trapezoidal wing due to flow separation N91-14330
LOW CONCENTRATIONS
A balloon-borne aerosol spectrometer for high altitude low aerosol concentration measurements
[DE91-002563] N91-14661
LOW CURRENTS
Low dark current photovoltaic multiquantum well long wavelength infrared detectors N91-14396
LOW SPEED
The effect of wing planform on low speed buffet N91-14336
LOW TEMPERATURE ENVIRONMENTS
Development of an animal model of human non-freezing cold injury: Changes in thermal sensitivity following cold exposure
[AD-A227174] N91-14705

LUBRICATION
A continuum approach toward modeling the mechanics of solid lubricating films
[AD-A226961] N91-14486
LUBRICATION SYSTEMS
A continuum approach toward modeling the mechanics of solid lubricating films
[AD-A226961] N91-14486
LUMINESCENCE
Solid state radioluminescent sources using zeolites
[DE91-002703] N91-14857
LUMINOSITY
The wavelength dependence of polarization in NGC 2023 N91-14923
Temperature distribution of dust in luminous IRAS galaxies N91-14982
LUNAR SOIL
Type of silicate feature in oxygen rich stellar envelopes N91-15024

M

M STARS
Dust formation around M-type stars N91-15017
MACH NUMBER
Investigations of aerothermodynamic effects on axisymmetric bodies at high Mach numbers N91-14302
MACHINE LEARNING
Intelligent manipulation technique for multi-branch robotic systems
[NASA-CR-187651] N91-14603
MACHINING
Manufacturing Technology: A Sandia Technology Bulletin, Volume 1, No. 1
[DE91-002518] N91-14504
A vibrating razor blade machining tool for material removal on low-density foams
[DE91-002996] N91-14507
MAGELLANIC CLOUDS
Multicolor optical polarimetry of reddened stars in the small Magellanic cloud N91-14986
MAGNESIUM ALLOYS
Processing studies of aluminum-magnesium and aluminum-copper-lithium alloys
[AD-A227255] N91-14465
MAGNESIUM CELLS
In-line sensors for electrolytic magnesium cells
[DE91-002561] N91-14438
MAGNESIUM CHLORIDES
In-line sensors for electrolytic magnesium cells
[DE91-002561] N91-14438
MAGNESIUM OXIDES
A LEED study of the MgO(001) surface structure
[DE91-002811] N91-14879
MAGNETIC COILS
Improved high power/high frequency inductor
[NASA-CASE-NPO-17830-1-CU] N91-14539
MAGNETIC DIFFUSION
Fast electron studies in the ZT-40M edge plasma
[DE91-002323] N91-14838
MAGNETIC DIPOLES
Experiments with collision of vortices in rotating and still free-surface shallow water N91-15080
MAGNETIC DISTURBANCES
Nonstationary processes in the front of high Mach number collisionless quasiperpendicular shock: Dynamics of the ion distribution N91-15067
MAGNETIC EFFECTS
Determination of SPEAR-1 rocket body potential during high-voltage experiments
[AD-A226971] N91-14417
MAGNETIC FIELD CONFIGURATIONS
HEM(sub 11) modes revisited
[DE91-001028] N91-14819
A two micron polarization survey toward dark clouds N91-14952
MAGNETIC FIELD RECONNECTION
Three-dimensional magnetic reconnection at the Earth's magnetopause N91-15059
Interrelationship between the tearing-instability and magnetic island merging N91-15109
MAGNETIC FIELDS
Task reports on developing techniques for scattering by 3D composite structures and to generate new solutions in diffraction theory using higher order boundary conditions
[NASA-CR-186899] N91-14475
Measurement of the gravitomagnetic field using a pair of laser ranged satellites N91-14670
Fast electron studies in the ZT-40M edge plasma
[DE91-002323] N91-14838
A characterization of internal-Sn Nb3 Sn superconductors for use in the Proof of Priciples (PoP) coil
[DE91-001743] N91-14852
On the polarization mechanism in the R Mon/NGC 2261 complex N91-14969
Does the far-infrared/radio correlation in spiral galaxies extend to the spatial domain N91-14985
Hydrodynamics of collisionless relativistic plasma in a strong magnetic field N91-15072
Amplification of Alfven waves in free shear flows N91-15074
Generation of inductive fields by an oblique magnetic rotator in collisionless plasma N91-15077
Observation of electron hole, double layer, and turbulent heating in a laboratory plasma N91-15079
A model for one-sided extragalactic jets N91-15097
On the generation of magnetic fields in active star atmospheres N91-15099
Influence of the parameter distribution of the solar wind near the Sun upon its structure at the Earth's orbit N91-15108
Interrelationship between the tearing-instability and magnetic island merging N91-15109
Nonlinear magnetosonic waves in an inhomogeneous plasma N91-15110
MAGNETIC FLUX
Irradiation-induced pinning in single-crystal and thin-film Tl2Ca2Ba2Cu3O10 superconductors
[DE91-001342] N91-14877
Solar magnetic flux-tubes and coronal loops N91-15047
Influence of the parameter distribution of the solar wind near the Sun upon its structure at the Earth's orbit N91-15108
MAGNETIC INDUCTION
Generation of inductive fields by an oblique magnetic rotator in collisionless plasma N91-15077
MAGNETIC MIRRORS
Observation of electron hole, double layer, and turbulent heating in a laboratory plasma N91-15079
MAGNETIC MOMENTS
Sterile neutrinos and astrophysical and cosmological constraints on the parameters of the extended electroweak models N91-15083
Neutrino scattering by nuclei in imperfect media N91-15104
MAGNETIC MONOPOLES
Initial data from the Soudan 2 experiment
[DE91-004454] N91-14815
MAGNETIC RESONANCE
Nonlinearity influence in local resonance regions on the Alfven waves propagation in solar corona N91-15055
MAGNETIC STORMS
A numerical calculation of parameters of explosion MHD shock waves from moderate solar flares N91-15066
MAGNETOACOUSTIC WAVES
Solar flares and particle acceleration N91-15049
Accretion disk instability and spokes in Saturn's rings N91-15094
Nonlinear magnetosonic waves in an inhomogeneous plasma N91-15110
MAGNETOHYDRODYNAMIC FLOW
Solitary vortices in the vicinity of comets N91-15062
Gradient catastrophe of the supersonic mass-loaded magnetised plasma flow and the formation of bow shock N91-15065
MAGNETOHYDRODYNAMIC GENERATORS
Wave collapse at lower hybrid resonance N91-15073
MAGNETOHYDRODYNAMIC STABILITY
Physics data base for the Beam Plasma Neutron Source (BPNS)
[DE91-002796] N91-14842
ITER global stability limits
[DE91-001488] N91-14845
A new kind of magnetic buoyancy instability N91-15050
Linear stability and MHD wave propagation in plasmas with solar abundances N91-15056
On the thermal stability of slabs, cylinders, and spheres N91-15057
Plasma waves associated with the space shuttle N91-15064
Maser cyclotron instability in a plasma with anisotropic distribution function N91-15075
Accretion disk instability and spokes in Saturn's rings N91-15094
Large-scale vortices in compressible turbulent medium with the magnetic field N91-15095
MAGNETOHYDRODYNAMIC TURBULENCE
A new kind of magnetic buoyancy instability N91-15050
Large-scale vortices in compressible turbulent medium with the magnetic field N91-15095
MAGNETOHYDRODYNAMIC WAVES
Nonlinear surface MHD waves in the inhomogeneous plasma with cusp-resonance in upper solar atmosphere N91-15052
Filamentary structures in the Sun's atmosphere as singular Alfven waves N91-15053
Nonlinearity influence in local resonance regions on the Alfven waves propagation in solar corona N91-15055
Linear stability and MHD wave propagation in plasmas with solar abundances N91-15056
A numerical calculation of parameters of explosion MHD shock waves from moderate solar flares N91-15066
Nonstationary processes in the front of high Mach number collisionless quasiperpendicular shock: Dynamics of the ion distribution N91-15067
Evolution of high amplitude Alfven waves near a bow shock N91-15068
Energy dissipation of shear Alfven waves in extended cosmic jets N91-15086
Large-scale vortices in compressible turbulent medium with the magnetic field N91-15095
MAGNETOHYDRODYNAMICS
Three-dimensional magnetic reconnection at the Earth's magnetopause N91-15059
Detection of nonlinear features in plasma and field measurements by PROGNOZ-8 N91-15063
Description of nonlinear effects in a relativistic plasma using Hamiltonian formalism N91-15071
Hydrodynamics of collisionless relativistic plasma in a strong magnetic field N91-15072
Magnetically driven jets and winds N91-15084
Radiation-driven diskons as a new astrophysical object N91-15105
MAGNETOPAUSE
Three-dimensional magnetic reconnection at the Earth's magnetopause N91-15059
Detection of nonlinear features in plasma and field measurements by PROGNOZ-8 N91-15063
MAGNETOPLASMADYNAMICS
Solitary vortices in the vicinity of comets N91-15062
MAGNETRON SPUTTERING
Superconducting properties of Tl-Ba-Ca-Cu-O films on silver substrates
[DE91-002304] N91-14856
MAIN SEQUENCE STARS
The discovery of a highly polarized bipolar nebula N91-15031
MAINTAINABILITY
Human factors engineering. Part 1: Test procedures
[AD-A226480] N91-14720
MAN-COMPUTER INTERFACE
Adaptive human-computer interfaces using expert profiles
[AD-A226906] N91-14721
Developing portable user interfaces for Ada command control software
[AD-A226712] N91-14747
MANEUVERABILITY
Investigation of a semi-empirical method to predict limit cycle oscillations of modern fighter aircraft N91-14333
Development of an unmanned air research vehicle for supermaneuverability studies
[AD-A227165] N91-14342
MANGANESE ALLOYS
Fundamental studies on microstructural evolution of two-phase titanium alloys N91-14452
MANGANESE COMPOUNDS
High efficiency cadmium and zinc telluride-based thin film solar cells
[DE91-002112] N91-14643
MANIPULATORS
Manipulation hardware for microgravity research
[NASA-TM-103423] N91-14498
Variation of wall shear stress and Reynolds stress over a flat plate downstream of a boundary layer manipulator
[AD-A226875] N91-14565
Contribution to the specification and implementation of complex robot tasks
[ETN-90-98209] N91-14604
Robot control strategies
[OUEL-1754/89] N91-14605
Spiral lead platen robotic end effector
[NASA-CASE-LAR-13855-1] N91-14615
Multi-fingered robotic hand
[NASA-CASE-NPO-15959-2] N91-14616
Reasoning of the geometric and uncertainty constraints in planning robot manipulation tasks
[LAAS-90143] N91-14775
MANUFACTURING
Method for manufacturing composite material
[EP-PATENT-0-314-353-A2] N91-14421
Manufacturing Technology: A Sandia Technology Bulletin, Volume 1, No. 1
[DE91-002518] N91-14504
A materials database for Li(Si)/FeS2 thermal batteries
[DE91-002592] N91-14531
MAPPING
Measurement of hydrodynamic forces and moments and flow field mapping of a model in coning motion
[AD-A226684] N91-14355

Feasibility study of the seismic reflection method in Amargosa Desert, Nye County, Nevada
[DE91-001646] N91-14676
Hidden surface removal for axis-parallel polyhedra
[RUU-CS-90-21] N91-14736
Mappings and accuracy for Chebyshev pseudo-spectral approximations
[NASA-TM-103630] N91-14781
On the polarization mechanism in the R Mon/NGC 2261 complex N91-14969

MARKOV PROCESSES
Minimization on stochastic matroids
[AD-A227413] N91-14799

MARS (PLANET)
Proceedings of the Mars Global Network Mission Workshop
[NASA-CR-186844] N91-14359
Specification goals for a Mars seismic network N91-14360
A global view of lander-to-orbiter communications accessibility for a Mars Global Network Mission N91-14362

MARS ATMOSPHERE
Solar radiation on Mars: Update 1990
[NASA-TM-103623] N91-15117

MARS LANDING
Space transfer concepts and analysis for exploration missions
[NASA-CR-183943] N91-14358
Proceedings of the Mars Global Network Mission Workshop
[NASA-CR-186844] N91-14359

MARS PROBES
Proceedings of the Mars Global Network Mission Workshop
[NASA-CR-186844] N91-14359
A polar orbit for the Mars Global Network Mission N91-14361
A global view of lander-to-orbiter communications accessibility for a Mars Global Network Mission N91-14362
Analysis of success probability/cost trades for small landers in a Mars network N91-14363
A GNM mission and system design proposal N91-14364

MARS SAMPLE RETURN MISSIONS
Mars Rover/Sample Return (MRSR) Mission: Mars Rover Technology Workshop
[NASA-TM-101129] N91-14600

MARS SURFACE
A polar orbit for the Mars Global Network Mission N91-14361
A global view of lander-to-orbiter communications accessibility for a Mars Global Network Mission N91-14362
Mars Rover/Sample Return (MRSR) Mission: Mars Rover Technology Workshop
[NASA-TM-101129] N91-14600
Solar radiation on Mars: Update 1990
[NASA-TM-103623] N91-15117

MASER OUTPUTS
Maser cyclotron instability in a plasma with anisotropic distribution function N91-15075

MASS DISTRIBUTION
Compact object masses in active galactic nuclei and quasars and duration of activity stage N91-15096

MASS SPECTRA
The composition of heavy molecular ions inside the ionopause of Comet Halley N91-15010

MASS SPECTROMETERS
Apparatus and method for characterizing the transmission efficiency of a mass spectrometer
[NASA-CASE-NPO-16989-1-CU] N91-14587

MASS SPECTROSCOPY
Characterization of phenolic resins with thermogravimetry-mass spectrometry
[DE91-002710] N91-14492

MASS TRANSFER
Coupled transport processes in semipermeable media. Part 1: Analytical solutions of the linearized governing equations
[DE91-004138] N91-14887

MASSIVELY PARALLEL PROCESSORS
Massively parallel network architectures for automatic recognition of visual speech signals
[AD-A226968] N91-14805

MATERIALS RECOVERY
Electroless nickel bath recovery by cation exchange and precipitation
[DE91-001988] N91-14457

MATHEMATICAL LOGIC
Capturing strong reduction in director string calculus
[AD-A226738] N91-14783

MATHEMATICAL MODELS
Missile Aerodynamics
[AGARD-CP-493] N91-14278
Store carriage, integration, and release N91-14281
Supersonic tactical missile computation using Euler's equation with crossflow separation modeling N91-14284
Systematic investigations of body-wing-tail interference at high angles of attack N91-14290
Asymmetric supersonic flow around cones with noncircular sections N91-14292
Computational models with advanced thermochemistry for the analysis of missile/plume flowfield interactions N91-14305
Numerical simulation of ice growth on a MS-317 swept wing geometry
[NASA-TM-103705] N91-14310
Task reports on developing techniques for scattering by 3D composite structures and to generate new solutions in diffraction theory using higher order boundary conditions
[NASA-CR-186899] N91-14475
Analytical solutions with Generalized Impedance Boundary Conditions (GIBC) N91-14477
On the modeling and control of slewing flexible structures N91-14499
Perspectives on modeling electromagnetic sea scatter
[AD-A226939] N91-14520
Computer aided design models for millimeter-wave suspended substrate microstrip line
[AD-A227259] N91-14547
A discussion of the results of an in-situ comparison of three full-vector anemometers
[DE91-002113] N91-14572
Validation of a computational model for autogenous arc welding
[AD-A227258] N91-14611
Methods for evaluating the predictive accuracy of structural dynamic models
[NASA-CR-187649] N91-14630
Remote sensing of Earth terrain
[NASA-CR-186904] N91-14635
Estimability of geodetic parameters from space VLBI observables
[NASA-CR-187413] N91-14636
The synthesis of solar radiation data for sizing stand-alone photovoltaic systems
[DE90-012758] N91-14652
Measurement of the gravitomagnetic field using a pair of laser ranged satellites N91-14670
Theory and measurements of nighttime horizontal gradients in the mid-latitude F region N91-14671
Crustal Dynamics Project data analysis, 1990
[NASA-TM-100765] N91-14679
Discrete event simulation tool for analysis of qualitative models of continuous processing systems
[NASA-CASE-MSC-21465-1] N91-14741
An analysis of input/output paradigms for real-time systems
[AD-A226724] N91-14748
Engineering design with decision support: An application of goal decomposition
[AD-A226730] N91-14782
Control of distributed parameter systems
[AD-A227306] N91-14787
Planning the behavior of dynamical systems
[AD-A227381] N91-14788
Approximately integrable linear statistical models in non-parametric estimation
[AD-A227395] N91-14798
An investigation of the diffraction of an acoustic plane wave by a curved surface of finite impedance N91-14800
Equilibrium composition of interphase boundaries
[DE91-002470] N91-14814
Tokamak fluidlike equations, with applications to turbulence and transport in H mode discharges
[DE91-002632] N91-14849
The evaluation of long range consequences in decision making
[AD-A226949] N91-14888
New results in the theory of dust grain alignment N91-14906
Grain growth, optical polarisation, and extinction in interstellar clouds N91-14959
Grains charges in interstellar clouds N91-14967
Dust coagulation in ISM N91-14968
Infrared studies of dust grains in infrared reflection nebulae N91-14970
Dust in regions of massive star formation N91-14972
IR emission from circumstellar envelopes of C-rich stars N91-15019
Continuum radiative transfer in accretion-powered pulsars N91-15043
A new model of spicule formation in the Sun chromosphere N91-15051
Laboratory and computer simulations of wave generation processes in non-stationary astrophysical phenomena N91-15082
On the existence of circular polarisation in the pulsar radiation N91-15088
On the theory of large-scale micropulse structure of pulsar radio radiation N91-15092
Structure of accretion flow in close binary system: A two dimensional numerical model N91-15093
Accretion disk instability and spokes in Saturn's rings N91-15094
A model for one-sided extragalactic jets N91-15097
On the generation of magnetic fields in active star atmospheres N91-15099
The plasma model of radioemission from SN 1987A N91-15101
A mesoscale planetary boundary layer numerical model for simulations of topographically induced circulations N91-15113
Studies of the chemistry of the nightside ionosphere of Venus
[NASA-CR-187714] N91-15114

MATHEMATICAL PROGRAMMING
Multivariable methods for the design, identification, and control of large space structures. Volume 2: Optimal and sub-optimal estimation applied to large flexible structures
[AD-A226699] N91-14375
Engineering design with decision support: An application of goal decomposition
[AD-A226730] N91-14782

MATRICES
Minimization on stochastic matroids
[AD-A227413] N91-14799

MATRICES (MATHEMATICS)
Computational equipment for the development of numerical algorithms computation
[AD-A226702] N91-14729
Covers by polars of arrangements
[DE91-001358] N91-14764
An accurate product SVD (singular value decomposition) algorithm
[DE91-004448] N91-14765
Matrix techniques for faster routing of affine permutations on a mesh interconnection network
[RUU-CS-90-19] N91-14767
A combined finite element-boundary element formulation for solution of axially symmetric bodies
[NASA-CR-185852] N91-14789

MATRIX MATERIALS
Fundamentals of interfacial strength in composite materials
[AD-A226701] N91-14431

MAXIMA
Extremal rays of convex cones and complementary inequalities
[ETN-91-98166] N91-14778

MAXWELL EQUATION
The inclusion of wall loss in electromagnetic finite-difference time-domain thin-slot algorithms
[DE91-001046] N91-14524

MEASURING INSTRUMENTS
Eddy current method for measuring electrical resistivity and device for providing accurate phase detection
[AD-D014571] N91-14530
Superconducting current transducer
[DE91-004674] N91-14554
NOVA 201 ultrasonic thickness gage (NOVA Gage)
[NASA-CR-184031] N91-14581
Automated system for measuring the strength of optical fibers
[AD-D014626] N91-14824

MECHANICAL DEVICES
Sensor based control of robotic mechanisms
[AD-A226784] N91-14776

MECHANICAL DRIVES
Robot control strategies
[OUEL-1754/89] N91-14605

MECHANICAL PROPERTIES
Adhesion at ceramic interfaces
[DE91-001660] N91-14480

MELTING
Irreversibility temperatures in oxide- and metallic superconductors
[DE91-004021] N91-14861

MEMBRANE STRUCTURES
Fabrication by filament winding with an elastomeric material
[AD-D014570] N91-14478

MEMORY
Air traffic controller memory enhancement
[DOT/FAA/CT-TN90/38] N91-14713

MEMORY (COMPUTERS)
Method of up-front load balancing for local memory parallel processors
[NASA-CASE-MSC-21348-1] N91-14769

MENTAL PERFORMANCE
The effects of sleep loss on individual and group performance
[AD-A226963] N91-14708

Empirical network model of human higher cognitive brain functions
[AD-A227193] N91-14718
Investigations of probabilistic inference
[AD-A226882] N91-14795
The object display: Principles and review of experimental findings
[AD-A226883] N91-14796
Interpretation of conditional probabilities in probabilistic interference word problems
[AD-A226907] N91-14797

MERCURY (METAL)
HgZnTe-based detectors for LWIR NASA applications N91-14404
Small band gap superlattices as intrinsic long wavelength infrared detector materials N91-14405

MERCURY (PLANET)
The rotation of Venus and its atmosphere N91-15112

MERCURY CADMIUM TELLURIDES
Status of LWIR HgCdTe infrared detector technology N91-14383
LWIR HgCdTe: Innovative detectors in an incumbent technology N91-14384
HgCdTe for NASA EOS missions and detector uniformity benchmarks N91-14385
Radiation response issues for infrared detectors N91-14388
MBE HgCdTe heterostructure detectors N91-14402

MERCURY TELLURIDES
MBE HgCdTe heterostructure detectors N91-14402
Growth and properties of Hg-based quantum well structures and superlattices N91-14403

MESOSCALE PHENOMENA
Mesoscale features of a winter storm: Dual Doppler velocity fields and differential reflectivity
[AD-A227342] N91-14692
Oceanographic expert system validation using GOAP mesoscale products and Gulf/DART validation test data
[AD-A226929] N91-14693
A mesoscale planetary boundary layer numerical model for simulations of topographically induced circulations N91-15113

METABOLISM
Cosmos 2044
[NASA-CR-187003] N91-14702

METAL BONDING
Fracture analysis of cathodic delamination in rubber-to-metal bonds N91-14627

METAL FATIGUE
Directional solidification of superalloys
[NASA-CASE-MFS-28314-1] N91-14462

METAL FILMS
Ion-induced grain growth in multilayer and coevaporated metal alloy thin films
[DE91-004489] N91-14472

METAL IONS
Conductivity fluctuations in fast ionic conductors
[AD-A227379] N91-14549

METAL MATRIX COMPOSITES
Fatigue and fracture of titanium aluminides, volume 2
[AD-A227353] N91-14351
Optimization of interface layers in the design of ceramic fiber reinforced metal matrix composites
[NASA-CR-185307] N91-14422
Dynamic consolidation of aluminum-silicon carbide composites
[DE91-001929] N91-14427
Thermomechanical processing and ambient temperature properties of a 6061 aluminum 10 volume percent alumina metal matrix composite
[AD-A227004] N91-14433

METAL OXIDE SEMICONDUCTORS
Method and apparatus for determining time, direction, and composition of impacting space particles
[NASA-CASE-LAR-13392-1-CU] N91-14412

METAL OXIDES
LWIR HgCdTe: Innovative detectors in an incumbent technology N91-14384
Irreversibility temperatures in oxide- and metallic superconductors
[DE91-004021] N91-14861
Laboratory studies of refractory metal oxide smokes N91-14993

METAL PARTICLES
Properties of grains derived from IRAS observations of dust N91-15001

METAL PLATES
A modification of 4330 alloy steel
[DE91-001764] N91-14455
The response and failure mechanisms of circular metal and composite plates subjected to underwater shock loading
[AD-A226759] N91-14631

METAL SHEETS
Application of ultrasonic guided waves to the characterization of texture in metal sheets of cubic and hexagonal crystallites
[DE91-001107] N91-14466

METAL SURFACES
Photodissociation near a rough metal surface: Effect of reaction fields
[AD-A227030] N91-14445
Surface treatment of metals
[EP-PATENT-0-367-504-A2] N91-14453
He atom surface spectroscopy: Surface lattice dynamics of insulators, metals, and metal overlayers
[DE91-001993] N91-14855

METAL VAPOR LASERS
Joining alumina to sapphire for copper vapor laser tubes
[AD-A226619] N91-14501

METAL-METAL BONDING
Heteronuclear metal cluster compounds synthesis and reactivity
[AD-A226815] N91-14463

METALLOGRAPHY
Thermal stability of the microstructure of an aged Nb-Zr-C alloy
[NASA-TM-103647] N91-14454

METALLOIDS
LWIR detector research in InAsSb/InAs N91-14406

METALS
Elucidation of fundamental properties of helium in metals by nuclear magnetic resonance techniques
[DE91-002715] N91-14460

METEORITES
Superaromatics: The key to a unified cosmic dust theory N91-14999

METEOROID DUST CLOUDS
Dust of Orionid meteor shower in the Earth atmosphere before and after Halley's Comet N91-15012

METEOROID SHOWERS
Dust of Orionid meteor shower in the Earth atmosphere before and after Halley's Comet N91-15012

METEOROIDS
A study of extended zodiacal structures
[NASA-CR-187687] N91-15044

METEOROLOGICAL PARAMETERS
Aircraft measurements of electrified clouds at Kennedy Space Center
[NASA-CR-186536] N91-14680
Aircraft measurements of electrified clouds at Kennedy Space Center. Part 1: 1988 flights N91-14681
Aircraft measurements of electrified clouds at Kennedy Space Center. Part 2: Case study: 4 November 1988 (88309) N91-14682

METEOROLOGICAL RADAR
Polarization radar studies of precipitation: Implementation of the technique and data interpretation
[AD-A227073] N91-14690
Mesoscale features of a winter storm: Dual Doppler velocity fields and differential reflectivity
[AD-A227342] N91-14692

METHANE
Diffusion and infrared properties of molecules in ice mantles N91-14963

METHOD OF MOMENTS
The application of deterministic spectral domain method to the analysis of planar circuit discontinuities on open substrates
[AD-A226901] N91-14542

METRIC SPACE
Finding shortest paths in the presence of orthogonal obstacles using a combined L sub 1 and link metric
[RUU-CS-90-20] N91-14777

MICROCOMPUTERS
Position requirements for space station personnel and linkages to portable microcomputer performance assessment
[NASA-CR-185606] N91-14719
Development of phenomenological fitting procedure for the fast microcomputer
[AD-A227168] N91-14759
Hybrid optical processor
[AD-A227163] N91-14834

MICROCRACKS
A statistically-based model of the interacting processes which lead to creep-rupture in filament-wound composite pressure vessels N91-14420
Flow behavior of Ti-24Al-11Nb at high strain rates
[DE91-004506] N91-14473

MICROELECTRONICS
Heterocycles based on group 3, 4, and 5 elements: Precursors for novel glasses and ceramics
[AD-A226988] N91-14487

MICROMECHANICS
A statistically-based model of the interacting processes which lead to creep-rupture in filament-wound composite pressure vessels N91-14420
Failure in laminated composite plates containing a hole
[AD-A227307] N91-14435

MICROMETEORITES
Size distribution of dust grains: A problem of self-similarity N91-14997

MICROPLASMAS
Development and testing of radiation and electromagnetic pulse hardened silicon carbide based electronics
[AD-A227309] N91-14548

MICROPULSATIONS
On the theory of large-scale micropulse structure of pulsar radio radiation N91-15092

MICROSTRIP ANTENNAS
The application of deterministic spectral domain method to the analysis of planar circuit discontinuities on open substrates
[AD-A226901] N91-14542

MICROSTRIP TRANSMISSION LINES
The application of deterministic spectral domain method to the analysis of planar circuit discontinuities on open substrates
[AD-A226901] N91-14542
Computer aided design models for millimeter-wave suspended substrate microstrip line
[AD-A227259] N91-14547

MICROSTRUCTURE
Aluminum nitride-silicon carbide whisker composites: Processing, properties, and microstructural stability
[DE91-001907] N91-14425
Fundamentals of interfacial strength in composite materials
[AD-A226701] N91-14431
Thermomechanical processing and ambient temperature properties of a 6061 aluminum 10 volume percent alumina metal matrix composite
[AD-A227004] N91-14433
Fundamental studies on microstructural evolution of two-phase titanium alloys N91-14452
Thermal stability of the microstructure of an aged Nb-Zr-C alloy
[NASA-TM-103647] N91-14454
Use of anomalous small angle x ray scattering to investigate microstructural features in complex alloys
[DE91-002397] N91-14471
Flow behavior of Ti-24Al-11Nb at high strain rates
[DE91-004506] N91-14473
Effect of hydrogen on the strength and microstructure of selected ceramics
[NASA-TM-103674] N91-14482
Ground boundaries
[DE91-004027] N91-14880

MICROWAVE ANTENNAS
The application of deterministic spectral domain method to the analysis of planar circuit discontinuities on open substrates
[AD-A226901] N91-14542

MICROWAVE CIRCUITS
MMIC compensation network for phased array element mismatch
[AD-A227437] N91-14522
Universal nondestructive mm-wave integrated circuit test fixture
[NASA-CASE-LEW-14746-1] N91-14552

MICROWAVE IMAGERY
Remote sensing of Earth terrain
[NASA-CR-186904] N91-14635

MICROWAVE RESONANCE
Characteristics and potential applications of an ORNL microwave ECR multicusp plasma ion source
[DE91-002649] N91-14840

MILITARY TECHNOLOGY
A system architecture for long duration free floating flight for military applications
[NASA-CR-187435] N91-14513
National software capacity: Near-term study
[AD-A226694] N91-14743
A performance study of the concurrency control algorithms in hierarchical network with partitioned database
[AD-A227055] N91-14756

MILLIMETER WAVES
Millimeter-wave monolithic diode-grid frequency multiplier
[NASA-CASE-NPO-17258-1-CU] N91-14551
Universal nondestructive mm-wave integrated circuit test fixture
[NASA-CASE-LEW-14746-1] N91-14552

MINERALOGY
Steps toward interstellar silicate dust mineralogy N91-14991

MINIMA
Extremal rays of convex cones and complementary inequalities
[ETN-91-98166] N91-14778

MINORITY CARRIERS
LWIR HgCdTe: Innovative detectors in an incumbent technology N91-14384
MIRA VARIABLES
Dust formation around M-type stars N91-15017
Dust around Mira variables: An analysis of IRAS LRS spectra N91-15026
MIRRORS
Nonlinear dynamics of broad-band lasers [DE91-001143] N91-14596
Characterization of semiconductor surface-emitting laser wafers [DE91-001336] N91-14598
Scattering by anisotropic grains in beryllium mirrors [DE91-001724] N91-14826
MISMATCH (ELECTRICAL)
MMIC compensation network for phased array element mismatch [AD-A227437] N91-14522
MISSILE BODIES
Application of Euler and Navier-Stokes codes to missile type bodies with high L/D ratios N91-14286
Supersonic vortex flows around a missile body: Basic experiment and Euler numerical computation N91-14291
MISSILE CONFIGURATIONS
Comparison of different calculation methods applied to a lenticular fuselage section N91-14293
MISSILE CONTROL
Review of the spring 1988 AGARD FMP symposium N91-14280
Device and method for monitoring the presence of an object in space [AD-D014621] N91-14823
MISSILE DESIGN
Missile Aerodynamics [AGARD-CP-493] N91-14278
Some trends in missile aerodynamics N91-14279
Review of the spring 1988 AGARD FMP symposium N91-14280
Supersonic tactical missile computation using Euler's equation with crossflow separation modeling N91-14284
Application of Euler and Navier-Stokes codes to missile type bodies with high L/D ratios N91-14286
A semi-empirical prediction method for missile aerodynamics N91-14288
Supersonic vortex flows around a missile body: Basic experiment and Euler numerical computation N91-14291
Overview of propulsion concepts for tactical missiles N91-14296
Computation of axisymmetric base flow with different turbulence models N91-14298
Results of GARTEUR action group AG09 on flow past missile afterbodies N91-14299
Experimental aerodynamics for hot gas jet reaction control systems N91-14300
Laminar/turbulent flow transition effects on high-speed missile domes N91-14301
MISSILE SYSTEMS
Overview of propulsion concepts for tactical missiles N91-14296
MISSILE TRACKING
Device and method for monitoring the presence of an object in space [AD-D014621] N91-14823
MISSILES
Supersonic tactical missile computation using Euler's equation with crossflow separation modeling N91-14284
A semi-empirical prediction method for missile aerodynamics N91-14288
Overview of propulsion concepts for tactical missiles N91-14296
Anticipation of aerodynamic coefficients of missile air intakes N91-14297
Computation of axisymmetric base flow with different turbulence models N91-14298
Results of GARTEUR action group AG09 on flow past missile afterbodies N91-14299
Laminar/turbulent flow transition effects on high-speed missile domes N91-14301
Thermal imaging on missiles in hypersonic flow N91-14303
Chordwise and spanwise centers of pressure of missile fins N91-14304
Computational models with advanced thermochemistry for the analysis of missile/plume flowfield interactions N91-14305
MISSION PLANNING
Space transfer concepts and analysis for exploration missions [NASA-CR-183943] N91-14358
Proceedings of the Mars Global Network Mission Workshop [NASA-CR-186844] N91-14359
A polar orbit for the Mars Global Network Mission N91-14361
A GNM mission and system design proposal N91-14364
Mars Rover/Sample Return (MRSR) Mission: Mars Rover Technology Workshop [NASA-TM-101129] N91-14600
MODELS
Improved estimation of variance components in mixed models [AD-A226854] N91-14794
Prediction of XV-15 tilt rotor discrete frequency aeroacoustic noise with WOPWOP [NASA-CR-187684] N91-14803
MODULARITY
Planning the behavior of dynamical systems [AD-A227381] N91-14788
MODULATORS
Optical phase conjugate beam modulator and method therefor [AD-D014569] N91-14820
MOLDS
Method for manufacturing composite material [EP-PATENT-0-314-353-A2] N91-14421
MOLECULAR BEAM EPITAXY
LWIR HgCdTe: Innovative detectors in an incumbent technology N91-14384
New heterojunction LWIR detector options N91-14398
Possibilities for LWIR detectors using MBE-grown Si(/Si(1-x)Ge(x) structures N91-14400
Novel Si(1-x)Ge(x)/Si heterojunction internal photoemission long wavelength infrared detectors N91-14401
MBE HgCdTe heterostructure detectors N91-14402
Growth and properties of Hg-based quantum well structures and superlattices N91-14403
InAs/Ga(1-x)In(x)Sb superlattices for infrared detector applications N91-14407
InAs/GaAs and InAs doping superlattices N91-14409
Kinetics of molecular beam epitaxy: Effect of ion-induced sputtering [DE91-004511] N91-14493
Pseudomorphic InGaAs materials [AD-A226895] N91-14864
MOLECULAR BEAMS
LWIR HgCdTe: Innovative detectors in an incumbent technology N91-14384
Laser studies of the interaction of SiO with the surface of a thin film [DE91-004562] N91-14450
MOLECULAR CHAINS
Heteronuclear metal cluster compounds synthesis and reactivity [AD-A226815] N91-14463
MOLECULAR CLOUDS
Interstellar Dust: Contributed Papers [NASA-CP-3036] N91-14897
Small scale variations of abundances of transiently heated grains in molecular clouds N91-14927
Dust emission from high latitude cirrus clouds N91-14930
The spatial distribution of infrared radiation from visible reflection nebulae N91-14931
Dust clouds in Orion and the interstellar neutral hydrogen distribution N91-14941
Dust in a few southern H II regions N91-14943
Distribution of dust in W31 complex N91-14944
Longwave spectral dependence of emission from warm dust clouds N91-14945
H I and dust in the high latitude dark cloud L1642 N91-14946
Dust emission in the Sagittarius B2 molecular cloud core N91-14947
The embedded objects in epsilon Cha I cloud N91-14949
Dust emission from Barnard 35: Gas heating anomaly resolved N91-14951
High resolution observations of compact H II regions at 230 GHz N91-14954
New insights in the photochemistry of grain mantles: The identification of the 4.62 and 6.87 micron bands N91-14957
Distribution of the 3.1 micron feature in Cepheus A N91-14958
Grain growth, optical polarisation, and extinction in interstellar clouds N91-14959
Molecular and mass spectroscopic analysis of isotopically labeled organic residues N91-14961
Synthesis of H2 in dirty ice mantles by fast ion energy loss: New experimental results increase the relevance of this mechanism N91-14962
Diffusion and infrared properties of molecules in ice mantles N91-14963
The evolution of organic mantles on interstellar grains N91-14964
Production and transfer of UV photons in non-homogeneous spherical clouds N91-14966
Grains charges in interstellar clouds N91-14967
Does CO trace H2 at high galactic latitude N91-14973
The origin of the galactic emission in IRAS data N91-14974
Molecules, grains, and shocks: A comparison of CO, H I, and IRAS data N91-14975
Molecules in an infrared cirrus cloud N91-14977
Thermal emission from interstellar dust in and near the Pleiades N91-14981
Size distribution of dust grains: A problem of self-similarity N91-14997
Stochastic histories of dust grains in the interstellar medium N91-14998
Sublimating comets as the source of nucleation seeds for grain condensation in the gas outflow from AGB stars N91-15018
IR emission from circumstellar envelopes of C-rich stars N91-15019
Type of silicate feature in oxygen rich stellar envelopes N91-15024
An interferometric study of molecular emission around NGC 7538 at millimeter wavelengths N91-15042
MOLECULAR COLLISIONS
State-to-state dynamics of molecular energy transfer [DE91-004589] N91-14599
MOLECULAR DIFFUSION
Dynamics of an unsteady diffusion flame: Effects of heat release and gravity [AD-A227348] N91-14447
MOLECULAR EXCITATION
State-to-state dynamics of molecular energy transfer [DE91-004589] N91-14599
MOLECULAR GASES
New results in the theory of dust grain alignment N91-14906
Infrared images of reflection nebulae and Orion's bar: Fluorescent molecular hydrogen and the 3.3 micron feature N91-14918
MOLECULAR INTERACTIONS
Angular motion of a PAH molecule in interstellar environment N91-14938
PAHs molecules and heating of the interstellar gas N91-14939
Interferometric molecular line observations of W51 N91-14950
MOLECULAR IONS
The composition of heavy molecular ions inside the ionopause of Comet Halley N91-15010
Theoretical studies of important processes in planetary and comet atmospheres [NASA-CR-187692] N91-15045
MOLECULAR ORBITALS
The effect of ionization on the infrared absorption spectra of PAHs: A preliminary report N91-14937
MOLECULAR RELAXATION
A LEED study of the MgO(001) surface structure [DE91-002811] N91-14879
MOLECULAR ROTATION
State-to-state dynamics of molecular energy transfer [DE91-004589] N91-14599
MOLECULAR SPECTRA
State-to-state dynamics of molecular energy transfer [DE91-004589] N91-14599
Influence of temperature on the infrared spectrum of the coronene molecule N91-14932
The nature of cometary dust as determined from infrared observations N91-15003
MOLECULAR STRUCTURE
Synthesis and properties of novel organometallic polymers [DE91-001978] N91-14491
Theory of the electronic and structural properties of solid state oxides [DE91-001192] N91-14874
Spectral structure near the 11.3 micron emission feature N91-14926
MOLECULES
Development of laser-ion beam photodissociation methods [DE91-000680] N91-14448
New results in the theory of dust grain alignment N91-14906
Red fluorescence and 3-12 micron emission in NGC 2023, HD 44179, M 82, and Lynds 1780 N91-14924
The 3.4 micron emission in comets N91-15006
MOLTEN SALTS
In-line sensors for electrolytic magnesium cells [DE91-002561] N91-14438

Organic cathode for a secondary battery
[NASA-CASE-NPO-17604-1-CU] N91-14536
MOLYBDENUM OXIDES
Mechanism of hydrodenitrogenation. Part 4: Infrared spectroscopy of acidic molybdena catalysts
[DE91-002496] N91-14440
MONITORS
Atmospheric source-receptor relationships: Concepts and terminology
[DE91-001033] N91-14656
A beam position monitor for low current dc beams
[CEBAF-PR-89-004] N91-14816
MONTE CARLO METHOD
Equilibrium composition of interphase boundaries
[DE91-002470] N91-14814
Effect of step edge transition rates and anisotropy in simulations of epitaxial growth
[DE91-001251] N91-14875
New results in the theory of dust grain alignment N91-14906
Stochastic histories of dust grains in the interstellar medium N91-14998
MOTION SICKNESS
Prediction of helicopter simulator sickness
[DE90-016530] N91-14710
MOTION STABILITY
The effects of liquid propellant motion on the attitude stability of spin stabilized spacecraft
[AD-A227002] N91-14376
MOUNTING
Thermal compensating mount
[NASA-CASE-LAR-14207-1] N91-14590
Post clamp
[NASA-CASE-LEW-14862-1] N91-14617
MOUTH
Bioreactivity: Studies on a simple brain stem reflex in behaving animals
[AD-A226823] N91-14704
MRCA AIRCRAFT
In-flight measurements on a Tornado aircraft for stores carriage and release research
[RAE-TM-AERO-2180] N91-14341
MULTIGRID METHODS
Acceleration techniques for explicit Euler codes N91-14555
MULTIPLEXING
Adaptive data acquisition multiplexing system and method
[NASA-CASE-MSC-21170-1] N91-14371
Issues and directions in IR detector readout electronics N91-14387
Unidirectional amplitude sensitive noise riding threshold circuit
[AD-D014568] N91-14529
MULTIPROCESSING (COMPUTERS)
Nonlinear finite element dynamics on multiprocessor computers
[AD-A227409] N91-14761
Literature survey on tools
[AD-A226933] N91-14770
MULTISENSOR APPLICATIONS
Development of a taction system using piezoelectric film
[AD-A227076] N91-14544
MULTISPECTRAL BAND CAMERAS
The optical parametrization of an aerial multispectral camera
[DE91-003017] N91-14593
MULTISPECTRAL BAND SCANNERS
Multispectral imagery support for ocean venture 90
[AD-A227119] N91-14697
MULTISTATIC RADAR
Description of the bistatic radar terrain measurements system equipment
[AD-A226808] N91-14517
MUONS
On the primary cosmic ray nuclei spectra behaviour in the 10(exp 16) eV energy region N91-15069
MUSCLES
Cosmos 2044
[NASA-CR-187003] N91-14702

N

NASA PROGRAMS
Proceedings of the Mars Global Network Mission Workshop
[NASA-CR-186844] N91-14359
HgCdTe for NASA EOS missions and detector uniformity benchmarks N91-14385
NASA-UVA light aerospace alloy and structures technology program
[NASA-CR-187321] N91-14474
The NASA/DOD aerospace knowledge diffusion research project: A research agenda
[NASA-TM-103439] N91-14892
Chronology: MSFC Space Station program, 1982 - present. Major events
[NASA-CR-184014] N91-15119
Chronology: MSFC Space Shuttle program development, assembly, and testing major events (1969 - April, 1981)
[NASA-CR-184013] N91-15120
NASTRAN
Low velocity impact analysis with NASTRAN
[NASA-TM-103169] N91-14426
NATIONAL AIRSPACE SYSTEM
DATAS hardware diagnostic tests
[DOT/FAA/CT-TN90/44] N91-14728
NATURAL LANGUAGE (COMPUTERS)
DEMON: A media object model incorporating natural language descriptions for retrieval support
[AD-A226711] N91-14893
NAVIER-STOKES EQUATION
Numerical investigations in three-dimensional internal flows
[NASA-CR-187373] N91-14277
Aerodynamic design of Pegasus (trademark): Concept to flight with CFD N91-14285
Application of Euler and Navier-Stokes codes to missile type bodies with high L/D ratios N91-14286
Asymmetric supersonic flow around cones with noncircular sections N91-14292
Three dimensional flow calculations for a projectile with standard and dome bases N91-14294
Navier-Stokes predictions of static and dynamic aerodynamic derivatives for high L/D finned projectiles N91-14295
Computational models with advanced thermochemistry for the analysis of missile/plume flowfield interactions N91-14305
Dynamics of an unsteady diffusion flame: Effects of heat release and gravity
[AD-A227348] N91-14447
Acceleration techniques for explicit Euler codes N91-14555
CFD code evaluation for internal flow modeling
[NASA-CR-187677] N91-14557
Computation of thermochemical nonequilibrium flows around a simple and a double ellipse
[NASA-CR-187702] N91-14558
NAVIGATION AIDS
Flight data acquisition methodology for validation of passive ranging algorithms for obstacle avoidance
[NASA-TM-102809] N91-14322
NAVIGATION TECHNOLOGY SATELLITES
Feasibility study of the seismic reflection method in Amargosa Desert, Nye County, Nevada
[DE91-001646] N91-14676
NEAR INFRARED RADIATION
IR and FIR laser diagnostics for plasma thrusters using a CW CO2 radiation source
[AD-A226816] N91-14843
A two micron polarization survey toward dark clouds N91-14952
Infrared studies of dust grains in infrared reflection nebulae N91-14970
NEBULAE
The spectral energy distribution of the scattered light from dark clouds N91-14911
Spatial variations of the 3 micron emission features within nebulae N91-14922
The wavelength dependence of polarization in NGC 2023 N91-14923
Red fluorescence and 3-12 micron emission in NGC 2023, HD 44179, M 82, and Lynds 1780 N91-14924
An interferometric study of molecular emission around NGC 7538 at millimeter wavelengths N91-15042
NEODYMIUM
A characterization of internal-Sn Nb3 Sn superconductors for use in the Proof of Priciples (PoP) coil
[DE91-001743] N91-14852
NEPHELOMETERS
A balloon-borne integrating nephelometer
[DE91-001037] N91-14687
NETWORK ANALYSIS
Electro-optic network analyzer
[NASA-CR-186613] N91-14527
Matrix techniques for faster routing of affine permutations on a mesh interconnection network
[RUU-CS-90-19] N91-14767
Efficient parallel algorithms on the network model
[AD-A227144] N91-14771
Finding shortest paths in the presence of orthogonal obstacles using a combined L sub 1 and link metric
[RUU-CS-90-20] N91-14777
Defense Data Network (DDN) performance analysis using probability modeling
[AD-A226856] N91-14894
NETWORK CONTROL
Space station common module network topology and hardware development
[NASA-CR-184034] N91-14373
A performance study of the concurrency control algorithms in hierarchical network with partitioned database
[AD-A227055] N91-14756
NETWORK SYNTHESIS
Space station common module network topology and hardware development
[NASA-CR-184034] N91-14373
NEUMANN PROBLEM
Boundary value problems of the elasticity theory for polyhedra: Singularities and approximation with boundary element methods
[ETN-91-98168] N91-14780
NEURAL NETS
International Symposium on Information Theory
[AD-A226957] N91-14521
Empirical network model of human higher cognitive brain functions
[AD-A227193] N91-14718
Method of up-front load balancing for local memory parallel processors
[NASA-CASE-MSC-21348-1] N91-14769
Analogue computation using VLSI neural network devices
[OUEL-1835/90] N91-14773
The definition of necessary hidden units in neural networks for combinatorial optimization
[AD-A227142] N91-14786
NEUROLOGY
Bioreactivity: Studies on a simple brain stem reflex in behaving animals
[AD-A226823] N91-14704
NEUROTRANSMITTERS
Bioreactivity: Studies on a simple brain stem reflex in behaving animals
[AD-A226823] N91-14704
NEUTRAL BEAMS
Physics data base for the Beam Plasma Neutron Source (BPNS)
[DE91-002796] N91-14842
NEUTRAL CURRENTS
Sterile neutrinos and astrophysical and cosmological constraints on the parameters of the extended electroweak models N91-15083
NEUTRAL GASES
Diffuse galactic light observations at 206 selected areas N91-14914
Dust clouds in Orion and the interstellar neutral hydrogen distribution N91-14941
NEUTRINOS
Initial data from the Soudan 2 experiment
[DE91-004454] N91-14815
Sterile neutrinos and astrophysical and cosmological constraints on the parameters of the extended electroweak models N91-15083
Neutrino scattering by nuclei in imperfect media N91-15104
NEUTRON BEAMS
Status of the advanced neutron source
[DE91-002870] N91-14810
NEUTRON DIFFRACTION
Status of the advanced neutron source
[DE91-002870] N91-14810
NEUTRON SCATTERING
Status of the advanced neutron source
[DE91-002870] N91-14810
NEUTRON SOURCES
Status of the advanced neutron source
[DE91-002870] N91-14810
Data requirements for intermediate energy nuclear applications
[DE91-004005] N91-14812
Physics data base for the Beam Plasma Neutron Source (BPNS)
[DE91-002796] N91-14842
NEUTRON STARS
Continuum radiative transfer in accretion-powered pulsars N91-15043
Maser cyclotron instability in a plasma with anisotropic distribution function N91-15075
Annihilation radiation of strongly-magnetised electron-positron plasma with power-law distributions of particles N91-15078
Matter penetration and motion through the magnetosphere of neutron star N91-15087
Thirty-five-day cycle of Her X-1: Synthesised optical light curves in the model of freely processing neutron star N91-15089
On the braking mechanisms of pulsars N91-15090

On the nature of cosmic gamma ray bursts N91-15098

NICKEL PLATE
Electroless nickel bath recovery by cation exchange and precipitation
[DE91-001988] N91-14457

NIOBIUM
Thermal stability of the microstructure of an aged Nb-Zr-C alloy
[NASA-TM-103647] N91-14454
Experimental results in superconducting niobium resonators for high-brightness ion beam acceleration
[DE91-004478] N91-14882
First tests of a superconducting RFQ (radio frequency quadrupole) structure
[DE91-004483] N91-14883

NITRATES
Electrophoretic and electrolytic deposition of ceramic particles on porous substrates
[AD-A227371] N91-14488

NITRIC ACID
The effects of climate change on the nitrogen cycle and acid deposition
[DE91-002785] N91-14659

NITROGEN
Laboratory studies of refractory metal oxide smokes N91-14993

NOAA 9 SATELLITE
NA-9 Solar Backscatter Ultraviolet (SBUV/2) instrument and derived ozone data
[AD-A227449] N91-15118

NOISE PREDICTION (AIRCRAFT)
Prediction of XV-15 tilt rotor discrete frequency aeroacoustic noise with WOPWOP
[NASA-CR-187684] N91-14803

NOISE REDUCTION
Low-noise nozzle valve
[NASA-CASE-MFS-28383-1] N91-14563
Innovative methodology for cancelling contaminating noise in turbulent fluid flow environments
[AD-A227028] N91-14567

NOISE THRESHOLD
Unidirectional amplitude sensitive noise riding threshold circuit
[AD-D014568] N91-14529

NONDESTRUCTIVE TESTS
Use of anomalous small angle x ray scattering to investigate microstructural features in complex alloys
[DE91-002397] N91-14471
Universal nondestructive mm-wave integrated circuit test fixture
[NASA-CASE-LEW-14746-1] N91-14552
Validation of a computational model for autogenous arc welding
[AD-A227258] N91-14611
Quality control and nondestructive test procedures for welded products
[DE91-004530] N91-14623

NONEQUILIBRIUM FLOW
Computation of thermochemical nonequilibrium flows around a simple and a double ellipse
[NASA-CR-187702] N91-14558

NONLINEAR EQUATIONS
Nonlinear magnetosonic waves in an inhomogeneous plasma N91-15110

NONLINEAR OPTICS
Approaches to the design of a novel macromolecular system with tailored optical properties
[AD-A226952] N91-14485
Nonlinear dynamics of broad-band lasers
[DE91-001143] N91-14596
Optoelectronic devices
[AD-D014618] N91-14822
Nonlinear optics and organic materials
[AD-A226953] N91-14831

NONLINEAR SYSTEMS
Adaptive control of large space structures
[AD-A227304] N91-14377
Quantum 1/f noise in high technology applications including ultrasmall structures and devices
[AD-A226739] N91-14515
Spontaneous and induced coherent radiation generation in atomic vapors
[AD-A226776] N91-14830
Optical phase conjugation via stimulated Brillouin scattering in multimode optical fiber
[AD-A227054] N91-14833

NONLINEARITY
Nonlinear finite element dynamics on multiprocessor computers
[AD-A227409] N91-14761
Nonlinearity influence in local resonance regions on the Alfven waves propagation in solar corona N91-15055
Detection of nonlinear features in plasma and field measurements by PROGNOZ-8 N91-15063
Excitation of Langmuir wave by transversal nonlinear wave in the electron-positron inhomogeneous plasma in the presence of positron beam N91-15076
Observation of electron hole, double layer, and turbulent heating in a laboratory plasma N91-15079

NONUNIFORM PLASMAS
Nonlinear surface MHD waves in the inhomogeneous plasma with cusp-resonance in upper solar atmosphere N91-15052

NORTHERN HEMISPHERE
The autocorrelation function of the North Pole dust N91-14901

NOSE CONES
Aerodynamic characteristics of cylindrical bodies with pointed and truncated conical noses N91-14289

NOVAE
PAH emission from Nova Cen 1986 N91-14921
Sublimating icy planetesimals as the source of nucleation seeds for grain condensation in classical novae N91-15016
The influence of grain growth in circumstellar dust envelopes on observed colors and polarization of some eruptive stars N91-15020
The optical observations of x ray Nova GS2023+33 = V404 Cyg N91-15103

NOZZLE DESIGN
Low-noise nozzle valve
[NASA-CASE-MFS-28383-1] N91-14563

NOZZLE GEOMETRY
Internal performance of a hybrid axisymmetric/nonaxisymmetric convergent-divergent nozzle
[NASA-TM-4230] N91-14275

NUCLEAR ELECTRIC PROPULSION
Space transfer concepts and analysis for exploration missions
[NASA-CR-183943] N91-14358

NUCLEAR INTERACTIONS
Nucleus-nucleus collisions at very high energies
[DE91-004003] N91-14811

NUCLEAR MAGNETIC RESONANCE
Elucidation of fundamental properties of helium in metals by nuclear magnetic resonance techniques
[DE91-002715] N91-14460

NUCLEAR REACTORS
ITER global stability limits
[DE91-001488] N91-14845

NUCLEAR SCATTERING
Neutrino scattering by nuclei in imperfect media N91-15104

NUCLEAR STRUCTURE
Intermediate energy nuclear physics
[DE91-002758] N91-14809

NUCLEATION
Low-energy electron diffraction investigation of epitaxial growth: Pt and Pd(100)
[DE91-000750] N91-14873
Sublimating icy planetesimals as the source of nucleation seeds for grain condensation in classical novae N91-15016
Sublimating comets as the source of nucleation seeds for grain condensation in the gas outflow from AGB stars N91-15018

NUCLEON-NUCLEON INTERACTIONS
Nucleus-nucleus collisions at very high energies
[DE91-004003] N91-14811

NUCLEONS
Intermediate energy nuclear physics
[DE91-002758] N91-14809
Initial data from the Soudan 2 experiment
[DE91-004454] N91-14815

NUMERICAL ANALYSIS
A numerical and experimental analysis of reactor performance and deposition rates for CVD on monofilaments
[NASA-TM-103631] N91-14500
Studying quantum phase-based electronic devices
[AD-A226809] N91-14541
Scale-invariant theory of optical properties of fractal clusters
[AD-A227031] N91-14832

NUMERICAL CONTROL
Smart tunnel: Docking mechanism
[NASA-CASE-MSC-21360-1] N91-14374
Automated system for measuring the strength of optical fibers
[AD-D014626] N91-14824

O

O RING SEALS
Axisymmetric shell analysis of the space shuttle solid rocket booster field joint
[NASA-TP-3033] N91-14618
A parametric shell analysis of the shuttle 51-L SRB AFT field joint
[NASA-TM-102748] N91-14629

O STARS
Properties of interstellar dust in the region of the CEP OB4 association N91-14903
Additional red and reddened stars in Cyg OB2 association N91-14948

OBLIQUE SHOCK WAVES
Generation of inductive fields by an oblique magnetic rotator in collisionless plasma N91-15077

OBSTACLE AVOIDANCE
Flight data acquisition methodology for validation of passive ranging algorithms for obstacle avoidance
[NASA-TM-102809] N91-14322

OCEAN CURRENTS
The SYNOP experiment: Inverted echo sounder data report for October 1987 to May 1988
[AD-A227232] N91-14699

OCEAN MODELS
Climate and atmospheric modeling studies. Climate applications of Earth and planetary observations. Chemistry of Earth and environment
[NASA-CR-187326] N91-14684

OCEAN SURFACE
Perspectives on modeling electromagnetic sea scatter
[AD-A226939] N91-14520
Oceanographic expert system validation using GOAP mesoscale products and Gulf/DART validation test data
[AD-A226929] N91-14693
Shipboard and satellite observations of upper ocean velocity and transport variability in the Gulf Stream
[AD-A226974] N91-14694
The distribution of wave heights and periods for seas with unimodal bimodal power density spectra
[AD-A227040] N91-14696

OCEANOGRAPHIC PARAMETERS
Oceanographic expert system validation using GOAP mesoscale products and Gulf/DART validation test data
[AD-A226929] N91-14693

OCEANS
Shipboard and satellite observations of upper ocean velocity and transport variability in the Gulf Stream
[AD-A226974] N91-14694
The SYNOP experiment: Inverted echo sounder data report for October 1987 to May 1988
[AD-A227232] N91-14699

OCTANE NUMBER
CRC program for quantifying performance of knock-sensor-equipped vehicles with varying octane level
[AD-A227340] N91-14612

OHMIC DISSIPATION
Joule heating investigations using the sondrestrom radar and DMSP satellites
[AD-A227425] N91-14677

OLIGOMERS
N-(3-ethynylphenyl)maleimide
[NASA-CASE-LAR-14188-2] N91-14419

OLIVINE
Infrared spectra of crystalline and glassy silicates and application to interstellar dust N91-14994

ON-LINE PROGRAMMING
Feature set evaluation for classifiers
[AD-A226903] N91-14751
Feature set evaluation for classifiers
[AD-A226904] N91-14752
Feature set evaluation for classifiers
[AD-A226905] N91-14753

ON-LINE SYSTEMS
Adaptive control of large space structures
[AD-A227304] N91-14377
Feature set evaluation for classifiers
[AD-A226903] N91-14751
Feature set evaluation for classifiers
[AD-A226904] N91-14752
Feature set evaluation for classifiers
[AD-A226905] N91-14753

OPACITY
Neutrino scattering by nuclei in imperfect media N91-15104

OPEN CLUSTERS
IR emission and UV extinction in two open clusters N91-14929

OPERATING COSTS
Automatic dependent surveillance benefit and cost analysis
[DOT/FAA/RD-90/34] N91-14320

OPERATING SYSTEMS (COMPUTERS)
Graphics software for the HP825/9000 IFSI system
[IFSI-89-18] N91-14735

OPERATIONAL PROBLEMS
Software management issues — superconducting super collider detectors
[DE91-001031] N91-14763

OPERATORS (MATHEMATICS)
Studies in statistical signal processing
[AD-A226825] N91-14518
Nonlinear finite element dynamics on multiprocessor computers
[AD-A227409] N91-14761
A study of strong stability of distributed systems
[NASA-CR-187421] N91-14766
OPTICAL COMMUNICATION
Tapered fiber amplifier
[AD-D014629] N91-14512
International Symposium on Information Theory
[AD-A226957] N91-14521
Optical encoding of imaging data
[AD-D014617] N91-14821
Optoelectronic devices
[AD-D014618] N91-14822
OPTICAL COUPLING
Tapered fiber amplifier
[AD-D014629] N91-14512
OPTICAL DATA PROCESSING
Hybrid optical processor
[AD-A227163] N91-14834
OPTICAL FIBERS
Automated system for measuring the strength of optical fibers
[AD-D014626] N91-14824
Optical phase conjugation via stimulated Brillouin scattering in multimode optical fiber
[AD-A227054] N91-14833
OPTICAL MATERIALS
Approaches to the design of a novel macromolecular system with tailored optical properties
[AD-A226952] N91-14485
Nonlinear optics and organic materials
[AD-A226953] N91-14831
OPTICAL MEASUREMENT
Picosecond laser system for high speed characterization of monolithic devices
[AD-A227372] N91-14595
Scattering by anisotropic grains in beryllium mirrors
[DE91-001724] N91-14826
OPTICAL MEMORY (DATA STORAGE)
Spontaneous and induced coherent radiation generation in atomic vapors
[AD-A226776] N91-14830
OPTICAL POLARIZATION
Grain growth, optical polarisation, and extinction in interstellar clouds N91-14959
Multicolor optical polarimetry of reddened stars in the small Magellanic cloud N91-14986
The influence of grain growth in circumstellar dust envelopes on observed colors and polarization of some eruptive stars N91-15020
Polarization due to dust scattering in the planetary nebula Cn1-1 N91-15027
OPTICAL PROPERTIES
Adhesion at ceramic interfaces
[DE91-001660] N91-14480
Approaches to the design of a novel macromolecular system with tailored optical properties
[AD-A226952] N91-14485
Nonlinear optics and organic materials
[AD-A226953] N91-14831
Scale-invariant theory of optical properties of fractal clusters
[AD-A227031] N91-14832
Investigation of new semiinsulating behavior of 3-5 compounds
[AD-A226787] N91-14862
The relationship between IR, optical, and UV extinction N91-14899
The autocorrelation function of the North Pole dust N91-14901
Interstellar circular polarization and the dielectric nature of dust grains N91-14905
Optical properties of irregular interstellar grains N91-14995
Properties of grains derived from IRAS observations of dust N91-15001
OPTICAL PUMPING
An intense optically pumped H(-) ion source
[DE91-002949] N91-14827
Spontaneous and induced coherent radiation generation in atomic vapors
[AD-A226776] N91-14830
OPTICAL RADAR
Helicopter lidar bathymeter system. Conceptual design
[AD-A227057] N91-14348
OPTICAL RESONATORS
Characterization of semiconductor surface-emitting laser wafers
[DE91-001336] N91-14598
OPTICAL THICKNESS
Reddening and extinction towards H II regions N91-14898
Infrared emission from ultracompact H II regions N91-14942
Solar radiation on Mars: Update 1990
[NASA-TM-103623] N91-15117
OPTIMAL CONTROL
Randomly sampled-data control systems
[NASA-CR-187425] N91-14734
Projected implicit Runge-Kutta methods for differential-algebraic boundary value problems
[DE91-000660] N91-14791
OPTIMIZATION
Efficient parallel algorithms on the network model
[AD-A227144] N91-14771
The definition of necessary hidden units in neural networks for combinatorial optimization
[AD-A227142] N91-14786
Minimization on stochastic matroids
[AD-A227413] N91-14799
OPTOELECTRONIC DEVICES
Optoelectronic devices
[AD-D014618] N91-14822
ORBIT TRANSFER VEHICLES
Gamma guidance of trajectories for coplanar, aeroassisted orbital transfer
[NASA-CR-187732] N91-14365
Properties of the optimal trajectories for coplanar, aeroassisted orbital transfer
[NASA-CR-187733] N91-14366
Decomposition technique and optimal trajectories for the aeroassisted flight experiment
[NASA-CR-187734] N91-14367
Guidance trajectories for aeroassisted orbital transfer
[NASA-CR-187735] N91-14368
ORBITAL ASSEMBLY
Mechanical end joint system for connecting structural column elements
[NASA-CASE-LAR-14465-1] N91-14614
ORBITAL ELEMENTS
The Astronomical Almanac for the year 1989
[ISBN-0-11-886932-9] N91-15038
The Astronomical Almanac for the year 1990
[ISBN-0-11-886934-5] N91-15039
ORBITAL POSITION ESTIMATION
Satellite situation report, volume 30, no. 1
[NASA-TM-101105] N91-14372
ORBITAL SERVICING
System for connecting fluid couplings
[NASA-CASE-MFS-26042-1-SB] N91-14613
ORGANIC COMPOUNDS
Molecular and mass spectroscopic analysis of isotopically labeled organic residues N91-14961
The 3.4 micron emission in comets N91-15006
ORGANIC MATERIALS
Nonlinear optics and organic materials
[AD-A226953] N91-14831
ORGANIC SEMICONDUCTORS
Spontaneous and induced coherent radiation generation in atomic vapors
[AD-A226776] N91-14830
ORGANOMETALLIC COMPOUNDS
Program to study the process parameters of OMVPE and their relationship to the properties of Ga(0.47)In(0.53) as ON InP substrates
[AD-A226618] N91-14851
ORGANOMETALLIC POLYMERS
Synthesis and properties of novel organometallic polymers
[DE91-001978] N91-14491
ORION NEBULA
Dust clouds in Orion and the interstellar neutral hydrogen distribution N91-14941
ORIONID METEOROIDS
Dust of Orionid meteor shower in the Earth atmosphere before and after Halley's Comet N91-15012
ORTHOGONALITY
Studies in statistical signal processing
[AD-A226825] N91-14518
ORTHOTROPIC PLATES
Low velocity impact analysis with NASTRAN
[NASA-TM-103169] N91-14426
ORTHOTROPIC SHELLS
The buckling of off-axis, orthotropic, cylindrical shells in torsion N91-14628
OSCILLATING FLOW
Unsteady aerodynamic forces on an oscillating wing at high incidences and flow separation N91-14331
One- and two-dimensional Stirling machine simulation using experimentally generated flow turbulence models
[NASA-CR-185285] N91-14414
OSCILLATIONS
Investigation of a semi-empirical method to predict limit cycle oscillations of modern fighter aircraft N91-14333
Unsteady separated flow phenomena causing self-excited structural oscillations N91-14339
OSMOSIS
Coupled transport processes in semipermeable media. Part 1: Analytical solutions of the linearized governing equations
[DE91-004138] N91-14887
OUTGASSING
Outgassing data for selecting spacecraft materials, revision 2
[NASA-RP-1124-REV-2] N91-14437
OVER-THE-HORIZON RADAR
Radio Frequency Interference (RFI) measurements made near the proposed Alaska OTH receiving site
[AD-A226922] N91-14519
OXIDE FILMS
Fabrication of sensitive high Tc bolometers N91-14389
OXIDIZERS
Definition of experiments to investigate fire suppressants in microgravity
[NASA-CR-185295] N91-14378
OXYACETYLENE
An investigation of diamond synthesis in an oxygen-acetylene diffusion flame
[AD-A227224] N91-14870
OXYGEN
Laboratory studies of refractory metal oxide smokes N91-14993
Theoretical studies of important processes in planetary and comet atmospheres
[NASA-CR-187692] N91-15045
OXYGEN SPECTRA
New circumstellar dust component in oxygen rich environments N91-15023
OZONE
Next-generation fire extinguishing agent. Phase 2: Laboratory tests and scoping trials
[AD-A227347] N91-14510
Studies of the observed and theoretical variations of atmospheric ozone
[NASA-CR-187703] N91-14657
Acidic deposition: Its nature and impacts
[DE91-001984] N91-14658
NA-9 Solar Backscatter Ultraviolet (SBUV/2) instrument and derived ozone data
[AD-A227449] N91-15118
OZONOMETRY
NA-9 Solar Backscatter Ultraviolet (SBUV/2) instrument and derived ozone data
[AD-A227449] N91-15118

P

P-N JUNCTIONS
MBE HgCdTe heterostructure detectors N91-14402
Silicon carbide, a semiconductor for space power electronics
[NASA-TM-103655] N91-14850
PACIFIC OCEAN
Observations of ocean fluctuations between 15 and 23 hour periods in the Pacific
[AD-A227017] N91-14695
PACKET SWITCHING
Defense Data Network (DDN) performance analysis using probability modeling
[AD-A226856] N91-14894
PACKET TRANSMISSION
Defense Data Network (DDN) performance analysis using probability modeling
[AD-A226856] N91-14894
PACKETS (COMMUNICATION)
Defense Data Network (DDN) performance analysis using probability modeling
[AD-A226856] N91-14894
PAIN SENSITIVITY
Development of an animal model of human non-freezing cold injury: Changes in thermal sensitivity following cold exposure
[AD-A227174] N91-14705
PAINTS
An evaluation of two flat-black silicone paints for space application
[NASA-TM-100768] N91-14494
PALEOMAGNETISM
Block rotations, fault domains and crustal deformation in the western US N91-14666
Distributed deformation and block rotation in 3D N91-14667
PALLADIUM COMPOUNDS
Elucidation of fundamental properties of helium in metals by nuclear magnetic resonance techniques
[DE91-002715] N91-14460
PANEL METHOD (FLUID DYNAMICS)
Comparison of different calculation methods applied to a lenticular fuselage section N91-14293

PANELS
Structural response of marine sandwich panels to uniform pressure loading
[AD-A227038] N91-14434
PARALLEL PROCESSING (COMPUTERS)
Systolic emulator experimentation
[AD-A226746] N91-14516
CFD code evaluation for internal flow modeling
[NASA-CR-187677] N91-14557
NASA's supercomputing experience
[NASA-TM-102890] N91-14727
ISIS and META projects
[NASA-CR-186413] N91-14731
Nonlinear finite element dynamics on multiprocessor computers
[AD-A227409] N91-14761
Method of up-front load balancing for local memory parallel processors
[NASA-CASE-MSC-21348-1] N91-14769
Literature survey on tools
[AD-A226933] N91-14770
Efficient parallel algorithms on the network model
[AD-A227144] N91-14771
Massively parallel network architectures for automatic recognition of visual speech signals
[AD-A226968] N91-14805
PARALLEL PROGRAMMING
Boolean Grobner bases, calculation methods. Applications and parallel processing
[ETN-90-98208] N91-14768
Literature survey on tools
[AD-A226933] N91-14770
PARAMAGNETISM
Alignment mechanisms of paramagnetic grains revisited N91-14908
PARAMETER IDENTIFICATION
Efficient detection and signal parameter estimation with application to high dynamic GPS receiver
[NASA-CASE-NPO-17820-1-CU] N91-14321
The effect of wing planform on low speed buffet N91-14336
Research in progress in applied mathematics, numerical analysis, and computer science
[NASA-CR-187474] N91-14726
Control of distributed parameter systems
[AD-A227306] N91-14787
PARAMETERIZATION
Parametric study of afterbody/nozzle drag on twin two-dimensional convergent-divergent nozzles at Mach numbers from 0.60 to 1.20
[NASA-TP-2640] N91-14316
The optical parametrization of an aerial multispectral camera
[DE91-003017] N91-14593
PARTIAL DIFFERENTIAL EQUATIONS
Mappings and accuracy for Chebyshev pseudo-spectral approximations
[NASA-TM-103630] N91-14781
Control of distributed parameter systems
[AD-A227306] N91-14787
The computer algebra approach of the finite difference methods for PDEs
[DE90-631581] N91-14790
Stochastic histories of dust grains in the interstellar medium N91-14998
PARTICLE ACCELERATION
High-energy particle acceleration during the implosion driven by 3-dimensional X-type current loop coalescence in solar flares N91-15048
Solar flares and particle acceleration N91-15049
Bursts of energetic protons in the Earth's magnetotail N91-15058
PARTICLE ACCELERATORS
Data requirements for intermediate energy nuclear applications
[DE91-004005] N91-14812
PARTICLE COLLISIONS
Interstellar dust as generator of x ray radiation N91-14910
Grains charges in interstellar clouds N91-14967
Dust coagulation in ISM N91-14968
PARTICLE DENSITY (CONCENTRATION)
Annihilation radiation of strongly-magnetised electron-positron plasma with power-law distributions of particles N91-15078
PARTICLE ENERGY
Interstellar dust as generator of x ray radiation N91-14910
PARTICLE INTERACTIONS
Surface modification using low energy ground state ion beams
[NASA-CASE-NPO-17498-1-CU] N91-14813
PARTICLE MOTION
Method and apparatus for determining time, direction, and composition of impacting space particles
[NASA-CASE-LAR-13392-1-CU] N91-14412
PARTICLE PRECIPITATION
Polarization radar studies of precipitation: Implementation of the technique and data interpretation
[AD-A227073] N91-14690
PARTICLE PRODUCTION
Nucleus-nucleus collisions at very high energies
[DE91-004003] N91-14811
PARTICLE SIZE DISTRIBUTION
A balloon-borne aerosol spectrometer for high altitude low aerosol concentration measurements
[DE91-002563] N91-14661
PARTICLE SPIN
Study of spin-temperature effects using energy-ordered continuum gamma ray spectroscopy technique
[DE91-002854] N91-14818
PARTICLES
Polarization and extinction by aligned grains N91-14907
Alignment mechanisms of paramagnetic grains revisited N91-14908
Scattering by fluffy grains N91-14992
PATTERN RECOGNITION
Information extraction from visual displays and the event-related brain potential
[AD-A227063] N91-14722
Feature set evaluation for classifiers
[AD-A226903] N91-14751
Feature set evaluation for classifiers
[AD-A226904] N91-14752
Feature set evaluation for classifiers
[AD-A226905] N91-14753
PELLETS
Fueling of magnetically confined plasmas by single- and two-stage repeating pneumatic pellet injectors
[DE91-002635] N91-14839
PENETRATION
Experimental investigation of buffet onset and penetration on a supercritical airfoil at transonic speeds N91-14328
Unsteady separated flow phenomena causing self-excited structural oscillations N91-14339
Matter penetration and motion through the magnetosphere of neutron star N91-15087
PEPTIDES
Development of laser-ion beam photodissociation methods
[DE91-000680] N91-14448
PERFORMANCE PREDICTION
A unified approach to buffet response of fighter aircraft empennage N91-14326
Experimental investigation and semi-empirical prediction of the dynamic response of a low-aspect-ratio trapezoidal wing due to flow separation N91-14330
Reliability of photovoltaic concentrator modules
[DE90-012754] N91-14651
PERFORMANCE TESTS
An evaluation of two flat-black silicone paints for space application
[NASA-TM-100768] N91-14494
Position requirements for space station personnel and linkages to portable microcomputer performance assessment
[NASA-CR-185606] N91-14719
PERMEABILITY
Coupled transport processes in semipermeable media. Part 1: Analytical solutions of the linearized governing equations
[DE91-004138] N91-14887
PERMITTIVITY
Process for lowering the dielectric constant of polyimides using diamic acid additives
[NASA-CASE-LAR-13902-1] N91-14484
PERMUTATIONS
Matrix techniques for faster routing of affine permutations on a mesh interconnection network
[RUU-CS-90-19] N91-14767
PERSONAL COMPUTERS
Integration of sneak analysis with design, volume 1
[AD-A226902] N91-14543
PETRI NETS
Prototyping of a protocol validation environment: Application to the Estelle approach
[LAAS-90113] N91-14774
PHARMACOLOGY
Bioreactivity: Studies on a simple brain stem reflex in behaving animals
[AD-A226823] N91-14704
PHASE CHANGE MATERIALS
High-temperature thermal storage systems for advanced solar receivers materials selections
[NASA-CR-187750] N91-14647
PHASE CONJUGATION
Optical phase conjugation via stimulated Brillouin scattering in multimode optical fiber
[AD-A227054] N91-14833
PHASE DETECTORS
Eddy current method for measuring electrical resistivity and device for providing accurate phase detection
[AD-D014571] N91-14530
PHASE DIAGRAMS
Chemical vapor deposition modeling: An assessment of current status
[NASA-CR-185301] N91-14511
PHASE MODULATION
Optical phase conjugate beam modulator and method therefor
[AD-D014569] N91-14820
Spontaneous and induced coherent radiation generation in atomic vapors
[AD-A226776] N91-14830
PHASE SHIFT KEYING
Trellis coded modulation for transmission over fading mobile satellite channel
[NASA-CASE-NPO-16904-2-CU] N91-14523
PHASE TRANSFORMATIONS
The effect of scandium on the phase stability of Al3Nb and Al3Zr
[DE91-002657] N91-14459
New multiphase equation of state for polycrystalline quartz
[DE91-001048] N91-14490
Phase changes during plasma spray deposition
[IPPCZ-297] N91-14837
Effect of step edge transition rates and anisotropy in simulations of epitaxial growth
[DE91-001251] N91-14875
An ion-channeling study of irradiation-induced amorphization of YBa2Cu3O(7-x)
[DE91-004488] N91-14884
PHASED ARRAYS
MMIC compensation network for phased array element mismatch
[AD-A227437] N91-14522
Millimeter-wave monolithic diode-grid frequency multiplier
[NASA-CASE-NPO-17258-1-CU] N91-14551
PHENOLIC RESINS
Characterization of phenolic resins with thermogravimetry-mass spectrometry
[DE91-002710] N91-14492
PHENYLS
Bis (4-(3,4-dimethylene-pyrrolidyl)-phenyl) methane
[NASA-CASE-LAR-13965-2-CU] N91-14418
PHONETICS
Perception and temporal properties of speech
[AD-A226958] N91-14716
PHOSPHORIC ACID FUEL CELLS
Prospects of new energy
[DE91-727567] N91-14654
PHOSPHORS
X ray sensitive area detection device
[NASA-CASE-MFS-28232-1] N91-14835
PHOSPHORUS
Processing experiments for development of high-efficiency silicon solar cells
[DE91-002698] N91-14645
PHOTOCHEMICAL REACTIONS
Development of laser-ion beam photodissociation methods
[DE91-000680] N91-14448
New insights in the photochemistry of grain mantles: The identification of the 4.62 and 6.87 micron bands N91-14957
PHOTOCONDUCTIVITY
LWIR detector research in InAsSb/InAs N91-14406
InAs/Ga(1-x)In(x)Sb superlattices for infrared detector applications N91-14407
PHOTOCONDUCTORS
HgCdTe for NASA EOS missions and detector uniformity benchmarks N91-14385
HgZnTe-based detectors for LWIR NASA applications N91-14404
Rise time and recovery of GaAs photoconductive semiconductor switches
[DE91-001267] N91-14854
PHOTODIODES
InAs/GaAs and InAs doping superlattices N91-14409
Optically-triggered GaAs thyristor switch s: Integrated structures for environmental hardening
[DE91-001355] N91-14553
The design of optical sensor for the pinhole/occulter facility
[NASA-CR-187694] N91-14825
PHOTODISSOCIATION
Photodissociation near a rough metal surface: Effect of reaction fields
[AD-A227030] N91-14445
Development of laser-ion beam photodissociation methods
[DE91-000680] N91-14448

The evolution of organic mantles on interstellar grains N91-14964

PHOTOELECTRIC EMISSION
New heterojunction LWIR detector options N91-14398
Novel Si(1-x)Ge(x)/Si heterojunction internal photoemission long wavelength infrared detectors N91-14401
Photogenerated carrier-induced reaction on semiconductor surfaces
[DE91-001349] N91-14878

PHOTOGRAMMETRY
Fitting of photogrammetry and field completion
[ETN-91-98144] N91-14640

PHOTOIONIZATION
PAHs molecules and heating of the interstellar gas N91-14939
Spectral synthesis code LINESPEC: Ionisation equilibrium of plasma and absorption spectra formation N91-15106

PHOTOLUMINESCENCE
InAs/Ga(1-x)In(x)Sb superlattices for infrared detector applications N91-14407

PHOTOLYSIS
Molecular and mass spectroscopic analysis of isotopically labeled organic residues N91-14961

PHOTOMAPPING
Fitting of photogrammetry and field completion
[ETN-91-98144] N91-14640

PHOTOMETERS
Innovative Long Wavelength Infrared Detector Workshop Proceedings
[NASA-CR-187433] N91-14379
Detector array evaluation and figures of merit N91-14386
Quantum Well Infrared Photodetectors (QWIP) N91-14392
Photovoltaic quantum well infrared photodetectors N91-14393
Resonant tunneling IR detectors N91-14395
LWIR detector research in InAsSb/InAs N91-14406
IR detectors based on n-i-p-i superlattices N91-14408
Monolithic multichannel detector amplifier arrays and circuit
[AD-D014566] N91-14528

PHOTOMETRY
Far infrared structure of spiral galaxies from the IRAS CPC images N91-14988
The optical observations of x ray Nova GS2023+33 = V404 Cyg N91-15103

PHOTONICS
Integrated optical devices for photonics instrumentation systems
[DE91-004192] N91-14828

PHOTONS
Production and transfer of UV photons in non-homogeneous spherical clouds N91-14966

PHOTOSYNTHESIS
Comparison of ground and satellite based measurements of the fraction of photosynthetically active radiation intercepted by tall-grass prairie
[NASA-CR-187696] N91-14639

PHOTOTRANSISTORS
Optically-triggered GaAs thyristor switch s: Integrated structures for environmental hardening
[DE91-001355] N91-14553

PHOTOVOLTAIC CELLS
Status of LWIR HgCdTe infrared detector technology N91-14383
Reliability of photovoltaic concentrator modules
[DE90-012754] N91-14651
The synthesis of solar radiation data for sizing stand-alone photovoltaic systems
[DE90-012758] N91-14652

PHOTOVOLTAIC CONVERSION
HgCdTe for NASA EOS missions and detector uniformity benchmarks N91-14385

PHOTOVOLTAIC EFFECT
Photovoltaic quantum well infrared photodetectors N91-14393

PHYSICS
Construction of large-scale simulation codes using ALPAL (A Livermore Physics Applications Language)
[DE91-002783] N91-14740

PHYSIOLOGY
Initial blood storage experiment
[NASA-CR-185513-PT-2] N91-14701
Bioreactivity: Studies on a simple brain stem reflex in behaving animals
[AD-A226823] N91-14704
Dual physiological rate measurement instrument
[NASA-CASE-MSC-20078-3] N91-14709

PICOSECOND PULSES
Picosecond laser system for high speed characterization of monolithic devices
[AD-A227372] N91-14595

PIEZOELECTRICITY
Development of a taction system using piezoelectric film
[AD-A227076] N91-14544
Piezoelectrostatic generator
[NASA-CASE-MFS-28298-1] N91-14872

PILOT PERFORMANCE
Interaction of feel system and flight control system dynamics on lateral flying qualities
[NASA-CR-179445] N91-14353
Prediction of helicopter simulator sickness
[DE90-016530] N91-14710

PINCH EFFECT
On the generation of magnetic fields in active star atmospheres N91-15099

PINHOLE CAMERAS
The design of optical sensor for the pinhole/occulter facility
[NASA-CR-187694] N91-14825

PINHOLE OCCULTER FACILITY
The design of optical sensor for the pinhole/occulter facility
[NASA-CR-187694] N91-14825

PIONS
Intermediate energy nuclear physics
[DE91-002758] N91-14809

PIPE FLOW
Dynamic stability of a spinning tube conveying a fluid through a symmetrical noncircular cross-section
[DE91-004146] N91-14573

PIPES (TUBES)
Dynamic stability of a spinning tube conveying a fluid through a symmetrical noncircular cross-section
[DE91-004146] N91-14573
Enable Kit (MC-4246) for the DOT Charged Line System: Welding development report for 1/4-inch tubes and fittings
[DE91-002577] N91-14606
Quick connect coupling
[NASA-CASE-MSC-21539-1] N91-14610
Axial-torsional fatigue: A study of tubular specimen thickness effects
[NASA-TM-103637] N91-14632

PITCH (INCLINATION)
Modeling and control design of a wind tunnel model support
[NASA-TM-103829] N91-14540

PITCHING MOMENTS
Measurement of hydrodynamic forces and moments and flow field mapping of a model in coning motion
[AD-A226684] N91-14355

PLANE WAVES
A simple plane-wave explosive lens
[DE91-004297] N91-14526
An investigation of the diffraction of an acoustic plane wave by a curved surface of finite impedance N91-14800

PLANETARY ATMOSPHERES
Theoretical studies of important processes in planetary and comet atmospheres
[NASA-CR-187692] N91-15045

PLANETARY BOUNDARY LAYER
A mesoscale planetary boundary layer numerical model for simulations of topographically induced circulations N91-15113

PLANETARY CRUSTS
Specification goals for a Mars seismic network N91-14360

PLANETARY GEOLOGY
A bibliography of planetary geology and geophysics principal investigators and their associates, 1989-1990
[NASA-TM-4221] N91-15034

PLANETARY IONOSPHERES
Studies of the chemistry of the nightside ionosphere of Venus
[NASA-CR-187714] N91-15114

PLANETARY MAPPING
Method for detecting surface motions and mapping small terrestrial or planetary surface deformations with synthetic aperture radar
[NASA-CASE-NPO-17831-1-CU] N91-14642

PLANETARY NEBULAE
The capability of the ultraviolet imaging telescope for observing interstellar dust N91-14913
Airborne observations of the infrared emission bands N91-14919
A survey for PAH emission in H II regions, planetary and proto-planetary nebulae N91-14920
Carbon stars with alpha-C:H emission N91-15022
Polarization due to dust scattering in the planetary nebula Cn1-1 N91-15027
Compact reflection nebulae, a transit phase of evolution from post-AGB to planetary nebulae N91-15029
Continuous infrared emission of proto- and young-planetary nebulae N91-15030
The discovery of a highly polarized bipolar nebula N91-15031

PLANETARY ROTATION
The rotation of Venus and its atmosphere N91-15112

PLANETARY SURFACES
Method for detecting surface motions and mapping small terrestrial or planetary surface deformations with synthetic aperture radar
[NASA-CASE-NPO-17831-1-CU] N91-14642

PLANNING
Human factors engineering. Part 1: Test procedures
[AD-A226480] N91-14720
Planning the behavior of dynamical systems
[AD-A227381] N91-14788

PLASMA CLOUDS
Laboratory and computer simulations of wave generation processes in non-stationary astrophysical phenomena N91-15082

PLASMA COMPRESSION
On the generation of magnetic fields in active star atmospheres N91-15099

PLASMA CONTROL
Recent long-pulse and high-average-power tests on a 140 GHz gyrotron
[DE91-001680] N91-14592
LLE (Laboratory for Laser Energetics) review
[DE91-001254] N91-14597
Fast electron studies in the ZT-40M edge plasma
[DE91-002323] N91-14838
Characteristics and potential applications of an ORNL microwave ECR multicusp plasma ion source
[DE91-002649] N91-14840
Wall conditioning and plasma surface interactions in DIII-D
[DE91-001547] N91-14846
DIII-D results and plans
[DE91-001548] N91-14847

PLASMA CURRENTS
Generation of inductive fields by an oblique magnetic rotator in collisionless plasma N91-15077

PLASMA DIAGNOSTICS
LLE (Laboratory for Laser Energetics) review
[DE91-001254] N91-14597
IR and FIR laser diagnostics for plasma thrusters using a CW CO2 radiation source
[AD-A226816] N91-14843
Characterization of electron cyclotron resonance hydrogen plasmas
[DE91-001250] N91-14844

PLASMA ENGINES
High temperature refractory member with radiation emissive overcoat
[NASA-CASE-NPO-17122-1-CU] N91-14489
IR and FIR laser diagnostics for plasma thrusters using a CW CO2 radiation source
[AD-A226816] N91-14843

PLASMA EQUILIBRIUM
Spectral synthesis code LINESPEC: Ionisation equilibrium of plasma and absorption spectra formation N91-15106

PLASMA HEATING
Characteristics and potential applications of an ORNL microwave ECR multicusp plasma ion source
[DE91-002649] N91-14840

PLASMA INTERACTIONS
Wall conditioning and plasma surface interactions in DIII-D
[DE91-001547] N91-14846
Laboratory simulation of the astrophysical burst processes in non-uniform magnetised media N91-15081
Nonlinear plasma effects in the environment of active galactic nuclei N91-15085

PLASMA JETS
Magnetically driven jets and winds N91-15084

PLASMA OSCILLATIONS
The plasma model of radioemission from SN 1987A N91-15101

PLASMA PINCH
Generation of cosmic rays in pinches N91-15070

PLASMA RADIATION
Maser cyclotron instability in a plasma with anisotropic distribution function N91-15075

PLASMA RESONANCE
Wave collapse at lower hybrid resonance N91-15073

PLASMA SPRAYING
Phase changes during plasma spray deposition
[IPPCZ-297] N91-14837

PLASMA TURBULENCE
Tokamak fluidlike equations, with applications to turbulence and transport in H mode discharges
[DE91-002632] N91-14849
Plasma waves associated with the space shuttle N91-15064
Nonlinear plasma effects in the environment of active galactic nuclei N91-15085
PLASMA WAVES
Detection of nonlinear features in plasma and field measurements by PROGNOZ-8 N91-15063
Plasma waves associated with the space shuttle N91-15064
Laboratory and computer simulations of wave generation processes in non-stationary astrophysical phenomena N91-15082
Magnetically driven jets and winds N91-15084
Ultrarelativistic low-frequency electromagnetic waves in pulsar magnetospheres N91-15091
PLASMAS (PHYSICS)
Fueling of magnetically confined plasmas by single- and two-stage repeating pneumatic pellet injectors
[DE91-002635] N91-14839
Plasma Astrophysics
[ESA-SP-311] N91-15046
Experiments with collision of vortices in rotating and still free-surface shallow water N91-15080
PLASTICS
Thermal analyses for quality control of plastics, ceramics, and explosives
[DE91-002701] N91-14622
PLATELETS
Initial blood storage experiment
[NASA-CR-185513-PT-1] N91-14700
Initial blood storage experiment
[NASA-CR-185513-PT-2] N91-14701
PLATES (STRUCTURAL MEMBERS)
Failure in laminated composite plates containing a hole
[AD-A227307] N91-14435
PLATINUM ALLOYS
Anomalous surface phase formation on Pt3Sn with zone axes group (100)
[DE91-001794] N91-14456
PLOTTING
Color palette: Plotting guide for use with GSMAP and GSDRAW digital cartographic software
[DE91-001643] N91-14737
PLUMES
Computational models with advanced thermochemistry for the analysis of missile/plume flowfield interactions N91-14305
PLY ORIENTATION
An analysis of interlaminar stresses in unsymmetrically laminated plates
[NASA-CR-187657] N91-14424
Structural response of marine sandwich panels to uniform pressure loading
[AD-A227038] N91-14434
PNEUMATICS
Fueling of magnetically confined plasmas by single- and two-stage repeating pneumatic pellet injectors
[DE91-002635] N91-14839
POINT SOURCES
IRAS results on outer galaxy star formation N91-14953
Infrared cirrus point sources N91-14978
POINTING CONTROL SYSTEMS
Device and method for monitoring the presence of an object in space
[AD-D014621] N91-14823
The design of optical sensor for the pinhole/occulter facility
[NASA-CR-187694] N91-14825
POLAR ORBITS
A polar orbit for the Mars Global Network Mission N91-14361
POLAR REGIONS
The autocorrelation function of the North Pole dust N91-14901
Diffuse galactic light observations at 206 selected areas N91-14914
Continuum radiative transfer in accretion-powered pulsars N91-15043
POLARIMETERS
Earth Observing Scanning Polarimeter (EOSP), phase B
[NASA-CR-187715] N91-14586
POLARIMETRY
Remote sensing of Earth terrain
[NASA-CR-186904] N91-14635
Multicolor optical polarimetry of reddened stars in the small Magellanic cloud N91-14986
POLARIZATION (WAVES)
The wavelength dependence of polarization in NGC 2023 N91-14923
A two micron polarization survey toward dark clouds N91-14952
Annihilation radiation of strongly-magnetised electron-positron plasma with power-law distributions of particles N91-15078
POLARIZATION CHARACTERISTICS
Polarization and extinction by aligned grains N91-14907
POLICIES
Environmental impact assessment as applied to policies, plans, and programs
[DE91-001372] N91-14664
Information technology and the conduct of research: The user's view. Report of the Panel on Information Technology and the Conduct of Research
[ISBN-0-309-03888-X] N91-14890
POLLUTION CONTROL
Combined air and water pollution control system
[NASA-CASE-NST-00007-1] N91-14662
POLLUTION TRANSPORT
Validity of environmental transfer models
[DE91-002929] N91-14660
POLOIDAL FLUX
A method for estimating tokamak poloidal field coil currents which incorporates engineering constraints
[DE91-001662] N91-14848
POLYAMIDE RESINS
Mesomechanical model for fibre composites
[AD-A226792] N91-14432
POLYCRYSTALS
Application of ultrasonic guided waves to the characterization of texture in metal sheets of cubic and hexagonal crystallites
[DE91-001107] N91-14466
New multiphase equation of state for polycrystalline quartz
[DE91-001048] N91-14490
High efficiency cadmium and zinc telluride-based thin film solar cells
[DE91-002112] N91-14643
Investigations of ultrasonic wave interactions with grain boundaries and grain imperfections
[DE91-002695] N91-14804
Growth, characterization and device development in monocrystalline diamond films
[AD-A227238] N91-14871
POLYETHYLENES
Mesomechanical model for fibre composites
[AD-A226792] N91-14432
POLYHEDRONS
Hidden surface removal for axis-parallel polyhedra
[RUU-CS-90-21] N91-14736
Boundary value problems of the elasticity theory for polyhedra: Singularities and approximation with boundary element methods
[ETN-91-98168] N91-14780
POLYIMIDES
Bis (4-(3,4-dimethylene-pyrrolidyl)-phenyl) methane
[NASA-CASE-LAR-13965-2-CU] N91-14418
Process for lowering the dielectric constant of polyimides using diamic acid additives
[NASA-CASE-LAR-13902-1] N91-14484
POLYMER CHEMISTRY
N-(3-ethynylphenyl)maleimide
[NASA-CASE-LAR-14188-2] N91-14419
Approaches to the design of a novel macromolecular system with tailored optical properties
[AD-A226952] N91-14485
Characterization of phenolic resins with thermogravimetry-mass spectrometry
[DE91-002710] N91-14492
POLYMER MATRIX COMPOSITES
Surface and interfacial properties of carbon fibers
[NASA-CR-184916] N91-14429
Structural response of marine sandwich panels to uniform pressure loading
[AD-A227038] N91-14434
POLYMERIC FILMS
Development of a taction system using piezoelectric film
[AD-A227076] N91-14544
POLYMERS
Approaches to the design of a novel macromolecular system with tailored optical properties
[AD-A226952] N91-14485
Nonlinear optics and organic materials
[AD-A226953] N91-14831
POLYNOMIALS
Studies in statistical signal processing
[AD-A226825] N91-14518
Mappings and accuracy for Chebyshev pseudo-spectral approximations
[NASA-TM-103630] N91-14781
POROSITY
Electrophoretic and electrolytic deposition of ceramic particles on porous substrates
[AD-A227371] N91-14488
Scattering by fluffy grains N91-14992
POROUS MATERIALS
Coupled transport processes in semipermeable media. Part 1: Analytical solutions of the linearized governing equations
[DE91-004138] N91-14887
PORTABLE EQUIPMENT
Developing portable user interfaces for Ada command control software
[AD-A226712] N91-14747
POSITION (LOCATION)
A global view of lander-to-orbiter communications accessibility for a Mars Global Network Mission N91-14362
Effect of atmospherics on beamforming accuracy
[NASA-CR-187695] N91-14802
Acoustic positioning and orientation prediction
[NASA-CASE-NPO-17511-1-CU] N91-14807
A beam position monitor for low current dc beams
[CEBAF-PR-89-004] N91-14816
POSITION SENSING
Contribution to the specification and implementation of complex robot tasks
[ETN-90-98209] N91-14604
POSITIONING
Modeling and control design of a wind tunnel model support
[NASA-TM-103829] N91-14540
Acoustic positioning and orientation prediction
[NASA-CASE-NPO-17511-1-CU] N91-14807
POTASSIUM COMPOUNDS
On the crystal structure of KInS2-I
[AD-A226940] N91-14866
POTENTIAL THEORY
Aerodynamic characteristics of cylindrical bodies with pointed and truncated conical noses N91-14289
POWDER (PARTICLES)
Aluminum nitride-silicon carbide whisker composites: Processing, properties, and microstructural stability
[DE91-001907] N91-14425
POWDERED ALUMINUM
Dynamic consolidation of aluminum-silicon carbide composites
[DE91-001929] N91-14427
POWER EFFICIENCY
Recent long-pulse and high-average-power tests on a 140 GHz gyrotron
[DE91-001680] N91-14592
Effects of wind shear and turbulence on wind turbine power curves
[DE91-004072] N91-14648
POWER SPECTRA
The distribution of wave heights and periods for seas with unimodal bimodal power density spectra
[AD-A227040] N91-14696
POWERED MODELS
Results of a sub-scale model rotor icing test
[NASA-TM-103709] N91-14309
PRECIPITATION (CHEMISTRY)
Electroless nickel bath recovery by cation exchange and precipitation
[DE91-001988] N91-14457
PRECIPITATION HARDENING
An examination of delta prime growth in an aluminum-lithium alloy by x ray diffraction
[AD-A227254] N91-14464
PRECIPITATION PARTICLE MEASUREMENT
An examination of delta prime growth in an aluminum-lithium alloy by x ray diffraction
[AD-A227254] N91-14464
Polarization radar studies of precipitation: Implementation of the technique and data interpretation
[AD-A227073] N91-14690
PREDICTION ANALYSIS TECHNIQUES
Missile Aerodynamics
[AGARD-CP-493] N91-14278
Review of the spring 1988 AGARD FMP symposium N91-14280
Store carriage, integration, and release N91-14281
Computation of viscous supersonic flows N91-14283
NUFA: A semi-empirical method for the prediction of isolated weapon aerodynamics N91-14287
A semi-empirical prediction method for missile aerodynamics N91-14288
Systematic investigations of body-wing-tail interference at high angles of attack N91-14290
Comparison of different calculation methods applied to a lenticular fuselage section N91-14293
Anticipation of aerodynamic coefficients of missile air intakes N91-14297
Chordwise and spanwise centers of pressure of missile fins N91-14304

Results of a sub-scale model rotor icing test
[NASA-TM-103709] N91-14309
Aircraft Dynamic Loads Due to Flow Separation
[AGARD-CP-483] N91-14324
Unsteady aerodynamic forces on an oscillating wing at high incidences and flow separation N91-14331
Investigation of a semi-empirical method to predict limit cycle oscillations of modern fighter aircraft N91-14333
Predictions of F-111 TACT aircraft buffet response N91-14335
Methods for evaluating the predictive accuracy of structural dynamic models
[NASA-CR-187649] N91-14630
Fatigue reliability of wind turbine components
[DE91-001262] N91-14650
Plate motions and deformations from geologic and geodetic data
[NASA-CR-187379] N91-14672
Cyclomatic complexity as a utility for predicting software faults
[AD-A227313] N91-14760
Semi-implicit time integration in limited area model
[AD-A226818] N91-14785

PREDICTIONS
Acoustic positioning and orientation prediction
[NASA-CASE-NPO-17511-1-CU] N91-14807

PREMIXING
Numerical study of shock-wave/boundary layer interactions in premixed hydrogen-air hypersonic flows
[NASA-TM-103273] N91-14559

PREPARATION
Procedures for the preparation of samples for cross-sectional transmission electron microscopy
[AD-A227013] N91-14444

PRESERVING
Initial blood storage experiment
[NASA-CR-185513-PT-1] N91-14700

PRESSURE MEASUREMENT
Pressure measurements on slender bodies at supersonic speeds and development of flow separation critera for Euler codes N91-14282
Comparison of different calculation methods applied to a lenticular fuselage section N91-14293
Wind tunnel investigation and flight tests of tail buffet on the CF-18 aircraft N91-14325

PRESSURE OSCILLATIONS
Investigation of combustion in large vortices
[AD-A226791] N91-14441

PRESSURE REGULATORS
Bio-reactor chamber
[NASA-CASE-MSC-20929-1] N91-14703

PRESSURE SENSORS
Wind tunnel balance
[NASA-CASE-ARC-11877-1-SB] N91-14357
Dynamic behavior of thin silicon plate: Application to silicon sensors
[LAAS-90144] N91-14582
The SYNOP experiment: Inverted echo sounder data report for October 1987 to May 1988
[AD-A227232] N91-14699

PRESSURE VESSELS
Hazards and safeguards of high pressure hydraulic fatigue testing
[AD-A226767] N91-14509

PRIMARY COSMIC RAYS
On the primary cosmic ray nuclei spectra behaviour in the 10(exp 16) eV energy region N91-15069

PROBABILITY DISTRIBUTION FUNCTIONS
On probability intervals and their updating
[RUU-CS-90-22] N91-14793

PROBABILITY THEORY
Analysis of success probability/cost trades for small landers in a Mars network N91-14363
Fatigue reliability of wind turbine components
[DE91-001262] N91-14650
Investigations of probabilistic inference
[AD-A226882] N91-14795
Interpretation of conditional probabilities in probabilistic interference word problems
[AD-A226907] N91-14797
Defense Data Network (DDN) performance analysis using probability modeling
[AD-A226856] N91-14894
Dust coagulation in ISM N91-14968

PROBLEM SOLVING
Planning the behavior of dynamical systems
[AD-A227381] N91-14788
Investigations of probabilistic inference
[AD-A226882] N91-14795

PROCESS CONTROL (INDUSTRY)
N-(3-ethynylphenyl)maleimide
[NASA-CASE-LAR-14188-2] N91-14419
A numerical and experimental analysis of reactor performance and deposition rates for CVD on monofilaments
[NASA-TM-103631] N91-14500
Processing experiments for development of high-efficiency silicon solar cells
[DE91-002698] N91-14645

PRODUCTION COSTS
Tips on how to cut technical publications costs
[AD-A227334] N91-14895

PROGRAM VERIFICATION (COMPUTERS)
Oceanographic expert system validation using GOAP mesoscale products and Gulf/DART validation test data
[AD-A226929] N91-14693
Methodology investigation of software maturity model validation
[AD-A226697] N91-14746
Mechanizing proof theory: Resource-aware logics and proof transformations to extract implicit information
[AD-A227147] N91-14758
Development of phenomenological fitting procedure for the fast microcomputer
[AD-A227168] N91-14759

PROGRAMMING LANGUAGES
A CLOS (Common Lisp Object System) implementation on top of KEE (Knowledge Engineering Environment)
[DE91-001957] N91-14739
Construction of large-scale simulation codes using ALPAL (A Livermore Physics Applications Language)
[DE91-002783] N91-14740
Capturing strong reduction in director string calculus
[AD-A226738] N91-14783

PROJECT MANAGEMENT
Environmental impact assessment as applied to policies, plans, and programs
[DE91-001372] N91-14664

PROJECT PLANNING
Environmental impact assessment as applied to policies, plans, and programs
[DE91-001372] N91-14664
A proposed astronomical reference catalog of infrared sources
[AD-A226757] N91-15041

PROJECTILES
Three dimensional flow calculations for a projectile with standard and dome bases N91-14294
Navier-Stokes predictions of static and dynamic aerodynamic derivatives for high L/D finned projectiles N91-14295
AC-130H Gunship Armor Upgrade Project
[DE91-002567] N91-14428
Direct numerical simulation of turbulent couette flow, part 2
[AD-A226770] N91-14564
Data requirements for intermediate energy nuclear applications
[DE91-004005] N91-14812

PROPAGATION MODES
HEM(sub 11) modes revisited
[DE91-001028] N91-14819

PROPAGATION VELOCITY
Effect of atmospherics on beamforming accuracy
[NASA-CR-187695] N91-14802

PROPELLANT CHEMISTRY
Analysis of hydroxylammonium nitrate based liquid propellants
[AD-A227300] N91-14497

PROPELLANT TRANSFER
System for connecting fluid couplings
[NASA-CASE-MFS-26042-1-SB] N91-14613

PROPULSION
Anticipation of aerodynamic coefficients of missile air intakes N91-14297
Research as part of the Air Force Research in Aero-Propulsion Technology (AFRAPT) program
[AD-A226893] N91-14350

PROPULSION SYSTEM CONFIGURATIONS
Overview of propulsion concepts for tactical missiles N91-14296

PROPULSION SYSTEM PERFORMANCE
Overview of propulsion concepts for tactical missiles N91-14296
CRC program for quantifying performance of knock-sensor-equipped vehicles with varying octane level
[AD-A227340] N91-14612

PROTECTION
A cable vehicle barrier for alert aircraft protection
[DE91-001723] N91-14354

PROTECTIVE COATINGS
High temperature refractory member with radiation emissive overcoat
[NASA-CASE-NPO-17122-1-CU] N91-14489
An evaluation of two flat-black silicone paints for space application
[NASA-TM-100768] N91-14494

PROTOCOL (COMPUTERS)
Prototyping of a protocol validation environment: Application to the Estelle approach
[LAAS-90113] N91-14774

PROTONS
High-energy particle acceleration during the implosion driven by 3-dimensional X-type current loop coalescence in solar flares N91-15048
Solar flares and particle acceleration N91-15049
Bursts of energetic protons in the Earth's magnetotail N91-15058

PROTOPLANETS
A survey for PAH emission in H II regions, planetary and proto-planetary nebulae N91-14920
Sublimating icy planetesimals as the source of nucleation seeds for grain condensation in classical novae N91-15016
The discovery of a highly polarized bipolar nebula N91-15031

PROTOSTARS
High resolution observations of compact H II regions at 230 GHz N91-14954
Distribution of the 3.1 micron feature in Cepheus A N91-14958
Absorption features in the 3 micron spectra of highly obscured objects N91-14965
Dust in regions of massive star formation N91-14972

PROVING
Mechanizing proof theory: Resource-aware logics and proof transformations to extract implicit information
[AD-A227147] N91-14758

PSYCHOACOUSTICS
Perception and temporal properties of speech
[AD-A226958] N91-14716

PSYCHOLOGICAL EFFECTS
The effects of sleep loss on individual and group performance
[AD-A226963] N91-14708

PSYCHOLOGICAL FACTORS
The object display: Principles and review of experimental findings
[AD-A226883] N91-14796

PSYCHOMETRICS
Interpretation of conditional probabilities in probabilistic interference word problems
[AD-A226907] N91-14797

PSYCHOMOTOR PERFORMANCE
Validation of dichotic listening and psychomotor task performance as predictors of primary flight training criteria: Highlighting relevant statistical issues
[AD-A227010] N91-14717

PSYCHOPHYSICS
Eye movements and visual information processing
[AD-A226782] N91-14714

PULLEYS
A cable vehicle barrier for alert aircraft protection
[DE91-001723] N91-14354

PULSAR MAGNETOSPHERES
Matter penetration and motion through the magnetosphere of neutron star N91-15087
On the existence of circular polarisation in the pulsar radiation N91-15088
Ultrarelativistic low-frequency electromagnetic waves in pulsar magnetospheres N91-15091
On the possibility of discovering pulsed radiation from SN 1987A N91-15102

PULSARS
On the existence of circular polarisation in the pulsar radiation N91-15088
On the braking mechanisms of pulsars N91-15090
Ultrarelativistic low-frequency electromagnetic waves in pulsar magnetospheres N91-15091
On the theory of large-scale micropulse structure of pulsar radio radiation N91-15092

PULSE COMMUNICATION
Trellis coded modulation for transmission over fading mobile satellite channel
[NASA-CASE-NPO-16904-2-CU] N91-14523

PULSE DURATION
Recent long-pulse and high-average-power tests on a 140 GHz gyrotron
[DE91-001680] N91-14592

PULSE GENERATORS
Rise time and recovery of GaAs photoconductive semiconductor switches
[DE91-001267] N91-14854

PULSE RATE
Dual physiological rate measurement instrument
[NASA-CASE-MSC-20078-3] N91-14709

PULSED LASERS
Study of diamond film growth and properties
[NASA-CR-187709] N91-14483

PULSED RADIATION
On the theory of large-scale micropulse structure of pulsar radio radiation N91-15092
On the possibility of discovering pulsed radiation from SN 1987A N91-15102

PURIFICATION
In-line sensors for electrolytic magnesium cells
[DE91-002561] N91-14438

PYROELECTRICITY
Pyroelectric detectors N91-14390
PYROXENES
Steps toward interstellar silicate dust mineralogy N91-14991

Q

QUADRUPOLES
Design and application possibilities of superconducting radio-frequency quadrupoles [DE91-004477] N91-14881
First tests of a superconducting RFQ (radio frequency quadrupole) structure [DE91-004483] N91-14883
QUALIFICATIONS
Space shuttle redesigned solid rocket motor Certificate of Qualification (COQ) data report [NASA-CR-184051] N91-14416
QUALITY CONTROL
The high cost of low quality in R/D (Research and Development) [DE91-002118] N91-14621
Thermal analyses for quality control of plastics, ceramics, and explosives [DE91-002701] N91-14622
Quality control and nondestructive test procedures for welded products [DE91-004530] N91-14623
QUANTITATIVE ANALYSIS
In-line sensors for electrolytic magnesium cells [DE91-002561] N91-14438
QUANTUM EFFICIENCY
Detector array evaluation and figures of merit N91-14386
QUANTUM ELECTRODYNAMICS
Quantum 1/f noise in high technology applications including ultrasmall structures and devices [AD-A226739] N91-14515
QUANTUM MECHANICS
Superaromatics: The key to a unified cosmic dust theory N91-14999
QUANTUM WELLS
Innovative Long Wavelength Infrared Detector Workshop Proceedings [NASA-CR-187433] N91-14379
Quantum Well Infrared Photodetectors (QWIP) N91-14392
Photovoltaic quantum well infrared photodetectors N91-14393
Characteristics of AlGaAs/GaAs multiple quantum well infrared detectors N91-14394
Resonant tunneling IR detectors N91-14395
Low dark current photovoltaic multiquantum well long wavelength infrared detectors N91-14396
Fundamental limits to performance of quantum well infrared detectors N91-14397
Growth and properties of Hg-based quantum well structures and superlattices N91-14403
LWIR detector research in InAsSb/InAs N91-14406
AlSb/InAs/AlSb quantum wells N91-14411
Quantum well laser [AD-A227303] N91-14594
Characterization of semiconductor surface-emitting laser wafers [DE91-001336] N91-14598
QUARTZ
New multiphase equation of state for polycrystalline quartz [DE91-001048] N91-14490
A numerical and experimental analysis of reactor performance and deposition rates for CVD on monofilaments [NASA-TM-103631] N91-14500
QUASARS
Compact object masses in active galactic nuclei and quasars and duration of activity stage N91-15096
Spectral synthesis code LINESPEC: Ionisation equilibrium of plasma and absorption spectra formation N91-15106

R

R CORONAE BOREALIS STARS
The influence of grain growth in circumstellar dust envelopes on observed colors and polarization of some eruptive stars N91-15020
RADAR ECHOES
Cloud cover statistics [AD-A226892] N91-14689
Mesoscale features of a winter storm: Dual Doppler velocity fields and differential reflectivity [AD-A227342] N91-14692
RADAR EQUIPMENT
Description of the bistatic radar terrain measurements system equipment [AD-A226808] N91-14517
RADAR IMAGERY
Remote sensing of Earth terrain [NASA-CR-186904] N91-14635
Multiband radar characterization of forest biomes [NASA-CR-185101] N91-14638
Method for detecting surface motions and mapping small terrestrial or planetary surface deformations with synthetic aperture radar [NASA-CASE-NPO-17831-1-CU] N91-14642
RADAR MEASUREMENT
Description of the bistatic radar terrain measurements system equipment [AD-A226808] N91-14517
RADAR RECEIVERS
Radio Frequency Interference (RFI) measurements made near the proposed Alaska OTH receiving site [AD-A226922] N91-14519
Unidirectional amplitude sensitive noise riding threshold circuit [AD-D014568] N91-14529
RADAR SCATTERING
Perspectives on modeling electromagnetic sea scatter [AD-A226939] N91-14520
RADAR SIGNATURES
Polarization radar studies of precipitation: Implementation of the technique and data interpretation [AD-A227073] N91-14690
RADIATION ABSORPTION
Evolution of high amplitude Alfven waves near a bow shock N91-15068
Maser cyclotron instability in a plasma with anisotropic distribution function N91-15075
RADIATION DAMAGE
Radiation response issues for infrared detectors N91-14388
RADIATION DETECTORS
LWIR HgCdTe: Innovative detectors in an incumbent technology N91-14384
Software management issues --- superconducting super collider detectors [DE91-001031] N91-14763
Device and method for monitoring the presence of an object in space [AD-D014621] N91-14823
X ray sensitive area detection device [NASA-CASE-MFS-28232-1] N91-14835
RADIATION DISTRIBUTION
The spectral energy distribution of the scattered light from dark clouds N91-14911
Observations of the diffuse UV radiation field N91-14912
Distribution of dust in W31 complex N91-14944
H I and dust in the high latitude dark cloud L1642 N91-14946
Does the far-infrared/radio correlation in spiral galaxies extend to the spatial domain N91-14985
Scattering by fluffy grains N91-14992
RADIATION DOSAGE
Radiation response issues for infrared detectors N91-14388
Corrosion behavior of copper-base materials in a gamma-irradiated environment [DE91-001286] N91-14468
Total-dose radiation hardness assurance for space electronics [DE91-002425] N91-14533
Data requirements for intermediate energy nuclear applications [DE91-004005] N91-14812
RADIATION EFFECTS
Effects of irradiation on initiation and crack-arrest toughness of two high-copper welds and on stainless steel cladding [DE91-001272] N91-14467
Corrosion behavior of copper-base materials in a gamma-irradiated environment [DE91-001286] N91-14468
Ion-induced grain growth in multilayer and coevaporated metal alloy thin films [DE91-004489] N91-14472
Data requirements for intermediate energy nuclear applications [DE91-004005] N91-14812
Irradiation-induced pinning in single-crystal and thin-film Tl2Ca2Ba2Cu3O10 superconductors [DE91-001342] N91-14877
An ion-channeling study of irradiation-induced amorphization of YBa2Cu3O(7-x) [DE91-004488] N91-14884
RADIATION HARDENING
Radiation response issues for infrared detectors N91-14388
Total-dose radiation hardness assurance for space electronics [DE91-002425] N91-14533
Optically-triggered GaAs thyristor switch s: Integrated structures for environmental hardening [DE91-001355] N91-14553
RADIATION PRESSURE
Radiation-driven diskons as a new astrophysical object N91-15105
RADIATION PROTECTION
Space transfer concepts and analysis for exploration missions [NASA-CR-183943] N91-14358
RADIATION SHIELDING
Data requirements for intermediate energy nuclear applications [DE91-004005] N91-14812
DIII-D results and plans [DE91-001548] N91-14847
RADIATION SPECTRA
Annihilation radiation of strongly-magnetised electron-positron plasma with power-law distributions of particles N91-15078
RADIATION THERAPY
Data requirements for intermediate energy nuclear applications [DE91-004005] N91-14812
RADIATION TOLERANCE
Radiation resistance of copper alloys at high exposure levels [DE91-001563] N91-14470
RADIATION TRANSPORT
On the thermal stability of slabs, cylinders, and spheres N91-15057
RADIATIVE TRANSFER
Studies of the observed and theoretical variations of atmospheric ozone [NASA-CR-187703] N91-14657
In-flight methods for satellite sensor absolute radiometric calibration N91-14801
New measurements of the far ultraviolet scattering properties of interstellar dust N91-14909
IR emission from circumstellar envelopes of C-rich stars N91-15019
Using infrared spectral features to probe circumstellar dust shells around cool stars N91-15021
Continuous infrared emission of proto- and young-planetary nebulae N91-15030
Continuum radiative transfer in accretion-powered pulsars N91-15043
Radiation-driven diskons as a new astrophysical object N91-15105
RADIO EMISSION
Angular motion of a PAH molecule in interstellar environment N91-14938
Longwave spectral dependence of emission from warm dust clouds N91-14945
Does the far-infrared/radio correlation in spiral galaxies extend to the spatial domain N91-14985
The plasma model of radioemission from SN 1987A N91-15101
RADIO FREQUENCIES
A versatile RF cavity mode damper [DE91-002947] N91-14534
Design and application possibilities of superconducting radio-frequency quadrupoles [DE91-004477] N91-14881
First tests of a superconducting RFQ (radio frequency quadrupole) structure [DE91-004483] N91-14883
RADIO FREQUENCY INTERFERENCE
Radio Frequency Interference (RFI) measurements made near the proposed Alaska OTH receiving site [AD-A226922] N91-14519
RADIO INTERFEROMETERS
Estimability of geodetic parameters from space VLBI observables [NASA-CR-187413] N91-14636
RADIO JETS (ASTRONOMY)
Piecewise-parabolic methods for systems of hyperbolic conservation laws in multiprocessing environments [DE91-004582] N91-14792
Nonlinear plasma effects in the environment of active galactic nuclei N91-15085
Energy dissipation of shear Alfven waves in extended cosmic jets N91-15086
A model for one-sided extragalactic jets N91-15097
RADIO OBSERVATION
Nonlinear plasma effects in the environment of active galactic nuclei N91-15085
RADIO RECEIVERS
Efficient detection and signal parameter estimation with application to high dynamic GPS receiver [NASA-CASE-NPO-17820-1-CU] N91-14321

RADIOACTIVE ISOTOPES
Short term creep rupture predictions for Tantalum alloy T-3
[DE91-002338] N91-14458
Validity of environmental transfer models
[DE91-002929] N91-14660
RADIOACTIVE WASTES
Office of Basic Energy Sciences 1990 summary report
[DE91-002971] N91-14653
Feasibility study of the seismic reflection method in Amargosa Desert, Nye County, Nevada
[DE91-001646] N91-14676
Data requirements for intermediate energy nuclear applications
[DE91-004005] N91-14812
RADIOMETERS
HgCdTe for NASA EOS missions and detector uniformity benchmarks N91-14385
Limb-darkening functions as derived from along-track operation of the ERBE scanning radiometers for August 1985
[NASA-RP-1243] N91-14683
RADIOMETRIC CORRECTION
In-flight methods for satellite sensor absolute radiometric calibration N91-14801
RAINDROPS
Polarization radar studies of precipitation: Implementation of the technique and data interpretation
[AD-A227073] N91-14690
RAMAN SPECTRA
Raman properties of various carbonaceous materials and their astrophysical implications N91-14933
RAMJET ENGINES
Investigation of combustion in large vortices
[AD-A226791] N91-14441
RAMPS (STRUCTURES)
Dynamics of separation and reattachment in a Mach 5 unswept compression ramp flow N91-14276
RANDOM SAMPLING
Randomly sampled-data control systems
[NASA-CR-187425] N91-14734
RANGEFINDING
Flight data acquisition methodology for validation of passive ranging algorithms for obstacle avoidance
[NASA-TM-102809] N91-14322
Status of LWIR HgCdTe infrared detector technology N91-14383
Measurement of the gravitomagnetic field using a pair of laser ranged satellites N91-14670
RASTER SCANNING
Reconstruction of vectorized raster data
[ETN-91-98143] N91-14738
RAZOR BLADES
A vibrating razor blade machining tool for material removal on low-density foams
[DE91-002996] N91-14507
REACTION KINETICS
Use of D2 to elucidate OMVPE growth mechanisms
[AD-A226966] N91-14443
Chemical vapor deposition modeling: An assessment of current status
[NASA-CR-185301] N91-14511
Effect of step edge transition rates and anisotropy in simulations of epitaxial growth
[DE91-001251] N91-14875
Superaromatics: The key to a unified cosmic dust theory N91-14999
Gas-phase formation of silicon carbides, oxides, and sulphides from atomic silicon ions N91-15014
PAH formation in carbon-rich circumstellar envelopes N91-15015
REACTIVITY
Heteronuclear metal cluster compounds synthesis and reactivity
[AD-A226815] N91-14463
REACTOR DESIGN
ITER global stability limits
[DE91-001488] N91-14845
REACTOR MATERIALS
Radiation resistance of copper alloys at high exposure levels
[DE91-001563] N91-14470
REACTOR SAFETY
Preliminary survey of 21st century civil mission applications of space nuclear power
[NASA-TM-101249] N91-14817
READOUT
Issues and directions in IR detector readout electronics N91-14387
Novel Si(1-x)Ge(x)/Si heterojunction internal photoemission long wavelength infrared detectors N91-14401
REAGENTS
Electroless nickel bath recovery by cation exchange and precipitation
[DE91-001988] N91-14457
REAL GASES
Hypersonic aerodynamics: An approximation method for the calculation of real gas effects and wall temperatures
[MBB/FE127/S/PUB/0403] N91-14306
REAL TIME OPERATION
Experimental investigation of buffet onset and penetration on a supercritical airfoil at transonic speeds N91-14328
ISIS and META projects
[NASA-CR-186413] N91-14731
The ISIS project: Real experience with a fault tolerant programming system
[NASA-CR-187029] N91-14732
Distributed systems status and control
[NASA-CR-187014] N91-14733
Experiences porting the distributed Ada real-time kernel
[AD-A226693] N91-14742
An analysis of input/output paradigms for real-time systems
[AD-A226724] N91-14748
Evaluations of some scheduling algorithms for hard real-time systems
[AD-A226930] N91-14755
Sensor based control of robotic mechanisms
[AD-A226784] N91-14776
RECIPROCAL THEOREMS
Some problems in elastic contact and fracture N91-14625
RECOMBINATION REACTIONS
The evolution of organic mantles on interstellar grains N91-14964
Theoretical studies of important processes in planetary and comet atmospheres
[NASA-CR-187692] N91-15045
RECONSTRUCTION
Reconstruction of vectorized raster data
[ETN-91-98143] N91-14738
RECTANGULAR WINGS
Coupled aerodynamic loads due to unsteady stall on a large aspect ratio wing oscillating at great amplitude N91-14338
RED SHIFT
The detection of a broad interstellar extinction feature near 1700 A N91-14900
REDUCED GRAVITY
Definition of experiments to investigate fire suppressants in microgravity
[NASA-CR-185295] N91-14378
Manipulation hardware for microgravity research
[NASA-TM-103423] N91-14498
Transient analysis of a two-phase hydrogen heat switch
[DE91-002314] N91-14506
Surface settling in partially filled containers upon step reduction in gravity
[NASA-TM-103641] N91-14556
Initial blood storage experiment
[NASA-CR-185513-PT-2] N91-14701
Cosmos 2044
[NASA-CR-187003] N91-14702
Acoustic transducer apparatus with reduced thermal conduction
[NASA-CASE-NPO-17620-1-CU] N91-14808
REFLECTION NEBULAE
The capability of the ultraviolet imaging telescope for observing interstellar dust N91-14913
Infrared images of reflection nebulae and Orion's bar: Fluorescent molecular hydrogen and the 3.3 micron feature N91-14918
Airborne observations of the infrared emission bands N91-14919
The spatial distribution of infrared radiation from visible reflection nebulae N91-14931
Angular motion of a PAH molecule in interstellar environment N91-14938
Infrared studies of dust grains in infrared reflection nebulae N91-14970
The origin of micrograins N91-15000
Compact reflection nebulae, a transit phase of evolution from post-AGB to planetary nebulae N91-15029
The discovery of a highly polarized bipolar nebula N91-15031
REFLEXES
Bioreactivity: Studies on a simple brain stem reflex in behaving animals
[AD-A226823] N91-14704
REFRACTION
Investigations of ultrasonic wave interactions with grain boundaries and grain imperfections
[DE91-002695] N91-14804
REFRACTORY MATERIALS
Fatigue and fracture of titanium aluminides, volume 2
[AD-A227353] N91-14351
High-temperature thermal storage systems for advanced solar receivers materials selections
[NASA-CR-187750] N91-14647
REFRACTORY METALS
High temperature refractory member with radiation emissive overcoat
[NASA-CASE-NPO-17122-1-CU] N91-14489
Laboratory studies of refractory metal oxide smokes N91-14993
REFUELING
System for connecting fluid couplings
[NASA-CASE-MFS-26042-1-SB] N91-14613
Fueling of magnetically confined plasmas by single- and two-stage repeating pneumatic pellet injectors
[DE91-002635] N91-14839
REGRESSION ANALYSIS
Improved estimation of variance components in mixed models
[AD-A226854] N91-14794
REINFORCING FIBERS
Optimization of interface layers in the design of ceramic fiber reinforced metal matrix composites
[NASA-CR-185307] N91-14422
RELATIVISTIC PLASMAS
Description of nonlinear effects in a relativistic plasma using Hamiltonian formalism N91-15071
Hydrodynamics of collisionless relativistic plasma in a strong magnetic field N91-15072
RELATIVISTIC VELOCITY
Ultrarelativistic low-frequency electromagnetic waves in pulsar magnetospheres N91-15091
RELIABILITY ANALYSIS
Fatigue reliability of wind turbine components
[DE91-001262] N91-14650
Reliability of photovoltaic concentrator modules
[DE90-012754] N91-14651
Methodology investigation of software maturity model validation
[AD-A226697] N91-14746
REMOTE SENSING
Sensor requirements for Earth and planetary observations N91-14380
Advanced technology needs for a global change science program: Perspective of the Langley Research Center
[NASA-TM-4196] N91-14634
Remote sensing of Earth terrain
[NASA-CR-186904] N91-14635
Strategic plan commercialization remote sensing by NEDECO
[BCRS-89-35] N91-14637
Multiband radar characterization of forest biomes
[NASA-CR-185101] N91-14638
Evaluation of data reduction and composing of the NOAA global vegetation index product: A case study
[AD-A227397] N91-14641
Method for detecting surface motions and mapping small terrestrial or planetary surface deformations with synthetic aperture radar
[NASA-CASE-NPO-17831-1-CU] N91-14642
Analysis of the boreal forest-tundra ecotone: A test of AVIRIS capabilities in the Eastern Canadian subarctic
[NASA-CR-187335] N91-14655
REQUIREMENTS
Space transfer concepts and analysis for exploration missions
[NASA-CR-183943] N91-14358
Advanced technology needs for a global change science program: Perspective of the Langley Research Center
[NASA-TM-4196] N91-14634
RESEARCH
Office of Basic Energy Sciences 1990 summary report
[DE91-002971] N91-14653
RESEARCH AND DEVELOPMENT
Manufacturing Technology: A Sandia Technology Bulletin, Volume 1, No. 1
[DE91-002518] N91-14504
The high cost of low quality in R/D (Research and Development)
[DE91-002118] N91-14621
JPRS Report: Science and technology. USSR: Life sciences
[JPRS-ULS-89-003] N91-14706
National software capacity: Near-term study
[AD-A226694] N91-14743
Experimental development, testing and research work in support of the inertial confinement fusion program
[DE91-002771] N91-14841
The NASA/DOD aerospace knowledge diffusion research project: A research agenda
[NASA-TM-103439] N91-14892
Chronology: MSFC Space Station program, 1982 - present. Major events
[NASA-CR-184014] N91-15119
Air Force Office of Scientific Research technical report summaries: April-June 1990
[AD-A227367] N91-15121

Air Force Office of Scientific Research technical report summaries: January-March 1990
[AD-A227368] N91-15122

RESEARCH FACILITIES
Chronology: MSFC Space Shuttle program development, assembly, and testing major events (1969 - April, 1981)
[NASA-CR-184013] N91-15120

RESEARCH MANAGEMENT
Research as part of the Air Force Research in Aero-Propulsion Technology (AFRAPT) program
[AD-A226893] N91-14350
The NASA/DOD aerospace knowledge diffusion research project: A research agenda
[NASA-TM-103439] N91-14892

RESEARCH VEHICLES
Development of an unmanned air research vehicle for supermaneuverability studies
[AD-A227165] N91-14342

RESIN MATRIX COMPOSITES
Failure in laminated composite plates containing a hole
[AD-A227307] N91-14435
The response and failure mechanisms of circular metal and composite plates subjected to underwater shock loading
[AD-A226759] N91-14631

RESISTANCE HEATING
Joule heating investigations using the sondrestrom radar and DMSP satellites
[AD-A227425] N91-14677

RESONANT FREQUENCIES
Acoustic positioning and orientation prediction
[NASA-CASE-NPO-17511-1-CU] N91-14807

RESONANT TUNNELING
Resonant tunneling IR detectors N91-14395
MBE HgCdTe heterostructure detectors N91-14402

RESONATORS
Computer aided design models for millimeter-wave suspended substrate microstrip line
[AD-A227259] N91-14547

RETICLES
Multiple axis reticle
[NASA-CASE-ARC-11886-1-SB] N91-14591

REVERSE FIELD PINCH
Fast electron studies in the ZT-40M edge plasma
[DE91-002323] N91-14838

REYNOLDS STRESS
Variation of wall shear stress and Reynolds stress over a flat plate downstream of a boundary layer manipulator
[AD-A226875] N91-14565

RHEOLOGY
A continuum approach toward modeling the mechanics of solid lubricating films
[AD-A226961] N91-14486

RIGID STRUCTURES
Mechanical end joint system for connecting structural column elements
[NASA-CASE-LAR-14465-1] N91-14614

ROBOT ARMS
Spiral lead platen robotic end effector
[NASA-CASE-LAR-13855-1] N91-14615
Multi-fingered robotic hand
[NASA-CASE-NPO-15959-2] N91-14616

ROBOT CONTROL
Spiral lead platen robotic end effector
[NASA-CASE-LAR-13855-1] N91-14615
Planning monotone paths to visit a set of obstacles
[AD-A226923] N91-14754

ROBOT DYNAMICS
Spiral lead platen robotic end effector
[NASA-CASE-LAR-13855-1] N91-14615
Multi-fingered robotic hand
[NASA-CASE-NPO-15959-2] N91-14616
Planning monotone paths to visit a set of obstacles
[AD-A226923] N91-14754

ROBOTICS
Manipulation hardware for microgravity research
[NASA-TM-103423] N91-14498
Intelligent manipulation technique for multi-branch robotic systems
[NASA-CR-187651] N91-14603
Contribution to the specification and implementation of complex robot tasks
[ETN-90-98209] N91-14604
Robot control strategies
[OUEL-1754/89] N91-14605
Analogue computation using VLSI neural network devices
[OUEL-1835/90] N91-14773
Sensor based control of robotic mechanisms
[AD-A226784] N91-14776

ROBOTS
Optimal sensor fusion for land vehicle navigation
[DE91-002586] N91-14319
Manipulation hardware for microgravity research
[NASA-TM-103423] N91-14498
Reasoning of the geometric and uncertainty constraints in planning robot manipulation tasks
[LAAS-90143] N91-14775
Sensor based control of robotic mechanisms
[AD-A226784] N91-14776

ROCKET ENGINE CASES
A parametric shell analysis of the shuttle 51-L SRB AFT field joint
[NASA-TM-102748] N91-14629

ROCKET ENGINE DESIGN
Space shuttle redesigned solid rocket motor Certificate of Qualification (COQ) data report
[NASA-CR-184051] N91-14416

ROCKS
Reports on block rotations, fault domains and crustal deformation
[NASA-CR-186756] N91-14665
Block rotations, fault domains and crustal deformation in the western US N91-14666
Distributed deformation and block rotation in 3D N91-14667
Stress field rotation or block rotation: An example from the Lake Mead fault system N91-14668

RODS
Low velocity impact analysis with NASTRAN
[NASA-TM-103169] N91-14426

ROLL
Interaction of feel system and flight control system dynamics on lateral flying qualities
[NASA-CR-179445] N91-14353
A continuum approach toward modeling the mechanics of solid lubricating films
[AD-A226961] N91-14486

ROLLING
A modification of 4330 alloy steel
[DE91-001764] N91-14455

ROLLING MOMENTS
Measurement of hydrodynamic forces and moments and flow field mapping of a model in coning motion
[AD-A226684] N91-14355

ROOM TEMPERATURE
Flow behavior of Ti-24Al-11Nb at high strain rates
[DE91-004506] N91-14473

ROTARY WING AIRCRAFT
Flight data acquisition methodology for validation of passive ranging algorithms for obstacle avoidance
[NASA-TM-102809] N91-14322

ROTARY WINGS
Tabulation of data from the tip aerodynamics and acoustics test
[NASA-TM-102280] N91-14273
Results of a sub-scale model rotor icing test
[NASA-TM-103709] N91-14309
Feasibility investigation of general time-domain unsteady aerodynamics of rotors
[NASA-CR-177570] N91-14311

ROTATING DISKS
Electrostatically suspended rotor for angular encoder
[NASA-CASE-MFS-28294-1] N91-14508

ROTATION
Hybrid butterfly valve
[NASA-CASE-SSC-00004-1] N91-14609
Reports on block rotations, fault domains and crustal deformation
[NASA-CR-186756] N91-14665
Block rotations, fault domains and crustal deformation in the western US N91-14666
Distributed deformation and block rotation in 3D N91-14667
Stress field rotation or block rotation: An example from the Lake Mead fault system N91-14668
Multiple strike slip faults sets: A case study from the Dead Sea transform N91-14669

ROTOR AERODYNAMICS
Tabulation of data from the tip aerodynamics and acoustics test
[NASA-TM-102280] N91-14273
Results of a sub-scale model rotor icing test
[NASA-TM-103709] N91-14309
Prediction of XV-15 tilt rotor discrete frequency aeroacoustic noise with WOPWOP
[NASA-CR-187684] N91-14803

ROTORS
Feasibility investigation of general time-domain unsteady aerodynamics of rotors
[NASA-CR-177570] N91-14311
Electrostatically suspended rotor for angular encoder
[NASA-CASE-MFS-28294-1] N91-14508
Turbomachinery rotor support with damping
[NASA-CASE-MFS-28345-1] N91-14608

ROVING VEHICLES
Optimal sensor fusion for land vehicle navigation
[DE91-002586] N91-14319
Mars Rover/Sample Return (MRSR) Mission: Mars Rover Technology Workshop
[NASA-TM-101129] N91-14600

RUNGE-KUTTA METHOD
Projected implicit Runge-Kutta methods for differential-algebraic boundary value problems
[DE91-000680] N91-14791

S

S WAVES
Energy dissipation of shear Alfven waves in extended cosmic jets N91-15086

SAFETY
Overview of propulsion concepts for tactical missiles N91-14296

SAFETY MANAGEMENT
Snow avalanche hazards and mitigation in the United States
[LC-90-62814] N91-14686

SAGITTARIUS CONSTELLATION
Dust emission in the Sagittarius B2 molecular cloud core N91-14947

SALINITY
Ion implantation for corrosion inhibition of aluminum alloys in saline media
[DE91-002887] N91-14461

SAMPLED DATA SYSTEMS
Evaluation of data reduction and composing of the NOAA global vegetation index product: A case study
[AD-A227397] N91-14641
Randomly sampled-data control systems
[NASA-CR-187425] N91-14734

SAMPLING
Procedures for the preparation of samples for cross-sectional transmission electron microscopy
[AD-A227013] N91-14444

SAND CASTING
Expendable Pattern Casting Technology
[DE91-001348] N91-14503

SANDWICH STRUCTURES
Structural response of marine sandwich panels to uniform pressure loading
[AD-A227038] N91-14434

SAPPHIRE
Joining alumina to sapphire for copper vapor laser tubes
[AD-A226619] N91-14501

SATELLITE ATTITUDE CONTROL
The effects of liquid propellant motion on the attitude stability of spin stabilized spacecraft
[AD-A227002] N91-14376

SATELLITE COMMUNICATION
Automatic dependent surveillance benefit and cost analysis
[DOT/FAA/RD-90/34] N91-14320
Trellis coded modulation for transmission over fading mobile satellite channel
[NASA-CASE-NPO-16904-2-CU] N91-14523

SATELLITE IMAGERY
Evaluation of data reduction and composing of the NOAA global vegetation index product: A case study
[AD-A227397] N91-14641
In-flight methods for satellite sensor absolute radiometric calibration N91-14801

SATELLITE INSTRUMENTS
In-flight methods for satellite sensor absolute radiometric calibration N91-14801

SATELLITE NETWORKS
Data transmission networks N91-14576

SATELLITE OBSERVATION
Comparison of ground and satellite based measurements of the fraction of photosynthetically active radiation intercepted by tall-grass prairie
[NASA-CR-187696] N91-14639
Multispectral imagery support for ocean venture 90
[AD-A227119] N91-14697

SATELLITE ORBITS
Satellite situation report, volume 30, no. 1
[NASA-TM-101105] N91-14372

SATELLITE-BORNE INSTRUMENTS
Advanced technology needs for a global change science program: Perspective of the Langley Research Center
[NASA-TM-4196] N91-14634

SATURN RINGS
Accretion disk instability and spokes in Saturn's rings N91-15094

SCALE MODELS
Development of an unmanned air research vehicle for supermaneuverability studies
[AD-A227165] N91-14342

SCANDIUM
The effect of scandium on the phase stability of Al3Nb and Al3Zr
[DE91-002657] N91-14459

SCANNERS
Earth Observing Scanning Polarimeter (EOSP), phase B
[NASA-CR-187715] N91-14586
SCATTERING
Studies in statistical signal processing
[AD-A226825] N91-14518
He atom surface spectroscopy: Surface lattice dynamics of insulators, metals, and metal overlayers
[DE91-001993] N91-14855
New measurements of the far ultraviolet scattering properties of interstellar dust N91-14909
The spectral energy distribution of the scattered light from dark clouds N91-14911
Observations of the diffuse UV radiation field N91-14912
On the polarization mechanism in the R Mon/NGC 2261 complex N91-14969
Scattering by fluffy grains N91-14992
Atomic environments in iron meteorites using EXAFS N91-15011
Solar radiation on Mars: Update 1990
[NASA-TM-103623] N91-15117
SCATTERING CROSS SECTIONS
Intermediate energy nuclear physics
[DE91-002758] N91-14809
Sterile neutrinos and astrophysical and cosmological constraints on the parameters of the extended electroweak models N91-15083
SCHEDULES
Advanced technology needs for a global change science program: Perspective of the Langley Research Center
[NASA-TM-4196] N91-14634
Evaluations of some scheduling algorithms for hard real-time systems
[AD-A226930] N91-14755
SCHEDULING
An analysis of input/output paradigms for real-time systems
[AD-A226724] N91-14748
Evaluations of some scheduling algorithms for hard real-time systems
[AD-A226930] N91-14755
SCHOOLS
Outer space: What should be the US Government policy toward the region beyond Earth's atmosphere. National debate topic for high schools, 1990-1991
[PB90-255464] N91-14896
SCHWASSMANN-WACHMANN COMET
A study of extended zodiacal structures
[NASA-CR-187687] N91-15044
SCIENTISTS
The high cost of low quality in R/D (Research and Development)
[DE91-002118] N91-14621
SCINTILLATION COUNTERS
A study of liquid scintillator and fiber materials for use in a fiber calorimeter
[DE91-004229] N91-14585
SEA SURFACE TEMPERATURE
Explosive cyclogenesis: A case study of the Veterans' Day storm of 11-12 November 1987
[AD-A227077] N91-14691
SEALING
Joining alumina to sapphire for copper vapor laser tubes
[AD-A226619] N91-14501
SEALS (STOPPERS)
Turbomachinery rotor support with damping
[NASA-CASE-MFS-28345-1] N91-14608
SEARCH PROFILES
Adaptive human-computer interfaces using expert profiles
[AD-A226906] N91-14721
SEAS
The distribution of wave heights and periods for seas with unimodal bimodal power density specira
[AD-A227040] N91-14696
SECURITY
Optimal sensor fusion for land vehicle navigation
[DE91-002586] N91-14319
SEISMIC WAVES
Stable explicit depth extrapolation of seismic wavefields
[DE91-001445] N91-14674
The 3-D depth migration via McClellan transformations
[DE91-001446] N91-14675
Feasibility study of the seismic reflection method in Amargosa Desert, Nye County, Nevada
[DE91-001646] N91-14676
SEISMOLOGY
Specification goals for a Mars seismic network N91-14360
Reports on block rotations, fault domains and crustal deformation
[NASA-CR-186756] N91-14665
Plate motions and deformations from geologic and geodetic data
[NASA-CR-187379] N91-14672
SEMICONDUCTOR DEVICES
Total-dose radiation hardness assurance for space electronics
[DE91-002425] N91-14533
Characterization of semiconductor surface-emitting laser wafers
[DE91-001336] N91-14598
FTIR (Fourier Transform Infrared) spectrophotometry for thin film monitors: Computer and equipment integration for enhanced capabilities
[DE91-001228] N91-14853
Rise time and recovery of GaAs photoconductive semiconductor switches
[DE91-001267] N91-14854
SEMICONDUCTOR DIODES
Millimeter-wave monolithic diode-grid frequency multiplier
[NASA-CASE-NPO-17258-1-CU] N91-14551
SEMICONDUCTOR JUNCTIONS
Investigation of redox processes at semiconductor electrode liquid junctions
[DE91-001787] N91-14858
SEMICONDUCTOR LASERS
Triggering GaAs lock-on switches with laser diode arrays
[DE91-002419] N91-14532
Field induced gap infrared detector
[NASA-CASE-NPO-17526-1-CU] N91-14588
Quantum well laser
[AD-A227303] N91-14594
Characterization of semiconductor surface-emitting laser wafers
[DE91-001336] N91-14598
Integrated optical devices for photonics instrumentation systems
[DE91-004192] N91-14828
SEMICONDUCTORS (MATERIALS)
Innovative Long Wavelength Infrared Detector Workshop Proceedings
[NASA-CR-187433] N91-14379
SDIO long wavelength infrared detector requirements N91-14381
Characteristics of AlGaAs/GaAs multiple quantum well infrared detectors N91-14394
Resonant tunneling IR detectors N91-14395
Low dark current photovoltaic multiquantum well long wavelength infrared detectors N91-14396
New heterojunction LWIR detector options N91-14398
LWIR detector research in InAsSb/InAs N91-14406
InAs/GaAs and InAs doping superlattices N91-14409
InAsSbBi, a direct band-gap, III-V, LWIR material N91-14410
Quantum 1/f noise in high technology applications including ultrasmall structures and devices
[AD-A226739] N91-14515
Triggering GaAs lock-on switches with laser diode arrays
[DE91-002419] N91-14532
Silicon carbide, a semiconductor for space power electronics
[NASA-TM-103655] N91-14850
Program to study the process parameters of OMVPE and their relationship to the properties of Ga(0.47)In(0.53) as ON InP substrates
[AD-A226618] N91-14851
Rise time and recovery of GaAs photoconductive semiconductor switches
[DE91-001267] N91-14854
Magnetic properties of doped semiconductors
[DE91-002395] N91-14859
Investigation of new semiinsulating behavior of 3-5 compounds
[AD-A226787] N91-14862
Ultra high speed compound semiconductors and real time signal processing
[AD-A226790] N91-14863
Photogenerated carrier-induced reaction on semiconductor surfaces
[DE91-001349] N91-14878
SEPARATED FLOW
Dynamics of separation and reattachment in a Mach 5 unswept compression ramp flow N91-14276
Pressure measurements on slender bodies at supersonic speeds and development of flow separation critera for Euler codes N91-14282
Supersonic tactical missile computation using Euler's equation with crossflow separation modeling N91-14284
Aircraft Dynamic Loads Due to Flow Separation
[AGARD-CP-483] N91-14324
Effects of trailing-edge flap on buffet characteristics of a supercritical airfoil N91-14327
Experimental investigation and semi-empirical prediction of the dynamic response of a low-aspect-ratio trapezoidal wing due to flow separation N91-14330
Unsteady aerodynamic forces on an oscillating wing at high incidences and flow separation N91-14331
The forward mounted spoiler as a source of buffet excitation N91-14332
Interaction between the canard and wing flow on a model of a typical combat aircraft N91-14334
Unsteady separated flow phenomena causing self-excited structural oscillations N91-14339
Unsteady airloads due to separated flow on airfoils and wings N91-14340
SEQUENCING
Acceleration techniques for explicit Euler codes N91-14555
SERPENTINE
Infrared spectra of crystalline and glassy silicates and application to interstellar dust N91-14994
SERVOMECHANISMS
On the modeling and control of slewing flexible structures N91-14499
SET THEORY
Adaptive control of large space structures
[AD-A227304] N91-14377
On probability intervals and their updating
[RUU-CS-90-22] N91-14793
SETTLING
Surface settling in partially filled containers upon step reduction in gravity
[NASA-TM-103641] N91-14556
SHADOWGRAPH PHOTOGRAPHY
Investigation of combustion in large vortices
[AD-A226791] N91-14441
SHAFTS (MACHINE ELEMENTS)
Straddle design of spiral bevel and hypoid pinions and gears
[NASA-TM-103621] N91-14602
SHAPED CHARGES
A modification of 4330 alloy steel
[DE91-001764] N91-14455
SHAPES
Some trends in missile aerodynamics N91-14279
Asymmetric supersonic flow around cones with noncircular sections N91-14292
SHEAR FLOW
Direct numerical simulation of turbulent couette flow, part 2
[AD-A226770] N91-14564
Amplification of Alfven waves in free shear flows N91-15074
SHEAR STRENGTH
The interlaminar shear strength of woven carbon, woven glass and woven carbon/glass hybrid laminates under static and impact loading
[OUEL-1831/90] N91-14423
SHEAR STRESS
Variation of wall shear stress and Reynolds stress over a flat plate downstream of a boundary layer manipulator
[AD-A226875] N91-14565
SHOCK ABSORBERS
A cable vehicle barrier for alert aircraft protection
[DE91-001723] N91-14354
SHOCK FRONTS
Structure of accretion flow in close binary system: A two dimensional numerical model N91-15093
SHOCK LAYERS
Numerical study of shock-wave/boundary layer interactions in premixed hydrogen-air hypersonic flows
[NASA-TM-103273] N91-14559
SHOCK LOADS
The response and failure mechanisms of circular metal and composite plates subjected to underwater shock loading
[AD-A226759] N91-14631
SHOCK WAVE ATTENUATION
A numerical calculation of parameters of explosion MHD shock waves from moderate solar flares N91-15066
SHOCK WAVE INTERACTION
Dynamics of separation and reattachment in a Mach 5 unswept compression ramp flow N91-14276
Numerical investigations in three-dimensional internal flows
[NASA-CR-187373] N91-14277
Numerical study of shock-wave/boundary layer interactions in premixed hydrogen-air hypersonic flows
[NASA-TM-103273] N91-14559
SHOCK WAVE PROPAGATION
A simple plane-wave explosive lens
[DE91-004297] N91-14526
Shot report, Holo-17-Holo-22 Rex-9
[DE91-002575] N91-14583
SHOCK WAVES
CFD code evaluation for internal flow modeling
[NASA-CR-187677] N91-14557

Numerical study of shock-wave/boundary layer interactions in premixed hydrogen-air hypersonic flows [NASA-TM-103273] N91-14559
Dust in stellar wind bow shocks N91-14979
The origin of micrograins N91-15000
Gradient catastrophe of the supersonic mass-loaded magnetised plasma flow and the formation of bow shock N91-15065
Nonstationary processes in the front of high Mach number collisionless quasiperpendicular shock: Dynamics of the ion distribution N91-15067

SHORT CIRCUITS
Thermal switch disc for short circuit protection of batteries [NASA-CASE-MSC-21428-1] N91-14537

SHOT NOISE
Characteristics of AlGaAs/GaAs multiple quantum well infrared detectors N91-14394

SIDELOBES
Effect of atmospherics on beamforming accuracy [NASA-CR-187695] N91-14802

SIGNAL ANALYSIS
The forward mounted spoiler as a source of buffet excitation N91-14332

SIGNAL DETECTION
Vibration analyzer [NASA-CASE-MSC-21408-1] N91-14607

SIGNAL ENCODING
System integration of a block code [ETN-91-98169] N91-14514
Trellis coded modulation for transmission over fading mobile satellite channel [NASA-CASE-NPO-16904-2-CU] N91-14523
Optical encoding of imaging data [AD-D014617] N91-14821

SIGNAL PROCESSING
Efficient detection and signal parameter estimation with application to high dynamic GPS receiver [NASA-CASE-NPO-17820-1-CU] N91-14321
Systolic emulator experimentation [AD-A226746] N91-14516
Studies in statistical signal processing [AD-A226825] N91-14518
Unidirectional amplitude sensitive noise riding threshold circuit [AD-D014568] N91-14529
Development of a taction system using piezoelectric film [AD-A227076] N91-14544
The 3-D depth migration via McClellan transformations [DE91-001446] N91-14675
Demodulation processes in auditory perception [AD-A226824] N91-14707
Optoelectronic devices [AD-D014618] N91-14822
Hybrid optical processor [AD-A227163] N91-14834
Ultra high speed compound semiconductors and real time signal processing [AD-A226790] N91-14863

SIGNAL REFLECTION
A model of the acoustic interactions occurring under Arctic ice [AD-A227128] N91-14806

SIGNAL TO NOISE RATIOS
Unidirectional amplitude sensitive noise riding threshold circuit [AD-D014568] N91-14529

SIGNAL TRANSMISSION
Observations of ocean fluctuations between 15 and 23 hour periods in the Pacific [AD-A227017] N91-14695

SIGNATURE ANALYSIS
Coronal mass ejections [NASA-CR-186579] N91-15115

SIGNS AND SYMPTOMS
Development of an animal model of human non-freezing cold injury: Changes in thermal sensitivity following cold exposure [AD-A227174] N91-14705

SIKORSKY AIRCRAFT
Results of a sub-scale model rotor icing test [NASA-TM-103709] N91-14309

SILANES
A numerical and experimental analysis of reactor performance and deposition rates for CVD on monofilaments [NASA-TM-103631] N91-14500

SILICA GEL
Conversion of alkoxide solutions to oxides: Evaporation of products [AD-A226927] N91-14442

SILICATES
Steps toward interstellar silicate dust mineralogy N91-14991
Infrared spectra of crystalline and glassy silicates and application to interstellar dust N91-14994
Optical properties of irregular interstellar grains N91-14995
Size distribution of dust grains: A problem of self-similarity N91-14997
A spectral difference between silicates in Comet Halley and interstellar silicates N91-15002
The nature of cometary dust as determined from infrared observations N91-15003
A comparative study of the continuum and emission characteristics of comet dust. 1: Are the silicates in Comet Halley and Kohoutek amorphous or crystalline N91-15005
Dust formation around M-type stars N91-15017
Type of silicate feature in oxygen rich stellar envelopes N91-15024
Interstellar extinction at 10-20 microns N91-15025
Dust around Mira variables: An analysis of IRAS LRS spectra N91-15026

SILICON
Intersubband absorption in Si(1-x)Ge(x/Si superlattices for long wavelength infrared detectors N91-14399
Possibilities for LWIR detectors using MBE-grown Si(/Si(1-x)Ge(x) structures N91-14400
Novel Si(1-x)Ge(x)/Si heterojunction internal photoemission long wavelength infrared detectors N91-14401
InAs/GaAs and InAs doping superlattices N91-14409
Optically-triggered GaAs thyristor switch s: Integrated structures for environmental hardening [DE91-001355] N91-14553
Processing experiments for development of high-efficiency silicon solar cells [DE91-002698] N91-14645
ion beam induced diffusion and crystallization in high dose Er implanted Si [DE91-002869] N91-14860
Defect and impurity effects on the initial growth of Ag on Si(111) [DE91-001277] N91-14876

SILICON CARBIDES
Fatigue and fracture of titanium aluminides, volume 2 [AD-A227353] N91-14351
Aluminum nitride-silicon carbide whisker composites: Processing, properties, and microstructural stability [DE91-001907] N91-14425
Dynamic consolidation of aluminum-silicon carbide composites [DE91-001929] N91-14427
Fundamentals of interfacial strength in composite materials [AD-A226701] N91-14431
Interfacial push-out measurements of fully-bonded SiC/SC composites [DE91-004527] N91-14436
Development and testing of radiation and electromagnetic pulse hardened silicon carbide based electronics [AD-A227309] N91-14548
Silicon carbide, a semiconductor for space power electronics [NASA-TM-103655] N91-14850
Gas-phase formation of silicon carbides, oxides, and sulphides from atomic silicon ions N91-15014

SILICON COMPOUNDS
Gas-phase formation of silicon carbides, oxides, and sulphides from atomic silicon ions N91-15014

SILICON DIOXIDE
Theory of the electronic and structural properties of solid state oxides [DE91-001192] N91-14874

SILICON NITRIDES
Si3N4 emissivity and the unidentified infrared bands N91-14935

SILICON OXIDES
Laser studies of the interaction of SiO with the surface of a thin film [DE91-004562] N91-14450
Gas-phase formation of silicon carbides, oxides, and sulphides from atomic silicon ions N91-15014

SILICONES
An evaluation of two flat-black silicone paints for space application [NASA-TM-100768] N91-14494

SILVER
Superconducting properties of Tl-Ba-Ca-Cu-O films on silver substrates [DE91-002304] N91-14856
Defect and impurity effects on the initial growth of Ag on Si(111) [DE91-001277] N91-14876

SIMULATION
The response of atmospheric CO2 to changes in land use [DE91-001212] N91-14663
The definition of necessary hidden units in neural networks for combinatorial optimization [AD-A227142] N91-14786
The evolution of organic mantles on interstellar grains N91-14964
Laboratory investigation of electric charging of dust particles by electrons, ions, and UV radiation N91-14971
Laboratory simulation of the astrophysical burst processes in non-uniform magnetised media N91-15081

SINGLE CRYSTALS
Anomalous surface phase formation on Pt3Sn with zone axes group (100) [DE91-001794] N91-14456
Conductivity fluctuations in fast ionic conductors [AD-A227379] N91-14549
On the crystal structure of KInS2-I [AD-A226940] N91-14866
Irradiation-induced pinning in single-crystal and thin-film Tl2Ca2Ba2Cu3O10 superconductors [DE91-001342] N91-14877

SINGULARITY (MATHEMATICS)
Boundary value problems of the elasticity theory for polyhedra: Singularities and approximation with boundary element methods [ETN-91-98168] N91-14780

SINTERING
Aluminum nitride-silicon carbide whisker composites: Processing, properties, and microstructural stability [DE91-001907] N91-14425

SITE SELECTION
Radio Frequency Interference (RFI) measurements made near the proposed Alaska OTH receiving site [AD-A226922] N91-14519

SIZE DISTRIBUTION
Size distribution of dust grains: A problem of self-similarity N91-14997
The nature of cometary dust as determined from infrared observations N91-15003

SKIN (STRUCTURAL MEMBER)
Fabrication by filament winding with an elastomeric material [AD-D014570] N91-14478

SKY SURVEYS (ASTRONOMY)
The detection of a broad interstellar extinction feature near 1700 A N91-14900

SLABS
Continuum radiative transfer in accretion-powered pulsars N91-15043

SLEEP DEPRIVATION
The effects of sleep loss on individual and group performance [AD-A226963] N91-14708

SLENDER BODIES
Pressure measurements on slender bodies at supersonic speeds and development of flow separation critera for Euler codes N91-14282

SLEWING
On the modeling and control of slewing flexible structures N91-14499

SLIDING
Hybrid butterfly valve [NASA-CASE-SSC-00004-1] N91-14609

SLIDING FRICTION
Interfacial push-out measurements of fully-bonded SiC/SC composites [DE91-004527] N91-14436

SLOT ANTENNAS
The application of deterministic spectral domain method to the analysis of planar circuit discontinuities on open substrates [AD-A226901] N91-14542

SLOTS
The inclusion of wall loss in electromagnetic finite-difference time-domain thin-slot algorithms [DE91-001046] N91-14524

SMELTING
Thin steel section casting on a near-horizontal twin-belt caster [DE91-001883] N91-14505

SMOKE
Smoke and extinguisher agent dissipation in a small pressurized fuselage [DOT/FAA/CT-89/31] N91-14317
Laboratory studies of refractory metal oxide smokes N91-14993
Infrared spectra of crystalline and glassy silicates and application to interstellar dust N91-14994

SMOOTHING
Modified seasonal factors in exponential smoothing [DE91-002802] N91-14688

SNEAK CIRCUIT ANALYSIS
Integration of sneak analysis with design, volume 1 [AD-A226902] N91-14543

SNOW
Mesoscale features of a winter storm: Dual Doppler velocity fields and differential reflectivity
[AD-A227342] N91-14692
SNOW COVER
Snow avalanche hazards and mitigation in the United States
[LC-90-62814] N91-14686
SOFTWARE ENGINEERING
National software capacity: Near-term study
[AD-A226694] N91-14743
Classifying software design methods
[AD-A226696] N91-14745
An analysis of input/output paradigms for real-time systems
[AD-A226724] N91-14748
The role of assessment in software process improvement
[AD-A227426] N91-14762
SOFTWARE TOOLS
ISIS and META projects
[NASA-CR-186413] N91-14731
The ISIS project: Real experience with a fault tolerant programming system
[NASA-CR-187029] N91-14732
Classifying software design methods
[AD-A226696] N91-14745
A software-system visualization tool
[AD-A227145] N91-14757
Literature survey on tools
[AD-A226933] N91-14770
SOI (SEMICONDUCTORS)
Dynamic behavior of thin silicon plate: Application to silicon sensors
[LAAS-90144] N91-14582
SOIL MAPPING
Climate and atmospheric modeling studies. Climate applications of Earth and planetary observations. Chemistry of Earth and environment
[NASA-CR-187326] N91-14684
SOIL SCIENCE
Acidic deposition: Its nature and impacts
[DE91-001984] N91-14658
Climate and atmospheric modeling studies. Climate applications of Earth and planetary observations. Chemistry of Earth and environment
[NASA-CR-187326] N91-14684
SOL-GEL PROCESSES
Conversion of alkoxide solutions to oxides: Evaporation of products
[AD-A226927] N91-14442
SOLAR ACTIVITY
On some peculiarities of solar differential rotation N91-15054
SOLAR ARRAYS
Status of LWIR HgCdTe infrared detector technology N91-14383
The synthesis of solar radiation data for sizing stand-alone photovoltaic systems
[DE90-012758] N91-14652
SOLAR ATMOSPHERE
A new model of spicule formation in the Sun chromosphere N91-15051
Nonlinear surface MHD waves in the inhomogeneous plasma with cusp-resonance in upper solar atmosphere N91-15052
Filamentary structures in the Sun's atmosphere as singular Alfven waves N91-15053
Interrelationship between the tearing-instability and magnetic island merging N91-15109
Nonlinear magnetosonic waves in an inhomogeneous plasma N91-15110
Flare heating and ionization of the low solar chromosphere N91-15116
SOLAR CELLS
High efficiency cadmium and zinc telluride-based thin film solar cells
[DE91-002112] N91-14643
Processing experiments for development of high-efficiency silicon solar cells
[DE91-002698] N91-14645
Preliminary survey of 21st century civil mission applications of space nuclear power
[NASA-TM-101249] N91-14817
SOLAR COLLECTORS
High-temperature thermal storage systems for advanced solar receivers materials selections
[NASA-CR-187750] N91-14647
Solar concentrator development in the US
[DE91-001232] N91-14649
SOLAR CORONA
The design of optical sensor for the pinhole/occulter facility
[NASA-CR-187694] N91-14825
Solar magnetic flux-tubes and coronal loops N91-15047
Nonlinearity influence in local resonance regions on the Alfven waves propagation in solar corona N91-15055
Coronal mass ejections
[NASA-CR-186579] N91-15115
SOLAR CYCLES
On some peculiarities of solar differential rotation N91-15054
SOLAR ELECTRIC PROPULSION
Space transfer concepts and analysis for exploration missions
[NASA-CR-183943] N91-14358
SOLAR ENERGY
Solar concentrator development in the US
[DE91-001232] N91-14649
SOLAR ENERGY CONVERSION
Solar concentrator development in the US
[DE91-001232] N91-14649
SOLAR FLARES
Solar magnetic flux-tubes and coronal loops N91-15047
High-energy particle acceleration during the implosion driven by 3-dimensional X-type current loop coalescence in solar flares N91-15048
Solar flares and particle acceleration N91-15049
A numerical calculation of parameters of explosion MHD shock waves from moderate solar flares N91-15066
Flare heating and ionization of the low solar chromosphere N91-15116
SOLAR MAGNETIC FIELD
Solar magnetic flux-tubes and coronal loops N91-15047
SOLAR PROMINENCES
Filamentary structures in the Sun's atmosphere as singular Alfven waves N91-15053
SOLAR RADIATION
The synthesis of solar radiation data for sizing stand-alone photovoltaic systems
[DE90-012758] N91-14652
Studies of the observed and theoretical variations of atmospheric ozone
[NASA-CR-187703] N91-14657
Solar radiation on Mars: Update 1990
[NASA-TM-103623] N91-15117
SOLAR ROTATION
On some peculiarities of solar differential rotation N91-15054
SOLAR TEMPERATURE
Flare heating and ionization of the low solar chromosphere N91-15116
SOLAR WIND
Solar wind dynamic pressure variations: Quantifying the statistical magnetospheric response N91-15060
Solitary vortices in the vicinity of comets N91-15062
Gradient catastrophe of the supersonic mass-loaded magnetised plasma flow and the formation of bow shock N91-15065
Influence of the parameter distribution of the solar wind near the Sun upon its structure at the Earth's orbit N91-15108
SOLDERED JOINTS
Effect of laser fluctuations in automated solder joint inspection
[AD-A226685] N91-14620
SOLID ELECTROLYTES
Conductivity fluctuations in fast ionic conductors
[AD-A227379] N91-14549
Prospects of new energy
[DE91-727567] N91-14654
SOLID LUBRICANTS
A continuum approach toward modeling the mechanics of solid lubricating films
[AD-A226961] N91-14486
SOLID MECHANICS
NASA-UVA light aerospace alloy and structures technology program
[NASA-CR-187321] N91-14474
SOLID PROPELLANT COMBUSTION
Solid fuel combustion
[AD-A227170] N91-14496
Effects of turbulence on stationary and nonstationary processes in C-systems
[AD-A227067] N91-14569
SOLID PROPELLANT ROCKET ENGINES
Axisymmetric shell analysis of the space shuttle solid rocket booster field joint
[NASA-TP-3033] N91-14618
SOLID PROPELLANTS
CFD code evaluation for internal flow modeling
[NASA-CR-187677] N91-14557
SOLID STATE
Solid state radioluminescent sources using zeolites
[DE91-002703] N91-14857
Theory of the electronic and structural properties of solid state oxides
[DE91-001192] N91-14874
SOLID STATE LASERS
Nonlinear dynamics of broad-band lasers
[DE91-001143] N91-14596
SOLID-SOLID INTERFACES
Some problems in elastic contact and fracture N91-14625
SOLVENT EXTRACTION
Characterization of phenolic resins with thermogravimetry-mass spectrometry
[DE91-002710] N91-14492
SOLVENTS
N-(3-ethynylphenyl)maleimide
[NASA-CASE-LAR-14138-2] N91-14419
SONIC ANEMOMETERS
A discussion of the results of an in-situ comparison of three full-vector anemometers
[DE91-002113] N91-14572
SOOT
Solid fuel combustion
[AD-A227170] N91-14496
SOUND FIELDS
Acoustic positioning and orientation prediction
[NASA-CASE-NPO-17511-1-CU] N91-14807
SOUND PRESSURE
Effects of turbulence on stationary and nonstationary processes in C-systems
[AD-A227067] N91-14569
SOUND WAVES
An investigation of the diffraction of an acoustic plane wave by a curved surface of finite impedance N91-14800
Effect of atmospherics on beamforming accuracy
[NASA-CR-187695] N91-14802
Acoustic positioning and orientation prediction
[NASA-CASE-NPO-17511-1-CU] N91-14807
Acoustic transducer apparatus with reduced thermal conduction
[NASA-CASE-NPO-17620-1-CU] N91-14808
SPACE COMMERCIALIZATION
Outer space: What should be the US Government policy toward the region beyond Earth's atmosphere. National debate topic for high schools, 1990-1991
[PB90-255464] N91-14896
SPACE ERECTABLE STRUCTURES
Mechanical end joint system for connecting structural column elements
[NASA-CASE-LAR-14465-1] N91-14614
SPACE EXPLORATION
Outer space: What should be the US Government policy toward the region beyond Earth's atmosphere. National debate topic for high schools, 1990-1991
[PB90-255464] N91-14896
SPACE HABITATS
Space transfer concepts and analysis for exploration missions
[NASA-CR-183943] N91-14358
SPACE LABORATORIES
Exobiology in Earth orbit: The results of science workshops held at NASA, Ames Research Center
[NASA-SP-500] N91-14725
SPACE MISSIONS
Preliminary survey of 21st century civil mission applications of space nuclear power
[NASA-TM-101249] N91-14817
SPACE PLASMAS
Nonlinearity influence in local resonance regions on the Alfven waves propagation in solar corona N91-15055
Detection of nonlinear features in plasma and field measurements by PROGNOZ-8 N91-15063
Laboratory and computer simulations of wave generation processes in non-stationary astrophysical phenomena N91-15082
Nonlinear magnetosonic waves in an inhomogeneous plasma N91-15110
SPACE POWER REACTORS
Preliminary survey of 21st century civil mission applications of space nuclear power
[NASA-TM-101249] N91-14817
SPACE SHUTTLE BOOSTERS
Space shuttle redesigned solid rocket motor Certificate of Qualification (COQ) data report
[NASA-CR-184051] N91-14416
Axisymmetric shell analysis of the space shuttle solid rocket booster field joint
[NASA-TP-3033] N91-14618
A parametric shell analysis of the shuttle 51-L SRB AFT field joint
[NASA-TM-102748] N91-14629
SPACE SHUTTLE MISSION 51-L
A parametric shell analysis of the shuttle 51-L SRB AFT field joint
[NASA-TM-102748] N91-14629

SPACE SHUTTLE MISSIONS
Flight Set 360L006 STS-34 field joint protection system, thermal protection system, and systems tunnel components, volume 4
[NASA-CR-184050] N91-14415
SPACE SHUTTLE PAYLOADS
Initial blood storage experiment
[NASA-CR-185513-PT-2] N91-14701
SPACE SHUTTLES
The AIS: A spectrograph/imager ensemble for space flight
[AD-A227009] N91-14413
State of the art in video system performance N91-14578
Plasma waves associated with the space shuttle N91-15064
Chronology: MSFC Space Shuttle program development, assembly, and testing major events (1969 - April, 1981)
[NASA-CR-184013] N91-15120
SPACE STATION STRUCTURES
Smart tunnel: Docking mechanism
[NASA-CASE-MSC-21360-1] N91-14374
SPACE STATIONS
Space station common module network topology and hardware development
[NASA-CR-184034] N91-14373
Definition of experiments to investigate fire suppressants in microgravity
[NASA-CR-185295] N91-14378
Liquid hydrogen polygeneration system and process
[NASA-CASE-KSC-11304-2] N91-14495
Position requirements for space station personnel and linkages to portable microcomputer performance assessment
[NASA-CR-185606] N91-14719
Chronology: MSFC Space Shuttle program development, assembly, and testing major events (1969 - April, 1981)
[NASA-CR-184013] N91-15120
SPACE SURVEILLANCE (SPACEBORNE)
SDIO long wavelength infrared detector requirements N91-14381
LWIR detector requirements for low-background space applications N91-14382
Radiation response issues for infrared detectors N91-14388
SPACE WEAPONS
SDIO long wavelength infrared detector requirements N91-14381
SPACEBORNE ASTRONOMY
A rocket-borne measurement of interstellar dust emission at high galactic latitude N91-14976
SPACEBORNE EXPERIMENTS
Determination of SPEAR-1 rocket body potential during high-voltage experiments
[AD-A226971] N91-14417
Exobiology in Earth orbit: The results of science workshops held at NASA, Ames Research Center
[NASA-SP-500] N91-14725
SPACEBORNE TELESCOPES
Exobiology in Earth orbit: The results of science workshops held at NASA, Ames Research Center
[NASA-SP-500] N91-14725
SPACECRAFT CHARGING
Determination of SPEAR-1 rocket body potential during high-voltage experiments
[AD-A226971] N91-14417
SPACECRAFT CONSTRUCTION MATERIALS
Outgassing data for selecting spacecraft materials, revision 2
[NASA-RP-1124-REV-2] N91-14437
SPACECRAFT CONTROL
Adaptive control of large space structures
[AD-A227304] N91-14377
SPACECRAFT DESIGN
Advanced technology needs for a global change science program: Perspective of the Langley Research Center
[NASA-TM-4196] N91-14634
SPACECRAFT DOCKING
Smart tunnel: Docking mechanism
[NASA-CASE-MSC-21360-1] N91-14374
SPACECRAFT EQUIPMENT
System for connecting fluid couplings
[NASA-CASE-MFS-26042-1-SB] N91-14613
SPACECRAFT GUIDANCE
Gamma guidance of trajectories for coplanar, aeroassisted orbital transfer
[NASA-CR-187732] N91-14365
Properties of the optimal trajectories for coplanar, aeroassisted orbital transfer
[NASA-CR-187733] N91-14366
Decomposition technique and optimal trajectories for the aeroassisted flight experiment
[NASA-CR-187734] N91-14367
Guidance trajectories for aeroassisted orbital transfer
[NASA-CR-187735] N91-14368
SPACECRAFT INSTRUMENTS
Earth Observing Scanning Polarimeter (EOSP), phase B
[NASA-CR-187715] N91-14586
SPACECRAFT MODULES
Space station common module network topology and hardware development
[NASA-CR-184034] N91-14373
SPACECRAFT POWER SUPPLIES
Space station common module network topology and hardware development
[NASA-CR-184034] N91-14373
Liquid hydrogen polygeneration system and process
[NASA-CASE-KSC-11304-2] N91-14495
Preliminary survey of 21st century civil mission applications of space nuclear power
[NASA-TM-101249] N91-14817
Silicon carbide, a semiconductor for space power electronics
[NASA-TM-103655] N91-14850
SPACECRAFT STABILITY
The effects of liquid propellant motion on the attitude stability of spin stabilized spacecraft
[AD-A227002] N91-14376
SPACECRAFT TRACKING
Efficient detection and signal parameter estimation with application to high dynamic GPS receiver
[NASA-CASE-NPO-17820-1-CU] N91-14321
Satellite situation report, volume 30, no. 1
[NASA-TM-101105] N91-14372
SPACECRAFT TRAJECTORIES
Gamma guidance of trajectories for coplanar, aeroassisted orbital transfer
[NASA-CR-187732] N91-14365
Properties of the optimal trajectories for coplanar, aeroassisted orbital transfer
[NASA-CR-187733] N91-14366
Guidance trajectories for aeroassisted orbital transfer
[NASA-CR-187735] N91-14368
SPACECREWS
Position requirements for space station personnel and linkages to portable microcomputer performance assessment
[NASA-CR-185606] N91-14719
SPALLATION
Data requirements for intermediate energy nuclear applications
[DE91-004005] N91-14812
SPARK IGNITION
CRC program for quantifying performance of knock-sensor-equipped vehicles with varying octane level
[AD-A227340] N91-14612
SPATIAL DISTRIBUTION
Studies of the observed and theoretical variations of atmospheric ozone
[NASA-CR-187703] N91-14657
Optical phase conjugate beam modulator and method therefor
[AD-D014569] N91-14820
The spatial distribution of infrared radiation from visible reflection nebulae N91-14931
Studying the spatial distribution of interstellar dust N91-14980
Does the far-infrared/radio correlation in spiral galaxies extend to the spatial domain N91-14985
SPATIAL FILTERING
Systolic emulator experimentation
[AD-A226746] N91-14516
SPATIAL RESOLUTION
Statistical errors in the fractal analysis of flame boundaries
[DE91-001795] N91-14439
SPECIFIC HEAT
An automated flow calorimeter for heat capacity and enthalpy measurements at elevated temperatures and pressures
[DE91-002759] N91-14584
SPECTRA
A spectral difference between silicates in Comet Halley and interstellar silicates N91-15002
The pre- and post-accretion irradiation history of cometary ices N91-15007
SPECTRAL BANDS
New insights in the photochemistry of grain mantles: The identification of the 4.62 and 6.87 micron bands N91-14957
SPECTRAL ENERGY DISTRIBUTION
The spectral energy distribution of the scattered light from dark clouds N91-14911
SPECTRAL METHODS
The application of deterministic spectral domain method to the analysis of planar circuit discontinuities on open substrates
[AD-A226901] N91-14542
Mappings and accuracy for Chebyshev pseudo-spectral approximations
[NASA-TM-103630] N91-14781
SPECTRAL REFLECTANCE
In-line sensors for electrolytic magnesium cells
[DE91-002561] N91-14438
Comparison of ground and satellite based measurements of the fraction of photosynthetically active radiation intercepted by tall-grass prairie
[NASA-CR-187696] N91-14639
SPECTRAL RESOLUTION
High resolution spectroscopy of the 11.3 micron emission band N91-14917
SPECTROGRAPHS
The AIS: A spectrograph/imager ensemble for space flight
[AD-A227009] N91-14413
SPECTROMETERS
A balloon-borne aerosol spectrometer for high altitude low aerosol concentration measurements
[DE91-002563] N91-14661
SPECTROPHOTOMETRY
FTIR (Fourier Transform Infrared) spectrophotometry for thin film monitors: Computer and equipment integration for enhanced capabilities
[DE91-001228] N91-14853
SPECTROSCOPY
He atom surface spectroscopy: Surface lattice dynamics of insulators, metals, and metal overlayers
[DE91-001993] N91-14855
Three-micron spectroscopy of highly reddened field stars N91-14904
Observational constraints on interstellar dust models N91-14996
SPECTRUM ANALYSIS
A spectral difference between silicates in Comet Halley and interstellar silicates N91-15002
The 10 micron spectral structure in comets N91-15004
A comparative study of the continuum and emission characteristics of comet dust. 1: Are the silicates in Comet Halley and Kohoutek amorphous or crystalline N91-15005
SPEECH
Perception and temporal properties of speech
[AD-A226958] N91-14716
SPEECH RECOGNITION
Perception and temporal properties of speech
[AD-A226958] N91-14716
Massively parallel network architectures for automatic recognition of visual speech signals
[AD-A226968] N91-14805
SPHERICAL SHELLS
Infrared emission from ultracompact H II regions N91-14942
SPICULES
A new model of spicule formation in the Sun chromosphere N91-15051
SPIN STABILIZATION
Role of separation autopilots for modern missile concepts
[MBB/FE121/S/PUB/409/A] N91-14352
The effects of liquid propellant motion on the attitude stability of spin stabilized spacecraft
[AD-A227002] N91-14376
SPIN-LATTICE RELAXATION
Elucidation of fundamental properties of helium in metals by nuclear magnetic resonance techniques
[DE91-002715] N91-14460
SPIRAL GALAXIES
Grains in galactic halos N91-14984
Does the far-infrared/radio correlation in spiral galaxies extend to the spatial domain N91-14985
Far infrared structure of spiral galaxies from the IRAS CPC images N91-14988
SPLINE FUNCTIONS
Intelligent manipulation technique for multi-branch robotic systems
[NASA-CR-187651] N91-14603
The evaluation of long range consequences in decision making
[AD-A226949] N91-14888
SPOILERS
The forward mounted spoiler as a source of buffet excitation N91-14332
SPOKES
Accretion disk instability and spokes in Saturn's rings N91-15094
SPRAYED COATINGS
Phase changes during plasma spray deposition
[IPPCZ-297] N91-14837

SPREAD SPECTRUM TRANSMISSION
International Symposium on Information Theory
[AD-A226957] N91-14521
SPUTTERING
Kinetics of molecular beam epitaxy: Effect of ion-induced sputtering
[DE91-004511] N91-14493
SQUALLS
Modeling study of tropical nonsquall and squall clusters N91-14685
STABILITY
The effect of scandium on the phase stability of Al3Nb and Al3Zr
[DE91-002657] N91-14459
Randomly sampled-data control systems
[NASA-CR-187425] N91-14734
STABILITY TESTS
HgZnTe-based detectors for LWIR NASA applications N91-14404
STABILIZATION
Snow avalanche hazards and mitigation in the United States
[LC-90-62814] N91-14686
Phase changes during plasma spray deposition
[IPPCZ-297] N91-14837
STAGE SEPARATION
Flight Set 360L006 STS-34 field joint protection system, thermal protection system, and systems tunnel components, volume 4
[NASA-CR-184050] N91-14415
STAGNATION FLOW
Prospects of new energy
[DE91-727567] N91-14654
STAINLESS STEELS
Effects of irradiation on initiation and crack-arrest toughness of two high-copper welds and on stainless steel cladding
[DE91-001272] N91-14467
Axial-torsional fatigue: A study of tubular specimen thickness effects
[NASA-TM-103637] N91-14632
STANDARD DEVIATION
Vibrational testing of optical fiber connector joints
[NASA-TM-103654] N91-14829
STANDARDS
Quality control and nondestructive test procedures for welded products
[DE91-004530] N91-14623
STAR FORMATION
Interstellar Dust: Contributed Papers
[NASA-CP-3036] N91-14897
The compact far infrared emission from the young stellar object IRAS 16293-2422 N91-14940
Dust in a few southern H II regions N91-14943
Distribution of dust in W31 complex N91-14944
The embedded objects in epsilon Cha I cloud N91-14949
Interferometric molecular line observations of W51 N91-14950
Dust emission from Barnard 35: Gas heating anomaly resolved N91-14951
A two micron polarization survey toward dark clouds N91-14952
IRAS results on outer galaxy star formation N91-14953
High resolution observations of compact H II regions at 230 GHz N91-14954
Infrared studies of dust grains in infrared reflection nebulae N91-14970
Dust in regions of massive star formation N91-14972
STAR TRACKERS
Graphics software for the HP825/9000 IFSI system
[IFSI-89-18] N91-14735
STATIC LOADS
The interlaminar shear strength of woven carbon, woven glass and woven carbon/glass hybrid laminates under static and impact loading
[OUEL-1831/90] N91-14423
STATIC TESTS
Internal performance of a hybrid axisymmetric/nonaxisymmetric convergent-divergent nozzle
[NASA-TM-4230] N91-14275
STATISTICAL ANALYSIS
Statistical errors in the fractal analysis of flame boundaries
[DE91-001795] N91-14439
Opposed jet turbulent diffusion flames
[AD-A227048] N91-14446
Studies in statistical signal processing
[AD-A226825] N91-14518
Multiple strike slip faults sets: A case study from the Dead Sea transform N91-14669
Initial blood storage experiment
[NASA-CR-185513-PT-1] N91-14700
Position requirements for space station personnel and linkages to portable microcomputer performance assessment
[NASA-CR-185606] N91-14719
Approximately integrable linear statistical models in non-parametric estimation
[AD-A227395] N91-14798
The detection of a broad interstellar extinction feature near 1700 A N91-14900
STATISTICAL DISTRIBUTIONS
Cloud cover statistics
[AD-A226892] N91-14689
The autocorrelation function of the North Pole dust N91-14901
STATORS
Turbomachinery rotor support with damping
[NASA-CASE-MFS-28345-1] N91-14608
STEADY STATE
Atmospheric source-receptor relationships: Concepts and terminology
[DE91-001033] N91-14656
Linear resonant interaction of an electromagnetic wave with a collisional inhomogeneous plasma
[IPPCZ-298] N91-14836
STEELS
A modification of 4330 alloy steel
[DE91-001764] N91-14455
Amorphization of C-implanted Fe(Cr) alloys
[DE91-001338] N91-14469
Use of anomalous small angle x ray scattering to investigate microstructural features in complex alloys
[DE91-002397] N91-14471
Thin steel section casting on a near-horizontal twin-belt caster
[DE91-001883] N91-14505
STELLAR ACTIVITY
Compact object masses in active galactic nuclei and quasars and duration of activity stage N91-15096
STELLAR ATMOSPHERES
The origin of micrograins N91-15000
On the generation of magnetic fields in active star atmospheres N91-15099
Radiation-driven diskons as a new astrophysical object N91-15105
STELLAR COLOR
Small scale variations of abundances of transiently heated grains in molecular clouds N91-14927
Additional red and reddened stars in Cyg OB2 association N91-14948
The influence of grain growth in circumstellar dust envelopes on observed colors and polarization of some eruptive stars N91-15020
STELLAR CORES
A two micron polarization survey toward dark clouds N91-14952
STELLAR ENVELOPES
Observational constraints on interstellar dust models N91-14996
Superaromatics: The key to a unified cosmic dust theory N91-14999
The origin of micrograins N91-15000
A spectral difference between silicates in Comet Halley and interstellar silicates N91-15002
PAH formation in carbon-rich circumstellar envelopes N91-15015
Dust formation around M-type stars N91-15017
IR emission from circumstellar envelopes of C-rich stars N91-15019
The influence of grain growth in circumstellar dust envelopes on observed colors and polarization of some eruptive stars N91-15020
Using infrared spectral features to probe circumstellar dust shells around cool stars N91-15021
New circumstellar dust component in oxygen rich environments N91-15023
Type of silicate feature in oxygen rich stellar envelopes N91-15024
Dust around Mira variables: An analysis of IRAS LRS spectra N91-15026
Polarization due to dust scattering in the planetary nebula Cn1-1 N91-15027
Circumstellar grain extinction properties of recently discovered post AGB stars N91-15028
The discovery of a highly polarized bipolar nebula N91-15031
STELLAR EVOLUTION
Reddening and extinction towards H II regions N91-14898
Grain mantles: The impact on grain evolution and selective extinction N91-14960
Sublimating icy planetesimals as the source of nucleation seeds for grain condensation in classical novae N91-15016
Dust formation around M-type stars N91-15017
Sublimating comets as the source of nucleation seeds for grain condensation in the gas outflow from AGB stars N91-15018
Carbon stars with alpha-C:H emission N91-15022
Circumstellar grain extinction properties of recently discovered post AGB stars N91-15028
Compact reflection nebulae, a transit phase of evolution from post-AGB to planetary nebulae N91-15029
Continuous infrared emission of proto- and young-planetary nebulae N91-15030
On the braking mechanisms of pulsars N91-15090
STELLAR LUMINOSITY
The embedded objects in epsilon Cha I cloud N91-14949
The 100 and 160 micron maps of the dust reemission from the nucleus and inner-arm regions of NGC 6946 N91-14983
On the possibility of discovering pulsed radiation from SN 1987A N91-15102
STELLAR MAGNETIC FIELDS
A two micron polarization survey toward dark clouds N91-14952
A new kind of magnetic buoyancy instability N91-15050
Matter penetration and motion through the magnetosphere of neutron star N91-15087
On the existence of circular polarisation in the pulsar radiation N91-15088
STELLAR MASS
The embedded objects in epsilon Cha I cloud N91-14949
Size distribution of dust grains: A problem of self-similarity N91-14997
STELLAR MASS ACCRETION
Continuum radiative transfer in accretion-powered pulsars N91-15043
Matter penetration and motion through the magnetosphere of neutron star N91-15087
The optical observations of x ray Nova GS2023+33 = V404 Cyg N91-15103
STELLAR MASS EJECTION
Sublimating icy planetesimals as the source of nucleation seeds for grain condensation in classical novae N91-15016
Coronal mass ejections
[NASA-CR-186579] N91-15115
STELLAR MODELS
Using infrared spectral features to probe circumstellar dust shells around cool stars N91-15021
Infrared emission from the supernova remnant Puppis A: Dust and gas parameters N91-15032
STELLAR RADIATION
On the existence of circular polarisation in the pulsar radiation N91-15088
Thirty-five-day cycle of Her X-1: Synthesised optical light curves in the model of freely processing neutron star N91-15089
On the theory of large-scale micropulse structure of pulsar radio radiation N91-15092
On the possibility of discovering pulsed radiation from SN 1987A N91-15102
STELLAR ROTATION
On the braking mechanisms of pulsars N91-15090
STELLAR SPECTRA
Reddening and extinction towards H II regions N91-14898
Dust in a few southern H II regions N91-14943
Survey observations of emission-line stars in the Orion region N91-14955
Using infrared spectral features to probe circumstellar dust shells around cool stars N91-15021
Carbon stars with alpha-C:H emission N91-15022
New circumstellar dust component in oxygen rich environments N91-15023
Interstellar extinction at 10-20 microns N91-15025
Dust around Mira variables: An analysis of IRAS LRS spectra N91-15026
Infrared emission from the supernova remnant Puppis A: Dust and gas parameters N91-15032
A proposed astronomical reference catalog of infrared sources
[AD-A226757] N91-15041
STELLAR SPECTROPHOTOMETRY
On the detectability of infrared echo arcs around supernova 1987A N91-15033
STELLAR STRUCTURE
The discovery of a highly polarized bipolar nebula N91-15031
Thirty-five-day cycle of Her X-1: Synthesised optical light curves in the model of freely processing neutron star N91-15089
STELLAR TEMPERATURE
PAHs molecules and heating of the interstellar gas N91-14939
Dust emission from Barnard 35: Gas heating anomaly resolved N91-14951

On the braking mechanisms of pulsars N91-15090
STELLAR WINDS
Dust in stellar wind bow shocks N91-14979
STEP FUNCTIONS
On probability intervals and their updating [RUU-CS-90-22] N91-14793
STIRLING CYCLE
One- and two-dimensional Stirling machine simulation using experimentally generated flow turbulence models [NASA-CR-185285] N91-14414
STOCHASTIC PROCESSES
Randomly sampled-data control systems [NASA-CR-187425] N91-14734
Stochastic histories of dust grains in the interstellar medium N91-14998
STOICHIOMETRY
Anomalous surface phase formation on Pt3Sn with zone axes group (100) [DE91-001794] N91-14456
STORMS (METEOROLOGY)
Explosive cyclogenesis: A case study of the Veterans' Day storm of 11-12 November 1987 [AD-A227077] N91-14691
Implications of multipoint observations of substorms in the inner magnetotail N91-15061
STRAIN GAGES
Wind tunnel balance [NASA-CASE-ARC-11877-1-SB] N91-14357
Computer-assisted strain-gage monitoring and data reduction system [AD-A226894] N91-14589
Damping measurements using operational data [DE91-002781] N91-14646
STRAPS
A cable vehicle barrier for alert aircraft protection [DE91-001723] N91-14354
STRATOSPHERE
A balloon-borne aerosol spectrometer for high altitude low aerosol concentration measurements [DE91-002563] N91-14661
STREAK CAMERAS
Avalanche transistor selection for long term stability in streak camera sweep and pulser applications [DE91-004195] N91-14535
Integrated optical devices for photonics instrumentation systems [DE91-004192] N91-14828
STRESS (PSYCHOLOGY)
The effects of sleep loss on individual and group performance [AD-A226963] N91-14708
STRESS ANALYSIS
An analysis of interlaminar stresses in unsymmetrically laminated plates [NASA-CR-187657] N91-14424
A boundary element method for elastostatic and elastodynamic crack problems in two and three dimensions N91-14626
STRESS DISTRIBUTION
An analysis of interlaminar stresses in unsymmetrically laminated plates [NASA-CR-187657] N91-14424
Reports on block rotations, fault domains and crustal deformation [NASA-CR-186756] N91-14665
Block rotations, fault domains and crustal deformation in the western US N91-14666
Distributed deformation and block rotation in 3D N91-14667
Stress field rotation or block rotation: An example from the Lake Mead fault system N91-14668
STRESS INTENSITY FACTORS
A boundary element method for elastostatic and elastodynamic crack problems in two and three dimensions N91-14626
STRING THEORY
Capturing strong reduction in director string calculus [AD-A226738] N91-14783
STRUCTURAL ANALYSIS
Investigation of combustion in large vortices [AD-A226791] N91-14441
A parametric shell analysis of the shuttle 51-L SRB AFT field joint [NASA-TM-102748] N91-14629
Research in progress in applied mathematics, numerical analysis, and computer science [NASA-CR-187474] N91-14726
NASA's supercomputing experience [NASA-TM-102890] N91-14727
STRUCTURAL DESIGN
Structural development of laminar flow control aircraft chordwise wing joint designs [NASA-CR-181888] N91-14346
NASA-UVA light aerospace alloy and structures technology program [NASA-CR-187321] N91-14474
Hybrid butterfly valve [NASA-CASE-SSC-00004-1] N91-14609
The synthesis of solar radiation data for sizing stand-alone photovoltaic systems [DE90-012758] N91-14652
Bio-reactor chamber [NASA-CASE-MSC-20929-1] N91-14703
STRUCTURAL FAILURE
A statistically-based model of the interacting processes which lead to creep-rupture in filament-wound composite pressure vessels N91-14420
STRUCTURAL VIBRATION
Computer-assisted strain-gage monitoring and data reduction system [AD-A226894] N91-14589
STUDENTS
Research as part of the Air Force Research in Aero-Propulsion Technology (AFRAPT) program [AD-A226893] N91-14350
SUBLIMATION
Sublimating icy planetesimals as the source of nucleation seeds for grain condensation in classical novae N91-15016
SUBMARINES
Measurement of hydrodynamic forces and moments and flow field mapping of a model in coning motion [AD-A226684] N91-14355
SUBMILLIMETER WAVES
Millimeter-wave monolithic diode-grid frequency multiplier [NASA-CASE-NPO-17258-1-CU] N91-14551
A rocket-borne measurement of interstellar dust emission at high galactic latitude N91-14976
SUBROUTINES
Prediction of XV-15 tilt rotor discrete frequency aeroacoustic noise with WOPWOP [NASA-CR-187684] N91-14803
SUBSTRATES
Method of growing diamond film on substrates [AD-D014632] N91-14479
SULFIDES
Gas-phase formation of silicon carbides, oxides, and sulphides from atomic silicon ions N91-15014
SUPERCOMPUTERS
NASA's supercomputing experience [NASA-TM-102890] N91-14727
SUPERCONDUCTING FILMS
Fabrication of sensitive high Tc bolometers N91-14389
Superconducting properties of Tl-Ba-Ca-Cu-O films on silver substrates [DE91-002304] N91-14856
Irradiation-induced pinning in single-crystal and thin-film Tl2Ca2Ba2Cu3O10 superconductors [DE91-001342] N91-14877
SUPERCONDUCTING SUPER COLLIDER
Software management issues --- superconducting super collider detectors [DE91-001031] N91-14763
SUPERCONDUCTIVITY
Superconducting current transducer [DE91-004674] N91-14554
Design and application possibilities of superconducting radio-frequency quadrupoles [DE91-004477] N91-14881
Experimental results in superconducting niobium resonators for high-brightness ion beam acceleration [DE91-004478] N91-14882
First tests of a superconducting RFQ (radio frequency quadrupole) structure [DE91-004483] N91-14883
SUPERCONDUCTORS
SDIO long wavelength infrared detector requirements N91-14381
Fabrication of sensitive high Tc bolometers N91-14389
A characterization of internal-Sn Nb3 Sn superconductors for use in the Proof of Priciples (PoP) coil [DE91-001743] N91-14852
Irreversibility temperatures in oxide- and metallic superconductors [DE91-004021] N91-14861
SUPERCRITICAL AIRFOILS
Effects of trailing-edge flap on buffet characteristics of a supercritical airfoil N91-14327
Experimental investigation of buffet onset and penetration on a supercritical airfoil at transonic speeds N91-14328
SUPERFLUIDITY
On the braking mechanisms of pulsars N91-15090
SUPERGIANT STARS
Three-micron spectroscopy of highly reddened field stars N91-14904
SUPERHIGH FREQUENCIES
Description of the bistatic radar terrain measurements system equipment [AD-A226808] N91-14517
SUPERLATTICES
Innovative Long Wavelength Infrared Detector Workshop Proceedings [NASA-CR-187433] N91-14379
Intersubband absorption in Si(1-x)Ge(x/Si superlattices for long wavelength infrared detectors N91-14399
Growth and properties of Hg-based quantum well structures and superlattices N91-14403
Small band gap superlattices as inrinsic long wavelength infrared detector materials N91-14405
LWIR detector research in InAsSb/InAs N91-14406
InAs/Ga(1-x)In(x)Sb superlattices for infrared detector applications N91-14407
IR detectors based on n-i-p-i superlattices N91-14408
InAs/GaAs and InAs doping superlattices N91-14409
AlSb/InAs/AlSb quantum wells N91-14411
Pseudomorphic InGaAs materials [AD-A226895] N91-14864
Defect and impurity effects on the initial growth of Ag on Si(111) [DE91-001277] N91-14876
SUPERNOVA REMNANTS
Laboratory investigation of electric charging of dust particles by electrons, ions, and UV radiation N91-14971
Stochastic histories of dust grains in the interstellar medium N91-14998
Infrared emission from the supernova remnant Puppis A: Dust and gas parameters N91-15032
Laboratory simulation of the astrophysical burst processes in non-uniform magnetised media N91-15061
SUPERNOVA 1987A
On the detectability of infrared echo arcs around supernova 1987A N91-15033
The plasma model of radioemission from SN 1987A N91-15101
On the possibility of discovering pulsed radiation from SN 1987A N91-15102
SUPERNOVAE
Does the far-infrared/radio correlation in spiral galaxies extend to the spatial domain N91-14985
SUPERPLASTICITY
Processing studies of aluminum-magnesium and aluminum-copper-lithium alloys [AD-A227255] N91-14465
SUPERSONIC COMBUSTION
Investigation of combustion in large vortices [AD-A226791] N91-14441
SUPERSONIC FLOW
Computation of viscous supersonic flows N91-14283
Supersonic vortex flows around a missile body: Basic experiment and Euler numerical computation N91-14291
Asymmetric supersonic flow around cones with noncircular sections N91-14292
The inviscid stability of supersonic flow past heated or cooled axisymmetric bodies [NASA-CR-187475] N91-14307
SUPERSONIC SPEED
Pressure measurements on slender bodies at supersonic speeds and development of flow separation critera for Euler codes N91-14282
Computation of viscous supersonic flows N91-14283
Supersonic tactical missile computation using Euler's equation with crossflow separation modeling N91-14284
Comparison of different calculation methods applied to a lenticular fuselage section N91-14293
SUPPORTS
Turbomachinery rotor support with damping [NASA-CASE-MFS-28345-1] N91-14608
Post clamp [NASA-CASE-LEW-14862-1] N91-14617
SUPPRESSORS
Investigating individual differences in general comprehension skill: The role of suppression and enhancement [AD-A226788] N91-14715
SURFACE DIFFUSION
Effect of step edge transition rates and anisotropy in simulations of epitaxial growth [DE91-001251] N91-14875
SURFACE DISTORTION
Method for detecting surface motions and mapping small terrestrial or planetary surface deformations with synthetic aperture radar [NASA-CASE-NPO-17831-1-CU] N91-14642
SURFACE FINISHING
Surface treatment of metals [EP-PATENT-0-367-504-A2] N91-14453

SURFACE LAYERS
A LEED study of the MgO(001) surface structure
[DE91-002811] N91-14879
SURFACE NAVIGATION
Optimal sensor fusion for land vehicle navigation
[DE91-002586] N91-14319
SURFACE PROPERTIES
Surface and interfacial properties of carbon fibers
[NASA-CR-184916] N91-14429
Anomalous surface phase formation on Pt3Sn with zone axes group (100)
[DE91-001794] N91-14456
Application of ultrasonic guided waves to the characterization of texture in metal sheets of cubic and hexagonal crystallites
[DE91-001107] N91-14466
Some problems in elastic contact and fracture
N91-14625
SURFACE REACTIONS
Photodissociation near a rough metal surface: Effect of reaction fields
[AD-A227030] N91-14445
Laser studies of the interaction of SiO with the surface of a thin film
[DE91-004562] N91-14450
Wall conditioning and plasma surface interactions in DIII-D
[DE91-001547] N91-14846
Defect and impurity effects on the initial growth of Ag on Si(111)
[DE91-001277] N91-14876
Photogenerated carrier-induced reaction on semiconductor surfaces
[DE91-001349] N91-14878
SURFACE ROUGHNESS
Photodissociation near a rough metal surface: Effect of reaction fields
[AD-A227030] N91-14445
SURFACE ROUGHNESS EFFECTS
A mesoscale planetary boundary layer numerical model for simulations of topographically induced circulations
N91-15113
SURFACE WATER
Acidic deposition: Its nature and impacts
[DE91-001984] N91-14658
SURFACE WAVES
The application of deterministic spectral domain method to the analysis of planar circuit discontinuities on open substrates
[AD-A226901] N91-14542
The distribution of wave heights and periods for seas with unimodal bimodal power density spectra
[AD-A227040] N91-14696
SURVEILLANCE
Automatic dependent surveillance benefit and cost analysis
[DOT/FAA/RD-90/34] N91-14320
A system architecture for long duration free floating flight for military applications
[NASA-CR-187435] N91-14513
SURVEYS
Results of the users' requirements survey
N91-14575
State of the art in video system performance
N91-14578
Position requirements for space station personnel and linkages to portable microcomputer performance assessment
[NASA-CR-185606] N91-14719
A survey for PAH emission in H II regions, planetary and proto-planetary nebulae N91-14920
SUSPENDING (HANGING)
Electrostatically suspended rotor for angular encoder
[NASA-CASE-MFS-28294-1] N91-14508
SUSPENSION SYSTEMS (VEHICLES)
Evaluation of performance and feedback control design for vehicle suspensions with variable compliance elements N91-14601
SWEPT WINGS
Flow visualization studies of blowing from the tip of a swept wing
[NASA-TM-4217] N91-14274
SWITCHES
Transient analysis of a two-phase hydrogen heat switch
[DE91-002314] N91-14506
Triggering GaAs lock-on switches with laser diode arrays
[DE91-002419] N91-14532
Thermal switch disc for short circuit protection of batteries
[NASA-CASE-MSC-21428-1] N91-14537
A study of two control methods for full bridge converters: Soft switch bypass and current mode control
[AD-A227136] N91-14546
SWITCHING
A study of two control methods for full bridge converters: Soft switch bypass and current mode control
[AD-A227136] N91-14546
SWITCHING CIRCUITS
Optically-triggered GaAs thyristor switch s: Integrated structures for environmental hardening
[DE91-001355] N91-14553
Rise time and recovery of GaAs photoconductive semiconductor switches
[DE91-001267] N91-14854
SYLLABLES
Perception and temporal properties of speech
[AD-A226958] N91-14716
SYNAPSES
Bioreactivity: Studies on a simple brain stem reflex in behaving animals
[AD-A226823] N91-14704
SYNCHRONISM
Digitized synchronous demodulator
[NASA-CASE-GSC-13237-1] N91-14550
SYNCHROTRONS
A versatile RF cavity mode damper
[DE91-002947] N91-14534
SYNTHESIS (CHEMISTRY)
N-(3-ethynylphenyl)maleimide
[NASA-CASE-LAR-14188-2] N91-14419
Process for lowering the dielectric constant of polyimides using diamic acid additives
[NASA-CASE-LAR-13902-1] N91-14484
Approaches to the design of a novel macromolecular system with tailored optical properties
[AD-A226952] N91-14485
Heterocycles based on group 3, 4, and 5 elements: Precursors for novel glasses and ceramics
[AD-A226988] N91-14487
Synthesis and properties of novel organometallic polymers
[DE91-001978] N91-14491
An investigation of diamond synthesis in an oxygen-acetylene diffusion flame
[AD-A227224] N91-14870
SYNTHETIC APERTURE RADAR
Multiband radar characterization of forest biomes
[NASA-CR-185101] N91-14638
Method for detecting surface motions and mapping small terrestrial or planetary surface deformations with synthetic aperture radar
[NASA-CASE-NPO-17831-1-CU] N91-14642
SYNTHETIC RESINS
N-(3-ethynylphenyl)maleimide
[NASA-CASE-LAR-14188-2] N91-14419
SYSTEM FAILURES
Integration of sneak analysis with design, volume 1
[AD-A226902] N91-14543
SYSTEMS ENGINEERING
Human factors engineering. Part 1: Test procedures
[AD-A226480] N91-14720
NASA's supercomputing experience
[NASA-TM-102890] N91-14727
SYSTEMS INTEGRATION
System integration of a block code
[ETN-91-98169] N91-14514
The ISIS project: Real experience with a fault tolerant programming system
[NASA-CR-187029] N91-14732
SYSTEMS SIMULATION
Prototyping of a protocol validation environment: Application to the Estelle approach
[LAAS-90113] N91-14774
SYSTEMS STABILITY
Stable explicit depth extrapolation of seismic wavefields
[DE91-001445] N91-14674
SYSTOLIC ARRAYS
Systolic emulator experimentation
[AD-A226746] N91-14516

T

TACTILE DISCRIMINATION
Development of a taction system using piezoelectric film
[AD-A227076] N91-14544
TAIL ASSEMBLIES
Wind tunnel investigation and flight tests of tail buffet on the CF-18 aircraft N91-14325
A unified approach to buffet response of fighter aircraft empennage N91-14326
TANTALUM ALLOYS
Short term creep rupture predictions for Tantalum alloy T-3
[DE91-002338] N91-14458
TARGET ACQUISITION
Device and method for monitoring the presence of an object in space
[AD-D014621] N91-14823
TARGET RECOGNITION
Feature set evaluation for classifiers
[AD-A226903] N91-14751
Feature set evaluation for classifiers
[AD-A226904] N91-14752
Feature set evaluation for classifiers
[AD-A226905] N91-14753
TARGETS
Low velocity impact analysis with NASTRAN
[NASA-TM-103169] N91-14426
TASKS
Interaction of feel system and flight control system dynamics on lateral flying qualities
[NASA-CR-179445] N91-14353
Validation of dichotic listening and psychomotor task performance as predictors of primary flight training criteria: Highlighting relevant statistical issues
[AD-A227010] N91-14717
TAYLOR SERIES
Stable explicit depth extrapolation of seismic wavefields
[DE91-001445] N91-14674
TECHNICAL WRITING
Tips on how to cut technical publications costs
[AD-A227334] N91-14895
TECHNOLOGIES
Manufacturing Technology: A Sandia Technology Bulletin, Volume 1, No. 1
[DE91-002518] N91-14504
TECHNOLOGY ASSESSMENT
Expendable Pattern Casting Technology
[DE91-001348] N91-14503
Chemical vapor deposition modeling: An assessment of current status
[NASA-CR-185301] N91-14511
National software capacity: Near-term study
[AD-A226694] N91-14743
TECHNOLOGY TRANSFER
Space transfer concepts and analysis for exploration missions
[NASA-CR-183943] N91-14358
Manufacturing Technology: A Sandia Technology Bulletin, Volume 1, No. 1
[DE91-002518] N91-14504
The NASA/DOD aerospace knowledge diffusion research project: A research agenda
[NASA-TM-103439] N91-14892
TECHNOLOGY UTILIZATION
An evaluation of two flat-black silicone paints for space application
[NASA-TM-100768] N91-14494
NASA's supercomputing experience
[NASA-TM-102890] N91-14727
TECTONICS
Method for detecting surface motions and mapping small terrestrial or planetary surface deformations with synthetic aperture radar
[NASA-CASE-NPO-17831-1-CU] N91-14642
Stress field rotation or block rotation: An example from the Lake Mead fault system N91-14668
Multiple strike slip faults sets: A case study from the Dead Sea transform N91-14669
Plate motions and deformations from geologic and geodetic data
[NASA-CR-187379] N91-14672
Crustal dynamics project: The interpretation of crustal dynamics data in terms of plate motions and regional deformation near plate boundaries
[NASA-CR-187691] N91-14673
Crustal Dynamics Project data analysis, 1990
[NASA-TM-100765] N91-14679
TELECOMMUNICATION
Information technology and the conduct of research: The user's view. Report of the Panel on Information Technology and the Conduct of Research
[ISBN-0-309-03888-X] N91-14890
TELEMETRY
The vertical Van de Graaff telemetry system
[DE91-001960] N91-14370
Adaptive data acquisition multiplexing system and method
[NASA-CASE-MSC-21170-1] N91-14371
TELESCOPES
Wind tunnel study of an observatory dome with a circular aperture
[NASA-TM-102888] N91-15040
TELEVISION SYSTEMS
State of the art in video system performance
N91-14578
TELLURIDES
Small band gap superlattices as intrinsic long wavelength infrared detector materials N91-14405

TEMPERATURE CONTROL
Thermal switch disc for short circuit protection of batteries
[NASA-CASE-MSC-21428-1] N91-14537
TEMPERATURE DISTRIBUTION
A numerical and experimental analysis of reactor performance and deposition rates for CVD on monofilaments
[NASA-TM-103631] N91-14500
Temperature distribution of dust in luminous IRAS galaxies N91-14982
TEMPERATURE EFFECTS
Laminar/turbulent flow transition effects on high-speed missile domes N91-14301
Fundamental studies on microstructural evolution of two-phase titanium alloys N91-14452
Use of anomalous small angle x ray scattering to investigate microstructural features in complex alloys
[DE91-002397] N91-14471
Flow behavior of Ti-24Al-11Nb at high strain rates
[DE91-004506] N91-14473
Development of an animal model of human non-freezing cold injury: Changes in thermal sensitivity following cold exposure
[AD-A227174] N91-14705
Study of spin-temperature effects using energy-ordered continuum gamma ray spectroscopy technique
[DE91-002854] N91-14818
Influence of temperature on the infrared spectrum of the coronene molecule N91-14932
TEMPERATURE GRADIENTS
Explosive cyclogenesis: A case study of the Veterans' Day storm of 11-12 November 1987
[AD-A227077] N91-14691
TEMPERATURE MEASUREMENT
Irreversibility temperatures in oxide- and metallic superconductors
[DE91-004021] N91-14861
TEMPERATURE PROFILES
A numerical and experimental analysis of reactor performance and deposition rates for CVD on monofilaments
[NASA-TM-103631] N91-14500
Validation of a computational model for autogenous arc welding
[AD-A227258] N91-14611
TEMPERATURE SENSORS
Wind tunnel balance
[NASA-CASE-ARC-11877-1-SB] N91-14357
TENSILE PROPERTIES
Ultrasonic detection of fatigue damage in glass-epoxy composites
[DE91-002652] N91-14619
TENSILE STRENGTH
Directional solidification of superalloys
[NASA-CASE-MFS-28314-1] N91-14462
TEPHIGRAMS
The rotation of Venus and its atmosphere N91-15112
TERNARY SYSTEMS
On the crystal structure of KInS2-I
[AD-A226940] N91-14866
TERRAIN
Description of the bistatic radar terrain measurements system equipment
[AD-A226808] N91-14517
Remote sensing of Earth terrain
[NASA-CR-186904] N91-14635
TEST EQUIPMENT
Electro-optical spin measurement system
[NASA-CASE-LAR-13629-1] N91-14356
TEST FACILITIES
Chronology: MSFC Space Shuttle program development, assembly, and testing major events (1969 - April, 1981)
[NASA-CR-184013] N91-15120
TEST VEHICLES
CRC program for quantifying performance of knock-sensor-equipped vehicles with varying octane level
[AD-A227340] N91-14612
THALLIUM COMPOUNDS
Superconducting properties of Tl-Ba-Ca-Cu-O films on silver substrates
[DE91-002304] N91-14856
THERMAL ABSORPTION
An investigation of using a phase-change material to improve the heat transfer in a small electronic module for an airborne radar application
[DE91-002597] N91-14525
THERMAL ANALYSIS
Thermal analyses for quality control of plastics, ceramics, and explosives
[DE91-002701] N91-14622
THERMAL BATTERIES
A materials database for Li(Si)/FeS2 thermal batteries
[DE91-002592] N91-14531
THERMAL CONDUCTIVITY
Heterocycles based on group 3, 4, and 5 elements: Precursors for novel glasses and ceramics
[AD-A226988] N91-14487
High-temperature thermal storage systems for advanced solar receivers materials selections
[NASA-CR-187750] N91-14647
THERMAL DEGRADATION
Characterization of phenolic resins with thermogravimetry-mass spectrometry
[DE91-002710] N91-14492
THERMAL EMISSION
The wavelength dependence of polarization in NGC 2023 N91-14923
Studying the spatial distribution of interstellar dust N91-14980
Thermal emission from interstellar dust in and near the Pleiades N91-14981
The pre- and post-accretion irradiation history of cometary ices N91-15007
THERMAL EXPANSION
A novel electron tunneling infrared detector N91-14391
Optimization of interface layers in the design of ceramic fiber reinforced metal matrix composites
[NASA-CR-185307] N91-14422
Thermal compensating mount
[NASA-CASE-LAR-14207-1] N91-14590
THERMAL MAPPING
Thermal imaging on missiles in hypersonic flow N91-14303
THERMAL NEUTRONS
Status of the advanced neutron source
[DE91-002870] N91-14810
THERMAL PLASMAS
Continuum radiative transfer in accretion-powered pulsars N91-15043
THERMAL PROTECTION
Flight Set 360L006 STS-34 field joint protection system, thermal protection system, and systems tunnel components, volume 4
[NASA-CR-184050] N91-14415
Thermal switch disc for short circuit protection of batteries
[NASA-CASE-MSC-21428-1] N91-14537
THERMAL SHOCK
An evaluation of two flat-black silicone paints for space application
[NASA-TM-100768] N91-14494
THERMAL STABILITY
Thermal stability of the microstructure of an aged Nb-Zr-C alloy
[NASA-TM-103647] N91-14454
On the thermal stability of slabs, cylinders, and spheres N91-15057
THERMAL STRESSES
Optimization of interface layers in the design of ceramic fiber reinforced metal matrix composites
[NASA-CR-185307] N91-14422
Study of diamond film growth and properties
[NASA-CR-187709] N91-14483
THERMOCHEMISTRY
Missile Aerodynamics
[AGARD-CP-493] N91-14278
Computational models with advanced thermochemistry for the analysis of missile/plume flowfield interactions N91-14305
Chemical vapor deposition modeling: An assessment of current status
[NASA-CR-185301] N91-14511
Computation of thermochemical nonequilibrium flows around a simple and a double ellipse
[NASA-CR-187702] N91-14558
THERMOCLINES
The SYNOP experiment: Inverted echo sounder data report for October 1987 to May 1988
[AD-A227232] N91-14699
THERMODYNAMIC CYCLES
Design of a He4 cooling system for a cryostat working at 1K
[IFSI-89-17] N91-14502
THERMODYNAMIC PROPERTIES
Transient analysis of a two-phase hydrogen heat switch
[DE91-002314] N91-14506
New accurate, vectorized approximations of state surfaces for the thermodynamic and transport properties of equilibrium air
[MBB/FE122/S/PUB/0389] N91-14886
THERMODYNAMICS
The definition of necessary hidden units in neural networks for combinatorial optimization
[AD-A227142] N91-14786
THERMOELASTICITY
An analysis of interlaminar stresses in unsymmetrically laminated plates
[NASA-CR-187657] N91-14424
THERMOELECTRIC GENERATORS
Short term creep rupture predictions for Tantalum alloy T-3
[DE91-002338] N91-14458
THERMOGRAVIMETRY
Characterization of phenolic resins with thermogravimetry-mass spectrometry
[DE91-002710] N91-14492
THERMOMECHANICAL TREATMENT
Thermomechanical processing and ambient temperature properties of a 6061 aluminum 10 volume percent alumina metal matrix composite
[AD-A227004] N91-14433
Processing studies of aluminum-magnesium and aluminum-copper-lithium alloys
[AD-A227255] N91-14465
THERMONUCLEAR REACTIONS
ITER global stability limits
[DE91-001488] N91-14845
On the generation of magnetic fields in active star atmospheres N91-15099
THERMOPLASTIC RESINS
Surface and interfacial properties of carbon fibers
[NASA-CR-184916] N91-14429
Mesomechanical model for fibre composites
[AD-A226792] N91-14432
THERMOREGULATION
Development of an animal model of human non-freezing cold injury: Changes in thermal sensitivity following cold exposure
[AD-A227174] N91-14705
THICKNESS
NOVA 201 ultrasonic thickness gage (NOVA Gage)
[NASA-CR-184031] N91-14581
THIN FILMS
Conversion of alkoxide solutions to oxides: Evaporation of products
[AD-A226927] N91-14442
Laser studies of the interaction of SiO with the surface of a thin film
[DE91-004562] N91-14450
Ion-induced grain growth in multilayer and coevaporated metal alloy thin films
[DE91-004489] N91-14472
Method of growing diamond film on substrates
[AD-D014632] N91-14479
A continuum approach toward modeling the mechanics of solid lubricating films
[AD-A226961] N91-14486
Effect of interline heat flow parameter on contact line heat transfer
[AD-A226944] N91-14566
High efficiency cadmium and zinc telluride-based thin film solar cells
[DE91-002112] N91-14643
FTIR (Fourier Transform Infrared) spectrophotometry for thin film monitors: Computer and equipment integration for enhanced capabilities
[DE91-001226] N91-14853
Growth, characterization and device development in monocrystalline diamond films
[AD-A227238] N91-14871
Low-energy electron diffraction investigation of epitaxial growth: Pt and Pd(100)
[DE91-000750] N91-14873
Irradiation-induced pinning in single-crystal and thin-film Tl2Ca2Ba2Cu3O10 superconductors
[DE91-001342] N91-14877
Ground boundaries
[DE91-004027] N91-14880
THIN WALLED SHELLS
The buckling of off-axis, orthotropic, cylindrical shells in torsion N91-14628
Interstellar extinction at 10-20 microns N91-15025
THREE DIMENSIONAL BODIES
Task reports on developing techniques for scattering by 3D composite structures and to generate new solutions in diffraction theory using higher order boundary conditions
[NASA-CR-186899] N91-14475
A finite element conjugate gradient FFT method for scattering N91-14476
THREE DIMENSIONAL FLOW
Numerical investigations in three-dimensional internal flows
[NASA-CR-187373] N91-14277
Three dimensional flow calculations for a projectile with standard and dome bases N91-14294
Navier-Stokes predictions of static and dynamic aerodynamic derivatives for high L/D finned projectiles N91-14295

THREE DIMENSIONAL MODELS
Reports on block rotations, fault domains and crustal deformation
[NASA-CR-186756] N91-14665
Climate and atmospheric modeling studies. Climate applications of Earth and planetary observations. Chemistry of Earth and environment
[NASA-CR-187326] N91-14684
Modeling study of tropical nonsquall and squall clusters N91-14685
THROTTLING
Hybrid butterfly valve
[NASA-CASE-SSC-00004-1] N91-14609
THRUST
Internal performance of a hybrid axisymmetric/nonaxisymmetric convergent-divergent nozzle
[NASA-TM-4230] N91-14275
THYRISTORS
Optically-triggered GaAs thyristor switch s: Integrated structures for environmental hardening
[DE91-001355] N91-14553
TILT ROTOR AIRCRAFT
Prediction of XV-15 tilt rotor discrete frequency aeroacoustic noise with WOPWOP
[NASA-CR-187684] N91-14803
TIME DEPENDENCE
Evaluations of some scheduling algorithms for hard real-time systems
[AD-A226930] N91-14755
TIME MARCHING
Acceleration techniques for explicit Euler codes N91-14555
TIME MEASUREMENT
Electro-optic network analyzer
[NASA-CR-186613] N91-14527
The evaluation of long range consequences in decision making
[AD-A226949] N91-14888
TIME RESPONSE
Rise time and recovery of GaAs photoconductive semiconductor switches
[DE91-001267] N91-14854
TIME SERIES ANALYSIS
The SYNOP experiment: Inverted echo sounder data report for October 1987 to May 1988
[AD-A227232] N91-14699
TIME SHARING
Data transmission networks N91-14576
TIME TEMPERATURE PARAMETER
A novel approach to determine the heat transfer coefficient in directional solidification furnaces
[NASA-CR-187648] N91-14885
TIN ALLOYS
Anomalous surface phase formation on Pt3Sn with zone axes group (100)
[DE91-001794] N91-14456
A characterization of internal-Sn Nb3 Sn superconductors for use in the Proof of Priciples (PoP) coil
[DE91-001743] N91-14852
TITANIUM
Investigation of new semiinsulating behavior of 3-5 compounds
[AD-A226787] N91-14862
TITANIUM ALLOYS
Fundamental studies on microstructural evolution of two-phase titanium alloys N91-14452
Amorphization of C-implanted Fe(Cr) alloys
[DE91-001338] N91-14469
TITANIUM COMPOUNDS
Fatigue and fracture of titanium aluminides, volume 2
[AD-A227353] N91-14351
TOILETS
Valve for waste collection and storage
[NASA-CASE-MSC-21025-4] N91-14723
Method for waste collection and storage
[NASA-CASE-MSC-21025-2] N91-14724
TOKAMAK DEVICES
ITER global stability limits
[DE91-001488] N91-14845
Wall conditioning and plasma surface interactions in DIII-D
[DE91-001547] N91-14846
DIII-D results and plans
[DE91-001548] N91-14847
A method for estimating tokamak poloidal field coil currents which incorporates engineering constraints
[DE91-001662] N91-14848
Tokamak fluidlike equations, with applications to turbulence and transport in H mode discharges
[DE91-002632] N91-14849
TOMOGRAPHY
Statistical errors in the fractal analysis of flame boundaries
[DE91-001795] N91-14439
TOPOGRAPHY
A mesoscale planetary boundary layer numerical model for simulations of topographically induced circulations N91-15113
TOPOLOGY
(DURIP) exploring and controlling spatio temporal chaos under complex structures through visualization: A mini-supercomputer approach
[AD-A226793] N91-14784
TOROIDAL DISCHARGE
Tokamak fluidlike equations, with applications to turbulence and transport in H mode discharges
[DE91-002632] N91-14849
TOROIDAL PLASMAS
Fast electron studies in the ZT-40M edge plasma
[DE91-002323] N91-14838
Tokamak fluidlike equations, with applications to turbulence and transport in H mode discharges
[DE91-002632] N91-14849
TOROIDS
Improved high power/high frequency inductor
[NASA-CASE-NPO-17830-1-CU] N91-14539
TORQUE
New results in the theory of dust grain alignment N91-14906
TORSION
The buckling of off-axis, orthotropic, cylindrical shells in torsion N91-14628
TOTAL OZONE MAPPING SPECTROMETER
NA-9 Solar Backscatter Ultraviolet (SBUV/2) instrument and derived ozone data
[AD-A227449] N91-15118
TOWNSEND AVALANCHE
Avalanche transistor selection for long term stability in streak camera sweep and pulser applications
[DE91-004195] N91-14535
TOXICITY
Smoke and extinguisher agent dissipation in a small pressurized fuselage
[DOT/FAA/CT-89/31] N91-14317
Definition of experiments to investigate fire suppressants in microgravity
[NASA-CR-185295] N91-14378
TRAILING EDGE FLAPS
Effects of trailing-edge flap on buffet characteristics of a supercritical airfoil N91-14327
TRAINING EVALUATION
Pedagogical strategies for human and computer tutoring
[AD-A226886] N91-14750
TRAJECTORY CONTROL
Modeling and control design of a wind tunnel model support
[NASA-TM-103829] N91-14540
Planning monotone paths to visit a set of obstacles
[AD-A226923] N91-14754
TRAJECTORY OPTIMIZATION
Gamma guidance of trajectories for coplanar, aeroassisted orbital transfer
[NASA-CR-187732] N91-14365
Properties of the optimal trajectories for coplanar, aeroassisted orbital transfer
[NASA-CR-187733] N91-14366
Decomposition technique and optimal trajectories for the aeroassisted flight experiment
[NASA-CR-187734] N91-14367
Guidance trajectories for aeroassisted orbital transfer
[NASA-CR-187735] N91-14368
Robot control strategies
[OUEL-1754/89] N91-14605
Planning monotone paths to visit a set of obstacles
[AD-A226923] N91-14754
TRAJECTORY PLANNING
Contribution to the specification and implementation of complex robot tasks
[ETN-90-98209] N91-14604
Planning monotone paths to visit a set of obstacles
[AD-A226923] N91-14754
TRANSDUCERS
Superconducting current transducer
[DE91-004674] N91-14554
TRANSFER FUNCTIONS
Studies in statistical signal processing
[AD-A226825] N91-14518
Pregalactic inhomogeneity in hot dark matter model of the universe N91-15100
TRANSFER ORBITS
Gamma guidance of trajectories for coplanar, aeroassisted orbital transfer
[NASA-CR-187732] N91-14365
Properties of the optimal trajectories for coplanar, aeroassisted orbital transfer
[NASA-CR-187733] N91-14366
Decomposition technique and optimal trajectories for the aeroassisted flight experiment
[NASA-CR-187734] N91-14367
Guidance trajectories for aeroassisted orbital transfer
[NASA-CR-187735] N91-14368
TRANSFORMATIONS (MATHEMATICS)
The 3-D depth migration via McClellan transformations
[DE91-001446] N91-14675
TRANSIENT HEATING
On the origin of extinction in the Coma cluster of galaxies N91-14987
TRANSIENT PRESSURES
Solar wind dynamic pressure variations: Quantifying the statistical magnetospheric response N91-15060
TRANSIENT RESPONSE
Low velocity impact analysis with NASTRAN
[NASA-TM-103169] N91-14426
TRANSISTOR CIRCUITS
Avalanche transistor selection for long term stability in streak camera sweep and pulser applications
[DE91-004195] N91-14535
TRANSISTORS
Avalanche transistor selection for long term stability in streak camera sweep and pulser applications
[DE91-004195] N91-14535
TRANSITION FLOW
One- and two-dimensional Stirling machine simulation using experimentally generated flow turbulence models
[NASA-CR-185285] N91-14414
TRANSITION METALS
The effect of scandium on the phase stability of Al3Nb and Al3Zr
[DE91-002657] N91-14459
Investigation of new semiinsulating behavior of 3-5 compounds
[AD-A226787] N91-14862
TRANSITION TEMPERATURE
Irreversibility temperatures in oxide- and metallic superconductors
[DE91-004021] N91-14861
Transient x ray irradiation of high transition temperature superconducting material
[AD-A227090] N91-14869
TRANSMISSION EFFICIENCY
Apparatus and method for characterizing the transmission efficiency of a mass spectrometer
[NASA-CASE-NPO-16989-1-CU] N91-14587
TRANSMISSION LINES
One- and two-dimensional Stirling machine simulation using experimentally generated flow turbulence models
[NASA-CR-185285] N91-14414
TRANSMITTER RECEIVERS
Electro-optical spin measurement system
[NASA-CASE-LAR-13629-1] N91-14356
TRANSONIC FLOW
Acceleration techniques for explicit Euler codes N91-14555
TRANSONIC SPEED
A method for the design of transonic flexible wings
[NASA-TP-3045] N91-14323
Experimental investigation of buffet onset and penetration on a supercritical airfoil at transonic speeds N91-14328
TRANSONIC WIND TUNNELS
Internal performance of a hybrid axisymmetric/nonaxisymmetric convergent-divergent nozzle
[NASA-TM-4230] N91-14275
TRANSPORT PROPERTIES
AlSb/InAs/AlSb quantum wells N91-14411
New accurate, vectorized approximations of state surfaces for the thermodynamic and transport properties of equilibrium air
[MBB/FE122/S/PUB/0389] N91-14886
TRANSPORT THEORY
Tokamak fluidlike equations, with applications to turbulence and transport in H mode discharges
[DE91-002632] N91-14849
TRANSVERSE WAVES
Excitation of Langmuir wave by transversal nonlinear wave in the electron-positron inhomogeneous plasma in the presence of positron beam N91-15076
TRAPEZOIDAL WINGS
Experimental investigations of buffet excitation forces on a low aspect ratio trapezoidal half wing in incompressible flow N91-14329
Experimental investigation and semi-empirical prediction of the dynamic response of a low-aspect-ratio trapezoidal wing due to flow separation N91-14330
TRAPPED PARTICLES
Method and apparatus for determining time, direction, and composition of impacting space particles
[NASA-CASE-LAR-13392-1-CU] N91-14412
TRENDS
Some trends in missile aerodynamics N91-14279
Information technology and the conduct of research: The user's view. Report of the Panel on Information Technology and the Conduct of Research
[ISBN-0-309-03888-X] N91-14890

TRIETHYL COMPOUNDS
Analysis of hydroxylammonium nitrate based liquid propellants
[AD-A227300] N91-14497
TRIGGER CIRCUITS
Optically-triggered GaAs thyristor switch s: Integrated structures for environmental hardening
[DE91-001355] N91-14553
TRISONIC WIND TUNNELS
Wind tunnel investigation and flight tests of tail buffet on the CF-18 aircraft N91-14325
TRITIUM
Elucidation of fundamental properties of helium in metals by nuclear magnetic resonance techniques
[DE91-002715] N91-14460
Physics data base for the Beam Plasma Neutron Source (BPNS)
[DE91-002796] N91-14842
TROPICAL REGIONS
Modeling study of tropical nonsquall and squall clusters N91-14685
TRUSSES
Multivariable methods for the design, identification, and control of large space structures. Volume 2: Optimal and sub-optimal estimation applied to large flexible structures
[AD-A226699] N91-14375
Methods for evaluating the predictive accuracy of structural dynamic models
[NASA-CR-187649] N91-14630
TUNABLE LASERS
Field induced gap infrared detector
[NASA-CASE-NPO-17526-1-CU] N91-14588
TUNDRA
Analysis of the boreal forest-tundra ecotone: A test of AVIRIS capabilities in the Eastern Canadian subarctic
[NASA-CR-187335] N91-14655
TUNNELS
Smart tunnel: Docking mechanism
[NASA-CASE-MSC-21360-1] N91-14374
TURBINE BLADES
A discussion of the results of an in-situ comparison of three full-vector anemometers
[DE91-002113] N91-14572
Load response of horizontal-axis wind turbines to turbulence
[DE90-000375] N91-14644
TURBINE ENGINES
Fatigue and fracture of titanium aluminides, volume 2
[AD-A227353] N91-14351
TURBINES
Wingtip vortex turbine
[NASA-CASE-LAR-14116-1] N91-14345
TURBOCOMPRESSORS
CRC program for quantifying performance of knock-sensor-equipped vehicles with varying octane level
[AD-A227340] N91-14612
TURBOGENERATORS
Wingtip vortex turbine
[NASA-CASE-LAR-14116-1] N91-14345
TURBULENCE
Statistical errors in the fractal analysis of flame boundaries
[DE91-001795] N91-14439
CFD code evaluation for internal flow modeling
[NASA-CR-187677] N91-14557
Active control of boundary layer transition and turbulence
[NASA-CASE-LAR-13532-1] N91-14562
Load response of horizontal-axis wind turbines to turbulence
[DE90-000375] N91-14644
Effects of wind shear and turbulence on wind turbine power curves
[DE91-004072] N91-14648
(DURIP) exploring and controlling spatio temporal chaos under complex structures through visualization: A mini-supercomputer approach
[AD-A226793] N91-14784
Size distribution of dust grains: A problem of self-similarity N91-14997
TURBULENCE EFFECTS
Opposed jet turbulent diffusion flames
[AD-A227048] N91-14446
Effects of turbulence on stationary and nonstationary processes in C-systems
[AD-A227067] N91-14569
TURBULENCE MODELS
Computation of viscous supersonic flows N91-14283
Computation of axisymmetric base flow with different turbulence models N91-14298
Computational models with advanced thermochemistry for the analysis of missile/plume flowfield interactions N91-14305
One- and two-dimensional Stirling machine simulation using experimentally generated flow turbulence models
[NASA-CR-185285] N91-14414
Solid fuel combustion
[AD-A227170] N91-14496
TURBULENT BOUNDARY LAYER
Dynamics of separation and reattachment in a Mach 5 unswept compression ramp flow N91-14276
Solid fuel combustion
[AD-A227170] N91-14496
Effects of turbulence on stationary and nonstationary processes in C-systems
[AD-A227067] N91-14569
TURBULENT DIFFUSION
Opposed jet turbulent diffusion flames
[AD-A227048] N91-14446
TURBULENT FLOW
Laminar/turbulent flow transition effects on high-speed missile domes N91-14301
One- and two-dimensional Stirling machine simulation using experimentally generated flow turbulence models
[NASA-CR-185285] N91-14414
The application of the turbulent burning speed concept to laboratory flames
[DE91-001789] N91-14449
Direct numerical simulation of turbulent couette flow, part 2
[AD-A226770] N91-14564
Innovative methodology for cancelling contaminating noise in turbulent fluid flow environments
[AD-A227028] N91-14567
Phase portrait methods for verifying fluid dynamic simulations
[DE91-001129] N91-14571
A discussion of the results of an in-situ comparison of three full-vector anemometers
[DE91-002113] N91-14572
Piecewise-parabolic methods for systems of hyperbolic conservation laws in multiprocessing environments
[DE91-004582] N91-14792
TURBULENT HEAT TRANSFER
Observation of electron hole, double layer, and turbulent heating in a laboratory plasma N91-15079
TVD SCHEMES
Numerical study of shock-wave/boundary layer interactions in premixed hydrogen-air hypersonic flows
[NASA-TM-103273] N91-14559
TWO DIMENSIONAL FLOW
A numerical and experimental analysis of reactor performance and deposition rates for CVD on monofilaments
[NASA-TM-103631] N91-14500
TWO DIMENSIONAL MODELS
One- and two-dimensional Stirling machine simulation using experimentally generated flow turbulence models
[NASA-CR-185285] N91-14414
Modeling study of tropical nonsquall and squall clusters N91-14685
Linear resonant interaction of an electromagnetic wave with a collisional inhomogeneous plasma
[IPPCZ-298] N91-14836

U

ULTRAHIGH VACUUM
Photogenerated carrier-induced reaction on semiconductor surfaces
[DE91-001349] N91-14878
ULTRASHORT PULSED LASERS
Picosecond laser system for high speed characterization of monolithic devices
[AD-A227372] N91-14595
ULTRASONIC RADIATION
Investigations of ultrasonic wave interactions with grain boundaries and grain imperfections
[DE91-002695] N91-14804
ULTRASONIC TESTS
Application of ultrasonic guided waves to the characterization of texture in metal sheets of cubic and hexagonal crystallites
[DE91-001107] N91-14486
ULTRASONICS
NOVA 201 ultrasonic thickness gage (NOVA Gage)
[NASA-CR-184031] N91-14581
ULTRAVIOLET ASTRONOMY
The dependence of UV extinction properties on dust environment N91-14902
Correlation properties of interstellar dust: Diffuse interstellar bands N91-14916
Spatial variations of the 3 micron emission features within nebulae N91-14922
ULTRAVIOLET RADIATION
The relationship between IR, optical, and UV extinction N91-14899
New measurements of the far ultraviolet scattering properties of interstellar dust N91-14909
Observations of the diffuse UV radiation field N91-14912
Simultaneous infrared and UV-visible absorption spectra of matrix-isolated carbon vapor N91-14915
The evolution of organic mantles on interstellar grains N91-14964
Production and transfer of UV photons in non-homogeneous spherical clouds N91-14966
Grains charges in interstellar clouds N91-14967
Laboratory investigation of electric charging of dust particles by electrons, ions, and UV radiation N91-14971
Does CO trace H2 at high galactic latitude N91-14973
Galaxy formation by dust N91-14989
VUV-visible measurements on different samples of amorphous carbon N91-14990
ULTRAVIOLET SPECTRA
IR emission and UV extinction in two open clusters N91-14929
Laboratory studies of refractory metal oxide smokes N91-14993
Circumstellar grain extinction properties of recently discovered post AGB stars N91-15028
ULTRAVIOLET SPECTROMETERS
NA-9 Solar Backscatter Ultraviolet (SBUV/2) instrument and derived ozone data
[AD-A227449] N91-15118
ULTRAVIOLET TELESCOPES
The capability of the ultraviolet imaging telescope for observing interstellar dust N91-14913
UNDERWATER ACOUSTICS
Observations of ocean fluctuations between 15 and 23 hour periods in the Pacific
[AD-A227017] N91-14695
A model of the acoustic interactions occurring under Arctic ice
[AD-A227128] N91-14806
UNITED NATIONS
Environmental impact assessment as applied to policies, plans, and programs
[DE91-001372] N91-14664
UNITED STATES
Cloud cover statistics
[AD-A226892] N91-14689
Outer space: What should be the US Government policy toward the region beyond Earth's atmosphere. National debate topic for high schools, 1990-1991
[PB90-255464] N91-14896
UNIVERSE
Pregalactic inhomogeneity in hot dark matter model of the universe N91-15100
UNIVERSITY PROGRAM
Research as part of the Air Force Research in Aero-Propulsion Technology (AFRAPT) program
[AD-A226893] N91-14350
UNSTEADY AERODYNAMICS
Feasibility investigation of general time-domain unsteady aerodynamics of rotors
[NASA-CR-177570] N91-14311
An experimental investigation into the use of hot-film anemometry to measure vortical velocity behind a pitching wing
[AD-A227177] N91-14313
Control of unsteady aerodynamic forces
[AD-A227365] N91-14315
Experimental investigation and semi-empirical prediction of the dynamic response of a low-aspect-ratio trapezoidal wing due to flow separation N91-14330
Unsteady aerodynamic forces on an oscillating wing at high incidences and flow separation N91-14331
Unsteady separated flow phenomena causing self-excited structural oscillations N91-14339
Unsteady airloads due to separated flow on airfoils and wings N91-14340
UNSTEADY FLOW
Asymmetric supersonic flow around cones with noncircular sections N91-14292
Coupled aerodynamic loads due to unsteady stall on a large aspect ratio wing oscillating at great amplitude N91-14338
Unsteady separated flow phenomena causing self-excited structural oscillations N91-14339
One- and two-dimensional Stirling machine simulation using experimentally generated flow turbulence models
[NASA-CR-185285] N91-14414
Dynamics of an unsteady diffusion flame: Effects of heat release and gravity
[AD-A227348] N91-14447
A fast solver for systems of axisymmetric ring vortices
[DE91-002594] N91-14561

UPWELLING WATER
Upwelling southwest of Iceland due to quasi-geostrophic flow
[AD-A227129] N91-14698
USER MANUALS (COMPUTER PROGRAMS)
Development of phenomenological fitting procedure for the fast microcomputer
[AD-A227168] N91-14759
USER REQUIREMENTS
Some trends in missile aerodynamics N91-14279
Results of the users' requirements survey N91-14575

V

VACANCIES (CRYSTAL DEFECTS)
Crystal structure of ZnGa2S4, a defect sphalerite-derivative
[AD-A226937] N91-14865
VACUUM TESTS
Outgassing data for selecting spacecraft materials, revision 2
[NASA-RP-1124-REV-2] N91-14437
VALVES
Valve for waste collection and storage
[NASA-CASE-MSC-21025-4] N91-14723
VAN DE GRAAFF ACCELERATORS
The vertical Van de Graaff telemetry system
[DE91-001960] N91-14370
VANADIUM
Investigation of new semiinsulating behavior of 3-5 compounds
[AD-A226787] N91-14862
VANADIUM ALLOYS
Fundamental studies on microstructural evolution of two-phase titanium alloys N91-14452
VAPOR DEPOSITION
LWIR HgCdTe: Innovative detectors in an incumbent technology N91-14384
Possibilities for LWIR detectors using MBE-grown Si(/Si(1-x)Ge(x) structures N91-14400
Method of growing diamond film on substrates
[AD-D014632] N91-14479
Study of diamond film growth and properties
[NASA-CR-187709] N91-14483
A numerical and experimental analysis of reactor performance and deposition rates for CVD on monofilaments
[NASA-TM-103631] N91-14500
Chemical vapor deposition modeling: An assessment of current status
[NASA-CR-185301] N91-14511
Silicon carbide, a semiconductor for space power electronics
[NASA-TM-103655] N91-14850
Program to study the process parameters of OMVPE and their relationship to the properties of Ga(0.47)In(0.53) as ON InP substrates
[AD-A226618] N91-14851
FTIR (Fourier Transform Infrared) spectrophotometry for thin film monitors: Computer and equipment integration for enhanced capabilities
[DE91-001228] N91-14853
VAPOR PHASE EPITAXY
InAsSbBi, a direct band-gap, III-V, LWIR material N91-14410
Use of D2 to elucidate OMVPE growth mechanisms
[AD-A226966] N91-14443
Quantum well laser
[AD-A227303] N91-14594
Program to study the process parameters of OMVPE and their relationship to the properties of Ga(0.47)In(0.53) as ON InP substrates
[AD-A226618] N91-14851
Ultra high speed compound semiconductors and real time signal processing
[AD-A226790] N91-14863
VAPOR PHASES
Chemical vapor deposition modeling: An assessment of current status
[NASA-CR-185301] N91-14511
The pre- and post-accretion irradiation history of cometary ices N91-15007
Gas-phase formation of silicon carbides, oxides, and sulphides from atomic silicon ions N91-15014
PAH formation in carbon-rich circumstellar envelopes N91-15015
VAPORS
Spontaneous and induced coherent radiation generation in atomic vapors
[AD-A226776] N91-14830
Simultaneous infrared and UV-visible absorption spectra of matrix-isolated carbon vapor N91-14915
VARIABILITY
Shipboard and satellite observations of upper ocean velocity and transport variability in the Gulf Stream
[AD-A226974] N91-14694
VARIATIONS
Conductivity fluctuations in fast ionic conductors
[AD-A227379] N91-14549
Observations of ocean fluctuations between 15 and 23 hour periods in the Pacific
[AD-A227017] N91-14695
Improved estimation of variance components in mixed models
[AD-A226854] N91-14794
VECTOR PROCESSING (COMPUTERS)
CFD code evaluation for internal flow modeling
[NASA-CR-187677] N91-14557
VECTORS (MATHEMATICS)
Acceleration techniques for explicit Euler codes N91-14555
Reconstruction of vectorized raster data
[ETN-91-98143] N91-14738
VEGETATIVE INDEX
Comparison of ground and satellite based measurements of the fraction of photosynthetically active radiation intercepted by tall-grass prairie
[NASA-CR-187696] N91-14639
Evaluation of data reduction and composing of the NOAA global vegetation index product: A case study
[AD-A227397] N91-14641
VELOCITY DISTRIBUTION
Vibration isolation technology: Sensitivity of selected classes of experiments to residual accelerations
[NASA-CR-186902] N91-14624
Mesoscale features of a winter storm: Dual Doppler velocity fields and differential reflectivity
[AD-A227342] N91-14692
Shipboard and satellite observations of upper ocean velocity and transport variability in the Gulf Stream
[AD-A226974] N91-14694
VELOCITY MEASUREMENT
An experimental investigation into the use of hot-film anemometry to measure vortical velocity behind a pitching wing
[AD-A227177] N91-14313
Investigation of combustion in large vortices
[AD-A226791] N91-14441
On the breakdown of a vortex
[AD-A227066] N91-14568
A discussion of the results of an in-situ comparison of three full-vector anemometers
[DE91-002113] N91-14572
Mesoscale features of a winter storm: Dual Doppler velocity fields and differential reflectivity
[AD-A227342] N91-14692
VENTILATION
Smoke and extinguisher agent dissipation in a small pressurized fuselage
[DOT/FAA/CT-89/31] N91-14317
VENUS (PLANET)
The rotation of Venus and its atmosphere N91-15112
VENUS ATMOSPHERE
The rotation of Venus and its atmosphere N91-15112
Studies of the chemistry of the nightside ionosphere of Venus
[NASA-CR-187714] N91-15114
VERBAL COMMUNICATION
Investigations of probabilistic inference
[AD-A226882] N91-14795
Interpretation of conditional probabilities in probabilistic interference word problems
[AD-A226907] N91-14797
VERY LARGE SCALE INTEGRATION
Analogue computation using VLSI neural network devices
[OUEL-1835/90] N91-14773
VERY LONG BASE INTERFEROMETRY
Estimability of geodetic parameters from space VLBI observables
[NASA-CR-187413] N91-14636
Crustal Dynamics Project data analysis, 1990
[NASA-TM-100765] N91-14679
VIBRATION
Tabulation of data from the tip aerodynamics and acoustics test
[NASA-TM-102280] N91-14273
A vibrating razor blade machining tool for material removal on low-density foams
[DE91-002996] N91-14507
Vibrational testing of optical fiber connector joints
[NASA-TM-103654] N91-14829
Spatial variations of the 3 micron emission features within nebulae N91-14922
Red fluorescence and 3-12 micron emission in NGC 2023, HD 44179, M 82, and Lynds 1780 N91-14924
VIBRATION ISOLATORS
Evaluation of performance and feedback control design for vehicle suspensions with variable compliance elements N91-14601
Vibration isolation technology: Sensitivity of selected classes of experiments to residual accelerations
[NASA-CR-186902] N91-14624
VIBRATION MEASUREMENT
Vibration analyzer
[NASA-CASE-MSC-21408-1] N91-14607
VIBRATION TESTS
Vibrational testing of optical fiber connector joints
[NASA-TM-103654] N91-14829
VIBRATIONAL SPECTRA
Dynamic behavior of thin silicon plate: Application to silicon sensors
[LAAS-90144] N91-14582
Theoretical studies of important processes in planetary and comet atmospheres
[NASA-CR-187692] N91-15045
VIDEO DATA
High Resolution, High Frame Rate Video Technology
[NASA-CP-3080] N91-14574
Results of the users' requirements survey N91-14575
Data transmission networks N91-14576
Data compression applied to HHVT N91-14577
Advanced technology development for image gathering, coding, and processing N91-14579
High resolution, high frame rate video technology development plan and the near-term system conceptual design N91-14580
VIDEO EQUIPMENT
High resolution, high frame rate video technology development plan and the near-term system conceptual design N91-14580
VIDEO SIGNALS
State of the art in video system performance N91-14578
VISCOSITY
Dynamics of an unsteady diffusion flame: Effects of heat release and gravity
[AD-A227348] N91-14447
Evolution of high amplitude Alfven waves near a bow shock N91-15068
VISCOUS FLOW
Computation of viscous supersonic flows N91-14283
Aerodynamic characteristics of cylindrical bodies with pointed and truncated conical noses N91-14289
Computation of thermochemical nonequilibrium flows around a simple and a double ellipse
[NASA-CR-187702] N91-14558
VISCOUS FLUIDS
The effect of wall compliance on the Goertler vortex instability
[NASA-CR-187477] N91-14308
VISIBILITY
Smoke and extinguisher agent dissipation in a small pressurized fuselage
[DOT/FAA/CT-89/31] N91-14317
VISUAL PERCEPTION
Eye movements and visual information processing
[AD-A226782] N91-14714
(DURIP) exploring and controlling spatio temporal chaos under complex structures through visualization: A mini-supercomputer approach
[AD-A226793] N91-14784
The object display: Principles and review of experimental findings
[AD-A226883] N91-14796
VISUAL SIGNALS
Massively parallel network architectures for automatic recognition of visual speech signals
[AD-A226968] N91-14805
VOICE COMMUNICATION
Perception and temporal properties of speech
[AD-A226958] N91-14716
VOLTAGE CONTROLLED OSCILLATORS
Dual physiological rate measurement instrument
[NASA-CASE-MSC-20078-3] N91-14709
VOLTAGE CONVERTERS (DC TO DC)
A study of two control methods for full bridge converters: Soft switch bypass and current mode control
[AD-A227136] N91-14546
VOLTAGE GENERATORS
Avalanche transistor selection for long term stability in streak camera sweep and pulser applications
[DE91-004195] N91-14535
VORTEX BREAKDOWN
On the breakdown of a vortex
[AD-A227066] N91-14568
VORTEX GENERATORS
Large-scale vortices in compressible turbulent medium with the magnetic field N91-15095

VORTICES
Supersonic vortex flows around a missile body: Basic experiment and Euler numerical computation N91-14291
The effect of wall compliance on the Goertler vortex instability
[NASA-CR-187477] N91-14308
Control of unsteady aerodynamic forces
[AD-A227365] N91-14315
Wingtip vortex turbine
[NASA-CASE-LAR-14116-1] N91-14345
A fast solver for systems of axisymmetric ring vortices
[DE91-002594] N91-14561
Investigations of equilibria, lattices, and chaotic dynamics of 2-D Hamiltonian point vortices
[AD-A227364] N91-14570
Explosive cyclogenesis: A case study of the Veterans' Day storm of 11-12 November 1987
[AD-A227077] N91-14691
Oceanographic expert system validation using GOAP mesoscale products and Gulf/DART validation test data
[AD-A226929] N91-14693
Piecewise-parabolic methods for systems of hyperbolic conservation laws in multiprocessing environments
[DE91-004582] N91-14792
Solitary vortices in the vicinity of comets N91-15062
Experiments with collision of vortices in rotating and still free-surface shallow water N91-15080
Large-scale vortices in compressible turbulent medium with the magnetic field N91-15095
VORTICITY
An experimental investigation into the use of hot-film anemometry to measure vortical velocity behind a pitching wing
[AD-A227177] N91-14313

W

WAFERS
HgCdTe for NASA EOS missions and detector uniformity benchmarks N91-14385
Characterization of semiconductor surface-emitting laser wafers
[DE91-001336] N91-14598
Silicon carbide, a semiconductor for space power electronics
[NASA-TM-103655] N91-14850
WAKES
Feasibility investigation of general time-domain unsteady aerodynamics of rotors
[NASA-CR-177570] N91-14311
WALL FLOW
Variation of wall shear stress and Reynolds stress over a flat plate downstream of a boundary layer manipulator
[AD-A226875] N91-14565
WALL PRESSURE
Dynamics of separation and reattachment in a Mach 5 unswept compression ramp flow N91-14276
Variation of wall shear stress and Reynolds stress over a flat plate downstream of a boundary layer manipulator
[AD-A226875] N91-14565
Innovative methodology for cancelling contaminating noise in turbulent fluid flow environments
[AD-A227028] N91-14567
WALL TEMPERATURE
Hypersonic aerodynamics: An approximation method for the calculation of real gas effects and wall temperatures
[MBB/FE127/S/PUB/0403] N91-14306
The inviscid stability of supersonic flow past heated or cooled axisymmetric bodies
[NASA-CR-187475] N91-14307
WALLS
The effect of wall compliance on the Goertler vortex instability
[NASA-CR-187477] N91-14308
Surface settling in partially filled containers upon step reduction in gravity
[NASA-TM-103641] N91-14556
NOVA 201 ultrasonic thickness gage (NOVA Gage)
[NASA-CR-184031] N91-14581
Axial-torsional fatigue: A study of tubular specimen thickness effects
[NASA-TM-103637] N91-14632
Wall conditioning and plasma surface interactions in DIII-D
[DE91-001547] N91-14846
WARHEADS
Device and method for monitoring the presence of an object in space
[AD-D014621] N91-14823
WARNING SYSTEMS
Unidirectional amplitude sensitive noise riding threshold circuit
[AD-D014568] N91-14529
Computer-assisted strain-gage monitoring and data reduction system
[AD-A226894] N91-14589
WASTE DISPOSAL
Feasibility study of the seismic reflection method in Amargosa Desert, Nye County, Nevada
[DE91-001646] N91-14676
Valve for waste collection and storage
[NASA-CASE-MSC-21025-4] N91-14723
Method for waste collection and storage
[NASA-CASE-MSC-21025-2] N91-14724
WASTE WATER
Combined air and water pollution control system
[NASA-CASE-NST-00007-1] N91-14662
WATER
Synthesis of H2 in dirty ice mantles by fast ion energy loss: New experimental results increase the relevance of this mechanism N91-14962
Diffusion and infrared properties of molecules in ice mantles N91-14963
WATER CIRCULATION
Shipboard and satellite observations of upper ocean velocity and transport variability in the Gulf Stream
[AD-A226974] N91-14694
WATER DEPTH
The SYNOP experiment: Inverted echo sounder data report for October 1987 to May 1988
[AD-A227232] N91-14699
WATER POLLUTION
Acidic deposition: Its nature and impacts
[DE91-001984] N91-14658
Combined air and water pollution control system
[NASA-CASE-NST-00007-1] N91-14662
WATER PRESSURE
The SYNOP experiment: Inverted echo sounder data report for October 1987 to May 1988
[AD-A227232] N91-14699
WATER TEMPERATURE
The SYNOP experiment: Inverted echo sounder data report for October 1987 to May 1988
[AD-A227232] N91-14699
WATER TREATMENT
Combined air and water pollution control system
[NASA-CASE-NST-00007-1] N91-14662
WATER TUNNEL TESTS
Measurement of hydrodynamic forces and moments and flow field mapping of a model in coning motion
[AD-A226684] N91-14355
WATER WAVES
Perspectives on modeling electromagnetic sea scatter
[AD-A226939] N91-14520
The distribution of wave heights and periods for seas with unimodal bimodal power density spectra
[AD-A227040] N91-14696
WAVE AMPLIFICATION
Amplification of Alfven waves in free shear flows N91-15074
WAVE DIFFRACTION
Analytical solutions with Generalized Impedance Boundary Conditions (GIBC) N91-14477
WAVE DRAG
Effects of trailing-edge flap on buffet characteristics of a supercritical airfoil N91-14327
WAVE EQUATIONS
Linear stability and MHD wave propagation in plasmas with solar abundances N91-15056
A numerical calculation of parameters of explosion MHD shock waves from moderate solar flares N91-15066
Evolution of high amplitude Alfven waves near a bow shock N91-15068
WAVE EXCITATION
Excitation of Langmuir wave by transversal nonlinear wave in the electron-positron inhomogeneous plasma in the presence of positron beam N91-15076
WAVE GENERATION
Generation of cosmic rays in pinches N91-15070
Laboratory and computer simulations of wave generation processes in non-stationary astrophysical phenomena N91-15082
WAVE INTERACTION
Investigations of ultrasonic wave interactions with grain boundaries and grain imperfections
[DE91-002695] N91-14804
Experiments with collision of vortices in rotating and still free-surface shallow water N91-15080
WAVE PROPAGATION
Investigations of ultrasonic wave interactions with grain boundaries and grain imperfections
[DE91-002695] N91-14804
Nonlinear surface MHD waves in the inhomogeneous plasma with cusp-resonance in upper solar atmosphere N91-15052
Linear stability and MHD wave propagation in plasmas with solar abundances N91-15056
Excitation of Langmuir wave by transversal nonlinear wave in the electron-positron inhomogeneous plasma in the presence of positron beam N91-15076
Ultrarelativistic low-frequency electromagnetic waves in pulsar magnetospheres N91-15091
WAVE REFLECTION
Feasibility study of the seismic reflection method in Amargosa Desert, Nye County, Nevada
[DE91-001646] N91-14676
WAVE SCATTERING
Remote sensing of Earth terrain
[NASA-CR-186904] N91-14635
WAVEFORMS
An investigation of the diffraction of an acoustic plane wave by a curved surface of finite impedance N91-14800
WAVEGUIDES
Universal nondestructive mm-wave integrated circuit test fixture
[NASA-CASE-LEW-14746-1] N91-14552
HEM(sub 11) modes revisited
[DE91-001028] N91-14819
WEAK ENERGY INTERACTIONS
Sterile neutrinos and astrophysical and cosmological constraints on the parameters of the extended electroweak models N91-15083
WEAPON SYSTEMS
NUFA: A semi-empirical method for the prediction of isolated weapon aerodynamics N91-14287
WEAPONS
Thermal analyses for quality control of plastics, ceramics, and explosives
[DE91-002701] N91-14622
WEATHER FORECASTING
Aircraft measurements of electrified clouds at Kennedy Space Center. Part 1: 1988 flights N91-14681
Aircraft measurements of electrified clouds at Kennedy Space Center. Part 2: Case study: 4 November 1988 (88309) N91-14682
Semi-implicit time integration in limited area model
[AD-A226818] N91-14785
WEIGHTLESSNESS
Valve for waste collection and storage
[NASA-CASE-MSC-21025-4] N91-14723
Method for waste collection and storage
[NASA-CASE-MSC-21025-2] N91-14724
Acoustic positioning and orientation prediction
[NASA-CASE-NPO-17511-1-CU] N91-14807
WELDED JOINTS
Effects of irradiation on initiation and crack-arrest toughness of two high-copper welds and on stainless steel cladding
[DE91-001272] N91-14467
Enable Kit (MC-4246) for the DOT Charged Line System: Welding development report for 1/4-inch tubes and fittings
[DE91-002577] N91-14606
Validation of a computational model for autogenous arc welding
[AD-A227258] N91-14611
Quality control and nondestructive test procedures for welded products
[DE91-004530] N91-14623
WELDING
Enable Kit (MC-4246) for the DOT Charged Line System: Welding development report for 1/4-inch tubes and fittings
[DE91-002577] N91-14606
Quality control and nondestructive test procedures for welded products
[DE91-004530] N91-14623
WHISKER COMPOSITES
Aluminum nitride-silicon carbide whisker composites: Processing, properties, and microstructural stability
[DE91-001907] N91-14425
WHISTLERS
Laboratory and computer simulations of wave generation processes in non-stationary astrophysical phenomena N91-15082
WHITE DWARF STARS
On the nature of cosmic gamma ray bursts N91-15098
WINCHES
A cable vehicle barrier for alert aircraft protection
[DE91-001723] N91-14354
WIND EFFECTS
Effects of wind shear and turbulence on wind turbine power curves
[DE91-004072] N91-14648
Upwelling southwest of Iceland due to quasi-geostrophic flow
[AD-A227129] N91-14698
Effect of atmospherics on beamforming accuracy
[NASA-CR-187695] N91-14802

WIND SHEAR
Effects of wind shear and turbulence on wind turbine power curves
[DE91-004072] N91-14648
WIND TUNNEL APPARATUS
Electro-optical spin measurement system
[NASA-CASE-LAR-13629-1] N91-14356
Wind tunnel balance
[NASA-CASE-ARC-11877-1-SB] N91-14357
Modeling and control design of a wind tunnel model support
[NASA-TM-103829] N91-14540
Multiple axis reticle
[NASA-CASE-ARC-11886-1-SB] N91-14591
WIND TUNNEL MODELS
Aerodynamic design of Pegasus (trademark): Concept to flight with CFD N91-14285
A unified approach to buffet response of fighter aircraft empennage N91-14326
Wind tunnel balance
[NASA-CASE-ARC-11877-1-SB] N91-14357
Modeling and control design of a wind tunnel model support
[NASA-TM-103829] N91-14540
Multiple axis reticle
[NASA-CASE-ARC-11886-1-SB] N91-14591
WIND TUNNEL TESTS
Dynamics of separation and reattachment in a Mach 5 unswept compression ramp flow N91-14276
Aerodynamic design of Pegasus (trademark): Concept to flight with CFD N91-14285
Anticipation of aerodynamic coefficients of missile air intakes N91-14297
Wind tunnel investigation and flight tests of tail buffet on the CF-18 aircraft N91-14325
A unified approach to buffet response of fighter aircraft empennage N91-14326
Investigation of a semi-empirical method to predict limit cycle oscillations of modern fighter aircraft N91-14333
New method to determine in wind tunnel the buffeting forces N91-14337
Modeling and control design of a wind tunnel model support
[NASA-TM-103829] N91-14540
Wind tunnel study of an observatory dome with a circular aperture
[NASA-TM-102888] N91-15040
WIND TUNNELS
New method to determine in wind tunnel the buffeting forces N91-14337
Wind tunnel balance
[NASA-CASE-ARC-11877-1-SB] N91-14357
WIND TURBINES
A discussion of the results of an in-situ comparison of three full-vector anemometers
[DE91-002113] N91-14572
Load response of horizontal-axis wind turbines to turbulence
[DE90-000375] N91-14644
Damping measurements using operational data
[DE91-002781] N91-14646
Effects of wind shear and turbulence on wind turbine power curves
[DE91-004072] N91-14648
Fatigue reliability of wind turbine components
[DE91-001262] N91-14650
WIND VELOCITY
Mesoscale features of a winter storm: Dual Doppler velocity fields and differential reflectivity
[AD-A227342] N91-14692
WINDPOWERED GENERATORS
Effects of wind shear and turbulence on wind turbine power curves
[DE91-004072] N91-14648
WING PANELS
Structural development of laminar flow control aircraft chordwise wing joint designs
[NASA-CR-181888] N91-14346
WING TIPS
Flow visualization studies of blowing from the tip of a swept wing
[NASA-TM-4217] N91-14274
Wingtip vortex turbine
[NASA-CASE-LAR-14116-1] N91-14345
WINGS
Supersonic vortex flows around a missile body: Basic experiment and Euler numerical computation N91-14291
An experimental investigation into the use of hot-film anemometry to measure vortical velocity behind a pitching wing
[AD-A227177] N91-14313
Unsteady aerodynamic forces on an oscillating wing at high incidences and flow separation N91-14331
The forward mounted spoiler as a source of buffet excitation N91-14332
Interaction between the canard and wing flow on a model of a typical combat aircraft N91-14334
Predictions of F-111 TACT aircraft buffet response N91-14335
The effect of wing planform on low speed buffet N91-14336
New method to determine in wind tunnel the buffeting forces N91-14337
WIRE WINDING
Improved high power/high frequency inductor
[NASA-CASE-NPO-17830-1-CU] N91-14539
WORKLOADS (PSYCHOPHYSIOLOGY)
Information extraction from visual displays and the event-related brain potential
[AD-A227063] N91-14722
WORKSTATIONS
Computational equipment for the development of numerical algorithms computation
[AD-A226702] N91-14729

X

X RAY ABSORPTION
Atomic environments in iron meteorites using EXAFS N91-15011
X RAY ANALYSIS
Thermal stability of the microstructure of an aged Nb-Zr-C alloy
[NASA-TM-103647] N91-14454
X RAY BINARIES
Thirty-five-day cycle of Her X-1: Synthesised optical light curves in the model of freely processing neutron star N91-15089
The optical observations of x ray Nova GS2023+33 = V404 Cyg N91-15103
X RAY DIFFRACTION
An examination of delta prime growth in an aluminum-lithium alloy by x ray diffraction
[AD-A227254] N91-14464
X RAY FLUORESCENCE
X ray sensitive area detection device
[NASA-CASE-MFS-28232-1] N91-14835
X RAY IMAGERY
The design of optical sensor for the pinhole/occulter facility
[NASA-CR-187694] N91-14825
X ray sensitive area detection device
[NASA-CASE-MFS-28232-1] N91-14835
X RAY IRRADIATION
Transient x ray irradiation of high transition temperature superconducting material
[AD-A227090] N91-14869
X RAY SCATTERING
Use of anomalous small angle x ray scattering to investigate microstructural features in complex alloys
[DE91-002397] N91-14471
X RAY SPECTRA
Infrared emission from the supernova remnant Puppis A: Dust and gas parameters N91-15032
X WING ROTORS
Results of a sub-scale model rotor icing test
[NASA-TM-103709] N91-14309
XENON
A novel electron tunneling infrared detector N91-14391
XV-15 AIRCRAFT
Prediction of XV-15 tilt rotor discrete frequency aeroacoustic noise with WOPWOP
[NASA-CR-187684] N91-14803

Y

YAWING MOMENTS
Measurement of hydrodynamic forces and moments and flow field mapping of a model in coning motion
[AD-A226684] N91-14355
YIELD POINT
Study of diamond film growth and properties
[NASA-CR-187709] N91-14483
YIELD STRENGTH
Computer studies of the dynamic strength of ceramics
[DE91-002568] N91-14481
YTTRIUM
Surface treatment of metals
[EP-PATENT-0-367-504-A2] N91-14453
YTTRIUM OXIDES
Fabrication of sensitive high Tc bolometers N91-14389
An ion-channeling study of irradiation-induced amorphization of YBa2Cu3O(7-x)
[DE91-004488] N91-14884

Z

ZEOLITES
Solid state radioluminescent sources using zeolites
[DE91-002703] N91-14857
ZINC
HgZnTe-based detectors for LWIR NASA applications N91-14404
ZINC SULFIDES
Crystal structure of ZnGa2S4, a defect sphalerite-derivative
[AD-A226937] N91-14865
ZINC TELLURIDES
High efficiency cadmium and zinc telluride-based thin film solar cells
[DE91-002112] N91-14643
ZINCBLENDE
Crystal structure of ZnGa2S4, a defect sphalerite-derivative
[AD-A226937] N91-14865
ZIRCONIUM
Thermal stability of the microstructure of an aged Nb-Zr-C alloy
[NASA-TM-103647] N91-14454
ZIRCONIUM ALLOYS
An examination of delta prime growth in an aluminum-lithium alloy by x ray diffraction
[AD-A227254] N91-14464
ZIRCONIUM COMPOUNDS
High temperature refractory member with radiation emissive overcoat
[NASA-CASE-NPO-17122-1-CU] N91-14489
ZIRCONIUM OXIDES
Electrophoretic and electrolytic deposition of ceramic particles on porous substrates
[AD-A227371] N91-14488
ZODIACAL DUST
A study of extended zodiacal structures
[NASA-CR-187687] N91-15044
ZODIACAL LIGHT
Observations of the diffuse UV radiation field N91-14912
Infrared emission from interplanetary dust N91-15013
ZONAL FLOW (METEOROLOGY)
Theory and measurements of nighttime horizontal gradients in the mid-latitude F region N91-14671
ZONE MELTING
Validation of a computational model for autogenous arc welding
[AD-A227258] N91-14611

Typical Personal Author Index Listing

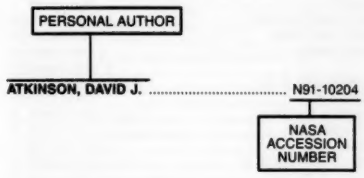

Listings in this index are arranged alphabetically by personal author. The NASA accession number denotes the number by which the citation is identified.

A

AARON, JAMES N91-14563
ABELL, G. C. N91-14460
ABEUOV, B. A. N91-14706
ABRAMOWITZ, A. N91-14317
ACHTERMANN, JEFF M. N91-14917
ADAM, JOZSEF N91-14636
ADAMS, PAUL M. N91-14444
ADDERLEY, P. N91-14816
AHLERS, STEPHEN T. N91-14705
AHMED, B. N91-14713
AHMED, I. N91-14851
AIELLO, ROBERT A. N91-14426
AIELLO, SANTI N91-14966
N91-14984
ALAVI, KAMBIZ N91-14393
ALBIN, SACHARIAL N91-14483
ALEXANDER, D. E. N91-14472
ALEXANDER, J. IWAN D. N91-14624
ALEXANDER, RICHARD M. N91-14802
ALEXOVICH, ROBERT N91-14576
ALLAMANDOLA, LOUIS J. N91-14897
N91-14919
N91-14922
N91-14926
N91-15003
ALLEN, C. N91-14980
ALLGOOD, GLENN O. N91-14710
ALLREAD, J. S. N91-14572
ALPERT, D. J. N91-14649
ALSOP, D. N91-14976
ALTER, WENDY SUE N91-14462
ALTICE, PETER PARKER, JR. N91-14585
ALTYNTSEV, A. T. N91-15109
AMOS, DONALD E. N91-14561
ANDERSON, GORDON E. N91-14528
ANDERSON, K. A. N91-15010
ANDERSON, MELVIN S. N91-14618
ANDERSON, P. N91-14373
N91-14847
ANDERSON, R. W. N91-14457
ANTONOV, V. M. N91-15081
ANTONOVA, R. A. N91-15080
APPELBAUM, JOSEPH N91-15117
APPLE, M. L. N91-14687
ARENDT, P. N. N91-14856
ARENDT, RICHARD G. N91-15032
ARMSTRONG, J. SCOTT N91-14688
ARNOLD, DAVID V. N91-14635
AROCENA, INAKI N91-14605
ASCHER, U. N91-14791
ASHOUR-ABDALLA, M. N91-15073
ASSENDORP, R. N91-14949
ASSEO, E. N91-15085
ATCHABAROV, B. A. N91-14706
ATLI, V. N91-14289
AVENI, GLENN N91-14807
AVERNA, D. A. N91-14962
AVIS, LEE M. N91-14683
AYDIN, ATILLA N91-14668
AYRES, DAVID S. N91-14815

B

BAER, D. R. N91-14879
BAFFES, PAUL THOMAS N91-14769
BAILEY, F. RON N91-14727
BAILEY, MICHAEL P. N91-14799
BAILEY, R. E. N91-14353
BAILEY, STEPHEN N91-14364
BAILLIEUL, JOHN N91-14776
BAKER, DOUGLAS ALAN N91-14601
BAKER, J. H. N91-14505
BAKTASH, C. N91-14818
BALDETTI, P. N91-14502
BALDO, P. M. N91-14884
BALL, DAVID W. N91-14956
BALLINGALL, J. M. N91-14864
BALLUFFI, R. W. N91-14880
BAMBERGER, JUDY N91-14744
BANAN, MOHSEN N91-14885
BANDY, JEFF N91-14688
BANKS, H. T. N91-14787
BANKSTON, CLYDE P. N91-14536
N91-14538
BARBOUR, J. C. N91-14844
N91-14877
BARDI, UGO N91-14456
BARE, E. ANN N91-14316
BARKER, JOHN R. N91-14934
BARMATZ, MARTIN B. N91-14807
BARNAVELI, T. T. N91-15069
BARNETT, BARBARA N91-14889
BARNS, CHRIS E. N91-14591
BARRATT, P. S. N91-14287
BARREAU, ROLAND N91-14337
BARRY, W. N91-14816
BARSELLA, BRUNO N91-14966
N91-14984
BASCOM, WILLARD D. N91-14429
BASHAM, BRYAN D. N91-14741
BASLER, D. N91-14328
BASORE, P. A. N91-14645
BASTIEN, PIERRE N91-14969
BAUDIN, D. N91-14297
BAYBA, ANDREW J. N91-14620
BAYLISS, ALVIN N91-14781
BAZELL, DAVID N91-14973
BEALS, DAVID C. N91-14615
BEAMON, WILLIAM S. N91-14347
BEAUBOUEF, T. N91-14697
BECKER, BRIGITTE KARIN N91-14779
BEDDINI, ROBERT A. N91-14569
BEEMAN, JEFFREY N91-14390
BEL, N. N91-14967
BELLIN, GIANLUIGI N91-14758
BELOV, A. N91-14827
BENEDETTI, G. A. N91-14573
BERNARD, JEAN-PHILLIPE N91-14932
BERNSTEIN, I. M. N91-14431
BESPALOV, P. A. N91-15105
BEZCHASTANOV, V. G. N91-15075
BHAT, BALAKRISHNA T. N91-14808
BHATT, HARISH C. N91-15027
BIDWELL, C. S. N91-14310
BIGGAR, STUART FRICK N91-14801
BIGLARI, H. N91-14849
BIRCH, T. J. N91-14282
BIRDSALL, D. L. N91-14332
BIRDWELL, J. DOUGLAS N91-14710
BIRMAN, KENNETH N91-14731
N91-14732
BISNOVATYI-KOGAN, G. S. N91-15101
BLANCHARD, D. L. N91-14879
BLANCO, A. N91-14933
N91-14990
N91-14994
N91-15008
N91-15019
BLANDING, WAYNE RICHARD N91-14695
BLAYLOCK, B. GORDON N91-14660
BLITZ, L. N91-14973
BLOSS, WALTER L. N91-14394
BLUMSTEIN, A. N91-14485
BOCK, K.-W. N91-14288
BODO, G. N91-15097
BOETTGER, J. C. N91-14490
BOHME, DIETHARD K. N91-15014
BOHN, C. L. N91-14882
BOJANCZYK, ADAM W. N91-14765
BOLOTIN, GARY S. N91-14772
BONACUSE, PETER J. N91-14632
BOND, THOMAS H. N91-14309
BOOS, JOHN B. N91-14528
BORENSTAIN, S. N91-14397
BORGHESI, A. N91-14933
N91-14990
N91-14994
N91-15008
N91-15019
BOSCO, CARLA N91-14722
BOSSLER, ROBERT N91-14602
BOSTOW, DUWAYNE N91-14519
BOULANGER, F. N91-14927
BOURCIER, R. J. N91-14473
BOWER, ALLAN N91-14867
BOWMAN, LYNN M. N91-14629
BOWYER, STUART N91-14909
BOYD, DAVID A. N91-14936
BOZEMAN, RICHARD J., JR. N91-14607
BRAGG, BOBBY J. N91-14537
BRAND, P. W. J. L. N91-14918
BRAUNAGEL, L. N91-14373
BREGMAN, JESSE D. N91-14919
N91-14926
N91-15003
BRENNAN, T. M. N91-14553
N91-14598
BRESSLER, STEVEN L. N91-14718
BRICKETT, PAUL A. N91-14718
BRIGGS, R. N91-14961
BRISTOWE, P. D. N91-14880
BRITTON, RANDALL K. N91-14309
BROADFOOT, A. L. N91-14413
BROCHER, THOMAS M. N91-14676
BROOKE, TIM Y. N91-15006
BROPHY, JAMES J. N91-14549
BROUILLET, NATHALIE N91-14977
BROWN, BRUCE B. N91-14509
BROWN, C. R. N91-14622
BROWN, D. N91-14325
BROWN, G. S N91-14661
N91-14687
BROWN, J. F. N91-14641
BROWN, W. L. N91-14962
BROWNLEE, D. N91-14725
BROWNLOW, MICHAEL N91-14773
BRUCE, D. E. N91-14917
BRUNO, R. N91-14735
BUBLITZ, P. N91-14329
BUCHANAN, R. A. N91-14461
BUCHMANN, L. N91-14827
BUCK, M. E. N91-14645
BUGGA, RATNAKUMAR V. N91-14536
N91-14538
BULLOCK, J. W. N91-14680
N91-14681
N91-14682
BURGE, R. N91-14827
BURLEY, JAMES R., II N91-14316
BURNARD, DAVID JAMES N91-15043
BURNS, F. C. N91-14461
BURTON, MICHAEL G. N91-14918
BUSH, HAROLD G. N91-14614
BUSS, RICHARD H., JR. N91-15000
N91-15028
BUSS, RICHARD J. N91-14450
BUSSOLETTI, E. N91-14933
N91-14990
N91-14994
N91-15008
N91-15019
BUTCHER, ROBERT L. N91-14575
BUTLER, P. L. N91-14498
BUTNER, HAROLD M. N91-14940
BUTTRAM, M. T. N91-14532

BYMAN, D. N91-14697
BYSTROVA, N. V. N91-14941

C

CADOGAN, J. B. N91-14648
CAHAY, M. N91-14541
CAIRNS, I. H. N91-15064
CALLAHAN, JOHN R. N91-14757
CALLEN, J. D. N91-14849
CALLIS, R. N91-14847
CAMELIO, FRANCIS JAMES N91-14565
CAMPBELL, M. F. N91-14940
CAMPBELL, RICHARD L. N91-14323
CAMPBELL, SCOTT R. N91-14590
CAMPBELL, WILLIAM A., JR. N91-14437
CAMPINS, HUMBERTO N91-15002
N91-15004
CAPLAN, JAMES N91-14898
CAPPELLI, M. A. N91-14870
CAPRETTE, D. S. N91-14679
CARASSO, M. N91-14649
CARDELLI, JASON A. N91-14899
CARICO, DAVID P. N91-14982
CARLE, STEVEN F. N91-14676
CARLSON, C. W. N91-15010
CARNAHAN, CHALON L. N91-14887
CARNE, T. G. N91-14646
CARNOCHAN, DAVID J. N91-14900
CARRERAS, B. A. N91-14849
CARRINGTON, WILLIAM A. N91-14479
CARSON, R. F. N91-14553
CARTER, DANIEL C. N91-14835
CARTER, JOYCE G. N91-14702
CARUSO, STEVEN C. N91-14285
CARYOTAKIS, G. N91-14369
CASPER, T. A. N91-14842
CASSINELLI, J. P. N91-14972
CATALTEPE, TAYFUN N91-14766
CAUX, EMANUEL N91-14928
N91-14974
CAVICCHI, ELIZABETH N91-14831
CAYLESS, RICHARD ARTHUR N91-14453
CECCARELLI, C. N91-14502
CECCHI-PESTELLINI, C. N91-14966
CHAGELISHVILI, G. D. N91-15074
N91-15097
CHAHINE, MOUSTAFA T. N91-14380
CHAIT, A. N91-14500
CHAMPIGNY, P. N91-14297
CHANDLER, JOSEPH A. N91-14703
CHANG, CHERNG N91-14492
CHANG, Z. N91-14849
CHANISHVILI, R. G. N91-15074
CHAPMAN, RICHARD N. N91-14652
CHAR, K. N91-14389
CHARGEISHVILI, B. B. N91-15051
CHASON, E. N91-14875
CHATELAIN, M. A. N91-14935
CHAUDHURI, SURAJIT N91-14730
CHELIKOWSKY, J. R. N91-14874
CHEN, ALEXANDER Y. K. N91-14603
CHEN, EUGENE Y. S. N91-14603
CHENG, ROBERT K. N91-14439
N91-14449
CHERCHNEFF, ISABELLE N91-14934
CHI, MAGGIE M. Y. N91-14702
CHIANG, CLEMENT J. N91-14651
CHILDRESS, C. E. N91-14623
CHIN, HUNG-NENG STEVE N91-14685
CHLEWICKI, GRZEGORZ N91-14905
N91-14930
N91-15001
CHOI, MAN S. N91-14547
CHOKSHI, ARATI N91-14968
N91-14988
CHOKSI, RATI N91-14702
CHOW, D. H. N91-14407
CHRASKA, P. N91-14837
CHRIST, D. N91-14300
CHRISTIE, W. H. N91-14860
CHROSTOWSKI, JON D. N91-14630
CHUNG, T. J. N91-14557
CHURCH, EUGENE L. N91-14826
CHURCHWELL, ED N91-14942
CHUTJIAN, ARA N91-14813
CHWIRKA, S. N91-14373
CHYBA, CHRISTOPHER N91-15007
CIUFOLINI, IGNAZIO N91-14670
CLARK, F. O. N91-14930
CLATTERBUCK, CARROLL H. N91-14494
CLAYTON, D. D. N91-14998
CLAYTON, GEOFFREY C. N91-14899
CLEAVER, CHRISTOPHER M. N91-14342
CLIFFTON, ETHAN W. N91-15040
CLIPSHAM, DAVID F. N91-14759
CODY, JOSEPH C. N91-14613
COE, CHARLES F. N91-14335
COENSGEN, F. H. N91-14842
COFFEN, CHARLES D. N91-14803
COHEN, M. N91-14919
N91-14926
COLANGELI, LUIGI N91-14933
N91-14990
N91-15008
N91-15019
COLE, EDWARD I., JR. N91-14633
COLEMAN, D. J. N91-14442
COLES, MICHAEL N91-14722
COLLERAINE, A. N91-14847
COLLINS, JEFFERY D. N91-14476
N91-14789
COMBS, S. K. N91-14839
CONNELL, JOHN W. N91-14419
COOK, GRANT N91-14740
COOK, ROBERT B. N91-14658
COOPER, ROBERT N91-14731
N91-14732
COOPER, TOMMY G. N91-14709
CORRELL, D. L. N91-14842
COSTES, J.-J. N91-14338
COULURIS, G. J. N91-14320
COUTLEY, RAYMOND L. N91-14312
COX, J. N. N91-14853
COX, P. N91-14920
COYNE, G. V. N91-14986
CRAVENS, DENNIS J. N91-14545
CRESSEY, G. N91-15011
CREWS, JOHN H., JR. N91-14430
CROSS, JEFFREY L. N91-14273
CROSS, MICHAEL THOMAS N91-14425
CROSSMAN, J. W. N91-14649
CUGNON, PIERRE N91-14906
CULBERTSON, R. J. N91-14461
CUNNINGHAM, ATLEE M., JR. N91-14335
CUNNINGHAM, BRUCE J. N91-14455
CURTIS, D. W. N91-15010
CUTILLO, BRIAN A. N91-14718

D

DAMM, C. C. N91-14842
DANIEL, R. R. N91-14943
N91-14944
DANIEL, S. S. N91-14505
DAS, PURNA C. N91-14445
DASH, S. M. N91-14305
DAUGHERTY, MICHAEL J. N91-14394
DAVIS, PAUL M. N91-14360
DAVIS, RANDALL C. N91-14629
DAVIS, ROBERT F. N91-14871
DEATON, A. W. N91-14366
N91-14367
DEBERG, MARK N91-14736
N91-14777
DECOFANO, R. P. N91-14606
DEFOURNEAU, D. N91-14939
DEFREES, D. N91-14725
DEFREES, DOUG J. N91-14937
DEGROOT, M. S. N91-14961
DEHARVENG, LISE N91-14898
DEININGER, WILLIAM D. N91-14489
DEITINGHOFF, H. N91-14881
DELABEAUJARDIERE, ODILE N91-14677
DELANEY, HAROLD D. N91-14717
DELAYEN, J. R. N91-14881
N91-14882
N91-14883
DELERY, J. N91-14299
DELUCCIA, FRANK J. N91-14382
N91-14394
DEMETRIADES-SHAH, T. H. N91-14639
DEMICHIEL, LINDA N91-14730
DEMUIZON, M. N91-14920
DENIER, J. P. N91-14308
DENT, A. J. N91-15011
DEQUAY, LAURENCE N91-14609
DERENIAK, EUSTACE L. N91-14386
DESAQUI-SANNES, PIERRE N91-14774
DESERT, FRANCOIS-XAVIER N91-14973
DESLANDES, RONALD N91-14352
DESPINEY, P. N91-14293
DESTUYNDER, ROGER N91-14337
DEVAN, J. H. N91-14647
DEY, DIPAK K. N91-14794
DHENDECOURT, LOUIS B. N91-14924
N91-14932
N91-14939
DIAMOND, P. H. N91-14849
DIDEBULIDZE, G. G. N91-15107
DIETERICH, WILLIAM N91-14313
DILLENIUS, MARNIX F. E. N91-14285
N91-14304
DIMITROV, B. G. N91-15095
DIMITROVA, M. M. N91-15093
DIMPAULT-DARCY, ERIC C. N91-14537
DISTEFANO, SALVADOR N91-14536
N91-14538
DITMAN, L. S., JR. N91-14820
DIVASALAR, DARIUSH N91-14523
DOBSON, B. N91-15011
DOBSON, M. CRAIG N91-14638
DODSON, B. W. N91-14875
DOGHRI, I. N91-14422
DONCHIN, EMANUEL N91-14722
DONN, BERTRAM N91-14993
DORSCHNER, J. N91-14991
N91-14997
DOUGHERTY, D. R. N91-14354
DOVE, J. F. N91-14834
DOWNER, M. C. N91-14595
DOWNING, J. N. N91-14838
DOYLE, B. L. N91-14846
DOYLE, LAURANCE R. N91-14988
DRAKE, DOUGLAS N91-14841
DUBRULLE, BERENGERE N91-14950
DUBSKY, J. N91-14837
DUCK, PETER W. N91-14307
DUDNIKOVA, G. I. N91-15082
DUENAS, A. R. N91-14852
DUERSCH, FRED, JR. N91-14416
DUMBACHER, S. N91-14375
DUSTON, C. N91-15010
DUSTON, DWIGHT N91-14381
DUTUIT, O. N91-14939
DUURSMA, H. F. N91-14738
DWEK, ELI N91-14931
N91-14987
N91-15032
N91-15033
DYE, R. C. N91-14856
DYKES, C. D N91-14505
DYKSTRA, PHILLIP C. N91-14564

E

EASON, D. N91-14373
EAVES, B. CURTIS N91-14764
ECCLES, THOMAS JOHN N91-14355
ECKEL, ANDREW J. N91-14482
EDENBOROUGH, KEVIN L. N91-14374
EDMOND, J. A. N91-14548
EDWARDS, JOHN W. N91-14340
EFIMOV, YU. S. N91-15020
EGAN, MICHAEL P. N91-15021
EGDORF, H. W. N91-14739
EIROA, CARLOS N91-14958
ELDERING, C. N91-14834
ELKERTON, JAY N91-14721
ELLIOTT, C. THOMAS N91-14588
ELLIOTT, D. L. N91-14648
ELLIOTT, N. N91-14856
ELLIS, R. F. N91-14838
ELLZEY, JANET L. N91-14447
ELTON, ALTAMONT BRACY HAMILTON N91-14560
EMANUEL, W. R. N91-14663
ENEGREN, T. A. N91-14534
ENGARGIOLA, GREGORY N91-14983
ENOMOTO, M. N91-14451
EPLEY, L. E. N91-14513
ERBIL, A. N91-14643
ERICSSON, L. E. N91-14339
ERISTAVI, N. A. N91-15089
ESCALONA, O. B. N91-15056
ESTES, STEVEN A. N91-14519
ESTEVEZ, RAUL N91-14667
EVANS, A. N91-15011
EVANS, J. N91-14286
EVANS, N. J., III N91-14940
EWERBRING, MANGUS N91-14765
EYAL, Y. N91-14669

F

FAINSHTEIN, V. G. N91-15108
FALGARONE, E. N91-14927
FAN, BAO-HUA N91-14755
FANG, Y. N91-14884
FANT, K. S. N91-14369
FARE, JEAN-CHRISTOPHER N91-14291
FEDUTENKO, E. A. N91-15052
FEIGELSON, ERIC D. N91-15015
FELCH, K. N91-14592
FELDMAN, P. D. N91-14912

FELTEN, JAMES E. N91-15033
FENTON, MICHAEL W. N91-14516
FERMAN, M. A. N91-14326
FERRARA, ANDREA N91-14984
FERRARI-TONIOLO, M. N91-14904
FERRARI, A. N91-15097
FERRINI, F. N91-14966
N91-14984
FERRIS, J. P. N91-14961
FETH, LAWRENCE L. N91-14707
FICH, MICHEL N91-14953
FIELD, GOERGE B. N91-14989
FIELDS, ERIK N91-14699
FILIPOV, L. G. N91-15074
N91-15093
FILONCZUK, MARIA K. N91-14698
FISCHER, J. N91-14886
FISCHLER, J. E. N91-14346
FISHKOVA, L. M. N91-15107
FISHMAN, M. N91-14373
FITT, A. J. N91-14985
FLEETER, SANFORD N91-14350
FLEETWOOD, DANIEL M. N91-14533
FLEMING, SCOTT N91-14455
FLEMMING, ROBERT J. N91-14309
FLICKINGER, GREGORY C. N91-14936
FLITCROFT, I. N91-14639
FLOOD, DENNIS J. N91-15117
FLYNN-SANDERS, DIANE K. N91-14873
FODALE, ROBERT N91-14356
FOERSCHING, H. W. N91-14331
FOERSTER, HANS PETER N91-14514
FOING, B. H. N91-15047
FOLIAS, E. S. N91-14435
FOLLSTAEDT, D. M. N91-14469
FONTI, SERGIO N91-14933
N91-14990
N91-14994
N91-15008
N91-15019
FORD, W. K. N91-14879
FOSSUM, ERIC R. N91-14387
FOSTER, G. W. N91-14341
FOUST, C. R. N91-14839
FOX, ARNOLD N91-15014
FOX, J. L. N91-15114
FREEMAN, K. N91-14373
FRENKLACH, MICHAEL N91-15015
FREUND, L. B. N91-14867
FRIEDLANDER, ALAN L. N91-14362
N91-14363
FRIEDRICHS, R. N91-14300
FRITZ, J. N. N91-14526
FRODSHAM, JOHN N91-14410
FUTCH, A. H. N91-14842

G

GABRIEL, ANDREW K. N91-14642
GAINES, JAMES N91-14841
GAL-OR, L. N91-14488
GALEEV, A. A. N91-15062
N91-15065
GALINSKY, V. L. N91-15062
N91-15068
GALLIMORE, F. H., JR. N91-14346
GALLO, K. P. N91-14641
GALLOWAY, M. D. N91-14860
GAMBONE, M. L. N91-14351
GAMMELL, PAUL M. N91-14530
GANGLOFF, RICHARD P. N91-14474
GARCIA, EPHRAHIM N91-14499
GARCIA, JOSEPH P. N91-14821
GARDNER, ROBERT H. N91-14660
GARECHT, DIANE N91-14581
GARNER, F. A. N91-14470
GARROD, M. J. N91-14622
GATES, THOMAS G. N91-15119
N91-15120
GATLEY, I. N91-14952
GAVER, DONALD P. N91-14894
GEBALLE, T. R. N91-14918
N91-14922
GEE, J. M. N91-14645
GELFAND, ALAN E. N91-14794
GENTILE, ROBERT N91-14455
GENTRY, W. RONALD N91-14599
GEORGE, ALBERT R. N91-14803
GEORGE, THOMAS F. N91-14445
N91-14832
GERBAULT, FLORENCE N91-15022
N91-15023
GERNSBACHER, MORTON A. N91-14715
GEVINS, ALAN S. N91-14718
GEWALI, LAXMI P. N91-14754
GHOSH, A. K. N91-14861
GHOSH, SWARNA KANTI N91-14943
N91-14944
GIARD, MARTIN N91-14928
N91-14938
GIGOLASHVILI, M. SH. N91-15054
GILL, JOHN T. N91-14857
GINLEY, D. S. N91-14877
GLAESER, ANDREAS M. N91-14501
GLASSELL, R. L. N91-14498
GNEDIN, N. Y. N91-15106
GOEBEL, JOHN H. N91-15022
N91-15023
GOETTL, BARRY P. N91-14889
GOGOLEWSKI, RAYMOND P. N91-14455
GOKCEN, TAHIR N91-14558
GOKOGLU, S. A. N91-14500
GOKOGLU, SULEYMAN A. N91-14511
GOLANSKI, A. N91-14860
GOLDBERG, LOUIS F. N91-14414
GOLDSMITH, PAUL F. N91-14947
GOLDSTEIN, MOISE N91-14805
GOLDSTEIN, RICHARD M. N91-14642
GOLUB, GENE H. N91-14729
GONIDEC, P. N91-14297
GONZALES, A. N91-14461
GOOSSEN, KEITH N91-14393
GORDON, M. A. N91-14945
GORDON, PETER C. N91-14716
GOUGE, M. J. N91-14839
GOURLEY, P. L. N91-14598
GOWARD, SAMUEL N. N91-14655
GRABOSKE, B. C. N91-14659
GRADY, JOSEPH E. N91-14426
GRAHAM, J. M. R. N91-14283
GRAMANN, RICHARD ANTHONY N91-14276
GRAVE, I. N91-14397
GRAY, JEFF T. N91-14370
GRAY, ROSS T. N91-14885
GREAVES, G. N. N91-15011
GREENBERG, J. MAYO N91-14905
N91-14957
N91-14961
N91-14963
N91-14964
N91-14984
N91-14992
N91-15005
GREENE, MICHAEL E. N91-14825
GREGORY, E. N91-14852
GREWAL, GURPREET SINGH N91-14452
GRIFFITH, R. L. N91-14535
GRIM, RUUD N91-14957
N91-14963
GROEBNER, R. J. N91-14849
GROMELSKI, S. N91-14713
GRUBIN, H. L. N91-14541
GRUEN, E. N91-14971
GRUENER, GEORGE N91-14868
GRUNTHANER, FRANK J. N91-14379
N91-14409
GUBCHENKO, V. M. N91-15077
GUBERMAN, STEVEN L. N91-15045
GUCWA, J. R. N91-14517
GUERTLER, J. N91-14991
N91-14997
GUIDOTTI, RONALD A. N91-14531
GULENKO, V. V. N91-15071
GUMLICH, H. E. N91-14990
GUNTER, WILLIAM D. N91-14591
GUO, T. N91-14879
GURNETT, D. A. N91-15064
GUSHCHIN, V. V. N91-15071
GUTKOWSKI, GARY P. N91-14495
GUYENNE, T. DUC N91-15046
GVARAMADZE, V. V. N91-15095
GWIN, HAL S. N91-14563

H

HAALAND, D. M. N91-14853
HABER, S. N91-14488
HACKWELL, JAMES A. N91-14929
N91-14996
HADDICK, CLYDE M., JR. N91-14371
HAGE, J. I. N91-14992
N91-15005
HAGGAG, FAHMY M. N91-14467
HAINES, A. B. N91-14281
HAKIEL, ZBIGNIEW N91-14628
HALBERSTAM, ISIDORE N91-14785
HALBERT, M. L. N91-14818
HALE, DAVE N91-14674
N91-14675
HALES, J. M. N91-14656
HALL, PHILIP N91-14308
HALLER, EUGENE E. N91-14390
HAMILL, P. E. N91-14505
HAMILTON, WILLIAM DAVID N91-14462
HAMM, ROBERT M. N91-14795
N91-14797
HAMMONS, B. E. N91-14553
N91-14598
HAMPTON, HERBERT R. N91-14356
HAN, HSIU C. N91-14635
HAN, KUORUEY N91-14734
HANCOCK, BRUCE R. N91-14409
HANDEL, PETER H. N91-14515
HANDLER, ROBERT A. N91-14567
HANDSCHUH, ROBERT F. N91-14602
HANER, ALEXANDRA N. N91-14456
HANSEN, OLE N91-14811
HANSEN, WILLIAM L. N91-14390
HARBISON, L. S. N91-14473
HARDING, J. N91-14423
HARMON, C. BRUCE N91-14313
HARMON, H. E. N91-14860
HARPER, D. A. N91-14983
HARRIS, RICHARD A. N91-14741
HARSACKY, FRANK J., JR. N91-14465
HART, PATRICK E. N91-14676
HARTIN, J. R. N91-14644
HARTMANN, K. N91-14290
HARTMANN, SVEN N91-14830
HARVEY, P. M. N91-14940
HASSELMAN, T. K. N91-14630
HAUENSTEIN, ROBERT J. N91-14400
HAUGE, ROBERT H. N91-14956
HAVENS, STEPHEN J. N91-14419
HAVILAND, JOHN K. N91-14474
HAWKINS, CHARLES F. N91-14633
HAWKINS, DANIEL B. N91-14857
HAYAKAWA, S. N91-14976
HAYES, BRIAN C. N91-14721
HAYES, PETER N91-14589
HAYRAPETYAN, V. S. N91-15099
HAYTER, JOHN B. N91-14810
HECHT, JAMES H. N91-14929
N91-14935
N91-14996
HECHT, MICHAEL H. N91-14813
HEEFNER, J. N91-14816
HEILES, CARL N91-14975
N91-14978
HELGESON, W. D. N91-14532
N91-14854
HELLSTROM, BENJAMIN J. N91-14786
HELOU, G. N91-14927
HENDERSON, C. M. B. N91-15011
HENNING, TH. N91-14991
N91-14997
HENRIKSEN, R. N. N91-15094
HENRY, R. C. N91-14912
N91-14980
HENSLEY, D. C. N91-14818
HEPENSTAL, A. N91-14817
HERAKOVICH, CARL T. N91-14424
N91-14474
HERBELL, THOMAS P. N91-14482
HERGENROTHER, PAUL M. N91-14419
HERNDON, J. N. N91-14498
HESS, C. N91-14592
HEY, N. S. N91-14504
HILL, D. N. N91-14846
HILLIER, R. N91-14283
HILLYER, D. F., JR. N91-14507
HINGST, UWE G. N91-14301
HO, CHIH-MING N91-14315
HO, P. N91-14864
HO, PAULINE N91-14450
HOAG, LYLE E. N91-14544
HOPPE, KLAUS-WERNER N91-14958
HODGES, J. N91-14282
HOFERKAMP, L. A. N91-14487
HOFFMAN, ALAN J. N91-14764
HOFFMAN, F. OWEN N91-14660
HOGAN, J. T. N91-14845
HOLLENBACH, DAVID N91-14968
HOLLENBERG, J. B. N91-14849
HOLTKAMP, BERNHARD N91-14893
HORN, ROGER D. N91-14710
HORNE, MICHAEL P. N91-14567
HORNE, WARREN L. N91-14357
HOUGH, J. H. N91-14952
HOUSER, R. M. N91-14649
HOUSTON, J. E. N91-14480
HOWARD, FRANK S. N91-14495
HOWARTH, NEIL A. N91-14985
HOWE, DAVID A. N91-14540
HOWELL, M. N91-14647
HSA, CHANG-YU N91-14476

HSU, W. L. N91-14846
HU, J. Y. N91-15029
HU, M. N91-14396
HU, QING N91-14389
HUANG, CHING-YUANG ALBERT N91-15113
HUBBARD, G. SCOTT N91-14390
HUBBARD, K. M. N91-14856
HUBERMAN, MARK L. N91-14401
HUCK, FRIEDRICH O. N91-14579
HUEY, H. N91-14592
HUFFMAN, DONALD R. N91-14915
HUGHES, R. C. N91-14553
HUGHES, ROBERT M., IV N91-14629
HULL, DAVID R. N91-14482
HUMES, DONALD H. N91-14412
HUMPHREY, WATTS S. N91-14762
HUNSUCKER, ROBERT D. N91-14519
HUNT, JAMES J. N91-15046
HUNTLEY, WILLIAM P. N91-14529
HUNYADY, S. J. N91-14680
N91-14681
N91-14682
HURWITZ, MARK N91-14909
HUSS, J. ROWLAND N91-14434
HUTCHISON, R. N91-15011
HWANG, HO-LING N91-14688
HYLAND, A. R. HARRY N91-14921

I

IBADOV, SUBHON N91-14910
IBANEZ, M. H. N91-15056
N91-15057
ILLARIONOV, A. F. N91-15101
ILLES, JUDY N91-14718
ILLINGWORTH, ANTHONY J. N91-14690
INDUSI, J. P. N91-14354
INGRAHAM, J. C. N91-14838
INUZUKA, H. N91-15079
IRVINE, W. N91-14725
ISKANDER, SHAFIK K. N91-14467
ITOH, TATSUO N91-14542
ITOL, T. N91-14595
IYENGAR, K. V. K. N91-14943
N91-14944
N91-15024

J

JACHIM, S. N91-14816
JACKSON, BRIAN J. N91-14629
JACKSON, G. L. N91-14846
JACKSON, TODD A. N91-14527
JACOBS, BARRY L. N91-14704
JACOBS, PATRICIA A. N91-14894
JACOBSEN, JANET S. N91-14887
JAFFE, D. T. N91-14383
JAIN, HIMANSHU N91-14822
JAIN, S. K. N91-14948
JALINK, ANTONY, JR. N91-14590
JAMES, G. H. N91-14646
JAMIESON, DAVID W. N91-14708
JANOUSEK, BRUCE K. N91-14394
JANSSON, S. N91-14422
JARRELL, LAMONT N91-14662
JAVAKHISHVILI, J. I. N91-15072
JEANNERET, P. R. N91-14719
JENKINS, R. N. N91-15011
JERSTAD, N. M. N91-14346
JIA, ZHENHONG N91-14626
JINCHARADZE, P. G. N91-15087
JOCOY, EDWARD H. N91-14517
JOHNSON, N. R. N91-14818
JOHNSON, ROY N91-14841
JOHNSON, WAYNE N91-14311
JONES, A. P. N91-14959
JONES, COLIN E. N91-14410
JONES, D. J. N91-14286
JONES, J. J. N91-14680
N91-14681
N91-14682
JONES, ROBERT A. N91-14631
JONGEWAARD, E. N91-14592
JORDAN, THOMAS H. N91-14672
JORGENSEN, G. N91-14649
JORY, H. N91-14592
JOSAFATSSON, KARL N91-15000
JOSEPH, CHARLES L. N91-14960
JOYCE, S. A. N91-14480
JUNG, CH. N91-14990

K

KADTKE, JAMES N91-14570
KAHNIASHVILI, T. A. N91-15100
KAIGORODOV, A. P. N91-15108
KAILATH, THOMAS N91-14518
KAISER, W. J. N91-14391
KAISIG, M. N91-15110
KAKUEVA, E. ILYINA N91-14702
KALCIC, M. T. N91-14697
KALINEN, V. P. N91-15073
KALISHER, MURRAY H. N91-14404
KALLURI, SREERAMESH N91-14632
KALMA, ARNE H. N91-14388
KAMINKER, A. D. N91-15078
KANAL, LAVEEN N. N91-14786
KANDIL, OSAMA A. N91-14292
KANEMASU, E. T. N91-14639
KANTER, HELMUT N91-14394
KARLSEN, C. E. N91-14852
KASSEL, PHILIP C., JR. N91-14412
KAUTZ, D. D. N91-14606
KAZBEGI, A. Z. N91-15088
N91-15102
KEARNS, JAMES ANDREW N91-14800
KELLEY, N. D. N91-14572
KENNEDY, JOHN M. N91-14892
KENNY, T. W. N91-14391
KERAUS, R. N91-14886
KHABIBRAKHMANOV, I. KH. N91-15062
N91-15063
N91-15065
KHALDEEVA, I. V. N91-15069
KHODACHENKO, M. L. N91-15077
KHRISTOV, T. S. N91-15074
KHUTSISHVILI, E. V. N91-15054
KIEFFER, JONATHAN N91-14602
KIM, Y. B. N91-14849
KIMBLE, R. N91-14980
KINARD, WILLIAM H. N91-14412
KINCH, MICHAEL N91-14397
KING, A. W. N91-14663
KING, D. L. N91-14645
KING, DAVID Q. N91-14489
KING, JULIAN V. N91-14495
KIPP, D. O. N91-14866
KIRCHNER, T. M. N91-15086
KITSON, DAVID H. N91-14762
KLEEORIN, N. I. N91-15050
KLEIN, H. N91-14725
KLEIN, MARK H. N91-14748
KLOEPPEL, P. N91-14816
KNACKE, ROGER F. N91-15006
KNAPP, J. A. N91-14469
KNECHT, D. J. N91-14413
KNOCKE, PHILIP N91-14361
KNOTTS, L. H. N91-14353
KNUDE, JENS N91-14901
KOGURE, T. N91-14955
KOLLER, DAVID C. N91-14869
KOLMAN, B. N91-14837
KONDA, SURESH N91-14743
KONG, JIN AU N91-14635
KONOTCHICK, JOHN N91-14751
N91-14753
KOO, BON-CHUL N91-14975
N91-14978
KOONTZ, R. F. N91-14369
KORTH, A. N91-15010
KORTH, G. E. N91-14427
KOSS, D. A. N91-14473
KOSUT, ROBERT L. N91-14377
KOVAL, CARL A. N91-14858
KOWLER, EILEEN N91-14714
KRABACH, T. N. N91-14401
KRAMER, ARTHUR F. N91-14722
N91-14889
KRASNOSELSKIKH, V. V. N91-15067
KRASNOV, IGOR N91-14702
KRATZER, R. H. N91-14487
KREIDLER, DAVID N91-14733
KRESKOVSKY, J. P. N91-14541
KROEMER, HERBERT N91-14411
KRUSIUS, J. PETER N91-14863
KSENDZOV, A. N91-14401
KUAN, CHIHPING N91-14602
KUCHNIR, M. N91-14554
KUCZMARSKI, M. N91-14500
KUHN, GARY D. N91-14285
KUMAR, JAYANT N91-14485
N91-14831
KUMAR, R. SAL N91-14485
KUMAR, RAJENDRA N91-14321
KUMPAN, S. A. N91-14597
KUNZ, NANS N91-14357
KUNZ, PAUL F. N91-14763
KURTZ, JOE N91-14915
KUZAN, JOHN D. N91-14564
KUZNETSOVA, M. M. N91-15063
KWON, O. J. N91-14849

L

LACAU, R. G. N91-14279
LACINA, J. N91-14836
LACY, J. H. N91-14917
LAFAW, D. A. N91-14828
LAFEMINA, J. P. N91-14879
LAFON, J. P. N91-14967
LAGACE, LAWRENCE N91-14589
LAGOWSKI, JACEK N91-14862
LAKSHINA, G. S. N91-15091
LAMARRE, J. M. N91-14928
LAMERS, HENNY J. G. L. M. N91-15028
LAMY, P. L. N91-14995
LANDINGHAM, ROBERT L. N91-14428
LANDIS, D. N91-14373
LANG, BRUNO N91-15009
LANGE, ANDREW E. N91-14976
LANZEROTTI, L. J. N91-14962
LAPSHIN, V. I. N91-15052
N91-15055
LARKEY, PATRICK D. N91-14743
LAUREIJS, RENE J. N91-14930
N91-15001
LEBEDEV, N. V. N91-15109
LECH, L. N91-14373
LECKIE, F. A. N91-14422
LEE, B. H. K. N91-14325
N91-14327
LEE, I. Y. N91-14818
LEE, I.-S. N91-14461
LEE, MICHAEL E. N91-14510
LEFEBVRE, JEAN-MARC N91-14604
LEGER, ALAIN N91-14932
N91-14938
N91-14939
LEIJTEN, J. C. M. N91-14640
LEINSON, L. B. N91-15104
LEMAIRE, J. N91-15063
LEMAITRE, J. N91-14422
LEONARD, J. A. N91-14504
LEQUEUX, J. N91-14920
LESCEUX, J. M. N91-15063
LESIEUTRE, DANIEL J. N91-14285
N91-14304
LESSOR, D. L. N91-14879
LESTER, D. F. N91-14940
LEUNG, CHUN MING N91-15021
LEUNG, EMILY W. N91-14808
LEVINE, B. F. N91-14392
LEVIT, B. YA. N91-14798
LEVSHAKOV, S. A. N91-15106
LEVY, C. D. P. N91-14827
LEVY, M. N91-14461
LEWIS, BLAIR F. N91-14772
LEWIS, MICHAEL J. N91-14578
LEWIS, T. W. N91-14505
LI, Y. L. N91-14423
LI, YAN N91-14466
LIERKE, ERNST G. N91-14808
LIFFMAN, KURT N91-14998
LILJESTROEM, TARJA N91-14946
LIM, HAROLD H. N91-14635
LIN, CHIH N91-14627
LIN, R. P. N91-15010
LIN, T. L. N91-14401
LIPELES, R. A. N91-14442
LIS, DARIUSZ C. N91-14947
LITVIN, FAYDOR L. N91-14602
LIU, C. H. N91-14292
LIUBOVICH, S. N91-14488
LOBZIN, V. V. N91-15067
LOEW, G. A. N91-14819
LOMINADZE, J. G. N91-15072
N91-15074
N91-15080
N91-15097
LONDON, JULIUS N91-14657
LONG, JOHN P. N91-14745
LOPEZ, R. E. N91-15061
LORDON, JEROME N91-14291
LOUBRIEL, G. M. N91-14532
N91-14854
LOVELACE, DONALD E. N91-14823
LOVELACE, R. V. E. N91-15084
LOWE-MA, CHARLOTTE K. N91-14865
N91-14866
LOWRY, M. N91-14828
LOWRY, OLIVER H. N91-14702
LU, XIAOPING N91-14625
LUAN, LING N91-14931
LUCKHARDT, RUTH N91-14841
LUGARA, M. N91-14933

LUK, FRANKLIN T. N91-14765
LUM, VINCENT Y. N91-14893
LUNA, PHILLIP M. N91-14357
LYBANON, MATTHEW N91-14693
LYNCH, DAVID K. N91-15004
LYON, S. P. N91-14490
LYON, STEVE A. N91-14393

M

MA, C. N91-14679
MA, DAVID I. N91-14528
MABEY, D. G. N91-14334
MACHABELI, G. Z. N91-15087
N91-15088
N91-15102
MACK, INGHAM A. N91-14528
MADZSAP, GEORGE C. N91-14829
MAESTRELLO, LUCIO N91-14562
MAGAGNATO, F. N91-14298
MAGALHAES, ANTONIO M. N91-14986
MAILHIOT, C. N91-14405
MALIN, JANE T. N91-14741
MAMANTOV, GLEB N91-14438
MAMRADZE, P. G. N91-15078
MANALO, NATIVIDAD D. N91-14683
MANCHESTER, JILL K. N91-14702
MANCINI, T. R. N91-14649
MANE, AMIR N91-14722
MANFREDI, LAWRENCE N91-14495
MANKINS, JOHN C. N91-14817
MANNING, ROBERT M. N91-14772
MANUEL, LAWRENCE R. N91-14999
MANUKJAN, K. A. N91-15100
MARGRAVE, JOHN L. N91-14956
MARKEL, VADIM A. N91-14832
MARSHALL, A. C. N91-14594
MARTIN, CHRISTOPHER N91-14909
MARTIN, J. N91-14373
MARTIN, J. A. N91-14856
MARTIN, P. N91-14864
MARZULLO, KEITH N91-14731
MASERJIAN, JOSEPH N91-14398
N91-14401
N91-14409
N91-14551
MASSA, DERCK N91-14902
MASUDA, S. R. N91-14487
MATESE, JOHN J. N91-15016
N91-15018
MATESHVILI, G. N91-15012
MATESHVILI, YU. N91-15012
MATHER, JOHN C. N91-14987
MATHIS, JOHN S. N91-14899
MATSUMOTO, T. N91-14976
MATSUMURA, MASAFUMI N91-14907
MATSUO, H. N91-14976
MATSUZAWA, S. N91-14451
MATTHEWS, PAUL R. N91-14613
MATTILA, KALEVI N91-14911
N91-14946
MATUS, LAWRENCE G. N91-14850
MAULL, D. J. N91-14336
MAY, JOHN H. N91-14510
MAYDEW, R. C. N91-14504
MAZON, ISABELLE N91-14775
MCANDREW, MARK P. N91-14705
MCBRAYER, J. D. N91-14645
MCCAIN, P. N91-14961
MCCLUNG, R. W. N91-14619
MCCONNELL, J. W. N91-14818
MCCORKLE, J. N91-14373
MCCORMACK, RUSSELL S. N91-14691
MCCUE, JOHN N91-15112
MCDONALD, M. N91-14827
MCDOUGAL, DAVID B., JR. N91-14702
MCDOUGALL, S. N91-14287
MCGILL, TOM C. N91-14399
N91-14407
MCGOWAN, F. K. N91-14818
MCGREGOR, P. J. N91-14921
MCKINLEY, SARAH L. N91-15119
N91-15120
MCLAUGHLIN, D. L. N91-14532
N91-14854
MCLEAN, JAMES STUART N91-14542
MCLYMAN, W. T. N91-14539
MCMILLAN, CHARLES N91-14583
MCMURRAY, ROBERT E., JR. N91-14390
MCWRIGHT, G. M. N91-14828
MEIJER, J. J. N91-14333
MELENDEZ-ALVIRA, DANIEL J. N91-14671
MELIKIDZE, G. I. N91-15088
N91-15102
MELTON, ADRIAN WILFRED N91-14421
MENARD, FRANCOIS N91-14969
MENCARAGLIA, FRANCESCO N91-14966
MENDENHALL, MICHAEL R. N91-14285
MENDIS, D. A. N91-15010
MENDOZA-GOMEZ, CELIA X. N91-14961
MENZIES, J. N91-15031
METCALF, JAMES I. N91-14692
METCALF, THOMAS ROBERT N91-15116
MEYERDIERKS, HORST N91-14977
MEYN, ERWIN H. N91-14617
MEZGER, P. G. N91-14954
MICHALSKE, T. A. N91-14480
MIELE, A. N91-14365
N91-14366
N91-14367
N91-14368
MIKULAS, MARTIN M., JR. N91-14614
MILES, RICHARD H. N91-14400
N91-14407
MILLER, G. N91-14838
MILLER, J. H. N91-14498
MILLER, JEFF N91-14543
MILLER, M. D. N91-14937
MILLER, MICHELLE A. N91-14797
MILLER, WALTER E., JR. N91-14823
MILORA, S. L. N91-14839
MINDERMAN, PETER A. N91-14495
MINECK, RAYMOND E. N91-14274
MIRAM, G. N91-14369
MIRANDA, RAUL N91-14440
MISRA, AJAY K. N91-14482
MITCHELL, DAVID L. N91-15010
MITCHELL, ROBERT R. N91-14823
MOLVIK, A. W. N91-14842
MOONEY, T. J. N91-14974
MOORE, C. B. N91-14680
N91-14681
N91-14682
MOORE, J. L. N91-14860
MOORE, JOANNE P. N91-14510
MOORHOUSE, ALAN N91-14918
N91-14922
MORAN, SUSANNA I. N91-14347
MORRISH, ARTHUR A. N91-14479
MORROW, J. DAN N91-14319
MUNDT, C. N91-14886
MUNDY, L. G. N91-14940
MUNSON, C. P. N91-14838
MURAKAMI, H. N91-14976
MURATOV, LEONID S. N91-14832
MURPHY, C. G. N91-14770
MURPHY, CLARENCE J. N91-14822
MURRAY, ALAN N91-14773
MURTHY, JAYANT N91-14912
N91-14980
MUSCETTOLA, NICOLA N91-14788
MYERS, JACK W., JR. N91-14376
MYERS, P. G. N91-14332

N

NAGASUBRAMANIAN, GANESAN N91-14538
NAGATA, T. N91-14925
NAHUM, MICHAEL N91-14389
NAKADA, Y. N91-14925
NAKAHARA, J. H. N91-14487
NAKAMURA, E. N91-14451
NAKAMURA, WAYNE H. N91-14478
NAKANO, M. N91-14955
NANOBASHVILI, J. I. N91-15080
NANSHENG, ZHAO N91-15005
NANSTAD, RANDY K. N91-14467
NATISHAN, PAUL M. N91-14479
NEESE, W. N91-14317
NEFF, W. A. N91-14457
NEILSON, J. N91-14592
NELKIRK, D. P. N91-14595
NELSON, R. N. N91-14993
NEMETH, MICHAEL P. N91-14618
NEMETH, PATTI M. N91-14702
NEUHART, DAN H. N91-14274
NEWMAN, N. N91-14389
NGHIEM, SON V. N91-14635
NICHOLSON, D. M. N91-14459
NIETUBICZ, CHARLES J. N91-14294
NIKOLITSCH, D. N91-14290
NILSSON, BENGT J. N91-14777
NISINI, B. N91-14502
NOGUCHI, Y. N91-14283
NOOR, AHMED K. N91-14761
NORTON, PAUL R. N91-14385
NORWOOD, D. S. N91-14424
NUR, AMOS N91-14665
N91-14666
N91-14667
N91-14668
N91-14669
NUTH, JOSEPH A. N91-14993

O

OGURA, K. N91-14955
OHSAWA, Y. N91-15049
OLIVIERI, J. N91-14817
OLOUGHLIN, MICHAEL J. N91-14394
OMALLEY, M. W. N91-14532
N91-14854
OMONT, A. N91-14938
ONAKA, TAKASHI N91-14925
N91-15017
ONERMARS, MARK H. N91-14777
ONISHCHENKO, O. G. N91-15092
ORAN, ELAINE S. N91-14447
ORIENT, OTTO J. N91-14813
ORISHICH, A. M. N91-15081
N91-15082
OROFINO, VINCENSO N91-14933
N91-14990
N91-15008
N91-15019
ORTMAN, BRYAN J. N91-14956
OSGOOD, RICHARD M., JR. N91-14878
OSMINKIN, E. YU. N91-15103
OSMINKINA, O. A. N91-15103
OTTENBRITE, RAPHAEL M. N91-14418
OTTO, A. N91-15059
OUTTEN, C. A. N91-14844
OVERMARS, MARK H. N91-14736
OWEN, T. C. N91-15006
OZELIS, J. P. N91-14554
OZERYANSKY, G. M. N91-14852

P

PACIOREK, K. L. N91-14487
PAGAN, DIDIER N91-14291
PAJOT, F. N91-14928
PALMER, PATRICK N91-14950
PALMOUR, J. W. N91-14548
PAPANICOLAOU, NICHOLAS A. N91-14528
PARIHAR, SANJAY N91-14393
PARK, J. L. N91-14860
PARTHASARATHY, M. N91-14948
PASK, JOSEPH A. N91-14501
PATARAYA, A. D. N91-15051
N91-15076
N91-15107
PATARAYA, T. A. N91-15076
PATEL, S. R. N91-14326
PATTEN, ELIZABETH A. N91-14404
PATTERSON, JAMES C., JR. N91-14345
PAUL, LEE E. N91-14318
PAVLOV, G. G. N91-15075
N91-15078
PEARLSTEIN, SOL N91-14812
PEERCY, PAUL S. N91-14406
PELLAT, R. N91-15094
PELLETIER, G. N91-15085
PELZL, ROBERT M. N91-14869
PENDERGRAFT, ODIS C., JR. N91-14316
PENDLETON, R. N91-14592
PENDLETON, YVONNE J. N91-14970
PENNER, J. E. N91-14659
PENNYCOOK, S. J. N91-14860
PERRIN, J. M. N91-14995
PERRY, L. ELAINE N91-14394
PERSI, P. N91-14904
PETERSEN, P. I. N91-14846
N91-14847
PETOT, D. N91-14338
PETRE, R N91-15032
PETSCHKE, MARTIN N91-14778
PETVIASHVILI, N. V. N91-15053
PETVIASHVILI, V. I. N91-15080
PETZOID, L. N91-14791
PETZOLD, DONALD E. N91-14655
PICKRELL, M. M. N91-14838
PIGGOTT, MICHAEL R. N91-14432
PIIROLA, VALERO N91-14986
PILKEY, WALTER D. N91-14474
PINDERA, MAREK-JERZY N91-14474
PINELLI, THOMAS E. N91-14892
PINTER, S. N91-14971
PIRRANELLO, VALERO N91-14962
PLACHCO, F. N91-15057
PLANET, WALTER G. N91-15118
POIREL, D. N91-14325
POIRIER, R. L. N91-14534
POKER, D. B. N91-14860
POLLARD, T. J. N91-14346

POLSTORFF, WALTER N91-14508
POLUSHKIN, V. G. N91-14827
PONOMARENKO, A. G. N91-15081
N91-15082
PONS, PATRICK N91-14582
POPE, L. E. N91-14469
POST, W. M. N91-14663
POSTNOV, K. A. N91-15089
POSUKH, V. G. N91-15081
POTAPCZUK, M. G. N91-14310
POWELL, J. ANTHONY N91-14850
POZGAY, R. N91-14522
PRATAP, PREETHI N91-15042
PRENGER, COYNE N91-14506
PRESS, A. J. N91-14287
PRIOLO, F. J. N91-14284
N91-14286
PROKHOROV, M. E. N91-15089
PRUSTI, TIMO N91-14949
PUGET, J. L. N91-14927
PURI, ASHOK N91-14445
PURTILO, JAMES M. N91-14757
PUSATERI, MARY ELLEN N91-14702
PUSEY, MARC L. N91-14835
PUTTERMAN, SETH N91-14807
PYNE, C. R. N91-14334

Q

QIAN, XIAOSHU N91-14699
QUINTANA, J. N91-14461

R

RABIN, B. H. N91-14427
RAJAKARUNANAYAKE, YASANTHA N91-14399
RALYA, THOMAS N91-14748
RAMIREZ, JEAN-CLAUDE N91-14867
RAMSEY, JOHN K. N91-14617
RANK, D. N91-14919
RASMUSSEN, ROBERT D. N91-14772
RAST, HOWARD E. N91-14824
RATHMANN, PETER N91-14730
RAUS, P. N91-14837
RAYMER, MICHAEL G. N91-14596
REACH, WILLIAM T. N91-14975
N91-14978
N91-15013
RECKAMP, DOUGLAS E. N91-14568
REEDER, JAMES R. N91-14430
REEVES, G. N91-14856
REGAN, J. D. N91-14302
REHN, L. E. N91-14472
N91-14884
REINE, M. B. N91-14383
REISER, BRIAN J. N91-14750
REME, H. N91-15010
RENGARAJAN, T. N. N91-14943
N91-14944
N91-15024
RENNE, D. S. N91-14656
RENSCHLER, CLIFFORD L. N91-14857
REPHAELI, Y. N91-14987
REUTHER, JAMES J. N91-14378
REYNOLDS, J. K. N91-14391
REYNOLDS, R. T. N91-15016
N91-15018
REZ, A. I. N91-15083
RICHARDS, ELIZABETH H. N91-14651
RICHARDS, PAUL L. N91-14389
N91-14976
RICHARDS, PETER M. N91-14493
RICOY, MARK A. N91-14477
RILEY, DOUGLAS J. N91-14524
RINGEL, S. N91-14643
RISCH, TORE N91-14730
ROBBINS, D. J. N91-14594
ROBERT, M. N91-14279
ROBERTS, ANDREW C. N91-14357
ROBERTS, TED A. N91-14569
ROBERTSON, GLEN A. N91-14872
ROCHE, C. T. N91-14882
ROCHE, PATRICK F. N91-14918
RODRIGUES, C. V. N91-14986
ROGACHEVSKII, I. V. N91-15050
ROHATGI, A. N91-14643
ROHN, D. A. N91-14498
ROLPH, C. D. N91-14923
ROMANOFSKY, ROBERT R. N91-14552
ROMANOVA, M. N91-15096
RON, HAGAI N91-14668
N91-14669
ROOKE, T. J. N91-14302
ROSE, WILLIAM C. N91-14277
ROSEN, A. N91-14532
ROSEN, WARREN A. N91-14822
ROSENBLUTH, MARY L. N91-14394
ROSS, HOWARD D. N91-14556
ROSS, PHILIP N. N91-14456
ROSSMANITH, R. N91-14816
ROTH, M. N91-14904
N91-15063
ROUAN, D. N91-14938
ROWE, NEIL C. N91-14893
ROWELL, LAWRENCE F. N91-14634
ROZNOV, V. B. N91-15067
RUBIN, ROBERT H. N91-15025
RUBY, D. S. N91-14645
RUDE, M. A. N91-14517
RUDEN, P. PAUL N91-14408
RUDNICK, JOSEPH N91-14807
RUDOLPH, ALEXANDER N91-14950
RUEGG, R. N91-14827
RUGGIERO, FRANK H. N91-14692
RUOFF, CARL F. N91-14616
RUSSELL, D. H. N91-14448
RUSSELL, RAY W. N91-14935
N91-14996
N91-15004
RUSSELL, STEPHEN D. N91-14512
RUXUN, LIU N91-14790
RYAN, EILEEN V. N91-15002
RYAN, J. W. N91-14679
RYAN, PATRICK F. N91-14658
RYAN, PATRICK T. N91-14833
RYTER, CHARLES N91-14924
RYU, KWAN WOO N91-14771
RYUTOVA, M. N91-15110

S

SABHERWAL, RAJIV N91-14891
SACHTJEN, SCOTT A. N91-14389
SAFRON, S. A. N91-14855
SAGAN, CARL N91-15007
SAGDEEV, R. Z. N91-15073
SAHU, JUBARAJ N91-14294
SAIKUMAR, R. SAI N91-14831
SAKAI, JUN-ICHI N91-15048
SAKATA, AKIRA N91-14925
SALAZAR, GEORGE A. N91-14371
SALISBURY, KENNETH, JR. N91-14616
SANDEL, B. N91-14413
SANDFORD, SCOTT A. N91-14926
N91-15003
SANTOS, MIKE N91-14393
SARACENO, E. N91-14502
SASSE, RONALD N91-14497
SATO, M. N91-14451
SATO, R. N. N91-14396
SATO, S. N91-14451
N91-14952
N91-14976
SAUVAUD, J. A. N91-15010
SCAMARCIO, G. N91-14933
SCARROTT, S. M. N91-14923
N91-15031
SCHAEFER, THOMAS A. N91-14433
SCHAEFFER, E. N91-14713
SCHAFFER, M. S. N91-14846
SCHEMPP, A. N91-14881
SCHETZINA, J. F. N91-14403
SCHEVE, M. N91-14649
SCHILLING, H. N91-14300
SCHILLING, STEVEN P. N91-14737
SCHINDLER, M. N91-14522
SCHISSEL, P. N91-14649
SCHLIESING, JOHN A. N91-14374
SCHMIDT, DEBORAH DIANE N91-14462
SCHMITT, BERNARD N91-14957
N91-14963
SCHMOR, P. W. N91-14827
SCHNEIBEL, J. H. N91-14459
SCHNUR, G. F. O. N91-14911
SCHOELER, HENNING N91-14303
SCHOENBERG, K. F. N91-14838
SCHREINER, ROLAND N91-14306
SCHROT, JOHN N91-14705
SCHUBERT, DAVID MICHAEL, JR. N91-14694
SCHULMAN, JOEL N. N91-14402
N91-14407
SCHUTTE, WILLEM A. N91-14957
N91-14961
N91-14964
SCHWEHM, G. N91-14990
N91-15008
SCHWEITZER, N. E. N91-14517
SCIALDONE, JOHN J. N91-14437
N91-14494
SCOTT, G. N. N91-14572
SCOTTI, OONA N91-14667
SEAB, C. GREGORY N91-15000
SEDAYAO, J. N91-14853
SEDRAKYAN, A. D. N91-15090
SEDRAKYAN, D. M. N91-15090
SEDY, EUGENE B. N91-14611
SEJNOWSKI, TERRENCE J. N91-14805
SEKI, MUNEZO N91-14907
N91-14908
SELLGREN, KRIS N91-14925
N91-14931
N91-14965
N91-15000
SEMIKOZ, V. B. N91-15083
SEN, J. K. N91-14343
N91-14344
SENECHAUD, PASCALE N91-14768
SERBER, A. V. N91-15105
SERRA, G. N91-14928
SETOGUCHI, O. N91-14451
SHAHABASYAN, K. M. N91-15090
SHAKURA, N. I. N91-15089
N91-15098
N91-15103
SHAKURA, N. N. N91-15098
SHALKHAUSER, KURT A. N91-14552
SHAPIRO, V. D. N91-15073
SHARGELASHVILI, S. T. N91-15069
SHARMA, R. P. N91-14884
SHARPE, MATTHEW MICHAEL N91-14696
SHAW, STEPHEN J. N91-14307
SHAYEGAN, MANSOUR N91-14393
SHELDON, L. M. N91-14517
SHELL, THOMAS E. N91-14428
SHELTON, W. A. N91-14459
SHEPARD, K. W. N91-14881
N91-14883
SHEPHERD, IAN G. N91-14439
SHERGILL, G. N91-14853
SHEVCHENKO, V. I. N91-15073
SHIH, J. G. N91-14487
SHIMIZU, Y. N91-14451
SHIN, EON S. N91-14756
SHIN, ROBERT T. N91-14635
SHUART, M. J. N91-14424
SHUGAROV, S. YU. N91-15103
SHUMAN, EDWIN A., IV N91-14760
SIBECK, D. G. N91-15060
SIBEYN, JOP F. N91-14767
SIEGEL, JANE A. L. N91-14743
SIGAL, LORENE L. N91-14664
SILVENNOINEN, R. N91-14593
SILVER, AARON N. N91-14749
SIMON, K. N91-14522
SIMON, MARVIN K. N91-14523
SIMPSON, JANET P. N91-15025
SIMPSON, W. A., JR. N91-14619
SINDERSON, RICHARD L. N91-14371
SINGER, FRED S. N91-14412
SINHA, N. N91-14305
SKOFRONICK, J. G. N91-14855
SLATTERY, KERRY TIMOTHY N91-14420
SLIJKHUIS, S. N91-15026
N91-15029
SLUSHER, G. N91-14317
SLYSH, V. I. N91-15101
SMITH, BRIAN N91-14742
SMITH, DARRYL L. N91-14405
SMITH, G. LOUIS N91-14683
SMITH, HOWARD A. N91-14951
SMITH, J. N91-14847
SMITH, JEANNETTE W. N91-14274
SMITH, KENNETH M. N91-14357
SMITH, LEIGH ANN N91-14323
SMITH, PHILLIP N. N91-14322
SMITH, RICHARD N. N91-14516
SMITH, ROBERT G. N91-14965
SMITH, RONALD C. N91-14357
SMITH, T. P., III N91-14395
SMYTHE, W. R. N91-14534
SNEAD, LANCE L. N91-14436
SNOW, THEODORE P., JR. N91-15000
N91-15028
SNYDER, ERIC S. N91-14633
SNYDER, KEITH W. N91-14525
SNYTNIKOV, V. N. N91-15081
SODEN, JERRY M. N91-14633
SOKOLOV, A. YU. N91-15063
SOL, H. N91-15085
SOLOMON, P. M. N91-14974
SOLOMON, SEAN C. N91-14673
SOLOVIEV, G. I. N91-15073
SOMERVILLE, W. B. N91-14916
SORENSEN, N. R. N91-14469
SORVARI, J. M. N91-15041

SOVIE, AMY L. N91-14829
SPAHN, CAROLL J. N91-14371
SPERLING, LESLIE H. N91-14822
SPONG, D. A. N91-14849
SPRAGUE, BENNY B. N91-14610
SREEDHAR, VUGRANAM N91-14783
SRIVASYTAVA, SANTASH N91-14587
ST.CLAIR, ANNE K. N91-14484
STABILE, P. J. N91-14532
STAMNITZ, TIMOTHY C. N91-14512
STANEWSKY, E. N91-14328
STANLEY, JOHN E. N91-14412
STECHER, THEODORE P. N91-14913
STEINBERG, DANIEL N91-14481
STEINER, DON N91-14436
STEINOLFSON, R. S. N91-15115
STEPANOV, K. N. N91-15052
N91-15055
STEPHENS, JOHN J. N91-14458
STEPHENS, JOHN R. N91-14935
N91-14994
STERNE, P. N91-14459
STETSON, KENNETH F. N91-14314
STEVENSON-BUSEMEYER, MARY KAY N91-14888
STEWART, H. BRUCE N91-14571
STEWART, WALTER N91-14506
STEWART, WILLIAM ANDREW N91-14848
STEWMAN, SHELBY N91-14743
STOAKLEY, DIANE M. N91-14484
STOCKMAN, MARK I. N91-14832
STOKES, GERALD M. N91-14678
STONE, F. G. N91-14463
STONER, GLENN E. N91-14474
STOVER, J. C. N91-14826
STOYANOVSKY, V. O. N91-15081
STRASSER, V. O. N91-15055
STRETCH, ROBERT H. N91-14708
STRICKLAND, JAMES H. N91-14561
STRINGER, P. N91-14713
STRINGFELLOW, G. B. N91-14410
N91-14443
STUART, THOMAS A. N91-14546
STUREK, WALTER B. N91-14286
N91-14295
STURMS, FRANCIS M., JR. N91-14359
SU, H. N91-14639
SUDHARSANAN, R. N91-14643
SUDZIUS, J. N91-14903
SUENAGA, M. N91-14861
SUMMERS, C. J. N91-14643
SUMMERS, L. T. N91-14852
SUN, CHIEN HSIUNG N91-14747
SURGENOR, DOUGLAS MACN. N91-14700
N91-14701
SVESTKA, JIRI N91-14971
SWAMY, K. S. KRISHNA N91-15003
SWANSON, ROBERT E. N91-14474
SWISSLER, THOMAS J. N91-14634
SYKES, MARK V. N91-15044
SZCZERBA, RYSZARD N91-15030

T

TACINA, ROBERT R. N91-14349
TACKETT, JUANITA R. N91-14492
TAGGER, M. N91-15094
TAGHVA, KAZEM N91-14783
TAI, CHANG HSIEN N91-14555
TAJIMA, T. N91-15110
TAKACS, PETER Z. N91-14826
TAKAHASHI, S. N91-14451
TAKTAKISHVILI, A. L. N91-15051
N91-15058
TALBOT, L. N91-14446
TAMURA, M. N91-14451
N91-14952
TANDON, S. N. N91-14943
N91-14944
TAPIA, MAURICIO N91-14904
TAPSCOTT, ROBERT E. N91-14510
TARASSENKO, LIONEL N91-14773
TARTER, J. N91-14725
TAYLOR, JOHN G. N91-14275
TAYLOR, M. E. C. N91-14423
TAYLOR, P. L. N91-14846
N91-14847
TAYLOR, T. S. N91-14846
TEMMERMAN, W. M. N91-14459
TENG, SUE Y. N91-14444
TENNANT, WILLIAM E. N91-14384
TENNYSON, P. D. N91-14912
TERASHIMA, Y. N91-15049
TEREBEY, SUSAN N91-14953
TERHUNE, R. N91-14401
TERRY, NANCY N91-14841
TERUYA, A. T. N91-14535
THOMAS, JOHN R. N91-14705
THOMAS, S. W. N91-14535
THOMPSON, A. W. N91-14431
THOMPSON, REN A. N91-14737
THOMPSON, S. P. N91-15011
THOMPSON, WILLIAM K. N91-14577
THORNTON, EARL A. N91-14474
THORNTON, WILLIAM E., JR. N91-14723
N91-14724
TICHLER, JOYCE L. N91-14678
TIELENS, ALEXANDER G. G. M. N91-14897
N91-14919
N91-14968
N91-14970
TIEN, JAMES S. N91-14496
TINDALL, W. N91-14828
TINGLEY, J. W. N91-14645
TITRAN, ROBERT H. N91-14454
TOKUNAGA, ALAN T. N91-14925
N91-14965
N91-15006
TOLLER, GARY N. N91-14914
TOMAYKO, JAMES E. N91-14742
TOMSIA, ANTONIA P. N91-14501
TORODE, H. A. N91-14280
TOROSHELIDZE, T. I. N91-15107
TRACEY, KAREN N91-14699
TREGLIO, J. R. N91-14461
TRIPATHY, SUKANT N91-14485
N91-14831
TROTTER, WILLIAM T. N91-14784
TROUBNIKOV, B. N91-15070
TROWBRIDGE, DANIEL A. N91-14426
TRUSSONI, E. N91-15097
TSAI, C. C. N91-14840
TSIKARISHVILI, E. G. N91-15072
TSINTSADZE, L. N. N91-15091
TSINTSADZE, N. L. N91-15091
TSIRULNIKOV, M. N91-14592
TSUI, P. N91-14500
TSUKISHIMA, T. N91-15079
TU, WILSON N91-14273
TURKEL, ELI N91-14781
TURNER, C. DAVID N91-14524
TURNER, MICHAEL S. N91-15111
TURNER, ROBERT S. N91-14658
TYRRELL, DEBRA L. N91-15122

U

UCKAN, N. A. N91-14845
ULABY, FAWWAZ T. N91-14638
ULLMAN, ROGER R., II N91-14806
URALOVA, S. V. N91-15066
UROLOV, A. M. N91-15066
USHER, D. N91-14725
UZ, MEHMET N91-14454

V

VANBUREN, DAVE N91-14979
VANCE, PETER N91-14583
VANDERAH, TERRELL A. N91-14865
N91-14866
VANDERGAAG, LINDA N91-14793
VANDOOREN, PAUL N91-14765
VANHORN, THURSTON N91-14417
VANKARSEN, KEN N91-14746
VANKREVELD, MARC N91-14777
VANORDEN, KARL F. N91-14705
VASSILICOS, A. N91-14505
VAWTER, G. A. N91-14598
VEERS, P. S. N91-14646
N91-14650
VEITCH, L. N91-14500
VENKATESH, CHIKKABELARANGALA N. N91-14371
VENTURINI, E. L. N91-14877
VERGHESE, S. N91-14389
VERHEEST, F. N91-15063
VERMA, R. P. N91-14943
N91-14944
VERNER, D. A. N91-15106
VERNON, SUSAN N. N91-14530
VERSTRAETE, LAURENT N91-14939
VIALA, Y. P. N91-14967
VICENTE, KIM J. N91-14721
VICKERS, DAVID N91-14733
VIERECK, R. A. N91-14413
VIKHAREV, V. V. N91-15099
VILLASOL, R. N91-14853
VINGELIS, P. J. N91-14713
VLIEKS, A. E. N91-14369
VOLAKIS, JOHN L. N91-14475
N91-14476
N91-14477
N91-14789
VONPETERSDORFF, TOBIAS N91-14780
VONPRAGENAU, GEORGE L. N91-14608
VSHIVKOV, V. A. N91-15082

W

WADA, S. N91-14925
WAGNER, B. N91-14299
WAGNER, W. GARY N91-14743
WAIDE, C. H. N91-14354
WAINSCOAT, RICHARD J. N91-14988
WALKER, C. L. N91-14697
WALKER, HELEN J. N91-14980
WALKER, JOSEPH L. N91-14510
WALKER, S. N. N91-14844
WALLSOM, RICHARD E. N91-14614
WALOWIT, JED A. N91-14486
WALSH, D. S. N91-14846
WALTMAN, S. B. N91-14391
WALTON, J. J. N91-14659
WAMPLER, W. R. N91-14844
WANG, BOQI N91-14989
WANG, J. W. N91-14819
WANG, T. N91-14365
N91-14366
N91-14367
WARD, L. C. N91-14282
WARD, RICHARD S. N91-14772
WARDLAW, A. B., JR. N91-14284
N91-14286
WAS, G. S. N91-14472
WATERMANN, JUERGEN N91-14677
WATTS, D. RANDOLPH N91-14699
WAWNER, FRANKLIN E., JR. N91-14474
WAYNER, PETER C., JR. N91-14566
WDOWIAK, THOMAS J. N91-14936
WEAVER, H. T. N91-14553
WEBER, M. E. N91-14450
WEBER, P. G. N91-14838
WEBER, T. L. N91-14644
WEERTMAN, J. R. N91-14471
WEINACHT, PAUL N91-14295
WEISLOGEL, MARL M. N91-14556
WEISS, R. E. N91-14661
N91-14687
WELCH, D. O. N91-14861
WELCH, WILLIAM J. N91-14950
WELLS, CHARLES E. N91-14782
WELLS, CHESTER V. N91-14621
WELSH, B. L. N91-14334
WEN, CHENG P. N91-14396
WENDELKEN, J. F. N91-14876
WENDLER, J. N91-14522
WERNER, MICHAEL W. N91-14931
N91-14970
N91-14980
WERT, JOHN A. N91-14474
WESSELIUS, P. R. N91-14930
N91-14949
N91-15001
WETZEL, LEWIS B. N91-14520
WHALEN, JESSIE E. N91-15119
N91-15120
WHIPKEY, RICHARD N91-14583
WHITAKER, R. B. N91-14622
WHITE, C. W. N91-14860
WHITE, RICHARD E. N91-14981
WHITMAN, CLARK E. N91-14464
WHITMIRE, D. P. N91-15016
N91-15018
WHITMORE, HENRY B. N91-14723
N91-14724
WICKENS, CHRISTOPHER D. N91-14722
N91-14796
N91-14889
WIEDERHOLD, GIO N91-14730
WILCOX, WILLIAM R. N91-14885
WILKINSON, J. P. N91-14415
WILLIAMS, D. M. N91-14498
WILLIAMS, J. M. N91-14461
WILLIAMS, P. J. N91-14594
WILLIAMS, ROGER M. N91-14536
WILLIAMSON, R. L. N91-14427
WILLIGES, ROBERT C. N91-14721
WILSON, D. F. N91-14647
WILSON, R. E. N91-14644
WINK, JOERN-E. N91-14954
WINN, W. P. N91-14680
N91-14681
N91-14682
WINOKUR, PETER S. N91-14533
WINTER, J. N91-14846
WIRAMIHARDJA, SUHARDJA D. N91-14955

WISE, M. N91-14816
WITHEROW, WILLIAM K. N91-14835
WITTEBORN, FRED C. N91-14919
N91-14926
N91-15003
WLODEK, STANISLAW N91-15014
WOFFORD, J. N91-14980
WOLFIRE, MARK G. N91-14942
N91-14972
WOLSTENCROFT, RAMON D. N91-15031
WOLVERTON, BILLY C. N91-14662
WONG, TIN-CHEE N91-14292
WOOD, DAVID P. N91-14745
WOOD, DOUGLAS O. S. N91-14942
WOOD, WILLIAM G. N91-14745
WOODALL, JERRY M. N91-14395
WOODEN, DIANE N91-14919
N91-14926
WOODHOUSE, CHRISTOPHER E. N91-14550
WOODWARD, PAUL R. N91-14792
WORTMAN, JIM J. N91-14412
WU, C. S. N91-14396
WU, OWEN K. N91-14402
WURDEN, G. A. N91-14838
WYLIE, DONALD P. N91-14689
WYNBLATT, PAUL N91-14814

X

XU, YOUWEN N91-14861

Y

YAKOVLEV, D. G. N91-15106
YAMAMOTO, T. N91-14451
YARIV, AMNON N91-14397
YESAVAGE, VICTOR F. N91-14584
YORK, B. J. N91-14305
YORK, THOMAS M. N91-14843
YOSHIDA, S. N91-14955
YOST, VAUGHN H. N91-14835
YOUNG, J. P. N91-14438
YOUNG, MARY H. N91-14400
YU, F. T. N91-14834
YU, T. N91-14864
YUEH, HERNG-AUNG N91-14635
YUNGSTER, SHAYE N91-14559
YUNKER, WAYNE H. N91-14468

Z

ZAKHAROV, YU. P. N91-15081
N91-15082
ZAN, S. J. N91-14336
ZAPP, JOHN N91-14476
ZARLINGO, FREDERICK C. N91-14296
ZEBKER, HOWARD A. N91-14642
ZEDGINIDZE, M. Z. N91-15076
ZELENYI, L. M. N91-15058
ZELINSKII, A. N91-14827
ZGELA, M. N91-14325
ZHELEZNYAKOV, V. V. N91-15105
ZHU, R. N91-15011
ZHVANIA, B. P. N91-15080
ZIEMKE, ROBERT A. N91-14580
ZILLIAC, GREGORY G. N91-15040
ZIMMERMAN, N. H. N91-14326
ZINGEL, H. N91-14329
N91-14330
ZINKLE, STEVEN J. N91-14436
N91-14470
ZIPPERIAN, T. E. N91-14553
ZUKOSKI, EDWARD E. N91-14441
ZUO, J.-K. N91-14876
ZUTAVERN, F. J. N91-14532
N91-14854
ZVANYA, JOHN N91-14728
ZWAAN, R. J. N91-14333
ZYLKA, R. N91-14954

Typical Corporate Source Index Listing

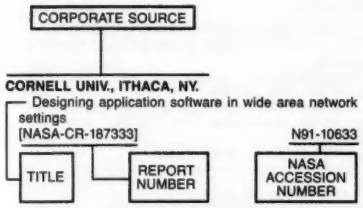

Listings in this index are arranged alphabetically by corporate source. The title of the document provides the user with a brief description of the subject matter. The report number helps to indicate the type of document cited (e.g., NASA report, translation, NASA contractor report). The NASA accession number denotes the number by which the citation is identified. The titles are arranged under each corporate source in ascending accession number order.

A

ABASTUMANI ASTROPHYSICAL OBSERVATORY, GEORGIA (USSR).
Dust of Orionid meteor shower in the Earth atmosphere before and after Halley's Comet N91-15012
A new model of spicule formation in the Sun chromosphere N91-15051
On some peculiarities of solar differential rotation N91-15054
Bursts of energetic protons in the Earth's magnetotail N91-15058
Hydrodynamics of collisionless relativistic plasma in a strong magnetic field N91-15072
Amplification of Alfven waves in free shear flows N91-15074
Excitation of Langmuir wave by transversal nonlinear wave in the electron-positron inhomogeneous plasma in the presence of positron beam N91-15076
Experiments with collision of vortices in rotating and still free-surface shallow water N91-15080
Matter penetration and motion through the magnetosphere of neutron star N91-15087
On the existence of circular polarisation in the pulsar radiation N91-15088
Large-scale vortices in compressible turbulent medium with the magnetic field N91-15095
Pregalactic inhomogeneity in hot dark matter model of the universe N91-15100
On the possibility of discovering pulsed radiation from SN 1987A N91-15102
Investigation of the night sky airglow near the epicenter of the earthquake N91-15107

ACADEMY OF PEDAGOGICAL SCIENCES OF THE USSR, MOSCOW.
A new kind of magnetic buoyancy instability N91-15050

ACADEMY OF SCIENCES, POTSDAM (GERMAN D.R.).
Energy dissipation of shear Alfven waves in extended cosmic jets N91-15086

ACADEMY OF SCIENCES OF THE GEORGIAN SSR, TBILISI.
On the primary cosmic ray nuclei spectra behaviour in the 10(exp 16) eV energy region N91-15069
Ultrarelativistic low-frequency electromagnetic waves in pulsar magnetospheres N91-15091

ACADEMY OF SCIENCES (USSR), DUSHANBE.
Interstellar dust as generator of x ray radiation N91-14910

ACADEMY OF SCIENCES (USSR), GORKY.
Generation of inductive fields by an oblique magnetic rotator in collisionless plasma N91-15077
Radiation-driven diskons as a new astrophysical object N91-15105

ACADEMY OF SCIENCES (USSR), IRKUTSK.
A numerical calculation of parameters of explosion MHD shock waves from moderate solar flares N91-15066
Influence of the parameter distribution of the solar wind near the Sun upon its structure at the Earth's orbit N91-15108
Interrelationship between the tearing-instability and magnetic island merging N91-15109

ACADEMY OF SCIENCES (USSR), LENINGRAD.
Dust clouds in Orion and the interstellar neutral hydrogen distribution N91-14941
Maser cyclotron instability in a plasma with anisotropic distribution function N91-15075
Annihilation radiation of strongly-magnetised electron-positron plasma with power-law distributions of particles N91-15078
Spectral synthesis code LINESPEC: Ionisation equilibrium of plasma and absorption spectra formation N91-15106

ACADEMY OF SCIENCES (USSR), MOSCOW.
Filamentary structures in the Sun's atmosphere as singular Alfven waves N91-15053
Solitary vortices in the vicinity of comets N91-15062
Detection of nonlinear features in plasma and field measurements by PROGNOZ-8 N91-15063
Gradient catastrophe of the supersonic mass-loaded magnetised plasma flow and the formation of bow shock N91-15065
Evolution of high amplitude Alfven waves near a bow shock N91-15068
Wave collapse at lower hybrid resonance N91-15073
Sterile neutrinos and astrophysical and cosmological constraints on the parameters of the extended electroweak models N91-15083
On the theory of large-scale micropulse structure of pulsar radio radiation N91-15092
Compact object masses in active galactic nuclei and quasars and duration of activity stage N91-15096
The plasma model of radioemission from SN 1987A N91-15101

ACADEMY OF SCIENCES (USSR), NOVOSIBIRSK.
Laboratory simulation of the astrophysical burst processes in non-uniform magnetised media N91-15081
Laboratory and computer simulations of wave generation processes in non-stationary astrophysical phenomena N91-15082
Nonlinear magnetosonic waves in an inhomogeneous plasma N91-15110

ACADEMY OF SCIENCES (USSR), TROITSK.
Nonstationary processes in the front of high Mach number collisionless quasiperpendicular shock: Dynamics of the ion distribution N91-15067
Neutrino scattering by nuclei in imperfect media N91-15104

ADVISORY GROUP FOR AEROSPACE RESEARCH AND DEVELOPMENT, NEUILLY-SUR-SEINE (FRANCE).
Missile Aerodynamics [AGARD-CP-493] N91-14278
Aircraft Dynamic Loads Due to Flow Separation [AGARD-CP-483] N91-14324

AEROSPACE CORP., EL SEGUNDO, CA.
Conversion of alkoxide solutions to oxides: Evaporation of products [AD-A226927] N91-14442
Procedures for the preparation of samples for cross-sectional transmission electron microscopy [AD-A227013] N91-14444

AEROSPACE CORP., LOS ANGELES, CA.
LWIR detector requirements for low-background space applications N91-14382
Characteristics of AlGaAs/GaAs multiple quantum well infrared detectors N91-14394
IR emission and UV extinction in two open clusters N91-14929
Si3N4 emissivity and the unidentified infrared bands N91-14935
Observational constraints on interstellar dust models N91-14996
The 10 micron spectral structure in comets N91-15004

AEROSPATIALE, CHATILLON (FRANCE).
Some trends in missile aerodynamics N91-14279
Supersonic vortex flows around a missile body: Basic experiment and Euler numerical computation N91-14291

AIR FORCE ACADEMY, CO.
An experimental investigation into the use of hot-film anemometry to measure vortical velocity behind a pitching wing [AD-A227177] N91-14313

AIR FORCE GEOPHYSICS LAB., HANSCOM AFB, MA.
The AIS: A spectrograph/imager ensemble for space flight [AD-A227009] N91-14413
Mesoscale features of a winter storm: Dual Doppler velocity fields and differential reflectivity [AD-A227342] N91-14692

AIR FORCE INST. OF TECH., WRIGHT-PATTERSON AFB, OH.
Optical phase conjugation via stimulated Brillouin scattering in multimode optical fiber [AD-A227054] N91-14833

AIR FORCE OFFICE OF SCIENTIFIC RESEARCH, BOLLING AFB, WASHINGTON, DC.
Air Force Office of Scientific Research technical report summaries: April-June 1990 [AD-A227367] N91-15121
Air Force Office of Scientific Research technical report summaries: January-March 1990 [AD-A227368] N91-15122

AIR FORCE WEAPONS LAB., KIRTLAND AFB, NM.
Transient x ray irradiation of high transition temperature superconducting material [AD-A227090] N91-14869

ALABAMA UNIV., BIRMINGHAM.
PAH in the laboratory and interstellar space N91-14936

ALABAMA UNIV., HUNTSVILLE.
CFD code evaluation for internal flow modeling [NASA-CR-187677] N91-14557
Vibration isolation technology: Sensitivity of selected classes of experiments to residual accelerations [NASA-CR-186902] N91-14624

ALASKA UNIV., FAIRBANKS.
Radio Frequency Interference (RFI) measurements made near the proposed Alaska OTH receiving site [AD-A226922] N91-14519

AMERICAN FOUNDREYMENS' SOCIETY, DES PLAINES, IL.
Expendable Pattern Casting Technology [DE91-001348] N91-14503

AMES LAB., IA.
Application of ultrasonic guided waves to the characterization of texture in metal sheets of cubic and hexagonal crystallites [DE91-001107] N91-14466
Low-energy electron diffraction investigation of epitaxial growth: Pt and Pd(100) [DE91-000750] N91-14873

AMSTERDAM UNIV. (NETHERLANDS).
Dust around Mira variables: An analysis of IRAS LRS spectra N91-15026

ANALEX CORP., CLEVELAND, OH.
Data transmission networks N91-14576
Data compression applied to HHVT N91-14577

APPLIED RESEARCH CORP., LANDOVER, MD.
The dependence of UV extinction properties on dust environment N91-14902
Diffuse galactic light observations at 206 selected areas N91-14914

ARGONNE NATIONAL LAB., IL.
Ion-induced grain growth in multilayer and coevaporated metal alloy thin films [DE91-004489] N91-14472
An accurate product SVD (singular value decomposition) algorithm [DE91-004448] N91-14765
Initial data from the Soudan 2 experiment [DE91-004454] N91-14815
Design and application possibilities of superconducting radio-frequency quadrupoles [DE91-004477] N91-14881

Experimental results in superconducting niobium resonators for high-brightness ion beam acceleration [DE91-004478] N91-14882
First tests of a superconducting RFQ (radio frequency quadrupole) structure [DE91-004483] N91-14883
An ion-channeling study of irradiation-induced amorphization of YBa2Cu3O(7-x) [DE91-004488] N91-14884

ARIZONA STATE UNIV., TEMPE.
(DURIP) exploring and controlling spatio temporal chaos under complex structures through visualization: A mini-supercomputer approach [AD-A226793] N91-14784

ARIZONA UNIV., TUCSON.
Detector array evaluation and figures of merit N91-14386
In-flight methods for satellite sensor absolute radiometric calibration N91-14801
Simultaneous infrared and UV-visible absorption spectra of matrix-isolated carbon vapor N91-14915
A study of extended zodiacal structures [NASA-CR-187687] N91-15044

ARMY ARMAMENT RESEARCH AND DEVELOPMENT COMMAND, WATERVLIET, NY.
Hazards and safeguards of high pressure hydraulic fatigue testing [AD-A226767] N91-14509

ARMY ELECTRONIC PROVING GROUND, FORT HUACHUCA, AZ.
Methodology investigation of software maturity model validation [AD-A226697] N91-14746

ARMY RESEARCH INST. OF ENVIRONMENTAL MEDICINE, NATICK, MA.
The effects of sleep loss on individual and group performance [AD-A226963] N91-14708

AUBURN UNIV., AL.
The design of optical sensor for the pinhole/occulter facility [NASA-CR-187694] N91-14825

B

BALLISTIC RESEARCH LABS., ABERDEEN PROVING GROUND, MD.
Three dimensional flow calculations for a projectile with standard and dome bases N91-14294
Navier-Stokes predictions of static and dynamic aerodynamic derivatives for high L/D finned projectiles N91-14295
Analysis of hydroxylammonium nitrate based liquid propellants [AD-A227300] N91-14497
Direct numerical simulation of turbulent couette flow, part 2 [AD-A226770] N91-14564

BANDUNG INST. OF TECH. (INDONESIA).
Survey observations of emission-line stars in the Orion region N91-14955

BATTELLE COLUMBUS LABS., OH.
Definition of experiments to investigate fire suppressants in microgravity [NASA-CR-185295] N91-14378

BEIJING OBSERVATORY, HUAIROU (CHINA).
Compact reflection nebulae, a transit phase of evolution from post-AGB to planetary nebulae N91-15029

BELEIDSCOMMISSIE REMOTE SENSING, DELFT (NETHERLANDS).
Strategic plan commercialization remote sensing by NEDECO [BCRS-89-35] N91-14637

BELGIAN ROYAL OBSERVATORY, BRUSSELS.
New results in the theory of dust grain alignment N91-14906

BELL TELEPHONE LABS., INC., MURRAY HILL, NJ.
Quantum Well Infrared Photodetectors (QWIP) N91-14392

BODENSEEWERK GERAETETECHNIK G.M.B.H., UEBERLINGEN (GERMANY, F.R.).
Laminar/turbulent flow transition effects on high-speed missile domes N91-14301

BOEING AEROSPACE CO., HUNTSVILLE, AL.
Space transfer concepts and analysis for exploration missions [NASA-CR-183943] N91-14358

BONN UNIV. (GERMANY, F.R.).
Molecules in an infrared cirrus cloud N91-14977

BOSTON UNIV., MA.
Sensor based control of robotic mechanisms [AD-A226784] N91-14776

BRANDEIS UNIV., WALTHAM, MA.
Synthesis and properties of novel organometallic polymers [DE91-001978] N91-14491

BRISTOL UNIV. (ENGLAND).
The forward mounted spoiler as a source of buffet excitation N91-14332
Heteronuclear metal cluster compounds synthesis and reactivity [AD-A226815] N91-14463

BRITISH AEROSPACE PUBLIC LTD. CO., BRISTOL (ENGLAND).
NUFA: A semi-empirical method for the prediction of isolated weapon aerodynamics N91-14287

BRITISH COLUMBIA UNIV., VANCOUVER.
An intense optically pumped H(-) ion source [DE91-002949] N91-14827

BRITISH MUSEUM OF NATURAL HISTORY, LONDON (ENGLAND).
Atomic environments in iron meteorites using EXAFS N91-15011

BRITISH PETROLEUM CO. LTD., LONDON (ENGLAND).
Method for manufacturing composite material [EP-PATENT-0-314-353-A2] N91-14421
Surface treatment of metals [EP-PATENT-0-367-504-A2] N91-14453

BROOKHAVEN NATIONAL LAB., UPTON, NY.
A cable vehicle barrier for alert aircraft protection [DE91-001723] N91-14354
Phase portrait methods for verifying fluid dynamic simulations [DE91-001129] N91-14571
Overview of the US Department of Energy's ARM (Atmospheric Radiation Measurement) program [DE91-001126] N91-14678
Nucleus-nucleus collisions at very high energies [DE91-004003] N91-14811
Data requirements for intermediate energy nuclear applications [DE91-004005] N91-14812
Scattering by anisotropic grains in beryllium mirrors [DE91-001724] N91-14826
Irreversibility temperatures in oxide- and metallic superconductors [DE91-004021] N91-14861

BROWN UNIV., PROVIDENCE, RI.
Control of distributed parameter systems [AD-A227306] N91-14787
Simulation of transient glide of a threading dislocation in an embedded strained expitaxial layer [AD-A226965] N91-14867

BULGARIAN ACADEMY OF SCIENCES, SOFIA.
Structure of accretion flow in close binary system: A two dimensional numerical model N91-15093

BYURAKAN OBSERVATORY, MOUNT ARAGATZ (USSR).
On the braking mechanisms of pulsars N91-15090
On the generation of magnetic fields in active star atmospheres N91-15099

C

CALABRIA UNIV., ARCAVACTA DI RENDE (ITALY).
Synthesis of H2 in dirty ice mantles by fast ion energy loss: New experimental results increase the relevance of this mechanism N91-14962

CALIFORNIA INST. OF TECH., PASADENA.
Intersubband absorption in Si(1-x)Ge(x/Si superlattices for long wavelength infrared detectors N91-14399
Investigation of combustion in large vortices [AD-A226791] N91-14441
IRAS results on outer galaxy star formation N91-14953
Temperature distribution of dust in luminous IRAS galaxies N91-14982

CALIFORNIA UNIV., BERKELEY.
Fabrication of sensitive high Tc bolometers N91-14389
Opposed jet turbulent diffusion flames [AD-A227048] N91-14446
New measurements of the far ultraviolet scattering properties of interstellar dust N91-14909
Interferometric molecular line observations of W51 N91-14950
Molecules, grains, and shocks: A comparison of CO, H I, and IRAS data N91-14975
A rocket-borne measurement of interstellar dust emission at high galactic latitude N91-14976
Infrared cirrus point sources N91-14978
The composition of heavy molecular ions inside the ionopause of Comet Halley N91-15010
Infrared emission from interplanetary dust N91-15013
Continuum radiative transfer in accretion-powered pulsars N91-15043

CALIFORNIA UNIV., BERKELEY. LAWRENCE BERKELEY LAB.
Fabrication of sensitive high Tc bolometers N91-14389
Statistical errors in the fractal analysis of flame boundaries [DE91-001795] N91-14439
The application of the turbulent burning speed concept to laboratory flames [DE91-001789] N91-14449
Anomalous surface phase formation on Pt3Sn with zone axes group (100) [DE91-001794] N91-14456
Coupled transport processes in semipermeable media. Part 1: Analytical solutions of the linearized governing equations [DE91-004138] N91-14887

CALIFORNIA UNIV., DAVIS.
Evaluation of performance and feedback control design for vehicle suspensions with variable compliance elements N91-14601

CALIFORNIA UNIV., LOS ANGELES.
Specification goals for a Mars seismic network N91-14360
Randomly sampled-data control systems [NASA-CR-187425] N91-14734
A study of strong stability of distributed systems [NASA-CR-187421] N91-14766
Electromagnetic properties of high Tc superconductors [AD-A227006] N91-14868

CALIFORNIA UNIV., SAN DIEGO.
Flare heating and ionization of the low solar chromosphere N91-15116

CALIFORNIA UNIV., SAN DIEGO, LA JOLLA.
Investigations of equilibria, lattices, and chaotic dynamics of 2-D Hamiltonian point vortices [AD-A227364] N91-14570

CALIFORNIA UNIV., SANTA BARBARA.
AlSb/InAs/AlSb quantum wells N91-14411
Optimization of interface layers in the design of ceramic fiber reinforced metal matrix composites [NASA-CR-185307] N91-14422

CALSPAN ADVANCED TECHNOLOGY CENTER, BUFFALO, NY.
Description of the bistatic radar terrain measurements system equipment [AD-A226808] N91-14517

CALSPAN-STATE UNIV. OF NEW YORK JOINT VENTURE, BUFFALO, NY.
Interaction of feel system and flight control system dynamics on lateral flying qualities [NASA-CR-179445] N91-14353

CARLOW ASSOCIATES, INC., FAIRFAX, VA.
Human factors engineering. Part 1: Test procedures [AD-A226480] N91-14720

CARNEGIE INST. OF TECH., PITTSBURGH, PA.
Fundamentals of interfacial strength in composite materials [AD-A226701] N91-14431

CARNEGIE-MELLON UNIV., PITTSBURGH, PA.
Experiences porting the distributed Ada real-time kernel [AD-A226693] N91-14742
National software capacity: Near-term study [AD-A226694] N91-14743
DARK technology transition plan [AD-A226695] N91-14744
Classifying software design methods [AD-A226696] N91-14745
An analysis of input/output paradigms for real-time systems [AD-A226724] N91-14748
The role of assessment in software process improvement [AD-A227426] N91-14762
Planning the behavior of dynamical systems [AD-A227381] N91-14788
Equilibrium composition of interphase boundaries [DE91-002470] N91-14814

CASE WESTERN RESERVE UNIV., CLEVELAND, OH.
Solid fuel combustion [AD-A227170] N91-14496
Chemical vapor deposition modeling: An assessment of current status [NASA-CR-185301] N91-14511

CENTER FOR BLOOD RESEARCH, BOSTON, MA.
Initial blood storage experiment [NASA-CR-185513-PT-1] N91-14700
Initial blood storage experiment [NASA-CR-185513-PT-2] N91-14701

CENTRE D'ETUDE SPATIALE DES RAYONNEMENTS, TOULOUSE (FRANCE).
The 3.3 micron emission feature: Map of the galactic disk, 10 deg less than l less than 35 deg, - 6 deg less than b less than 6 deg N91-14928

The origin of the galactic emission in IRAS data N91-14974

CENTRE NATIONAL DE LA RECHERCHE SCIENTIFIQUE, VERRIERES-LE BUISSON (FRANCE).
Influence of temperature on the infrared spectrum of the coronene molecule N91-14932

CESKOSLOVENSKA AKADEMIE VED, PRAGUE.
Linear resonant interaction of an electromagnetic wave with a collisional inhomogeneous plasma [IPPCZ-298] N91-14836
Phase changes during plasma spray deposition [IPPCZ-297] N91-14837

CHICAGO UNIV., IL.
Dust in regions of massive star formation N91-14972
Particle physics and cosmology [DE91-001946] N91-15111

CHILDRENS HOSPITAL MEDICAL CENTER, BOSTON, MA.
Initial blood storage experiment [NASA-CR-185513-PT-1] N91-14700
Initial blood storage experiment [NASA-CR-185513-PT-2] N91-14701

CINCINNATI UNIV., OH.
Multivariable methods for the design, identification, and control of large space structures. Volume 2: Optimal and sub-optimal estimation applied to large flexible structures [AD-A226699] N91-14375

CITY UNIV. OF NEW YORK RESEARCH FOUNDATION, NY.
Magnetic properties of doped semiconductors [DE91-002395] N91-14859

CLARKSON UNIV., POTSDAM, NY.
A novel approach to determine the heat transfer coefficient in directional solidification furnaces [NASA-CR-187648] N91-14885

COLORADO SCHOOL OF MINES, GOLDEN.
An automated flow calorimeter for heat capacity and enthalpy measurements at elevated temperatures and pressures [DE91-002759] N91-14584
Stable explicit depth extrapolation of seismic wavefields [DE91-001445] N91-14674
The 3-D depth migration via McClellan transformations [DE91-001446] N91-14675

COLORADO UNIV., BOULDER.
Studies of the observed and theoretical variations of atmospheric ozone [NASA-CR-187703] N91-14657
Investigations of probabilistic inference [AD-A226882] N91-14795
Interpretation of conditional probabilities in probabilistic interference word problems [AD-A226907] N91-14797
Intermediate energy nuclear physics [DE91-002758] N91-14809
Investigation of redox processes at semiconductor electrode liquid junctions [DE91-001787] N91-14858
The origin of micrograins N91-15000
Circumstellar grain extinction properties of recently discovered post AGB stars N91-15028

COLUMBIA UNIV., NEW YORK, NY.
Issues and directions in IR detector readout electronics N91-14387
Climate and atmospheric modeling studies. Climate applications of Earth and planetary observations. Chemistry of Earth and environment [NASA-CR-187326] N91-14684
Spontaneous and induced coherent radiation generation in atomic vapors [AD-A226776] N91-14830
Photogenerated carrier-induced reaction on semiconductor surfaces [DE91-001349] N91-14878

COMMISSARIAT A L'ENERGIE ATOMIQUE, GIF-SUR-YVETTE (FRANCE).
Red fluorescence and 3-12 micron emission in NGC 2023, HD 44179, M 82, and Lynds 1780 N91-14924

COMMISSARIAT A L'ENERGIE ATOMIQUE, SACLAY (FRANCE).
Accretion disk instability and spokes in Saturn's rings N91-15094

CONGRESSIONAL RESEARCH SERVICE, WASHINGTON, DC.
Outer space: What should be the US Government policy toward the region beyond Earth's atmosphere. National debate topic for high schools, 1990-1991 [PB90-255464] N91-14896

CONSIGLIO NAZIONALE DELLE RICERCHE, FRASCATI (ITALY).
Design of a He4 cooling system for a cryostat working at 1K [IFSI-89-17] N91-14502
Measurement of the gravitomagnetic field using a pair of laser ranged satellites N91-14670
Graphics software for the HP825/9000 IFSI system [IFSI-89-18] N91-14735

CONTINUOUS ELECTRON BEAM ACCELERATOR FACILITY, NEWPORT NEW, VA.
A beam position monitor for low current dc beams [CEBAF-PR-89-004] N91-14816

COORDINATING RESEARCH COUNCIL, INC., ATLANTA, GA.
CRC program for quantifying performance of knock-sensor-equipped vehicles with varying octane level [AD-A227340] N91-14612

COPENHAGEN OBSERVATORY (DENMARK).
The autocorrelation function of the North Pole dust N91-14901

CORNELL UNIV., ITHACA, NY.
ISIS and META projects [NASA-CR-186413] N91-14731
The ISIS project: Real experience with a fault tolerant programming system [NASA-CR-187029] N91-14732
Prediction of XV-15 tilt rotor discrete frequency aeroacoustic noise with WOPWOP [NASA-CR-187684] N91-14803
Ultra high speed compound semiconductors and real time signal processing [AD-A226790] N91-14863
The pre- and post-accretion irradiation history of cometary ices N91-15007

COUNCIL FOR NATIONAL ACADEMIC AWARDS (ENGLAND).
The rotation of Venus and its atmosphere N91-15112

CREE RESEARCH, INC., DURHAM, NC.
Development and testing of radiation and electromagnetic pulse hardened silicon carbide based electronics [AD-A227309] N91-14548

CRIMEAN ASTROPHYSICAL OBSERVATORY (USSR).
The influence of grain growth in circumstellar dust envelopes on observed colors and polarization of some eruptive stars N91-15020

D

DEPARTMENT OF DEFENSE, WASHINGTON, DC.
Office of Basic Energy Sciences 1990 summary report [DE91-002971] N91-14653

DEPARTMENT OF THE ARMY, WASHINGTON, DC.
Device and method for monitoring the presence of an object in space [AD-D014621] N91-14823

DEPARTMENT OF THE NAVY, WASHINGTON, DC.
Fabrication by filament winding with an elastomeric material [AD-D014570] N91-14478
Method of growing diamond film on substrates [AD-D014632] N91-14479
Tapered fiber amplifier [AD-D014629] N91-14512
Monolithic multichannel detector amplifier arrays and circuit [AD-D014566] N91-14528
Unidirectional amplitude sensitive noise riding threshold circuit [AD-D014568] N91-14529
Eddy current method for measuring electrical resistivity and device for providing accurate phase detection [AD-D014571] N91-14530
Optical phase conjugate beam modulator and method therefor [AD-D014569] N91-14820
Optical encoding of imaging data [AD-D014617] N91-14821
Optoelectronic devices [AD-D014618] N91-14822
Automated system for measuring the strength of optical fibers [AD-D014626] N91-14824

DETROIT DIESEL ALLISON, INDIANAPOLIS, IN.
Fatigue and fracture of titanium aluminides, volume 2 [AD-A227353] N91-14351

DEUTSCHE AIRBUS G.M.B.H., BREMEN (GERMANY, F.R.).
Experimental investigation and semi-empirical prediction of the dynamic response of a low-aspect-ratio trapezoidal wing due to flow separation N91-14330

DEUTSCHE FORSCHUNGS- UND VERSUCHSANSTALT FUER LUFT- UND RAUMFAHRT, GOETTINGEN (GERMANY, F.R.).
Thermal imaging on missiles in hypersonic flow N91-14303

DEUTSCHE FORSCHUNGSANSTALT FUER LUFT- UND RAUMFAHRT, GOETTINGEN (GERMANY, F.R.).
Systematic investigations of body-wing-tail interference at high angles of attack N91-14290
Experimental investigation of buffet onset and penetration on a supercritical airfoil at transonic speeds N91-14328
Experimental investigations of buffet excitation forces on a low aspect ratio trapezoidal half wing in incompressible flow N91-14329
Unsteady aerodynamic forces on an oscillating wing at high incidences and flow separation N91-14331

DEVCOM, INC., FRAMINGHAM, MA.
Program to study the process parameters of OMVPE and their relationship to the properties of Ga(0.47)In(0.53) as ON InP substrates [AD-A226618] N91-14851

DORNIER-WERKE G.M.B.H., FRIEDRICHSHAFEN (GERMANY, F.R.).
A semi-empirical prediction method for missile aerodynamics N91-14288
Computation of axisymmetric base flow with different turbulence models N91-14296

DOUGLAS AIRCRAFT CO., INC., LONG BEACH, CA.
Structural development of laminar flow control aircraft chordwise wing joint designs [NASA-CR-181888] N91-14346

DOVE ELECTRONICS, INC., ROME, NY.
Hybrid optical processor [AD-A227163] N91-14834

DURHAM UNIV. (ENGLAND).
The wavelength dependence of polarization in NGC 2023 N91-14923

E

ECOLE NORMALE SUPERIEURE, PARIS (FRANCE).
Small scale variations of abundances of transiently heated grains in molecular clouds N91-14927

ECOLE POLYTECHNIQUE, PALAISEAU (FRANCE).
Nonlinear plasma effects in the environment of active galactic nuclei N91-15085

EDGERTON, GERMESHAUSEN AND GRIER, INC., IDAHO FALLS, ID.
Dynamic consolidation of aluminum-silicon carbide composites [DE91-001929] N91-14427
Thin steel section casting on a near-horizontal twin-belt caster [DE91-001883] N91-14505

EEG SYSTEMS LAB., SAN FRANCISCO, CA.
Empirical network model of human higher cognitive brain functions [AD-A227193] N91-14718

EG AND G MOUND APPLIED TECHNOLOGIES, MIAMISBURG, OH.
Characterization of phenolic resins with thermogravimetry-mass spectrometry [DE91-002710] N91-14492
Thermal analyses for quality control of plastics, ceramics, and explosives [DE91-002701] N91-14622

ELORET CORP., PALO ALTO, CA.
Computation of thermochemical nonequilibrium flows around a simple and a double ellipse [NASA-CR-187702] N91-14558

ENGINEERING MECHANICS ASSOCIATION, INC., TORRANCE, CA.
Methods for evaluating the predictive accuracy of structural dynamic models [NASA-CR-187649] N91-14630

EROS DATA CENTER, SIOUX FALLS, SD.
Evaluation of data reduction and composing of the NOAA global vegetation index product: A case study [AD-A227397] N91-14641

ESSEX CORP., ALEXANDRIA, VA.
Air traffic controller memory enhancement [DOT/FAA/CT-TN90/38] N91-14713

ESSEX CORP., ORLANDO, FL.
Position requirements for space station personnel and linkages to portable microcomputer performance assessment [NASA-CR-185606] N91-14719

EUROPEAN SPACE AGENCY, PARIS (FRANCE).
Plasma Astrophysics [ESA-SP-311] N91-15046

EUROPEAN SPACE AGENCY. EUROPEAN SPACE RESEARCH AND TECHNOLOGY CENTER, ESTEC, NOORDWIJK (NETHERLANDS).
Experimental evidence for amorphous carbon grains in comets N91-15008
Solar magnetic flux-tubes and coronal loops N91-15047

F

FAIL-SAFE TECHNOLOGY CORP., LOS ANGELES, CA.
Integration of sneak analysis with design, volume 1
[AD-A226902] N91-14543
FEDERAL AVIATION ADMINISTRATION, ATLANTIC CITY, NJ.
Smoke and extinguisher agent dissipation in a small pressurized fuselage
[DOT/FAA/CT-89/31] N91-14317
Using simulation to evaluate the safety of proposed ATC operations and procedures
[DOT/FAA/CT-TN90/22] N91-14318
DATAS hardware diagnostic tests
[DOT/FAA/CT-TN90/44] N91-14728
FERMI NATIONAL ACCELERATOR LAB., BATAVIA, IL.
Superconducting current transducer
[DE91-004674] N91-14554
FIVE-COLLEGE ASTRONOMY DEPT., AMHERST, MA.
Dust emission in the Sagittarius B2 molecular cloud core N91-14947
Thermal emission from interstellar dust in and near the Pleiades N91-14981
FLORENCE UNIV. (ITALY).
Production and transfer of UV photons in non-homogeneous spherical clouds N91-14966
FLORIDA STATE UNIV., TALLAHASSEE.
He atom surface spectroscopy: Surface lattice dynamics of insulators, metals, and metal overlayers
[DE91-001993] N91-14855

G

GENERAL ATOMIC CO., SAN DIEGO, CA.
Wall conditioning and plasma surface interactions in DIII-D
[DE91-001547] N91-14846
DIII-D results and plans
[DE91-001548] N91-14847
GENERAL DYNAMICS CORP., FORT WORTH, TX.
Predictions of F-111 TACT aircraft buffet response N91-14335
GENERAL ELECTRIC CO., DAYTONA BEACH, FL.
Raster graphic helmet-mounted display study
[NASA-CR-4331] N91-14347
GENERAL ELECTRIC CO., SYRACUSE, NY.
Pseudomorphic InGaAs materials
[AD-A226895] N91-14864
GEOLOGICAL SURVEY, DENVER, CO.
Color palette: Plotting guide for use with GSMAP and GSDRAW digital cartographic software
[DE91-001643] N91-14737
GEOLOGICAL SURVEY, MENLO PARK, CA.
Feasibility study of the seismic reflection method in Amargosa Desert, Nye County, Nevada
[DE91-001646] N91-14676
GEORGE WASHINGTON UNIV., WASHINGTON, DC.
Nonlinear finite element dynamics on multiprocessor computers
[AD-A227409] N91-14761
GEORGIA INST. OF TECH., ATLANTA.
High efficiency cadmium and zinc telluride-based thin film solar cells
[DE91-002112] N91-14643
An investigation of the diffraction of an acoustic plane wave by a curved surface of finite impedance N91-14800
GEORGIA UNIV., ATHENS.
Comparison of ground and satellite based measurements of the fraction of photosynthetically active radiation intercepted by tall-grass prairie
[NASA-CR-187696] N91-14639
GRONINGEN RIJKSUNIV. (NETHERLANDS).
The embedded objects in epsilon Cha I cloud N91-14949

H

HARRY DIAMOND LABS., ADELPHI, MD.
Effect of laser fluctuations in automated solder joint inspection
[AD-A226685] N91-14620
HARVARD-SMITHSONIAN CENTER FOR ASTROPHYSICS, CAMBRIDGE, MA.
Galaxy formation by dust N91-14989
HARVARD UNIV., CAMBRIDGE, MA.
Perception and temporal properties of speech
[AD-A226958] N91-14716
HAWAII UNIV., HONOLULU.
High-spectral resolution observations of the 3.29 micron emission feature: Comparison to QCC and PAHs N91-14925
Distribution of the 3.1 micron feature in Cepheus A N91-14958
HELSINKI UNIV. (FINLAND).
The spectral energy distribution of the scattered light from dark clouds N91-14911
H I and dust in the high latitude dark cloud L1642 N91-14946
HUGHES AIRCRAFT CO., TORRANCE, CA.
Low dark current photovoltaic multiquantum well long wavelength infrared detectors N91-14396
MBE HgCdTe heterostructure detectors N91-14402
InAs/Ga(1-x)In(x)Sb superlattices for infrared detector applications N91-14407
HUGHES RESEARCH LABS., MALIBU, CA.
Possibilities for LWIR detectors using MBE-grown Si(/Si(1-x)Ge(x) structures N91-14400

I

IAT, MENLO PARK, CA
Automatic dependent surveillance benefit and cost analysis
[DOT/FAA/RD-90/34] N91-14320
ILLINOIS UNIV., CHAMPAIGN.
Information extraction from visual displays and the event-related brain potential
[AD-A227063] N91-14722
The object display: Principles and review of experimental findings
[AD-A226883] N91-14796
The object display in decision making and judgment
[AD-A227059] N91-14889
ILLINOIS UNIV., CHICAGO.
Straddle design of spiral bevel and hypoid pinions and gears
[NASA-TM-103621] N91-14602
ILLINOIS UNIV., URBANA.
Effects of turbulence on stationary and nonstationary processes in C-systems
[AD-A227067] N91-14569
ILLINOIS UNIV., URBANA-CHAMPAIGN.
Aluminum nitride-silicon carbide whisker composites: Processing, properties, and microstructural stability
[DE91-001907] N91-14425
Modeling study of tropical nonsquall and squall clusters N91-14685
An interferometric study of molecular emission around NGC 7538 at millimeter wavelengths N91-15042
IMPERIAL COLL. OF SCIENCE AND TECHNOLOGY, LONDON (ENGLAND).
Computation of viscous supersonic flows N91-14283
INDIAN INST. OF ASTROPHYSICS, BANGALORE.
Additional red and reddened stars in Cyg OB2 association N91-14948
Polarization due to dust scattering in the planetary nebula Cn1-1 N91-15027
INSTITUT NATIONAL POLYTECHNIQUE, GRENOBLE (FRANCE).
Contribution to the specification and implementation of complex robot tasks
[ETN-90-98209] N91-14604
Boolean Grobner bases, calculation methods. Applications and parallel processing
[ETN-90-98208] N91-14768
INSTITUTE FOR COMPUTER APPLICATIONS IN SCIENCE AND ENGINEERING, HAMPTON, VA.
The inviscid stability of supersonic flow past heated or cooled axisymmetric bodies
[NASA-CR-187475] N91-14307
The effect of wall compliance on the Goertler vortex instability
[NASA-CR-187477] N91-14308
Research in progress in applied mathematics, numerical analysis, and computer science
[NASA-CR-187474] N91-14726
INSTITUTE FOR SCIENTIFIC RESEARCH, LEXINGTON, MA.
Theoretical studies of important processes in planetary and comet atmospheres
[NASA-CR-187692] N91-15045
INSTITUTE OF APPLIED ENERGY, TOKYO (JAPAN).
Prospects of new energy
[DE91-727567] N91-14654
INSTITUTE OF ELECTRICAL AND ELECTRONICS ENGINEERS, NEW YORK, NY.
International Symposium on Information Theory
[AD-A226957] N91-14521
INTEGRATED SYSTEMS, INC., SANTA CLARA, CA.
Adaptive control of large space structures
[AD-A227304] N91-14377
INTEL CORP., SANTA CLARA, CA.
FTIR (Fourier Transform Infrared) spectrophotometry for thin film monitors: Computer and equipment integration for enhanced capabilities
[DE91-001228] N91-14853
INTERNATIONAL BUSINESS MACHINES CORP., YORKTOWN HEIGHTS, NY.
Resonant tunneling IR detectors N91-14395
INTERNATIONAL CENTRE FOR THEORETICAL PHYSICS, TRIESTE (ITALY).
The computer algebra approach of the finite difference methods for PDEs
[DE90-631581] N91-14790
IOWA UNIV., IOWA CITY.
Plasma waves associated with the space shuttle N91-15064
ISTANBUL UNIV. (TURKEY).
Aerodynamic characteristics of cylindrical bodies with pointed and truncated conical noses N91-14289

J

JEANNERET AND ASSOCIATES, INC., HOUSTON, TX.
Position requirements for space station personnel and linkages to portable microcomputer performance assessment
[NASA-CR-185606] N91-14719
JET PROPULSION LAB., CALIFORNIA INST. OF TECH., PASADENA.
Efficient detection and signal parameter estimation with application to high dynamic GPS receiver
[NASA-CASE-NPO-17820-1-CU] N91-14321
Proceedings of the Mars Global Network Mission Workshop
[NASA-CR-186844] N91-14359
A polar orbit for the Mars Global Network Mission N91-14361
Innovative Long Wavelength Infrared Detector Workshop Proceedings
[NASA-CR-187433] N91-14379
Sensor requirements for Earth and planetary observations N91-14380
A novel electron tunneling infrared detector N91-14391
Fundamental limits to performance of quantum well infrared detectors N91-14397
New heterojunction LWIR detector options N91-14398
Novel Si(1-x)Ge(x)/Si heterojunction internal photoemission long wavelength infrared detectors N91-14401
InAs/GaAs and InAs doping superlattices N91-14409
High temperature refractory member with radiation emissive overcoat
[NASA-CASE-NPO-17122-1-CU] N91-14489
Trellis coded modulation for transmission over fading mobile satellite channel
[NASA-CASE-NPO-16904-2-CU] N91-14523
Organic cathode for a secondary battery
[NASA-CASE-NPO-17604-1-CU] N91-14536
Copper chloride cathode for a secondary battery
[NASA-CASE-NPO-17640-1-CU] N91-14538
Improved high power/high frequency inductor
[NASA-CASE-NPO-17830-1-CU] N91-14539
Millimeter-wave monolithic diode-grid frequency multiplier
[NASA-CASE-NPO-17258-1-CU] N91-14551
Apparatus and method for characterizing the transmission efficiency of a mass spectrometer
[NASA-CASE-NPO-16989-1-CU] N91-14587
Field induced gap infrared detector
[NASA-CASE-NPO-17526-1-CU] N91-14588
Mars Rover/Sample Return (MRSR) Mission: Mars Rover Technology Workshop
[NASA-TM-101129] N91-14600
Multi-fingered robotic hand
[NASA-CASE-NPO-15959-2] N91-14616
Method for detecting surface motions and mapping small terrestrial or planetary surface deformations with synthetic aperture radar
[NASA-CASE-NPO-17831-1-CU] N91-14642
Distributed computing system with dual independent communications paths between computers and employing split tokens
[NASA-CASE-NPO-17185-1-CU] N91-14772
Acoustic positioning and orientation prediction
[NASA-CASE-NPO-17511-1-CU] N91-14807
Acoustic transducer apparatus with reduced thermal conduction
[NASA-CASE-NPO-17620-1-CU] N91-14808
Surface modification using low energy ground state ion beams
[NASA-CASE-NPO-17498-1-CU] N91-14813
Preliminary survey of 21st century civil mission applications of space nuclear power
[NASA-TM-101249] N91-14817
JOENSUU UNIV. (FINLAND).
The optical parametrization of an aerial multispectral camera
[DE91-003017] N91-14593

JOHNS HOPKINS UNIV., BALTIMORE, MD.
Massively parallel network architectures for automatic recognition of visual speech signals
[AD-A226968] N91-14805
Dust in stellar wind bow shocks N91-14979
JOHNS HOPKINS UNIV., LAUREL, MD.
Solar wind dynamic pressure variations: Quantifying the statistical magnetospheric response N91-15060
Implications of multipoint observations of substorms in the inner magnetotail N91-15061
JOHNSON AERONAUTICS, PALO ALTO, CA.
Feasibility investigation of general time-domain unsteady aerodynamics of rotors
[NASA-CR-177570] N91-14311
JOINT PUBLICATIONS RESEARCH SERVICE, ARLINGTON, VA.
JPRS Report: Science and technology. USSR: Life sciences
[JPRS-ULS-89-003] N91-14706

K

KAB LABS, INC., SAN DIEGO, CA.
Feature set evaluation for classifiers
[AD-A226903] N91-14751
Feature set evaluation for classifiers
[AD-A226904] N91-14752
Feature set evaluation for classifiers
[AD-A226905] N91-14753
KAPTEYN ASTRONOMICAL LAB., GRONINGEN (NETHERLANDS).
Interstellar circular polarization and the dielectric nature of dust grains N91-14905
Dust emission from high latitude cirrus clouds N91-14930
Properties of grains derived from IRAS observations of dust N91-15001
KENTUCKY UNIV., LEXINGTON.
A boundary element method for elastostatic and elastodynamic crack problems in two and three dimensions N91-14626
KHARKOV STATE UNIV. (USSR).
Nonlinear surface MHD waves in the inhomogeneous plasma with cusp-resonance in upper solar atmosphere N91-15052
Nonlinearity influence in local resonance regions on the Alfven waves propagation in solar corona N91-15055
Description of nonlinear effects in a relativistic plasma using Hamiltonian formalism N91-15071
KMS FUSION, INC., ANN ARBOR, MI.
Experimental development, testing and research work in support of the inertial confinement fusion program
[DE91-002771] N91-14841
KURCHATOV (I. V.) INST. OF ATOMIC ENERGY, MOSCOW (USSR).
Generation of cosmic rays in pinches N91-15070
KYOTO UNIV. (JAPAN).
A two micron polarization survey toward dark clouds N91-14952

L

LABORATOIRE D'ASTRONOMIE SPATIALE, MARSEILLE (FRANCE).
Optical properties of irregular interstellar grains N91-14995
LABORATOIRE D'AUTOMATIQUE ET D'ANALYSE DES SYSTEMES, TOULOUSE (FRANCE).
Dynamic behavior of thin silicon plate: Application to silicon sensors
[LAAS-90144] N91-14582
Prototyping of a protocol validation environment: Application to the Estelle approach
[LAAS-90113] N91-14774
Reasoning of the geometric and uncertainty constraints in planning robot manipulation tasks
[LAAS-90143] N91-14775
LAHEY CLINIC MEDICAL CENTER, BOSTON, MA.
Initial blood storage experiment
[NASA-CR-185513-PT-1] N91-14700
Initial blood storage experiment
[NASA-CR-185513-PT-2] N91-14701
LAWRENCE LIVERMORE NATIONAL LAB., CA.
AC-130H Gunship Armor Upgrade Project
[DE91-002567] N91-14428
A modification of 4330 alloy steel
[DE91-001764] N91-14455
Computer studies of the dynamic strength of ceramics
[DE91-002568] N91-14481
A vibrating razor blade machining tool for material removal on low-density foams
[DE91-002996] N91-14507
A system architecture for long duration free floating flight for military applications
[NASA-CR-187435] N91-14513
Avalanche transistor selection for long term stability in streak camera sweep and pulser applications
[DE91-004195] N91-14535
A numerical theory of lattice gas and lattice Boltzmann methods in the computation of solutions to nonlinear advective-diffusive systems
[DE91-002566] N91-14560
Shot report, Holo-17-Holo-22 Rex-9
[DE91-002575] N91-14583
Recent long-pulse and high-average-power tests on a 140 GHz gyrotron
[DE91-001680] N91-14592
Enable Kit (MC-4246) for the DOT Charged Line System: Welding development report for 1/4-inch tubes and fittings
[DE91-002577] N91-14606
The effects of climate change on the nitrogen cycle and acid deposition
[DE91-002785] N91-14659
Construction of large-scale simulation codes using ALPAL (A Livermore Physics Applications Language)
[DE91-002783] N91-14740
Projected implicit Runge-Kutta methods for differential-algebraic boundary value problems
[DE91-000660] N91-14791
Integrated optical devices for photonics instrumentation systems
[DE91-004192] N91-14828
Physics data base for the Beam Plasma Neutron Source (BPNS)
[DE91-002796] N91-14842
A characterization of internal-Sn Nb3 Sn superconductors for use in the Proof of Priciples (PoP) coil
[DE91-001743] N91-14852
LECCE UNIV. (ITALY).
Raman properties of various carbonaceous materials and their astrophysical implications N91-14933
VUV-visible measurements on different samples of amorphous carbon N91-14990
IR emission from circumstellar envelopes of C-rich stars N91-15019
LEIDEN UNIV. (NETHERLANDS).
A survey for PAH emission in H II regions, planetary and proto-planetary nebulae N91-14920
New insights in the photochemistry of grain mantles: The identification of the 4.62 and 6.87 micron bands N91-14957
Molecular and mass spectroscopic analysis of isotopically labeled organic residues N91-14961
Diffusion and infrared properties of molecules in ice mantles N91-14963
The evolution of organic mantles on interstellar grains N91-14964
Scattering by fluffy grains N91-14992
A comparative study of the continuum and emission characteristics of comet dust. 1: Are the silicates in Comet Halley and Kohoutek amorphous or crystalline N91-15005
LITTLE (ARTHUR D.), INC., BOSTON, MA.
Initial blood storage experiment
[NASA-CR-185513-PT-1] N91-14700
Initial blood storage experiment
[NASA-CR-185513-PT-2] N91-14701
LOCKHEED MISSILES AND SPACE CO., SUNNYVALE, CA.
Unsteady separated flow phenomena causing self-excited structural oscillations N91-14339
LORAL INFRARED AND IMAGING SYSTEMS, LEXINGTON, MA.
Status of LWIR HgCdTe infrared detector technology N91-14383
LOS ALAMOS NATIONAL LAB., NM.
The vertical Van de Graaff telemetry system
[DE91-001960] N91-14370
Small band gap superlattices as intrinsic long wavelength infrared detector materials N91-14405
Short term creep rupture predictions for Tantalum alloy T-3
[DE91-002338] N91-14458
New multiphase equation of state for polycrystalline quartz
[DE91-001048] N91-14490
Transient analysis of a two-phase hydrogen heat switch
[DE91-002314] N91-14506
A simple plane-wave explosive lens
[DE91-004297] N91-14526
A CLOS (Common Lisp Object System) implementation on top of KEE (Knowledge Engineering Environment)
[DE91-001957] N91-14739
Fast electron studies in the ZT-40M edge plasma
[DE91-002323] N91-14838
Superconducting properties of Tl-Ba-Ca-Cu-O films on silver substrates
[DE91-002304] N91-14856
Infrared spectra of crystalline and glassy silicates and application to interstellar dust N91-14994
LOUISVILLE UNIV., KY.
Mechanism of hydrodenitrogenation. Part 4: Infrared spectroscopy of acidic molybdena catalysts
[DE91-002496] N91-14440
LOWELL UNIV., MA.
Approaches to the design of a novel macromolecular system with tailored optical properties
[AD-A226952] N91-14485
Nonlinear optics and organic materials
[AD-A226953] N91-14831

M

MANAGEMENT SERVICES, INC., HUNTSVILLE, AL.
Chronology: MSFC Space Station program, 1982 - present. Major events
[NASA-CR-184014] N91-15119
Chronology: MSFC Space Shuttle program development, assembly, and testing major events (1969 - April, 1981)
[NASA-CR-184013] N91-15120
MANCHESTER COLL. OF SCIENCE AND TECHNOLOGY (ENGLAND).
Grain growth, optical polarisation, and extinction in interstellar clouds N91-14959
MANCHESTER UNIV. (ENGLAND).
Polarization radar studies of precipitation: Implementation of the technique and data interpretation
[AD-A227073] N91-14690
MANUEL (LAWRENCE R.), BERKELEY, CA.
Superaromatics: The key to a unified cosmic dust theory N91-14999
MARTIN MARIETTA AEROSPACE, DENVER, CO.
Software cost estimation study
[AD-A226777] N91-14749
MARTIN MARIETTA CORP., DENVER, CO.
Space station common module network topology and hardware development
[NASA-CR-184034] N91-14373
MARYLAND UNIV., COLLEGE PARK.
Fundamental studies on microstructural evolution of two-phase titanium alloys N91-14452
Analysis of the boreal forest-tundra ecotone: A test of AVIRIS capabilities in the Eastern Canadian subarctic
[NASA-CR-187335] N91-14655
A software-system visualization tool
[AD-A227145] N91-14757
Efficient parallel algorithms on the network model
[AD-A227144] N91-14771
The definition of necessary hidden units in neural networks for combinatorial optimization
[AD-A227142] N91-14786
MASSACHUSETTS INST. OF TECH., CAMBRIDGE.
Measurement of hydrodynamic forces and moments and flow field mapping of a model in coning motion
[AD-A226684] N91-14355
Structural response of marine sandwich panels to uniform pressure loading
[AD-A227038] N91-14434
Variation of wall shear stress and Reynolds stress over a flat plate downstream of a boundary layer manipulator
[AD-A226875] N91-14565
Remote sensing of Earth terrain
[NASA-CR-186904] N91-14635
Plate motions and deformations from geologic and geodetic data
[NASA-CR-187379] N91-14672
Crustal dynamics project: The interpretation of crustal dynamics data in terms of plate motions and regional deformation near plate boundaries
[NASA-CR-187691] N91-14673
Shipboard and satellite observations of upper ocean velocity and transport variability in the Gulf Stream
[AD-A226974] N91-14694
Observations of ocean fluctuations between 15 and 23 hour periods in the Pacific
[AD-A227017] N91-14695
The distribution of wave heights and periods for seas with unimodal bimodal power density spectra
[AD-A227040] N91-14696
A method for estimating tokamak poloidal field coil currents which incorporates engineering constraints
[DE91-001662] N91-14848
Investigation of new semiinsulating behavior of 3-5 compounds
[AD-A226787] N91-14862
Ground boundaries
[DE91-004027] N91-14880

MASSACHUSETTS INST. OF TECH., LEXINGTON.
A proposed astronomical reference catalog of infrared sources
[AD-A226757] N91-15041
MASSACHUSETTS UNIV., BOSTON.
Initial blood storage experiment
[NASA-CR-185513-PT-1] N91-14700
Initial blood storage experiment
[NASA-CR-185513-PT-2] N91-14701
MAX-PLANCK-INST. FUER EXTRATERRESTRISCHE PHYSIK, GARCHING (GERMANY, F.R.).
Absorption features in the 3 micron spectra of highly obscured objects N91-14965
MAX-PLANCK-INST. FUER RADIOASTRONOMIE, BONN (GERMANY, F.R.).
High resolution observations of compact H II regions at 230 GHz N91-14954
MCDONNELL AIRCRAFT CO., SAINT LOUIS, MO.
A unified approach to buffet response of fighter aircraft empennage N91-14326
MCDONNELL-DOUGLAS HELICOPTER CO., MESA, AZ.
Advanced technology landing gear. Volume 1: Design
[AD-A227196] N91-14343
Advanced technology landing gear. Volume 2: Test
[AD-A227197] N91-14344
MECHANICAL TECHNOLOGY, INC., LATHAM, NY.
Computer-assisted strain-gage monitoring and data reduction system
[AD-A226894] N91-14589
MESSERSCHMITT-BOELKOW-BLOHM G.M.B.H., MUNICH (GERMANY, F.R.).
Hypersonic aerodynamics: An approximation method for the calculation of real gas effects and wall temperatures
[MBB/FE127/S/PUB/0403] N91-14306
Role of separation autopilots for modern missile concepts
[MBB/FE121/S/PUB/409/A] N91-14352
New accurate, vectorized approximations of state surfaces for the thermodynamic and transport properties of equilibrium air
[MBB/FE122/S/PUB/0389] N91-14886
MICHIGAN UNIV., ANN ARBOR.
Task reports on developing techniques for scattering by 3D composite structures and to generate new solutions in diffraction theory using higher order boundary conditions
[NASA-CR-186899] N91-14475
A finite element conjugate gradient FFT method for scattering N91-14476
Analytical solutions with Generalized Impedance Boundary Conditions (GIBC) N91-14477
Acceleration techniques for explicit Euler codes N91-14555
Some problems in elastic contact and fracture N91-14625
Multiband radar characterization of forest biomes
[NASA-CR-185101] N91-14638
Theory and measurements of nighttime horizontal gradients in the mid-latitude F region N91-14671
A combined finite element-boundary element formulation for solution of axially symmetric bodies
[NASA-CR-185852] N91-14789
Infrared fluorescence from PAHs in the laboratory N91-14934
MIDWEST RESEARCH INST., GOLDEN, CO.
A discussion of the results of an in-situ comparison of three full-vector anemometers
[DE91-002113] N91-14572
The high cost of low quality in R/D (Research and Development)
[DE91-002118] N91-14621
High efficiency cadmium and zinc telluride-based thin film solar cells
[DE91-002112] N91-14643
Load response of horizontal-axis wind turbines to turbulence
[DE90-000375] N91-14644
MINNESOTA UNIV., MINNEAPOLIS.
IR detectors based on n-i-p-i superlattices N91-14408
One- and two-dimensional Stirling machine simulation using experimentally generated flow turbulence models
[NASA-CR-185285] N91-14414
State-to-state dynamics of molecular energy transfer
[DE91-004589] N91-14599
Piecewise-parabolic methods for systems of hyperbolic conservation laws in multiprocessing environments
[DE91-004582] N91-14792
Theory of the electronic and structural properties of solid state oxides
[DE91-001192] N91-14874
MISSION RESEARCH CORP., COLORADO SPRINGS, CO.
Radiation response issues for infrared detectors N91-14388
MISSISSIPPI UNIV., UNIVERSITY.
A statistically-based model of the interacting processes which lead to creep-rupture in filament-wound composite pressure vessels N91-14420
MISSOURI UNIV., SAINT LOUIS.
Quantum 1/f noise in high technology applications including ultrasmall structures and devices
[AD-A226739] N91-14515
MITECH, INC., WASHINGTON, DC.
Automatic dependent surveillance benefit and cost analysis
[DOT/FAA/RD-90/34] N91-14320
MOLECULAR RESEARCH INST., PALO ALTO, CA.
The effect of ionization on the infrared absorption spectra of PAHs: A preliminary report N91-14937
MONTREAL UNIV. (QUEBEC).
On the polarization mechanism in the R Mon/NGC 2261 complex N91-14969
MOUND LAB., MIAMISBURG, OH.
Elucidation of fundamental properties of helium in metals by nuclear magnetic resonance techniques
[DE91-002715] N91-14460
Solid state radioluminescent sources using zeolites
[DE91-002703] N91-14857
MOUNT STROMLO AND SIDING SPRING OBSERVATORY, CANBERRA (AUSTRALIA).
PAH emission from Nova Cen 1986 N91-14921
MULLARD RADIO ASTRONOMY OBSERVATORY, CAMBRIDGE (ENGLAND).
Does the far-infrared/radio correlation in spiral galaxies extend to the spatial domain N91-14985

N

NAGOYA UNIV. (JAPAN).
Solar flares and particle acceleration N91-15049
Observation of electron hole, double layer, and turbulent heating in a laboratory plasma N91-15079
NATIONAL ACADEMY OF SCIENCES - NATIONAL RESEARCH COUNCIL, WASHINGTON, DC.
Snow avalanche hazards and mitigation in the United States
[LC-90-62814] N91-14686
Information technology and the conduct of research: The user's view. Report of the Panel on Information Technology and the Conduct of Research
[ISBN-0-309-03888-X] N91-14890
NATIONAL AERONAUTICAL ESTABLISHMENT, OTTAWA (ONTARIO).
Application of Euler and Navier-Stokes codes to missile type bodies with high L/D ratios N91-14286
Wind tunnel investigation and flight tests of tail buffet on the CF-18 aircraft N91-14325
Effects of trailing-edge flap on buffet characteristics of a supercritical airfoil N91-14327
The effect of wing planform on low speed buffet N91-14336
NATIONAL AERONAUTICS AND SPACE ADMINISTRATION, WASHINGTON, DC.
Aerospace medicine and biology: A continuing bibliography with indexes (supplement 343)
[NASA-SP-7011(343)] N91-14711
Aerospace medicine and biology: A continuing bibliography with indexes (supplement 344)
[NASA-SP-7011(344)] N91-14712
A bibliography of planetary geology and geophysics principal investigators and their associates, 1989-1990
[NASA-TM-4221] N91-15034
NATIONAL AERONAUTICS AND SPACE ADMINISTRATION. AMES RESEARCH CENTER, MOFFETT FIELD, CA.
Tabulation of data from the tip aerodynamics and acoustics test
[NASA-TM-102280] N91-14273
Flight data acquisition methodology for validation of passive ranging algorithms for obstacle avoidance
[NASA-TM-102809] N91-14322
Wind tunnel balance
[NASA-CASE-ARC-11877-1-SB] N91-14357
Pyroelectric detectors N91-14390
Modeling and control design of a wind tunnel model support
[NASA-TM-103829] N91-14540
Multiple axis reticle
[NASA-CASE-ARC-11886-1-SB] N91-14591
Exobiology in Earth orbit: The results of science workshops held at NASA, Ames Research Center
[NASA-SP-500] N91-14725
NASA's supercomputing experience
[NASA-TM-102890] N91-14727
Interstellar Dust: Contributed Papers
[NASA-CP-3036] N91-14897
Infrared images of reflection nebulae and Orion's bar: Fluorescent molecular hydrogen and the 3.3 micron feature N91-14918
Airborne observations of the infrared emission bands N91-14919
Spatial variations of the 3 micron emission features within nebulae N91-14922
Spectral structure near the 11.3 micron emission feature N91-14926
The spatial distribution of infrared radiation from visible reflection nebulae N91-14931
Dust coagulation in ISM N91-14968
Infrared studies of dust grains in infrared reflection nebulae N91-14970
Studying the spatial distribution of interstellar dust N91-14980
Far infrared structure of spiral galaxies from the IRAS CPC images N91-14988
Stochastic histories of dust grains in the interstellar medium N91-14998
The nature of cometary dust as determined from infrared observations N91-15003
Sublimating icy planetesimals as the source of nucleation seeds for grain condensation in classical novae N91-15016
Sublimating comets as the source of nucleation seeds for grain condensation in the gas outflow from AGB stars N91-15018
Carbon stars with alpha-C:H emission N91-15022
New circumstellar dust component in oxygen rich environments N91-15023
Interstellar extinction at 10-20 microns N91-15025
Wind tunnel study of an observatory dome with a circular aperture
[NASA-TM-102888] N91-15040
NATIONAL AERONAUTICS AND SPACE ADMINISTRATION. GODDARD SPACE FLIGHT CENTER, GREENBELT, MD.
Satellite situation report, volume 30, no. 1
[NASA-TM-101105] N91-14372
Outgassing data for selecting spacecraft materials, revision 2
[NASA-RP-1124-REV-2] N91-14437
An evaluation of two flat-black silicone paints for space application
[NASA-TM-100768] N91-14494
Digitized synchronous demodulator
[NASA-CASE-GSC-13237-1] N91-14550
Crustal Dynamics Project data analysis, 1990
[NASA-TM-100765] N91-14679
Observations of the diffuse UV radiation field N91-14912
The capability of the ultraviolet imaging telescope for observing interstellar dust N91-14913
Does CO trace H2 at high galactic latitude N91-14973
On the origin of extinction in the Coma cluster of galaxies N91-14987
Laboratory studies of refractory metal oxide smokes N91-14993
Infrared emission from the supernova remnant Puppis A: Dust and gas parameters N91-15032
On the detectability of infrared echo arcs around supernova 1987A N91-15033
NATIONAL AERONAUTICS AND SPACE ADMINISTRATION. JOHN C. STENNIS SPACE CENTER, BAY SAINT LOUIS, MS.
Hybrid butterfly valve
[NASA-CASE-SSC-00004-1] N91-14609
Combined air and water pollution control system
[NASA-CASE-NST-00007-1] N91-14662
NATIONAL AERONAUTICS AND SPACE ADMINISTRATION. JOHN F. KENNEDY SPACE CENTER, COCOA BEACH, FL.
Liquid hydrogen polygeneration system and process
[NASA-CASE-KSC-11304-2] N91-14495
NATIONAL AERONAUTICS AND SPACE ADMINISTRATION. LYNDON B. JOHNSON SPACE CENTER, HOUSTON, TX.
A GNM mission and system design proposal N91-14364
Adaptive data acquisition multiplexing system and method
[NASA-CASE-MSC-21170-1] N91-14371
Smart tunnel: Docking mechanism
[NASA-CASE-MSC-21360-1] N91-14374
Thermal switch disc for short circuit protection of batteries
[NASA-CASE-MSC-21428-1] N91-14537
Vibration analyzer
[NASA-CASE-MSC-21408-1] N91-14607
Quick connect coupling
[NASA-CASE-MSC-21539-1] N91-14610
Bio-reactor chamber
[NASA-CASE-MSC-20929-1] N91-14703
Dual physiological rate measurement instrument
[NASA-CASE-MSC-20078-3] N91-14709
Valve for waste collection and storage
[NASA-CASE-MSC-21025-4] N91-14723

Method for waste collection and storage
[NASA-CASE-MSC-21025-2] N91-14724
Discrete event simulation tool for analysis of qualitative models of continuous processing systems
[NASA-CASE-MSC-21465-1] N91-14741
Method of up-front load balancing for local memory parallel processors
[NASA-CASE-MSC-21348-1] N91-14769

NATIONAL AERONAUTICS AND SPACE ADMINISTRATION. LANGLEY RESEARCH CENTER, HAMPTON, VA.

Flow visualization studies of blowing from the tip of a swept wing
[NASA-TM-4217] N91-14274
Internal performance of a hybrid axisymmetric/nonaxisymmetric convergent-divergent nozzle
[NASA-TM-4230] N91-14275
Asymmetric supersonic flow around cones with noncircular sections N91-14292
Parametric study of afterbody/nozzle drag on twin two-dimensional convergent-divergent nozzles at Mach numbers from 0.60 to 1.20
[NASA-TP-2640] N91-14316
A method for the design of transonic flexible wings
[NASA-TP-3045] N91-14323
Unsteady airloads due to separated flow on airfoils and wings N91-14340
Wingtip vortex turbine
[NASA-CASE-LAR-14116-1] N91-14345
Electro-optical spin measurement system
[NASA-CASE-LAR-13629-1] N91-14356
Method and apparatus for determining time, direction, and composition of impacting space particles
[NASA-CASE-LAR-13392-1-CU] N91-14412
Bis (4-(3,4-dimethylene-pyrrolidyl)-phenyl) methane
[NASA-CASE-LAR-13965-2-CU] N91-14418
N-(3-ethynylphenyl)maleimide
[NASA-CASE-LAR-14188-2] N91-14419
Delamination test apparatus and method
[NASA-CASE-LAR-13985-1] N91-14430
Process for lowering the dielectric constant of polyimides using diamic acid additives
[NASA-CASE-LAR-13902-1] N91-14484
Active control of boundary layer transition and turbulence
[NASA-CASE-LAR-13532-1] N91-14562
Advanced technology development for image gathering, coding, and processing N91-14579
Thermal compensating mount
[NASA-CASE-LAR-14207-1] N91-14590
Mechanical end joint system for connecting structural column elements
[NASA-CASE-LAR-14465-1] N91-14614
Spiral lead platen robotic end effector
[NASA-CASE-LAR-13855-1] N91-14615
Axisymmetric shell analysis of the space shuttle solid rocket booster field joint
[NASA-TP-3033] N91-14618
A parametric shell analysis of the shuttle 51-L SRB AFT field joint
[NASA-TM-102748] N91-14629
Advanced technology needs for a global change science program: Perspective of the Langley Research Center
[NASA-TM-4196] N91-14634
Limb-darkening functions as derived from along-track operation of the ERBE scanning radiometers for August 1985
[NASA-RP-1243] N91-14683
The NASA/DOD aerospace knowledge diffusion research project: A research agenda
[NASA-TM-103439] N91-14892

NATIONAL AERONAUTICS AND SPACE ADMINISTRATION. LEWIS RESEARCH CENTER, CLEVELAND, OH.

Results of a sub-scale model rotor icing test
[NASA-TM-103709] N91-14309
Numerical simulation of ice growth on a MS-317 swept wing geometry
[NASA-TM-103705] N91-14310
Combustor technology for future aircraft
[NASA-TM-103268] N91-14349
Low velocity impact analysis with NASTRAN
[NASA-TM-103169] N91-14426
Thermal stability of the microstructure of an aged Nb-Zr-C alloy
[NASA-TM-103647] N91-14454
Effect of hydrogen on the strength and microstructure of selected ceramics
[NASA-TM-103674] N91-14482
Manipulation hardware for microgravity research
[NASA-TM-103423] N91-14498
A numerical and experimental analysis of reactor performance and deposition rates for CVD on monofilaments
[NASA-TM-103631] N91-14500
Universal nondestructive mm-wave integrated circuit test fixture
[NASA-CASE-LEW-14746-1] N91-14552
Surface settling in partially filled containers upon step reduction in gravity
[NASA-TM-103641] N91-14556
Numerical study of shock-wave/boundary layer interactions in premixed hydrogen-air hypersonic flows
[NASA-TM-103273] N91-14559
High Resolution, High Frame Rate Video Technology
[NASA-CP-3080] N91-14574
Results of the users' requirements survey N91-14575
State of the art in video system performance N91-14578
High resolution, high frame rate video technology development plan and the near-term system conceptual design N91-14580
Post clamp
[NASA-CASE-LEW-14862-1] N91-14617
Axial-torsional fatigue: A study of tubular specimen thickness effects
[NASA-TM-103637] N91-14632
Mappings and accuracy for Chebyshev pseudo-spectral approximations
[NASA-TM-103630] N91-14781
Vibrational testing of optical fiber connector joints
[NASA-TM-103654] N91-14829
Silicon carbide, a semiconductor for space power electronics
[NASA-TM-103655] N91-14850
Solar radiation on Mars: Update 1990
[NASA-TM-103623] N91-15117

NATIONAL AERONAUTICS AND SPACE ADMINISTRATION. MARSHALL SPACE FLIGHT CENTER, HUNTSVILLE, AL.

Directional solidification of superalloys
[NASA-CASE-MFS-28314-1] N91-14462
Electrostatically suspended rotor for angular encoder
[NASA-CASE-MFS-28294-1] N91-14508
Low-noise nozzle valve
[NASA-CASE-MFS-28383-1] N91-14563
Turbomachinery rotor support with damping
[NASA-CASE-MFS-28345-1] N91-14608
System for connecting fluid couplings
[NASA-CASE-MFS-26042-1-SB] N91-14613
X ray sensitive area detection device
[NASA-CASE-MFS-28232-1] N91-14835
Piezoelectrostatic generator
[NASA-CASE-MFS-28298-1] N91-14872

NATIONAL AERONAUTICS AND SPACE ADMINISTRATION. PASADENA OFFICE, CA.

Efficient detection and signal parameter estimation with application to high dynamic GPS receiver
[NASA-CASE-NPO-17820-1-CU] N91-14321
High temperature refractory member with radiation emissive overcoat
[NASA-CASE-NPO-17122-1-CU] N91-14489
Trellis coded modulation for transmission over fading mobile satellite channel
[NASA-CASE-NPO-16904-2-CU] N91-14523
Organic cathode for a secondary battery
[NASA-CASE-NPO-17604-1-CU] N91-14536
Copper chloride cathode for a secondary battery
[NASA-CASE-NPO-17640-1-CU] N91-14538
Improved high power/high frequency inductor
[NASA-CASE-NPO-17830-1-CU] N91-14539
Millimeter-wave monolithic diode-grid frequency multiplier
[NASA-CASE-NPO-17258-1-CU] N91-14551
Apparatus and method for characterizing the transmission efficiency of a mass spectrometer
[NASA-CASE-NPO-16989-1-CU] N91-14587
Field induced gap infrared detector
[NASA-CASE-NPO-17526-1-CU] N91-14588
Multi-fingered robotic hand
[NASA-CASE-NPO-15959-2] N91-14616
Method for detecting surface motions and mapping small terrestrial or planetary surface deformations with synthetic aperture radar
[NASA-CASE-NPO-17831-1-CU] N91-14642
Distributed computing system with dual independent communications paths between computers and employing split tokens
[NASA-CASE-NPO-17185-1-CU] N91-14772
Acoustic positioning and orientation prediction
[NASA-CASE-NPO-17511-1-CU] N91-14807
Acoustic transducer apparatus with reduced thermal conduction
[NASA-CASE-NPO-17620-1-CU] N91-14808
Surface modification using low energy ground state ion beams
[NASA-CASE-NPO-17498-1-CU] N91-14813

NATIONAL AEROSPACE LAB., AMSTERDAM (NETHERLANDS).

Investigation of a semi-empirical method to predict limit cycle oscillations of modern fighter aircraft N91-14333

NATIONAL ENVIRONMENTAL SATELLITE SERVICE, WASHINGTON, DC.

Evaluation of data reduction and composing of the NOAA global vegetation index product: A case study
[AD-A227397] N91-14641
NA-9 Solar Backscatter Ultraviolet (SBUV/2) instrument and derived ozone data
[AD-A227449] N91-15118

NATIONAL RADIO ASTRONOMY OBSERVATORY, TUCSON, AZ.

Longwave spectral dependence of emission from warm dust clouds N91-14945

NATIONAL RESEARCH INST. FOR POLLUTION AND RESOURCES, TOKYO (JAPAN).

Hydrocarbon group-type analysis of petroleum distillates and residues by high-performance liquid chromatography
[DE91-727527] N91-14451

NAUTICAL ALMANAC OFFICE, WASHINGTON, DC.

Astronomical phenomena for the year 1990 N91-15035
The Air Almanac, 1990 N91-15036
The Astronomical Almanac for the year 1989
[ISBN-0-11-886932-9] N91-15038
The Astronomical Almanac for the year 1990
[ISBN-0-11-886934-5] N91-15039

NAVAL ACADEMY, ANNAPOLIS, MD.

Development of a taction system using piezoelectric film
[AD-A227076] N91-14544
On the breakdown of a vortex
[AD-A227066] N91-14568
Explosive cyclogenesis: A case study of the Veterans' Day storm of 11-12 November 1987
[AD-A227077] N91-14691
Upwelling southwest of Iceland due to quasi-geostrophic flow
[AD-A227129] N91-14698
Development of phenomenological fitting procedure for the fast microcomputer
[AD-A227168] N91-14759
A model of the acoustic interactions occurring under Arctic ice
[AD-A227128] N91-14806

NAVAL AEROSPACE MEDICAL RESEARCH LAB., PENSACOLA, FL.

Validation of dichotic listening and psychomotor task performance as predictors of primary flight training criteria: Highlighting relevant statistical issues
[AD-A227010] N91-14717

NAVAL MEDICAL RESEARCH INST., BETHESDA, MD.

Development of an animal model of human non-freezing cold injury: Changes in thermal sensitivity following cold exposure
[AD-A227174] N91-14705

NAVAL OBSERVATORY, WASHINGTON, DC.

The Air Almanac, 1989 N91-15037

NAVAL OCEANOGRAPHIC AND ATMOSPHERIC RESEARCH LAB., BAY SAINT LOUIS, MS.

Oceanographic expert system validation using GOAP mesoscale products and Gulf/DART validation test data
[AD-A226929] N91-14693
Multispectral imagery support for ocean venture 90
[AD-A227119] N91-14697

NAVAL POSTGRADUATE SCHOOL, MONTEREY, CA.

Numerical studies of compressible flow over a double-delta wing at high angles of attack
[AD-A226931] N91-14312
Development of an unmanned air research vehicle for supermaneuverability studies
[AD-A227165] N91-14342
The effects of liquid propellant motion on the attitude stability of spin stabilized spacecraft
[AD-A227002] N91-14376
Determination of SPEAR-1 rocket body potential during high-voltage experiments
[AD-A226971] N91-14417
Thermomechanical processing and ambient temperature properties of a 6061 aluminum 10 volume percent alumina metal matrix composite
[AD-A227004] N91-14433
An examination of delta prime growth in an aluminum-lithium alloy by x ray diffraction
[AD-A227254] N91-14464
Processing studies of aluminum-magnesium and aluminum-copper-lithium alloys
[AD-A227255] N91-14465
Computer aided design models for millimeter-wave suspended substrate microstrip line
[AD-A227259] N91-14547
Validation of a computational model for autogenous arc welding
[AD-A227258] N91-14611

The response and failure mechanisms of circular metal and composite plates subjected to underwater shock loading
[AD-A226759] N91-14631
Developing portable user interfaces for Ada command control software
[AD-A226712] N91-14747
Evaluations of some scheduling algorithms for hard real-time systems
[AD-A226930] N91-14755
A performance study of the concurrency control algorithms in hierarchical network with partitioned database
[AD-A227055] N91-14756
Cyclomatic complexity as a utility for predicting software faults
[AD-A227313] N91-14760
Minimization on stochastic matroids
[AD-A227413] N91-14799
DEMON: A media object model incorporating natural language descriptions for retrieval support
[AD-A226711] N91-14893
Defense Data Network (DDN) performance analysis using probability modeling
[AD-A226856] N91-14894

NAVAL RESEARCH LAB., WASHINGTON, DC.
Dynamics of an unsteady diffusion flame: Effects of heat release and gravity
[AD-A227348] N91-14447
Perspectives on modeling electromagnetic sea scatter
[AD-A226939] N91-14520
Innovative methodology for cancelling contaminating noise in turbulent fluid flow environments
[AD-A227028] N91-14567
Dust emission from Barnard 35: Gas heating anomaly resolved N91-14951

NAVAL SURFACE WARFARE CENTER, SILVER SPRING, MD.
Supersonic tactical missile computation using Euler's equation with crossflow separation modeling
N91-14284

NAVAL UNDERWATER SYSTEMS CENTER, NEWPORT, RI.
Tips on how to cut technical publications costs
[AD-A227334] N91-14895

NAVAL WEAPONS CENTER, CHINA LAKE, CA.
Overview of propulsion concepts for tactical missiles
N91-14296
Crystal structure of ZnGa2S4, a defect sphalerite-derivative
[AD-A226937] N91-14865
On the crystal structure of KInS2-I
[AD-A226940] N91-14866

NEVADA UNIV., LAS VEGAS.
Planning monotone paths to visit a set of obstacles
[AD-A226923] N91-14754
Capturing strong reduction in director string calculus
[AD-A226738] N91-14783

NEVADA UNIV., RENO.
Numerical investigations in three-dimensional internal flows
[NASA-CR-187373] N91-14277

NEW MEXICO INST. OF MINING AND TECHNOLOGY, SOCORRO.
Aircraft measurements of electrified clouds at Kennedy Space Center
[NASA-CR-186536] N91-14680
Aircraft measurements of electrified clouds at Kennedy Space Center. Part 1: 1988 flights N91-14681
Aircraft measurements of electrified clouds at Kennedy Space Center. Part 2: Case study: 4 November 1988 (88309) N91-14682

NEW MEXICO UNIV., ALBUQUERQUE.
Next-generation fire extinguishing agent. Phase 2: Laboratory tests and scoping trials
[AD-A227347] N91-14510

NIELSEN ENGINEERING AND RESEARCH, INC., MOUNTAIN VIEW, CA.
Aerodynamic design of Pegasus (trademark): Concept to flight with CFD N91-14285
Chordwise and spanwise centers of pressure of missile fins N91-14304

NORTH CAROLINA STATE UNIV., RALEIGH.
Growth and properties of Hg-based quantum well structures and superlattices N91-14403
Growth, characterization and device development in monocrystalline diamond films
[AD-A227238] N91-14871
A mesoscale planetary boundary layer numerical model for simulations of topographically induced circulations
N91-15113

NORTHWESTERN UNIV., EVANSTON, IL.
Use of anomalous small angle x ray scattering to investigate microstructural features in complex alloys
[DE91-002397] N91-14471

O

OAK RIDGE GASEOUS DIFFUSION PLANT, TN.
Electroless nickel bath recovery by cation exchange and precipitation
[DE91-001988] N91-14457

OAK RIDGE NATIONAL LAB., TN.
Interfacial push-out measurements of fully-bonded SiC/SC composites
[DE91-004527] N91-14436
In-line sensors for electrolytic magnesium cells
[DE91-002561] N91-14438
The effect of scandium on the phase stability of Al3Nb and Al3Zr
[DE91-002657] N91-14459
Ion implantation for corrosion inhibition of aluminum alloys in saline media
[DE91-002887] N91-14461
Effects of irradiation on initiation and crack-arrest toughness of two high-copper welds and on stainless steel cladding
[DE91-001272] N91-14467
Ultrasonic detection of fatigue damage in glass-epoxy composites
[DE91-002652] N91-14619
Quality control and nondestructive test procedures for welded products
[DE91-004530] N91-14623
High-temperature thermal storage systems for advanced solar receivers materials selections
[NASA-CR-187750] N91-14647
Acidic deposition: Its nature and impacts
[DE91-001984] N91-14658
Validity of environmental transfer models
[DE91-002929] N91-14660
The response of atmospheric CO2 to changes in land use
[DE91-001212] N91-14663
Environmental impact assessment as applied to policies, plans, and programs
[DE91-001372] N91-14664
Modified seasonal factors in exponential smoothing
[DE91-002802] N91-14688
Prediction of helicopter simulator sickness
[DE90-016530] N91-14710
Status of the advanced neutron source
[DE91-002870] N91-14810
Study of spin-temperature effects using energy-ordered continuum gamma ray spectroscopy technique
[DE91-002854] N91-14818
Fueling of magnetically confined plasmas by single- and two-stage repeating pneumatic pellet injectors
[DE91-002635] N91-14839
Characteristics and potential applications of an ORNL microwave ECR multicusp plasma ion source
[DE91-002649] N91-14840
ITER global stability limits
[DE91-001488] N91-14845
Tokamak fluidlike equations, with applications to turbulence and transport in H mode discharges
[DE91-002632] N91-14849
Ion beam induced diffusion and crystallization in high dose Er implanted Si
[DE91-002869] N91-14860
Defect and impurity effects on the initial growth of Ag on Si(111)
[DE91-001277] N91-14876

OBSERVATOIRE DE MARSEILLE (FRANCE).
Reddening and extinction towards H II regions
N91-14898

OBSERVATOIRE DE PARIS-MEUDON (FRANCE).
Angular motion of a PAH molecule in interstellar environment N91-14938
Grains charges in interstellar clouds N91-14967

OFFICE NATIONAL D'ETUDES ET DE RECHERCHES AEROSPATIALES, PARIS (FRANCE).
Comparison of different calculation methods applied to a lenticular fuselage section N91-14293
Anticipation of aerodynamic coefficients of missile air intakes N91-14297
Results of GARTEUR action group AG09 on flow past missile afterbodies N91-14299
New method to determine in wind tunnel the buffeting forces N91-14337
Coupled aerodynamic loads due to unsteady stall on a large aspect ratio wing oscillating at great amplitude
N91-14338

OHIO STATE UNIV., COLUMBUS.
Estimability of geodetic parameters from space VLBI observables
[NASA-CR-187413] N91-14636
Demodulation processes in auditory perception
[AD-A226824] N91-14707
Investigations of ultrasonic wave interactions with grain boundaries and grain imperfections
[DE91-002695] N91-14804
IR and FIR laser diagnostics for plasma thrusters using a CW CO2 radiation source
[AD-A226816] N91-14843

OLD DOMINION UNIV., NORFOLK, VA.
Study of diamond film growth and properties
[NASA-CR-187709] N91-14483

OPTECH, INC., DOWNSVIEW (ONTARIO).
Helicopter lidar bathymeter system. Conceptual design
[AD-A227057] N91-14348

OREGON STATE UNIV., CORVALLIS.
Load response of horizontal-axis wind turbines to turbulence
[DE90-000375] N91-14644

OREGON UNIV., EUGENE.
Nonlinear dynamics of broad-band lasers
[DE91-001143] N91-14596
Investigating individual differences in general comprehension skill: The role of suppression and enhancement
[AD-A226788] N91-14715

OSSERVATORIO ASTRONOMICO, TURIN (ITALY).
A model for one-sided extragalactic jets N91-15097

OXFORD UNIV. (ENGLAND).
The interlaminar shear strength of woven carbon, woven glass and woven carbon/glass hybrid laminates under static and impact loading
[OUEL-1831/90] N91-14423
Robot control strategies
[OUEL-1754/89] N91-14605
Analogue computation using VLSI neural network devices
[OUEL-1835/90] N91-14773

P

PACIFIC NORTHWEST LAB., RICHLAND, WA.
Radiation resistance of copper alloys at high exposure levels
[DE91-001563] N91-14470
Effects of wind shear and turbulence on wind turbine power curves
[DE91-004072] N91-14648
Atmospheric source-receptor relationships: Concepts and terminology
[DE91-001033] N91-14656
A LEED study of the MgO(001) surface structure
[DE91-002811] N91-14879

PARIS VII UNIV. (FRANCE).
PAHs molecules and heating of the interstellar gas
N91-14939

PASK RESEARCH AND ENGINEERING, INC., PINOLE, CA.
Joining alumina to sapphire for copper vapor laser tubes
[AD-A226619] N91-14501

PENNSYLVANIA STATE UNIV., UNIVERSITY PARK.
PAH formation in carbon-rich circumstellar envelopes
N91-15015

PERI, INC., PRINCETON, NJ.
Air traffic controller memory enhancement
[DOT/FAA/CT-TN90/38] N91-14713

PISA UNIV. (ITALY).
Grains in galactic haloes N91-14984

PITTSBURGH UNIV., PA.
Strategic utilization of information resources: A contingency approach N91-14891

PLANETARY SCIENCE INST., TUCSON, AZ.
A spectral difference between silicates in Comet Halley and interstellar silicates N91-15002

PLESSCOR OPTRONICS, INC., CHATSWORTH, CA.
Quantum well laser
[AD-A227303] N91-14594

POLISH ACADEMY OF SCIENCES, TORUN.
Continuous infrared emission of proto- and young-planetary nebulae N91-15030

PRAGUE OBSERVATORY (CZECHOSLOVAKIA).
Laboratory investigation of electric charging of dust particles by electrons, ions, and UV radiation
N91-14971

PRINCETON UNIV., NJ.
Photovoltaic quantum well infrared photodetectors
N91-14393
Bioreactivity: Studies on a simple brain stem reflex in behaving animals
[AD-A226823] N91-14704
Pedagogical strategies for human and computer tutoring
[AD-A226886] N91-14750

PRINCETON UNIV. OBSERVATORY, NJ.
Grain mantles: The impact on grain evolution and selective extinction N91-14960

PURDUE UNIV., WEST LAFAYETTE, IN.
Research as part of the Air Force Research in Aero-Propulsion Technology (AFRAPT) program
[AD-A226893] N91-14350
Approximately integrable linear statistical models in non-parametric estimation
[AD-A227395] N91-14798
The evaluation of long range consequences in decision making
[AD-A226949] N91-14888

R

RAYTHEON CO., LEXINGTON, MA.
MMIC compensation network for phased array element mismatch
[AD-A227437] N91-14522
RENSSELAER POLYTECHNIC INST., TROY, NY.
Effect of interline heat flow parameter on contact line heat transfer
[AD-A226944] N91-14566
Using infrared spectral features to probe circumstellar dust shells around cool stars N91-15021
RHEINMETALL G.M.B.H., DUESSELDORF (GERMANY, F.R.).
Experimental aerodynamics for hot gas jet reaction control systems N91-14300
RHODE ISLAND UNIV., NARRAGANSETT.
The SYNOP experiment: Inverted echo sounder data report for October 1987 to May 1988
[AD-A227232] N91-14699
RICE UNIV., HOUSTON, TX.
Gamma guidance of trajectories for coplanar, aeroassisted orbital transfer
[NASA-CR-187732] N91-14365
Properties of the optimal trajectories for coplanar, aeroassisted orbital transfer
[NASA-CR-187733] N91-14366
Decomposition technique and optimal trajectories for the aeroassisted flight experiment
[NASA-CR-187734] N91-14367
Guidance trajectories for aeroassisted orbital transfer
[NASA-CR-187735] N91-14368
Matrix isolation as a tool for studying interstellar chemical reactions N91-14956
ROCHESTER UNIV., NY.
Electro-optic network analyzer
[NASA-CR-186613] N91-14527
LLE (Laboratory for Laser Energetics) review
[DE91-001254] N91-14597
The buckling of off-axis, orthotropic, cylindrical shells in torsion N91-14628
ROCKWELL INTERNATIONAL SCIENCE CENTER, THOUSAND OAKS, CA.
LWIR HgCdTe: Innovative detectors in an incumbent technology N91-14384
ROME AIR DEVELOPMENT CENTER, GRIFFISS AFB, NY.
Systolic emulator experimentation
[AD-A226746] N91-14516
ROYAL AERONAUTICAL SOCIETY, LONDON (ENGLAND).
Store carriage, integration, and release N91-14281
ROYAL AEROSPACE ESTABLISHMENT, BEDFORD (ENGLAND).
Pressure measurements on slender bodies at supersonic speeds and development of flow separation critera for Euler codes N91-14282
Interaction between the canard and wing flow on a model of a typical combat aircraft N91-14334
ROYAL AEROSPACE ESTABLISHMENT, FARNBOROUGH (ENGLAND).
Review of the spring 1988 AGARD FMP symposium N91-14280
Investigations of aerothermodynamic effects on axisymmetric bodies at high Mach numbers N91-14302
In-flight measurements on a Tornado aircraft for stores carriage and release research
[RAE-TM-AERO-2180] N91-14341
ROYAL GREENWICH OBSERVATORY, CAMBRIDGE (ENGLAND).
Astronomical phenomena for the year 1990 N91-15035
The Air Almanac, 1990 N91-15036
The Air Almanac, 1989 N91-15037
ROYAL OBSERVATORY, EDINBURGH (SCOTLAND).
The discovery of a highly polarized bipolar nebula N91-15031
RUHR UNIV., BOCHUM (GERMANY, F.R.).
Three-dimensional magnetic reconnection at the Earth's magnetopause N91-15059
RUTGERS - THE STATE UNIV., NEW BRUNSWICK, NJ.
Eye movements and visual information processing
[AD-A226782] N91-14714

S

SANDIA NATIONAL LABS., ALBUQUERQUE, NM.
Optimal sensor fusion for land vehicle navigation
[DE91-002586] N91-14319
LWIR detector research in InAsSb/InAs N91-14406
Laser studies of the interaction of SiO with the surface of a thin film
[DE91-004562] N91-14450
Amorphization of C-implanted Fe(Cr) alloys
[DE91-001338] N91-14469
Flow behavior of Ti-24Al-11Nb at high strain rates
[DE91-004508] N91-14473
Adhesion at ceramic interfaces
[DE91-001660] N91-14480
Kinetics of molecular beam epitaxy: Effect of ion-induced sputtering
[DE91-004511] N91-14493
Manufacturing Technology: A Sandia Technology Bulletin, Volume 1, No. 1
[DE91-002518] N91-14504
The inclusion of wall loss in electromagnetic finite-difference time-domain thin-slot algorithms
[DE91-001046] N91-14524
An investigation of using a phase-change material to improve the heat transfer in a small electronic module for an airborne radar application
[DE91-002597] N91-14525
A materials database for Li(Si)/FeS2 thermal batteries
[DE91-002592] N91-14531
Triggering GaAs lock-on switches with laser diode arrays
[DE91-002419] N91-14532
Total-dose radiation hardness assurance for space electronics
[DE91-002425] N91-14533
Optically-triggered GaAs thyristor switch s: Integrated structures for environmental hardening
[DE91-001355] N91-14553
A fast solver for systems of axisymmetric ring vortices
[DE91-002594] N91-14561
Dynamic stability of a spinning tube conveying a fluid through a symmetrical noncircular cross-section
[DE91-004146] N91-14573
Characterization of semiconductor surface-emitting laser wafers
[DE91-001336] N91-14598
The use of light emission in failure analysis of CMOS ICs
[DE91-001234] N91-14633
Processing experiments for development of high-efficiency silicon solar cells
[DE91-002698] N91-14645
Damping measurements using operational data
[DE91-002781] N91-14646
Solar concentrato: development in the US
[DE91-001232] N91-14649
Fatigue reliability of wind turbine components
[DE91-001262] N91-14650
Reliability of photovoltaic concentrator modules
[DE90-012754] N91-14651
The synthesis of solar radiation data for sizing stand-alone photovoltaic systems
[DE90-012758] N91-14652
A balloon-borne aerosol spectrometer for high altitude low aerosol concentration measurements
[DE91-002563] N91-14661
A balloon-borne integrating nephelometer
[DE91-001037] N91-14687
Characterization of electron cyclotron resonance hydrogen plasmas
[DE91-001250] N91-14844
FTIR (Fourier Transform Infrared) spectrophotometry for thin film monitors: Computer and equipment integration for enhanced capabilities
[DE91-001228] N91-14853
Rise time and recovery of GaAs photoconductive semiconductor switches
[DE91-001267] N91-14854
Effect of step edge transition rates and anisotropy in simulations of epitaxial growth
[DE91-001251] N91-14875
Irradiation-induced pinning in single-crystal and thin-film Tl2Ca2Ba2Cu3O10 superconductors
[DE91-001342] N91-14877
SANTA BARBARA RESEARCH CENTER, CA.
HgZnTe-based detectors for LWIR NASA applications N91-14404
Earth Observing Scanning Polarimeter (EOSP), phase B
[NASA-CR-187715] N91-14586
SANTA BARBARA RESEARCH CENTER, GOLETA, CA.
HgCdTe for NASA EOS missions and detector uniformity benchmarks N91-14385

SAO PAULO UNIV. (BRAZIL).
Multicolor optical polarimetry of reddened stars in the small Magellanic cloud N91-14986
SCIENCE APPLICATIONS INTERNATIONAL CORP., FORT WASHINGTON, PA.
Computational models with advanced thermochemistry for the analysis of missile/plume flowfield interactions N91-14305
SCIENCE APPLICATIONS INTERNATIONAL CORP., SAN DIEGO, CA.
Literature survey on tools
[AD-A226933] N91-14770
SCIENCE APPLICATIONS INTERNATIONAL CORP., SCHAUMBURG, IL.
A global view of lander-to-orbiter communications accessibility for a Mars Global Network Mission N91-14362
Analysis of success probability/cost trades for small landers in a Mars network N91-14363
SCIENCE APPLICATIONS INTERNATIONAL CORP., TORRANCE, CA.
Electric propulsion study
[AD-A227121] N91-14545
SCIENCE RESEARCH COUNCIL, LONDON (ENGLAND).
The Astronomical Almanac for the year 1989
[ISBN-0-11-886932-9] N91-15038
The Astronomical Almanac for the year 1990
[ISBN-0-11-886934-5] N91-15039
SCIENTIFIC RESEARCH ASSOCIATES, INC., GLASTONBURY, CT.
Studying quantum phase-based electronic devices
[AD-A226809] N91-14541
Intelligent manipulation technique for multi-branch robotic systems
[NASA-CR-187651] N91-14603
SOHAR, INC., LOS ANGELES, CA.
Integration of sneak analysis with design, volume 1
[AD-A226902] N91-14543
SOUTHWEST RESEARCH INST., SAN ANTONIO, TX.
Distributed systems status and control
[NASA-CR-187014] N91-14733
SPACE TELESCOPE SCIENCE INST., BALTIMORE, MD.
Dust in stellar wind bow shocks N91-14979
SRI INTERNATIONAL CORP., MENLO PARK, CA.
Joule heating investigations using the sondrestrom radar and DMSP satellites
[AD-A227425] N91-14677
ST SYSTEMS CORP., LEXINGTON, MA.
Semi-implicit time integration in limited area model
[AD-A226818] N91-14785
STANFORD LINEAR ACCELERATOR CENTER, CA.
High gradient electron guns
[DE91-000056] N91-14369
Software management issues
[DE91-001031] N91-14763
HEM(sub 11) modes revisited
[DE91-001028] N91-14819
STANFORD UNIV., CA.
Studies in statistical signal processing
[AD-A226825] N91-14518
Reports on block rotations, fault domains and crustal deformation
[NASA-CR-186756] N91-14665
Block rotations, fault domains and crustal deformation in the western US N91-14666
Distributed deformation and block rotation in 3D N91-14667
Stress field rotation or block rotation: An example from the Lake Mead fault system N91-14668
Multiple strike slip faults sets: A case study from the Dead Sea transform N91-14669
Computational equipment for the development of numerical algorithms computation
[AD-A226702] N91-14729
A mediator architecture for abstract data access
[AD-A227362] N91-14730
Mechanizing proof theory: Resource-aware logics and proof transformations to extract implicit information
[AD-A227147] N91-14758
Covers by polars of arrangements
[DE91-001358] N91-14764
Improved estimation of variance components in mixed models
[AD-A226854] N91-14794
An investigation of diamond synthesis in an oxygen-acetylene diffusion flame
[AD-A227224] N91-14870
STATE UNIV. OF NEW YORK, BUFFALO.
Photodissociation near a rough metal surface: Effect of reaction fields
[AD-A227030] N91-14445
On the modeling and control of slewing flexible structures N91-14499
Scale-invariant theory of optical properties of fractal clusters
[AD-A227031] N91-14832

STATE UNIV. OF NEW YORK, STONY BROOK.
The 3.4 micron emission in comets N91-15006
Studies of the chemistry of the nightside ionosphere of Venus
[NASA-CR-187714] N91-15114
STERNBERG ASTRONOMICAL INST., MOSCOW (USSR).
Thirty-five-day cycle of Her X-1: Synthesised optical light curves in the model of freely processing neutron star N91-15089
On the nature of cosmic gamma ray bursts N91-15098
The optical observations of x ray Nova GS2023+33 = V404 Cyg N91-15103
STRATEGIC DEFENSE INITIATIVE ORGANIZATION, WASHINGTON, DC.
SDIO long wavelength infrared detector requirements N91-14381

T

TATA INST. OF FUNDAMENTAL RESEARCH, BOMBAY (INDIA).
Dust in a few southern H II regions N91-14943
Distribution of dust in W31 complex N91-14944
Type of silicate feature in oxygen rich stellar envelopes N91-15024
TECHNION RESEARCH AND DEVELOPMENT FOUNDATION LTD., HAIFA (ISRAEL).
Electrophoretic and electrolytic deposition of ceramic particles on porous substrates
[AD-A227371] N91-14488
TECHNISCHE HOCHSCHULE, DARMSTADT (GERMANY, F.R.).
System integration of a block code
[ETN-91-98169] N91-14514
Extremal rays of convex cones and complementary inequalities
[ETN-91-98166] N91-14778
The integral equation method for an elliptic boundary value of the half integer characteristic
[ETN-91-98167] N91-14779
Boundary value problems of the elasticity theory for polyhedra: Singularities and approximation with boundary element methods
[ETN-91-98168] N91-14780
TECHNISCHE UNIV., DELFT (NETHERLANDS).
Fitting of photogrammetry and field completion
[ETN-91-98144] N91-14640
Reconstruction of vectorized raster data
[ETN-91-98143] N91-14738
TEXAS A&M UNIV., COLLEGE STATION.
Development of laser-ion beam photodissociation methods
[DE91-000680] N91-14448
A study of liquid scintillator and fiber materials for use in a fiber calorimeter
[DE91-004229] N91-14585
Effect of atmospherics on beamforming accuracy
[NASA-CR-187695] N91-14802
TEXAS UNIV., AUSTIN.
Dynamics of separation and reattachment in a Mach 5 unswept compression ramp flow N91-14276
The application of deterministic spectral domain method to the analysis of planar circuit discontinuities on open substrates
[AD-A226901] N91-14542
Picosecond laser system for high speed characterization of monolithic devices
[AD-A227372] N91-14585
Fracture analysis of cathodic delamination in rubber-to-metal bonds N91-14627
High resolution spectroscopy of the 11.3 micron emission band N91-14917
The compact far infrared emission from the young stellar object IRAS 16293-2422 N91-14940
Magnetically driven jets and winds N91-15084
Coronal mass ejections
[NASA-CR-186579] N91-15115
THIOKOL CORP., BRIGHAM CITY, UT.
Flight Set 360L006 STS-34 field joint protection system, thermal protection system, and systems tunnel components, volume 4
[NASA-CR-184050] N91-14415
Space shuttle redesigned solid rocket motor Certificate of Qualification (COQ) data report
[NASA-CR-184051] N91-14416
NOVA 201 ultrasonic thickness gage (NOVA Gage)
[NASA-CR-184031] N91-14581
TOHOKU UNIV., SENDAI (JAPAN).
Polarization and extinction by aligned grains N91-14907
Alignment mechanisms of paramagnetic grains revisited N91-14908
TOKYO UNIV. (JAPAN).
Dust formation around M-type stars N91-15017
TOLEDO UNIV., OH.
A study of two control methods for full bridge converters: Soft switch bypass and current mode control
[AD-A227136] N91-14546
TORONTO UNIV. (ONTARIO).
Mesomechanical model for fibre composites
[AD-A226792] N91-14432
TOYAMA UNIV. (JAPAN).
High-energy particle acceleration during the implosion driven by 3-dimensional X-type current loop coalescence in solar flares N91-15048
TRI-UNIV. MESON FACILITY, VANCOUVER (BRITISH COLUMBIA).
A versatile RF cavity mode damper
[DE91-002947] N91-14534

U

ULTRASYSTEMS DEFENSE AND SPACE SYSTEMS, INC., IRVINE, CA.
Heterocycles based on group 3, 4, and 5 elements: Precursors for novel glasses and ceramics
[AD-A226988] N91-14487
UNIVERSAL ENERGY SYSTEMS, INC., DAYTON, OH.
Engineering design with decision support: An application of goal decomposition
[AD-A226730] N91-14782
UNIVERSIDAD DE LOS ANDES, MERIDA (VENEZUELA).
Linear stability and MHD wave propagation in plasmas with solar abundances N91-15056
On the thermal stability of slabs, cylinders, and spheres N91-15057
UNIVERSIDAD NACIONAL AUTONOMA DE MEXICO, ENSENADA.
Three-micron spectroscopy of highly reddened field stars N91-14904
UNIVERSITAETS-STERNWARTE, JENA (GERMAN D.R.).
Steps toward interstellar silicate dust mineralogy N91-14991
Size distribution of dust grains: A problem of self-similarity N91-14997
UNIVERSITY COLL., LONDON (ENGLAND).
The detection of a broad interstellar extinction feature near 1700 A N91-14900
Correlation properties of interstellar dust: Diffuse interstellar bands N91-14916
UNIVERSITY OF SOUTHERN CALIFORNIA, LOS ANGELES.
Control of unsteady aerodynamic forces
[AD-A227365] N91-14315
UTAH UNIV., SALT LAKE CITY.
InAsSbBi, a direct band-gap, III-V, LWIR material N91-14410
Surface and interfacial properties of carbon fibers
[NASA-CR-184916] N91-14429
Failure in laminated composite plates containing a hole
[AD-A227307] N91-14435
Use of D2 to elucidate OMVPE growth mechanisms
[AD-A226966] N91-14443
Conductivity fluctuations in fast ionic conductors
[AD-A227379] N91-14549
UTRECHT STATE UNIV. (NETHERLANDS).
Hidden surface removal for axis-parallel polyhedra
[RUU-CS-90-21] N91-14736
Matrix techniques for faster routing of affine permutations on a mesh interconnection network
[RUU-CS-90-19] N91-14767
Finding shortest paths in the presence of orthogonal obstacles using a combined L sub 1 and link metric
[RUU-CS-90-20] N91-14777
On probability intervals and their updating
[RUU-CS-90-22] N91-14793

V

VILNIUS KAPSUKAS STATE UNIV. (LITHUANIA).
Properties of interstellar dust in the region of the CEP OB4 association N91-14903
VIRGINIA POLYTECHNIC INST. AND STATE UNIV., BLACKSBURG.
An analysis of interlaminar stresses in unsymmetrically laminated plates
[NASA-CR-187657] N91-14424
Adaptive human-computer interfaces using expert profiles
[AD-A226906] N91-14721
VIRGINIA UNIV., CHARLOTTESVILLE.
NASA-UVA light aerospace alloy and structures technology program
[NASA-CR-187321] N91-14474

W

WALOWIT (JED A.), INC., CLIFTON PARK, NY.
A continuum approach toward modeling the mechanics of solid lubricating films
[AD-A226961] N91-14486
WARSAW UNIV. (POLAND).
Vega-Giotto flyby missions and cometary cosmogony N91-15009
WASHINGTON UNIV., SAINT LOUIS, MO.
Cosmos 2044
[NASA-CR-187003] N91-14702
WESTINGHOUSE HANFORD CO., RICHLAND, WA.
Corrosion behavior of copper-base materials in a gamma-irradiated environment
[DE91-001286] N91-14468
WISCONSIN UNIV., MADISON.
Cloud cover statistics
[AD-A226892] N91-14689
The relationship between IR, optical, and UV extinction N91-14899
Infrared emission from ultracompact H II regions N91-14942
WOODS HOLE OCEANOGRAPHIC INST., MA.
Shipboard and satellite observations of upper ocean velocity and transport variability in the Gulf Stream
[AD-A226974] N91-14694
Observations of ocean fluctuations between 15 and 23 hour periods in the Pacific
[AD-A227017] N91-14695
The distribution of wave heights and periods for seas with unimodal bimodal power density spectra
[AD-A227040] N91-14696
WRIGHT RESEARCH DEVELOPMENT CENTER, WRIGHT-PATTERSON AFB, OH.
Comments on hypersonic boundary-layer transition
[AD-A227242] N91-14314
WYOMING UNIV., LARAMIE.
Thermal emission from interstellar dust in and near the Pleiades N91-14981

Y

YERKES OBSERVATORY, WILLIAMS BAY, WI.
The 100 and 160 micron maps of the dust reemission from the nucleus and inner-arm regions of NGC 6946 N91-14983
YORK UNIV. (ONTARIO).
Gas-phase formation of silicon carbides, oxides, and sulphides from atomic silicon ions N91-15014

Typical Contract Number Index Listing

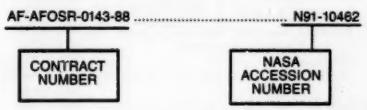

Listings in this index are arranged alphanumerically by contract number. Under each contract number the NASA accession numbers denoting documents that have been produced as a result of research done under that contract are arranged in ascending order. The NASA accession number denotes the number by which the citation is identified.

AF PROJ. 691X N91-14517
AF PROJ. 0581 ..... N91-14566
AF PROJ. 2302 ..... N91-14375
N91-14377
N91-14432
N91-14435
AF PROJ. 2303 ..... N91-14463
AF PROJ. 2304 ..... N91-14518
N91-14570
N91-14761
AF PROJ. 2305 ..... N91-14515
N91-14595
N91-14805
N91-14834
N91-14864
AF PROJ. 2306 ..... N91-14431
N91-14443
N91-14488
N91-14594
N91-14862
AF PROJ. 2307 ..... N91-14313
N91-14314
AF PROJ. 2308 ..... N91-14350
N91-14441
N91-14446
N91-14496
N91-14569
N91-14843
AF PROJ. 2310 ..... N91-14690
AF PROJ. 2312 ..... N91-14704
AF PROJ. 2313 ..... N91-14707
N91-14714
N91-14715
N91-14716
N91-14718
AF PROJ. 2338 ..... N91-14543
AF PROJ. 2386 ..... N91-14541
AF PROJ. 2420 ..... N91-14351
AF PROJ. 2917 ..... N91-14729
AF PROJ. 3066 ..... N91-14589
AF PROJ. 3145 ..... N91-14546
AF PROJ. 3484 ..... N91-14787
AF PROJ. 3842 ..... N91-14595
N91-14776
N91-14784
AF PROJ. 4140 ..... N91-14519
AF PROJ. 4519 ..... N91-14516
AF PROJ. 4600 ..... N91-14851
AF PROJ. 6670 ..... N91-14689
AF PROJ. 7601 ..... N91-14413
AF-AFOSR-0011-88 ..... N91-14446
AF-AFOSR-0072-87 ..... N91-14570
AF-AFOSR-0084-87 ..... N91-14729
AF-AFOSR-0121-88 ..... N91-14690
AF-AFOSR-0125-86 ..... N91-14463
AF-AFOSR-0129-87 ..... N91-14423
AF-AFOSR-0132-86 ..... N91-14766
AF-AFOSR-0135-89 ..... N91-14776
AF-AFOSR-0136-88 ..... N91-14761
AF-AFOSR-0155-89 ..... N91-14784
AF-AFOSR-0171-88 ..... N91-14714
AF-AFOSR-0204-87 ..... N91-14435
AF-AFOSR-0209-89 ..... N91-14595
AF-AFOSR-0227-89 ..... N91-14707
AF-AFOSR-0233-80 ..... N91-14443
AF-AFOSR-0238-86 ..... N91-14431
AF-AFOSR-0246-86 ..... N91-14805
AF-AFOSR-0261-88 ..... N91-14350
AF-AFOSR-0286-84 ..... N91-14441
AF-AFOSR-0297-89 ..... N91-14843
AF-AFOSR-0301-87 ..... N91-14704
AF-AFOSR-0305-89 ..... N91-14715
AF-AFOSR-0319-86 ..... N91-14569
AF-AFOSR-0327-87 ..... N91-14597
AF-AFOSR-0327-88 ..... N91-14518
AF-AFOSR-0340-85 ..... N91-14496
AF-AFOSR-0342-86 ..... N91-14862
AF-AFOSR-0365-89 ..... N91-14432
AF-AFOSR-0416-89 ..... N91-14515
AF-AFOSR-0461-89 ..... N91-14716
AF-AFOSR-0474-89 ..... N91-14488
ARPA ORDER 6037 ..... N91-14731
DA PROJ. 1L1-62211-A-47-A N91-14602
DA PROJ. 3M1-61102-BS-15 ..... N91-14708
DAAB07-88-C-F415 ..... N91-14751
N91-14752
N91-14753
DAAJ02-85-C-0049 ..... N91-14343
N91-14344
DAAK70-89-C-0022 ..... N91-14612
DAAL03-87-G-0004 ..... N91-14754
N91-14783
DAAL03-90-G-0092 ..... N91-14765
DACW39-88-D-0039 ..... N91-14348
DE-AC02-76CH-00016 ..... N91-14354
N91-14571
N91-14678
N91-14811
N91-14812
N91-14826
N91-14861
DE-AC02-76CH-03000 ..... N91-14554
DE-AC02-76ER-01198 ..... N91-14425
DE-AC02-78ET-51013 ..... N91-14848
DE-AC02-83CH-10093 ..... N91-14572
N91-14621
N91-14643
N91-14644
N91-14649
DE-AC03-76SF-00098 ..... N91-14389
N91-14439
N91-14449
N91-14456
N91-14887
DE-AC03-76SF-00515 ..... N91-14369
N91-14763
N91-14819
DE-AC03-87DP-10560 ..... N91-14841
DE-AC03-89ER-51114 ..... N91-14846
N91-14847
DE-AC04-76DP-00789 ..... N91-14319
N91-14450
N91-14458
N91-14469
N91-14473
N91-14480
N91-14493
N91-14504
N91-14524
N91-14525
N91-14531
N91-14532
N91-14533
N91-14553
N91-14561
N91-14573
N91-14598
N91-14633
N91-14645
N91-14646
N91-14649
N91-14650
N91-14651
N91-14652
N91-14661
N91-14687
N91-14844
N91-14853
N91-14854
N91-14857
N91-14875
N91-14877
DE-AC04-88DP-43495 ..... N91-14460
N91-14492
N91-14622
N91-14857
DE-AC05-84OR-21400 ..... N91-14436
N91-14438
N91-14459
N91-14461
N91-14467
N91-14470
N91-14498
N91-14619
N91-14623
N91-14647
N91-14658
N91-14660
N91-14663
N91-14664
N91-14688
N91-14710
N91-14810
N91-14818
N91-14839
N91-14840
N91-14845
N91-14849
N91-14860
N91-14876
DE-AC05-84OT-21400 ..... N91-14457
DE-AC06-76RL-01830 ..... N91-14470
N91-14648
N91-14656
N91-14879
DE-AC06-87RL-10930 ..... N91-14468
DE-AC07-76ID-01570 ..... N91-14427
DE-AI08-78ET-44802 ..... N91-14676
N91-14737
DE-AS05-81ER-40039 ..... N91-14585
DE-A103-86SF-16310 ..... N91-14454
DE-FC03-85DP-40200 ..... N91-14597
DE-FC07-84ID-12545 ..... N91-14505
DE-FC07-89ID-12869 ..... N91-14503
DE-FG02-84ER-13247 ..... N91-14858
DE-FG02-84ER-45057 ..... N91-14804
DE-FG02-84ER-45153 ..... N91-14859
DE-FG02-85ER-45193 ..... N91-14491
DE-FG02-86ER-13515 ..... N91-14599
DE-FG02-86ER-40269 ..... N91-14809
DE-FG02-86ER-45229 ..... N91-14471
DE-FG02-87ER-13683 ..... N91-14584
DE-FG02-87ER-25035 ..... N91-14792
DE-FG02-87ER-40335 ..... N91-14809
DE-FG02-87ER-45310 ..... N91-14880
DE-FG02-88ER-45358 ..... N91-14814
DE-FG02-88ER-45376 ..... N91-14597
DE-FG02-89ER-14079 ..... N91-14674
N91-14675
DE-FG02-89ER-45391 ..... N91-14874
DE-FG02-90ER-14104 ..... N91-14878
DE-FG02-90ER-40560 ..... N91-15111
DE-FG03-87ER-25028 ..... N91-14764
DE-FG05-80ET-53088 ..... N91-15084
N91-15110
DE-FG05-85ER-13434 ..... N91-14448
DE-FG05-85ER-45208 ..... N91-14855
DE-FG06-88ER-13973 ..... N91-14596
DE-FG22-89PC-89771 ..... N91-14440
DI-J-5130-137 ..... N91-14686
DOE-1886-8189-8L N91-14467
DTFA01-88-Y-D-01025 ..... N91-14320
DTFA08-89-0050 ..... N91-14713
DTFH61-85-P-00311 ..... N91-14686
EMW-85-K-2202 ..... N91-14686
FAA-F2006-D N91-14318
FAA-T-2001-F N91-14728

F04611-86-K-0081 ..... N91-14569
F04611-88-C-0014 ..... N91-14545
F04701-88-C-0089 ..... N91-14442
N91-14444
F19628-84-C-0066 ..... N91-14851
F19628-85-C-0003 ..... N91-14762
F19628-85-C-0172 ..... N91-14594
F19628-87-C-0086 ..... N91-14834
F19628-87-K-0006 ..... N91-14677
F19628-87-K-0048 ..... N91-14519
F19628-88-C-0072 ..... N91-14785
F19628-89-C-0003 ..... N91-14742
N91-14743
F19628-89-K-0031 ..... N91-14689
F19628-90-C-0002 ..... N91-15041
F19628-90-C-0003 ..... N91-14748
F29601-84-C-0080 ..... N91-14510
F30602-87-C-0193 ..... N91-14543
F33615-84-C-1517 ..... N91-14517
F33615-85-C-2503 ..... N91-14589
F33615-85-C-5111 ..... N91-14351
F33615-86-C-2720 ..... N91-14546
F33615-86-C-3216 ..... N91-14375
F33615-86-C-3626 ..... N91-14304
F33615-88-C-2821 ..... N91-14566
F33615-88-C-5448 ..... N91-14450
F49620-85-C-0013 ..... N91-14782
F49620-85-C-0042 ..... N91-14487
F49620-86-C-0111 ..... N91-14787
F49620-87-C-0044 ..... N91-14863
F49620-87-C-0047 ..... N91-14718
F49620-87-C-0055 ..... N91-14541
F49620-88-C-0054 ..... N91-14864
F49620-88-C-0061 ..... N91-14315
F49620-89-C-0043 ..... N91-14377
F729601-88-C-0025 ..... N91-14388
GA PROJ. 3466 ..... N91-14846
N91-14847
GS-14-08-0001-G1101 ..... N91-14686
MDA903-83-K-0255 ..... N91-14722
N91-14796
N91-14889
MDA903-84-C-2017 ..... N91-14721
MDA903-85-K-0366 ..... N91-14868
MDA903-86-K-0265 ..... N91-14795
N91-14797
MDA903-87-K-0652 ..... N91-14750
NAGW-496 ..... N91-15045
NAGW-733 ..... N91-14638
NAGW-749 ..... N91-14936
NAGW-1103 ..... N91-15021
NAGW-1142 ..... N91-14655
NAGW-1324 ..... N91-15115
NAGW-1404 ..... N91-15045
NAGW-1488 ..... N91-15064
NAGW-1617 ..... N91-14635
NAGW-2022 ..... N91-15117
NAG1-343 ..... N91-14424
NAG1-745 ..... N91-14474
NAG1-791 ..... N91-14483
NAG1-911 ..... N91-14802
NAG1-1049 ..... N91-14429
NAG2-303 ..... N91-14766
NAG2-523 ..... N91-15114
NAG2-541 ..... N91-14475
N91-14789
NAG2-554 ..... N91-14803
NAG2-593 ..... N91-14731
N91-14732
NAG2-615 ..... N91-14702
NAG3-449 ..... N91-15064
NAG3-693 ..... N91-14414
NAG3-894 ..... N91-14422
NAG5-459 ..... N91-14672
NAG5-619 ..... N91-14912
NAG5-814 ..... N91-14673
NAG5-926 ..... N91-14665
N91-14666
NAG5-1092 ..... N91-15115
NAG5-1192 ..... N91-14639
NAG5-1236 ..... N91-15044
NAG8-095 ..... N91-14557
NAG8-636 ..... N91-14825
NAG8-724 ..... N91-14624
NAG8-751 ..... N91-14680
NAG8-820 ..... N91-14365
N91-14366
N91-14367
N91-14368
NAG8-831 ..... N91-14885
NAG9-387 ..... N91-14733
NASA ORDER A-43049-C N91-14353
NASA ORDER C-99066-G N91-14559
N91-14781
NAS1-18037 ..... N91-14346
NAS1-18584 ..... N91-14292
NAS1-18605 ..... N91-14307
N91-14308
N91-14726
NAS1-18711 ..... N91-14347
NAS2-11420 ..... N91-14335
NAS2-12370 ..... N91-15004
NAS2-13125 ..... N91-14311
NAS3-25266 ..... N91-14500
NAS3-25362 ..... N91-14378
NAS5-30756 ..... N91-14586
NAS7-918 ..... N91-14359
N91-14379
NAS7-1072 ..... N91-14603
NAS8-30490 ..... N91-14415
N91-14416
N91-14581
NAS8-35900 ..... N91-15119
N91-15120
NAS8-36583 ..... N91-14373
NAS8-37857 ..... N91-14358
NAS9-17222 ..... N91-14700
N91-14701
NAS9-17326 ..... N91-14719
NCA2-269 ..... N91-14931
NCC2-374 ..... N91-14734
NCC2-420 ..... N91-14558
NCC2-507 ..... N91-14277
NCC3-73 ..... N91-14511
NCC3-107 ..... N91-14527
NCC5-29 ..... N91-14684
NGL-05-003-497 ..... N91-14976
NGR-05-003-805 ..... N91-14909
NGR-33-018-148 ..... N91-14961
NGT-50185 ..... N91-14909
NR PROJ. 042-267 ..... N91-14794
NSF ASC-87-19573 ..... N91-14781
NSF ATM-88-11128 ..... N91-15110
NSF CCR-87-18605 ..... N91-14758
NSF CHE-89-22288 ..... N91-14445
NSF DCR-85-04011 ..... N91-14786
NSF DMR-86-03174 ..... N91-14472
NSF DMR-87-14665 ..... N91-14867
NSF DMR-88-13525 ..... N91-14403
NSF DMR-89-03138 ..... N91-14472
NSF DMS-87-01543 ..... N91-14781
NSF DMS-89-02662 ..... N91-14764
NSF DMS-89-23071 ..... N91-14798
NSF NAS-82-05616 ..... N91-14686
NSF OCE-87-17144 ..... N91-14699
NSG-5153 ..... N91-14657
NSG-5265 ..... N91-14636
N00014-80-C-0700 ..... N91-14304
N00014-82-K-0603 ..... N91-14549
N00014-85-C-0892 ..... N91-14749
N00014-85-K-0617 ..... N91-14868
N00014-87-C-0549 ..... N91-14305
N00014-87-C-2517 ..... N91-14522
N00014-87-K-0235 ..... N91-14699
N00014-87-K-0481 ..... N91-14867
N00014-88-K-0299 ..... N91-14830
N00014-89-C-1006 ..... N91-14542
N00014-89-J-1197 ..... N91-14870
N00014-89-J-1627 ..... N91-14794
N00014-89-K-0170 ..... N91-14798
N00014-89-5-2024 ..... N91-14403
N00014-90-C-0037 ..... N91-14548
N00014-90-C-0087 ..... N91-14486
N00014-90-J-1148 ..... N91-14485
N91-14831
N00014-90-J-1193 ..... N91-14445
N91-14832
N00014-90-J-1604 ..... N91-14871
N00039-84-C-0211 ..... N91-14730
N91-14758
N00039-87-C-5301 ..... N91-15060
N00123-89-G-0580 ..... N91-14355
N91-14434
N91-14694
N91-14695
N91-14696
N00140-87-C-8904 ..... N91-14731
N61331-90-C-0005 ..... N91-14501
N66001-87-D-0039 ..... N91-14770
SNL-06-9583 ..... N91-14473
SUNYRF-4313159A N91-15114
SWRI PROJ. 05-2985 ..... N91-14733
W-31-109-ENG-38 ..... N91-14472
N91-14765
N91-14815
N91-14881
N91-14882
N91-14883
N91-14884
W-7405-ENG-36 ..... N91-14370
N91-14490
N91-14506
N91-14526
N91-14739
N91-14838
N91-14856
W-7405-ENG-48 ..... N91-14428
N91-14455
N91-14481
N91-14507
N91-14513
N91-14535
N91-14560
N91-14583
N91-14592
N91-14606
N91-14659
N91-14740
N91-14791
N91-14828
N91-14842
N91-14852
W-7405-ENG-82 ..... N91-14466
N91-14873
186-30-00-00-00 ..... N91-14359
199-52-12-01 ..... N91-14725
505-59-00 ..... N91-14727
505-60-11 ..... N91-15040
505-60-41-01 ..... N91-14346
505-61-21-03 ..... N91-14323
505-61-51 ..... N91-14273
N91-14311
505-62-21 ..... N91-14559
N91-14781
505-62-50 ..... N91-14850
505-62-71-01 ..... N91-14275
505-62-91-01 ..... N91-14316
505-63-1A N91-14511
505-63-1B N91-14632
505-63-01-08 ..... N91-14618
505-63-11 ..... N91-14426
505-63-51 ..... N91-14602
505-66-51 ..... N91-14322
505-67-01 ..... N91-14353
505-67-01-04 ..... N91-14347
505-68-10 ..... N91-14310
505-68-11 ..... N91-14309
505-90-21-01 ..... N91-14307
N91-14308
N91-14726
506-41-11 ..... N91-15117
506-43-71-04 ..... N91-14629
506-48-4A N91-14378
506-49-21-02 ..... N91-14634
510-01-01 ..... N91-14422
N91-14500
535-03-01-01 ..... N91-14274
535-05-01 ..... N91-14349
553-13-00 ..... N91-14829
582-01-11 ..... N91-14482
590-13-11 ..... N91-14414
N91-14454
672-40-05-70 ..... N91-14683
674-24-05 ..... N91-14556
694-03-03 ..... N91-14574

Typical Report Number Index Listing

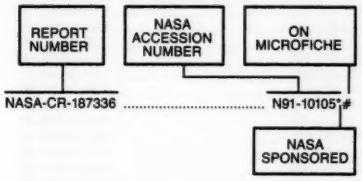

Listings in this index are arranged alphanumerically by report number. The NASA accession number denotes the number by which the citation is identified. An asterisk (*) indicates that the item is a NASA report. A pound sign (#) indicates that the item is available on microfiche.

A-89050 ..... N91-14897* #
A-90069 ..... N91-14273* #
A-90124 ..... N91-14322* #
A-90304 ..... N91-14311* #
A-91008 ..... N91-14540* #
A-91019 ..... N91-15040* #
A-91024 ..... N91-14727* #

AA-246 ..... N91-14365* #
AA-249 ..... N91-14366* #
AA-250 ..... N91-14367* #
AA-251 ..... N91-14368* #

AAE-87-1 ..... N91-14569 #

AD-A226480 ..... N91-14720 #
AD-A226502 ..... N91-14892* #
AD-A226618 ..... N91-14851 #
AD-A226619 ..... N91-14501 #
AD-A226684 ..... N91-14355 #
AD-A226685 ..... N91-14620 #
AD-A226693 ..... N91-14742 #
AD-A226694 ..... N91-14743 #
AD-A226695 ..... N91-14744 #
AD-A226696 ..... N91-14745 #
AD-A226697 ..... N91-14746 #
AD-A226699 ..... N91-14375 #
AD-A226701 ..... N91-14431 #
AD-A226702 ..... N91-14729 #
AD-A226711 ..... N91-14893 #
AD-A226712 ..... N91-14747 #
AD-A226724 ..... N91-14748 #
AD-A226730 ..... N91-14782 #
AD-A226738 ..... N91-14783 #
AD-A226739 ..... N91-14515 #
AD-A226742 ..... N91-14341 #
AD-A226746 ..... N91-14516 #
AD-A226757 ..... N91-15041 #
AD-A226759 ..... N91-14631 #
AD-A226767 ..... N91-14509 #
AD-A226770 ..... N91-14564 #
AD-A226776 ..... N91-14830 #
AD-A226777 ..... N91-14749 #
AD-A226782 ..... N91-14714 #
AD-A226784 ..... N91-14776 #
AD-A226787 ..... N91-14862 #
AD-A226788 ..... N91-14715 #
AD-A226790 ..... N91-14863 #
AD-A226791 ..... N91-14441 #
AD-A226792 ..... N91-14432 #
AD-A226793 ..... N91-14784 #
AD-A226808 ..... N91-14517 #
AD-A226809 ..... N91-14541 #
AD-A226815 ..... N91-14463 #
AD-A226816 ..... N91-14843 #
AD-A226818 ..... N91-14785 #
AD-A226823 ..... N91-14704 #
AD-A226824 ..... N91-14707 #
AD-A226825 ..... N91-14518 #
AD-A226854 ..... N91-14794 #
AD-A226856 ..... N91-14894 #
AD-A226875 ..... N91-14565 #
AD-A226882 ..... N91-14795 #
AD-A226883 ..... N91-14796 #
AD-A226886 ..... N91-14750 #
AD-A226892 ..... N91-14689 #
AD-A226893 ..... N91-14350 #
AD-A226894 ..... N91-14589 #
AD-A226895 ..... N91-14864 #
AD-A226901 ..... N91-14542 #
AD-A226902 ..... N91-14543 #
AD-A226903 ..... N91-14751 #
AD-A226904 ..... N91-14752 #
AD-A226905 ..... N91-14753 #
AD-A226906 ..... N91-14721 #
AD-A226907 ..... N91-14797 #
AD-A226922 ..... N91-14519 #
AD-A226923 ..... N91-14754 #
AD-A226927 ..... N91-14442 #
AD-A226929 ..... N91-14693 #
AD-A226930 ..... N91-14755 #
AD-A226931 ..... N91-14312 #
AD-A226933 ..... N91-14770 #
AD-A226937 ..... N91-14865 #
AD-A226939 ..... N91-14520 #
AD-A226940 ..... N91-14866 #
AD-A226944 ..... N91-14506 #
AD-A226949 ..... N91-14888 #
AD-A226952 ..... N91-14485 #
AD-A226953 ..... N91-14831 #
AD-A226957 ..... N91-14521 #
AD-A226958 ..... N91-14716 #
AD-A226961 ..... N91-14486 #
AD-A226963 ..... N91-14708 #
AD-A226965 ..... N91-14867 #
AD-A226966 ..... N91-14443 #
AD-A226968 ..... N91-14805 #
AD-A226971 ..... N91-14417 #
AD-A226974 ..... N91-14694 #
AD-A226988 ..... N91-14487 #
AD-A227002 ..... N91-14376 #
AD-A227004 ..... N91-14433 #
AD-A227006 ..... N91-14868 #
AD-A227009 ..... N91-14413 #
AD-A227010 ..... N91-14717 #
AD-A227013 ..... N91-14444 #
AD-A227017 ..... N91-14695 #
AD-A227028 ..... N91-14567 #
AD-A227030 ..... N91-14445 #
AD-A227031 ..... N91-14832 #
AD-A227038 ..... N91-14434 #
AD-A227040 ..... N91-14696 #
AD-A227048 ..... N91-14446 #
AD-A227054 ..... N91-14833 #
AD-A227055 ..... N91-14756 #
AD-A227057 ..... N91-14348 #
AD-A227059 ..... N91-14889 #
AD-A227063 ..... N91-14722 #
AD-A227066 ..... N91-14568 #
AD-A227067 ..... N91-14569 #
AD-A227073 ..... N91-14690 #
AD-A227076 ..... N91-14544 #
AD-A227077 ..... N91-14691 #
AD-A227090 ..... N91-14869 #
AD-A227119 ..... N91-14697 #
AD-A227121 ..... N91-14545 #
AD-A227128 ..... N91-14806 #
AD-A227129 ..... N91-14698 #
AD-A227136 ..... N91-14546 #
AD-A227142 ..... N91-14786 #
AD-A227144 ..... N91-14771 #
AD-A227145 ..... N91-14757 #
AD-A227147 ..... N91-14758 #
AD-A227163 ..... N91-14834 #
AD-A227165 ..... N91-14342 #
AD-A227168 ..... N91-14759 #
AD-A227170 ..... N91-14496 #
AD-A227174 ..... N91-14705 #
AD-A227177 ..... N91-14313 #
AD-A227193 ..... N91-14718 #
AD-A227196 ..... N91-14343 #
AD-A227197 ..... N91-14344 #
AD-A227224 ..... N91-14870 #
AD-A227232 ..... N91-14699 #
AD-A227238 ..... N91-14871 #
AD-A227242 ..... N91-14314 #
AD-A227254 ..... N91-14464 #
AD-A227255 ..... N91-14465 #
AD-A227258 ..... N91-14611 #
AD-A227259 ..... N91-14547 #
AD-A227300 ..... N91-14497 #
AD-A227303 ..... N91-14591 #
AD-A227304 ..... N91-14377 #
AD-A227306 ..... N91-14787 #
AD-A227307 ..... N91-14435 #
AD-A227309 ..... N91-14548 #
AD-A227313 ..... N91-14760 #
AD-A227334 ..... N91-14895 #
AD-A227340 ..... N91-14612 #
AD-A227342 ..... N91-14692 #
AD-A227347 ..... N91-14510 #
AD-A227348 ..... N91-14447 #
AD-A227353 ..... N91-14351 #
AD-A227362 ..... N91-14730 #
AD-A227364 ..... N91-14570 #
AD-A227365 ..... N91-14315 #
AD-A227367 ..... N91-15121 #
AD-A227368 ..... N91-15122 #
AD-A227371 ..... N91-14488 #
AD-A227372 ..... N91-14595 #
AD-A227379 ..... N91-14549 #
AD-A227381 ..... N91-14788 #
AD-A227395 ..... N91-14798 #
AD-A227397 ..... N91-14641 #
AD-A227409 ..... N91-14761 #
AD-A227413 ..... N91-14799 #
AD-A227425 ..... N91-14677 #
AD-A227426 ..... N91-14762 #
AD-A227437 ..... N91-14522 #
AD-A227449 ..... N91-15118 #

AD-D014566 ..... N91-14528
AD-D014568 ..... N91-14529
AD-D014569 ..... N91-14820
AD-D014570 ..... N91-14478
AD-D014571 ..... N91-14530
AD-D014617 ..... N91-14821 #
AD-D014618 ..... N91-14822 #
AD-D014621 ..... N91-14823 #
AD-D014626 ..... N91-14824
AD-D014629 ..... N91-14512
AD-D014632 ..... N91-14479 #

AFESC/ESL-TR-87-03 ..... N91-14510 #

AFHRL-TP-90-65 ..... N91-14782 #

AFIT/GEP/ENP/90S-1 ..... N91-14833 #

AFOSR-90-0914TR ..... N91-14863 #
AFOSR-90-0917TR ..... N91-14487 #
AFOSR-90-0921TR ..... N91-14377 #
AFOSR-90-0923TR ..... N91-14541 #
AFOSR-90-0924TR ..... N91-14315 #
AFOSR-90-0927TR ..... N91-14787 #
AFOSR-90-0928TR ..... N91-15121 #
AFOSR-90-0929TR ..... N91-15122 #
AFOSR-90-0936TR ..... N91-14569 #
AFOSR-90-0937TR ..... N91-14435 #
AFOSR-90-0938TR ..... N91-14515 #
AFOSR-90-0939TR ..... N91-14862 #
AFOSR-90-0941TR ..... N91-14690 #
AFOSR-90-0943TR ..... N91-14716 #
AFOSR-90-0944TR ..... N91-14570 #
AFOSR-90-0945TR ..... N91-14715 #
AFOSR-90-0946TR ..... N91-14496 #
AFOSR-90-0949TR ..... N91-14805 #
AFOSR-90-0950TR ..... N91-14443 #
AFOSR-90-0955TR ..... N91-14518 #
AFOSR-90-0960TR ..... N91-14463 #
AFOSR-90-0961TR ..... N91-14350 #
AFOSR-90-0966TR ..... N91-14707 #
AFOSR-90-0967TR ..... N91-14704 #
AFOSR-90-0970TR ..... N91-14776 #
AFOSR-90-0978TR ..... N91-14714 #
AFOSR-90-0998TR ..... N91-14729 #
AFOSR-90-1002TR ..... N91-14431 #

AFOSR-90-1026TR ..... N91-14446 #
AFOSR-90-1028TR ..... N91-14718 #
AFOSR-90-1030TR ..... N91-14843 #
AFOSR-90-1033TR ..... N91-14761 #
AFOSR-90-1035TR ..... N91-14784 #
AFOSR-90-1037TR ..... N91-14864 #
AFOSR-90-1038TR ..... N91-14441 #
AFOSR-90-1040TR ..... N91-14432 #
AFOSR-90-1046TR ..... N91-14595 #
AFOSR-90-1047TR ..... N91-14488 #

AGARD-CP-483 ..... N91-14324 #
AGARD-CP-493 ..... N91-14278 #

AIAA-90-2400 ..... N91-14349* #
AIAA-91-0263 ..... N91-14310* #
AIAA-91-0413 ..... N91-14559* #
AIAA-91-0660 ..... N91-14309* #

AL-TR-89-040 ..... N91-14545 #

ALLISON-EDR-14249-VOL-2 ..... N91-14351 #

ANL-HEP-CP-90-87 ..... N91-14815 #

ARCCB-TR-90020 ..... N91-14509 #

ARI-RN-90-63 ..... N91-14797 #
ARI-RN-90-73 ..... N91-14795 #
ARI-RN-90-83 ..... N91-14721 #
ARI-RN-90-90 ..... N91-14750 #
ARI-RN-90-112 ..... N91-14889 #
ARI-RN-90-113 ..... N91-14888 #
ARI-RN-90-119 ..... N91-14796 #
ARI-RN-90-120 ..... N91-14722 #

ARO-24960.50-MA-REP ..... N91-14754 #
ARO-24960.52-MA-REP ..... N91-14783 #

AVSCOM-TM-90-C-014 ..... N91-14632* #

AVSCOM-TR-90-B-008 ..... N91-14347* #
AVSCOM-TR-90-C-010 ..... N91-14602* #

BCO-JJR-90-1348 ..... N91-14378* #

BCRS-89-35 ..... N91-14637 #

BNL-44375 ..... N91-14678 #
BNL-44994 ..... N91-14354 #
BNL-45154 ..... N91-14826 #
BNL-45182 ..... N91-14571 #
BNL-45308 ..... N91-14812 #
BNL-45312 ..... N91-14811 #
BNL-45324 ..... N91-14861 #

BRL-MR-3857 ..... N91-14564 #

BRL-TR-3154 ..... N91-14497 #

BR114548 ..... N91-14341 #

CALSPAN-7205-26 ..... N91-14353* #

CCMS-90-11 ..... N91-14424* #

CEBAF-PR-89-004 ..... N91-14816 #

CERC-90-2 ..... N91-14348 #

CMU-RI-TR-90-10 ..... N91-14788 #

CMU/SEI-89-TR-3 ..... N91-14762 #
CMU/SEI-89-TR-25 ..... N91-14745 #
CMU/SEI-90-SR-6 ..... N91-14744 #
CMU/SEI-90-TR-12 ..... N91-14743 #
CMU/SEI-90-TR-17 ..... N91-14742 #
CMU/SEI-90-TR-19 ..... N91-14748 #

CONF-890415-14 ..... N91-14763 #
CONF-900206-12 ..... N91-14427 #
CONF-900355-1 ..... N91-14663 #
CONF-900368-11 ..... N91-14828 #
CONF-900450-12 ..... N91-14818 #
CONF-900466-92 ..... N91-14459 #
CONF-900542-11 ..... N91-14651 #
CONF-900542-12 ..... N91-14652 #
CONF-900603-45 ..... N91-14827 #
CONF-900603-46 ..... N91-14534 #
CONF-900756-52 ..... N91-14826 #
CONF-900762-1 ..... N91-14678 #
CONF-900822-15 ..... N91-14815 #
CONF-900857-2 ..... N91-14811 #
CONF-900918-13 ..... N91-14847 #
CONF-900918-14 ..... N91-14846 #
CONF-900936-14 ..... N91-14877 #
CONF-900936-15 ..... N91-14469 #
CONF-900936-18 ..... N91-14861 #
CONF-900936-19 ..... N91-14860 #
CONF-900936-21 ..... N91-14884 #
CONF-900936-22 ..... N91-14472 #
CONF-900944-13 ..... N91-14852 #
CONF-900944-15 ..... N91-14856 #
CONF-900989-2 ..... N91-14648 #
CONF-901007-19 ..... N91-14845 #
CONF-901025-21 ..... N91-14849 #
CONF-901029-3 ..... N91-14506 #
CONF-901035-8 ..... N91-14876 #
CONF-901035-9 ..... N91-14844 #
CONF-901035-10 ..... N91-14875 #
CONF-901035-12 ..... N91-14879 #
CONF-901073-8 ..... N91-14598 #
CONF-901101-46 ..... N91-14498* #
CONF-901102-1 ..... N91-14553 #
CONF-901105-25 ..... N91-14493 #
CONF-901105-26 ..... N91-14450 #
CONF-901169-1 ..... N91-14861 #
CONF-901209-2 ..... N91-14710 #
CONF-901209-5 ..... N91-14791 #
CONF-910108-1 ..... N91-14659 #
CONF-910108-2 ..... N91-14572 #
CONF-910116-3 ..... N91-14458 #
CONF-910116-5 ..... N91-14533 #
CONF-910147-1 ..... N91-14457 #
CONF-910154-1 ..... N91-14646 #
CONF-8706159-4 ..... N91-14456 #
CONF-8909178-2 ..... N91-14571 #
CONF-9004189-2 ..... N91-14740 #
CONF-9005284-1 ..... N91-14853 #
CONF-9006295-1 ..... N91-14765 #
CONF-9007106-75 ..... N91-14354 #
CONF-9008139-2 ..... N91-14649 #
CONF-9009107-3 ..... N91-14650 #
CONF-9009123-37 ..... N91-14819 #
CONF-9009123-54 ..... N91-14883 #
CONF-9009123-56 ..... N91-14881 #
CONF-9009123-58 ..... N91-14882 #
CONF-9009153-4 ..... N91-14621 #
CONF-9009192-14 ..... N91-14369 #
CONF-9009201-9 ..... N91-14857 #
CONF-9009223-3 ..... N91-14622 #
CONF-9009223-4 ..... N91-14492 #
CONF-9009248-4 ..... N91-14535 #
CONF-9009256-2 ..... N91-14460 #
CONF-9009264-2 ..... N91-14470 #
CONF-9010148-1 ..... N91-14633 #
CONF-9010190-2 ..... N91-14455 #
CONF-9010199-2 ..... N91-14812 #
CONF-9010207-3 ..... N91-14439 #
CONF-9010207-4 ..... N91-14449 #
CONF-9010209-5 ..... N91-14842 #
CONF-9010211-2 ..... N91-14739 #
CONF-9010217-1 ..... N91-14467 #
CONF-9010227-2 ..... N91-14839 #
CONF-9010228-1 ..... N91-14370 #
CONF-9010230-4 ..... N91-14838 #
CONF-9010240-1 ..... N91-14505 #
CONF-9010243-2 ..... N91-14810 #
CONF-9010258-1 ..... N91-14473 #
CONF-9011122-2 ..... N91-14436 #
CONF-9011123-1 ..... N91-14480 #
CONF-9011125-1 ..... N91-14854 #
CONF-9011125-2 ..... N91-14532 #
CONF-9011135-1 ..... N91-14619 #
CONF-9011136-1 ..... N91-14840 #
CONF-9011138-1 ..... N91-14645 #

CPL-86-7 ..... N91-14889 #

CS-TR-2388 ..... N91-14786 #
CS-TR-2426 ..... N91-14771 #
CS-TR-2450 ..... N91-14757 #

CSR-90-36 ..... N91-14754 #
CSR-90-38 ..... N91-14783 #

CWP-095 ..... N91-14674 #
CWP-096 ..... N91-14675 #

DE90-000375 ..... N91-14644 #
DE90-012754 ..... N91-14651 #
DE90-012758 ..... N91-14652 #
DE90-016530 ..... N91-14710 #
DE90-631581 ..... N91-14790 #
DE91-000056 ..... N91-14369 #
DE91-000660 ..... N91-14791 #
DE91-000680 ..... N91-14448 #
DE91-000750 ..... N91-14873 #
DE91-001028 ..... N91-14819 #
DE91-001031 ..... N91-14763 #
DE91-001033 ..... N91-14656 #
DE91-001037 ..... N91-14687 #
DE91-001046 ..... N91-14524 #
DE91-001048 ..... N91-14490 #
DE91-001107 ..... N91-14466 #
DE91-001126 ..... N91-14678 #
DE91-001129 ..... N91-14571 #
DE91-001143 ..... N91-14596 #
DE91-001192 ..... N91-14874 #
DE91-001212 ..... N91-14663 #
DE91-001228 ..... N91-14853 #
DE91-001232 ..... N91-14649 #
DE91-001234 ..... N91-14633 #
DE91-001250 ..... N91-14844 #
DE91-001251 ..... N91-14875 #
DE91-001254 ..... N91-14597 #
DE91-001262 ..... N91-14650 #
DE91-001267 ..... N91-14854 #
DE91-001272 ..... N91-14467 #
DE91-001277 ..... N91-14876 #
DE91-001286 ..... N91-14468 #
DE91-001336 ..... N91-14598 #
DE91-001338 ..... N91-14469 #
DE91-001342 ..... N91-14877 #
DE91-001348 ..... N91-14503 #
DE91-001349 ..... N91-14878 #
DE91-001355 ..... N91-14553 #
DE91-001358 ..... N91-14764 #
DE91-001372 ..... N91-14664 #
DE91-001445 ..... N91-14674 #
DE91-001446 ..... N91-14675 #
DE91-001488 ..... N91-14845 #
DE91-001547 ..... N91-14846 #
DE91-001548 ..... N91-14847 #
DE91-001563 ..... N91-14470 #
DE91-001643 ..... N91-14737 #
DE91-001646 ..... N91-14676 #
DE91-001660 ..... N91-14480 #
DE91-001662 ..... N91-14848 #
DE91-001680 ..... N91-14592 #
DE91-001723 ..... N91-14354 #
DE91-001724 ..... N91-14826 #
DE91-001743 ..... N91-14852 #
DE91-001764 ..... N91-14455 #
DE91-001787 ..... N91-14858 #
DE91-001789 ..... N91-14449 #
DE91-001794 ..... N91-14456 #
DE91-001795 ..... N91-14439 #
DE91-001883 ..... N91-14505 #
DE91-001907 ..... N91-14425 #
DE91-001929 ..... N91-14427 #
DE91-001946 ..... N91-15111 #
DE91-001957 ..... N91-14739 #
DE91-001960 ..... N91-14370 #
DE91-001978 ..... N91-14491 #
DE91-001984 ..... N91-14658 #
DE91-001988 ..... N91-14457 #
DE91-001993 ..... N91-14855 #
DE91-002112 ..... N91-14643 #
DE91-002113 ..... N91-14572 #
DE91-002118 ..... N91-14621 #
DE91-002304 ..... N91-14856 #
DE91-002314 ..... N91-14506 #
DE91-002323 ..... N91-14838 #
DE91-002338 ..... N91-14458 #
DE91-002395 ..... N91-14859 #
DE91-002397 ..... N91-14471 #
DE91-002419 ..... N91-14532 #
DE91-002425 ..... N91-14533 #
DE91-002470 ..... N91-14814 #
DE91-002496 ..... N91-14440 #
DE91-002518 ..... N91-14504 #
DE91-002561 ..... N91-14438 #
DE91-002563 ..... N91-14661 #
DE91-002566 ..... N91-14560 #
DE91-002567 ..... N91-14428 #
DE91-002568 ..... N91-14481 #
DE91-002575 ..... N91-14583 #
DE91-002577 ..... N91-14606 #
DE91-002586 ..... N91-14319 #
DE91-002592 ..... N91-14531 #
DE91-002594 ..... N91-14561 #
DE91-002597 ..... N91-14525 #
DE91-002632 ..... N91-14849 #
DE91-002635 ..... N91-14839 #
DE91-002649 ..... N91-14840 #
DE91-002652 ..... N91-14619 #
DE91-002657 ..... N91-14459 #
DE91-002668 ..... N91-14513* #
DE91-002695 ..... N91-14804 #
DE91-002698 ..... N91-14645 #
DE91-002701 ..... N91-14622 #
DE91-002703 ..... N91-14857 #
DE91-002710 ..... N91-14492 #
DE91-002715 ..... N91-14460 #
DE91-002758 ..... N91-14809 #
DE91-002759 ..... N91-14584 #
DE91-002771 ..... N91-14841 #

ISBN-9-51696-8678

DE91-002781 ..... N91-14646 #
DE91-002783 ..... N91-14740 #
DE91-002785 ..... N91-14659 #
DE91-002796 ..... N91-14842 #
DE91-002802 ..... N91-14688 #
DE91-002811 ..... N91-14879 #
DE91-002854 ..... N91-14818 #
DE91-002869 ..... N91-14860 #
DE91-002870 ..... N91-14810 #
DE91-002871 ..... N91-14498* #
DE91-002887 ..... N91-14461 #
DE91-002929 ..... N91-14660 #
DE91-002947 ..... N91-14534 #
DE91-002949 ..... N91-14827 #
DE91-002969 ..... N91-14647* #
DE91-002971 ..... N91-14653 #
DE91-002996 ..... N91-14507 #
DE91-003017 ..... N91-14593 #
DE91-004003 ..... N91-14811 #
DE91-004005 ..... N91-14812 #
DE91-004021 ..... N91-14861 #
DE91-004027 ..... N91-14880 #
DE91-004072 ..... N91-14648 #
DE91-004138 ..... N91-14887 #
DE91-004146 ..... N91-14573 #
DE91-004192 ..... N91-14828 #
DE91-004195 ..... N91-14535 #
DE91-004229 ..... N91-14585 #
DE91-004297 ..... N91-14526 #
DE91-004448 ..... N91-14765 #
DE91-004454 ..... N91-14815 #
DE91-004477 ..... N91-14881 #
DE91-004478 ..... N91-14882 #
DE91-004483 ..... N91-14883 #
DE91-004488 ..... N91-14884 #
DE91-004489 ..... N91-14472 #
DE91-004506 ..... N91-14473 #
DE91-004511 ..... N91-14493 #
DE91-004527 ..... N91-14436 #
DE91-004530 ..... N91-14623 #
DE91-004562 ..... N91-14450 #
DE91-004582 ..... N91-14792 #
DE91-004589 ..... N91-14599 #
DE91-004674 ..... N91-14554 #
DE91-727527 ..... N91-14451 #
DE91-727567 ..... N91-14654 #

DMLB87-0016 ..... N91-14586* #

DOC-101-24 ..... N91-14896 #

DOE/DP-40200/132 ..... N91-14597 #

DOE/ER-0475P ..... N91-14653 #
DOE/ER-01198/T43 ..... N91-14425 #
DOE/ER-13247/6 ..... N91-14858 #
DOE/ER-13434/5 ..... N91-14448 #
DOE/ER-13515/6 ..... N91-14599 #
DOE/ER-13683/3 ..... N91-14584 #
DOE/ER-13973/3 ..... N91-14596 #
DOE/ER-14079/2 ..... N91-14674 #
DOE/ER-14079/3 ..... N91-14675 #
DOE/ER-14104/1 ..... N91-14878 #
DOE/ER-25035/2 ..... N91-14792 #
DOE/ER-40039/45 ..... N91-14585 #
DOE/ER-40269/7 ..... N91-14809 #
DOE/ER-40560/T2 ..... N91-15111 #
DOE/ER-45057/6 ..... N91-14804 #
DOE/ER-45153/T3 ..... N91-14859 #
DOE/ER-45193/1 ..... N91-14491 #
DOE/ER-45208/6 ..... N91-14855 #
DOE/ER-45229/T3 ..... N91-14471 #
DOE/ER-45310/21 ..... N91-14880 #
DOE/ER-45358/2 ..... N91-14814 #
DOE/ER-45391/1 ..... N91-14874 #

DOE/ET-51013/T231 ..... N91-14848 #

DOE/ID-12869/1 ..... N91-14503 #

DOE/NASA/16310-14 ..... N91-14454* #

DOE/PC-89771/4 ..... N91-14440 #

DOT/FAA/CT-TN90/22 ..... N91-14318 #
DOT/FAA/CT-TN90/38 ..... N91-14713 #
DOT/FAA/CT-TN90/44 ..... N91-14728 #

DOT/FAA/CT-89/31 ..... N91-14317 #

DOT/FAA/RD-90/34 ..... N91-14320 #

D615-10009 ..... N91-14358* #

E-4998 ..... N91-14556* #
E-5044 ..... N91-14574* #
E-5541 ..... N91-14426* #
E-5702 ..... N91-14482* #
E-5707 ..... N91-14349* #
E-5715 ..... N91-14559* #
E-5783 ..... N91-15117* #
E-5792 ..... N91-14511* #
E-5798 ..... N91-14781* #
E-5801 ..... N91-14500* #
E-5814 ..... N91-14632* #
E-5829 ..... N91-14454* #
E-5845 ..... N91-14829* #
E-5928 ..... N91-14310* #
E-5935 ..... N91-14309* #

EEG-88001 ..... N91-14718 #

EGG-M-89129 ..... N91-14427 #
EGG-M-90402 ..... N91-14505 #

EMA-TR-89-1152-6 ..... N91-14630* #

EOTR-88-11 ..... N91-14719* #

EP-PATENT-APPL-SN-88309670-3 ..... N91-14421
EP-PATENT-APPL-SN-89311025-9 ..... N91-14453

EP-PATENT-0-314-353-A2 ..... N91-14421
EP-PATENT-0-367-504-A2 ..... N91-14453

ERP-1061 ..... N91-14692 #

ESA-SP-311 ..... N91-15046 #

ESD-TR-89-3 ..... N91-14762 #
ESD-TR-90-085 ..... N91-15041 #

ESD-89-TR-33 ..... N91-14745 #
ESD-90-TR-13 ..... N91-14743 #
ESD-90-TR-217 ..... N91-14742 #
ESD-90-TR-220 ..... N91-14748 #

ETDE/JP-MF-1727527 ..... N91-14451 #
ETDE/JP-MF-1727567 ..... N91-14654 #

ETN-90-97605 ..... N91-14421
ETN-90-97684 ..... N91-14637 #
ETN-90-97778 ..... N91-14502 #
ETN-90-97779 ..... N91-14735 #
ETN-90-97972 ..... N91-14453
ETN-90-98132 ..... N91-14767 #
ETN-90-98133 ..... N91-14777 #
ETN-90-98134 ..... N91-14736 #
ETN-90-98135 ..... N91-14793 #
ETN-90-98150 ..... N91-14352 #
ETN-90-98151 ..... N91-14886 #
ETN-90-98153 ..... N91-14306 #
ETN-90-98208 ..... N91-14768 #
ETN-90-98209 ..... N91-14604 #
ETN-90-98221 ..... N91-14605 #
ETN-90-98222 ..... N91-14423 #
ETN-90-98223 ..... N91-14773 #
ETN-91-98143 ..... N91-14738 #
ETN-91-98144 ..... N91-14640 #
ETN-91-98166 ..... N91-14778 #
ETN-91-98167 ..... N91-14779 #
ETN-91-98168 ..... N91-14780 #
ETN-91-98169 ..... N91-14514 #
ETN-91-98210 ..... N91-14774 #
ETN-91-98211 ..... N91-14775 #
ETN-91-98212 ..... N91-14582 #
ETN-91-98344 ..... N91-15046 #
ETN-91-98366 ..... N91-14341 #

FDA-90-10 ..... N91-14803* #

FJSRL-TR-90-0002 ..... N91-14313 #

FNAL-TM-1688 ..... N91-14554 #

GA-A-20219 ..... N91-14847 #
GA-A-20250 ..... N91-14846 #

GL-IP-340 ..... N91-14413 #

GL-TR-89-0296 ..... N91-14519 #
GL-TR-89-0324 ..... N91-14785 #
GL-TR-90-0091 ..... N91-14692 #
GL-TR-90-0146 ..... N91-14689 #
GL-TR-90-0158 ..... N91-14413 #
GL-TR-90-0172 ..... N91-14677 #

GSO-TR-90-3 ..... N91-14699 #

H-1584 ..... N91-14353* #

HCI-87-01 ..... N91-14721 #

HDL-TM-90-13 ..... N91-14620 #

IAEA-CN-53/D-4-13 ..... N91-14849 #

IAT-ADS-BC-1 ..... N91-14320 #

IC-90/12 ..... N91-14790 #

ICASE-90-81 ..... N91-14307* #
ICASE-90-84 ..... N91-14308* #

ICOMP-90-22 ..... N91-14559* #
ICOMP-90-24 ..... N91-14781* #

ICS-88-15 ..... N91-14797 #

IEEE-90CH2711-0 ..... N91-14521 #

IFSI-89-17 ..... N91-14502 #
IFSI-89-18 ..... N91-14735 #

INT-PATENT-CLASS-A47K-11/00 ..... N91-14724*

INT-PATENT-CLASS-B01D-29/04 ..... N91-14703*
INT-PATENT-CLASS-B01D-29/42 ..... N91-14703*
INT-PATENT-CLASS-B22D-27/04 ..... N91-14462*
INT-PATENT-CLASS-B23K-26/00 ..... N91-14508*
INT-PATENT-CLASS-B25G-3/00 ..... N91-14610*
INT-PATENT-CLASS-B25G-3/18 ..... N91-14614*
INT-PATENT-CLASS-B25J-15/08 ..... N91-14615*
INT-PATENT-CLASS-B29C-33/00 ..... N91-14421
INT-PATENT-CLASS-B29C-67/18 ..... N91-14421
INT-PATENT-CLASS-B29D-28/00 ..... N91-14421
INT-PATENT-CLASS-B64B-21/00 ..... N91-14562*
INT-PATENT-CLASS-B64D-33/00 ..... N91-14345*
INT-PATENT-CLASS-B64G-1/64 ..... N91-14374*

INT-PATENT-CLASS-C07D-207/44 ..... N91-14419*
INT-PATENT-CLASS-C08G-73/10 ..... N91-14418*
INT-PATENT-CLASS-C23C-22/68 ..... N91-14453
INT-PATENT-CLASS-C23C-22/83 ..... N91-14453

INT-PATENT-CLASS-E03D-9/04 ..... N91-14723*

INT-PATENT-CLASS-F01D-11/08 ..... N91-14608*
INT-PATENT-CLASS-F16B-1/00 ..... N91-14610*
INT-PATENT-CLASS-F16K-1/22 ..... N91-14609*
INT-PATENT-CLASS-F16K-3/32 ..... N91-14563*
INT-PATENT-CLASS-F16K-3/316 ..... N91-14563*
INT-PATENT-CLASS-F16K-37/00 ..... N91-14563*
INT-PATENT-CLASS-F16L-35/00 ..... N91-14613*
INT-PATENT-CLASS-F16M-13/00 ..... N91-14617*
INT-PATENT-CLASS-F41G-11/00 ..... N91-14591*

INT-PATENT-CLASS-G01K-15/00 ..... N91-14807*
INT-PATENT-CLASS-G01M-9/00 ..... N91-14357*
INT-PATENT-CLASS-G01N-3/00 ..... N91-14430*
INT-PATENT-CLASS-G01N-23/20 ..... N91-14835*
INT-PATENT-CLASS-G01R-1/04 ..... N91-14552*
INT-PATENT-CLASS-G01S-5/02 ..... N91-14321*
INT-PATENT-CLASS-G01S-13/90 ..... N91-14642*
INT-PATENT-CLASS-G01W-1/00 ..... N91-14412*
INT-PATENT-CLASS-G02B-7/18 ..... N91-14590*
INT-PATENT-CLASS-G02B-23/00 ..... N91-14591*
INT-PATENT-CLASS-G02B-27/64 ..... N91-14590*
INT-PATENT-CLASS-G06F-9/46 ..... N91-14769*
INT-PATENT-CLASS-G06F-15/16 ..... N91-14769*
INT-PATENT-CLASS-G06F-15/18 ..... N91-14741*
INT-PATENT-CLASS-G06F-15/20 ..... N91-14371*
INT-PATENT-CLASS-G08B-21/00 ..... N91-14607*

INT-PATENT-CLASS-H01F-27/30 ..... N91-14539*
INT-PATENT-CLASS-H01L-27/14 ..... N91-14551*
INT-PATENT-CLASS-H01L-41/08 ..... N91-14808*
INT-PATENT-CLASS-H01L-41/08 ..... N91-14872*
INT-PATENT-CLASS-H01L-43/00 ..... N91-14537*
INT-PATENT-CLASS-H01M-6/20 ..... N91-14538*
INT-PATENT-CLASS-H02K-44/10 ..... N91-14489*
INT-PATENT-CLASS-H03D-1/00 ..... N91-14550*
INT-PATENT-CLASS-H04J-3/02 ..... N91-14772*
INT-PATENT-CLASS-H04L-27/18 ..... N91-14523*
INT-PATENT-CLASS-H05B-33/00 ..... N91-14835*
INT-PATENT-CLASS-H07M-4/60 ..... N91-14536*
INT-PATENT-CLASS-H07M-10/39 ..... N91-14536*

IPPCZ-297 ..... N91-14837 #
IPPCZ-298 ..... N91-14836 #

IS-T-1415 ..... N91-14873 #
IS-T-1515 ..... N91-14466 #

ISBN-0-11-886932-9 ..... N91-15038 #
ISBN-0-11-886934-5 ..... N91-15039 #
ISBN-0-309-03888-X ..... N91-14690 #
ISBN-0-309-04335-2 ..... N91-14686 #
ISBN-9-51696-8678 ..... N91-14593 #

ISBN-92-835-0582-4 ..... N91-14324 #
ISBN-92-835-0589-1 ..... N91-14278 #
ISBN-92-9092-086-6 ..... N91-15046 #

ISI-5877-01 ..... N91-14377 #

ISSN-0781-0342 ..... N91-14593 #
ISSN-0879-6566 ..... N91-15046 #
ISSN-0924-3275 ..... N91-14793 #

JAW-90-TR-1 ..... N91-14486 #

JOY-LT-16 ..... N91-14593 #

JPL-D-3547 ..... N91-14817* #
JPL-D-4788 ..... N91-14600* #

JPL-PUBL-90-5 ..... N91-14359* #
JPL-PUBL-90-22 ..... N91-14379* #

JPRS-ULS-89-003 ..... N91-14706 #

KMSF-U-2375 ..... N91-14841 #

L-5467 ..... N91-14602* #
L-16156 ..... N91-14316* #
L-16705 ..... N91-14634* #
L-16746 ..... N91-14618* #
L-16762 ..... N91-14323* #
L-16767 ..... N91-14274* #
L-16779 ..... N91-14683* #
L-16816 ..... N91-14275* #

LA-UR-90-2156 ..... N91-14506 #
LA-UR-90-3408 ..... N91-14856 #
LA-UR-90-3456 ..... N91-14838 #
LA-UR-90-3535 ..... N91-14370 #
LA-UR-90-3541 ..... N91-14739 #

LA-11918-MS ..... N91-14490 #
LA-11956-MS ..... N91-14526 #

LAAS-90113 ..... N91-14774 #
LAAS-90143 ..... N91-14775 #
LAAS-90144 ..... N91-14582 #

LBL-24725-PT-1 ..... N91-14887 #
LBL-29473 ..... N91-14456 #
LBL-29665 ..... N91-14449 #
LBL-29666 ..... N91-14439 #

LC-72-179437 ..... N91-14521 #
LC-88-28903 ..... N91-14890 #
LC-90-62814 ..... N91-14686 #

MBB/FE121/S/PUB/409/A ..... N91-14352 #
MBB/FE122/S/PUB/0389 ..... N91-14886 #
MBB/FE127/S/PUB/0403 ..... N91-14306 #

MCR-90-523 ..... N91-14749 #
MCR-90-536 ..... N91-14373* #

MDHC-89-17-VOL-1 ..... N91-14343 #
MDHC-89-17-VOL-2 ..... N91-14344 #

MEMS-ACL-13 ..... N91-14431 #

MHR-12 ..... N91-15119* #
MHR-15 ..... N91-15120* #

MLM-3658(OP) ..... N91-14460 #
MLM-3663(OP) ..... N91-14857 #
MLM-3667(OP) ..... N91-14622 #
MLM-3668(OP) ..... N91-14492 #

MTI-89TR19 ..... N91-14589 #

MW-90-P-5 ..... N91-14542 #

NAMRL-1357 ..... N91-14717 #

NAS 1.15:4196 ..... N91-14634* #
NAS 1.15:4217 ..... N91-14274* #
NAS 1.15:4221 ..... N91-15034* #
NAS 1.15:4230 ..... N91-14275* #
NAS 1.15:100765 ..... N91-14679* #
NAS 1.15:100768 ..... N91-14494* #
NAS 1.15:101105 ..... N91-14372* #
NAS 1.15:101129 ..... N91-14600* #
NAS 1.15:101249 ..... N91-14817* #
NAS 1.15:102280 ..... N91-14273* #
NAS 1.15:102748 ..... N91-14629* #
NAS 1.15:102809 ..... N91-14322* #
NAS 1.15:102868 ..... N91-15040* #
NAS 1.15:102890 ..... N91-14727* #
NAS 1.15:103169 ..... N91-14426* #
NAS 1.15:103268 ..... N91-14349* #
NAS 1.15:103273 ..... N91-14559* #
NAS 1.15:103423 ..... N91-14498* #
NAS 1.15:103439 ..... N91-14892* #
NAS 1.15:103621 ..... N91-14602* #
NAS 1.15:103623 ..... N91-15117* #
NAS 1.15:103630 ..... N91-14781* #
NAS 1.15:103631 ..... N91-14500* #
NAS 1.15:103637 ..... N91-14632* #
NAS 1.15:103641 ..... N91-14556* #
NAS 1.15:103647 ..... N91-14454* #
NAS 1.15:103654 ..... N91-14829* #
NAS 1.15:103655 ..... N91-14850* #
NAS 1.15:103674 ..... N91-14482* #
NAS 1.15:103705 ..... N91-14310* #
NAS 1.15:103709 ..... N91-14309* #
NAS 1.15:103829 ..... N91-14540* #
NAS 1.21:500 ..... N91-14725* #
NAS 1.21:7011(343) N91-14711*
NAS 1.21:7011(344) N91-14712*
NAS 1.26:4331 ..... N91-14347* #
NAS 1.26:177570 ..... N91-14311* #
NAS 1.26:179445 ..... N91-14353* #
NAS 1.26:181888 ..... N91-14346* #
NAS 1.26:183943 ..... N91-14358* #
NAS 1.26:184013 ..... N91-15120* #
NAS 1.26:184014 ..... N91-15119* #
NAS 1.26:184031 ..... N91-14581* #
NAS 1.26:184034 ..... N91-14373* #
NAS 1.26:184050 ..... N91-14415* #
NAS 1.26:184051 ..... N91-14416* #
NAS 1.26:184916 ..... N91-14429* #
NAS 1.26:185101 ..... N91-14638* #
NAS 1.26:185285 ..... N91-14414* #
NAS 1.26:185295 ..... N91-14378* #
NAS 1.26:185301 ..... N91-14511* #
NAS 1.26:185307 ..... N91-14422* #
NAS 1.26:185513-PT-1 ..... N91-14700* #
NAS 1.26:185513-PT-2 ..... N91-14701* #
NAS 1.26:185606 ..... N91-14719* #
NAS 1.26:185852 ..... N91-14789* #
NAS 1.26:186413 ..... N91-14731* #
NAS 1.26:186536 ..... N91-14680* #
NAS 1.26:186579 ..... N91-15115* #
NAS 1.26:186613 ..... N91-14527* #
NAS 1.26:186756 ..... N91-14665* #
NAS 1.26:186844 ..... N91-14359* #
NAS 1.26:186899 ..... N91-14475* #
NAS 1.26:186902 ..... N91-14624* #
NAS 1.26:186904 ..... N91-14635* #
NAS 1.26:187003 ..... N91-14702* #
NAS 1.26:187014 ..... N91-14733* #
NAS 1.26:187029 ..... N91-14732* #
NAS 1.26:187321 ..... N91-14474* #
NAS 1.26:187326 ..... N91-14684* #
NAS 1.26:187335 ..... N91-14655* #
NAS 1.26:187373 ..... N91-14277* #
NAS 1.26:187379 ..... N91-14672* #
NAS 1.26:187413 ..... N91-14636* #
NAS 1.26:187421 ..... N91-14766* #
NAS 1.26:187425 ..... N91-14734* #
NAS 1.26:187433 ..... N91-14379* #
NAS 1.26:187435 ..... N91-14513* #
NAS 1.26:187474 ..... N91-14726* #
NAS 1.26:187475 ..... N91-14307* #
NAS 1.26:187477 ..... N91-14308* #
NAS 1.26:187648 ..... N91-14885* #
NAS 1.26:187649 ..... N91-14630* #
NAS 1.26:187651 ..... N91-14603* #
NAS 1.26:187657 ..... N91-14424* #
NAS 1.26:187677 ..... N91-14557* #
NAS 1.26:187684 ..... N91-14803* #
NAS 1.26:187687 ..... N91-15044* #
NAS 1.26:187691 ..... N91-14673* #
NAS 1.26:187692 ..... N91-15045* #
NAS 1.26:187694 ..... N91-14825* #
NAS 1.26:187695 ..... N91-14802* #
NAS 1.26:187696 ..... N91-14639* #
NAS 1.26:187702 ..... N91-14558* #
NAS 1.26:187703 ..... N91-14657* #
NAS 1.26:187709 ..... N91-14483* #
NAS 1.26:187714 ..... N91-15114* #
NAS 1.26:187715 ..... N91-14586* #
NAS 1.26:187732 ..... N91-14365* #
NAS 1.26:187733 ..... N91-14366* #
NAS 1.26:187734 ..... N91-14367* #
NAS 1.26:187735 ..... N91-14368* #
NAS 1.26:187750 ..... N91-14647* #
NAS 1.55:3036 ..... N91-14897* #
NAS 1.55:3080 ..... N91-14574* #
NAS 1.60:2640 ..... N91-14316* #
NAS 1.60:3033 ..... N91-14618* #
NAS 1.60:3045 ..... N91-14323* #
NAS 1.61:1124-REV-2 ..... N91-14437* #
NAS 1.61:1243 ..... N91-14683* #

NASA-CASE-ARC-11877-1-SB N91-14357*
NASA-CASE-ARC-11886-1-SB N91-14591*

NASA-CASE-GSC-13237-1 ..... N91-14550*

NASA-CASE-KSC-11304-2 ..... N91-14495*

NASA-CASE-LAR-13392-1-CU N91-14412*
NASA-CASE-LAR-13532-1 ..... N91-14562*
NASA-CASE-LAR-13629-1 ..... N91-14356*
NASA-CASE-LAR-13855-1 ..... N91-14615*
NASA-CASE-LAR-13902-1 ..... N91-14484*
NASA-CASE-LAR-13965-2-CU N91-14418*
NASA-CASE-LAR-13985-1 ..... N91-14430*
NASA-CASE-LAR-14116-1 ..... N91-14345*
NASA-CASE-LAR-14188-2 ..... N91-14419*
NASA-CASE-LAR-14207-1 ..... N91-14590*
NASA-CASE-LAR-14465-1 ..... N91-14614*

NASA-CASE-LEW-14746-1 ..... N91-14552*
NASA-CASE-LEW-14862-1 ..... N91-14617*

NASA-CASE-MFS-26042-1-SB N91-14613*
NASA-CASE-MFS-28232-1 ..... N91-14835*
NASA-CASE-MFS-28294-1 ..... N91-14508*
NASA-CASE-MFS-28298-1 ..... N91-14872*
NASA-CASE-MFS-28314-1 ..... N91-14462*
NASA-CASE-MFS-28345-1 ..... N91-14608*
NASA-CASE-MFS-28383-1 ..... N91-14563*

NASA-CASE-MSC-20078-3 ..... N91-14709*
NASA-CASE-MSC-20929-1 ..... N91-14703*
NASA-CASE-MSC-21025-2 ..... N91-14724*
NASA-CASE-MSC-21025-4 ..... N91-14723*
NASA-CASE-MSC-21170-1 ..... N91-14371*
NASA-CASE-MSC-21348-1 ..... N91-14769*
NASA-CASE-MSC-21360-1 ..... N91-14374*
NASA-CASE-MSC-21408-1 ..... N91-14607*
NASA-CASE-MSC-21428-1 ..... N91-14537*
NASA-CASE-MSC-21465-1 ..... N91-14741*
NASA-CASE-MSC-21539-1 ..... N91-14610*

NASA-CASE-NPO-15959-2 ..... N91-14616*
NASA-CASE-NPO-16904-2-CU N91-14523*
NASA-CASE-NPO-16989-1-CU N91-14587*
NASA-CASE-NPO-17122-1-CU N91-14489*
NASA-CASE-NPO-17185-1-CU N91-14772*
NASA-CASE-NPO-17258-1-CU N91-14551*
NASA-CASE-NPO-17498-1-CU N91-14813*
NASA-CASE-NPO-17511-1-CU N91-14807*
NASA-CASE-NPO-17526-1-CU N91-14588*
NASA-CASE-NPO-17604-1-CU N91-14536*
NASA-CASE-NPO-17620-1-CU N91-14808*
NASA-CASE-NPO-17640-1-CU N91-14538*
NASA-CASE-NPO-17820-1-CU N91-14321*
NASA-CASE-NPO-17830-1-CU N91-14539*
NASA-CASE-NPO-17831-1-CU N91-14642*

NASA-CASE-NST-00007-1 ..... N91-14662*

NASA-CASE-SSC-00004-1 ..... N91-14609*

NASA-CP-3036 ..... N91-14897* #
NASA-CP-3060 ..... N91-14574* #

NASA-CR-4331 ..... N91-14347* #
NASA-CR-177570 ..... N91-14311* #
NASA-CR-179445 ..... N91-14353* #
NASA-CR-181888 ..... N91-14346* #
NASA-CR-183943 ..... N91-14358* #
NASA-CR-184013 ..... N91-15120* #
NASA-CR-184014 ..... N91-15119* #
NASA-CR-184031 ..... N91-14581* #
NASA-CR-184034 ..... N91-14373* #
NASA-CR-184050 ..... N91-14415* #
NASA-CR-184051 ..... N91-14416* #
NASA-CR-184916 ..... N91-14429* #
NASA-CR-185101 ..... N91-14638* #
NASA-CR-185285 ..... N91-14414* #
NASA-CR-185295 ..... N91-14378* #
NASA-CR-185301 ..... N91-14511* #
NASA-CR-185307 ..... N91-14422* #
NASA-CR-185513-PT-1 ..... N91-14700* #
NASA-CR-185513-PT-2 ..... N91-14701* #
NASA-CR-185606 ..... N91-14719* #
NASA-CR-185852 ..... N91-14789* #
NASA-CR-186413 ..... N91-14731* #
NASA-CR-186536 ..... N91-14680* #
NASA-CR-186579 ..... N91-15115* #
NASA-CR-186613 ..... N91-14527* #
NASA-CR-186756 ..... N91-14665* #
NASA-CR-186844 ..... N91-14359* #
NASA-CR-186899 ..... N91-14475* #
NASA-CR-186902 ..... N91-14624* #
NASA-CR-186904 ..... N91-14635* #
NASA-CR-187003 ..... N91-14702* #

NASA-CR-187014 N91-14733* #
NASA-CR-187029 N91-14732* #
NASA-CR-187321 N91-14474* #
NASA-CR-187326 N91-14684* #
NASA-CR-187335 N91-14655* #
NASA-CR-187373 N91-14277* #
NASA-CR-187379 N91-14672* #
NASA-CR-187413 N91-14636* #
NASA-CR-187421 N91-14766* #
NASA-CR-187425 N91-14734* #
NASA-CR-187433 N91-14379* #
NASA-CR-187435 N91-14513* #
NASA-CR-187474 N91-14726* #
NASA-CR-187475 N91-14307* #
NASA-CR-187477 N91-14308* #
NASA-CR-187648 N91-14885* #
NASA-CR-187649 N91-14630* #
NASA-CR-187651 N91-14603* #
NASA-CR-187657 N91-14424* #
NASA-CR-187677 N91-14557* #
NASA-CR-187684 N91-14803* #
NASA-CR-187687 N91-15044* #
NASA-CR-187691 N91-14673* #
NASA-CR-187692 N91-15045* #
NASA-CR-187694 N91-14825* #
NASA-CR-187695 N91-14802* #
NASA-CR-187696 N91-14639* #
NASA-CR-187702 N91-14558* #
NASA-CR-187703 N91-14657* #
NASA-CR-187709 N91-14483* #
NASA-CR-187714 N91-15114* #
NASA-CR-187715 N91-14586* #
NASA-CR-187732 N91-14365* #
NASA-CR-187733 N91-14366* #
NASA-CR-187734 N91-14367* #
NASA-CR-187735 N91-14368* #
NASA-CR-187750 N91-14647* #

NASA-RP-1124-REV-2 N91-14437* #
NASA-RP-1243 N91-14683* #

NASA-SP-500 N91-14725* #
NASA-SP-7011(343) N91-14711*
NASA-SP-7011(344) N91-14712*

NASA-TM-4196 N91-14634* #
NASA-TM-4217 N91-14274* #
NASA-TM-4221 N91-15034* #
NASA-TM-4230 N91-14275* #
NASA-TM-100765 N91-14679* #
NASA-TM-100768 N91-14494* #
NASA-TM-101105 N91-14372* #
NASA-TM-101129 N91-14600* #
NASA-TM-101249 N91-14817* #
NASA-TM-102280 N91-14273* #
NASA-TM-102748 N91-14629* #
NASA-TM-102809 N91-14322* #
NASA-TM-102888 N91-15040* #
NASA-TM-102890 N91-14727* #
NASA-TM-103169 N91-14426* #
NASA-TM-103268 N91-14349* #
NASA-TM-103273 N91-14559* #
NASA-TM-103423 N91-14498* #
NASA-TM-103439 N91-14892* #
NASA-TM-103621 N91-14602* #
NASA-TM-103623 N91-15117* #
NASA-TM-103630 N91-14781* #
NASA-TM-103631 N91-14500* #
NASA-TM-103637 N91-14632* #
NASA-TM-103641 N91-14556* #
NASA-TM-103647 N91-14454* #
NASA-TM-103654 N91-14829* #
NASA-TM-103655 N91-14850* #
NASA-TM-103674 N91-14482* #
NASA-TM-103705 N91-14310* #
NASA-TM-103709 N91-14309* #
NASA-TM-103829 N91-14540* #

NASA-TP-2640 N91-14316* #
NASA-TP-3033 N91-14618* #
NASA-TP-3045 N91-14323* #

NAVY-CASE-72146 N91-14821 #
NAVY-CASE-72676 N91-14822 #

NESDIS-53 N91-15118 #

NESIDS-54 N91-14641 #

NMERI-WA3-78-(3.21) N91-14510 #

NMRI-90-63 N91-14705 #

NOARL-SP-058-351-90 N91-14697 #

NOARL-5 N91-14693 #

NOSC/TD-1853 N91-14770 #

NPS52-90-019 N91-14893 #
NPS55-90-13 N91-14894 #
NPS55-90-14 N91-14799 #

NRL-MR-6683 N91-14567 #
NRL-MR-6716 N91-14447 #
NRL-MR-6720 N91-14520 #

NUSC-TD-6771 N91-14895 #

ORNL/FTR-3784 N91-14664 #
ORNL/FTR-3791 N91-14658 #
ORNL/FTR-3812 N91-14660 #
ORNL/FTR-3815 N91-14623 #

ORNL/M-1262 N91-14688 #
ORNL/M-1323 N91-14438 #

ORNL/TM-11587 N91-14647* #

OSU-406 N91-14636* #

OUEL-1754/89 N91-14605 #
OUEL-1831/90 N91-14423 #
OUEL-1835/90 N91-14773 #

PB90-255464 N91-14896 #

PFC/RR-90-8 N91-14848 #

PNL-SA-18242 N91-14879 #
PNL-SA-18354 N91-14648 #
PNL-SA-18576 N91-14470 #

PNL-7470 N91-14656 #

PUBL-90654 N91-14581* #
PUBL-91211 N91-14415* #

RADC-TR-89-224 N91-14851 #
RADC-TR-89-352 N91-14594 #
RADC-TR-90-109-VOL-1 N91-14543 #
RADC-TR-90-181 N91-14516 #
RADC-TR-90-256 N91-14834 #

RAE-TM-AERO-2180 N91-14341 #

RAY/RD/S-4248A N91-14522 #

REPT-90B00138-REV-2 N91-14437* #
REPT-91E00700 N91-14494* #
REPT-91E00714 N91-14679* #
REPT-7277-1 N91-14517 #
REPT-025921-18-T N91-14789* #

RPI-CHE/PCW-89-01 N91-14566 #

RUU-CS-90-19 N91-14767 #
RUU-CS-90-20 N91-14777 #
RUU-CS-90-21 N91-14736 #
RUU-CS-90-22 N91-14793 #

R90-900077-4 N91-14603* #

SAF/AQT-SR-90-011 N91-14892* #

SAND-88-2466 N91-14661 #
SAND-89-0816 N91-14319 #
SAND-89-2738C N91-14853 #
SAND-90-0404 N91-14687 #
SAND-90-0736C N91-14553 #
SAND-90-0903C N91-14649 #
SAND-90-0953C N91-14532 #
SAND-90-1068C N91-14469 #
SAND-90-1094C N91-14877 #
SAND-90-1131C N91-14854 #
SAND-90-1169C N91-14633 #
SAND-90-1201C N91-14652 #
SAND-90-1239C N91-14875 #
SAND-90-1259C N91-14651 #
SAND-90-1302 N91-14531 #
SAND-90-1387C N91-14844 #
SAND-90-1770C N91-14598 #
SAND-90-1789C N91-14450 #
SAND-90-1925 N91-14561 #
SAND-90-2091 N91-14524 #
SAND-90-2168 N91-14504 #
SAND-90-2316 N91-14525 #
SAND-90-2538C N91-14650 #
SAND-90-2557C N91-14480 #
SAND-90-2587C N91-14645 #
SAND-90-2670C N91-14646 #
SAND-90-2724C N91-14533 #
SAND-90-2778C N91-14458 #

SAND-90-2884C N91-14493 #
SAND-90-2909C N91-14473 #
SAND-90-8015 N91-14573 #

SERI/TP-211-3952 N91-14643 #
SERI/TP-215-3975 N91-14621 #
SERI/TP-257-3891 N91-14644 #
SERI/TP-257-4019 N91-14572 #

SN-3503-F N91-14487 #

SR-1 N91-14519 #
SR-1 N91-14785 #

SRA/R90-910023-F N91-14541 #

SSD-TR-90-18 N91-14444 #
SSD-TR-90-27 N91-14442 #

SU-SLAC-PUB-5293 N91-14763 #
SU-SLAC-PUB-5321 N91-14819 #
SU-SLAC-PUB-5325 N91-14369 #

SU-SOL-90-14 N91-14764 #

SU-STAN-CS-90-1303 N91-14730 #
SU-STAN-CS-90-1319 N91-14758 #

SU-TR-4 N91-14870 #
SU-TR-434 N91-14794 #

TOP-1-2-610-PT-1 N91-14720 #

TR-5 N91-14831 #
TR-6 N91-14485 #
TR-90-37C N91-14798 #
TR-90-1138 N91-14732* #
TR-884 N91-15041 #
TR-0089(4945-02)-1 N91-14442 #
TR-0090(5945-07)-1 N91-14444 #
TR-901008-4 N91-14548 #

TRI-PP-90-42 N91-14827 #
TRI-PP-90-43 N91-14534 #

TTC-0836 N91-14661 #
TTC-0959 N91-14687 #

TWR-17545-VOL-4 N91-14415* #
TWR-18764/13 N91-14416* #
TWR-60533 N91-14581* #

UBUFFALO/DC/90/TR-23 N91-14445 #
UBUFFALO/DC/90/TR-25 N91-14832 #

UCRL-CR-104813 N91-14592 #
UCRL-CR-105118 N91-14513* #

UCRL-ID-104523 N91-14606 #
UCRL-ID-105063 N91-14507 #
UCRL-ID-105117 N91-14583 #
UCRL-ID-106004 N91-14481 #
UCRL-ID-106022 N91-14428 #

UCRL-JC-103491 N91-14852 #
UCRL-JC-103736 N91-14842 #
UCRL-JC-104926 N91-14791 #
UCRL-JC-106083 N91-14659 #

UCRL-LR-105090 N91-14560 #

UCRL-101486 N91-14828 #
UCRL-102469 N91-14740 #
UCRL-102844 N91-14535 #
UCRL-103008 N91-14455 #

UILU-ENG-870501 N91-14569 #

UM-022486-1-F N91-14638* #

UMIACS-TR-90-6 N91-14786 #
UMIACS-TR-90-37 N91-14771 #
UMIACS-TR-90-51 N91-14757 #

UMICH-025921-13-T N91-14475* #

US-PATENT-APPL-SN-004304 N91-14345*
US-PATENT-APPL-SN-035401 N91-14723*
US-PATENT-APPL-SN-035401 N91-14724*
US-PATENT-APPL-SN-085833 N91-14772*
US-PATENT-APPL-SN-087358 N91-14703*
US-PATENT-APPL-SN-087375 N91-14419*
US-PATENT-APPL-SN-087376 N91-14489*
US-PATENT-APPL-SN-161682 N91-14613*
US-PATENT-APPL-SN-168065 N91-14590*
US-PATENT-APPL-SN-182266 N91-14371*

US-PATENT-APPL-SN-183475 ..... N91-14709*
US-PATENT-APPL-SN-195563 ..... N91-14357*
US-PATENT-APPL-SN-209143 ..... N91-14478
US-PATENT-APPL-SN-219295 ..... N91-14741*
US-PATENT-APPL-SN-221386 ..... N91-14418*
US-PATENT-APPL-SN-223122 ..... N91-14614*
US-PATENT-APPL-SN-239158 ..... N91-14512
US-PATENT-APPL-SN-239259 ..... N91-14484*
US-PATENT-APPL-SN-239498 ..... N91-14820
US-PATENT-APPL-SN-243685 ..... N91-14345*
US-PATENT-APPL-SN-246032 ..... N91-14523*
US-PATENT-APPL-SN-250662 ..... N91-14615*
US-PATENT-APPL-SN-251411 ..... N91-14356*
US-PATENT-APPL-SN-260762 ..... N91-14813*
US-PATENT-APPL-SN-262765 ..... N91-14528
US-PATENT-APPL-SN-264993 ..... N91-14345*
US-PATENT-APPL-SN-271265 ..... N91-14807*
US-PATENT-APPL-SN-283106 ..... N91-14769*
US-PATENT-APPL-SN-283673 ..... N91-14551*
US-PATENT-APPL-SN-292131 ..... N91-14374*
US-PATENT-APPL-SN-294622 ..... N91-14530
US-PATENT-APPL-SN-304154 ..... N91-14607*
US-PATENT-APPL-SN-304155 ..... N91-14835*
US-PATENT-APPL-SN-311551 ..... N91-14418*
US-PATENT-APPL-SN-326756 ..... N91-14808*
US-PATENT-APPL-SN-328392 ..... N91-14419*
US-PATENT-APPL-SN-343652 ..... N91-14537*
US-PATENT-APPL-SN-343656 ..... N91-14872*
US-PATENT-APPL-SN-357938 ..... N91-14662*
US-PATENT-APPL-SN-358027 ..... N91-14587*
US-PATENT-APPL-SN-364743 ..... N91-14608*
US-PATENT-APPL-SN-364774 ..... N91-14616*
US-PATENT-APPL-SN-366205 ..... N91-14590*
US-PATENT-APPL-SN-369403 ..... N91-14588*
US-PATENT-APPL-SN-369490 ..... N91-14412*
US-PATENT-APPL-SN-373955 ..... N91-14529
US-PATENT-APPL-SN-386172 ..... N91-14430*
US-PATENT-APPL-SN-388264 ..... N91-14614*
US-PATENT-APPL-SN-391692 ..... N91-14419*
US-PATENT-APPL-SN-391911 ..... N91-14724*
US-PATENT-APPL-SN-392228 ..... N91-14723*
US-PATENT-APPL-SN-392239 ..... N91-14552*
US-PATENT-APPL-SN-394343 ..... N91-14709*
US-PATENT-APPL-SN-396262 ..... N91-14508*
US-PATENT-APPL-SN-397074 ..... N91-14824
US-PATENT-APPL-SN-404288 ..... N91-14536*
US-PATENT-APPL-SN-404289 ..... N91-14462*
US-PATENT-APPL-SN-404290 ..... N91-14563*
US-PATENT-APPL-SN-404292 ..... N91-14609*
US-PATENT-APPL-SN-405169 ..... N91-14538*
US-PATENT-APPL-SN-414816 ..... N91-14617*
US-PATENT-APPL-SN-418374 ..... N91-14591*
US-PATENT-APPL-SN-418612 ..... N91-14550*
US-PATENT-APPL-SN-429734 ..... N91-14321*
US-PATENT-APPL-SN-443297 ..... N91-14539*
US-PATENT-APPL-SN-470665 ..... N91-14642*
US-PATENT-APPL-SN-501910 ..... N91-14614*
US-PATENT-APPL-SN-503410 ..... N91-14610*
US-PATENT-APPL-SN-516585 ..... N91-14479 #
US-PATENT-APPL-SN-518620 ..... N91-14823 #
US-PATENT-APPL-SN-553058 ..... N91-14821 #
US-PATENT-APPL-SN-554051 ..... N91-14822 #
US-PATENT-APPL-SN-585627 ..... N91-14709*
US-PATENT-APPL-SN-603375 ..... N91-14495*
US-PATENT-APPL-SN-680605 ..... N91-14616*
US-PATENT-APPL-SN-798713 ..... N91-14495*
US-PATENT-APPL-SN-838649 ..... N91-14562*
US-PATENT-APPL-SN-929876 ..... N91-14523*

US-PATENT-CLASS-4-DIG.9 ..... N91-14724*
US-PATENT-CLASS-4-209R N91-14723*
US-PATENT-CLASS-4-316 ..... N91-14723*
US-PATENT-CLASS-4-316 ..... N91-14724*
US-PATENT-CLASS-4-482 ..... N91-14723*
US-PATENT-CLASS-4-482 ..... N91-14724*
US-PATENT-CLASS-4-661 ..... N91-14724*
US-PATENT-CLASS-14-71.5 ..... N91-14374*
US-PATENT-CLASS-33-261 ..... N91-14591*
US-PATENT-CLASS-33-263 ..... N91-14356*
US-PATENT-CLASS-48-77 ..... N91-14495*
US-PATENT-CLASS-48-197R N91-14495*
US-PATENT-CLASS-48-203 ..... N91-14495*
US-PATENT-CLASS-55-68 ..... N91-14662*
US-PATENT-CLASS-55-74 ..... N91-14662*
US-PATENT-CLASS-55-84 ..... N91-14662*
US-PATENT-CLASS-55-89 ..... N91-14662*
US-PATENT-CLASS-55-228 ..... N91-14662*
US-PATENT-CLASS-55-242 ..... N91-14662*
US-PATENT-CLASS-60-39.12 ..... N91-14495*
US-PATENT-CLASS-60-39.182 ..... N91-14495*
US-PATENT-CLASS-73-147 ..... N91-14356*
US-PATENT-CLASS-73-147 ..... N91-14357*
US-PATENT-CLASS-73-170R N91-14412*
US-PATENT-CLASS-73-505 ..... N91-14807*
US-PATENT-CLASS-73-658 ..... N91-14607*
US-PATENT-CLASS-73-794 ..... N91-14430*

US-PATENT-CLASS-74-479 ..... N91-14616*
US-PATENT-CLASS-74-665G N91-14616*
US-PATENT-CLASS-114-67A N91-14562*
US-PATENT-CLASS-128-671 ..... N91-14709*
US-PATENT-CLASS-128-689 ..... N91-14709*
US-PATENT-CLASS-128-706 ..... N91-14709*
US-PATENT-CLASS-128-716 ..... N91-14709*
US-PATENT-CLASS-137-556 ..... N91-14563*
US-PATENT-CLASS-156-169 ..... N91-14478
US-PATENT-CLASS-164-122.1 ..... N91-14462*
US-PATENT-CLASS-164-338.1 ..... N91-14462*
US-PATENT-CLASS-181-0.5 ..... N91-14808*
US-PATENT-CLASS-210-355 ..... N91-14703*
US-PATENT-CLASS-210-414 ..... N91-14703*
US-PATENT-CLASS-210-615 ..... N91-14662*
US-PATENT-CLASS-219-121.68 ..... N91-14508*
US-PATENT-CLASS-244-58 ..... N91-14345*
US-PATENT-CLASS-244-130 ..... N91-14562*
US-PATENT-CLASS-244-137.2 ..... N91-14374*
US-PATENT-CLASS-244-161 ..... N91-14374*
US-PATENT-CLASS-244-199 ..... N91-14345*
US-PATENT-CLASS-244-203 ..... N91-14562*
US-PATENT-CLASS-244-204 ..... N91-14562*
US-PATENT-CLASS-248-229 ..... N91-14617*
US-PATENT-CLASS-248-230 ..... N91-14617*
US-PATENT-CLASS-250-227.15 ..... N91-14824
US-PATENT-CLASS-250-281 ..... N91-14587*
US-PATENT-CLASS-250-282 ..... N91-14587*
US-PATENT-CLASS-250-286 ..... N91-14587*
US-PATENT-CLASS-250-287 ..... N91-14587*
US-PATENT-CLASS-250-288 ..... N91-14587*
US-PATENT-CLASS-250-305 ..... N91-14587*
US-PATENT-CLASS-250-327.2 ..... N91-14835*
US-PATENT-CLASS-250-338.1 ..... N91-14588*
US-PATENT-CLASS-250-338.2 ..... N91-14588*
US-PATENT-CLASS-250-370.12 ..... N91-14588*
US-PATENT-CLASS-250-370.13 ..... N91-14588*
US-PATENT-CLASS-250-423 ..... N91-14587*
US-PATENT-CLASS-250-484.1 ..... N91-14835*
US-PATENT-CLASS-250-493.1 ..... N91-14588*
US-PATENT-CLASS-251-160 ..... N91-14609*
US-PATENT-CLASS-251-163 ..... N91-14609*
US-PATENT-CLASS-251-212 ..... N91-14563*
US-PATENT-CLASS-252-62.2 ..... N91-14536*
US-PATENT-CLASS-285-82 ..... N91-14613*
US-PATENT-CLASS-285-327 ..... N91-14610*
US-PATENT-CLASS-285-361 ..... N91-14613*
US-PATENT-CLASS-290-44 ..... N91-14345*
US-PATENT-CLASS-290-55 ..... N91-14345*
US-PATENT-CLASS-294-106 ..... N91-14616*
US-PATENT-CLASS-294-111 ..... N91-14616*
US-PATENT-CLASS-294-119.1 ..... N91-14615*
US-PATENT-CLASS-310-11 ..... N91-14489*
US-PATENT-CLASS-310-323 ..... N91-14808*
US-PATENT-CLASS-310-325 ..... N91-14808*
US-PATENT-CLASS-310-330 ..... N91-14872*
US-PATENT-CLASS-310-331 ..... N91-14872*
US-PATENT-CLASS-310-334 ..... N91-14808*
US-PATENT-CLASS-310-339 ..... N91-14872*
US-PATENT-CLASS-310-340 ..... N91-14872*
US-PATENT-CLASS-320-51 ..... N91-14537*
US-PATENT-CLASS-320-236 ..... N91-14530
US-PATENT-CLASS-324-115 ..... N91-14371*
US-PATENT-CLASS-324-158F N91-14552*
US-PATENT-CLASS-324-158P N91-14552*
US-PATENT-CLASS-324-601 ..... N91-14552*
US-PATENT-CLASS-328-151 ..... N91-14550*
US-PATENT-CLASS-329-306 ..... N91-14321*
US-PATENT-CLASS-329-363 ..... N91-14550*
US-PATENT-CLASS-331-1 ..... N91-14709*
US-PATENT-CLASS-333-247 ..... N91-14552*
US-PATENT-CLASS-336-198 ..... N91-14539*
US-PATENT-CLASS-336-205 ..... N91-14539*
US-PATENT-CLASS-336-229 ..... N91-14539*
US-PATENT-CLASS-338-32 ..... N91-14537*
US-PATENT-CLASS-338-221 ..... N91-14537*
US-PATENT-CLASS-340-683 ..... N91-14607*
US-PATENT-CLASS-340-825.5 ..... N91-14772*
US-PATENT-CLASS-342-25 ..... N91-14642*
US-PATENT-CLASS-342-54 ..... N91-14356*
US-PATENT-CLASS-342-91 ..... N91-14529
US-PATENT-CLASS-342-352 ..... N91-14321*
US-PATENT-CLASS-342-357 ..... N91-14321*
US-PATENT-CLASS-342-418 ..... N91-14321*
US-PATENT-CLASS-350-287 ..... N91-14590*
US-PATENT-CLASS-350-354 ..... N91-14820
US-PATENT-CLASS-350-500 ..... N91-14590*
US-PATENT-CLASS-350-576 ..... N91-14591*
US-PATENT-CLASS-350-9615 ..... N91-14512
US-PATENT-CLASS-356-1 ..... N91-14356*
US-PATENT-CLASS-356-141 ..... N91-14356*
US-PATENT-CLASS-356-152 ..... N91-14356*
US-PATENT-CLASS-357-15 ..... N91-14551*
US-PATENT-CLASS-357-27 ..... N91-14588*
US-PATENT-CLASS-357-29 ..... N91-14551*
US-PATENT-CLASS-357-30 ..... N91-14528

US-PATENT-CLASS-357-30 ..... N91-14551*
US-PATENT-CLASS-357-30 ..... N91-14588*
US-PATENT-CLASS-357-32 ..... N91-14551*
US-PATENT-CLASS-357-58 ..... N91-14551*
US-PATENT-CLASS-364-228.3 ..... N91-14769*
US-PATENT-CLASS-364-231.9 ..... N91-14769*
US-PATENT-CLASS-364-280 ..... N91-14769*
US-PATENT-CLASS-364-281 ..... N91-14769*
US-PATENT-CLASS-364-300 ..... N91-14769*
US-PATENT-CLASS-364-433 ..... N91-14356*
US-PATENT-CLASS-364-487 ..... N91-14371*
US-PATENT-CLASS-364-513 ..... N91-14741*
US-PATENT-CLASS-364-550 ..... N91-14371*
US-PATENT-CLASS-364-578 ..... N91-14741*
US-PATENT-CLASS-370-85.4 ..... N91-14772*
US-PATENT-CLASS-370-85.6 ..... N91-14772*
US-PATENT-CLASS-370-85.9 ..... N91-14772*
US-PATENT-CLASS-370-94.3 ..... N91-14772*
US-PATENT-CLASS-371-43 ..... N91-14523*
US-PATENT-CLASS-375-53 ..... N91-14523*
US-PATENT-CLASS-375-57 ..... N91-14523*
US-PATENT-CLASS-375-80 ..... N91-14321*
US-PATENT-CLASS-375-94 ..... N91-14321*
US-PATENT-CLASS-403-171 ..... N91-14614*
US-PATENT-CLASS-403-317 ..... N91-14610*
US-PATENT-CLASS-403-322 ..... N91-14614*
US-PATENT-CLASS-403-327 ..... N91-14610*
US-PATENT-CLASS-403-327 ..... N91-14614*
US-PATENT-CLASS-403-331 ..... N91-14610*
US-PATENT-CLASS-403-331 ..... N91-14614*
US-PATENT-CLASS-403-381 ..... N91-14610*
US-PATENT-CLASS-403-385 ..... N91-14617*
US-PATENT-CLASS-403-391 ..... N91-14617*
US-PATENT-CLASS-405-188 ..... N91-14374*
US-PATENT-CLASS-414-7 ..... N91-14616*
US-PATENT-CLASS-414-729 ..... N91-14616*
US-PATENT-CLASS-415-170.1 ..... N91-14608*
US-PATENT-CLASS-415-174.5 ..... N91-14608*
US-PATENT-CLASS-415-229 ..... N91-14608*
US-PATENT-CLASS-423-655 ..... N91-14495*
US-PATENT-CLASS-429-103 ..... N91-14538*
US-PATENT-CLASS-429-104 ..... N91-14536*
US-PATENT-CLASS-429-120 ..... N91-14538*
US-PATENT-CLASS-429-213 ..... N91-14536*
US-PATENT-CLASS-435-311 ..... N91-14703*
US-PATENT-CLASS-435-316 ..... N91-14703*
US-PATENT-CLASS-437-225 ..... N91-14813*
US-PATENT-CLASS-437-228 ..... N91-14813*
US-PATENT-CLASS-437-235 ..... N91-14813*
US-PATENT-CLASS-437-238 ..... N91-14813*
US-PATENT-CLASS-437-239 ..... N91-14813*
US-PATENT-CLASS-437-930 ..... N91-14813*
US-PATENT-CLASS-437-936 ..... N91-14813*
US-PATENT-CLASS-526-262 ..... N91-14418*
US-PATENT-CLASS-528-125 ..... N91-14484*
US-PATENT-CLASS-528-126 ..... N91-14484*
US-PATENT-CLASS-528-128 ..... N91-14484*
US-PATENT-CLASS-528-172 ..... N91-14484*
US-PATENT-CLASS-528-185 ..... N91-14484*
US-PATENT-CLASS-528-188 ..... N91-14484*
US-PATENT-CLASS-528-322 ..... N91-14418*
US-PATENT-CLASS-528-353 ..... N91-14484*
US-PATENT-CLASS-548-549 ..... N91-14419*
US-PATENT-CLASS-901-38 ..... N91-14615*
US-PATENT-CLASS-901-39 ..... N91-14615*

US-PATENT-4,839,046 ..... N91-14703*
US-PATENT-4,845,993 ..... N91-14357*
US-PATENT-4,860,975 ..... N91-14374*
US-PATENT-4,895,430 ..... N91-14590*
US-PATENT-4,895,915 ..... N91-14418*
US-PATENT-4,895,972 ..... N91-14484*
US-PATENT-4,902,647 ..... N91-14813*
US-PATENT-4,917,332 ..... N91-14345*
US-PATENT-4,920,346 ..... N91-14529
US-PATENT-4,920,487 ..... N91-14769*
US-PATENT-4,921,212 ..... N91-14609*
US-PATENT-4,921,293 ..... N91-14616*
US-PATENT-4,921,335 ..... N91-14820
US-PATENT-4,921,557 ..... N91-14478
US-PATENT-4,922,201 ..... N91-14530
US-PATENT-4,924,285 ..... N91-14528
US-PATENT-4,926,694 ..... N91-14430*
US-PATENT-4,927,326 ..... N91-14608*
US-PATENT-4,928,027 ..... N91-14489*
US-PATENT-4,932,610 ..... N91-14562*
US-PATENT-4,932,688 ..... N91-14613*
US-PATENT-4,932,777 ..... N91-14356*
US-PATENT-4,933,558 ..... N91-14835*
US-PATENT-4,933,936 ..... N91-14772*
US-PATENT-4,936,309 ..... N91-14709*
US-PATENT-4,936,869 ..... N91-14495*
US-PATENT-4,937,356 ..... N91-14419*
US-PATENT-4,937,891 ..... N91-14723*
US-PATENT-4,940,891 ..... N91-14824
US-PATENT-4,941,726 ..... N91-14512

US-PATENT-4,942,632 ..... N91-14724*
US-PATENT-4,945,012 ..... N91-14538*
US-PATENT-4,945,549 ..... N91-14523*
US-PATENT-4,946,122 ..... N91-14617*
US-PATENT-4,952,811 ..... N91-14588*
US-PATENT-4,952,836 ..... N91-14872*
US-PATENT-4,954,864 ..... N91-14551*
US-PATENT-4,955,653 ..... N91-14615*
US-PATENT-4,957,139 ..... N91-14563*
US-PATENT-4,957,357 ..... N91-14591*
US-PATENT-4,959,084 ..... N91-14662*
US-PATENT-4,959,656 ..... N91-14321*
US-PATENT-4,962,330 ..... N91-14808*
US-PATENT-4,963,052 ..... N91-14614*
US-PATENT-4,964,300 ..... N91-14412*
US-PATENT-4,964,303 ..... N91-14807*
US-PATENT-4,964,453 ..... N91-14462*
US-PATENT-4,965,429 ..... N91-14508*
US-PATENT-4,965,743 ..... N91-14741*
US-PATENT-4,966,823 ..... N91-14536*
US-PATENT-4,971,474 ..... N91-14610*
US-PATENT-4,973,840 ..... N91-14587*
US-PATENT-4,973,914 ..... N91-14550*
US-PATENT-4,974,181 ..... N91-14371*
US-PATENT-4,975,672 ..... N91-14539*
US-PATENT-4,975,704 ..... N91-14642*
US-PATENT-4,977,395 ..... N91-14607*
US-PATENT-4,980,636 ..... N91-14552*

USAAVSCOM-TR-89-D-13A-VOL-1 ..... N91-14343 #
USAAVSCOM-TR-89-D-13B-VOL-2 ..... N91-14344 #

USAF-STINFO-CONTRIB-90/6 ..... N91-14892* #

USARIEM-T16-90 ..... N91-14708 #

USGS-OFR-88-553 ..... N91-14737 #
USGS-OFR-89-133 ..... N91-14676 #

USNA-TSPR-166 ..... N91-14759 #
USNA-TSPR-167 ..... N91-14698 #
USNA-TSPR-168 ..... N91-14544 #
USNA-TSPR-169 ..... N91-14691 #
USNA-TSPR-171 ..... N91-14568 #
USNA-TSPR-173 ..... N91-14806 #

UVA/528266/MS90/104 ..... N91-14474* #

VPI-E-90-18 ..... N91-14424* #

WHC-EP-0188 ..... N91-14468 #

WL-TR-90-47 ..... N91-14869 #

WRDC-TR-89-4145-VOL-2 ..... N91-14351 #
WRDC-TR-90-1067 ..... N91-14517 #
WRDC-TR-90-2008 ..... N91-14566 #
WRDC-TR-90-2026 ..... N91-14546 #
WRDC-TR-90-2064 ..... N91-14589 #
WRDC-TR-90-3037-VOL-2 ..... N91-14375 #
WRDC-TR-90-3057 ..... N91-14314 #

Appendix

NASA SCIENTIFIC AND TECHNICAL INFORMATION PROGRAM PRODUCTS AND SERVICES

The NASA Scientific and Technical Information (STI) program provides for the collection and announcement of aerospace-related reports and literature obtained worldwide through agreements and exchanges. The result of the collection is the comprehensive NASA STI Database that covers aeronautics, space, and supporting disciplines.

The STI Database, documents generated or obtained by NASA, and products and services derived from or supporting the database are made available to the NASA research community and to the public. Descriptions and sources of these items are presented in the following pages.

Scientific and Technical Aerospace Reports (*STAR*) is an abstract journal, listing citations with abstracts for aerospace-related reports obtained from worldwide sources. *STAR* is issued on the 8th and 23rd of each month and announces current documents that have been entered into the NASA STI Database during the previous two weeks. The reports are of the following types:

- NASA, NASA contractor, and NASA grantee reports;
- Reports issued by other U.S. Government agencies, domestic and foreign institutions, universities, and private firms;
- Translations in report form;
- NASA-owned patents and patent applications;
- Other U.S. Government agency and foreign patents and patent applications;
- Domestic and foreign dissertations and theses.

Journal, book, and conference literature, journal translations, and certain foreign dissertations having the same subject scope as *STAR* are announced in a companion journal, *International Aerospace Abstracts* (*IAA*). *IAA* is issued on the 1st and 15th of each month and is available from the American Institute of Aeronautics and Astronautics, Technical Information Service, 555 West 57th Street, 12th Floor, New York, NY 10019.

ELIGIBILITY AND REGISTRATION FOR NASA STI PRODUCTS AND SERVICES

Organizations of the type listed below that have registered with NASA can receive products and services.

- NASA offices and installations, contractors, subcontractors, grantees, and consultants;
- Other U.S. Government agencies and their contractors;
- Libraries in the United States that have arrangements with NASA to maintain collections of NASA documents for public reference;
- Other organizations in the United States having a need for NASA documents in work related to aeronautics and space research;
- Organizations abroad that have established reciprocal documents exchange arrangements with NASA.

Only the central service points or central points of document acquisition and control within qualified organizations are eligible to register for NASA STI products and services. Domestic organizations that may be eligible to receive various classes of NASA publications and services should address their requests for registration or further information to:

NASA Scientific and Technical Information Facility
ATTN: Registration Services
P.O. Box 8757
BWI Airport, MD 21240
301-621-0153

Organizations abroad should direct requests to:

National Aeronautics and Space Administration
Director, Scientific and Technical Information Divison
Code NTT
Washington, DC 20546
USA
703-271-5640

SUBJECT SCOPE

The subject scope of *STAR* and *IAA* includes all aspects of aeronautics and space research and development, supporting basic and applied research, and applications. Aerospace aspects of Earth resources, energy development, conservation, oceanography, environmental protection, urban transportation, and other topics of high national priority are also covered.

HOW TO USE *STAR* SUBJECT CATEGORIES

Abstracts in *STAR* are categorized by 10 major subject divisions that are divided further into 76 specific subject categories. The subject divisions and categories are listed in the Table of Contents together with a note for each that defines its scope and provides any cross-references. For example:

16 SPACE TRANSPORTATION
Includes passenger and cargo space transportation, e.g., shuttle operations; and space rescue techniques. For related information see also *03 Air Transportation and Safety* and *18 Spacecraft Design, Testing and Performance.* For space suits see *54 Man/System Technology and Life Support.*

CROSS-REFERENCES

Individual *STAR* abstracts are not ordinarily cross-referenced, except for certain conference reports or book translations that have had separate abstracts written for their component papers or chapters. Citations and abstracts of the components follow immediately after those of the parent document. When the subject content of a component differs sufficiently from the general content of the parent, a cross-reference citation also is printed at the end of the category to which it normally would have been assigned if it were independent.

DOCUMENTS ON MICROFICHE

Documents available on microfiche are designated by a pound sign (#) following the accession number.

LIMITED REPRODUCIBILITY

A note of limited reproducibility appears in the citation, if there are factors affecting the reproducibility of more than 20% of the document. These factors include faint or broken type, color photographs, black and white photographs, foldouts, dot matrix print, or some other factor that limits the reproducibility of the document. This notation also appears on the microfiche header with the specific factor checked off on a list visible in the second frame.

COLOR COPIES

An increasing number of NASA scientific and technical reports are being produced with color graphs, charts, illustrations, and photographs. An indication that a document has color pages follows the source and pricing (SAP) information in the *STAR* citation.

Registered users of the NASA Scientific and Technical Information Program will receive ordered documents with color at no additional cost, as long as stock copies of the document are available. Otherwise, an additional fee of $2.00 per color page will be charged. The NASA STI Facility staff will contact registered users to determine individual user's needs.

NASA PATENTS AND PATENT APPLICATIONS

Patents and patent applications owned by NASA are announced in *STAR* under appropriate subject categories and are referenced in the *STAR* indexes. In the Report/Accession Number Index, patents are indexed by the NASA Case Number, and the U.S. Patent Class. Patent applications are indexed by the NASA Case Number and the U.S. Patent Application Serial Number.

Printed copies of patents (which are not microfiched) are available for purchase from the U.S. Patent and Trademark Office.

NASA patent application specifications are sold in both paper copy and microfiche by the National Technical Information Service (NTIS). The US-Patent-Appl-SN-number should be used in ordering either paper copy or microfiche from NTIS.

When ordering patents, the U.S. Patent Number should be used, and payment must be remitted in advance, by money order or check payable to the Commissioner of Patents and Trademarks. Prepaid purchase coupons for ordering are also available from the U.S. Patent and Trademark Office.

The patents and patent applications announced in *STAR* are owned by NASA and are available for royalty-free licensing. Requests for licensing terms and further information should be addressed to:

National Aeronautics and Space Administration
Associate General Counsel for Intellectual Property
Code GP
Washington, DC 20546

SOURCES FOR DOCUMENTS

One or more sources from which a document announced in *STAR* is available to the public is given in each citation. The most commonly indicated sources and their acronyms or abbreviations are listed on page A-6. If the publication is available from a source other than those listed, the publisher and address will be displayed on the availability line or in combination with the corporate source line.

Avail: NTIS. Sold by the National Technical Information Service. Prices for hard copy (HC) and microfiche (MF) are indicated by a price code following the letters HC or MF in the *STAR* citation. Current values for the price codes are given in the tables on page A-7.

Initially distributed microfiche under the NTIS SRIM (Selected Research in Microfiche) is available at greatly reduced unit prices. For this service and for information concerning subscription to NASA printed reports, consult the NTIS Subscription Section, Springfield, VA 22161.

NOTE ON ORDERING DOCUMENTS: When ordering NASA publications (those followed by the * symbol), use the N accession number. NASA patent applications (only the specifications are offered) should be ordered by the US-Patent-Appl-SN number. Non-NASA publications (no asterisk) should be ordered by the AD, PB, or other *report number* shown on the last line of the citation, not by the N accession number. It is also advisable to cite the title and other bibliographic identification.

Avail: SOD (or GPO). Sold by the Superintendent of Documents, U.S. Government Printing Office, in hard copy. The current price and order number are given following the availability line. (NTIS will fill microfiche requests, as indicated above, for those documents identified by a # symbol.)

Avail: BLL (formerly NLL): British Library Lending Division, Boston Spa, Wetherby, Yorkshire, England. Photocopies available from this organization at the price shown. (If none is given, address inquiry to the BLL.)

Avail: DOE Depository Libraries. Organizations in U.S. cities and abroad that maintain collections of Department of Energy reports, usually in microfiche form, are listed in *Energy Research Abstracts.* Services available from the DOE and its depositories are described in a booklet, *DOE Technical Information Center - Its Functions and Services* (TID-4660), which may be obtained without charge from the DOE Technical Information Center.

Avail: ESDU. Pricing information on specific data, computer programs, and details on Engineering Sciences Data Unit (ESDU) topic categories can be obtained from ESDU International Ltd. Requesters in North America should use the Virginia address while all other requesters should use the London address, both of which are on page A-6.

Avail: Fachinformationszentrum, Karlsruhe. Sold by the Fachinformationszentrum Energie, Physik, Mathematik GMBH, Eggenstein Leopoldshafen, Federal Republic of Germany, at the price shown in deutschmarks (DM).

Avail: HMSO. Publications of Her Majesty's Stationery Office are sold in the U.S. by Pendragon House, Inc. (PHI), Redwood City, CA. The U.S. price (including a service and mailing charge) is given, or a conversion table may be obtained from PHI.

Avail: NASA Public Document Rooms. Documents so indicated may be examined at or purchased from the National Aeronautics and Space Administration, Public Documents Room (Room 126), 600 Independence Ave., S.W., Washington, DC 20546, or public document rooms located at NASA installations, and the NASA Pasadena Office at the Jet Propulsion Laboratory.

Avail: Univ. Microfilms. Documents so indicated are dissertations selected from *Dissertation Abstracts* and are sold by University Microfilms as xerographic copy (HC) and microfilm. All requests should cite the author and the Order Number as they appear in the citation.

Avail: US Patent and Trademark Office. Sold by Commissioner of Patents and Trademarks, U.S. Patent and Trademark Office, at the standard price of $1.50 each, postage free. (See discussion of NASA patents and patent applications below.)

Avail: (US Sales Only). These foreign documents are available to users within the United States from the National Technical Information Service (NTIS). They are available to users outside the United States through the International Nuclear Information Service (INIS) representative in their country, or by applying directly to the issuing organization.

Avail: USGS. Originals of many reports from the U.S. Geological Survey, which may contain color illustrations, or otherwise may not have the quality of illustrations preserved in the microfiche or facsimile reproduction, may be examined by the public at the libraries of the USGS field offices whose addresses are listed on page A-6. The libraries may be queried concerning the availability of specific documents and the possible utilization of local copying services, such as color reproduction.

Avail: Issuing Activity, or Corporate Author, or no indication of availability. Inquiries as to the availability of these documents should be addressed to the organization shown in the citation as the corporate author of the document.

PUBLIC COLLECTIONS OF NASA DOCUMENTS

DOMESTIC: NASA and NASA-sponsored documents and a large number of aerospace publications are available to the public for reference purposes at the library maintained by the American Institute of Aeronautics and Astronautics, Technical Information Service, 555 West 57th Street, 12th Floor, New York, NY 10019.

EUROPEAN: An extensive collection of NASA and NASA-sponsored publications is maintianed by the British Library Lending Divison, Boston Spa, Wetherby, Yorkshire, England, for public access. The British Library Lending Division also has available many of the non-NASA publications cited in *STAR*.

European requesters may purchase facsimile copy or microfiche of NASA and NASA-sponsored documents, those identified by both the symbols # and * from ESA—Information Retrieval Service, European Space Agency, 8-10 rue Mario-Nikis, 75738 Paris CEDEX 15, France.

FEDERAL DEPOSITORY LIBRARIES: To provide the general public with greater access to U.S. Government publications, Congress established the Federal Depository Library Program under the Government Printing Office (GPO), with 51 regional depositories responsible for permanent retention of material, inter-library loan, and reference services. (These libraries are not sales outlets.) At least one copy of nearly every NASA and NASA-sponsored publication, either in printed or microfiche format, is received and retained by the 51 regional depositories. A list of the regional GPO libraries, appears on page A-8. A local library can contact a regional depository library to help locate specific reports, or direct contact may be made by an individual.

SUBMITTING DOCUMENTS

All users of this abstract service are urged to forward reports to be considered for announcement in *STAR*. This will aid NASA in its efforts to provide the fullest possible coverage of all scientific and technical publications that might support aeronautics and space research and development. If you have prepared relevant reports (other than those you will transmit to NASA, DOD, or DOE through the usual contract- or grant-reporting channels), please send them for consideration to the NASA Scientific and Technical Information Facility, P.O. Box 8757, BWI Airport, MD 21240.

Reprints of journal articles, book chapters, and conference papers are also welcome. These will be considered for announcement in *STAR*'s companion journal, *IAA*.

You may specify a particular source to be included in a report announcement if you wish; otherwise the report will be placed on a public sale at the National Technical Information Service. Copyrighted publications will be announced but not distributed or sold.

PURCHASE OF *STAR*

STAR is publicly available on annual subscription from the Superintendent of Documents, U.S. Government Printing Office, Washington, DC 20402.

STAR is available to registered users on annual subscription from the NASA Scientific and Technical Information Facility, ATTN: Registration Services, P.O. Box 8757, BWI Airport, MD 21240.

Microfiche of the abstract sections of *STAR* are available, on annual subscription only, from NTIS as PB91-911300, Attn: Subscriptions, 5285 Port Royal Road, Springfield, VA 22161. Annual subscription rates are $85.00 North America; $170.00 foreign. Abstract sections for previous years retroactive to 1964 are available at the current rates.

ADDRESSES OF ORGANIZATIONS

American Institute of Aeronautics and Astronautics
Technical Information Service
555 West 57th Street, 12th Floor
New York, New York 10019

British Library Lending Division,
Boston Spa, Wetherby, Yorkshire,
England

Commissioner of Patents and Trademarks
U.S. Patent and Trademark Office
Washington, DC 20231

Department of Energy
Technical Information Center
P.O. Box 62
Oak Ridge, Tennessee 37830

European Space Agency-Information Retrieval Service
ESRIN
Via Galileo Galilei
00044 Frascati (Rome) Italy

Engineering Sciences Data Unit International
P.O. Box 1633
Manassas, Virginia 22110

Engineering Sciences Data Unit International, Ltd.
251-259 Regent Street
London, W1R 7AD, England

Fachinformationszentrum Energie, Physik, Mathematik
GMBH
7514 Eggenstein Leopoldshafen
Federal Republic of Germany

Her Majesty's Stationery Office
P.O. Box 569, S.E. 1
London, England

NASA Scientific and Technical Information Facility
P.O. Box 8757
BWI Airport, Maryland 21240

National Aeronautics and Space Administration
Scientific and Technical Information Division (NTT)
Washington, DC 20546

National Technical Information Service
5285 Port Royal Road
Springfield, Virginia 22161

Pendragon House, Inc.
899 Broadway Avenue
Redwood City, California 94063

Superintendent of Documents
U.S. Government Printing Office
Washington, DC 20402

University Microfilms
A Xerox Company
300 North Zeeb Road
Ann Arbor, Michigan 48106

University Microfilms, Ltd.
Tylers Green
London, England

U.S. Geological Survey Library National Center
MS 950
12201 Sunrise Valley Drive
Reston, Virginia 22092

U.S. Geological Survey Library
2255 North Gemini Drive
Flagstaff, Arizona 86001

U.S. Geological Survey
345 Middlefield Road
Menlo Park, California 94025

U.S. Geological Survey Library
Box 25046
Denver Federal Center, MS914
Denver, Colorado 80225

NTIS PRICE SCHEDULES

(Effective January 1, 1991)

Schedule A
STANDARD PRICE DOCUMENTS AND MICROFICHE**

PRICE CODE	NORTH AMERICAN PRICE	FOREIGN PRICE
A01	$ 8.00	$ 16.00
A02	11.00	22.00
A03	15.00	30.00
A04-A05	17.00	34.00
A06-A09	23.00	46.00
A10-A13	31.00	62.00
A14-A17	39.00	78.00
A18-A21	45.00	90.00
A22-A25	53.00	106.00
A99	*	*
N01	60.00	120.00
N02	59.00	118.00
N03	20.00	40.00

Schedule E
EXCEPTION PRICE DOCUMENTS AND MICROFICHE**

PRICE CODE	NORTH AMERICAN PRICE	FOREIGN PRICE
E01	$10.00	$ 20.00
E02	12.00	24.00
E03	14.00	28.00
E04	16.50	33.00
E05	18.50	37.00
E06	21.50	43.00
E07	24.00	48.00
E08	27.00	54.00
E09	29.50	59.00
E10	32.50	65.00
E11	35.00	70.00
E12	38.50	77.00
E13	41.00	82.00
E14	45.00	90.00
E15	48.50	97.00
E16	53.00	106.00
E17	57.50	115.00
E18	62.00	124.00
E19	69.00	138.00
E20	80.00	160.00
E99	*	*

* Contact NTIS for price quote.

** Effective January 1, 1991, the microfiche copy of any new document entering the NTIS collection will be priced the same as the paper copy of the document.

IMPORTANT NOTICE

NTIS Shipping and Handling Charges

U.S., Canada, Mexico — ADD $3.00 per TOTAL ORDER

All Other Countries — ADD $4.00 per TOTAL ORDER

Exceptions — Does NOT apply to:

ORDERS REQUESTING NTIS RUSH HANDLING
ORDERS FOR SUBSCRIPTION OR STANDING ORDER PRODUCTS *ONLY*

NOTE: Each additional delivery address on an order requires a separate shipping and handling charge.

FEDERAL REGIONAL DEPOSITORY LIBRARIES

ALABAMA

AUBURN UNIV. AT MONTGOMERY LIBRARY
Documents Department
Montgomery, AL 36193
(205) 279-9110 ext.253

UNIV. OF ALABAMA LIBRARY
Reference Department/Documents
Box S
Tuscaloosa, AL 35486
(205) 348-6046

ARIZONA

DEPT. OF LIBRARY, ARCHIVES, AND PUBLIC RECORDS
Third Floor State Capitol
1700 West Washington
Phoenix, AZ 85007
(602) 255-4121

ARKANSAS

ARKANSAS STATE LIBRARY
Documents Service Section
One Capitol Mall
Little Rock, AR 72201
(501) 371-2090

CALIFORNIA

CALIFORNIA STATE LIBRARY
Govt. Publications Section
914 Capitol Mall
Sacramento, CA 95814
(916) 322-4572

COLORADO

UNIV. OF COLORADO
Norlin Library
Government Publications Division
Campus Box 184
Boulder, CO 80309
(303) 492-8834

DENVER PUBLIC LIBRARY
Govt. Pub. Department
1357 Broadway
Denver, CO 80203
(303) 571-2346

CONNECTICUT

CONNECTICUT STATE LIBRARY
231 Capitol Avenue
Hartford, CT 06106
(203) 566-4971

FLORIDA

UNIV. OF FLORIDA LIBRARIES
Documents Department
Library West
Gainesville, FL 32611
(904) 392-0367

GEORGIA

UNIV. OF GEORGIA LIBRARIES
Government Documents Dept.
Athens, GA 30602
(404) 542-8949

HAWAII

UNIV. OF HAWAII
Hamilton Library
Government Documents Collection
2550 The Mall
Honolulu, HI 96822
(808) 948-8230

IDAHO

UNIV. OF IDAHO LIBRARY
Documents Section
Moscow, ID 83843
(208) 885-6344

ILLINOIS

ILLINOIS STATE LIBRARY
Federal Documents
Centennial Building
Springfield, IL 62756
(217) 782-5012

INDIANA

INDIANA STATE LIBRARY
Serials Section
140 North Senate Avenue
Indianapolis, IN 46204
(317) 232-3686

IOWA

UNIV. OF IOWA LIBRARIES
Government Publications Dept.
Iowa City, IA 52242
(319) 335-5926

KANSAS

UNIVERSITY OF KANSAS
Spencer Research Library
Government Documents
Lawrence, KS 66045
(913) 864-4662

KENTUCKY

UNIV. OF KENTUCKY LIBRARIES
Government Publications/Maps Dept.
Lexington, KY 40506
(606) 257-8400

LOUISIANA

LOUISIANA STATE UNIVERSITY
Middleton Library
Government Documents Dept.
Baton Rouge, LA 70803
(504) 388-2570

LOUISIANA TECHNICAL UNIV.
Prescott Memorial Library
Government Documents Dept.
Ruston, LA 71272
(318) 257-4962

MAINE

UNIVERSITY OF MAINE
Raymond H. Fogler Library
Govt. Documents & Microforms Dept.
Orono, ME 04469
(207) 581-1680

MARYLAND

UNIVERSITY OF MARYLAND
McKeldin Library
Documents/Maps Room
College Park, MD 20742
(301) 454-3034

MASSACHUSETTS

BOSTON PUBLIC LIBRARY
Government Documents Dept.
666 Boylston Street
Boston, MA 02117
(617) 536-5400 ext.226

MICHIGAN

DETROIT PUBLIC LIBRARY
5201 Woodward Avenue
Detroit, MI 48202
(313) 833-1409

LIBRARY OF MICHIGAN
Government Documents
P.O. Box 30007
735 E. Michigan Avenue
Lansing, MI 48909
(517) 373-1593

MINNESOTA

UNIVERSITY OF MINNESOTA
Wilson Library
Government Publications
309 Nineteenth Avenue South
Minneapolis, MN 55455
(612) 373-7813

MISSISSIPPI

UNIV. OF MISSISSIPPI LIB.
Government Documents Dept.
106 Old Gym Bldg.
University, MS 38677
(601) 232-5857

MISSOURI

University of Missouri at Columbia Library
Government Documents
Columbia, MO 65201
(314) 882-6733

MONTANA

UNIV. OF MONTANA
Mansfield Library
Documents Division
Missoula, MT 59812
(406) 243-6700

NEBRASKA

UNIVERSITY OF NEBRASKA - LINCOLN
Love Memorial Library
Documents Department
Lincoln, NE 68588
(402) 472-2562

NEVADA

UNIV. OF NEVADA-RENO LIB.
Govt. Pub. Department
Reno, NV 89557
(702) 784-6579

NEW JERSEY

NEWARK PUBLIC LIBRARY
U.S. Documents Division
5 Washington Street
P.O. Box 630
Newark, NJ 07101
(201) 733-7812

NEW MEXICO

UNIVERSITY OF NEW MEXICO
General Library
Government Publications/Maps Dept.
Albuquerque, NM 87131
(505) 277-5441

NEW MEXICO STATE LIBRARY
325 Don Gaspar Avenue
Santa Fe, NM 87501
(505) 827-3826

NEW YORK

NEW YORK STATE LIBRARY
Documents Sect. Cultural Educ. Ctr.
Empire State Plaza
Albany, NY 12230
(518) 474-5563

NORTH CAROLINA

UNIVERSITY OF NORTH CAROLINA AT CHAPEL HILL
Davis Library 080A
BA/SS Department Documents
Chapel Hill, NC 27514
(919) 962-1151

NORTH DAKOTA

NORTH DAKOTA STATE UNIVERSITY LIBRARY
Government Documents Dept.
Fargo, ND 58105
(701) 237-8352
In cooperation with Univ. of North Dakota, Chester Fritz Library Grand Forks

OHIO

STATE LIBRARY OF OHIO
Documents Section
65 South Front Street
Columbus, OH 43266
(614) 644-7051

OKLAHOMA

OKLAHOMA DEPT. OF LIBRARIES
Government Documents
200 NE 18th Street
Oklahoma City, OK 73105
(405) 521-2502, ext. 252

OKLAHOMA STATE UNIV. LIB.
Documents Department
Stillwater, OK 74078
(405) 624-0489

OREGON

PORTLAND STATE UNIV.
Millar Library
934 SW Harrison - P.O. Box 1151
Portland, OR 97207
(503) 229-3673

PENNSYLVANIA

STATE LIBRARY OF PENN.
Government Publications Section
Box 1601
Walnut St. & Commonwealth Ave.
Harrisburg, PA 17105
(717) 787-3752

SOUTH CAROLINA

CLEMSON UNIV. COOPER LIB.
Documents Department
Clemson, SC 29634
(803) 656-5174
In cooperation with Univ. of South Carolina, Thomas Cooper Library, Columbia

TEXAS

TEXAS STATE LIBRARY
Public Services Department
P.O. Box 12927 - 1201 Brazos
Austin, TX 78711
(512) 463-5455

TEXAS TECH. UNIV. LIBRARY
Documents Department
Lubbock, TX 79409
(806) 742-2268

UTAH

UTAH STATE UNIVERSITY
Merrill Library & Learning Resources Center, UMC-30
Documents Department
Logan, UT 84322
(801) 750-2682

VIRGINIA

UNIVERSITY OF VIRGINIA
Alderman Library
Government Documents
Charlottesville, VA 22903
(804) 924-3133

WASHINGTON

WASHINGTON STATE LIBRARY
Document Section
Olympia, WA 98504
(206) 753-4027

WEST VIRGINIA

WEST VIRGINIA UNIV. LIB.
Government Documents Section
P.O. Box 6069
Morgantown, WV 26506
(304) 293-3640

WISCONSIN

ST. HIST SOC. OF WISCONSIN LIB.
Government Pub. Section
816 State Street
Madison, WI 53706
(608) 262-2781
In cooperation with Univ. of Wisconsin-Madison, Memorial Library

MILWAUKEE PUBLIC LIBRARY
Documents Division
814 West Wisconsin Avenue
Milwaukee, WI 53233
(414) 278-3065

WYOMING

WYOMING STATE LIBRARY
Supreme Court & Library Bldg.
Cheyenne, WY 82002
(307) 777-5919

TYPICAL CITATION AND ABSTRACT

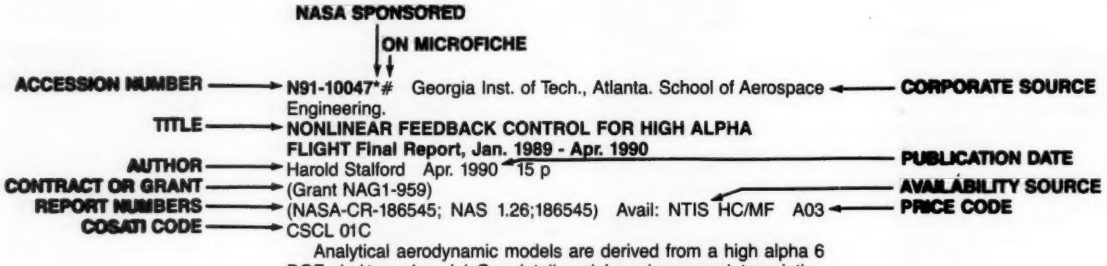

Analytical aerodynamic models are derived from a high alpha 6 DOF wind tunnel model. One detail model requires some interpolation between nonlinear functions of alpha. One analytical model requires no interpolation and as such is a completely continuous model. Flight path optimization is conducted on the basic maneuvers: half-loop, 90 degree pitch-up, and level turn. The optimal control analysis uses the derived analytical model in the equations of motion and is based on both moment and force equations. The maximum principle solution for the half-loop is poststall trajectory performing the half-loop in 13.6 seconds. The agility induced by thrust vectoring capability provided a minimum effect on reducing the maneuver time. By means of thrust vectoring control the 90 degrees pitch-up maneuver can be executed in a small place over a short time interval. The agility capability of thrust vectoring is quite beneficial for pitch-up maneuvers. The level turn results are based currently on only outer layer solutions of singular pertrubation. Poststall solutions provide high turn rates but generate higher losses of energy than that of classical sustained solutions.

Author

National Aeronautics and
Space Administration
Code NTT
Washington, D.C.
20546
Official Business
Penalty for Private Use, $300

SPECIAL FOURTH-CLASS RATE
POSTAGE & FEES PAID
NASA
PERMIT No. G27

NASA

POSTMASTER: If Undeliverable (Section 158
Postal Manual) Do Not Return